

NASA Technical Memorandum 100842

Engine Structures

A Bibliography of Lewis Research Center's Research for 1980-1987

SEPTEMBER 1988



PREFACE

The Structures Technology Bibliography covers the years during which the Structures Division of the NASA Lewis Research Center has had its individual identity (1980 to present). During 1980, the Materials and Structures Division was split into two divisions, the Materials Division and the Structures and Mechanical Technologies Division (under the direction of J.A. Ziemianski). Then, in August 1984 a reorganization occurred that gave the discipline of structures its single identity and title. Dr. Lester D. Nichols was appointed to the position of Division Chief. Although not stated in its name, the principal types of structures to be addressed by the division are engine structures, and, more specifically, aerospace propulsion engines.

This extensive bibliography contains over 1000 citations to technical publications written by the division's staff, its contractors, and its grantees. The bibliographical information is a printout of detailed information contained in the NASA computerized data bank. As each NASA sponsored technical publication is generated, pertinent information is entered into the system for future retrieval. Titles, authors, affiliations, reporting categories, key words, and abstracts are entered into the system. Sorting of stored information can take place by subject, author, author's organization, contract number, and publication report number.

Each year, the NASA Lewis bibliographic information from all divisions is collected and printed in a single NASA Technical Memorandum containing several hundred citations. These volumes were initiated in 1965 and have been published for the calendar years 1965 through 1968 and 1976 through 1987. They have been steadily improved upon through the dedicated efforts of Lewis' George Mandel, Chief of the Technical Information Services Division. The bibliographic information is also published in the biweekly abstracting publications, STAR (Scientific and Technical Aerospace Reports) and IAA (International Aerospace Abstracts).

The information concerning Lewis structures technology contained herein has been gleaned from Lewis publications from 1980 through 1987. Only certain STAR categories were scanned for structures related reports: 7, 24, 26, 27, 37, 38,39,61, and 64. In fact, every citation from categories 38 and 39 is contained in the current compilation. Owing to the lead time for preparation of this volume, few 1988 listings are included.

We trust the bibliographic information will be helpful in identifying publications of value to your scientific and engineering needs.

G.R. Halford
Chairman, Committee for LST '88

TABLE OF CONTENTS

	Page
Category 7 Aircraft Propulsion and Power	1
Includes prime propulsion systems and systems components, e.g., gas turbine engines and compressors; and onboard auxiliary power plants for aircraft.	
Category 24 Composite Materials	12
Includes physical, chemical, and mechanical properties of laminates and other composite materials.	
Category 26 Metallic Materials	32
Includes physical, chemical, and mechanical properties of metals, e.g., corrosion; and metallurgy.	
Category 27 Nonmetallic Materials	45
Includes physical, chemical, and mechanical properties of plastics, elastomers, lubricants, polymers, textiles, adhesives, and ceramic materials.	
Category 37 Mechanical Engineering	47
Includes auxiliary systems (nonpower); machine elements and processes; and mechanical equipment..	
Category 38 Quality Assurance and Reliability	50
Includes product sampling procedures and techniques; and quality control..	
Category 39 Structural Mechanics	63
Includes structural element design and weight analysis; fatigue; and thermal stress..	
Category 61 Computer Programming and Software	126
Includes computer programs, routines, algorithms, and specific applications, e.g., CAD/CAM..	
Category 64 Numerical Analysis	126
Includes iteration, difference equations, and numerical approximation..	
Subject Index	A-1
Personal Author Index	B-1
Corporate Source Index	C-1
Contract Number Index	D-1
Report / Accession Number Index	E-1

Engine Structures

A Bibliography of Lewis Research Center's Research for 1980-1987

07

AIRCRAFT PROPULSION AND POWER

Includes prime propulsion systems and systems components, e.g., gas turbine engines and compressors; and onboard auxiliary power plants for aircraft.

A80-35101*# National Aeronautics and Space Administration. Lewis Research Center, Cleveland, Ohio.

ENGINE ENVIRONMENTAL EFFECTS ON COMPOSITE BEHAVIOR

C. C. CHAMIS and G. T. SMITH (NASA, Lewis Research Center, Cleveland, Ohio) In: Structures, Structural Dynamics, and Materials Conference, 21st, Seattle, Wash., May 12-14, 1980, Technical Papers. Part 2. New York, American Institute of Aeronautics and Astronautics, Inc., 1980, p. 987-997. refs (AIAA 80-0695)

The effects of turbojet engine environmental saturation moisture and temperatures up to 300 F on composites were investigated. It was found that epoxy resin composites absorbed the most moisture (2 wt %), while polyimide resin composites absorbed 0.8%. High moisture and 250 F degraded the flexural and interlaminar shear properties, and the environmental and impact conditions severely damaged epoxy composites. The impact damage of fiber composites in moisture-temperature environments can be assessed with finite element and composite mechanics analyses. Engine operation environmental conditions of 0.8% moisture and 140 F had no discernible effect on the fatigue resistance of composite fan exit guide vanes, which can be designed to exceed engine operational requirements using composite materials. A.T.

A81-29940*# National Aeronautics and Space Administration. Lewis Research Center, Cleveland, Ohio.

SUPERHYBRID COMPOSITE BLADE IMPACT STUDIES

C. C. CHAMIS, R. F. LARK, and J. H. SINCLAIR (NASA, Lewis Research Center, Cleveland, Ohio) American Society of Mechanical Engineers, Gas Turbine Conference and Products Show, Houston, Tex., Mar. 9-12, 1981, 8 p. refs (ASME PAPER 81-GT-24)

An investigation was conducted to determine the feasibility of superhybrid composite blades for meeting the mechanical design and impact resistance requirements of large fan blades for aircraft turbine engine applications. Two design concepts were evaluated: (1) leading edge spar (TiCom) and (2) center spar (TiCore), both with superhybrid composite shells. The investigation was both analytical and experimental. The results obtained show promise that superhybrid composites can be used to make light-weight, high-quality, large fan blades with good structural integrity. The blades tested successfully demonstrated their ability to meet steady-state operating conditions, overspeed, and small bird impact requirements. (Author)

A83-29024*# General Electric Co., Cincinnati, Ohio.

TURBINE BLADE NONLINEAR STRUCTURAL AND LIFE ANALYSIS

R. L. MCKNIGHT, J. H. LAFLEN (General Electric Co., Aircraft Engine Business Group, Cincinnati, OH), G. R. HALFORD, and A. KAUFMAN (NASA, Lewis Research Center, Structures and Mechanical Technologies Div., Cleveland, OH) Journal of Aircraft (ISSN 0021-8669), vol. 20, May 1983, p. 475-480. refs

Previously cited in issue 17, p. 2687, Accession no. A82-34981

A83-29737*# Pratt and Whitney Aircraft Group, East Hartford, Conn.

STRUCTURAL TAILORING OF ENGINE BLADES (STAEBL)

K. W. BROWN, T. K. PRATT (United Technologies Corp., Pratt and Whitney Aircraft Group, East Hartford, CT), and C. C. CHAMIS (NASA Lewis Research Center, Cleveland, OH) In: Structures, Structural Dynamics and Materials Conference, 24th, Lake Tahoe, NV, May 2-4, 1983, Collection of Technical Papers. Part 1. New York, American Institute of Aeronautics and Astronautics, 1983, p. 79-88. refs

(Contract NAS3-22525)

(AIAA 83-0828)

Mathematical optimization is applied to the design of gas turbine fan blades. The automated procedure replaces the current manual process which requires experience and intuition on the part of the designer to achieve successful blade designs. The optimization procedure that is developed utilizes the COPES/CONMIN optimization code. Approximate vibration and stress analyses are used for the optimization process. Analysis recalibrations are achieved through the application of more detailed, refined analysis. Optimizations of a hollow titanium fan blade with composite inlays and of a superhybrid composite blade are demonstrated. Author

A83-32791*# Carnegie-Mellon Univ., Pittsburgh, Pa.

EFFECTS OF FRICTION DAMPERS ON AERODYNAMICALLY UNSTABLE ROTOR STAGES

J. H. GRIFFIN (Carnegie-Mellon University, Pittsburgh, PA) and A. SINHA AIAA, ASME, ASCE, and AHS, Structures, Structural Dynamics and Materials Conference, Lake Tahoe, NV, May 2-4, 1983, 12 p. refs

(Contract NAG3-231)

(AIAA PAPER 83-0848)

Attention is given to the physical concepts and mathematical techniques useful in the analysis of the stabilizing effect of friction on aerodynamically unstable rotor stages. Results are presented for three-, four-, and five-bladed disks. In the present multidegree-of-freedom model of an aerodynamically unstable rotor stage, a harmonic steady state solution due to the friction dampers may be either a stability limit, a stable cycle limit, or neither. A criterion is established in the form of an energy function which determines whether the solution is a stability limit. In the event that the initial displacement and velocity exceed those associated with the steady state solution corresponding to a stability limit, the response becomes unbounded. O.C.

07 AIRCRAFT PROPULSION AND POWER

A83-35883*# Princeton Univ., N. J.
DESIGN OF DRY-FRICTION DAMPERS FOR TURBINE BLADES

W. ANCONA and E. H. DOWELL (Princeton University, Princeton, NJ) IN: International Symposium on Air Breathing Engines, 6th, Paris, France, June 6-10, 1983, Symposium Papers. New York, American Institute of Aeronautics and Astronautics, 1983, p. 708-722. refs
(Contract NAG3-221)

A study is conducted of turbine blade forced response, where the blade has been modeled as a cantilever beam with a generally dry friction damper attached, and where the minimization of blade root strain as the excitation frequency is varied over a given range is the criterion for the evaluation of the effectiveness of the dry friction damper. Attempts are made to determine the location of the damper configuration best satisfying the design criterion, together with the best damping force (assuming that the damper location has been fixed). Results suggest that there need not be an optimal value for the damping force, or an optimal location for the dry friction damper, although there is a range of values which should be avoided. O.C.

A83-40864*# General Electric Co., Cincinnati, Ohio.
BLADE LOSS TRANSIENT DYNAMIC ANALYSIS OF TURBOMACHINERY

M. J. STALLONE, V. GALLARDO, A. F. STORACE, L. J. BACH, G. BLACK, and E. F. GAFFNEY (General Electric Co, Aircraft Engine Business Group, Cincinnati, OH) AIAA Journal (ISSN 0001-1452), vol. 21, Aug. 1983, p. 1134-1138. refs
(Contract NAS3-22053)

Previously cited in issue 17, p. 2687, Accession no. A82-34982

A83-47970*# Lehigh Univ., Bethlehem, Pa.
ANALYSIS OF AN AXIAL COMPRESSOR BLADE VIBRATION BASED ON WAVE REFLECTION THEORY

J. A. OWCZAREK (Lehigh University, Bethlehem, PA) American Society of Mechanical Engineers, International Gas Turbine Conference and Exhibit, 28th, Phoenix, AZ, Mar. 27-31, 1983.

8 p
(Contract NAG3-135)
(ASME PAPER 83-GT-151)

The paper describes application of the theory of wave reflection in turbomachines to rotor blade vibrations measured in an axial compressor stage. The blade vibrations analyzed could not be predicted using various flutter prediction techniques. The wave reflection theory, first advanced in 1966, is expanded, and more general equations for the rotor blade excitation frequencies are derived. The results of the analysis indicate that all examined rotor blade vibrations can be explained by forced excitations caused by reflecting waves (pressure pulses). Wave reflections between the rotor blades and both the upstream and downstream stator vanes had to be considered. Author

A83-48331*# National Aeronautics and Space Administration. Lewis Research Center, Cleveland, Ohio.
DESIGN CONCEPTS FOR LOW COST COMPOSITE ENGINE FRAMES

C. C. CHAMIS (NASA, Lewis Research Center, Cleveland, OH) American Institute of Aeronautics and Astronautics, Aircraft Design, Systems and Technology Meeting, Fort Worth, TX, Oct. 17-19, 1983. 16 p.
(AIAA PAPER 83-2445)

Design concepts for low-cost, lightweight composite engine frames were applied to the design requirements for the frame of commercial, high-bypass turbine engines. The concepts consist of generic-type components and subcomponents that could be adapted for use in different locations in the engine and to different engine sizes. A variety of materials and manufacturing methods were assessed with a goal of having the lowest number of parts possible at the lowest possible cost. The evaluation of the design concepts resulted in the identification of a hybrid composite frame

which would weigh about 70 percent of the state-of-the-art metal frame and cost would be about 60 percent. Author

A84-22877*# Pratt and Whitney Aircraft Group, East Hartford, Conn.

SIMPLIFIED ANALYTICAL PROCEDURES FOR REPRESENTING MATERIAL CYCLIC RESPONSE

V. MORENO (United Technologies Corp., Pratt and Whitney Group, East Hartford, CT) and A. KAUFMAN (NASA, Lewis Research Center, Cleveland, OH) Auburn University, Southeastern Conference on Theoretical and Applied Mechanics, 12th, Callaway Gardens, GA, May 10, 11, 1984, Paper. 5 p. refs

Requirements for increased durability of gas turbine hot section structural components have made it necessary to place greater emphasis on accurate structural analysis and life prediction. Linear finite-element analysis is generally sufficient for structural analysis applications. However, for structures in the hot part of the engine, nonlinear structural analysis may be required under certain conditions for the accurate prediction of the local stress-strain response. Nonlinear finite element analysis represents a costly effort which is generally incompatible with the iterative nature of the design process. The present investigation is, therefore, concerned with two simplified procedures for estimating the local hysteretic response produced by cyclic thermal loading. These procedures reduce the need for nonlinear finite-element analysis. G.R.

A84-26959*# National Aeronautics and Space Administration. Lewis Research Center, Cleveland, Ohio.

THE COUPLED RESPONSE OF TURBOMACHINERY BLADING TO AERODYNAMIC EXCITATIONS

D. HOYNIK (NASA, Lewis Research Center, Cleveland, OH; Purdue University, West Lafayette, IN) and S. FLEETER (Purdue University, West Lafayette, IN) (Structures, Structural Dynamics and Materials Conference, 24th, Lake Tahoe, NV, May 2-4, 1983, Collection of Technical Papers. Part 2, p. 137-148) Journal of Aircraft (ISSN 0021-8669), vol. 21, April 1984, p. 278-286. USAF-supported research. refs

Previously cited in issue 12, p. 1742, Accession no. A83-29822

A84-31905*# Carnegie-Mellon Univ., Pittsburgh, Pa.
MODEL DEVELOPMENT AND STATISTICAL INVESTIGATION OF TURBINE BLADE MISTUNING

J. H. GRIFFIN (Carnegie-Mellon University, Pittsburgh, PA) and T. M. HOOSAC (ASME, Transactions, Journal of Vibration, Acoustics, Stress and Reliability in Design (ISSN 0739-3717), vol. 106, April 1984, p. 204-210. refs
(Contract NAG3-231)

This paper discusses the development of an efficient algorithm which calculates the individual blade response of a bladed turbine disk, the subsequent statistical investigation to establish mistuning dependencies, and procedures which reduce the increase in blade amplitudes caused by mistuning. Author

A85-18792*# General Electric Co., Cincinnati, Ohio.
CONSIDERATIONS FOR DAMAGE ANALYSIS OF GAS TURBINE HOT SECTION COMPONENTS

T. S. COOK and J. H. LAFLIN (General Electric Co., Cincinnati, OH) American Society of Mechanical Engineers, Pressure Vessels and Piping Conference and Exhibition, San Antonio, TX, June 17-21, 1984. 7 p. refs

(Contract NAS3-22534)
(ASME PAPER 84-PVP-77)

The hot flowpath of a gas turbine engine contains static and rotating components operating in a very hostile environment. Since the reliable operation of these components is critical to the safe and efficient performance of the engine, structural life analysis of these members is carried out with great care. However, the complex nature of the strain-temperature-time cycle affecting the engine makes a general analysis procedure difficult and usually leads to separating the damage into regimes where one damage mode dominates. In particular, cycle dependent, time dependent, and

thermomechanical fatigue regimes have been identified and some general considerations of each region are discussed. This discussion includes both the damage models themselves and the application of the models. Specific examples of several models are given and important factors affecting each are presented.

Author

A85-21866*# Pennsylvania State Univ., University Park.
EFFECTS OF FRICTION DAMPERS ON AERODYNAMICALLY UNSTABLE ROTOR STAGES

A. SINHA (Pennsylvania State University, University Park, PA) and J. H. GRIFFIN (Carnegie-Mellon University, Pittsburgh, PA) AIAA Journal (ISSN 0001-1452), vol. 23, Feb. 1985, p. 262-270. Previously cited in issue 14, p. 1976, Accession no. A83-32791. refs

(Contract NAG3-231)

A85-30378*# National Aeronautics and Space Administration. Lewis Research Center, Cleveland, Ohio.

THE EFFECT OF AERODYNAMIC AND STRUCTURAL DETUNING ON TURBOMACHINE SUPERSONIC UNSTALLED TORSIONAL FLUTTER

D. HOYNIK (NASA, Lewis Research Center, Cleveland, OH) and S. FLEETER (Purdue University, West Lafayette, IN) IN: Structures, Structural Dynamics, and Materials Conference, 26th, Orlando, FL, April 15-17, 1985, Technical Papers. Part 2. New York, American Institute of Aeronautics and Astronautics, 1985, p. 500-514. refs (AIAA PAPER 85-0761)

The effects of alternate-blade structural detuning and adjacent-blade alternate-circumferential-spacing aerodynamic detuning on the supersonic unstalled torsional flutter stability of a turbomachine rotor are investigated analytically. An unsteady aerodynamic model employing influence coefficients is constructed for the case of a flat-plate-airfoil cascade in torsion-mode harmonic oscillation in a supersonic inviscid isentropic adiabatic irrotational perfect-gas inlet flow with a subsonic leading-edge locus. The influence coefficients and equations of motion are derived; the model is verified by applying it to the 12-blade cascade-B flow geometry studied by Verdon and McCune (1975); and the results are presented graphically. It is found that the rotor can be stabilized over the entire reduced frequency range by applying a combination of structural and aerodynamic detuning as the passive flutter-control mechanism.

T.K.

A85-42365*# Virginia Polytechnic Inst. and State Univ., Blacksburg.

OPTIMIZATION OF CASCADE BLADE MISTUNING. I - EQUATIONS OF MOTION AND BASIC INHERENT PROPERTIES

E. NISSIM (Virginia Polytechnic Institute and State University, Blacksburg) AIAA Journal (ISSN 0001-1452), vol. 23, Aug. 1985, p. 1213-1222. refs (Contract NAG3-347)

Attention is given to the derivation of the equations of motion of mistuned compressor blades, interpolating aerodynamic coefficients by means of quadratic expressions in the reduced frequency. If the coefficients of the quadratic expressions are permitted to assume complex values, excellent accuracy is obtained and Pade rational expressions are obviated. On the basis of the resulting equations, it is shown analytically that the sum of all the real parts of the eigenvalues is independent of the mistuning introduced into the system. Blade mistuning is further treated through the aerodynamic energy approach, and the limiting vibration modes associated with alternative mistunings are identified.

O.C.

A85-45715*# Virginia Polytechnic Inst. and State Univ., Blacksburg.

OPTIMIZATION OF CASCADE BLADE MISTUNING. II - GLOBAL OPTIMUM AND NUMERICAL OPTIMIZATION

E. NISSIM and R. T. HAFTKA (Virginia Polytechnic Institute and State University, Blacksburg) AIAA Journal (ISSN 0001-1452), vol. 23, Sept. 1985, p. 1402-1410. (Contract NAG3-347)

The values of the mistuning which yield the most stable eigenvectors are analytically determined, using the simplified equations of motion which were developed in Part I of this work. It is shown that random mistunings, if large enough, may lead to the maximal stability, whereas the alternate mistunings cannot. The problem of obtaining maximum stability for minimal mistuning is formulated, based on numerical optimization techniques. Several local minima are obtained using different starting mistuning vectors. The starting vectors which lead to the global minimum are identified. It is analytically shown that all minima appear in multiplicities which are equal to the number of compressor blades. The effect of mistuning on the flutter speed is studied using both an optimum mistuning vector and an alternate mistuning vector. Effects of mistunings in elastic axis locations are shown to have a negligible effect on the eigenvalues. Finally, it is shown that any general two-dimensional bending-torsion system can be reduced to an equivalent uncoupled torsional system.

Author

A85-45854*# National Aeronautics and Space Administration. Lewis Research Center, Cleveland, Ohio.

VIBRATION AND FLUTTER OF MISTUNED BLADED-DISK ASSEMBLIES

K. R. V. KAZA and R. E. KIELB (NASA, Lewis Research Center, Cleveland, OH) Journal of Propulsion and Power (ISSN 0748-4658), vol. 1, Sept.-Oct. 1985, p. 336-344. Previously cited in issue 05, p. 602, Accession no. A85-16095. refs

A86-14338* National Aeronautics and Space Administration. Lewis Research Center, Cleveland, Ohio.

VIBRATION ANALYSIS OF ROTATING TURBOMACHINERY BLADES BY AN IMPROVED FINITE DIFFERENCE METHOD

K. B. SUBRAHMANYAM and K. R. V. KAZA (NASA, Lewis Research Center, Cleveland, OH) International Journal for Numerical Methods in Engineering (ISSN 0029-5981), vol. 21, Oct. 1985, p. 1871-1886. refs

The problem of calculating the natural frequencies and mode shapes of rotating blades is solved by an improved finite difference procedure based on second-order central differences. Lead-lag, flapping and coupled bending-torsional vibration cases of untwisted blades are considered. Results obtained by using the present improved theory have been observed to be close lower bound solutions. The convergence has been found to be rapid in comparison with the classical first-order finite difference method. While the computational space and time required by the present approach is observed to be almost the same as that required by the first-order theory for a given mesh size, accuracies of practical interest can be obtained by using the improved finite difference procedure with a relatively smaller matrix size, in contrast to the classical finite difference procedure which requires either a larger matrix or an extrapolation procedure for improvement in accuracy.

Author

A86-14430*# Army Propulsion Lab., Cleveland, Ohio.

DEAN - A PROGRAM FOR DYNAMIC ENGINE ANALYSIS

G. G. SADLER (U.S. Army, Propulsion Laboratory, Cleveland, OH) and K. J. MELCHER (NASA, Lewis Research Center, Cleveland, OH) AIAA, SAE, and ASME, Joint Propulsion Conference, 21st, Monterey, CA, July 8-10, 1985. 17 p. Previously announced in STAR as N85-28945. refs (AIAA PAPER 85-1354)

The Dynamic Engine Analysis Program, DEAN, is a FORTRAN code implemented on the IBM/370 mainframe at NASA Lewis Research Center for digital simulation of turbofan engine dynamics. DEAN is an interactive program which allows the user to simulate engine subsystems as well as full engine systems with relative

ease. The nonlinear first order ordinary differential equations which define the engine model may be solved by one of four integration schemes, a second order Runge-Kutta, a fourth order Runge-Kutta, an Adams Predictor-Corrector, or Gear's method for stiff systems. The numerical data generated by the model equations are displayed a specified intervals between which the user may choose to modify various parameters affecting the model equations and transient execution. Following the transient run, versatile graphics capabilities allow close examination of the data. DEAN's modeling procedure and capabilities are demonstrated by generating a model of simple compressor rig. Author

A86-19198* Pennsylvania State Univ., University Park.
STABILITY OF LIMIT CYCLES IN FRICTIONALLY DAMPED AND AERODYNAMICALLY UNSTABLE ROTOR STAGES
A. SINHA (Pennsylvania State University, University Park) and J. H. GRIFFIN (Carnegie-Mellon University, Pittsburgh, PA) Journal of Sound and Vibration (ISSN 0022-460X), vol. 103, Dec. 8, 1985, p. 341-356. refs
(Contract NAG3-231)

This paper deals with the stability of limit cycles (Steady-State Oscillations) associated with the multi-degree-of-freedom model of a frictionally damped and aerodynamically unstable rotor stage. By using the first order averaging technique, a generalized criterion has been established to sort out those unstable limit cycles which govern the maximum transient amplitude beyond which the rotor stage becomes unstable. The stability of the remaining steady-state solutions is analyzed by linearizing the averaged system of differential equations. Numerical results are discussed for three-, four- and five-bladed disks. Author

A86-22068*# Princeton Univ., N. J.
VIBRATION CHARACTERISTICS OF MISTUNED SHROUDED BLADE ASSEMBLIES
O. O. BENDIKSEN (Princeton University, NJ) and N. A. VALERO ASME, International Gas Turbine Conference and Exhibit, 30th, Houston, TX, Mar. 18-21, 1985. 7 p. refs
(Contract NAG3-308)
(ASME PAPER 85-GT-115)

An investigation of the mode localization phenomenon associated with mistuning is presented for shrouded blade assemblies. The calculations are based on a generic finite element model, which permits modeling of arbitrary mistuning and both slipping and nonslipping shroud interfaces. The results presented indicate that interactions occur between mistuning and slip effects, with maximum mode localization occurring when the shrouds slip freely. Certain modes are found to be very sensitive to shroud slip, and in some cases completely change character when slip occurs. Mode localization is most pronounced in the predominantly bending modes, and varies considerably from mode to mode. As the ratio of interblade coupling strength to mistuning strength is increased, the effect of mistuning is observed to decrease significantly. This result has important implications for the flutter problem, since it suggests that the stabilization effect available from mistuning is significantly less for a shrouded rotor as compared to an unshrouded rotor. Author

A86-24677* Massachusetts Inst. of Tech., Cambridge.
AEROELASTIC FORMULATIONS FOR TURBOMACHINES AND PROPELLERS
E. F. CRAWLEY (MIT, Cambridge, MA) IN: Unsteady aerodynamics of turbomachines and propellers; Proceedings of the Symposium, Cambridge, England, September 24-27, 1984. Cambridge, Cambridge University, 1984, p. 13-28. Navy-supported research. refs
(Contract NSG-3079)

The task of the aeroelastic analysis is to combine the formulations of the structural dynamic and unsteady aerodynamic models in a consistent manner, to solve the resulting aeroelastic model to determine the dynamic behavior (e.g., stability, forced vibration), and to interpret those results for both qualitative trends, and quantitative detail. A review of the various formulations of the aeroelastic problem and a comparison of their relative advantages

will be the subject of this paper. Specifically, the topics to be addressed are: the formulation of the aeroelastic problem, including a summary of the relations necessary to transform various diverse structural and aerodynamic models to a consistent notation for oscillatory motion; an approximate transformation for arbitrary temporal behavior; and a brief review of the applicable solution techniques. Author

A86-25743* General Electric Co., Cincinnati, Ohio.
THE DYNAMICS OF A FLEXIBLE BLADED DISC ON A FLEXIBLE ROTOR IN A TWO-ROTOR SYSTEM
V. C. GALLARDO and M. J. STALLONE (General Electric Co., Aircraft Engine Business Group, Cincinnati, OH) IN: International Conference on Vibrations in Rotating Machinery, 3rd, Hestington, England, September 11-13, 1984, Proceedings. London, Mechanical Engineering Publications, Ltd., 1984, p. 383-390. refs
(Contract NAS3-23281)

This paper describes the development of the analysis of the transient dynamic response of a bladed disk on a flexible rotor. The rotating flexible bladed disk is considered as a module in a complete turbine engine structure. The analysis of the flexible bladed disk (FBD) module is developed for the non-equilibrated one-diameter axial mode. The FBD motion is considered as a sum of two standing axial waves constrained to the rotor. The FBD is coupled inertially and gyroscopically to its rotor support, and indirectly through connecting elements, to the adjacent rotor and/or other supporting structures. Incorporated in the basic Turbine Engine Transient Response Analysis program (TETRA), the FBD module is demonstrated with a two-rotor model where the FBD can be excited into resonance by an unbalance in the adjacent rotor and at a frequency equal to the differential rotor speed. The FBD module also allows the analysis of two flexible bladed disks in the same rotor. Author

A86-26893*# Toledo Univ., Ohio.
THE EFFECTS OF STRONG SHOCK LOADING ON COUPLED BENDING-TORSION FLUTTER OF TUNED AND MISTUNED CASCADES
B. C. BUSBEY (Toledo University; Teledyne CAE, OH), T. G. KEITH, JR. (NASA, Lewis Research Center, Cleveland, OH), and K. R. V. KAZA (Toledo, University, OH) IN: Fluid-structure interaction and aerodynamics damping; Proceedings of the Tenth Biennial Conference on Mechanical Vibration and Noise, Cincinnati, OH, September 10-13, 1985. New York, American Society of Mechanical Engineers, 1985, p. 93-108. refs
(Contract NSG-3139)

This paper presents an investigation of the effects of strong in-passage shock waves on coupled bending-torsion flutter of both tuned and mistuned cascades. The aerodynamic and inertial coupling between the bending and torsional motions of each blade are included in the analytical model. Analysis revealed (1) that the shock loading has a beneficial effect on torsional flutters of both tuned and mistuned cascades and (2) that alternating bending mistuning has a beneficial effect on shock load induced bending flutter. The latter finding becomes important when shock induced bending flutter is a problem. Author

A86-26901* National Aeronautics and Space Administration. Lewis Research Center, Cleveland, Ohio.
VIBRATIONS OF BLADES AND BLADED DISK ASSEMBLIES; PROCEEDINGS OF THE TENTH BIENNIAL CONFERENCE ON MECHANICAL VIBRATION AND NOISE, CINCINNATI, OH, SEPTEMBER 10-13, 1985
R. E. KIELB, ED. (NASA, Lewis Research Center, Cleveland, OH) and N. F. RIEGER, ED. Conference sponsored by ASME. New York, American Society of Mechanical Engineers, 1985, 123 p. For individual items see A86-26902 to A86-26914.

The papers presented in this volume provide an overview of recent theoretical and analytical research in bladed disk assemblies, with particular attention given to forced response, mistuning, and damping. Specific topics discussed include the response of mistuned bladed disk assemblies; forced response analysis of an

aerodynamically detuned supersonic turbomachine rotor; dynamic analysis of blade groups using component mode synthesis; and pendulum dynamic vibration absorbers for reducing blade vibration in industrial fans. V.L.

A86-26902*# National Aeronautics and Space Administration. Lewis Research Center, Cleveland, Ohio.

FORCED RESPONSE ANALYSIS OF AN AERODYNAMICALLY DETUNED SUPERSONIC TURBOMACHINE ROTOR

D. HOYNIK (NASA, Lewis Research Center, Cleveland, OH) and S. FLEETER (Purdue University, West Lafayette, IN) IN: Vibrations of blades and bladed disk assemblies; Proceedings of the Tenth Biennial Conference on Mechanical Vibration and Noise, Cincinnati, OH, September 10-13, 1985. New York, American Society of Mechanical Engineers, 1985, p. 1-13. NASA-supported research. refs

The effect of aerodynamic detuning on the supersonic flow induced forced response behavior of a turbomachine blade row is analyzed using an aeroelastic model. The rotor is modeled as a flat plate airfoil cascade representing an unwrapped rotor annulus; the aerodynamic detuning is achieved by alternating the circumferential spacing of adjacent rotor blades. The total unsteady aerodynamic loading on the blading, due to the convection of the transverse gust past the airfoil cascade as well as that resulting from the motion of the cascade, is developed in terms of influence coefficients. The model developed here is then used to analyze the effect of aerodynamic detuning on the flow induced forced response behavior of a twelve-bladed rotor with Verdon's Cascade B flow geometry. V.L.

A86-26905*# Carnegie-Mellon Univ., Pittsburgh, Pa.

THE EFFECT OF LIMITING AERODYNAMIC AND STRUCTURAL COUPLING IN MODELS OF MISTUNED BLADED DISK VIBRATION

P. BASU and J. H. GRIFFIN (Carnegie-Mellon University, Pittsburgh, PA) IN: Vibrations of blades and bladed disk assemblies; Proceedings of the Tenth Biennial Conference on Mechanical Vibration and Noise, Cincinnati, OH, September 10-13, 1985. New York, American Society of Mechanical Engineers, 1985, p. 31-40. refs

(Contract NAG3-367)

A model has been developed for studying the effect of mistuning on bladed disk vibration which has the unique feature that the extent of aerodynamic and structural interaction which it simulates can be readily varied from full coupling of all blades on the disk to coupling of each blade with only its nearest neighbors. Simulations utilizing the resulting algorithm show that limited coupling models may be used to predict the statistical distribution of blade amplitudes that characterizes the mistuning effect, which in turn determines stage durability. This approach is used to study the effect of changing various system parameters on amplitude scatter. Gas density, the number of blades on the disk, disk stiffness, and the engine order of the excitation are considered. The results are used to draw some conclusions about how to improve laboratory tests and component design. Author

A86-31595*# National Aeronautics and Space Administration. Lewis Research Center, Cleveland, Ohio.

AERODYNAMIC AND STRUCTURAL DETUNING OF SUPERSONIC TURBOMACHINE ROTORS

D. HOYNIK (NASA, Lewis Research Center, Cleveland, OH) and S. FLEETER (Purdue University, West Lafayette, IN) (Structures, Structural Dynamics, and Materials Conference, 26th, Orlando, FL, April 15-17, 1985, Technical Papers. Part 2, p. 500-514) Journal of Propulsion and Power (ISSN 0748-4658), vol. 2, Mar.-Apr. 1986, p. 161-167. Previously cited in issue 13, p. 1850, Accession no. A85-30378. refs

A86-32956*# United Technologies Research Center, East Hartford, Conn.

DYNAMIC CHARACTERISTICS OF AN ASSEMBLY OF PROP-FAN BLADES

A. V. SRINIVASAN (United Technologies Research Center, East Hartford, CT), R. E. KIELB, and C. LAWRENCE (NASA, Lewis Research Center, Cleveland, OH) ASME, Transactions, Journal of Engineering for Gas Turbines and Power (ISSN 0022-0825), vol. 108, April 1986, p. 306-312. refs (ASME PAPER 85-GT-134)

In contrast to conventional propellers, propfan blades are thin and highly swept-back, thereby giving rise to large bending and twisting deformations and complex vibratory characteristics. Aerodynamic performance depends on the extent of steady state deformation, and the aeroelastic response depends on the vibratory frequency and mode shape. Attention is presently given to the principal results of structural analyses for a five-bladed propfan assembly; these results are compared with test data. The results encompass both steady deformations and vibratory frequencies and mode shapes in a vacuum centrifugal environment. O.C.

A86-32957*# Pennsylvania State Univ., University Park.

INFLUENCE OF FRICTION DAMPERS ON TORSIONAL BLADE FLUTTER

A. SINHA (Pennsylvania State University, University Park), J. H. GRIFFIN (Carnegie-Mellon University, Pittsburgh, PA), and R. E. KIELB (NASA, Lewis Research Center, Cleveland, OH) ASME, Transactions, Journal of Engineering for Gas Turbines and Power (ISSN 0022-0825), vol. 108, April 1986, p. 313-318. refs (ASME PAPER 85-GT-170)

This paper deals with the stabilizing effects of dry friction on torsional blade flutter. A lumped parameter model with single degree of freedom per blade has been used to represent the rotor stage. The well-known cascade theories for incompressible and supersonic flows have been used to determine the allowable increase in fluid velocity relative to the blade. It has been found that the effectiveness of friction dampers in controlling flutter can be substantial. Author

A86-38894*# Purdue Univ., West Lafayette, Ind.

THREE DIMENSIONAL UNSTEADY AERODYNAMICS AND AEROELASTIC RESPONSE OF ADVANCED TURBOPROPS

M. H. WILLIAMS and C.-C. HWANG (Purdue University, West Lafayette, IN) IN: Structures, Structural Dynamics and Materials Conference, 27th, San Antonio, TX, May 19-21, 1986, Technical Papers. Part 2. New York, American Institute of Aeronautics and Astronautics, 1986, p. 116-124. refs (Contract NAG3-499)

(AIAA PAPER 86-0846)

A method for the prediction of steady and unsteady aerodynamic loads and aeroelastic response of advanced turboprops is presented. The aerodynamic analysis uses three dimensional unsteady linearized compressible flow theory to compute the blade pressure distribution. The aeroelastic analysis is based on a normal mode representation of the structure. The method is applicable to both conventional and advanced turbo-prop configurations, provided that blade stall and transonic shock waves are not important factors. Aerodynamic results are presented which validate the model in various limits by comparisons to alternative theories and experimental data. Finally, results of a stability analysis of an advanced turboprop are given, with comparisons to measurements made at NASA Lewis Research Center. Author

A86-48141*# National Aeronautics and Space Administration. Lewis Research Center, Cleveland, Ohio.

COMPUTATIONAL ENGINE STRUCTURAL ANALYSIS

C. C. CHAMIS and R. H. JOHNS (NASA, Lewis Research Center, Cleveland, OH) ASME, International Gas Turbine Conference and Exhibit, 31st, Duesseldorf, West Germany, June 8-12, 1986. 12 p. Previously announced in STAR as N86-19663. refs (ASME PAPER 86-GT-70)

A significant research activity at the NASA Lewis Research Center is the computational simulation of complex multidisciplinary

engine structural problems. This simulation is performed using computational engine structural analysis (CESA) which consists of integrated multidisciplinary computer codes in conjunction with computer post-processing for problem-specific application. A variety of the computational simulations of specific cases are described in some detail in this paper. These case studies include: (1) aeroelastic behavior of bladed rotors, (2) high velocity impact of fan blades, (3) blade-loss transient response, (4) rotor/stator/squeeze-film/bearing interaction, (5) blade-fragment/rotor-burst containment, and (6) structural behavior of advanced swept turboprops. These representative case studies are selected to demonstrate the breath of the problems analyzed and the role of the computer including post-processing and graphical display of voluminous output data.

Author

A86-48163*# Massachusetts Inst. of Tech., Cambridge.
ANALYTICAL AND EXPERIMENTAL INVESTIGATION OF THE COUPLED BLADED DISK/SHAFT WHIRL OF A CANTILEVERED TURBOFAN

E. F. CRAWLEY, E. H. DUCHARME, and D. R. MOKADAM (MIT, Cambridge, MA) ASME, International Gas Turbine Conference and Exhibit, 31st, Duesseldorf, West Germany, June 8-12, 1986. 9 p. refs

(Contract NAG3-200)
 (ASME PAPER 86-GT-98)

A simple analytical model for the structural dynamics of a rotating flexible blade/rigid disk/flexible cantilevered shaft system yields the equations of motion expressed in the rotating frame, showing that the blade's one-nodal diameter modes dynamically couple to the rigid body whirling motion of the shaft-disk system. This analytical model is correlated with the results of a structural dynamic experiment performed on an aeroelastic rotor fan that is similar to a high bypass ratio shroudless turbofan. The agreement between the predicted and experimental natural frequencies is good, and suggests significant interaction of the one-nodal diameter blade modes with the shaft-disk modes.

O.C.

A86-48224*# National Aeronautics and Space Administration. Lewis Research Center, Cleveland, Ohio.

TOWARD IMPROVED DURABILITY IN ADVANCED COMBUSTORS AND TURBINES - PROGRESS IN PREDICTION OF THERMOMECHANICAL LOADS

D. E. SOKOLOWSKI and C. R. ENSIGN (NASA, Lewis Research Center, Cleveland, OH) ASME, International Gas Turbine Conference and Exhibit, 31st, Duesseldorf, West Germany, June 8-12, 1986. 13 p. refs

(ASME PAPER 86-GT-172)

NASA is sponsoring the Turbine Engine Hot Section Technology (HOST) Project to address the need for improved durability in advanced combustors and turbines. Analytical and experimental activities aimed at more accurate prediction of the aerothermal environment, the thermomechanical loads, the material behavior and structural responses to such loading, and life predictions for high temperature cyclic operation have been underway for several years and are showing promising results. Progress is reported in the development of advanced instrumentation and in the improvement of combustor aerothermal and turbine heat transfer models that will lead to more accurate prediction of thermomechanical loads.

Author

A87-25396*# National Aeronautics and Space Administration. Lewis Research Center, Cleveland, Ohio.

THE EFFECT OF CIRCUMFERENTIAL AERODYNAMIC DETUNING ON COUPLED BENDING-TORSION UNSTALLED SUPERSONIC FLUTTER

D. HOYNIK (NASA, Lewis Research Center, Cleveland, OH) and S. FLEETER (Purdue University, West Lafayette, IN) ASME, Transactions, Journal of Turbomachinery (ISSN 0889-504X), vol. 108, Oct. 1986, p. 253-260. Previously announced in STAR as N86-21513. refs

(ASME PAPER 86-GT-100)

A mathematical model developed to predict the enhanced coupled bending-torsion unstalled supersonic flutter stability due

to alternate circumferential spacing aerodynamic detuning of a turbomachine rotor. The translational and torsional unsteady aerodynamic coefficients are developed in terms of influence coefficients, with the coupled bending-torsion stability analysis developed by considering the coupled equations of this aerodynamic detuning on coupled bending-torsion unstalled supersonic flutter as well as the verification of the modeling are then demonstrated by considering an unstable 12 bladed rotor, with Verdon's uniformly spaced Cascade B flow geometry as a baseline. However, with the elastic axis and center of gravity at 60 percent of the chord, this type of aerodynamic detuning has a minimal effect on stability. For both uniform and nonuniform circumferentially spaced rotors, a single degree of freedom torsion mode analysis was shown to be appropriate for values of the bending-torsion natural frequency ratio lower than 0.6 and higher 1.2. When the elastic axis and center of gravity are not coincident, the effect of detuning on cascade stability was found to be very sensitive to the location of the center of gravity with respect to the elastic axis. In addition, it was determined that when the center of gravity was forward of an elastic axis located at midchord, a single degree of freedom torsion model did not accurately predict cascade stability.

Author

A87-46228*# National Aeronautics and Space Administration. Lewis Research Center, Cleveland, Ohio.

INFLUENCE OF THIRD-DEGREE GEOMETRIC NONLINEARITIES ON THE VIBRATION AND STABILITY OF PRETWISTED, PRECONED, ROTATING BLADES

K. B. SUBRAHMANYAM and K. R. V. KAZA (NASA, Lewis Research Center, Cleveland, OH) IN: International Symposium on Air Breathing Engines, 8th, Cincinnati, OH, June 14-19, 1987, Proceedings. New York, American Institute of Aeronautics and Astronautics, 1987, p. 465-479. Previously announced in STAR as N86-31920. refs

The governing coupled flapwise bending, edgewise bending, and torsional equations are derived including third-degree geometric nonlinear elastic terms by making use of the geometric nonlinear theory of elasticity in which the elongations and shears are negligible compared to unity. These equations are specialized for blades of doubly symmetric cross section with linear variation of Pretwist over the blade length. The nonlinear steady state equations and the linearized perturbation equations are solved by using the Galerkin method, and by utilizing the nonrotating normal modes for the shape functions. Parametric results obtained for various cases of rotating blades from the present theoretical formulation are compared to those produced from the finite element code MSC/NASTRAN, and also to those produced from an in-house experimental test rig. It is shown that the spurious instabilities, observed for thin, rotating blades when second degree geometric nonlinearities are used, can be eliminated by including the third-degree elastic nonlinear terms. Furthermore, inclusion of third degree terms improves the correlation between the theory and experiment.

M.G.

N80-21330*# IIT Research Inst., Chicago, Ill.

THERMAL FATIGUE AND OXIDATION DATA FOR DIRECTIONALLY SOLIDIFIED MAR-M 246 TURBINE BLADES

V. L. HILL and V. E. HUMPHREYS Jan. 1980 45 p refs

(Contract NAS3-19696)

(NASA-CR-159798; IITRI-M6003-53) Avail: NTIS HC A03/MF A01 CSCL 21E

Thermal fatigue and oxidation data were obtained for 11 plasma spray coated and 13 uncoated directionally solidified and single crystal MAR-M 246 blades. Blade coatings on the airfoil included several metal-oxide thermal barrier layers based on Al₂O₃, Cr₂O₃, or ZrO₂. The 24 turbine blades were tested simultaneously for 3000 cycles in fluidized beds maintained at 950 and 25 C using a symmetrical 360 set thermal cycle. In 3000 cycles, only uncoated turbine blades exhibited cracking on the trailing edge near the platform; 3 of the 13 uncoated blades did not crack. Cracking occurred over the range 400 to 2750 cycles, with single crystal blades indicating the poorest thermal fatigue resistance. Oxidation of the uncoated blades was limited in 3000 cycles. All coatings

indicated microscopically visible spalling at the trailing edge radius after 3000 cycles. Severe general spalling on the airfoil was observed for two multilayered coatings. Author

N81-17079*# Pratt and Whitney Aircraft Group, East Hartford, Conn.

COMBUSTOR LINER DURABILITY ANALYSIS Final Report

V. MORENO Feb. 1981 84 p refs

(Contract NAS3-21836)

(NASA-CR-165250; PWA-5684-19) Avail: NTIS HC A05/MF A01 CSCL 21E

An 18 month combustor liner durability analysis program was conducted to evaluate the use of advanced three dimensional transient heat transfer and nonlinear stress-strain analyses for modeling the cyclic thermomechanical response of a simulated combustor liner specimen. Cyclic life prediction technology for creep/fatigue interaction is evaluated for a variety of state-of-the-art tools for crack initiation and propagation. The sensitivity of the initiation models to a change in the operating conditions is also assessed. A.R.H.

N82-22266*# National Aeronautics and Space Administration. Lewis Research Center, Cleveland, Ohio.

STRUCTURAL DYNAMICS OF SHROUDLESS, HOLLOW FAN BLADES WITH COMPOSITE IN-LAYS

R. A. AIELLO, M. S. HIRSCHBEIN, and C. C. CHAMIS 1982 12 p refs Presented at the 27th Ann. Intern. Gas Turbine Conf., London, 18-22 Apr. 1982; sponsored by ASME

(NASA-TM-82816; E-1163; NAS 1.15:82816) Avail: NTIS HC A02/MF A01 CSCL 21E

Structural and dynamic analyses are presented for a shroudless, hollow titanium fan blade proposed for future use in aircraft turbine engines. The blade was modeled and analyzed using the composite blade structural analysis computer program (COBSTRAN); an integrated program consisting of mesh generators, composite mechanics codes, NASTRAN, and pre- and post-processors. Vibration and impact analyses are presented. The vibration analysis was conducted with COBSTRAN. Results show the effect of the centrifugal force field on frequencies, twist, and blade camber. Bird impact analysis was performed with the multi-mode blade impact computer program. This program uses the geometric model and modal analysis from the COBSTRAN vibration analysis to determine the gross impact response of the fan blades to bird strikes. The structural performance of this blade is also compared to a blade of similar design but with composite in-lays on the outer surface. Results show that the composite in-lays can be selected (designed) to substantially modify the mechanical performance of the shroudless, hollow fan blade. Author

N82-25257*# United Technologies Corp., East Hartford, Conn. Commercial Products Div.

FRACTURE MECHANICS CRITERIA FOR TURBINE ENGINE HOT SECTION COMPONENTS Final Report

G. J. MEYERS May 1982 123 p refs

(Contract NAS3-22550)

(NASA-CR-167896; NAS 1.26:167896; PWA-5772-23) Avail: NTIS HC A06/MF A01 CSCL 21E

The application of several fracture mechanics data correlation parameters to predicting the crack propagation life of turbine engine hot section components was evaluated. An engine survey was conducted to determine the locations where conventional fracture mechanics approaches may not be adequate to characterize cracking behavior. Both linear and nonlinear fracture mechanics analyses of a cracked annular combustor liner configuration were performed. Isothermal and variable temperature crack propagation tests were performed on Hastelloy X combustor liner material. The crack growth data was reduced using the stress intensity factor, the strain intensity factor, the J integral, crack opening displacement, and Tomkins' model. The parameter which showed the most effectiveness in correlation high temperature and variable temperature Hastelloy X crack growth data was crack opening displacement. S.L.

N82-33390*# Akron Univ., Ohio. Dept. of Mechanical and Civil Engineering.

ENGINE DYNAMIC ANALYSIS WITH GENERAL NONLINEAR FINITE ELEMENT CODES. PART 2: BEARING ELEMENT IMPLEMENTATION OVERALL NUMERICAL CHARACTERISTICS AND BENCHMARKING

J. PADOVAN, M. ADAMS, J. FERTIS, I. ZEID, and P. LAM Oct. 1982 229 p refs

(Contract NSG-3283)

(NASA-CR-167944; NAS 1.26:167944) Avail: NTIS HC A11/MF A01 CSCL 21E

Finite element codes are used in modelling rotor-bearing-stator structure common to the turbine industry. Engine dynamic simulation is used by developing strategies which enable the use of available finite element codes. benchmarking the elements developed are benchmarked by incorporation into a general purpose code (ADINA); the numerical characteristics of finite element type rotor-bearing-stator simulations are evaluated through the use of various types of explicit/implicit numerical integration operators. Improving the overall numerical efficiency of the procedure is improved. S.L.

N82-33391*# Pratt and Whitney Aircraft Group, East Hartford, Conn. Commercial Products Div.

STRUCTURAL TAILORING OF ENGINE BLADES (STAEBL) Interim Report

C. E. PLATT, T. K. PRATT, and K. W. BROWN Jun. 1982 359 p refs

(Contract NAS3-22525)

(NASA-CR-167949; NAS 1.26:167949; PWA-5774-21) Avail: NTIS HC A16/MF A01 CSCL 21E

A mathematical optimization procedure was developed for the structural tailoring of engine blades and was used to structurally tailor two engine fan blades constructed of composite materials without midspan shrouds. The first was a solid blade made from superhybrid composites, and the second was a hollow blade with metal matrix composite inlays. Three major computerized functions were needed to complete the procedure: approximate analysis with the established input variables, optimization of an objective function, and refined analysis for design verification. S.L.

N84-13193*# General Electric Co., Cincinnati, Ohio. Aircraft Engine Business Group.

BLADE LOSS TRANSIENT DYNAMICS ANALYSIS WITH FLEXIBLE BLADED DISK Final Report

V. C. GALLARDO, G. BLACK, L. BACH, S. CLINE, and A. STORACE Apr. 1983 269 p refs

(Contract NAS3-23281)

(NASA-CR-168176; NAS 1.26:168176) Avail: NTIS HC A12/MF A01 CSCL 21E

The transient dynamic response of a flexible bladed disk on a flexible rotor in a two rotor system is formulated by modal synthesis and a Lagrangian approach. Only the nonequilibrated one diameter flexible mode is considered for the flexible bladed disk, while the two flexible rotors are represented by their normal modes. The flexible bladed disk motion is modeled as a combination of two one diameter standing waves, and is coupled inertially and gyroscopically to the flexible rotors. Application to a two rotor model shows that a flexible bladed disk on one rotor can be driven into resonance by an unbalance in the other rotor, and at a frequency equal to the difference in the rotor speeds. Author

N84-15152*# General Electric Co., Cincinnati, Ohio. Aircraft Engine Business Group.

AEROTHERMAL MODELING. EXECUTIVE SUMMARY Final Report

M. K. KENWORTHY, S. M. CORREA, and D. L. BURRUS Dec. 1983 55 p refs

(Contract NAS3-23525)

(NASA-CR-168330; NAS 1.26:168330) Avail: NTIS HC A04/MF A01 CSCL 21E

One of the significant ways in which the performance level of aircraft turbine engines has been improved is by the use of

07 AIRCRAFT PROPULSION AND POWER

advanced materials and cooling concepts that allow a significant increase in turbine inlet temperature level, with attendant thermodynamic cycle benefits. Further cycle improvements have been achieved with higher pressure ratio compressors. The higher turbine inlet temperatures and compressor pressure ratios with corresponding higher temperature cooling air has created a very hostile environment for the hot section components. To provide the technology needed to reduce the hot section maintenance costs, NASA has initiated the Hot Section Technology (HOST) program. One key element of this overall program is the Aerothermal Modeling Program. The overall objective of this program is to evolve and validate improved analysis methods for use in the design of aircraft turbine engine combustors. The use of such combustor analysis capabilities can be expected to provide significant improvement in the life and durability characteristics of both combustor and turbine components. B.W.

N84-15153*# Textron Bell Aerospace Co., Buffalo, N. Y.
NASTRAN DOCUMENTATION FOR FLUTTER ANALYSIS OF ADVANCED TURBOPROPELLERS Final Report
V. ELCHURI, A. M. GALLO, and S. C. SKALSKI Apr. 1982
216 p refs
(Contract NAS3-22533)
(NASA-CR-167927; NAS 1.26:167927; D2536-941010) Avail:
NTIS HC A10/MF A01 CSCL 20K

An existing capability developed to conduct modal flutter analysis of tuned bladed-shrouded discs was modified to facilitate investigation of the subsonic unstalled flutter characteristics of advanced turbopropellers. The modifications pertain to the inclusion of oscillatory modal aerodynamic loads of blades with large (backward and forward) varying sweep. Author

N84-15154*# Textron Bell Aerospace Co., Buffalo, N. Y.
BLADED-SHROUDED-DISC AEROELASTIC ANALYSES: COMPUTER PROGRAM UPDATES IN NASTRAN LEVEL 17.7 Final Report
A. M. GALLO, V. ELCHURI, and S. C. SKALSKI Dec. 1981
348 p
(Contract NAS3-22533)
(NASA-CR-165428; NAS 1.26:165428; D2536-941006) Avail:
NTIS HC A15/MF A01 CSCL 21E

In October 1979, a computer program based on the state-of-the-art compressor and structural technologies applied to bladed-shrouded-disc was developed. The program was more operational in NASTRAN Level 16. The bladed disc computer program was updated for operation in NASTRAN Level 17.7. The supersonic cascade unsteady aerodynamics routine UCAS, delivered as part of the NASTRAN Level 16 program was recorded to improve its execution time. These improvements are presented. Author

N84-16181*# National Aeronautics and Space Administration.
Lewis Research Center, Cleveland, Ohio.
DYNAMIC BEHAVIOR OF SPIRAL-GROOVE AND RAYLEIGH-STEP SELF-ACTING FACE SEALS
E. DIRUSSO Jan. 1984 19 p refs
(NASA-TP-2266; NAS 1.60:2266; E-1754) Avail: NTIS HC
A02/MF A01 CSCL 21E

Tests were performed to determine the dynamic behavior and establish baseline dynamic data for five self-acting face seals employing Rayleigh-step lift-pads and inward pumping as well as outward-pumping spiral grooves for the lift-generating mechanism. The primary parameters measured in the tests were film thickness, seal seat axial motion, and seal frictional torque. The data show the dynamic response of the film thickness to the motion of the seal seat. The inward-pumping spiral-groove seals exhibited a high-amplitude film thickness vibratory mode with a frequency of four times the shaft speed. This mode was not observed in the other seals tested. The tests also revealed that high film thickness vibration amplitude produces considerably higher average film thickness than do low amplitude film thickness vibrations. The seals were tested at a constant face load of 73 N (16.4 lb) with ambient air at room temperature and atmospheric pressure as the

fluid medium. The test speed range was from 7000 to 17000 rpm. Seal tangential speed range was 34.5 to 83.7 m/sec (113 to 274 ft/sec). Author

N84-16185*# National Aeronautics and Space Administration.
Lewis Research Center, Cleveland, Ohio.
DIGITAL COMPUTER PROGRAM FOR GENERATING DYNAMIC TURBOFAN ENGINE MODELS (DIGTEM)
C. J. DANIELE, S. M. KROSEL, J. R. SZUCH, and E. J. WESTERKAMP Sep. 1983 109 p refs
(NASA-TM-83446; E-1748; NAS 1.15:83446) Avail: NTIS HC
A06/MF A01 CSCL 21E

This report describes DIGTEM, a digital computer program that simulates two spool, two-stream turbofan engines. The turbofan engine model in DIGTEM contains steady-state performance maps for all of the components and has control volumes where continuity and energy balances are maintained. Rotor dynamics and duct momentum dynamics are also included. Altogether there are 16 state variables and state equations. DIGTEM features a backward-difference integration scheme for integrating stiff systems. It trims the model equations to match a prescribed design point by calculating correction coefficients that balance out the dynamic equations. It uses the same coefficients at off-design points and iterates to a balanced engine condition. Transients can also be run. They are generated by defining controls as a function of time (open-loop control) in a user-written subroutine (TMRSF). DIGTEM has run on the IBM 370/3033 computer using implicit integration with time steps ranging from 1.0 msec to 1.0 sec. DIGTEM is generalized in the aerothermodynamic treatment of components. B.W.

N84-16186*# National Aeronautics and Space Administration.
Lewis Research Center, Cleveland, Ohio.
DESIGN CONCEPTS FOR LOW-COST COMPOSITE ENGINE FRAMES
C. C. CHAMIS 1983 28 p refs Presented at Aircraft Design Systems and Operations Meeting, Fort Worth, Tex., 17-19 Oct. 1983; sponsored by AIAA and AHS Previously announced in IAA as A83-48331
(NASA-TM-83544; E-1916; NAS 1.15:83544) Avail: NTIS HC
A03/MF A01 CSCL 21E

Design concepts for low-cost, lightweight composite engine frames were applied to the design requirements for the frame of commercial, high-bypass turbine engines. The concepts consist of generic-type components and subcomponents that could be adapted for use in different locations in the engine and to different engine sizes. A variety of materials and manufacturing methods were assessed with a goal of having the lowest number of parts possible at the lowest possible cost. The evaluation of the design concepts resulted in the identification of a hybrid composite frame which would weigh about 70 percent of the state-of-the-art metal frame and cost would be about 60 percent. Author (IAA)

N84-20562*# National Aeronautics and Space Administration.
Lewis Research Center, Cleveland, Ohio.
FORMULATION OF BLADE-FLUTTER SPECTRAL ANALYSES IN STATIONARY REFERENCE FRAME
A. P. KURKOV Mar. 1984 32 p refs
(NASA-TP-2296; E-1888; NAS 1.60:2296) Avail: NTIS HC
A03/MF A01 CSCL 21E

Analytic representations are developed for the discrete blade deflection and the continuous tip static pressure fields in a stationary reference frame. Considered are the sampling rates equal to the rotational frequency, equal to blade passing frequency, and for the pressure, equal to a multiple of the blade passing frequency. For the last two rates the expressions for determining the nodal diameters from the spectra are included. A procedure is presented for transforming the complete unsteady pressure field into a rotating frame of reference. The determination of the true flutter frequency by using two sensors is described. To illustrate their use, the developed procedures are used to interpret selected experimental results. Author

N84-24578*# National Aeronautics and Space Administration. Lewis Research Center, Cleveland, Ohio.

LEWIS RESEARCH CENTER SPIN RIG AND ITS USE IN VIBRATION ANALYSIS OF ROTATING SYSTEMS

G. V. BROWN, R. E. KIELB, E. H. MEYN, R. E. MORRIS, and S. J. POSTA May 1984 19 p refs
(NASA-TP-2304; E-1829; NAS 1.60:2304) Avail: NTIS HC A02/MF A01 CSCL 21E

The Lewis Research Center spin rig was constructed to provide experimental evaluation of analysis methods developed under the NASA Engine Structural Dynamics Program. Rotors up to 51 cm (20 in.) in diameter can be spun to 16,000 rpm in vacuum by an air motor. Vibration forcing functions are provided by shakers that apply oscillatory axial forces or transverse moments to the shaft, by a natural whirling of the shaft, and by an air jet. Blade vibration is detected by strain gages and optical blade-tip motion sensors. A variety of analog and digital processing equipment is used to display and analyze the signals. Results obtained from two rotors are discussed. A 56-blade compressor disk was used to check proper operation of the entire spin rig system. A special two-blade rotor was designed and used to hold flat and twisted plates at various setting and sweep angles. Accurate Southwell coefficients have been obtained for several modes of a flat plate oriented parallel to the plane of rotation. Author

N84-24586*# Massachusetts Inst. of Tech., Cambridge. Gas Turbine and Plasma Dynamics Lab.

FLUTTER AND FORCED RESPONSE OF MISTUNED ROTORS USING STANDING WAVE ANALYSIS

D. J. BUNDAS and J. DUNGUNDJI Mar. 1983 155 p refs
Previously announced as A83-29823
(Contract NAG3-214)

(NASA-CR-173555; NAS 1.26:173555; GT/PDL-170) Avail: NTIS HC A08/MF A01 CSCL 21E

A standing wave approach is applied to the analysis of the flutter and forced response of tuned and mistuned rotors. The traditional traveling wave cascade airforces are recast into standing wave arbitrary motion form using Pade approximants, and the resulting equations of motion are written in the matrix form. Applications for vibration modes, flutter, and forced response are discussed. It is noted that the standing wave methods may prove to be more versatile for dealing with certain applications, such as coupling flutter with forced response and dynamic shaft problems, transient impulses on the rotor, low-order engine excitation, bearing motion, and mistuning effects in rotors. V.L. (IAA)

N85-10951*# National Aeronautics and Space Administration. Lewis Research Center, Cleveland, Ohio.

TURBINE ENGINE HOT SECTION TECHNOLOGY (HOST)

Washington Oct. 1982 356 p refs Workshop held in Cleveland, 19-20 Oct. 1982

(NASA-TM-83022; E-1458; NAS 1.15:83022) Avail: NTIS HC A16/MF A01 CSCL 21E

Research and plans concerning aircraft gas turbine engine hot section durability problems were discussed. Under the topics of structural analysis, fatigue and fracture, surface protective coatings, combustion, turbine heat transfer, and instrumentation specific points addressed were the thermal and fluid environment around liners, blades, and vanes, material coatings, constitutive behavior, stress-strain response, and life prediction methods for the three components.

N85-10954*# National Aeronautics and Space Administration. Lewis Research Center, Cleveland, Ohio.

NONLINEAR STRUCTURAL AND LIFE ANALYSES OF A TURBINE BLADE

A. KAUFMAN *In its* Turbine Eng. Hot Sect. Technol. (HOST) p 39-44 Oct. 1982

Avail: NTIS HC A16/MF A01 CSCL 21E

The most critical structural requirements that aircraft gas turbine engines must meet result from the diversity of extreme environmental conditions in the turbine section components. Accurate life assessment of the components under these conditions

requires sound analytical tools and techniques. The utility of advanced structural analysis techniques and advanced life prediction techniques in the life assessment of hot-section components was evaluated. The extent to which a three-dimensional cyclic isoparametric finite element analysis of a hot-section component would improve the accuracy of component life predictions was assessed. At the same time, high temperature life prediction theories such as strainrange partitioning and the frequency modified approaches were applied and their efficiency judged. A stress analysis was performed on a commercial air-cooled turbine blade. The evaluation of the life prediction methods indicated that none of those studied were satisfactory. R.S.F.

N85-10955*# National Aeronautics and Space Administration. Lewis Research Center, Cleveland, Ohio.

NONLINEAR STRUCTURAL AND LIFE ANALYSES OF A COMBUSTOR LINER

A. KAUFMAN *In its* Turbine Eng. Hot Sect. Technol. (HOST) p 45-53 Oct. 1982

Avail: NTIS HC A16/MF A01 CSCL 21E

Three-dimensional, nonlinear, finite element structural analyses were performed for a simulated aircraft combustor liner specimen in order to assess the capability of nonlinear analyses using classical inelastic material models to represent the thermoplastic-creep response of the component. In addition, the computed stress-strain history at the critical location was input into life prediction methods in order to evaluate the ability of these procedures to predict crack initiation life. It is concluded that: (1) elastic analysis is adequate for obtaining strain range and critical location; (2) inelastic analyses did not accurately represent cyclic behavior of materials; and (3) none of the crack initiation life prediction methods were satisfactory. R.S.F.

N85-10956*# National Aeronautics and Space Administration. Lewis Research Center, Cleveland, Ohio.

PRE-HOST HIGH TEMPERATURE CRACK PROPAGATION

T. W. ORANGE *In its* Turbine Eng. Hot Sect. Technol. (HOST) p 55-63 Oct. 1982

Avail: NTIS HC A16/MF A01 CSCL 21E

The highlights of NASA contract CR-167896, Fracture Mechanics Criteria for Turbine Engine Hot Section Components, are presented. The five technical tasks of the program are reviewed. Results of several tasks are presented. R.S.F.

N85-10969*# National Aeronautics and Space Administration. Lewis Research Center, Cleveland, Ohio.

STRUCTURAL ANALYSIS

R. H. JOHNS *In its* Turbine Eng. Hot Sect. Technol. (HOST) p 181-184 Oct. 1982

Avail: NTIS HC A16/MF A01 CSCL 21E

Hot section components of aircraft gas turbine engines are subjected to severe thermal-structural loading conditions, especially during the start-up and take-off portions of the engine cycle. The most severe and damaging stresses and strains are those induced by the steep thermal gradients induced during the start-up transient. These transient stresses and strains are also the most difficult to predict, in part because the temperature gradients and distributions are not well known or predictable, and also because the cyclic elasto-viscoplastic behavior of the materials at these extremes of temperature and strain are not well known or predictable. One element of the structures program will develop improved time-varying thermal-mechanical load models for the entire engine mission cycle from start-up to shutdown. The thermal model refinements will be consistent with those required by the structural code including considerations of mesh-point density, strain concentrations, and thermal gradients. Models will be developed for the burner liner, turbine vane and turbine blade. B.G.

07 AIRCRAFT PROPULSION AND POWER

N85-10971*# National Aeronautics and Space Administration. Lewis Research Center, Cleveland, Ohio.

COMPONENT-SPECIFIC MODELING

M. S. HIRSCHBEIN *In its* Turbine Eng. Hot Sect. Technol. (HOST) p 197-202 Oct. 1982

Avail: NTIS HC A16/MF A01 CSCL 21E

The ability to accurately structurally analyze engine components to assure that they can survive for their designed lifetime in an increasingly harsh environment is discussed. Under the HOST (HOT Section Technology) program, advanced component-specific modeling methods, with built-in analysis capability, will be developed separately for burner liners, turbine blades and vanes. These modeling methods will make maximum use of, but will not rely solely on, existing analysis methods and techniques, to analyze the three identified components. Nor will the complete structural analysis of a component necessarily be performed as a single analysis. The approach to be taken will develop complete software analysis packages with internal, component-specific, self-adaptive solution strategies. Each package will contain a set of modeling and analysis tools. The selection and order of specific methods and techniques within the set to be applied will depend on the specific-component, the current thermo-mechanical loading, and the current state of the component. All modeling and analysis decisions will be made internally based on developed decision criteria within the solution strategies; minimal user intervention will be required. B.W.

N85-10972*# National Aeronautics and Space Administration. Lewis Research Center, Cleveland, Ohio.

THE 3-D INELASTIC ANALYSIS METHODS FOR HOT SECTION COMPONENTS: BRIEF DESCRIPTION

C. C. CHAMIS *In its* Turbine Eng. Hot Sect. Technol. (HOST) p 203-208 Oct. 1982

Avail: NTIS HC A16/MF A01

Advanced 3-D inelastic structural/stress analysis methods and solution strategies for more accurate yet more cost-effective analysis of components subjected to severe thermal gradients and loads in the presence of mechanical loads, with steep stress and strain gradients are being developed. Anisotropy, time and temperature dependent plasticity and creep effects are also addressed. The approach is to develop four different theories, one linear and three higher order theories (polynomial function, special function, general function). The theories are progressively more complex from linear to general function in order to provide streamlined analysis capability with increasing accuracy for each hot section component and for different parts of the same component according to the severity of the local stress, strain and temperature gradients associated with hot spots, cooling holes and surface coating cracks. To further enhance the computational effectiveness, the higher order theories will have embedded singularities (cooling passages, for example) in the generic modeling region. Each of the four theories consists of three formulation models derivable from independent theoretical formulations. These formulation models are based on: (1) mechanics of materials; (2) special finite elements; and (3) an advanced formulation to be recommended by the contractor. B.W.

N85-10973*# National Aeronautics and Space Administration. Lewis Research Center, Cleveland, Ohio.

LIFE PREDICTION AND CONSTITUTIVE BEHAVIOR: OVERVIEW

G. R. HALFORD *In its* Turbine Eng. Hot Sect. Technol. (HOST) p 209-212 Oct. 1982

Avail: NTIS HC A16/MF A01 CSCL 21E

The evolution of programs to investigate high temperature constitutive behavior and develop cyclic life prediction methods is reviewed. Contracts granted for developing and verifying workable engineering methods for the calculation, in advance of service, of the local stress-strain response at the critical life governing location in typical hot section components as well as the resultant cyclic crack initiation and crack growth lifetimes are listed. The Langley fatigue facility is being upgraded to include: (1) a servocontrolled

testing machine for high temperature crack growth; (2) three servocontrolled tension/torsion machines for biaxial studies; (3) a HOST/satellite computer for data acquisition, processing, storage, and retrieval; and (4) HCV/LOF machines for cumulative damage studies. A.R.H.

N85-10975*# National Aeronautics and Space Administration. Lewis Research Center, Cleveland, Ohio.

CONSTITUTIVE MODEL DEVELOPMENT FOR ISOTROPIC MATERIALS

A. KAUFMAN *In its* Turbine Eng. Hot Sect. Technol. (HOST) p 215-221 Oct. 1982

Avail: NTIS HC A16/MF A01 CSCL 21E

The objective is to develop a unified constitutive model for finite-element structural analysis of turbine engine hot section components. This effort constitutes a different approach for nonlinear finite-element computer codes which were heretofore based on classical inelastic methods. A unified constitutive theory will avoid the simplifying assumptions of classical theory and should more accurately represent the behavior of superalloy materials under cyclic loading conditions and high temperature environments. Model development will be directed toward isotropic, cast nickel-base alloys used for aircooled turbine blades and vanes. The contractor will select a base material for model development and an alternate material for verification purposes from a list of three alloys specified by NASA. The candidate alloys represent a cross-section of turbine blade and vane materials of interest to both large and small size engine manufacturers. Material stock for the base and alternate materials will be supplied to the Contractor by the government. R.J.F.

N85-10977*# National Aeronautics and Space Administration. Lewis Research Center, Cleveland, Ohio.

HOST HIGH TEMPERATURE CRACK PROPAGATION

T. W. ORANGE *In its* Turbine Eng. Hot Sect. Technol. (HOST) p 227-229 Oct. 1982

Avail: NTIS HC A16/MF A01 CSCL 21E

Methods for characterizing and predicting crack growth at elevated temperatures are discussed. Nonlinear behavior, thermal gradients, and thermomechanical cycling are discussed. R.J.F.

N85-10987*# National Aeronautics and Space Administration. Lewis Research Center, Cleveland, Ohio.

VALIDATION OF STRUCTURAL ANALYSIS METHODS USING THE IN-HOUSE LINER CYCLIC RIGS

R. L. THOMPSON *In its* Turbine Eng. Hot Sect. Technol. (HOST) p 335-344 Oct. 1982

Avail: NTIS HC A16/MF A01 CSCL 21E

Test conditions and variables to be considered in each of the test rigs and test configurations, and also used in the validation of the structural predictive theories and tools, include: thermal and mechanical load histories (simulating an engine mission cycle; different boundary conditions; specimens and components of different dimensions and geometries; different materials; various cooling schemes and cooling hole configurations; several advanced burner liner structural design concepts; and the simulation of hot streaks. Based on these test conditions and test variables, the test matrices for each rig and configurations can be established to verify the predictive tools over as wide a range of test conditions as possible using the simplest possible tests. A flow chart for the thermal/structural analysis of a burner liner and how the analysis relates to the tests is shown schematically. The chart shows that several nonlinear constitutive theories are to be evaluated. A.R.H.

N85-10988*# National Aeronautics and Space Administration. Lewis Research Center, Cleveland, Ohio.

HOST LINER CYCLIC FACILITIES: FACILITY DESCRIPTION

D. SCHULTZ *In its* Turbine Eng. Hot Sect. Technol. (HOST) p 345-360 Oct. 1982

Avail: NTIS HC A16/MF A01 CSCL 21E

A quartz lamp box, a quartz lamp annular rig, and a low pressure liner cyclic can rig planned for liner cyclic tests are described.

Special test instrumentation includes an IR-TV camera system for measuring liner cold side temperatures, thin film thermocouples for measuring liner hot side temperatures, and laser and high temperature strain gages for obtaining local strain measurements. A plate temperature of 2,000 F was obtained in an initial test of an apparatus with three quartz lamps. Lamp life, however, appeared to be limited for the standard commercial quartz lamps available. The design of vitiated and nonvitiated preheaters required for the quartz lamp annular rig and the cyclic can test rigs is underway.

A.R.H.

N85-15744*# National Aeronautics and Space Administration. Lewis Research Center, Cleveland, Ohio.

ENGINE CYCLIC DURABILITY BY ANALYSIS AND MATERIAL TESTING

A. KAUFMAN and G. R. HALFORD *In* AGARD Eng. Cyclic Durability by Analysis and Testing 12 p Sep. 1984 refs
Previously announced as N84-18683

Avail: NTIS HC A12/MF A01 CSCL 21E

The problem of calculating turbine engine component durability is addressed. Nonlinear, finite-element structural analyses, cyclic constitutive behavior models, and an advanced creep-fatigue life prediction method called strainrange partitioning were assessed for their applicability to the solution of durability problems in hot-section components of gas turbine engines. Three different component or subcomponent geometries are examined: a stress concentration in a turbine disk; a lower lip of a half-scale combustor liner; and a squealer tip of a first-stage high-pressure turbine blade. Cyclic structural analyses were performed for all three problems. The computed strain-temperature histories at the critical locations of the combustor liner and turbine blade components were imposed on smooth specimens in uniaxial, strain-controlled, thermomechanical fatigue tests of evaluate the structural and life analysis methods.

Author

N85-21165*# Massachusetts Inst. of Tech., Cambridge. Dept. of Aeronautics and Astronautics.

ADVANCED STRESS ANALYSIS METHODS APPLICABLE TO TURBINE ENGINE STRUCTURES Final Report

T. H. H. PIAN Mar. 1985 44 p refs

(Contract NAG3-33)

(NASA-CR-175573; NAS 1.26:175573) Avail: NTIS HC A03/MF A01 CSCL 21E

Advanced stress analysis methods applicable to turbine engine structures are investigated. Constructions of special elements which containing traction-free circular boundaries are investigated. New versions of mixed variational principle and version of hybrid stress elements are formulated. A method is established for suppression of kinematic deformation modes. semiLoof plate and shell elements are constructed by assumed stress hybrid method. An elastic-plastic analysis is conducted by viscoplasticity theory using the mechanical subelement model.

B.W.

N85-22391*# Massachusetts Inst. of Tech., Cambridge. Gas Turbine Lab.

STRUCTURAL RESPONSE OF A ROTATING BLADED DISK TO ROTOR WHIRL Final Report

E. F. CRAWLEY Apr. 1985 140 p refs

(Contract NAG3-200)

(NASA-CR-175605; NAS 1.26:175605) Avail: NTIS HC A07/MF A01 CSCL 21E

A set of high speed rotating whirl experiments were performed in the vacuum of the MIT Blowdown Compressor Facility on the MIT Aeroelastic Rotor, which is structurally typical of a modern high bypass ratio turbofan stage. These tests identified the natural frequencies of whirl of the rotor system by forcing its response using an electromagnetic shaker whirl excitation system. The excitation was slowly swept in frequency at constant amplitude for several constant rotor speeds in both a forward and backward whirl direction. The natural frequencies of whirl determined by these experiments were compared to those predicted by an analytical 6 DOF model of a flexible blade-rigid disk-flexible shaft rotor. The model is also presented in terms of nondimensional

parameters in order to assess the importance of the interaction between the bladed disk dynamics and the shaft-disk dynamics. The correlation between the experimental and predicted natural frequencies is reasonable, given the uncertainty involved in determining the stiffness parameters of the system.

Author

N85-27868*# Ohio State Univ., Columbus. Dept. of Engineering Mechanics.

A STUDY OF INTERNAL AND DISTRIBUTED DAMPING FOR VIBRATING TURBOMACHINERY BLADES Final Report, 15 Apr. 1983 - 15 Apr. 1985

A. W. LEISSA Jun. 1985 24 p refs

(Contract NAG3-424)

(NASA-CR-175901; NAS 1.26:175901) Avail: NTIS HC A02/MF A01 CSCL 21E

Internal and distributed damping as possible methods for reducing the vibration response of turbomachine blades and theoretical methods for analyzing damped vibration were studied. It is demonstrated how the Ritz-Galerkin methods may be used to straightforwardly analyze forced vibrations with damping. This is done directly without requiring the free vibration eigenfunctions. The Galerkin method is an effective technique for these types of problems. The Ritz method has the further advantage of not needing to satisfy the force type boundary conditions, which is particularly important for plates and shells. But proper functionals representing the forcing and damping terms must be developed, and this is done. Two types of damping--viscous and material (hysteretic) are considered. Both distributed and concentrated exciting forces are treated. Numerical results are obtained for cantilevered beams and rectangular plates. Studies showing the rates of convergence of the solutions are made. In the case of the cantilever beam, approximate solutions from the present methods are compared with the exact solutions.

R.J.F.

N85-28945*# National Aeronautics and Space Administration. Lewis Research Center, Cleveland, Ohio.

DEAN: A PROGRAM FOR DYNAMIC ENGINE ANALYSIS

G. G. SADLER and K. J. MELCHER 1985 18 p refs Proposed for presentation at the 21st Joint Propulsion Conf., Monterey, Calif., 8-10 Jul. 1985; sponsored by AIAA, SAE and ASME Prepared in cooperation with Army Research and Technology Labs.

(NASA-TM-87033; E-2588; NAS 1.15:87033;

USAAVSCOM-TR-85-C-10) Avail: NTIS HC A02/MF A01

CSCL 21E

The Dynamic Engine Analysis program, DEAN, is a FORTRAN code implemented on the IBM/370 mainframe at NASA Lewis Research Center for digital simulation of turbofan engine dynamics. DEAN is an interactive program which allows the user to simulate engine subsystems as well as a full engine systems with relative ease. The nonlinear first order ordinary differential equations which define the engine model may be solved by one of four integration schemes, a second order Runge-Kutta, a fourth order Runge-Kutta, an Adams Predictor-Corrector, or Gear's method for stiff systems. The numerical data generated by the model equations are displayed at specified intervals between which the user may choose to modify various parameters affecting the model equations and transient execution. Following the transient run, versatile graphics capabilities allow close examination of the data. DEAN's modeling procedure and capabilities are demonstrated by generating a model of simple compressor rig.

Author

N85-31057*# Pratt and Whitney Aircraft, East Hartford, Conn. Commercial Products Div.

CREEP FATIGUE LIFE PREDICTION FOR ENGINE HOT SECTION MATERIALS (ISOTROPIC) Annual Report

V. MORENO Aug. 1983 89 p refs

(Contract NAS3-23288)

(NASA-CR-168228; NAS 1.26:168228; PWA-5894-17; AR-1)

Avail: NTIS HC A05/MF A01 CSCL 21E

The Hot Section Technology (HOST) program, creep fatigue life prediction for engine hot section materials (isotropic), is reviewed. The program is aimed at improving the high temperature crack initiation life prediction technology for gas turbine hot section

07 AIRCRAFT PROPULSION AND POWER

components. Significant results include: (1) cast B1900 and wrought IN 718 selected as the base and alternative materials respectively; (2) fatigue test specimens indicated that measurable surface cracks appear early in the specimen lives, i.e., 15% of total life at 871 C and 50% of life at 538 C; (3) observed crack initiation sites are all surface initiated and are associated with either grain boundary carbides or local porosity, transgranular cracking is observed at the initiation site for all conditions tested; and (4) an initial evaluation of two life prediction models, representative of macroscopic (Coffin-Manson) and more microscopic (damage rate) approaches, was conducted using limited data generated at 871 C and 538 C. It is found that the microscopic approach provides a more accurate regression of the data used to determine crack initiation model constants, but overpredicts the effect of strain rate on crack initiation life for the conditions tested. E.A.K.

N85-32119*# General Electric Co., Cincinnati, Ohio. Aircraft Engine Business Group.

COMPONENT-SPECIFIC MODELING Annual Status Report, 1 Jan. - 31 Dec. 1984

R. L. MCKNIGHT 1985 131 p

(Contract NAS3-23687)

(NASA-CR-174925; NAS 1.26:174925; ASR-2) Avail: NTIS HC A07/MF A01 CSCL 21E

Accomplishments are described for the second year effort of a 3-year program to develop methodology for component specific modeling of aircraft engine hot section components (turbine blades, turbine vanes, and burner liners). These accomplishments include: (1) engine thermodynamic and mission models; (2) geometry model generators; (3) remeshing; (4) specialty 3-D inelastic structural analysis; (5) computationally efficient solvers, (6) adaptive solution strategies; (7) engine performance parameters/component response variables decomposition and synthesis; (8) integrated software architecture and development, and (9) validation cases for software developed. Author

N85-34140*# General Electric Co., Cincinnati, Ohio. Aircraft Engine Business Group.

COMPONENT-SPECIFIC MODELING Annual Status Report

R. L. MCKNIGHT May 1985 162 p refs

(Contract NAS3-23687)

(NASA-CR-174765; NAS 1.26:174765; ASR-1) Avail: NTIS HC A08/MF A01 CSCL 21E

A series of interdisciplinary modeling and analysis techniques that were specialized to address three specific hot section components are presented. These techniques will incorporate data as well as theoretical methods from many diverse areas including cycle and performance analysis, heat transfer analysis, linear and nonlinear stress analysis, and mission analysis. Building on the proven techniques already available in these fields, the new methods developed will be integrated into computer codes to provide an accurate, and unified approach to analyzing combustor burner liners, hollow air cooled turbine blades, and air cooled turbine vanes. For these components, the methods developed will predict temperature, deformation, stress and strain histories throughout a complete flight mission. Author

N86-11513*# National Aeronautics and Space Administration. Lewis Research Center, Cleveland, Ohio.

HOST STRUCTURAL ANALYSIS PROGRAM OVERVIEW

R. H. JOHNS *In its* Turbine Eng. Hot Sect. Technol. (HOST) p 153-158 Oct. 1983

Avail: NTIS HC A11/MF A01 CSCL 21E

Hot section components of aircraft gas turbine engines are subjected to severe thermal structural loading conditions, especially during the start up and take off portions of the engine cycle. The most severe and damaging stresses and strains are those induced by the steep thermal gradients induced during the start up transient. These transient stresses and strains are also the most difficult to predict, in part because of the temperature gradients and distributions are not well known or readily predictable, and also because the cyclic elastic viscoplastic behavior of the materials at these extremes of temperature and strain are not well known

or readily predictable. A broad spectrum of structures related technology programs is underway to address these deficiencies. One element of the structures program is developing improved time varying thermal mechanical load models for the entire engine mission cycle from start up to shutdown. Another major part of the program is the development of new and improved nonlinear 3-D finite elements and associated structural analysis programs, including the development of temporal elements with time dependent properties to account for creep effects in the materials and components. Author

N86-11515*# General Electric Co., Cincinnati, Ohio.

COMPONENT-SPECIFIC MODELING

M. L. ROBERTS *In* NASA. Lewis Research Center Turbine Eng. Hot Sect. Technol. (HOST) p 165-173 Oct. 1983 (Contract NAS3-23687)

Avail: NTIS HC A11/MF A01 CSCL 21E

The overall objective of this program is to develop and verify a series of interdisciplinary modeling and analysis techniques which have been specialized to address three specific hot section components. These techniques will incorporate data as well as theoretical methods from many diverse areas, including cycle and performance analysis, heat transfer analysis, linear and nonlinear stress analysis, and mission analysis. Building on the proven techniques already available in these fields, the new methods developed through this contract will be integrated to provide an accurate, efficient, and unified approach to analyzing combustor burner liners, hollow air cooled turbine blades, and air cooled turbine vanes. For these components, the methods developed will predict temperature, deformation, stress, and strain histories throughout a complete flight mission. Author

N86-24693*# United Technologies Research Center, East Hartford, Conn.

ADVANCED TURBOPROP VIBRATORY CHARACTERISTICS Final Report

A. V. SRINIVASAN and G. B. FULTON Apr. 1984 104 p refs

(Contract NAS3-23533)

(NASA-CR-174708; NAS 1.26:174708; R84-956627-1) Avail:

NTIS HC A06/MF A01 CSCL 21E

The assembly of SR5 advanced turboprop blades to develop a structural dynamic data base for swept props is reported. Steady state blade deformation under centrifugal loading and vibratory characteristics of the rotor assembly were measured. Vibration was induced through a system of piezoelectric crystals attached to the blades. Data reduction procedures are used to provide deformation, mode shape, and frequencies of the assembly at predetermined speeds. Author

N86-27283*# Pratt and Whitney Aircraft, East Hartford, Conn. Commercial Products Div.

STRUCTURAL TAILORING OF ENGINE BLADES (STAEBL) THEORETICAL MANUAL

K. W. BROWN Mar. 1985 51 p

(Contract NAS3-22525)

(NASA-CR-175112; NAS 1.26:175112; PWA-5774-40) Avail:

NTIS HC A04/MF A01 CSCL 21E

This Theoretical Manual includes the theories included in the Structural Tailoring of Engine Blades (STAEBL) computer program which was developed to perform engine fan and compressor blade numerical optimizations. These blade optimizations seek a minimum weight or cost design that satisfies practical blade design constraints, by controlling one to twenty design variables. The STAEBL constraint analyses include blade stresses, vibratory response, flutter, and foreign object damage. Blade design variables include airfoil thickness at several locations, blade chord, and construction variables: hole size for hollow blades, and composite material layout for composite blades. Author

N86-27284*# Pratt and Whitney Aircraft, East Hartford, Conn. Commercial Products Div.

STRUCTURAL TAILORING OF ENGINE BLADES (STAEBL) USER'S MANUAL

K. W. BROWN Mar. 1985 106 p

(Contract NAS3-22525)

(NASA-CR-175113; NAS 1.26:175113; PWA-5774-39) Avail:

NTIS HC A06/MF A01 CSCL 21E

This User's Manual contains instructions and demonstration case to prepare input data, run, and modify the Structural Tailoring of Engine Blades (STAEBL) computer code. STAEBL was developed to perform engine fan and compressor blade numerical optimizations. This blade optimization seeks a minimum weight or cost design that satisfies realistic blade design constraints, by tuning one to twenty design variables. The STAEBL constraint analyses include blade stresses, vibratory response, flutter, and foreign object damage. Blade design variables include airfoil thickness at several locations, blade chord, and construction variables: hole size for hollow blades, and composite material layup for composite blades.

Author

N86-32433*# National Aeronautics and Space Administration. Lewis Research Center, Cleveland, Ohio.

STRUCTURAL DYNAMIC MEASUREMENT PRACTICES FOR TURBOMACHINERY AT THE NASA LEWIS RESEARCH CENTER

L. J. KIRALY 1986 30 p Presented at the Symposium on Propulsion Instrumentation, Jiangyou, China, 6-10 Oct. 1986; sponsored by NASA and Chinese Aeronautical Establishment (NASA-TM-88857; E-3245; NAS 1.15:88857) Avail: NTIS HC A03/MF A01 CSCL 51C

Methods developed for measuring blade and rotor-shaft system response include optical systems, transient instruments, and special digital data processing equipment. Optical methods offer some distinct benefits for blade vibration measurement. Transient and steady state measurements of the response of rotor-shaft systems strongly affect analytical methods development. Digital computing systems allow processing of large volumes of high speed data from rotating blade sets. Also, digital systems develop useful vibration response signatures from randomly excited systems. Research facilities include the spin rig facility and the transient rotor response lab.

Author

N87-11731*# National Aeronautics and Space Administration. Lewis Research Center, Cleveland, Ohio.

STAEBL: STRUCTURAL TAILORING OF ENGINE BLADES, PHASE 2

M. S. HIRSCHBEIN and K. W. BROWN (Pratt and Whitney Aircraft, East Hartford, Conn.) /n NASA. Langley Research Center Recent Experiences in Multidisciplinary Analysis and Optimization, Part 1 13 p 1984

Avail: NTIS HC A22/MF A01 CSCL 21E

The Structural Tailoring of Engine Blades (STAEBL) program was initiated at NASA Lewis Research Center in 1980 to introduce optimal structural tailoring into the design process for aircraft gas turbine engine blades. The standard procedure for blade design is highly iterative with the engineer directly providing most of the decisions that control the design process. The goal of the STAEBL program has been to develop an automated approach to generate structurally optimal blade designs. The program has evolved as a three-phase effort with the developmental work being performed contractually by Pratt & Whitney Aircraft. Phase 1 was intended as a proof of concept in which two fan blades were structurally tailored to meet a full set of structural design constraints while minimizing DOC+I (direct operating cost plus interest) for a representative aircraft. This phase was successfully completed and was reported in reference 1 and 2. Phase 2 has recently been completed and is the basis for this discussion. During this phase, three tasks were accomplished: (1) a nonproprietary structural tailoring computer code was developed; (2) a dedicated approximate finite-element analysis was developed; and (3) an approximate large-deflection analysis was developed to assess local foreign object damage. Phase 3 is just beginning and is

designed to incorporate aerodynamic analyses directly into the structural tailoring system in order to relax current geometric constraints.

Author

N87-28551*# National Aeronautics and Space Administration. Lewis Research Center, Cleveland, Ohio.

TOWARD IMPROVED DURABILITY IN ADVANCED COMBUSTORS AND TURBINES: PROGRESS IN THE PREDICTION OF THERMOMECHANICAL LOADS

DANIEL E. SOKOLOWSKI and C. ROBERT ENSIGN 1986 31 p Presented at the 31st International Gas Turbine Conference and Exhibition, Dusseldorf, West Germany, 8-12 Jun. 1986; sponsored by ASME Previously announced in IAA as A86-48224

(NASA-TM-88932; E-3374; NAS 1.15:88932) Avail: NTIS HC

A03/MF A01 CSCL 21E

NASA is sponsoring the Turbine Engine Hot Section Technology (HOST) Project to address the need for improved durability in advanced combustors and turbines. Analytical and experimental activities aimed at more accurate prediction of the aerothermal environment, the thermomechanical loads, the material behavior and structural responses to such loading, and life predictions for high temperature cyclic operation have been underway for several years and are showing promising results. Progress is reported in the development of advanced instrumentation and in the improvement of combustor aerothermal and turbine heat transfer models that will lead to more accurate prediction of thermomechanical loads.

Author

24

COMPOSITE MATERIALS

Includes physical, chemical, and mechanical properties of laminates and other composite materials.

A80-10036*# National Aeronautics and Space Administration. Lewis Research Center, Cleveland, Ohio.

FATIGUE BEHAVIOR OF SIC REINFORCED TITANIUM COMPOSITES

R. T. BHATT and H. H. GRIMES (NASA, Lewis Research Center, Cleveland, Ohio) American Society for Testing and Materials, Symposium on Fatigue of Fibrous Composite Materials, San Francisco, Calif., May 22, 23, 1979, Paper. 18 p. refs

The low cycle axial fatigue properties of 25 and 44 fiber volume percent SiC/Ti(6Al-4V) composites were measured at room temperature and at 650 C. At room temperature, the S-N curves for the composites showed no anticipated improvement over bulk matrix behavior. Although axial and transverse tensile strength results suggest a degradation in SiC fiber strength during composite fabrication, it appears that the poor fatigue life of the composites was caused by a reduced fatigue resistance of the reinforced Ti(6Al-4V) matrix. Microstructural studies indicate that the reduced matrix behavior was due, in part, to the presence of flawed and fractured fibers created near the specimen surfaces by preparation techniques. Another possible contributing factor is the large residual tensile stresses that can exist in fiber-reinforced matrices. These effects, as well as the effects of fatigue testing at high temperature, are discussed.

(Author)

A80-20954*# National Aeronautics and Space Administration. Lewis Research Center, Cleveland, Ohio.

MECHANICAL PROPERTY CHARACTERIZATION OF INTRAPLY HYBRID COMPOSITES

C. C. CHAMIS, R. F. LARK, and J. H. SINCLAIR (NASA, Lewis Research Center, Cleveland, Ohio) American Society for Testing and Materials, Symposium, Dearborn, Mich., Oct. 2, 3, 1979, Paper. 24 p. refs

An investigation of the mechanical properties of intraply hybrids made from graphite fiber/epoxy matrix hybridized with secondary

24 COMPOSITE MATERIALS

S-glass or Kevlar 49 fiber composites is presented. The specimen stress-strain behavior was determined, showing that mechanical properties of intraply hybrid composites can be measured with available methods such as the ten-degree off-axis test for intralaminar shear, and conventional tests for tensile, flexure, and Izod impact properties. The results also showed that combinations of high modulus graphite/S-glass/epoxy matrix composites exist which yield intraply hybrid laminates with the best 'balanced' properties, and that the translation efficiency of mechanical properties from the constituent composites to intraply hybrids may be assessed with a simple equation. A.T.

A80-27982*# National Aeronautics and Space Administration. Lewis Research Center, Cleveland, Ohio.

DYNAMIC RESPONSE OF DAMAGED ANGLEPLIED FIBER COMPOSITES

C. C. CHAMIS, J. H. SINCLAIR, and R. F. LARK (NASA, Lewis Research Center, Cleveland, Ohio) In: Modern developments in composite materials and structures; Proceedings of the Winter Annual Meeting, New York, N.Y., December 2-7, 1979. New York, American Society of Mechanical Engineers, 1979, p. 31-51.

An investigation was conducted to determine the effects of low level damage induced by monotonic load, cyclic load and/or residual stresses on the vibration frequencies and damping factors of fiber composite angleplied laminates. Two different composite systems were studied - low modulus fiber and ultra high modulus fiber composites. The results obtained showed that the frequencies and damping factors of angleplied laminates made from low modulus fiber composites are sensitive to low level damage while those made from ultra high modulus composites are not. Also, vibration tests may not be sufficiently sensitive to assess concentrated local damage in angleplied laminates. And furthermore, dynamic response determined from low-velocity impact coupled with the Fast Fourier Transform and packaged in a minicomputer can be a convenient procedure for assessing low-level damage in fiber composite angleplied laminates.

(Author)

A80-27994*# National Aeronautics and Space Administration. Lewis Research Center, Cleveland, Ohio.

MICROMECHANICS OF INTRAPLY HYBRID COMPOSITES: ELASTIC AND THERMAL PROPERTIES

C. C. CHAMIS and J. H. SINCLAIR (NASA, Lewis Research Center, Cleveland, Ohio) In: Modern developments in composite materials and structures; Proceedings of the Winter Annual Meeting, New York, N.Y., December 2-7, 1979. New York, American Society of Mechanical Engineers, 1979, p. 253-267.

Composite micromechanics are used to derive equations for predicting the elastic and thermal properties of unidirectional intraply hybrid composites. The results predicted using these equations are compared with those predicted using approximate equations based on the rule of mixtures, linear laminate theory, finite element analysis and limited experimental data. The comparisons for three different intraply hybrids indicate that all four methods predict approximately the same elastic properties and are in good agreement with measured data. The micromechanics equations and linear laminate theory predict about the same values for thermal expansion coefficients. The micromechanics equations predict through-the-thickness properties which are in good agreement with the finite element results.

(Author)

A80-32069*# National Aeronautics and Space Administration. Lewis Research Center, Cleveland, Ohio.

FRACTURE MODES OF HIGH MODULUS GRAPHITE/EPOXY ANGLEPLIED LAMINATES SUBJECTED TO OFF-AXIS TENSILE LOADS

J. H. SINCLAIR (NASA, Lewis Research Center, Cleveland, Ohio) In: Rising to the challenge of the '80s; Annual Conference and Exhibit, 35th, New Orleans, La., February 4-8, 1980, Preprints. New York, Society of the Plastics Industry, Inc., 1980, p. 12-C 1 to 12-C 8. refs

Angleplied laminates of high modulus graphite fiber/epoxy were examined in several ply configurations at various tensile loading angles to the zero ply direction to determine the effects of ply orientations on tensile properties, fracture modes, and fracture surface characteristics of the various plies. Experimental results consist of stress-strain data, selected plots, fracture stresses and strains, and scanning electron microscope (SEM) photographs of fracture surfaces. It was found that the stress-strain curves were linear to fracture, and that although fracture surface characteristics for a given fracture mode are similar to those for the same fracture mode in uniaxial specimens, no simple load angle range can be associated with a given fracture mode. It was also concluded that SEM results must be supplemented with ply stress calculations in order to identify ranges of fracture modes occurring as a function of ply orientation with respect to the load direction. J.P.B.

A80-34764* National Aeronautics and Space Administration. Lewis Research Center, Cleveland, Ohio.

A REVIEW OF ISSUES AND STRATEGIES IN NONDESTRUCTIVE EVALUATION OF FIBER REINFORCED STRUCTURAL COMPOSITES

A. VARY (NASA, Lewis Research Center, Materials and Structures Div., Cleveland, Ohio) In: New horizons - Materials and processes for the eighties; Proceedings of the Eleventh National Conference, Boston, Mass., November 13-15, 1979. Azusa, Calif., Society for the Advancement of Material and Process Engineering, 1979, p. 166-177. refs

The need for advanced nondestructive evaluation (NDE) techniques for quantitative assessment of the mechanical strength and integrity of fiber composites during manufacture and service and following repair operations is stressed. The discussion covers problems and different approaches in regard to acceptance criteria, calibration standards, and methods for NDE of composites in strength critical applications. Finally, it is concluded that acousto-ultrasonic techniques provide the 'methods of choice' in this area. M.E.P.

A80-35494*# National Aeronautics and Space Administration. Lewis Research Center, Cleveland, Ohio.

PREDICTING THE TIME-TEMPERATURE DEPENDENT AXIAL FAILURE OF B/AL COMPOSITES

J. A. DICARLO (NASA, Lewis Research Center, Cleveland, Ohio) Metallurgical Society of AIME, Symposium on Fracture Modes in Metal Matrix Composites, Las Vegas, Nev., Feb. 25-28, 1980, Paper. 26 p. refs

Theoretical and experimental studies are reviewed whose objective was to gain insight into and predict the effects of time, temperature, and stress on the axial failure modes of boron fibers and B/Al composites. Owing to the inelastic nature of boron fiber deformation, it proved possible to develop simple creep functions which can be used to describe accurately the creep and fracture stress of as-produced fibers. Analysis of damping and stress data for B/6061 Al composites indicates that fiber creep and the effects of creep of fiber fracture are measurably reduced by the composite fabrication process. V.P.

A80-44236*# National Aeronautics and Space Administration. Lewis Research Center, Cleveland, Ohio.

DYNAMIC MODULUS AND DAMPING OF BORON, SILICON CARBIDE, AND ALUMINA FIBERS

J. A. DICARLO (NASA, Lewis Research Center, Cleveland, Ohio) and W. WILLIAMS (Lincoln University, Lincoln University, Pa.) American Ceramic Society, Annual Conference on Composites and Advanced Materials, 4th, Cocoa Beach, Fla., Jan. 21-24, 1980, Paper. 42 p. refs

The dynamic modulus and damping capacity for boron, silicon carbide, and silicon carbide-coated boron fibers were measured from -190 to 800 C. The single fiber vibration test also allowed measurement of transverse thermal conductivity for the silicon carbide fibers. Temperature-dependent damping capacity data for alumina fibers were calculated from axial damping results for alumina-aluminum composites. The dynamic fiber data indicate essentially elastic behavior for both the silicon carbide and alumina fibers. In contrast, the boron-based fibers are strongly anelastic, displaying frequency-dependent moduli and very high microstructural damping. The single fiber damping results were compared with composite damping data in order to investigate the practical and basic effects of employing the four fiber types as reinforcement for aluminum and titanium matrices. (Author)

A81-29411*# National Aeronautics and Space Administration. Lewis Research Center, Cleveland, Ohio.

NONLINEAR LAMINATE ANALYSIS FOR METAL MATRIX FIBER COMPOSITES

C. C. CHAMIS and J. H. SINCLAIR (NASA, Lewis Research Center, Structures and Mechanical Technologies Div., Cleveland, Ohio) In: Structures, Structural Dynamics and Materials Conference, 22nd, Atlanta, Ga., April 6-8, 1981, Technical Papers. Part 1. New York, American Institute of Aeronautics and Astronautics, Inc., 1981, p. 313-324. refs (AIAA 81-0579)

A nonlinear laminate analysis is described for predicting the mechanical behavior (stress-strain relationships) of angle-ply laminates in which the matrix is strained nonlinearly by both the residual stress and the mechanical load and in which additional nonlinearities are induced due to progressive fiber fractures and ply relative rotations. The nonlinear laminate analysis is based on linear composite mechanics and a piece-wise linear laminate analysis to handle the nonlinear responses. Results obtained by using this nonlinear analysis on boron-fiber/aluminum-matrix angle-ply laminates agree well with experimental data. The results shown illustrate the in situ ply stress-strain behavior and synergistic strength enhancement. (Author)

A81-44662*# National Aeronautics and Space Administration. Lewis Research Center, Cleveland, Ohio.

COMPUTER CODE FOR INTRAPLY HYBRID COMPOSITE DESIGN

C. C. CHAMIS and J. H. SINCLAIR (NASA, Lewis Research Center, Cleveland, OH) U.S. Department of Defense and NASA, Conference on Fibrous Composites in Structural Design, 5th, New Orleans, LA, Jan. 27-29, 1981, Paper. 13 p. refs

A computer program has been developed and is described herein for intraply hybrid composite design (INHYD). The program includes several composite micromechanics theories, intraply hybrid composite theories and a hygrothermomechanical theory. These theories provide INHYD with considerable flexibility and capability which the user can exercise through several available options. Key features and capabilities of INHYD are illustrated through selected samples. (Author)

A82-37101*# National Aeronautics and Space Administration. Lewis Research Center, Cleveland, Ohio.

SENSITIVITY ANALYSIS RESULTS OF THE EFFECTS OF VARIOUS PARAMETERS ON COMPOSITE DESIGN

C. C. CHAMIS (NASA, Lewis Research Center, Structures and Mechanical Technologies Div., Cleveland, OH) In: Reinforced Plastics/Composites Institute, Annual Conference, 37th, Washington, DC, January 11-15, 1982, Preprints. New York, Society of the Plastics Industry, Inc., 1982 (Session 20-B). 8 p.

Sensitivity analysis results are presented to assess the effects of a multitude of important parameters on fiber composite design and structural response. These results were obtained by using optimum design procedures in conjunction with sensitivity analyses. Sensitivity analyses were performed to assess the effects on composite optimum design and structural response of parameters such fiber transverse and shear properties, in situ matrix elastic and strength properties, correlation coefficients used in composite micromechanics and in combined strength predictions, processing variables, and perturbations of loading conditions. The results show that matrix properties, fiber volume ratio and small perturbations of the loading conditions have significant effects on certain composite structural responses. The remaining parameters have negligible effect. (Author)

A83-12414* National Aeronautics and Space Administration. Lewis Research Center, Cleveland, Ohio.

FATIGUE BEHAVIOR OF SIC REINFORCED Ti/6AL-4V/ AT 650 C

R. T. BHATT (U.S. Army, Propulsion Laboratory, Cleveland, OH) and H. H. GRIMES (NASA, Lewis Research Center, Cleveland, OH) Metallurgical Transactions A - Physical Metallurgy and Materials Science, vol. 13A, Nov. 1982, p. 1933-1938. refs

Axial, low cycle fatigue properties of 25 and 44 fiber vol pct SiC/Ti(6Al-4V) composites, measured at 650 C, were compared with the fatigue properties of unreinforced Ti(6Al-4V) at the same temperature. A prior study of the fatigue behavior of this composite system at room temperature indicated that the SiC fiber reinforcement did not provide the anticipated improvement of fatigue resistance of this alloy. At 650 C, the composite fatigue properties degraded somewhat from those at room temperature. However, these properties degraded more for the unreinforced matrix at 650 C with the result that the composite fatigue strength was two to three times the fatigue strength of the matrix alloy. The reasons for this reversal are discussed in terms of crack initiation at broken fibers and residual matrix stresses. (Author)

A83-12734* Northwestern Univ., Evanston, Ill.

COMPOSITES WITH PERIODIC MICROSTRUCTURE

T. IWAKUMA and S. NEMAT-NASSER (Northwestern University, Evanston, IL) (Symposium on Advances and Trends in Structural and Solid Mechanics, Washington, DC, Oct. 4-7, 1982.) Computers and Structures, vol. 16, no. 1-4, 1983, p. 13-19. refs (Contract NAG3-134)

For an elastic body containing periodically distributed inhomogeneities, a general procedure is developed for estimating the overall properties of the composite in terms of several infinite series which, for the isotropic matrix (but anisotropic inclusions), depend only on the geometry of the inhomogeneities and hence can be calculated once and for all for each geometry. These infinite series are obtained and tabulated for ellipsoidal inhomogeneities, and the results are used to estimate the overall elastic moduli of composites which contain spherical or ellipsoidal voids or elastic inclusions. (Author)

24 COMPOSITE MATERIALS

A83-29886*# National Aeronautics and Space Administration. Lewis Research Center, Cleveland, Ohio.

LOW CYCLE FATIGUE BEHAVIOR OF ALUMINUM/STAINLESS STEEL COMPOSITES

R. B. BHAGAT (NASA, Lewis Research Center, Cleveland, OH; Indian Institute of Technology, Bombay, India) IN: Structures, Structural Dynamics and Materials Conference, 24th, Lake Tahoe, NV, May 2-4, 1983, Collection of Technical Papers. Part 2. New York, American Institute of Aeronautics and Astronautics, 1983, p. 744-752. refs
(AIAA 83-0806)

Composites consisting of an aluminum matrix reinforced with various volume fractions of stainless steel wire were fabricated by hot die pressing under various conditions of temperature, time, and pressure. The composites were tested in plane bending to complete fracture under cycle loading, and the results were analyzed on a computer to obtain a statistically valid mathematical relationship between the low-cycle fatigue life and the fiber volume fraction of the composite. The fractured surfaces of the composites were examined by scanning electron microscopy to identify the characteristic features of fatigue damage. Fatigue damage mechanisms are proposed and discussed. V.L.

A84-10430* Virginia Polytechnic Inst. and State Univ., Blacksburg.

CHARACTERIZATION OF COMPOSITE MATERIALS BY MEANS OF THE ULTRASONIC STRESS WAVE FACTOR

J. C. DUKE, JR., E. G. HENNEKE, W. W. STINCHCOMB, and K. L. REIFSNIDER (Virginia Polytechnic Institute and State University, Blacksburg, VA) IN: Composite structures 2; Proceedings of the Second International Conference, Paisley, Scotland, September 14-16, 1983. London, Applied Science Publishers, 1983, p. 53-60.

(Contract NAG3-172; NAG3-323)

The usual approach to nondestructively evaluating a composite structure involves inspection and mechanical analysis of the inspection results. Such an approach has met with only limited success. On the other hand, the ultrasonic stress wave factor technique directly evaluates the material. Despite requiring access to only one surface of the material, the technique interrogates the material in the directions of applied load. Using the stress wave factor technique it is possible to determine the failure location in the material. The correlation of the stress wave factor with stiffness is shown. In addition, the use of the technique for determining the strength or life of composite material structures is discussed.

Author

A84-14285* National Aeronautics and Space Administration. Lewis Research Center, Cleveland, Ohio.

PREDICTION OF COMPOSITE HYGRAL BEHAVIOR MADE SIMPLE

C. C. CHAMIS and J. H. SINCLAIR (NASA, Lewis Research Center, Cleveland, OH) (Society of Plastics Industry, Annual Conference, 37th, Washington, DC, Jan. 1982) SAMPE Quarterly (ISSN 0036-0821), vol. 14, Oct. 1982, p. 30-39. refs

A convenient procedure is described to determine the hygral behavior (moisture expansion coefficients and moisture stresses) of angleplied fiber composites using a pocket calculator. The procedure consists of equations and appropriate graphs for various (+ or - theta) ply combinations. These graphs present reduced stiffness and moisture expansion coefficients as functions of (+ or - theta) in order to simplify and expedite the use of the equations. The procedure is applicable to all types of balanced, symmetric fiber composites including interply and intraply hybrids. The versatility and generality of the procedure is illustrated using several step-by-step numerical examples. Previously announced in STAR as N82-16181

Author

A84-17444*# National Aeronautics and Space Administration. Lewis Research Center, Cleveland, Ohio.

ENVIRONMENTAL AND HIGH STRAIN RATE EFFECTS ON COMPOSITES FOR ENGINE APPLICATIONS

C. C. CHAMIS and G. T. SMITH (NASA, Lewis Research Center, Cleveland, OH) (Structures, Structural Dynamics and Materials Conference, 23rd, New Orleans, LA, May 10-12, 1982, Collection of Technical Papers, Part 1, p. 405-419) AIAA Journal (ISSN 0001-1452), vol. 22, Jan. 1984, p. 128-134. refs

Previously cited in issue 13, p. 2034, Accession no. A82-30118

A84-27356* Purdue Univ., West Lafayette, Ind. INDENTATION LAW FOR COMPOSITE LAMINATES

S. H. YANG and C. T. SUN (Purdue University, West Lafayette, IN) IN: Composite materials: Testing and design (Sixth Conference). Philadelphia, PA, American Society for Testing and Materials, 1982, p. 425-449.

(Contract NSG-3185)

Static indentation tests are described for glass/epoxy and graphite/epoxy composite laminates with steel balls as the indenter. Beam specimens clamped at various spans were used for the tests. Loading, unloading, and reloading data were obtained and fitted into power laws. Results show that: (1) contact behavior is not appreciably affected by the span; (2) loading and reloading curves seem to follow the 1.5 power law; and (3) unloading curves are described quite well by a 2.5 power law. In addition, values were determined for the critical indentation, α sub cr which can be used to predict permanent indentations in unloading. Since α sub cr only depends on composite material properties, only the loading and an unloading curve are needed to establish the complete loading-unloading-reloading behavior. Previously announced in STAR as N82-15123

Author

A84-27359* National Aeronautics and Space Administration. Lewis Research Center, Cleveland, Ohio.

DURABILITY/LIFE OF FIBER COMPOSITES IN HYGROTHERMOMECHANICAL ENVIRONMENTS

C. C. CHAMIS and J. H. SINCLAIR (NASA, Lewis Research Center, Cleveland, OH) IN: Composite materials: Testing and design (Sixth Conference). Philadelphia, PA, American Society for Testing and Materials, 1982, p. 498-512. refs

Statistical analysis and multiple regression were used to determine and quantify the significant hygrothermomechanical variables which influence the tensile durability/life (cycle loading, fatigue) of boron-fiber/epoxy-matrix (B/E) and high-modulus-fiber/epoxy-matrix (HMS/E) composites. The use of the multiple regression analysis reduced the variables from fifteen, assumed initially, to six or less with a probability of greater than 0.999. The reduced variables were used to derive predictive models for compression and intralaminar shear durability/life of B/E and HMS/E composites assuming isoparametric fatigue behavior. The predictive models were subsequently generalized to predict the durability/life of graphite/fiber-r generalized model is of simple form, predicts conservative values compared with measured data and should be adequate for use in preliminary designs. Previously announced in STAR as N82-14287

B.W.

A84-29894* National Aeronautics and Space Administration. Lewis Research Center, Cleveland, Ohio.

COMPRESSIVE BEHAVIOR OF UNIDIRECTIONAL FIBROUS COMPOSITES

J. H. SINCLAIR and C. C. CHAMIS (NASA, Lewis Research Center, Cleveland, OH) IN: Compression testing of homogeneous materials and composites; Proceedings of the Symposium, Williamsburg, VA, March 10, 11, 1982. Philadelphia, PA, American Society for Testing and Materials, 1983, p. 155-174. refs

The longitudinal compressive behavior of unidirectional fiber composites was investigated by using the Illinois Institute of Technology Research Institute (IITRI) test method with thick and thin test specimens. The test data obtained are interpreted by means of stress/strain curves from back-to-back strain gages, examination of fracture surfaces by scanning electron microscope,

and predictive equations for distinct failure modes including fiber compression failure. Euler buckling, delamination, and flexure. The results show that longitudinal compressive fracture is induced by a combination of delamination, flexure, and fiber tier breaks. No distinct fracture surface characteristics can be associated with unique failure modes. An equation is described that can be used to extract the longitudinal compressive strength from the longitudinal tensile and flexural strengths of the same composite system. Author

A84-33389* Illinois Univ., Urbana.

ELASTICITY SOLUTIONS FOR A CLASS OF COMPOSITE LAMINATE PROBLEMS WITH STRESS SINGULARITIES

S. S. WANG (Illinois, University, Urbana, IL) IN: Mechanics of composite materials: Recent advances; Proceedings of the Symposium, Blacksburg, VA, August 16-19, 1982. New York and Oxford, Pergamon Press, 1983, p. 259-281. refs (Contract NSG-3044; N00014-79-C-0579)

A study on the fundamental mechanics of fiber-reinforced composite laminates with stress singularities is presented. Based on the theory of anisotropic elasticity and Lekhnitskii's complex-variable stress potentials, a system of coupled governing partial differential equations are established. An eigenfunction expansion method is introduced to determine the orders of stress singularities in composite laminates with various geometric configurations and material systems. Complete elasticity solutions are obtained for this class of singular composite laminate mechanics problems. Homogeneous solutions in eigenfunction series and particular solutions in polynomials are presented for several cases of interest. Three examples are given to illustrate the method of approach and the basic nature of the singular laminate elasticity solutions. The first problem is the well-known laminate free-edge stress problem, which has a rather weak stress singularity. The second problem is the important composite delamination problem, which has a strong crack-tip stress singularity. The third problem is the commonly encountered bonded composite joints, which has a complex solution structure with moderate orders of stress singularities. Author

A84-41858* National Aeronautics and Space Administration. Lewis Research Center, Cleveland, Ohio.

SIMPLIFIED COMPOSITE MICROMECHANICS EQUATIONS FOR STRENGTH, FRACTURE TOUGHNESS AND ENVIRONMENTAL EFFECTS

C. C. CHAMIS (NASA, Lewis Research Center, Cleveland, OH) SAMPE Quarterly (ISSN 0036-0821), vol. 15, July 1984, p. 41-55. refs

A unified set of composite micromechanics equations of simple form is summarized and described. This unified set includes composite micromechanics equations for predicting: (1) ply in-plane uniaxial strengths; (2) through-the-thickness strength (interlaminar and flexural); (3) in-plane fracture toughness; (4) in-plane impact resistance; and (5) through-the-thickness (interlaminar and flexural) impact resistance. Equations are also included for predicting the hygrothermal effects on strength, fracture toughness and impact resistance. Several numerical examples are worked out to illustrate the ease of use of the various composite micromechanics equations. Author

A84-49377* National Aeronautics and Space Administration. Lewis Research Center, Cleveland, Ohio.

SIMPLIFIED COMPOSITE MICROMECHANICS EQUATIONS OF HYGRAL, THERMAL, AND MECHANICAL PROPERTIES

C. C. CHAMIS (NASA, Lewis Research Center, Cleveland, OH) SAMPE Quarterly (ISSN 0036-0821), vol. 15, April 1984, p. 14-23. Previously announced in STAR as N83-19817. refs

A unified set of composite micromechanics equations of simple form is summarized and described. This unified set can be used to predict unidirectional composite (ply) geometric, mechanical, thermal and hygral properties using constituent material (fiber/matrix) properties. This unified set also includes approximate equations for predicting (1) moisture absorption; (2) glass transition temperature of wet resins; and (3) hygrothermal degradation effects.

Several numerical examples are worked-out to illustrate ease of use and versatility of these equations. These numerical examples also demonstrate the interrelationship of the various factors (geometric to environmental) and help provide insight into composite behavior at the micromechanistic level. Author

A85-11926* Ohio State Univ., Columbus.

ULTRASONIC WAVE PROPAGATION IN TWO-PHASE MEDIA - SPHERICAL INCLUSIONS

L. S. FU and Y. C. SHEU (Ohio State University, Columbus, OH) Composite Structures (ISSN 0263-8223), vol. 2, no. 4, 1984, p. 289-303. Previously announced in STAR as N83-36500. refs (Contract NAG3-340)

The scattering theory, recently developed via the extended method of equivalent inclusion, is used to study the propagation of time-harmonic waves in two-phase media of elastic matrix with randomly distributed elastic spherical inclusion materials. The elastic moduli and mass density of the composite medium are determined as functions of frequencies when given properties and concentration of the spheres and the matrix. Velocity and attenuation of ultrasonic waves in two-phase media are determined for cases of distributed spheres and localized damage. An averaging theorem that requires the equivalence of the strain energy and the kinetic energy between the effective medium and the original matrix with spherical inhomogeneities is employed to derive the effective moduli and mass density. The functional dependency of these quantities upon frequencies and concentration provides a method of data analysis in ultrasonic evaluation of material properties. Numerical results or moduli, velocity and/or attenuation as functions of concentration of inclusion material, or porosity, are graphically displayed. Author

A85-15632*# National Aeronautics and Space Administration. Lewis Research Center, Cleveland, Ohio.

HYGROTHERMOMECHANICAL EVALUATION OF TRANSVERSE FILAMENT TAPE EPOXY/POLYESTER FIBERGLASS COMPOSITES

R. F. LARK and C. C. CHAMIS (NASA, Lewis Research Center, Cleveland, OH) IN: Reinforced Plastics/Composites Institute, Annual Conference, 38th, Houston, TX, February 7-11, 1983, Preprints. New York, Society of the Plastics Industry, Inc., 1984, p. 12-C-1 to 12-C-15. refs

Transverse filament tape (TFT) fiberglass/epoxy and TFT polyester composites intended for low cost wind turbine blade fabrication have been subjected to static and cyclic load behavior tests whose results are presently evaluated on the basis of an integrated hygrothermomechanical response theory. Laminate testing employed simulated filament winding procedures. The results obtained show that the predicted hygrothermomechanical environmental effects on TFT composites are in good agreement with measured data for various properties, including fatigue at different R-ratio values. O.C.

A85-15636*# National Aeronautics and Space Administration. Lewis Research Center, Cleveland, Ohio.

DESIGN PROCEDURES FOR FIBER COMPOSITE STRUCTURAL COMPONENTS - RODS, BEAMS, AND BEAM COLUMNS

C. C. CHAMIS (NASA, Lewis Research Center, Cleveland, OH) IN: Reinforced Plastics/Composites Institute, Annual Conference, 38th, Houston, TX, February 7-11, 1983, Preprints. New York, Society of the Plastics Industry, Inc., 1984, p. 16-C-1 to 16-C-9. Previously announced in STAR as N83-24559. refs

Step by step procedures are described which are used to design structural components (rods, columns, and beam columns) subjected to steady state mechanical loads and hydrothermal environments. Illustrative examples are presented for structural components designed for static tensile and compressive loads, and fatigue as well as for moisture and temperature effects. Each example is set up as a sample design illustrating the detailed steps that are used to design similar components. Author

24 COMPOSITE MATERIALS

A85-16040* National Aeronautics and Space Administration. Lewis Research Center, Cleveland, Ohio.

SELECT FIBER COMPOSITES FOR SPACE APPLICATIONS - A MECHANISTIC ASSESSMENT

C. A. GINTY and C. C. CHAMIS (NASA, Lewis Research Center, Cleveland, OH) IN: Technology vectors; Proceedings of the Twenty-ninth National SAMPE Symposium and Exhibition, Reno, NV, April 3-5, 1984. Covina, CA, Society for the Advancement of Material and Process Engineering, 1984, p. 979-993. Previously announced in STAR as N84-22702. refs

Three fiber composites (graphite-fiber epoxy, graphite-fiber aluminum, and graphite-fiber magnesium) are evaluated for their possible use in space applications. Using the composite mechanics theories for thermomechanical behavior embodied in the ICAN (Integrated Composites Analyzer) computer code, select composite thermal and mechanical properties are predicted and also their response to cryogenic temperatures, resembling those which occur in space applications. The predicted results are presented in graphical form as a function of the composite's laminate configuration, fiber volume ratio and the selected use temperature. These results are suitable for preliminary design purposes only and should serve as an aid in selecting controlled experiments for obtaining corresponding measured data. Author

A85-16094*# National Aeronautics and Space Administration. Lewis Research Center, Cleveland, Ohio.

ICAN - INTEGRATED COMPOSITES ANALYZER

P. L. N. MURTHY and C. C. CHAMIS (NASA, Lewis Research Center, Cleveland, OH) AIAA, ASME, ASCE, and AHS, Structures, Structural Dynamics and Materials Conference, 25th, Palm Springs, CA, May 14-16, 1984. 24 p. Previously announced in STAR as N84-26755. refs
(AIAA PAPER 84-0974)

The ICAN computer program performs all the essential aspects of mechanics/analysis/design of multilayered fiber composites. Modular, open-ended and user friendly, the program can handle a variety of composite systems having one type of fiber and one matrix as constituents as well as intraply and interply hybrid composite systems. It can also simulate isotropic layers by considering a primary composite system with negligible fiber volume content. This feature is specifically useful in modeling thin interply matrix layers. Hygrothermal conditions and various combinations of in-plane and bending loads can also be considered. Usage of this code is illustrated with a sample input and the generated output. Some key features of output are stress concentration factors around a circular hole, locations of probable delamination, a summary of the laminate failure stress analysis, free edge stresses, microstresses and ply stress/strain influence coefficients. These features make ICAN a powerful, cost-effective tool to analyze/design fiber composite structures and components. A.R.H.

A85-16096*# National Aeronautics and Space Administration. Lewis Research Center, Cleveland, Ohio.

INTERPLY LAYER DEGRADATION EFFECTS ON COMPOSITE STRUCTURAL RESPONSE

C. C. CHAMIS (NASA, Lewis Research Center, Cleveland, OH) and G. C. WILLIAMS (Arizona, University, Tucson, AZ) AIAA, ASME, ASCE, and AHS, Structures, Structural Dynamics and Materials Conference, 25th, Palm Springs, CA, May 14-16, 1984. 29 p. Previously announced in STAR as N84-26756.
(AIAA PAPER 84-0849)

Recent research activities at NASA Lewis Research Center to computationally evaluate the effects of interply layer progressive weakening (degradation) on the structural response of a composite beam are summarized. The structural responses of interest include: (1) bending, (2) buckling, (3) free vibrations, (4) periodic excitation, and (5) impact. Finite element analysis was used for the computational evaluations. The interply layer degradation effects on the various structural responses were determined and assessed as a function of the interply layer modulus varying from 1 million psi down to 1000 psi and even lower for some limiting cases. The results obtained show that the interply layer degradation has

generally negligible effects on composite structural response and, therefore, structural integrity, unless the interply layer modulus degrades to about 10,000 psi or less. Author

A85-29133*# Drexel Univ., Philadelphia, Pa.

USE OF STATICAL INDENTATION LAWS IN THE IMPACT ANALYSIS OF LAMINATED COMPOSITE PLATES

T. M. TAN (Drexel University, Philadelphia, PA; Purdue University, West Lafayette, IN) and C. T. SUN (Purdue University, West Lafayette, IN) ASME, Transactions, Journal of Applied Mechanics (ISSN 0021-8936), vol. 52, March 1985, p. 6-12.
(Contract NSG-3185)

The low-velocity impact response of graphite/epoxy laminates was investigated theoretically and experimentally. A nine-node isoparametric plate finite element in conjunction with an empirical contact law was used for the theoretical investigation. Theoretical results are in good agreement with strain-gage experimental data. The results of the investigation indicate that the present theoretical procedure describes the impact response of laminate for low-impact velocities. Author

A85-41127* National Aeronautics and Space Administration. Lewis Research Center, Cleveland, Ohio.

A STUDY OF INTERPLY LAYER EFFECTS ON THE FREE EDGE STRESS FIELD OF ANGLEPLY LAMINATES

P. L. N. MURTHY and C. C. CHAMIS (NASA, Lewis Research Center, Cleveland, OH) (George Washington University and NASA, Symposium on Advances and Trends in Structures and Dynamics, Washington, DC, Oct. 22-25, 1984) Computers and Structures (ISSN 0045-7949), vol. 20, no. 1-3, 1985, p. 431-441. Previously announced in STAR as N85-15822. refs

The general-purpose finite-element program MSC/NASTRAN is used to study the interply layer effects on the free-edge stress field of symmetric angleply laminates subjected to uniform tensile stress. The free-edge region is modeled as a separate substructure (superelement) which enables easy mesh refinement and provides the flexibility to move the superelement along the edge. The results indicate that the interply layer reduces the stress intensity significantly at the free edge. Another important observation of the study is that the failures observed near free edges of these types of laminates could have been caused by the interlaminar shear stresses. Author

A85-46543* National Aeronautics and Space Administration. Lewis Research Center, Cleveland, Ohio.

IMPACT RESISTANCE OF FIBER COMPOSITES - ENERGY-ABSORBING MECHANISMS AND ENVIRONMENTAL EFFECTS

C. C. CHAMIS and J. H. SINCLAIR (NASA, Lewis Research Center, Cleveland, OH) IN: Recent advances in composites in the United States and Japan; Proceedings of the Symposium, Hampton, VA, June 6-8, 1983. Philadelphia, PA, ASTM, 1985, p. 326-345. Previously announced in STAR as N84-24712. refs

Energy absorbing mechanisms were identified by several approaches. The energy absorbing mechanisms considered are those in unidirectional composite beams subjected to impact. The approaches used include: mechanic models, statistical models, transient finite element analysis, and simple beam theory. Predicted results are correlated with experimental data from Charpy impact tests. The environmental effects on impact resistance are evaluated. Working definitions for energy absorbing and energy releasing mechanisms are proposed and a dynamic fracture progression is outlined. Possible generalizations to angle-ply laminates are described. E.A.K.

A85-47022* National Aeronautics and Space Administration. Lewis Research Center, Cleveland, Ohio.

TEN YEAR ENVIRONMENTAL TEST OF GLASS FIBER/EPOXY PRESSURE VESSELS

J. R. FADDOUL (NASA, Lewis Research Center, Cleveland, OH) AIAA, SAE, ASME, and ASCE, Joint Propulsion Conference, 21st, Monterey, CA, July 8-10, 1985. 10 p. Previously announced in STAR as N85-30034. refs (AIAA PAPER 85-1198)

By the beginning of the 1970's composite pressure vessels had received a significant amount of development effort, and applications were beginning to be investigated. One of the first applications grew out of NASA Johnson Space Center efforts to develop a superior emergency breathing system for firemen. While the new breathing system provided improved wearer comfort and an improved mask and regulator, the primary feature was low weight which was achieved by using a glass fiber reinforced aluminum pressure vessel. Part of the development effort was to evaluate the long term performance of the pressure vessel and as a consequence, some 30 bottles for a test program were procured. These bottles were then provided to NASA Lewis Research Center where they were maintained in an outdoor environment in a pressurized condition for a period of up to 10 yr. During this period, bottles were periodically subjected to cyclic and burst testing. There was no protective coating applied to the fiberglass/epoxy composite, and significant loss in strength did occur as a result of the environment. Similar bottles stored indoors showed little, if any, degradation. This report contains a description of the pressure vessels, a discussion of the test program, data for each bottle, and appropriate plots, comparisons, and conclusions. Author

A85-47970* Martin Marietta Aerospace, Denver, Colo.
FIBERGLASS EPOXY LAMINATE FATIGUE PROPERTIES AT 300 AND 20 K

J. M. TOTH, JR., W. J. BAILEY, and D. A. BOYCE (Martin Marietta Aerospace, Denver, CO) IN: Fatigue at low temperatures; Proceedings of the Symposium, Louisville, KY, May 10, 1983. Philadelphia, PA, ASTM, 1985, p. 163-172. (Contract NAS3-23245)

A subcritical liquid hydrogen orbital storage and supply experiment is being designed for flight in the Space Shuttle cargo bay. The Cryogenic Fluid Management Experiment (CFME) includes a liquid hydrogen tank supported in a vacuum jacket by two fiberglass epoxy composite trunnion mounts. The ability of the CFME to last for the required seven missions depends primarily on the fatigue life of the composite trunnions at cryogenic temperatures. To verify the trunnion design and test the performance of the composite material, fatigue property data at 300 and 20 K were obtained for the specific E-glass fabric/S-glass unidirectional laminate that will be used for the CFME trunnions. The fatigue life of this laminate was greater at 20 K than at 300 K, and was satisfactory for the intended application. Author

A86-19999* National Aeronautics and Space Administration. Lewis Research Center, Cleveland, Ohio.

LONGITUDINAL COMPRESSIVE FAILURE MODES IN FIBER COMPOSITES END ATTACHMENT EFFECTS ON IITRI TYPE TEST SPECIMENS

C. C. CHAMIS (NASA, Lewis Research Center, Cleveland, OH) and J. H. SINCLAIR Journal of Composites Technology and Research, vol. 7, Winter 1985, p. 129-135.

The end-attachment effects on longitudinal compressive strength of IITRI type specimen unidirectional fiber composites are formally assessed using finite-element analysis (FEA) in conjunction with composite mechanics. Sixteen different cases were analyzed to evaluate end-attachment effects (such as degree of misalignment, type of misalignment, progressive end-tab debonding, and specimen thickness) on stress distribution, peak stresses, buckling loads, and buckling mode shapes. The results obtained from the FEA and comparisons with fractured specimens show that eccentricities induce bending-type stresses which peak near the end-tabs and cause flexural type fracture. Also, guidelines

are included for placing back-to-back strain gages to measure the presence/absence of possible end-attachment and eccentricity effects. Author

A86-27734* National Aeronautics and Space Administration. Lewis Research Center, Cleveland, Ohio.

DESIGNING FOR FIBER COMPOSITE STRUCTURAL DURABILITY IN HYGROTHERMOMECHANICAL ENVIRONMENTS

C. C. CHAMIS (NASA, Lewis Research Center, Cleveland, OH) IN: ICCM - V; Proceedings of the Fifth International Conference on Composite Materials, San Diego, CA, July 29-August 1, 1985. Warrendale, PA, Metallurgical Society, Inc., 1985, p. 1101-1113. Previously announced in STAR as N85-27978. refs

A methodology is described which can be used to design/analyze fiber composite structures subjected to complex hygrothermomechanical environments. This methodology includes composite mechanics and advanced structural analysis methods (finite element). Select examples are described to illustrate the application of the available methodology. The examples include: (1) composite progressive fracture; (2) composite design for high cycle fatigue combined with hot-wet conditions; and (3) general laminate design. Author

A86-35809* National Aeronautics and Space Administration. Lewis Research Center, Cleveland, Ohio.

PROGRESSIVE FRACTURE OF FIBER COMPOSITES

T. B. IRVINE and C. A. GINTY (NASA, Lewis Research Center, Cleveland, OH) Journal of Composite Materials (ISSN 0021-9983), vol. 20, March 1986, p. 166-184. refs

Refined models and procedures are described for determining progressive composite fracture in graphite/epoxy angleplied laminates. Unique Lewis Research Center capabilities are utilized including the Real-Time Ultrasonic C-San (RUSCAN) experimental facility and the Composite Durability Structural Analysis (CODSTRAN) computer code. CODSTRAN is used to predict the fracture progression based on composite mechanics, finite element stress analysis, and fracture criteria modules. The RUSCAN facility, CODSTRAN computer code, and scanning electron microscope are used to determine durability and identify failure mechanisms in graphite/epoxy composites. Results indicate that RUSCAN/CODSTRAN is an effective method of studying progressive fracture of composites. Author

A86-40596* National Aeronautics and Space Administration. Lewis Research Center, Cleveland, Ohio.

COMPUTATIONAL COMPOSITE MECHANICS FOR AEROSPACE PROPULSION STRUCTURES

C. C. CHAMIS (NASA, Lewis Research Center, Cleveland, OH) IN: Space Systems Technology Conference, San Diego, CA, June 9-12, 1986, Technical Papers. New York, American Institute of Aeronautics and Astronautics, 1986, p. 145-155. refs (AIAA PAPER 86-1190)

Specialty methods are presented for the computational simulation of specific composite behavior. These methods encompass all aspects of composite mechanics, impact, progressive fracture and component specific simulation. Some of these methods are structured to computationally simulate, in parallel, the composite behavior and history from the initial fabrication through several missions and even to fracture. Select methods and typical results obtained from such simulations are described in detail in order to demonstrate the effectiveness of computationally simulating (1) complex composite structural behavior in general and (2) specific aerospace propulsion structural components in particular. Author

A86-41070* National Aeronautics and Space Administration. Lewis Research Center, Cleveland, Ohio.

DYNAMIC STRESS ANALYSIS OF SMOOTH AND NOTCHED FIBER COMPOSITE FLEXURAL SPECIMENS

P. L. N. MURTHY and C. C. CHAMIS (NASA, Lewis Research Center, Cleveland, OH) IN: Composite materials: Testing and design; Proceedings of the Seventh Conference, Philadelphia, PA, April 2-4, 1984. Philadelphia, PA, American Society for Testing and Materials, 1986, p. 368-391. Previously announced in STAR as N84-25770.

A detailed analysis of the dynamic stress field in smooth and notched fiber composite (Charpy-type) specimens is reported in this paper. The analysis is performed with the aid of the direct transient response analysis solution sequence of MSC/NASTRAN. Three unidirectional composites were chosen for the study. They are S-Glass/Epoxy, Kevlar/Epoxy and T-300/Epoxy composite systems. The specimens are subjected to an impact load which is modeled as a triangular impulse with a maximum of 2000 lb and a duration of 1 ms. The results are compared with those of static analysis of the specimens subjected to a peak load of 2000 lb. For the geometry and type of materials studied, the static analysis results gave close conservative estimates for the dynamic stresses. Another interesting inference from the study is that the impact induced effects are felt by S-Glass/Epoxy specimens sooner than Kevlar/Epoxy or T-300/Epoxy specimens. Author

A86-43010* Purdue Univ., West Lafayette, Ind.

DYNAMIC DELAMINATION CRACK PROPAGATION IN A GRAPHITE/EPOXY LAMINATE

C. T. SUN (Purdue University, West Lafayette, IN) and J. E. GRADY IN: Composite materials: Fatigue and fracture; Proceedings of the Symposium, Dallas, TX, October 24, 25, 1984. Philadelphia, PA, American Society for Testing and Materials, 1986, p. 5-31. refs (Contract NAG3-211)

The dynamic delamination crack propagation behavior during ballistic tests of (90/0)5s T-300/934 graphite/epoxy laminates with embedded interfacial cracks was investigated using high speed photography. The impact on the beam-like specimen was produced with a silicon rubber ball, and the crack propagation speeds and the threshold impact velocities required to initiate dynamic crack propagation were determined for several crack positions. The results suggest that the mode of crack propagation depends on the specimen geometry as well as the loading condition. A simplified finite element analysis of the experimental data obtained from one of the midplane-cracked specimens was used to estimate the critical strain energy release rate, which may determine the onset of unstable crack propagation. I.S.

A87-19121* National Aeronautics and Space Administration. Lewis Research Center, Cleveland, Ohio.

ASSESSMENT OF SIMPLIFIED COMPOSITE MICROMECHANICS USING THREE-DIMENSIONAL FINITE-ELEMENT ANALYSIS

J. J. CARUSO and C. C. CHAMIS (NASA, Lewis Research Center, Cleveland, OH) Journal of Composites Technology and Research (ISSN 0885-6804), vol. 8, Fall 1986, p. 77-83. refs

Three-dimensional finite-element analyses are used to assess the accuracy of simplified composite micromechanics equations (SME) for hygral, thermal, and mechanical properties of unidirectional composites with orthotropic fibers. The properties predicted by the SME are in reasonably good agreement with those predicted by the three-dimensional finite-element analyses. This correlation demonstrates that the SME can be used with confidence in predicting the hygral, thermal, and mechanical behavior of unidirectional fiber composites. Author

A87-19123* National Aeronautics and Space Administration. Lewis Research Center, Cleveland, Ohio.

FABRICATION AND QUALITY ASSURANCE PROCESSES FOR SUPERHYBRID COMPOSITE FAN BLADES

R. F. LARK and C. C. CHAMIS (NASA, Lewis Research Center, Cleveland, OH) Journal of Composites Technology and Research (ISSN 0885-6804), vol. 8, Fall 1986, p. 98-102. Previously announced in STAR as N85-14882. refs

The feasibility of fabricating full-scale fan blades from superhybrid composites (SHC) for use large, commercial gas turbine engines was evaluated. The type of blade construction selected was a metal-spar/SHC-shell configuration, in which the outer shell was adhesively bonded to a short, internal, titanium spar. Various aspects of blade fabrication, inspection, and quality assurance procedures developed in the investigation are described. It is concluded that the SHC concept is feasible for the fabrication of prototype, full-scale, metal-spar/SHC-shell fan blades that have good structural properties and meet dimensional requirements. R.S.F.

A87-20090*# National Aeronautics and Space Administration. Lewis Research Center, Cleveland, Ohio.

SIMPLIFIED COMPOSITE MICROMECHANICS FOR PREDICTING MICROSTRESSES

CHRISTOS C. CHAMIS (NASA, Lewis Research Center, Cleveland, OH) IN: Reinforced Plastics/Composites Institute, Annual Conference, 41st, Atlanta, GA, January 27-31, 1986, Preprint. Lancaster, PA, Technomic Publishing Co., 1986, 11 p. Previously announced in STAR as N86-24759. refs

A unified set of composite micromechanics equations is summarized and described. This unified set is for predicting the ply microstresses when the ply stresses are known. The set consists of equations of simple form for predicting three-dimensional stresses (six each) in the matrix, fiber, and interface. Several numerical examples are included to illustrate use and computational effectiveness of the equations in this unified set. Numerical results from these examples are discussed with respect to their significance on microcrack formation and, therefore, damage initiation in fiber composites. Author

A87-38610* National Aeronautics and Space Administration. Lewis Research Center, Cleveland, Ohio.

COMPOSITE SPACE ANTENNA STRUCTURES - PROPERTIES AND ENVIRONMENTAL EFFECTS

C. A. GINTY (NASA, Lewis Research Center, Cleveland, OH) and N. M. ENDRES (Sverdrup Technology, Inc., Middleburg Heights, OH) IN: International SAMPE Technical Conference, 18th, Seattle, WA, Oct. 7-9, 1986, Proceedings. Covina, CA, Society for the Advancement of Material and Process Engineering, 1986, p. 545-560. Previously announced in STAR as N87-16880. refs

The thermal behavior of composite spacecraft antenna reflectors has been investigated with the integrated Composites Analyzer (ICAN) computer code. Parametric studies have been conducted on the face sheets and honeycomb core which constitute the sandwich-type structures. Selected thermal and mechanical properties of the composite faces and sandwich structures are presented graphically as functions of varying fiber volume ratio, temperature, and moisture content. The coefficients of thermal expansion are discussed in detail since these are the critical design parameters. In addition, existing experimental data are presented and compared to the ICAN predictions. Author

A87-38615* National Aeronautics and Space Administration. Langley Research Center, Hampton, Va.

THERMAL EXPANSION BEHAVIOR OF GRAPHITE/GLASS AND GRAPHITE/MAGNESIUM

STEPHEN S. TOMPKINS (NASA, Langley Research Center, Hampton, VA), K. E. ARD (Harris Corp., Aerospace Systems Div., Melbourne, FL), and G. RICHARD SHARP (NASA, Lewis Research Center, Cleveland, OH) IN: International SAMPE Technical Conference, 18th, Seattle, WA, Oct. 7-9, 1986, Proceedings. Covina, CA, Society for the Advancement of Material and Process Engineering, 1986, p. 623-637. refs

The thermal expansion behavior of n (+/- 8)s graphite fiber reinforced magnesium laminate and four graphite reinforced glass-matrix laminates (a unidirectional laminate, a quasi-isotropic laminate, a symmetric low angle-ply laminate, and a random chopped-fiber mat laminate) was determined, and was found, in all cases, to not be significantly affected by thermal cycling. Specimens were cycled up to 100 times between -200 F and 100 F, and the thermal expansion coefficients determined for each material as a function of temperature were found to be low. Some dimensional changes as a function of thermal cycling, and some thermal-strain hysteresis, were observed. R.R.

N80-11143*# National Aeronautics and Space Administration. Lewis Research Center, Cleveland, Ohio.

MICROMECHANICS OF INTRAPLY HYBRID COMPOSITES: ELASTIC AND THERMAL PROPERTIES

C. C. CHAMIS and J. H. SINCLAIR Washington 1979 19 p refs Presented at the Winter Ann. Meeting of the Am. Soc. of Mech. Engr., New York, 2-7 Dec. 1979 (NASA-TM-79253; E-164) Avail: NTIS HC A02/MF A01 CSCL 11D

Composite micromechanics are used to derive equations for predicting the elastic and thermal properties of unidirectional intraply hybrid composites. The results predicted using these equations are compared with those predicted using approximate equations based on the rule of mixtures, linear laminate theory, finite element analysis and limited experimental data. The comparisons for three different intraply hybrids indicate that all four methods predict approximately the same elastic properties and are in good agreement with measured data. The micromechanics equations and linear laminate theory predict about the same values for thermal expansion coefficients. The micromechanics equations predict through-the-thickness properties which are in good agreement with the finite element results.

Author

N80-11144*# National Aeronautics and Space Administration. Lewis Research Center, Cleveland, Ohio.

TENSILE AND FLEXURAL STRENGTH OF NON-GRAPHITIC SUPERHYBRID COMPOSITES: PREDICTIONS AND COMPARISONS

C. C. CHAMIS, J. H. SINCLAIR, and R. F. LARK 1979 27 p refs Presented at 11th Natl. Tech. Conf., Boston, Mass., 13-15 Nov. 1979; sponsored by Soc. for the Advancement of Material and Process Engr. (NASA-TM-79276; E-203) Avail: NTIS HC A03/MF A01 CSCL 11D

Equations are presented and described which can be used to predict bounds on the tensile and flexural strengths of nongraphitic superhybrid (NGSH) composites. These equations are derived by taking into account the measured stress-strain behavior, the lamination residual stresses and the sequence of events leading to fracture. The required input for using these equations includes constituents, properties (elastic and strength), NGSH elastic properties, cure temperature, and ply stress influence coefficients. Results predicted by these equations are in reasonably good agreement with measured data for strength and for the apparent knees in the nonlinear stress-strain curve. The lower bound values are conservative compared to measured data. These equations are relatively simple and are suitable for use in the preliminary design and initial sizing of structural components made from NGSH composites. Author

N80-11145*# National Aeronautics and Space Administration. Lewis Research Center, Cleveland, Ohio.

DYNAMIC RESPONSE OF DAMAGED ANGLEPLY FIBER COMPOSITES

C. C. CHAMIS, J. H. SINCLAIR, and R. F. LARK 1979 17 p refs Presented at the Winter Ann. Meeting of the Am. Soc. of Mech. Engr., New York, 2-7 Dec. 1979 (NASA-TM-79281; E-182) Avail: NTIS HC A02/MF A01 CSCL 11D

The effects of low level damage induced by monotonic load, cyclic load and/or residual stresses on the vibration frequencies and damping factors of fiber composite angleply laminates were investigated. Two different composite systems were studied - low modulus fiber and ultra high modulus fiber composites. The results obtained show that the frequencies and damping factors of angleply laminates made from low modulus fiber composites are sensitive to low level damage while those made from ultra high modulus composites are not. Vibration tests may not be sufficiently sensitive to assess concentrated local damage in angleply laminates. Dynamic response determined from low-velocity impact coupled with the Fast Fourier Transform and packaged in a minicomputer can be a convenient procedure for assessing low-level damage. A.R.H.

N80-12120*# National Aeronautics and Space Administration. Lewis Research Center, Cleveland, Ohio.

MECHANICAL PROPERTY CHARACTERIZATION OF INTRAPLY HYBRID COMPOSITES

C. C. CHAMIS, R. F. LARK, and J. H. SINCLAIR 1979 26 p refs Presented at the Am. Soc. for Testing and Materials Symp., Dearborn, Mich., 2-3 Oct. 1979 (NASA-TM-79306; E-261) Avail: NTIS HC A03/MF A01 CSCL 11D

An investigation was conducted to characterize the mechanical properties of intraply hybrids made from graphite fiber/epoxy matrix (primary composites) hybridized with varying amounts of secondary composites made from S-glass or Kevlar 49 fibers. The tests were conducted using thin laminates having the same thickness. The specimens for these tests were instrumented with strain gages to determine stress-strain behavior. Significant results are included.

R.C.T.

N80-16102*# National Aeronautics and Space Administration. Lewis Research Center, Cleveland, Ohio.

FRACTURE MODES OF HIGH MODULUS GRAPHITE/EPOXY ANGLEPLY LAMINATES SUBJECTED TO OFF-AXIS TENSILE LOADS

J. H. SINCLAIR 1980 22 p refs Presented at 35th Ann. Conf. of the Reinforced Plastics/Composites Inst., New Orleans, 4-8 Feb. 1980; sponsored by Soc. of Plastics Ind. (NASA-TM-81405; E-319) Avail: NTIS HC A02/MF A01 CSCL 11D

Angleply laminates of high modulus graphite fiber/epoxy were studied in several ply configurations at various tensile loading angles to the zero ply direction in order to determine the effects of ply orientations on tensile properties, fracture modes, and fracture surface characteristics of the various plies. It was found that fracture modes in the plies of angleply laminates can be characterized by scanning electron microscope observation. The characteristics for a given fracture mode are similar to those for the same fracture mode in unidirectional specimens. However, no simple load angle range can be associated with a given fracture mode. Author

24 COMPOSITE MATERIALS

N80-16107*# National Aeronautics and Space Administration. Lewis Research Center, Cleveland, Ohio.

PREDICTION OF FIBER COMPOSITE MECHANICAL BEHAVIOR MADE SIMPLE

C. C. CHAMIS 1980 26 p refs Presented at the 35th Ann. Conf. of the Reinforced Plastics/Composites Inst., New Orleans, 4-8 Feb. 1980; sponsored by the Soc. of Plastics Ind. (NASA-TM-81404; E-331) Avail: NTIS HC A03/MF A01 CSCL 11D

The elastic properties and failure stresses of angleplied fiber composite laminates were determined using a pocket calculator. The procedure uses simple equations and appropriate graphs of elastic properties versus angle plies, and can handle all types of fiber composites including hybrids. The versatility and generality of the method is illustrated in several step-by-step numerical examples. A.R.H.

N80-18106*# National Aeronautics and Space Administration. Lewis Research Center, Cleveland, Ohio.

APPLICATION OF COMPOSITE MATERIALS TO TURBOFAN ENGINE FAN EXIT GUIDE VANES

G. T. SMITH 1980 19 p refs Presented at 35th Ann. Conf. of the Reinforced Plastics/Composite Inst., New Orleans, 4-8 Feb. 1980; sponsored by Soc. of Plastics Industries (NASA-TM-81432; E-356) Avail: NTIS HC A02/MF A01 CSCL 11D

A program was conducted by NASA with the JT9D engine manufacturer to develop a lightweight, cost effective, composite material fan exit guide vane design having satisfactory structural durability for commercial engine use. Based on the results of a previous company supported program, eight graphite/epoxy and graphite-glass/epoxy guide vane designs were evaluated and four were selected for fabrication and testing. Two commercial fabricators each fabricated 13 vanes. Fatigue tests were used to qualify the selected design configurations under nominally dry, 38 C (100 F) and fully wet and 60 C (140 F) environmental conditions. Cost estimates for a production rate of 1000 vanes per month ranged from 1.7 to 2.6 times the cost of an all aluminum vane. This cost is 50 to 80 percent less than the initial program target cost ratio which was 3 times the cost of an aluminum vane. Application to the JT9D commercial engine is projected to provide a weight savings of 236 N (53 lb) per engine. Author

N80-20313*# National Aeronautics and Space Administration. Lewis Research Center, Cleveland, Ohio.

DYNAMIC MODULUS AND DAMPING OF BORON, SILICON CARBIDE, AND ALUMINA FIBERS

J. A. DICARLO and W. WILLIAMS 1980 44 p refs Presented at the 4th Ann. Conf. on Composites and Advanced Mater., Cocoa Beach, Fla. 20-24 Jan. 1980; sponsored by the Am. Ceram. Soc. (NASA-TM-81422; E-345) Avail: NTIS HC A03/MF A01 CSCL 11D

The dynamic modulus and damping capacity for boron, silicon carbide, and silicon carbide coated boron fibers were measured from -190 to 800 C. The single fiber vibration test also allowed measurement of transverse thermal conductivity for the silicon carbide fibers. Temperature dependent damping capacity data for alumina fibers were calculated from axial damping results for alumina-aluminum composites. The dynamics fiber data indicate essentially elastic behavior for both the silicon carbide and alumina fibers. In contrast, the boron based fibers are strongly anelastic, displaying frequency dependent moduli and very high microstructural damping. This single fiber damping results were compared with composite damping data in order to investigate the practical and basic effects of employing the four fiber types as reinforcement for aluminum and titanium matrices. K.L.

N80-20314*# National Aeronautics and Space Administration. Lewis Research Center, Cleveland, Ohio.

CALCULATION OF RESIDUAL PRINCIPAL STRESSES IN CVD BORON ON CARBON FILAMENTS

D. R. BEHRENDT 1980 15 p refs Prepared for the 4th Ann. Conf. on Composites and Advanced Mater., Cocoa Beach, Fla., 21-24 Jan. 1980; sponsored by the Am. Ceram. Soc. (NASA-TM-81456; E-386) Avail: NTIS HC A02/MF A01 CSCL 11D

A three-dimensional finite element model of the chemical vapor deposition of boron on a carbon substrate (B/C) is developed. The model includes an expansion of the boron after deposition due to atomic rearrangement and includes creep of the boron and carbon. Curves are presented showing the variation of the principal residual stresses and the filament elongation with the parameters defining deposition strain and creep. The calculated results are compared with experimental axial residual stress and elongation measurements made on B/C filaments. For good agreement between calculated and experimental results, the deposited boron must continue to expand after deposition, and the build up of residual stresses must be limited by significant boron and carbon creep rates. K.L.

N80-21452*# National Aeronautics and Space Administration. Lewis Research Center, Cleveland, Ohio.

PREDICTING THE TIME-TEMPERATURE DEPENDENT AXIAL FAILURE OF B/A1 COMPOSITES

J. A. DICARLO 1980 28 p refs Presented at Symp. on Failure Modes in Composites, Las Vegas, Nev., 25-26 Feb. 1980, sponsored by Metallurgical Soc. of the Am. Inst. of Mining, Metallurgical and Petroleum Engr. (NASA-TM-81474; E-408) Avail: NTIS HC A03/MF A01 CSCL 11D

Experimental and theoretical studies were conducted in order to understand and predict the effects of time, temperature, and stress on the axial failure modes of boron fibers and B/A1 composites. Due to the anelastic nature of boron fiber deformation, it was possible to determine simple creep functions which can be employed to accurately describe creep and fracture stress of as-produced fibers. Analysis of damping and strength data for B/6061 A1 composites indicates that fiber creep effects of creep on fiber fracture are measurably reduced by the composite fabrication process. The creep function appropriate for fibers with B/A1 composites was also determined. A fracture theory is presented for predicting the time-temperature dependence of the axial tensile strength for metal matrix composites in general and B/A1 composites in particular. Author

N80-23370*# National Aeronautics and Space Administration. Lewis Research Center, Cleveland, Ohio.

ENGINE ENVIRONMENTAL EFFECTS ON COMPOSITE BEHAVIOR

C. C. CHAMIS and G. T. SMITH 1980 20 p refs Presented at the 21st Struct., Structural Dyn. and Mater. Conf., Seattle, 12-14 May 1980; sponsored by AIAA, ASME, ASCE, and AHS (NASA-TM-81508; E-446) Avail: NTIS HC A02/MF A01 CSCL 11D

A series of programs were conducted to investigate and develop the application of composite materials to turbojet engines. A significant part of that effort was directed to establishing the impact resistance and defect growth characteristics of composite materials over the wide range of environmental conditions found in commercial turbojet engine operations. Both analytical and empirical efforts were involved. The experimental programs and the analytical methodology development as well as an evaluation program for the use of composite materials as fan exit guide vanes are summarized. R.C.T.

N80-25382*# Hamilton Standard, Windsor Locks, Conn.
DIFFUSION BONDED BORON/ALUMINUM SPAR-SHELL FAN BLADE Final Report, Jun. 1977 - May 1978
 C. E. K. CARLSON, J. L. CUTLER, W. J. FISHER, and J. V. W. MEMMOTT Jun. 1980 114 p refs
 (Contract NAS3-20407)
 (NASA-CR-159571; HSER-7698) Avail: NTIS HC A06/MF A01 CSCL 11D

Design and process development tasks intended to demonstrate composite blade application in large high by-pass ratio turbofan engines are described. Studies on a 3.0 aspect ratio space and shell construction fan blade indicate a potential weight savings for a first stage fan rotor of 39% when a hollow titanium spar is employed. An alternate design which featured substantial blade internal volume filled with titanium honeycomb inserts achieved a 14% potential weight savings over the B/M rotor system. This second configuration requires a smaller development effort and entails less risk to translate a design into a successful product. The feasibility of metal joining large subsonic spar and shell fan blades was demonstrated. Initial aluminum alloy screening indicates a distinct preference for AA6061 aluminum alloy for use as a joint material. The simulated airfoil pressings established the necessity of rigid air surfaces when joining materials of different compressive rigidities. The two aluminum alloy matrix choices both were successfully formed into blade shells. A.R.H.

N80-25383*# Lehigh Univ., Bethlehem, Pa. Inst. of Fracture and Solid Mechanics.
SUDDEN STRETCHING OF A FOUR LAYERED COMPOSITE PLATE Interim Report
 G. C. SIH and E. P. CHEN Mar. 1980 42 p refs
 (Contract NSG-3197)
 (NASA-CR-159870; IFSM-80-102) Avail: NTIS HC A03/MF A01 CSCL 11D

An approximate theory of laminated plates is developed by assuming that the extensorial and thickness mode of vibration are coupled. The mixed boundary value crack problem of a four layered composite plate is solved. Dynamic stress intensity factors for a crack subjected to suddenly applied stress are found to vary as a function of time and depend on the material properties of the laminate. Stress intensification in the region near the crack front can be reduced by having the shear modulus of the inner layers to be larger than that of the outer layers. Author

N80-25384*# Lehigh Univ., Bethlehem, Pa. Inst. of Fracture and Solid Mechanics.
SUDDEN BENDING OF CRACKED LAMINATES Interim Report
 G. C. SIH and E. P. CHEN Feb. 1980 53 p refs
 (Contract NSG-3197)
 (NASA-CR-159860; IFSM-80-103) Avail: NTIS HC A04/MF A01 CSCL 11D

A dynamic approximate laminated plate theory is developed with emphasis placed on obtaining effective solution for the crack configuration where the $1/\text{square root of } r$ stress singularity and the condition of plane strain are preserved. The radial distance r is measured from the crack edge. The results obtained show that the crack moment intensity tends to decrease as the crack length to laminate plate thickness is increased. Hence, a laminated plate has the desirable feature of stabilizing a through crack as it increases its length at constant load. Also, the level of the average load intensity transmitted to a through crack can be reduced by making the inner layers to be stiffer than the outer layers. The present theory, although approximate, is useful for analyzing laminate failure to crack propagation under dynamic load conditions. Author

N80-29432*# George Washington Univ., Washington, D.C. School of Engineering and Applied Science.
STATISTICAL ASPECTS OF CARBON FIBER RISK ASSESSMENT MODELING
 D. GROSS, D. R. MILLER, and R. M. SOLAND Jul. 1980 127 p refs
 (Contract NSG-1556)
 (NASA-CR-159318) Avail: NTIS HC A07/MF A01 CSCL 11D

The probabilistic and statistical aspects of the carbon fiber risk assessment modeling of fire accidents involving commercial aircraft are examined. Three major sources of uncertainty in the modeling effort are identified. These are: (1) imprecise knowledge in establishing the model; (2) parameter estimation; and (3) Monte Carlo sampling error. All three sources of uncertainty are treated and statistical procedures are utilized and/or developed to control them wherever possible. A.R.H.

N81-12171*# National Aeronautics and Space Administration. Lewis Research Center, Cleveland, Ohio.
LAMINATES AND REINFORCED METALS
 C. C. CHAMIS Oct. 1980 47 p refs
 (NASA-TM-81591; E-570) Avail: NTIS HC A03/MF A01 CSCL 11D

A selective review is presented of the state of the art of metallic laminates and fiber reinforced metals called metallic matrix laminates (MMLs). Design and analysis procedures that are used for, and typical structural components that have been made from MMLs are emphasized. Selected MMLs, constituent materials, typical material properties and fabrication procedures are briefly described, including hybrids and superhybrids. Advantages, disadvantages, and special considerations required during design, analysis, and fabrication of MMLs are examined. Tabular and graphical data are included to illustrate key aspects of MMLs. Appropriate references are cited to provide a selective bibliography of a rapidly expanding and very promising research and development field. J.M.S.

N81-16132*# National Aeronautics and Space Administration. Lewis Research Center, Cleveland, Ohio.
PREDICTION OF COMPOSITE THERMAL BEHAVIOR MADE SIMPLE
 C. C. CHAMIS 1981 33 p refs Presented at the 36th Ann. Conf. of the Soc. of the Plastics Ind. (SPI) Reinforced Plastics/Composites Inst., Washington, D.C., 16-20 Feb. 1981
 (NASA-TM-81618; E-624) Avail: NTIS HC A03/MF A01 CSCL 11D

A convenient procedure is described to determine the thermal behavior (thermal expansion coefficients and thermal stresses) of angledply fiber composites using a pocket calculator. The procedure consists of equations and appropriate graphs for various (+ or - theta) ply combinations. These graphs present reduced stiffness and thermal expansion coefficients as functions of (+ or - theta) in order to simplify and expedite the use of the equations. The procedure is applicable to all types of balanced, symmetric fiber composites including interply and intraply hybrids. The versatility and generality of the procedure is illustrated using several step-by-step numerical examples. Author

N81-17170* National Aeronautics and Space Administration. Lewis Research Center, Cleveland, Ohio.
METHOD FOR ALLEVIATING THERMAL STRESS DAMAGE IN LAMINATES Patent
 C. A. HOFFMAN, J. W. WEETON, and N. W. ORTH, inventors (to NASA) 8 Jul. 1980 6 p Filed 6 Apr. 1978 Supersedes N78-22163 (16 - 13, p 1675)
 (NASA-CASE-LEW-12493-1; US-PATENT-4,211,354; US-PATENT-APPL-SN-893857; US-PATENT-CLASS-228-118; US-PATENT-CLASS-228-170; US-PATENT-CLASS-228-174; US-PATENT-CLASS-228-190; US-PATENT-CLASS-156-292)
 Avail: US Patent and Trademark Office CSCL 11D

A method is provided for alleviating the stress damage in metallic matrix composites, such as laminated sheet or foil composites. Discontinuities are positively introduced into the

24 COMPOSITE MATERIALS

interface between the layers so as to reduce the thermal stress produced by unequal expansion of the materials making up the composite. Although a number of discrete elements could be used to form one of the layers and thus carry out this purpose, the discontinuities are preferably produced by simply drilling holes in the metallic matrix layer or by forming grooves in a grid pattern in this layer.

Official Gazette of the U.S. Patent and Trademark Office

N81-25149*# National Aeronautics and Space Administration. Lewis Research Center, Cleveland, Ohio.

NONLINEAR LAMINATE ANALYSIS FOR METAL MATRIX FIBER COMPOSITES

C. C. CHAMIS and J. H. SINCLAIR 1981 18 p refs Presented at the 22d Structural Dyn. and Mater. Conf., Atlanta 6-8 Apr. 1981; sponsored by AIAA; ASME; American Society of Civil Engineers and AHS (NASA-TM-82596; E-763) Avail: NTIS HC A02/MF A01 CSCL 11D

A nonlinear laminate analysis is described for predicting the mechanical behavior (stress-strain relationships) of angleplied laminates in which the matrix is strained nonlinearly by both the residual stress and the mechanical load and in which additional nonlinearities are induced due to progressive fiber fractures and ply relative rotations. The nonlinear laminate analysis (NLA) is based on linear composite mechanics and a piece wise linear laminate analysis to handle the nonlinear responses. Results obtained by using this nonlinear analysis on boron fiber/aluminum matrix angleplied laminates agree well with experimental data. The results shown illustrate the in situ ply stress-strain behavior and synergistic strength enhancement. Author

N81-25151*# National Aeronautics and Space Administration. Lewis Research Center, Cleveland, Ohio.

COMPUTER CODE FOR INTRAPLY HYBRID COMPOSITE DESIGN

C. C. CHAMIS and J. H. SINCLAIR 1981 15 p refs Presented at the 5th Conf. on Fibrous Composites in Struct. Design, New Orleans, 27-29 Jan. 1981; sponsored by DOD and NASA (NASA-TM-82593; E-841) Avail: NTIS HC A02/MF A01 CSCL 11D

A computer program is described for intraply hybrid composite design (INHYD). The program includes several composite micromechanics theories, intraply hybrid composite theories, and a hygrothermomechanical theory. These theories provide INHYD with considerable flexibility and capability which the user can exercise through several available options. Key features and capabilities of INHYD are illustrated through selected samples. E.D.K.

N81-26179* National Aeronautics and Space Administration. Lewis Research Center, Cleveland, Ohio.

METHOD FOR ALLEVIATING THERMAL STRESS DAMAGE IN LAMINATES Patent

C. A. HOFFMAN, J. W. WEETON, and N. W. ORTH, inventors (to NASA) 19 May 1981 5 p Filed 20 Feb. 1980 Division of US Patent Appl. SN-893857, filed 6 Apr. 1979, US Patent-4,211,354 (NASA-CASE-LEW-12493-2; US-PATENT-4,267,953; US-PATENT-APPL-SN-122967; US-PATENT-4,211,354; US-PATENT-APPL-SN-893857; US-PATENT-CLASS-228-118; US-PATENT-CLASS-228-190) Avail: US Patent and Trademark Office CSCL 11D

The method is for metallic matrix composites, such as laminated sheet or foil composites. Non-intersecting discrete discontinuities are positively introduced into the interface between the layers so as to reduce the thermal stress produced by unequal expansion of the materials making up the composite. The discontinuities are preferably produced by drilling holes in the metallic matrix layer. However, a plurality of discrete elements may be used between the layers to carry out this purpose.

Official Gazette of the U.S. Patent and Trademark Office

N82-14287*# National Aeronautics and Space Administration. Lewis Research Center, Cleveland, Ohio.

DURABILITY/LIFE OF FIBER COMPOSITES IN HYGROTHERMOMECHANICAL ENVIRONMENTS

C. C. CHAMIS and J. H. SINCLAIR 1981 28 p refs Presented at the Sixth Conf. on Composite Mater.: Testing and Design sponsored by the Am. Soc. for Testing and Mater., Phoenix, Ariz., 12-13 May 1981

(NASA-TM-82749; E-1065) Avail: NTIS HC A03/MF A01 CSCL 11D

Statistical analysis and multiple regression were used to determine and quantify the significant hygrothermomechanical variables which influence the tensile durability/life (cycle loading, fatigue) of boron-fiber/epoxy-matrix (B/E) and high-modulus-fiber/epoxy-matrix (HMS/E) composites. The use of the multiple regression analysis reduced the variables from fifteen, assumed initially, to six or less with a probability of greater than 0.999. The reduced variables were used to derive predictive models for compression an intralaminar shear durability/life of B/E and HMS/E composites assuming isoparametric fatigue behavior. The predictive models were subsequently generalized to predict the durability/life of graphite-fiber-r generalized model is of simple form, predicts conservative values compared with measured data and should be adequate for use in preliminary designs. B.W.

N82-14288*# Wyoming Univ., Laramie. Composite Materials Research Group.

ANALYSIS OF CRACK PROPAGATION AS AN ENERGY ABSORPTION MECHANISM IN METAL MATRIX COMPOSITES Interim Report, Sep. 1979 - Dec. 1980

D. F. ADAMS and D. P. MURPHY Feb. 1981 159 p refs (Contract NSG-3217) (NASA-CR-165051; UWME-DR-101-102-1) Avail: NTIS HC A08/MF A01 CSCL 11D

The crack initiation and crack propagation capability was extended to the previously developed generalized plane strain, finite element micromechanics analysis. Also, an axisymmetric analysis was developed, which contains all of the general features of the plane analysis, including elastoplastic material behavior, temperature-dependent material properties, and crack propagation. These analyses were used to generate various example problems demonstrating the inelastic response of, and crack initiation and propagation in, a boron/aluminum composite. B.W.

N82-16181*# National Aeronautics and Space Administration. Lewis Research Center, Cleveland, Ohio.

PREDICTION OF COMPOSITE HYGRAL BEHAVIOR MADE SIMPLE

C. C. CHAMIS and J. H. SINCLAIR 1982 30 p refs Presented at the 37th Ann. Conf. of the Soc. of the Plastics Ind. (SPI), Washington, D.C., 12-15 Jan. 1982 (NASA-TM-82780; E-1022) Avail: NTIS HC A03/MF A01 CSCL 11D

A convenient procedure is described to determine the hygral behavior (moisture expansion coefficients and moisture stresses) of angleplied fiber composites using a pocket calculator. The procedure consists of equations and appropriate graphs for various (+ or - theta) ply combinations. These graphs present reduced stiffness and moisture expansion coefficients as functions of (+ or - theta) in order to simplify and expedite the use of the equations. The procedure is applicable to all types of balanced, symmetric fiber composites including interply and intraply hybrids. The versatility and generality of the procedure is illustrated using several step-by-step numerical examples. Author

N82-18326*# Wyoming Univ., Laramie. Composite Materials Research Group.

MICROMECHANICAL PREDICTIONS OF CRACK PROPAGATION AND FRACTURE ENERGY IN A SINGLE FIBER BORON/ALUMINUM MODEL COMPOSITE

D. F. ADAMS and J. M. MAHISHI Feb. 1982 65 p refs (Contract NSG-3217)
(NASA-CR-168550; UWME-DR-201-101-1) Avail: NTIS HC A04/MF A01 CSCL 11D

The axisymmetric finite element model and associated computer program developed for the analysis of crack propagation in a composite consisting of a single broken fiber in an annular sheath of matrix material was extended to include a constant displacement boundary condition during an increment of crack propagation. The constant displacement condition permits the growth of a stable crack, as opposed to the catastrophic failure in an earlier version. The finite element model was refined to respond more accurately to the high stresses and steep stress gradients near the broken fiber end. The accuracy and effectiveness of the conventional constant strain axisymmetric element for crack problems was established by solving the classical problem of a penny-shaped crack in a thick cylindrical rod under axial tension. The stress intensity factors predicted by the present finite element model are compared with existing continuum results. S.L.

N82-21259*# National Aeronautics and Space Administration. Lewis Research Center, Cleveland, Ohio.

TUNGSTEN FIBER REINFORCED SUPERALLOY COMPOSITE HIGH TEMPERATURE COMPONENT DESIGN CONSIDERATIONS

E. A. WINSA 1982 23 p refs Presented at the 111th Ann. Meeting of the Am. Inst. of Mining, Met. and Petrol. Engr., Dallas, 14-18 Feb. 1982
(NASA-TM-82811; E-1152; NAS 1.15:82811) Avail: NTIS HC A02/MF A01 CSCL 11D

Tungsten fiber reinforced superalloy composites (TFRS) are intended for use in high temperature turbine components. Current turbine component design methodology is based on applying the experience, sometimes semiempirical, gained from over 30 years of superalloy component design. Current composite component design capability is generally limited to the methodology for low temperature resin matrix composites. Often the tendency is to treat TFRS as just another superalloy or low temperature composite. However, TFRS behavior is significantly different than that of superalloys, and the high environment adds consideration not common in low temperature composite component design. The methodology used for preliminary design of TFRS components are described. Considerations unique to TFRS are emphasized.

Author

N82-22313*# National Aeronautics and Space Administration. Lewis Research Center, Cleveland, Ohio.

COMPRESSION BEHAVIOR OF UNIDIRECTIONAL FIBROUS COMPOSITE

J. H. SINCLAIR and C. C. CHAMIS 1982 20 p refs Presented at Symp. on Compression Testing of Homogeneous Mater. and Composites, Williamsburg, Va., 10-11 Mar. 1982; sponsored by Am. Soc. for Testing and Materials
(NASA-TM-82833; E-1145; NAS 1.15:82833) Avail: NTIS HC A02/MF A01 CSCL 11D

The longitudinal compression behavior of unidirectional fiber composites is investigated using a modified Celanese test method with thick and thin test specimens. The test data obtained are interpreted using the stress/strain curves from back-to-back strain gages, examination of fracture surfaces by scanning electron microscope, and predictive equations for distinct failure modes including fiber compression failure, Euler buckling, delamination, and flexure. The results show that the longitudinal compression fracture is induced by a combination of delamination, flexure, and fiber tier breaks. No distinct fracture surface characteristics can be associated with unique failure modes. An equation is described which can be used to extract the longitudinal compression strength

knowing the longitudinal tensile and flexural strengths of the same composite system. M.G.

N82-24300*# National Aeronautics and Space Administration. Lewis Research Center, Cleveland, Ohio.

DESIGNING WITH FIBER-REINFORCED PLASTICS (PLANAR RANDOM COMPOSITES)

C. C. CHAMIS Washington Mar. 1982 26 p refs (NASA-TM-82812; E-1155; NAS 1.15:82812) Avail: NTIS HC A03/MF A01 CSCL 11D

The use of composite mechanics to predict the hygrothermomechanical behavior of planar random composites (PRC) is reviewed and described. These composites are usually made from chopped fiber reinforced resins (thermoplastics or thermosets). The hygrothermomechanical behavior includes mechanical properties, physical properties, thermal properties, fracture toughness, creep and creep rupture. Properties are presented in graphical form with sample calculations to illustrate their use. Concepts such as directional reinforcement and strip hybrids are described. Typical data that can be used for preliminary design for various PRCs are included. Several resins and molding compounds used to make PRCs are described briefly. Pertinent references are cited that cover analysis and design methods, materials, data, fabrication procedures and applications. Author

N82-31449*# National Aeronautics and Space Administration. Lewis Research Center, Cleveland, Ohio.

ENVIRONMENTAL AND HIGH-STRAIN RATE EFFECTS ON COMPOSITES FOR ENGINE APPLICATIONS

C. C. CHAMIS and G. T. SMITH 1982 20 p refs Presented at the 23rd Struct. Dyn. and Mater. Conf., New Orleans, 10-12 May 1982; sponsored by AIAA, ASME, ASCE, and AHS Previously announced in IAA as A82-30118
(NASA-TM-82882; NAS 1.15:82882) Avail: NTIS HC A02/MF A01 CSCL 11D

The Lewis Research Center is conducting a series of programs intended to investigate and develop the application of composite materials to structural components for turbojet engines. A significant part of that effort is directed to establishing resistance, defect growth, and strain rate characteristics of composite materials over the wide range of environmental and load conditions found in commercial turbojet engine operations. Both analytical and experimental efforts are involved. Author

N83-13173*# Purdue Univ., West Lafayette, Ind. Composite Materials Lab.

DYNAMIC RESPONSES OF GRAPHITE/EPOXY LAMINATED BEAM TO IMPACT OF ELASTIC SPHERES

C. T. SUN and T. WANG Sep. 1982 59 p refs (Contract NSG-3185)
(NASA-CR-165461; NAS 1.26:165461; CML-82-4) Avail: NTIS HC A04/MF A01 CSCL 11D

Wave propagation in 90/45/90/-45/90/2s and 0/45/0/-45/0/2s laminates of a graphite/epoxy composite due to impact of a steel ball was investigated experimentally and also by using a high order beam finite element. Dynamic strain responses at several locations were obtained using strain gages. The finite element program which incorporated statically determined contact laws was employed to calculate the contact force history as well as the target beam dynamic deformation. The comparison of the finite element solutions with the experimental data indicated that the static contact laws for loading and unloading (developed under this grant) are adequate for the dynamic impact analysis. It was found that for the 0/45/0/-45/0/2s laminate which has a much larger longitudinal bending rigidity, the use of beam finite elements is not suitable and plate finite element should be used instead.

Author

24 COMPOSITE MATERIALS

N83-15362*# National Aeronautics and Space Administration. Lewis Research Center, Cleveland, Ohio.

HYGROTHERMOMECHANICAL EVALUATION OF TRANSVERSE FILAMENT TAPE EPOXY/POLYESTER FIBERGLASS COMPOSITES

R. L. LARK and C. C. CHAMIS 1983 24 p refs Proposed for presentation at the 38th Ann. Conf. of the Society of Plastics Industry (SPI) Reinforced Plastics/Composites Inst., Houston, Tex., 7-11 Feb. 1983

(NASA-TM-83044; E-1491; NAS 1.15:83044) Avail: NTIS HC A02/MF A01 CSCL 11D

The static and cyclic load behavior of transverse filament tape (TFT) fiberglass/epoxy and TFY fiberglass/polyester composites, intended for use in the design of low-cost wind turbine blades, are presented. The data behavior is also evaluated with respect to predicted properties based on an integrated hygrothermomechanical response theory. Experimental TFT composite data were developed by the testing of laminates made by using composite layups typical of those used for the fabrication of TFT fiberglass wind turbine blades. Static properties include tension, compression, and interlaminar shear strengths at ambient conditions and at high humidity/elevated temperature conditions after a 500 hour exposure. Cyclic fatigue data were obtained using similar environmental conditions and a range of cyclic stresses. The environmental (temperature and moisture) and cyclic load effects on composite strength degradation are subsequently compared with the predictions obtained by using the composite life/durability theory. The results obtained show that the predicted hygrothermomechanical environmental effects on TFT composites are in good agreement with measured data for various properties including fatigue at different cyclic stresses. S.L.

N83-19817*# National Aeronautics and Space Administration. Lewis Research Center, Cleveland, Ohio.

SIMPLIFIED COMPOSITE MICROMECHANICS EQUATIONS FOR HYGRAL, THERMAL AND MECHANICAL PROPERTIES

C. C. CHAMIS 1983 20 p refs Presented at the 38th Ann. Conf. of the Society of the Plastics Industry (SPI) Reinforced Plastics/Composites Inst., Houston, Tex., 7-11 Feb. 1983

(NASA-TM-83320; E-1561; NAS 1.15:83320) Avail: NTIS HC A02/MF A01 CSCL 11D

A unified set of composite micromechanics equations of simple form is summarized and described. This unified set can be used to predict unidirectional composite (ply) geometric, mechanical, thermal and hygral properties using constituent material (fiber/matrix) properties. This unified set also includes approximate equations for predicting (1) moisture absorption; (2) glass transition temperature of wet resins; and (3) hygrothermal degradation effects. Several numerical examples are worked-out to illustrate ease of use and versatility of these equations. These numerical examples also demonstrate the interrelationship of the various factors (geometric to environmental) and help provide insight into composite behavior at the micromechanistic level. Author

N83-22325*# Purdue Univ., West Lafayette, Ind. School of Aeronautics and Astronautics.

WAVE PROPAGATION IN GRAPHITE/EPOXY LAMINATES DUE TO IMPACT Interim Report

T. M. TAN and C. T. SUN Dec. 1982 171 p refs (Contract NSG-3185)

(NASA-CR-168057; NAS 1.26:168057; CML-82-5) Avail: NTIS HC A08/MF A01 CSCL 11D

The low velocity impact response of graphite-epoxy laminates is investigated theoretically and experimentally. A nine-node isoparametric finite element in conjunction with an empirical contact law was used for the theoretical investigation. Flat laminates subjected to pendulum impact were used for the experimental investigation. Theoretical results are in good agreement with strain gage experimental data. The collective results of the investigation indicate that the theoretical procedure describes the impact response of the laminate up to about 150 in/sec. impact velocity. S.L.

N83-24559*# National Aeronautics and Space Administration. Lewis Research Center, Cleveland, Ohio.

DESIGN PROCEDURES FOR FIBER COMPOSITE STRUCTURAL COMPONENTS: RODS, COLUMNS AND BEAM COLUMNS

C. C. CHAMIS 1983 32 p refs Presented at the 38th Ann. Conf. of the Soc. of the Plastics Ind. (SPI) Reinforced Plastics/Composites Inst., Houston, Tex., 7-11 Feb. 1983

(NASA-TM-83321; E-1562; NAS 1.15:83321) Avail: NTIS HC A03/MF A01 CSCL 11D

Step by step procedures are described which are used to design structural components (rods, columns, and beam columns) subjected to steady state mechanical loads and hydrothermal environments. Illustrative examples are presented for structural components designed for static tensile and compressive loads, and fatigue as well as for moisture and temperature effects. Each example is set up as a sample design illustrating the detailed steps that are used to design similar components. Author

N84-13224*# National Aeronautics and Space Administration. Lewis Research Center, Cleveland, Ohio.

INHYD: COMPUTER CODE FOR INTRAPLY HYBRID COMPOSITE DESIGN. A USERS MANUAL

C. C. CHAMIS and J. H. SINCLAIR Dec. 1983 41 p refs (NASA-TP-2239; E-1755; NAS 1.60:2239) Avail: NTIS HC A03/MF A01 CSCL 11D

A computer program (INHYD) was developed for intraply hybrid composite design. A users manual for INHYD is presented. In INHYD embodies several composite micromechanics theories, intraply hybrid composite theories, and an integrated hygrothermomechanical theory. The INHYD can be run in both interactive and batch modes. It has considerable flexibility and capability, which the user can exercise through several options. These options are demonstrated through appropriate INHYD runs in the manual. S.C.L.

N84-22702*# National Aeronautics and Space Administration. Lewis Research Center, Cleveland, Ohio.

SELECT FIBER COMPOSITES FOR SPACE APPLICATIONS: A MECHANISTIC ASSESSMENT

C. A. GINTY and C. C. CHAMIS 1984 26 p refs Presented at the 29th SAMPE Symp. and Exhibition, Reno, Nev., 3-5 Apr. 1984

(NASA-TM-83631; E-2069; NAS 1.15:83631) Avail: NTIS HC A03/MF A01 CSCL 11D

Three fiber composites (graphite-fiber epoxy, graphite-fiber aluminum, and graphite-fiber magnesium) are evaluated for their possible use in space applications. Using the composite mechanics theories for thermomechanical behavior embodied in the ICAN (Integrated Composites Analyzer) computer code, select composite thermal and mechanical properties are predicted and also their response to cryogenic temperatures, resembling those which occur in space applications. The predicted results are presented in graphical form as a function of the composite's laminate configuration, fiber volume ratio and the selected use temperature. These results are suitable for preliminary design purposes only and should serve as an aid in selecting controlled experiments for obtaining corresponding measured data. Author

N84-24712*# National Aeronautics and Space Administration. Lewis Research Center, Cleveland, Ohio.

IMPACT RESISTANCE OF FIBER COMPOSITES: ENERGY ABSORBING MECHANISMS AND ENVIRONMENTAL EFFECTS

C. C. CHAMIS and J. H. SINCLAIR 1983 25 p refs Presented at the 2nd US/Japan Conf. on Composite Mater.: Mech. Properties, Processing Sci. and Technol. and Appl., Hampton, Va., 6-8 Jun. 1983

(NASA-TM-83594; E-1996; NAS 1.15:83594) Avail: NTIS HC A02/MF A01 CSCL 11D

Energy absorbing mechanisms were identified by several approaches. The energy absorbing mechanisms considered are those in unidirectional composite beams subjected to impact. The approaches used include: mechanic models, statistical models, transient finite element analysis, and simple beam theory. Predicted

results are correlated with experimental data from Charpy impact tests. The environmental effects on impact resistance are evaluated. Working definitions for energy absorbing and energy releasing mechanisms are proposed and a dynamic fracture progression is outlined. Possible generalizations to angle-ply laminates are described. E.A.K.

N84-25770*# National Aeronautics and Space Administration. Lewis Research Center, Cleveland, Ohio.

DYNAMIC STRESS ANALYSIS OF SMOOTH AND NOTCHED FIBER COMPOSITE FLEXURAL SPECIMENS

P. L. N. MURTHY and C. C. CHAMIS 1984 27 p refs Presented at the 7th Conf. on Composite Mater.: Testing and Design, Philadelphia, 2-5 Apr. 1984; sponsored by the American Society for Testing and Materials (NASA-TM-83694; E-2152; NAS 1.15:83694) Avail: NTIS HC A03/MF A01 CSCL 11D

A detailed analysis of the dynamic stress field in smooth and notched fiber composite (Charpy-type) specimens is reported in this paper. The analysis is performed with the aid of the direct transient response analysis solution sequence of MSC/NASTRAN. Three unidirectional composites were chosen for the study. They are S-Glass/Epoxy, Kevlar/Epoxy and T-300/Epoxy composite systems. The specimens are subjected to an impact load which is modeled as a triangular impulse with a maximum of 2000 lb and a duration of 1 ms. The results are compared with those of static analysis of the specimens subjected to a peak load of 2000 lb. For the geometry and type of materials studied, the static analysis results gave close conservative estimates for the dynamic stresses. Another interesting inference from the study is that the impact induced effects are felt by S-Glass/Epoxy specimens sooner than Kevlar/Epoxy or T-300/Epoxy specimens. Author

N84-26755*# National Aeronautics and Space Administration. Lewis Research Center, Cleveland, Ohio.

ICAN: INTEGRATED COMPOSITES ANALYZER

P. L. N. MURTHY and C. C. CHAMIS 1984 25 p refs Presented at the 25th Struct., Struct. Dyn. and Mater. Conf., Palm Springs, Calif., 14-16 May 1984; sponsored by the AIAA, ASME, ASCE and AHS (NASA-TM-83700; E-2158; NAS 1.15:83700) Avail: NTIS HC A02/MF A01 CSCL 11D

The ICAN computer program performs all the essential aspects of mechanics/analysis/design of multilayered fiber composites. Modular, open-ended and user friendly, the program can handle a variety of composite systems having one type of fiber and one matrix as constituents as well as intraply and interply hybrid composite systems. It can also simulate isotropic layers by considering a primary composite system with negligible fiber volume content. This feature is specifically useful in modeling thin interply matrix layers. Hygrothermal conditions and various combinations of in-plane and bending loads can also be considered. Usage of this code is illustrated with a sample input and the generated output. Some key features of output are stress concentration factors around a circular hole, locations of probable delamination, a summary of the laminate failure stress analysis, free edge stresses, microstresses and ply stress/strain influence coefficients. These features make ICAN a powerful, cost-effective tool to analyze/design fiber composite structures and components. A.R.H.

N84-26756*# National Aeronautics and Space Administration. Lewis Research Center, Cleveland, Ohio.

INTERPLY LAYER DEGRADATION EFFECTS ON COMPOSITE STRUCTURAL RESPONSE

C. C. CHAMIS and G. C. WILLIAMS 1983 30 p Presented at the 25th Struct., Struct. Dyn. and Mater. Conf., Palm Springs, Calif., 14-16 May 1984; cosponsored by AIAA, ASME, ASCE, and AHS (NASA-TM-83702; E-2160; NAS 1.15:83702) Avail: NTIS HC A03/MF A01 CSCL 11D

Recent research activities at NASA Lewis Research Center to computationally evaluate the effects of interply layer progressive

weakening (degradation) on the structural response of a composite beam are summarized. The structural responses of interest include: (1) bending, (2) buckling, (3) free vibrations, (4) periodic excitation, and (5) impact. Finite element analysis was used for the computational evaluations. The interply layer degradation effects on the various structural responses were determined and assessed as a function of the interply layer modulus varying from 1 million psi down to 1000 psi and even lower for some limiting cases. The results obtained show that the interply layer degradation has generally negligible effects on composite structural response and, therefore, structural integrity, unless the interply layer modulus degrades to about 10,000 psi or less. Author

N84-27832*# National Aeronautics and Space Administration. Lewis Research Center, Cleveland, Ohio.

SIMPLIFIED COMPOSITE MICROMECHANICS EQUATIONS FOR STRENGTH, FRACTURE TOUGHNESS AND ENVIRONMENTAL EFFECTS

C. C. CHAMIS 1984 27 p refs Presented at the 39th Ann. Conf. of the Soc. of the Plastics Ind. (SPI) Reinforced Plastics/Composites Inst., Houston, 16-20 Jan. 1984 (NASA-TM-83696; E-2154; NAS 1.15:83696) Avail: NTIS HC A03/MF A01 CSCL 11D

A unified set of composite micromechanics equations of simple form is summarized and described. This unified set includes composite micromechanics equations for predicting: (1) ply in plane uniaxial strengths, (2) through the thickness strength, (3) in plane fracture toughness, (4) in plane impact resistance, and (5) through the thickness impact resistance. Equations are also included for predicting the hygrothermal effects on strength, fracture toughness and impact resistance. Several numerical examples are worked out. The numerical examples are selected to demonstrate the interrelationships of the various constituent properties in composite strength and strength related behavior, to make comparisons with available experimental data and to provide insight into composite strength behavior. M.A.C.

N84-28918*# National Aeronautics and Space Administration. Lewis Research Center, Cleveland, Ohio.

HYGROTHERMOMECHANICAL FRACTURE STRESS CRITERIA FOR FIBER COMPOSITES WITH SENSE-PARITY

C. C. CHAMIS and C. A. GINTY 1983 15 p refs Presented at the 7th Conf. on Composite Mater.: Testing and Design, Philadelphia, 2-5 Apr. 1984; sponsored by Am. Soc. for Testing and Mater. (NASA-TM-83691; E-2146; NAS 1.15:83691) Avail: NTIS HC A02/MF A01 CSCL 11D

Hygrothermomechanical fracture stress criteria are developed and evaluated for unidirectional composites (plies) with sense-parity. These criteria explicitly quantify the individual contributions of applied, hygral and thermal stresses as well as couplings among these stresses. The criteria are for maximum stress, maximum strain, internal friction, work-to-fracture and combined-stress fracture. Predicted results obtained indicate that first ply failure will occur at stress levels lower than those predicted using criteria currently available in the literature. Also, the contribution of the various stress couplings (predictable only by fracture criteria with sense-parity) is significant to first ply failure and attendant fracture modes. Author

N84-31288*# National Aeronautics and Space Administration. Lewis Research Center, Cleveland, Ohio.

APPLICATION OF FINITE ELEMENT SUBSTRUCTURING TO COMPOSITE MICROMECHANICS M.S. Thesis - Akron Univ., May 1984

J. J. CARUSO Aug. 1984 70 p refs (Contract NSG-350) (NASA-TM-83729; E-2203; NAS 1.15:83729) Avail: NTIS HC A04/MF A01 CSCL 11D

Finite element substructuring is used to predict unidirectional fiber composite hygral (moisture), thermal, and mechanical properties. COSMIC NASTRAN and MSC/NASTRAN are used to perform the finite element analysis. The results obtained from the

24 COMPOSITE MATERIALS

finite element model are compared with those obtained from the simplified composite micromechanics equations. A unidirectional composite structure made of boron/HM-epoxy, S-glass/IMHS-epoxy and AS/IMHS-epoxy are studied. The finite element analysis is performed using three dimensional isoparametric brick elements and two distinct models. The first model consists of a single cell (one fiber surrounded by matrix) to form a square. The second model uses the single cell and substructuring to form a nine cell square array. To compare computer time and results with the nine cell superelement model, another nine cell model is constructed using conventional mesh generation techniques. An independent computer program consisting of the simplified micromechanics equation is developed to predict the hygral, thermal, and mechanical properties for this comparison. The results indicate that advanced techniques can be used advantageously for fiber composite micromechanics.

Author

N84-33522*# National Aeronautics and Space Administration. Lewis Research Center, Cleveland, Ohio.

FRACTURE SURFACE CHARACTERISTICS OF NOTCHED ANGLEPLIED GRAPHITE/EPOXY COMPOSITES

C. A. GINTY and T. B. IRVINE 1984 25 p refs Presented at the Intern. Symp. on Composites: Mater. and Eng., Newark, Del., 24-28 Sep. 1984; sponsored by the Center for Composite Materials (NASA-TM-83786; E-2284; NAS 1.15:83786) Avail: NTIS HC A02/MF A01 CSCL 11D

Composite fracture surface characteristics and related fracture modes have been investigated through extensive microscopic inspections of the fracture surfaces of notched angleplied graphite/epoxy laminates. The investigation involved 4 ply laminates of the configuration \pm or θ (s) where $\theta = 0$ deg, 3 deg, 5 deg, 10 deg, 15 deg, 30 deg, 45 deg, 60 deg, 75 deg, and 90 deg. Two-inch wide tensile specimens with 0.25 in. by 0.05 in. through-slits centered across the width were tested to fracture. The fractured surfaces were then removed and examined using a scanning electron microscope. Evaluation of the photomicrographs combined with analytical results obtained using the CODSTRAN computer code culminated in a unified set of fracture criteria for determining the mode of fracture in notched angleplied graphite/epoxy laminates.

Author

N84-34575*# Case Western Reserve Univ., Cleveland, Ohio.
MECHANICAL BEHAVIOR OF CARBON-CARBON COMPOSITES
Final Report

G. A. ROZAK Sep. 1984 31 p refs (Contract NAG3-464) (NASA-CR-174767; NAS 1.26:174767) Avail: NTIS HC A03/MF A01 CSCL 11D

A general background, test plan, and some results of preliminary examinations of a carbon-carbon composite material are presented with emphasis on mechanical testing and inspection techniques. Experience with testing and evaluation was gained through tests of a low modulus carbon-carbon material, K-Karb C. The properties examined are the density - 1.55 g/cc; four point flexure strength in the warp - 137 MPa (19,800 psi) and the fill - 95.1 MPa (13,800 psi) directions; and the warp interlaminar shear strength - 14.5 MPa (2100 psi). Radiographic evaluation revealed thickness variations and the thinner areas of the composite were scrapped. The ultrasonic C-scan showed attenuation variations, but these did not correspond to any of the physical and mechanical properties measured. Based on these initial tests and a survey of the literature, a plan has been devised to examine the effect of stress on the oxidation behavior, and the strength degradation of coated carbon-carbon composites. This plan will focus on static fatigue tests in the four point flexure mode in an elevated temperature, oxidizing environment.

Author

N84-34576*# National Aeronautics and Space Administration. Lewis Research Center, Cleveland, Ohio.

FRACTURE MODES IN NOTCHED ANGLEPLIED COMPOSITE LAMINATES

T. B. IRVINE and C. A. GINTY 1984 27 p refs Presented at Symp. on Composite Fatigue and Fracture, Dallas, 24-25 Oct. 1984; sponsored by American Society for Testing and Materials (NASA-TM-83802; E-2307; NAS 1.15:83802) Avail: NTIS HC A03/MF A01 CSCL 11D

The Composite Durability Structural Analysis (CODSTRAN) computer code is used to determine composite fracture. Fracture modes in solid and notched, unidirectional and angleplied graphite/epoxy composites were determined by using CODSTRAN. Experimental verification included both nondestructive (ultrasonic C-Scanning) and destructive (scanning electron microscopy) techniques. The fracture modes were found to be a function of ply orientations and whether the composite is notched or unnotched. Delaminations caused by stress concentrations around notch tips were also determined. Results indicate that the composite mechanics, structural analysis, laminate analysis, and fracture criteria modules embedded in CODSTRAN are valid for determining composite fracture modes.

R.J.F.

N85-14882*# National Aeronautics and Space Administration. Lewis Research Center, Cleveland, Ohio.

FABRICATION AND QUALITY ASSURANCE PROCESSES FOR SUPERHYBRID COMPOSITE FAN BLADES

R. F. LARK and C. C. CHAMIS 1983 15 p refs Presented at the 15th Ann. SAMPE Tech. Conf., Cincinnati, 4-5 Oct. 1983 (NASA-TM-83354; E-1611; NAS 1.15:83354) Avail: NTIS HC A02/MF A01 CSCL 11D

The feasibility of fabricating full-scale fan blades from superhybrid composites (SHC) for use large, commercial gas turbine engines was evaluated. The type of blade construction selected was a metal-spar/SHC-shell configuration, in which the outer shell was adhesively bonded to a short, internal, titanium spar. Various aspects of blade fabrication, inspection, and quality assurance procedures developed in the investigation are described. It is concluded that the SHC concept is feasible for the fabrication of prototype, full-scale, metal-spar/SHC-shell fan blades that have good structural properties and meet dimensional requirements.

R.S.F.

N85-15822*# National Aeronautics and Space Administration. Lewis Research Center, Cleveland, Ohio.

A STUDY OF INTERPLY LAYER EFFECTS ON THE FREE-EDGE STRESS FIELD OF ANGLEPLIED LAMINATES

P. L. N. MURTHY and C. C. CHAMIS 1984 31 p refs Presented at the Symp. on Adv. and Trends in Struct. Dyn., Washington, D.C., 22-25 Oct. 1984; sponsored by NASA and George Washington Univ. (NASA-TM-86924; E-2201; NAS 1.15:86924) Avail: NTIS HC A03/MF A01 CSCL 11D

The general-purpose finite-element program MSC/NASTRAN is used to study the interply layer effects on the free-edge stress field of symmetric angleplied laminates subjected to uniform tensile stress. The free-edge region is modeled as a separate substructure (superelement) which enables easy mesh refinement and provides the flexibility to move the superelement along the edge. The results indicate that the interply layer reduces the stress intensity significantly at the free edge. Another important observation of the study is that the failures observed near free edges of these types of laminates could have been caused by the interlaminar shear stresses.

Author

N85-15823*# National Aeronautics and Space Administration. Lewis Research Center, Cleveland, Ohio.

DESIGN PROCEDURES FOR FIBER COMPOSITE STRUCTURAL COMPONENTS: PANELS SUBJECTED TO COMBINED IN-PLANE LOADS

C. C. CHAMIS 1985 29 p refs Presented at the 40th Ann. Conf. of the Society of the Plastics Industry (SPI) Reinforced Plastics/Composites Inst., Atlanta, 28 Jan. - 1 Feb. 1985 (NASA-TM-86909; E-2319; NAS 1.15:86909) Avail: NTIS HC A03/MF A01 CSCL 11D

Step by step procedures are described which can be used to design panels made from fiber composite angleplied laminates and subjected to combined in plane loads. The procedures are set up as a multistep sample design. Steps in the sample design procedure range from selection of the laminate configuration to the subsequent analyses required to check design requirements for: (1) displacement, (2) ply stresses, and (3) buckling. The sample design steps are supplemented with appropriate tabular and graphical data which can be used to expedite the design process.

Author

N85-21273*# National Aeronautics and Space Administration. Lewis Research Center, Cleveland, Ohio.

NONLINEAR ANALYSIS FOR HIGH-TEMPERATURE MULTILAYERED FIBER COMPOSITE STRUCTURES M.S. Thesis

D. A. HOPKINS Aug. 1984 120 p refs (NASA-TM-83754; E-2242; NAS 1.15:83754) Avail: NTIS HC A06/MF A01 CSCL 11D

A unique upward-integrated top-down-structured approach is presented for nonlinear analysis of high-temperature multilayered fiber composite structures. Based on this approach, a special purpose computer code was developed (nonlinear COBSTRAN) which is specifically tailored for the nonlinear analysis of tungsten-fiber-reinforced superalloy (TFRS) composite turbine blade/vane components of gas turbine engines. Special features of this computational capability include accounting of; micro- and macro-heterogeneity, nonlinear (stress-temperature-time dependent) and anisotropic material behavior, and fiber degradation. A demonstration problem is presented to manifest the utility of the upward-integrated top-down-structured approach, in general, and to illustrate the present capability represented by the nonlinear COBSTRAN code. Preliminary results indicate that nonlinear COBSTRAN provides the means for relating the local nonlinear and anisotropic material behavior of the composite constituents to the global response of the turbine blade/vane structure.

Author

N85-27978*# National Aeronautics and Space Administration. Lewis Research Center, Cleveland, Ohio.

DESIGNING FOR FIBER COMPOSITE STRUCTURAL DURABILITY IN HYGROTHERMOMECHANICAL ENVIRONMENT

C. C. CHAMIS 1985 23 p refs Proposed for presentation at the 5th Intern. Conf. on Composite Mater., San Diego, Calif., 30 Jul. - 1 Aug. 1985; sponsored by American Society of Mining Engineers (NASA-TM-87045; E-2606; NAS 1.15:87045) Avail: NTIS HC A02/MF A01 CSCL 11D

A methodology is described which can be used to design/analyze fiber composite structures subjected to complex hygrothermomechanical environments. This methodology includes composite mechanics and advanced structural analysis methods (finite element). Select examples are described to illustrate the application of the available methodology. The examples include: (1) composite progressive fracture; (2) composite design for high cycle fatigue combined with hot-wet conditions; and (3) general laminate design.

E.A.K.

N85-30034*# National Aeronautics and Space Administration. Lewis Research Center, Cleveland, Ohio.

TEN YEAR ENVIRONMENTAL TEST OF GLASS FIBER/EPOXY PRESSURE VESSELS

J. R. FADDOUL 1985 18 p refs Presented at the 21st Joint Propulsion Conf., Monterey, Calif., 8-10 Jul. 1985; sponsored by AIAA, SAE, ASME, and ASEE (NASA-TM-87058; E-2625; NAS 1.15:87058) Avail: NTIS HC A02/MF A01 CSCL 11D

By the beginning of the 1970's composite pressure vessels had received a significant amount of development effort, and applications were beginning to be investigated. One of the first applications grew out of NASA Johnson Space Center efforts to develop a superior emergency breathing system for firemen. While the new breathing system provided improved wearer comfort and an improved mask and regulator, the primary feature was low weight which was achieved by using a glass fiber reinforced aluminum pressure vessel. Part of the development effort was to evaluate the long term performance of the pressure vessel and as a consequence, some 30 bottles for a test program were procured. These bottles were then provided to NASA Lewis Research Center where they were maintained in an outdoor environment in a pressurized condition for a period of up to 10 yr. During this period, bottles were periodically subjected to cyclic and burst testing. There was no protective coating applied to the fiberglass/epoxy composite, and significant loss in strength did occur as a result of the environment. Similar bottles stored indoors showed little, if any, degradation. This report contains a description of the pressure vessels, a discussion of the test program, data for each bottle, and appropriate plots, comparisons, and conclusions.

R.J.F.

N85-30035*# Virginia Polytechnic Inst. and State Univ., Blacksburg.

A STUDY OF THE STRESS WAVE FACTOR TECHNIQUE FOR THE CHARACTERIZATION OF COMPOSITE MATERIALS Final Report

A. K. GOVADA, J. C. DUKE, JR., E. G. HENNEKE, II, and W. W. STINCHCOMB Feb. 1985 103 p refs (Contract NAG3-172) (NASA-CR-174870; NAS 1.26:174870; CCMS-84-13) Avail: NTIS HC A06/MF A01 CSCL 11D

This study has investigated the potential of the Stress Wave Factor as an NDT technique for thin composite laminates. The conventional SWF and an alternate method for quantifying the SWF were investigated. Agreement between the initial SWF number, ultrasonic C-scan, inplane displacements as obtained by full field moire interferometry, and the failure location have been observed. The SWF number was observed to be the highest when measured along the fiber direction and the lowest when measured across the fibers. The alternate method for quantifying the SWF used square root of the zeroth moment (square root of M_{00}) of the frequency spectrum of the received signal as a quantitative parameter. From this study it therefore appears that the stress wave factor has an excellent potential to monitor damage development in thin composite laminates.

B.W.

N86-10290*# National Aeronautics and Space Administration. Lewis Research Center, Cleveland, Ohio.

PROGRESSIVE DAMAGE, FRACTURE PREDICTIONS AND POST MORTEM CORRELATIONS FOR FIBER COMPOSITES

1985 21 p refs Presented at Intern. Conf.: Post Failure Anal. Tech. Fiber Reinforced Composites, Dayton, Ohio, 1-3 Jul. 1985; sponsored by Air Force (NASA-TM-87101; E-2695; NAS 1.15:87101) Avail: NTIS HC A02/MF A01 CSCL 11D

Lewis Research Center is involved in the development of computational mechanics methods for predicting the structural behavior and response of composite structures. In conjunction with the analytical methods development, experimental programs including post failure examination are conducted to study various factors affecting composite fracture such as laminate thickness effects, ply configuration, and notch sensitivity. Results indicate

24 COMPOSITE MATERIALS

that the analytical capabilities incorporated in the CODSTRAN computer code are effective in predicting the progressive damage and fracture of composite structures. In addition, the results being generated are establishing a data base which will aid in the characterization of composite fracture. Author

N86-21614*# National Aeronautics and Space Administration. Lewis Research Center, Cleveland, Ohio.

INTEGRATED COMPOSITE ANALYZER (ICAN): USERS AND PROGRAMMERS MANUAL

P. L. N. MURTHY and C. C. CHAMIS Mar. 1986 77 p refs (NASA-TP-2515; E-2035; NAS 1.60:2515) Avail: NTIS HC A05/MF A01 CSCL 11D

The use of and relevant equations programmed in a computer code designed to carry out a comprehensive linear analysis of multilayered fiber composites is described. The analysis contains the essential features required to effectively design structural components made from fiber composites. The inputs to the code are constituent material properties, factors reflecting the fabrication process, and composite geometry. The code performs micromechanics, macromechanics, and laminate analysis, including the hygrothermal response of fiber composites. The code outputs are the various ply and composite properties, composite structural response, and composite stress analysis results with details on failure. The code is in Fortran IV and can be used efficiently as a package in complex structural analysis programs. The input-output format is described extensively through the use of a sample problem. The program listing is also included. The code manual consists of two parts. Author

N86-24756*# National Aeronautics and Space Administration. Lewis Research Center, Cleveland, Ohio.

THERMOVISCOPLASTIC NONLINEAR CONSTITUTIVE RELATIONSHIPS FOR STRUCTURAL ANALYSIS OF HIGH TEMPERATURE METAL MATRIX COMPOSITES

C. C. CHAMIS and D. A. HOPKINS 1985 25 p refs Presented at First Symposium on Testing Technology of Metal Matrix Composites, Nashville, Tenn., 18-20, 1985; sponsored by American Society for Testing Materials (NASA-TM-87291; E-2998; NAS 1.15:87291) Avail: NTIS HC A02/MF A01 CSCL 11D

A set of thermoviscoplastic nonlinear constitutive relationships (1VP-NCR) is presented. The set was developed for application to high temperature metal matrix composites (HT-MMC) and is applicable to thermal and mechanical properties. Formulation of the TVP-NCR is based at the micromechanics level. The TVP-NCR are of simple form and readily integrated into nonlinear composite structural analysis. It is shown that the set of TVP-NCR is computationally effective. The set directly predicts complex materials behavior at all levels of the composite simulation, from the constituent materials, through the several levels of composite mechanics, and up to the global response of complex HT-MMC structural components. E.A.K.

N86-24757*# National Aeronautics and Space Administration. Lewis Research Center, Cleveland, Ohio.

A UNIQUE SET OF MICROMECHANICS EQUATIONS FOR HIGH TEMPERATURE METAL MATRIX COMPOSITES

D. A. HOPKINS and C. C. CHAMIS 1985 27 p refs Presented at the 1st Symposium on Testing Technology of Metal Matrix Composites, Nashville, Tenn., 18-20 Nov. 1985; sponsored by American Society for Testing and Materials (NASA-TM-87154; E-2780; NAS 1.15:87154) Avail: NTIS HC A03/MF A01 CSCL 11D

A unique set of micromechanic equations is presented for high temperature metal matrix composites. The set includes expressions to predict mechanical properties, thermal properties and constituent microstresses for the unidirectional fiber reinforced ply. The equations are derived based on a mechanics of materials formulation assuming a square array unit cell model of a single fiber, surrounding matrix and an interphase to account for the chemical reaction which commonly occurs between fiber and matrix. A three-dimensional finite element analysis was used to

perform a preliminary validation of the equations. Excellent agreement between properties predicted using the micromechanics equations and properties simulated by the finite element analyses are demonstrated. Implementation of the micromechanics equations as part of an integrated computational capability for nonlinear structural analysis of high temperature multilayered fiber composites is illustrated. E.A.K.

N86-24759*# National Aeronautics and Space Administration. Lewis Research Center, Cleveland, Ohio.

SIMPLIFIED COMPOSITE MICROMECHANICS FOR PREDICTING MICROSTRESSES

C. C. CHAMIS 1986 27 p refs Presented at 41st Annual Conference of the Society of the Plastics Industry (SPI) Reinforced Plastics/Composites Inst., Atlanta, Ga., 27-31 Jan. 1986 (NASA-TM-87295; E-2782; NAS 1.15:87295) Avail: NTIS HC A03/MF A01 CSCL 11D

A unified set of composite micromechanics equations is summarized and described. This unified set is for predicting the ply microstresses when the ply stresses are known. The set consists of equations of simple form for predicting three-dimensional stresses (six each) in the matrix, fiber, and interface. Several numerical examples are included to illustrate use and computational effectiveness of the equations in this unified set. Numerical results from these examples are discussed with respect to their significance on microcrack formation and, therefore, damage initiation in fiber composites. Author

N86-25417*# National Aeronautics and Space Administration. Lewis Research Center, Cleveland, Ohio.

FRACTURE CHARACTERISTICS OF ANGLEPLIED LAMINATES FABRICATED FROM OVERAGED GRAPHITE/EPOXY PREPREG

C. A. GINTY and C. C. CHAMIS 1985 22 p refs Presented at Symposium on Fractography of Modern Engineering Materials, Nashville, Tenn., 18-19 Nov. 1985; Sponsored by American Society for Testing and Materials (NASA-TM-87266; E-2968; NAS 1.15:87266) Avail: NTIS HC A02/MF A01 CSCL 11D

A series of angleplied graphite/epoxy laminates was fabricated from overaged prepreg and tested in tension to investigate the effects of overaged or advanced cure material on the degradation of laminate strength. Results, which include fracture stresses, indicate a severe degradation in strength. In addition, the fracture surfaces and microstructural characteristics are distinctly unlike any features observed in previous tests of this prepreg and laminate configuration. Photographs of the surfaces and microstructures reveal flat morphologies consisting of alternate rows of fibers and hackles. These fracture surface characteristics are independent of the laminate configurations. The photomicrographs are presented and compared with data from similar studies to show the unique characteristics produced by the overage prepreg. Analytical studies produced results which agreed with those from the experimental investigations. Author

N86-26376*# National Aeronautics and Space Administration. Lewis Research Center, Cleveland, Ohio.

COMPUTATIONAL SIMULATION OF PROGRESSIVE FRACTURE IN FIBER COMPOSITES

C. C. CHAMIS 1986 12 p refs Presented at the International Conference on Computational Mechanics, Tokyo, Japan, 25-28 May 1986 (NASA-TM-87341; E-3090; NAS 1.15:87341) Avail: NTIS HC A02/MF A01 CSCL 11D

Computational methods for simulating and predicting progressive fracture in fiber composite structures are presented. These methods are integrated into a computer code of modular form. The modules include composite mechanics, finite element analysis, and fracture criteria. The code is used to computationally simulate progressive fracture in composite laminates with and without defects. The simulation tracks the fracture progression in terms of modes initiating fracture, damage growth, and imminent global (catastrophic) laminate fracture. Author

N86-31663*# National Aeronautics and Space Administration. Lewis Research Center, Cleveland, Ohio.

FIBER COMPOSITE SANDWICH THERMOSTRUCTURAL BEHAVIOR: COMPUTATIONAL SIMULATION

C. C. CHAMIS, R. A. AIELLO, and P. L. N. MURTHY (Cleveland State Univ., Ohio) 1986 18 p Presented at the 27th Structures, Structural Dynamics and Materials Conference (SDM), San Antonio, Tex., 19-21 May 1986; sponsored by AIAA, ASME, ASCE and AHS

(NASA-TM-88787; E-3112; NAS 1.15:88787) Avail: NTIS HC A02/MF A01 CSCL 11D

Several computational levels of progressive sophistication/simplification are described to computationally simulate composite sandwich hygral, thermal, and structural behavior. The computational levels of sophistication include: (1) three-dimensional detailed finite element modeling of the honeycomb, the adhesive and the composite faces; (2) three-dimensional finite element modeling of the honeycomb assumed to be an equivalent continuous, homogeneous medium, the adhesive and the composite faces; (3) laminate theory simulation where the honeycomb (metal or composite) is assumed to consist of plies with equivalent properties; and (4) derivations of approximate, simplified equations for thermal and mechanical properties by simulating the honeycomb as an equivalent homogeneous medium. The approximate equations are combined with composite hygrothermomechanical and laminate theories to provide a simple and effective computational procedure for simulating the thermomechanical/thermostrostructural behavior of fiber composite sandwich structures. Author

N86-31664*# National Aeronautics and Space Administration. Lewis Research Center, Cleveland, Ohio.

ICAN: A VERSATILE CODE FOR PREDICTING COMPOSITE PROPERTIES

C. A. GINTY and C. C. CHAMIS 1986 20 p Presented at the 31st National SAMPE Symposium and Exhibition, Las Vegas, Nev., 7-10 Apr. 1986

(NASA-TM-87334; E-2017; NAS 1.15:87334) Avail: NTIS HC A02/MF A01 CSCL 11D

The Integrated Composites ANalyzer (ICAN), a stand-alone computer code, incorporates micromechanics equations and laminate theory to analyze/design multilayered fiber composite structures. Procedures for both the implementation of new data in ICAN and the selection of appropriate measured data are summarized for: (1) composite systems subject to severe thermal environments; (2) woven fabric/cloth composites; and (3) the selection of new composite systems including those made from high strain-to-fracture fibers. The comparisons demonstrate the versatility of ICAN as a reliable method for determining composite properties suitable for preliminary design. M.G.

N87-13491*# National Aeronautics and Space Administration. Lewis Research Center, Cleveland, Ohio.

COMPOSITE INTERLAMINAR FRACTURE TOUGHNESS: THREE-DIMENSIONAL FINITE ELEMENT MODELING FOR MIXED MODE 1, 2 AND 3 FRACTURE

P. L. N. MURTHY (Cleveland State Univ., Ohio) and C. C. CHAMIS 1986 27 p Presented at the 8th Symposium on Composite Materials Testing and Design, Charleston, S. Car., 28-30 Apr. 1986; sponsored by the American Society for Testing and Materials

(NASA-TM-88872; E-3278; NAS 1.15:88872) Avail: NTIS HC A03/MF A01 CSCL 71F

A computational method/procedure is described which can be used to simulate individual and mixed mode interlaminar fracture progression in fiber composite laminates. Different combinations of Modes 1, 2, and 3 fracture are simulated by varying the crack location through the specimen thickness and by selecting appropriate unsymmetric laminate configurations. The contribution of each fracture mode to strain energy release rate is determined by the local crack closure methods while the mixed mode is determined by global variables. The strain energy release rates are plotted versus extending crack length, where slow crack growth,

stable crack growth, and rapid crack growth regions are easily identified. Graphical results are presented to illustrate the effectiveness and versatility of the computational simulation for: (1) evaluating mixed-mode interlaminar fracture, (2) for identifying respective dominant parameters, and (3) for selecting possible simple test methods. Author

N87-16880*# National Aeronautics and Space Administration. Lewis Research Center, Cleveland, Ohio.

COMPOSITE SPACE ANTENNA STRUCTURES: PROPERTIES AND ENVIRONMENTAL EFFECTS

CAROL A. GINTY and NED M. ENDRES (Sverdrup Technology, Inc., Cleveland, Ohio) 1986 22 p Presented at the 18th International SAMPE Technical Conference, Seattle, Wash., 7-9 Oct. 1986

(NASA-TM-88859; E-3225; NAS 1.15:88859) Avail: NTIS HC A02/MF A01 CSCL 11D

The thermal behavior of composite spacecraft antenna reflectors has been investigated with the integrated Composites Analyzer (ICAN) computer code. Parametric studies have been conducted on the face sheets and honeycomb core which constitute the sandwich-type structures. Selected thermal and mechanical properties of the composite faces and sandwich structures are presented graphically as functions of varying fiber volume ratio, temperature, and moisture content. The coefficients of thermal expansion are discussed in detail since these are the critical design parameters. In addition, existing experimental data are presented and compared to the ICAN predictions. Author

N87-18614*# National Aeronautics and Space Administration. Lewis Research Center, Cleveland, Ohio.

COMPUTATIONAL COMPOSITE MECHANICS FOR AEROSPACE PROPULSION STRUCTURES

CHRISTOS C. CHAMIS 1987 19 p Presented at the 3rd Space Systems Technology Conference, San Diego, Calif., 9-12 Jun. 1986; sponsored by the AIAA Previously announced in IAA as A86-40596

(NASA-TM-88965; E-3023; NAS 1.15:88965) Avail: NTIS HC A02/MF A01 CSCL 11D

Specialty methods are presented for the computational simulation of specific composite behavior. These methods encompass all aspects of composite mechanics, impact, progressive fracture and component specific simulation. Some of these methods are structured to computationally simulate, in parallel, the composite behavior and history from the initial fabrication through several missions and even to fracture. Select methods and typical results obtained from such simulations are described in detail in order to demonstrate the effectiveness of computationally simulating: (1) complex composite structural behavior in general, and (2) specific aerospace propulsion structural components in particular. Author

N87-28611*# National Aeronautics and Space Administration. Lewis Research Center, Cleveland, Ohio.

DYNAMIC DELAMINATION BUCKLING IN COMPOSITE LAMINATES UNDER IMPACT LOADING: COMPUTATIONAL SIMULATION

JOSEPH E. GRADY, CHRISTOS C. CHAMIS, and ROBERT A. AIELLO 1987 14 p Presented at the 2nd Symposium on Composite Materials: Fatigue and Fracture, Cincinnati, Ohio, 26-30 Apr. 1987; sponsored by the American Society for Testing and Materials

(NASA-TM-100192; E-3779; NAS 1.15:100192) Avail: NTIS HC A02/MF A01 CSCL 11D

A unique dynamic delamination buckling and delamination propagation analysis capability has been developed and incorporated into a finite element computer program. This capability consists of the following: (1) a modification of the direct time integration solution sequence which provides a new analysis algorithm that can be used to predict delamination buckling in a laminate subjected to dynamic loading, and (2) a new method of modeling the composite laminate using plate bending elements and multipoint constraints. This computer program is used to predict

24 COMPOSITE MATERIALS

both impact induced buckling in composite laminates with initial delaminations and the strain energy release rate due to extension of the delamination. It is shown that delaminations near the outer surface of a laminate are susceptible to local buckling and buckling-induced delamination propagation when the laminate is subjected to transverse impact loading. The capability now exists to predict the time at which the onset of dynamic delamination buckling occurs, the dynamic buckling mode shape, and the dynamic delamination strain energy release rate. Author

N88-12551*# National Aeronautics and Space Administration. Lewis Research Center, Cleveland, Ohio.

FREE-EDGE DELAMINATION: LAMINATE WIDTH AND LOADING CONDITIONS EFFECTS

P. L. N. MURTHY (Cleveland State Univ., Ohio.) and C. C. CHAMIS Dec. 1987 28 p

(NASA-TM-100238; E-3862; NAS 1.15:100238) Avail: NTIS HC A03/MF A01 CSCL 11D

The width and loading conditions effects on free-edge stress fields in composite laminates are investigated using a three-dimensional finite element analysis. This analysis includes a special free-edge region refinement or superelement with progressive substructuring (mesh refinement) and finite thickness interply layers. The different loading conditions include in-plane and out-of-plane bending, combined axial tension and in-plane shear, twisting, uniform temperature and uniform moisture. Results obtained indicate that: axial tension causes the smallest magnitude of interlaminar free edge stress compared to other loading conditions; free-edge delamination data obtained from laboratory specimens cannot be scaled to structural components; and composite structural components are not likely to delaminate. Author

N88-12552*# National Aeronautics and Space Administration. Lewis Research Center, Cleveland, Ohio.

COMPOSITE MECHANICS FOR ENGINE STRUCTURES

CHRISTOS C. CHAMIS 1987 35 p Presented at the 32nd International Gas Turbine Conference and Exhibition, Anaheim, Calif., 31- May - 4 Jun. 1987; sponsored by ASME

(NASA-TM-100176; E-3750; NAS 1.15:100176) Avail: NTIS HC A03/MF A01 CSCL 11D

Recent research activities and accomplishments at Lewis Research Center on composite mechanics for engine structures are summarized. The activities focused mainly on developing procedures for the computational simulation of composite intrinsic and structural behavior. The computational simulation encompasses all aspects of composite mechanics, advanced three-dimensional finite-element methods, damage tolerance, composite structural and dynamic response, and structural tailoring and optimization. Author

26

METALLIC MATERIALS

Includes physical, chemical, and mechanical properties of metals, e.g., corrosion; and metallurgy.

A80-35495*# National Aeronautics and Space Administration. Lewis Research Center, Cleveland, Ohio.

EFFECTS OF FINE POROSITY ON THE FATIGUE BEHAVIOR OF A POWDER METALLURGY SUPERALLOY

R. V. MINER and R. L. DRESHFIELD (NASA, Lewis Research Center, Cleveland, Ohio) American Institute of Mining, Metallurgical and Petroleum Engineers, Annual Meeting, 109th, Las Vegas, Nev., Feb. 25-28, 1980, Paper. 23 p. refs

Hot-isostatically-pressed powder-metallurgy Astroloy was obtained which contained 1.4 percent porosity at the grain boundaries produced by argon entering the powder container during pressing. This material was tested at 650 C in fatigue, creep-fatigue, tension, and stress-rupture and the results compared with data

on sound Astroloy. They influenced fatigue crack initiation and produced a more intergranular mode of propagation but fatigue life was not drastically reduced. Fatigue behavior of the porous material showed typical correlation with tensile behavior. The plastic strain range-life relation was reduced proportionately with the reduction in tensile ductility, but the elastic strain range-life relation was changed little. (Author)

A81-12266*# Pratt and Whitney Aircraft Group, West Palm Beach, Fla.

CYCLIC BEHAVIOR OF TURBINE DISK ALLOYS AT 650 C

B. A. COWLES, D. L. SIMS, J. R. WARREN (United Technologies Corp. Pratt and Whitney Aircraft Group, West Palm Beach, Fla.), and R. V. MINER, JR. (NASA, Lewis Research Center, Cleveland, Ohio) ASME, Transactions, Journal of Engineering Materials and Technology, vol. 102, Oct. 1980, p. 356-363. refs

Five gas turbine disk alloys representing a range of strengths and processing methods were tested for resistance to both cyclic crack initiation and propagation at 650 C using a 0.33 Hz fatigue cycle and a cycle incorporating a 900 s tensile dwell. At the low strain ranges pertinent to disks, resistance to crack initiation increased with increasing tensile yield strength among the alloys, though the advantage was somewhat smaller for the creep fatigue cycle. Cyclic crack growth resistance, however, decreased with increasing strength and very markedly so for the dwell cycle. (Author)

A82-11399* National Aeronautics and Space Administration. Lewis Research Center, Cleveland, Ohio.

COMPARATIVE THERMAL FATIGUE RESISTANCE OF SEVERAL OXIDE DISPERSION STRENGTHENED ALLOYS

J. D. WHITTENBERGER and P. T. BIZON (NASA, Lewis Research Center, Cleveland, OH) International Journal of Fatigue, vol. 3, Oct. 1981, p. 173-180. refs

The thermal fatigue resistance of several oxide dispersion strengthened (ODS) alloys has been evaluated through cyclic exposure in fluidized beds. The ODS nickel-base alloy MA 754 and ODS iron-base alloy MA 956 as well as four experimental ODS Ni-16Cr-4.5Al base alloys with and without Ta additions were examined. Both bare and coated alloys were subjected to up to 6000 cycles where each cycle consisted of a 3 minute immersion in a fluidized bed at 1130 C followed by a 3 minute immersion in a bed at 357 C. Testing revealed that the thermal fatigue resistance of the ODS nickel-base alloys was excellent and about equal to that of directionally solidified superalloys. However, the thermal fatigue resistance of MA 956 was found to be poor. Metallographic examination of tested specimens revealed that, in general, the post-test microstructures can be rationalized on the basis of previous diffusion, mechanical property, and oxidation studies. (Author)

A82-47398* National Aeronautics and Space Administration. Lewis Research Center, Cleveland, Ohio.

FATIGUE AND CREEP-FATIGUE DEFORMATION OF SEVERAL NICKEL-BASE SUPERALLOYS AT 650 C

R. V. MINER, J. GAYDA (NASA, Lewis Research Center, Cleveland, OH), and R. D. MAIER (Chase Brass and Copper Co., Solon, OH) Metallurgical Transactions A - Physical Metallurgy and Materials Science, vol. 13A, Oct. 1982, p. 1755-1765. refs

Transmission electron microscopy has been used to study the bulk deformation characteristics of seven nickel-base superalloys tested in fatigue and creep-fatigue at 650 C. The alloys were Waspalloy, HIP Astroloy, H plus F Astroloy, H plus F Rene 95, IN 100, MERL 76, and NASA IIB-7. The amount of bulk deformation observed in all the alloys was low. In tests with inelastic strain amplitudes less than about 0.003, only some grains exhibited yielding and the majority of those had the 110 line near the tensile axis. Deformation occurred on octahedral systems for all of the alloys except MERL 76 which also showed abundant primary cube slip. Creep-fatigue cycling occasionally produced extended faults between partial dislocations, but otherwise deformation was much the same as for fatigue cycling. V.L.

A83-21071* General Electric Co., Cincinnati, Ohio.
REQUIREMENTS OF CONSTITUTIVE MODELS FOR TWO NICKEL-BASE SUPERALLOYS

J. H. LAFLIN and T. S. COOK (General Electric Co., Aircraft Engine Business Group, Cincinnati, OH) International Conference on Constitutive Laws of Engineering Materials: Theory and Application, University of Arizona, Tucson, AZ, Jan. 1983, Paper. 3 p. refs
 (Contract NAS3-22534)

The constitutive behavior of two nickel-base superalloys, Rene '80 and Inconel 718, utilized in gas turbine blade and disk components, respectively, is presented. In turbine blade applications, the high homologous temperatures result in strain-rate effects dominating behavior. In turbine disks, the temperatures are cooler so that mean stress effects become important. The impact of these two variables on the overall crack initiation lifetime and analysis methodology is discussed. (Author)

A83-22019* Cincinnati Univ., Ohio.
METALLURGICAL INSTABILITIES DURING THE HIGH TEMPERATURE LOW CYCLE FATIGUE OF NICKEL-BASE SUPERALLOYS

S. D. ANTOLOVICH and N. JAYARAMAN (Cincinnati, University, Cincinnati, OH) Materials Science and Engineering, vol. 57, Jan. 1983, p. L9-L12. refs
 (Contract AF-AFOSR-80-0065; NSG-3263)

An investigation is made of the microstructural instabilities that affect the high temperature low cycle fatigue (LCF) life of nickel-base superalloys. Crack initiation processes, provoked by the formation of carbides and the coarsening of the grains of the material at high temperatures are discussed. Experimental results are examined, and it is concluded that LCF behavior can be understood more fully only if details of the material and its dynamic behavior at high temperatures are considered. The effects of high stress, dislocation debris, and increasing environmental damage on the life of the alloy are discussed. M.I.I.

A83-36166* Cincinnati Univ., Ohio.
THE EFFECT OF MICROSTRUCTURE ON THE FATIGUE BEHAVIOR OF NI BASE SUPERALLOYS

S. D. ANTOLOVICH (Cincinnati, University, Cincinnati, OH) and N. JAYARAMAN IN: Fatigue: Environment and temperature effects. New York, Plenum Press, 1983, p. 119-144. refs
 (Contract AF-AFOSR-80-0065; NSG-3263)

Nickel-base superalloys are used in jet engine components such as disks, turbine blades, and vanes. Improvements in the fatigue behavior will allow the life to be extended or the payloads to be increased. The first part of the present investigation deals primarily with the effects of microstructural variations on the fatigue crack propagation (FCP) behavior of nickel-base alloys, while the second part is concerned with low-cycle fatigue (LCF) behavior of Ni base systems. Waspaloy at low temperature is considered, taking into account material heat treatment and test procedures, a composite plot of Waspaloy FCP data, Paris law fatigue crack propagation constants, monotonic tensile data, and overload FCP test results for Waspaloy. It is found that the FCP and overload behavior of nickel-base alloys may be markedly improved by heat treating. Attention is given to effects of cyclic deformation on microstructure and substructure, environmental damage, and an environmental/deformation model of high temperature LCF. G.R.

A83-41199* National Aeronautics and Space Administration. Lewis Research Center, Cleveland, Ohio.
FATIGUE CRACK INITIATION AND PROPAGATION IN SEVERAL NICKEL-BASE SUPERALLOYS AT 650 C

J. GAYDA and R. V. MINER (NASA, Lewis Research Center, Materials Div., Cleveland, OH) International Journal of Fatigue (ISSN 0142-1123), vol. 5, July 1983, p. 135-143. refs

The modes of crack initiation and propagation of several nickel-base superalloys have been examined after fatigue and creep-fatigue testing at 650 C. In fatigue, crack initiation was transgranular and frequently associated with porosity or inclusions in the higher strength alloys. These defects were usually located

at the surface, except for tests at low strain ranges where larger, internal defects often initiated failure. Although fatigue crack initiation was transgranular, in those alloys with grain sizes of less than 15 microns, fatigue crack growth quickly became intergranular. This transition was environmentally assisted and did not occur for subsurface cracks until the crack broke through to the atmosphere. In the creep-fatigue cycle, which included a 900 s tensile dwell, crack initiation and propagation were both intergranular in all alloys. Author

A84-11194*# Louisiana State Univ., Baton Rouge.
BENCHMARK CYCLIC PLASTIC NOTCH STRAIN MEASUREMENTS

W. N. SHARPE, JR. and M. WARD (Louisiana State University, Baton Rouge, LA) ASME, Transactions, Journal of Engineering Materials and Technology (ISSN 0094-4289), vol. 105, Oct. 1983, p. 235-241. Research supported by the General Electric Co., and Louisiana State University. refs
 (Contract NAS3-22522)

Plastic strains at the roots of notched specimens of Inconel 718 subjected to tension-compression cycling at 650 C are reported. These strains were measured with a laser-based technique over a gage length of 0.1 mm and are intended to serve as 'benchmark' data for further development of experimental, analytical, and computational approaches. The specimens were 250 mm by 2.5 mm in the test section with double notches of 4.9 mm radius subjected to axial loading sufficient to cause yielding at the notch root on the tensile portion of the first cycle. The tests were run for 1000 cycles at 10 cpm or until cracks initiated at the notch root. The experimental techniques are described, and then representative data for the various load spectra are presented. All the data for each cycle of every test are available on floppy disks from NASA. Author

A84-12395*# National Aeronautics and Space Administration. Lewis Research Center, Cleveland, Ohio.
THE EFFECT OF MICROSTRUCTURE ON 650 C FATIGUE CRACK GROWTH IN P/M ASTROLOY

J. GAYDA and R. V. MINER (NASA, Lewis Research Center, Cleveland, OH) Metallurgical Transactions A - Physical Metallurgy and Materials Science (ISSN 0360-2133), vol. 14A, Nov. 1983, p. 2301-2308. refs

The effect of microstructure on fatigue crack propagation at 650 C has been studied in a P/M nickel-base superalloy, Astroloy. Crack propagation data were obtained in air and vacuum at 20 cpm with a modified compact tension specimen. The rate of crack growth, da/dN, was correlated with the stress intensity range. Key microstructural variables examined were grain size and the distribution and size of the strengthening gamma prime phase. A fine grain size less than 20 microns always promoted rapid, intergranular failure, while a large grain size promoted slower, transgranular failure which decreased as the size and volume fraction of aging gamma prime was manipulated so as to increase alloy strength. The rapid, intergranular mode of failure of the fine grain microstructures was suppressed in vacuum. Author

A84-14286* National Aeronautics and Space Administration. Lewis Research Center, Cleveland, Ohio.
HIGH-TEMPERATURE FATIGUE IN METALS - A BRIEF REVIEW OF LIFE PREDICTION METHODS DEVELOPED AT THE LEWIS RESEARCH CENTER OF NASA

G. R. HALFORD (NASA, Lewis Research Center, Cleveland, OH) SAMPE Quarterly (ISSN 0036-0821), vol. 14, April 1983, p. 17-25. refs

The presentation focuses primarily on the progress we at NASA Lewis Research Center have made. The understanding of the phenomenological processes of high temperature fatigue of metals for the purpose of calculating lives of turbine engine hot section components is discussed. Improved understanding resulted in the development of accurate and physically correct life prediction methods such as Strain-Range partitioning for calculating creep fatigue interactions and the Double Linear Damage Rule for predicting potentially severe interactions between high and low

cycle fatigue. Examples of other life prediction methods are also discussed. Previously announced in STAR as A83-12159 Author

A84-18733* Rensselaer Polytechnic Inst., Troy, N.Y.
THE EFFECTS OF FREQUENCY AND HOLD TIMES ON FATIGUE CRACK PROPAGATION RATES IN A NICKEL BASE SUPERALLOY

S. GOLWALKAR, N. S. STOLOFF, and D. J. DUQUETTE (Rensselaer Polytechnic Institute, Troy, NY) IN: Strength of metals and alloys (ICSMA 6); Proceedings of the Sixth International Conference, Melbourne, Australia, August 16-20, 1982. Volume 2. Oxford, Pergamon Press, 1983, p. 879-885. (Contract NAG3-22)

The elevated temperature cyclic crack propagation behavior of a nickel base superalloy, Astroloy, produced by a hot isostatic pressing technique has been evaluated. Environment, frequency and peak load hold times have been controlled to evaluate the effects of creep and environment of fatigue crack propagation rates at several temperatures. Author

A84-43872* Northwestern Univ., Evanston, Ill.
FINITE ELASTIC-PLASTIC DEFORMATION OF POLYCRYSTALLINE METALS

T. IWAKUMA and S. NEMAT-NASSER (Northwestern University, Evanston, IL) Royal Society (London), Proceedings, Series A - Mathematical and Physical Sciences (ISSN 0080-4630), vol. 394, no. 1806, July 9, 1984, p. 87-119. refs (Contract NAG3-134)

Applying Hill's self-consistent method to finite elastic-plastic deformations, the overall moduli of polycrystalline solids are estimated. The model predicts a Bauschinger effect, hardening, and formation of vertex or corner on the yield surface for both microscopically non-hardening and hardening crystals. The changes in the instantaneous moduli with deformation are examined, and their asymptotic behavior, especially in relation to possible localization of deformations, is discussed. An interesting conclusion is that small second-order quantities, such as shape changes of grains and residual stresses (measured relative to the crystal elastic moduli), have a first-order effect on the overall response, as they lead to a loss of the overall stability by localized deformation. The predicted incipience of localization for a uniaxial deformation in two dimensions depends on the initial yield strain, but the orientation of localization is slightly less than 45 deg with respect to the tensile direction, although the numerical instability makes it very difficult to estimate this direction accurately. Author

A84-48715* National Aeronautics and Space Administration, Lewis Research Center, Cleveland, Ohio.
EFFECTS OF PROCESSING AND MICROSTRUCTURE ON THE FATIGUE BEHAVIOUR OF THE NICKEL-BASE SUPERALLOY RENE95

R. V. MINER and J. GAYDA (NASA, Lewis Research Center, Processing Science Section, Cleveland, OH) International Journal of Fatigue (ISSN 0142-1123), vol. 6, July 1984, p. 189-193. refs

Forms of the nickel-base superalloy Rene95 produced by three processing methods were evaluated in tensile, low cycle fatigue and fatigue crack propagation tests at 540 and 650 C. Two powder-metallurgy (PM) forms, hot-isostatically-pressed and extruded-and-forged, and a conventionally cast-and-wrought form were all given the same heat treatment. The extruded-and-forged form showed superior fatigue life in low strain range tests though the two PM forms exhibited nearly identical mechanical behavior in all other respects. Further, this life difference could not be explained by significant differences in the types, sizes or shapes of the defects initiating failure. The cast-and-wrought Rene95, however, had lower strength, ductility and fatigue life, but higher fatigue crack propagation resistance because of a larger grain size. It did not exhibit the environmentally-assisted intergranular mode of propagation which occurs in PM Rene95 and other fine-grained superalloys at these test temperatures and frequencies. Author

A85-11603*# National Aeronautics and Space Administration, Lewis Research Center, Cleveland, Ohio.

STRAINRANGE PARTITIONING - A TOTAL STRAIN RANGE VERSION

G. R. HALFORD and J. F. SALTSMAN (NASA, Lewis Research Center, Cleveland, OH) IN: International Conference on Advances in Life Prediction Methods, Albany, NY, April 18-20, 1983, Proceedings. New York, American Society of Mechanical Engineers, 1983, p. 17-26. Previously announced in STAR as N83-14246. refs

Procedures are presented for expressing the Strainrange Partitioning (SRP) method for creep fatigue life prediction in terms of total strain range. Inelastic and elastic strain-range - life relations are summed to give total strain-range - life relations. The life components due to inelastic strains are dealt with using conventional SRP procedures while the life components due to elastic strains are expressed as families of time-dependent terms for each type of SRP cycle. Cyclic constitutive material behavior plays an important role in establishing the elastic strain-range life relations as well as the partitioning of the inelastic strains. To apply the approach, however, it is not necessary to have to determine the magnitude of the inelastic strain range. The total strain SRP approach is evaluated and verified using two nickel base superalloys, AF2-1DA and Rene 95. Excellent agreement is demonstrated between observed and predicted cyclic lifetimes with 70 to 80 percent of the predicted lives falling within factors of two of the observed lives. The total strain-range SRP approach should be of considerable practical value to designers who are faced with creep-fatigue problems for which the inelastic strains cannot be calculated with sufficient accuracy to make reliable life predictions by the conventional inelastic strain range SRP approach. Author

A85-12098* Max-Planck-Inst. fuer Metallforschung, Stuttgart (West Germany).

A STUDY OF FATIGUE DAMAGE MECHANISMS IN WASPALOY FROM 25 TO 800 C

B. A. LERCH (Max-Planck-Institut fuer Metallforschung, Stuttgart, West Germany; Cincinnati, University, Cincinnati, OH), N. JAYARAMAN (Cincinnati, University, Cincinnati, OH), and S. D. ANTOLOVICH (Georgia Institute of Technology, Atlanta, GA) Materials Science and Engineering (ISSN 0025-5416), vol. 66, Sept. 15, 1984, p. 151-166. refs (Contract NSG-3263)

The objective of the study was to examine the effect of various microstructures on the fatigue and damage accumulation behavior of Waspaloy, a nickel-base alloy commonly used in aircraft engines. Shearing was the dominant deformation mode in specimens with coarse grains and small (50-80 A) gamma prime particles, whereas Orowan looping was dominant in fine-grained specimens with large (about 900 A) gamma prime particles. At temperatures up to 500 C, cracks initiated transgranularly, while at 800 C the failure process was intergranular for both coarse-grained and fine-grained specimens. At temperatures above 500 C, a significant decrease in the fatigue life was observed for both coarse-grained and fine-grained material. V.L.

A85-25835* Ball Aerospace Systems Div., Boulder, Colo.
FRACTURE TOUGHNESS OF HOT-PRESSED BERYLLIUM

D. D. LEMON (Ball Corp., Ball Aerospace Systems Div., Boulder, CO) and W. F. BROWN, JR. (NASA, Lewis Research Center, Cleveland, OH) Journal of Testing and Evaluation (ISSN 0090-3973), vol. 13, March 1985, p. 152-161. refs

This paper presents the results of an investigation into the fracture toughness, sustained-load flaw growth, and fatigue-crack propagation resistance of S200E hot-pressed beryllium at room temperature. It also reviews the literature pertaining to the influence of various factors on the fracture toughness of hot-pressed beryllium determined using fatigue-cracked specimens. Author

A85-32399* Rockwell International Corp., Canoga Park, Calif.
THE EFFECT OF MICROSTRUCTURE, TEMPERATURE, AND HOLD-TIME ON LOW-CYCLE FATIGUE OF AS HIP P/M RENE 95

S. BASHIR (Rockwell International Corp., Rocketdyne Div., Canoga Park, CA) and S. D. ANTOLOVICH (Georgia Institute of Technology, Atlanta, GA) IN: Superalloys 1984; Proceedings of the Fifth International Symposium, Champion, PA, October 7-11, 1984. Warrendale, PA, Metallurgical Society of AIME, 1984, p. 295-307. refs

(Contract NSG-3147)

The effects of microstructure, temperature, plastic strain range, and hold time on the low-cycle fatigue (LCF) life were studied for Rene 95, an important Ni base superalloy used in jet engine disks. It was shown that the life could be varied by approximately an order of magnitude at elevated temperatures by simple heat treatments. The life was largest for the microstructure that promoted the most homogeneous deformation mode. The results are explained using the concept of a synergistic interaction between the deformation mode and boundary oxidation. Author

A85-32400* Rensselaer Polytechnic Inst., Troy, N.Y.
THE INFLUENCE OF HOLD TIMES ON LCF AND FCG BEHAVIOR IN A P/M NI-BASE SUPERALLOY

S. J. CHOE, S. V. GOLWALKER, D. J. DUQUETTE, and N. S. STOLOFF (Rensselaer Polytechnic Institute, Troy, NY) IN: Superalloys 1984; Proceedings of the Fifth International Symposium, Champion, PA, October 7-11, 1984. Warrendale, PA, Metallurgical Society of AIME, 1984, p. 309-318. refs (Contract NAG3-22)

The relative importance of creep and environmental interactions in high temperature fatigue behavior has been investigated for as-HIP Rene 95. Strain-controlled low cycle fatigue and load-controlled fatigue crack growth tests were performed at elevated temperatures in argon, followed by fractographic analyses of the fracture surfaces by scanning electron microscopy. Fatigue lives were drastically reduced and crack growth rates increased one hundred fold as a result of superposition of hold times on continuous cycling. A change in fracture mode with hold time also was noted. Chromium oxide was detected on the fracture surface by Auger electron spectroscopy. The drastic changes in fatigue resistance due to hold times were attributed primarily to environmental interactions with fatigue processes. Author

A85-32434* National Aeronautics and Space Administration, Lewis Research Center, Cleveland, Ohio.

ON THE FATIGUE CRACK PROPAGATION BEHAVIOR OF SUPERALLOYS AT INTERMEDIATE TEMPERATURES

J. GAYDA, R. V. MINER, and T. P. GABB (NASA, Lewis Research Center, Cleveland, OH) IN: Superalloys 1984; Proceedings of the Fifth International Symposium, Champion, PA, October 7-11, 1984. Warrendale, PA, Metallurgical Society of AIME, 1984, p. 731-740. refs

Two superalloys used in gas-turbine disks, Rene 95 and IN-100 were tested in several forms at 0.33 Hz in air, and the results were compared with earlier data on Astroloy to gain a better understanding of the effects of grain size, strength, and alloy composition on the fatigue crack propagation behavior. In addition, selected forms of Rene 95 were tested at 0.33 Hz in vacuum and in air using a cycle with a 120-sec tensile dwell to evaluate the effects of environment and creep. Results of the study emphasize the beneficial effect of large grain size on the fatigue and creep-fatigue crack growth resistance of the superalloys in the temperature range corresponding to the operating temperatures of aircraft gas-turbine engine disk rims. V.L.

A85-43979*# Pratt and Whitney Aircraft Group, East Hartford, Conn.

APPLICATION OF TWO CREEP FATIGUE LIFE MODELS FOR THE PREDICTION OF ELEVATED TEMPERATURE CRACK INITIATION OF A NICKEL BASE ALLOY

V. MORENO, D. M. NISSLEY (United Technologies Corp., Pratt and Whitney Group, East Hartford, CT), G. R. HALFORD, and J. F. SALTSMAN (NASA, Lewis Research Center, Cleveland, OH) AIAA, SAE, ASME, and ASCE, Joint Propulsion Conference, 21st, Monterey, CA, July 8-10, 1985. 15 p. refs

(Contract NAS3-23288)

(AIAA PAPER 85-1420)

Cyclic Damage Accumulation (CDA) and Total Strain-Strain Range Partitioning (TS-SRP) models for predicting the creep-fatigue crack initiation life of high temperature alloys are presented. The models differ in their fundamental assumptions regarding the controlling parameters for fatigue crack initiation and in the amount of data required to determine model constants. The CDA model represents a ductility exhaustion approach and uses stress quantities to calculate the cyclic fatigue damage. The TS-SRP model is based on the use of total mechanical strain and earlier concepts of the Strain Range Partitioning Method. Both models were applied to a well controlled fatigue data set at a high temperature nickel base alloy, B1900 + Hf, tested at 1600 F and 1800 F. The tests were divided into a baseline data set required to determine model constants and a verification data set for evaluation of the predictive capability of the models. Both models correlated the baseline data set to within factors of two in life, and predicted the verification data set to within a factor of three or better. In addition, sample calculations to demonstrate the application of each model and discussions of the predictive capabilities and areas requiring further development are presented. Author

A85-47972* Lockheed-California Co., Burbank.

EFFECT OF LOW TEMPERATURE ON FATIGUE AND FRACTURE PROPERTIES OF Ti-5Al-2.5Sn(ELI) FOR USE IN ENGINE COMPONENTS

J. T. RYDER (Lockheed-California Co., Burbank) and W. E. WITZELL (General Dynamics Corp., Convair Div., San Diego, CA) IN: Fatigue at low temperatures; Proceedings of the Symposium, Louisville, KY, May 10, 1983. Philadelphia, PA, ASTM, 1985, p. 210-237. refs

(Contract NAS3-18896)

Experiments were conducted to evaluate the characteristics of the Ti-5Al-2.5Sn (ELI) alloy used in a fuel pump impeller at cryogenic temperatures. Tension, fracture toughness, and fatigue crack propagation data were collected determining the effect of frequency and load ratio on crack propagation. The results revealed that tensile strength increased significantly at 20 K compared to room temperature and fracture toughness was reduced at cryogenic temperatures. The fatigue crack growth rate was not sensitive to experimental conditions and there were only minimal crack orientation effects. Different frequencies produced no effect. At various temperatures and frequencies a load ratio increase resulted in higher crack growth rates. At low stress intensity levels the fatigue rate for both temperatures was the same; however, at high stress intensity levels the crack growth rate at 20 K increased because of the decrease in fracture toughness. The results correlated well with previous data. I.F.

A86-20982* Massachusetts Inst. of Tech., Cambridge.

THERMAL-MECHANICAL FATIGUE CRACK GROWTH IN INCONEL X-750

N. MARCHAND and R. M. PELLOUX (MIT, Cambridge, MA) IN: Time-dependent fracture; Proceedings of the Eleventh Canadian Fracture Conference, Ottawa, Canada, June 14, 15, 1984. Dordrecht, Martinus Nijhoff Publishers, 1985, p. 167-178. Previously announced in STAR as N85-15877. refs

(Contract NAG3-280)

Thermal-mechanical fatigue crack growth (TMFCG) was studied in a 'gamma-gamma' nickel base superalloy Inconel X-750 under controlled load amplitude in the temperature range from 300 to

650 C. In-phase (T_{sub} max at σ_{sub} max), out-of-phase (T_{sub} min at σ_{sub} max), and isothermal tests at 650 C were performed on single-edge notch bars under fully reversed cyclic conditions. A dc electrical potential method was used to measure crack length. The electrical potential response obtained for each cycle of a given wave form and R value yields information on crack closure and crack extension per cycle. The macroscopic crack growth rates are reported as a function of ΔK and the relative magnitude of the TMFCG are discussed in the light of the potential drop information and of the fractographic observations.

R.S.F.

A86-28951* Connecticut Univ., Storrs.

FRACTURE MECHANICS APPLIED TO NONISOTHERMAL FATIGUE CRACK GROWTH

E. H. JORDAN (Connecticut, University, Storrs) and G. J. MEYERS (McGraw-Edison Co., Worthington Compressors Div., Buffalo, NY) Engineering Fracture Mechanics (ISSN 0013-7944), vol. 23, no. 2, 1986, p. 345-358. refs
(Contract NAS3-22550)

Twelve nonisothermal fatigue crack growth tests were performed on Hastelloy-X tubular specimens in which strain and temperature varied simultaneously. Conditions were selected to include nominally elastic and nominally plastic conditions and temperatures up to 982 C. A number of parameters, including the stress intensity factor, strain intensity factor, and J-integral, were examined for their ability to correlate the data. There was no decisive difference between the success of the three parameters. Each parameter correlated data from different strain ranges to within no worse than a factor of 2.1 on da/dN . The effect of strain temperature cycle shape was investigated and found to be moderate, while a strain hold of 1 min had very little effect. An attempt was made to predict nonisothermal test results from isothermal data. These predictions were better than those made by using peak test temperature isothermal data but still not within scatter.

Author

A86-30010* Case Western Reserve Univ., Cleveland, Ohio.

THE CRACK LAYER APPROACH TO TOUGHNESS CHARACTERIZATION IN STEEL

M. BESSENDORFF and A. CHUDNOVSKY (Case Western Reserve University, Cleveland, OH) IN: Advances in fracture research (Fracture 84). Volume 3. Oxford and New York, Pergamon Press, 1986, p. 1663-1670. refs
(Contract NAG3-223)

In a study of the laws of crack propagation and toughness characterization, it is feasible to employ two alternative approaches, including the fracture mechanics approach and the material science approach. The crack layer (CL) theory discussed by Khandogin and Chudnovsky (1978) and Chudnovsky (1980) considers the crack together with the surrounding defects as one system which has several degrees of freedom. It is pointed out that the CL theory defines the relationship between the parameters of fracture mechanics and the characteristics of microstructural changes which are the subject of material science. Experiments are described, taking into account a toughness characterization test and microscopic studies. Attention is given to a phenomenological study of toughness characterization, the morphology of crack layer, and the evaluation of energy stored in the dislocation network. G.R.

A86-35697* National Aeronautics and Space Administration. Lewis Research Center, Cleveland, Ohio.

THE TENSILE AND FATIGUE DEFORMATION STRUCTURES IN A SINGLE CRYSTAL NI-BASE SUPERALLOY

T. P. GABB, R. V. MINER, and J. GAYDA (NASA, Lewis Research Center, Cleveland, OH) Scripta Metallurgica (ISSN 0036-9748), vol. 20, April 1986, p. 513-518. refs

Dislocation structures produced in Rene N4 crystals of various orientations deformed in tension and low cycle fatigue (LCF) at 760 and 980 degrees C were examined in order to elucidate the observed differences in stress-strain behavior. Specimens tensile tested at 760 degrees C displayed significant crystallographic orientation dependences in mechanical response but comparable

inhomogeneous dislocation structures. LCF specimens of various orientations had comparable cyclic stress-strain curves and generally similar somewhat more homogeneous dislocation structures. Tensile specimens at the higher temperature had comparable mechanical response and corresponding similar quite homogeneous dislocation structures with gamma' faulting; and LCF specimens had orientation-dependent mechanical response but comparable homogeneous loose dislocation networks. D.H.

A86-45715* National Aeronautics and Space Administration. Lewis Research Center, Cleveland, Ohio.

THE CYCLIC STRESS-STRAIN BEHAVIOR OF A NICKEL-BASE SUPERALLOY AT 650 C

T. P. GABB (NASA, Lewis Research Center, Cleveland, OH) and G. E. WELSCH (Case Western Reserve University, Cleveland, OH) Scripta Metallurgica (ISSN 0036-9748), vol. 20, July 1986, p. 1049-1054. refs

It is pointed out that examinations of the monotonic tensile and fatigue behaviors of single crystal nickel-base superalloys have disclosed orientation-dependent tension-compression anisotropies and significant differences in the mechanical response of octahedral and cube slip at intermediate temperatures. An examination is conducted of the cyclic hardening response of the single crystal superalloy PWA 1480 at 650 C. In the considered case, tension-compression anisotropy is present, taking into account primarily conditions under which a single slip system is operative. Aspects of a deformation by single slip are considered along with cyclic hardening anisotropy in tension and compression. It is found that specimens deforming by octahedral slip on a single slip system have similar hardening responses in tensile and low cycle fatigue loading. Cyclic strain hardening is very low for specimens displaying single slip. G.R.

A86-48973* National Aeronautics and Space Administration. Lewis Research Center, Cleveland, Ohio.

A STUDY OF SPECTRUM FATIGUE CRACK PROPAGATION IN TWO ALUMINUM ALLOYS. I - SPECTRUM SIMPLIFICATION. II - INFLUENCE OF MICROSTRUCTURES

J. TELESMA (NASA, Lewis Research Center, Cleveland, OH) and S. D. ANTOLOVICH (Georgia Institute of Technology, Atlanta) Engineering Fracture Mechanics (ISSN 0013-7944), vol. 24, no. 3, 1986, p. 453-459, 461-473, 475-477. Research supported by Northrop Corp. refs

An investigation of the fatigue crack propagation FCP behavior of two aluminum alloys is performed to simulate spectrum loading conditions found at critical locations in high performance fighter aircraft. Negative loads are shown to be eliminated for the tension-compression spectrum for low to intermediate maximum stress intensities, and load interactions are found to be more significant at higher stress intensities and with more plasticity at the crack tip. In the second part, the influence of microstructural features including grain size, inclusions, and dispersoids on constant amplitude and spectrum crack growth behavior in aluminum alloys is studied. At low stress intensities the I/M alloy demonstrated better FCP resistance than the P/M 7091 alloy for both constant amplitude and spectrum testing, and the inhomogeneous planar slip and large grain size of 7050 limit dislocation interactions, thereby improving FCP performance. R.R.

A86-49690* National Aeronautics and Space Administration. Lewis Research Center, Cleveland, Ohio.

THE PLASTIC COMPRESSIBILITY OF 7075-T651 ALUMINUM-ALLOY PLATE

A. D. FREED (NASA, Lewis Research Center, Cleveland, OH) and B. I. SANDOR (Wisconsin, University, Madison) Experimental Mechanics (ISSN 0014-4851), vol. 26, June 1986, p. 119-121. Research supported by the Lockheed-Georgia Co. refs

The change in volume, and therefore the change in mass density, of an aluminum alloy was measured in uniaxial tension using clip-on extensometers. The experimental data do not agree with the assumption of plastic incompressibility found in the classical theories of plasticity. In fact, the elastic and plastic volume

changes are of the same order of magnitude. Plastic anisotropy is thought to be the prime cause of this plastic compressibility.

Author

A86-50322*# National Aeronautics and Space Administration. Lewis Research Center, Cleveland, Ohio.

ORIENTATION AND TEMPERATURE DEPENDENCE OF SOME MECHANICAL PROPERTIES OF THE SINGLE-CRYSTAL NICKEL-BASE SUPERALLOY RENE N4. II - LOW CYCLE FATIGUE BEHAVIOR

T. P. GABB, J. GAYDA, and R. V. MINER (NASA, Lewis Research Center, Cleveland, OH) Metallurgical Transactions A - Physical Metallurgy and Materials Science (ISSN 0360-2133), vol. 17A, March 1986, p. 497-505. refs

The low cycle fatigue (LCF) properties of a single-crystal nickel-base superalloy Rene N4, have been examined at 760 and 980 C in air. Specimens having crystallographic orientations near the 001, 011, -111, 023, -236, and -145 lines were tested in fully reversed, total-strain-controlled LCF tests at a frequency of 0.1 Hz. At 760 C, this alloy exhibited orientation dependent tension-compression anisotropies of yielding which continued to failure. Also at 760 C, orientations exhibiting predominately single slip exhibited serrated yielding for many cycles. At 980 C, orientation dependencies of yielding behavior were smaller. In spite of the tension-compression anisotropies, cyclic stress range-strain range behavior was not strongly orientation dependent for either test temperature. Fatigue life on a total strain range basis was highly orientation dependent at 760 and 980 C and was related chiefly to elastic modulus, low modulus orientations having longer lives. Stage I crack growth on 111 planes was dominant at 760 C, while Stage II crack growth occurred at 980 C. Crack initiation generally occurred at near-surface micropores, but occasionally at oxidation spikes in the 980 C tests.

Author

A87-54370* National Aeronautics and Space Administration. Lewis Research Center, Cleveland, Ohio.

RESULTS OF AN INTERLABORATORY FATIGUE TEST PROGRAM CONDUCTED ON ALLOY 800H AT ROOM AND ELEVATED TEMPERATURES

J. R. ELLIS (NASA, Lewis Research Center, Cleveland; Akron, University, OH) Journal of Testing and Evaluation (ISSN 0090-3973), vol. 15, Sept. 1987, p. 249-256. Research sponsored by the General Atomic Co. Previously announced in STAR as N85-32340.

(Contract NAG3-379)

The experimental approach adopted for low cycle fatigue tests of alloy 800H involved the use of electrohydraulic test systems, hour glass geometry specimens, diametral extensometers, and axial strain computers. Attempts to identify possible problem areas were complicated by the lack of reliable data for the heat of Alloy 800H under investigation. The method adopted was to generate definitive test data in an Interlaboratory Fatigue Test Program. The laboratories participating in the program were Argonne National Laboratory, Battelle Columbus, Mar-Test, and NASA Lewis. Fatigue tests were conducted on both solid and tubular specimens at temperatures of 20, 593, and 760 C and strain ranges of 2.0, 1.0, and 0.5 percent. The subject test method can, under certain circumstances, produce fatigue data which are serious in error. This approach subsequently was abandoned at General Atomic Company in favor of parallel gage length specimens and axial extensometers.

F.M.R.

N80-21493*# National Aeronautics and Space Administration. Lewis Research Center, Cleveland, Ohio.

EFFECTS OF FINE POROSITY ON THE FATIGUE BEHAVIOR OF A POWDER METALLURGY SUPERALLOY

R. V. MINER, JR. and R. L. DRESHFIELD 1980 25 p refs Presented at Ann. Meeting of the Am. Inst. of Mining, Met. and Petroleum Engr., Las Vegas, Nev., 24-28 Feb. 1980

(NASA-TM-81448; E-367) Avail: NTIS HC A02/MF A01 CSCL 11F

Hot isostatically pressed powder metallurgy Astroloy was obtained which contained 1.4 percent fine porosity at the grain

boundaries produced by argon entering the powder container during pressing. This material was tested at 650 C in fatigue, creep fatigue, tension, and stress-rupture and the results compared with previous data on sound Astroloy. The pores averaged about 2 micrometers diameter and 20 micrometers spacing. They did influence fatigue crack initiation and produced a more intergranular mode of propagation. However, fatigue life was not drastically reduced. A large 25 micrometers pore in one specimen resulting from a hollow particle did not reduce life by 60 percent. Fatigue behavior of the porous material showed typical correlation with tensile behavior. The plastic strain range life relation was reduced proportionately with the reduction in tensile ductility, but the elastic strain range-life relation was little changed reflecting the small reduction in sigma sub u/E for the porous material.

R.C.T.

N80-25415*# IIT Research Inst., Chicago, Ill. Materials Technology Div.

THERMAL FATIGUE AND OXIDATION DATA OF OXIDE DISPERSION-STRENGTHENED ALLOYS

K. E. HOFER, V. L. HILL, and V. E. HUMPHREYS Mar. 1980 42 p refs

(Contract NAS3-17787)

(NASA-CR-159842; IITRI-M6001-82) Avail: NTIS HC A03/MF A01 CSCL 11F

Thermal fatigue and oxidation data were obtained 24 specimens representing 9 discrete oxide dispersion-strengthened alloy compositions or fabricating techniques. Double edge wedge specimens, both bare metal and coated for each system, were cycled between fluidized beds maintained at 1130 C with a three minute immersion in each bed. The systems included alloys identified as 262 in hardness of HRC 38; 264 in hardness of HRC 38, 40 and 43; 265 HRC 39, 266 of HRC 37 and 40; 754; and 956. Specimens in the bare condition of 265 HRC 39 and 266 HRC 37 survived 6000 cycles without cracking on the small radius of the double edge wedge specimen. A coated specimen of 262 HRC 38, 266 HRC 37 and 266 HRC40 also survived 6000 cycles without cracking. A duplicate coated specimen of 262 HRC 38 alloy survived 5250 cycles before cracks appeared. All the alloys showed little weight change compared compared to alloys tested in prior programs.

Author

N80-26433*# National Aeronautics and Space Administration. Lewis Research Center, Cleveland, Ohio.

THREE DIMENSIONAL FINITE-ELEMENT ELASTIC ANALYSIS OF A THERMALLY CYCLED DOUBLE-EDGE WEDGE GEOMETRY SPECIMEN Final Report, 1 Jun. 1977 - 1 Jan. 1979

S. K. DRAKE, R. J. HILL, P. T. BIZON, J. L. KLADDEN, and B. P. GUILLIAMS Mar. 1980 49 p refs Prepared in cooperation with AF Wright Aeronautical Labs., Wright-Patterson AFB, Ohio

(Contract AF PROJ. 3066)

(NASA-TM-80980; AD-A083245; AFWAL-TR-80-2013) Avail: NTIS HC A03/MF A01 CSCL 11F

An elastic stress analysis was performed on a wedge specimen (prismatic bar with double-edge wedge cross-section) subjected to thermal cycles in fluidized beds. Five alloys (IN 100, Mar-M 200, Mar-M 302, NASA TAZ-8A, and Rene 80) subjected to the same thermal cycling condition were analyzed. This condition was alternate 3 minute immersions in fluidized beds maintained at 316 C and 1088 C (600 and 1990 F). The analyses were performed as a joint effort of two laboratories using different models and computer programs (NASTRAN and IS03DQ). Stress, strain, and temperature results are presented.

GRA

N80-30482*# Pratt and Whitney Aircraft Group, West Palm Beach, Fla.

EVALUATION OF THE CYCLIC BEHAVIOR OF AIRCRAFT TURBINE DISK ALLOYS, PART 2 Contractor Report, Jul. 1978 - Mar. 1980

B. A. COWLES and J. R. WARREN Jul. 1980 196 p refs (Contract NAS3-21379)
(NASA-CR-165123; PWA-FR-13153-PT-2) Avail: NTIS HC A09/MF A01 CSCL 11F

Several nickel-base aircraft turbine disk superalloys were evaluated at 650 C for resistance to fatigue crack initiation and propagation under cyclic and cyclic/dwell conditions. Controlled strain low cycle fatigue (LCF) and controlled load crack propagation tests were performed and results utilized to provide a direct comparison among the alloys. Tests were performed on selected alloys to evaluate the effects of hold times, mean stresses, stress-dwell cycle types, inert environment, and contractor test methods. At the lower total strain ranges of interest, the alloys exhibited generally increasing initiation life with increasing tensile strength for both cyclic (0.33 Hz) and cyclic/dwell (900-sec hold per cycle) conditions. Rank order of the alloys by LCF initiation life changed substantially at higher strain ranges, approaching the rank order expected from monotonic tensile ductilities. The effect of the 900 sec (15 min) hold time fatigue life varied significantly from alloy to alloy. Generally, the higher-strength, finer-grained alloys exhibited more significant reductions in fatigue life due to the dwell. The effects of mean strain were found to be negligible and the effects of mean stress were pronounced. At high strain ranges the mean stress was near zero and did not contribute to reduction in life. At low strain ranges, however, mean stresses were large and significant reductions in LCF lives occurred.

L.F.M.

N80-32486*# National Aeronautics and Space Administration. Lewis Research Center, Cleveland, Ohio.

FRACTURE TOUGHNESS OF BRITTLE MATERIALS DETERMINED WITH CHEVRON NOTCH SPECIMENS

J. L. SHANNON, JR., R. T. BURSEY, D. MUNZ (Karlsruhe Univ.), and W. S. PIERCE 1980 17 p refs Proposed for presentation at the 5th Intern. Conf. on Fracture, Cannes, France, 29 Mar. - 3 Apr. 1981; sponsored by the International Congress on Fracture (NASA-TM-81607; E-600) Avail: NTIS HC A02/MF A01 CSCL 11F

The use of chevron-notch specimens for determining the plane strain fracture toughness ($K_{sub Ic}$) of brittle materials is discussed. Three chevron-notch specimens were investigated: short bar, short rod, and four-point-bend. The dimensionless stress intensity coefficient used in computing $K_{sub Ic}$ is derived for the short bar specimen from the superposition of ligament-dependent and ligament-independent solutions for the straight through crack, and also from experimental compliance calibrations. Coefficients for the four-point-bend specimen were developed by the same superposition procedure, and with additional refinement using the slice model of Bluhm. Short rod specimen stress intensity coefficients were determined only by experimental compliance calibration. Performance of the three chevron-notch specimens and their stress intensity factor relations were evaluated by tests on hot-pressed silicon nitride and sintered aluminum oxide. Results obtained with the short bar and the four-point-bend specimens on silicon nitride are in good agreement and relatively free of specimen geometry and size effects within the range investigated. Results on aluminum oxide were affected by specimen size and chevron-notch geometry, believed due to a rising crack growth resistance curve for the material. Only the results for the short bar specimen are presented in detail.

M.G.

N81-21174*# National Aeronautics and Space Administration. Lewis Research Center, Cleveland, Ohio.

ION BEAM SPUTTER ETCHING OF ORTHOPEDIC IMPLANTED ALLOY MP35N AND RESULTING EFFECTS ON FATIGUE

E. G. WINTUCKY, M. CHRISTOPHER, E. BAHNUIK, and S. WANG Mar. 1981 35 p refs Presented at 15th Intern. Electric Propulsion Conf., Las Vegas, 21-23 Apr. 1981; sponsored by AIAA, Japan Soc. for Aeron. and Space Sci. and DGLR (NASA-TM-81747; E-782) Avail: NTIS HC A03/MF A01 CSCL 11F

The effects of two types of argon ion sputter etched surface structures on the tensile stress fatigue properties of orthopedic implant alloy MP35N were investigated. One surface structure was a natural texture resulting from direct bombardment by 1 keV argon ions. The other structure was a pattern of square holes milled into the surface by a 1 keV argon ion beam through a Ni screen mask. The etched surfaces were subjected to tensile stress only in fatigue tests designed to simulate the cyclic load conditions experienced by the stems of artificial hip joint implants. Both types of sputter etched surface structures were found to reduce the fatigue strength below that of smooth surface MP35N. Author

N82-10193*# IIT Research Inst., Chicago, Ill. Materials Technology Div.

THERMAL FATIGUE AND OXIDATION DATA OF TAZ-8A AND M22 ALLOYS AND VARIATIONS Technical Report, 1 Feb. - 30 Apr. 1980

K. E. HOFER and V. E. HUMPHREYS Sep. 1981 44 p refs (Contract NAS3-17787)
(NASA-CR-165407; IITRI-M06001-89) Avail: NTIS HC A03/MF A01 CSCL 11F

Thermal fatigue and oxidation data were obtained on 36 specimens, representing 18 distinct variations (including the base systems) of TAZ-8A and M22 alloys. Double-edge wedge specimens for these systems were cycled between fluidized beds maintained at 1088 C and 316 C with a 180 s immersion in each bed. The systems included alloys TAZ-8A, M22, and 16 variations of these alloys. Each alloy variation consisted of a unique composition with an alternation in the percentage of carbon (C1 and C2), molybdenum (M1 and M2), tungsten (W1 and W2), columbium (CB1, CB2, and CB3), tantalum (T1, T2, and T3), or boron (B1, B2, and B3) present. All of the alloys showed little weight change due to oxidation compared with other alloys previously tested in fluidized beds. Only both C1 alloy variation specimens survived 3500 cycles without cracking in the small radius, although substantial cracks were present, emanating from the end notches which were used for holding the specimens.

Author

N82-13281*# National Aeronautics and Space Administration. Lewis Research Center, Cleveland, Ohio.

ELEVATED TEMPERATURE FATIGUE TESTING OF METALS

M. H. HIRSCHBERG In AGARD Fatigue Test Methodology 18 p Oct. 1981 refs
Avail: NTIS HC A12/MF A01

Material characterization and evaluation conducted for the purpose of calculating fatigue crack initiation lives of components operating at elevated temperatures are discussed. The major technology areas needed to perform a life prediction of an aircraft turbine engine hot section component and the steps required for life prediction are outlined. These include: the determination of the operating environment, the calculation of the thermal and mechanical loading of the component, the cyclic stress strain and creep behavior of the material required for structural analysis, the structural analysis to determine the local stress strain temperature time response of the material at the critical location in the component, and from a knowledge of the fatigue, creep, and failure resistance of the material, a prediction of the life of the component.

E.A.K.

N82-26436*# Cincinnati Univ., Ohio. Dept. of Materials Science and Metallurgical Engineering.

HIGH TEMPERATURE LOW CYCLE FATIGUE MECHANISMS FOR NICKEL BASE AND A COPPER BASE ALLOY M.S. Thesis Final Report

C. I. SHIH Washington NASA Jun. 1982 110 p refs (Contract NSG-3263)

(NASA-CR-3543; NAS 1.26:3543) Avail: NTIS HC A06/MF A01 CSCL 11F

Damage mechanisms were studied in Rene' 95 and NARloy Z, using optical, scanning and transmission in microscopy. In necklace Rene' 95, crack initiation was mainly associated with cracking of surface MC carbides, except for hold time tests at higher strain ranges where initiation was associated more with a grain boundary mechanism. A mixed mode of propagation with a faceted fracture morphology was typical for all cycle characters. The dependence of life on maximum tensile stress can be demonstrated by the data falling onto three lines corresponding to the three tensile hold times, in the life against maximum tensile stress plot. In NARloy Z, crack initiation was always at the grain boundaries. The mode of crack propagation depended on the cycle character. The life decreased with decreasing strain rate and with tensile holds. In terms of damage mode, different life prediction laws may be applicable to different cycle characters. A.R.H.

N83-11289*# National Aeronautics and Space Administration. Lewis Research Center, Cleveland, Ohio.

THERMAL FATIGUE RESISTANCE OF COBALT-MODIFIED UDIMET 700

P. T. BIZON *In its* COSAM (Conserv. Of Strategic Aerospace Mater.) Program Overview p 77-81 Oct. 1982

Avail: NTIS HC A11/MF A01 CSCL 11F

The determination of comparative thermal fatigue resistances of five cobalt composition modifications of UDIMET 700 from fluidized bed tests is described. Cobalt compositional levels of 0.1, 4.3, 8.6, 12.8, 17.0 percent were being investigated in both the bare and coated (NiCrAlY overlay) conditions. Triplicate tests of each variation including duplicate tests of three control alloys are under investigation. Fluidized beds were maintained at 550 and 1850 F for the first 5500 cycles at which time the hot bed was increased to 1922 F. Immersion time in each bed is always 3 minutes. Upon the completion of 10,000 cycles, it appears that the 8.6 percent cobalt level gives the best thermal fatigue life. Considerable deformation of the test bars was observed. Author

N83-11290*# National Aeronautics and Space Administration. Lewis Research Center, Cleveland, Ohio.

CREEP-FATIGUE OF LOW COBALT SUPERALLOYS

G. R. HALFORD *In its* COSAM (Conserv. Of Strategic Aerospace Mater.) Program Overview p 83-88 Oct. 1982

Avail: NTIS HC A11/MF A01 CSCL 11F

Testing for the low cycle fatigue and creep fatigue resistance of superalloys containing reduced amounts of cobalt is described. The test matrix employed involves a single high temperature appropriate for each alloy. A single total strain range, again appropriate to each alloy, is used in conducting strain controlled, low cycle, creep fatigue tests. The total strain range is based upon the level of straining that results in about 10,000 cycles to failure in a high frequency (0.5 Hz) continuous strain-cycling fatigue test. No creep is expected to occur in such a test. To bracket the influence of creep on the cyclic strain resistance, strain hold time tests with one minute hold periods are introduced. One test per composition is conducted with the hold period in tension only, one in compression only, and one in both tension and compression. The test temperatures, alloys, and their cobalt compositions that are under study are given. J.D.

N83-14246*# National Aeronautics and Space Administration. Lewis Research Center, Cleveland, Ohio.

STRAINRANGE PARTITIONING: A TOTAL STRAIN RANGE VERSION

G. R. HALFORD and J. F. SALTSMAN 1983 12 p refs Proposed for presentation at the Intern. Conf. on Advan. in Life Prediction, Albany, N.Y., 18-21 Apr. 1983; sponsored by ASME (NASA-TM-83023; E-1459; NAS 1.15:83023) Avail: NTIS HC A02/MF A01 CSCL 11F

Procedures are presented for expressing the Strainrange Partitioning (SRP) method for creep fatigue life prediction in terms of total strain range. Inelastic and elastic strain-range - life relations are summed to give total strain-range - life relations. The life components due to inelastic strains are dealt with using conventional SRP procedures while the life components due to elastic strains are expressed as families of time-dependent terms for each type of SRP cycle. Cyclic constitutive material behavior plays an important role in establishing the elastic strain-range - life relations as well as the partitioning of the inelastic strains. To apply the approach, however, it is not necessary to have to determine the magnitude of the inelastic strain range. The total strain SRP approach is evaluated and verified using two nickel base superalloys, AF2-1DA and Rene 95. Excellent agreement is demonstrated between observed and predicted cyclic lifetimes with 70 to 80 percent of the predicted lives falling within factors of two of the observed lives. The total strain-range SRP approach should be of considerable practical value to designers who are faced with creep-fatigue problems for which the inelastic strains cannot be calculated with sufficient accuracy to make reliable life predictions by the conventional inelastic strain range SRP approach. Author

N83-35103*# National Aeronautics and Space Administration. Lewis Research Center, Cleveland, Ohio.

THE THERMAL FATIGUE RESISTANCE OF H-13 DIE STEEL FOR ALUMINUM DIE CASTING DIES

7 Aug. 1982 22 p refs Presented at Let's Do It Ourselves: In Sci. and Technol., Baltimore, 2-7 Aug. 1982, sponsored by National Technical Association

(NASA-TM-83331; E-1578; NAS 1.15:83331) Avail: NTIS HC A02/MF A01 CSCL 11F

The effects of welding, five selected surface coatings, and stress relieving on the thermal fatigue resistance of H-13 Die Steel for aluminum die casting dies were studied using eleven thermal fatigue specimens. Stress relieving was conducted after each 5,000 cycle interval at 1050 F for three hours. Four thermal fatigue specimens were welded with H-13 or maraging steel welding rods at ambient and elevated temperatures and subsequently, subjected to different post-weld heat treatments. Crack patterns were examined at 5,000, 10,000, and 15,000 cycles. The thermal fatigue resistance is expressed by two crack parameters which are the average maximum crack and the average cracked area. The results indicate that a significant improvement in thermal fatigue resistance over the control was obtained from the stress-relieving treatment. Small improvements were obtained from the H-13 welded specimens and from a salt bath nitrogen and carbon-surface treatment. The other surface treatments and welded specimens either did not affect or had a detrimental influence on the thermal fatigue properties of the H-13 die steel. A.R.H.

N84-10267*# Rensselaer Polytechnic Inst., Troy, N.Y. Dept. of Materials Engineering.

FATIGUE CRACK GROWTH AND LOW CYCLE FATIGUE OF TWO NICKEL BASE SUPERALLOYS Final Report

N. S. STOLOFF, D. J. DUQUETTE, S. J. CHOE, and S. GOLWALKAR 16 Sep. 1983 51 p refs (Contract NAG3-22)

(NASA-CR-174534; NAS 1.26:174534) Avail: NTIS HC A04/MF A01 CSCL 11F

The fatigue crack growth and low cycle fatigue behavior of two P/M superalloys, Rene 95 and Astrology, in the hot isostatically pressed (HIP) condition, was determined. Test variables included frequency, temperature, environment, and hold times at peak tensile

26 METALLIC MATERIALS

loads (or strains). Crack initiation sites were identified in both alloys. Crack growth rates were shown to increase in argon with decreasing frequency or with the imposition of hold times. This behavior was attributed to the effect of oxygen in the argon. Auger analyses were performed on oxide films formed in argon. Low cycle fatigue lives also were degraded by tensile hold, contrary to previous reports in the literature. The role of environment in low cycle fatigue behavior is discussed. M.G.

N84-10268*# Pratt and Whitney Aircraft Group, West Palm Beach, Fla. Government Products Div.

LOW STRAIN, LONG LIFE CREEP FATIGUE OF AF2-1DA AND INCO 718

A. B. THAKKER and B. A. COWLES Apr. 1983 152 p refs
(Contract NAS3-22387)
(NASA-CR-167989; NAS 1.26:167989; FR-15652) Avail: NTIS
HC A08/MF A01 CSCL 11F

Two aircraft turbine disk alloys, GATORIZED AF2-DA and INCO 718 were evaluated for their low strain long life creep-fatigue behavior. Static (tensile and creep rupture) and cyclic properties of both alloys were characterized. The controlled strain LCF tests were conducted at 760 C (1400 F) and 649 C (1200 F) for AF2-1DA and INCO 718, respectively. Hold times were varied for tensile, compressive and tensile/compressive strain dwell (relaxation) tests. Stress (creep) hold behavior of AF2-1DA was also evaluated. Generally, INCO 718 exhibited more pronounced reduction in cyclic life due to hold than AF2-1DA. The percent reduction in life for both alloys for strain dwell tests was greater at low strain ranges (longer life regime). Changing hold time from 0 to 0.5, 2.0 and 15.0 min. resulted in corresponding reductions in life. The continuous cycle and cyclic/dwell initiation failure mechanism was predominantly transgranular for AF2-1DA and intergranular for INCO 718. Author

N84-13265*# Battelle Columbus Labs., Ohio.
CREEP FATIGUE OF LOW-COBALT SUPERALLOYS: WASPALLOY, PM U 700 AND WROUGHT U 700 Final Report
B. N. LEIS, R. RUNGTA, and A. T. HOPPER 1 Sep. 1983
61 p refs
(Contract NAS3-23289)
(NASA-CR-168260; NAS 1.26:168260) Avail: NTIS HC A04/MF
A01 CSCL 11F

The influence of cobalt content on the high temperature creep fatigue crack initiation resistance of three primary alloys was evaluated. These were Waspalloy, Powder U 700, and Cast U 700, with cobalt contents ranging from 0 up to 17 percent. Waspalloy was studied at 538 C whereas the U 700 was studied at 760 C. Constraints of the program required investigation at a single strain range using diametral strain control. The approach was phenomenological, using standard low cycle fatigue tests involving continuous cycling tension hold cycling, compression hold cycling, and symmetric hold cycling. Cycling in the absence of or between holds was done at 0.5 Hz, whereas holds when introduced lasted 1 minute. The plan was to allocate two specimens to the continuous cycling, and one specimen to each of the hold time conditions. Data was taken to document the nature of the cracking process, the deformation response, and the resistance to cyclic loading to the formation of small cracks and to specimen separation. The influence of cobalt content on creep fatigue resistance was not judged to be very significant based on the results generated. Specific conclusions were that the hold time history dependence of the resistance is as significant as the influence of cobalt content and increased cobalt content does not produce increased creep fatigue resistance on a one to one basis. S.L.

N84-17350*# National Aeronautics and Space Administration. Lewis Research Center, Cleveland, Ohio.

PRELIMINARY STUDY OF THERMOMECHANICAL FATIGUE OF POLYCRYSTALLINE MAR-M 200

R. C. BILL (USAAVSCOM Research and Technology Labs.), M. J. VERRILLI (Northwestern Univ.), M. A. MCGAW, and G. R. HALFORD Feb. 1984 17 p refs
(NASA-TP-2280; E-1795; NAS 1.60:2280; AVSCOM-TR-83-C-6)
Avail: NTIS HC A02/MF A01 CSCL 11F

Thermomechanical fatigue (TMF) experiments were conducted on polycrystalline MAR-M 200 over a cyclic temperature range of 500 to 1000 C. Inelastic strain ranges of 0.03 to 0.2 percent were imposed on the specimens. The TMF lives were found to be significantly shorter than isothermal low-cycle-fatigue (LCF) life at the maximum cycle temperature, and in-phase cycling was more damaging than out-of-phase cycling. Extensive crack tip oxidation appeared to play a role in promoting the severity of in-phase cycling. Carbide particle - matrix interface cracking was also observed after in-phase TMF cycling. The applicability of various life prediction models to the TMF results obtained was assessed. It was concluded that current life prediction models based on isothermal data as input must be modified to be applicable to the TMF results. M.G.

N84-20674*# Syracuse Univ., N. Y. Dept. of Chemical Engineering and Materials Science.

LITERATURE SURVEY ON OXIDATIONS AND FATIGUE LIVES AT ELEVATED TEMPERATURES Final Report

H. W. LIU and Y. OSHIDA Apr. 1984 52 p refs
(Contract NAG3-348)
(NASA-CR-174639; NAS 1.26:174639) Avail: NTIS HC A04/MF
A01 CSCL 11F

Nickel-base superalloys are the most complex and the most widely used for high temperature applications such as aircraft engine components. The desirable properties of nickel-base superalloys at high temperatures are tensile strength, thermomechanical fatigue resistance, low thermal expansion, as well as oxidation resistance. At elevated temperature, fatigue cracks are often initiated by grain boundary oxidation, and fatigue cracks often propagate along grain boundaries, where the oxidation rate is higher. Oxidation takes place at the interface between metal and gas. Properties of the metal substrate, the gaseous environment, as well as the oxides formed all interact to make the oxidation behavior of nickel-base superalloys extremely complicated. The important topics include general oxidation, selective oxidation, internal oxidation, grain boundary oxidation, multilayer oxide structure, accelerated oxidation under stress, stress-generation during oxidation, composition and substrate microstructural changes due to prolonged oxidation, fatigue crack initiation at oxidized grain boundaries and the oxidation accelerated fatigue crack propagation along grain boundaries. S.L.

N84-31348*# National Aeronautics and Space Administration. Lewis Research Center, Cleveland, Ohio.

EVALUATION OF THE EFFECT OF CRACK CLOSURE ON FATIGUE CRACK GROWTH OF SIMULATED SHORT CRACKS

J. TELESMA and D. M. FISHER Aug. 1984 12 p refs
(NASA-TM-83778; E-2063; NAS 1.15:83778) Avail: NTIS HC
A02/MF A01 CSCL 11F

A test program was performed to determine the influence of crack closure on fatigue crack growth (FCG) rates of short cracks. By use of the standard compact tension specimen, test procedures were devised to evaluate closure loads in the wake of the crack behind its tip. The first procedure determined the magnitude of crack closure as a function of the fatigued crack wave by incrementally removing the contacting wake surfaces and measuring closure load at each increment. The second procedure used a low-high loading sequence to simulate short crack behavior. Based on the results, it was concluded that crack closure is not the major reason for the more rapid growth of short cracks as compared to long crack growth. Author

N84-32503*# Syracuse Univ., N. Y.

CRACK TIP FIELD AND FATIGUE CRACK GROWTH IN GENERAL YIELDING AND LOW CYCLE FATIGUE Final Report
Z. MINZHONG (Aircraft Strength Research Inst., Xian, China) and H. W. LIU Sep. 1984 94 p refs
(Contract NAG3-348)
(NASA-CR-174686; NAS 1.26:174686) Avail: NTIS HC A05/MF A01 CSCL 11F

Fatigue life consists of crack nucleation and crack propagation periods. Fatigue crack nucleation period is shorter relative to the propagation period at higher stresses. Crack nucleation period of low cycle fatigue might even be shortened by material and fabrication defects and by environmental attack. In these cases, fatigue life is largely crack propagation period. The characteristic crack tip field was studied by the finite element method, and the crack tip field is related to the far field parameters: the deformation work density, and the product of applied stress and applied strain. The cyclic crack growth rates in specimens in general yielding as measured by Solomon are analyzed in terms of J-integral. A generalized crack behavior in terms of delta is developed. The relations between J and the far field parameters and the relation for the general cyclic crack growth behavior are used to analyze fatigue lives of specimens under general-yielding cyclic-load. Fatigue life is related to the applied stress and strain ranges, the deformation work density, crack nucleus size, fracture toughness, fatigue crack growth threshold, Young's modulus, and the cyclic yield stress and strain. The fatigue lives of two aluminum alloys correlate well with the deformation work density as depicted by the derived theory. The general relation is reduced to Coffin-Manson low cycle fatigue law in the high strain region.

Author

N84-33564*# National Aeronautics and Space Administration. Lewis Research Center, Cleveland, Ohio.

LOW CYCLE FATIGUE BEHAVIOR OF CONVENTIONALLY CAST MAR-M 200 AT 1000 DEG C
W. W. MILLIGAN (Georgia Inst. of Technology) and R. C. BILL Sep. 1984 15 p refs
(NASA-TM-83769; E-2260; NAS 1.15:83769; USAAVSCOM-TR-84-C-16; AD-A149178) Avail: NTIS HC A02/MF A01 CSCL 11F

The low cycle fatigue behavior of the nickel-based superalloy MAR-M 200 in conventionally cast form was studied at 1000 C. Continuous cycling tests, without hold times, were conducted with inelastic strain ranges of from 0.04 to 0.33 percent. Tests were also conducted which included a hold time at peak strain in either tension or compression. For the conditions studied, it was determined that imposition of hold times did not significantly affect the fatigue life. Also, for continuous cycling tests, increasing or decreasing the cycle frequency did not affect life. Metallographic analysis revealed that the most significant damage mechanism involved environmentally assisted intergranular crack initiation and propagation, regardless of the cycle type. Changes in the gamma morphology (rafting and rod formation) were observed, but did not significantly affect the failure.

Author

N85-15877*# Massachusetts Inst. of Tech., Cambridge. Dept. of Materials Science and Engineering.

THERMAL-MECHANICAL FATIGUE CRACK GROWTH IN INCONEL X-750 Final Report
N. MARCHAND and R. M. PELLOUX Oct. 1984 17 p refs
(Contract NAG3-280)
(NASA-CR-174740; NAS 1.26:174740) Avail: NTIS HC A02/MF A01 CSCL 11F

Thermal-mechanical fatigue crack growth (TMFCG) was studied in a gamma-gamma' nickel base superalloy Inconel X-750 under controlled load amplitude in the temperature range from 300 to 650 C. In-phase (T sub max at sigma sub max), out-of-phase (T sub min at sigma sub max), and isothermal tests at 650 C were performed on single-edge notch bars under fully reversed cyclic conditions. A dc electrical potential method was used to measure crack length. The electrical potential response obtained for each cycle of a given wave form and R value yields information on

crack closure and crack extension per cycle. The macroscopic crack growth rates are reported as a function of delta k and the relative magnitude of the TMFCG are discussed in the light of the potential drop information and of the fractographic observations.
R.S.F.

N85-18124*# National Aeronautics and Space Administration. Lewis Research Center, Cleveland, Ohio.

A STUDY OF SPECTRUM FATIGUE CRACK PROPAGATION IN TWO ALUMINUM ALLOYS. 1: SPECTRUM SIMPLIFICATION
J. TELESMA and S. D. ANTOLOVICH (Georgia Inst. of Technology) Jan. 1985 16 p refs 2 Vol.
(NASA-TM-86929; E-2348; NAS 1.15:86929) Avail: NTIS HC A02/MF A01 CSCL 11F

The fatigue crack propagation behavior of two commercial Al alloys was studied using spectrum loading conditions characteristics of those encountered at critical locations in high performance fighter aircraft. A tension dominated (TD) and tension compression (TC) spectrum were employed for each alloy. Using a mechanics-based analysis, it was suggested that negative loads could be eliminated for the TC spectrum for low to intermediate maximum stress intensities. The suggestion was verified by subsequent testing. Using fractographic evidence, it was suggested that a further simplification in the spectra could be accomplished by eliminating low and intermediate peak load points resulting in near or below threshold maximum peak stress intensity values. It is concluded that load interactions become more important at higher stress intensities and more plasticity at the crack tip. These results suggest that a combined mechanics/fractographic mechanisms approach can be used to simplify other complex spectra.
M.G.

N85-18125*# National Aeronautics and Space Administration. Lewis Research Center, Cleveland, Ohio.

A STUDY OF SPECTRUM FATIGUE CRACK PROPAGATION IN TWO ALUMINUM ALLOYS. 2: INFLUENCE OF MICROSTRUCTURES
J. TELESMA and S. D. ANTOLOVICH (Georgia Inst. of Technology) Jan. 1985 19 p refs 2 Vol.
(NASA-TM-86930; E-2439; NAS 1.15:86930) Avail: NTIS HC A02/MF A01 CSCL 11F

The important metallurgical factors that influence both constant amplitude and spectrum crack growth behavior in aluminum alloys were investigated. The effect of microstructural features such as grain size, inclusions, and dispersoids was evaluated. It was shown that a lower stress intensities, the I/M 7050 alloy showed better fatigue crack propagation (FCP) resistance than P/M 7091 alloy for both constant amplitude and spectrum testing. It was suggested that the most important microstructural variable accounting for superior FCP resistance of 7050 alloy is its large grain size. It was further postulated that the inhomogeneous planar slip and large grain size of 7050 limit dislocation interactions and thus increase slip reversibility which improves FCP performance. The hypothesis was supported by establishing that the cyclic strain hardening exponent for the 7091 alloy is higher than that of 7050.
M.G.

N85-19074*# National Aeronautics and Space Administration. Lewis Research Center, Cleveland, Ohio.

LOW CYCLE FATIGUE OF MAR-M 200 SINGLE CRYSTALS AT 760 AND 870 DEG C
W. W. MILLIGAN (Georgia Inst. of Tech., Atlanta), N. JAYARAMAN (Cincinnati Univ.), and R. C. BILL 1984 31 p refs Presented at the TMS-AIME Fall Meeting, Detroit, 17-19 Sep. 1984 Prepared in cooperation with Army Research and Technology Labs., Cleveland
(Contract DA PROJ. 1L1-61101-AH-45)
(NASA-TM-86933; E-2444; NAS 1.15:86933; USAAVSCOM-TR-85-C-1) Avail: NTIS HC A03/MF A01 CSCL 11F

Fully reversed low cycle fatigue tests were conducted on single crystals of the nickel-base superalloys Mar-M 200 at 760 C and 870 C. At 760 C, planar slip (octohedral) lead to orientation-dependent strain hardening and cyclic lives. Multiple slip crystals strain hardened the most, resulting in relatively high stress ranges and low

lives. Single slip crystals strain hardened the least, resulting in relatively low stress ranges and higher lives. A preferential crack initiation site which was related to slip plane geometry was observed in single slip orientated crystals. At 870 C, the trends were quite different, and the slip character was much more homogeneous. As the tensile axis orientation deviated from 001, the stress ranges increased and the cyclic lives decreased. Two possible mechanisms were proposed to explain the behavior; one is based on Takeuchi and Kuramoto's cube cross-slip model, and the other is based on orientation-dependent creep rates. EAK

N85-26964*# National Aeronautics and Space Administration. Lewis Research Center, Cleveland, Ohio.

MULTIAXIAL AND THERMOMECHANICAL FATIGUE CONSIDERATIONS IN DAMAGE TOLERANT DESIGN

G. E. LEESE (TRW, Inc., Cleveland) and R. C. BILL 1985 21 p refs Presented at the 60th Meeting of the Struct. and Mater. Panel, San Antonio, 21-26 Apr. 1985; sponsored by AGARD Prepared in cooperation with Army Research and Technology Labs., Cleveland (NASA-TM-87022; E-2514; NAS 1.15:87022; USAAVSCOM-TR-85-C-5; AD-A157112) Avail: NTIS HC A02/MF A01 CSCL 11F

In considering damage tolerant design concepts for gas turbine hot section components, several challenging concerns arise: Complex multiaxial loading situations are encountered; Thermomechanical fatigue loading involving very wide temperature ranges is imposed on components; Some hot section materials are extremely anisotropic; and coatings and environmental interactions play an important role in crack propagation. The effects of multiaxiality and thermomechanical fatigue are considered from the standpoint of their impact on damage tolerant design concepts. Recently obtained research results as well as results from the open literature are examined and their implications for damage tolerant design are discussed. Three important needs required to advance analytical capabilities in support of damage tolerant design become readily apparent: (1) a theoretical basis to account for the effect of nonproportional loading (mechanical and mechanical/thermal); (2) the development of practical crack growth parameters that are applicable to thermomechanical fatigue situations; and (3) the development of crack growth models that address multiple crack failures. Author

N86-10311*# National Aeronautics and Space Administration. Lewis Research Center, Cleveland, Ohio.

CREEP-FATIGUE BEHAVIOR OF NICOCRALY COATED PWA 1480 SUPERALLOY SINGLE CRYSTALS

R. V. MINER, J. GAYDA, and M. G. HEBSUR 1985 20 p refs Presented at the Symp. on Low-Cycle Fatigue Directions for the Future, Bolton Landing, N.Y., 30 Sep. - 4 Oct. 1985; sponsored by American Society for Testing Materials (NASA-TM-87110; E-2710; NAS 1.15:87110) Avail: NTIS HC A02/MF A01 CSCL 11F

Single crystal specimens of a Ni base superalloy, PWA 1480, with a low pressure plasma sprayed NiCoCrAlY coating were tested in various 0.1 Hz fatigue and creep fatigue cycles both at 1015 and 1050 C. Creep fatigue tests of the cp, pc, and cc types were conducted with various constant total strain ranges employing creep dwells at various constant stresses. Considerable cyclic softening occurred as was evidenced particularly by rapidly increasing creep rates in the creep fatigue tests. The cycle time in the creep fatigue tests typically decreased by more than 80 percent at 0.5 N sub f. Though cyclic life did correlate with delta epsilon sub in a better correlation existed with sub f for both the fatigue and creep fatigue tests, and poor correlations were observed with either sigma sub max or the average cycle time. A model containing both delta sigma and delta sigma (sub in), N sub f = alpha delta sigma (sub in) beta delta sigma gamma, with best fit values of sigma for each cycle type, but the same values of beta and gamma, was found to provide good correlations. Life lines were not greatly different among the cycle types, differing only by a factor of about three. The cp cycle life line was lowest for both test temperatures,

however among the other three cycle types there was no consistent ranking. For all test types failure occurred predominately by multiple internal cracking originating at pores. The strong correlation of life with delta sigma may reflect a significant crack growth period in the life of the specimens. B.W.

N86-12292*# National Aeronautics and Space Administration. Lewis Research Center, Cleveland, Ohio.

INFLUENCE OF LOAD INTERACTIONS ON CRACK GROWTH AS RELATED TO STATE OF STRESS AND CRACK CLOSURE

J. TELESMA Sep. 1985 22 p refs (NASA-TM-87117; E-2724; NAS 1.15:87117) Avail: NTIS HC A02/MF A01 CSCL 11F

Fatigue crack propagation (FCP) after an application of a low-high loading sequence was investigated as a function of specimen thickness and crack closure. No load interaction effects were detected for specimens in a predominant plane strain state. However, for the plane stress specimens, initially high FCP rates after transition to a higher stress intensity range were observed. The difference in observed behavior was explained by examining the effect of the resulting closure stress intensity values on the effective stress intensity range. Author

N86-12294*# National Aeronautics and Space Administration. Lewis Research Center, Cleveland, Ohio.

FATIGUE CRACK PROPAGATION OF NICKEL-BASE SUPERALLOYS AT 650 DEG C

J. GAYDA, T. P. GABB, and R. V. MINER Oct. 1985 22 p refs Presented at the Symp. on Low-Cycle Fatigue Directions for the Future, Bolton Landing, N.Y., 30 Sep. - 4 Oct. 1985; sponsored by American Society for Testing and Materials (NASA-TM-87150; E-2778; NAS 1.15:87150) Avail: NTIS HC A02/MF A01 CSCL 11F

The 650 C fatigue crack propagation behavior of two nickel-base superalloys, Rene 95 and Waspaloy, is studied with particular emphasis placed on understanding the roles of creep, environment, and two key grain boundary alloying additions, boron and zirconium. Comparison of air and vacuum data shows the air environment to be detrimental over a wide range of frequencies for both alloys. More in-depth analysis on Rene 95 shows at lower frequencies, such as 0.02 Hz, failure in air occurs by intergranular, environmentally-assisted creep crack growth, while at higher frequencies, up to 5.0 Hz, environmental interactions are still evident but creep effects are minimized. The effect of B and Zr in Waspaloy is found to be important where environmental and/or creep interactions are presented. In those instances, removal of B and Zr dramatically increases crack growth and it is therefore plausible that effective dilution of these elements may explain a previously observed trend in which crack growth rates increase with decreasing grain size. Author

N86-12295*# National Aeronautics and Space Administration. Lewis Research Center, Cleveland, Ohio.

AN UPDATE OF THE TOTAL-STRAIN VERSION OF SRP

J. F. SALTSMAN and G. R. HALFORD Oct. 1985 27 p refs Presented at the Symp. on Low Cycle Fatigue: Direc. for the Future, Lake George, N.Y., 30 Sep. - 4 Oct. 1985; sponsored by American Society for Testing and Materials, American Inst. of Mining, Metallurgical and Petroleum Engineers, and American Society for Metals (NASA-TF-2499; E-2575; NAS 1.60:2499) Avail: NTIS HC A03/MF A01 CSCL 11F

An updated procedure for characterizing an alloy and predicting cyclic life by using the total strain range version of strainrange partitioning (TS-SRP) has been developed. The principal feature of this update is a new procedure for determining the intercept of time dependent elastic strain range versus cyclic life lines. The procedure is based on an established relation between failure and the cyclic stress-strain response of an alloy. The stress-strain response is characterized by empirical equations presented in this report. These equations were determined with the aid of a cyclic constitutive model. The procedures presented herein reduce the testing required to characterize an alloy. Failure testing is done

only in the high strain, low life regime; cyclic stress-strain response is determined from tests conducted in both the high and low strain regimes. These tests are carried out to stability of the stress-strain hysteresis loop but not to failure. Thus both the time and costs required to characterize an alloy are greatly reduced. This approach was evaluated and verified for two nickel base superalloys, AF2-1DA and Inconel 718. Author

N86-14356*# Texas A&M Univ., College Station. Dept. of Aerospace Engineering.

DEVELOPMENT OF CONSTITUTIVE MODELS FOR CYCLIC PLASTICITY AND CREEP BEHAVIOR OF SUPER ALLOYS AT HIGH TEMPERATURE Final Report

W. E. HAISLER 30 Sep. 1983 161 p refs
(Contract NAG3-31; RESEARCH FOUNDATION PROJ. 4246)
(NASA-CR-176418; NAS 1.26:176418) Avail: NTIS HC A08/MF A01 CSCL 11F

An uncoupled constitutive model for predicting the transient response of thermal and rate dependent, inelastic material behavior was developed. The uncoupled model assumes that there is a temperature below which the total strain consists essentially of elastic and rate insensitive inelastic strains only. Above this temperature, the rate dependent inelastic strain (creep) dominates. The rate insensitive inelastic strain component is modelled in an incremental form with a yield function, flow rule and hardening law. Revisions to the hardening rule permit the model to predict temperature-dependent kinematic-isotropic hardening behavior, cyclic saturation, asymmetric stress-strain response upon stress reversal, and variable Bauschinger effect. The rate dependent inelastic strain component is modelled using a rate equation in terms of back stress, drag stress and exponent n as functions of temperature and strain. A sequence of hysteresis loops and relaxation tests are utilized to define the rate dependent inelastic strain rate. Evaluation of the model has been performed by comparison with experiments involving various thermal and mechanical load histories on 5086 aluminum alloy, 304 stainless steel and Hastelloy X. Author

N86-20542*# Syracuse Univ., N. Y. Dept. of Mechanical and Aerospace Engineering.

GRAIN BOUNDARY OXIDATION AND OXIDATION ACCELERATED FATIGUE CRACK NUCLEATION AND PROPAGATION

H. W. LIU and Y. OSHIDA Jan. 1986 19 p refs Presented at the Minnowbrook Conference on Life Prediction for High Temperature Gas Turbine Materials, Blue Mountain Lake, N.Y., 27-30 Aug. 1985 Sponsored in part by the HOST Program (Contract NAG3-348)
(NASA-CR-175050; NAS 1.26:175050) Avail: NTIS HC A02/MF A01 CSCL 11F

Fatigue life at elevated temperatures is often shortened by oxidation. Grain boundary oxidation penetrates deeper than the surface oxidation. Therefore, grain boundary oxide penetration could be the primary cause of accelerated fatigue crack nucleation and propagation, and the shortened fatigue life at elevated temperatures. Grain boundary oxidation kinetics was studied and its statistical scatter was analyzed by the Weibull's distribution function. The effects of grain boundary oxidation on shortened fatigue life was analyzed and discussed. A model of intermittent microcracks of the grain boundary oxide was proposed for the fatigue crack growth in the low frequency region. The proposed model is consistent with the observations that fatigue crack growth rate in the low frequency region with hold time at K_{sub} max is inversely proportional to cyclic frequency and that crack growth is intergranular. Author

N86-21661*# National Aeronautics and Space Administration. Lewis Research Center, Cleveland, Ohio.

VARIABLES CONTROLLING FATIGUE CRACK GROWTH OF SHORT CRACKS

J. TELESMA, D. M. FISHER, and D. HOLKA (Michigan Technological Univ., Houghton) Dec. 1985 20 p refs Presented at the International Conference on Fatigue, Corrosion Cracking, Fracture Mechanics, and Failure Analysis, Salt Lake City, Utah, 2-6 Dec. 1985; sponsored by American Society for Metals (NASA-TM-87208; E-2865; NAS 1.15:87208) Avail: NTIS HC A02/MF A01 CSCL 11F

A study was conducted to evaluate the roles of crack closure and microstructure in the fatigue growth of short cracks. Testing was performed at R ratios of 0.1, 0.5, and 0.7. At all R ratios short cracks exhibited accelerated growth rates in comparison to long cracks. It was concluded that crack closure could not entirely account for the accelerated growth rates of short cracks. The accelerated growth rates occurred over crack lengths on the order of grain size, suggesting a strong influence of microstructure. A significant effect of grain boundaries and inclusions on short crack FCG behavior was observed. For very short crack lengths, fatigue growth rates do not appear to be a function of either ΔK or R ratio. Author

N86-22686*# National Aeronautics and Space Administration. Lewis Research Center, Cleveland, Ohio.

INFLUENCE OF FATIGUE CRACK WAKE LENGTH AND STATE OF STRESS ON CRACK CLOSURE

J. TELESMA and D. M. FISHER 1986 27 p refs Presented at the International Symposium on Fatigue Crack Closure, 1-2 May 1986; sponsored by the American Society for Testing and Materials (NASA-TM-87292; E-2999; NAS 1.15:87292) Avail: NTIS HC A03/MF A01 CSCL 11F

The location of crack closure with respect to crack wake and specimen thickness under different loading conditions was determined. The rate of increase of K_{sub} CL in the crack wake was found to be significantly higher for plasticity induced closure in comparison to roughness induced closure. Roughness induced closure was uniform throughout the thickness of the specimen while plasticity induced closure levels were 50 percent higher in the near surface region than in the midthickness. The influence of state of stress on low-high load interaction effects was also examined. Load interaction effects differed depending upon the state of stress and were explained in terms of ΔK sub eff. Author

N86-24818*# Massachusetts Inst. of Tech., Cambridge. Dept. of Materials Science and Engineering.

THERMAL-MECHANICAL FATIGUE BEHAVIOR OF NICKEL-BASE SUPERALLOYS Final Report

R. M. PELLOUX and N. MARCHAND Mar. 1986 186 p refs (Contract NAG3-280)
(NASA-CR-175048; NAS 1.26:175048; USAAVSCOM-TR-86-C-4) Avail: NTIS HC A09/MF A01 CSCL 11F

The main achievements of a 36-month research program are presented. The main objective was to gain more insight into the problem of crack growth under thermal mechanical fatigue (TMF) conditions. This program was conducted at M.I.T. for the period of September 1982 to September 1985. The program was arranged into five technical tasks. Under Task I, the literature of TMF data was reviewed. The goal was to identify the crack propagation conditions in aircraft engines (hot section) and to assess the validity of conventional fracture mechanics parameters to address TMF crack growth. The second task defined the test facilities, test specimen and the testing conditions needed to establish the effectiveness of data correlation parameters identified in Task I. Three materials (Inconel X-750, Hastelloy-X, and B-1900) were chosen for the program. Task II was accomplished in collaboration with Pratt & Whitney Aircraft engineers. Under Task III, a computerized testing system to measure the TMF behavior (LCF and CG behaviors) of various alloys systems was built. The software used to run isothermal and TMF tests was also developed. Built

26 METALLIC MATERIALS

around a conventional servohydraulic machine, the system is capable of push-pull tests under stress or strain and temperature controlled conditions in the temperature range of 25C to 1050C. A crack propagation test program was defined and conducted under Task IV. The test variables included strain range, strain rate (frequency) and temperature. Task V correlated and generalized the Task IV data for isothermal and variable temperature conditions so that several crack propagation parameters could be compared and evaluated. The structural damage (mode of cracking and dislocation substructure) under TMF cycling was identified and contrasted with the isothermal damage to achieve a sound fundamental mechanistic understanding of TMF. Author

N86-25454*# Pennsylvania State Univ., University Park. Dept. of Engineering Science and Mechanics.

AXIAL AND TORSIONAL FATIGUE BEHAVIOR OF WASPALOY Final Report

S. ZAMRIK, M. MIRDAMADI, and F. ZAHIRI Apr. 1986 27 p (Contract NAG3-264)
(NASA-CR-175052; NAS 1.26:175052; USAAVSCOM-TR-86-C-14)
Avail: NTIS HC A02/MF A01 CSCL 11F

The cyclic flow response and crack growth behavior of Waspaloy at room temperature and 650 C under tensile loading and torsional loading was studied, for two conditions of Waspaloy: fine grain, large gamma prime size; coarse grain, small gamma prime size. The fine grain material showed 5 to 10 percent hardening after about 10 percent of life, with sequent softening to failure at both temperature levels. The coarse grain material showed either stable response or monotonic softening to failure. Early crack initiation was observed on planes of maximum shear, with eventual branching to principle planes under torsional loading; cracks were always normal to load axis under tensile loading. Also, crack paths were intergranular at 650 C, mostly transgranular at room temperature. Author

N86-25455*# Georgia Inst. of Tech., Atlanta. School of Materials Engineering.

YIELDING AND DEFORMATION BEHAVIOR OF THE SINGLE CRYSTAL NICKEL-BASE SUPERALLOY PWA 1480

W. W. MILLIGAN, JR. May 1986 96 p refs
(Contract NAG3-503)
(NASA-CR-175100; NAS 1.26:175100; USAAVSCOM-TR-86-C-18; AD-A171035) Avail: NTIS HC A05/MF A01 CSCL 11F

Interrupted tensile tests were conducted to fixed plastic strain levels in 100 ordered single crystals of the nickel based superalloy PWA 1480. Testing was done in the range of 20 to 1093 C, at strain rate of 0.5 and 50%/min. The yield strength was constant from 20 to 760 C, above which the strength dropped rapidly and became a strong function of strain rate. The high temperature data were represented very well by an Arrhenius type equation, which resulted in three distinct temperature regimes. The deformation substructures were grouped in the same three regimes, indicating that there was a fundamental relationship between the deformation mechanisms and activation energies. Models of the yielding process were considered, and it was found that no currently available model was fully applicable to this alloy. It was also demonstrated that the initial deformation mechanism (during yielding) was frequently different from that which would be inferred by examining specimens which were tested to failure. Author

N86-28164*# National Aeronautics and Space Administration. Lewis Research Center, Cleveland, Ohio.

MICROMECHANISMS OF THERMOMECHANICAL FATIGUE: A COMPARISON WITH ISOTHERMAL FATIGUE

R. C. BILL 1986 21 p Presented at the International Spring Conference Fatigue at High Temperatures, Paris, France, 9-11 Jun. 1986; sponsored by the Societe Francaise de Metallurgie Prepared in cooperation with Army Aviation Research and Technology Activity, Cleveland, Ohio
(NASA-TM-87331; E-3075; NAS 1.15:87331;
USAAVSCOM-TR-86-C-7; AD-A180176) Avail: NTIS HC
A02/MF A01 CSCL 11F

Thermomechanical Fatigue (TMF) experiments were conducted on Mar-M 200, B-1900, and PWA-1480 (single crystals) over temperature ranges representative of gas turbine airfoil environments. The results were examined from both a phenomenological basis and a micromechanical basis. Depending on constituents present in the superalloy system, certain micromechanisms dominated the crack initiation process and significantly influenced the TMF lives as well as sensitivity of the material to the type TMF cycle imposed. For instance, high temperature cracking around grain boundary carbides in Mar-M 200 resulted in short in-phase TMF lives compared to either out-of-phase or isothermal lives. In single crystal PWA-1480, the type of coating applied was seen to be the controlling factor in determining sensitivity to the type of TMF cycle imposed. Micromechanisms of deformation were observed over the temperature range of interest to the TMF cycles, and provided some insight as to the differences between TMF damage mechanisms and isothermal damage mechanisms. Finally, the applicability of various life prediction models to TMF results was reviewed. Current life prediction models based on isothermal data must be modified before being generally applied to TMF. Author

N86-31699*# National Aeronautics and Space Administration. Lewis Research Center, Cleveland, Ohio.

THE LOW CYCLE FATIGUE BEHAVIOR OF A PLASMA-SPRAYED COATING MATERIAL

J. GAYDA, T. P. GABB, and R. V. MINER, JR. 1986 17 p Presented at the 1986 TMS-AIME Annual Meeting, New Orleans, La., 2-6 Mar. 1986
(NASA-TM-87318; E-3050; NAS 1.15:87318) Avail: NTIS HC
A02/MF A01 CSCL 11F

Single crystal nickel-base superalloys employed in turbine blade applications are often used with a plasma spray coating for oxidation and hot corrosion resistance. These coatings may also affect fatigue life of the superalloy substrate. As part of a large program to understand the fatigue behavior of coated single crystals, fully reversed, total strain controlled fatigue tests were run on a free standing NiCoCrAlY coating alloy, PWA 276, at 0.1 Hz. Fatigue tests were conducted at 650 C, where the NiCoCrAlY alloy has modest ductility, and at 1050 C, where it is extremely ductile, showing tensile elongation in excess of 100 percent. At the lower test temperature, deformation induced disordering softened the NiCoCrAlY alloy, while at the higher test temperature cyclic hardening was observed which was linked to gradual coarsening of the two phase microstructure. Fatigue life of the NiCoCrAlY alloy was significantly longer at the higher temperature. Further, the life of the NiCoCrAlY alloy exceeds that of coated, /001/-oriented PWA 1480 single crystals at 1050 C, but at 650 C the life of the coated crystal is greater than that of the NiCoCrAlY alloy on a total strain basis. Author

N87-14489*# National Aeronautics and Space Administration. Lewis Research Center, Cleveland, Ohio.

ESTIMATION OF HIGH TEMPERATURE LOW CYCLE FATIGUE ON THE BASIS OF INELASTIC STRAIN AND STRAINRATE

A. BERKOVITS Sep. 1986 13 p
(NASA-TM-88841; E-3168; NAS 1.15:88841) Avail: NTIS HC
A02/MF A01 CSCL 11F

Fatigue life at elevated temperature can be predicted by introducing parametric values obtained from monotonic constitutive behavior into the Universal-Slopes Equation. For directionally

NONMETALLIC MATERIALS

solidified MAR-M200+HF at 975 C, these parameters are the maximum stress achievable under entirely plastic (time-independent) and purely creep (time-dependent) conditions and the corresponding inelastic strains, as well as the elastic modulus. For materials which exhibit plasticity/creep interaction, two more pairs of monotonic parameters must be evaluated for fatigue life prediction. This life-prediction method based on the Universal-Slopes Equation, resulted from a constitutive model characterizing monotonic and cyclic data as inelastic strainrate as a function of inelastic strain. Characterizing monotonic data is this way, permitted distinction between different material responses such as strain-hardening, strain-softening, and dynamic recovery effects. Understanding and defining the region of influence of each of these effects facilitated formulation of the constitutive model in relation to the mechanical and microstructural processes occurring in the material under cyclic loading. Author

N87-20408*# National Aeronautics and Space Administration. Lewis Research Center, Cleveland, Ohio.

BITHERMAL LOW-CYCLE FATIGUE BEHAVIOR OF A NICOCRALY-COATED SINGLE CRYSTAL SUPERALLOY

J. GAYDA, T. P. GABB, R. V. MINER, and G. R. HALFORD
1987 25 p Presented at the 1987 TMS-AIME Annual Meeting, Denver, Colo., 22-26 Feb. 1987
(NASA-TM-89831; E-3484; NAS 1.15:89831) Avail: NTIS HC A02/MF A01 CSCL 20B

Specimens of a single crystal superalloy, PWA 1480, both bare and coated with a NiCoCrAlY alloy, PWA 276, were tested in low-cycle fatigue at 650 and 1050 C, and in bithermal thermomechanical fatigue tests. In the two bithermal test types, tensile strain was imposed at one of the two temperatures and reversed in compression at the other. In the high-strain regime, lives for both bithermal test types approached that for the 650 C isothermal test on an inelastic strain basis, all being controlled by the low ductility of the superalloy at 650 C. In the low-strain regime, coating cracking reduced life in the 650 C isothermal test. The bithermal test imposing tension at 650 C, termed out-of-phase, also produced rapid surface cracking, but in both coated and bare specimens. Increased crack growth rates also occurred for the out-of-phase test. Increased lives in vacuum suggested that there is a large environmental contribution to damage in the out-of-phase test due to the 1050 C exposure followed by tensile straining at the low temperature. Author

N87-22777*# National Aeronautics and Space Administration. Lewis Research Center, Cleveland, Ohio.

FATIGUE DAMAGE INTERACTION BEHAVIOR OF PWA 1480
MICHAEL A. MCGAW *In its Structural Integrity and Durability of Reusable Space Propulsion Systems* p 83-87 1987
Avail: NTIS HC A10/MF A01 CSCL 11F

The fatigue damage interaction behavior of PWA 1480 single crystal alloy has been experimentally established for the two-level loading case in which a block of low-cycle fatigue loading is followed by high-cycle fatigue loading to failure. A relative life ratio N_1/N_2 (where N_1 and N_2 are the low- and high-cycle fatigue baseline lives, respectively) of approximately 0.002 was explored to assess the interaction behavior. The experimental results thus far show evidence of a loading order interaction effect to a similar degree of detriment as has been observed in polycrystalline materials. Current generation single crystal alloys in general, and PWA 1480 in particular, contain pores; indeed, it was observed in all cases that specimen failure initiated from pores connected with or immediately below the surface. Detailed fractographic and metallographic studies are currently being made to assess the nature of the porosity in terms of its effect on fatigue life. Author

Includes physical, chemical, and mechanical properties of plastics, elastomers, lubricants, polymers, textiles, adhesives, and ceramic materials.

A80-42085* National Aeronautics and Space Administration. Lewis Research Center, Cleveland, Ohio.

FRACTURE TOUGHNESS DETERMINATION OF AL₂O₃ USING FOUR-POINT-BEND SPECIMENS WITH STRAIGHT-THROUGH AND CHEVRON NOTCHES

D. MUNZ, R. T. BUBSEY, and J. L. SHANNON, JR. (NASA, Lewis Research Center, Strength of Materials Section, Cleveland, Ohio)
American Ceramic Society, Journal, vol. 63, May-June 1980, p. 300-305. refs

A80-50696* Deutsche Forschungs- und Versuchsanstalt fuer Luft- und Raumfahrt, Cologne (West Germany).

PERFORMANCE OF CHEVRON-NOTCH SHORT BAR SPECIMEN IN DETERMINING THE FRACTURE TOUGHNESS OF SILICON NITRIDE AND ALUMINUM OXIDE

D. MUNZ (Deutsche Forschungs- und Versuchsanstalt fuer Luft- und Raumfahrt, Cologne, West Germany), R. T. BUBSEY, and J. L. SHANNON, JR. (NASA, Lewis Research Center, Strength of Materials Section, Cleveland, Ohio) *Journal of Testing and Evaluation*, vol. 8, May 1980, p. 103-107. refs

Ease of preparation and testing are advantages unique to the chevron-notch specimen used for the determination of the plane strain fracture toughness of extremely brittle materials. During testing, a crack develops at the notch tip and extends stably as the load is increased. For a given specimen and notch configuration, maximum load always occurs at the same relative crack length independent of the material. Fracture toughness is determined from the maximum load with no need for crack length measurement. Chevron notch acuity is relatively unimportant since a crack is produced during specimen loading. In this paper, the authors use their previously determined stress intensity factor relationship for the chevron-notch short bar specimen to examine the performance of that specimen in determining the plane strain fracture toughness of silicon nitride and aluminum oxide. (Author)

A81-32545*# National Aeronautics and Space Administration. Lewis Research Center, Cleveland, Ohio.

FRACTURE TOUGHNESS OF BRITTLE MATERIALS DETERMINED WITH CHEVRON NOTCH SPECIMENS

J. L. SHANNON, JR., R. T. BUBSEY, W. S. PIERCE (NASA, Lewis Research Center, Cleveland, Ohio), and D. MUNZ (Karlsruhe, Universitat; Kernforschungszentrum Karlsruhe GmBH, Karlsruhe, West Germany) *Societe Francaise de Metallurgie, International Conference on Fracture*, 5th, Cannes, France, Mar. 29-Apr. 3, 1981, Paper. 15 p. refs

Short bar, short rod, and four-point-bend chevron-notch specimens were used to determine the plane strain fracture toughness of hot-pressed silicon nitride and sintered aluminum oxide brittle ceramics. The unique advantages of this specimen type are: (1) the production of a sharp natural crack during the early stage of test loading, so that no precracking is required, and (2) the load passes through a maximum at a constant, material-independent crack length-to-width ratio for a specific geometry, so that no post-test crack measurement is required. The plane strain fracture toughness is proportional to the maximum test load and functions of the specimen geometry and elastic compliance. Although results obtained for silicon nitride are in good mutual agreement and relatively free of geometry and size effects, aluminum oxide results were affected in both these respects by the rising crack growth resistance curve of the material. O.C.

27 NONMETALLIC MATERIALS

A83-29734* National Aeronautics and Space Administration. Lewis Research Center, Cleveland, Ohio.

RESIN SELECTION CRITERIA FOR TOUGH COMPOSITE STRUCTURES

C. C. CHAMIS (NASA, Lewis Research Center, Cleveland, OH) and G. T. SMITH IN: Structures, Structural Dynamics and Materials Conference, 24th, Lake Tahoe, NV, May 2-4, 1983, Collection of Technical Papers. Part 1. New York, American Institute of Aeronautics and Astronautics, 1983, p. 45-60. refs (AIAA 83-0801)

Resin selection criteria are derived using a structured methodology consisting of an upward integrated mechanistic theory and its inverse (top-down structured theory). These criteria are expressed in a 'criteria selection space' which can be used to identify resin bulk properties for improved composite 'toughness'. The resin selection criteria correlate with a variety of experimental data including laminate strength, elevated temperature effects and impact resistance. Author

A84-11676* National Aeronautics and Space Administration. Lewis Research Center, Cleveland, Ohio.

DEVELOPMENT OF PLANE STRAIN FRACTURE TOUGHNESS TEST FOR CERAMICS USING CHEVRON NOTCHED SPECIMENS

R. T. BUBSEY, J. L. SHANNON, JR. (NASA, Lewis Research Center, Cleveland, OH), and D. MUNZ (Deutsche Forschungs- und Versuchsanstalt fuer Luft- und Raumfahrt, Cologne, West Germany) IN: Ceramics for high-performance applications III: Reliability. New York, Plenum Press, 1983, p. 753-771. refs

Chevron-notched four-point-bend and short-bar specimens have been used to determine the fracture toughness of sintered aluminum oxide and hot-pressed silicon nitride ceramics. The fracture toughness for Si₃N₄ is found to be essentially independent of the specimen size and chevron notch configuration, with values ranging from 4.6 to 4.9 MNm exp -3/2. In contrast, significant specimen size and notch geometry effects have been observed for Al₂O₃, with the fracture toughness ranging from 3.1 to 4.7 MNm exp -3/2. These effects are attributed to a rising crack growth resistance curve for the Al₂O₃ tested. V.L.

A86-15226* Case Western Reserve Univ., Cleveland, Ohio. **FINITE ELEMENT ANALYSIS OF RESIDUAL STRESS IN PLASMA-SPRAYED CERAMIC**

R. L. MULLEN (Case Western Reserve University, Cleveland, OH), R. C. HENDRICKS, and G. McDONALD (NASA, Lewis Research Center, Cleveland, OH) Ceramic Engineering and Science Proceedings (ISSN 0196-6219), vol. 6, July-Aug. 1985, p. 871-879. refs

Residual stress in a ZrO₂-Y₂O₃ ceramic coating resulting from the plasma spraying operation is calculated. The calculations were done using the finite element method. Both thermal and mechanical analysis were performed. The resulting residual stress field was compared to the measurements obtained by Hendricks and McDonald. Reasonable agreement between the predicted and measured moment occurred. However, the resulting stress field is not in pure bending. Author

A86-37141* National Aeronautics and Space Administration. Lewis Research Center, Cleveland, Ohio.

NONDESTRUCTIVE CHARACTERIZATION OF STRUCTURAL CERAMICS

S. J. KLIMA and G. Y. BASKLINI (NASA, Lewis Research Center, Cleveland, OH) SAMPE Quarterly (ISSN 0036-0821), vol. 17, April 1986, p. 13-19. Previously announced in STAR as N86-22970. refs

Ultrasonic velocity and attenuation measurements were used to characterize density and microstructure in monolithic silicon nitride and silicon carbide. Research samples of these structural ceramics exhibited a wide range of density and microstructural variations. It was shown that bulk density variations correlate with and can be estimated by velocity measurements. Variations in microstructural features such as grain size or shape and pore morphology had a minor effect on velocity. However, these features

had a pronounced effect on ultrasonic attenuation. The ultrasonic results are supplemented by low-energy radiography and scanning laser acoustic microscopy. Author

A87-12938* National Aeronautics and Space Administration. Lewis Research Center, Cleveland, Ohio.

CORRELATION OF PROCESSING AND SINTERING VARIABLES WITH THE STRENGTH AND RADIOGRAPHY OF SILICON NITRIDE

W. A. SANDERS (NASA, Lewis Research Center, Cleveland, OH) and G. Y. BAKLINI (Cleveland State University, OH) Ceramic Engineering and Science Proceedings (ISSN 0196-6219), vol. 7, July-Aug. 1986, p. 839-859. refs

A sintered Si₃N₄-SiO₂-Y₂O₃ composition, NASA 6Y, was developed that reached four-point flexural average strength/standard deviation values of 857/36, 544/33, and 462/59 MPa at room temperature, 1200 and 1370 C, respectively. These strengths represented improvements of 56, 38, and 21 percent over baseline properties at the three test temperatures. At room temperature the standard deviation was reduced by over a factor of three. These accomplishments were realized by the iterative utilization of conventional X-radiography to characterize structural (density) uniformity as affected by systematic changes in powder processing and sintering parameters. Accompanying the improvement in mechanical properties was a change in the type of flaw causing failure from a pore to a large columnar beta-Si₃N₄ grain typically 40-80 micron long, 10-30 micron wide, and with an aspect ratio of 5:1. Author

A87-30621* National Aeronautics and Space Administration. Lewis Research Center, Cleveland, Ohio.

FRACTURE TOUGHNESS OF Si₃N₄ MEASURED WITH SHORT BAR CHEVRON-NOTCHED SPECIMENS

JONATHAN A. SALEM and JOHN L. SHANNON, JR. (NASA, Lewis Research Center, Cleveland, OH) Journal of Materials Science (ISSN 0022-2461), vol. 22, Jan. 1987, p. 321-324. Previously announced in STAR as N86-13495. refs

The short bar chevron-notched specimen is used to measure the plane strain fracture toughness of hot pressed Si₃N₄. Specimen proportions and chevron-notch angle are varied, thereby varying the amount of crack extension to maximum load (upon which K sub IC is based). The measured toughness (4.68 ± 0.19 MNm to the 3/2 power) is independent of these variations, inferring that the material has a flat crack growth resistance curve. Author

N82-14359* National Aeronautics and Space Administration. Lewis Research Center, Cleveland, Ohio.

ULTRASONIC VELOCITY FOR ESTIMATING DENSITY OF STRUCTURAL CERAMICS

S. J. KLIMA, G. K. WATSON, T. P. HERBELL, and T. J. MOORE 1981 12 p refs Presented at the Automotive Technol. Develop. Contractor Coord. Meeting, Dearborn, Mich., 26-29 Oct. 1981

(Contract DE-AI01-77CS-51040)

(NASA-TM-82765; DOE/NASA/51040-35; E-1026-5) Avail:

NTIS HC A02/MF A01 CSCL 11B

The feasibility of using ultrasonic velocity as a measure of bulk density of sintered alpha silicon carbide was investigated. The material studied was either in the as-sintered condition or hot isostatically pressed in the temperature range from 1850 to 2050 C. Densities varied from approximately 2.8 to 3.2 g cu cm. Results show that the bulk, nominal density of structural grade silicon carbide articles can be estimated from ultrasonic velocity measurements to within 1 percent using 20 MHz longitudinal waves and a commercially available ultrasonic time intervalometer. The ultrasonic velocity measurement technique shows promise for screening out material with unacceptably low density levels. Author

N83-19902*# National Aeronautics and Space Administration. Lewis Research Center, Cleveland, Ohio.

SPECIMEN SIZE AND GEOMETRY EFFECTS ON FRACTURE TOUGHNESS OF AL2O3 MEASURED WITH SHORT ROD AND SHORT BAR CHEVRON-NOTCH SPECIMENS

J. L. SHANNON, JR. and D. G. MUNZ (Karlsruhe Univ.) 1983 14 p refs Proposed for presentation at the Symp. on Chevron-Notched Specimens: Testing and Stress Anal., Louisville, Ky., 21 Apr. 1983; sponsored by American Society for Testing and Materials

(NASA-TM-83319; E-1560; NAS 1.15:83319) Avail: NTIS HC A02/MF A01 CSCL 07C

Plane strain fracture toughness measurements were made on Al₂O₃ using short rod and short bar chevron notch specimens previously calibrated by the authors for their dimensionless stress intensity factor coefficients. The measured toughness varied systematically with variations in specimen size, proportions, and chevron notch angle apparently due to their influence on the amount of crack extension to maximum load (the measurement point). The toughness variations are explained in terms of a suspected rising R curve for the material tested, along with a discussion of an unavoidable imprecision in the calculation of K sub Ic for materials with rising R curves when tested with chevron notch specimens. Author

N86-13495*# National Aeronautics and Space Administration. Lewis Research Center, Cleveland, Ohio.

FRACTURED TOUGHNESS OF Si3N4 MEASURED WITH SHORT BAR CHEVRON-NOTCHED SPECIMENS

J. A. SALEM and J. L. SHANNON, JR. 1985 19 p refs Presented at Basic Sci. Meeting of the Am. Ceram. Soc., Baltimore, 17-19 Nov. 1985

(NASA-TM-87153; E-2749; NAS 1.15:87153) Avail: NTIS HC A02/MF A01 CSCL 11G

The short bar chevron-notched specimen is used to measure the plane strain fracture toughness of hot pressed Si₃N₄. Specimen proportions and chevron-notch angle are varied, thereby varying the amount of crack extension to maximum load (upon which K sub IC is based). The measured toughness (4.68 + or - 0.19 MNm to the 3/2 power) is independent of these variations, inferring that the material has a flat crack growth resistance curve. Author

37

MECHANICAL ENGINEERING

Includes auxiliary systems (nonpower); machine elements and processes; and mechanical equipment.

A81-33867* National Aeronautics and Space Administration. Lewis Research Center, Cleveland, Ohio.

SELF-ACTING GEOMETRY FOR NONCONTACT SEALS

G. P. ALLEN (NASA, Lewis Research Center, Cleveland, Ohio) American Society of Lubrication Engineers, Annual Meeting, 36th, Pittsburgh, Pa., May 11-14, 1981, 5 p. refs (ASLE PREPRINT 81-AM-5B-2)

Two hydrodynamic self-acting seal designs for a LOX turbopump were analyzed in order to predict performance. A radial face seal-to-seal LOX at 310 N/sq cm and 32,000 rpm (130 m/s) was analyzed for pressure differentials of 172 to 448 N/sq cm and speeds from 98 to 147 m/s. A segmented circumferential seal-to-seal helium at 34.5 or 69 N/sq cm and 157 m/s was analyzed for pressures of 35 to 86 N/sq cm (10 N/sq cm ambient) and speeds from 94 to 189 m/s. Test results confirmed noncontact operation near the design speed and pressure, and relatively good qualitative agreement between test and analysis. The face seal was found to operate with mostly liquid in the pads and mostly gas across the dam. E.B.

A82-14400* Virginia Univ., Charlottesville.

A PAD PERTURBATION METHOD FOR THE DYNAMIC COEFFICIENTS OF TILTING-PAD JOURNAL BEARINGS

P. E. ALLAIRE, J. K. PARSELL, and L. E. BARRETT (Virginia, University, Charlottesville, VA) Wear, vol. 72, Oct. 1, 1981, p. 29-44. refs

(Contract EF-76-5-01-2479; NSG-3105)

A pad assembly method for analyzing tilting-pad bearings is presented. The method results in the complete coefficient matrix for a tilting-pad bearing; the matrix is independent of the pad inertia, the pitch frequency and the number of degrees of freedom of the pad. A pad assembly method is used because it allows the collection of more bearing data with less computer time than a brute force iterative procedure. The results given show the complete dynamical matrices for a five-pad tilting-pad bearing both including and ignoring the damping effects of the unloaded (top) pads. For a symmetrical tilting-pad bearing the reduced cross-coupling coefficients are zero when the moment of inertia of the pad is ignored. (Author)

A82-35462*# Akron Univ., Ohio.

ENGINE DYNAMIC ANALYSIS WITH GENERAL NONLINEAR FINITE ELEMENT CODES. II - BEARING ELEMENT IMPLEMENTATION, OVERALL NUMERICAL CHARACTERISTICS AND BENCHMARKING

J. PADOVAN, M. ADAMS, P. LAM (Akron, University, Akron, OH), D. FERTIS, and I. ZEID (Northeastern University, Boston, MA) American Society of Mechanical Engineers, International Gas Turbine Conference and Exhibit, 27th, London, England, Apr. 18-22, 1982, 9 p. refs

(Contract NSG-3283)

(ASME PAPER 82-GT-292)

Second-year efforts within a three-year study to develop and extend finite element (FE) methodology to efficiently handle the transient/steady state response of rotor-bearing-stator structure associated with gas turbine engines are outlined. The two main areas aim at (1) implanting the squeeze film damper element into a general purpose FE code for testing and evaluation; and (2) determining the numerical characteristics of the FE-generated rotor-bearing-stator simulation scheme. The governing FE field equations are set out and the solution methodology is presented. The choice of ADINA as the general-purpose FE code is explained, and the numerical operational characteristics of the direct integration approach of FE-generated rotor-bearing-stator simulations is determined, including benchmarking, comparison of explicit vs. implicit methodologies of direct integration, and demonstration problems. C.D.

A82-48243*# Boeing Vertol Co., Philadelphia, Pa.

ON THE AUTOMATIC GENERATION OF FEM MODELS FOR COMPLEX GEARS - A WORK-IN-PROGRESS REPORT

R. J. DRAGO (Boeing Vertol Co., Philadelphia, PA) American Gear Manufacturers Association, Meeting, San Diego, CA, Feb. 1982, Paper. 36 p.

(Contract NAS3-22143)

A description is presented of the development and use of a preprocessor to create a NASTRAN finite element model of a complex spur, helical, or spiral bevel gear quickly, inexpensively, and accurately. The preprocessor creates a ready to run NASTRAN input deck including the executive, case control, and bulk data sections. It generates nodes and solid elements to model spur, helical, or spiral bevel gear teeth with integral shafting. Either a complete gear shafting model or a symmetric model is created. The fundamental building block of the gear model is the base layer. The base layer is the mesh configuration of one layer of one tooth segment which is in turn duplicated, translated, and rotated to create the completed model of the gear. Once the base layer is created, the construction of the finite element model is straightforward. G.R.

37 MECHANICAL ENGINEERING

A84-20580* Akron Univ., Ohio.

NONLINEAR TRANSIENT FINITE ELEMENT ANALYSIS OF ROTOR-BEARING-STATOR SYSTEMS

J. PADOVAN, M. ADAMS, D. FERTIS, I. ZEID, and P. LAM (Akron, University, Akron, OH) Computers and Structures (ISSN 0045-7949), vol. 18, no. 4, 1984, p. 629-639. refs (Contract NSG-3283)

This paper extends the finite element scheme to handle the highly nonlinear interfacial fields generated in the fluid filled annuli of squeeze film and journal bearings so as to model the transient response of rotor-bearing-stator systems. Since such simulations are highly nonlinear, direct numerical integration schemes are employed to generate the overall response. In this context, the paper gives consideration to such items as (1) numerical efficiency/stability, (2) comparison of implicit and explicit schemes, (3) determines extent of response nonlinearity as well as (4) extensively benchmarks the overall concept/methodologies.

Author

A84-46893*# Arizona State Univ., Tempe.

A BLADE LOSS RESPONSE SPECTRUM FOR FLEXIBLE ROTOR SYSTEMS

H. D. NELSON (Arizona State University, Tempe, AZ) and M. ALAM. American Society of Mechanical Engineers, International Gas Turbine Conference and Exhibit, 29th, Amsterdam, Netherlands, June 4-7, 1984. 8 p. refs (Contract NAG3-6) (ASME PAPER 84-GT-29)

A shock spectrum procedure is developed to estimate the peak displacement response of linear flexible rotor-bearing systems subjected to a step change in unbalance (i.e., a blade loss). A progressive and a retrograde response spectrum are established. These blade loss response spectra are expressed in a unique non-dimensional form and are functions of the modal damping ratio and the ratio of rotor spin speed to modal damped whirl speed. Modal decomposition using complex modes is utilized to make use of the unique feature of the spectra for the calculation of the peak blade loss displacement response of the rotor system. The procedure is applied to three example systems using several modal superposition strategies. The results of each are compared to true peak displacement obtained by a separate transient response program.

Author

A84-47046*# National Aeronautics and Space Administration. Lewis Research Center, Cleveland, Ohio.

ACOUSTIC EMISSION EVALUATION OF PLASMA-SPRAYED THERMAL BARRIER COATINGS

C. C. BERNDT (NASA, Lewis Research Center, Cleveland, OH) American Society of Mechanical Engineers, International Gas Turbine Conference and Exhibit, 29th, Amsterdam, Netherlands, June 4-7, 1984. 5 p. refs (Contract NAG3-164; NCC3-27) (ASME PAPER 84-GT-292)

Acoustic emission techniques have recently been used in a number of studies to investigate the performance and failure behavior of plasma-sprayed thermal barrier coatings. Failure of the coating is a complex phenomena, especially when the composite nature of the coating is considered in the light of possible failure mechanisms. Thus it can be expected that both the metal and ceramic components (i.e., the bond coat and ceramic overlay) of a composite thermal protection system influence the macroscopic behavior and performance of the coating. The aim of the present work is to summarize the 'state-of-the-art' in terms of this initial work and indicate where future progress may be made.

Author

A87-14656*# National Aeronautics and Space Administration. Lewis Research Center, Cleveland, Ohio.

FACTORS THAT AFFECT THE FATIGUE STRENGTH OF POWER TRANSMISSION SHAFTING AND THEIR IMPACT ON DESIGN

S. H. LEOWENTHAL (NASA, Lewis Research Center, Cleveland, OH) ASME, Transactions, Journal of Mechanisms, Transmission, and Automation in Design, vol. 108, March 1986, p. 106-114; Discussion, p. 115-118; Author's Closure, p. 118. Previously announced in STAR as N84-26029. refs

A long standing objective in the design of power transmission shafting is to eliminate excess shaft material without compromising operational reliability. A shaft design method is presented which accounts for variable amplitude loading histories and their influence on limited life designs. The effects of combined bending and torsional loading are considered along with a number of application factors known to influence the fatigue strength of shafting materials. Among the factors examined are surface condition, size, stress concentration, residual stress and corrosion fatigue.

Author

A87-37686* National Aeronautics and Space Administration. Lewis Research Center, Cleveland, Ohio.

EFFECT OF INTERFERENCE FITS ON ROLLER BEARING FATIGUE LIFE

HAROLD H. COE and ERWIN V. ZARETSKY (NASA, Lewis Research Center, Cleveland, OH) ASLE Transactions (ISSN 0569-8197), vol. 30, April 1987, p. 131-140; Discussion, p. 140. Previously announced in STAR as N86-19616. refs

An analysis was performed to determine the effects of inner-ring speed and press fits on roller bearing fatigue life. The effects of the resultant hoop and radial stresses on the principal stresses were considered. The maximum shear stresses below the Hertzian contact were determined for different conditions of inner-ring speed and load, and were applied to a conventional roller bearing life analysis. The effect of mean stress was determined using Goodman diagram approach. Hoop stresses caused by press fits and centrifugal force can reduce bearing life by as much as 90 percent. Use of a Goodman diagram predicts life reduction of 20 to 30 percent. The depth of the maximum shear stress remains virtually unchanged.

Author

N82-28646*# National Aeronautics and Space Administration. Lewis Research Center, Cleveland, Ohio.

A FINITE ELEMENT STRESS ANALYSIS OF SPUR GEARS INCLUDING FILLET RADII AND RIM THICKNESS EFFECTS

S. H. CHANG (Cincinnati Univ.), R. L. HUSTON (Cincinnati Univ.), and J. J. COY. 1982 12 p refs Proposed for presentation at Ann. Meeting of ASME, Phoenix, Ariz., 14-19 Nov. 1982 Prepared in cooperation with Army Aviation Research and Development Command, Cleveland, Ohio (NASA-TM-82865; E-1234; NAS 1.15:82865; AVRADCOM-TR-82-C-8) Avail: NTIS HC A02/MF A01 CSCL 13I

Spur gear stress analysis results are presented for a variety of loading conditions, support conditions, fillet radii, and rim thickness. These results are obtained using the SAP IV finite-element code. The maximum stresses, occurring at the root surface, substantially increase with decreasing rim thickness for partially supported rims (that is, with loose-fitting hubs). For fully supported rims (that is, with tight-fitting hubs), the root surface stresses slightly decrease with decreasing rim thickness. The fillet radius is found to have a significant effect upon the maximum stresses at the root surface. These stresses increase with increasing fillet radius. The fillet radius has little effect upon the internal root section stresses.

Author

N82-29607*# Cincinnati Univ., Ohio. Dept. of Mechanical Engineering.

ON FINITE ELEMENT STRESS ANALYSIS OF SPUR GEARS

S. H. CHANG and R. L. HUSTON Jul. 1982 53 p refs (Contract NSG-3188) (NASA-CR-167938; NAS 1.26:167938) Avail: NTIS HC A04/MF A01 CSCL 13I

Spur gear stress analysis results are presented for a variety of loading conditions, support conditions, root radii, and rime

thicknesses. These results are obtained using the SAP-IV finite element code. The maximum stresses, occurring at the root surface, substantially increase with decreasing rim thickness for partially supported rims (that is, with loose fitting hubs). For fully supported rims (that is, with tight fitting hubs), the root surface stresses slightly decrease with decreasing rim thickness. The fillet radius has a significant effect upon the maximum stresses at the root surface. These stresses increase with decreasing fillet radius. Finally, the fillet radius has little effect upon the internal root section stresses. S.L.

N85-27226*# National Aeronautics and Space Administration. Lewis Research Center, Cleveland, Ohio.

FATIGUE CRITERION TO SYSTEM DESIGN, LIFE AND RELIABILITY

E. V. ZARETSKY 10 Jul. 1985 22 p refs Presented at the 21st Joint Propulsion Conf., Monterey, Calif., 8-10 Jul. 1985; sponsored by AIAA, SAE and ASME (NASA-TM-87017; E-2562; NAS 1.15:87017) Avail: NTIS HC A02/MF A01 CSCL 14D

A generalized methodology to structural life prediction, design, and reliability based upon a fatigue criterion is advanced. The life prediction methodology is based in part on work of W. Weibull and G. Lundberg and A. Palmgren. The approach incorporates the computed life of elemental stress volumes of a complex machine element to predict system life. The results of coupon fatigue testing can be incorporated into the analysis allowing for life prediction and component or structural renewal rates with reasonable statistical certainty. Author

N85-30333* National Aeronautics and Space Administration. Lewis Research Center, Cleveland, Ohio.

VARIABLE FORCE, EDDY-CURRENT OR MAGNETIC DAMPER Patent

R. E. CUNNINGHAM, inventor (to NASA) 14 May 1985 6 p Filed 3 Feb. 1983 (NASA-CASE-LEW-13717-1; US-PATENT-4,517,505; US-PATENT-APPL-SN-463456; US-PATENT-CLASS-318-611; US-PATENT-CLASS-310-77; US-PATENT-CLASS-310-93; US-PATENT-CLASS-335-100) Avail: US Patent and Trademark Office CSCL 13I

An object of the invention is to provide variable damping for resonant vibrations which may occur at different rotational speeds in the range of rpms in which a rotating machine is operated. A variable force damper in accordance with the invention includes a rotating mass carried on a shaft which is supported by a bearing in a resilient cage. The cage is attached to a support plate whose rim extends into an annular groove in a housing. Variable damping is effected by tabs of electrically conducting nonmagnetic material which extend radially from the cage. The tabs at an index position lie between the pole face of respective C shaped magnets. The magnets are attached by cantilever spring members to the housing. Author

N87-11993*# National Aeronautics and Space Administration. Lewis Research Center, Cleveland, Ohio.

SELECTION OF ROLLING-ELEMENT BEARING STEELS FOR LONG-LIFE APPLICATION

E. V. ZARETSKY 1986 76 p Presented at International Symposium on the Effect of Steel Manufacturing Processes on the Quality of Bearing Steels, Phoenix, Ariz., 4-6 Nov. 1986; sponsored by American Society for Testing and Materials (NASA-TM-88881; E-3288; NAS 1.15:88881) Avail: NTIS HC A05/MF A01 CSCL 13I

Nearly four decades of research in bearing steel metallurgy and processing have resulted in improvements in bearing life by a factor of 100 over that obtained in the early 1940's. For critical applications such as aircraft, these improvements have resulted in longer lived, more reliable commercial aircraft engines. Material factors such as hardness, retained austenite, grain size and carbide size, number, and area can influence rolling-element fatigue life. Bearing steel processing such as double vacuum melting can have a greater effect on bearing life than material chemistry. The selection

and specification of a bearing steel is dependent on the integration of all these considerations into the bearing design and application. The paper reviews rolling-element fatigue data and analysis which can enable the engineer or metallurgist to select a rolling-element bearing steel for critical applications where long life is required.

Author

N87-13755*# National Aeronautics and Space Administration. Lewis Research Center, Cleveland, Ohio.

EFFECT OF DESIGN VARIABLES, TEMPERATURE GRADIENTS AND SPEED OF LIFE AND RELIABILITY OF A ROTATING DISK

E. V. ZARETSKY, T. E. SMITH (Sverdrup Technology, Inc., Cleveland, Ohio), and R. AUGUST 1986 26 p Proposed for presentation at the 2nd Thermal Engineering Conference, Honolulu, Hawaii, 22-27 Mar. 1987; sponsored by ASME and JSME (NASA-TM-88883; E-3291; NAS 1.15:88883) Avail: NTIS HC A03/MF A01 CSCL 94O

A generalized methodology to predict the fatigue life and reliability of a rotating disk such as used for aircraft engine turbines and compressors is advanced. The approach incorporates the computed life of elemental stress volumes to predict system life and reliability. Disk speed and thermal gradients as well as design variables such as disk diameter and thickness and bolt hole size, number and location are considered. Author

N87-15467*# National Aeronautics and Space Administration. Lewis Research Center, Cleveland, Ohio.

LUBRICANT EFFECTS ON BEARING LIFE

ERWIN V. ZARETSKY Dec. 1986 22 p Presented at the OEM Design Conference, New York, N.Y., 9-11 Dec. 1986 (NASA-TM-88875; E-3253; NAS 1.15:88875) Avail: NTIS HC A02/MF A01 CSCL 11H

Lubricant considerations for rolling-element bearings have within the last two decades taken on added importance in the design and operation of mechanical systems. The phenomenon which limits the useful life of bearings is rolling-element or surface pitting fatigue. The elastohydrodynamic (EHD) film thickness which separates the ball or roller surface from those of the raceways of the bearing directly affects bearing life. Chemical additives added to the lubricant can also significantly affect bearings life and reliability. The interaction of these physical and chemical effects is important to the design engineer and user of these systems. Design methods and lubricant selection for rolling-element bearings are presented and discussed. Author

N87-16336*# National Aeronautics and Space Administration. Lewis Research Center, Cleveland, Ohio.

EVALUATION OF A HIGH-TORQUE BACKLASH-FREE ROLLER ACTUATOR

BRUCE M. STEINETZ, DOUGLAS A. ROHN, and WILLIAM ANDERSON (NASTEC, Inc., Cleveland, Ohio) In its The 20th Aerospace Mechanics Symposium p 205-230 May 1986 Avail: NTIS HC A14/MF A01 CSCL 13I

The results are presented of a test program that evaluated the stiffness, accuracy, torque ripple, frictional losses, and torque holding capability of a 16:1 ratio, 430 N-m (320 ft-lb) planetary roller drive for a potential space vehicle actuator application. The drive's planet roller supporting structure and bearings were found to be the largest contributors to overall drive compliance, accounting for more than half of the total. In comparison, the traction roller contacts themselves contributed only 9 percent of the drive's compliance based on an experimentally verified stiffness model. The drive exhibited no backlash although 8 arc sec of hysteresis deflection were recorded due to microcreep within the contact under torque load. Because of these load-dependent displacements, some form of feedback control would be required for arc second positioning applications. Torque ripple tests showed the drive to be extremely smooth, actually providing some damping of input torsional oscillations. The drive also demonstrated the ability to hold static torque with drifts of 7 arc sec or less over a 24 hr period at 35 percent of full load. Author

37 MECHANICAL ENGINEERING

N87-18820*# National Aeronautics and Space Administration. Lewis Research Center, Cleveland, Ohio.

EFFECTS OF SURFACE REMOVAL ON ROLLING-ELEMENT FATIGUE

ERWIN V. ZARETSKY 1987 20 p Prepared for presentation at the International Conference on Tribology, Lubrication and Wear; 50 Years On, London, England, 1-3 Jul. 1987; sponsored by Inst. of Mechanical Engineers. (NASA-TM-88871; E-3231; NAS 1.15:88871) Avail: NTIS HC A02/MF A01 CSCL 131

The Lundberg-Palmgren equation was modified to show the effect on rolling-element fatigue life of removing by grinding a portion of the stressed volume of the raceways of a rolling-element bearing. Results of this analysis show that depending on the amount of material removed, and depending on the initial running time of the bearing when material removal occurs, the 10-percent life of the reground bearings ranges from 74 to 100 percent of the 10-percent life of a brand new bearing. Three bearing types were selected for testing. A total of 250 bearings were reground. Of this matter, 30 bearings from each type were endurance tested to 1600 hr. No bearing failure occurred related to material removal. Two bearing failures occurred due to defective rolling elements and were typical of those which may occur in new bearings.

Author

N87-23978*# National Aeronautics and Space Administration. Lewis Research Center, Cleveland, Ohio.

THE IMPACT DAMPED HARMONIC OSCILLATOR IN FREE DECAY

G. V. BROWN and C. M. NORTH 1987 23 p Prepared for presentation at the Vibrations Conference, Boston, Mass., 27-30 Sep. 1987; sponsored by the ASME (NASA-TM-89897; E-3587; NAS 1.15:89897) Avail: NTIS HC A02/MF A01 CSCL 131

The impact-damped oscillator in free decay is studied by using time history solutions. A large range of oscillator amplitude is covered. The amount of damping is correlated with the behavior of the impacting mass. There are three behavior regimes: (1) a low amplitude range with less than one impact per cycle and very low damping, (2) a useful middle amplitude range with a finite number of impacts per cycle, and (3) a high amplitude range with an infinite number of impacts per cycle and progressively decreasing damping. For light damping the impact damping in the middle range is: (1) proportional to impactor mass, (2) additive to proportional damping, (3) a unique function of vibration amplitude, (4) proportional to 1-epsilon, where epsilon is the coefficient of restitution, and (5) very roughly inversely proportional to amplitude. The system exhibits jump phenomena and period doublings. An impactor with 2 percent of the oscillator's mass can produce a loss factor near 0.1.

Author

38

QUALITY ASSURANCE AND RELIABILITY

Includes product sampling procedures and techniques; and quality control.

A80-39641*# National Aeronautics and Space Administration. Lewis Research Center, Cleveland, Ohio.

QUANTITATIVE ULTRASONIC EVALUATION OF ENGINEERING PROPERTIES IN METALS, COMPOSITES, AND CERAMICS

A. VARY (NASA, Lewis Research Center, Cleveland, Ohio) National Research Council of Canada, Seminar on Advanced Ultrasonic Technology, 1st, Longueuil, Quebec, Canada, June 9, 10, 1980, Paper. 16 p. refs

Ultrasonic techniques that have demonstrated potential for material characterization are reviewed. These techniques rely on physical acoustic properties of materials and the interaction of elastic stress waves with morphological factors in the ultrasonic

regime. The speed of wave propagation and energy loss by interaction with material microstructure and geometrical factors underlie ultrasonic determination of material properties. Two categories of ultrasonic measurements are discussed: those related to material strengths (e.g., elastic moduli, tensile strength, and fracture toughness) and those related to morphology and material conditions that govern strength and performance (e.g., microstructure, void content, residual stress, fatigue damage). It is shown that large-scale industrial application of ultrasonic NDE will depend on advancement in such areas as theory development, instrumentation, system automation, standardization, and coordination with design. V.L.

A80-51575*# National Aeronautics and Space Administration. Lewis Research Center, Cleveland, Ohio.

CONCEPTS AND TECHNIQUES FOR ULTRASONIC EVALUATION OF MATERIAL MECHANICAL PROPERTIES

A. VARY (NASA, Lewis Research Center, Cleveland, Ohio) Virginia Polytechnic Institute and State University, Conference on Mechanics of Nondestructive Testing, Virginia Polytechnic Institute and State University, Blacksburg, Va., Sept. 10-12, 1980, Paper. 19 p. refs

The ultrasonic nondestructive evaluation techniques discussed in the present paper indicate potentials for material characterization and property prediction. Stress wave interaction and material transfer function concepts are examined as a basis for explaining correlations between material mechanical behavior and ultrasonically measured quantities. It is observed that the effect and criticality of any discrete flaw, such as crack, inclusion, or any other stress raiser, is definable only in terms of its material microstructural environment. This underscores the importance of ultrasonic techniques capable of characterizing the stress wave energy transfer properties of a material. V.P.

A81-19656* National Aeronautics and Space Administration. Lewis Research Center, Cleveland, Ohio.

ULTRASONIC MEASUREMENT OF MATERIAL PROPERTIES

A. VARY (NASA, Lewis Research Center, Materials and Structures Div., Cleveland, Ohio) In: Research techniques in nondestructive testing. Volume 4. London, Academic Press, 1980, p. 159-204. refs

The state-of-the-art of ultrasonic methods is reviewed with reference to the basic measurements, signal acquisition and processing, strength property and morphological condition measurements, and industrial applications. The emphasis is placed on techniques that indicate quantitative ultrasonic correlations with material strength and morphology relevant to the reliability of load-bearing structures. V.L.

A81-44660*# National Aeronautics and Space Administration. Lewis Research Center, Cleveland, Ohio.

ACOUSTO-ULTRASONIC CHARACTERIZATION OF FIBER REINFORCED COMPOSITES

A. VARY (NASA, Lewis Research Center, Cleveland, OH) U.S. Navy, Conference on a Critical Review: Technique for the Characterization of Composite Materials, Cambridge, MA, June 8-10, 1981, Paper. 13 p. refs

The acousto-ultrasonic technique combines advantageous aspects of acoustic emission and ultrasonic methodologies. Acousto-ultrasonics operates by introducing a repeating series of ultrasonic pulses into a material. The waves introduced simulate the spontaneous stress waves that would arise if the material were put under stress as in the case of acoustic emission measurements. These benign stress waves are detected by an acoustic emission sensor. The physical arrangement of the ultrasonic (input) transducer and acoustic emission (output) sensor is such that the resultant waveform carries an imprint of morphological factors that govern or contribute to material performance. The output waveform is quite complex, but it can be quantitized in terms of a 'stress wave factor'. The stress wave factor, which can be defined in a number of ways, is essentially a relative measure of the efficiency of energy dissipation in a material. If flaws or other material anomalies exist in the volume being

examined, their combined effect will appear in the stress wave factor. (Author)

A83-22265* Carborundum Co., Niagara Falls, N. Y.
COMPARISON OF NDE TECHNIQUES FOR SINTERED-SiC COMPONENTS

M. SRINIVASAN, D. LAWLER (Carborundum Co., Niagara Falls, NY), L. J. INGLEHART, R. L. THOMAS (Wayne State University, Detroit, MI), and D. YUHAS (Sonoscan, Inc., Bensenville, IL) Ceramic Engineering and Science Proceedings, vol. 3, Sept.-Oct. 1982, p. 654-679. Research supported by the U.S. Department of Energy (Contract DEN3-168; DEN3-167)

High frequency, bulk-wave ultrasonics detected defects in manufactured SiC components. In addition, gas-turbine blades and vanes were examined by scanning laser acoustic microscopy (SLAM). Comparative results obtained on simple shapes such as disks and bars by microfocus X-ray radiography, ultrasonics, scanning photoacoustic spectroscopy, and SLAM are discussed. (Author)

A83-25571* Ohio State Univ., Columbus.
MECHANICS ASPECTS OF NDE BY SOUND AND ULTRASOUND

L. S. FU (Ohio State University, Columbus, OH) Applied Mechanics Reviews, vol. 35, Aug. 1982, p. 1047-1057. refs (Contract NSG-3269)

Nondestructive evaluation (NDE) is considered as a means to detect the energy release mechanism of defects and the interaction of microstructures within materials with sound waves and/or ultrasonic waves. Ultrasonic inspection involves the frequency range 20 kHz-1 GHz with amplitudes depending on the sensitivity of the test instrumentation. Pulse echo systems are most frequently used in NDE. Information is extracted from the signals through measurements of the signal velocity, attenuation, the acoustic emission when stress is applied, and calculation of the acoustoelastic coefficients. Fracture properties, tensile and shear strengths, the interlaminar shear strength, the cohesive strength, yield and impact strengths, the hardness, and the residual stress can be assayed by ultrasonic methods. Finally, attention is given to analytical treatment of the derived data, with mention given to transition matrix, integral equation, and eigenstrain approaches. M.S.K.

A83-39620*# National Aeronautics and Space Administration. Lewis Research Center, Cleveland, Ohio.

METAL HONEYCOMB TO POROUS WIREFORM SUBSTRATE DIFFUSION BOND EVALUATION

A. VARY, P. E. MOORHEAD, and D. R. HULL (NASA, Lewis Research Center, Nondestructive Evaluation Section, Cleveland, OH) Materials Evaluation (ISSN 0025-5327), vol. 41, July 1983, p. 942-945. refs

Two nondestructive techniques were used to evaluate diffusion bond quality between a metal foil honeycomb and porous wireform substrate. The two techniques, cryographics and acousto-ultrasonics, are complementary in revealing variations of bond integrity and quality in shroud segments from an experimental aircraft turbine engine. Previously announced in STAR as N82-18612 Author

A84-17546* National Aeronautics and Space Administration. Lewis Research Center, Cleveland, Ohio.

FAILURE ANALYSIS OF A TOOL STEEL TORQUE SHAFT

J. R. REAGAN (NASA, Lewis Research Center, Cleveland, OH) IN: Technology advances in engineering and their impact on detection, diagnosis and prognosis methods; Proceedings of the Thirty-sixth Meeting, Scottsdale, AZ, December 6-10, 1982. Cambridge and New York, Cambridge University Press, 1983, p. 287-291.

A low design load drive shaft used to deliver power from an experimental exhaust heat recovery system to the crankshaft of an experimental diesel truck engine failed during highway testing. An independent testing laboratory analyzed the failure by routine

metallography and attributed the failure to fatigue induced by a banded microstructure. Visual examination by NASA of the failed shaft plus the knowledge of the torsional load that it carried pointed to a 100 percent ductile failure with no evidence of fatigue. Scanning electron microscopy confirmed this. Previously announced in STAR as N82-11184 A.R.H.

A85-42151*# National Aeronautics and Space Administration. Lewis Research Center, Cleveland, Ohio.

THE ROLE OF THE REFLECTION COEFFICIENT IN PRECISION MEASUREMENT OF ULTRASONIC ATTENUATION

E. R. GENERAZIO (NASA, Lewis Research Center, Cleveland, OH) (DARPA, Annual Review of Progress in Quantitative Nondestructive Evaluation, La Jolla, CA, July 8-13, 1984) Materials Evaluation (ISSN 0025-5327), vol. 43, July 1985, p. 995-1004. Previously announced in STAR as N84-32849. refs

Ultrasonic attenuation measurements using contact, pulse-echo techniques are sensitive to surface roughness and couplant thickness variations. This can reduce considerable inaccuracies in the measurement of the attenuation coefficient for broadband pulses. Inaccuracies arise from variations in the reflection coefficient at the buffer-couplant-sample interface. The reflection coefficient is examined as a function of the surface roughness and corresponding couplant thickness variations. Interrelations with ultrasonic frequency are illustrated. Reliable attenuation measurements are obtained only when the frequency dependence of the reflection coefficient is incorporated in signal analysis. Data are given for nickel 200 samples and a silicon nitride ceramic bar having surface roughness variations in the 0.3 to 3.0 microns range for signal bandwidths in the 50 to 100 MHz range. Author

A86-13192*# National Aeronautics and Space Administration. Lewis Research Center, Cleveland, Ohio.

MEASUREMENT OF ULTRASONIC VELOCITY USING PHASE-SLOPE AND CROSS-CORRELATION METHODS

D. R. HULL, H. E. KAUTZ, and A. VARY (NASA, Lewis Research Center, Cleveland, OH) Materials Evaluation (ISSN 0025-5327), vol. 43, Oct. 1985, p. 1455-1460. Previously announced in STAR as N84-34769. refs

Computer implemented phase-slope and cross-correlation methods are introduced for measuring time delays between pairs of broadband ultrasonic pulse-echo signals for determining velocity in engineering materials. The phase-slope and cross-correlation methods are compared with the overlap method which is currently in wide use. Comparison of digital versions of the three methods shows similar results for most materials having low ultrasonic attenuation. However, the cross-correlation method is preferred for highly attenuating materials. An analytical basis for the cross-correlation method is presented. Examples are given for the three methods investigated to measure velocity in representative materials in the megahertz range. Author

A86-31745* National Aeronautics and Space Administration. Lewis Research Center, Cleveland, Ohio.

RADIOGRAPHIC DETECTABILITY LIMITS FOR SEEDED VOIDS IN SINTERED SILICON CARBIDE AND SILICON NITRIDE

G. Y. BAAKLINI, J. D. KISER, and D. J. ROTH (NASA, Lewis Research Center, Cleveland, OH) Advanced Ceramic Materials (ISSN 0883-5551), vol. 1, Jan. 1986, p. 43-49. Previously announced in STAR as N85-21674. refs

Conventional and microfocus X-radiographic techniques were compared to determine relative detectability limits for voids in green and sintered SiC and Si₃N₄. The relative sensitivity of the techniques was evaluated by comparing their ability to detect voids that were artificially introduced by a seeding process. For projection microfocus radiography the sensitivity of void detection at a 90/95 probability of detection/confidence level is 1.5 percent of specimen thickness in sintered SiC and Si₃N₄. For conventional contact radiography the sensitivity is 2.5 percent of specimen thickness. It appears that microfocus projection radiography is preferable to conventional contact radiography in cases where increased sensitivity is required and where the additional complexity of the technique can be tolerated. E.A.K.

38 QUALITY ASSURANCE AND RELIABILITY

A86-35575* National Aeronautics and Space Administration. Lewis Research Center, Cleveland, Ohio.

NDE OF ADVANCED CERAMICS

S. J. KLIMA (NASA, Lewis Research Center, Cleveland, OH) Materials Evaluation (ISSN 0025-5327), vol. 44, April 1986, p. 571-576. refs

Radiographic, ultrasonic, and scanning laser acoustic microscopy (SLAM) techniques were used to characterize silicon nitride and silicon carbide modulus-of-rupture test specimens in various stages of fabrication. Conventional and microfocus X-ray techniques were found capable of detecting minute high-density inclusions in as-received powders, green compacts, and fully densified specimens. Significant density gradients in sintered bars were observed by radiography, ultrasonic velocity, and SLAM. Ultrasonic attenuation was found sensitive to microstructural variations due to grain and void morphology and distribution. SLAM was capable also of detecting voids, inclusions, and cracks in finished test bars. Consideration is given to the potential for applying thermoacoustic microscopy techniques to green and densified ceramics. Some limitations and the detection probability statistics of the aforementioned nondestructive evaluation (NDE) processes are also discussed. Author

A86-39027*# National Aeronautics and Space Administration. Lewis Research Center, Cleveland, Ohio.

RELIABILITY OF VOID DETECTION IN STRUCTURAL CERAMICS BY USE OF SCANNING LASER ACOUSTIC MICROSCOPY

D. J. ROTH, S. J. KLIMA, J. D. KISER (NASA, Lewis Research Center, Cleveland, OH), and G. Y. BAAKLINI (Cleveland State University, OH) Materials Evaluation (ISSN 0025-5327), vol. 44, May 1986, p. 762-769, 761. Previously announced in STAR as N85-32337. refs

The reliability of scanning laser acoustic microscopy (SLAM) for detecting surface voids in structural ceramic test specimens was statistically evaluated. Specimens of sintered silicon nitride and sintered silicon carbide, seeded with surface voids, were examined by SLAM at an ultrasonic frequency of 100 MHz in the as fired condition and after surface polishing. It was observed that polishing substantially increased void detectability. Voids as small as 100 micrometers in diameter were detected in polished specimens with 0.90 probability at a 0.95 confidence level. In addition, inspection times were reduced up to a factor of 10 after polishing. The applicability of the SLAM technique for detection of naturally occurring flaws of similar dimensions to the seeded voids is discussed. A FORTRAN program listing is given for calculating and plotting flaw detection statistics. Author

A86-45150*# National Aeronautics and Space Administration. Lewis Research Center, Cleveland, Ohio.

QUANTITATIVE FLAW CHARACTERIZATION WITH SCANNING LASER ACOUSTIC MICROSCOPY

E. R. GENERAZIO and D. J. ROTH (NASA, Lewis Research Center, Cleveland, OH) Materials Evaluation (ISSN 0025-5327), vol. 44, June 1986, p. 863-870. Previously announced in STAR as N86-22983. refs

Surface roughness and diffraction are two factors that have been observed to affect the accuracy of flaw characterization with scanning laser acoustic microscopy. Inaccuracies can arise when the surface of the test sample is acoustically rough. It is shown that, in this case, Snell's law is no longer valid for determining the direction of sound propagation within the sample. The relationship between the direction of sound propagation within the sample, the apparent flaw depth, and the sample's surface roughness is investigated. Diffraction effects can mask the acoustic images of minute flaws and make it difficult to establish their size, depth, and other characteristics. It is shown that for Fraunhofer diffraction conditions the acoustic image of a subsurface defect corresponds to a two-dimensional Fourier transform. Transforms based on simulated flaws are used to infer the size and shape of the actual flaw. Author

A86-48143*# National Aeronautics and Space Administration. Lewis Research Center, Cleveland, Ohio.

NONDESTRUCTIVE TECHNIQUES FOR CHARACTERIZING MECHANICAL PROPERTIES OF STRUCTURAL MATERIALS - AN OVERVIEW

A. VARY and S. J. KLIMA (NASA, Lewis Research Center, Cleveland, OH) ASME, International Gas Turbine Conference and Exhibit, 31st, Duesseldorf, West Germany, June 8-12, 1986. 10 p. Previously announced in STAR as N86-19636. refs (ASME PAPER 86-GT-75)

An overview of nondestructive evaluation (NDE) is presented to indicate the availability and application potentials of techniques for quantitative characterization of the mechanical properties of structural materials. The purpose is to review NDE techniques that go beyond the usual emphasis on flow detection and characterization. Discussed are current and emerging NDE techniques that can verify and monitor intrinsic properties (e.g., tensile, shear, and yield strengths; fracture toughness, hardness, ductility; elastic moduli) and underlying microstructural and morphological factors. Most of the techniques described are, at present, neither widely applied nor widely accepted in commerce and industry because they are still emerging from the laboratory. The limitations of the techniques may be overcome by advances in applications research and instrumentation technology and perhaps by accommodations for their use in the design of structural parts. Author

A86-48298*# National Aeronautics and Space Administration. Lewis Research Center, Cleveland, Ohio.

NDE OF STRUCTURAL CERAMICS

S. J. KLIMA and A. VARY (NASA, Lewis Research Center, Cleveland, OH) ASME, International Gas Turbine Conference and Exhibit, 31st, Duesseldorf, West Germany, June 8-12, 1986. 8 p. Previously announced in STAR as N86-16598. refs (ASME PAPER 86-GT-279)

Radiographic, ultrasonic, scanning laser acoustic microscopy (SLAM), and thermo-acoustic microscopy techniques were used to characterize silicon nitride and silicon carbide modulus-of-rupture test specimens in various stages of fabrication. Conventional and microfocus X-ray techniques were found capable of detecting minute high density inclusions in as-received powders, green compacts, and fully densified specimens. Significant density gradients in sintered bars were observed by radiography, ultrasonic velocity, and SLAM. Ultrasonic attenuation was found sensitive to microstructural variations due to grain and void morphology and distribution. SLAM was also capable of detecting voids, inclusions and cracks in finished test bars. Consideration is given to the potential for applying thermo-acoustic microscopy techniques to green and densified ceramics. The detection probability statistics and some limitations of radiography and SLAM also are discussed. Author

A87-14300* Cleveland State Univ., Ohio.

PROBABILITY OF DETECTION OF INTERNAL VOIDS IN STRUCTURAL CERAMICS USING MICROFOCUS RADIOGRAPHY

G. Y. BAAKLINI (Cleveland State University, OH) and D. J. ROTH (NASA, Lewis Research Center, Cleveland, OH) Journal of Materials Research (ISSN 0884-2914), vol. 1, May-June 1986, p. 457-467. Previously announced in STAR as N86-13749. refs

The reliability of microfocus X-radiography for detecting subsurface voids in structural ceramic test specimens was statistically evaluated. The microfocus system was operated in the projection mode using low X-ray photon energies (20 keV) and a 10 micro m focal spot. The statistics were developed for implanted subsurface voids in green and sintered silicon carbide and silicon nitride test specimens. These statistics were compared with previously-obtained statistics for implanted surface voids in similar specimens. Problems associated with void implantation are discussed. Statistical results are given as probability-of-detection curves at a 95 percent confidence level for voids ranging in size from 20 to 528 micro m in diameter. Author

A87-32200* Illinois Univ., Urbana.

NONDESTRUCTIVE EVALUATION OF ADHESIVE BOND

STRENGTH USING THE STRESS WAVE FACTOR TECHNIQUE

HENRIQUE L. M. DOS REIS (Illinois, University, Urbana) and HAROLD E. KRAUTZ (NASA, Lewis Research Center, Cleveland, OH) Journal of Acoustic Emission (ISSN 0730-0050), vol. 5, Oct.-Dec. 1986, p. 144-147. refs

Acousto-ultrasonic nondestructive evaluation has been conducted to evaluate the adhesive bond strength between rubber and steel plates using the stress wave factor (SWF) measurement technique. Specimens with different bond strength were manufactured and tested using the SWF technique. Two approaches were used to define the SWF. One approach defines the SWF as the signal energy and the other approach defines the SWF as the square root of the zero moment of the frequency spectrum of the received signal. The strength of the rubber-steel adhesive joint was then evaluated using the destructive peel strength test method. It was observed that in both approaches higher values of the SWF measurements correspond to higher values of the peel strength test data. Therefore, these results show that the stress wave factor technique has the potential of being used in quality assurance of the adhesive bond strength between rubber and steel substrates.

Author

A87-48702*# National Aeronautics and Space Administration. Lewis Research Center, Cleveland, Ohio.

NDE RELIABILITY AND PROCESS CONTROL FOR STRUCTURAL CERAMICS

G. Y. BAAKLINI (NASA, Lewis Research Center, Cleveland, OH) ASME, Transactions, Journal of Engineering for Gas Turbines and Power (ISSN 0022-0825), vol. 109, July 1987, p. 263-266. Previously announced in STAR as N87-12910. refs (ASME PAPER 87-GT-8)

The reliability of microfocus X-radiography and scanning laser acoustic microscopy for detecting microvoids in silicon nitride and silicon carbide was statistically evaluated. Materials- and process-related parameters that influenced the statistical findings in research samples are discussed. The use of conventional X-radiography in controlling and optimizing the processing and sintering of an Si₃N₄-SiO₂-Y₂O₃ composition designated NASA 6Y is described. Radiographic evaluation and guidance helped develop uniform high-density Si₃N₄ modulus-of-rupture bars with improved four-point flexural strength (857, 544, and 462 MPa at room temperature, 1200 C, and 1370 C, respectively) and reduced strength scatter.

Author

A87-51974*# National Aeronautics and Space Administration. Lewis Research Center, Cleveland, Ohio.

QUANTITATIVE VOID CHARACTERIZATION IN STRUCTURAL CERAMICS BY USE OF SCANNING LASER ACOUSTIC MICROSCOPY

D. J. ROTH, E. R. GENERAZIO (NASA, Lewis Research Center, Cleveland, OH), and G. Y. BAAKLINI (Cleveland State University, OH) Materials Evaluation (ISSN 0025-5327), vol. 45, Aug. 1987, p. 958-966. Previously announced in STAR as N86-31913. refs

The ability of scanning laser acoustic microscopy (SLAM) to characterize artificially seeded voids in sintered silicon nitride structural ceramic specimens was investigated. Using trigonometric relationships and Airy's diffraction theory, predictions of internal void depth and size were obtained from acoustic diffraction patterns produced by the voids. Agreement was observed between actual and predicted void depths. However, predicted void diameters were generally much greater than actual diameters. Precise diameter predictions are difficult to obtain due to measurement uncertainty and the limitations of 100 MHz SLAM applied to typical ceramic specimens.

Author

N80-15422*# National Aeronautics and Space Administration. Lewis Research Center, Cleveland, Ohio.

PHOTOVOLTAIC POWER SYSTEM RELIABILITY CONSIDERATIONS

V. R. LALLI 1980 9 p refs Presented at the Ann. Reliability and Maintainability Symp., San Francisco, 22-24 Jan. 1980 (Contract DE-AB29-76EI-20370)

(NASA-TM-79291; DOE/NASA/20370-79/19; E-235) Avail: NTIS HC A02/MF A01 CSCL 14D

An example of how modern engineering and safety techniques can be used to assure the reliable and safe operation of photovoltaic power systems is presented. This particular application is for a solar cell power system demonstration project designed to provide electric power requirements for remote villages. The techniques utilized involve a definition of the power system natural and operating environment, use of design criteria and analysis techniques, an awareness of potential problems via the inherent reliability and FMEA methods, and use of fail-safe and planned spare parts engineering philosophy.

J.M.S.

N80-22714*# National Aeronautics and Space Administration. Lewis Research Center, Cleveland, Ohio.

SIMULATION OF TRANSDUCER-COUPPLANT EFFECTS ON BROADBAND ULTRASONIC SIGNALS

A. VARY 1980 36 p refs Presented at Spring Meeting of the Am. Soc. of Nondestructive Testing, Philadelphia, 24-27 Mar. 1980

(NASA-TM-81489; E-427) Avail: NTIS HC A03/MF A01 CSCL 14D

The increasing use of broadband, pulse-echo ultrasonics in nondestructive evaluation of flaws and material properties has generated a need for improved understanding of the way signals are modified by coupled and bonded thin-layer interfaces associated with transducers. This understanding is most important when using frequency spectrum analyses for characterizing material properties. In this type of application, signals emanating from material specimens can be strongly influenced by couplant and bond-layers in the acoustic path. Computer synthesized waveforms were used to simulate a range of interface conditions encountered in ultrasonic transducer systems operating in the 20 to 80 MHz regime. The adverse effects of thin-layer multiple reflections associated with various acoustic impedance conditions are demonstrated. The information presented is relevant to ultrasonic transducer design, specimen preparation, and couplant selection.

Author

N80-24634*# National Aeronautics and Space Administration. Lewis Research Center, Cleveland, Ohio.

CONCEPTS AND TECHNIQUES FOR ULTRASONIC EVALUATION OF MATERIAL MECHANICAL PROPERTIES

A. VARY 1980 21 p refs To be presented at the Conf. on Mech. of Nondestructive Testing, Blacksburg, Va., 10-12 Sep. 1980

(NASA-TM-81523; E-467) Avail: NTIS HC A02/MF A01 CSCL 14D

Ultrasonic methods that can be used for material strength are reviewed. Emergency technology involving advanced ultrasonic techniques and associated measurements is described. It is shown that ultrasonic NDE is particularly useful in this area because it involves mechanical elastic waves that are strongly modulated by morphological factors that govern mechanical strength and also dynamic failure modes. These aspects of ultrasonic NDE are described in conjunction with advanced approaches and theoretical concepts for signal acquisition and analysis for materials characterization. It is emphasized that the technology is in its infancy and that much effort is still required before the techniques and concepts can be transferred from laboratory to field conditions.

A.R.H.

38 QUALITY ASSURANCE AND RELIABILITY

N80-26682*# National Aeronautics and Space Administration. Lewis Research Center, Cleveland, Ohio.

QUANTITATIVE ULTRASONIC EVALUATION OF ENGINEERING PROPERTIES IN METALS, COMPOSITES AND CERAMICS

A. VARY 1980 18 p refs Presented at First Seminar on Advanced Ultrasonic Tech., Longueuil, Quebec, 9-10 Jun. 1980; sponsored by National Research Council of Canada (NASA-TM-81530; E-482) Avail: NTIS HC A02/MF A01 CSCL 14D

Ultrasonic technology from the perspective of nondestructive evaluation approaches to material strength prediction and property verification is reviewed. Emergent advanced technology involving quantitative ultrasonic techniques for materials characterization is described. Ultrasonic methods are particularly useful in this area because they involve mechanical elastic waves that are strongly modulated by the same morphological factors that govern mechanical strength and dynamic failure processes. It is emphasized that the technology is in its infancy and that much effort is still required before all the available techniques can be transferred from laboratory to industrial environments. E.D.K.

N81-28458*# National Aeronautics and Space Administration. Lewis Research Center, Cleveland, Ohio.

ACOUSTO-ULTRASONIC CHARACTERIZATION OF FIBER REINFORCED COMPOSITES

A. VARY 1981 14 p refs Presented at the Office of Naval Res. Conf. A Critical Rev: Tech. for the Characterization of Composite Mater., Cambridge, Mass., 8-10 Jun. 1981 (NASA-TM-82651; E-910) Avail: NTIS HC A02/MF A01 CSCL 14D

The acousto-ultrasonic technique combines advantageous aspects of acoustic emission and ultrasonic methodologies. Acousto-ultrasonics operates by introducing a repeating series of ultrasonic pulses into a material. The waves introduced simulate the spontaneous stress waves that would arise if the material were put under stress as in the case of acoustic emission measurements. These benign stress waves are detected by an acoustic emission sensor. The physical arrangement of the ultrasonic (input) transducer and acoustic emission (output) sensor is such that the resultant waveform carries an imprint of morphological factors that govern or contribute to material performance. The output waveform is complex, but it can be quantitized in terms of a 'stress wave factor.' The stress wave factor, which can be defined in a number of ways, is a relative measure of the efficiency of energy dissipation in a material. If flaws or other material anomalies exist in the volume being examined, their combined effect appears in the stress wave factor. S.F.

N81-33492*# National Aeronautics and Space Administration. Lewis Research Center, Cleveland, Ohio.

RELIABILITY AND QUALITY ASSURANCE ON THE MOD 2 WIND SYSTEM

W. E. B. MASON and B. G. JONES (Boeing Engineering and Construction Co., Seattle, Wash.) 1981 16 p refs Presented at 5th Biennial Wind Energy Conf. and Workshop, Washington, 5-7 Oct. 1981; sponsored by Solar Energy Res. Inst. and DOE (Contract DE-AL01-79ET-20305) (NASA-TM-82717; DOE/NASA/20305-6; E-1015) Avail: NTIS HC A02/MF A01 CSCL 14D

The Safety, Reliability, and Quality Assurance (R&QA) approach developed for the largest wind turbine generator, the Mod 2, is described. The R&QA approach assures that the machine is not hazardous to the public or to the operating personnel, is operated unattended on a utility grid, demonstrates reliable operation, and helps establish the quality assurance and maintainability requirements for future wind turbine projects. The significant guideline consisted of a failure modes and effects analysis (FMEA) during the design phase, hardware inspections during parts fabrication, and three simple documents to control activities during machine construction and operation. E.A.K.

N82-18612*# National Aeronautics and Space Administration. Lewis Research Center, Cleveland, Ohio.

METAL HONEYCOMB TO POROUS WIREFORM SUBSTRATE DIFFUSION BOND EVALUATION

A. VARY, P. E. MOORHEAD, and D. R. HULL 1982 12 p refs Presented at the Spring Conf. of the Am. Soc. for Nondestructive Testing, Boston, 22-25 Mar. 1982 (NASA-TM-82793; E-959) Avail: NTIS HC A02/MF A01 CSCL 14D

Two nondestructive techniques were used to evaluate diffusion bond quality between a metal foil honeycomb and porous wireform substrate. The two techniques, cryographics and acousto-ultrasonics, are complementary in revealing variations of bond integrity and quality in shroud segments from an experimental aircraft turbine engine. S.L.

N82-18613*# Massachusetts Inst. of Tech., Cambridge. Dept. of Mechanical Engineering.

ULTRASONIC INPUT-OUTPUT FOR TRANSMITTING AND RECEIVING LONGITUDINAL TRANSDUCERS COUPLED TO SAME FACE OF ISOTROPIC ELASTIC PLATE Final Report

J. H. WILLIAMS, JR., H. KARAGULLE, and S. S. LEE Washington, D.C. NASA Feb. 1982 29 p refs (Contract NSG-3210)

(NASA-CR-3506) Avail: NTIS HC A03/MF A01 CSCL 14D

The quantitative understanding of ultrasonic nondestructive evaluation parameters such as the stress wave factor were studied. Ultrasonic input/output characteristics for an isotropic elastic plate with transmitting and receiving longitudinal transducers coupled to the same face were analyzed. The asymptotic normal stress is calculated for an isotropic elastic half space subjected to a uniform harmonic normal stress applied to a circular region at the surface. The radiated stress waves are traced within the plate by considering wave reflections at the top and bottom faces. The output voltage amplitude of the receiving transducer is estimated by considering only longitudinal waves. Agreement is found between the output voltage wave packet amplitudes and times of arrival due to multiple reflections of the longitudinal waves. E.A.K.

N82-19550*# National Aeronautics and Space Administration. Lewis Research Center, Cleveland, Ohio.

EXPERIENCE WITH MODIFIED AEROSPACE RELIABILITY AND QUALITY ASSURANCE METHOD FOR WIND TURBINES

W. E. KLEIN 1982 11 p refs Proposed for Presentation at 9th Ann. Engr. Conf. on Reliability, Hershey, Penn., 16-18 Jun. 1982 Revised (Contract DE-AL01-76ET-20320)

(NASA-TM-82803; DOE/NASA/20320-38; E-1142) Avail: NTIS HC A02/MF A01 CSCL 14D

The SR&QA approach assures that the machine is not hazardous to the public or operating personnel, can operate unattended on a utility grid, demonstrates reliability operation, and helps establish the quality assurance and maintainability requirements for future wind turbine projects. The approach consisted of modified failure modes and effects analysis (FMEA) during the design phase, minimal hardware inspection during parts fabrication, and three simple documents to control activities during machine construction and operation. Five years experience shows that this low cost approach works well enough that it should be considered by others for similar projects. T.M.

N82-20551*# National Aeronautics and Space Administration. Lewis Research Center, Cleveland, Ohio.

INTERRELATION OF MATERIAL MICROSTRUCTURE, ULTRASONIC FACTORS, AND FRACTURE TOUGHNESS OF TWO PHASE TITANIUM ALLOY

A. VARY and D. R. HULL 1982 25 p refs Presented at the Spring Conf. of the Am. Soc. for Nondestructive Testing, Boston, 22-25 Mar. 1982

(NASA-TM-82810; E-1151; NAS 1.15:82810) Avail: NTIS HC A02/MF A01 CSCL 14D

The pivotal role of an alpha-beta phase microstructure in governing fracture toughness in a titanium alloy, Ti-662, is

demonstrated. The interrelation of microstructure and fracture toughness is demonstrated using ultrasonic measurement techniques originally developed for nondestructive evaluation and material property characterization. It is shown that the findings determined from ultrasonic measurements agree with conclusions based on metallurgical, metallographic, and fractographic observations concerning the importance of alpha-beta morphology in controlling fracture toughness in two phase titanium alloys.

Author

N83-11506*# Ohio State Univ., Columbus. Dept. of Engineering Mechanics.

PHENOMENOLOGICAL AND MECHANICS ASPECTS OF NONDESTRUCTIVE EVALUATION AND CHARACTERIZATION BY SOUND AND ULTRASOUND OF MATERIAL AND FRACTURE PROPERTIES Final Report

L. S. W. FU Washington NASA Oct. 1982 32 p refs
(Contract NSG-3269)

(NASA-CR-3623; NAS 1.26:3623) Avail: NTIS HC A03/MF A01 CSCL 14D

Developments in fracture mechanics and elastic wave theory enhance the understanding of many physical phenomena in a mathematical context. Available literature in the material, and fracture characterization by NDT, and the related mathematical methods in mechanics that provide fundamental underlying principles for its interpretation and evaluation are reviewed. Information on the energy release mechanism of defects and the interaction of microstructures within the material is basic in the formulation of the mechanics problems that supply guidance for nondestructive evaluation (NDE).

A.R.H.

N83-11507*# Ohio State Univ., Columbus. Dept. of Engineering Mechanics.

FUNDAMENTAL ASPECTS IN QUANTITATIVE ULTRASONIC DETERMINATION OF FRACTURE TOUGHNESS: THE SCATTERING OF A SINGLE ELLIPSOIDAL INHOMOGENEITY Final Report

L. S. W. FU Washington NASA Oct. 1981 37 p refs
(Contract NSG-3269)

(NASA-CR-3625; NAS 1.26:3625) Avail: NTIS HC A03/MF A01 CSCL 14D

The scattering of a single ellipsoidal inhomogeneity is studied via an eigenstrain approach. The displacement field is given in terms of volume integrals that involve eigenstrains that are related to mismatch in mass density and that in elastic moduli. The governing equations for these unknown eigenstrains are derived. Agreement with other approaches for the scattering problem is shown. The formulation is general and both the inhomogeneity and the host medium can be anisotropic. The axisymmetric scattering of an ellipsoidal inhomogeneity in a linear elastic isotropic medium is given as an example. The angular and frequency dependence of the scattered displacement field, the differential and total cross sections are formally given in series expansions for the case of uniformly distributed eigenstrains.

Author

N83-16773*# Ohio State Univ., Columbus. Dept. of Engineering Mechanics.

THE TRANSMISSION OR SCATTERING OF ELASTIC WAVES BY AN INHOMOGENEITY OF SIMPLE GEOMETRY: A COMPARISON OF THEORIES Final Report

Y. C. SHEU and L. S. FU Washington NASA Jan. 1983 91 p refs

(Contract NSG-3269)

(NASA-CR-3659; E-1394; NAS 1.26:3659; RF-TECH-104) Avail: NTIS HC A05/MF A01 CSCL 20N

The extended method of equivalent inclusions is applied to study the specific wave problems: (1) the transmission of elastic waves in an infinite medium containing a layer of inhomogeneity, and (2) the scattering of elastic waves in an infinite medium containing a perfect spherical inhomogeneity. Eigenstrains are expanded as a geometric series and a method of integration based on the inhomogeneous Helmholtz operator is adopted. This study compares results, obtained by using limited number of terms in

the eigenstrain expansion, with exact solutions for the layer problem and that for a perfect sphere.

S.L.

N83-21373*# Massachusetts Inst. of Tech., Cambridge. Dept. of Mechanical Engineering.

EFFECTS OF SPECIMEN RESONANCES ON ACOUSTIC-ULTRASONIC TESTING Final Report

J. H. WILLIAMS, JR., E. B. KAHN, and S. S. LEE Washington NASA Mar. 1983 36 p refs

(Contract NSG-3210)

(NASA-CR-3679; NAS 1.26:3679) Avail: NTIS HC A03/MF A01 CSCL 14D

The effects of specimen resonances on acoustic ultrasonic (AU) nondestructive testing were investigated. Selected resonant frequencies and the corresponding normal mode nodal patterns of the aluminum block are measured up to 75.64 kHz. Prominent peaks in the pencil lead fracture and sphere impact spectra from the two transducer locations corresponded exactly to resonant frequencies of the block. It is established that the resonant frequencies of the block dominated the spectral content of the output signal. The spectral content of the output signals is further influenced by the transducer location relative to the resonant frequency nodal lines. Implications of the results are discussed in relation to AU parameters and measurements.

E.A.K.

N83-23620*# National Aeronautics and Space Administration. Lewis Research Center, Cleveland, Ohio.

ULTRASONIC RANKING OF TOUGHNESS OF TUNGSTEN CARBIDE

A. VARY and D. R. HULL Apr. 1983 11 p refs Presented at the 14th Symp. on Nondestructive Evaluation, San Antonio, Tex., 19-21 Apr. 1983

(NASA-TM-83358; E-1619; NAS 1.15:83358) Avail: NTIS HC A02/MF A01 CSCL 14D

The feasibility of using ultrasonic attenuation measurements to rank tungsten carbide alloys according to their fracture toughness was demonstrated. Six samples of cobalt-cemented tungsten carbide (WC-Co) were examined. These varied in cobalt content from approximately 2 to 16 weight percent. The toughness generally increased with increasing cobalt content. Toughness was first determined by the Palmqvist and short rod fracture toughness tests. Subsequently, ultrasonic attenuation measurements were correlated with both these mechanical test methods. It is shown that there is a strong increase in ultrasonic attenuation corresponding to increased toughness of the WC-Co alloys. A correlation between attenuation and toughness exists for a wide range of ultrasonic frequencies. However, the best correlation for the WC-Co alloys occurs when the attenuation coefficient measured in the vicinity of 100 megahertz is compared with toughness as determined by the Palmqvist technique.

Author

N83-27248*# Virginia Polytechnic Inst. and State Univ., Blacksburg. Dept. of Engineering Science and Mechanics.

A STUDY OF THE STRESS WAVE FACTOR TECHNIQUE FOR THE CHARACTERIZATION OF COMPOSITE MATERIALS Final Report

E. G. HENNEKE, II, J. C. DUKE, JR., W. W. STINCHCOMB, A. GOVADA, and A. LEMASCON Washington Feb. 1983 74 p refs

(Contract NSG-3172)

(NASA-CR-3670; NAS 1.26:3670) Avail: NTIS HC A04/MF A01 CSCL 14D

A testing program was undertaken to provide an independent investigation and evaluation of the stress wave factor for characterizing the mechanical behavior of composite laminates. Some of the data which was obtained after performing a very large number of tests to determine the reproducibility of the SWF measurement is presented. It was determined that, with some optimizing of experimental parameters, the SWF value can be reproduced to within + or - 10%. Results are also given which show that, after careful calibration procedures, the lowest SWF value along the length of a specimen will correlate very closely to the site of final failure when the specimen is loaded in tension.

38 QUALITY ASSURANCE AND RELIABILITY

Finally, using a moire interferometry technique, it was found that local regions having the highest in plane strains under tensile loading also had the lowest SWF values. S.L.

N83-28466*# Massachusetts Inst. of Tech., Cambridge. Dept. of Mechanical Engineering.

ULTRASONIC ATTENUATION OF A VOID-CONTAINING MEDIUM FOR VERY LONG WAVELENGTHS Final Report

J. H. WILLIAMS, JR., S. S. LEE, and H. YUECE NASA Washington Jun. 1983 22 p refs
(Contract NSG-3210)
(NASA-CR-3693; NAS 1.26:3693) Avail: NTIS HC A02/MF A01 CSCL 14D

Ultrasonic longitudinal through-thickness attenuation in an isotropic medium due to scattering by randomly distributed voids is considered analytically. The attenuation is evaluated on the assumption of no interaction between voids. The scattered power is assumed to be entirely lost, thus accounting for the ultrasonic attenuation. The scattered power due to the presence of a void is described in terms of the scattering cross section of the void. An exact solution exists for the scattering cross section of a spherical void. An approximate solution for the scattering cross section of an ellipsoidal void is developed based on the so-called Born approximation commonly used in quantum mechanics. This approximate solution is valid for $k \sin \theta \ll 1$, where k is the wave number of the incident longitudinal wave and $\sin \theta$ is the largest dimension of the void. It is found that the shape of the void has negligible effect on the scattering cross section and that only the volume of the void is important. Thus, it is noted that in cases where $k \sin \theta \ll 1$, the exact scattering cross section of a spherical void having the same volume as an arbitrarily shaped void can be used for evaluating ultrasonic attenuation. M.G.

N83-33180*# Cleveland State Univ., Ohio. Coll. of Engineering. **THE EFFECT OF STRESS ON ULTRASONIC PULSES IN FIBER REINFORCED COMPOSITES Final Report**

J. H. HEMANN and G. Y. BAAKLINI Washington NASA Aug. 1983 80 p refs
(Contract NAG3-106)
(NASA-CR-3724; NAS 1.26:3724) Avail: NTIS HC A05/MF A01 CSCL 20K

An acoustical-ultrasonic technique was used to demonstrate relationships existing between changes in attenuation of stress waves and tensile stress for an eight ply 0 degree graphite-epoxy fiber reinforced composite. All tests were conducted in the linear range of the material for which no mechanical or macroscopic damage was evident. Changes in attenuation were measured as a function of tensile stress in the frequency domain and in the time domain. Stress wave propagation in these specimens was dispersive, i.e., the wave speed depends on frequency. Wave speeds varied from 267 400 cm/sec to 680 000 cm/sec as the frequency of the signal was varied from 150 kHz to 1.9 MHz which strongly suggests that flexural/lamb wave modes of propagation exist. The magnitude of the attenuation changes depended strongly on tensile stress. It was further observed that the wave speeds increased slightly for all tested frequencies as the stress was increased. Author

N83-33182*# Pratt and Whitney Aircraft Group, East Hartford, Conn.

SENSOR FAILURE DETECTION FOR JET ENGINES Final Report

E. C. BEATTIE, R. F. LAPRAD, M. M. AKHTER (Systems Control Technology), and S. M. ROCK (Systems Control Technology) May 1983 152 p refs
(Contract NAS3-23282)

(NASA-CR-168190; NAS 1.26:168190; PWA-5891-18) Avail: NTIS HC A08/MF A01 CSCL 14D

Revisions to the advanced sensor failure detection, isolation, and accommodation (DIA) algorithm, developed under the sensor failure detection system program were studied to eliminate the steady state errors due to estimation filter biases. Three algorithm

revisions were formulated and one revision for detailed evaluation was chosen. The selected version modifies the DIA algorithm to feedback the actual sensor outputs to the integral portion of the control for the nofailure case. In case of a failure, the estimates of the failed sensor output is fed back to the integral portion. The estimator outputs are fed back to the linear regulator portion of the control all the time. The revised algorithm is evaluated and compared to the baseline algorithm developed previously. E.A.K.

N84-14525*# Ohio State Univ., Columbus.

VOLUME INTEGRALS ASSOCIATED WITH THE INHOMOGENEOUS HELMHOLTZ EQUATION. PART 1: ELLIPSOIDAL REGION Final Report

L. S. FU and T. MURA Washington NASA Dec. 1983 19 p refs

(Contract NSG-3269)

(NASA-CR-3749; NAS 1.26:3749) Avail: NTIS HC A02/MF A01 CSCL 14D

Problems of wave phenomena in fields of acoustics, electromagnetics and elasticity are often reduced to an integration of the inhomogeneous Helmholtz equation. Results are presented for volume integrals associated with the Helmholtz operator, $\nabla^2 + \alpha^2$, for the case of an ellipsoidal region. By using appropriate Taylor series expansions and multinomial theorem, these volume integrals are obtained in series form for regions $r < r'$ and $r > r'$, where r and r' are distances from the origin to the point of observation and source, respectively. Derivatives of these integrals are easily evaluated. When the wave number approaches zero, the results reduce directly to the potentials of variable densities. M.G.

N84-14526*# Ohio State Univ., Columbus.

VOLUME INTEGRALS ASSOCIATED WITH THE INHOMOGENEOUS HELMHOLTZ EQUATION. PART 2: CYLINDRICAL REGION; RECTANGULAR REGION Final Report

W. F. ZHONG and L. S. FU Dec. 1983 22 p refs

(Contract NAG3-340)

(NASA-CR-3750; NAS 1.26:3750) Avail: NTIS HC A02/MF A01 CSCL 20K

Results are presented for volume integrals associated with the Helmholtz operator, $\nabla^2 + \alpha^2$, for the cases of a finite cylindrical region and a region of rectangular parallelepiped. By using appropriate Taylor series expansions and multinomial theorem, these volume integrals are obtained in series form for regions $r < r'$ and $r > r'$, where r and r' are distances from the origin to the point of observation and source, respectively. When the wave number approaches zero, the results reduce directly to the potentials of variable densities. M.G.

N84-15565*# Massachusetts Inst. of Tech., Cambridge. Dept. of Mechanical Engineering.

INPUT-OUTPUT CHARACTERIZATION OF AN ULTRASONIC TESTING SYSTEM BY DIGITAL SIGNAL ANALYSIS Final Report

H. KARAGUELLE, S. S. LEE, and J. WILLIAMS, JR. Washington NASA Jan. 1984 46 p refs

(Contract NAG3-328)

(NASA-CR-3756; E-1873; NAS 1.26:3756) Avail: NTIS HC A03/MF A01 CSCL 14D

The input/output characteristics of an ultrasonic testing system used for stress wave factor measurements were studied. The fundamentals of digital signal processing are summarized. The inputs and outputs are digitized and processed in a microcomputer using digital signal processing techniques. The entire ultrasonic test system, including transducers and all electronic components, is modeled as a discrete-time linear shift-invariant system. Then the impulse response and frequency response of the continuous time ultrasonic test system are estimated by interpolating the defining points in the unit sample response and frequency response of the discrete time system. It is found that the ultrasonic test system behaves as a linear phase bandpass filter. Good results were obtained for rectangular pulse inputs of various amplitudes and durations and for tone burst inputs whose center frequencies

are within the passband of the test system and for single cycle inputs of various amplitudes. The input/output limits on the linearity of the system are determined. E.A.K.

N84-17606*# Cleveland State Univ., Ohio. Coll. of Engineering.
PRELIMINARY INVESTIGATION OF AN ELECTRICAL NETWORK MODEL FOR ULTRASONIC SCATTERING Final Report

J. E. MAISEL Washington NASA Jan. 1984 46 p refs
(Contract NAG3-362)
(NASA-CR-3770; E-1895; NAS 1.26:3770) Avail: NTIS HC
A03/MF A01 CSCL 14D

The behavior of acoustic attenuation in a solid is related to the electrical transmission line model where the electrical shunt conductance, which is frequency dependent, represents the loss due to the scattering sites in the solid. Results indicate that the absolute value of attenuation at a given frequency depends on both the normalized mean square deviation of the density and bulk modulus of the scattering sites from the ambient medium and the spatial scattering correlation function. Besides establishing the absolute value of attenuation, the spatial correlation function determines the attenuation profile as a function of frequency.

S.L.

N84-32849*# National Aeronautics and Space Administration.
Lewis Research Center, Cleveland, Ohio.

THE ROLE OF THE REFLECTION COEFFICIENT IN PRECISION MEASUREMENT OF ULTRASONIC ATTENUATION

E. R. GENERAZIO 1984 30 p refs Presented at the Ann. Rev. of Progr. in Quantitative Nondestructive Evaluation, La Jolla, Calif., 8-13 Jul. 1984; sponsored by DARPA
(NASA-TM-83788; E-2185; NAS 1.15:83788) Avail: NTIS HC
A03/MF A01 CSCL 14D

Ultrasonic attenuation measurements using contact, pulse-echo techniques are sensitive to surface roughness and couplant thickness variations. This can reduce considerable inaccuracies in the measurement of the attenuation coefficient for broadband pulses. Inaccuracies arise from variations in the reflection coefficient at the buffer-couplant-sample interface. The reflection coefficient is examined as a function of the surface roughness and corresponding couplant thickness variations. Interrelations with ultrasonic frequency are illustrated. Reliable attenuation measurements are obtained only when the frequency dependence of the reflection coefficient is incorporated in signal analysis. Data are given for nickel 200 samples and a silicon nitride ceramic bar having surface roughness variations in the 0.3 to 3.0 microns range for signal bandwidths in the 50 to 100 MHz range. Author

N84-34769*# National Aeronautics and Space Administration.
Lewis Research Center, Cleveland, Ohio.

ULTRASONIC VELOCITY MEASUREMENT USING PHASE-SLOPE CROSS-CORRELATION METHODS

D. R. HULL, H. E. KAUTZ, and A. VARY 1984 20 p refs
Presented at 1984 Spring Conf. of the Am. Soc. for Nondestructive Testing, Denver, 21-24 May 1984
(NASA-TM-83794; E-2290; NAS 1.15:83794) Avail: NTIS HC
A02/MF A01 CSCL 14D

Computer implemented phase-slope and cross-correlation methods are introduced for measuring time delays between pairs of broadband ultrasonic pulse-echo signals for determining velocity in engineering materials. The phase-slope and cross-correlation methods are compared with the overlap method which is currently in wide use. Comparison of digital versions of the three methods shows similar results for most materials having low ultrasonic attenuation. However, the cross-correlation method is preferred for highly attenuating materials. An analytical basis for the cross-correlation method is presented. Examples are given for the three methods investigated to measure velocity in representative materials in the megahertz range. Author

N85-10371*# National Aeronautics and Space Administration.
Lewis Research Center, Cleveland, Ohio.

ULTRASONIC NONDESTRUCTIVE EVALUATION, MICROSTRUCTURE, AND MECHANICAL PROPERTY INTERRELATIONS

A. VARY Washington Oct. 1984 30 p refs
(NASA-TM-86876; E-2337; NAS 1.15:86876) Avail: NTIS HC
A03/MF A01 CSCL 14D

Ultrasonic techniques for mechanical property characterizations are reviewed and conceptual models are advanced for explaining and interpreting the empirically based results. At present, the technology is generally empirically based and is emerging from the research laboratory. Advancement of the technology will require establishment of theoretical foundations for the experimentally observed interrelations among ultrasonic measurements, mechanical properties, and microstructure. Conceptual models are applied to ultrasonic assessment of fracture toughness to illustrate an approach for predicting correlations found among ultrasonic measurements, microstructure, and mechanical properties.

R.S.F.

N85-16195*# Ohio State Univ., Columbus.

FUNDAMENTALS OF MICROCRACK NUCLEATION MECHANICS Final Report

L. S. FU, Y. C. SHEU, C. M. CO, W. F. ZHONG, and H. D. SHEN
NASA Washington Jan. 1985 86 p refs
(Contract NAG3-340)

(NASA-CR-3851; E-2296; NAS 1.26:3851; RFP763340/714952)
Avail: NTIS HC A05/MF A01 CSCL 20K

A foundation for ultrasonic evaluation of microcrack nucleation mechanics is identified in order to establish a basis for correlations between plane strain fracture toughness and ultrasonic factors through the interaction of elastic waves with material microstructures. Since microcracking is the origin of (brittle) fracture, it is appropriate to consider the role of stress waves in the dynamics of microcracking. Therefore, the following topics are discussed: (1) microstress distributions with typical microstructural defects located in the stress field; (2) elastic wave scattering from various idealized defects; and (3) dynamic effective-properties of media with randomly distributed inhomogeneities.

R.S.F.

N85-20389*# National Aeronautics and Space Administration.
Lewis Research Center, Cleveland, Ohio.

NDE FOR HEAT ENGINE CERAMICS

S. J. KLIMA 1984 13 p refs Presented at 22nd Automotive Technol. Develop. Contractors Coordination Meeting (ATD/CCM), 29 Oct. - 2 Nov. 1984, Dearborn, Mich.; sponsored by Society of Automotive Engineers
(NASA-TM-86949; E-2470; NAS 1.15:86949) Avail: NTIS HC
A02/MF A01 CSCL 14B

Radiographic, ultrasonic, and scanning laser acoustic microscopy (SLAM) techniques were used to characterize silicon nitride and silicon carbide MOR bars in various stages of fabrication. Conventional and microfocus x-ray techniques were found capable of detecting minute high density inclusions in as-received powders, green compacts, and fully densified specimens. Significant density gradients in sintered bars were observed by radiography, ultrasonic velocity, and SLAM. Ultrasonic attenuation was found sensitive to microstructural variations due to grain and void morphology and distribution. SLAM was also capable of detecting voids, inclusions, and cracks in finished test bars. It was determined that thermoacoustic microscopy techniques have promise for application to green and densified ceramics.

R.J.F.

38 QUALITY ASSURANCE AND RELIABILITY

N85-20390*# Massachusetts Inst. of Tech., Cambridge.
STRESS WAVES IN AN ISOTROPIC ELASTIC PLATE EXCITED BY A CIRCULAR TRANSDUCER Final Report

H. KARAGULLE, J. H. WILLIAMS, JR., and S. S. LEE
Washington NASA Mar. 1985 52 p refs

(Contract NAG3-328)

(NASA-CR-3877; NAS 1.26:3877) Avail: NTIS HC A04/MF A01 CSCL 14D

Steady state harmonic stress waves in an isotropic elastic plate excited on one face by a circular transducer are analyzed theoretically. The transmitting transducer transforms an electrical voltage into a uniform normal stress at the top of the plate. To solve the boundary value problem, the radiation into a half-space is considered. The receiving transducer produces an electrical voltage proportional to the average spatially integrated normal stress over its face due to an incident wave. A numerical procedure is given to evaluate the frequency response at a receiving point due to a multiply reflected wave in the near field. Its stability and convergence are discussed. Parameterization plots which determine the particular wave whose frequency response has maximum magnitude compared with other multiple reflected waves are given for a range of values of dimensionless parameters. The effects of changes in the values of the parameters are discussed.

B.G.

N85-21673*# Massachusetts Inst. of Tech., Cambridge. Dept. of Mechanical Engineering.

APPLICATION OF HOMOMORPHIC SIGNAL PROCESSING TO STRESS WAVE FACTOR ANALYSIS

H. KARAGULLE, J. H. WILLIAMS, JR., and S. S. LEE Feb. 1985 48 p refs

(Contract NSG-3328)

(NAS 1.26:174871; NASA-CR-174871) Avail: NTIS HC A03/MF A01 CSCL 14D

The stress wave factor (SWF) signal, which is the output of an ultrasonic testing system where the transmitting and receiving transducers are coupled to the same face of the test structure, is analyzed in the frequency domain. The SWF signal generated in an isotropic elastic plate is modeled as the superposition of successive reflections. The reflection which is generated by the stress waves which travel p times as a longitudinal (P) wave and s times as a shear (S) wave through the plate while reflecting back and forth between the bottom and top faces of the plate is designated as the reflection with p, s . Short-time portions of the SWF signal are considered for obtaining spectral information on individual reflections. If the significant reflections are not overlapped, the short-time Fourier analysis is used. A summary of the relevant points of homomorphic signal processing, which is also called cepstrum analysis, is given. Homomorphic signal processing is applied to short-time SWF signals to obtain estimates of the log spectra of individual reflections for cases in which the reflections are overlapped. Two typical SWF signals generated in aluminum plates (overlapping and non-overlapping reflections) are analyzed.

M.G.

N85-21674*# National Aeronautics and Space Administration. Lewis Research Center, Cleveland, Ohio.

RADIOGRAPHIC DETECTABILITY LIMITS FOR SEEDED VOIDS IN SINTERED SILICON CARBIDE AND SILICON NITRIDE

G. Y. BAAKLINI (Cleveland State Univ.), J. D. KISER, and D. J. ROTH 1984 19 p refs Presented at the Regional Meeting of the American Ceramic Society, San Francisco, 28-31 Oct. 1984

(NASA-TM-86945; E-2464; NAS 1.15:86945) Avail: NTIS HC A02/MF A01 CSCL 14D

Conventional and microfocus X-radiographic techniques were compared to determine relative detectability limits for voids in green and sintered SiC and Si₃N₄. The relative sensitivity of the techniques was evaluated by comparing their ability to detect voids that were artificially introduced by a seeding process. For projection microfocus radiography the sensitivity of void detection at a 90/95 probability of detection/confidence level is 1.5% of specimen thickness in sintered SiC and Si₃N₄. For conventional contact

radiography the sensitivity is 2.5% of specimen thickness. It appears that microfocus projection radiography is preferable to conventional contact radiography in cases where increased sensitivity is required and where the additional complexity of the technique can be tolerated.

E.A.K.

N85-29307*# Massachusetts Inst. of Tech., Cambridge. Dept. of Mechanical Engineering.

ULTRASONIC TESTING OF PLATES CONTAINING EDGE CRACKS Final Report

J. H. WILLIAMS, JR., H. KARAGULLE, and S. S. LEE
Washington NASA Jun. 1985 37 p refs

(Contract NAG3-328)

(NASA-CR-3904; E-2550; NAS 1.26:3904) Avail: NTIS HC A03/MF A01 CSCL 14D

The stress wave factor (SWF) signal is utilized for the nondestructive evaluation of plates containing perpendicular edge cracks. The effects of the existence lateral location and depth of the crack on the magnitude spectra of individual reflections in the SWF signal are studied. If the reflections in the SWF signal are not overlapped the short time Fourier analysis is applied. If the reflections are overlapped the short time homomorphic analysis (cepstrum analysis) is applied. Several reflections which have average resonant frequencies approximately at 0.9, 1.3, and 1.7 MHz are analyzed. It is observed that the magnitude ratios evaluated at average resonant frequencies decrease more with increasing d/h if the crack is located between the transducers, where h is plate thickness and d is crack depth. Moreover, for the plates, crack geometries, reflections, and frequencies considered, the average decibel drop depends mainly on the dimensionless parameter d/h and it is approximately -1 dB per 0.07 d/h . Changes in the average resonant frequencies of the magnitude spectra are also observed due to changes in the location of the crack.

B.W.

N85-32337*# National Aeronautics and Space Administration. Lewis Research Center, Cleveland, Ohio.

RELIABILITY OF VOID DETECTION IN STRUCTURAL CERAMICS USING SCANNING LASER ACOUSTIC MICROSCOPY

D. J. ROTH, S. J. KLIMA, J. D. KISER, and G. Y. BAAKLINI (Cleveland State Univ.) 1985 54 p refs Presented at the Spring Meeting of the Am. Soc. for Nondestructive Testing, Washington, D.C., 11-14 Mar. 1985

(NASA-TM-87035; E-2591; NAS 1.15:87035) Avail: NTIS HC A04/MF A01 CSCL 14D

The reliability of scanning laser acoustic microscopy (SLAM) for detecting surface voids in structural ceramic test specimens was statistically evaluated. Specimens of sintered silicon nitride and sintered silicon carbide, seeded with surface voids, were examined by SLAM at an ultrasonic frequency of 100 MHz in the as fired condition and after surface polishing. It was observed that polishing substantially increased void detectability. Voids as small as 100 micrometers in diameter were detected in polished specimens with 0.90 probability at a 0.95 confidence level. In addition, inspection times were reduced up to a factor of 10 after polishing. The applicability of the SLAM technique for detection of naturally occurring flaws of similar dimensions to the seeded voids is discussed. A FORTRAN program listing is given for calculating and plotting flaw detection statistics.

Author

N86-10561*# National Aeronautics and Space Administration. Lewis Research Center, Cleveland, Ohio.

ULTRASONIC EVALUATION OF MECHANICAL PROPERTIES OF THICK, MULTILAYERED, FILAMENT WOUND COMPOSITES

H. E. KAUTZ Sep. 1985 36 p refs

(NASA-TM-87088; E-2676; NAS 1.15:87088) Avail: NTIS HC A03/MF A01 CSCL 14D

A preliminary investigation is conducted to define capabilities and limitations of ultrasonic and acousto-ultrasonic measurements related to mechanical properties of filament wound graphite/epoxy composite structures. The structures studied are segments of filament wound cylinders formed of multiple layers of hoop and

helical windings. The segments consist of 24 to 35 layers and range from 3.02 to 3.34 cm in wall thickness. The resultant structures are anisotropic, heterogeneous, porous, and highly attenuating to ultrasonic frequencies greater than 1 MHz. The segments represent structures to be used for space shuttle booster cases. Ultrasonic velocity and acousto-ultrasonic stress wave factor measurement approaches are discussed. Correlations among velocity, density, and porosity, and between the acousto-ultrasonic stress wave factor and interlaminar shear strength are presented.

Author

N86-13749*# National Aeronautics and Space Administration. Lewis Research Center, Cleveland, Ohio.

PROBABILITY OF DETECTION OF INTERNAL VOIDS IN STRUCTURAL CERAMICS USING MICROFOCUS RADIOGRAPHY

G. Y. BAAKLINI and D. J. ROTH Nov. 1985 23 p refs (NASA-TM-87164; E-2800; NAS 1.15:87164) Avail: NTIS HC A02/MF A01 CSCL 14D

The reliability of microfocus x-radiography for detecting subsurface voids in structural ceramic test specimens was statistically evaluated. The microfocus system was operated in the projection mode using low X-ray photon energies (20 keV) and a 10 micro m focal spot. The statistics were developed for implanted subsurface voids in green and sintered silicon carbide and silicon nitride test specimens. These statistics were compared with previously-obtained statistics for implanted surface voids in similar specimens. Problems associated with void implantation are discussed. Statistical results are given as probability-of-detection curves at a 95 percent confidence level for voids ranging in size from 20 to 528 micro m in diameter.

Author

N86-16598*# National Aeronautics and Space Administration. Lewis Research Center, Cleveland, Ohio.

NDE OF STRUCTURAL CERAMICS

S. J. KLIMA and A. VARY 1986 14 p refs Proposed for presentation at the 31st International Gas Turbine Conference, Dusseldorf, West Germany, 8-12 Jun. 1986; sponsored by ASME (NASA-TM-87186; E-2840; NAS 1.15:87186) Avail: NTIS HC A02/MF A01 CSCL 14D

Radiographic, ultrasonic, scanning laser acoustic microscopy (SLAM), and thermo-acoustic microscopy techniques were used to characterize silicon nitride and silicon carbide modulus-of-rupture test specimens in various stages of fabrication. Conventional and microfocus X-ray techniques were found capable of detecting minute high density inclusions in as-received powders, green compacts, and fully densified specimens. Significant density gradients in sintered bars were observed by radiography, ultrasonic velocity, and SLAM. Ultrasonic attenuation was found sensitive to microstructural variations due to grain and void morphology and distribution. SLAM was also capable of detecting voids, inclusions and cracks in finished test bars. Consideration is given to the potential for applying thermo-acoustic microscopy techniques to green and densified ceramics. The detection probability statistics and some limitations of radiography and SLAM also are discussed.

Author

N86-16599*# National Aeronautics and Space Administration. Lewis Research Center, Cleveland, Ohio.

RELIABILITY OF SCANNING LASER ACOUSTIC MICROSCOPY FOR DETECTING INTERNAL VOIDS IN STRUCTURAL CERAMICS

D. J. ROTH and G. Y. BAAKLINI 1986 36 p refs Presented at the 10th Annual Conference on Composites and Advanced Ceramic Materials, Cocoa Beach, Fla., 19-22 Jan. 1986; sponsored by the American Ceramic Society (NASA-TM-87222; E-2864; NAS 1.15:87222) Avail: NTIS HC A03/MF A01 CSCL 14D

The reliability of 100 MHz scanning laser acoustic microscopy (SLAM) for detecting internal voids in sintered specimens of silicon nitride and silicon carbide was evaluated. The specimens contained artificially implanted voids and were positioned at depths ranging up to 2 mm below the specimen surface. Detection probability of

0.90 at a 0.95 confidence level was determined as a function of material, void diameter, and void depth. The statistical results presented for void detectability indicate some of the strengths and limitations of SLAM as a nondestructive evaluation technique for structural ceramics.

Author

N86-19636*# National Aeronautics and Space Administration. Lewis Research Center, Cleveland, Ohio.

NONDESTRUCTIVE TECHNIQUES FOR CHARACTERIZING MECHANICAL PROPERTIES OF STRUCTURAL MATERIALS: AN OVERVIEW

A. VARY and S. J. KLIMA Dec. 1985 21 p refs Proposed for presentation at the 31st International Gas Turbine Conference, Dusseldorf, West Germany, 8-12 Jun. 1986; sponsored by ASME (NASA-TM-87203; E-2858; NAS 1.15:87203) Avail: NTIS HC A02/MF A01 CSCL 14D

An overview of nondestructive evaluation (NDE) is presented to indicate the availability and application potentials of techniques for quantitative characterization of the mechanical properties of structural materials. The purpose is to review NDE techniques that go beyond the usual emphasis on flaw detection and characterization. Discussed are current and emerging NDE techniques that can verify and monitor intrinsic properties (e.g., tensile, shear, and yield strengths; fracture toughness, hardness, ductility; elastic moduli) and underlying microstructural and morphological factors. Most of the techniques described are, at present, neither widely applied nor widely accepted in commerce and industry because they are still emerging from the laboratory. The limitations of the techniques may be overcome by advances in applications research and instrumentation technology and perhaps by accommodations for their use in the design of structural parts.

Author

N86-22962*# National Aeronautics and Space Administration. Lewis Research Center, Cleveland, Ohio.

ANALYTICAL ULTRASONICS IN MATERIALS RESEARCH AND TESTING

A. VARY Jan. 1986 357 p refs Conference held in Cleveland, Ohio, 13-14 Nov. 1984 (NASA-CP-2383; E-2486; NAS 1.55:2383) Avail: NTIS HC A16/MF A01 CSCL 20A

Research results in analytical ultrasonics for characterizing structural materials from metals and ceramics to composites are presented. General topics covered by the conference included: status and advances in analytical ultrasonics for characterizing material microstructures and mechanical properties; status and prospects for ultrasonic measurements of microdamage, degradation, and underlying morphological factors; status and problems in precision measurements of frequency-dependent velocity and attenuation for materials analysis; procedures and requirements for automated, digital signal acquisition, processing, analysis, and interpretation; incentives for analytical ultrasonics in materials research and materials processing, testing, and inspection; and examples of progress in ultrasonics for interrelating microstructure, mechanical properties, and dynamic response.

N86-25002*# Massachusetts Inst. of Tech., Cambridge. Dept. of Mechanical Engineering.

STRESS WAVES IN TRANSVERSELY ISOTROPIC MEDIA: THE HOMOGENEOUS PROBLEM Final Report

E. R. C. MARQUES and J. H. WILLIAMS, JR. Washington NASA May 1986 48 p refs (Contract NAG3-328) (NASA-CR-3977; E-2949; NAS 1.26:3977) Avail: NTIS HC A03/MF A01 CSCL 14D

The homogeneous problem of stress wave propagation in unbounded transversely isotropic media is analyzed. By adopting plane wave solutions, the conditions for the existence of the solution are established in terms of phase velocities and directions of particle displacements. Dispersion relations and group velocities are derived from the phase velocity expressions. The deviation angles (e.g., angles between the normals to the adopted plane waves and the actual directions of their propagation) are numerically

38 QUALITY ASSURANCE AND RELIABILITY

determined for a specific fiber-glass epoxy composite. A graphical method is introduced for the construction of the wave surfaces using magnitudes of phase velocities and deviation angles. The results for the case of isotropic media are shown to be contained in the solutions for the transversely isotropic media. Author

N86-25003*# Pratt and Whitney Aircraft, East Hartford, Conn. Engineering Div.

LIFE PREDICTION AND CONSTITUTIVE MODELS FOR ENGINE HOT SECTION ANISOTROPIC MATERIALS PROGRAM Annual Status Report

G. A. SWANSON, I. LINASK, D. M. NISSLEY, P. P. NORRIS, T. G. MEYER, and K. P. WALKER Feb. 1986 203 p refs (Contract NAS3-23939)

(NASA-CR-174952; NAS 1.26:174952; PWA-5968-19) Avail:

NTIS HC A09/MF A01 CSCL 14D

This report presents the results of the first year of a program designed to develop life prediction and constitutive models for two coated single crystal alloys used in gas turbine airfoils. The two alloys are PWA 1480 and Alloy 185. The two oxidation resistant coatings are PWA 273, an aluminide coating, and PWA 286, an overlay NiCoCrAlY coating. To obtain constitutive and/or fatigue data, tests were conducted on coated and uncoated PWA 1480 specimens tensile loaded in the 100, 110, 111, and 123 directions. A literature survey of constitutive models was completed for both single crystal alloys and metallic coating materials; candidate models were selected. One constitutive model under consideration for single crystal alloys applies Walker's micromechanical viscoplastic formulation to all slip systems participating in the single crystal deformation. The constitutive models for the overlay coating correlate the viscoplastic data well. For the aluminide coating, a unique test method is under development. LCF and TMF tests are underway. The two coatings caused a significant drop in fatigue life, and each produced a much different failure mechanism. Author

N86-25812*# National Aeronautics and Space Administration. Lewis Research Center, Cleveland, Ohio.

CONCEPTS FOR INTERRELATING ULTRASONIC ATTENUATION, MICROSTRUCTURE AND FRACTURE TOUGHNESS IN POLYCRYSTALLINE SOLIDS

A. VARY May 1986 30 p refs Presented at the Symposium on Solid Mechanics Research of Quantitative NDE, Evanston, Ill., 18-20 Sep. 1985

(NASA-TM-87339; E-3086; NAS 1.15:87339) Avail: NTIS HC A03/MF A01 CSCL 14D

Conceptual models are advanced for explaining and predicting empirical correlations found between ultrasonic measurements and fracture toughness of polycrystalline solids. The models lead to insights concerning microstructural factors governing fracture processes and associated stress wave interactions. Analysis of the empirical correlations suggested by the models indicate that, in addition to grain size and shape, grain boundary reflections, elastic anisotropy, and dislocation damping are factors that underly both fracture toughness and ultrasonic attenuation. One outcome is that ultrasonic attenuation can predict the size of crack blunting or process zones that develop in the vicinity active cracks in metals. This forms a basis for ultrasonic ranking according to variations in fracture toughness. Author

N86-27665*# Virginia Polytechnic Inst. and State Univ., Blacksburg. Dept. of Engineering Science and Mechanics.

ULTRASONIC STRESS WAVE CHARACTERIZATION OF COMPOSITE MATERIALS Final Report

J. C. DUKE, JR., E. G. HENNEKE, II, and W. W. STINCHCOMB Washington NASA May 1986 161 p (Contract NAG3-323)

(NASA-CR-3976; E-2948; NAS 1.26:3976) Avail: NTIS HC A08/MF A01 CSCL 14D

The report covered three simultaneous projects. The first project was concerned with: (1) establishing the sensitivity of the acousto-ultrasonic method for evaluating subtle forms of damage development in cyclically loaded composite materials, (2)

establishing the ability of the acousto-ultrasonic method for detecting initial material imperfections that lead to localized damage growth and final specimen failure, and (3) characteristics of the NBS/Proctor sensor/receiver for acousto-ultrasonic evaluation of laminated composite materials. The second project was concerned with examining the nature of the wave propagation that occurs during acoustic-ultrasonic evaluation of composite laminates and demonstrating the role of Lamb or plate wave modes and their utilization for characterizing composite laminates. The third project was concerned with the replacement of contact-type receiving piezotransducers with noncontacting laser-optical sensors for acousto-ultrasonic signal acquisition. Author

N86-27666*# Massachusetts Inst. of Tech., Cambridge. Dept. of Mechanical Engineering.

WAVE PROPAGATION IN ANISOTROPIC MEDIUM DUE TO AN OSCILLATORY POINT SOURCE WITH APPLICATION TO UNIDIRECTIONAL COMPOSITES Final Report

J. H. WILLIAMS, JR., E. R. C. MARQUES, and S. S. LEE Washington NASA Jul. 1986 59 p

(Contract NAG3-328)

(NASA-CR-4001; E-3093; NAS 1.26:4001) Avail: NTIS HC A04/MF A01 CSCL 14D

The far-field displacements in an infinite transversely isotropic elastic medium subjected to an oscillatory concentrated force are derived. The concepts of velocity surface, slowness surface and wave surface are used to describe the geometry of the wave propagation process. It is shown that the decay of the wave amplitudes depends not only on the distance from the source (as in isotropic media) but also depends on the direction of the point of interest from the source. As an example, the displacement field is computed for a laboratory fabricated unidirectional fiberglass epoxy composite. The solution for the displacements is expressed as an amplitude distribution and is presented in polar diagrams. This analysis has potential usefulness in the acoustic emission (AE) and ultrasonic nondestructive evaluation of composite materials. For example, the transient localized disturbances which are generally associated with AE sources can be modeled via this analysis. In which case, knowledge of the displacement field which arrives at a receiving transducer allows inferences regarding the strength and orientation of the source, and consequently perhaps the degree of damage within the composite. Author

N86-28250*# Aerojet Technical Systems Co., Sacramento, Calif.

LONGITUDINAL MODE COMBUSTION INSTABILITIES OF A HIGH-PRESSURE FUEL-RICH LOX/RP-1 PREBURNER

J. J. FANG In Johns Hopkins Univ. The 22nd JANNAF Combustion Meeting, Vol. 1 p 429-441 Oct. 1985

(Contract NAS3-22647)

Avail: CPIA, Laurel, Md. 20707 HC \$70.00 CSCL 21B

During the hot-fire testing of a high-pressure fuel-rich LOX/RP-1 preburner, longitudinal mode combustion instabilities were observed. The experimental data showing how the instability varied with the chamber pressure, mixture ratio, chamber length and turbulence ring are given. Technical rationales are given for the test-to-test hardware configuration changes that eventually led to the stable result. Author

N86-28445*# Virginia Polytechnic Inst. and State Univ., Blacksburg. Dept. of Engineering Science and Mechanics.

A STUDY OF THE STRESS WAVE FACTOR TECHNIQUE FOR NONDESTRUCTIVE EVALUATION OF COMPOSITE MATERIALS Final Report

A. SARRAFZADEH-KHOEE, M. T. KIERNAN, J. C. DUKE, JR., and E. G. HENNEKE, II Washington NASA Jul. 1986 33 p (Contract NAG3-172)

(NASA-CR-4002; E-3081; NAS 1.26:4002) Avail: NTIS HC A03/MF A01 CSCL 14D

The acousto-ultrasonic method of nondestructive evaluation is an extremely sensitive means of assessing material response. Efforts continue to complete the understanding of this method. In order to achieve the full sensitivity of the technique, extreme care

must be taken in its performance. This report provides an update of the efforts to advance the understanding of this method and to increase its application to the nondestructive evaluation of composite materials. Included are descriptions of a novel optical system that is capable of measuring in-plane and out-of-plane displacements, an IBM PC-based data acquisition system, an extensive data analysis software package, the azimuthal variation of acousto-ultrasonic behavior in graphite/epoxy laminates, and preliminary examination of processing variation in graphite-aluminum tubes. Author

N86-31065*# National Aeronautics and Space Administration. Lewis Research Center, Cleveland, Ohio.

DETERMINATION OF GRAIN SIZE DISTRIBUTION FUNCTION USING TWO-DIMENSIONAL FOURIER TRANSFORMS OF TONE PULSE ENCODED IMAGES

E. R. GENERAZIO Jun. 1986 24 p
(NASA-TM-88790; E-3125; NAS 1.15:88790) Avail: NTIS HC A02/MF A01 CSCL 11F

Microstructural images may be tone pulse encoded and subsequently Fourier transformed to determine the two-dimensional density of frequency components. A theory is developed relating the density of frequency components to the density of length components. The density of length components corresponds directly to the actual grain size distribution function from which the mean grain shape, size, and orientation can be obtained. Author

N86-31912*# National Aeronautics and Space Administration. Lewis Research Center, Cleveland, Ohio.

FACTORS THAT AFFECT RELIABILITY OF NONDESTRUCTIVE DETECTION OF FLAWS IN STRUCTURAL CERAMICS

S. J. KLIMA, G. Y. BAAKLINI (Cleveland State Univ., Ohio), and D. J. ROTH 1986 11 p Presented at the 2nd International Symposium on Ceramic Materials and Components for Engines, Luebeck-Travemuende, West Germany, 14-17 Apr. 1986; sponsored by the German Ceramic Society and the American Ceramic Society
(NASA-TM-87348; E-3096; NAS 1.15:87348) Avail: NTIS HC A02/MF A01 CSCL 14D

The factors that affect reliability of nondestructive detection of flaws in structural ceramics by microfocus radiography and scanning laser acoustic microscopy (SLAM) were investigated. Reliability of void detection in silicon nitride and silicon carbide by microfocus X-rays was affected by photon energy level, material chemistry in the immediate vicinity of the void, and the presence of loose powder aggregates inside the void cavity. The sensitivity of SLAM to voids was affected by material microstructure, the level of porosity, and the condition of the specimen surfaces. Statistical results are presented in the form of probability of detection as a function of void diameter for green compacts and sintered materials. Author

N86-31913*# National Aeronautics and Space Administration. Lewis Research Center, Cleveland, Ohio.

QUANTITATIVE VOID CHARACTERIZATION IN STRUCTURAL CERAMICS USING SCANNING LASER ACOUSTIC MICROSCOPY

D. J. ROTH, E. R. GENERAZIO, and G. Y. BAAKLINI (Cleveland State Univ., Ohio) 1986 23 p Proposed for presentation at the Basic Science, Electronics and Glass Divisions Joint Meeting, New Orleans, La., 2-5 Nov. 1986; sponsored by American Ceramic Society
(NASA-TM-88797; E-3166; NAS 1.15:88797) Avail: NTIS HC A02/MF A01 CSCL 14D

The ability of scanning laser acoustic microscopy (SLAM) to characterize artificially seeded voids in sintered silicon nitride structural ceramic specimens was investigated. Using trigonometric relationships and Airy's diffraction theory, predictions of internal void depth and size were obtained from acoustic diffraction patterns produced by the voids. Agreement was observed between actual and predicted void depths. However, predicted void diameters were generally much greater than actual diameters. Precise diameter

predictions are difficult to obtain due to measurement uncertainty and the limitations of 100 MHz SLAM applied to typical ceramic specimens. Author

N86-32764*# National Aeronautics and Space Administration. Lewis Research Center, Cleveland, Ohio.

ACOUSTO-ULTRASONIC VERIFICATION OF THE STRENGTH OF FILAMENT WOUND COMPOSITE MATERIAL

H. E. KAUTZ 1986 24 p Presented at the Pressure Vessel Conference, Chicago, Ill., 21-24 Jul. 1986; sponsored by the American Society of Mechanical Engineers
(NASA-TM-88827; E-3201; NAS 1.15:88827) Avail: NTIS HC A02/MF A01 CSCL 14D

The concept of acousto-ultrasonic (AU) waveform partitioning was applied to nondestructive evaluation of mechanical properties in filament wound composites (FWC). A series of FWC test specimens were subjected to AU analysis and the results were compared with destructively measured interlaminar shear strengths (ISS). AU stress-wave factor (SWF) measurements gave greater than 90 percent correlation coefficient upon regression against the ISS. This high correlation was achieved by employing the appropriate time and frequency domain partitioning as dictated by wave propagation path analysis. There is indication that different SWF frequency partitions are sensitive to ISS at different depths below the surface. Author

N87-10399*# National Aeronautics and Space Administration. Lewis Research Center, Cleveland, Ohio.

ULTRASONIC DETERMINATION OF RECRYSTALLIZATION

E. R. GENERAZIO 1986 15 p Presented at the Review of Progress in Quantitative NDE, La Jolla, Calif. 3-8 Aug. 1986; sponsored by Ames Lab. and Iowa State Univ.
(NASA-TM-88855; E-3248; NAS 1.15:88855) Avail: NTIS HC A02/MF A01 CSCL 14D

Ultrasonic attenuation was measured for cold worked Nickel 200 samples annealed at increasing temperatures. Localized dislocation density variations, crystalline order and volume percent of recrystallized phase were determined over the anneal temperature range using transmission electron microscopy, X-ray diffraction, and metallurgy. The exponent of the frequency dependence of the attenuation was found to be a key variable relating ultrasonic attenuation to the thermal kinetics of the recrystallization process. Identification of this key variable allows for the ultrasonic determination of onset, degree, and completion of recrystallization. B.G.

N87-12910*# National Aeronautics and Space Administration. Lewis Research Center, Cleveland, Ohio.

NDE RELIABILITY AND PROCESS CONTROL FOR STRUCTURAL CERAMICS

G. Y. BAAKLINI 1986 17 p Proposed for presentation at the 32nd International Gas Turbine Conference and Exhibition, Anaheim, Calif., 31 May - 4 Jun. 1987; sponsored by ASME
(NASA-TM-88870; E-3276; NAS 1.15:88870) Avail: NTIS HC A02/MF A01 CSCL 14D

The reliability of microfocus x-radiography and scanning laser acoustic microscopy for detecting microvoids in silicon nitride and silicon carbide was statistically evaluated. Materials- and process-related parameters that influenced the statistical findings in research samples are discussed. The use of conventional x-radiography in controlling and optimizing the processing and sintering of an Si₃N₄-SiO₂-Y₂O₃ composition designated NASA 6Y is described. Radiographic evaluation and guidance helped develop uniform high-density Si₃N₄ modulus-of-rupture bars with improved four-point flexural strength (857, 544, and 462 MPa at room temperature, 1200 C, and 1370 C, respectively) and reduced strength scatter. Author

N87-18109*# National Aeronautics and Space Administration. Lewis Research Center, Cleveland, Ohio.

NONDESTRUCTIVE EVALUATION OF STRUCTURAL CERAMICS

STANLEY J. KLIMA, GEORGE Y. BAAKLINI (Cleveland State Univ., Ohio), and PHILLIP B. ABEL 1987 23 p Presented at the 24th Automotive Technology Development Contractors Coordination Meeting, Dearborn, Mich., 27-30 Oct. 1986; sponsored by DOE

(NASA-TM-88978; E-3446; NAS 1.15:88978) Avail: NTIS HC A02/MF A01 CSCL 14D

A review is presented on research and development of techniques for nondestructive evaluation and characterization of advanced ceramics for heat engine applications. Highlighted in this review are Lewis Research Center efforts in microfocus radiography, scanning laser acoustic microscopy (SLAM), scanning acoustic microscopy (SAM), scanning electron acoustic microscopy (SEAM), and photoacoustic microscopy (PAM). The techniques were evaluated by applying them to research samples of green and sintered silicon nitride and silicon carbide in the form of modulus-of-rupture bars containing seeded voids. Probabilities of detection of voids were determined for diameters as small as 20 microns for microfocus radiography, SLAM, and SAM. Strengths and limitations of the techniques for ceramic applications are identified. Application of ultrasonics for characterizing ceramic microstructures is also discussed. Author

N87-20562*# National Aeronautics and Space Administration. Lewis Research Center, Cleveland, Ohio.

THE ACOUSTO-ULTRASONIC APPROACH

ALEX VARY 1987 30 p Prepared for presentation at the Conference on Acousto-Ultrasonics: Theory and Application, Blacksburg, Va., 12-15 Jul. 1987; sponsored in part by NASA and American Society for Nondestructive Testing (NASA-TM-89843; E-3504; NAS 1.15:89843) Avail: NTIS HC A03/MF A01 CSCL 14D

The nature and underlying rationale of the acousto-ultrasonic approach is reviewed, needed advanced signal analysis and evaluation methods suggested, and application potentials discussed. Acousto-ultrasonics is an NDE technique combining aspects of acoustic emission methodology with ultrasonic simulation of stress waves. This approach uses analysis of simulated stress waves for detecting and mapping variations of mechanical properties. Unlike most NDE, acousto-ultrasonics is less concerned with flaw detection than with the assessment of the collective effects of various flaws and material anomalies. Acousto-ultrasonics has been applied chiefly to laminated and filament-wound fiber reinforced composites. It has been used to assess the significant strength and toughness reducing effects that can be wrought by combinations of essentially minor flaws and diffuse flaw populations. Acousto-ultrasonics assesses integrated defect states and the resultant variations in properties such as tensile, shear, and flexural strengths and fracture resistance. Matrix cure state, porosity, fiber orientation, fiber volume fraction, fiber-matrix bonding, and interlaminar bond quality are underlying factors. Author

N87-23987*# National Aeronautics and Space Administration. Lewis Research Center, Cleveland, Ohio.

APPLICATION OF SCANNING ACOUSTIC MICROSCOPY TO ADVANCED STRUCTURAL CERAMICS

ALEX VARY and STANLEY J. KLIMA Jul. 1987 14 p Prepared for presentation at the Symposium on Characterization of Advanced Materials, Monterey, Calif., 27-28 Jul. 1987; sponsored by International Metallographic Society (NASA-TM-89929; E-3632; NAS 1.15:89929) Avail: NTIS HC A02/MF A01 CSCL 14D

A review is presented of research investigations of several acoustic microscopy techniques for application to structural ceramics for advanced heat engines. Results obtained with scanning acoustic microscopy (SAM), scanning laser acoustic microscopy (SLAM), scanning electron acoustic microscopy (SEAM), and photoacoustic microscopy (PAM) are compared. The

techniques were evaluated on research samples of green and sintered monolithic silicon nitrides and silicon carbides in the form of modulus-of-rupture bars containing deliberately introduced flaws. Strengths and limitations of the techniques are described with emphasis on statistics of detectability of flaws that constitute potential fracture origins. Author

N87-25589*# National Aeronautics and Space Administration. Lewis Research Center, Cleveland, Ohio.

RAY PROPAGATION PATH ANALYSIS OF ACOUSTO-ULTRASONIC SIGNALS IN COMPOSITES

HAROLD E. KAUTZ 1987 20 p Presented at Acousto-Ultrasonics: Theory and Application, Blacksburg, Va., 12-15 Jul. 1987; sponsored by NASA (NASA-TM-100148; E-3706; NAS 1.15:100148) Avail: NTIS HC A02/MF A01 CSCL 14D

The most important result was the demonstration that acousto-ultrasonic (AU) energy introduced into a laminated graphite/resin propagates by two modes through the structure. The first mode, along the graphite fibers, is the faster. The second mode, through the resin matrix, besides being slower is also more strongly attenuated at the higher frequencies. This demonstration was accomplished by analyzing the time and frequency domain of the composite AU signal and comparing them to the same for a neat resin specimen of the same chemistry and geometry as the composite matrix. Analysis of the fine structure of AU spectra was accomplished by various geometrical strategies. It was shown that the multitude of narrow peaks associated with AU spectra are the effect of the many pulse arrivals in the signal. The shape and distribution of the peaks is mainly determined by the condition of nonnormal reflections of ray paths. A cepstrum analysis was employed which can be useful in detecting characteristic times. Analysis of propagation modes can be accomplished while ignoring the fine structure. Author

N87-26362*# National Aeronautics and Space Administration. Lewis Research Center, Cleveland, Ohio.

ULTRASONIC NDE OF STRUCTURAL CERAMICS FOR POWER AND PROPULSION SYSTEMS

ALEX VARY, EDWARD R. GENERAZIO, DON J. ROTH, and GEORGE Y. BAAKLINI (Cleveland State Univ., Ohio.) 1987 12 p Presented at the 4th European Conference on Non-Destructive Testing, London, England, 13-18 Sep. 1987; sponsored by the British Inst. of Non-Destructive Testing (NASA-TM-100147; E-3705; NAS 1.15:100147) Avail: NTIS HC A02/MF A01 CSCL 14D

A review of research investigations of several ultrasonic evaluation techniques applicable to structural ceramics for advanced heat engines is presented. This review highlights recent work conducted under the sponsorship of and at the Lewis Research Center. Results obtained with scanning acoustic microscopy, scanning laser acoustic microscopy, photo acoustic microscopy, and scanning electron acoustic microscopy are compared. In addition to these flaw imaging techniques, microstructure characterization by analytical ultrasonics is described. The techniques were evaluated by application to research samples of monolithic silicon nitride and silicon carbide in the form of discs and bars containing naturally occurring and deliberately-introduced flaws and microstructural anomalies. Strengths and limitations of the techniques are discussed. Author

N88-12106*# National Aeronautics and Space Administration. Lewis Research Center, Cleveland, Ohio.

FLAW IMAGING AND ULTRASONIC TECHNIQUES FOR CHARACTERIZING SINTERED SILICON CARBIDE

GEORGE Y. BAAKLINI (Cleveland State Univ., Ohio.) and PHILLIP B. ABEL Aug. 1987 21 p Presented at the Conference on Nondestructive Testing of High-Performance Ceramics, Boston, Mass., 25-27 Aug. 1987; sponsored in part by American Ceramic Society and the American Society for Nondestructive Testing (NASA-TM-100177; E-3753; NAS 1.15:100177) Avail: NTIS HC A03/MF A01 CSCL 14D

The capabilities were investigated of projection microfocus x-radiography, ultrasonic velocity and attenuation, and reflection scanning acoustic microscopy for characterizing silicon carbide specimens. Silicon carbide batches covered a range of densities and different microstructural characteristics. Room temperature, four point flexural strength tests were conducted. Fractography was used to identify types, sizes, and locations of fracture origins. Fracture toughness values were calculated from fracture strength and flaw characterization data. Detection capabilities of radiography and acoustic microscopy for fracture-causing flaws were evaluated. Applicability of ultrasonics for verifying material strength and toughness was examined. Author

39

STRUCTURAL MECHANICS

Includes structural element design and weight analysis; fatigue; and thermal stress.

A80-10832* National Aeronautics and Space Administration. Lewis Research Center, Cleveland, Ohio.

SIMPLE SPLINE-FUNCTION EQUATIONS FOR FRACTURE MECHANICS CALCULATIONS

T. W. ORANGE (NASA, Lewis Research Center, Cleveland, Ohio) International Journal of Fracture, vol. 15, Oct. 1979, p. R161-R163. refs

The paper presents simple spline-function equations for fracture mechanics calculations. A spline function is a sequence of piecewise polynomials of degree n greater than 1 whose coefficients are such that the function and its first $n-1$ derivatives are continuous. Second-degree spline equations are presented for the compact, three point bend, and crack-line wedge-loaded specimens. Some expressions can be used directly, so that for a cyclic crack propagation test using a compact specimen, the equation given allows the cracklength to be calculated from the slope of the load-displacement curve. For an R-curve test, equations allow the crack length and stress intensity factor to be calculated from the displacement and the displacement ratio.

A.T.

A80-20149* Army Structures Lab., Hampton, Va.
BUCKLING OF ROTATING BEAMS

W. F. WHITE, JR. (U.S. Army, Structures Laboratory, Hampton, Va.), R. G. KVATERNIK (NASA, Langley Research Center, Hampton, Va.), and K. R. V. KAZA (NASA, Lewis Research Center, Cleveland; Toledo, University, Toledo, Ohio) International Journal of Mechanical Sciences, vol. 21, no. 12, 1979, p. 739-745. refs

The stability of a beam subjected to compressive centrifugal forces arising from steady rotation about an axis which does not pass through the clamped end of the beam is analyzed to determine the critical rotational speeds for buckling in the inplane and out-of-plane directions. The differential equations of motion are solved numerically using an integrating matrix method in combination with an eigenanalysis to determine the eigenvalues from which stability is assessed. The results clarify several differences which have been identified in the literature relating to the proper behavior of the critical rotational speed for buckling as

the radius of rotation of the clamped end of the beam is reduced. (Author)

A80-27958*# National Aeronautics and Space Administration. Lewis Research Center, Cleveland, Ohio.

STRAINRANGE PARTITIONING LIFE PREDICTIONS OF THE LONG TIME METAL PROPERTIES COUNCIL CREEP-FATIGUE TESTS

J. F. SALTSMAN and G. R. HALFORD (NASA, Lewis Research Center, Cleveland, Ohio) In: Methods for predicting material life in fatigue; Proceedings of the Winter Annual Meeting, New York, N.Y., December 2-7, 1979. New York, American Society of Mechanical Engineers, 1979, p. 101-132. refs

The method of Strainrange Partitioning is used to predict the cyclic lives of the Metal Properties Council's long time creep-fatigue interspersed tests of several steel alloys. Comparisons are made with predictions based upon the Time- and Cycle-Fraction approach. The method of Strainrange Partitioning is shown to give consistently more accurate predictions of cyclic life than is given by the Time- and Cycle-Fraction approach. (Author)

A80-32067*# National Aeronautics and Space Administration. Lewis Research Center, Cleveland, Ohio.

PREDICTION OF FIBER COMPOSITE MECHANICAL BEHAVIOR MADE SIMPLE

C. C. CHAMIS (NASA, Lewis Research Center, Materials and Structures Div., Cleveland, Ohio) In: Rising to the challenge of the '80s; Annual Conference and Exhibit, 35th, New Orleans, La., February 4-8, 1980, Preprints. New York, Society of the Plastics Industry, Inc., 1980, p. 12-A 1 to 12-A 10.

A convenient procedure is described for the determination of the mechanical behavior (elastic properties and failure stresses of angleplied fiber composite laminates using a pocket calculator. The procedure consists of simple equations and appropriate graphs of (plus or minus theta) ply combinations. The procedure can handle all types of fiber composites including hybrids. The versatility and generality of the procedure is illustrated using several step-by-step numerical examples. (Author)

A80-35906*# National Aeronautics and Space Administration. Lewis Research Center, Cleveland, Ohio.

STATUS OF NASA FULL-SCALE ENGINE AEROELASTICITY RESEARCH

J. F. LUBOMSKI (NASA, Lewis Research Center, Cleveland, Ohio) In: Structures, Structural Dynamics, and Materials Conference, 21st, Seattle, Wash., May 12-14, 1980, Technical Papers. Conference sponsored by AIAA, ASME, ASCE, and AHS. New York, American Institute of Aeronautics and Astronautics, Inc., 1980, 18 p. refs

The paper presents data relevant to several types of aeroelastic instabilities which have been obtained using several types of turbojet and turbofan engines. Special attention is given to data relative to separated flow (stall) flutter, choke flutter, and system mode instabilities. The discussion covers the characteristics of these instabilities, and a number of correlations are presented that help identify the nature of the phenomena. M.E.P.

A80-38142*# Case Western Reserve Univ., Cleveland, Ohio.

A QUARTER-CENTURY OF PROGRESS IN THE DEVELOPMENT OF CORRELATION AND EXTRAPOLATION METHODS FOR CREEP RUPTURE DATA

S. S. MANSON (Case Western Reserve University, Cleveland, Ohio) and C. R. ENSIGN (NASA, Lewis Research Center, Cleveland, Ohio) ASME, Transactions, Journal of Engineering Materials and Technology, vol. 101, Oct. 1979, p. 317-325. refs

Developments in the analysis of creep-rupture data are reviewed with particular reference to time temperature relations for the correlation and extrapolation of creep and stress rupture data, the minimum commitment method, and successive regression methods. Some contributions to the development of time-temperature parameters are noted. V.P.

A80-45364* National Aeronautics and Space Administration. Lewis Research Center, Cleveland, Ohio.

VIBRATION AND BUCKLING OF RECTANGULAR PLATES UNDER IN-PLANE HYDROSTATIC LOADING

R. E. KIELB (NASA, Lewis Research Center, Cleveland, Ohio) and L. S. HAN (Ohio State University, Columbus, Ohio) *Journal of Sound and Vibration*, vol. 70, June 22, 1980, p. 543-555. refs

Numerical solutions are presented for the fundamental natural frequency and mode shape of a rectangular plate loaded by in-plane hydrostatic forces for a wide variety of aspect ratios, boundary conditions, and load magnitudes. All six possible combinations of simply supported and clamped edges are considered. The limiting conditions of unloaded vibration and buckling are discussed in detail, with emphasis on the preferred mode shape. Design curves and approximate formulae are presented which provide a simple means of determining the fundamental frequency parameter.

(Author)

A80-46032* National Aeronautics and Space Administration. Lewis Research Center, Cleveland, Ohio.

COMPLIANCE AND STRESS INTENSITY COEFFICIENTS FOR SHORT BAR SPECIMENS WITH CHEVRON NOTCHES

D. MUNZ (NASA, Lewis Research Center, Cleveland, Ohio; Deutsche Forschungs- und Versuchsanstalt fuer Luft- und Raumfahrt, Cologne, West Germany), R. T. BUBSEY, and J. E. SRAWLEY (NASA, Lewis Research Center, Cleveland, Ohio) *International Journal of Fracture*, vol. 16, Aug. 1980, p. 359-374. refs

(Contract EC-77-A-31-1040)

For the determination of fracture toughness especially with brittle materials, a short bar specimen with rectangular cross section and chevron notch can be used. As the crack propagates from the tip of the triangular notch, the load increases to a maximum then decreases. To obtain the relation between the fracture toughness and maximum load, calculations of Srawley and Gross for specimens with a straight-through crack were applied to the specimens with chevron notches. For the specimens with a straight-through crack, an analytical expression was obtained. This expression was used for the calculation of the fracture toughness versus maximum load relation under the assumption that the change of the compliance with crack length for the specimen with a chevron notch is the same as for a specimen with a straight-through crack.

(Author)

A81-14162* Battelle Columbus Labs., Ohio.

CONTINUOUS ANALYSIS OF STRESSES FROM ARBITRARY SURFACE LOADS ON A HALF SPACE

J. C. BELL (Battelle Columbus Laboratories, Columbus, Ohio) *International Journal of Solids and Structures*, vol. 16, no. 12, 1980, p. 1069-1091. Research supported by Battelle Memorial Institute and Bell Aerospace Co. refs

(Contract F33615-72-C-1739; NAS3-17760; NAS3-21020)

A new form of elemental surface load on a half space is introduced, presuming a quasi-pyramidal variation of load which is doubly linear in each of four rectangular parts of a surface rectangle. Approximations of arbitrary load distributions by sums of such elements are continuous, piecewise linear in two directions and well adaptable. The loads may be normal or tangential. The explicit solutions obtained for all stress and displacement components due to each elemental load involve only elementary functions, are free of the discontinuities which arise with stepwise elements, and are suitable for computing. Some illustrative stress distributions are presented for elemental loads and for multiple pyramidal loads involving both normal and tangential loads. The value of the load continuity in the more complicated analyses of surface cracks is also illustrated.

(Author)

A81-18792* National Aeronautics and Space Administration. Lewis Research Center, Cleveland, Ohio.

ON THE EQUIVALENCE BETWEEN SEMIEMPIRICAL FRACTURE ANALYSES AND R-CURVES

T. W. ORANGE (NASA, Lewis Research Center, Cleveland, Ohio) In: *Fracture mechanics; Proceedings of the Twelfth National Symposium*, Washington University, St. Louis, Mo., May 21-23, 1979. Philadelphia, Pa., American Society for Testing and Materials, 1980, p. 478-499. refs

The relationship between the R-curves and semiempirical fracture analyses (SEFA) is investigated theoretically using a hypothetical material. Equivalent R-curves (ERC) are developed for real materials using data from the literature. It is shown that for each SEFA there is an ERC whose magnitude and shape are determined by the SEFA formulation and its empirical parameters. The ERC is equivalent in that it predicts exactly the same relationship between the fracture stress and the initial crack length (residual strength) as the SEFA. If the effective R-curve is unique, then the various empirical parameters cannot be constant, and vice versa. However, for one of the SEFA examined, Newman's SEFA, parameter variations are small enough to be within the range of normal data scatter for real materials.

V.L.

A81-22526*# National Aeronautics and Space Administration. Lewis Research Center, Cleveland, Ohio.

STABILITY OF LARGE HORIZONTAL-AXIS AXISYMMETRIC WIND TURBINES

M. S. HIRSCHBEIN (NASA, Lewis Research Center, Cleveland, Ohio) and M. I. YOUNG (Delaware University, Newark, Del.) *Miami International Conference on Alternative Energy Sources*, 3rd, Miami, Fla., Dec. 15-17, 1980, Paper. 35 p. refs

The stability of large horizontal-axis, axisymmetric, power producing wind turbines is examined within the framework of an analytical model which includes dynamic coupling of the rotor, tower, and power generating system. The aerodynamic loading is derived from blade element theory. Stability is determined by the eigenvalues of a set of linearized constant-coefficient differential equations. All results presented are based on a 3-bladed, 300-ft diameter, 2.0-MW wind turbine. It is shown that unstable or weakly stable behavior can be caused by aerodynamic forces due to motion of the rotor blades and tower in the plane of rotation or by mechanical coupling between the rotor system and the tower.

V.L.

A81-29095*# United Technologies Research Center, East Hartford, Conn.

EFFECTS OF MISTUNING ON BLADE TORSIONAL FLUTTER

A. V. SRINIVASAN (United Technologies Research Center, East Hartford, Conn.) and A. KURKOV (NASA, Lewis Research Center, Cleveland, Ohio) In: *International Symposium on Air Breathing Engines*, 5th, Bangalore, India, February 16-22, 1981, Proceedings. Bangalore, National Aeronautical Laboratory, 1981, p. 59-1 to 59-8. refs

(Contract NAS3-21603)

An analytical model for the prediction of fan blade flutter is presented and evaluated using data from NASA tests on an advanced high performance engine. For the cascade conditions appropriate to the test points studied, the aerodynamic theory cannot predict subcritical flutter. Under the assumptions of a tuned assembly, the imaginary part of the aerodynamic coefficients does indicate flutter for a limited number of interblade phase angles, but these interblade phase angles are close to those at which the acoustic resonance is predicted. Upon using the individual blade frequencies and solving the mistuned system with aerodynamic coupling only, the results show a stable system. Eigenvectors calculated for the mistuned system demonstrate the presence of several harmonics in each mistuned mode. Inclusion of both mechanical and aerodynamic coupling in the solution of the eigenproblem influences not only the frequencies but also damping in the system with a trend toward stability.

L.S.

A81-29465* National Aeronautics and Space Administration. Lewis Research Center, Cleveland, Ohio.

EFFECTS OF MISTUNING ON BENDING-TORSION FLUTTER AND RESPONSE OF A CASCADE IN INCOMPRESSIBLE FLOW
K. R. V. KAZA (NASA, Lewis Research Center, Cleveland; Toledo, University, Toledo, Ohio) and R. E. KIELB (NASA, Lewis Research Center, Structures Branch, Cleveland, Ohio) In: Structures, Structural Dynamics and Materials Conference, 22nd, Atlanta, Ga., April 6-8, 1981, and AIAA Dynamics Specialists Conference, Atlanta, Ga., April 9, 10, 1981, Technical Papers. Part 2. New York, American Institute of Aeronautics and Astronautics, Inc., 1981, p. 320-331. refs
(AIAA 81-0602)

This paper presents an investigation of the effects of blade mistuning on the aeroelastic stability and response of a cascade in incompressible flow. The aerodynamic, inertial, and structural coupling between the bending and torsional motions of each blade and the aerodynamic coupling between the blades are included in the formulation. A digital computer program was developed to conduct parametric studies. Results indicate that the mistuning has a beneficial effect on the coupled bending-torsion and uncoupled torsion flutter. The effect of mistuning on forced response, however, may be either beneficial or adverse, depending on the engine order of the forcing function. Additionally, the results illustrate that it may be feasible to utilize mistuning as a passive control to increase flutter speed while maintaining forced response at an acceptable level. (Author)

A82-11298* Ohio State Univ., Columbus.
VIBRATIONS OF CANTILEVERED SHALLOW CYLINDRICAL SHELLS OF RECTANGULAR PLANFORM

A. W. LEISSA, J. K. LEE, and A. J. WANG (Ohio State University, Columbus, OH) Journal of Sound and Vibration, vol. 78, Oct. 8, 1981, p. 311-328. refs
(Contract NAG3-36)

A cantilevered, shallow shell of circular cylindrical curvature and rectangular planform exhibits free vibration behavior which differs considerably from that of a cantilevered beam or of a flat plate. Some numerical results can be found for the problem in the previously published literature, mainly obtained by using various finite element methods. The present paper is the first definitive study of the problem, presenting accurate non-dimensional frequency parameters for wide ranges of aspect ratio, shallowness ratio and thickness ratio. The analysis is based upon shallow shell theory. Numerical results are obtained by using the Ritz method, with algebraic polynomial trial functions for the displacements. Convergence is investigated, with attention being given both to the number of terms taken for each co-ordinate direction and for each of the three components of displacement. Accuracy of the results is also established by comparison with finite element results for shallow shells and with other accurate flat plate solutions. (Author)

A82-19341* Ohio State Univ., Columbus.
VIBRATIONS OF TWISTED ROTATING BLADES

A. W. LEISSA, J. K. LEE (Ohio State University, Columbus, OH), and A. J. WANG American Society of Mechanical Engineers, Design Engineering Technical Conference, Hartford, CT, Sept. 20-23, 1981, 8 p. refs
(Contract NAG3-36)
(ASME PAPER 81-DET-127)

The literature dealing with vibrations of turbomachinery blades is voluminous, but the vast majority of it treats the blades as beams. In a previous paper a two-dimensional analytical procedure was developed and demonstrated on simple models of blades having camber. The procedure utilizes shallow shell theory along with the classical Ritz method for solving the vibration problem. Displacement functions are taken as algebraic polynomials. In the present paper the method is demonstrated on blade models having camber. Comparisons are first made with results in the literature for nonrotating twisted plates and various disagreements between results are pointed out. A method for depicting mode shape information is demonstrated, permitting one to examine all three

components of displacement. Finally, the analytical procedure is demonstrated on rotating twisted blade modes, both without and with camber. (Author)

A82-32303* Georgia Inst. of Tech., Atlanta.
PATH-INDEPENDENT INTEGRALS IN FINITE ELASTICITY AND INELASTICITY, WITH BODY FORCES, INERTIA, AND ARBITRARY CRACK-FACE CONDITIONS

S. N. ATLURI (Georgia Institute of Technology, Atlanta, GA) Engineering Fracture Mechanics, vol. 16, no. 3, 1982, p. 341-364. refs

(Contract N00014-78-C-0636; AF-AFOSR-81-0057; NAG3-38)
(Previously announced in STAR as N81-32547)

A82-35408* Ohio State Univ., Columbus.
COMPARISON OF BEAM AND SHELL THEORIES FOR THE VIBRATIONS OF THIN TURBOMACHINERY BLADES

A. W. LEISSA (Ohio State University, Columbus, OH) and M. S. EWING (U.S. Air Force Academy, Colorado Springs, CO) American Society of Mechanical Engineers, International Gas Turbine Conference and Exhibit, 27th, London, England, Apr. 18-22, 1982, 12 p. refs

(Contract NAG3-36)
(ASME PAPER 82-GT-223)

Vibration analysis of turbomachinery blades has traditionally been carried out by means of beam theory. In recent years two-dimensional methods of blade vibration analysis have been developed, most of which utilize finite elements and tend to require considerable computation time. More recently a two-dimensional method of blade analysis has evolved which does not require finite elements and is based upon shell equations. The present investigation has the primary objective to demonstrate the accuracy and limitations of blade vibration analyses which utilize one-dimensional, beam theories. It is found that beam theory is generally inadequate to determine the free vibration frequencies and mode shapes of moderate to low aspect ratio turbomachinery blades. The shallow shell theory, by contrast, is capable of representing all the vibration modes accurately. However, the one-dimensional beam theory has an important advantage over the two-dimensional shell theory for blades and vibration modes. It uses fewer degrees of freedom, thus requiring less computer time. G.R.

A82-36782* Georgia Inst. of Tech., Atlanta.
ON A STUDY OF THE $\Delta T/C$ AND $C/ASTERISK$ INTEGRALS FOR FRACTURE ANALYSIS UNDER NON-STEADY CREEP

R. B. STONESIFER and S. N. ATLURI (Georgia Institute of Technology, Atlanta, GA) Engineering Fracture Mechanics, vol. 16, no. 5, 1982, p. 625-643. refs
(Contract NAG3-38; AF-AFOSR-81-0057)

Applications of a vector quantity, path-independent integral which has an energy interpretation to the characterization of crack-tip fields in the range from fast to slow crack propagation are examined. The crack tip characterization parameter is defined in terms of a conservation integral for an area around the crack tip in a two-dimensional cracked body. The actual physical interpretation of the parameter is shown to be the difference in crack lengths displayed by two identical bodies which have equal load histories. A steady-state value is obtained for the parameter for cases of steady-state creep and is shown to be related to the standard path-independent integral for macroscopic self-similar crack growth under mode I conditions. A finite element model is developed for viscoplastic material models, using an initial strain approach with steps in a size employed in tangent stiffness methods. M.S.K.

A82-39514* Akron Univ., Ohio.

ON THE SOLUTION OF CREEP INDUCED BUCKLING IN GENERAL STRUCTURE

J. PADOVAN and S. TOVICHAKCHAIKUL (Akron, University, Akron, OH) Computers and Structures, vol. 15, no. 4, 1982, p. 379-392. refs

(Contract NAG3-54)

This paper considers the pre and post buckling behavior of general structures exposed to high temperature fields for long durations wherein creep effects become significant. The solution to this problem is made possible through the use of closed upper bounding constraint surfaces which enable the development of a new time stepping algorithm. This permits the stable and efficient solution of structural problems which exhibit indefinite tangent properties. Due to the manner of constraining/bounding successive iterates, the algorithm developed herein is largely self adaptive, inherently stable, sufficiently flexible to handle geometric material and boundary induced nonlinearity, and can be incorporated into either finite element or difference simulations. To illustrate the capability of the procedure, as well as, the physics of creep induced pre and post buckling behavior, the results of several numerical experiments are included. (Author)

A82-39852* National Aeronautics and Space Administration. Lewis Research Center, Cleveland, Ohio.

IMPACT RESISTANCE OF FIBER COMPOSITES

C. C. CHAMIS and J. H. SINCLAIR (NASA, Lewis Research Center, Cleveland, OH) In: Composite materials: Mechanics, mechanical properties and fabrication; Proceedings of the Japan-U.S. Conference, Tokyo, Japan, January 12-14, 1981. Barking, Essex, England, Applied Science Publishers, 1982, p. 1-11.

Stress-strain curves are obtained for a variety of glass fiber and carbon fiber reinforced plastics in dynamic tension, over the stress-strain range of 0.00087-2070/sec. The test method is of the one-bar block-to-bar type, using a rotating disk or a pendulum as the loading apparatus and yielding accurate stress-strain curves up to the breaking strain. In the case of glass fiber reinforced plastic, the tensile strength, strain to peak impact stress, total strain and total absorbed energy all increase significantly as the strain rate increases. By contrast, carbon fiber reinforced plastics show lower rates of increase with strain rate. It is recommended that hybrid composites incorporating the high strength and rigidity of carbon fiber reinforced plastic with the high impact absorption of glass fiber reinforced plastics be developed for use in structures subjected to impact loading. O.C.

A82-40066* Georgia Inst. of Tech., Atlanta.

MOVING SINGULARITY CREEP CRACK GROWTH ANALYSIS WITH THE $\Delta T/c$ AND C^* INTEGRALS

R. B. STONESIFER and S. N. ATLURI (Georgia Institute of Technology, Atlanta, GA) Engineering Fracture Mechanics, vol. 16, no. 6, 1982, p. 769-782. refs

(Contract NAG3-38)

The physical meaning of $\Delta T/c$ and its applicability to creep crack growth are reviewed. Numerical evaluation of $\Delta T/c$ and C^* is discussed with results being given for compact specimen and strip geometries. A moving crack-tip singularity, creep crack growth simulation procedure is described and demonstrated. The results of several crack growth simulation analyses indicate that creep crack growth in 304 stainless steel occurs under essentially steady-state conditions. Based on this result, a simple methodology for predicting creep crack growth behavior is summarized. (Author)

A82-40357* National Aeronautics and Space Administration. Lewis Research Center, Cleveland, Ohio.

EXTENDED RANGE STRESS INTENSITY FACTOR EXPRESSIONS FOR CHEVRON-NOTCHED SHORT BAR AND SHORT ROD FRACTURE TOUGHNESS SPECIMENS

J. L. SHANNON, JR., R. T. BUBSEY, W. S. PIERCE (NASA, Lewis Research Center, Cleveland, OH), and D. MUNZ (Karlsruhe, Universitaet, Karlsruhe, West Germany) International Journal of Fracture, vol. 19, July 1982, p. R55-R58.

A82-40358* National Aeronautics and Space Administration. Lewis Research Center, Cleveland, Ohio.

CRACK DISPLACEMENTS FOR J/I TESTING WITH COMPACT SPECIMENS

T. W. ORANGE (NASA, Lewis Research Center, Cleveland, OH) International Journal of Fracture, vol. 19, July 1982, p. R59-R61. refs

The suggestion is made that the standard compact specimen (with opening displacement measured at the crack mouth) may be entirely suitable for J-integral determinations if a very simple conversion factor is used. Experimental determination of J-integral values requires the measurement of displacements at the points of load application. For the compact specimen this is a difficult task. On the basis of studies reported by Newman (1979) and Fisher and Buzzard (1980), it is suggested that for any J-based test the standard compact specimen can be used. A very good approximation to the load point displacement (within 3.4 percent) can be obtained by measuring the crack mouth displacement and multiplying by 0.773. G.R.

A82-42863*# Ohio State Univ., Columbus.

ON ULTRASONIC FACTORS AND FRACTURE TOUGHNESS

L. S. FU (Ohio State University, Columbus, OH) In: Symposium on Nondestructive Evaluation, 13th, San Antonio, TX, April 21-23, 1981, Proceedings. San Antonio, TX, Southwest Research Institute, 1982, p. 149-160. refs

(Contract NSG-3269)

Recent experimental and theoretical studies on ultrasonics have shown that the scattering of elastic waves by material defects yields data which characterize crack properties, such as size and orientation, and also the mechanical properties of the given material. In the present study, elastodynamic fields due to the presence of a pair of inhomogeneities in a material of plate geometry are investigated by the method of equivalent inclusions. The stress amplitude change of the plates during the passage of plane time-harmonic waves is found, and the relation between fracture toughness and ultrasonic factors is determined. The approach used does not assume the existence of a sharp crack in the material. O.C.

A82-45869* Northwestern Univ., Evanston, Ill.

ON FINITE DEFORMATION ELASTO-PLASTICITY

S. NEMAT-NASSER (Northwestern University, Evanston, IL) International Journal of Solids and Structures, vol. 18, no. 10, 1982, p. 857-872. refs

(Contract NAG3-134)

Lee (1969) has proposed a theory based on the decomposition of the total deformation gradient to an elastic and plastic part, and from it has concluded that the additive decomposition of the strain rates holds only approximately. Lubarda and Lee (1981) have declared that Lee's 'exact finite-deformation kinematics shows the almost universal assumption that the total velocity strain or rate of deformation is the sum of elastic and plastic rates to be in error'. Hence questions are raised regarding the validity of essentially all finite deformation elasto-plasticity theories. The present investigation is concerned with these questions. It is shown that the additive decomposition of the strain rates follows from all common finite elasto-plasticity concepts. Lee's theory is examined, and it is shown that this theory also leads to an additive strain rate decomposition, and therefore, his conclusion stems from misinterpretation. It is found that the elastic and the plastic strain rates considered by Lee do not correspond to the same configuration. They are, therefore, not compatible measures. G.R.

A82-46109* Illinois Univ., Urbana.

INTERFACE CRACKS IN ADHESIVELY BOUNDED LAP-SHEAR JOINTS

S. S. WANG and J. F. YAU (Illinois, University, Urbana, IL) International Journal of Fracture, vol. 19, Aug. 1982, p. 295-309. refs
(Contract NSG-3044)

A study on the elastic behavior of interface cracks in adhesively bonded lap-shear joints is presented. The problem is investigated by using a recently developed method of analysis based on conservation laws in elasticity for nonhomogeneous solids and fundamental relationships in fracture mechanics of dissimilar materials. The formulation leads to a pair of linear algebraic equations in mixed-mode stress intensity factors. Singular crack-tip stress intensity solutions are determined directly by information extracted from the far field. Stress intensity factors and associated energy release rates are obtained for various cases of interest. Fundamental nature of the interfacial flaw behavior in lap-shear adhesive joints is examined in detail. (Author)

A82-46806*# Illinois Univ., Urbana.

BOUNDARY-LAYER EFFECTS IN COMPOSITE LAMINATES. I - FREE-EDGE STRESS SINGULARITIES. II - FREE-EDGE STRESS SOLUTIONS AND BASIC CHARACTERISTICS

S. S. WANG and I. CHOI (Illinois, University, Urbana, IL) ASME, Transactions, Journal of Applied Mechanics, vol. 49, Sept. 1982, p. 541-560. refs
(Contract NSG-3044)

The fundamental nature of the boundary-layer effect in fiber-reinforced composite laminates is formulated in terms of the theory of anisotropic elasticity. The basic structure of the boundary-layer field solution is obtained by using Lekhnitskii's stress potentials (1963). The boundary-layer stress field is found to be singular at composite laminate edges, and the exact order or strength of the boundary layer stress singularity is determined using an eigenfunction expansion method. A complete solution to the boundary-layer problem is then derived, and the convergence and accuracy of the solution are analyzed, comparing results with existing approximate numerical solutions. The solution method is demonstrated for a symmetric graphite-epoxy composite. V.L.

A83-10283* Northwestern Univ., Evanston, Ill.

ON COMPOSITES WITH PERIODIC STRUCTURE

S. NEMAT-NASSER, T. IWAKUMA, and M. HEJAZI (Northwestern University, Evanston, IL) Mechanics of Materials, vol. 1, Sept. 1982, p. 239-267. refs
(Contract DAAG29-79-C-0168; NAG3-134)

The overall moduli of a composite with an isotropic elastic matrix containing periodically distributed (anisotropic) inclusions or voids, can be expressed in terms of several infinite series which only depend on the geometry of the inclusions or voids, and hence can be computed once and for all for given geometries. For solids with periodic structures these infinite series play exactly the same role as does Eshelby's tensor for a single inclusion or void in an unbounded elastic medium. For spherical and circular-cylindrical geometries, the required infinite series are calculated and the results are tabulated. These are then used to estimate the overall elastic moduli when either the overall strains or the overall stresses are prescribed, obtaining the same results. These results are compared with other estimates and with experimental data. It is found that the model of composites with periodic structure yields estimates in excellent agreement with the experimental observations. (Author)

A83-10900*# National Aeronautics and Space Administration, Lewis Research Center, Cleveland, Ohio.

TENSILE BUCKLING OF ADVANCED TURBOPROPS

C. C. CHAMIS and R. A. AIELLO (NASA, Lewis Research Center, Cleveland, OH) AIAA, ASME, ASCE, and AHS, Structures, Structural Dynamics and Materials Conference, 23rd New Orleans, LA, May 10-12, 1982, AIAA 23 p. refs
(AIAA PAPER 82-0776)

(Previously announced in STAR as N82-31708)

A83-12048* Lehigh Univ., Bethlehem, Pa.

MOVING CRACKS IN LAYERED COMPOSITES

G. C. SIH (Lehigh University, Bethlehem, PA) and E. P. CHEN (Sandia National Laboratory, Albuquerque, NM) International Journal of Engineering Science, vol. 20, no. 11, 1982, p. 1181-1192. refs
(Contract NSG-3179)

A three-layered composite with a crack spreading in the center layer has been analytically examined to evaluate the effect of material nonhomogeneity on a constant velocity crack. Two different loading characteristics are considered. In the first case, crack motion is maintained by uniform tensile stresses. In the other, crack deformation is caused by anti-plane shear stresses. Galilean transformation and Fourier sine and cosine transforms are used to determine dynamic crack tip stress fields. Standard Fredholm integral equations yield the dynamic stress intensity factors. The results show that the intensity of local dynamic stresses increases or decreases with crack length to layer thickness as a function of the relative magnitudes of the adjoining layer's material properties. Crack speed tends to increase the effect of material nonhomogeneity. S.C.S.

A83-12514* Illinois Univ., Urbana.

EXTENDING THE LASER-SPECKLEGRAM TECHNIQUE TO STRAIN ANALYSIS OF ROTATING COMPONENTS

C. H. CHIEN (Illinois, University, Urbana, IL), J. L. TURNER, W. F. SWINSON (Auburn University, Auburn, AL), and W. F. RANSON (South Carolina, University, Columbia, SC) (Society for Experimental Stress Analysis, Spring Meeting, Dearborn, MI, May 30-June 4, 1981.) Experimental Mechanics, vol. 22, Nov. 1982, p. 434-440. refs
(Contract NAG3-103)

A technique involving sandwich-speckle interferometry has been investigated for application in making strain measurements on rotating structures. The technique has proven to be effective in relaxing stringent timing requirements for recording laser photographs and provides extended ranges of displacement measurement. Application of the technique to an experimental rotating specimen has demonstrated the potential of the method for making accurate strain measurements. (Author)

A83-12739* Massachusetts Inst. of Tech., Cambridge.

A NEW FORMULATION OF HYBRID/MIXED FINITE ELEMENT

T. H. H. PIAN, D. KANG (MIT, Cambridge, MA), and D.-P. CHEN (Symposium on Advances and Trends in Structural and Solid Mechanics, Washington, DC, Oct. 4-7, 1982.) Computers and Structures, vol. 16, no. 1-4, 1983, p. 81-87. refs
(Contract NAG3-33)

A new formulation of finite element method is accomplished by the Hellinger-Reissner principle for which the stress equilibrium conditions are not introduced initially but are brought-in through the use of additional internal displacement parameters. The method can lead to the same result as the assumed stress hybrid model. However, it is more general and more flexible. The use of natural coordinates for stress assumptions leads to elements which are less sensitive to the choice of reference coordinates. Numerical solutions by 3-D solid element indicate that more efficient elements can be constructed by assumed stresses which only partially satisfy the equilibrium conditions. (Author)

A83-12746* Akron Univ., Ohio.

ON THE SOLUTION OF ELASTIC-PLASTIC STATIC AND DYNAMIC POSTBUCKLING COLLAPSE OF GENERAL STRUCTURE

J. PADOVAN and S. TOVICHAKCHAIKUL (Akron, University, Akron, OH) (Symposium on Advances and Trends in Structural and Solid Mechanics, Washington, DC, Oct. 4-7, 1982.) Computers and Structures, vol. 16, no. 1-4, 1983, p. 199-205. refs
(Contract NAG3-54)

Many investigations have considered structural collapse from strictly the transient point of view. While such an approach is ideally correct, certain difficulties have to be overcome in its implementation. The present investigation is concerned with the

development of self-adaptive algorithms which make it possible to conduct the analysis of both static elastic and elastic-plastic postbuckling, as well as static loading to the onset of buckling followed by subsequent dynamic postbuckling. The approach employed to solve the static portion of loading is to extend the constrained Incremental Newton-Raphson (INR) algorithm by incorporating elastic-plastic constitutive characterizations. Large deformation moderate strain theory is adopted to establish the overall strategy. Attention is given to governing field equations, aspects of algorithmic development, and numerical experiments conducted to illustrate the efficiency and stability of the developed schemes. G.R.

A83-12764* Pratt and Whitney Aircraft Group, East Hartford, Conn.

NONLINEAR STRUCTURAL AND LIFE ANALYSES OF A COMBUSTOR LINER

V. MORENO, G. J. MEYERS (United Technologies Corp., Pratt and Whitney Group, East Hartford, CT), A. KAUFMAN, and G. R. HALFORD (NASA, Lewis Research Center, Cleveland, OH) (Symposium on Advances and Trends in Structural and Solid Mechanics, Washington, DC, Oct. 4-7, 1982.) Computers and Structures, vol. 16, no. 1-4, 1983, p. 509-515. refs (Previously announced in STAR as N82-24501)

A83-14710* Massachusetts Inst. of Tech., Cambridge.
ALTERNATIVE WAYS FOR FORMULATION OF HYBRID STRESS ELEMENTS

T. H. H. PIAN (MIT, Cambridge, MA) and D.-P. CHEN International Journal for Numerical Methods in Engineering, vol. 18, Nov. 1982, p. 1679-1684. refs (Contract NAG3-33)

An element stiffness matrix can be derived by the conventional potential energy principle and, indirectly, also by generalized variational principles, such as the Hu-Washizu principle and the Hellinger-Reissner principle. The present investigation has the objective to show an approach which is concerned with the formulation of incompatible elements for solid continuum and for plate bending problems by the Hellinger-Reissner principle. It is found that the resulting scheme is equivalent to that considered by Tong (1982) for the construction of hybrid stress elements. In Tong's scheme the inversion of a large flexibility matrix can be avoided. It is concluded that the introduction of additional internal displacement modes in mixed finite element formulations by the Hellinger-Reissner principle and the Hu-Washizu principle can lead to element stiffness matrices which are equivalent to the assumed stress hybrid method. G.R.

A83-15060* Northwestern Univ., Evanston, Ill.
GROWTH AND STABILITY OF INTERACTING SURFACE FLAWS OF ARBITRARY SHAPE

Y. MURAKAMI and S. NEMAT-NASSER (Northwestern University, Evanston, IL) Engineering Fracture Mechanics, vol. 17, no. 3, 1983, p. 193-210. refs (Contract NSF CME-80-06265; NAG3-134)

Growth regimes of interacting surface flaws of arbitrary shape are analyzed with the aid of the body force method, and the stability of the process is assessed on the basis of the variation of the load during the growth. It is shown that irregularly shaped flaws are often associated with very high stress intensity factors locally, which tend to change as the flaws grow into more regular shapes. Several examples of various flaw shapes are worked out for illustration, and it is shown that a simple formula seems to provide an accurate estimate of the maximum stress intensity factor for surface flaws of various shapes, which are not very slender. The formula involves the overall maximum tension, as well as the area of the projection of the flaw on the plane normal to the maximum tension. (Author)

A83-18383* Rensselaer Polytechnic Inst., Troy, N.Y.
NATURAL FREQUENCY OF ROTATING BEAMS USING NON-ROTATING MODES

R. G. LOEWY (Rensselaer Polytechnic Institute, Troy, NY) and N. KHADER American Helicopter Society, Journal, vol. 27, Apr. 1982, p. 75-78. refs (Contract NAG3-37)

A Lagrangian approach is formulated for predicting the rotating natural frequencies of a beam from the nonrotating modes and frequencies. Using the first two nonrotating mode shapes in one case and the first four such modes in the other case the frequencies of the rotating modes are calculated for a short tapered beam and a typical helicopter blade, respectively. In each case the beam is represented by lumped parameters. The number of mass points representing the beam and the accuracy of the calculated slopes of the nonrotating mode shapes at those points are both shown to affect the accuracy of the resulting frequencies, but the number of stations is shown to be more important. (Author)

A83-27431* Virginia Polytechnic Inst. and State Univ., Blacksburg.

GEOMETRICALLY NONLINEAR ANALYSIS OF LAYERED COMPOSITE SHELLS

W. C. CHAO and J. N. REDDY (Virginia Polytechnic Institute and State University, Blacksburg, VA) In: 1982 advances in aerospace structures and materials; Proceedings of the Winter Annual Meeting, Phoenix, AZ, November 14-19, 1982. New York, American Society of Mechanical Engineers, 1982, p. 25-28. refs (Contract N00014-78-C-0647; NAG3-208)

Two kinds of finite-element analyses are developed for the geometrically nonlinear study of the large deformations in laminated composite structures, especially shells. The first kind of finite-element analysis utilizes the general incremental variational formulation as well as the total Lagrangian description of motion, and a three-dimensional degenerate element is adopted. The second kind of analysis employs a formulation based on deformable shell theory, and the plate-bending element is used. Numerical results for bending are presented for five plate and shell structures of isotropic as well as orthotropic composition, including an isotropic cylindrical panel with uniform loading and a laminated cylindrical panel with uniform loading. The results obtained using these analyses are found to be in good agreement with those available in the literature. N.B.

A83-27432* Virginia Polytechnic Inst. and State Univ., Blacksburg.

THREE-DIMENSIONAL FINITE-ELEMENT ANALYSIS OF LAYERED COMPOSITE PLATES

N. S. PUTCHA and J. N. REDDY (Virginia Polytechnic Institute and State University, Blacksburg, VA) In: 1982 advances in aerospace structures and materials; Proceedings of the Winter Annual Meeting, Phoenix, AZ, November 14-19, 1982. New York, American Society of Mechanical Engineers, 1982, p. 29-35. refs (Contract N00014-78-C-0647; NAG3-208)

Results are presented for an investigation of the three-dimensional, geometrically nonlinear, finite-element analysis of the bending of laminated anisotropic composite plates. The individual laminae are treated as homogeneous, transversely isotropic, and linearly elastic. A fully three-dimensional isoparametric finite element with eight nodes (i.e., linear element) and 24 degrees of freedom (three displacement components per node) is used. The numerical results obtained using this linear analysis are compared with the exact solutions given in Pagano (1969, 1970). It is found that the results of the linear analysis converge to the exact solution as the mesh is refined. N.B.

A83-29798*# Texas A&M Univ., College Station.

AN UNCOUPLED VISCOPLASTIC CONSTITUTIVE MODEL FOR METALS AT ELEVATED TEMPERATURE

W. E. HAISLER and J. CRONENWORTH (Texas A & M University, College Station, TX) IN: Structures, Structural Dynamics and Materials Conference, 24th, Lake Tahoe, NV, May 2-4, 1983, Collection of Technical Papers. Part 1. New York, American Institute of Aeronautics and Astronautics, 1983, p. 664-673. refs (Contract NAG3-31) (AIAA 83-1016)

An uncoupled constitutive model for predicting the transient response of thermal and rate dependent, inelastic material behavior is presented. The uncoupled model assumes that there is a temperature below which the total strain consists essentially of elastic and rate insensitive inelastic strains only. Above this temperature, the rate dependent inelastic strain (creep) dominates. The rate insensitive inelastic strain component is modeled in an incremental form with a yield function, flow rule and hardening law. Revisions to the hardening rule permit the model to predict temperature-dependent kinematic-isotropic hardening behavior, cyclic saturation, asymmetric stress-strain response upon stress reversal, and variable Bauschinger effect. The rate dependent inelastic strain component is modeled using a rate equation in terms of back stress, drag stress and exponent n as functions of temperature and strain. A sequence of hysteresis loops and relaxation tests are utilized to define the rate dependent inelastic strain rate. Evaluation of the model is performed by comparison with experiments involving various thermal and mechanical load histories on 5086 aluminum alloy, 304 stainless steel and Hastelloy-X. Author

A83-29822*# National Aeronautics and Space Administration. Lewis Research Center, Cleveland, Ohio.

THE COUPLED AEROELASTIC RESPONSE OF TURBOMACHINE-ERY BLADING TO AERODYNAMIC EXCITATIONS

D. HOYNIK (NASA, Lewis Research Center, Cleveland, OH; Purdue University, West Lafayette, IN) and S. FLEETER (Purdue University, West Lafayette, IN) IN: Structures, Structural Dynamics and Materials Conference, 24th, Lake Tahoe, NV, May 2-4, 1983, Collection of Technical Papers. Part 2. New York, American Institute of Aeronautics and Astronautics, 1983, p. 137-148. refs (AIAA 83-0844)

An energy balance technique is developed to predict the coupled bending-torsion mode aerodynamically forced response of an airfoil. In this technique, the energy input to the airfoil system per cycle of oscillation is generated by gust forces and moments and, under certain conditions, the self-induced aerodynamic forces and moments. The energy dissipation per cycle is associated with the structural damping, the static moment term for coupled motions, and under certain conditions, the self-induced aerodynamic forces and moments. The effects of the various aerodynamic parameters on the coupled forced response are then considered. In particular, the effects of the inlet Mach number, the interblade phase angle, the level of structural damping, and the cascade geometry on the coupled bending-torsion aerodynamically forced response of a flat plate airfoil cascade are demonstrated. Author

A83-29823*# Massachusetts Inst. of Tech., Cambridge.

FLUTTER AND FORCED RESPONSE OF MISTUNED ROTORS USING STANDING WAVE ANALYSIS

J. DUGUNDJI and D. J. BUNDAS (MIT, Cambridge, MA) IN: Structures, Structural Dynamics and Materials Conference, 24th, Lake Tahoe, NV, May 2-4, 1983, Collection of Technical Papers. Part 2. New York, American Institute of Aeronautics and Astronautics, 1983, p. 149-159. refs (Contract NAG3-214) (AIAA 83-0845)

A standing wave approach is applied to the analysis of the flutter and forced response of tuned and mistuned rotors. The traditional traveling wave cascade airforces are recast into standing wave arbitrary motion form using Pade approximants, and the resulting equations of motion are written in the matrix form.

Applications for vibration modes, flutter, and forced response are discussed. It is noted that the standing wave methods may prove to be more versatile for dealing with certain applications, such as coupling flutter with forced response and dynamic shaft problems, transient impulses on the rotor, low-order engine excitation, bearing motions, and mistuning effects in rotors. V.L.

A83-29824*# Textron Bell Aerospace Co., Buffalo, N. Y.

FLUTTER ANALYSIS OF ADVANCED TURBOPROPELLERS

V. ELCHURI and G. C. C. SMITH (Bell Aerospace Textron, Buffalo, NY) IN: Structures, Structural Dynamics and Materials Conference, 24th, Lake Tahoe, NV, May 2-4, 1983, Collection of Technical Papers. Part 2. New York, American Institute of Aeronautics and Astronautics, 1983, p. 160-165. refs (Contract NAS3-22533) (AIAA 83-0846)

The two-dimensional subsonic cascade unsteady aerodynamic theory of Jones and Rao (1975) has been modified to account for the variable sweep angles of the blades of advanced turbopropellers. The aerodynamics and the structural modal properties have been formally integrated to determine the generalized aerodynamic coefficients matrix for the blade modes. Modal flutter analysis has been conducted for two SR-5 five- and ten-blade propellers, and analytical results have been found to be in very good agreement with wind tunnel test data. V.L.

A83-32987*# Massachusetts Inst. of Tech., Cambridge.

SOME ANALYSIS METHODS FOR ROTATING SYSTEMS WITH PERIODIC COEFFICIENTS

J. DUGUNDJI (MIT, Cambridge, MA) and J. H. WENDELL AIAA Journal (ISSN 0001-1452), vol. 21, June 1983, p. 890-897. refs (Contract NSG-3303)

Two of the more common procedures for analyzing the stability and forced response of equations with periodic coefficients are reviewed: the use of Floquet methods, and the use of multiblade coordinate and harmonic balance methods. The analysis procedures of these periodic coefficient systems are compared with those of the more familiar constant coefficient systems. Previously announced in STAR as N82-23702 Author

A83-36958* Ohio State Univ., Columbus.

VIBRATIONS OF CANTILEVERED CIRCULAR CYLINDRICAL SHELLS SHALLOW VERSUS DEEP SHELL THEORY

J. K. LEE, A. W. LEISSA, and A. J. WANG (Ohio State University, Columbus, OH) International Journal of Mechanical Sciences (ISSN 0020-7403), vol. 25, no. 5, 1983, p. 361-383. refs (Contract NAG3-36)

Free vibrations of cantilevered circular cylindrical shells having rectangular planforms are studied in this paper by means of the Ritz method. The deep shell theory of Novozhilov and Goldenveizer is used and compared with the usual shallow shell theory for a wide range of shell parameters. A thorough convergence study is presented along with comparisons to previously published finite element solutions and experimental results. Accurately computed frequency parameters and mode shapes for various shell configurations are presented. The present paper appears to be the first comprehensive study presenting rigorous comparisons between the two shell theories in dealing with free vibrations of cantilevered cylindrical shells. Author

A83-37388*# Ohio State Univ., Columbus.

THE DETERMINATION OF THE ELASTODYNAMIC FIELDS OF AN ELLIPSOIDAL INHOMOGENEITY

L. S. FU (Ohio State University, Columbus, OH) and T. MURA (Northwestern University, Evanston, IL) ASME, Transactions, Journal of Applied Mechanics (ISSN 0021-8936), vol. 50, June 1983, p. 390-396. refs (Contract NSG-3269) (ASME PAPER 83-APM-19)

The determination of the elastodynamic fields of an ellipsoidal inhomogeneity is studied in detail via the eigenstrain approach. A complete formulation and a treatment of both types of eigenstrains for equivalence between the inhomogeneity problem and the

inclusion problem are given. This approach is shown to be mathematically identical to other approaches such as the direct volume integral formulation. Expanding the eigenstrains and applied strains in the polynomial form in the position vector and satisfying the equivalence conditions at every point, the governing simultaneous algebraic equations for the unknown coefficients in the eigenstrain expansion are derived. The elastodynamic field outside an ellipsoidal inhomogeneity in a linear elastic isotropic medium is given as an example. The angular and frequency dependence of the induced displacement field, as well as the differential and total cross sections are formally given in series expansion form for the case of uniformly distributed eigenstrains. C.D.

A83-37729* Ohio State Univ., Columbus.
ON THE THREE-DIMENSIONAL VIBRATIONS OF THE CANTILEVERED RECTANGULAR PARALLELEPIPED
 A. LEISSA (Ohio State University, Columbus, OH) and Z.-D. ZHANG Acoustical Society of America, Journal (ISSN 0001-4966), vol. 73, June 1983, p. 2013-2021. refs
 (Contract NAG3-36)

A solution is presented for the three-dimensional problem of determining the free vibration frequencies and mode shapes for a rectangular parallelepiped which is completely fixed on one face and free on the other five faces. This problem apparently is previously unsolved in the published literature. The Ritz method is used, with displacements assumed in the form of algebraic polynomials. Convergence is studied. Numerical results are given for the first five frequencies of each of the four symmetry classes of vibration, for five thick parallelepiped configurations, including the cube. Contour plots are exhibited for the modal displacements of the cube. The effects of varying Poisson's ratio are also observed. Author

A83-38528* Northwestern Univ., Evanston, Ill.
DYNAMIC FIELDS NEAR A CRACK TIP GROWING IN AN ELASTIC-PERFECTLY-PLASTIC SOLID
 S. NEMAT-NASSER (Northwestern University, Evanston, IL) and Y. C. GAO Mechanics of Materials (ISSN 0167-6636), vol. 2, April 1983, p. 47-60. refs
 (Contract NAG3-134)

A full asymptotic solution is presented for the fields in the neighborhood of the tip of a steadily advancing crack in an incompressible elastic-perfectly-plastic solid. There are four findings for mode I crack growth in the plane strain condition. The first is that the entire crack tip in steady crack growth is surrounded by a plastic region and that no elastic unloading is predicted by the complete dynamic asymptotic solution. The second is that, in contrast to the quasi-static solution, the dynamic solution yields strain fields with a logarithmic singularity everywhere near the crack tip. The third is that whereas the stress field varies throughout the entire crack tip neighborhood, it does not exhibit behavior that can be approximated by a constant field followed by an essentially centered-fan field and then by another constant field, especially for small crack growth speeds. The fourth finding is that there are two shock fronts emanating from the crack tip across which certain stress and strain components undergo jump discontinuities. After reviewing the mode III steady-state crack growth, it is concluded that ductile fracture criteria for nonstationary cracks must be based on solutions that include the inertia effects and that for this purpose quasi-static solutions may be inadequate. C.R.

A83-39557* Ohio State Univ., Columbus.
VIBRATIONS OF CANTILEVERED DOUBLY-CURVED SHALLOW SHELLS
 A. W. LEISSA, J. K. LEE, and A. J. WANG (Ohio State University, Columbus, OH) International Journal of Solids and Structures (ISSN 0020-7683), vol. 19, no. 5, 1983, p. 411-424. refs
 (Contract NAG3-36)

Vibrational characteristics are determined for a previously unsolved class of problems, that of doubly-curved shallow shells having rectangular planforms, clamped along one edge and free

on the other three. The solution procedure uses the Ritz method with algebraic polynomial trial functions. Convergence studies are made, and accurate frequencies and contour plots of mode shapes are presented for various curvature ratios, including spherical, circular cylindrical and hyperbolic paraboloidal shells. Particular emphasis is given to the effect of adding spanwise curvature to shells having chordwise curvature; numerous published references already exist for the case of zero spanwise curvature. The effects of changing aspect ratio, thickness ratio and Poisson's ratio are also studied. Author

A83-44050* Purdue Univ., West Lafayette, Ind.
WAVE PROPAGATION IN A GRAPHITE/EPOXY LAMINATE
 C. T. SUN and T. M. TAN (Purdue University, West Lafayette, IN) IN: Engineering science and mechanics; Proceedings of the International Symposium, Tainan, Republic of China, December 29-31, 1981. Part 2. San Diego, American Astronautical Society, 1983, p. 1290-1307. refs
 (Contract NSG-3185)

Harmonic wave and wave front propagations in a graphite/epoxy laminate are investigated using a plate theory that includes transverse shear deformation. Transient waves produced by impact of a steel ball are studied experimentally and by using finite elements. The statically measured law of contact between the steel ball and the laminate is used in the finite element program to compute the dynamic contact force. It is found that use of this contact law in conjunction with the finite element modeling of the laminate yields excellent agreement with the experimental results. Author

A83-47978*# Ohio State Univ., Columbus.
VIBRATIONS OF BLADES WITH VARIABLE THICKNESS AND CURVATURE BY SHELL THEORY
 J. K. LEE, A. W. LEISSA, and A. J. WANG (Ohio State University, Columbus, OH) American Society of Mechanical Engineers, International Gas Turbine Conference and Exhibit, 28th, Phoenix, AZ, Mar. 27-31, 1983. 6 p. refs
 (Contract NAG3-36)
 (ASME PAPER 83-GT-152)

A procedure for analyzing the vibrations of rotating turbomachinery blades has been previously developed. This procedure is based upon shallow shell theory, and utilizes the Ritz method to determine frequencies and mode shapes. However, it has been limited heretofore to blades of uniform thickness, uniform curvature, and/or twist and rectangular planform. The present work shows how the procedure may be generalized to eliminate the aforementioned restrictions. Nonrectangular planforms are dealt with by a suitable coordinate transformation. This, as well as variable thickness, curvature and twist, require using numerical integration. The procedure is demonstrated on four examples of cantilevered blades for which theoretical and experimental data have been previously published: (1) flat plate with spanwise taper, (2) flat plate with chordwise taper, (3) twisted plate with chordwise taper, and (4) cylindrical shell with chordwise taper. Author

A83-49437* Akron Univ., Ohio.
FINITE ELEMENT ANALYSIS OF STEADILY MOVING CONTACT FIELDS
 J. PADOVAN, S. TOVICHAKCHAIKUL (Akron, University, Akron, OH), and I. ZEID (North Eastern University, Boston, MA) Computers and Structures (ISSN 0045-7949), vol. 18, no. 2, 1984, p. 191-200. refs
 (Contract NAG3-54)

By introducing a moving updated Lagrangian observer, this paper develops traveling finite elements with the capacity to handle the global response resulting from steadily moving contact fields. The generality of the results is such that large deformation kinematics and kinetics as well as the full compliment of inertial fields can be handled. To streamline the handling of nonlinear behavior, an elliptically constrained solution algorithm is also developed. Employing this algorithm, the results of several numerical benchmarking studies are presented which illustrate the

capacity of the moving updated Lagrangian formulation as well as the potential effects of nonlinearity. Author

A84-11039* National Aeronautics and Space Administration. Lewis Research Center, Cleveland, Ohio.

TENSILE BUCKLING OF ADVANCED TURBOPROPS

C. C. CHAMIS and R. A. AIELLO (NASA, Lewis Research Center, Cleveland, OH) Journal of Aircraft (ISSN 0021-8669), vol. 20, Nov. 1983, p. 907-912. refs

Previously cited in issue 01, p. 60, Accession no. A83-10900

A84-13248* Georgia Inst. of Tech., Atlanta.

INELASTIC STRESS ANALYSES AT FINITE DEFORMATION THROUGH COMPLEMENTARY ENERGY APPROACHES

S. N. ATLURI (Georgia Institute of Technology, Atlanta, GA) and K. W. REED IN: Computer methods for nonlinear solids and structural mechanics; Proceedings of the Applied Mechanics, Bioengineering, and Fluids Engineering Conference, Houston, TX, June 20-22, 1983. New York, American Society of Mechanical Engineers, 1983, p. 191-226. refs

(Contract NAG3-346)

A new hybrid-stress finite element algorithm, suitable for analyses of large, quasistatic, inelastic deformations, is presented. The algorithm is based upon a generalization of de Veubeke's (1972) complementary energy principle. The principal variables in the formulation are the nominal stress rate and spin, and the resulting finite element equations are discrete versions of the equations of compatibility and angular momentum balance. The algorithm produces true rates, time derivatives, as opposed to 'increments'. There results a boundary value problem (for stress rate and velocity) and an initial value problem (for total stress and deformation). A discussion of the numerical treatment of the boundary value problem is followed by a detailed examination of the numerical treatment of the initial value problem, covering the topics of efficiency, stability, and objectivity. The paper is closed with a set of examples, finite homogeneous deformation problems, which serve to bring out important aspects of the algorithm.

Author

A84-13545* Texas Univ., Austin.

COMMENTS ON SOME PROBLEMS IN COMPUTATIONAL PENETRATION MECHANICS

J. T. ODEN (Texas, University, Austin, TX) IN: Computational aspects of penetration mechanics; Proceedings of the Workshop, Aberdeen Proving Ground, MD, April 27-29, 1982. Berlin, Springer-Verlag, 1983, p. 149-165. refs

(Contract NAG3-329; F49620-78-C-0083)

Three problem areas in the computer simulation of large-scale penetration mechanics problems are briefly discussed. These are numerical instabilities due to incomplete integration of the momentum or continuity equations, constitutive modelling, and friction effects. Author

A84-16874* Georgia Inst. of Tech., Atlanta.

ANALYSES OF LARGE QUASISTATIC DEFORMATIONS OF INELASTIC BODIES BY A NEW HYBRID-STRESS FINITE ELEMENT ALGORITHM

K. W. REED and S. N. ATLURI (Georgia Institute of Technology, Atlanta, GA) Computer Methods in Applied Mechanics and Engineering (ISSN 0045-7825), vol. 39, Sept. 1983, p. 245-295. refs

(Contract NAG3-38)

A new hybrid-stress finite element algorithm, suitable for analyses of large, quasistatic, inelastic deformations, is presented. The algorithm is based upon a generalization of de Veubeke's complementary energy principle. The principal variables in the formulation are the nominal stress rate and spin, and the resulting finite element equations are discrete versions of the equations of compatibility and angular momentum balance. The algorithm produces true rates, time derivatives, as opposed to 'increments'. There results a complete separation of the boundary value problem (for stress rate and velocity) and the initial value problem (for total stress and deformation); hence, their numerical treatments

are essentially independent. After a fairly comprehensive discussion of the numerical treatment of the boundary value problem, we launch into a detailed examination of the numerical treatment of the initial value problem, covering the topics of efficiency, stability and objectivity. The paper is closed with a set of examples, finite homogeneous deformation problems, which serve to bring out important aspects of the algorithm. Author

A84-16884* Georgia Inst. of Tech., Atlanta.

ANALYSES OF LARGE QUASISTATIC DEFORMATIONS OF INELASTIC BODIES BY A NEW HYBRID-STRESS FINITE ELEMENT ALGORITHM - APPLICATIONS

K. W. REED and S. N. ATLURI (Georgia Institute of Technology, Atlanta, GA) Computer Methods in Applied Mechanics and Engineering (ISSN 0045-7825), vol. 40, Oct. 1983, p. 171-198. refs

(Contract NAG3-38)

A new hybrid-stress finite element algorithm suitable for analyzing large quasistatic deformations of inelastic solids is presented and its feasibility and performance are demonstrated with examples. The algorithm provides extremely accurate bifurcation analysis which is stable with respect to variation in the finite element mesh, so long as the same type of element is used in every mesh. When the mesh element is varied, the result changes in a predictable manner. The method does not necessarily lead to an upper or lower bound for the critical load. An explicit forward gradient scheme is used to improve stability and is shown to be useful also for elongation-dominated deformations. The application of the method to the onset of necking in plane extension and to deformation and stress in plane extension of an elasticoviscous fluid with an array of cylindrical voids is given in detail. C.D.

A84-18691* National Aeronautics and Space Administration. Lewis Research Center, Cleveland, Ohio.

ANALYSIS OF AN INTERNALLY RADially CRACKED RING SEGMENT SUBJECT TO THREE-POINT RADIAL LOADING

B. GROSS and J. E. SRAWLEY (NASA, Lewis Research Center, Cleveland, OH) Journal of Testing and Evaluation (ISSN 0090-3973), vol. 11, Nov. 1983, p. 357-359. refs

The boundary collocation method was used to generate Mode I stress intensity and crack mouth opening displacement coefficients for externally radially cracked ring segments subjected to three point radial loading. Numerical results were obtained for ring segment outer-to-inner radius ratios ($R_{\text{sub } o}/R_{\text{sub } i}$) ranging from 1.10 to 2.50 and crack length to segment width ratios (a/W) ranging from 0.1 to 0.8. Stress intensity and crack mouth displacement coefficients were found to depend on the ratios $R_{\text{sub } o}/R_{\text{sub } i}$ and a/W as well as the included angle between the directions of the reaction forces. Previously announced in STAR as N83-35413 Author

A84-21267* Princeton Univ., N. J.

FORCED RESPONSE OF A CANTILEVER BEAM WITH A DRY FRICTION DAMPER ATTACHED. I - THEORY. II - EXPERIMENT

E. H. DOWELL and H. B. SCHWARTZ (Princeton University, Princeton, NJ) Journal of Sound and Vibration (ISSN 0022-460X), vol. 91, Nov. 22, 1983, p. 255-267, 269-291. refs

(Contract NAG3-221)

A theoretical and experimental study of the forced vibration response of a cantilevered beam with Coulomb damping nonlinearity is described. Viscous damping in the beam is neglected. Beam and dry friction damper configurations of interest for applications to turbine blade vibrations are considered. It is shown that the basic phenomena found by Dowell (1983) for a simply supported beam with an attached dry friction damper of specific geometry also apply to a cantilevered beam and a more general representation of the dry friction damper and its associated mass and stiffness. C.D.

A84-21541* Massachusetts Inst. of Tech., Cambridge.
ON THE SUPPRESSION OF ZERO ENERGY DEFORMATION MODES

T. H. H. PIAN (MIT, Cambridge, MA) and D. CHEN International Journal for Numerical Methods in Engineering (ISSN 0029-5981), vol. 19, Dec. 1983, p. 1741-1752. refs
 (Contract NAG3-33)

Based on the Hellinger-Reissner principle and the deformation energy due to assumed stresses and displacements, the problem of the kinematic deformation modes in assumed stress hybrid/mixed finite elements has been examined. Basic schemes are developed for the choice of assumed stress terms that will suppress all kinematic deformation modes. Quadrilateral membrane and axisymmetric elements, and three-dimensional hexahedral elements, are used to illustrate the suggested procedure. Author

A84-27370* Texas Univ., Austin.
A NUMERICAL ANALYSIS OF CONTACT AND LIMIT-POINT BEHAVIOR IN A CLASS OF PROBLEMS OF FINITE ELASTIC DEFORMATION

T. ENDO, J. T. ODEN, E. B. BECKER, and T. MILLER (Texas, University, Austin, TX) Computers and Structures (ISSN 0045-7949), vol. 18, no. 5, 1984, p. 899-910. refs
 (Contract NAG3-329)

Finite element methods for the analysis of bifurcations, limit-point behavior, and unilateral frictionless contact of elastic bodies undergoing finite deformation are presented. Particular attention is given to the development and application of Riks-type algorithms for the analysis of limit points and exterior penalty methods for handling the unilateral constraints. Applications focus on the problem of finite axisymmetric deformations, snap-through, and inflation of thick rubber spherical shells. Author

A84-29103*# Textron Bell Aerospace Co., Buffalo, N. Y.
NASTRAN FORCED VIBRATION ANALYSIS OF ROTATING CYCLIC STRUCTURES

V. ELCHURI, G. C. C. SMITH, and A. M. GALLO (Bell Aerospace Textron, Buffalo, NY) American Society of Mechanical Engineers, Design and Production Engineering Technical Conference, Dearborn, MI, Sept. 11-14, 1983. 11 p. refs
 (Contract NAS3-22533)
 (ASME PAPER 83-DET-20)

Theoretical aspects of a new capability, developed and added to the general purpose finite element program NASTRAN Level 17.7, to conduct forced vibration analysis of turned cyclic structures rotating about their axis of symmetry, are presented. The effects of Coriolis and centripetal accelerations as well as those due to the translational acceleration of the axis of rotation, are included. The equations of motion are first derived for an arbitrary grid point of the cyclic sector finite element model and then extended for the complete model. The equations are solved by four principal steps: (1) transformation of applied loads at frequency-dependent circumferential harmonic components; (2) application of circumferential harmonic-dependent intersegment compatibility constraints; (3) solution of frequency-dependent circumferential harmonic components of displacements; and (4) recovery of frequency-dependent response in various segments of the total structure. Five interrelated examples are presented to illustrate the various features of the development. C.D.

A84-31596* Arizona Univ., Tucson.
ADVANCED RELIABILITY METHOD FOR FATIGUE ANALYSIS

Y.-T. WU and P. H. WIRSCHING (Arizona, University, Tucson, AZ) Journal of Engineering Mechanics (ISSN 0733-9399), vol. 110, April 1984, p. 536-553. Research supported by the Cummins Engine Co. refs
 (Contract NAG3-41)

When design factors are considered as random variables and the failure condition cannot be expressed by a closed form algebraic inequality, computations of risk (or probability of failure) may become extremely difficult or very inefficient. This study suggests using a simple and easily constructed second degree polynomial to approximate the complicated limit state in the neighborhood of

the design point; a computer analysis relates the design variables at selected points. Then a fast probability integration technique (i.e., the Rackwitz-Fiessler algorithm) can be used to estimate risk. The capability of the proposed method is demonstrated in an example of a low cycle fatigue problem for which a computer analysis is required to perform local strain analysis to relate the design variables. A comparison of the performance of this method is made with a far more costly Monte Carlo solution. Agreement of the proposed method with Monte Carlo is considered to be good. Author

A84-31903*# Massachusetts Inst. of Tech., Cambridge.
STAGGER ANGLE DEPENDENCE OF INERTIAL AND ELASTIC COUPLING IN BLADED DISKS

E. F. CRAWLEY and D. R. MOKADAM (MIT, Cambridge, MA) ASME, Transactions, Journal of Vibration, Acoustics, Stress and Reliability in Design (ISSN 0739-3717), vol. 106, April 1984, p. 181-188. refs
 (Contract NAG3-200; F33615-81-K-2036)

Conditions which necessitate the inclusion of disk and shaft flexibility in the analysis of blade response in rotating blade-disk-shaft systems are derived in terms of nondimensional parameters. A simple semianalytical Rayleigh-Ritz model is derived in which the disk possesses all six rigid body degrees of freedom, which are elastically constrained by the shaft. Inertial coupling by the rigid body motion of the disk on a flexible shaft and out-of-plane elastic coupling due to disk flexure are included. Frequency ratios and mass ratios, which depend on the stagger angle, are determined for three typical rotors: a first stage high-pressure core compressor, a high bypass ratio fan, and an advanced turboprop. The stagger angle controls the degree of coupling in the blade-disk system. In the blade-disk-shaft system, the stagger angle determines whether blade-disk motion couples principally to the out-of-plane or in-plane motion of the disk on the shaft. The Ritz analysis shows excellent agreement with experimental results. J.N.

A84-32039* National Aeronautics and Space Administration.
 Lewis Research Center, Cleveland, Ohio.

THE STRUCTURAL RESPONSE OF A RAIL ACCELERATION
 S. Y. WANG (NASA, Lewis Research Center, Cleveland, OH) (Institute of Electrical and Electronics Engineers, Symposium on Electromagnetic Launch Technology, 2nd, Boston, MA, Oct. 10-13, 1983) IEEE Transactions on Magnetics (ISSN 0018-9464), vol. MAG-20, March 1984, p. 356-359. refs

The transient response of a 0.4 by 0.6 cm rectangular bore rail accelerator was analyzed by a three dimensional finite element code. The copper rail deflected to a peak value of 0.08 mm in compression and then oscillated at an amplitude of 0.02 mm. Simultaneously the insulating side wall of glass fabric base, epoxy resin laminate (G-10) was compressed to a peak value of 0.13 mm and rebounded to a steady state in extension. Projectile pinch or blowby due to the rail extension or compression, respectively, can be identified by examining the time history of the rail displacement. The effect of blowby was most significant at the side wall characterized by mm size displacement in compression. Dynamic stress calculations indicate that the G-10 supporting material behind the rail is subjected to over 21 MPa at which the G-10 could fail if the laminate was not carefully oriented. Results for a polycarbonate resin (Lexan) side wall show much larger displacements and stresses than for G-10. The tradeoff between the transparency of Lexan and the mechanical strength of G-10 for sidewall material is obvious. Displacement calculations from the modal method are smaller than the results from the direct integration method by almost an order of magnitude, because the high frequency effect is neglected. Previously announced in STAR as N83-35412 E.A.K.

A84-33701* National Aeronautics and Space Administration. Lewis Research Center, Cleveland, Ohio.

EFFECTS OF STRUCTURAL COUPLING ON MISTUNED CASCADE FLUTTER AND RESPONSE

R. E. KIELB and K. R. V. KAZA (NASA, Lewis Research Center, Cleveland, OH) ASME, Transactions, Journal of Engineering for Gas Turbines and Power (ISSN 0022-0825), vol. 106, Jan. 1984, p. 17-24. refs
(ASME PAPER 83-GT-117)

The effects of structural coupling on mistuned cascade flutter and response are analytically investigated using an extended typical section model. This model includes both structural and aerodynamic coupling between the blades. The model assumes that the structurally coupled system natural modes were determined and are represented in the form of N bending and N torsional uncoupled modes for each blade, where N is the number of blades and, hence, is only valid for blade dominated motion. The aerodynamic loads are calculated by using two dimensional unsteady cascade theories in the subsonic and supersonic flow regimes. The results show that the addition of structural coupling can affect both the aeroelastic stability and frequency. The stability is significantly affected only when the system is mistuned. The resonant frequencies can be significantly changed by structural coupling in both tuned and mistuned systems, however, the peak response is significantly affected only in the latter. Previously announced in STAR as N83-15672 S.L.

A84-33702* National Aeronautics and Space Administration. Lewis Research Center, Cleveland, Ohio.

MEASUREMENTS OF SELF-EXCITED ROTOR-BLADE VIBRATIONS USING OPTICAL DISPLACEMENTS

A. P. KURKOV (NASA, Lewis Research Center, Cleveland, OH) ASME, Transactions, Journal of Engineering for Gas Turbines and Power (ISSN 0022-0825), vol. 106, Jan. 1984, p. 44-49. refs
(ASME PAPER 83-GT-132)

The characteristics of optical displacement spectra and their role of monitoring rotor blade vibrations are discussed. During the operation of a turbofan engine at part speed, near stall, and elevated inlet pressure and temperature, several vibratory instabilities were excited simultaneously on the first fan rotor. The torsional and bending contributions to the main flutter mode were resolved by using casing-mounted optical displacement sensors. Other instabilities in the blade deflection spectra were identified. Previously announced in STAR as N83-14523 E.A.K.

A84-36492*# Bell Aerospace Co., Buffalo, N. Y.

FLUTTER ANALYSIS OF ADVANCED TURBOPROPELLERS

V. ELCHURI and G. C. C. SMITH (Bell Aerospace Textron, Buffalo, NY) (Structures, Structural Dynamics and Materials Conference, 24th, Lake Tahoe, NV, May 2-4, 1983, Collection of Technical Papers. Part 2, p. 160-165) AIAA Journal (ISSN 0001-1452), vol. 22, June 1984, p. 801, 802. refs
(Contract NAS3-22533)

Previously cited in issue 12, p. 1742, Accession no. A83-29824

A84-38480* Akron Univ., Ohio

ALGORITHMS FOR ELASTO-PLASTIC-CREEP POSTBUCKLING

J. PADOVAN (Akron, University, Akron, OH) and S. TOVICHAKCHAIKUL (IBM, Thailand) Journal of Engineering Mechanics (ISSN 0733-9399), vol. 110, June 1984, p. 911-929. refs
(Contract NAG3-54)

This paper considers the development of an improved constrained time stepping scheme which can efficiently and stably handle the pre-post-buckling behavior of general structure subject to high temperature environments. Due to the generality of the scheme, the combined influence of elastic-plastic behavior can be handled in addition to time dependent creep effects. This includes structural problems exhibiting indefinite tangent properties. To illustrate the capability of the procedure, several benchmark problems employing finite element analyses are presented. These

demonstrate the numerical efficiency and stability of the scheme. Additionally, the potential influence of complex creep histories on the buckling characteristics is considered. Author

A84-45994* Virginia Polytechnic Inst. and State Univ., Blacksburg.

A MIXED SHEAR FLEXIBLE FINITE ELEMENT FOR THE ANALYSIS OF LAMINATED PLATES

N. S. PUTCHA and J. N. REDDY (Virginia Polytechnic Institute and State University, Blacksburg, VA) Computer Methods in Applied Mechanics and Engineering (ISSN 0045-7825), vol. 44, July 1984, p. 213-227. refs
(Contract NAG3-208; AF-AFOSR-81-0142)

A mixed shear flexible finite element based on the Hencky-Mindlin type shear deformation theory of laminated plates is presented and their behavior in bending is investigated. The element consists of three displacements, two rotations, and three moments as the generalized degrees of freedom per node. The numerical convergence and accuracy characteristics of the element are investigated by comparing the finite element solutions with the exact solutions. The present study shows that reduced-order integration of the stiffness coefficients due to shear is necessary to obtain accurate results for thin plates. Author

A84-46937*# Air Force Aero Propulsion Lab., Wright-Patterson AFB, Ohio.

VIBRATIONS OF TWISTED CANTILEVERED PLATES - EXPERIMENTAL INVESTIGATION

J. C. MACBAIN (USAF, Aero Propulsion Laboratory, Wright-Patterson AFB, OH), R. E. KIELB (NASA, Lewis Research Center, Structural and Mechanical Technology Div., Cleveland, OH), and A. W. LEISSA (Ohio State University, Columbus, OH) American Society of Mechanical Engineers, International Gas Turbine Conference and Exhibit, 29th, Amsterdam, Netherlands, June 4-7, 1984. 10 p. refs
(ASME PAPER 84-GT-96)

The experimental portion of a joint government/industry/university research study on the vibrational characteristics of twisted cantilevered plates is presented. The overall purpose of the research study was to assess the capabilities and limitations of existing analytical methods in predicting the vibratory characteristics of twisted plates. Thirty cantilevered plates were precision machined at the Air Force's Aero Propulsion Laboratory. These plates, having five different degrees of twist, two thicknesses, and three aspect ratios representative of turbine engine blade geometries, were tested for their vibration mode shapes and frequencies. The resulting nondimensional frequencies and selected mode shapes are presented as a function of plate tip twist. The trends of the natural frequencies as a function of the governing geometric parameters are discussed. The effect of support compliance on the plate natural frequency and its impact on numerically modeling twisted plates is also presented. Author

A84-46957*# Carnegie-Mellon Univ., Pittsburgh, Pa.

THE INTERACTION BETWEEN MISTUNING AND FRICTION IN THE FORCED RESPONSE OF BLADED DISK ASSEMBLIES

J. H. GRIFFIN (Carnegie-Mellon University, Pittsburgh, PA) and A. SINHA (Pennsylvania State University, University Park, PA) American Society of Mechanical Engineers, International Gas Turbine Conference and Exhibit, 29th, Amsterdam, Netherlands, June 4-7, 1984. 7 p. refs
(Contract NAG3-231)
(ASME PAPER 84-GT-139)

This paper summarizes the results of an investigation to establish the impact of mistuning on the performance and design of blade-to-blade friction dampers of the type used to control the resonant response of turbine blades in gas turbine engines. In addition, it discusses the importance of friction slip force variations on the dynamic response of shrouded fan blades. Author

A84-48565* Akron Univ., Ohio.

HIGH TEMPERATURE THERMOMECHANICAL ANALYSIS OF CERAMIC COATINGS

J. PADOVAN, M. J. BRAUN, B. T. F. CHUNG (Akron, University, Akron, OH), D. DOUGHERTY (General Tire and Rubber Co., Akron, OH), and R. HENDRICKS (NASA, Lewis Research Center, Cleveland, OH) *Journal of Thermal Stresses* (ISSN 0149-5739), vol. 7, no. 1, 1984, p. 51-74. refs
(Contract NAG3-265)

This paper investigates the thermomechanical response of ceramically coated metal parts in elevated thermal environments. This is made possible through the development of an improved finite element algorithm that enables the efficient and stable solution of the inherently nonlinear elastic-creep (inelastic) type thermomechanical field equations associated with high temperature. Based on the improved algorithm, the results of several numerical experiments are presented. These illustrate the significant influence of inelastic behavior in generating residual stress fields. Author

A85-11125* Texas Univ., Austin.

ANALYSIS OF HOURGLASS INSTABILITIES AND CONTROL IN UNDERINTEGRATED FINITE ELEMENT METHODS

O.-P. JACQUOTTE and J. T. ODEN (Texas, University, Austin, TX) *Computer Methods in Applied Mechanics and Engineering* (ISSN 0045-7825), vol. 44, Aug. 1984, p. 339-363. refs
(Contract NAG3-329)

Belytschko et al. (1981, 1984) has developed stabilization methods for the treatment of underintegrated FEM problems; these methods involve the computation of an underintegrated stiffness matrix, which is rank-deficient, and the addition of a stabilization matrix which effectively eliminates the spurious modes. An attempt is presently made to give this a priori stabilization method a mathematical means of support. Attention is also given to an a posteriori stabilization method for hourglass control, in which an approximate solution of the underintegrated system is obtained and then subjected to a special projection in order to eliminate the hourglass modes. A proof is obtained for the convergence of this stabilized underintegrated approximation to the exact solution of a model problem at almost the same rate (as the mesh is refined) as the fully integrated solutions. O.C.

A85-12029* Massachusetts Inst. of Tech., Cambridge.

RATIONAL APPROACH FOR ASSUMED STRESS FINITE ELEMENTS

T. H. H. PIAN (MIT, Cambridge, MA) and K. SUMIHARA *International Journal for Numerical Methods in Engineering* (ISSN 0029-5981), vol. 20, Sept. 1984, p. 1685-1695. refs
(Contract NAG3-33)

A new method for the formulation of hybrid elements by the Hellinger-Reissner principle is established by expanding the essential terms of the assumed stresses as complete polynomials in the natural coordinates of the element. The equilibrium conditions are imposed in a variational sense through the internal displacements which are also expanded in the natural co-ordinates. The resulting element possesses all the ideal qualities, i.e. it is invariant, it is less sensitive to geometric distortion, it contains a minimum number of stress parameters and it provides accurate stress calculations. For the formulation of a 4-node plane stress element, a small perturbation method is used to determine the equilibrium constraint equations. The element has been proved to be always rank sufficient. Author

A85-12716* National Aeronautics and Space Administration, Lewis Research Center, Cleveland, Ohio.

FLUTTER OF TURBOFAN ROTORS WITH MISTUNED BLADES

K. R. V. KAZA and R. E. KIELB (NASA, Lewis Research Center, Cleveland, OH) (Structures, Structural Dynamics and Materials Conference, 23rd, New Orleans, LA, May 10-12, 1982, Collection of Technical Papers. Part 2, p. 446-461) *AIAA Journal* (ISSN 0001-1452), vol. 22, Nov. 1984, p. 1618-1625. Previously cited in issue 13, p. 2111, Accession no. A82-30175. refs

A85-12721* Massachusetts Inst. of Tech., Cambridge.

FLUTTER AND FORCED RESPONSE OF MISTUNED ROTORS USING STANDING WAVE ANALYSIS

J. DUGUNDJI and D. J. BUNDAS (MIT, Cambridge, MA) (Structures, Structural Dynamics and Materials Conference, 24th, Lake Tahoe, NV, May 2-4, 1983, Collection of Technical Papers. Part 2, p. 149-159) *AIAA Journal* (ISSN 0001-1452), vol. 22, Nov. 1984, p. 1652-1661. Previously cited in issue 12, p. 1742, Accession no. A83-29823. refs
(Contract NAG3-214)

A85-13942* Babcock and Wilcox Co., New York, N.Y.

EXTENSION OF CONSTRAINED INCREMENTAL NEWTON-RAPHSON SCHEME TO GENERALIZED LOADING FIELDS

J. PADOVAN (Akron, University, Akron, OH) and S. PAI (Babcock and Wilcox Co., New York, NY; Akron, University, Akron, OH) *Franklin Institute, Journal* (ISSN 0016-0032), vol. 318, Sept. 1984, p. 165-186. refs
(Contract NAG3-54)

This paper develops numerical strategies which enable the constrained incremental Newton-Raphson scheme to handle the static response of structure to loading fields with completely generalized histories. This is made possible through the use of specially warped hyperelliptic constraint surfaces which control successive or clustered load steps in the vicinity of loading events with specific timing schedules. Such an approach enables improved convergence and stability characteristics. Due to the generality of the methodology, pre- and postbuckling behavior caused by both kinematic and material nonlinearity can be handled. To demonstrate the scheme, the results of several bench-mark problems are also presented. These include situations involving nonlinear kinematics as well as highly history-dependent elastic-plastic and thermoelastic-plastic material behavior. Author

A85-15893* Massachusetts Inst. of Tech., Cambridge.

HYBRID SEMILOOF ELEMENTS FOR PLATES AND SHELLS BASED UPON A MODIFIED HU-WASHIZU PRINCIPLE

T. H. H. PIAN (MIT, Cambridge, MA) and K. SUMIHARA *Computers and Structures* (ISSN 0045-7949), vol. 19, no. 1-2, 1984, p. 165-173. refs
(Contract NAG3-33)

Hybrid SemiLoof elements for plates and shells are developed based upon modified Hu-Washizu principle. In the new version of the assumed stress hybrid formulation the equilibrium equations are satisfied through the introduction of internal displacement parameters as Lagrange multipliers. The inversion of the resulting H-matrices is simplified particularly when the stresses are expressed in terms of natural coordinates. A 24-DOF triangular element and a 32-DOF quadrilateral element based on shallow shell theory are derived and evaluated. Author

A85-15894* Georgia Inst. of Tech., Atlanta.

HYBRID STRESS FINITE ELEMENTS FOR LARGE DEFORMATIONS OF INELASTIC SOLIDS

K. W. REED and S. N. ATLURI (Georgia Institute of Technology, Atlanta, GA) *Computers and Structures* (ISSN 0045-7949), vol. 19, no. 1-2, 1984, p. 175-182. refs
(Contract NAG3-38)

A new hybrid stress finite element algorithm, based on a generalization of Fraeijs de Veubeke's complementary energy principle is presented. Analyses of large quasistatic deformation of inelastic solids (hypoelastic, plastic, viscoplastic) are within its capability. Principle variables in the formulation are the nominal stress rate and spin. A brief account is given of the boundary value problem in these variables, and the 'equivalent' variational principle. The finite element equation, along with initial positions and stresses, comprise an initial value problem. Factors affecting the choice of time integration schemes are discussed. Results found by application of the new algorithm are compared to those obtained by a velocity based finite element algorithm. Author

A85-16095*# National Aeronautics and Space Administration. Lewis Research Center, Cleveland, Ohio.

VIBRATION AND FLUTTER OF MISTUNED BLADED-DISK ASSEMBLIES

K. RAO, V. KAZA (NASA, Lewis Research Center, Cleveland, OH), and R. E. KIELB AIAA, ASME, ASCE, and AHS, Structures, Structural Dynamics and Materials Conference, 25th, Palm Springs, CA, May 14-16, 1984. 16 p. Previously announced in STAR as N84-23923. refs (AIAA PAPER 84-0991)

An analytical model for investigating vibration and flutter of mistuned bladed disk assemblies is presented. This model accounts for elastic, inertial and aerodynamic coupling between bending and torsional motions of each individual blade, elastic and inertial couplings between the blades and the disk, and aerodynamic coupling among the blades. The disk was modeled as a circular plate with constant thickness and each blade was represented by a twisted, slender, straight, nonuniform, elastic beam with a symmetric cross section. The elastic axis, inertia axis, and the tension axis were taken to be noncoincident and the structural warping of the section was explicitly considered. The blade aerodynamic loading in the subsonic and supersonic flow regimes was obtained from two-dimensional unsteady, cascade theories. All the possible standing wave modes of the disk and traveling wave modes of the blades were included. The equations of motion were derived by using the energy method in conjunction with the assumed mode shapes for the disk and the blades. Continuities of displacement and slope at the blade-disk junction were maintained. The equations were solved to investigate the effects of blade-disk coupling and blade frequency mistuning on vibration and flutter. Results showed that the flexibility of practical disks such as those used for current generation turbopumps did not have a significant influence on either the tuned or mistuned flutter characteristics. However, the disk flexibility may have a strong influence on some of the system frequencies and on forced response. Author

A85-17039*# Rice Univ., Houston, Tex.

OSCILLATOR RESPONSE TO NONSTATIONARY EXCITATION

P.-T. D. SPANOS (Rice University, Houston, TX) and G. P. SOLOMOS ASME, Transactions, Journal of Applied Mechanics (ISSN 0021-8936), vol. 51, Dec. 1984, p. 907-912. refs (Contract NAG3-210) (ASME PAPER 84-WA/APM-38)

Analytical solutions are presented regarding probability density distributions of various response parameters of a lightly damped oscillator. The oscillator is subjected to a broad-band stochastic excitation which possesses a time-variant power spectrum. The analytical solutions are derived by utilizing appropriate Fokker-Planck equations which govern Markovian approximations of the response parameters considered. The reliability of the approximate analytical solution is tested by using pertinent data generated by a digital Monte Carlo study. Author

A85-17040*# National Aeronautics and Space Administration. Lewis Research Center, Cleveland, Ohio.

EFFECTS OF WARPING AND PRETWIST ON TORSIONAL VIBRATION OF ROTATING BEAMS

K. R. V. KAZA and R. E. KIELB (NASA, Lewis Research Center, Cleveland, OH) ASME, Transactions, Journal of Applied Mechanics (ISSN 0021-8936), vol. 51, Dec. 1984, p. 913-920. refs (ASME PAPER 84-WA/APM-41)

The effect of pretwist and warping on the torsional vibration of short-aspect-ratio rotating beams is examined for application to the modeling of turbofan, turboprop, and compressor blades. The equations of motion and the associated boundary conditions by using both Wagner's hypothesis and Washizu's theory are derived and a few minor limitations of the Wagner's hypothesis, as applied to thick blades, are pointed out and discussed. The equations for several special cases are solved in a closed form. Results are presented indicating the effect of warping, pretwist, and rotation on torsional vibration of beams as aspect ratio is varied. The

results show that the structural warping and pretwist terms have a significant effect on torsional frequency and mode shapes of short-aspect-ratio blades whereas the inertial warping terms have negligible effect. Since the torsional frequencies and mode shapes are very important in aeroelastic analyses by using modal methods, the structural warping terms should be included in modeling turbofan, turboprop, compressor, and turbine blades. Author

A85-18795*# Battelle Columbus Labs., Ohio.

A HISTORY DEPENDENT DAMAGE MODEL FOR LOW CYCLE FATIGUE

B. N. LEIS (Battelle Columbus Laboratories, Columbus, OH) American Society of Mechanical Engineers, Pressure Vessels and Piping Conference and Exhibition, San Antonio, TX, June 17-21, 1984. 10 p. Research supported by the Battelle Columbus Laboratories, and Battelle Memorial Institute. refs (Contract NAS3-22825) (ASME PAPER 84-PVP-112)

This paper examines damage assessment and accumulation. A nonlinear damage postulate is advanced that embodies the dependence of the damage rate on cycle-dependent changes in the bulk microstructure and the surface topography. The postulate is analytically formulated in terms of the deformation history dependence of the bulk behavior. This formulation is used in conjunction with baseline data in accordance with the damage postulate to predict the low cycle fatigue resistance of OFE copper. Close comparison of the predictions with observed behavior suggests the postulate offers a viable basis for nonlinear damage analysis. Author

A85-19433* Case Western Reserve Univ., Cleveland, Ohio.

STATISTICS AND THERMODYNAMICS OF FRACTURE

A. CHUDNOVSKY (Case Western Reserve University, Cleveland, OH) (Michigan Technological University, Workshop on Media with Microstructure and Wave Propagation, Michigan Technological University, Houghton, MI, Jan. 24, 25, 1983) International Journal of Engineering Science (ISSN 0020-7225), vol. 22, no. 8-10, 1984, p. 989-997. refs (Contract NAG3-223)

A probabilistic model of the fracture processes unifying the phenomenological study of long term strength of materials, fracture mechanics and statistical approaches to fracture is briefly outlined. The general framework of irreversible thermodynamics is employed to model the deterministic side of the failure phenomenon. The stochastic calculus is used to account for the failure mechanisms controlled by chance; particularly, the random roughness of fracture surfaces. Author

A85-19899* Georgia Inst. of Tech., Atlanta.

DEVELOPMENT AND TESTING OF STABLE, INVARIANT, ISOPARAMETRIC CURVILINEAR 2- AND 3-D HYBRID-STRESS ELEMENTS

E. F. PUNCH (Georgia Institute of Technology, Atlanta, GA; GM Research Laboratories, Warren, MI) and S. N. ATLURI (Georgia Institute of Technology, Atlanta, GA) Computer Methods in Applied Mechanics and Engineering (ISSN 0045-7825), vol. 47, Dec. 1984, p. 331-356. refs (Contract NAG3-346)

Linear and quadratic Serendipity hybrid-stress elements are examined in respect of stability, coordinate invariance, and optimality. A formulation based upon symmetry group theory successfully addresses these issues in undistorted geometries and is fully detailed for plane elements. The resulting least-order stable invariant stress polynomials can be applied as astute approximations in distorted cases through a variety of tensor components and variational principles. A distortion sensitivity study for two- and three-dimensional elements provides favorable numerical comparisons with the assumed displacement method. Author

39 STRUCTURAL MECHANICS

A85-22069* Ohio State Univ., Cleveland.

VIBRATIONS OF TWISTED CANTILEVERED PLATES - SUMMARY OF PREVIOUS AND CURRENT STUDIES

A. W. LEISSA (Ohio State University, Columbus, OH), J. C. MACBAIN (USAF, Aero Propulsion Laboratory, Wright-Patterson AFB, OH), and R. E. KIELB (NASA, Lewis Research Center, Structural and Mechanical Technology Div., Cleveland, OH) *Journal of Sound and Vibration* (ISSN 0022-460X), vol. 96, Sept. 22, 1984, p. 159-173. refs

This work summarizes a comprehensive study made of the free vibrations of twisted, cantilevered plates of rectangular planform. Numerous theoretical and experimental investigations previously made by others have resulted in frequency results which disagree considerably. To clarify the problem a joint industry/government/university research effort was initiated to obtain comprehensive theoretical and experimental results for models having useful ranges of aspect ratios, thickness ratios and twist angles. Theoretical data came from 19 independent computer analyses, including finite element, shell theory and beam theory idealizations. Two independent sets of experimental data were also obtained. The theoretical and experimental results are summarized and compared. Author

A85-23150*# National Aeronautics and Space Administration. Lewis Research Center, Cleveland, Ohio.

A SIMPLIFIED METHOD FOR ELASTIC-PLASTIC-CREEP STRUCTURAL ANALYSIS

A. KAUFMAN (NASA, Lewis Research Center, Cleveland, OH) *ASME, Transactions, Journal of Engineering for Gas Turbines and Power* (ISSN 0022-0825), vol. 107, Jan. 1985, p. 231-237. refs (ASME PAPER 84-GT-191)

A simplified inelastic analysis computer program (ANSYPM) was developed for predicting the stress-strain history at the critical location of a thermomechanically cycled structure from an elastic solution. The program uses an iterative and incremental procedure to estimate the plastic strains from the material stress-strain properties and a plasticity hardening model. Creep effects are calculated on the basis of stress relaxation at constant strain, creep at constant stress or a combination of stress relaxation and creep accumulation. The simplified method was exercised on a number of problems involving uniaxial and multiaxial loading, isothermal and nonisothermal conditions, dwell times at various points in the cycles, different materials and kinematic hardening. Good agreement was found between these analytical results and nonlinear finite element solutions for these problems. The simplified analysis program used less than 1 percent of the CPU time required for a nonlinear finite element analysis. Author

A85-24532* Northwestern Univ., Evanston, Ill.

ON STRESS FIELD NEAR A STATIONARY CRACK TIP

S. NEMAT-NASSER and M. OBATA (Northwestern University, Evanston, IL) *Mechanics of Materials* (ISSN 0167-6636), vol. 3, Sept. 1984, p. 235-243. refs (Contract NAG3-134; DAAG29-82-K-0147) (AD-A152863)

It is well known that the stress and elastic-plastic deformation fields near a crack tip have important roles in the corresponding fracture process. For elastic-perfectly-plastic solids, different solutions are given in the literature. In this work several of these solutions are examined and compared for Mode I (tension), Mode II (shear), and mixed Modes I and II loading conditions in plane strain. By consideration of the dynamic solution, it is shown that the assumption that the material is yielding all around a crack tip may not be reasonable in all cases. By admitting the existence of some elastic sectors, continuous stress fields are obtained even for mixed Modes I and II. Author

A85-27935* Materials Research Lab., Inc., Glenwood, Ill.

FRACTURE OF COMPOSITE-ADHESIVE-COMPOSITE SYSTEMS

E. J. RIPLING, J. S. SANTNER, and P. B. CROSLLEY (Materials Research Laboratory, Inc., Glenwood, IL) *IN: Adhesive joints: Formation, characteristics, and testing*. New York, Plenum Press, 1984, p. 755-787. refs (Contract NAS3-21824)

This program was undertaken to initiate the development of a test method for testing adhesive joints in metal-adhesive-composite systems. The uniform double cantilever beam (UDCB) and the width tapered beam (WTB) specimen geometries were evaluated for measuring Mode I fracture toughness in these systems. The WTB specimen is the preferred geometry in spite of the fact that it is more costly to machine than the UDCB specimen. The use of loading tabs attached to thin sheets of composites proved to be experimentally unsatisfactory. Consequently, a new system was developed to load thin sheets of adherends. This system allows for the direct measurement of displacement along the load line. In well made joints separation occurred between the plies rather than in the adhesive. Author

A85-30313*# Pratt and Whitney Aircraft Group, East Hartford, Conn.

FINITE ELEMENT ENGINE BLADE STRUCTURAL OPTIMIZATION

K. W. BROWN (United Technologies Corp., Pratt and Whitney Group, East Hartford, CT), M. S. HIRSCHBEIN, and C. C. CHAMIS (NASA, Lewis Research Center, Cleveland, OH) *IN: Structures, Structural Dynamics, and Materials Conference, 26th, Orlando, FL, April 15-17, 1985, Technical Papers. Part 1*. New York, American Institute of Aeronautics and Astronautics, 1985, p. 793-803. refs (Contract NAS3-22525) (AIAA PAPER 85-0645)

The Structural Tailoring of Engine Blades (STAEBL) computer program was developed to perform engine fan blade numerical optimizations. These blade optimizations seek a minimum weight or cost design that satisfies realistic blade design constraints, by tuning one to twenty design variables. The STAEBL system has been generalized to include both fan and compressor blade numerical optimizations. The system analyses have been significantly improved through the inclusion of an efficient plate finite element analysis for blade stress and frequency determinations. Additionally, a finite element based approximate severe foreign object damage (FOD) analysis has been included. The new FOD analysis gives very accurate estimates of the full nonlinear bird ingestion solution. Optimizations of fan and compressor blades have been performed using the system, showing significant cost and weight reductions, while comparing very favorably with refined design validation procedures. Author

A85-32343* Indian Inst. of Tech., Madras.

NATURAL FREQUENCIES OF TWISTED ROTATING PLATES

V. RAMAMURTI (Indian Institute of Technology, Madras, India) and R. KIELB (NASA, Lewis Research Center, Cleveland, OH) *Journal of Sound and Vibration* (ISSN 0022-460X), vol. 97, Dec. 8, 1984, p. 429-449. refs

A detailed comparison is presented of the predicted eigenfrequencies of twisted rotating plates as obtained by using two different shape functions. Primarily, rotating twisted plates of two different aspect ratios and two different thickness ratios are considered. The effects of rotation are included by using a 'stress smoothing' technique when calculating the augmented stiffness matrix. In addition, the effects of Coriolis acceleration, contributions from membrane behavior, setting angle and sweep angle are considered. The effects of geometric nonlinearity are briefly discussed. Finally, results of a brief study of cambered plates are presented. Author

A85-32962*# National Aeronautics and Space Administration. Lewis Research Center, Cleveland, Ohio.

FLUTTER OF SWEEP FAN BLADES

R. E. KIELB and K. R. V. KAZA (NASA, Lewis Research Center, Cleveland, OH) ASME, Transactions, Journal of Engineering for Gas Turbines and Power (ISSN 0022-0825), vol. 107, April 1985, p. 394-398. Previously announced in STAR as N84-16587. refs (ASME PAPER 84-GT-138)

The effect of sweep on fan blade flutter is studied by applying the analytical methods developed for aeroelastic analysis of advance turboprops. Two methods are used. The first method utilizes an approximate structural model in which the blade is represented by a swept, nonuniform beam. The second method utilizes a finite element technique to conduct modal flutter analysis. For both methods the unsteady aerodynamic loads are calculated using two dimensional cascade theories which are modified to account for sweep. An advanced fan stage is analyzed with 0, 15 and 30 degrees of sweep. It is shown that sweep has a beneficial effect on predominantly torsional flutter and a detrimental effect on predominantly bending flutter. This detrimental effect is shown to be significantly destabilizing for 30 degrees of sweep. M.G.

A85-33847* Georgia Inst. of Tech., Atlanta.

ON THE EXISTENCE AND STABILITY CONDITIONS FOR MIXED-HYBRID FINITE ELEMENT SOLUTIONS BASED ON REISSNER'S VARIATIONAL PRINCIPLE

L. A. KARLOVITZ, S. N. ATLURI (Georgia Institute of Technology, Atlanta, GA), and W.-M. XUE International Journal of Solids and Structures (ISSN 0020-7683), vol. 21, no. 1, 1985, p. 97-116. refs

(Contract NAG3-346)

The extensions of Reissner's two-field (stress and displacement) principle to the cases wherein the displacement field is discontinuous and/or the stress field results in unreciprocated tractions, at a finite number of surfaces ('interelement boundaries') in a domain (as, for instance, when the domain is discretized into finite elements), is considered. The conditions for the existence, uniqueness, and stability of mixed-hybrid finite element solutions based on such discontinuous fields, are summarized. The reduction of these global conditions to local ('element') level, and the attendant conditions on the ranks of element matrices, are discussed. Two examples of stable, invariant, least-order elements - a four-node square planar element and an eight-node cubic element - are discussed in detail. Author

A85-35046*# Massachusetts Inst. of Tech., Cambridge.

EVOLUTION OF ASSUMED STRESS HYBRID FINITE ELEMENT

T. H. H. PIAN (MIT, Cambridge, MA) World Congress and Exhibition on Finite Element Methods, 4th, Interlaken, Switzerland, Sept. 17-21, 1984, Preprint. 18 p. refs (Contract NAG3-33; F33615-83-K-5016)

Early versions of the assumed stress hybrid finite elements were based on the a priori satisfaction of stress equilibrium conditions. In the new version such conditions are relaxed but are introduced through additional internal displacement functions as Lagrange multipliers. A rational procedure is to choose the displacement terms such that the resulting strains are now of complete polynomials up to the same degree as that of the assumed stresses. Several example problems indicate that optimal element properties are resulted by this method. Author

A85-35048*

PLASTICITY, VISCOPLASTICITY, AND CREEP OF SOLIDS BY MECHANICAL SUBELEMENT MODELS

T. H. H. PIAN IN: Numerical methods in coupled systems. Chichester, Sussex, England, John Wiley and Sons, Ltd., 1984, p. 119-126. refs

(Contract NAG3-33)

This paper discusses the modelling by mechanical subelements, the general plasticity, the viscoplasticity, and the creep behavior of solids under multiaxial loading conditions. The formulation of a time-independent elastic-plastic analysis is based on the viscoplasticity theory and the assumed stress finite element

method. An example of an in-plane stress problem is included.

Author

A85-37440* Akron Univ., Ohio.

PANTOGRAPHING SELF ADAPTIVE GAP ELEMENTS

J. PADOVAN, R. MOSCARELLO (Akron, University, Akron, OH), J. STAFFORD, and F. TABADDOR (B.F. Goodrich Co., Akron, OH) Computers and Structures (ISSN 0045-7949), vol. 20, no. 4, 1985, p. 745-758. refs

(Contract NAG3-54)

This paper develops a so-called pantographing self adaptive gap element type contact strategy. Due to the manner of formulation, the scheme has the capability to handle large deformations in the contact zone; contact initiation in structure exhibiting either positive or indefinite stiffness characteristics; kinematic and material nonlinearity as well as; self adaptively adjusts load/time stepping. In this context, contact in pre and postbuckling structure can be treated. To illustrate the scheme, several benchmark problems are presented. These include contacting structure involving large deformation kinematics, inelastic behavior as well as pre and postbuckling stiffness characteristics. Author

A85-38425*# Technion - Israel Inst. of Tech., Haifa.

THERMODYNAMICALLY CONSISTENT CONSTITUTIVE EQUATIONS FOR NONISOTHERMAL LARGE STRAIN, ELASTO-PLASTIC, CREEP BEHAVIOR

R. RIFF (Technion - Israel Institute of Technology, Haifa, Israel; Georgia Institute of Technology, Atlanta, GA), R. L. CARLSON, and G. J. SIMITSES (Georgia Institute of Technology, Atlanta, GA) American Institute of Aeronautics and Astronautics, Structures, Structural Dynamics and Materials Conference, 26th, Orlando, FL, Apr. 15-17, 1985. 11 p.

(Contract NAG3-534)

(AIAA PAPER 85-0621)

The paper is concerned with the development of constitutive relations for large nonisothermal elastic-viscoplastic deformations for metals. The kinematics of elastic-plastic deformation, valid for finite strains and rotations, is presented. The resulting elastic-plastic uncoupled equations for the deformation rate combined with use of the incremental elasticity law permits a precise and purely deductive development of elastic-viscoplastic theory. It is shown that a phenomenological thermodynamic theory in which the elastic deformation and the temperature are state variables, including few internal variables, can be utilized to construct elastic-viscoplastic constitutive equations, which are appropriate for metals. The limiting case of inviscid plasticity is examined. Author

A85-39769*# National Aeronautics and Space Administration. Lewis Research Center, Cleveland, Ohio.

UNIFIED CONSTITUTIVE MATERIAL MODELS FOR NONLINEAR FINITE-ELEMENT STRUCTURAL ANALYSIS

A. KAUFMAN (NASA, Lewis Research Center, Cleveland, OH), J. H. LAFFLE (General Electric Co., Cincinnati, OH), and U. S. LINDHOLM (Southwest Research Institute, San Antonio, TX) AIAA, SAE, ASME, and ASEE, Joint Propulsion Conference, 21st, Monterey, CA, July 8-10, 1985. 10 p. Previously announced in STAR as N85-24338. refs

(AIAA PAPER 85-1418)

Unified constitutive material models were developed for structural analyses of aircraft gas turbine engine components with particular application to isotropic materials used for high-pressure stage turbine blades and vanes. Forms or combinations of models independently proposed by Bodner and Walker were considered. These theories combine time-dependent and time-independent aspects of inelasticity into a continuous spectrum of behavior. This is in sharp contrast to previous classical approaches that partition inelastic strain into uncoupled plastic and creep components. Predicted stress-strain responses from these models were evaluated against monotonic and cyclic test results for uniaxial specimens of two cast nickel-base alloys, B1900+Hf and Rene 80. Previously obtained tension-torsion test results for Hastelloy X alloy were used to evaluate multiaxial stress-strain cycle predictions.

The unified models, as well as appropriate algorithms for integrating the constitutive equations, were implemented in finite-element computer codes. Author

A85-39770*# South Carolina State Coll., Orangeburg.
ON LOCAL TOTAL STRAIN REDISTRIBUTION USING A SIMPLIFIED CYCLIC INELASTIC ANALYSIS BASED ON AN ELASTIC SOLUTION

S. Y. HWANG (South Carolina State College, Orangeburg, SC) and A. KAUFMAN (NASA, Lewis Research Center, Cleveland, OH) AIAA, SAE, ASME, and ASEE, Joint Propulsion Conference, 21st, Monterey, CA, July 8-10, 1985. 10 p. Previously announced in STAR as N85-21690. refs (AIAA PAPER 85-1419)

Strain redistribution corrections were developed for a simplified inelastic analysis procedure to economically calculate material cyclic response at the critical location of a structure for life prediction purposes. The method was based on the assumption that the plastic region in the structure is local and the total strain history required for input can be defined from elastic finite element analyses. Cyclic stress-strain behavior was represented by a bilinear kinematic hardening model. The simplified procedure has been found to predict stress-strain response with reasonable accuracy for thermally cycled problems but needs improvement for mechanically load cycled problems. This study derived and incorporated Neuber type corrections in the simplified procedure to account for local total strain redistribution under cyclic mechanical loading. The corrected simplified method was exercised on a mechanically load cycled benchmark notched plate problem. Excellent agreement was found between the predicted material response and nonlinear finite element solutions for the problem. The simplified analysis computer program used 0.3 percent of the CPU time required for a nonlinear finite element analysis. Author

A85-40814*# National Aeronautics and Space Administration. Lewis Research Center, Cleveland, Ohio.
FATIGUE CRITERION TO SYSTEM DESIGN, LIFE AND RELIABILITY

E. V. ZARETSKY (NASA, Lewis Research Center, Cleveland, OH) AIAA, SAE, ASME, and ASEE, Joint Propulsion Conference, 21st, Monterey, CA, July 8-10, 1985. 9 p. Previously announced in STAR as N85-27226. refs (AIAA PAPER 85-1140)

A generalized methodology to structural life prediction, design, and reliability based upon a fatigue criterion is advanced. The life prediction methodology is based in part on work of Weibull and Lundberg and Palmgren. The approach incorporates the computed life of elemental stress volumes of a complex machine element to predict system life. The results of coupon fatigue testing can be incorporated into the analysis allowing for life prediction and component or structural renewal rates with reasonable statistical certainty. Author

A85-40910* Southwest Research Inst., San Antonio, Tex.
CONSTITUTIVE MODELING AND COMPUTATIONAL IMPLEMENTATION FOR FINITE STRAIN PLASTICITY

K. W. REED (Southwest Research Institute, San Antonio, TX) and S. N. ATLURI (Georgia Institute of Technology, Atlanta) International Journal of Plasticity (ISSN 0749-6419), vol. 1, no. 1, 1985, p. 63-87. refs (Contract NAG3-346)

This paper describes a simple alternate approach to the difficult problem of modeling material behavior. Starting from a general representation for a rate-type constitutive equation, it is shown by example how sets of test data may be used to derive restrictions on the scalar functions appearing in the representation. It is not possible to determine these functions from experimental data, but the aforementioned restrictions serve as a guide in their eventual definition. The implications are examined for hypo-elastic, isotropically hardening plastic, and kinematically hardening plastic materials. A simple model for the evolution of the 'back-stress,' in a kinematic-hardening plasticity theory, that is entirely analogous to a hypoelastic stress-strain relation is postulated and examined

in detail in modeling finitely plastic tension-torsion test. The implementation of rate-type material models in finite element algorithms is also discussed. Author

A85-41109* Massachusetts Inst. of Tech., Cambridge.
AXISYMMETRIC SOLID ELEMENTS BY A RATIONAL HYBRID STRESS METHOD

Z. TIAN and T. H. H. PIAN (MIT, Cambridge, MA) (George Washington University and NASA, Symposium on Advances and Trends in Structures and Dynamics, Washington, DC, Oct. 22-25, 1984) Computers and Structures (ISSN 0045-7949), vol. 20, no. 1-3, 1985, p. 141-149. refs (Contract NAG3-33)

Four-node axisymmetric solid elements are derived by a new version of hybrid method for which the assumed stresses are expressed in complete polynomials in natural coordinates. The stress equilibrium conditions are introduced through the use of additional displacements as Lagrange multipliers. A rational procedure is to choose the displacement terms such that the resulting strains are also of complete polynomials of the same order. Example problems all indicate that elements obtained by this procedure lead to better results in displacements and stresses than that by other finite elements. Author

A85-41983* Akron Univ., Ohio.
QUASI-STATIC SOLUTION ALGORITHMS FOR KINEMATICALLY/MATERIALLY NONLINEAR THERMOMECHANICAL PROBLEMS

J. PADOVAN (Akron, University, OH) and S. S. PAI (Babcock and Wilcox Co., Akron, OH) Journal of Thermal Stresses (ISSN 0149-5739), vol. 7, no. 3-4, 1984, p. 227-257. Research supported by Babcock and Wilcox Corp. refs (Contract NAG3-54)

This paper develops an algorithmic solution strategy which allows the handling of positive/indefinite stiffness characteristics associated with the pre- and post-buckling of structures subject to complex thermomechanical loading fields. The flexibility of the procedure is such that it can be applied to both finite difference and element-type simulations. Due to the generality of the algorithmic approach developed, both kinematic and thermal/mechanical type material nonlinearity including inelastic effects can be treated. This includes the possibility of handling completely general thermomechanical boundary conditions. To demonstrate the scheme, the results of several benchmark problems is presented. Author

A85-42047* National Aeronautics and Space Administration. Lewis Research Center, Cleveland, Ohio.
FINITE DIFFERENCE ANALYSIS OF TORSIONAL VIBRATIONS OF PRETWISTED, ROTATING, CANTILEVER BEAMS WITH EFFECTS OF WARPING

K. B. SUBRAHMANYAM and K. R. V. KAZA (NASA, Lewis Research Center, Cleveland, OH) Journal of Sound and Vibration (ISSN 0022-460X), vol. 99, March 22, 1985, p. 213-224. refs

Theoretical natural frequencies of the first three modes of torsional vibration of pretwisted, rotating cantilever beams are determined for various thickness and aspect ratios. Conclusions concerning individual and collective effects of warping, pretwist, tension-torsion coupling and tennis racket effect (twist-rotational coupling) terms on the natural frequencies are drawn from numerical results obtained by using a finite difference procedure with first order central differences. The relative importance of structural warping, inertial warping, pretwist, tension-torsion and twist-rotational coupling terms is discussed for various rotational speeds. The accuracy of results obtained by using the finite difference approach is verified by a comparison with the exact solution for specialized simple cases of the equation of motion used in this paper. Author

A85-42566* Garrett Turbine Engine Co., Phoenix, Ariz.

CREEP-RUPTURE RELIABILITY ANALYSIS

A. PERALTA-DURAN (Garrett Turbine Engine Co., Phoenix, AZ) and P. H. WIRSCHING (Arizona, University, Phoenix) ASME, Transactions, Journal of Vibration, Acoustics, Stress, and Reliability in Design (ISSN 0739-3717), vol. 107, July 1985, p. 339-346. Previously announced in STAR as N84-19925. refs (Contract NAG3-41)

A probabilistic approach to the correlation and extrapolation of creep-rupture data is presented. Time temperature parameters (TTP) are used to correlate the data, and an analytical expression for the master curve is developed. The expression provides a simple model for the statistical distribution of strength and fits neatly into a probabilistic design format. The analysis focuses on the Larson-Miller and on the Manson-Haferd parameters, but it can be applied to any of the TTP's. A method is developed for evaluating material dependent constants for TTP's. It is shown that optimized constants can provide a significant improvement in the correlation of the data, thereby reducing modelling error. Attempts were made to quantify the performance of the proposed method in predicting long term behavior. Uncertainty in predicting long term behavior from short term tests was derived for several sets of data. Examples are presented which illustrate the theory and demonstrate the application of state of the art reliability methods to the design of components under creep. Author

A85-47626* National Aeronautics and Space Administration. Lewis Research Center, Cleveland, Ohio.

VIBRATIONS OF TWISTED CANTILEVER PLATES - A COMPARISON OF THEORETICAL RESULTS

R. E. KIELB (NASA, Lewis Research Center, Cleveland, OH), A. W. LEISSA (Ohio State University, Columbus), and J. C. MACBAIN (USAF, Aero Propulsion Laboratory, Wright-Patterson AFB, OH) International Journal for Numerical Methods in Engineering (ISSN 0029-5981), vol. 21, Aug. 1985, p. 1365-1380. refs

As a result of significant differences in the published results for various methods of analysis involving the use of finite element techniques, there are now some questions regarding the adequacy of these methods to predict accurately the vibratory characteristics of highly twisted cantilever plates. In an attempt to help in a resolution of the arising problems, a joint government/industry/university research effort was initiated. The primary objective of the present paper is to summarize the theoretical methods used in the study and show samples of the obtained results. The study provided 19 sets of theoretical results which are derived from beam theory, shell theory, and fine element methods. G.R.

A85-48703* Air Force Flight Dynamics Lab., Wright-Patterson AFB, Ohio.

STRUCTURAL OPTIMIZATION USING OPTIMALITY CRITERIA METHODS

N. S. KHOT (USAF, Flight Dynamics Laboratory, Wright-Patterson AFB, OH) and L. BERKE (NASA, Lewis Research Center, Cleveland, OH) IN: New directions in optimum structural design Chichester, England and New York, Wiley-Interscience, 1984, p. 47-74.

Optimality criteria methods take advantage of some concepts as those of statically determinate or indeterminate structures, and certain variational principles of structural dynamics, to develop efficient algorithms for the sizing of structures that are subjected to stiffness-related constraints. Some of the methods and iterative strategies developed over the last decade for calculations of the Lagrange multipliers in stress and displacement-limited problems, as well as for satisfying the appropriate optimality criterion, are discussed. The application of these methods are illustrated by solving problems with stress and displacement constraints. O.C.

A86-18123* Massachusetts Inst. of Tech., Cambridge.

FINITE ELEMENTS BASED ON CONSISTENTLY ASSUMED STRESSES AND DISPLACEMENTS

T. H. H. PIAN (MIT, Cambridge, MA) Finite Elements in Analysis and Design (ISSN 0168-874X), vol. 1, Aug. 1985, p. 131-140. refs

(Contract NAG3-33; F33615-83-K-5016)

Finite element stiffness matrices are derived using an extended Hellinger-Reissner principle in which internal displacements are added to serve as Lagrange multipliers to introduce the equilibrium constraint in each element. In a consistent formulation the assumed stresses are initially unconstrained and complete polynomials and the total displacements are also complete such that the corresponding strains are complete in the same order as the stresses. Several examples indicate that resulting properties for elements constructed by this consistent formulation are ideal and are less sensitive to distortions of element geometries. The method has been used to find the optimal stress terms for plane elements, 3-D solids, axisymmetric solids, and plate bending elements.

Author

A86-20706* Army Armament Research and Development Command, Watervliet, N. Y.

WIDE-RANGE DISPLACEMENT EXPRESSIONS FOR STANDARD FRACTURE MECHANICS SPECIMENS

J. A. KAPP (U.S. Army, Benet Weapons Laboratory, Watervliet, NY), B. GROSS (NASA, Lewis Research Center, Cleveland, OH), and G. S. LEGER IN: Fracture mechanics . Philadelphia, PA, American Society for Testing and Materials, 1985, p. 27-44.

Wide-range algebraic expressions for the displacement of cracked fracture mechanics specimens are developed. For each specimen two equations are given: one for the displacement as a function of crack length, the other for crack length as a function of displacement. All the specimens that appear in ASTM Test for Plane-Strain Fracture Toughness of Metallic Materials (E 399) are represented in addition to the crack mouth displacement for a pure bending specimen. For the compact tension sample and the disk-shaped compact tension sample, the displacement at the crack mouth and at the load line are both considered. Only the crack mouth displacements for the arc-shaped tension samples are presented. The agreement between the displacements or crack lengths predicted by the various equations and the corresponding numerical data from which they were developed are nominally about 3 percent or better. These expressions should be useful in all types of fracture testing including fracture toughness, K-resistance, and fatigue crack growth. Author

A86-20709* National Aeronautics and Space Administration. Lewis Research Center, Cleveland, Ohio.

WIDE-RANGE WEIGHT FUNCTIONS FOR THE STRIP WITH A SINGLE EDGE CRACK

T. W. ORANGE (NASA, Lewis Research Center, Cleveland, OH) IN: Fracture mechanics . Philadelphia, PA, American Society for Testing and Materials, 1985, p. 95-105. Previously announced in STAR as N84-11512. refs

A closed form expression for the weight function for a strip with a single edge crack is presented. The expression is valid for relative crack lengths from zero to unity. It is based on the assumption that the shape of an opened edge crack can be approximated by a conic section. The results agree well with published values for weight functions, stress intensity factors, and crack mouth opening displacements. S.L.

A86-20710* National Aeronautics and Space Administration. Lewis Research Center, Cleveland, Ohio.

ANALYSIS OF AN EXTERNALLY RADIAL CRACK RING SEGMENT SUBJECT TO THREE-POINT RADIAL LOADING

B. GROSS, J. E. SRAWLEY, and J. L. SHANNON, JR. (NASA, Lewis Research Center, Cleveland, OH) IN: Fracture mechanics . Philadelphia, PA, American Society for Testing and Materials, 1985, p. 106-112. refs

The boundary collocation method was used to generate Mode I stress intensity and crack mouth opening displacement

coefficients for externally radially (through-the-thickness) cracked ring segments subjected to three-point radial loading. Numerical results were obtained for ring segment outer-to-inner radius ratios (R_o/R_i) ranging from 1.10 to 2.50 and crack length to segment width ratios (a/W) ranging from 0.1 to 0.8. Stress intensity and crack mouth displacement coefficients were found to depend on the ratios R_o/R_i and a/W as well as the included angle between the directions of the reaction forces. Author

A86-22084*# National Aeronautics and Space Administration. Lewis Research Center, Cleveland, Ohio.

NASA LEWIS RESEARCH CENTER/UNIVERSITY GRADUATE RESEARCH PROGRAM ON ENGINE STRUCTURES

C. C. CHAMIS (NASA, Lewis Research Center, Cleveland, OH) ASME, International Gas Turbine Conference and Exhibit, 30th, Houston, TX, Mar. 18-21, 1985. 10 p. Previously announced in STAR as N85-18375. (ASME PAPER 85-GT-159)

NASA Lewis Research Center established a graduate research program in support of the Engine Structures Research activities. This graduate research program focuses mainly on structural and dynamics analyses, computational mechanics, mechanics of composites and structural optimization. The broad objectives of the program, the specific program, the participating universities and the program status are briefly described. Author

A86-24219* Syracuse Univ., N. Y.

SHEAR FATIGUE CRACK GROWTH - A LITERATURE SURVEY

H. W. LIU (Syracuse University, NY) Fatigue and Fracture of Engineering Materials and Structures (ISSN 8756-758X), vol. 8, no. 4, 1985, p. 295-313. refs (Contract NAG3-348)

Recent studies of shear crack growth are reviewed, emphasizing test methods and data analyses. The combined mode I and mode II elastic crack tip stress fields are considered. The development and design of the compact shear specimen are described, and the results of fatigue crack growth tests using compact shear specimens are reviewed. The fatigue crack growth tests are discussed and the results of inclined cracks in tensile panels, center cracks in plates under biaxial loading, cracked beam specimens with combined bending and shear loading, center-cracked panels and double edge-cracked plates under cyclic shear loading are examined and analyzed in detail. C.D.

A86-26689* Akron Univ., Ohio.

HIERARCHIAL IMPLICIT DYNAMIC LEAST-SQUARE SOLUTION ALGORITHM

J. PADOVAN and J. LACKNEY (Akron, University, OH) Computers and Structures (ISSN 0045-7949), vol. 22, no. 3, 1986, p. 479-489. refs (Contract NAG3-54)

This paper develops an implicit type transient solution strategy which possesses hierarchical levels of application. In particular, due to the manner of formulation, stiffness updating, assembly inversion, solution constraint, as well as iteration are all performed at a localized level. The level of iterative calculations depends on the type of hierarchical partitioning employed, namely degree of freedom, nodal, elemental, material/nonlinear group, substructural, and so on. Since the iterative solution process and application of constraints are applied at a local level, the resulting so-called hierarchical implicit solution algorithm possesses very stable and efficient numerical properties and is highly storage efficient. To demonstrate the scheme, the results of several benchmark examples are presented. These enable comparisons with the Newton-Raphson solved implicit transient solution method. Overall the comparisons illustrate the superior stability and efficiency of the hierarchical scheme. Author

A86-26896*# Illinois Univ., Urbana.

THREE-DIMENSIONAL HYBRID-STRESS FINITE ELEMENT ANALYSIS OF COMPOSITE LAMINATES WITH CRACKS AND CUTOUTS

S. S. WANG (Illinois, University, Urbana) IN: Pressure vessel components design and analysis; Proceedings of the Pressure Vessels and Piping Conference, New Orleans, LA, June 23-26, 1985. New York, American Society of Mechanical Engineers, 1985, p. 235-246. refs (Contract NSG-3044)

A three-dimensional hybrid-stress finite element analysis of composite laminates containing cutouts and cracks is presented. Fully three-dimensional, hexahedral isoparametric elements of the hybrid-stress model are formulated on the basis of the Hellinger-Reissner variational principle. Traction-free edges, cutouts, and crack surfaces are modeled by imposition of exact traction boundary conditions along element surfaces. Special boundary and surface elements are constructed by introducing proper constraints on assumed stress functions. The Lagrangian multiplier technique is used to enforce ply-interface continuity conditions in hybrid bimaterial composite elements for modeling the interface region in a composite laminate. Two examples are given to illustrate the capability of the present method of approach: (1) the well-known delamination problem in an angle-ply laminate, and (2) the important problem of a composite laminate containing a circular hole. Results are presented in detail for each case. Implications of interlaminar and intralaminar crack initiation, growth and fracture in composites containing cracks and cutouts are discussed. Author

A86-26910*# National Aeronautics and Space Administration. Lewis Research Center, Cleveland, Ohio.

VIBRATION AND BUCKLING OF ROTATING, PRETWISTED, PRECONED BEAMS INCLUDING CORIOLIS EFFECTS

K. B. SUBRAHMANYAM and K. R. V. KAZA (NASA, Lewis Research Center, Cleveland, OH) IN: Vibrations of blades and bladed disk assemblies; Proceedings of the Tenth Biennial Conference on Mechanical Vibration and Noise, Cincinnati, OH, September 10-13, 1985. New York, American Society of Mechanical Engineers, 1985, p. 75-87. Previously announced in STAR as N85-25893. refs

The effects of pretwist, precone, setting angle and Coriolis forces on the vibration and buckling behavior of rotating, torsionally rigid, cantilevered beams were studied. The beam is considered to be clamped on the axis of rotation in one case, and off the axis of rotation in the other. Two methods are employed for the solution of the vibration problem: (1) one based upon a finite-difference approach using second order central differences for solution of the equations of motion, and (2) based upon the minimum of the total potential energy functional with a Ritz type of solution procedure making use of complex forms of shape functions for the dependent variables. The individual and collective effects of pretwist, precone, setting angle, thickness ratio and Coriolis forces on the natural frequencies and the buckling boundaries are presented. It is shown that the inclusion of Coriolis effects is necessary for blades of moderate to large thickness ratios while these effects are not so important for small thickness ratio blades. The possibility of buckling due to centrifugal softening terms for large values of precone and rotation is shown. Author

A86-28653*# Northwestern Univ., Evanston, Ill.

PROBABILISTIC FINITE ELEMENTS FOR TRANSIENT ANALYSIS IN NONLINEAR CONTINUA

W. K. LIU, T. BELYTSCHKO, and A. MANI (Northwestern University, Evanston, IL) IN: Advances in aerospace structural analysis; Proceedings of the Winter Annual Meeting, Miami Beach, FL, November 17-22, 1985. New York, American Society of Mechanical Engineers, 1985, p. 9-24. refs (Contract NAG3-535)

The probabilistic finite element method (PFEM), which is a combination of finite element methods and second-moment analysis, is formulated for linear and nonlinear continua with inhomogeneous random fields. Analogous to the discretization of

the displacement field in finite element methods, the random field is also discretized. The formulation is simplified by transforming the correlated variables to a set of uncorrelated variables through an eigenvalue orthogonalization. Furthermore, it is shown that a reduced set of the uncorrelated variables is sufficient for the second-moment analysis. Based on the linear formulation of the PFEM, the method is then extended to transient analysis in nonlinear continua. The accuracy and efficiency of the method is demonstrated by application to a one-dimensional, elastic/plastic wave propagation problem. The moments calculated compare favorably with those obtained by Monte Carlo simulation. Also, the procedure is amenable to implementation in deterministic FEM based computer programs. Author

A86-28654*# Rice Univ., Houston, Tex.
NUMERICAL SYNTHESIS OF TRI-VARIATE VELOCITY REALIZATIONS OF TURBULENCE

P.-T. D. SPANOS (Rice University, Houston, TX) and K. P. SCHULTZ (Lockheed Engineering and Management Services Co., Houston, TX) IN: Advances in aerospace structural analysis; Proceedings of the Winter Annual Meeting, Miami Beach, FL, November 17-22, 1985. New York, American Society of Mechanical Engineers, 1985, p. 25-35. refs (Contract NAG3-210)

An approach for synthesizing trivariate turbulence velocity field spatial realizations is presented. Some of the spatial frequency characteristics of the random velocity field are described by the von Karman spectrum. The simulation algorithm is based on an efficient autoregressive-moving average (ARMA) scheme involving coefficient square matrices of order three. The determination of the efficient low order ARMA algorithm is preceded by the determination of a suitable high order autoregressive (AR) simulation algorithm. The numerical results are presented in a dimensionless form. Thus, they are applicable for any scale of turbulence. Author

A86-28655*# MARC Analysis Research Corp., Palo Alto, Calif.
EFFICIENT ALGORITHMS FOR USE IN PROBABILISTIC FINITE ELEMENT ANALYSIS

J. B. DIAS and J. C. NAGTEGAAL (MARC Analysis Research Corp., Palo Alto, CA) IN: Advances in aerospace structural analysis; Proceedings of the Winter Annual Meeting, Miami Beach, FL, November 17-22, 1985. New York, American Society of Mechanical Engineers, 1985, p. 37-50. refs (Contract NAS3-24389)

This paper investigates the use of Fast Probability Integration (FPI) algorithms in a Finite Element environment. A method allowing the representation of correlated fields in terms of a vector of uncorrelated transformed variables, based on the spectral decomposition of the variance-covariance matrix is developed. The response of the deterministic model corresponding to selected perturbations of these uncorrelated variables is then obtained via a Newton-type iterative scheme. The results of the perturbed problems are used to construct a local representation of the model's behavior in the neighborhood of the deterministic state, which the FPI algorithm will use to estimate the reliability of the system. Although the proposed strategy has thus far only been applied to linear elastostatics, the extension of the method to a broader class of problems appears to be feasible. Author

A86-28659*# Southwest Research Inst., San Antonio, Tex.
PROBABILISTIC STRUCTURAL ANALYSIS FOR SPACE PROPULSION SYSTEM COMPONENTS

O. H. BURNSIDE (Southwest Research Institute, San Antonio, TX) IN: Advances in aerospace structural analysis; Proceedings of the Winter Annual Meeting, Miami Beach, FL, November 17-22, 1985. New York, American Society of Mechanical Engineers, 1985, p. 87-102. refs (Contract NAS3-24389)

Probabilistic design and analysis methods for the achievement of greater reliability in structural systems are especially useful in those cases where the structure operates in such severe environments as that of the Space Shuttle. Attention is presently

given to the development status of a NASA-sponsored program for probabilistic structural analysis methods applicable to current and future reusable space propulsion systems. Methodologies for the assessment of structural response by means of integrated finite element and probabilistic analysis techniques are discussed, with illustrative examples. O.C.

A86-34257* Virginia Polytechnic Inst. and State Univ., Blacksburg.

FACTORS INFLUENCING THE ULTRASONIC STRESS WAVE FACTOR EVALUATION OF COMPOSITE MATERIAL STRUCTURES

C. J. REBELLO (National Technical Systems, Hartwood, VA) and J. C. DUKE, JR. (Virginia Polytechnic Institute and State University, Blacksburg) Journal of Composites Technology and Research (ISSN 0885-6804), vol. 8, Spring 1986, p. 18-23. refs (Contract NAG3-323)

To demonstrate that the finite-element model can be used to investigate some of the factors influencing the ultrasonic stress wave evaluation of materials, a hypothetical case was studied in which classical vibration theory was used. Vibration analysis and experiments for the undamaged case were conducted on an isotropic aluminum plate and a unidirectional graphite-epoxy plate, using a point source to excite the plates. The finite-element solution correlated within eight percent with the exact method. The frequencies predicted by the finite-element model were observed in the experiments in both plates, although in the composite plate, additional frequencies were observed which could not be accounted for. Damaged isotropic plates were also considered. The effects of increasing damage severity with constant damage area, and increasing damage area with constant severity on the resonant frequencies were analyzed. I.S.

A86-34444*# United Technologies Corp., East Hartford, Conn.
STRESS ANALYSIS OF GAS TURBINE ENGINE STRUCTURES USING THE BOUNDARY ELEMENT METHOD

R. B. WILSON, D. W. SNOW (United Technologies Corp., Engineering Div., Hartford, CT), and P. K. BANERJEE (New York, State University, Buffalo) IN: Advanced topics in boundary element analysis; Proceedings of the Winter Annual Meeting, Miami Beach, FL, November 17-22, 1985. New York, American Society of Mechanical Engineers, 1985, p. 45-63. refs (Contract NAS3-23697)

The theory of the boundary element method is briefly reviewed with particular reference to the feasibility of elastic and inelastic three-dimensional stress analysis of complex structures characteristic of gas turbine engine components. Particular requirements of gas turbine analysis are defined, and examples of the use of a boundary element code designed for the three-dimensional stress analysis of turbine components are presented. It is shown that the general-purpose boundary element code can accurately and efficiently analyze many of the gas turbine engine structures. V.L.

A86-34445*# State Univ. of New York, Buffalo.
ADVANCED THREE-DIMENSIONAL DYNAMIC ANALYSIS BY BOUNDARY ELEMENT METHODS

P. K. BANERJEE (New York, State University, Buffalo) and S. AHMA IN: Advanced topics in boundary element analysis; Proceedings of the Winter Annual Meeting, Miami Beach, FL, November 17-22, 1985. New York, American Society of Mechanical Engineers, 1985, p. 65-81. refs (Contract NAS3-23697)

Advanced formulations of boundary element method for periodic, transient transform domain and transient time domain solution of three-dimensional solids have been implemented using a family of isoparametric boundary elements. The necessary numerical integration techniques as well as the various solution algorithms are described. The developed analysis has been incorporated in a fully general purpose computer program BEST3D which can handle up to 10 subregions. A number of numerical examples are presented to demonstrate the accuracy of the dynamic analyses. Author

A86-34461*# MARC Analysis Research Corp., Palo Alto, Calif. ITERATIVE METHODS FOR MIXED FINITE ELEMENT EQUATIONS

S. NAKAZAWA, J. C. NAGTEGAAL (MARC Analysis Research Corp., Palo Alto, CA), and O. C. ZIENKIEWICZ (Swansea, University College, Wales) IN: Hybrid and mixed finite element methods; Proceedings of the Winter Annual Meeting, Miami Beach, FL, November 17-22, 1985. New York, American Society of Mechanical Engineers, 1985, p. 57-67. refs
(Contract NAS3-23697)

Iterative strategies for the solution of indefinite system of equations arising from the mixed finite element method are investigated in this paper with application to linear and nonlinear problems in solid and structural mechanics. The augmented Hu-Washizu form is derived, which is then utilized to construct a family of iterative algorithms using the displacement method as the preconditioner. Two types of iterative algorithms are implemented. Those are: constant metric iterations which does not involve the update of preconditioner; variable metric iterations, in which the inverse of the preconditioning matrix is updated. A series of numerical experiments is conducted to evaluate the numerical performance with application to linear and nonlinear model problems. Author

A86-34462*# Massachusetts Inst. of Tech., Cambridge. HYBRID SOLID ELEMENT WITH A TRACTION-FREE CYLINDRICAL SURFACE

T. H. H. PIAN (MIT, Cambridge, MA) and Z. TIAN (Chinese Academy of Sciences, Graduate School, Beijing, People's Republic of China) IN: Hybrid and mixed finite element methods; Proceedings of the Winter Annual Meeting, Miami Beach, FL, November 17-22, 1985. New York, American Society of Mechanical Engineers, 1985, p. 69-75. refs
(Contract NAG3-33)

An eight node solid element with two parallel faces and one traction-free cylindrical surface is derived using the assumed stress hybrid method. Cylindrical coordinates are used so that the assumed stresses satisfy the equilibrium equations as well as the traction-free condition over the cylindrical boundary. In the limiting case of plane stress conditions the assumed stresses also satisfy the compatibility conditions. Example solutions have demonstrated the advantage of using this special element for analyzing solids with circular holes. Author

A86-34464*# Georgia Inst. of Tech., Atlanta. EXISTENCE AND STABILITY, AND DISCRETE BB AND RANK CONDITIONS, FOR GENERAL MIXED-HYBRID FINITE ELEMENTS IN ELASTICITY

W.-M. XUE and S. N. ATLURI (Georgia Institute of Technology, Atlanta) IN: Hybrid and mixed finite element methods; Proceedings of the Winter Annual Meeting, Miami Beach, FL, November 17-22, 1985. New York, American Society of Mechanical Engineers, 1985, p. 91-112. refs
(Contract NAG3-346)

In this paper, all possible forms of mixed-hybrid finite element methods that are based on multi-field variational principles are examined as to the conditions for existence, stability, and uniqueness of their solutions. The reasons as to why certain 'simplified hybrid-mixed methods' in general, and the so-called 'simplified hybrid-displacement method' in particular (based on the so-called simplified variational principles), become unstable, are discussed. A comprehensive discussion of the 'discrete' BB-conditions, and the rank conditions, of the matrices arising in mixed-hybrid methods, is given. Some recent studies aimed at the assurance of such rank conditions, and the related problem of the avoidance of spurious kinematic modes, are presented. Author

A86-37799* Akron Univ., Ohio. INELASTIC HIGH-TEMPERATURE THERMOMECHANICAL RESPONSE OF CERAMIC COATED GAS TURBINE SEALS

J. PADOVAN (Akron, University, OH), D. DOUGHERTY (General Tire and Rubber Co., Akron, OH), and B. HENDRICKS (NASA, Lewis Research Center, Cleveland, OH) Journal of Thermal Stresses (ISSN 0149-5739), vol. 9, no. 1, 1986, p. 31-43. refs
(Contract NAG3-265)

Through the use of a constrained Newton-Raphson time stepping finite element scheme, the inelastic thermomechanical response of ceramic coated gas turbine parts is considered. Due to the generality of the solution procedure developed, the combined thermoelastic-plastic-creep properties associated with ceramics is treated. This includes the handling of temperature-dependent elastic-plastic creep and thermal material properties. To illustrate the procedure, the thermomechanical response of ceramic coated outer gas path seals is considered. This includes the evaluation of time-dependent thermal ratcheting and its concomitant residual stress and strain fields. Author

A86-38838*# Georgia Inst. of Tech., Atlanta. BOUNDING SOLUTIONS OF GEOMETRICALLY NONLINEAR VISCOELASTIC PROBLEMS

J. M. STUBSTAD and G. J. SIMITSES (Georgia Institute of Technology, Atlanta) IN: Structures, Structural Dynamics and Materials Conference, 27th, San Antonio, TX, May 19-21, 1986, Technical Papers. Part 1. New York, American Institute of Aeronautics and Astronautics, 1986, p. 343-352. Previously announced in STAR as N86-10860. refs
(Contract NAG3-534)
(AIAA PAPER 86-0943)

Integral transform techniques, such as the Laplace transform, provide simple and direct methods for solving viscoelastic problems formulated within a context of linear material response and using linear measures for deformation. Application of the transform operator reduces the governing linear integro-differential equations to a set of algebraic relations between the transforms of the unknown functions, the viscoelastic operators, and the initial and boundary conditions. Inversion either directly or through the use of the appropriate convolution theorem, provides the time domain response once the unknown functions have been expressed in terms of sums, products or ratios of known transforms. When exact inversion is not possible approximate techniques may provide accurate results. The overall problem becomes substantially more complex when nonlinear effects must be included. Situations where a linear material constitutive law can still be productively employed but where the magnitude of the resulting time dependent deformations warrants the use of a nonlinear kinematic analysis are considered. The governing equations will be nonlinear integro-differential equations for this class of problems. Thus traditional as well as approximate techniques, such as cited above, cannot be employed since the transform of a nonlinear function is not explicitly expressible. Author

A86-38842*# National Aeronautics and Space Administration. Lewis Research Center, Cleveland, Ohio.

COMPOSITE SANDWICH THERMOSTRUCTURAL BEHAVIOR - COMPUTATIONAL SIMULATION

C. C. CHAMIS, R. A. AIELLO (NASA, Lewis Research Center, Cleveland, OH), and P. L. N. MURTHY (Cleveland State University, OH) IN: Structures, Structural Dynamics and Materials Conference, 27th, San Antonio, TX, May 19-21, 1986, Technical Papers. Part 1. New York, American Institute of Aeronautics and Astronautics, 1986, p. 370-381. refs
(AIAA PAPER 86-0948)

Computational methods have been developed for simulating the thermomechanical behavior of composite sandwiches, in which the analyses with several levels of progressive sophistication were used in conjunction with composite hygrothermomechanical theory. The sophistication levels include: (1) three-dimensional detailed finite element modeling of the honeycomb, the adhesive, and the composite faces; (2) three-dimensional finite element modeling assuming a homogeneous core; (3) laminate theory simulation;

and (4) simple equations for predicting the equivalent properties of the honeycomb core. These levels have been packaged into a procedure embedded in a computer code streamlined for the simulation of the composite sandwich hygrothermal and structural behavior. It is shown that in order to properly simulate the thermomechanical response of the composite sandwich, all the honeycomb thermal and mechanical properties must be used.

I.S.

A86-38873* # Ohio State Univ., Columbus.

COMPUTER AIDED DERIVATION OF EQUATIONS FOR COMPOSITE MECHANICS PROBLEMS AND FINITE ELEMENT ANALYSES

N. SARIGUL (Ohio State University, Columbus) and C. C. CHAMIS (NASA, Lewis Research Center, Cleveland, OH) IN: Structures, Structural Dynamics and Materials Conference, 27th, San Antonio, TX, May 19-21, 1986, Technical Papers. Part 1. New York, American Institute of Aeronautics and Astronautics, 1986, p. 676-679. refs
(AIAA PAPER 86-1016)

Explicit equations are derived for analysis of multilayered fiber composites and for finite element analyses. The equations are obtained using a symbolic program and tested for various composite properties as well as for different fiber orientations. In order to analyze multilayered fiber composite structures, a variable thickness finite element is formulated. Examples of an airfoil geometry, simulated in a form of a cantilevered beam with various fiber orientations are studied.

Author

A86-39485* # Duke Univ., Durham, N. C.

FREQUENCY DOMAIN SOLUTIONS TO MULTI-DEGREE-OF-FREEDOM, DRY FRICTION DAMPED SYSTEMS UNDER PERIODIC EXCITATION

A. A. FERRI and E. H. DOWELL (Duke University, Durham, NC) IN: Dynamics and control of large structures; Proceedings of the Fifth Symposium, Blacksburg, VA, June 12-14, 1985. Blacksburg, VA, Virginia Polytechnic Institute and State University, 1985, p. 125-144. refs
(Contract AF-AFOSR-83-0346; NAG3-516)

The anticipated low damping level in large space structures (LSS) has been a major concern for the designers of these structures. Low damping degrades the free response and complicates the design of shape and attitude controllers for flexible spacecraft. Dry friction damping has been considered as a means of increasing the passive damping of LSS, by placing it in the joints and connecting junctures of structures. However, dry friction is highly nonlinear and, hence, analytical investigations are difficult to perform. Here, a multi-harmonic, frequency domain solution technique is developed and applied to a multi-DOF, dry friction damped system. It is seen that the multi-harmonic method is much more accurate than traditional, one harmonic solution methods. The method also compares well with time integration. Finally, comparisons are made with experimental results.

Author

A86-40695* # Georgia Inst. of Tech., Atlanta.

ON THE EQUIVALENCE OF THE INCREMENTAL HARMONIC BALANCE METHOD AND THE HARMONIC BALANCE-NEWTON RAPHSON METHOD

A. A. FERRI (Georgia Institute of Technology, Atlanta) ASME, Transactions, Journal of Applied Mechanics (ISSN 0021-8936), vol. 53, June 1986, p. 455-457. refs
(Contract NAG3-516)

A86-41673* Georgia Inst. of Tech., Atlanta.

CONSTITUTIVE MODELING OF CYCLIC PLASTICITY AND CREEP, USING AN INTERNAL TIME CONCEPT

O. WATANABE and S. N. ATLURI (Georgia Institute of Technology, Atlanta) International Journal of Plasticity (ISSN 0749-6419), vol. 2, no. 2, 1986, p. 107-134. refs
(Contract NAG3-46)

Using the concept of an internal time as related to plastic strains, a differential stress-strain relation for elastoplasticity is rederived, such that (1) the concept of a yield-surface is retained;

(2) the definitions of elastic and plastic processes are analogous to those in classical plasticity theory; and (3) its computational implementation, via a 'tangent-stiffness' finite element method and a 'generalized-midpoint-radial-return' stress-integration algorithm, is simple and efficient. Also, using the concept of an internal time, as related to both the inelastic strains as well as the Newtonian time, a constitutive model for creep-plasticity interaction, is discussed. The problem of modeling experimental data for plasticity and creep, by the present analytical relations, as accurately as desired, is discussed. Numerical examples which illustrate the validity of the present relations are presented for the cases of cyclic plasticity and creep.

Author

A86-43566* National Aeronautics and Space Administration. Lewis Research Center, Cleveland, Ohio.

MODE II FATIGUE CRACK GROWTH SPECIMEN DEVELOPMENT

R. J. BUZZARD, B. GROSS, and J. E. SRAWLEY (NASA, Lewis Research Center, Cleveland, OH) IN: Fracture mechanics; Proceedings of the Seventeenth National Symposium, Albany, NY, August 7-9, 1984. Philadelphia, PA, American Society for Testing and Materials, 1986, p. 329-345; Discussion, p. 345, 346. Previously announced in STAR as N84-29248. refs

A Mode II test specimen was developed which has potential application in understanding phenomena associated with mixed mode fatigue failures in high performance aircraft engine bearing races. The attributes of the specimen are: it contains one single ended notch, which simplifies data gathering and reduction; the fatigue crack grows in-line with the direction of load application; a single axis test machine is sufficient to perform testing; and the Mode I component is vanishingly small.

Author

A86-43771* Akron Univ., Ohio.

LOCALLY BOUND CONSTRAINED NEWTON-RAPHSON SOLUTION ALGORITHMS

J. PADOVAN and R. MOSCARELLO (Akron, University, OH) Computers and Structures (ISSN 0045-7949), vol. 23, no. 2, 1986, p. 181-197. refs
(Contract NAG3-54)

This paper develops strategies which enable the automatic adjustment of the constraint surfaces recently used to extend the range and numerical stability/efficiency of nonlinear finite-element equation solvers. In addition to handling kinematic and material induced nonlinearity, both pre- and postbuckling behavior can be treated. The scheme developed employs localized bounds on various hierarchical partitions of the field variables. These are used to resize, shape, and orient the global constraint surface, thereby enabling essentially automatic load/deflection incrementation. Due to the generality of the approach taken, it can be implemented in conjunction with constraints of arbitrary functional type. To benchmark the method, several numerical experiments are presented. These include problems involving kinematic and material nonlinearity, as well as, pre- and postbuckling characteristics.

Author

A86-43774* Akron Univ., Ohio.

CONSTRAINED HIERARCHICAL LEAST SQUARE NONLINEAR EQUATION SOLVERS

J. PADOVAN and J. LACKNEY (Akron, University, OH) Computers and Structures (ISSN 0045-7949), vol. 23, no. 2, 1986, p. 251-263. refs
(Contract NSG-3283)

The current paper develops a constrained hierarchical least square nonlinear equation solver. The procedure can handle the response behavior of systems which possess indefinite tangent stiffness characteristics. Due to the generality of the scheme, this can be achieved at various hierarchical application levels. For instance, in the case of finite element simulations, various combinations of either degree of freedom, nodal, elemental, substructural, and global level iterations are possible. Overall, this enables a solution methodology which is highly stable and storage efficient. To demonstrate the capability of the constrained hierarchical least square methodology, benchmarking examples are

presented which treat structure exhibiting highly nonlinear pre- and postbuckling behavior wherein several indefinite stiffness transitions occur. Author

A86-44339* # Syracuse Univ., N. Y.

FATIGUE CRACK GROWTH UNDER GENERAL-YIELDING CYCLIC-LOADING

Z. MINZHONG and H. W. LIU (Syracuse University, NY) ASME, Transactions, Journal of Engineering Materials and Technology (ISSN 0094-4289), vol. 108, July 1986, p. 201-205. refs (Contract NAG3-348)

In low cycle fatigue, cracks are initiated, and propagated under general-yielding cyclic loading. For general-yielding cyclic loading, Dowling and Begley (1976) have shown that fatigue crack growth rate correlates well with the measured Delta J. The correlation of da/dN with Delta J has also been studied by a number of other investigators. However, none of these studies has correlated da/dN with Delta J calculated specifically for the test specimens. Solomon measured fatigue crack growth in specimens in general-yielding cyclic loading. The crack tip fields for Solomon's specimens are calculated, using the finite element method, and the J-values of Solomon's tests are evaluated. The measured crack growth rate in Solomon's specimens correlates very well with the calculated Delta J. Author

A86-48245* # National Aeronautics and Space Administration. Lewis Research Center, Cleveland, Ohio.

MASS BALANCING OF HOLLOW FAN BLADES

R. E. KIELB (NASA, Lewis Research Center, Cleveland, OH) ASME, International Gas Turbine Conference and Exhibit, 31st, Duesseldorf, West Germany, June 8-12, 1986. 7 p. Previously announced in STAR as N86-16611. refs (ASME PAPER 86-GT-195)

A typical section model is used to analytically investigate the effect of mass balancing as applied to hollow, supersonic fan blades. A procedure to determine the best configuration of an internal balancing mass to provide flutter alleviation is developed. This procedure is applied to a typical supersonic shroudless fan blade which is unstable in both the solid configuration and when it is hollow with no balancing mass. The addition of an optimized balancing mass is shown to stabilize the blade at the design condition. Author

A86-48271* # Princeton Univ., N. J.

AEROELASTIC BEHAVIOR OF LOW ASPECT RATIO METAL AND COMPOSITE BLADES

J. F. WHITE, III and O. O. BENDIKSEN (Princeton University, NJ) ASME, International Gas Turbine Conference and Exhibit, 31st, Duesseldorf, West Germany, June 8-12, 1986. 10 p. refs (Contract NAG3-308) (ASME PAPER 86-GT-243)

The aeroelastic stability of titanium and composite blades of low aspect ratio is examined over a range of design parameters, using a Rayleigh-Ritz formulation. The blade modes include a plate-type mode to account for chordwise bending. Chordwise flexibility is found to have a significant effect on the unstalled supersonic flutter of low aspect ratio blades, and also on the stability of tip sections of shrouded fan blades. For blades with a thickness of less than approximately four percent of chord, the chordwise, second bending, and first torsion branches are all unstable at moderately high supersonic Mach numbers. For composite blades, the important structural coupling between bending and torsion cannot be modeled properly unless chordwise bending is accounted for. Typically, aft fiber sweep produces beneficial bending-torsion coupling that is stabilizing, whereas forward fiber sweep has the opposite effect. By using crossed-ply laminate configurations, critical aeroelastic modes can be stabilized. Author

A86-49133* # National Aeronautics and Space Administration. Lewis Research Center, Cleveland, Ohio.

UNIFIED CONSTITUTIVE MATERIALS MODEL DEVELOPMENT AND EVALUATION FOR HIGH-TEMPERATURE STRUCTURAL ANALYSIS APPLICATIONS

R. L. THOMPSON (NASA, Lewis Research Center, Cleveland, OH) and M. T. TONG (Sverdrup Technology, Inc., Cleveland, OH) IN: ICAS, Congress, 15th, London, England, September 7-12, 1986, Proceedings. Volume 2. New York, American Institute of Aeronautics and Astronautics, Inc., 1986, p. 1505a-1505s. refs

Unified constitutive material models were developed for structural analyses of aircraft gas turbine engine hot section components with particular application to an isotropic material used for combustor liners. Differential forms of models independently developed were considered in this study. These models combine the interactions of time-dependent (creep) and time-independent (plasticity) inelastic behavior of a material. Predicted stress-strain responses from these models were evaluated against cyclic isothermal and nonisothermal test results for uniaxial specimens of a nickel-base superalloy. The unified models were implemented in a nonlinear structural analysis code. Two unique NASA Lewis test facilities were used in the evaluation of the models for complex geometry specimens and evaluation of advanced temperature and high-temperature strain measurement instrumentation. Predicted nonlinear structural responses from one of the models for a flat plate and a segment of a conventional combustor liner are presented. Author

A87-17799* National Aeronautics and Space Administration. Lewis Research Center, Cleveland, Ohio.

ELASTIC ANALYSIS OF A MODE II FATIGUE CRACK TEST SPECIMEN

B. GROSS, R. J. BUZZARD, and W. F. BROWN, JR. (NASA, Lewis Research Center, Cleveland, OH) International Journal of Fracture (ISSN 0376-9429), vol. 31, June 1986, p. 151-157.

Elastic displacements and stress intensity measurements for a mode II specimen have been obtained over a range of a/W values between 0.500 and 0.900 using the MARC general purpose finite element program. Stress intensity factors were experimentally determined using load point displacement values. Good general agreement between numerical and experimental results for crack mouth, crack surface, and load point displacements, and for stress intensity factors, demonstrates the accuracy of the present method. R.R.

A87-17988* # National Aeronautics and Space Administration. Lewis Research Center, Cleveland, Ohio.

SCARE - A POSTPROCESSOR PROGRAM TO MSC/NASTRAN FOR RELIABILITY ANALYSIS OF STRUCTURAL CERAMIC COMPONENTS

J. P. GYKENYESI (NASA, Lewis Research Center, Cleveland, OH) ASME, Transactions, Journal of Engineering for Gas Turbines and Power (ISSN 0022-0825), vol. 108, July 1986, p. 540-546. Previously announced in STAR as N86-14688. refs (ASME PAPER 86-GT-34)

A computer program was developed for calculating the statistical fast fracture reliability and failure probability of ceramic components. The program includes the two-parameter Weibull material fracture strength distribution model, using the principle of independent action for polyaxial stress states and Batdorf's shear-sensitive as well as shear-insensitive crack theories, all for volume distributed flaws in macroscopically isotropic solids. Both penny-shaped cracks and Griffith cracks are included in the Batdorf shear-sensitive crack response calculations, using Griffith's maximum tensile stress or critical coplanar strain energy release rate criteria to predict mixed mode fracture. Weibull material parameters can also be calculated from modulus of rupture bar tests, using the least squares method with known specimen geometry and fracture data. The reliability prediction analysis uses MSC/NASTRAN stress, temperature and volume output, obtained from the use of three-dimensional, quadratic, isoparametric, or axisymmetric finite elements. The statistical fast fracture theories employed, along with selected input and output formats and options, are summarized. An example

problem to demonstrate various features of the program is included.
Author

A87-22128* Case Western Reserve Univ., Cleveland, Ohio.
RE-EXAMINATION OF CUMULATIVE FATIGUE DAMAGE ANALYSIS - AN ENGINEERING PERSPECTIVE

S. S. MANSON (Case Western Reserve University, Cleveland, OH) and G. R. HALFORD (NASA, Lewis Research Center, Cleveland, OH) (IUTAM, Israel Academy of Science and Humanities, U.S. Army, et al., Symposium on Mechanics of Damage and Fatigue, Haifa and Tel Aviv, Israel, July 1-4, 1985) Engineering Fracture Mechanics (ISSN 0013-7944), vol. 25, no. 5-6, 1986, p. 539-571. Previously announced in STAR as N86-27680. refs

A method which has evolved in the laboratories for the past 20 yr is re-examined with the intent of improving its accuracy and simplicity of application to engineering problems. Several modifications are introduced both to the analytical formulation of the Damage Curve Approach, and to the procedure for modifying this approach to achieve a Double Linear Damage Rule formulation which immensely simplifies the calculation. Improvements are also introduced in the treatment of mean stress for determining fatigue life of the individual events that enter into a complex loading history. While the procedure is completely consistent with the results of numerous two level tests that have been conducted on many materials, it is still necessary to verify applicability to complex loading histories. Caution is expressed that certain phenomenon can also influence the applicability - for example, unusual deformation and fracture modes inherent in complex loading especially if stresses are multiaxial. Residual stresses at crack tips, and metallurgical factors are also important in creating departures from the cumulative damage theories; examples of departures are provided.
Author

A87-25407* National Aeronautics and Space Administration. Lewis Research Center, Cleveland, Ohio.

DESIGN CONCEPTS/PARAMETERS ASSESSMENT AND SENSITIVITY ANALYSES OF SELECT COMPOSITE STRUCTURAL COMPONENTS

C. C. CHAMIS (NASA, Lewis Research Center, Cleveland, OH) International Journal of Materials and Product Technology (ISSN 0268-1900), vol. 1, Oct. 1986, p. 211-229. refs

Formal approaches are summarized to evaluate design concepts and perform sensitivity analyses on design parameters of composite structural components for vehicles. The formal approaches include structural analyses coupled with composite micromechanics to assess the structural response of beams made from various intraply hybrids, finite element analysis in conjunction with composite mechanics to assess the structural response of panels made from strip hybrids, and sensitivity analysis through optimization to assess the effects of various design parameters on the optimum design of a panel made from angleplyed composite laminates. Results obtained from these approaches are presented in graphical and tabular form to illustrate parametric studies and acceptable ranges of various design parameters.
Author

A87-27986*# National Aeronautics and Space Administration. Lewis Research Center, Cleveland, Ohio.

FATIGUE CRITERION TO SYSTEM DESIGN, LIFE, AND RELIABILITY

ERWIN Y. ZARETSKY (NASA, Lewis Research Center, Cleveland, OH) Journal of Propulsion and Power (ISSN 0748-4658), vol. 3, Jan.-Feb. 1987, p. 76-83. Previously cited in issue 19, p. 2818, Accession no. A85-40814. refs

A87-33581*# Sverdrup Technology, Inc., Cleveland, Ohio.
PROBABILISTIC STRUCTURAL ANALYSIS TO QUANTIFY UNCERTAINTIES ASSOCIATED WITH TURBOPUMP BLADES
VINOD K. NAGPAL, ROBERT RUBINSTEIN (Sverdrup Technology, Inc., Cleveland, OH), and CHRISTOS C. CHAMIS (NASA, Lewis Research Center, Cleveland, OH) IN: Structures, Structural Dynamics and Materials Conference, 28th, Monterey, CA, Apr. 6-8, 1987, Technical Papers. Part 1. New York, American Institute of Aeronautics and Astronautics, 1987, p. 268-274. refs
(AIAA PAPER 87-0766)

A probabilistic study of turbopump blades has been in progress at NASA Lewis Research Center for over the last two years. The objectives of this study are to evaluate the effects of uncertainties in geometry and material properties on the structural response of the turbopump blades to evaluate the tolerance limits on the design. A methodology based on probabilistic approach has been developed to quantify the effects of the random uncertainties. The results of this study indicate that only the variations in geometry have significant effects.
Author

A87-33645*# National Aeronautics and Space Administration. Lewis Research Center, Cleveland, Ohio.

ADVANCES IN 3-D INELASTIC ANALYSIS METHODS FOR HOT SECTION COMPONENTS

CHRISTOS C. CHAMIS (NASA, Lewis Research Center, Cleveland, OH) IN: Structures, Structural Dynamics and Materials Conference, 28th, Monterey, CA, Apr. 6-8, 1987, Technical Papers. Part 1. New York, American Institute of Aeronautics and Astronautics, 1987, p. 802-811.
(AIAA PAPER 87-0719)

3-D Inelastic Analysis Methods are described. These methods consist of a series of new computer codes embodying a progression of mathematical models (mechanics of materials, specialty finite element, boundary element) for streamlined analysis of: (1) combustor liners, (2) turbine blades, and (3) turbine vanes. These models address the effects of high temperatures and thermal/mechanical loadings on the local (stress/strain) and global (dynamics, buckling) structural behavior of the three selected components. Three computer codes, referred to as MOMM (Mechanics of Materials Model), MHOST (MARC-Hot Section Technology), and BEST (Boundary Element Stress Technology), have been developed and are briefly described in this paper.
Author

A87-33648*# Pratt and Whitney Aircraft Group, East Hartford, Conn.

STRUCTURAL TAILORING OF ADVANCED TURBOPROPS

K. W. BROWN, P. R. HARVEY (Pratt and Whitney, East Hartford, CT), and C. C. CHAMIS (NASA, Lewis Research Center, Cleveland, OH) IN: Structures, Structural Dynamics and Materials Conference, 28th, Monterey, CA, Apr. 6-8, 1987, Technical Papers. Part 1. New York, American Institute of Aeronautics and Astronautics, 1987, p. 827-837. refs
(AIAA PAPER 87-0753)

A computer program has been developed for the performance of numerical optimizations of highly swept propfan blades by minimizing an objective function that is defined either as direct operating cost or the aeroelastic difference between a blade and its scaled model. Three component analysis categories are employed: an optimization algorithm, approximate analysis procedures for objective function and constraint evaluation, and refined analysis procedures for optimum design validation. The analyses conducted by the program encompass aerodynamic efficiency evaluation, finite element stress and vibration analysis, acoustics, flutter, and forced response life prediction.
O.C.

A87-33719*# Georgia Inst. of Tech., Atlanta.

A TECHNIQUE FOR THE PREDICTION OF AIRFOIL FLUTTER CHARACTERISTICS IN SEPARATED FLOW

JIUNN-CHI WU, L. N. SANKAR (Georgia Institute of Technology, Atlanta), and K. R. V. KAZA (NASA, Lewis Research Center, Cleveland, OH) IN: Structures, Structural Dynamics and Materials Conference, 28th, Monterey, CA, Apr. 6-8, 1987 and AIAA Dynamics Specialists Conference, Monterey, CA, Apr. 9, 10, 1987, Technical Papers. Part 2B. New York, American Institute of Aeronautics and Astronautics, 1987, p. 664-673. refs
(Contract NAG3-730)
(AIAA PAPER 87-0910)

A solution procedure is described for determining the two-dimensional, one- or two-degree-of-freedom flutter characteristics of arbitrary airfoils at large angles of attack. The same procedure is used to predict stall flutter. This procedure requires a simultaneous integration in time of the solid and fluid equations of motion. The fluid equations of motion are the unsteady compressible Navier-Stokes equations, solved in a body-fitted moving coordinate system using an approximate factorization scheme. The solid equations of motion are integrated in time using an Euler implicit scheme. Flutter is said to occur if small disturbances imposed on the airfoil attitude lead to divergent oscillatory motions at subsequent times. Results for a number of special cases are presented to demonstrate the suitability of this scheme to predict flutter at large mean angles of attack. Some stall flutter applications are also presented. Author

A87-33756*# National Aeronautics and Space Administration. Lewis Research Center, Cleveland, Ohio.

APPROXIMATIONS TO EIGENVALUES OF MODIFIED GENERAL MATRICES

DURBHA V. MURTHY (NASA, Lewis Research Center, Cleveland; Toledo, University, OH) and RAPHAEL T. HAFTKA (Virginia Polytechnic Institute and State University, Blacksburg) IN: Structures, Structural Dynamics and Materials Conference, 28th, Monterey, CA, Apr. 6-8, 1987 and AIAA Dynamics Specialists Conference, Monterey, CA, Apr. 9, 10, 1987, Technical Papers. Part 2B. New York, American Institute of Aeronautics and Astronautics, 1987, p. 1032-1045. refs
(Contract NAG3-347; NAG1-224)
(AIAA PAPER 87-0947)

The reanalysis of non-self-adjoint dynamic models is computationally very expensive in design optimization applications. This paper describes several approximations that can be applied to eigenvalues of non-hermitian matrices to reduce that computational cost. Approximations based on eigenvalue derivatives, generalized Rayleigh quotient and the trace theorem are presented and their accuracy and computational cost are estimated. The accuracy and cost estimates are verified by applying the approximations to random matrices and matrices arising in flutter analysis of compressor blades. Recommendations are made for selection of the best approximation when the derivatives are available and when they are not. In particular, it is concluded that the quadratic approximation for eigenvalues should never be used as higher order approximations are always more accurate as well as more efficient. Author

A87-35656*# Indian Inst. of Science, Bangalore.

A HIGHER ORDER THEORY OF LAMINATED COMPOSITE CYLINDRICAL SHELLS

A. V. KRISHNA MURTHY (Indian Institute of Science, Bangalore, India) and T. S. R. REDDY (NASA, Lewis Research Center, Cleveland, OH) Aeronautical Society of India, Journal (ISSN 0001-9267), vol. 38, Aug. 1986, p. 161-171. Research supported by the Aeronautical Research and Development Board. refs

A new higher order theory has been proposed for the analysis of composite cylindrical shells. The formulation allows for arbitrary variation of inplane displacements. Governing equations are presented in the form of a hierarchy of sets of partial differential equations. Each set describes the shell behavior to a certain degree of approximation. The natural frequencies of simply-supported isotropic and laminated shells and stresses in a ring loaded

composite shell have been determined to various orders of approximation and compared with three dimensional solutions. These numerical studies indicate the improvements achievable in estimating the natural frequencies and the interlaminar shear stresses in laminated composite cylinders. Author

A87-39896*# National Aeronautics and Space Administration. Lewis Research Center, Cleveland, Ohio.

NONLINEAR VIBRATION AND STABILITY OF ROTATING, PRETWISTED, PRECONED BLADES INCLUDING CORIOLIS EFFECTS

K. B. SUBRAHMANYAM, K. R. V. KAZA, G. V. BROWN, and C. LAWRENCE (NASA, Lewis Research Center, Cleveland, OH) Journal of Aircraft (ISSN 0021-8669), vol. 24, May 1987, p. 342-352. Previously announced in STAR as N86-17789. refs

The coupled bending-bending-torsional equations of dynamic motion of rotating, linearly pretwisted blades are derived including large precone, second degree geometric nonlinearities and Coriolis effects. The equations are solved by the Galerkin method and a linear perturbation technique. Accuracy of the present method is verified by comparisons of predicted frequencies and steady state deflections with those from MSC/NASTRAN and from experiments. Parametric results are generated to establish where inclusion of only the second degree geometric nonlinearities is adequate. The nonlinear terms causing torsional divergence in thin blades are identified. The effects of Coriolis terms and several other structurally nonlinear terms are studied, and their relative importance is examined. Author

A87-40496*# National Aeronautics and Space Administration. Lewis Research Center, Cleveland, Ohio.

ANALYTICAL AND EXPERIMENTAL INVESTIGATION OF MISTUNING IN PROPFAN FLUTTER

KRISHNA RAO V. KAZA, ORAL MEHMED (NASA, Lewis Research Center, Cleveland, OH), MARC WILLIAMS (Purdue University, West Lafayette, IN), and LARRY A. MOSS (Sverdrup Technology, Inc., Cleveland, OH) IN: Structures, Structural Dynamics and Materials Conference, 28th, Monterey, CA, Apr. 6-8, 1987 and AIAA Dynamics Specialists Conference, Monterey, CA, Apr. 9, 10, 1987, Technical Papers. Part 2A. New York, American Institute of Aeronautics and Astronautics, 1987, p. 98-110. Previously announced in STAR as N87-18116. refs
(AIAA PAPER 87-0739)

An analytical and experimental investigation of the effects of mistuning on propfan subsonic flutter was performed. The analytical model is based on the normal modes of a rotating composite blade and a three-dimensional subsonic unsteady lifting surface aerodynamic theory. Theoretical and experimental results are compared for selected cases at different blade pitch angles, rotational speeds, and free-stream Mach numbers. The comparison shows a reasonably good agreement between theory and experiment. Both theory and experiment showed that combined mode shape, frequency, and aerodynamic mistuning can have a beneficial or adverse effect on blade damping depending on Mach number. Additional parametric results showed that alternative blade frequency mistuning does not have enough potential for it to be used as a passive flutter control in propfans similar to the one studied. It can be inferred from the results that a laminated composite propfan blade can be tailored to optimize its flutter speed by selecting the proper ply angles. Author

A87-40497*# National Aeronautics and Space Administration. Lewis Research Center, Cleveland, Ohio.

ANALYTICAL FLUTTER INVESTIGATION OF A COMPOSITE PROPFAN MODEL

K. R. V. KAZA, O. MEHMED (NASA, Lewis Research Center, Cleveland, OH), G. V. NARAYANAN (Sverdrup Technology, Inc., Cleveland, OH), and D. V. MURTHY (Toledo, University, OH) IN: Structures, Structural Dynamics and Materials Conference, 28th, Monterey, CA, Apr. 6-8, 1987 and AIAA Dynamics Specialists Conference, Monterey, CA, Apr. 9, 10, 1987, Technical Papers. Part 2A. New York, American Institute of Aeronautics and Astronautics, 1987, p. 84-97. Previously announced in STAR as N87-18115. refs
(AIAA PAPER 87-0738)

A theoretical model and an associated computer program for predicting subsonic bending-torsion flutter in propfans are presented. The model is based on two-dimensional unsteady cascade strip theory and three-dimensional steady and unsteady lifting surface aerodynamic theory in conjunction with a finite element structural model for the blade. The analytical results compare well with published experimental data. Additional parametric studies are also presented illustrating the effects on flutter speed of steady aeroelastic deformations, blade setting angle, rotational speed, number of blades, structural damping, and number of modes. Author

A87-49275* National Aeronautics and Space Administration. Lewis Research Center, Cleveland, Ohio.

SIMPLIFIED COMPOSITE MICROMECHANICS FOR PREDICTING MICROSTRESSES

CHRISTOS C. CHAMIS (NASA, Lewis Research Center, Cleveland, OH) (Society of Plastics Industry, Conference, 41st, Atlanta, GA, Jan. 1986) Journal of Reinforced Plastics and Composites (ISSN 0731-6844), vol. 6, July 1987, p. 268-284. refs

A unified set of composite micromechanics equations is summarized and described. This unified set is for predicting the ply microstresses when the ply stresses are known. The set consists of equations of simple form for predicting three-dimensional stresses (six each) in the matrix, fiber, and interface. Several numerical examples are included to illustrate use and computational effectiveness of the equations in this unified set. Numerical results from these examples are discussed with respect to their significance on microcrack formation and, therefore, damage initiation in fiber composites. Author

N80-10515*# Pratt and Whitney Aircraft Group, East Hartford, Conn. Commercial Products Div.

EFFECT OF TIME DEPENDENT FLIGHT LOADS ON JT9D-7 PERFORMANCE DETERIORATION

A. JAY and B. L. LEWIS 21 Aug. 1979 73 p refs
(Contract NAS3-20632)
(NASA-CR-159681; PWA-5512-45) Avail: NTIS HC A04/MF A01 CSCL 01C

The results of a modal transient analysis of the engine/aircraft system are presented. The response of the JT9D to analytically simulated vertical gusts and landings was predicted using a NASTRAN finite element mathematical model of the JT9D/747 propulsion system. The NASTRAN finite element model of the propulsion system included engine structural models of the fan, low/high pressure compressors, diffuser/turbine cases, and high/low pressure rotors, as well as nacelle models of the inlet cowl, tailcone, and wing pylon. The analysis conducted predicts that an insignificant level of JT9D-7 performance deterioration would occur due to a typical vertical gust encounter or a typical revenue service landing. Analysis of a high sink rate landing with a heavy fuel load indicates the possibility of local wear, however, the lack of an accurate dynamic rotor/seal interference model precludes an accurate quantitative evaluation of performance change for this once-per-airframe-life event. J.M.S.

N80-13503 Syracuse Univ., N. Y.

MODELLING OF CRACK TIP DEFORMATION WITH FINITE ELEMENT METHOD AND ITS APPLICATIONS Ph.D. Thesis

C. Y. YANG 1979 125 p
Avail: Univ. Microfilms Order No. 7925610

A finite element computer program using the initial stress approach of elastic-plastic analysis was developed. Crack closure stresses were calculated for three different models. It was concluded that: (1) the closure stress is highest in the strip necking model, lowest in the plane strain model, and intermediate in the plane stress model; and (2) the crack closure stress decreases if the separation occurs before the stress reaches the maximum value. Nonpropagating fatigue cracks in the two phase martensitic-ferritic steels were also investigated. Unzipping increments were calculated for different crack lengths. At a prescribed stress intensity level, the shorter the crack length, the greater the unzipping increment is. This means that the shorter crack will grow faster than the longer one if both are subjected to the same K-level. Dissert. Abstr.

N80-13513*# National Aeronautics and Space Administration. Lewis Research Center, Cleveland, Ohio.

COMPARISON TESTS AND EXPERIMENTAL COMPLIANCE CALIBRATION OF THE PROPOSED STANDARD ROUND COMPACT PLANE STRAIN FRACTURE TOUGHNESS SPECIMEN

D. M. FISHER and R. J. BUZZARD Nov. 1979 21 p refs
(NASA-TM-81379; E-284) Avail: NTIS HC A02/MF A01 CSCL 20K

Standard round specimen fracture test results compared satisfactorily with results from standard rectangular compact specimens machined from the same material. The location of the loading pin holes was found to provide adequate strength in the load bearing region for plane strain fracture toughness testing. Excellent agreement was found between the stress intensity coefficient values obtained from compliance measurements and the analytic solution proposed for inclusion in the standard test method. Load displacement measurements were made using long armed displacement gages and hollow loading cylinders. Gage points registered on the loading hole surfaces through small holes in the walls of the loading cylinders. Author

N80-15428*# National Aeronautics and Space Administration. Lewis Research Center, Cleveland, Ohio.

A RELATION BETWEEN SEMIEMPIRICAL FRACTURE ANALYSES AND R-CURVES

T. W. ORANGE Jan. 1980 45 p refs
(NASA-TP-1600; E-9963) Avail: NTIS HC A03/MF A01 CSCL 20K

The relations between several semiempirical fracture analyses (SEFA) and the R-curve concept of fracture mechanics are examined and the conditions for equivalence between a SEFA and an R-curve are derived. A hypothetical material is employed to study the relation analytically. Equivalent R-curves are developed for several real materials using data from the literature. For each SEFA there is an equivalent R-curve whose magnitude and shape are determined by the SEFA formulation and its empirical parameters. If the R-curve is indeed unique, then the various empirical parameters cannot be constant, and vice versa. However, for one SEFA the differences are small enough that they may be within the range of normal data scatter for real materials. Author

N80-22733*# Mechanical Technology, Inc., Latham, N. Y.

DEVELOPMENT OF PROCEDURES FOR CALCULATING STIFFNESS AND DAMPING OF ELASTOMERS IN ENGINEERING APPLICATIONS, PART 6

A. RIEGER, G. BURGESS, and E. ZORZI Apr. 1980 157 p refs
(Contract NAS3-18546)
(NASA-CR-159838; MTI-80TR29) Avail: NTIS HC A08/MF A01 CSCL 20K

An elastomer damper was designed, tested, and compared with the performance of a hydraulic damper for a power

39 STRUCTURAL MECHANICS

transmission shaft. The six button Viton-70 damper was designed so that the elastomer damper or the hydraulic damper could be activated without upsetting the imbalance condition of the assembly. This permitted a direct comparison of damper effectiveness. The elastomer damper consistently performed better than the hydraulic mount and permitted stable operation of the power transmission shaft to speeds higher than obtained with the squeeze film damper. Tests were performed on shear specimens of Viton-79, Buna-N, EPDM, and Neoprene to determine performance limitations imposed by strain, temperature, and frequency. Frequencies of between 110 Hz and 1100 Hz were surveyed with imposed strains between 0.0005 and 0.08 at temperatures of 32 C, 66 C, and 80 C. A set of design curves was generated in a unified format for each of the elastomer materials. E.D.K.

N80-22734*# National Aeronautics and Space Administration. Lewis Research Center, Cleveland, Ohio.

NONLINEAR, THREE-DIMENSIONAL FINITE-ELEMENT ANALYSIS OF AIR-COOLED GAS TURBINE BLADES

A. KAUFMAN and R. E. GAUGLER Apr. 1980 22 p refs (NASA-TP-1669; E-074) Avail: NTIS HC A02/MF A01 CSCL 21E

Cyclic stress-strain states in cooled turbine blades were calculated for a simulated mission of an advanced-technology commercial aircraft engine. The MARC, nonlinear, finite-element computer program was used for the analysis of impingement-cooled airfoils, with and without leading-edge film cooling. Creep was the predominant damage mode (ignoring hot corrosion), particularly around film-cooling holes. Radially angled holes exhibited less creep than holes with axes normal to the surface. Beam-theory analyses of all-impingement-cooled airfoils gave fair agreement with MARC results for initial creep. Author

N80-23678*# National Aeronautics and Space Administration. Lewis Research Center, Cleveland, Ohio.

STATUS OF NASA FULL-SCALE ENGINE AEROELASTICITY RESEARCH

J. F. LUBOMSKI 1980 21 p refs Presented at the 21st Struct., Structural Dyn., and Mater. Conf., Seattle, 12-14 May 1980; sponsored by AIAA, ASME, ASCE and AHS (NASA-TM-81500; E-437) Avail: NTIS HC A02/MF A01 CSCL 20K

Data relevant to several types of aeroelastic instabilities were obtained using several types of turbojet and turbofan engines. In particular, data relative to separated flow (stall) flutter, choke flutter, and system mode instabilities are presented. The unique characteristics of these instabilities are discussed, and a number of correlations are presented that help identify the nature of the phenomena. R.E.S.

N80-23684*# National Aeronautics and Space Administration. Lewis Research Center, Cleveland, Ohio.

PRACTICAL IMPLEMENTATION OF THE DOUBLE LINEAR DAMAGE RULE AND DAMAGE CURVE APPROACH FOR TREATING CUMULATIVE FATIGUE DAMAGE

S. S. MANSON (Case Western Reserve Univ.) and G. R. HALFORD Apr. 1980 50 p refs (NASA-TM-81517; E-387) Avail: NTIS HC A03/MF A01 CSCL 20K

Simple procedures are presented for treating cumulative fatigue damage under complex loading history using either the damage curve concept or the double linear damage rule. A single equation is provided for use with the damage curve approach; each loading event providing a fraction of damage until failure is presumed to occur when the damage sum becomes unity. For the double linear damage rule, analytical expressions are provided for determining the two phases of life. The procedure involves two steps, each similar to the conventional application of the commonly used linear damage rule. When the sum of cycle ratios based on phase 1 lives reaches unity, phase 1 is presumed complete, and further loadings are summed as cycle ratios on phase 2 lives. When the phase 2 sum reaches unity, failure is presumed to occur. No

other physical properties or material constants than those normally used in a conventional linear damage rule analysis are required for application of either of the two cumulative damage methods described. Illustrations and comparisons of both methods are discussed. Author

N80-27719*# National Aeronautics and Space Administration. Lewis Research Center, Cleveland, Ohio.

COMPARISON OF ELASTIC AND ELASTIC-PLASTIC STRUCTURAL ANALYSES FOR COOLED TURBINE BLADE AIRFOILS

A. KAUFMAN Jul. 1980 15 p refs (NASA-TP-1679; E-241) Avail: NTIS HC A02/MF A01 CSCL 20K

Elastic plastic stress strain states in cooled turbine blade airfoils were calculated by three methods for the initial takeoff transient of an advanced technology aircraft engine. The three analytical methods compared were a three dimensional elastic plastic, finite element analysis, a three dimensional, elastic, finite element analysis, and a one dimensional, elastic plastic, beam theory analysis. Structural analyses were performed for eight cases involving different combinations of mechanical and thermal loading on impingement cooled airfoils with and without leading edge film cooling holes. The von Mises effective total strains at maximum takeoff computed from the elastic and elastic plastic finite element analyses agreed with 9 percent for rotating airfoils and 28 percent for stationary airfoils with the elastic results on the conservative side. Author

N80-27720*# Massachusetts Inst. of Tech., Cambridge. Aeroelastic and Structures Research Lab.

INSTRUCTIONS FOR THE USE OF THE CIVM-JET 4C FINITE-STRAIN COMPUTER CODE TO CALCULATE THE TRANSIENT STRUCTURAL RESPONSES OF PARTIAL AND/OR COMPLETE ARBITRARILY-CURVED RINGS SUBJECTED TO FRAGMENT IMPACT

J. J. A. RODAL, S. E. FRENCH, E. A. WITMER, and T. R. STAGLIANO Dec. 1979 38 p refs (Contract NGR-22-009-339) (NASA-CR-159873; ASTL-MR-154-1) Avail: NTIS HC A03/MF A01

The CIVM-JET 4C computer program for the 'finite strain' analysis of 2 d transient structural responses of complete or partial rings and beams subjected to fragment impact stored on tape as a series of individual files. Which subroutines are found in these files are described in detail. All references to the CIVM-JET 4C program are made assuming that the user has a copy of NASA CR-134907 (ASRL TR 154-9) which serves as a user's guide to (1) the CIVM-JET 4B computer code and (2) the CIVM-JET 4C computer code 'with the use of the modified input instructions' attached hereto. L.F.M.

N80-29762*# Massachusetts Inst. of Tech., Cambridge.

FINITE-STRAIN LARGE-DEFLECTION ELASTIC-VISCOPLASTIC FINITE-ELEMENT TRANSIENT RESPONSE ANALYSIS OF STRUCTURES

J. J. A. RODAL and E. A. WITMER Jul. 1979 567 p refs (Contract NGR-22-009-339) (NASA-CR-159874; ASRL-TR-154-15) Avail: NTIS HC A24/MF A01 CSCL 20K

A method of analysis for thin structures that incorporates finite strain, elastic-plastic, strain hardening, time dependent material behavior implemented with respect to a fixed configuration and is consistently valid for finite strains and finite rotations is developed. The theory is formulated systematically in a body fixed system of convected coordinates with materially embedded vectors that deform in common with continuum. Tensors are considered as linear vector functions and use is made of the dyadic representation. The kinematics of a deformable continuum is treated in detail, carefully defining precisely all quantities necessary for the analysis. The finite strain theory developed gives much better predictions and agreement with experiment than does the traditional small strain theory, and at practically no additional cost.

This represents a very significant advance in the capability for the reliable prediction of nonlinear transient structural responses, including the reliable prediction of strains large enough to produce ductile metal rupture.
E.D.K.

N80-32753*# National Aeronautics and Space Administration. Lewis Research Center, Cleveland, Ohio.

THE METHOD OF LINES IN THREE DIMENSIONAL FRACTURE MECHANICS

J. GYEKENYESI and L. BERKE Washington 1980 19 p refs Presented at the Intern. Symp. on Absorbed Specific Energy and/or Strain Energy Density Criterion, Budapest, 17-19 Sep. 1980; sponsored by Lehigh Univ. and the Hungarian Acad. of Sci. (NASA-TM-81593; E-576) Avail: NTIS HC A02/MF A01 CSCL 20K

A review of recent developments in the calculation of design parameters for fracture mechanics by the method of lines (MOL) is presented. Three dimensional elastic and elasto-plastic formulations are examined and results from previous and current research activities are reported. The application of MOL to the appropriate partial differential equations of equilibrium leads to coupled sets of simultaneous ordinary differential equations. Solutions of these equations are obtained by the Peano-Baker and by the recurrence relations methods. The advantages and limitations of both solution methods from the computational standpoint are summarized.
R.K.G.

N81-11412*# National Aeronautics and Space Administration. Lewis Research Center, Cleveland, Ohio.

SUPERHYBRID COMPOSITE BLADE IMPACT STUDIES

C. C. CHAMIS, R. F. LARK, and J. H. SINCLAIR 1980 16 p refs Proposed for presentation at the 26th Ann. Intern. Gas Turbine Conf., Houston, Tex., 9-12 Mar. 1981 (NASA-TM-81597; E-580) Avail: NTIS HC A02/MF A01 CSCL 20K

The feasibility of superhybrid composite blades for meeting the mechanical design and impact resistance requirements of large fan blades for aircraft turbine engine applications was investigated. Two design concepts were evaluated: leading edge spar (TiCom) and center spar (TiCore), both with superhybrid composite shells. The investigation was both analytical and experimental. The results obtained show promise that superhybrid composites can be used to make light weight, high quality, large fan blades with good structural integrity. The blades tested successfully demonstrated their ability to meet steady state operating conditions, overspeed, and small bird impact requirements.
A.R.H.

N81-11417*# National Aeronautics and Space Administration. Lewis Research Center, Cleveland, Ohio.

METHOD FOR ESTIMATING CRACK-EXTENSION RESISTANCE CURVE FROM RESIDUAL STRENGTH DATA

T. W. ORANGE Nov. 1980 15 p refs (NASA-TP-1753; E-439) Avail: NTIS HC A02/MF A01 CSCL 20K

A method is presented for estimating the crack extension resistance curve (R curve) from residual strength (maximum load against initial crack length) data for precracked fracture specimens. The method allows additional information to be inferred from simple test results, and that information is used to estimate the failure loads of more complicated structures. Numerical differentiation of the residual strength data is required, and the problems that it may present are discussed.
R.C.T.

N81-12446*# National Aeronautics and Space Administration. Lewis Research Center, Cleveland, Ohio.

STABILITY OF LARGE HORIZONTAL-AXIS AXISYMMETRIC WIND TURBINES Ph.D. Thesis - Delaware Univ.

M. S. HIRSCHBEIN and M. I. YOUNG (Delaware Univ., Newark) 1980 37 p refs Presented at 3d Miami Conf. on Alternative Energy Sources, Miami, 15-17 Dec. 1980 (NASA-TM-81623; E-633) Avail: NTIS HC A03/MF A01 CSCL 20K

The stability of large horizontal axis, axis-symmetric, power producing wind turbines was examined. The analytical model used included the dynamic coupling of the rotor, tower and power generating system. The aerodynamic loading was derived from blade element theory. Each rotor blade was permitted two principal elastic bending degrees of freedom, one degree of freedom in torsion and controlled pitch as a rigid body. The rotor hub was mounted in a rigid nacelle which may yaw freely or in a controlled manner. The tower can bend in two principal directions and may twist. Also, the rotor speed can vary and may induce perturbation reactions within the power generating equipment. Stability was determined by the eigenvalues of a set of linearized constant coefficient differential equations. All results presented are based on a 3 bladed, 300 ft. diameter, 2.5 megawatt wind turbine. Some of the parameters varied were; wind speed, rotor speed structural stiffness and damping, the effective stiffness and damping of the power generating system and the principal bending directions of the rotor blades. Unstable or weakly stable behavior can be caused by aerodynamic forces due to motion of the rotor blades and tower in the plane of rotation or by mechanical coupling between the rotor system and the tower.
Author

N81-16492*# National Aeronautics and Space Administration. Lewis Research Center, Cleveland, Ohio.

EXPERIMENTAL COMPLIANCE CALIBRATION OF THE COMPACT FRACTURE TOUGHNESS SPECIMEN

D. M. FISHER and R. J. BUZZARD Dec. 1980 11 p refs (NASA-TM-81665; E-685) Avail: NTIS HC A02/MF A01 CSCL 20K

Compliances and stress intensity coefficients were determined over crack length to width ratios from 0.1 to 0.8. Displacements were measured at the load points, load line, and crack mouth. Special fixturing was devised to permit accurate measurement of load point displacement. The results are in agreement with the currently used results of boundary collocation analyses. The errors which occur in stress intensity coefficients or specimen energy input determinations made from load line displacement measurements rather than from load point measurements are emphasized.
Author

N81-16494*# National Aeronautics and Space Administration. Lewis Research Center, Cleveland, Ohio.

EFFECTS OF MISTUNING ON BENDING-TORSION FLUTTER AND RESPONSE OF A CASCADE IN INCOMPRESSIBLE FLOW

K. R. V. KAZA (Toledo Univ., Ohio) and R. E. KIELB 1981 20 p refs Proposed for presentation at Dyn. Specialists Conf., Atlanta, 9-11 Apr. 1981; sponsored by AIAA (Contract EX-76-I-01-1028) (NASA-TM-81674; DOE/NASA/1028-29; E-699) Avail: NTIS HC A02/MF A01 CSCL 20K

The effect of small differences between the individual blades (mistuning) on the aeroelastic stability and response of a cascade were studied. The aerodynamic, inertial, and structural coupling between the bending and torsional motions of each blade and the aerodynamic coupling between the blades was considered. A digital computer program was developed to conduct parametric studies. Results indicate that the mistuning has a beneficial effect on the coupled bending torsion and uncoupled torsion flutter. On forced response, however, the effect may be either beneficial or adverse, depending on the engine order of the forcing function. The results also illustrate that it may be feasible to utilize mistuning as a passive control to increase flutter speed while maintaining forced response at an acceptable level.
A.R.H.

39 STRUCTURAL MECHANICS

N81-17480*# National Aeronautics and Space Administration. Lewis Research Center, Cleveland, Ohio.

COMPOSITE CONTAINMENT SYSTEMS FOR JET ENGINE FAN BLADES

G. T. SMITH 1981 18 p refs Presented at the 36th Ann. Conf. of the Reinforced Plastics/Composites Inst. of the Soc. of the Plastics Ind., Inc., Washington, D.C., 16-20 Feb. 1981 (NASA-TM-81675; E-700) Avail: NTIS HC A02/MF A01 CSCL 21E

The use of composites in fan blade containment systems is investigated and the associated structural benefits of the composite system design are identified. Two basic types of containment structures were investigated. The short finned concept was evaluated using Kevlar/epoxy laminates for fins which were mounted in a 6061 T-6 aluminum ring. The long fin concept was evaluated with Kevlar/epoxy, 6Al4V titanium, and 2024 T-3 aluminum fins. The unfinned configurations consisted of the base-line steel sheet, a circumferentially oriented aluminum honeycomb, and a Kevlar cloth filled ring. Results obtained show that a substantial reduction in the fan blade containment system weight is possible. Minimization of damage within the engine arising from impact interaction between blade debris and the engine structure is also achieved. M.G.

N81-19479*# Textron Bell Aerospace Co., Buffalo, N. Y. **AEROELASTIC AND DYNAMIC FINITE ELEMENT ANALYSES OF A BLADDER SHROUDED DISK**

G. C. C. SMITH and V. ELCHURI Mar. 1980 152 p refs (Contract NAS3-20382) (NASA-CR-159728; D2536-941001) Avail: NTIS HC A08/MF A01 CSCL 20K

The delivery and demonstration of a computer program for the analysis of aeroelastic and dynamic properties is reported. Approaches to flutter and forced vibration of mistuned discs, and transient aerothermoelasticity are described. R.C.T.

N81-19480*# Textron Bell Aerospace Co., Buffalo, N. Y. **NASTRAN LEVEL 16 THEORETICAL MANUAL UPDATES FOR AEROELASTIC ANALYSIS OF BLADED DISCS**

V. ELCHURI and G. C. C. SMITH Mar. 1980 24 p refs (Contract NAS3-20382) (NASA-CR-159823; D2536-941002) Avail: NTIS HC A02/MF A01 CSCL 20K

A computer program based on state of the art compressor and structural technologies applied to bladed shrouded disc was developed and made operational in NASTRAN Level 16. Aeroelastic analyses, modes and flutter. Theoretical manual updates are included. S.F.

N81-19481*# Textron Bell Aerospace Co., Buffalo, N. Y. **NASTRAN LEVEL 16 USER'S MANUAL UPDATES FOR AEROELASTIC ANALYSIS OF BLADED DISCS**

V. ELCHURI and A. M. GALLO Mar. 1980 167 p refs (Contract NAS3-20382) (NASA-CR-159824; D2536-941003) Avail: NTIS HC A08/MF A01 CSCL 20K

The NASTRAN aeroelastic and flutter capability was extended to solve a class of problems associated with axial flow turbomachines. The capabilities of the program are briefly discussed. The aerodynamic data pertaining to the bladed disc sector, the associated aerodynamic modeling, the steady aerothermoelastic 'design/analysis' formulations, and the modal, flutter, and subcritical roots analyses are described. Sample problems and their solutions are included. R.C.T.

N81-19482*# Textron Bell Aerospace Co., Buffalo, N. Y. **NASTRAN LEVEL 16 PROGRAMMER'S MANUAL UPDATES FOR AEROELASTIC ANALYSIS OF BLADED DISCS**

A. M. GALLO and B. DALE Mar. 1980 88 p refs (Contract NAS3-20382) (NASA-CR-159825; D2536-941004) Avail: NTIS HC A05/MF A01 CSCL 20K

The programming routines for the NASTRAN Level 16 program are presented. Particular emphasis is placed on its application to aeroelastic analyses, mode development, and flutter analysis for turbomachine blades. R.C.T.

N81-19483*# Textron Bell Aerospace Co., Buffalo, N. Y. **NASTRAN LEVEL 16 DEMONSTRATION MANUAL UPDATES FOR AEROELASTIC ANALYSIS OF BLADED DISCS**

V. ELCHURI and A. M. GALLO Mar. 1980 15 p refs (Contract NAS3-20382) (NASA-CR-159826; D2536-941005) Avail: NTIS HC A02/MF A01 CSCL 20K

A computer program based on state of the art compressor and structural technologies applied to bladed shrouded discs was developed and made operational in NASTRAN level 16. The problems encompassed include aeroelastic analyses, modes, and flutter. The demonstration manual updates are described. L.F.M.

N81-26492*# National Aeronautics and Space Administration. Lewis Research Center, Cleveland, Ohio.

AEROELASTIC CHARACTERISTICS OF A CASCADE OF MISTUNED BLADES IN SUBSONIC AND SUPERSONIC FLOWS

R. E. KIELB and K. R. V. KAZA (Toledo Univ.) 1981 18 p refs Proposed for presentation at the 8th Biennial Eng. Div. Conf., Hartford, Conn., 20-23 Sep. 1981; sponsored by the American Society of Mechanical Engineers (Contract NSG-3139) (NASA-TM-82631; E-886) Avail: NTIS HC A02/MF A01 CSCL 20K

The effects of mistuning on flutter and forced response of a cascade in subsonic and supersonic flow were investigated. The aerodynamic and structural coupling between the bending and torsional motions and the aerodynamic coupling between the blades were studied. It is shown that frequency mistuning always has a beneficial effect on flutter. For the cascade considered, the potential for raising flutter speed is greater in subsonic than in supersonic flow. Preliminary results for structural damping mistuning show that there are no additional benefits over adding damping mistuning may have either a beneficial or an adverse effect on forced response, depending on the engine order of the excitation and Mach number. A.R.H.

N81-33497*# National Aeronautics and Space Administration. Lewis Research Center, Cleveland, Ohio.

STRUCTURAL DYNAMICS VERIFICATION FACILITY STUDY

L. J. KIRALY, M. S. HIRCHBEIN, J. M. MCALEESE, and D. P. FLEMING Aug. 1981 21 p refs (NASA-TM-82675; E-958) Avail: NTIS HC A02/MF A01 CSCL 20K

The need for a structural dynamics verification facility to support structures programs was studied. Most of the industry operated facilities are used for highly focused research, component development, and problem solving, and are not used for the generic understanding of the coupled dynamic response of major engine subsystems. Capabilities for the proposed facility include: the ability to both excite and measure coupled structural dynamic response of elastic blades on elastic shafting, the mechanical simulation of various dynamical loadings representative of those seen in operating engines, and the measurement of engine dynamic deflections and interface forces caused by alternative engine mounting configurations and compliances. E.A.K.

N82-11491*# National Aeronautics and Space Administration. Lewis Research Center, Cleveland, Ohio.

INTEGRATED ANALYSIS OF ENGINE STRUCTURES

C. C. CHAMIS 1981 24 p refs Presented at the Ann. Meeting of the ASME, Washington, D.C., 16-21 Nov. 1981 (NASA-TM-82713; E-995) Avail: NTIS HC A02/MF A01 CSCL 20K

The need for light, durable, fuel efficient, cost effective aircraft requires the development of engine structures which are flexible, made from advanced materials (including composites), resist higher temperatures, maintain tighter clearances and have lower maintenance costs. The formal quantification of any or several of these requires integrated computer programs (multilevel and/or interdisciplinary analysis programs interconnected) for engine structural analysis/design. Several integrated analysis computer programs are under development at Lewis Research Center. These programs include: (1) COBSTRAN-Composite Blade Structural Analysis, (2) CODSTRAN-Composite Durability Structural Analysis, (3) CISTRAN-Composite Impact Structural Analysis, (4) STAEBL-Strut Tailoring of Engine Blades, and (5) ESMOSS-Engine Structures Modeling Software System. Three other related programs, developed under Lewis sponsorship, are described.

Author

N82-14531*# Arizona Univ., Tucson. Dept. of Aerospace and Mechanical Engineering.

THE APPLICATION OF PROBABILISTIC DESIGN THEORY TO HIGH TEMPERATURE LOW CYCLE FATIGUE

P. H. WIRSCHING Nov. 1981 224 p refs

(Contract NAG3-41)

(NASA-CR-165488) Avail: NTIS HC A10/MF A01 CSCL 20K

Metal fatigue under stress and thermal cycling is a principal mode of failure in gas turbine engine hot section components such as turbine blades and disks and combustor liners. Designing for fatigue is subject to considerable uncertainty, e.g., scatter in cycles to failure, available fatigue test data and operating environment data, uncertainties in the models used to predict stresses, etc. Methods of analyzing fatigue test data for probabilistic design purposes are summarized. The general strain life as well as homo- and hetero-scedastic models are considered. Modern probabilistic design theory is reviewed and examples are presented which illustrate application to reliability analysis of gas turbine engine components.

A.R.H.

N82-16419*# National Aeronautics and Space Administration. Lewis Research Center, Cleveland, Ohio.

ELEVATED TEMPERATURE FATIGUE TESTING OF METALS

M. H. HIRSCHBERG Dec. 1981 24 p refs

(NASA-TM-82745; E-1058) Avail: NTIS HC A02/MF A01

CSCL 20K

The major technology areas needed to perform a life prediction of an aircraft turbine engine hot section component are discussed and the steps required for life prediction are outlined. These include the determination of the operating environment, the calculation of the thermal and mechanical loading of the component, the cyclic stress-strain and creep behavior of the material required for structural analysis, and the structural analysis to determine the local stress-strain-temperature-time response of the material at the critical location in the components. From a knowledge of the fatigue, creep, and failure resistance of the material, a prediction of the life of the component is made. Material characterization and evaluation conducted for the purpose of calculating fatigue crack initiation lives of components operating at elevated temperatures are emphasized.

J.D.H.

N82-17521*# Battelle Columbus Labs., Ohio.

STRESS EVALUATIONS UNDER ROLLING/SLIDING CONTACTS Final Report

J. W. KANNEL and J. L. TEVAARWERK 30 Oct. 1981 54 p refs

(Contract NAS3-22808)

(NASA-CR-165561; G7782) Avail: NTIS HC A04/MF A01

CSCL 20K

The state of stress beneath traction drive type of contacts were analyzed. Computing stresses and stress reversals on various planes for points beneath the surface were examined. The effect of tangential and axial friction under gross slip conditions is evaluated with the models. Evaluations were performed on an RC (rolling contact) tester configuration and it is indicated that the classical fatigue stresses are not altered by friction forces typical of lubricated contact. Higher values of friction can result in surface shear reversal that exceeds the stresses at the depth of maximum shear reversal under rolling contact.

E.A.K.

N82-19563*# Virginia Polytechnic Inst. and State Univ., Blacksburg. Dept. of Engineering Science and Mechanics.

FINITE-ELEMENT MODELING OF LAYERED, ANISOTROPIC COMPOSITE PLATES AND SHELLS: A REVIEW OF RECENT RESEARCH

J. N. REDDY In Shock and Vibration Information Center The Shock and Vibration Digest, Vol. 13, No. 12 p 3-12 Dec. 1981 refs

(Contract NAG3-208; AF-AFOSR-0142-81)

Avail: SVIC, Code 5804, Naval Research Lab., Washington, D.C.

20375; \$15.00/set CSCL 20K

Finite element papers published in the open literature on the static bending and free vibration of layered, anisotropic, and composite plates and shells are reviewed. A literature review of large-deflection bending and large-amplitude free oscillations of layered composite plates and shells is also presented. Non-finite element literature is cited for continuity of the discussion.

J.D.H.

N82-20564*# Case Western Reserve Univ., Cleveland, Ohio.

FATIGUE LIFE PREDICTION IN BENDING FROM AXIAL FATIGUE INFORMATION

S. S. MANSON and U. MURALIDHARAN Feb. 1982 38 p refs

(Contract NAG3-39)

(NASA-CR-165563; NAS 1.26:165563) Avail: NTIS HC A03/MF A01 CSCL 20K

Bending fatigue in the low cyclic life range differs from axial fatigue due to the plastic flow which alters the linear stress-strain relation normally used to determine the nominal stresses. An approach is presented to take into account the plastic flow in calculating nominal bending stress (S_{sub} bending) based on true surface stress. These functions are derived in closed form for rectangular and circular cross sections. The nominal bending stress and the axial fatigue stress are plotted as a function of life (N_{sub} S) and these curves are shown for several materials of engineering interest.

S.L.

N82-20565*# National Aeronautics and Space Administration. Lewis Research Center, Cleveland, Ohio.

ELASTIC-PLASTIC FINITE-ELEMENT ANALYSES OF THERMALLY CYCLED SINGLE-EDGE WEDGE SPECIMENS

A. KAUFMAN Mar. 1982 27 p refs

(NASA-TP-1982; E-687; NAS 1.60:1982) Avail: NTIS HC

A03/MF A01 CSCL 20K

Elastic-plastic stress-strain analyses were performed for single-edge wedge alloys subjected to thermal cycling in fluidized beds. Three cases (NASA TAZ-8A alloy under one cycling condition and 316 stainless steel alloy under two cycling conditions) were analyzed by using the MARC nonlinear, finite-element computer program. Elastic solutions from MARC showed good agreement with previously reported solutions that used the NASTRAN and ISO3DQ computer programs. The NASA TAZ-8A case exhibited no plastic strains, and the elastic and elastic-plastic analyses gave identical results. Elastic-plastic analyses of the 316 stainless steel

alloy showed plastic strain reversal with a shift of the mean stresses in the compressive direction. The maximum equivalent total strain ranges for these cases were 13 to 22 percent greater than that calculated from elastic analyses. Author

N82-20566*# National Aeronautics and Space Administration. Lewis Research Center, Cleveland, Ohio.

ELASTIC-PLASTIC FINITE-ELEMENT ANALYSES OF THERMALLY CYCLED DOUBLE-EDGE WEDGE SPECIMENS

A. KAUFMAN and L. E. HUNT Mar. 1982 31 p refs (NASA-TP-1973; E-626; NAS 1.60:1973) Avail: NTIS HC A03/MF A01 CSCL 20K

Elastic-plastic stress-strain analyses were performed for double-edge wedge specimens subjected to thermal cycling in fluidized beds at 316 and 1088 C. Four cases involving different nickel-base alloys (IN 100, Mar M-200, NASA TAZ-8A, and Rene 80) were analyzed by using the MARC nonlinear, finite element computer program. Elastic solutions from MARC showed good agreement with previously reported solutions obtained by using the NASTRAN and ISO3DQ computer programs. Equivalent total strain ranges at the critical locations calculated by elastic analyses agreed within 3 percent with those calculated from elastic-plastic analyses. The elastic analyses always resulted in compressive mean stresses at the critical locations. However, elastic-plastic analyses showed tensile mean stresses for two of the four alloys and an increase in the compressive mean stress for the highest plastic strain case. M.G.

N82-21604*# National Aeronautics and Space Administration. Lewis Research Center, Cleveland, Ohio.

COUPLED BENDING-BENDING-TORSION FLUTTER OF A MISTUNED CASCADE WITH NONUNIFORM BLADES

K. R. V. KAZA (Toledo Univ.) and R. E. KIELB 1982 20 p refs Presented at the 23rd Struct., Structural Dyn., and Mater. Conf., New Orleans, 10-12 May 1982 (NASA-TM-82813; E-1156; NAS 1.15:82813) Avail: NTIS HC A02/MF A01 CSCL 20K

A set of aeroelastic equations describing the motion of an arbitrarily mistuned cascade with flexible, pretwisted, nonuniform blades is developed using an extended Hamilton's principle. The derivation of the equations has its basis in the geometric nonlinear theory of elasticity in which the elongations and shears are negligible compared to unity. A general expression for foreshortening of a blade is derived and is explicitly used in the formulation. The blade aerodynamic loading in the subsonic and supersonic flow regimes is obtained from two dimensional, unsteady, cascade theories. The aerodynamic, inertial and structural coupling between the bending (in two planes) and torsional motions of the blade is included. The equations are used to investigate the aeroelastic stability and to quantify the effect of frequency mistuning on flutter in turbofans. Results indicate that a moderate amount of intentional mistuning has enough potential to alleviate flutter problems in unshrouded, high aspect ratio turbofans. S.L.

N82-24501*# National Aeronautics and Space Administration. Lewis Research Center, Cleveland, Ohio.

NONLINEAR STRUCTURAL AND LIFE ANALYSES OF A COMBUSTOR LINER

V. MORENO (Pratt and Whitney Aircraft Group, East Hartford, Conn.), G. J. MEYERS (Pratt and Whitney Aircraft Group, East Hartford, Conn.), A. KAUFMAN, and G. R. HALFORD 1982 23 p refs Proposed for presentation at the Symp. on Advances and Trends in Struct. and Solid Mech., 4-7 Oct. 1982, Washington, D.C.; sponsored by NASA and Georgetown Univ. (NASA-TM-82846; E-1216; NAS 1.15:82846) Avail: NTIS HC A02/MF A01 CSCL 20K

Three dimensional, nonlinear finite element structural analyses were performed for a simulated combustor liner specimen to assess the capability of nonlinear analyses using classical inelastic material models to represent the thermoplastic creep response of the one half scale component. Results indicate continued cyclic hardening and ratcheting while experimental data suggested a stable stress

strain response after only a few loading cycles. The computed stress strain history at the critical location was put into two life prediction methods, strainrange partitioning and a Pratt and Whitney combustor life prediction method to evaluate their ability to predict cyclic crack initiation. It is found that the life prediction analyses over predicted the observed cyclic crack initiation life. E.A.K.

N82-24502*# National Aeronautics and Space Administration. Lewis Research Center, Cleveland, Ohio.

EVALUATION OF INELASTIC CONSTITUTIVE MODELS FOR NONLINEAR STRUCTURAL ANALYSIS

A. KAUFMAN 1982 22 p refs Presented at the Symp. on Nonlinear Constitutive Relations for High Temp. Appl., Akron, Ohio, 19-20 May 1982; sponsored by NASA and Akron Univ. (NASA-TM-82845; E-1215; NAS 1.15:82845) Avail: NTIS HC A02/MF A01 CSCL 20K

The influence of inelastic material models on computed stress-strain states, and therefore predicted lives, was studied for thermomechanically loaded structures. Nonlinear structural analyses were performed on a fatigue specimen which had been subjected to thermal cycling in fluidized beds and on a mechanically load cycled benchmark notch specimen. Four incremental plasticity creep models (isotropic, kinematic, combined isotropic kinematic, combined plus transient creep) were exercised using the MARC program. Of the plasticity models, kinematic hardening gave results most consistent with experimental observations. Life predictions using the computed strain histories at the critical location with a strainrange partitioning approach considerably overpredicted the crack initiation life of the thermal fatigue specimen. S.L.

N82-24503*# Georgia Inst. of Tech., Atlanta. Center for the Advancement of Computational Mechanics.

CREEP CRACK-GROWTH: A NEW PATH-INDEPENDENT T SUB O AND COMPUTATIONAL STUDIES

R. B. STONESIFER and S. N. ATLURI Dec. 1981 141 p refs (Contract NAG3-38) (NASA-CR-168930; NAS 1.26:168930) Avail: NTIS HC A07/MF A01 CSCL 20K

Two path independent integral parameters which show some degree of promise as fracture criteria are the C^* and $\Delta T_{sub c}$ integrals. The mathematical aspects of these parameters are reviewed. This is accomplished by deriving generalized vector forms of the parameters using conservation laws which are valid for arbitrary, three dimensional, cracked bodies with crack surface tractions (or applied displacements), body forces, inertial effects and large deformations. Two principal conclusions are that $\Delta T_{sub c}$ is a valid crack tip parameter during nonsteady as well as steady state creep and that $\Delta T_{sub c}$ has an energy rate interpretation whereas C^* does not. An efficient, small displacement, infinitesimal strain, displacement based finite element model is developed for general elastic/plastic material behavior. For the numerical studies, this model is specialized to two dimensional plane stress and plane strain and to power law creep constitutive relations. S.L.

N82-26701*# National Aeronautics and Space Administration. Lewis Research Center, Cleveland, Ohio.

BIRD IMPACT ANALYSIS PACKAGE FOR TURBINE ENGINE FAN BLADES

M. S. HIRSCHBEIN 1982 20 p refs Presented at 23rd Struct. Dyn. and Mater. Conf., New Orleans, 10-12 Previously announced in IAA as A82-30162 May 1982; Sponsored by AIAA, ASME, ASCE, and AHS (NASA-TM-82831; NAS 1.15:82831) Avail: NTIS HC A02/MF A01 CSCL 20K

For abstract see A82-30162

N82-26702*# Cincinnati Univ., Ohio.

MICROSTRUCTURAL EFFECTS ON THE ROOM AND ELEVATED TEMPERATURE LOW CYCLE FATIGUE BEHAVIOR OF WASPALOY M.S. Thesis Final Report

B. A. LERCH May 1982 194 p refs

(Contract NSG-3263)

(NASA-CR-165497; NAS 1.26:165497) Avail: NTIS HC A09/MF A01 CSCL 20K

Longitudinal specimens of Waspaloy containing either coarse grains with small gamma or fine grains with large gamma were tested in air at a frequency of 0.33 Hz or 0.50 Hz. The coarse grained structures exhibited planar slip on (III) planes and precipitate shearing at all temperatures. Cracks initiated by a Stage 1 mechanism and propagated by a striation forming mechanism. At 700 C and 800 C, cleavage and intergranular cracking were observed. Testing at 500 C, 700 C, and 800 C caused precipitation of grain boundary carbides. At 700 C, carbides precipitated on slip bands. The fine grained structures exhibited planar slip on (111) planes. Dislocations looped the large gamma precipitates. This structure led to stress saturation and propagation was observed. Increasing temperatures resulted in increased specimen oxidation for both heat treatments. Slip band and grain boundary oxidation were observed. At 800 C, oxidized grain boundaries were cracked by intersecting slip bands which resulted in intergranular failure. The fine specimens had crack initiation later in the fatigue life, but with more rapid propagation crack propagation. A.R.H.

N82-26706*# Cincinnati Univ., Ohio. Dept. of Materials Science and Metallurgical Engineering.

MECHANISMS OF DEFORMATION AND FRACTURE IN HIGH TEMPERATURE LOW CYCLE FATIGUE OF RENE 80 AND IN 100 Final Report

G. R. ROMANOSKI, JR. Mar. 1982 227 p refs

(Contract NSG-3263)

(NASA-CR-165498; NAS 1.26:165498) Avail: NTIS HC A11/MF A01 CSCL 20K

Specimens tested for the AGARD strain range partitioning program were investigated. Rene 80 and IN 100 were tested in air and in vacuum; at 871 C, 925 C, and 1000 C; and in the coated and uncoated condition. The specimens exhibited a multiplicity of high-temperature low-cycle fatigue damage. Observations of the various forms of damage were consistent with material and testing conditions and were generally in agreement with previous studies. In every case observations support a contention that failure occurs at a particular combination of crack length and maximum stress. A failure criterion which is applicable in the regime of testing studied is presented. The predictive capabilities of this criterion are straight forward.

Author

N82-26713*# Illinois Univ., Urbana-Champaign. Dept. of Theoretical and Applied Mechanics.

BOUNDARY LAYER THERMAL STRESSES IN ANGLE-PLY COMPOSITE LAMINATES, PART 1 Final Report

S. S. WANG and I. CHOI Feb. 1981 56 p refs 6 Vol.

(Contract NSG-3044)

(NASA-CR-165412; NAS 1.26:165412) Avail: NTIS HC A04/MF A01 CSCL 20K

Thermal boundary-layer stresses (near free edges) and displacements were determined by an eigenfunction expansion technique and the establishment of an appropriate particular solution. Current solutions in the region away from the singular domain (free edge) are found to be excellent agreement with existing approximate numerical results. As the edge is approached, the singular term controls the near field behavior of the boundary layer. Results are presented for cases of various angle-ply graphite/epoxy laminates with $(\theta/\theta/\theta/\theta)$ configurations. These results show high interlaminar (through-the-thickness) stresses. Thermal boundary-layer thicknesses of different composite systems are determined by examining the strain energy density distribution in composites. It is shown that the boundary-layer thickness depends on the degree of anisotropy of each individual lamina, thermomechanical

properties of each ply, and the relative thickness of adjacent layers. The interlaminar thermal stresses are compressive with increasing temperature. The corresponding residual stresses are tensile and may enhance interply delaminations. A.R.H.

N82-26714*# Illinois Univ., Urbana-Champaign. Dept. of Theoretical and Applied Mechanics.

ANALYSIS OF CRACKS EMANATING FROM A CIRCULAR HOLE IN UNIDIRECTIONAL FIBER REINFORCED COMPOSITES, PART 2 Final Report

S. S. WANG and J. F. YAU Feb. 1981 35 p refs 6 Vol.

(Contract NSG-3044)

(NASA-CR-165433; NAS 1.26:165433) Avail: NTIS HC A03/MF A01 CSCL 20K

An analytical method is developed for cracks emanating from a circular hole in an off-axis unidirectional fiber-reinforced composite. The method which is formulated by using conservation laws of elasticity and fundamental relationships in anisotropic fracture mechanics, provides a convenient and accurate means to examine the complicated crack behavior, when used in conjunction with a suitable numerical scheme such as the finite element method. The formulation is eventually reduced to a system of linear algebraic equations of mixed-mode stress intensity factors. Fracture parameters, describing crack-tip deformation and fracture in the composite, are obtained explicitly. Effects of material anisotropy and crack/hole geometry are examined also. Of particular interest are the energy release rates associated with crack extension; their values are evaluated for various cases. Results show that mixed-mode stress intensity factors and energy release rates associated with the cracks emanating from a hole change very appreciably with fiber orientation in the composite. $K_{sub 1}$ and G increase monotonically with increasing θ ; but $K_{sub 2}$ reaches its maximum at $\theta = 45$ deg, and then decreases gradually as θ increases further. Author

N82-26715*# Illinois Univ., Urbana-Champaign. Dept. of Theoretical and Applied Mechanics.

INTERLAMINAR CRACK GROWTH IN FIBER REINFORCED COMPOSITES DURING FATIGUE, PART 3 Final Report

S. S. WANG and H. T. WANG Feb. 1981 37 p refs 6 Vol.

(Contract NSG-3044)

(NASA-CR-165434; NAS 1.26:165434) Avail: NTIS HC A03/MF A01 CSCL 20K

Interlaminar crack growth behavior in fiber-reinforced composites subjected to fatigue loading was investigated experimentally and theoretically. In the experimental phase, inter-laminar crack propagation rates and mechanisms were determined for the cases of various geometries, laminate parameters and cyclic stress levels. A singular hybrid-stress finite element method was used in conjunction with the experimental results to examine the local crack-tip behavior and to characterize the crack propagation during fatigue. Results elucidate the basic nature of the cyclic delamination damage, and relate the interlaminar crack growth rate to the range of mixed-mode crack-tip stress intensity factors. The results show that crack growth rates are directly related to the range of the mixed-mode cyclic stress intensity factors by a power law relationship. Author

N82-26716*# Illinois Univ., Urbana-Champaign. Dept. of Theoretical and Applied Mechanics.

ANALYSIS OF INTERFACE CRACKS IN ADHESIVELY BONDED LAP SHEAR JOINTS, PART 4 Final Report

S. S. WANG and J. F. YAU Feb. 1981 39 p refs 6 Vol.

(Contract NSG-3044)

(NASA-CR-165438; NAS 1.26:165438) Avail: NTIS HC A03/MF A01 CSCL 20K

Conservation laws of elasticity for nonhomogeneous materials were developed and were used to study the crack behavior in adhesively bonded lap shear joints. By using these laws and the fundamental relationships in fracture mechanics of interface cracks, the problem is reduced to a pair of linear algebraic equations, and stress intensity solutions can be determined directly by information extracted from the far field. The numerical results

obtained show that: (1) in the lap-shear joint with a given adherend, the opening-mode stress intensity factor, ($K_{sub 1}$) is always larger than that of the shearing-mode ($K_{sub 2}$); (2) ($K_{sub 1}$) is not sensitive to adherent thickness about ($K_{sub 2}$) increases rapidly with increasing thickness; and (3) ($K_{sub 1}$) and ($K_{sub 2}$) increase simultaneously as the interfacial crack length increases. Author

N82-26717* # Illinois Univ., Urbana-Champaign. Dept. of Theoretical and Applied Mechanics.
EDGE DELAMINATION IN ANGLE-PLY COMPOSITE LAMINATES, PART 5 Final Report
 S. S. WANG Feb. 1981 50 p refs 6 Vol.
 (Contract NSG-3044)
 (NASA-CR-165439; NAS 1.26:165439) Avail: NTIS HC A03/MF A01 CSCL 20K

A theoretical method was developed for describing the edge delamination stress intensity characteristics in angle-ply composite laminates. The method is based on the theory of anisotropic elasticity. The edge delamination problem is formulated using Lekhnitskii's complex-variable stress potentials and an especially developed eigenfunction expansion method. The method predicts exact orders of the three-dimensional stress singularity in a delamination crack tip region. With the aid of boundary collocation, the method predicts the complete stress and displacement fields in a finite-dimensional, delaminated composite. Fracture mechanics parameters such as the mixed-mode stress intensity factors and associated energy release rates for edge delamination can be calculated explicitly. Solutions are obtained for edge delaminated (θ - θ angle-ply composites under uniform axial extension. Effects of delamination lengths, fiber orientations, lamination and geometric variables are studied. Author

N82-26718* # Illinois Univ., Urbana-Champaign. Dept. of Theoretical and Applied Mechanics.
BOUNDARY-LAYER EFFECTS IN COMPOSITE LAMINATES: FREE-EDGE STRESS SINGULARITIES, PART 6 Final Report
 S. S. WANAN and I. CHOI Apr. 1981 38 p refs 6 Vol.
 (Contract NSG-3044)
 (NASA-CR-165440; NAS 1.26:165440) Avail: NTIS HC A03/MF A01 CSCL 20K

A rigorous mathematical model was obtained for the boundary-layer free-edge stress singularity in angleplied and crossplied fiber composite laminates. The solution was obtained using a method consisting of complex-variable stress function potentials and eigenfunction expansions. The required order of the boundary-layer stress singularity is determined by solving the transcendental characteristic equation obtained from the homogeneous solution of the partial differential equations. Numerical results obtained show that the boundary-layer stress singularity depends only upon material elastic constants and fiber orientation of the adjacent plies. For angleplied and crossplied laminates the order of the singularity is weak in general. Author

N82-29619* # Georgia Inst. of Tech., Atlanta. Center for the Advancement of Computational Mechanics.
CREEP CRACK-GROWTH: A NEW PATH-INDEPENDENT INTEGRAL ($T_{sub C}$), AND COMPUTATIONAL STUDIES Ph.D. Thesis Final Report
 R. B. STONESIFER and S. N. ATLURI Jul. 1982 112 p refs
 (Contract NAG3-38)
 (NASA-CR-167897; NAS 1.26:167897) Avail: NTIS HC A06/MF A01 CSCL 20K

The development of valid creep fracture criteria is considered. Two path-independent integral parameters which show some degree of promise are the C^* and (ΔT)_{sub c} integrals. The mathematical aspects of these parameters are reviewed by deriving generalized vector forms of the parameters using conservation laws which are valid for arbitrary, three dimensional, cracked bodies with crack surface tractions (or applied displacements), body forces, inertial effects, and large deformations. Two principal conclusions are that (ΔT)_{sub c} has an energy rate interpretation whereas C^* does not. The development and application of fracture criteria often involves the solution of boundary/initial value problems

associated with deformation and stresses. The finite element method is used for this purpose. An efficient, small displacement, infinitesimal strain, displacement based finite element model is specialized to two dimensional plane stress and plane strain and to power law creep constitutive relations. A mesh shifting/remeshing procedure is used for simulating crack growth. The model is implemented with the quartz-point node technique and also with specially developed, conforming, crack-tip singularity elements which provide for the r to the $n(1+n)$ power strain singularity associated with the HRR crack-tip field. Comparisons are made with a variety of analytical solutions and alternate numerical solutions for a number of problems. J.D.

N82-31707* # National Aeronautics and Space Administration. Lewis Research Center, Cleveland, Ohio.
LARGE DISPLACEMENTS AND STABILITY ANALYSIS OF NONLINEAR PROPELLER STRUCTURES
 R. A. AIELLO 1982 18 p refs Presented at the 10th NASTRAN User's Colloq., New Orleans, 13-14 May 1982
 (NASA-TM-82850; NAS 1.15:82850) Avail: NTIS HC A02/MF A01 CSCL 20K

The use of linear rigid formats in COSMIC NASTRAN without DMAP procedures for the analysis of nonlinear propeller structures is described. Approaches for updating geometry and applying follower forces for incremental loading are demonstrated. Comparisons are made with COSMIC NASTRAN rigid formats and other independent finite element programs. Specifically, the comparisons include results from the four approaches for updating the geometry using RIGID FORMAT 1, RIGID FORMATS 4 and 13, MARC and MSC/NASTRAN. It is shown that 'user friendly' updating approaches (without DMAPS) can be used to predict the large displacements and instability of these nonlinear structures. These user friendly approaches can be easily implemented by the user and predict conservative results. Author

N82-31708* # National Aeronautics and Space Administration. Lewis Research Center, Cleveland, Ohio.
TENSILE BUCKLING OF ADVANCED TURBOPROPS
 C. C. CHAMIS and R. A. AIELLO 1982 25 p refs Presented at the 23rd Struct., Struct. Dyn. and Mater. Conf., New Orleans, 10-12 May 1982; sponsored by AIAA, ASME, ASCE and AHS
 (NASA-TM-82896; E-1276; NAS 1.15:82896) Avail: NTIS HC A02/MF A01 CSCL 20K

Theoretical studies were conducted to determine analytically the tensile buckling of advanced propeller blades (turboprops) in centrifugal fields, as well as the effects of tensile buckling on other types of structural behavior, such as resonant frequencies and flutter. Theoretical studies were also conducted to establish the advantages of using high performance composite turboprops as compared to titanium. Results show that the vibration frequencies are not affected appreciably prior to 80 percent of the tensile speed. Some frequencies approach zero as the tensile buckling speed is approached. Composites provide a substantial advantage over titanium on a buckling speed to weight basis. Vibration modes change as the rotor speed is increased and substantial geometric coupling is present. R.J.F.

N82-33738* # Dayton Univ., Ohio. Dept. of Aerospace Mechanics.
A PRELIMINARY STUDY OF CRACK INITIATION AND GROWTH AT STRESS CONCENTRATION SITES Interim Technical Report, 1 Jan. - 31 Aug. 1982
 D. S. DAWICKE, J. P. GALLAGHER, G. A. HARTMAN, and A. M. RAJENDRAN Sep. 1982 30 p refs
 (Contract NAG3-246)
 (NASA-CR-169358; NAS 1.26:169358; UDR-TR-82-119; ITR-1)
 Avail: NTIS HC A03/MF A01 CSCL 20K

Crack initiation and propagation models for notches are examined. The Dowling crack initiation model and the E1 Haddad et al. crack propagation model were chosen for additional study. Existing data was used to make a preliminary evaluation of the crack propagation model. The results indicate that for the crack sizes in the test, the elastic parameter K gave good correlation

for the crack growth rate data. Additional testing, directed specifically toward the problem of small cracks initiating and propagating from notches is necessary to make a full evaluation of these initiation and propagation models. S.L.

N82-33744*# National Aeronautics and Space Administration. Lewis Research Center, Cleveland, Ohio.

NONLINEAR CONSTITUTIVE THEORY FOR TURBINE ENGINE STRUCTURAL ANALYSIS

R. L. THOMPSON /n NASA. Langley Research Center Res. in Struct. and Solid Mech., 1982 p 67-96 Oct. 1982 refs
 Avail: NTIS HC A19/MF A01 CSCL 20K

A number of viscoplastic constitutive theories and a conventional constitutive theory are evaluated and compared in their ability to predict nonlinear stress-strain behavior in gas turbine engine components at elevated temperatures. Specific application of these theories is directed towards the structural analysis of combustor liners undergoing transient, cyclic, thermomechanical load histories. The combustor liner material considered in this study is Hastelloy X. The material constants for each of the theories (as a function of temperature) are obtained from existing, published experimental data. The viscoplastic theories and a conventional theory are incorporated into a general purpose, nonlinear, finite element computer program. Several numerical examples of combustor liner structural analysis using these theories are given to demonstrate their capabilities. Based on the numerical stress-strain results, the theories are evaluated and compared.

Author

N83-11514*# National Aeronautics and Space Administration. Lewis Research Center, Cleveland, Ohio.

BENDING-TORSION FLUTTER OF A HIGHLY SWEEPED ADVANCED TURBOPROP

O. MEHMED, K. R. V. KAZA, J. F. LUBOMSKI, and R. E. KIELB 1981 24 p refs Prepared for presentation at the 1982 Aerospace Congr. and Exposition, Anaheim, Calif., 25-28 Oct., 1982; sponsored by the Soc. of Automotive Engr. (NASA-TM-82975; E-1404; NAS 1.15:82975) Avail: NTIS HC A02/MF A01 CSCL 20K

Experimental and analytical results are presented for a bending-torsion flutter phenomena encountered during wind-tunnel testing of a ten-bladed, advanced, high-speed propeller (turboprop) model with thin airfoil sections, high blade sweep, low aspect ratio, high solidity and transonic tip speeds. Flutter occurred at free-stream Mach numbers of 0.6 and greater and when the relative tip Mach number (based on vector sum of axial and tangential velocities) reached a value of about one. The experiment also included two- and five-blade configurations. The data indicate that aerodynamic cascade effects have a strong destabilizing influence on the flutter boundary. The data was correlated with analytical results which include aerodynamic cascade effects and good agreement was found.

Author

N83-12449*# National Aeronautics and Space Administration. Lewis Research Center, Cleveland, Ohio.

MATERIALS CONSTITUTIVE MODELS FOR NONLINEAR ANALYSIS OF THERMALLY CYCLED STRUCTURES

A. KAUFMAN and L. E. HUNT (Arizona Univ., Tucson) Oct. 1982 26 p refs
 (Contract NAG3-45)
 (NASA-TP-2055; E-1125; NAS 1.60:2055) Avail: NTIS HC A03/MF A01 CSCL 20K

Effects of inelastic materials models on computed stress-strain solutions for thermally loaded structures were studied by performing nonlinear (elastoplastic creep) and elastic structural analyses on a prismatic, double edge wedge specimen of IN 100 alloy that was subjected to thermal cycling in fluidized beds. Four incremental plasticity creep models (isotropic, kinematic, combined isotropic kinematic, and combined plus transient creep) were exercised for the problem by using the MARC nonlinear, finite element computer program. Maximum total strain ranges computed from the elastic and nonlinear analyses agreed within 5 percent. Mean cyclic stresses, inelastic strain ranges, and inelastic work were

significantly affected by the choice of inelastic constitutive model. The computing time per cycle for the nonlinear analyses was more than five times that required for the elastic analysis. S.L.

N83-12451*# General Electric Co., Cincinnati, Ohio. Aircraft Engine Business Group.

BENCHMARK NOTCH TEST FOR LIFE PREDICTION

P. A. DOMAS, W. N. SHARPE, M. WARD, and J. F. YAU Oct. 1982 212 p refs Prepared in cooperation with Louisiana State Univ., Baton Rouge
 (Contract NAS3-22522)
 (NASA-CR-165571; NAS 1.26:165571; R82AEB358) Avail: NTIS HC A10/MF A01 CSCL 20L

The laser Interferometric Strain Displacement Gage (ISDG) was used to measure local strains in notched Inconel 718 test bars subjected to six different load histories at 649 C (1200 F) and including effects of tensile and compressive hold periods. The measurements were compared to simplified Neuber notch analysis predictions of notch root stress and strain. The actual strains incurred at the root of a discontinuity in cyclically loaded test samples subjected to inelastic deformation at high temperature where creep deformations readily occur were determined. The steady state cyclic, stress-strain response at the root of the discontinuity was analyzed. Flat, double notched uniaxially loaded fatigue specimens manufactured from the nickel base, superalloy Inconel 718 were used. The ISDG was used to obtain cycle by cycle recordings of notch root strain during continuous and hold time cycling at 649 C. Comparisons to Neuber and finite element model analyses were made. The results obtained provide a benchmark data set in high technology design where notch fatigue life is the predominant component service life limitation. S.L.

N83-12460*# National Aeronautics and Space Administration. Lewis Research Center, Cleveland, Ohio.

LARGE DISPLACEMENTS AND STABILITY ANALYSIS OF NONLINEAR PROPELLER STRUCTURES

R. A. AIELLO and C. C. CHAMIS /n Georgia Univ. 10th NASTRAN User's Colloq. p 112-132 Nov. 1982
 Avail: NTIS HC A12/MF A01 CSCL 20K

The use of linear rigid formats in COSMIC NASTRAN without DMAP procedures for the analysis of nonlinear propeller structures is described. Approaches for updating geometry and applying follower forces for incremental loading are demonstrated. The COSMIC NASTRAN rigid formats and other independent finite element programs are compared. The comparisons include results from the four approaches for updating the geometry using RIGID FORMAT 1, RIGID FORMATS 4 and 13, MARC and MSC/NASTRAN. It is shown that user friendly updating approaches can be used to predict the large displacements and instability of these nonlinear structures. The approaches are easily implemented by the user and predict conservative results. E.A.K.

N83-14523*# National Aeronautics and Space Administration. Lewis Research Center, Cleveland, Ohio.

MEASUREMENTS OF SELF-EXCITED ROTOR-BLADE VIBRATIONS USING OPTICAL DISPLACEMENTS

A. P. KURKOV 1982 13 p refs Proposed for presentation at the 28th Ann. Intern. Gas Turbine Conf., Phoenix, Ariz., 27-31 Mar. 1983
 (NASA-TM-82953; E-1368; NAS 1.15:82953) Avail: NTIS HC A02/MF A01 CSCL 20K

The characteristics of optical displacement spectra and their role of monitoring rotor blade vibrations are discussed. During the operation of a turbofan engine at part speed, near stall, and elevated inlet pressure and temperature, several vibratory instabilities were excited simultaneously on the first fan rotor. The torsional and bending contributions to the main flutter mode were resolved by using casing-mounted optical displacement sensors. Other instabilities in the blade deflection spectra were identified.

E.A.K.

39 STRUCTURAL MECHANICS

N83-15672*# National Aeronautics and Space Administration. Lewis Research Center, Cleveland, Ohio.

EFFECTS OF STRUCTURAL COUPLING ON MISTUNED CASCADE FLUTTER AND RESPONSE

R. E. KIELB and K. R. V. KAZA (Toledo Univ.) 1983 17 p refs Proposed for presentation at the 28th Ann. Intern. Gas Turbine Conf., Phoenix, Ariz., 27-31 Mar. 1983; sponsored by ASME

(NASA-TM-83049; E-1500; NAS 1.15:83049) Avail: NTIS HC A02/MF A01 CSCL 20K

The effects of structural coupling on mistuned cascade flutter and response are analytically investigated using an extended typical section model. This model includes both structural and aerodynamic coupling between the blades. The model assumes that the structurally coupled system natural modes were determined and are represented in the form of N bending and N torsional uncoupled modes for each blade, where N is the number of blades and, hence, is only valid for blade dominated motion. The aerodynamic loads are calculated by using two dimensional unsteady cascade theories in the subsonic and supersonic flow regimes. The results show that the addition of structural coupling can affect both the aeroelastic stability and frequency. The stability is significantly affected only when the system is mistuned. The resonant frequencies can be significantly changed by structural coupling in both tuned and mistuned systems, however, the peak response is significantly affected only in the latter. S.L.

N83-19121*# Michigan State Univ., East Lansing.

EXPERIMENTAL VERIFICATION OF THE NEUBER RELATION AT ROOM AND ELEVATED TEMPERATURES M.S. Thesis

L. J. LUCAS 1982 100 p refs

(Contract NAG3-51)

(NASA-CR-167967; NAS 1.26:167967) Avail: NTIS HC A05/MF A01 CSCL 20K

The accuracy of the Neuber equation at room temperature and 1,200 F as experimentally determined under cyclic load conditions with hold times. All strains were measured with an interferometric technique at both the local and remote regions of notched specimens. At room temperature, strains were obtained for the initial response at one load level and for cyclically stable conditions at four load levels. Stresses in notched members were simulated by subjecting smooth specimens to the same strains as were recorded on the notched specimen. Local stress-strain response was then predicted with excellent accuracy by subjecting a smooth specimen to limits established by the Neuber equation. Data at 1,200 F were obtained with the same experimental techniques but only in the cyclically stable conditions. The Neuber prediction at this temperature gave relatively accurate results in terms of predicting stress and strain points. S.L.

N83-19246*# National Aeronautics and Space Administration. Lewis Research Center, Cleveland, Ohio.

STRUCTURAL FATIGUE TEST RESULTS FOR LARGE WIND TURBINE BLADE SECTIONS

J. R. FADDLOUL and T. L. SULLIVAN *In its* Large Horizontal-Axis Wind Turbines p 303-328 1982 refs

Avail: NTIS HC A99/MF A01 CSCL 20K

In order to provide quantitative information on the operating life capabilities of wind turbine rotor blade concepts for root-end load transfer, a series of cantilever beam fatigue tests was conducted. Fatigue tests were conducted on a laminated wood blade with bonded steel studs, a low cost steel spar (utility pole) with a welded flange, a utility pole with additional root-end thickness provided by a swaged collar, fiberglass spars with both bonded and nonbonded fittings, and, finally, an aluminum blade with a bolted steel fitting (Lockheed Mod-0 blade). Photographs, data, and conclusions for each of these tests are presented. In addition, the aluminum blade test results are compared to field failure information; these results provide evidence that the cantilever beam type of fatigue test is a satisfactory method for obtaining qualitative data on blade life expectancy and for identifying structurally underdesigned areas (hot spots). M.G.

N83-21390*# Pratt and Whitney Aircraft Group, East Hartford, Conn. Commercial Engineering.

DEVELOPMENT OF A SIMPLIFIED ANALYTICAL METHOD FOR REPRESENTING MATERIAL CYCLIC RESPONSE

V. MORENO Jan. 1983 91 p refs

(Contract NAS3-22821)

(NASA-CR-168100; NAS 1.26:168100; PWA-5843-13) Avail: NTIS HC A05/MF A01 CSCL 20K

Development of a simplified method for estimating structural inelastic stress and strain response to cyclic thermal loading is presented. The method assumes that high temperature structural response is the sum of time independent plastic and time dependent elastic/creep components. The local structural stress and strain response predicted by linear elastic analysis is modified by the simplified method to predict the inelastic response. The results with simulations by a nonlinear finite element analysis and used time independent plasticity and unified time dependent material model are compared. E.A.K.

N83-23629*# National Aeronautics and Space Administration. Lewis Research Center, Cleveland, Ohio. Dept. of Aerospace Mechanics.

A TOTAL LIFE PREDICTION MODEL FOR STRESS CONCENTRATION SITES Semiannual Engineering Technical Report, 1 Sep. 1982 - 31 Mar. 1983

G. A. HARTMAN and D. S. DAWICKE 11 Apr. 1983 35 p refs

(Contract NAG3-246)

(NASA-CR-170290; NAS 1.26:170290; UDR-TR-83-57; SATR-2)

Avail: NTIS HC A03/MF A01 CSCL 20K

Fatigue crack growth tests were performed on center crack panels and radial crack hole samples. The data were reduced and correlated with the elastic parameter-K taking into account finite width and corner crack corrections. The anomalous behavior normally associated with short cracks was not observed. Total life estimates for notches were made by coupling an initiation life estimate with a propagation life estimate. E.A.K.

N83-23631*# National Aeronautics and Space Administration. Lewis Research Center, Cleveland, Ohio.

ARRAY STRUCTURE DESIGN HANDBOOK FOR STAND ALONE PHOTOVOLTAIC APPLICATIONS

R. C. DIDELOT Oct. 1980 243 p refs

(Contract DE-AI01-79ET-20485)

(NASA-TM-82629; E-882; NAS 1.15:82629; DOE/NASA/20485-2)

Avail: NTIS HC A11/MF A01 CSCL 20K

This handbook will permit the user to design a low-cost structure for a variety of photovoltaic system applications under 10 kW. Any presently commercially available photovoltaic modules may be used. Design alternatives are provided for different generic structure types, structural materials, and electric interfaces. The use of a hand-held calculator is sufficient to perform the necessary calculations for the array designs. Author

N83-24874*# National Aeronautics and Space Administration. Lewis Research Center, Cleveland, Ohio.

STRESS INTENSITY AND DISPLACEMENT COEFFICIENTS FOR RADIALLY CRACKED RING SEGMENTS SUBJECT TO THREE-POINT BENDING

B. GROSS and J. E. SRAWLEY Mar. 1983 19 p refs

(NASA-TM-83059; E-1524; NAS 1.15:83059) Avail: NTIS HC A02/MF A01 CSCL 20K

The boundary collocation method was used to generate Mode I stress intensity and crack mouth displacement coefficients for internally and externally radially cracked ring segments (arc bend specimens) subjected to three point radial loading. Numerical results were obtained for ring segment outer to inner radius ratios ($R_{sub o}/R_{sub i}$) ranging from 1.10 to 2.50 and crack length to width ratios (a/W) ranging from 0.1 to 0.8. Stress intensity and crack mouth displacement coefficients were found to depend on the ratios $R_{sub o}/R_{sub i}$ and a/W as well as the included angle between the directions of the reaction forces. S.L.

N83-24875*# National Aeronautics and Space Administration. Lewis Research Center, Cleveland, Ohio.

VAPOR CAVITATION IN DYNAMICALLY LOADED JOURNAL BEARINGS

B. O. JACOBSON (Lulea Univ.) and B. J. HAMROCK 1983 14 p refs Proposed for presentation at the 2d Intern. Conf. on Cavitation, Edinburgh, 5-8 Sep. 1983
(NASA-TM-83366; E-1401; NAS 1.15:83366) Avail: NTIS HC A02/MF A01 CSCL 20K

High speed motion camera experiments were performed on dynamically loaded journal bearings. The length to diameter ratio of the bearing, the speed of the roller and the tube, the surface material of the roller, and the static and dynamic eccentricity of the bearing were varied. One hundred and thirty-four cases were filmed. The occurrence of vapor cavitation was clearly evident in the films and figures presented. Vapor cavitation was found to occur when the tensile stress applied to the oil exceeded the tensile strength of the oil or the binding of the oil to the surface. The physical situation in which vapor cavitation occurs is during the squeezing and sliding motion within a bearing. Besides being able to accurately capture the vapor cavitation on film, an analysis of the formation and collapse of the cavitation bubbles and characteristics of the bubble content are presented. S.L.

N83-27256*# Case Western Reserve Univ., Cleveland, Ohio.
CRACK LAYER MORPHOLOGY AND TOUGHNESS CHARACTERIZATION IN STEELS Final Report

A. CHUDNOVSKY and M. BESSENDORF May 1983 41 p refs
(Contract NAG3-223)
(NASA-CR-168154; NAS 1.26:168154) Avail: NTIS HC A03/MF A01 CSCL 20K

Both the macro studies of crack layer propagation are presented. The crack extension resistance parameter $R_{sub 1}$ based on the morphological study of microdefects is introduced. Experimental study of the history dependent nature of $G_{sub c}$ supports the representation of $G_{sub c}$ as a product of specific enthalpy of damage (material constant) and $R_{sub 1}$. The latter accounts for the history dependence. The observation of nonmonotonic crack growth under monotonic changes of J as well as statistical features of the critical energy release rate (variance of $G_{sub c}$) indicate the validity of the proposed damage characterization. S.L.

N83-28493*# National Aeronautics and Space Administration. Lewis Research Center, Cleveland, Ohio.

CONSTITUTIVE RELATIONSHIPS FOR ANISOTROPIC HIGH-TEMPERATURE ALLOYS

D. N. ROBINSON 1982 22 p refs Prepared for Presentation at the Intern. Post-Conf. Seminar on Inelastic Analysis and Life Prediction, Chicago, 29-30 Aug. 1983; sponsored by Commission of European Communities and Argonne Natl. Lab., Chicago
(NASA-TM-83437; E-1733; NAS 1.15:83437) Avail: NTIS HC A02/MF A01 CSCL 20K

A constitutive theory is presented for representing the anisotropic viscoplastic behavior of high temperature alloys that possess directional properties resulting from controlled grain growth or solidification. The theory is an extension of a viscoplastic model that was applied in structural analyses involving isotropic metals. Anisotropy is introduced through the definition of a vector field that identifies a preferential (solidification) direction at each material point. Following the development of a full multiaxial theory, application is made to homogeneously stressed elements in pure shear and to a uniaxially stressed rectangular block in plane stress with the stress direction oriented at an arbitrary angle with the material direction. It is shown that an additional material parameter introduced to characterize the degree of anisotropy can be determined on the basis of simple creep tests. S.L.

N83-29731*# Arizona Univ., Tucson. Dept. of Aerospace and Mechanical Engineering.

STATISTICAL SUMMARIES OF FATIGUE DATA FOR DESIGN PURPOSES Final Report

P. H. WIRSCHING Washington, D.C. NASA Jul. 1983 63 p refs
(Contract NAG3-41)
(NASA-CR-3697; NAS 1.26:3697) Avail: NTIS HC A04/MF A01 CSCL 20K

Two methods are discussed for constructing a design curve on the safe side of fatigue data. Both the tolerance interval and equivalent prediction interval (EPI) concepts provide such a curve while accounting for both the distribution of the estimators in small samples and the data scatter. The EPI is also useful as a mechanism for providing necessary statistics on S-N data for a full reliability analysis which includes uncertainty in all fatigue design factors. Examples of statistical analyses of the general strain life relationship are presented. The tolerance limit and EPI techniques for defining a design curve are demonstrated. Examples using WASPALOY B and RQC-100 data demonstrate that a reliability model could be constructed by considering the fatigue strength and fatigue ductility coefficients as two independent random variables. A technique given for establishing the fatigue strength for high cycle lives relies on an extrapolation technique and also accounts for 'runners.' A reliability model or design value can be specified. Author

N83-29734*# Arizona Univ., Tucson. Dept. of Aerospace and Mechanical Engineering.

APPLICATION OF ADVANCED RELIABILITY METHODS TO LOCAL STRAIN FATIGUE ANALYSIS Final Report

T. T. WU and P. H. WIRSCHING Washington Jul. 1983 52 p refs
(Contract NAG3-41)
(NASA-CR-168198; NAS 1.26:168198) Avail: NTIS HC A04/MF A01 CSCL 20K

When design factors are considered as random variables and the failure condition cannot be expressed by a closed form algebraic inequality, computations of risk (or probability of failure) might become extremely difficult or very inefficient. This study suggests using a simple, and easily constructed, second degree polynomial to approximate the complicated limit state in the neighborhood of the design point; a computer analysis relates the design variables at selected points. Then a fast probability integration technique (i.e., the Rackwitz-Fiessler algorithm) can be used to estimate risk. The capability of the proposed method is demonstrated in an example of a low cycle fatigue problem for which a computer analysis is required to perform local strain analysis to relate the design variables. A comparison of the performance of this method is made with a far more costly Monte Carlo solution. Agreement of the proposed method with Monte Carlo is considered to be good. Author

N83-33217*# National Aeronautics and Space Administration. Lewis Research Center, Cleveland, Ohio.

TEMPERATURE DISTRIBUTION IN AN AIRCRAFT TIRE AT LOW GROUND SPEEDS

J. L. MCCARTY and J. A. TANNER Aug. 1983 36 p refs
(NASA-TP-2195; L-15605; NAS 1.60:2195) Avail: NTIS HC A03/MF A01 CSCL 20K

An experimental study was conducted to define temperature profiles of 22 x 5.5, type 7, bias ply aircraft tires subjected to freely rolling, yawed rolling, and light braking conditions. Temperatures along the inner wall of freely rolling tires were greater than those near the outer surface. The effect of increasing tire deflection was to increase the temperature within the shoulder and sidewall areas of the tire carcass. The effect of cornering and braking was to increase the tread temperature. For taxi operations at fixed yaw angles, temperature profiles were not symmetric. Increasing the ground speed produced only moderate increases in tread temperature, whereas temperatures in the carcass shoulder and sidewall were essentially unaffected. Author

N83-33219*# Virginia Polytechnic Inst. and State Univ., Blacksburg. Dept. of Engineering Science and Mechanics.
GEOMETRICALLY NONLINEAR ANALYSIS OF LAYERED COMPOSITE PLATES AND SHELLS Interim Report
 W. C. CHAO and J. N. REDDY Feb. 1983 117 p refs
 (Contract NAG3-208)
 (NASA-CR-168182; NAS 1.26:168182; VPI-E-83.10) Avail: NTIS HC A06/MF A01 CSCL 20K

A degenerated three dimensional finite element, based on the incremental total Lagrangian formulation of a three dimensional layered anisotropic medium was developed. Its use in the geometrically nonlinear, static and dynamic, analysis of layered composite plates and shells is demonstrated. A two dimensional finite element based on the Sanders shell theory with the von Karman (nonlinear) strains was developed. It is shown that the deflections obtained by the 2D shell element deviate from those obtained by the more accurate 3D element for deep shells. The 3D degenerated element can be used to model general shells that are not necessarily doubly curved. The 3D degenerated element is computationally more demanding than the 2D shell theory element for a given problem. It is found that the 3D element is an efficient element for the analysis of layered composite plates and shells undergoing large displacements and transient motion.

E.A.K.

N83-34349*# National Aeronautics and Space Administration. Lewis Research Center, Cleveland, Ohio.
RELATION OF CYCLIC LOADING PATTERN TO MICROSTRUCTURAL FRACTURE IN CREEP FATIGUE
 S. S. MANSON (Case Western Reserve Univ.), G. R. HALFORD, and R. E. OLDRIEVE 1983 44 p refs Proposed for presentation at Fatigue 84 The 2nd Intern. Conf. on Fatigue and Fatigue Thresholds, Birmingham, England, 3-7 Sep. 1984
 (NASA-TM-83473; E-1787; NAS 1.15:83473) Avail: NTIS HC A03/MF A01 CSCL 20K

Creep-fatigue-environment interaction is discussed using the 'strainrange partitioning' (SRP) framework as a basis. The four generic SRP strainrange types are studied with a view of revealing differences in micromechanisms of deformation and fatigue degradation. Each combines in a different manner the degradation associated with slip-plane sliding, grain-boundary sliding, migration, cavitation, void development and environmental interaction; hence the approach is useful in delineating the relative importance of these mechanisms in the different loadings. Micromechanistic results are shown for a number of materials, including 316 SS, wrought heat resistant alloys, several nickel-base superalloys, and a tantalum base alloy, T-111. Although there is a commonality of basic behavior, the differences are useful in delineation several important principles of interpretation. Some quantitative results are presented for 316 SS, involving crack initiation and early crack growth, as well as the interaction of low-cycle fatigue with high-cycle fatigue.

M.G.

N83-34351*# National Aeronautics and Space Administration. Lewis Research Center, Cleveland, Ohio.
NONLINEAR CONSTITUTIVE RELATIONS FOR HIGH TEMPERATURE APPLICATIONS
 Mar. 1983 360 p refs Symp. held in Akron, Ohio, 19-20 May 1982; sponsored by Akron Univ.
 (NASA-CP-2271; E-1541; NAS 1.55:2271) Avail: NTIS HC A16/MF A01 CSCL 20K

The topics of discussion addressed were material behavior, design analysis, deformation kinetics, metallurgical characterization, mechanical subelement models, stress analysis, fracture mechanics, viscoplasticity, and thermal loading.

N83-34353*# National Aeronautics and Space Administration. Lewis Research Center, Cleveland, Ohio.

TENSILE AND COMPRESSIVE CONSTITUTIVE RESPONSE OF 316 STAINLESS STEEL AT ELEVATED TEMPERATURES
 S. S. MANSON, U. MURALIDHARAN, and G. R. HALFORD *In its* Nonlinear Constitutive Relations for High Temp. Appl. p 13-42
 Mar. 1983 refs Prepared in cooperation with Case Western Reserve Univ.

(Contract NAG3-46)

Avail: NTIS HC A16/MF A01 CSCL 20K

Creep rate in compression is lower by factors of 2 to 10 than in tension if the microstructure of the two specimens is the same and are tested at equal temperatures and equal but opposite stresses. Such behavior is characteristic for monotonic creep and conditions involving cyclic creep. In the latter case creep rate in both tension and compression progressively increases from cycle to cycle, rendering questionable the possibility of expressing a time stabilized constitutive relationship. The difference in creep rates in tension and compression is considerably reduced if the tension specimen is first subjected to cycles of tensile creep (reversed by compressive plasticity), while the compression specimen is first subjected to cycles of compressive creep (reversed by tensile plasticity). In both cases, the test temperature is the same and the stresses are equal and opposite. Such reduction is a reflection of differences in microstructure of the specimens resulting from different prior mechanical history.

Author

N83-34355*# Michigan State Univ., East Lansing.
EXPERIMENTAL VERIFICATION OF THE NUMBER RELATION AT ROOM AND ELEVATED TEMPERATURES

L. J. LUCAS and J. F. MARTIN *In* NASA. Lewis Research Center Nonlinear Constitutive Relations for High Temp. Appl. p 47-68 Mar. 1983 refs
 (Contract NAG3-51)

Avail: NTIS HC A16/MF A01 CSCL 20K

The accuracy of the Neuber equation for predicting notch root stress-strain behavior at room temperature and at 650 C was experimentally investigated. Strains on notched specimens were measured with a non-contacting, interferometric technique and stresses were simulated with smooth specimens. Predictions of notch root stress-strain response were made from the Neuber Equation and smooth specimen behavior. Neuber predictions gave very accurate results at room temperature. However, the predicted interaction of creep and stress relaxation differed from experimentally measured behavior at 650 C.

Author

N83-34357*# National Aeronautics and Space Administration. Lewis Research Center, Cleveland, Ohio.

EVALUATION OF INELASTIC CONSTITUTIVE MODELS FOR NONLINEAR STRUCTURAL ANALYSIS

A. KAUFMAN *In its* Nonlinear Constitutive Relations for High Temp. Appl. p 89-106 Mar. 1983 refs
 Avail: NTIS HC A16/MF A01 CSCL 20K

The influence of inelastic material models on computed stress-strain states, and therefore predicted lives, was studied for thermomechanically loaded structures. Nonlinear structural analyses were performed on a fatigue specimen which was subjected to thermal cycling in fluidized beds and on a mechanically load cycled benchmark notch specimen. Four incremental plasticity creep models (isotropic, kinematic, combined isotropic-kinematic, combined plus transient creep) were exercised. Of the plasticity models, kinematic hardening gave results most consistent with experimental observations. Life predictions using the computed strain histories at the critical location with a Strainrange Partitioning approach considerably overpredicted the crack initiation life of the thermal fatigue specimen.

Author

N83-34359*# Northwestern Univ., Evanston, Ill.
MICROMECHANICALLY BASED CONSTITUTIVE RELATIONS FOR POLYCRYSTALLINE SOLIDS

S. NEMAT-NASSER and T. IWAKUMA /in NASA. Lewis Research Center Nonlinear Constitutive Relations for High Temp. Appl. p 113-136 Mar. 1983 refs
 (Contract NAG3-134)

Avail: NTIS HC A16/MF A01 CSCL 20K

A basic method to estimate the overall mechanical response of solids which contain periodically distributed defects is presented. The method estimates the shape and growth pattern of voids periodically distributed over the grain boundaries in a viscous matrix. The relaxed moduli are obtained for a polycrystalline solid that undergoes relaxation by grain boundary sliding which accounts for the interaction effects. The overall inelastic nonlinear response at elevated temperatures in terms of a model which considers nonlinear power law creep within the grains, and linear viscous flow in the grain boundaries is discussed. E.A.K.

N83-34369*# Massachusetts Inst. of Tech., Cambridge.
TIME-INDEPENDENT ANISOTROPIC PLASTIC BEHAVIOR BY MECHANICAL SUBELEMENT MODELS

T. H. H. PIAN /in NASA. Lewis Research Center Nonlinear Constitutive Relations for High Temp. Appl. p 283-300 Mar. 1983 refs

(Contract NAG3-33)

Avail: NTIS HC A16/MF A01 CSCL 20K

The paper describes a procedure for modelling the anisotropic elastic-plastic behavior of metals in plane stress state by the mechanical sub-layer model. In this model the stress-strain curves along the longitudinal and transverse directions are represented by short smooth segments which are considered as piecewise linear for simplicity. The model is incorporated in a finite element analysis program which is based on the assumed stress hybrid element and the iscoplasticity-theory. Author

N83-34370*# Akron Univ., Ohio.
CONSTRAINED SELF-ADAPTIVE SOLUTIONS PROCEDURES FOR STRUCTURE SUBJECT TO HIGH TEMPERATURE ELASTIC-PLASTIC CREEP EFFECTS

J. PADOVAN and S. TOVICHAKCHAIKUL /in NASA. Lewis Research Center Nonlinear Constitutive Relations for High Temp. Appl. p 301-304 Mar. 1983 refs

(Contract NAG3-54)

Avail: NTIS HC A16/MF A01 CSCL 20K

This paper will develop a new solution strategy which can handle elastic-plastic-creep problems in an inherently stable manner. This is achieved by introducing a new constrained time stepping algorithm which will enable the solution of creep initiated pre/postbuckling behavior where indefinite tangent stiffnesses are encountered. Due to the generality of the scheme, both monotone and cyclic loading histories can be handled. The presentation will give a thorough overview of current solution schemes and their short comings, the development of constrained time stepping algorithms as well as illustrate the results of several numerical experiments which benchmark the new procedure. B.W.

N83-34371*# Georgia Inst. of Tech., Atlanta.
STRESS AND FRACTURE ANALYSES UNDER ELASTIC-PLASTIC CREEP CONDITIONS: SOME BASIC DEVELOPMENTS AND COMPUTATIONAL APPROACHES

K. W. REED, R. B. STONESIFER, and S. N. ATLURI /in NASA. Lewis Research Center Nonlinear Constitutive Relations for High Temp. Appl. p 305-366 Mar. 1983 refs

(Contract NAG3-38)

Avail: NTIS HC A16/MF A01 CSCL 20K

A new hybrid-stress finite element algorithm, suitable for analyses of large quasi-static deformations of inelastic solids, is presented. Principal variables in the formulation are the nominal stress-rate and spin. A such, a consistent reformulation of the constitutive equation is necessary, and is discussed. The finite element equations give rise to an initial value problem. Time integration has been accomplished by Euler and Runge-Kutta schemes and

the superior accuracy of the higher order schemes is noted. In the course of integration of stress in time, it has been demonstrated that classical schemes such as Euler's and Runge-Kutta may lead to strong frame-dependence. As a remedy, modified integration schemes are proposed and the potential of the new schemes for suppressing frame dependence of numerically integrated stress is demonstrated. The topic of the development of valid creep fracture criteria is also addressed. B.W.

N83-34372*# National Aeronautics and Space Administration. Lewis Research Center, Cleveland, Ohio.
SIMPLIFIED METHOD FOR NONLINEAR STRUCTURAL ANALYSIS

A. KAUFMAN Sep. 1983 15 p refs

(NASA-TP-2208; E-1646; NAS 1.60:2208) Avail: NTIS HC

A02/MF A01 CSCL 20K

A simplified inelastic analysis computer program was developed for predicting the stress-strain history of a thermomechanically cycled structure from an elastic solution. The program uses an iterative and incremental procedure to estimate the plastic strains from the material stress-strain properties and a simulated plasticity hardening model. The simplified method was exercised on a number of problems involving uniaxial and multiaxial loading, isothermal and nonisothermal conditions, and different materials and plasticity models. Good agreement was found between these analytical results and nonlinear finite element solutions for these problems. The simplified analysis program used less than 1 percent of the CPU time required for a nonlinear finite element analysis. Author

N83-34373*# National Aeronautics and Space Administration. Lewis Research Center, Cleveland, Ohio.

A SOLUTION PROCEDURE FOR BEHAVIOR OF THICK PLATES ON A NONLINEAR FOUNDATION AND POSTBUCKLING BEHAVIOR OF LONG PLATES

M. STEIN and P. A. STEIN Sep. 1978 40 p refs

(Contract NCC1-15)

(NASA-TP-2174; L-15587; NAS 1.60:2174) Avail: NTIS HC

A03/MF A01 CSCL 20K

Approximate solutions for three nonlinear orthotropic plate problems are presented: (1) a thick plate attached to a pad having nonlinear material properties which, in turn, is attached to a substructure which is then deformed; (2) a long plate loaded in inplane longitudinal compression beyond its buckling load; and (3) a long plate loaded in inplane shear beyond its buckling load. For all three problems, the two dimensional plate equations are reduced to one dimensional equations in the y-direction by using a one dimensional trigonometric approximation in the x-direction. Each problem uses different trigonometric terms. Solutions are obtained using an existing algorithm for simultaneous, first order, nonlinear, ordinary differential equations subject to two point boundary conditions. Ordinary differential equations are derived to determine the variable coefficients of the trigonometric terms. E.A.K.

N83-35412*# National Aeronautics and Space Administration. Lewis Research Center, Cleveland, Ohio.

THE STRUCTURAL RESPONSE OF A RAIL ACCELERATOR

S. Y. WANG 1983 15 p refs Presented at the 2nd Symp. on Electromagnetic Launch Technol., Boston, 1-14 Oct. 1983; sponsored by IEEE

(NASA-TM-83491; E-1820; NAS 1.15:83491) Avail: NTIS HC

A02/MF A01 CSCL 20G

The transient response of a 0.4 by 0.6 cm rectangular bore rail accelerator was analyzed by a three dimensional finite element code. The copper rail deflected to a peak value of 0.08 mm in compression and then oscillated at an amplitude of 0.02 mm. Simultaneously the insulating side wall of glass fabric base, epoxy resin laminate (G-10) was compressed to a peak value of 0.13 mm and rebounded to a steady state in extension. Projectile pinch or blowby due to the rail extension or compression, respectively, can be identified by examining the time history of the rail displacement. The effect of blowby was most significant at the side wall characterized by mm size displacement in compression. Dynamic stress calculations indicate that the G-10 supporting

material behind the rail is subjected to over 21 MPa at which the G-10 could fail if the laminate was not carefully oriented. Results for a polycarbonate resin (Lexan) side wall show much larger displacements and stresses than for G-10. The tradeoff between the transparency of Lexan and the mechanical strength of G-10 for sidewall material is obvious. Displacement calculations from the modal method are smaller than the results from the direct integration method by almost an order of magnitude, because the high frequency effect is neglected. E.A.K.

N83-35413*# National Aeronautics and Space Administration. Lewis Research Center, Cleveland, Ohio.

ANALYSIS OF AN EXTERNALLY RADially CRACKED RING SEGMENT SUBJECT TO THREE-POINT RADIAL LOADING

B. GROSS, J. E. SRAWLWY, and J. L. SHANNON, JR. 1983 12 p refs Presented at 16th Symp. on Fracture Mech., Columbus, Ohio, 15-17 Aug. 1983; sponsored by Battelle Columbus Labs. and ASTM

(NASA-TM-83482; E-1804; NAS 1.15:83482) Avail: NTIS HC A02/MF A01 CSCL 20K

The boundary collocation method was used to generate Mode 1 stress intensity and crack mouth opening displacement coefficients for externally radially cracked ring segments subjected to three point radial loading. Numerical results were obtained for ring segment outer-to-inner radius ratios ($R_{sub o}/R_{sub i}$) ranging from 1.10 to 2.50 and crack length to segment width ratios (a/W) ranging from 0.1 to 0.8. Stress intensity and crack mouth displacement coefficients were found to depend on the ratios $R_{sub o}/R_{sub i}$ and a/W as well as the included angle between the directions of the reaction forces. Author

N84-10612*# Dayton Univ., Ohio. Aerospace Mechanics Div. **A TOTAL LIFE PREDICTION MODEL FOR STRESS CONCENTRATION SITES Final Report**

G. A. HARTMAN and D. S. DAWICKE Sep. 1983 33 p refs (Contract NAG3-246)

(NASA-CR-168225; NAS 1.26:168225; UDR-TR-83-57) Avail: NTIS HC A03/MF A01 CSCL 20K

Fatigue crack growth tests were performed on center crack panels and radial crack hole samples. The data were reduced and correlated with the elastic parameter K taking into account finite width and corner crack corrections. The anomalous behavior normally associated with short cracks was not observed. Total life estimates for notches were made by coupling an initiation life estimate with a propagation life estimate. Author

N84-10613*# United Technologies Research Center, East Hartford, Conn.

RESEARCH AND DEVELOPMENT PROGRAM FOR THE DEVELOPMENT OF ADVANCED TIME-TEMPERATURE DEPENDENT CONSTITUTIVE RELATIONSHIPS. VOLUME 1: THEORETICAL DISCUSSION Final Report

B. N. CASSENTI Jul. 1983 127 p refs

(Contract NAS3-23273) (NASA-CR-168191-VOL-1; NAS 1.26:168191-VOL-1; R83-956077-1) Avail: NTIS HC A07/MF A01

The results of a 10-month research and development program for the development of advanced time-temperature constitutive relationships are presented. The program included (1) the effect of rate of change of temperature, (2) the development of a term to include time independent effects, and (3) improvements in computational efficiency. It was shown that rate of change of temperature could have a substantial effect on the predicted material response. A modification to include time-independent effects, applicable to many viscoplastic constitutive theories, was shown to reduce to classical plasticity. The computation time can be reduced by a factor of two if self-adaptive integration is used when compared to an integration using ordinary forward differences. During the course of the investigation, it was demonstrated that the most important single factor affecting the theoretical accuracy was the choice of material parameters. Author

N84-10614*# United Technologies Research Center, East Hartford, Conn.

RESEARCH AND DEVELOPMENT PROGRAM FOR THE DEVELOPMENT OF ADVANCED TIME-TEMPERATURE DEPENDENT CONSTITUTIVE RELATIONSHIPS. VOLUME 2: PROGRAMMING MANUAL Final Report

B. N. CASSENTI Jul. 1983 58 p refs

(Contract NAS3-23273) (NASA-CR-168191-VOL-2; NAS 1.26:168191-VOL-2; R83-956077-2) Avail: NTIS HC A04/MF A01

The results of a 10-month research and development program for nonlinear structural modeling with advanced time-temperature constitutive relationships are presented. The implementation of the theory in the MARC nonlinear finite element code is discussed, and instructions for the computational application of the theory are provided. Author

N84-11512*# National Aeronautics and Space Administration. Lewis Research Center, Cleveland, Ohio.

WIDE RANGE WEIGHT FUNCTIONS FOR THE STRIP WITH A SINGLE EDGE CRACK

T. W. ORANGE 1982 12 p refs Presented at the 16th Natl. Symp. on Fracture Mech., Columbus, Ohio, 15-18 Aug. 1983; sponsored by the Am. Soc. for Testing and Mater.

(NASA-TM-83478; E-1794; NAS 1.15:83478) Avail: NTIS HC A02/MF A01 CSCL 20K

A closed form expression for the weight function for a strip with a single edge crack is presented. The expression is valid for relative crack lengths from zero to unity. It is based on the assumption that the shape of an opened edge crack can be approximated by a conic section. The results agree well with published values for weight functions, stress intensity factors, and crack mouth opening displacements. S.L.

N84-11513*# Case Western Reserve Univ., Cleveland, Ohio. **EFFECT OF CRACK CURVATURE ON STRESS INTENSITY FACTORS FOR ASTM STANDARD COMPACT TENSION SPECIMENS Final Report**

J. ALAM and A. MENDELSON Oct. 1983 19 p refs (Contract NSG-3251)

(NASA-CR-168280; NAS 1.26:168280) Avail: NTIS HC A02/MF A01 CSCL 20K

The stress intensity factors (SIF) are calculated using the method of lines for the compact tension specimen in tensile and shear loading for curved crack fronts. For the purely elastic case, it was found that as the crack front curvature increases, the SIF value at the center of the specimen decreases while increasing at the surface. For the higher values of crack front curvatures, the maximum value of the SIF occurs at an interior point located adjacent to the surface. A thickness average SIF was computed for parabolically applied shear loading. These results were used to assess the requirements of ASTM standards E399-71 and E399-81 on the shape of crack fronts. The SIF is assumed to reflect the average stress environment near the crack edge. Author

N84-11514*# Textron Bell Aerospace Co., Buffalo, N. Y. **FORCED VIBRATION ANALYSIS OF ROTATING CYCLIC STRUCTURES IN NASTRAN Final Report**

V. ELCHURI, A. M. GALLO, and S. C. SKALSKI Dec. 1981 176 p

(Contract NAS3-22533) (NASA-CR-165429; NAS 1.26:165429; D2536-941007) Avail: NTIS HC A09/MF A01 CSCL 20K

A new capability was added to the general purpose finite element program NASTRAN Level 17.7 to conduct forced vibration analysis of tuned cyclic structures rotating about their axis of symmetry. The effects of Coriolis and centripetal accelerations together with those due to linear acceleration of the axis of rotation were included. The theoretical, user's, programmer's and demonstration manuals for this new capability are presented. Author

N84-11515*# Textron Bell Aerospace Co., Buffalo, N. Y.
FINITE ELEMENT FORCED VIBRATION ANALYSIS OF ROTATING CYCLIC STRUCTURES Final Technical Report
 V. ELCHURI and G. C. C. SMITH Dec. 1981 73 p refs
 (Contract NAS3-22533)
 (NASA-CR-165430; NAS 1.26:165430; D2536-941008) Avail: NTIS HC A04/MF A01 CSCL 20K

A capability was added to the general purpose finite element program NASTRAN Level 17.7 to conduct forced vibration analysis of tuned cyclic structures rotating about their axes of symmetry. The effects of Coriolis and centripetal accelerations together with those due to linear acceleration of the axis of rotation were included. The theoretical development of this capability is presented. S.L.

N84-12530*# United Technologies Research Center, East Hartford, Conn.
AEROELASTIC ANALYSIS FOR PROPELLERS - MATHEMATICAL FORMULATIONS AND PROGRAM USER'S MANUAL Final Report
 R. L. BIELAWA, S. A. JOHNSON, R. M. CHI, and S. T. GANGWANI Washington NASA Dec. 1983 255 p refs
 (Contract NAS3-22753)
 (NASA-CR-3729; NAS 1.26:3729; UTRC83-6) Avail: NTIS HC A12/MF A01 CSCL 20K

Mathematical development is presented for a specialized propeller dedicated version of the G400 rotor aeroelastic analysis. The G400PROP analysis simulates aeroelastic characteristics particular to propellers such as structural sweep, aerodynamic sweep and high subsonic unsteady airloads (both stalled and unstalled). Formulations are presented for these expanded propeller related methodologies. Results of limited application of the analysis to realistic blade configurations and operating conditions which include stable and unstable stall flutter test conditions are given. Sections included for enhanced program user efficiency and expanded utilization include descriptions of: (1) the structuring of the G400PROP FORTRAN coding; (2) the required input data; and (3) the output results. General information to facilitate operation and improve efficiency is also provided. Author

N84-13610*# National Aeronautics and Space Administration. Lewis Research Center, Cleveland, Ohio.
AN IMPROVED FINITE-DIFFERENCE ANALYSIS OF UNCOUPLED VIBRATIONS OF TAPERED CANTILEVER BEAMS
 K. B. SUBRAHMANYAM (NBKR Inst. of Science and Technology) and K. R. V. KAZA Sep. 1983 39 p refs
 (NASA-TM-83495; E-1828; NAS 1.15:83495) Avail: NTIS HC A03/MF A01 CSCL 20K

An improved finite difference procedure for determining the natural frequencies and mode shapes of tapered cantilever beams undergoing uncoupled vibrations is presented. Boundary conditions are derived in the form of simple recursive relations involving the second order central differences. Results obtained by using the conventional first order central differences and the present second order central differences are compared, and it is observed that the present second order scheme is more efficient than the conventional approach. An important advantage offered by the present approach is that the results converge to exact values rapidly, and thus the extrapolation of the results is not necessary. Consequently, the basic handicap with the classical finite difference method of solution that requires the Richardson's extrapolation procedure is eliminated. Furthermore, for the cases considered herein, the present approach produces consistent lower bound solutions. Author

N84-14541*# National Aeronautics and Space Administration. Lewis Research Center, Cleveland, Ohio.
COMPLEXITIES OF HIGH TEMPERATURE METAL FATIGUE: SOME STEPS TOWARD UNDERSTANDING
 S. S. MANSON and G. R. HALFORD 1983 47 p refs
 Presented at the 25th Ann. Conf. on Aeronautics and Astronautics, Haifa, Israel, 23-25 Feb. 1983
 (NASA-TM-83507; E-1852; NAS 1.15:83507) Avail: NTIS HC A03/MF A01 CSCL 20K

After pointing out many of the complexities that attend high temperature metal fatigue beyond those already studied in the sub-creep range, a description of the micromechanisms of deformation and fracture is presented for several classes of materials that were studied over the past dozen years. Strainrange Partitioning (SRP) is used as a framework for interpreting the results. Several generic types of behavior were observed with regard both to deformation and fracture and each is discussed in the context of the micromechanisms involved. Treatment of cumulative fatigue damage and the possibility of "healing" of damage in successive loading loops, has led to a new interpretation of the Interaction Damage Rule of SRP. Using the concept of "equivalent micromechanistic damage" -- that the same damage on a microscopic scale is induced if the same hysteresis loops are generated, element for element -- it turns out the Interaction Damage Rule essentially compounds a number of variants of hysteresis loops, all of which have the same damage according to SRP concepts, into a set of loops each containing only one of the generic SRP strainranges. Thus the damage associated with complex loops comprising several types of strainrange is analyzed by considering a combination of loops each containing only one type of strainrange. This concept is expanded to show how several independent loops can combine to "heal" creep damage in a complex loading history. Author

N84-14542*# National Aeronautics and Space Administration. Lewis Research Center, Cleveland, Ohio.
A SIMPLIFIED METHOD FOR ELASTIC-PLASTIC-CREEP STRUCTURAL ANALYSIS
 A. KAUFMAN 1984 19 p refs Proposed for presentation at the 29th Ann. Intern. Gas Turbine Conf., Amsterdam, 3-7 Jun. 1984; sponsored by ASME
 (NASA-TM-83509; E-1855-1; NAS 1.15:83509) Avail: NTIS HC A02/MF A01 CSCL 20K

A simplified inelastic analysis computer program (ANSYPM) was developed for predicting the stress-strain history at the critical location of a thermomechanically cycled structure from an elastic solution. The program uses an iterative and incremental procedure to estimate the plastic strains from the material stress-strain properties and a plasticity hardening model. Creep effects are calculated on the basis of stress relaxation at constant strain, creep at constant stress or a combination of stress relaxation and creep accumulation. The simplified method was exercised on a number of problems involving uniaxial and multiaxial loading, isothermal and nonisothermal conditions, dwell times at various points in the cycles, different materials and kinematic hardening. Good agreement was found between these analytical results and nonlinear finite element solutions for these problems. The simplified analysis program used less than 1 percent of the CPU time required for a nonlinear finite element analysis. Author

N84-15589*# Kansas Univ., Lawrence. Structural Engineering and Engineering Materials.
THEORETICAL AND SOFTWARE CONSIDERATIONS FOR NONLINEAR DYNAMIC ANALYSIS Interim Report
 R. J. SCHMIDT and R. H. DODDS, JR. Feb. 1983 299 p refs
 (Contract NAG3-32)
 (NASA-CR-174504; NAS 1.26:174504; SM-8) Avail: NTIS HC A13/MF A01 CSCL 20K

In the finite element method for structural analysis, it is generally necessary to discretize the structural model into a very large number of elements to accurately evaluate displacements, strains, and stresses. As the complexity of the model increases, the number of degrees of freedom can easily exceed the capacity of

present-day software system. Improvements of structural analysis software including more efficient use of existing hardware and improved structural modeling techniques are discussed. One modeling technique that is used successfully in static linear and nonlinear analysis is multilevel substructuring. This research extends the use of multilevel substructure modeling to include dynamic analysis and defines the requirements for a general purpose software system capable of efficient nonlinear dynamic analysis. The multilevel substructuring technique is presented, the analytical formulations and computational procedures for dynamic analysis and nonlinear mechanics are reviewed, and an approach to the design and implementation of a general purpose structural software system is presented. E.A.K.

N84-16587*# National Aeronautics and Space Administration. Lewis Research Center, Cleveland, Ohio.

FLUTTER OF SWEEPED FAN BLADES

R. E. KIELB and K. R. V. KAZA 1984 12 p refs Proposed for presentation at the 29th Intern. Gas Turbine Conf., Amsterdam, 3-7 Jun. 1984; sponsored by ASME (NASA-TM-83547; E-1921; NAS 1.15:83547) Avail: NTIS HC A02/MF A01 CSCL 20K

The effect of sweep on fan blade flutter is studied by applying the analytical methods developed for aeroelastic analysis of advance turboprops. Two methods are used. The first method utilizes an approximate structural model in which the blade is represented by a swept, nonuniform beam. The second method utilizes a finite element technique to conduct modal flutter analysis. For both methods the unsteady aerodynamic loads are calculated using two dimensional cascade theories which are modified to account for sweep. An advanced fan stage is analyzed with 0, 15 and 30 degrees of sweep. It is shown that sweep has a beneficial effect on predominantly torsional flutter and a detrimental effect on predominantly bending flutter. This detrimental effect is shown to be significantly destabilizing for 30 degrees of sweep. M.G.

N84-16588*# National Aeronautics and Space Administration. Lewis Research Center, Cleveland, Ohio.

IMPROVED FINITE-DIFFERENCE VIBRATION ANALYSIS OF PRETWISTED, TAPERED BEAMS

K. B. SUBRAHMANYAM and K. R. V. KAZA 1984 13 p refs To be presented at the Southeastern Conf. on Theoretical and Appl. Mech. (SECTAM 12), Pine Mountain, Ga., 10-11 May 1984 (NASA-TM-83549; NAS 1.15:83549; E-1923) Avail: NTIS HC A02/MF A01 CSCL 20K

An improved finite difference procedure based upon second order central differences is developed. Several difficulties encountered in earlier works with fictitious stations that arise in using second order central differences, are eliminated by developing certain recursive relations. The need for forward or backward differences at the beam boundaries or other similar procedures is eliminated in the present theory. By using this improved theory, the vibration characteristics of pretwisted and tapered beams are calculated. Results of the second order theory are compared with published theoretical and experimental results and are found to be in good agreement. The present method generally produces close lower bound solutions and shows fast convergence. Thus, extrapolation procedures that are customary with first order finite-difference methods are unnecessary. Furthermore, the computational time and effort needed for this improved method are almost the same as required for the conventional first order finite-difference approach. M.G.

N84-16589*# National Aeronautics and Space Administration. Lewis Research Center, Cleveland, Ohio.

BENDING FATIGUE OF ELECTRON-BEAM-WELDED FOILS. APPLICATION TO A HYDRODYNAMIC AIR BEARING IN THE CHRYSLER/DOE UPGRADED AUTOMOTIVE GAS TURBINE ENGINE Final Report

J. F. SALTSMAN and G. R. HALFORD Jan. 1984 27 p refs (Contract DE-AI01-77CS-51040) (NASA-TM-83539; DOE/NASA/51040-51; E-1910; NAS 1.15:83539) Avail: NTIS HC A03/MF A01 CSCL 20K

A hydrodynamic air bearing with a compliant surface is used in the gas generator of an upgraded automotive gas turbine engine. In the prototype design, the compliant surface is a thin foil spot welded at one end to the bearing cartridge. During operation, the foil failed along the line of spot welds which acted as a series of stress concentrators. Because of its higher degree of geometric uniformity, electron beam welding of the foil was selected as an alternative to spot welding. Room temperature bending fatigue tests were conducted to determine the fatigue resistance of the electron beam welded foils. Equations were determined relating cycles to crack initiation and cycles to failure to nominal total strain range. A scaling procedure is presented for estimating the reduction in cyclic life when the foil is at its normal operating temperature of 260 C (500 F). S.L.

N84-18683*# National Aeronautics and Space Administration. Lewis Research Center, Cleveland, Ohio.

ENGINE CYCLIC DURABILITY BY ANALYSIS AND MATERIAL TESTING

A. KAUFMAN and G. R. HALFORD 1983 19 p refs To be presented at the 61st Meeting of the Propulsion and Energetics Panel, Lisse, Netherlands, 30 May - 1 Jun. 1984; sponsored by AGARD (NASA-TM-83577; E-1964; NAS 1.15:83577) Avail: NTIS HC A02/MF A01 CSCL 20K

The problem of calculating turbine engine component durability is addressed. Nonlinear, finite-element structural analyses, cyclic constitutive behavior models, and an advanced creep-fatigue life prediction method called strainrange partitioning were assessed for their applicability to the solution of durability problems in hot-section components of gas turbine engines. Three different component or subcomponent geometries are examined: a stress concentration in a turbine disk; a louver lip of a half-scale combustor liner; and a squealer tip of a first-stage high-pressure turbine blade. Cyclic structural analyses were performed for all three problems. The computed strain-temperature histories at the critical locations of the combustor linear and turbine blade components were imposed on smooth specimens in uniaxial, strain-controlled, thermomechanical fatigue tests to evaluate the structural and life analysis methods. Author

N84-19925*# Arizona Univ., Tucson. Dept. of Aerospace and Mechanical Engineering.

CREEP-RUPTURE RELIABILITY ANALYSIS Final Report

A. PERALTA-DURAN and P. H. WIRSCHING Washington NASA Mar. 1984 31 p refs (Contract NAG3-41) (NASA-CR-3790; E-1982; NAS 1.26:3790) Avail: NTIS HC A03/MF A01 CSCL 20K

A probabilistic approach to the correlation and extrapolation of creep-rupture data is presented. Time temperature parameters (TTP) are used to correlate the data, and an analytical expression for the master curve is developed. The expression provides a simple model for the statistical distribution of strength and fits neatly into a probabilistic design format. The analysis focuses on the Larson-Miller and on the Manson-Haferd parameters, but it can be applied to any of the TTP's. A method is developed for evaluating material dependent constants for TTP's. It is shown that optimized constants can provide a significant improvement in the correlation of the data, thereby reducing modelling error. Attempts were made to quantify the performance of the proposed method in predicting long term behavior. Uncertainty in predicting long term behavior from short term tests was derived for several

sets of data. Examples are presented which illustrate the theory and demonstrate the application of state of the art reliability methods to the design of components under creep. Author

N84-19927*# Akron Univ., Ohio. Dept. of Mechanical Engineering.

EXPERIMENTAL STUDY OF UNCENTRALIZED SQUEEZE FILM DAMPERS

R. D. QUINN Dec. 1983 127 p refs
(Contract NSG-3283; NAG3-50)
(NASA-CR-168317; NAS 1.26:168317; NAUFP-202-2) Avail:
NTIS HC A07/MF A01 CSCL 20K

The vibration response of a rotor system supported by a squeeze film damper (SFD) was experimentally investigated in order to provide experimental data in support of the Rotor/Stator Interactive Finite Element theoretical development. Part of the investigation required the designing and building of a rotor/SFD system that could operate with or without end seals in order to accommodate different SFD lengths. SFD variables investigated included clearance, eccentricity mass, fluid pressure, and viscosity and temperature. The results show inlet pressure, viscosity and clearance have significant influence on the damper performance and accompanying rotor response. Author

N84-20878*# National Aeronautics and Space Administration. Lewis Research Center, Cleveland, Ohio.

DEVELOPMENT OF A SIMPLIFIED PROCEDURE FOR CYCLIC STRUCTURAL ANALYSIS

A. KAUFMAN Mar. 1984 20 p refs Proposed for presentation at the 29th ASME Intern. Gas Turbine Conf., Amsterdam, 3-7 Jun. 1984
(NASA-TP-2243; E-1855; NAS 1.60:2243) Avail: NTIS HC A02/MF A01 CSCL 20K

Development was extended of a simplified inelastic analysis computer program (ANSYMP) for predicting the stress-strain history at the critical location of a thermomechanically cycled structure from an elastic solution. The program uses an iterative and incremental procedure to estimate the plastic strains from the material stress-strain properties and a plasticity hardening model. Creep effects can be calculated on the basis of stress relaxation at constant strain, creep at constant stress, or a combination of stress relaxation and creep accumulation. The simplified method was exercised on a number of problems involving uniaxial and multiaxial loading, isothermal and nonisothermal conditions, dwell times at various points in the cycles, different materials, and kinematic hardening. Good agreement was found between these analytical results and nonlinear finite-element solutions for these problems. The simplified analysis program used less than 1 percent of the CPU time required for a nonlinear finite-element analysis. Author

N84-21903*# Toledo Univ., Ohio. Dept. of Civil Engineering.
THERMAL STRESS ANALYSIS FOR A WOOD COMPOSITE BLADE Report, 5 Dec. 1982 - 4 Apr. 1984

K. C. FU and A. HARB 4 Apr. 1984 117 p refs
(Contract NAG3-373)
(NASA-CR-173394; NAS 1.26:173394) Avail: NTIS HC A06/MF A01 CSCL 20K

Heat conduction throughout the blade and the distribution of thermal stresses caused by the temperature distribution were determined for a laminated wood wind turbine blade in both the horizontal and vertical positions. Results show that blade cracking is not due to thermal stresses induced by insulation. A method and practical example of thermal stress analysis for an engineering body of orthotropic materials is presented. A.R.H.

N84-21905*# Connecticut Univ., Storrs. Dept. of Mechanical Engineering.

ELEVATED TEMPERATURE BIAXIAL FATIGUE Semiannual Status Report, 15 Feb. - 15 Aug. 1983

E. H. JORDAN 15 Aug. 1983 21 p
(Contract NAG3-160)
(NASA-CR-173473; NAS 1.26:173473) Avail: NTIS HC A02/MF A01 CSCL 20K

Biaxial fatigue is often encountered in the complex thermo-mechanical loadings present in gas turbine engines. Engine strain histories can involve non-constant temperature, mean stress, creep, environmental effects, both isotropic and anisotropic materials and non-proportional loading. Life prediction for the general case involving all the above factors is not a practicable research project. The current research program is limited to isothermal fatigue at room temperature and 1200 F of Hastalloy-X for both proportional and non-proportional loading. An improved method for predicting the fatigue life and deformation response under biaxial cycle loading is sought. Author

N84-22980*# Case Western Reserve Univ., Cleveland, Ohio. Dept. of Civil Engineering.

CRACK LAYER THEORY

A. CHUDNOVSKY Mar. 1984 43 p refs
(Contract NAG3-23)
(NASA-CR-174634; NAS 1.26:174634) Avail: NTIS HC A03/MF A01 CSCL 20K

A damage parameter is introduced in addition to conventional parameters of continuum mechanics and consider a crack surrounded by an array of microdefects within the continuum mechanics framework. A system consisting of the main crack and surrounding damage is called crack layer (CL). Crack layer propagation is an irreversible process. The general framework of the thermodynamics of irreversible processes are employed to identify the driving forces (causes) and to derive the constitutive equation of CL propagation, that is, the relationship between the rates of the crack growth and damage dissemination from one side and the conjugated thermodynamic forces from another. The proposed law of CL propagation is in good agreement with the experimental data on fatigue CL propagation in various materials. The theory also elaborates material toughness characterization. M.A.C.

N84-23923*# National Aeronautics and Space Administration. Lewis Research Center, Cleveland, Ohio.

VIBRATION AND FLUTTER OF MISTUNED BLADED-DISK ASSEMBLIES

K. R. V. KAZA and R. E. KIELB 1984 17 p refs Presented at the 25th Struct., Dyn. and Mater. Conf., Palm Springs, Calif., 14-16 May 1984; sponsored by the AIAA, ASME, ASCE and AHS
(NASA-TM-83634; E-2074; NAS 1.15:83634; AIAA-84-0991)
Avail: NTIS HC A02/MF A01 CSCL 20K

An analytical model for investigating vibration and flutter of mistuned bladed disk assemblies is presented. This model accounts for elastic, inertial and aerodynamic coupling between bending and torsional motions of each individual blade, elastic and inertial couplings between the blades and the disk, and aerodynamic coupling among the blades. The disk was modeled as a circular plate with constant thickness and each blade was represented by a twisted, slender, straight, nonuniform, elastic beam with a symmetric cross section. The elastic axis, inertia axis, and the tension axis were taken to be noncoincident and the structural warping of the section was explicitly considered. The blade aerodynamic loading in the subsonic and supersonic flow regimes was obtained from two-dimensional unsteady, cascade theories. All the possible standing wave modes of the disk and traveling wave modes of the blades were included. The equations of motion were derived by using the energy method in conjunction with the assumed mode shapes for the disk and the blades. Continuities of displacement and slope at the blade-disk junction were maintained. The equations were solved to investigate the effects of blade-disk coupling and blade frequency mistuning on vibration

39 STRUCTURAL MECHANICS

and flutter. Results showed that the flexibility of practical disks such as those used for current generation turbfans did not have a significant influence on either the tuned or mistuned flutter characteristics. However, the disk flexibility may have a strong influence on some of the system frequencies and on forced response. Author

N84-29247*# National Aeronautics and Space Administration. Lewis Research Center, Cleveland, Ohio.

A COMPUTER PROGRAM FOR PREDICTING NONLINEAR UNIAXIAL MATERIAL RESPONSES USING VISCOPLASTIC MODELS

T. Y. CHANG (Akron Univ., Ohio) and R. L. THOMPSON Jul. 1984 65 p refs
(NASA-TM-83675; E-2120; NAS 1.15:83675) Avail: NTIS HC A04/MF A01 CSCL 20K

A computer program was developed for predicting nonlinear uniaxial material responses using viscoplastic constitutive models. Four specific models, i.e., those due to Miller, Walker, Krieg-Swearengen-Rhode, and Robinson, are included. Any other unified model is easily implemented into the program in the form of subroutines. Analysis features include stress-strain cycling, creep response, stress relaxation, thermomechanical fatigue loop, or any combination of these responses. An outline is given on the theoretical background of uniaxial constitutive models, analysis procedure, and numerical integration methods for solving the nonlinear constitutive equations. In addition, a discussion on the computer program implementation is also given. Finally, seven numerical examples are included to demonstrate the versatility of the computer program developed. Author

N84-29248*# National Aeronautics and Space Administration. Lewis Research Center, Cleveland, Ohio.

MODE 2 FATIGUE CRACK GROWTH SPECIMEN DEVELOPMENT

R. J. BUZZARD, B. GROSS, and J. E. SRAWLEY 1983 18 p refs Presented at the 17th Natl. Symp. on Fracture Mech., Albany, N.Y., 7-9 Aug. 1984; sponsored by Am. Soc. for Testing and Mater.
(NASA-TM-83722; E-2108; NAS 1.15:83722) Avail: NTIS HC A02/MF A01 CSCL 20K

A Mode II test specimen was developed which has potential application in understanding phenomena associated with mixed mode fatigue failures in high performance aircraft engine bearing races. The attributes of the specimen are: it contains one single ended notch, which simplifies data gathering and reduction; the fatigue crack grows in-line with the direction of load application; a single axis test machine is sufficient to perform testing; and the Mode I component is vanishingly small. Author

N84-29252*# Textron Bell Aerospace Co., Buffalo, N. Y. Structural Dynamics.

NASTRAN FORCED VIBRATION ANALYSIS OF ROTATING CYCLIC STRUCTURES Final Report

V. ELCHURI, G. C. C. SMITH, and A. M. GALLO 1983 31 p refs Presented at the ASME Conf. on Mech. Vibration and Noise, Dearborn, Mich., Sep. 1983
(Contract NAS3-22533)

(NASA-CR-173821; NAS 1.26:173821) Avail: NTIS HC A03/MF A01 CSCL 20K

Theoretical aspects of a new capability developed and implemented in NASTRAN level 17.7 to analyze forced vibration of a cyclic structure rotating about its axis of symmetry are presented. Fans, propellers, and bladed shrouded discs of turbomachines are some examples of such structures. The capability includes the effects of Coriolis and centripetal accelerations on the rotating structure which can be loaded with: (1) directly applied loads moving with the structure and (2) inertial loads due to the translational acceleration of the axis of rotation ("base" acceleration). Steady-state sinusoidal or general periodic loads are specified to represent: (1) the physical loads on various segments of the complete structure, or (2) the circumferential harmonic components of the loads in (1). The cyclic symmetry

feature of the rotating structure is used in deriving and solving the equations of forced motion. Consequently, only one of the cyclic sectors is modelled and analyzed using finite elements, yielding substantial savings in the analysis cost. Results, however, are obtained for the entire structure. A tuned twelve bladed disc example is used to demonstrate the various features of the capability. M.G.

N84-30329*# National Aeronautics and Space Administration. Lewis Research Center, Cleveland, Ohio.

IMPROVED METHODS OF VIBRATION ANALYSIS OF PRETWISTED, AIRFOIL BLADES

K. B. SUBRAHMANYAM and K. R. V. KAZA 1984 37 p refs Presented at the 16th Intern. Congr. of Theoretical and Appl. Mech., Lyngby, Denmark, 19-25 Aug. 1984; sponsored by the International Union of Theoretical and Applied Mechanics and the Technical Univ. of Denmark
(NASA-TM-83735; E-2175; NAS 1.15:83735) Avail: NTIS HC A03/MF A01 CSCL 20K

Vibration analysis of pretwisted blades of asymmetric airfoil cross section is performed by using two mixed variational approaches. Numerical results obtained from these two methods are compared to those obtained from an improved finite difference method and also to those given by the ordinary finite difference method. The relative merits, convergence properties and accuracies of all four methods are studied and discussed. The effects of asymmetry and pretwist on natural frequencies and mode shapes are investigated. The improved finite difference method is shown to be far superior to the conventional finite difference method in several respects. Close lower bound solutions are provided by the improved finite difference method for untwisted blades with a relatively coarse mesh while the mixed methods have not indicated any specific bound. Author

N84-31683*# National Aeronautics and Space Administration. Lewis Research Center, Cleveland, Ohio.

NONLINEAR DISPLACEMENT ANALYSIS OF ADVANCED PROPELLER STRUCTURES USING NASTRAN

C. LAWRENCE and R. E. KIELB Aug. 1984 12 p refs
(NASA-TM-83737; E-2222; NAS 1.15:83737) Avail: NTIS HC A02/MF A01 CSCL 20K

The steady state displacements of a rotating advanced turboprop are computed using the geometrically nonlinear capabilities of COSMIC NASTRAN Rigid Format 4 and MSC NASTRAN Solution 64. A description of the modified Newton-Raphson algorithm used by Solution 64 and the iterative scheme used by Rigid Format 4 is provided. A representative advanced turboprop, SR3, was used for the study. Displacements for SR3 are computed for rotational speeds up to 10,000 rpm. The results show Solution 64 to be superior for computing displacements of flexible rotating structures. This is attributed to its ability to update the displacement dependent centrifugal force during the solution process. Author

N84-31685*# Toledo Univ., Ohio. Dept. of Civil Engineering. **THERMAL-STRESS ANALYSIS FOR WOOD COMPOSITE BLADE Report, 5 Dec. 1982 - 4 Apr. 1984**

K. C. FU and A. HARB 20 Jul. 1984 117 p refs
(Contract NAG3-373)
(NASA-CR-173830; NAS 1.26:173830) Avail: NTIS HC A06/MF A01 CSCL 20K

The thermal-stress induced by solar insolation on a wood composite blade of a Mod-OA wind turbine was investigated. The temperature distribution throughout the blade (a heat conduction problem) was analyzed and the thermal-stress distribution of the blades caused by the temperature distribution (a thermal-stress analysis problem) was then determined. The computer programs used for both problems are included along with output examples. A.R.H.

N84-31687*# National Aeronautics and Space Administration. Lewis Research Center, Cleveland, Ohio.

CYCLIC TORSION TESTING

G. E. LEESE Aug. 1984 21 p refs Submitted for publication (NASA-TM-83756; E-2232; NAS 1.15:83756) Avail: NTIS HC A02/MF A01 CSCL 20K

Torsional fatigue testing and data analysis procedures are described. Since there are no standards governing cyclic torsion testing that are generally accepted on a widespread basis by the technical community, the different approaches that dominate current experimental activity, and the ramifications of each are discussed. Particular attention is given to the theoretical and experimental difficulties that have paced refinement and general acceptance of test procedures. Finally, specific quantities and nomenclature modeled after analogous axial fatigue properties are suggested as an effective way to communicate torsional fatigue results until accepted standards are established. Author

N84-31688*# National Aeronautics and Space Administration. Lewis Research Center, Cleveland, Ohio.

NONLINEAR STRUCTURAL ANALYSIS

Washington Jun. 1984 168 p Workshop held in Cleveland, 19-20 Apr. 1983

(NASA-CP-2297; E-1903; NAS 1.55:2297) Avail: NTIS HC A08/MF A01 CSCL 20K

Nonlinear structural analysis techniques for engine structures and components are addressed. The finite element method and boundary element method are discussed in terms of stress and structural analyses of shells, plates, and laminates.

N84-31689*# Textron Bell Aerospace Co., Buffalo, N. Y. **SLAVE FINITE ELEMENTS: THE TEMPORAL ELEMENT APPROACH TO NONLINEAR ANALYSIS**

S. GELLIN /in NASA. Lewis Research Center Nonlinear Struct. Anal. p 1-16 Jun. 1984 refs (Contract NAS3-23279)

Avail: NTIS HC A08/MF A01 CSCL 20K

A formulation method for finite elements in space and time incorporating nonlinear geometric and material behavior is presented. The method uses interpolation polynomials for approximating the behavior of various quantities over the element domain, and only explicit integration over space and time. While applications are general, the plate and shell elements that are currently being programmed are appropriate to model turbine blades, vanes, and combustor liners. Author

N84-31690*# Massachusetts Inst. of Tech., Cambridge. **NEW VARIATIONAL FORMULATIONS OF HYBRID STRESS ELEMENTS**

T. H. H. PIAN, K. SUMIHARA, and D. KANG /in NASA. Lewis Research Center Nonlinear Struct. Anal. p 17-29 Jun. 1984 refs

(Contract NAG3-33)

Avail: NTIS HC A08/MF A01 CSCL 20K

In the variational formulations of finite elements by the Hu-Washizu and Hellinger-Reissner principles the stress equilibrium condition is maintained by the inclusion of internal displacements which function as the Lagrange multipliers for the constraints. These versions permit the use of natural coordinates and the relaxation of the equilibrium conditions and render considerable improvements in the assumed stress hybrid elements. These include the derivation of invariant hybrid elements which possess the ideal qualities such as minimum sensitivity to geometric distortions, minimum number of independent stress parameters, rank sufficient, and ability to represent constant strain states and bending moments. Another application is the formulation of semiLoof thin shell elements which can yield excellent results for many severe test cases because the rigid body nodes, the momentless membrane strains, and the inextensional bending modes are all represented. Author

N84-31692*# Akron Univ., Ohio.

NONLINEAR FINITE ELEMENT ANALYSIS OF SHELLS WITH LARGE ASPECT RATIO

T. Y. CHANG and K. SAWAMIPHAKE /in NASA. Lewis Research Center Nonlinear Struct. Anal. p 45-54 Jun. 1984 refs (Contract NAG3-317)

Avail: NTIS HC A08/MF A01 CSCL 20K

A higher order degenerated shell element with nine nodes was selected for large deformation and post-buckling analysis of thick or thin shells. Elastic-plastic material properties are also included. The post-buckling analysis algorithm is given. Using a square plate, it was demonstrated that the none-node element does not have shear locking effect even if its aspect ratio was increased to the order 10 to the 8th power. Two sample problems are given to illustrate the analysis capability of the shell element. Author

N84-31693*# Akron Univ., Ohio.

SELF-ADAPTIVE SOLUTION STRATEGIES

J. PADOVAN /in NASA. Lewis Research Center Nonlinear Struct. Anal. p 55-63 Jun. 1984 refs

(Contract NAG3-54)

Avail: NTIS HC A08/MF A01 CSCL 20K

The development of enhancements to current generation nonlinear finite element algorithms of the incremental Newton-Raphson type was overviewed. Work was introduced on alternative formulations which lead to improve algorithms that avoid the need for global level updating and inversion. To quantify the enhanced Newton-Raphson scheme and the new alternative algorithm, the results of several benchmarks are presented. Author

N84-31694*# Stanford Univ., Calif.

ELEMENT-BY-ELEMENT SOLUTION PROCEDURES FOR NONLINEAR STRUCTURAL ANALYSIS

T. J. R. HUGHES, J. M. WINGET, and I. LEVIT /in NASA. Lewis Research Center Nonlinear Struct. Anal. p 65-84 Jun. 1984 refs

(Contract NAG3-319)

Avail: NTIS HC A08/MF A01 CSCL 20K

Element-by-element approximate factorization procedures are proposed for solving the large finite element equation systems which arise in nonlinear structural mechanics. Architectural and data base advantages of the present algorithms over traditional direct elimination schemes are noted. Results of calculations suggest considerable potential for the methods described. Author

N84-31695*# Kent State Univ., Ohio. Dept. of Mathematical Sciences.

AUTOMATIC FINITE ELEMENT GENERATORS

P. S. WANG /in NASA. Lewis Research Center Nonlinear Struct. Anal. p 85-94 Jun. 1984 refs

(Contract NAG3-298)

Avail: NTIS HC A08/MF A01 CSCL 20K

The design and implementation of a software system for generating finite elements and related computations are described. Exact symbolic computational techniques are employed to derive strain-displacement matrices and element stiffness matrices. Methods for dealing with the excessive growth of symbolic expressions are discussed. Automatic FORTRAN code generation is described with emphasis on improving the efficiency of the resultant code. Author

N84-31696*# Texas Univ., Austin.

STABILITY AND CONVERGENCE OF UNDERINTEGRATED FINITE ELEMENT APPROXIMATIONS

J. T. ODEN /in NASA. Lewis Research Center Nonlinear Struct. Anal. p 95-103 Jun. 1984 refs

(Contract NAG3-329)

Avail: NTIS HC A08/MF A01 CSCL 20K

The effects of underintegration on the numerical stability and convergence characteristics of certain classes of finite element approximations were analyzed. Particular attention is given to

hourglassing instabilities that arise from underintegrating the stiffness matrix entries and checkerboard instabilities that arise from underintegrating constrain terms such as those arising from incompressibility conditions. A fundamental result reported here is the proof that the fully integrated stiffness is restored in some cases through a post-processing operation. Author

N84-31697*# Georgia Inst. of Tech., Atlanta.
INELASTIC AND DYNAMIC FRACTURE AND STRESS ANALYSES

S. N. ATLURI /In NASA. Lewis Research Center Nonlinear Struct. Anal. p 105-118 Jun. 1984 refs (Contract NAG3-346)

Avail: NTIS HC A08/MF A01 CSCL 20K

Large deformation inelastic stress analysis and inelastic and dynamic crack propagation research work is summarized. The salient topics of interest in engine structure analysis that are discussed herein include: (1) a path-independent integral (T) in inelastic fracture mechanics, (2) analysis of dynamic crack propagation, (3) generalization of constitutive relations of inelasticity for finite deformations, (4) complementary energy approaches in inelastic analyses, and (5) objectivity of time integration schemes in inelastic stress analysis. Author

N84-31699*# National Aeronautics and Space Administration. Lewis Research Center, Cleveland, Ohio.

NONLINEAR ANALYSIS FOR HIGH-TEMPERATURE COMPOSITES: TURBINE BLADES/VANES

D. A. HOPKINS and C. C. CHAMIS /In its Nonlinear Struct. Anal. p 131-147 Jun. 1984 refs

Avail: NTIS HC A08/MF A01 CSCL 20K

An integrated approach to nonlinear analysis of high-temperature composites in turbine blade/vane applications is presented. The overall strategy of this approach and the key elements comprising this approach are summarized. Preliminary results for a tungsten-fiber-reinforced superalloy (TFRS) composite are discussed. Author

N84-31700*# Pratt and Whitney Aircraft, East Hartford, Conn.
THREE-DIMENSIONAL STRESS ANALYSIS USING THE BOUNDARY ELEMENT METHOD

R. B. WILSON and P. K. BANERJEE (State Univ. of New York, Buffalo) /In NASA. Lewis Research Center Nonlinear Struct. Anal. p 149-160 Jun. 1984 refs

(Contract NAS3-23697)

Avail: NTIS HC A08/MF A01 CSCL 20K

The boundary element method is to be extended (as part of the NASA Inelastic Analysis Methods program) to the three-dimensional stress analysis of gas turbine engine hot section components. The analytical basis of the method (as developed in elasticity) is outlined, its numerical implementation is summarized, and the approaches to be followed in extending the method to include inelastic material response indicated. Author

N84-34774*# Case Western Reserve Univ., Cleveland, Ohio. Dept. of Civil Engineering.

ON STRESS ANALYSIS OF A CRACK-LAYER Final Report

A. CHUDNOVSKY, A. DOLGOPOLSKY (Delaware Univ., Newark), and M. KACHANOV (Tufts Univ., Medford, Mass.) Oct. 1984 95 p refs

(Contract NAG3-223)

(NASA-CR-174774; NAS 1.26:174774) Avail: NTIS HC A05/MF A01 CSCL 20K

This work considers the problem of elastic interaction of a macrocrack with an array of microcracks in the vicinity of the macrocrack tip. Using the double layer potential techniques, the solution to the problem within the framework of the plane problem of elastostatics has been obtained. Three particular problems of interest to fracture mechanics have been analyzed. It follows from analysis that microcrack array can either amplify or reduce the resulting stress field of the macrocrack-microcrack array system depending on the array's configuration. Using the obtained elastic solution the energy release rate associated with the translational

motion of the macrocrack-microcrack array system has been evaluated. Author

N85-10384*# Stanford Univ., Calif.

AUGMENTED WEAK FORMS AND ELEMENT-BY-ELEMENT PRECONDITIONERS: EFFICIENT ITERATIVE STRATEGIES FOR STRUCTURAL FINITE ELEMENTS. A PRELIMINARY STUDY

A. MULLER and T. J. R. HUGHES /In NASA. Langley Research Center Res. in Struct. and Dyn., 1984 p 95-109 Oct. 1984 refs

(Contract NAG3-319)

Avail: NTIS HC A18/MF A01 CSCL 20K

A weak formulation in structural analysis that provides well conditioned matrices suitable for iterative solutions is presented. A mixed formulation ensures the proper representation of the problem and the constitutive relations are added in a penalized form. The problem is solved by a double conjugate gradient algorithm combined with an element by element approximate factorization procedure. The double conjugate gradient strategy resembles Uzawa's variable-length type algorithms the main difference is the presence of quadratic terms in the mixed variables. In the case of shear deformable beams these terms ensure that the proper finite thickness solution is obtained. E.A.K.

N85-11380*# Arizona Univ., Tucson. Dept. of Aerospace and Mechanical Engineering.

RELIABILITY CONSIDERATIONS FOR THE TOTAL STRAIN RANGE VERSION OF STRAINRANGE PARTITIONING Final Report

P. H. WIRSCHING and Y. T. WU Sep. 1984 85 p refs

(Contract NAG3-41)

(NASA-CR-174757; NAS 1.26:174757) Avail: NTIS HC A05/MF A01 CSCL 20K

A proposed total strainrange version of strainrange partitioning (SRP) to enhance the manner in which SRP is applied to life prediction is considered with emphasis on how advanced reliability technology can be applied to perform risk analysis and to derive safety check expressions. Uncertainties existing in the design factors associated with life prediction of a component which experiences the combined effects of creep and fatigue can be identified. Examples illustrate how reliability analyses of such a component can be performed when all design factors in the SRP model are random variables reflecting these uncertainties. The Rackwitz-Fiessler and Wu algorithms are used and estimates of the safety index and the probability of failure are demonstrated for a SRP problem. Methods of analysis of creep-fatigue data with emphasis on procedures for producing synoptic statistics are presented. An attempt to demonstrate the importance of the contribution of the uncertainties associated with small sample sizes (fatigue data) to risk estimates is discussed. The procedure for deriving a safety check expression for possible use in a design criteria document is presented. A.R.H.

N85-15184*# National Aeronautics and Space Administration. Lewis Research Center, Cleveland, Ohio.

THE USE OF AN OPTICAL DATA ACQUISITION SYSTEM FOR BLADED DISK VIBRATION ANALYSIS

C. LAWRENCE and E. H. MEYN Dec. 1984 23 p refs (NASA-TM-86891; E-2358; NAS 1.15:86891) Avail: NTIS HC A02/MF A01 CSCL 20K

A new concept in instrumentation was developed by engineers at NASA Lewis Research Center to collect vibration data from multi-bladed rotors. This new concept, known as the optical data acquisition system, uses optical transducers to measure bladed tip deflections by reflection light beams off the tips of the blades as they pass in front of the optical transducer. By using an array of transducers around the perimeter of the rotor, detailed vibration signals can be obtained. In this study, resonant frequencies and mode shapes were determined for a 56 bladed rotor using the optical system. Frequency data from the optical system was also compared to data obtained from strain gauge measurements and finite element analysis and was found to be in good agreement. Author

N85-16205*# National Aeronautics and Space Administration. Lewis Research Center, Cleveland, Ohio.

EXPERIMENTAL COMPLIANCE CALIBRATION OF THE NASA LEWIS RESEARCH CENTER MODE 2 FATIGUE SPECIMEN

R. J. BUZZARD 1985 11 p refs Proposed for presentation at the 18th Natl. Symp. on Fracture Mech., Boulder, Colo., 24-27 Jun. 1985; sponsored by American Society for Testing and Materials

(NASA-TM-86908; E-2398; NAS 1.15:86908) Avail: NTIS HC A02/MF A01 CSCL 20K

Calibration of the mode II aluminum fatigue specimen was performed experimentally to provide displacement and stress intensity coefficients over crack length to specimen width ratios (a/W) of 0.5 to 0.9. Displacements were measured both at the specimen notch mouth and at the intersection of the notch with the centerline of the loading pin holes.

R.S.F.

N85-18375*# National Aeronautics and Space Administration. Lewis Research Center, Cleveland, Ohio.

NASA LEWIS RESEARCH CENTER/UNIVERSITY GRADUATE RESEARCH PROGRAM ON ENGINE STRUCTURES

C. C. CHAMIS 1985 18 p Presented at the 30th Intern. Gas Turbine Conf. and Exhibit, Houston, Tex., 17-21 Mar. 1985; sponsored by ASME

(NASA-TM-86916; E-2393; NAS 1.15:86916) Avail: NTIS HC A02/MF A01 CSCL 20K

NASA Lewis Research Center established a graduate research program in support of the Engine Structures Research activities. This graduate research program focuses mainly on structural and dynamics analyses, computational mechanics, mechanics of composites and structural optimization. The broad objectives of the program, the specific program, the participating universities and the program status are briefly described.

Author

N85-20396*# National Aeronautics and Space Administration. Lewis Research Center, Cleveland, Ohio.

LOCAL STRAIN REDISTRIBUTION CORRECTIONS FOR A SIMPLIFIED INELASTIC ANALYSIS PROCEDURE BASED ON AN ELASTIC FINITE-ELEMENT ANALYSIS

A. KAUFMAN and S. Y. HWANG (South Carolina State Coll., Orangeburg) Mar. 1985 14 p refs To be presented at the 21st AIAA/SAE/ASME Joint Propulsion Conf., Monterey, Calif., 8-11 Jul. 1985

(NASA-TP-2421; E-2373; NAS 1.60:2421) Avail: NTIS HC A02/MF A01 CSCL 20K

Strain redistribution corrections were developed for a simplified inelastic analysis procedure to economically calculate material cyclic response at the critical location of a structure for life prediction purposes. The method was based on the assumption that the plastic region in the structure is local and the total strain history required for input can be defined from elastic finite-element analyses. Cyclic stress-strain behavior was represented by a bilinear kinematic hardening model. The simplified procedure predicts stress-strain response with reasonable accuracy for thermally cycled problems but needs improvement for mechanically load-cycled problems. Neuber-type corrections were derived and incorporated in the simplified procedure to account for local strain redistribution under cyclic mechanical loading. The corrected simplified method was used on a mechanically load-cycled benchmark notched-plate problem. The predicted material response agrees well with the nonlinear finite-element solutions for the problem. The simplified analysis computer program was 0.3% of the central processor unit time required for a nonlinear finite-element analysis.

EAK

N85-21685*# Case Western Reserve Univ., Cleveland, Ohio. Dept. of Civil Engineering.

TRANSLATIONAL AND EXTENSIONAL ENERGY RELEASE RATES (THE J- AND M-INTEGRALS) FOR A CRACK LAYER IN THERMOELASTICITY Final Report

A. CHUDNOVSKY and B. GOMMERSTADT Mar. 1985 9 p refs

(Contract NAG3-223)

(NASA-CR-174872; NAS 1.26:174872) Avail: NTIS HC A02/MF A01 CSCL 20K

A number of papers have been presented on the evaluation of energy release rate for thermoelasticity and corresponding J integral. Two main approaches were developed to treat energy release rate in elasticity. The first is based on direct calculation of the potential energy rate with respect to crack length. The second makes use of Lagrangian formalism. The translational and expansional energy release rates in thermoelasticity are studied by employing the formalism of irreversible thermodynamics and the Crack Layer Approach.

Author

N85-21686*# Pratt and Whitney Aircraft, East Hartford, Conn. Engineering Div.

3-D INELASTIC ANALYSIS METHODS FOR HOT SECTION COMPONENTS (BASE PROGRAM) Annual Status Report, 14 Feb. 1983 - 14 Feb. 1984

R. B. WILSON, M. J. BAK, S. NAKAZAWA, and P. K. BANERJEE Feb. 1984 167 p refs

(Contract NAS3-23697)

(NASA-CR-174700; NAS 1.26:174700; PWA-5940-19; ASR-1)

Avail: NTIS HC A08/MF A01 CSCL 20K

A 3-D inelastic analysis methods program consists of a series of computer codes embodying a progression of mathematical models (mechanics of materials, special finite element, boundary element) for streamlined analysis of combustor liners, turbine blades, and turbine vanes. These models address the effects of high temperatures and thermal/mechanical loadings on the local (stress/strain) and global (dynamics, buckling) structural behavior of the three selected components. These models are used to solve 3-D inelastic problems using linear approximations in the sense that stresses/strains and temperatures in generic modeling regions are linear functions of the spatial coordinates, and solution increments for load, temperature and/or time are extrapolated linearly from previous information. Three linear formulation computer codes, referred to as MOMM (Mechanics of Materials Model), MHOST (MARC-Hot Section Technology), and BEST (Boundary Element Stress Technology), were developed and are described.

Author

N85-21687*# Massachusetts Inst. of Tech., Cambridge. Dept. of Aeronautics and Astronautics.

RECENT ADVANCES IN HYBRID/MIXED FINITE ELEMENTS

T. H. H. PIAN 1985 8 p refs

(Contract NAG3-33)

(NASA-CR-175574; NAS 1.26:175574) Avail: NTIS HC A02/MF A01 CSCL 20K

In formulations of Hybrid/Mixed finite element methods respectively by the Hellinger-Reissner principle and the Hu-Washizu principle, the stress equilibrium equations are brought in as conditions of constraint through the introduction of additional internal displacement parameters. These two approaches are more flexible and have better computing efficiencies. A procedure for the choice of assumed stress terms for 3-D solids is suggested. Example solutions are given for plates and shells using the present formulations and the idea of semiloof elements.

Author

N85-21690*# National Aeronautics and Space Administration. Lewis Research Center, Cleveland, Ohio.

ON LOCAL TOTAL STRAIN REDISTRIBUTION USING A SIMPLIFIED CYCLIC INELASTIC ANALYSIS BASED ON AN ELASTIC SOLUTION

S. Y. HWANG (South Carolina State Coll.) and A. KAUFMAN 1985 16 p refs Proposed for presentation at the 21st Joint Propulsion Conf., Monterey, Calif., 9-11 Jul. 1985; sponsored by the AIAA, SAE and ASME (NASA-TM-86913; E-2406; NAS 1.15:86913) Avail: NTIS HC A02/MF A01 CSCL 20K

Strain redistribution corrections were developed for a simplified inelastic analysis procedure to economically calculate material cyclic response at the critical location of a structure for life prediction purposes. The method was based on the assumption that the plastic region in the structure is local and the total strain history required for input can be defined from elastic finite element analyses. Cyclic stress-strain behavior was represented by a bilinear kinematic hardening model. The simplified procedure has been found to predict stress-strain response with reasonable accuracy for thermally cycled problems but needs improvement for mechanically load cycled problems. This study derived and incorporated Neuber type corrections in the simplified procedure to account for local total strain redistribution under cyclic mechanical loading. The corrected simplified method was exercised on a mechanically load cycled benchmark notched plate problem. Excellent agreement was found between the predicted material response and nonlinear finite element solutions for the problem. The simplified analysis computer program used 0.3 percent of the CPU time required for a nonlinear finite element analysis. Author

N85-21691*# Akron Univ., Ohio. Dept. of Civil Engineering. VISCOPLASTIC CONSTITUTIVE RELATIONSHIPS WITH DEPENDENCE ON THERMOMECHANICAL HISTORY Final Report

D. N. ROBINSON and P. A. BARTOLOTTA Mar. 1985 42 p refs (Contract NAG3-379) (NASA-CR-174836; NAS 1.26:174836) Avail: NTIS HC A03/MF A01 CSCL 20K

Experimental evidence of thermomechanical history dependence in the cyclic hardening behavior of some common high-temperature structural alloys is presented with special emphasis on dynamic metallurgical changes. The inadequacy of formulating nonisothermal constitutive equations solely on the basis of isothermal testing is discussed. A representation of thermoviscoplasticity is proposed that qualitatively accounts for the observed hereditary behavior. This is achieved by formulating the scalar evolutionary equation in an established viscoplasticity theory to reflect thermomechanical path dependence. To assess the importance of accounting for thermomechanical history dependence in practical structural analyses, two qualitative models are specified: (1) formulated as if based entirely on isothermal information; (2) to reflect thermomechanical path dependence using the proposed thermoviscoplastic representation. Predictions of the two models are compared and the impact the calculated differences in deformation behavior may have on subsequent lifetime predictions is discussed. E.A.K.

N85-21720*# Virginia Polytechnic Inst. and State Univ., Blacksburg. Dept. of Engineering Science and Mechanics.

GEOMETRICALLY NONLINEAR ANALYSIS OF LAMINATED ELASTIC STRUCTURES Final Report

J. N. REDDY Nov. 1984 107 p refs (Contract NAG3-208) (NASA-CR-175609; NAS 1.26:175609; PB85-127173; VPI-E-84-36) Avail: NTIS HC A06/MF A01 CSCL 20K

Laminated composite plates and shells that can be used to model automobile bodies, aircraft wings and fuselages, and pressure vessels among many other were analyzed. The finite element method, a numerical technique for engineering analysis of structures, is used to model the geometry and approximate the solution. Various alternative formulations for analyzing laminated

plates and shells are developed and their finite element models are tested for accuracy and economy in computation. These include the shear deformation laminate theory and degenerated 3-D elasticity theory for laminates. GRA

N85-23096*# Massachusetts Inst. of Tech., Cambridge. ON HYBRID AND MIXED FINITE ELEMENT METHODS

T. H. H. PIAN 1981 19 p refs (Contract NAG3-33) (NASA-CR-175551; NAS 1.26:175551) Avail: NTIS HC A02/MF A01 CSCL 20K

Three versions of the assumed stress hybrid model in finite element methods and the corresponding variational principles for the formulation are presented. Examples of rank deficiency for stiffness matrices by the hybrid stress model are given and their corresponding kinematic deformation modes are identified. A discussion of the derivation of general semi-Loof elements for plates and shells by the hybrid stress method is given. It is shown that the equilibrium model by Fraeijs de Veubeke can be derived by the approach of the hybrid stress model as a special case of semi-Loof elements. Author

N85-24338*# National Aeronautics and Space Administration. Lewis Research Center, Cleveland, Ohio.

UNIFIED CONSTITUTIVE MATERIAL MODELS FOR NONLINEAR FINITE-ELEMENT STRUCTURAL ANALYSIS

A. KAUFMAN, J. H. LAFFLEN (General Electric Co., Cincinnati), and U. S. LINDHOLM (Southwest Research Inst., San Antonio) 10 Jul. 1985 16 p refs Proposed for presentation at 21st Joint Propulsion Conf., Monterey, Calif., 8-10 Jul. 1985; sponsored by AIAA, SAE and ASME (NASA-TM-86985; E-2529; NAS 1.15:86985) Avail: NTIS HC A02/MF A01 CSCL 20K

Unified constitutive material models were developed for structural analyses of aircraft gas turbine engine components with particular application to isotropic materials used for high-pressure stage turbine blades and vanes. Forms or combinations of models independently proposed by Bodner and Walker were considered. These theories combine time-dependent and time-independent aspects of inelasticity into a continuous spectrum of behavior. This is in sharp contrast to previous classical approaches that partition inelastic strain into uncoupled plastic and creep components. Predicted stress-strain responses from these models were evaluated against monotonic and cyclic test results for uniaxial specimens of two cast nickel-base alloys, B1900+Hf and Rene' 80. Previously obtained tension-torsion test results for Hastelloy X alloy were used to evaluate multiaxial stress-strain cycle predictions. The unified models, as well as appropriate algorithms for integrating the constitutive equations, were implemented in finite-element computer codes. Author

N85-24339*# National Aeronautics and Space Administration. Lewis Research Center, Cleveland, Ohio.

CYCLIC STRUCTURAL ANALYSES OF ANISOTROPIC TURBINE BLADES FOR REUSABLE SPACE PROPULSION SYSTEMS

J. M. MANDERSCHIED and A. KAUFMAN 12 Apr. 1985 13 p refs Presented at 1985 JANNAF Propulsion Meeting, San Diego, Calif., 9-12 Apr. 1985; sponsored by JANNAF (NASA-TM-86990; E-2534; NAS 1.15:86990) Avail: NTIS HC A02/MF A01 CSCL 20K

Turbine blades for reusable space propulsion systems are subject to severe thermomechanical loading cycles that result in large inelastic strains and very short lives. These components require the use of anisotropic high-temperature alloys to meet the safety and durability requirements of such systems. To assess the effects on blade life of material anisotropy, cyclic structural analyses are being performed for the first stage high-pressure fuel turbopump blade of the space shuttle main engine. The blade alloy is directionally solidified MAR-M 246 alloy. The analyses are based on a typical test stand engine cycle. Stress-strain histories at the airfoil critical location are computed using the MARC nonlinear finite-element computer code. The MARC solutions are compared to cyclic response predictions from a simplified structural

analysis procedure developed at the NASA Lewis Research Center.
Author

N85-25893*# National Aeronautics and Space Administration. Lewis Research Center, Cleveland, Ohio.

VIBRATION AND BUCKLING OF ROTATING, PRETWISTED, PRECONED BEAMS INCLUDING CORIOLIS EFFECTS

K. B. SUBRAHMANYAM and K. R. V. KAZA 1985 21 p refs
Proposed for presentation at the 10th Bien. Design Eng. Conf. and Exhibit on Mech. Vibration and Noise, Cincinnati, 10-13 Sep. 1985; sponsored by ASME
(NASA-TM-87004; E-2310; NAS 1.15:87004) Avail: NTIS HC A02/MF A01 CSCL 20K

The effects of pretwist, precone, setting angle and Coriolis forces on the vibration and buckling behavior of rotating, torsionally rigid, cantilevered beams were studied. The beam is considered to be clamped on the axis of rotation in one case, and off the axis of rotation in the other. Two methods are employed for the solution of the vibration problem: (1) one based upon a finite-difference approach using second order central differences for solution of the equations of motion, and (2) based upon the minimum of the total potential energy functional with a Ritz type of solution procedure making use of complex forms of shape functions for the dependent variables. The individual and collective effects of pretwist, precone, setting angle, thickness ratio and Coriolis forces on the natural frequencies and the buckling boundaries are presented. It is shown that the inclusion of Coriolis effects is necessary for blades of moderate to large thickness ratios while these effects are not so important for small thickness ratio blades. The possibility of buckling due to centrifugal softening terms for large values of precone and rotation is shown. E.A.K.

N85-25894*# Akron Univ., Ohio. Dept. of Civil Engineering.

ON THERMOMECHANICAL TESTING IN SUPPORT OF CONSTITUTIVE EQUATION DEVELOPMENT FOR HIGH TEMPERATURE ALLOYS Final Report

D. N. ROBINSON May 1985 32 p refs

(Contract NAG3-379)

(NASA-CR-174879; NAS 1.26:174879) Avail: NTIS HC A03/MF A01 CSCL 11F

Three major categories of testing are identified that are necessary to provide support for the development of constitutive equations for high temperature alloys. These are exploratory, characterization and verification tests. Each category is addressed and specific examples of each are given. An extensive, but not exhaustive, set of references is provided concerning pertinent experimental results and their relationships to theoretical development. This guide to formulating a meaningful testing effort in support of constitutive equation development can also aid in defining the necessary testing equipment and instrumentation for the establishment of a deformation and structures testing laboratory.
Author

N85-25896*# Georgia Inst. of Tech., Atlanta.

ANALYSIS OF SHELL TYPE STRUCTURES SUBJECTED TO TIME DEPENDENT MECHANICAL AND THERMAL LOADING Semiannual Status Report, 15 Aug. 1984 - 14 Apr. 1985

G. J. SIMITSES, R. L. CARLSON, and R. RIFF May 1985 4 p
(Contract NAG3-534)

(NASA-CR-175747; NAS 1.26:175747) Avail: NTIS HC A02/MF A01 CSCL 20K

A general mathematical model and solution methodologies for analyzing structural response of thin, metallic shell-type structures under large transient, cyclic or static thermomechanical loads is considered. Among the system responses, which are associated with these load conditions, are thermal buckling, creep buckling and ratchetting. Thus, geometric as well as material-type nonlinearities (of high order) can be anticipated and must be considered in the development of the mathematical model.
G.L.C.

N85-26885*# Wyle Labs., Inc., Huntsville, Ala.

FLOW DYNAMIC ENVIRONMENT DATA BASE DEVELOPMENT FOR THE SSME

C. V. SUNDARAM /in NASA. Marshall Space Flight Center Advan. High Pressure O2/H2 Technol. p 277-288 Apr. 1985 refs

Avail: NTIS HC A99/MF E03; SOD HC CSCL 20K

The fluid flow-induced vibration of the Space Shuttle main engine (SSME) components are being studied with a view to correlating the frequency characteristics of the pressure fluctuations in a rocket engine to its operating conditions and geometry. An overview of the data base development for SSME test firing results and the interactive computer software used to access, retrieve, and plot or print the results selectively for given thrust levels, engine numbers, etc., is presented. The various statistical methods available in the computer code for data analysis are discussed. Plots of test data, nondimensionalized using parameters such as fluid flow velocities, densities, and pressures, are presented. Results are compared with those available in the literature. Correlations between the resonant peaks observed at higher frequencies in power spectral density plots with pump geometry and operating conditions are discussed. An overview of the status of the investigation is presented and future directions are discussed.
A.R.H.

N85-26887*# National Aeronautics and Space Administration. Lewis Research Center, Cleveland, Ohio.

NONLINEAR STRUCTURAL ANALYSIS FOR FIBER-REINFORCED SUPERALLOY TURBINE BLADES

D. A. HOPKINS and C. C. CHAMIS /in NASA. Marshall Space Flight Center Advan. High Pressure O2/H2 Technol. p 318-340 Apr. 1985 refs

Avail: NTIS HC A99/MF E03; SOD HC CSCL 20K

A computational capability for predicting the nonlinear thermomechanical structural response of fiber-reinforced superalloy (FRS) turbine blades is described. This capability is embedded in a special purpose computer code (COBSTRAN) developed at the NASA Lewis Research Center. Special features of this computational capability include accounting for: fiber/matrix reaction, nonlinear and anisotropic material behavior, complex stress distribution due to local and global heterogeneity, and residual stresses due to initial fabrication and/or inelastic behavior during subsequent missions. Numerical results are presented from analyses of a hypothetical FRS turbine blade subjected to a fabrication process and subsequent mission cycle. The results demonstrate the capabilities of this computational tool to: predict local stress/strain response and capture trends of local nonlinear and anisotropic material behavior, relate the effects of this local behavior to the global response of a multilayered fiber-composite turbine blade, and trace material history from fabrication through successive missions.
Author

N85-27260*# Akron Univ., Ohio. Dept. of Civil Engineering.

SOME ADVANCES IN EXPERIMENTATION SUPPORTING DEVELOPMENT OF VISCOPLASTIC CONSTITUTIVE MODELS Final Report

J. R. ELLIS and D. N. ROBINSON May 1985 62 p refs

(Contract NAG3-379; W-7405-ENG-26)

(NASA-CR-174855; NAS 1.26:174855) Avail: NTIS HC A04/MF A01 CSCL 20K

The development of a biaxial extensometer capable of measuring axial, torsion, and diametral strains to near-microstrain resolution at elevated temperatures is discussed. An instrument with this capability was needed to provide experimental support to the development of viscoplastic constitutive models. The advantages gained when torsional loading is used to investigate inelastic material response at elevated temperatures are highlighted. The development of the biaxial extensometer was conducted in two stages. The first involved a series of bench calibration experiments performed at room temperature. The second stage involved a series of in-place calibration experiments conducted at room and elevated temperature. A review of the calibration data indicated that all performance requirements

39 STRUCTURAL MECHANICS

regarding resolution, range, stability, and crosstalk had been met by the subject instrument over the temperature range of interest, 21 C to 651 C. The scope of the in-place calibration experiments was expanded to investigate the feasibility of generating stress relaxation data under torsional loading. B.W.

N85-27261*# General Electric Co., Cincinnati, Ohio. Aircraft Engine Business Group.

COMPONENT-SPECIFIC MODELING Annual Status Report

R. L. MCKNIGHT 1984 115 p

(Contract NAS3-23687)

(NASA-CR-174765; NAS 1.26:174765; ASR-1) Avail: NTIS HC A06/MF A01 CSCL 20K

A series of interdisciplinary modeling and analysis techniques that were specialized to address three specific hot section components are presented. These techniques will incorporate data as well as theoretical methods from many diverse areas including cycle and performance analysis, heat transfer analysis, linear and nonlinear stress analysis, and mission analysis. Building on the proven techniques already available in these fields, the new methods developed will be integrated into computer codes to provide an accurate, efficient and unified approach to analyzing combustor burner liners, hollow air-cooled turbine blades and air-cooled turbine vanes. For these components, the methods developed will predict temperature, deformation, stress and strain histories throughout a complete flight mission. Author

N85-27263*# Connecticut Univ., Storrs. Dept. of Mechanical Engineering.

ELEVATED TEMPERATURE BIAxIAL FATIGUE Final Report, 15 Feb. 1981 - 31 Oct. 1984

E. H. JORDAN 31 Oct. 1984 167 p refs

(Contract NAG3-160)

(NASA-CR-175795; NAS 1.26:175795) Avail: NTIS HC A09/MF A01 CSCL 20K

A three year experimental program for studying elevated temperature biaxial fatigue of a nickel based alloy Hastelloy-X has been completed. A new high temperature fatigue test facility with unique capabilities has been developed. Effort was directed toward understanding multiaxial fatigue and correlating the experimental data to the existing theories of fatigue failure. The difficult task of predicting fatigue lives for non-proportional loading was used as an ultimate test for various life prediction methods being considered. The primary means of reaching improved understanding were through several critical non-proportional loading experiments. It was discovered that the cracking mode switched from primarily cracking on the maximum shear planes at room temperature to cracking on the maximum normal strain planes at 649 C. Author

N85-27264*# National Aeronautics and Space Administration. Lewis Research Center, Cleveland, Ohio.

A COMPUTER ANALYSIS PROGRAM FOR INTERFACING THERMAL AND STRUCTURAL CODES

R. L. THOMPSON and R. J. MAFFEO (GE, Cincinnati) 1985 17 p refs Proposed for presentation at the Intern. Computers in Eng. Conf. and Exhibition, Boston, 4-8 Aug. 1985; sponsored by ASME

(NASA-TM-87021; E-2571; NAS 1.15:87021) Avail: NTIS HC A02/MF A01 CSCL 20K

A software package has been developed to transfer three-dimensional transient thermal information accurately, efficiently, and automatically from a heat transfer analysis code to a structural analysis code. The code is called three-dimensional TRansfer ANalysis Code to Interface Thermal and Structural codes, or 3D TRANCITS. TRANCITS has the capability to couple finite difference and finite element heat transfer analysis codes to linear and nonlinear finite element structural analysis codes. TRANCITS currently supports the output of SINDA and MARC heat transfer codes directly. It will also format the thermal data output directly so that it is compatible with the input requirements of the NASTRAN and MARC structural analysis codes. Other thermal and structural codes can be interfaced using the transfer module with the neutral heat transfer input file and the neutral temperature output file.

The transfer module can handle different elemental mesh densities for the heat transfer analysis and the structural analysis. Author

N85-27952*# National Aeronautics and Space Administration. Lewis Research Center, Cleveland, Ohio.

OVERVIEW OF STRUCTURAL RESPONSE: PROBABILISTIC STRUCTURAL ANALYSIS Abstract Only

C. C. CHAMIS *In its* Struct. Integrity and Durability of Reusable Space Propulsion Systems p 63-66 May 1985

Avail: NTIS HC A09/MF A01 CSCL 20K

Advanced analysis methods are required to predict accurately the structural response (static, transient, cyclic, etc.) and accompanying local stresses in space propulsion system components operating in a fatigue environment consisting of complex thermal and mechanical load spectra. The probabilistic approach to structural response consists of the following program elements: (1) composite load spectra, (2) probabilistic structural analysis methods development, (3) probabilistic finite element theory, (4) probabilistic structural analysis application, (5) structural tailoring of turbopump blades, (6) unified theory of dynamic creep buckling/ratcheting, (7) creep buckling/ratcheting analyzer, and (8) nonlinear COBSTRAN development. Research activities on all of these program elements (except the creep buckling/ratcheting analyzer) are under way. G.L.C.

N85-27953*# Rockwell International Corp., Canoga Park, Calif. **COMPOSITE LOADS SPECTRA FOR SELECT SPACE PROPULSION STRUCTURAL COMPONENTS Abstract Only**

J. F. NEWELL *In* NASA. Lewis Research Center Struct. Integrity and Durability of Reusable Space Propulsion Systems p 67-75 May 1985

(Contract NAS3-24382)

Avail: NTIS HC A09/MF A01 CSCL 20K

Rocket engine technology continues to demand higher performance with lighter weight components that have man-rated reliability requirements. These requirements have yielded higher operating pressures, temperatures, and transient effects as well as markedly increased mechanical vibration and flow-related loads. The difficulty in installation, cost, and potential for destroying an engine severely limited the required instrumentation and measurements to adequately define loads of key components such as turbine blades. Also, accurate analytical methodologies for defining internal flow-related loads are just emerging for problems typically found in rocket engines. The difficulty of obtaining measured data and verified analysis methodologies has led to the probabilistic load definition approach. G.L.C.

N85-27954*# Battelle Columbus Labs., Ohio.

COMPOSITE LOADS SPECTRA FOR SELECT SPACE PROPULSION STRUCTURAL COMPONENTS: PROBABILISTIC LOAD MODEL DEVELOPMENT Abstract Only

R. KURTH *In* NASA. Lewis Research Center Struct. Integrity and Durability of Reusable Space Propulsion Systems p 77-83 May 1985

(Contract NAS3-24382)

Avail: NTIS HC A09/MF A01 CSCL 20K

This effort is in support of the development of the expert system of computer codes to predict the loads on select structural components of a space propulsion engine. The development will be based primarily on the space shuttle main engine (SSME) test data base. Because of random variations of the many different sources of the loadings on the selected structural components and transients, a probabilistic approach to the problems was adopted. The goal of this task is to characterize all of the individual sources of loads at critical structural locations, such as the turbine blades, the transfer ducts, and liquid oxygen posts, using state-of-the-art probabilistic methods with varying levels of sophistication. The second phase of this work is the development of a composite load model based on a probabilistic synthesis of the individual load model previously developed. This model will be based on the stochastic combination of the load variables and not on the physical process for the combination of the individual

loads to the composite load seen by the selected structural components.
R.J.F.

**N85-27955*# Southwest Research Inst., San Antonio, Tex.
PROBABILISTIC STRUCTURAL ANALYSIS THEORY
DEVELOPMENT Abstract Only**

O. H. BURNSIDE *In* NASA. Lewis Research Center Struct. Integrity and Durability of Reusable Space Propulsion Systems p 85-92 May 1985

(Contract NAS3-24389)

Avail: NTIS HC A09/MF A01 CSCL 20K

The objective of the Probabilistic Structural Analysis Methods (PSAM) project is to develop analysis techniques and computer programs for predicting the probabilistic response of critical structural components for current and future space propulsion systems. This technology will play a central role in establishing system performance and durability. The first year's technical activity is concentrating on probabilistic finite element formulation strategy and code development. Work is also in progress to survey critical materials and space shuttle main engine components. The probabilistic finite element computer program NESSUS (Numerical Evaluation of Stochastic Structures Under Stress) is being developed. The final probabilistic code will have, in the general case, the capability of performing nonlinear dynamic of stochastic structures. It is the goal of the approximate methods effort to increase problem solving efficiency relative to finite element methods by using energy methods to generate trial solutions which satisfy the structural boundary conditions. These approximate methods will be less computer intensive relative to the finite element approach.
R.J.F.

**N85-27956*# MARC Analysis Research Corp., Palo Alto, Calif.
PROBABILISTIC FINITE ELEMENT DEVELOPMENT Abstract Only**

J. NAGTEGAAL *In* NASA. Lewis Research Center Struct. Integrity and Durability of Reusable Space Propulsion Systems p 93-98 May 1985

(Contract NAS3-24389)

Avail: NTIS HC A09/MF A01 CSCL 20K

The probabilistic finite element computer program known as Numerical Evaluation of Stochastic Structures Under Stress (NESSUS) is being developed for the analysis of critical structural components for reusable space propulsion systems. First year efforts involve the formulation of the probabilistic analysis strategy and the development of a probabilistic linear analysis code. The ultimate goal of the 3-year program is the development of a finite element code capable of performing nonlinear dynamic analysis of structures having stochastic material properties, geometry, and boundary conditions and subjected to random loading. Three levels of sophistication are envisioned for the stochastic description of the structural problem, namely: (1) homogeneous random variable for stiffness, mass, damping, and external loading; (2) stochastic characterization of variables at the element level, with specified interelement correlations; and (3) stochastic interpolation of variables within a finite element. Two alternative probabilistic analysis methods will be developed, allowing for all three levels of modeling sophistication.
R.J.F.

**N85-27957*# Northwestern Univ., Evanston, Ill.
PROBABILISTIC FINITE ELEMENT: VARIATIONAL THEORY
Abstract Only**

T. BELYTSCHKO and W. K. LIU *In* NASA. Lewis Research Center Struct. Integrity and Durability of Reusable Propulsion Systems p 99-107 May 1985

(Contract NAG3-535)

Avail: NTIS HC A09/MF A01 CSCL 20K

The goal of this research is to provide techniques which are cost-effective and enable the engineer to evaluate the effect of uncertainties in complex finite element models. Embedding the probabilistic aspects in a variational formulation is a natural approach. In addition, a variational approach to probabilistic finite elements enables it to be incorporated within standard finite element methodologies. Therefore, once the procedures are

developed, they can easily be adapted to existing general purpose programs. Furthermore, the variational basis for these methods enables them to be adapted to a wide variety of structural elements and to provide a consistent basis for incorporating probabilistic features in many aspects of the structural problem. Tasks concluded include the theoretical development of probabilistic variational equations for structural dynamics, the development of efficient numerical algorithms for probabilistic sensitivity displacement and stress analysis, and integration of methodologies into a pilot computer code.
R.J.F.

**N85-27959*# Georgia Inst. of Tech., Atlanta.
DYNAMIC CREEP BUCKLING: ANALYSIS OF SHELL
STRUCTURES SUBJECTED TO TIME-DEPENDENT MECHANICAL AND THERMAL LOADING Abstract Only**

G. J. SIMITSES, R. L. CARLSON, and R. RIFF *In* NASA. Lewis Research Center Struct. Integrity and Durability of Reusable Space Propulsion Systems p 117-120 May 1985

(Contract NAG3-534)

Avail: NTIS HC A09/MF A01 CSCL 20K

The objective of the present research is to develop a general mathematical model and solution methodologies for analyzing the structural response of thin, metallic shell structures under large transient, cyclic, or static thermomechanical loads. Among the system responses associated with these loads and conditions are thermal buckling, creep buckling, and ratcheting. Thus geometric and material nonlinearities (of high order) can be anticipated and must be considered in developing the mathematical model. A complete, true ab-initio rate theory of kinematics and kinetics for continuum and curved thin structures, without any restriction on the magnitude of the strains or the deformations, was formulated. The time dependence and large strain behavior are incorporated through the introduction of the time rates of metric and curvature in two coordinate systems: fixed (spatial) and convected (material). The relations between the time derivative and the covariant derivative (gradient) were developed for curved space and motion, so the velocity components supply the connection between the equations of motion and the time rates of change of the metric and curvature tensors.
R.J.F.

**N85-27961*# National Aeronautics and Space Administration.
Lewis Research Center, Cleveland, Ohio.
INTERACTION OF HIGH-CYCLE AND LOW-CYCLE FATIGUE
OF HAYNES 188 ALLOY AT 1400 F DEG Abstract Only**

P. T. BIZON, D. J. THOMA, and G. R. HALFORD *In its* Struct. Integrity and Durability of Reusable Space Propulsion Systems p 129-138 May 1985

Avail: NTIS HC A09/MF A01 CSCL 20K

The interaction of low-cycle fatigue (LCF) and high-cycle fatigue (HCF) was evaluated at the NASA Lewis Research Center on Haynes 188 alloy at 1400 F. Completely reversed, axial-load, strain-controlled fatigue tests were performed to determine the baseline data for this study. Additional specimens for interaction tests were cycled first at a high strain range for various small portions of expected LCF life followed by a step change to a low strain range to failure in HCF. Failure was defined as complete specimen separation. The resultant lives varied between 10 and 5000 cycles for the low-cycle fatigue tests and between 4500 and 3 million for the high-cycle fatigue tests. For the interaction tests the low-cycle-life portion ranged from 30 and 1000 applied cycles while the high-frequency life ranged from 300 and 300,000 cycles to failure. The step change results showed a significant nonlinear interaction in expected life. Application of a small part of the LCF life drastically decreased the available HCF life as compared with what would have been expected by the classical linear damage rule (LDR).
B.W.

N85-27962*# National Aeronautics and Space Administration. Lewis Research Center, Cleveland, Ohio.

REEXAMINATION OF CUMULATIVE FATIGUE DAMAGE LAWS

Abstract Only

G. R. HALFORD and S. S. MANSON (Case Western Reserve Univ.) *In its* Struct. Integrity and Durability of Reusable Space Propulsion Systems p 139-145 May 1985 refs

Avail: NTIS HC A09/MF A01 CSCL 20K

Treatment of accumulated fatigue damage in materials and structures subjected to a history of nonsimple repetitive loadings has received a large amount of attention in recent years. A method used for the treatment of complex loading is known as linear damage rule. It was recognized that, this method could result in unconservative predictions of material and structural behavior. An intense flurry of activity followed in the pursuit of alternative methods of analysis that would predict behavior more accurately. So many methods were introduced that it became necessary periodically to prepare review papers placing all the new methods into perspective. The current integrated view regarding the state of the art as it applies to this effort is discussed. The more recently proposed cumulative damage life prediction methods are reviewed. The double linear damage rule (DLDR), which has evolved over the past 20 years, is reexamined with the intent of improving its accuracy and applicability to engineering problems. Modifications are introduced to the analytical formulation to achieve greater compatibility between the DLDR and the so-called damage curve approach, which is an alternative continuous representation of the DLDR. B.W.

N85-27963*# National Aeronautics and Space Administration. Lewis Research Center, Cleveland, Ohio.

CYCLIC STRUCTURAL ANALYSES OF SSME TURBINE BLADES

A. KAUFMAN and J. M. MANDERSCHIED *In its* Struct. Integrity and Durability of Reusable Space Propulsion Systems p 147-154 May 1985 refs

Avail: NTIS HC A09/MF A01 CSCL 20K

The problems of calculating the structural response of high-temperature space propulsion components such as turbine blades for the fuel turbopump are addressed. The first high-pressure-stage fuel turbine blade (HPFTB) in the liquid-hydrogen turbopump of the space shuttle main engine (SSME) was selected for this study. In the past these blades have cracked in the blade shank region and at the airfoil leading edge adjacent to the platform. To achieve the necessary durability, these blades are currently being cast by using directional solidification. Single-crystal alloys are also being investigated for future SSME applications. The study evaluated the utility of advanced structural analysis methods in assessing the low-cycle fatigue lives of these anisotropic components. The turbine blade airfoil of the high-pressure stage of the SSME fuel turbopump was analyzed because it has a history of rapid crack initiation. B.W.

N85-30361*# National Aeronautics and Space Administration. Lewis Research Center, Cleveland, Ohio.

STRUCTURAL ANALYSIS AND COST ESTIMATE OF AN EIGHT-LEG SPACE FRAME AS A SUPPORT STRUCTURE FOR HORIZONTAL AXIS WIND TURBINES Final Report

R. L. SIZEMORE, J. R. WINEMILLER, S. T. YEE, and G. R. FREDERICK (Toledo Univ.) Oct. 1983 27 p refs (Contract DE-A101-76ET-20320)

(NASA-TM-83470; E-1529; DOE/NASA/20320-49; NAS 1.15:83470) Avail: NTIS HC A03/MF A01 CSCL 20K

A structural analysis was performed and a cost estimate was prepared to determine if an eight-leg space frame tower in which the legs lie on the surface of a hyperboloid of revolution was a suitable alternative to the truss-type tower for application to an intermediate size horizontal axis wind turbine. This tower concept had eight straight pipe elements as its main structural members that lie on the surface of a hyperboloid of revolution. The structural analysis included: response to static loads, determination of vibration characteristics, and investigation of overall frame stability.

The design was lighter than the four-leg truss-type tower used for the Mod-O and Mod-OA wind turbines. The estimated cost for fabrication and erection of the hyperboloid tower is less than that for any of the four Mod-OA towers constructed to date. It is concluded that the hyperboloid tower concept is a suitable alternative to the truss-type tower for application to horizontal axis wind turbines. E.A.K.

N85-31530*# National Aeronautics and Space Administration. Lewis Research Center, Cleveland, Ohio.

NONLINEAR CONSTITUTIVE RELATIONS FOR HIGH TEMPERATURE APPLICATION, 1984

Jun. 1985 368 p refs Symp. held in Cleveland, 15-17 Jun. 1984

(NASA-CP-2369; E-2368; NAS 1.55:2369) Avail: NTIS HC A16/MF A01 CSCL 20K

Nonlinear constitutive relations for high temperature applications were discussed. The state of the art in nonlinear constitutive modeling of high temperature materials was reviewed and the need for future research and development efforts in this area was identified. Considerable research efforts are urgently needed in the development of nonlinear constitutive relations for high temperature applications prompted by recent advances in high temperature materials technology and new demands on material and component performance. Topics discussed include: constitutive modeling, numerical methods, material testing, and structural applications.

N85-31531*# Southwest Research Inst., San Antonio, Tex.

A SURVEY OF UNIFIED CONSTITUTIVE THEORIES

K. S. CHAN, U. S. LINDHOLM, S. R. BODNER (Technion - Israel Inst. of Tech., Haifa), and K. P. WALKER (Engineering Scientific Software, Inc., Smithfield, R.I.) *In* NASA. Lewis Research Center Nonlinear Constitutive Relations for High Temp. Appl., 1984 p 1-23 Jun. 1985 refs

(Contract NAS3-23925)

Avail: NTIS HC A16/MF A01 CSCL 20K

The state of the art of time temperature dependent elastic viscoplastic constitutive theories which are based on the unified approach were assessed. This class of constitutive theories is characterized by the use of kinetic equations and internal variables with appropriate evolutionary equations for treating all aspects of inelastic deformation including plasticity, creep, and stress relaxation. More than 10 such unified theories which are shown to satisfy the uniqueness and stability criteria imposed by Drucker's postulate and Ponter's inequalities are identified. The theories are compared for the types of flow law, kinetic equation, evolutionary equation of the internal variables, and treatment of temperature dependence. The similarities and differences of these theories are outlined in terms of mathematical formulations and illustrated by comparisons of theoretical calculations with experimental results which include monotonic stress-strain curves, cyclic hysteresis loops, creep and stress relaxation rates, and thermomechanical loops. Numerical methods used for integrating these stiff time temperature dependent constitutive equations are reviewed. E.A.K.

N85-31533*# Akron Univ., Ohio.

THERMOMECHANICAL DEFORMATION IN THE PRESENCE OF METALLURGICAL CHANGES

D. N. ROBINSON *In* NASA. Lewis Research Center Nonlinear Constitutive Relations for High Temp. Appl., 1984 p 51-54 Jun. 1985 refs

(Contract NAG3-379)

Avail: NTIS HC A16/MF A01 CSCL 20K

Nonisothermal testing that can be used as a basis of a nonisothermal representation is discussed. Related tests regarding metallurgical changes that occur in other high temperature structural alloys are discussed. A viscoplastic constitutive model capable of qualitatively representing the behavioral features was formulated. This model is used to assess the differences in ultimate life prediction in some typical nonisothermal structural problems when the constitutive model does or does not account for

metallurgically induced thermomechanical history dependence.

E.A.K.

N85-31536*# Texas A&M Univ., College Station. Aerospace Engineering Dept.

ON THE USE OF INTERNAL STATE VARIABLES IN THERMOVISCOPLASTIC CONSTITUTIVE EQUATIONS

D. H. ALLEN and J. M. BEEK *In* NASA. Lewis Research Center Nonlinear Constitutive Relations for High Temp. Appl., 1984 p 83-102 Jun. 1985 refs

(Contract NAG3-491)

Avail: NTIS HC A16/MF A01 CSCL 20K

The general theory of internal state variables are reviewed to apply it to inelastic metals in use in high temperature environments. In this process, certain constraints and clarifications will be made regarding internal state variables. It is shown that the Helmholtz free energy can be utilized to construct constitutive equations which are appropriate for metallic superalloys. Internal state variables are shown to represent locally averaged measures of dislocation arrangement, dislocation density, and intergranular fracture. The internal state variable model is demonstrated to be a suitable framework for comparison of several currently proposed models for metals and can therefore be used to exhibit history dependence, nonlinearity, and rate as well as temperature sensitivity. E.A.K.

N85-31538*# National Aeronautics and Space Administration. Lewis Research Center, Cleveland, Ohio.

A COMPARISON OF TWO CONTEMPORARY CREEP-FATIGUE LIFE PREDICTION METHODS Abstract Only

M. A. MCGAW *In* its Nonlinear Constitutive Relations for High Temp. Appl., 1984 p 125 Jun. 1985

Avail: NTIS HC A16/MF A01 CSCL 20K

A comparison of two contemporary approaches to creep fatigue life prediction, the Continuous Damage Mechanics as developed at ONERA, and Strain Range Partitioning, is presented. The general framework of each of these approaches, both being crack initiation life prediction tools, are examined. The basis for, and implications of each predictive method are discussed, relative to the material class(es) for which each was developed, as well as to their general applicability. Evident is a need for critical experiments capable of discriminating among the models; to this end, the question of choice of experiment and material is addressed. Author

N85-31541*# Texas A&M Univ., College Station. Aerospace Engineering Dept.

NUMERICAL CONSIDERATIONS IN THE DEVELOPMENT AND IMPLEMENTATION OF CONSTITUTIVE MODELS

W. E. HAILER and P. K. IMBRIE *In* NASA. Lewis Research Center Nonlinear Constitutive Relations for High Temp. Appl., 1984 p 169-185 Jun. 1985 refs

(Contract NAG3-491)

Avail: NTIS HC A16/MF A01 CSCL 20K

Several unified constitutive models were tested in uniaxial form by specifying input strain histories and comparing output stress histories. The purpose of the tests was to evaluate several time integration methods with regard to accuracy, stability, and computational economy. The sensitivity of the models to slight changes in input constants was also investigated. Results are presented for In100 at 1350 F and Hastelloy-X at 1800 F.

Author

N85-31542*# National Aeronautics and Space Administration. Lewis Research Center, Cleveland, Ohio.

ON NUMERICAL INTEGRATION AND COMPUTER IMPLEMENTATION OF VISCOPLASTIC MODELS

T. Y. CHANG (Akron Univ., Ohio), J. P. CHANG (Akron Univ., Ohio), and R. L. THOMPSON *In* its Nonlinear Constitutive Relations for High Temp. Appl., 1984 p 187-200 Jun. 1985 refs

Avail: NTIS HC A16/MF A01 CSCL 20K

Due to the stringent design requirement for aerospace or nuclear structural components, considerable research interests have been generated on the development of constitutive models for

representing the inelastic behavior of metals at elevated temperatures. In particular, a class of unified theories (or viscoplastic constitutive models) have been proposed to simulate material responses such as cyclic plasticity, rate sensitivity, creep deformations, strain hardening or softening, etc. This approach differs from the conventional creep and plasticity theory in that both the creep and plastic deformations are treated as unified time-dependent quantities. Although most of viscoplastic models give better material behavior representation, the associated constitutive differential equations have stiff regimes which present numerical difficulties in time-dependent analysis. In this connection, appropriate solution algorithm must be developed for viscoplastic analysis via finite element method. G.L.C.

N85-31543*# National Aeronautics and Space Administration. Lewis Research Center, Cleveland, Ohio.

TWO SIMPLIFIED PROCEDURES FOR PREDICTING CYCLIC MATERIAL RESPONSE FROM A STRAIN HISTORY

A. KAUFMAN and V. MORENO (Pratt and Whitney Aircraft, East Hartford, Conn.) *In* its Nonlinear Constitutive Relations for High Temp. Appl., 1984 p 201-219 Jun. 1985 refs

Avail: NTIS HC A16/MF A01 CSCL 20K

Simplified inelastic analysis procedures were developed at NASA Lewis and Pratt & Whitney Aircraft for predicting the stress-strain response at the critical location of a thermomechanically cycled structure. These procedures are intended primarily for use as economical structural analysis tools in the early design stages of aircraft engine hot section components where nonlinear finite-element analyses would be prohibitively expensive. Both simplified methods use as input the total strain history calculated from a linear elastic analysis. The elastic results are modified to approximate the characteristics of the inelastic cycle by incremental solution techniques. A von Mises yield criterion is used to determine the onset of active plasticity. The fundamental assumption of these methods is that the inelastic strain is local and constrained from redistribution by the surrounding elastic material. G.L.C.

N85-31545*# Akron Univ., Ohio. Dept. of Civil Engineering.

SOME ADVANCES IN EXPERIMENTATION SUPPORTING DEVELOPMENT OF VISCOPLASTIC CONSTITUTIVE MODELS

J. R. ELLIS and D. N. ROBINSON *In* NASA. Lewis Research Center Nonlinear Constitutive Relations for High Temp. Appl., 1984 p 237-271 Jun. 1985 refs Previously announced as N85-27260

(Contract NAG3-379; W-7405-ENG-26)

Avail: NTIS HC A16/MF A01 CSCL 20K

The development of a biaxial extensometer capable of measuring axial, torsion, and diametral strains to near-microstrain resolution at elevated temperatures is discussed. An instrument with this capability was needed to provide experimental support to the development of viscoplastic constitutive models. The advantages gained when torsional loading is used to investigate inelastic material response at elevated temperatures are highlighted. The development of the biaxial extensometer was conducted in two stages. The first involved a series of bench calibration experiments performed at room temperature. The second stage involved a series of in-place calibration experiments performed at room temperature. A review of the calibration data indicated that all performance requirements regarding resolution, range, stability, and crosstalk had been met by the subject instrument over the temperature range of interest, 21 C to 651 C. The scope of the in-placed calibration experiments was expanded to investigate the feasibility of generating stress relaxation data under torsional loading. B.W. (IAA)

39 STRUCTURAL MECHANICS

N85-31546*# Michigan State Univ., East Lansing. Dept. of Metallurgy, Mechanics, and Materials Science.

A COMPARISON OF SMOOTH SPECIMEN AND ANALYTICAL SIMULATION TECHNIQUES FOR NOTCHED MEMBERS AT ELEVATED TEMPERATURES

J. F. MARTIN /in NASA. Lewis Research Center Nonlinear Constitutive Relations for High Temp. Appl., 1984 p 273-281 Jun. 1985 refs

(Contract NAG3-51)

Avail: NTIS HC A16/MF A01 CSCL 20K

Experimental strain measurements have been made at the highly strained regions on notched plate specimens that were made of Hastelloy X. Tests were performed at temperatures up to 1,600 F. Variable load patterns were chosen so as to produce plastic and creep strains. Where appropriate, notch root stresses were experimentally estimated by subjecting a smooth specimen to the measured notch root strains. The results of three analysis techniques are presented and compared to the experimental data. The most accurate results were obtained from an analysis procedure that used a smooth specimen and the Neuber relation to simulate the notch root stress-strain response. When a generalized constitutive relation was used with the Neuber relation, good results were also obtained, however, these results were not as accurate as those obtained when the smooth specimen was used directly. Finally, a general finite element program, ANSYS, was used which resulted in acceptable solutions, but, these were the least accurate predictions. Author

N85-31548*# Cincinnati Univ., Ohio. Dept. of Aerospace Engineering and Applied Mechanics.

FINITE ELEMENT ANALYSIS OF NOTCH BEHAVIOR USING A STATE VARIABLE CONSTITUTIVE EQUATION

L. T. DAME, D. C. STOFFER, and N. ABUELFOUTOUH /in NASA. Lewis Research Center Nonlinear Constitutive Relations for High Temp. Appl., 1984 p 297-310 Jun. 1985 refs

(Contract NAS3-23698; NAS3-23927; NAG3-511)

Avail: NTIS HC A16/MF A01 CSCL 20K

The state variable constitutive equation of Bodner and Partom was used to calculate the load-strain response of Inconel 718 at 649 C in the root of a notch. The constitutive equation was used with the Bodner-Partom evolution equation and with a second evolution equation that was derived from a potential function of the stress and state variable. Data used in determining constants for the constitutive models was from one-dimensional smooth bar tests. The response was calculated for a plane stress condition at the root of the notch with a finite element code using constant strain triangular elements. Results from both evolution equations compared favorably with the observed experimental response. The accuracy and efficiency of the finite element calculations also compared favorably to existing methods. Author

N85-32340*# Akron Univ., Ohio. Dept. of Civil Engineering. RESULTS OF AN INTERLABORATORY FATIGUE TEST PROGRAM CONDUCTED ON ALLOY 800H AT ROOM AND ELEVATED TEMPERATURES Final Report

J. R. ELLIS Jul. 1985 38 p refs Sponsored in part by General Atomic Co.

(Contract NAG3-379)

(NASA-CR-174940; NAS 1.26:174940) Avail: NTIS HC A03/MF A01 CSCL 20K

The experimental approach adopted for low cycle fatigue tests of alloy 800H involved the use of electrohydraulic test systems, hour glass geometry specimens, diametral extensometers, and axial strain computers. Attempts to identify possible problem areas were complicated by the lack of reliable data for the heat of Alloy 800H under investigation. The method adopted was to generate definitive test data in an Interlaboratory Fatigue Test Program. The laboratories participating in the program were Argonne National Laboratory, Battelle Columbus, Mar-Test, and NASA Lewis. Fatigue tests were conducted on both solid and tubular specimens at temperatures of 20, 593, and 760 C and strain ranges of 2.0, 1.0, and 0.5 percent. The subject test method can, under certain circumstances, produce fatigue data which are serious in error.

This approach subsequently was abandoned at General Atomic Company in favor of parallel gage length specimens and axial extensometers. F.M.R.

N85-32341*# Akron Univ., Ohio. Dept. of Civil Engineering. A CONTINUOUS DAMAGE MODEL BASED ON STEPWISE-STRESS CREEP RUPTURE TESTS Final Report

D. N. ROBINSON Cleveland Jul. 1985 24 p refs

(Contract NAG3-379)

(NASA-CR-174941; NAS 1.26:174941) Avail: NTIS HC A02/MF A01 CSCL 20K

A creep damage accumulation model is presented that makes use of the Kachanov damage rate concept with a provision accounting for damage that results from a variable stress history. This is accomplished through the introduction of an additional term in the Kachanov rate equation that is linear in the stress rate. Specification of the material functions and parameters in the model requires two types of constituting a data base: (1) standard constant-stress creep rupture tests, and (2) a sequence of two-step creep rupture tests. Author

N85-33520*# National Aeronautics and Space Administration. Lewis Research Center, Cleveland, Ohio.

APPLICATION OF TRACTION DRIVES AS SERVO MECHANISMS

S. H. LOEWENTHAL, D. A. ROHN, and B. M. STEINETZ /in NASA. Ames Research Center 19th Aerospace Mech. Symp. p 119-139 Aug. 1985 refs

Avail: NTIS HC A17/MF A01 CSCL 20K

The suitability of traction drives for a wide class of aerospace control mechanisms is examined. Potential applications include antenna or solar array drive positioners, robotic joints, control moment gyro (CMG) actuators and propeller pitch change mechanisms. In these and similar applications the zero backlash, high torsional stiffness, low hysteresis and torque ripple characteristics of traction drives are of particular interest, as is the ability to run without liquid lubrication in certain cases. Wear and fatigue considerations for wet and dry operation are examined along with the tribological performance of several promising self lubricating polymers for traction contracts. The speed regulation capabilities of variable ratio traction drives are reviewed. A torsional stiffness analysis described suggests that traction contacts are relatively stiff compared to gears and are significantly stiffer than the other structural elements in the prototype CMG traction drive analyzed. Discussion is also given of an advanced turboprop propeller pitch change mechanism that incorporates a traction drive. Author

N85-33541*# General Electric Co., Cincinnati, Ohio. Advanced Technology Programs Dept.

A REVIEW OF PATH-INDEPENDENT INTEGRALS IN ELASTIC-PLASTIC FRACTURE MECHANICS, TASK 4 Interim Report

K. S. KIM Aug. 1985 33 p refs

(Contract NAS3-23940)

(NASA-CR-174956; NAS 1.26:174956) Avail: NTIS HC A03/MF A01 CSCL 20K

The path independent (P-I) integrals in elastic plastic fracture mechanics which have been proposed in recent years to overcome the limitations imposed on the J integral are reviewed. The P-I integrals considered herein are the J integral by Rice, the thermoelastic P-I integrals by Wilson and Yu and by Gurtin, the J* integral by Blackburn, the J sub theta integral by Ainsworth et al., the J integral by Kishimoto et al., and the delta T sub p and delta T* sub p integrals by Atluri et al. The theoretical foundation of these P-I integrals is examined with emphasis on whether or not path independence is maintained in the presence of nonproportional loading and unloading in the plastic regime, thermal gradients, and material inhomogeneities. The similarities, differences, salient features, and limitations of these P-I integrals are discussed. Comments are also made with regard to the physical meaning, the possibility of experimental measurement, and computational aspects. Author

N85-34427*# National Aeronautics and Space Administration. Lewis Research Center, Cleveland, Ohio.

NONLINEAR FLAP-LAG-EXTENSIONAL VIBRATIONS OF ROTATING, PRETWISTED, PRECONED BEAMS INCLUDING CORIOLIS EFFECTS

K. B. SUBRAHMANYAM (NBKR Inst. of Science and Tech.) and K. R. V. KAZA 1985 35 p refs Presented at the 19th Midwestern Mech. Conf., Columbus, Ohio, 9-11 Sep. 1985; sponsored by the Ohio State Univ.

(NASA-TM-87102; E-2598; NAS 1.15:87102) Avail: NTIS HC A03/MF A01 CSCL 20K

The effects of pretwist, precone, setting angle, Coriolis forces and second degree geometric nonlinearities on the natural frequencies, steady state deflections and mode shapes of rotating, torsionally rigid, cantilevered beams were studied. The governing coupled equations of flap lag extensional motion are derived including the effects of large precone and retaining geometric nonlinearities up to second degree. The Galerkin method, with nonrotating normal modes, is used for the solution of both steady state nonlinear equations and linear perturbation equations. Parametric indicating the individual and collective effects of pretwist, precone, Coriolis forces and second degree geometric nonlinearities on the steady state deflection, natural frequencies and mode shapes of rotating blades are presented. It is indicated that the second degree geometric nonlinear terms, which vanish for zero precone, can produce frequency changes of engineering significance. Further confirmation of the validity of including those generated by MSC NASTRAN. It is indicated that the linear and nonlinear Coriolis effects must be included in analyzing thick blades. The Coriolis effects are significant on the first flatwise and the first edgewise modes. E.A.K.

N86-10579*# National Aeronautics and Space Administration. Lewis Research Center, Cleveland, Ohio.

JOINT RESEARCH EFFORT ON VIBRATIONS OF TWISTED PLATES, PHASE 1: FINAL RESULTS

R. E. KIELB, A. W. LEISSA, J. C. MACBAIN, and K. S. CARNEY Washington Sep. 1985 100 p refs

(NASA-RP-1150; E-2576; NAS 1.61:1150) Avail: NTIS HC A05/MF A01 CSCL 20K

The complete theoretical and experimental results of the first phase of a joint government/industry/university research study on the vibration characteristics of twisted cantilever plates are given. The study is conducted to generate an experimental data base and to compare many different theoretical methods with each other and with the experimental results. Plates with aspect ratios, thickness ratios, and twist angles representative of current gas turbine engine blading are investigated. The theoretical results are generated by numerous finite element, shell, and beam analysis methods. The experimental results are obtained by precision matching a set of twisted plates and testing them at two laboratories. The second and final phase of the study will concern the effects of rotation. Author

N86-10582*# National Aeronautics and Space Administration. Lewis Research Center, Cleveland, Ohio.

IMPROVED STUD CONFIGURATIONS FOR ATTACHING LAMINATED WOOD WIND TURBINE BLADES Final Report

J. R. FADOUL Sep. 1985 29 p refs

(Contract DE-A101-76ET-20320)

(NASA-TM-87109; DOE/NASA/20320-66; E-2709; NAS 1.15:87109) Avail: NTIS HC A03/MF A01

A series of bonded stud design configurations was screened on the basis of tension-tension cyclic tests to determine the structural capability of each configuration for joining a laminated wood structure (wind turbine blade) to a steel flange (wind turbine hub). Design parameters which affected the joint strength (ultimate and fatigue) were systematically varied and evaluated through appropriate testing. Two designs showing the most promise were used to fabricate additave testing. Two designs showing the most promise were used to fabricate additional test specimens to determine ultimate strength and fatigue curves. Test results for the bonded stud designs demonstrated that joint strengths

approaching the 10,000 to 12,000 psi ultimate strength and 5000 psi high cycle fatigue strength of the wood epoxy composite could be achieved. Author

N86-10588*# Georgia Inst. of Tech., Atlanta.

ANALYSIS OF LARGE, NON-ISOTHERMAL ELASTIC-VISCO-PLASTIC DEFORMATIONS

R. RIFF, R. L. CARLSON, and G. J. SIMITSES 1984 4 p refs

(Contract NAG3-534)

(NASA-CR-176220; NAS 1.26:176220) Avail: NTIS HC A02/MF A01 CSCL 20K

The development of a general mathematical model and solutions of test problems to analyze large nonisothermal elasto-visco-plastic deformations of structures is discussed. Geometric and material type nonlinearities of higher order are present in the development of the mathematical model and in the developed solution methodology. DOE

N86-10589*# Southwest Research Inst., San Antonio, Tex.

CONSTITUTIVE MODELING FOR ISOTROPIC MATERIALS (HOST) Annual Status Report

U. S. LINDHOLM, K. S. CHAN, S. R. BODNER, R. M. WEBER, K. P. WALKER, and B. N. CASSENTI 20 Aug. 1985 185 p refs

(Contract NAS3-23925)

(NASA-CR-174980; NAS 1.26:174980; SWRI-7576/30; ASR-2) Avail: NTIS HC A09/MF A01 CSCL 20K

This report presents the results of the second year of work on a problem which is part of the NASA HOST Program. Its goals are: (1) to develop and validate unified constitutive models for isotropic materials, and (2) to demonstrate their usefulness for structural analyses of hot section components of gas turbine engines. The unified models selected for development and evaluation are that of Bodner-Partom and Walker. For model evaluation purposes, a large constitutive data base is generated for a B1900 + Hf alloy by performing uniaxial tensile, creep, cyclic, stress relation, and thermomechanical fatigue (TMF) tests as well as biaxial (tension/torsion) tests under proportional and nonproportional loading over a wide range of strain rates and temperatures. Systematic approaches for evaluating material constants from a small subset of the data base are developed. Correlations of the uniaxial and biaxial tests data with the theories of Bodner-Partom and Walker are performed to establish the accuracy, range of applicability, and integrability of the models. Both models are implemented in the MARC finite element computer code and used for TMF analyses. Benchmark notch round experiments are conducted and the results compared with finite-element analyses using the MARC code and the Walker model. Author

N86-11495*# National Aeronautics and Space Administration. Lewis Research Center, Cleveland, Ohio.

TURBINE ENGINE HOT SECTION TECHNOLOGY (HOST)

Oct. 1983 250 p refs Workshop held in Cleveland, Ohio, 25-26 Oct. 1983

(NASA-CP-2289; E-1816; NAS 1.55:2289) Avail: NTIS HC A11/MF A01 CSCL 21E

A two-day workshop on the research and plans for turbine engine hot section durability problems was held on October 25 and 26, 1983, at the NASA Lewis Research Center. Presentations were made during six sessions, including structural analysis, fatigue and fracture, surface protective coatings, combustion, turbine heat transfer, and instrumentation, that dealt with the thermal and fluid environment around liners, blades, and vanes, and with material coatings, constitutive behavior, stress-strain response, and life prediction methods for the three components. The principal objective of each session was to disseminate the research results to date, along with future plans, in each of the six areas. Contract and government researchers presented results of their work.

N86-16615*# National Aeronautics and Space Administration. Lewis Research Center, Cleveland, Ohio.

SIMPLIFIED CYCLIC STRUCTURAL ANALYSES OF SSME TURBINE BLADES

A. KAUFMAN and J. M. MANDERSCHIED 1986 17 p refs Proposed for presentation at the Conference on Advanced High Pressure Oxygen/Hydrogen Propulsion Technology, Huntsville, Ala., 14-16 May 1986; sponsored by NASA Marshall Space Flight Center

(NASA-TM-87214; E-2873; NAS 1.15:87214) Avail: NTIS HC A02/MF A01 CSCL 20K

Anisotropic high-temperature alloys are used to meet the safety and durability requirements of turbine blades for high-pressure turbopumps in reusable space propulsion systems. The applicability to anisotropic components of a simplified inelastic structural analysis procedure developed at the NASA Lewis Research Center is assessed. The procedure uses as input the history of the total strain at the critical crack initiation location computed from elastic finite-element analyses. Cyclic heat transfer and structural analyses are performed for the first stage high-pressure fuel turbopump blade of the space shuttle main engine. The blade alloy is directionally solidified MAR-M 246 (nickel base). The analyses are based on a typical test stand engine cycle. Stress-strain histories for the airfoil critical location are computed using both the MARC nonlinear finite-element computer code and the simplified procedure. Additional cases are analyzed in which the material yield strength is arbitrarily reduced to increase the plastic strains and, therefore, the severity of the problem. Good agreement is shown between the predicted stress-strain solutions from the two methods. The simplified analysis uses about 0.02 percent (5 percent with the required elastic finite-element analyses) of the CPU time used by the nonlinear finite element analysis. Author

N86-17788*# Virginia Polytechnic Inst. and State Univ., Blacksburg. Dept. of Engineering Science and Mechanics.

CLOSURE OF FATIGUE CRACKS AT HIGH STRAINS Final Report

N. S. IYER and N. E. DOWLING Dec. 1985 159 p refs (Contract NAG3-438)

(NASA-CR-175021; NAS 1.26:175021) Avail: NTIS HC A08/MF A01 CSCL 20K

Experiments were conducted on smooth specimens to study the closure behavior of short cracks at high cyclic strains under completely reversed cycling. Testing procedures and methodology, and closure measurement techniques, are described in detail. The strain levels chosen for the study cover from predominantly elastic to grossly plastic strains. Crack closure measurements are made at different crack lengths. The study reveals that, at high strains, cracks close only as the lowest stress level in the cycle is approached. The crack opening is observed to occur in the compressive part of the loading cycle. The applied stress needed to open a short crack under high strain is found to be less than for cracks under small scale yielding. For increased plastic deformations, the value of σ_{op}/σ_{max} is observed to decrease and approaches the value of R. Comparison of the experimental results with existing analysis is made and indicates the limitations of the small scale yielding approach where gross plastic deformation behavior occurs. Author

N86-17789*# National Aeronautics and Space Administration. Lewis Research Center, Cleveland, Ohio.

NONLINEAR BENDING-TORSIONAL VIBRATION AND STABILITY OF ROTATING, PRETWISTED, PRECONED BLADES INCLUDING CORIOLIS EFFECTS

K. B. SUBRAHMANYAM (Toledo Univ., Ohio), K. R. V. KAZA, G. V. BROWN, and C. LAWRENCE Jan. 1986 36 p refs Presented at Workshop on Dynamics and Aeroelastic Stability Modeling of Rotor Systems, Atlanta, Ga., 4-5 Dec. 1985; sponsored by Army and Georgia Inst. of Technology, Atlanta

(NASA-TM-87207; NAS 1.15:87207) Avail: NTIS HC A03/MF A01 CSCL 20K

The coupled bending-bending-torsional equations of dynamic motion of rotating, linearly pretwisted blades are derived including

large precone, second degree geometric nonlinearities and Coriolis effects. The equations are solved by the Galerkin method and a linear perturbation technique. Accuracy of the present method is verified by comparisons of predicted frequencies and steady state deflections with those from MSC/NASTRAN and from experiments. Parametric results are generated to establish where inclusion of only the second degree geometric nonlinearities is adequate. The nonlinear terms causing torsional divergence in thin blades are identified. The effects of Coriolis terms and several other structurally nonlinear terms are studied, and their relative importance is examined. Author

N86-18750*# National Aeronautics and Space Administration. Lewis Research Center, Cleveland, Ohio.

ESTIMATING THE R-CURVE FROM RESIDUAL STRENGTH DATA

T. W. ORANGE 1985 17 p refs Presented at the International Conference and Exhibition on Fatigue, Corrosion Cracking, Fracture Mechanics and Failure Analysis, Salt Lake City, Utah, 2-6 Dec. 1985; sponsored by the American Society for Metals

(NASA-TM-87182; E-2832; NAS 1.15:87182) Avail: NTIS HC A02/MF A01 CSCL 20K

A method is presented for estimating the crack-extension resistance curve (R-curve) from residual-strength (maximum load against original crack length) data for precracked fracture specimens. The method allows additional information to be inferred from simple test results, and that information can be used to estimate the failure loads of more complicated structures of the same material and thickness. The fundamentals of the R-curve concept are reviewed first. Then the analytical basis for the estimation method is presented. The estimation method has been verified in two ways. Data from the literature (involving several materials and different types of specimens) are used to show that the estimated R-curve is in good agreement with the measured R-curve. A recent predictive blind round-robin program offers a more crucial test. When the actual failure loads are disclosed, the predictions are found to be in good agreement. Author

N86-19663*# National Aeronautics and Space Administration. Lewis Research Center, Cleveland, Ohio.

COMPUTATIONAL ENGINE STRUCTURAL ANALYSIS

C. C. CHAMIS and R. H. JOHNS 1986 20 p refs Proposed for presentation at the 31st International Gas Turbine Conference and Exhibit, Dusseldorf, West Germany, 8-12 Jun. 1986; sponsored by American Society of Mechanical Engineers

(NASA-TM-87231; E-2898; NAS 1.15:87231) Avail: NTIS HC A02/MF A01 CSCL 20K

A significant research activity at the NASA Lewis Research Center is the computational simulation of complex multidisciplinary engine structural problems. This simulation is performed using computational engine structural analysis (CESA) which consists of integrated multidisciplinary computer codes in conjunction with computer post-processing for problem-specific application. A variety of the computational simulations of specific cases are described in some detail in this paper. These case studies include: (1) aeroelastic behavior of bladed rotors, (2) high velocity impact of fan blades, (3) blade-loss transient response, (4) rotor/stator/squeeze-film/bearing interaction, (5) blade-fragment/rotor-burst containment, and (6) structural behavior of advanced swept turboprops. These representative case studies are selected to demonstrate the breadth of the problems analyzed and the role of the computer including post-processing and graphical display of voluminous output data. Author

N86-21909*# Ohio State Univ., Columbus. Dept. of Engineering Mechanics.

EXTENSIONS OF THE RITZ-GALERKIN METHOD FOR THE FORCED, DAMPED VIBRATIONS OF STRUCTURAL ELEMENTS

A. W. LEISSA and T. H. YOUNG /in AFWAL Vibration Damping 1984 Workshop Proceedings 21 p Nov. 1984

(Contract NAG3-424)

Avail: NTIS HC A99/MF A01 CSCL 20K

The Ritz-Galerkin methods were used to obtain approximate solutions for free undamped, vibration problems. It is demonstrated that these same methods may be used straightforwardly to analyze forced vibrations with damping without requiring the free vibration eigenfunctions. It was shown that the Galerkin method is an effective technique for these types of problems. The Ritz method has the advantage that it does not need to satisfy the force-type boundary conditions, which is particularly important for plates and shells. Proper functionals representing the forcing and damping terms were developed. Two types of damping--viscous and material (hysteretic) are discussed. Distributed and concentrated exciting forces are treated. Numerical results are obtained for cantilevered beams and rectangular plates. The rates of convergence of the solutions are shown. Approximate solutions from the present methods are compared with the exact solutions for the cantilever beam.

E.A.K.

N86-21932*# General Electric Co., Cincinnati, Ohio. Aircraft Engine Business Group.

BURNER LINER THERMAL-STRUCTURAL LOAD MODELING

R. MAFFEO 1986 205 p

(Contract NAS3-23272)

(NASA-CR-174892; NAS 1.26:174892) Avail: NTIS HC A10/MF A01 CSCL 20K

The software package Transfer Analysis Code to Interface Thermal/Structural Problems (TRANCITS) was developed. The TRANCITS code is used to interface temperature data between thermal and structural analytical models. The use of this transfer module allows the heat transfer analyst to select the thermal mesh density and thermal analysis code best suited to solve the thermal problem and gives the same freedoms to the stress analyst, without the efficiency penalties associated with common meshes and the accuracy penalties associated with the manual transfer of thermal data.

E.A.K.

N86-21951*# Syracuse Univ., N. Y. Dept. of Mechanical and Aerospace Engineering.

FATIGUE CRACK GROWTH UNDER GENERAL-YIELDING CYCLIC-LOADING

Z. MINZHONG and H. W. LIU Feb. 1986 28 p refs

(Contract NAG3-348)

(NASA-CR-175049; NAS 1.26:175049) Avail: NTIS HC A03/MF A01 CSCL 20K

In low cycle fatigue, cracks are initiated and propagated under general yielding cyclic loading. For general yielding cyclic loading, Dowling and Begley have shown that fatigue crack growth rate correlates well with the measured delta J. The correlation of da/dN with delta J was also studied by a number of other investigators. However, none of these studies have correlated da/dN with delta J calculated specifically for the test specimens. Solomon measured fatigue crack growth in specimens in general yielding cyclic loading. The crack tips fields for Solomon's specimens are calculated using the finite element method and the J values of Solomon's tests are evaluated. The measured crack growth rate in Solomon's specimens correlates very well with the calculated delta J.

Author

N86-21952*# Cincinnati Univ., Ohio. Dept. of Aerospace Engineering and Engineering Mechanics.

ANISOTROPIC CONSTITUTIVE MODEL FOR NICKEL BASE SINGLE CRYSTAL ALLOYS: DEVELOPMENT AND FINITE ELEMENT IMPLEMENTATION Final Report

L. T. DAME and D. C. STOFFER Mar. 1986 130 p refs

(Contract NAG3-511)

(NASA-CR-175015; NAS 1.26:175015) Avail: NTIS HC A07/MF A01 CSCL 20K

A tool for the mechanical analysis of nickel base single crystal superalloys, specifically Rene N4, used in gas turbine engine components is developed. This is achieved by a rate dependent anisotropic constitutive model implemented in a nonlinear three dimensional finite element code. The constitutive model is developed from metallurgical concepts utilizing a crystallographic approach. A non Schmid's law formulation is used to model the tension/compression asymmetry and orientation dependence in octahedral slip. Schmid's law is a good approximation to the inelastic response of the material in cube slip. The constitutive equations model the tensile behavior, creep response, and strain rate sensitivity of these alloys. Methods for deriving the material constants from standard tests are presented. The finite element implementation utilizes an initial strain method and twenty noded isoparametric solid elements. The ability to model piecewise linear load histories is included in the finite element code. The constitutive equations are accurately and economically integrated using a second order Adams-Moulton predictor-corrector method with a dynamic time incrementing procedure. Computed results from the finite element code are compared with experimental data for tensile, creep and cyclic tests at 760 deg C. The strain rate sensitivity and stress relaxation capabilities of the model are evaluated.

Author

N86-25822*# National Aeronautics and Space Administration. Lewis Research Center, Cleveland, Ohio.

CYCLIC CREEP ANALYSIS FROM ELASTIC FINITE-ELEMENT SOLUTIONS

A. KAUFMAN and S. Y. HWANG (South Carolina State Coll., Orangeburg) 1986 21 p refs Presented at the Southeastern Conference on Theoretical and Applied Mechanics, Columbia, S.C., 17-18 Apr. 1986

(NASA-TM-87213; E-2872; NAS 1.15:87213) Avail: NTIS HC A02/MFA01 CSCL 20K

A uniaxial approach was developed for calculating cyclic creep and stress relaxation at the critical location of a structure subjected to cyclic thermomechanical loading. This approach was incorporated into a simplified analytical procedure for predicting the stress-strain history at a crack initiation site for life prediction purposes. An elastic finite-element solution for the problem was used as input for the simplified procedure. The creep analysis includes a self-adaptive time incrementing scheme. Cumulative creep is the sum of the initial creep, the recovery from the stress relaxation and the incremental creep. The simplified analysis was exercised for four cases involving a benchmark notched plate problem. Comparisons were made with elastic-plastic-creep solutions for these cases using the MARC nonlinear finite-element computer code.

Author

N86-25850*# Michigan State Univ., East Lansing. Dept. of Metallurgy, Mechanics and Materials Science.

EXPERIMENTAL EVALUATION CRITERIA FOR CONSTITUTIVE MODELS OF TIME DEPENDENT CYCLIC PLASTICITY Final Report, 1 Jun. 1980 - 30 Sep. 1983

J. F. MARTIN 1986 13 p

(Contract NAG3-51)

(NASA-CR-176821; NAS 1.26:176821) Avail: NTIS HC A02/MF A01 CSCL 20K

Notched members were tested at temperatures far above those recorded till now. Simulation of the notch root stress response was accomplished to establish notch stress-strain behavior. Cyclic stress-strain profiles across the net-section were recorded and on-line direct notch strain control was accomplished. Data are compared to three analysis techniques with good results. The

39 STRUCTURAL MECHANICS

objective of the study is to generate experimental data that can be used to evaluate the accuracy of constitutive models of time dependent cyclic plasticity. Author

N86-25851*# Case Western Reserve Univ., Cleveland, Ohio.
FATIGUE CRACK LAYER PROPAGATION IN SILICON-IRON Final Report
Y. BIROL, G. WELSCH, and A. CHUDNOVSKY May 1986 47 p refs
(Contract NAG3-223)
(NASA-CR-175115; NAS 1.26:175115) Avail: NTIS HC A03/MF A01 CSCL 20K

Fatigue crack propagation in metal is almost always accompanied by plastic deformation unless conditions strongly favor brittle fracture. The analysis of the plastic zone is crucial to the understanding of crack propagation behavior as it governs the crack growth kinetics. This research was undertaken to study the fatigue crack propagation in a silicon iron alloy. Kinetic and plasticity aspects of fatigue crack propagation in the alloy were obtained, including the characterization of damage evolution. Author

N86-26651*# National Aeronautics and Space Administration. Lewis Research Center, Cleveland, Ohio.
LOW-CYCLE THERMAL FATIGUE
G. R. HALFORD Feb. 1986 114 p refs
(NASA-TM-87225; E-2890; NAS 1.15:87225) Avail: NTIS HC A06/MF A01 CSCL 20K

A state-of-the-art review is presented of the field of thermal fatigue. Following a brief historical review, the concept is developed that thermal fatigue can be viewed as processes of unbalanced deformation and cracking. The unbalances refer to dissimilar mechanisms occurring in opposing halves of thermal fatigue loading and unloading cycles. Extensive data summaries are presented and results are interpreted in terms of the unbalanced processes involved. Both crack initiation and crack propagation results are summarized. Testing techniques are reviewed, and considerable discussion is given to a technique for thermal fatigue simulation, known as the bithermal fatigue test. Attention is given to the use of isothermal life prediction methods for the prediction of thermal fatigue lives. Shortcomings of isothermally-based life prediction methods are pointed out. Several examples of analyses and thermal fatigue life predictions of high technology structural components are presented. Finally, numerous dos and don'ts relative to design against thermal fatigue are presented. Author

N86-26652*# Battelle Columbus Labs., Ohio.
NONLINEAR DAMAGE ANALYSIS: POSTULATE AND EVALUATION Final Report, 30 Sep. 1981 - 6 Apr. 1983
B. N. LEIS and T. P. FORTE 6 Apr. 1983 101 p refs
(Contract NAS3-22825)
(NASA-CR-168171; NAS 1.26:168171) Avail: NTIS HC A06/MF A01 CSCL 20K

The objective of this program is to assess the viability of a damage postulate which asserts that the fatigue resistance curve of a metal is history dependent due to inelastic action. The study focusses on OFE copper because this simple model material accentuates the inelastic action central to the damage postulate. Data relevant to damage evolution and crack initiation are developed via a study of surface topography. The effects of surface layer residual stresses are explored via comparative testing as were the effects in initial prestraining. The results of the study very clearly show the deformation history dependence of the fatigue resistance of OFE copper. Furthermore the concept of deformation history dependence is shown to qualitatively explain the fatigue resistance of all histories considered. Likewise quantitative predictions for block cycle histories are found to accurately track the observed results. In this respect the assertion that damage per cycle for a given level of the damage parameter is deformation history dependent appears to be physically justified. Author

N86-27680*# National Aeronautics and Space Administration. Lewis Research Center, Cleveland, Ohio.

RE-EXAMINATION OF CUMULATIVE FATIGUE DAMAGE ANALYSIS: AN ENGINEERING PERSPECTIVE

S. S. MANSON and G. R. HALFORD 1986 71 p Presented at the Symposium on Mechanics of Damage and Fatigue, Haifa-Tel Aviv, Israel, 1-5 Jul. 1985; sponsored by the International Union of Theoretical and Applied Mechanics
(NASA-TM-87325; E-3066; NAS 1.15:87325) Avail: NTIS HC A04/MF A01 CSCL 20K

A method which has evolved in our laboratories for the past 20 yr is re-examined with the intent of improving its accuracy and simplicity of application to engineering problems. Several modifications are introduced both to the analytical formulation of the Damage Curve Approach, and to the procedure for modifying this approach to achieve a Double Linear Damage Rule formulation which immensely simplifies the calculation. Improvements are also introduced in the treatment of mean stress for determining fatigue life of the individual events that enter into a complex loading history. While the procedure is completely consistent with the results of numerous two level tests that have been conducted on many materials, it is still necessary to verify applicability to complex loading histories. Caution is expressed that certain phenomena can also influence the applicability - for example, unusual deformation and fracture modes inherent in complex loading - especially if stresses are multiaxial. Residual stresses at crack tips, and metallurgical factors are also important in creating departures from the cumulative damage theories; examples of departures are provided. Author

N86-27689*# Argonne National Lab., Ill. **EFFECTS OF A HIGH MEAN STRESS ON THE HIGH CYCLE FATIGUE LIFE OF PWA 1480 AND CORRELATION OF DATA BY LINEAR ELASTIC FRACTURE MECHANICS**

S. MAJUMDAR and R. KWASNY Nov. 1985 28 p
(Contract NASA ORDER C-91113-D; W-31-109-ENG-38)
(NASA-CR-175057; NAS 1.26:175057; ANL-85-74) Avail: NTIS HC A03/MF A01 CSCL 20K

High-cycle fatigue tests using 5-mm-diameter smooth specimens were performed on the single crystal alloy PWA 1480 (001 axis) at 70F (room temperature) in air and at 100F (538C) in vacuum (10 to the -6 power torr). Tests were conducted at zero mean stress as well as at high tensile mean stress. The results indicate that, although a tensile mean stress, in general, reduces life, the reduction in fatigue strength, for a given mean stress at a life of one million cycles, is much less than what is predicted by the usual linear Goodman plot. Further, the material appears to be significantly more resistant to mean stress effects at 1000F than at 70F. Metallographic examinations of failed specimens indicate that failures in all cases are initiated from micropores of sizes of the order of 30 to 40 microns. Since the macroscopic stress-strain response in all cases was observed to be linear elastic, linear elastic fracture mechanics (LEFM) analyses were carried out to determine the crack growth curves of the material assuming that crack initiation from a micropore (a sub $a = 40$ microns) occurs very early in life. The results indicate that the calculated crack growth rates at an R (defined as the ratio between minimum stress to maximum stress) value of zero are approximately the same at 70F as at 1000F. However, the calculated crack growth rates at other R ratios, both positive and negative, tend to be higher at 70F than at 1000F. Calculated threshold effects at large R values tend to be independent of temperature in the temperature regime studied. They are relatively constant with increasing R ratio up to a value of about 0.6, beyond which the calculated threshold stress intensity factor range decreases rapidly with increasing R ratios. Author

N86-28455*# Texas A&M Univ., College Station. Dept. of Aerospace Engineering.

INTEGRATED RESEARCH IN CONSTITUTIVE MODELLING AT ELEVATED TEMPERATURES, PART 2 Final Report

W. E. HAISLER and D. H. ALLEN Jun. 1986 224 p
(Contract NAG3-491)
(NASA-CR-177233; NAS 1.26:177233; MM-4998-86-13-PT-2)
Avail: NTIS HC A10/MF A01 CSCL 20K

Four current viscoplastic models are compared experimentally with Inconel 718 at 1100 F. A series of tests were performed to create a sufficient data base from which to evaluate material constants. The models used include Bodner's anisotropic model; Krieg, Swearingen, and Rhode's model; Schmidt and Miller's model; and Walker's exponential model.

N86-28461*# National Aeronautics and Space Administration. Lewis Research Center, Cleveland, Ohio.

STRUCTURAL ANALYSIS OF TURBINE BLADES USING UNIFIED CONSTITUTIVE MODELS

A. KAUFMAN, M. TONG, J. F. SALTSMAN, and G. R. HALFORD 1986 12 p Proposed for presentation at the International Conference on Computers in Engine Technology, Cambridge, England, 24-27 Mar. 1987; sponsored by the Institution of Mechanical Engineers
(NASA-TM-88807; E-3155; NAS 1.15:88807) Avail: NTIS HC A02/MF A01 CSCL 20K

The utility of advanced constitutive models and structural analysis methods in predicting the cyclic life of an air-cooled turbine blade is assessed. Five structural analysis methods were exercised in calculating the cyclic stress-strain response at the airfoil critical location. The methods studied were a cyclic elastic finite-element analysis, nonlinear finite-element analyses based on classical inelastic models and the unified models of Bodner and Walker, and a simplified inelastic procedure. These analyses were compared in terms of computing times and of predicted crack initiation lives using the Strainrange Partitioning method. Author

N86-28462*# Georgia Inst. of Tech., Atlanta. School of Engineering Science and Mechanics.

FORMULATION OF THE NONLINEAR ANALYSIS OF SHELL-LIKE STRUCTURES, SUBJECTED TO TIME-DEPENDENT MECHANICAL AND THERMAL LOADING Interim Technical Report, 15 Apr. 1984 - 14 Apr. 1986

G. J. SIMITSES, R. L. CARLSON, and R. RIFF 28 Jul. 1986 178 p
(Contract NAG3-534)
(NASA-CR-177194; NAS 1.26:177194) Avail: NTIS HC A09/MF A01 CSCL 20K

A general mathematical model and solution methodologies for analyzing the structural response of thin, metallic shell structures under large transient, cyclic, or static thermomechanical loads was sought. Among the system responses associated with these loads and conditions are thermal buckling, creep buckling, and ratcheting. Thus geometric and material nonlinearities (of high order) can be anticipated and must be considered in developing the mathematical model. A complete, true ab-initio rate theory of kinematics and kinetics for continuum ad curved thin structures, without any restriction on the magnitude of the strains or the deformations, was formulated. The time dependence and large strain behavior are incorporated through the introduction of the time rates of metric and curvature in two coordinate systems: fixed (spatial) and convected (material). The relations between the time derivative and the covariant derivative (gradient) was developed for curved space and motion, so the velocity components supply the connection between the equations of motion and the time rates of change of the metric and curvature tensors. A time and temperature dependent viscoplasticity model was formulated to account for finite strains and rotations. Author

N86-28464*# National Aeronautics and Space Administration. Lewis Research Center, Cleveland, Ohio.

THERMAL-FATIGUE AND OXIDATION RESISTANCE OF COBALT-MODIFIED UDIMET 700 ALLOY

P. T. BIZON and B. J. BARROW Apr. 1986 15 p
(NASA-TP-2591; E-2704; NAS 1.60:2591) Avail: NTIS HC A02/MF A01 CSCL 20K

Comparative thermal-fatigue and oxidation resistances of cobalt-modified wrought Udimet 700 alloy (obtained by reducing the cobalt level by direct substitution of nickel) were determined from fluidized-bed tests. Bed temperatures were 1010 and 288 C (1850 and 550 C) for the first 5500 symmetrical 6-min cycles. From cycle 5501 to the 14000-cycle limit of testing, the heating bed temperature was increased to 1050 C (1922 F). Cobalt levels between 0 and 17 wt% were studied in both the bare and NiCrAlY overlay coated conditions. A cobalt level of about 8 wt% gave the best thermal-fatigue life. The conventional alloy specification is for 18.5% cobalt, and hence, a factor of 2 in savings of cobalt could be achieved by using the modified alloy. After 13500 cycles, all bare cobalt-modified alloys lost 10 to 13 percent of their initial weight. Application of the NiCrAlY overlay coating resulted in weight losses of 1/20 to 1/100 of that of the corresponding bare alloy. Author

N86-28467*# Virginia Polytechnic Inst. and State Univ., Blacksburg. Dept. of Engineering Science and Mechanics.

J-INTEGRAL ESTIMATES FOR CRACKS IN INFINITE BODIES Final Report

N. E. DOWLING Jul. 1986 42 p
(Contract NAG3-438)
(NASA-CR-179474; NAS 1.26:179474) Avail: NTIS HC A03/MF A01 CSCL 20K

An analysis and discussion is presented of existing estimates of the J-integral for cracks in infinite bodies. Equations are presented which provide convenient estimates for Ramberg-Osgood type elastoplastic materials containing cracks and subjected to multiaxial loading. The relationship between J and the strain normal to the crack is noted to be only weakly dependent on state of stress. But the relationship between J and the stress normal to the crack is strongly dependent on state of stress. A plastic zone correction term often employed is found to be arbitrary, and its magnitude is seldom significant. Author

N86-29271*# National Aeronautics and Space Administration. Lewis Research Center, Cleveland, Ohio.

EXPERIMENTAL CLASSICAL FLUTTER RESULTS OF A COMPOSITE ADVANCED TURBOPROP MODEL

O. MEHMED and K. R. V. KAZA Jul. 1986 18 p Presented at the Bisplinghoff Memorial Symposium on Recent Trends in Aeroelasticity, Structures and Structural Dynamics, Gainesville, Fla., 6-7 Feb., 1986; sponsored by Fla. Univ.
(NASA-TM-88792; E-3127; NAS 1.15:88792) Avail: NTIS HC A02/MF A01 CSCL 20K

Experimental results are presented that show the effects of blade pitch angle and number of blades on classical flutter of a composite advanced turboprop (propfan) model. An increase in the number of blades on the rotor or the blade pitch angle is destabilizing which shows an aerodynamic coupling or cascade effect between blades. The flutter came in suddenly and all blades vibrated at the same frequency but at different amplitudes and with a common predominant phase angle between consecutive blades. This further indicates aerodynamic coupling between blades. The flutter frequency was between the first two blade normal modes, signifying an aerodynamic coupling between the normal modes. Flutter was observed at all blade pitch angles from small to large angles-of-attack of the blades. A strong blade response occurred, for four blades at the two-per-revolution (2P) frequency, when the rotor speed was near the crossing of the flutter mode frequency and the 2P order line. This is because the damping is low near the flutter condition and the interblade phase angle of the flutter mode and the 2P response are the same. Author

39 STRUCTURAL MECHANICS

N86-30227*# Texas A&M Univ., College Station. Dept. of Aerospace Engineering.

INTEGRATED RESEARCH IN CONSTITUTIVE MODELLING AT ELEVATED TEMPERATURES, PART 1 Final Report

W. E. HAISLER and D. H. ALLEN Jun. 1986 332 p
(Contract NAG3-491)
(NASA-CR-177237; NAS 1.26:177237; MM-4998-86-13-PT-1)
Avail: NTIS HC A15/MF A01 CSCL 20K

Topics covered include: numerical integration techniques; thermodynamics and internal state variables; experimental lab development; comparison of models at room temperature; comparison of models at elevated temperature; and integrated software development.

N86-30236*# Cleveland State Univ., Ohio. Dept. of Civil Engineering.

COMPLIANCE MATRICES FOR CRACKED BODIES Final Report

R. BALLARINI Jul. 1986 8 p
(Contract NCC3-46)
(NASA-CR-179478; E-3158; NAS 1.26:179478) Avail: NTIS HC A02/MF A01 CSCL 20K

An algorithm is presented which can be used to develop compliance matrices for cracked bodies. The method relies on the numerical solution of singular integral equations with Cauchy-type kernels and provides an efficient and accurate procedure for relating applied loadings to crack opening displacements. The algorithm should be of interest to those performing repetitive calculations in the analysis of experimental results obtained from fracture specimens. Author

N86-31920*# National Aeronautics and Space Administration. Lewis Research Center, Cleveland, Ohio.

INFLUENCE OF THIRD-DEGREE GEOMETRIC NONLINEARITIES ON THE VIBRATION AND STABILITY OF PRETWISTED, PRECONED, ROTATING BLADES

K. B. SUBRAHMANYAM and K. R. V. KAZA May 1986 43 p
(NASA-TM-87307; E-2988; NAS 1.15:87307) Avail: NTIS HC A03/MF A01 CSCL 20K

The governing coupled flapwise bending, edgewise bending, and torsional equations are derived including third-degree geometric nonlinear elastic terms by making use of the geometric nonlinear theory of elasticity in which the elongations and shears are negligible compared to unity. These equations are specialized for blades of doubly symmetric cross section with linear variation of pretwist over the blade length. The nonlinear steady state equations and the linearized perturbation equations are solved by using the Galerkin method, and by utilizing the nonrotating normal modes for the shape functions. Parametric results obtained for various cases of rotating blades from the present theoretical formulation are compared to those produced from the finite element code MSC/NASTRAN, and also to those produced from an in-house experimental test rig. It is shown that the spurious instabilities, observed for thin, rotating blades when second degree geometric nonlinearities are used, can be eliminated by including the third-degree elastic nonlinear terms. Furthermore, inclusion of third degree terms improves the correlation between the theory and experiment. M.G.

N87-11180*# National Aeronautics and Space Administration. Lewis Research Center, Cleveland, Ohio.

TURBINE ENGINE HOT SECTION TECHNOLOGY, 1984

Oct. 1984 400 p Conference held in Cleveland, Ohio, 23-24 Oct. 1984
(NASA-CP-2339; E-2267; NAS 1.55:2339) Avail: NTIS HC A17/MF A01 CSCL 20K

Presentations were made concerning the hot section environment and behavior of combustion liners, turbine blades, and waves. The presentations were divided into six sessions: instrumentation, combustion, turbine heat transfer, structural analysis, fatigue and fracture, and surface properties. The principal objective of each session was to disseminate research results to date, along with future plans. Topics discussed included modeling

of thermal and fluid flow phenomena, structural analysis, fatigue and fracture, surface protective coatings, constitutive behavior, stress-strain response, and life prediction methods.

N87-11183*# National Aeronautics and Space Administration. Lewis Research Center, Cleveland, Ohio.

FATIGUE AND FRACTURE: OVERVIEW

G. R. HALFORD *In its Turbine Engine Hot Section Technology*, 1984 4 p Oct. 1984

Avail: NTIS HC A17/MF A01 CSCL 20K

A brief overview of the status of the fatigue and fracture programs is given. The programs involve the development of appropriate analytic material behavior models for cyclic stress-strain-temperature-time/cyclic crack initiation, and cyclic crack propagation. The underlying thrust of these programs is the development and verification of workable engineering methods for the calculation, in advance of service, of the local cyclic stress-strain response at the critical life governing location in hot section compounds, and the resultant crack initiation and crack growth lifetimes. B.G.

N87-11209*# National Aeronautics and Space Administration. Lewis Research Center, Cleveland, Ohio.

HIGH TEMPERATURE STRESS-STRAIN ANALYSIS

R. L. THOMPSON *In its Turbine Engine Hot Section Technology*, 1984 14 p Oct. 1984

Avail: NTIS HC A17/MF A01 CSCL 20K

The objectives are threefold: to assist in developing predictive tools needed to improve design analyses and procedures for the efficient and accurate prediction of burner liner structural performance and response; to calibrate, validate, and evaluate these predictive tools by comparing the predicted results with the experimental data; and to evaluate existing as well as advanced temperature and strain measurement instrumentation, through both contact and noncontact efforts, in a simulated turbine engine combustor environment. As the predictive tool, tests, test methods, instrumentation, and data acquisition and reduction methods are developed and evaluated, a proven, integrated analysis/experiment method will be developed that will permit the accurate prediction of the cyclic life of a burner liner. Author

N87-12017*# National Aeronautics and Space Administration. Lewis Research Center, Cleveland, Ohio.

CONCENTRATED MASS EFFECTS ON THE FLUTTER OF A COMPOSITE ADVANCED TURBOPROP MODEL

J. K. RAMSEY and K. R. V. KAZA Oct. 1986 22 p
(NASA-TM-88854; E-3247; NAS 1.15:88854) Avail: NTIS HC A02/MF A01 CSCL 20K

The effects on bending-torsion flutter due to the addition of a concentrated mass to an advanced turboprop model blade with rigid hub are studied. Specifically the effects of the magnitude and location of added mass on the natural frequencies, mode shapes, critical interblade phase angle, and flutter Mach number are analytically investigated. The flutter of a propfan model is shown to be sensitive to the change in mass distribution. Static unbalance effects, like those for fixed wings, were shown to occur as the concentrated mass was moved from the leading edge to the trailing edge with the exception of one mass location. Mass balancing is also inferred to be a feasible method for increasing the flutter speed. Author

N87-12924*# National Aeronautics and Space Administration. Lewis Research Center, Cleveland, Ohio.

A CONSTITUTIVE LAW FOR FINITE ELEMENT CONTACT PROBLEMS WITH UNCLASSICAL FRICTION

M. E. PLESHA and B. M. STEINETZ Nov. 1986 19 p
(NASA-TM-88838; E-3181; NAS 1.15:88838; ICOMP-86-1) Avail: NTIS HC A02/MF A01 CSCL 20K

Techniques for modeling complex, unclassical contact-friction problems arising in solid and structural mechanics are discussed. A constitutive modeling concept is employed whereby analytic relations between increments of contact surface stress (i.e., traction) and contact surface deformation (i.e., relative

displacement) are developed. Because of the incremental form of these relations, they are valid for arbitrary load-deformation histories. The motivation for the development of such a constitutive law is that more realistic friction idealizations can be implemented in finite element analysis software in a consistent, straightforward manner. Of particular interest is modeling of two-body (i.e., unlubricated) metal-metal, ceramic-ceramic, and metal-ceramic contact. Interfaces involving ceramics are of engineering importance and are being considered for advanced turbine engines in which higher temperature materials offer potential for higher engine fuel efficiency. Author

N87-13794*# National Aeronautics and Space Administration. Lewis Research Center, Cleveland, Ohio.

PROBABILISTIC STRUCTURAL ANALYSIS METHODS FOR SPACE PROPULSION SYSTEM COMPONENTS

C. C. CHAMIS 1986 25 p Presented at the 3rd Space Systems Technology Conference, San Diego, Calif., 9-12 Jun. 1986; sponsored by the American Institute of Aeronautics and Astronautics (NASA-TM-88861; E-3015; NAS 1.15:88861) Avail: NTIS HC A02/MF A01 CSCL 46E

The development of a three-dimensional inelastic analysis methodology for the Space Shuttle main engine (SSME) structural components is described. The methodology is composed of: (1) composite load spectra, (2) probabilistic structural analysis methods, (3) the probabilistic finite element theory, and (4) probabilistic structural analysis. The methodology has led to significant technical progress in several important aspects of probabilistic structural analysis. The program and accomplishments to date are summarized. Author

N87-14730*# National Aeronautics and Space Administration. Lewis Research Center, Cleveland, Ohio.

A LOW-COST OPTICAL DATA ACQUISITION SYSTEM FOR VIBRATION MEASUREMENT

S. J. POSTA and G. V. BROWN Dec. 1986 21 p (NASA-TM-88907; E-3330; NAS 1.15:88907) Avail: NTIS HC A02/MF A01 CSCL 20K

A low cost optical data acquisition system was designed to measure deflection of vibrating rotor blade tips. The basic principle of the new design is to record raw data, which is a set of blade arrival times, in memory and to perform all processing by software following a run. This approach yields a simple and inexpensive system with the least possible hardware. Functional elements of the system were breadboarded and operated satisfactorily during rotor simulations on the bench, and during a data collection run with a two-bladed rotor in the Lewis Research Center Spin Rig. Software was written to demonstrate the sorting and processing of data stored in the system control computer, after retrieval from the data acquisition system. The demonstration produced an accurate graphical display of deflection versus time. Author

N87-16321*# National Aeronautics and Space Administration. Lewis Research Center, Cleveland, Ohio.

THE 20TH AEROSPACE MECHANICS SYMPOSIUM

May 1986 316 p Symposium held in Cleveland, Ohio, 7-9 May 1986; sponsored by NASA, the California Inst. of Tech. and LMSC (NASA-CP-2423-REV; E-2904; NAS 1.55:2423-REV) Avail: NTIS HC A14/MF A01 CSCL 20K

Numerous topics related to aerospace mechanisms were discussed. Deployable structures, electromagnetic devices, tribology, hydraulic actuators, positioning mechanisms, electric motors, communication satellite instruments, redundancy, lubricants, bearings, space stations, rotating joints, and teleoperators are among the topics covered.

N87-17087*# National Aeronautics and Space Administration. Lewis Research Center, Cleveland, Ohio.

SURFACE FLAW RELIABILITY ANALYSIS OF CERAMIC COMPONENTS WITH THE SCARE FINITE ELEMENT POSTPROCESSOR PROGRAM

JOHN P. GYKENYESI and NOEL N. NEMETH (WLT Corp., Cleveland, Ohio) 1987 17 p Proposed for presentation at the 32nd International Gas Turbine Conference and Exhibit, Anaheim, Calif., 31 May - 4 Jun. 1987; sponsored by ASME (NASA-TM-88901; E-3229; NAS 1.15:88901) Avail: NTIS HC A02/MF A01 CSCL 20K

The SCARE (Structural Ceramics Analysis and Reliability Evaluation) computer program on statistical fast fracture reliability analysis with quadratic elements for volume distributed imperfections is enhanced to include the use of linear finite elements and the capability of designing against concurrent surface flaw induced ceramic component failure. The SCARE code is presently coupled as a postprocessor to the MSC/NASTRAN general purpose, finite element analysis program. The improved version now includes the Weibull and Batdorf statistical failure theories for both surface and volume flaw based reliability analysis. The program uses the two-parameter Weibull fracture strength cumulative failure probability distribution model with the principle of independent action for poly-axial stress states, and Batdorf's shear-sensitive as well as shear-insensitive statistical theories. The shear-sensitive surface crack configurations include the Griffith crack and Griffith notch geometries, using the total critical coplanar strain energy release rate criterion to predict mixed-mode fracture. Weibull material parameters based on both surface and volume flaw induced fracture can also be calculated from modulus of rupture bar tests, using the least squares method with known specimen geometry and grouped fracture data. The statistical fast fracture theories for surface flaw induced failure, along with selected input and output formats and options, are summarized. An example problem to demonstrate various features of the program is included. Author

N87-18112*# National Aeronautics and Space Administration. Lewis Research Center, Cleveland, Ohio.

THE EFFECT OF NONLINEARITIES ON THE DYNAMIC RESPONSE OF A LARGE SHUTTLE PAYLOAD

TIMOTHY L. SULLIVAN and KELLY S. CARNEY 1987 31 p Proposed for presentation at the 28th Structures, Structural Dynamics and Materials Conference, Monterey, Calif., 6-8 Apr. 1987; sponsored by AIAA (NASA-TM-88941; E-3387; NAS 1.15:88941) Avail: NTIS HC A03/MF A01 CSCL 20K

The STS Centaur was designed to be a high energy upper stage for use with the Space Shuttle. Two versions were designed under development when the program was cancelled. The first version, designated G-prime, was for planetary missions. The second version, designated G, was to place spacecraft in geosynchronous orbit. As a part of the STS Centaur finite-element model verification effort, test articles of both versions were subjected to a series of static tests. In addition the Centaur G-prime test article was subjected to a series of dynamic tests including a modal survey. Both the static and dynamic tests showed that nonlinearities existed in the Centaur and its support system. The support system included flight-like latches. The nonlinearities were particularly apparent in tests that loaded the forward support structure of the Centaur. These test results were used to aid in the development of two improved finite-element models. The first was a linear model, while the second contained nonlinear elements at the boundaries. Results from both models were compared with the transient response obtained from a step-relaxation or twang test. The linear model was able to accurately match the low frequency response found in the test data. However, only the nonlinear model was able to match higher frequency response that was present in some of the test data. In addition the nonlinear model was able to predict other nonlinear behavior such as the dynamic jump that occurs in systems with nonlinear stiffness. Author

N87-18115*# National Aeronautics and Space Administration. Lewis Research Center, Cleveland, Ohio.

ANALYTICAL FLUTTER INVESTIGATION OF A COMPOSITE PROPFAN MODEL

K. R. V. KAZA, O. MEHMED, G. V. NARAYANAN (Sverdrup Technology, Inc., Cleveland, Ohio), and D. V. MURTHY (Toledo Univ., Ohio) 1987 24 p Proposed for presentation at the 28th Structures, Structural Dynamics and Materials Conference, Monterey, Calif., 6-8 Apr. 1987; sponsored by AIAA, ASME, AHS and ASEE

(NASA-TM-88944; E-3392; NAS 1.15:88944; AIAA-87-0738)

Avail: NTIS HC A02/MF A01 CSCL 20K

A theoretical model and an associated computer program for predicting subsonic bending-torsion flutter in propfans are presented. The model is based on two-dimensional unsteady cascade strip theory and three-dimensional steady and unsteady lifting surface aerodynamic theory in conjunction with a finite element structural model for the blade. The analytical results compare well with published experimental data. Additional parametric studies are also presented illustrating the effects on flutter speed of steady aeroelastic deformations, blade setting angle, rotational speed, number of blades, structural damping, and number of modes.

Author

N87-18116*# National Aeronautics and Space Administration. Lewis Research Center, Cleveland, Ohio.

ANALYTICAL AND EXPERIMENTAL INVESTIGATION OF MISTUNING IN PROPFAN FLUTTER

KRISHNA RAO V. KAZA, ORAL MEHMED, MARC WILLIAMS (Purdue Univ., West Lafayette, Ind.), and LARRY A. MOSS (Sverdrup Technology, Inc., Cleveland, Ohio) 1987 21 p Proposed for presentation at the 28th Structures, Structural Dynamics and Materials Conference, Monterey, Calif., 6-8 Apr. 1987; sponsored by AIAA, ASME, AHS and ASEE

(NASA-TM-88959; E-3412; NAS 1.15:88959; AIAA-87-0739)

Avail: NTIS HC A02/MF A01 CSCL 20K

An analytical and experimental investigation of the effects of mistuning on propfan subsonic flutter was performed. The analytical model is based on the normal modes of a rotating composite blade and a three-dimensional subsonic unsteady lifting surface aerodynamic theory. Theoretical and experimental results are compared for selected cases at different blade pitch angles, rotational speeds, and free-stream Mach numbers. The comparison shows a reasonably good agreement between theory and experiment. Both theory and experiment showed that combined mode shape, frequency, and aerodynamic mistuning can have a beneficial or adverse effect on blade damping depending on Mach number. Additional parametric results showed that alternative blade frequency mistuning does not have enough potential for it to be used as a passive flutter control in propfans similar to the one studied. It can be inferred from the results that a laminated composite propfan blade can be tailored to optimize its flutter speed by selecting the proper ply angles.

Author

N87-18881*# National Aeronautics and Space Administration. Lewis Research Center, Cleveland, Ohio.

THE EFFECTS OF CRACK SURFACE FRICTION AND ROUGHNESS ON CRACK TIP STRESS FIELDS

ROBERTO BALLARINI (Case Western Reserve Univ., Cleveland, Ohio) and MICHAEL E. PLESHA (Wisconsin Univ., Madison) Feb. 1987 19 p

(Contract NCC3-46; NASA ORDER C-99066-G;

DAAL03-86-K-0134)

(NASA-TM-88976; ICOMP-87-1; E-3445; NAS 1.15:88976) Avail:

NTIS HC A02/MF A01 CSCL 20K

A model is presented which can be used to incorporate the effects of friction and tortuosity along crack surfaces through a constitutive law applied to the interface between opposing crack surfaces. The problem of a crack with a saw-tooth surface in an infinite medium subjected to a far-field shear stress is solved and the ratios of Mode-I stress intensity to Mode-II stress intensity are calculated for various coefficients of friction and material properties. The results show that tortuosity and friction lead to an increase in

fracture loads and alter the direction of crack propagation.

Author

N87-18882*# National Aeronautics and Space Administration. Lewis Research Center, Cleveland, Ohio.

FATIGUE FAILURE OF REGENERATOR SCREENS IN A HIGH FREQUENCY STIRLING ENGINE

DAVID R. HULL, DONALD L. ALGER, THOMAS J. MOORE, and COULSON M. SCHEUERMANN Mar. 1987 22 p

(NASA-TM-88974; E-3443; NAS 1.15:88974) Avail: NTIS HC

A02/MF A01 CSCL 10B

Failure of Stirling Space Power Demonstrator Engine (SPDE) regenerator screens was investigated. After several hours of operation the SPDE was shut down for inspection and on removing the regenerator screens, debris of unknown origin was discovered along with considerable cracking of the screens in localized areas. Metallurgical analysis of the debris determined it to be cracked-off-deformed pieces of the 41 micron thickness Type 304 stainless steel wire screen. Scanning electron microscopy of the cracked screens revealed failures occurring at wire crossovers and fatigue striations on the fracture surface of the wires. Thus, the screen failure can be characterized as a fatigue failure of the wires. The crossovers were determined to contain a 30 percent reduction in wire thickness and a highly worked microstructure occurring from the manufacturing process of the wire screens. Later it was found that reduction in wire thickness occurred because the screen fabricator had subjected it to a light cold-roll process after weaving. Installation of this screen left a clearance in the regenerator allowing the screens to move. The combined effects of the reduction in wire thickness, stress concentration (caused by screen movement), and highly worked microstructure at the wire crossovers led to the fatigue failure of the screens.

Author

N87-18883*# National Aeronautics and Space Administration. Lewis Research Center, Cleveland, Ohio.

A COMPARATIVE STUDY OF SOME DYNAMIC STALL MODELS

T. S. R. REDDY (Toledo Univ., Ohio) and K. R. V. KAZA Mar. 1987 79 p

(NASA-TM-88917; E-3342; NAS 1.15:88917) Avail: NTIS HC

A05/MF A01 CSCL 20K

Three semi-empirical aerodynamic stall models are compared with respect to their lift and moment hysteresis loop prediction, limit cycle behavior, easy implementation, and feasibility in developing the parameters required for stall flutter prediction of advanced turbines. For the comparison of aeroelastic response prediction including stall, a typical section model and a plate structural model are considered. The response analysis includes both plunging and pitching motions of the blades. In model A, a correction to the angle of attack is applied when the angle of attack exceeds the static stall angle. In model B, a synthesis procedure is used for angles of attack above static stall angles and the time history effects are accounted through the Wagner function. In both models the life and moment coefficients for angle of attack below stall are obtained from tabular data for a given Mach number and angle of attack. In model C, referred to as the ONERA model, the life and moment coefficients are given in the form of two differential equations, one for angles below stall, and the other for angles above stall. The parameters of those equations are nonlinear functions of the angle of attack.

Author

N87-20565*# National Aeronautics and Space Administration. Lewis Research Center, Cleveland, Ohio.

CALCULATION OF THERMOMECHANICAL FATIGUE LIFE BASED ON ISOTHERMAL BEHAVIOR

GARY R. HALFORD and JAMES F. SALTSMAN 1987 22 p

Prepared for presentation at the 5th National Congress on Pressure Vessel and Piping Technology, San Diego, Calif., 28 Jun. - 2 Jul. 1987; sponsored by ASME

(NASA-TM-88864; E-2940; NAS 1.15:88864) Avail: NTIS HC

A02/MF A01 CSCL 20K

The isothermal and thermomechanical fatigue (TMF) crack initiation response of a hypothetical material was analyzed.

Expected thermomechanical behavior was evaluated numerically based on simple, isothermal, cyclic stress-strain - time characteristics and on strainrange versus cyclic life relations that have been assigned to the material. The attempt was made to establish basic minimum requirements for the development of a physically accurate TMF life-prediction model. A worthy method must be able to deal with the simplest of conditions: that is, those for which thermal cycling, per se, introduces no damage mechanisms other than those found in isothermal behavior. Under these assumed conditions, the TMF life should be obtained uniquely from known isothermal behavior. The ramifications of making more complex assumptions will be dealt with in future studies. Although analyses are only in their early stages, considerable insight has been gained in understanding the characteristics of several existing high-temperature life-prediction methods. The present work indicates that the most viable damage parameter is based on the inelastic strainrange. Author

N87-20566*# National Aeronautics and Space Administration. Lewis Research Center, Cleveland, Ohio.

SHOT PEENING FOR Ti-6Al-4V ALLOY COMPRESSOR BLADES

GERALD A. CAREK Apr. 1987 9 p
(NASA-TP-2711; E-3430; NAS 1.60:2711) Avail: NTIS HC A01/MF A01 CSCL 20K

A text program was conducted to determine the effects of certain shot-peening parameters on the fatigue life of the Ti-6Al-4V alloys as well as the effect of a demarcation line on a test specimen. This demarcation line, caused by an abrupt change from untreated surface to shot-peened surface, was thought to have caused the failure of several blades in a multistage compressor at the NASA Lewis Research Center. The demarcation line had no detrimental effect upon bending fatigue specimens tested at room temperature. Procedures for shot peening Ti-6Al-4V compressor blades are recommended for future applications. Author

N87-21375*# National Aeronautics and Space Administration. Lewis Research Center, Cleveland, Ohio.

A NASTRAN PRIMER FOR THE ANALYSIS OF ROTATING FLEXIBLE BLADES

CHARLES LAWRENCE, ROBERT A. AIELLO, MICHAEL A. ERNST, and OLIVER G. MCGEE (Ohio State Univ., Columbus) May 1987 23 p
(NASA-TM-89861; E-3528; NAS 1.15:89861) Avail: NTIS HC A02/MF A01 CSCL 20K

This primer provides documentation for using MSC NASTRAN in analyzing rotating flexible blades. The analysis of these blades includes geometrically nonlinear (large displacement) analysis under centrifugal loading, and frequency and mode shape (normal modes) determination. The geometrically nonlinear analysis using NASTRAN Solution sequence 64 is discussed along with the determination of frequencies and mode shapes using Solution Sequence 63. A sample problem with the complete NASTRAN input data is included. Items unique to rotating blade analyses, such as setting angle and centrifugal softening effects are emphasized. Author

N87-22273*# National Aeronautics and Space Administration. Lewis Research Center, Cleveland, Ohio.

STRUCTURAL AND AEROELASTIC ANALYSIS OF THE SR-7L PROPFAN

MURRAY HIRSCHBEIN, ROBERT KIELB, ROBERT AIELLO, MARSHA NALL, and CHARLES LAWRENCE Mar. 1985 31 p
(NASA-TM-86877; E-2338; NAS 1.15:86877) Avail: NTIS HC A03/MF A01 CSCL 20K

A structural and aeroelastic analysis of a large scale advanced turboprop rotor blade is presented. This 8-blade rotor is designed to operate at Mach 0.8 at an altitude of 35,000 ft. The blades are highly swept and twisted and of spar/shell construction. Due to the complexity of the blade geometry and its high performance, it is subjected to much higher loads and tends to be much less stable than conventional blades. Four specific analyses were conducted: (1) steady deflection; (2) natural frequencies and mode

shapes; (3) steady stresses; and (4) aeroelastic stability. State-of-the-art methods were used to analyze the blades including a large deflection, finite element structural analysis, and an aeroelastic analysis including interblade aerodynamic coupling (cascade effects). The study found the blade to be structurally sound and aeroelastically stable. However, it clearly indicated that advanced turboprop blades are much less robust than conventional blades and must be analyzed and fabricated much more carefully in order to assure that they are structurally sound and aeroelastically stable. Author

N87-22779*# National Aeronautics and Space Administration. Lewis Research Center, Cleveland, Ohio.

NONLINEAR HEAT TRANSFER AND STRUCTURAL ANALYSES OF SSME TURBINE BLADES

A. ABDUL-AZIZ (Sverdrup Technology, Inc., Middleburg Heights, Ohio.) and A. KAUFMAN *In its* Structural Integrity and Durability of Reusable Space Propulsion Systems p 95-104 1987
Avail: NTIS HC A10/MF A01 CSCL 20K

Three-dimensional nonlinear finite-element heat transfer and structural analyses were performed for the first stage high-pressure fuel turbopump blade of the space shuttle main engine (SSME). Directionally solidified (DS) MAR-M 246 material properties were considered for the analyses. Analytical conditions were based on a typical test stand engine cycle. Blade temperature and stress-strain histories were calculated using MARC finite-element computer code. The study was undertaken to assess the structural response of an SSME turbine blade and to gain greater understanding of blade damage mechanisms, convective cooling effects, and the thermal-mechanical effects. Author

N87-23010*# National Aeronautics and Space Administration. Lewis Research Center, Cleveland, Ohio.

FINITE ELEMENT IMPLEMENTATION OF ROBINSON'S UNIFIED VISCOPLASTIC MODEL AND ITS APPLICATION TO SOME UNIAXIAL AND MULTIAXIAL PROBLEMS

V. K. ARYA and A. KAUFMAN Jun. 1987 20 p
(NASA-TM-89891; E-3583; NAS 1.15:89891) Avail: NTIS HC A02/MF A01 CSCL 20K

A description of the finite element implementation of Robinson's unified viscoplastic model into the General Purpose Finite Element Program (MARC) is presented. To demonstrate its application, the implementation is applied to some uniaxial and multiaxial problems. A comparison of the results for the multiaxial problem of a thick internally pressurized cylinder, obtained using the finite element implementation and an analytical solution, is also presented. The excellent agreement obtained confirms the correct finite element implementation of Robinson's model. Author

N87-24006*# National Aeronautics and Space Administration. Lewis Research Center, Cleveland, Ohio.

IDENTIFICATION OF STRUCTURAL INTERFACE CHARACTERISTICS USING COMPONENT MODE SYNTHESIS

A. A. HUCKELBRIDGE (Case Western Reserve Univ., Cleveland, Ohio.) and C. LAWRENCE 1987 14 p Prepared for presentation at the Vibrations Conference, Boston, Mass., 27-30 Sep. 1987; sponsored by ASME
(NASA-TM-88960; E-3415; NAS 1.15:88960) Avail: NTIS HC A02/MF A01 CSCL 20K

The inability to adequately model connections has limited the ability to predict overall system dynamic response. Connections between structural components are often mechanically complex and difficult to accurately model analytically. Improved analytical models for connections are needed to improve system dynamic predictions. This study explores combining Component Mode synthesis methods for coupling structural components with Parameter Identification procedures for improving the analytical modeling of the connections. Improvements in the connection properties are computed in terms of physical parameters so the physical characteristics of the connections can be better understood, in addition to providing improved input for the system model. Two sample problems, one utilizing simulated data, the

other using experimental data from a rotor dynamic test rig are presented. Author

N87-24007*# National Aeronautics and Space Administration. Lewis Research Center, Cleveland, Ohio.

ENVIRONMENTAL DEGRADATION OF 316 STAINLESS STEEL IN HIGH TEMPERATURE LOW CYCLE FATIGUE

SREERAMESH KALLURI, S. STANFORD MANSON, and GARY R. HALFORD Apr. 1987 17 p Presented at the 3rd International Conference on Environmental Degradation of Engineering Materials, University Park, Pa., 13-15 Apr. 1987; sponsored by the Pennsylvania State Univ.

(Contract NAG3-337; NAG3-553)

(NASA-TM-89931; E-3636; NAS 1.15:89931) Avail: NTIS HC

A02/MF A01 CSCL 20K

Procedures based on modification of the conventional Strainrange Partitioning method are proposed to characterize the time-dependent degradation of engineering alloys in high-temperature, low-cycle fatigue. Creep-fatigue experiments were conducted in air using different waveforms of loading on 316 stainless steel at 816 C (1500 F) to determine the effect of exposure time on cyclic life. Reductions in the partitioned cyclic lives were observed with an increase in the time of exposure (or with the corresponding decrease in the steady-state creep rate) for all the waveforms involving creep strain. Excellent correlations of the experimental data were obtained by modifying the Conventional Strainrange Partitioning life relationships involving creep strain using a power-law term of either: (1) time of exposure, or (2) steady-state creep rate of the creep-fatigue test. Environmental degradation due to oxidation, material degradation due to the precipitation of carbides along the grain boundaries and detrimental deformation modes associated with the prolonged periods of creep were observed to be the main mechanisms responsible for life reductions at long exposure times. Author

N87-24722*# National Aeronautics and Space Administration. Lewis Research Center, Cleveland, Ohio.

HUB FLEXIBILITY EFFECTS ON PROPPAN VIBRATION

MICHAEL A. ERNST and CHARLES LAWRENCE Jul. 1987 16 p

(NASA-TM-89900; E-3596; NAS 1.15:89900) Avail: NTIS HC

A02/MF A01 CSCL 20K

The significance of hub flexibility in the nonlinear static and dynamic analyses of advanced turboprop blades is assessed. The chosen blade is the 0.175 scale model of the GE-A7-B4 unducted fan blade. A procedure for coupling the effective hub stiffness matrix to an MSC/NASTRAN finite element model is defined and verified. A series of nonlinear static and dynamic analyses are conducted on the blade for both rigid and flexible hub configurations. Results indicate that hub flexibility is significant in the nonlinear static and dynamic analyses of the GE-A7-B4. In order to insure accuracy in analyses of other blades, hub flexibility should always be considered. Author

N87-26385*# National Aeronautics and Space Administration. Lewis Research Center, Cleveland, Ohio.

FINITE ELEMENT ANALYSIS OF FLEXIBLE, ROTATING BLADES

OLIVER G. MCGEE Jul. 1987 40 p

(NASA-TM-89906; E-3674; NAS 1.15:89906) Avail: NTIS HC

A03/MF A01 CSCL 20K

A reference guide that can be used when using the finite element method to approximate the static and dynamic behavior of flexible, rotating blades is given. Important parameters such as twist, sweep, camber, co-planar shell elements, centrifugal loads, and inertia properties are studied. Comparisons are made between NASTRAN elements through published benchmark tests. The main purpose is to summarize blade modeling strategies and to document capabilities and limitations (for flexible, rotating blades) of various NASTRAN elements. Author

N87-26399*# National Aeronautics and Space Administration. Lewis Research Center, Cleveland, Ohio.

A HIGH TEMPERATURE FATIGUE AND STRUCTURES TESTING FACILITY

PAUL A. BARTOLOTTA and MICHAEL A. MCGAW Aug. 1987 24 p

(NASA-TM-100151; E-3712; NAS 1.15:100151) Avail: NTIS HC

A02/MF A01 CSCL 20K

As man strives for higher levels of sophistication in air and space transportation, awareness of the need for accurate life and material behavior predictions for advanced propulsion system components is heightened. Such sophistication will require complex operating conditions and advanced materials to meet goals in performance, thrust-to-weight ratio, and fuel efficiency. To accomplish these goals will require that components be designed using a high percentage of the material's ultimate capabilities. This serves only to complicate matters dealing with life and material behavior predictions. An essential component of material behavior model development is the underlying experimentation which must occur to identify phenomena. To support experimentation, the NASA Lewis Research Center's High Temperature Fatigue and Structures Laboratory has been expanded significantly. Several new materials testing systems have been added, as well as an extensive computer system. The intent of this paper is to present an overview of the laboratory, and to discuss specific aspects of the test systems. A limited discussion of computer capabilities will also be presented. Author

N87-27268*# National Aeronautics and Space Administration. Lewis Research Center, Cleveland, Ohio.

SINDA-NASTRAN INTERFACING PROGRAM THEORETICAL DESCRIPTION AND USER'S MANUAL

STEVEN R. WINEGAR Aug. 1987 31 p

(NASA-TM-100158; E-3720; NAS 1.15:100158) Avail: NTIS HC

A03/MF A01 CSCL 20K

The task of converting SINDA finite difference thermal model temperature results into NASTRAN finite element model thermal loads can be very labor intensive if there is not one node-to-one element, or systematic node-to-element, correlation between models. This paper describes the SINDA-NASTRAN Interfacing Program (SNIP), a FORTRAN computer code that generates NASTRAN structural model thermal load cards given by SINDA (or similar thermal model) temperature results and thermal model geometric data. SNIP generates NASTRAN thermal load cards for NASTRAN plate, shell, bar, and beam elements. The paper describes the interfacing procedures used by SNIP, and discusses set-up and operation of the program. Sample cases are included to demonstrate use of the program and show its performance under a variety of conditions. SNIP can provide structural model thermal loads that accurately reflect thermal model results while reducing the time required to interface thermal and structural models when compared to other methods. Author

N87-27269*# National Aeronautics and Space Administration. Lewis Research Center, Cleveland, Ohio.

FRACTURE MECHANICS CONCEPTS IN RELIABILITY ANALYSIS OF MONOLITHIC CERAMICS

JANE M. MANDERSCHIED and JOHN P. GYEKENYESI Aug. 1987 16 p Presented at the Testing High Performance Ceramics,

Boston, Mass., 25-27 Aug. 1987; sponsored in part by American Ceramic Society, and the American Society for Nondestructive Testing.

(NASA-TM-100174; E-3743; NAS 1.15:100174) Avail: NTIS HC

A02/MF A01 CSCL 20K

Basic design concepts for high-performance, monolithic ceramic structural components are addressed. The design of brittle ceramics differs from that of ductile metals because of the inability of ceramic materials to redistribute high local stresses caused by inherent flaws. Random flaw size and orientation requires that a probabilistic analysis be performed in order to determine component reliability. The current trend in probabilistic analysis is to combine linear elastic fracture mechanics concepts with the two parameter Weibull distribution function to predict component reliability under multiaxial

stress states. Nondestructive evaluation supports this analytical effort by supplying data during verification testing. It can also help to determine statistical parameters which describe the material strength variation, in particular the material threshold strength (the third Weibull parameter), which in the past was often taken as zero for simplicity. Author

N87-28058*# National Aeronautics and Space Administration. Lewis Research Center, Cleveland, Ohio.

A COMPUTATIONAL PROCEDURE FOR AUTOMATED FLUTTER ANALYSIS

DURBHA V. MURTHY (Toledo Univ., Ohio.) and KRISHNA RAO V. KAZA Aug. 1987 17 p
(NASA-TM-100171; E-3736; NAS 1.15:100171) Avail: NTIS HC A02/MF A01 CSCL 20K

A direct solution procedure for computing the flutter Mach number and the flutter frequency is applied to the aeroelastic analysis of propfans using a finite element structural model and an unsteady aerodynamic model based on a three-dimensional subsonic compressible lifting surface theory. An approximation to the Jacobian matrix that improves the efficiency of the iterative process is presented. The Jacobian matrix is indirectly approximated from approximate derivatives of the flutter matrix. Examples are used to illustrate the convergence properties. The direct solution procedure facilitates the automated flutter analysis in addition to contributing to the efficient use of computer time as well as the analyst's time. Author

N87-28944*# National Aeronautics and Space Administration. Lewis Research Center, Cleveland, Ohio.

EXPOSURE TIME CONSIDERATIONS IN HIGH TEMPERATURE LOW CYCLE FATIGUE

S. KALLURI, S. S. MANSON (Case Western Reserve Univ., Cleveland, Ohio.), and G. R. HALFORD Jun. 1987 12 p
Presented at the 5th International Conference on Mechanical Behaviour of Materials, Beijing, China, 3-6 Jun. 1987; sponsored in part by the Chinese Society of Metals, and the Chinese Society of Mechanics
(Contract NAG3-337; NAG3-553)
(NASA-TM-88934; E-3375; NAS 1.15:88934) Avail: NTIS HC A02/MF A01 CSCL 20K

The Conventional Strainrange Partitioning (CSRP) method for High-Temperature, Low-Cycle Fatigue (HTLCF) life prediction has its origins in the modeling of first-order, creep-fatigue waveform effects while treating as second-order effects, the influence of metallurgical or environmental time dependencies. Procedures are proposed to include the latter explicitly in the inelastic strainrange-life relations. For brevity, only the CP life relation will be presented in detail. The exposure-time effect within the CP inelastic strainrange (tensile creep reversed by compressive plasticity) was determined by tensile stresshold-time experiments for 316 SS at 816 C. Reductions in CP cyclic life of a factor of about two were observed with an increase in exposure time or a corresponding decrease in creep rate by a factor of about 100. The CP life relation has been modified to be expressed in terms of either Steady State Creep Rate (SSCR) or Exposure Time (ET). The applicability and accuracy of the time-dependent CP life relations is demonstrated by conducting verification experiments involving complex hysteresis loops. Metallographic examination revealed time-dependent degradation attributable to oxide formation and precipitation of carbides along grain boundaries. Author

N88-11140*# National Aeronautics and Space Administration. Lewis Research Center, Cleveland, Ohio.

TURBINE ENGINE HOT SECTION TECHNOLOGY, 1985

Oct. 1985 443 p Conference held in Cleveland, Ohio, 22-23 Oct. 1985
(NASA-CP-2405; E-2727; NAS 1.55:2405) Avail: NTIS HC A19/MF A01 CSCL 20K

The Turbine Engine Section Technology (HOST) Project Office of the Lewis Research Center sponsored a workshop to discuss current research pertinent to turbine engine hot section durability problems. Presentations were made concerning hot section

environment and the behavior of combustion liners, turbine blades, and turbine vanes.

N88-11170*# National Aeronautics and Space Administration. Lewis Research Center, Cleveland, Ohio.

HIGH TEMPERATURE STRESS-STRAIN ANALYSIS

ROBERT L. THOMPSON *In its* Turbine Engine Hot Section Technology, 1985 p 287-301 Oct. 1985
Avail: NTIS HC A19/MF A01 CSCL 20K

The objectives of the high temperature structures program are threefold: to assist in the development of analytical tools needed to improve design analysis and procedures for the efficient and accurate prediction of the nonlinear structural response of hot-section components; to aid in the calibration, validation, and evaluation of the analytical tools by comparing predictions with experimental data; and to evaluate existing as well as advanced temperature and strain measurement instrumentation. Author

N88-11177*# National Aeronautics and Space Administration. Lewis Research Center, Cleveland, Ohio.

LEWIS' ENHANCED LABORATORY FOR RESEARCH INTO THE FATIGUE AND CONSTITUTIVE BEHAVIOR OF HIGH TEMPERATURE MATERIALS

MICHAEL A. MCGAW *In its* Turbine Engine Hot Section Technology, 1985 p 361-371 Oct. 1985
Avail: NTIS HC A19/MF A01 CSCL 20K

Lewis Research Center's high temperature fatigue laboratory has undergone significant changes resulting in the addition of several new experimental capabilities. New materials testing systems have been installed enabling research to be conducted in multiaxial fatigue and deformation at high temperature, as well as cumulative creep-fatigue damage wherein the relative failure-life levels are widely separated. A key component of the new high-temperature fatigue and structures laboratory is a local, distributed computer system whose hardware and software architecture emphasizes a high degree of configurability, which in turn, enables the researcher to tailor a solution to the problem at hand. Author

N88-12825*# National Aeronautics and Space Administration. Lewis Research Center, Cleveland, Ohio.

CREEP LIFE PREDICTION BASED ON STOCHASTIC MODEL OF MICROSTRUCTURALLY SHORT CRACK GROWTH

TAKAYUKI KITAMURA and RYUICHI OHTANI (Kyoto Univ., Japan) 1988 23 p Proposed for presentation to the Summer Annual Meeting of the American Society of Mechanical Engineers, Berkeley, Calif., 20-22 Jun. 1988
(NASA-TM-100245; E-3867; NAS 1.15:100245) Avail: NTIS HC A03/MF A01 CSCL 20K

A nondimensional model of microstructurally short crack growth in creep is developed based on a detailed observation of the creep fracture process of 304 stainless steel. In order to deal with the scatter of small crack growth rate data caused by microstructural inhomogeneity, a random variable technique is used in the model. A cumulative probability of the crack length at an arbitrary time, $G(\bar{a}, \bar{t})$, and that of the time when a crack reaches an arbitrary length, $F(\bar{t}, \bar{a})$, are obtained numerically by means of a Monte Carlo method. $G(\bar{a}, \bar{t})$, and $F(\bar{t}, \bar{a})$ are the probabilities for a single crack. However, multiple cracks generally initiate on the surface of a smooth specimen from the early stage of creep life to the final stage. Taking into account the multiple crack initiations, the actual crack length distribution observed on the surface of a specimen is predicted by the combination of probabilities for a single crack. The prediction shows a fairly good agreement with the experimental result for creep of 304 stainless steel at 923 K. The probability of creep life is obtained from an assumption that creep fracture takes place when the longest crack reaches a critical length. The observed and predicted scatter of the life is fairly small for the specimens tested. Author

COMPUTER PROGRAMMING AND SOFTWARE

Includes computer programs, routines, and algorithms, and specific applications, e.g., CAD/CAM.

A86-36861*# National Aeronautics and Space Administration. Lewis Research Center, Cleveland, Ohio.

A COMPUTER ANALYSIS PROGRAM FOR INTERFACING THERMAL AND STRUCTURAL CODES

R. L. THOMPSON (NASA, Lewis Research Center, Cleveland, OH) and R. J. MAFFEO (General Electric Co., Cincinnati, OH) IN: Computers in engineering 1985; Proceedings of the International Computers in Engineering Conference and Exhibition, Boston, MA, August 4-8, 1985. Volume 2. New York, American Society of Mechanical Engineers, 1985, p. 289-295. Previously announced in STAR as N85-27264.

A software package has been developed to transfer three-dimensional transient thermal information accurately, efficiently, and automatically from a heat transfer analysis code to a structural analysis code. The code is called three-dimensional TRansfer ANalysis Code to Interface Thermal and Structural codes, or 3D TRANCITS. TRANCITS has the capability to couple finite difference and finite element heat transfer analysis codes to linear and nonlinear finite element structural analysis codes. TRANCITS currently supports the output of SINDA and MARC heat transfer codes directly. It will also format the thermal data output directly so that it is compatible with the input requirements of the NASTRAN and MARC structural analysis codes. Other thermal and structural codes can be interfaced using the transfer module with the neutral heat transfer input file and the neutral temperature output file. The transfer module can handle different elemental mesh densities for the heat transfer analysis and the structural analysis. Author

A87-33614*# University of Western Michigan, Kalamazoo. **OPTIMIZATION AND ANALYSIS OF GAS TURBINE ENGINE BLADES**

D. J. VANDENBRINK (Western Michigan University, Kalamazoo, MI) and D. A. HOPKINS (NASA, Lewis Research Center, Cleveland, OH) IN: Structures, Structural Dynamics and Materials Conference, 28th, Monterey, CA, Apr. 6-8, 1987, Technical Papers. Part 1. New York, American Institute of Aeronautics and Astronautics, 1987, p. 535-537. refs (AIAA PAPER 87-0827)

A gas turbine engine blade design is optimized using STAEBL. To validate the STAEBL analysis, the optimized blade design is analyzed using MARC, MHOST and BEST3D. The results show good agreement between STAEBL, MARC, and MHOST. The conclusion is that STAEBL can be used to optimize an engine blade design. Author

NUMERICAL ANALYSIS

Includes iteration, difference equations, and numerical approximation.

A83-10273* Akron Univ., Ohio. **FORMAL CONVERGENCE CHARACTERISTICS OF ELLIPTI-**

CALLY CONSTRAINED INCREMENTAL NEWTON-RAPHSON ALGORITHMS

J. PADOVAN (Akron, University, Akron, OH) and T. ARECHAGA International Journal of Engineering Science, vol. 20, no. 10, 1982, p. 1077-1097. refs (Contract NAG3-54)

Various aspects of the convergence, uniqueness, and existence properties associated with solutions generated via the elliptically constrained incremental Newton-Raphson (ECINR) algorithm are analyzed. Several theorems are developed, and the formal behavior of the elliptically constrained scheme developed by Padovan (1981) is discussed in detail. Consideration is given to global and local rates of convergence, to the determination of the occurrence of safety zones wherein the algorithm yields inherently convergent results, to formal limitations on the class of functions which the scheme can be applied to solve, and to single and multidimensional formalisms on existence uniqueness and convergence. Special attention is given to functions whose Jacobian matrix exhibit positive, negative, semi and indefinite properties. Several significant advantages of ECINR over the classical INR are mentioned.

C.D.

A85-21979* Akron Univ., Ohio. **ON THE DEVELOPMENT OF HIERARCHICAL SOLUTION STRATEGIES FOR NONLINEAR FINITE ELEMENT FORMULATIONS**

J. PADOVAN and J. LACKNEY (Akron, University, Akron, OH) Computers and Structures (ISSN 0045-7949), vol. 19, no. 4, 1984, p. 535-544. refs (Contract NSG-3283)

This paper develops a hierarchical type solution scheme which can handle the field equations associated with nonlinear finite element simulations. The overall procedure possesses various levels of application namely degree of freedom, nodal, elemental, substructural as well as global. In particular iteration, updating, assembly and solution control occurs at the various hierarchical levels. Due to the manner of formulation, the degree of matrix inversion depends on the size of the various hierarchical partitioned groups. In this context, degree of freedom partitioning requires no inversion. To benchmark the overall scheme, the results of several numerical examples are presented. Author

A86-30814* Cleveland State Univ., Ohio. **AN EMBEDDING METHOD FOR THE STEADY EULER EQUATIONS**

S.-H. CHANG (Cleveland State University, OH) and G. M. JOHNSON (Institute for Computational Studies, Fort Collins, CO) Journal of Computational Physics (ISSN 0021-9991), vol. 63, March 1986, p. 191-200. refs (Contract NAG3-339)

Certain difficulties arise in connection with the numerical solution of a direct finite difference representation of the steady Euler equations. Johnson (1979, 1981, 1982) has, therefore, proposed a surrogate-equation technique, in which the first-order steady Euler equations are embedded in a certain second-order system of equations. The present paper is concerned with the theoretical justification for such an embedding approach. For the numerical solution of the two-dimensional steady Euler equations, it is shown that, under a continuity restriction, it is possible to solve a second-order embedded system together with appropriate additional boundary conditions. The result indicates that a more direct and potentially more efficient approach to the steady

solutions exists than the alternative of solving the unsteady equations. G.R.

N83-23087# Iowa Univ., Iowa City. Inst. of Hydraulic Research.
THE FINITE ANALYTIC METHOD, VOLUME 3 Final Report

C. J. CHEN, M. Z. SHEIKHOLESAMI, B. KHALIGHI, and K. SINGH Aug. 1981 391 p refs 5 Vol.
(Contract NSG-3305)

(NASA-CR-170186; NAS 1.26:10186; IIHR-232-III-VOL-3) Avail:
NTIS HC A17/MF A01 CSCL 12A

The finite analytic (FA) method is applied to the numerical solution of two-point boundary value problems of ordinary differential equation. Convergence, stability, and accuracy of the method are examined and a comparison of the finite analytic solution with solutions obtained from the finite difference method is given for several numerical examples. In addition, the FA method is used to solve the two-dimensional Poisson and Laplace equations. Finally a general 9-point finite analytic formula is developed for the Navier-Stokes equation in a finite element. The Navier-Stokes equations are formulated using the primitive variables. An iterative scheme which solves the continuity equation, Poisson pressure equation and the momentum equations for the three primitive variables is devised. The FA numerical solution is first obtained for stagnation point flow and a comparison with the exact solution is made. Then the formula is used to obtain the numerical solution for a flat plate-wake combined problem and also for a square driven cavity flow. The results are obtained for Reynolds numbers 100, 400, and 800. M.G.

N83-23088# Iowa Univ., Iowa City. Inst. of Hydraulic Research.
THE FINITE ANALYTIC METHOD, VOLUME 4 Final Report

C. J. CHEN and H. C. CHEN Aug. 1982 424 p refs 5 Vol.
(Contract NSG-3305)

(NASA-CR-170187; NAS 1.26:170187; IIHR-232-IV-VOL-4) Avail:
NTIS HC A18/MF A01 CSCL 12A

Unsteady 1D, 2D, and 3D incompressible Navier-Stokes equations are numerically analyzed by a numerical scheme called the finite analytic method. The basic idea of the finite analytic method is the incorporation of a local analytic solution in the numerical solution of linear and nonlinear partial differential equations. The local analytic solutions for unsteady 1D, 2D and 3D convective transport equations are obtained from locally linearized governing equations by specifying suitable initial and boundary conditions for each local element. When the local analytic solution is evaluated at a given nodal point, it gives an analytic algebraic relationship between a nodal value in a local element to its neighboring nodal points. The solution of the problem is then achieved by solving the system of algebraic equations. Depending on the boundary and initial functions chosen to represent the boundary and initial conditions for each local element, a number of local analytic solutions are derived. The results show that the boundary approximation based on the combination of exponential and linear function is the best one since the boundary function thus constructed is the natural solution of the governing equation. The finite analytic coefficients thus obtained are shown to be relatively simple and do give the correct asymptotic behavior for both diffusion and convection dominated cases. M.G.

N83-23089# Iowa Univ., Iowa City. Inst. of Hydraulic Research.
THE FINITE ANALYTIC METHOD, VOLUME 5 Final Report

C. J. CHEN, K. S. HO, and W. S. CHENG Oct. 1982 438 p refs 5 Vol.

(Contract NSG-3305)

(NASA-CR-170188; NAS 1.26:170188; IIHR-232-V-VOL-5) Avail:
NTIS HC A19/MF A01 CSCL 12A

In order to solve practical engineering problems, a finite analytic (FA) method capable of solving flow and heat transfer problems involving complex geometries is developed. The boundary-fitted coordinate transformation is incorporated into the FA method. The FA method is employed to solve several flow and heat transfer problems. The problem of convective heat transfer in a cavity is studied with the Reynolds number ranging from 100 to 2,000 and the Peclet number ranging from 10 to 20,000 by using an equal

size grid in the physical plane. The separation of channel flow is examined at different Reynolds numbers over the range 25 to 229 with both equal and unequal size grids in the physical plane. For problems with complex geometries, flow past an airfoil and convective heat transfer in tube bundles, both are solved with the FA method for the boundary-fitted coordinate system. The FA results are compared with the experimental data, the theoretical calculation, and predictions by other numerical schemes. In addition, the FA numerical solution for two dimensional incompressible flows over an arbitrary body shape is discussed.

M.G.

N83-34656*# Virginia Polytechnic Inst. and State Univ., Blacksburg. Dept. of Mechanical Engineering.

THEORETICAL INVESTIGATION OF THE FORCE AND DYNAMICALLY COUPLED TORSIONAL-AXIAL-LATERAL DYNAMIC RESPONSE OF EARED ROTORS Annual Status Report

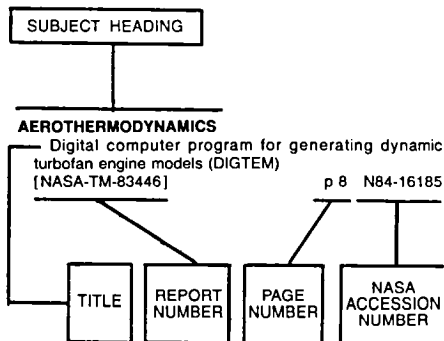
J. W. DAVID and L. D. MITCHELL 1982 33 p

(Contract NSG-3239)

(NASA-CR-173013; NAS 1.26:173013) Avail: NTIS HC A03/MF A01 CSCL 12A

Difficulties in solution methodology to be used to deal with the potentially higher nonlinear rotor equations when dynamic coupling is included. A solution methodology is selected to solve the nonlinear differential equations. The selected method was verified to give good results even at large nonlinearity levels. The transfer matrix methodology is extended to the solution of nonlinear problems. Author

Typical Subject Index Listing



The subject heading is a key to the subject content of the document. The title is used to provide a description of the subject matter. When the title is insufficiently descriptive of document content, a title extension is added, separated from the title by three hyphens. The (NASA or AIAA) accession number and the page number are included in each entry to assist the user in locating the abstract in the abstract section. If applicable, a report number is also included as an aid in identifying the document. Under any one subject heading, the accession numbers are arranged in sequence with the AIAA accession numbers appearing first.

A

ACCELERATED LIFE TESTS

Elevated temperature fatigue testing of metals
p 38 N82-13281

ACCURACY

Strainrange partitioning - A total strain range version
--- for creep fatigue life prediction by summing inelastic
and elastic strain-range-life relations for two Ni base
superalloys p 34 A85-11603

Strainrange partitioning: A total strain range version
[NASA-TM-83023] p 39 N83-14246

ACOUSTIC ATTENUATION

On ultrasonic factors and fracture toughness
p 66 A82-42863

Nondestructive characterization of structural ceramics
p 46 A86-37141

Ultrasonic attenuation of a void-containing medium for
very long wavelengths
[NASA-CR-3693] p 56 N83-28466

Preliminary investigation of an electrical network model
for ultrasonic scattering
[NASA-CR-3770] p 57 N84-17606

ACOUSTIC EMISSION

Acousto-ultrasonic characterization of fiber reinforced
composites p 50 A81-44660

Acoustic emission evaluation of plasma-sprayed thermal
barrier coatings
[ASME PAPER 84-GT-292] p 48 A84-47046

Nondestructive evaluation of adhesive bond strength
using the stress wave factor technique
p 53 A87-32200

Acousto-ultrasonic characterization of fiber reinforced
composites
[NASA-TM-82651] p 54 N81-28458

Fundamental aspects in quantitative ultrasonic
determination of fracture toughness: The scattering of a
single ellipsoidal inhomogeneity
[NASA-CR-3625] p 55 N83-11507

Effects of specimen resonances on acoustic-ultrasonic
testing
[NASA-CR-3679] p 55 N83-21373

Analytical Ultrasonics in Materials Research and
Testing
[NASA-CP-2383] p 59 N86-22962

Wave propagation in anisotropic medium due to an
oscillatory point source with application to unidirectional
composites
[NASA-CR-4001] p 60 N86-27666

ACOUSTIC MEASUREMENT
Phenomenological and mechanics aspects of
nondestructive evaluation and characterization by sound
and ultrasound of material and fracture properties
[NASA-CR-3623] p 55 N83-11506

Ultrasonic stress wave characterization of composite
materials
[NASA-CR-3976] p 60 N86-27665

A study of the stress wave factor technique for
nondestructive evaluation of composite materials
[NASA-CR-4002] p 60 N86-28445

Acousto-ultrasonic verification of the strength of filament
wound composite material
[NASA-TM-88827] p 61 N86-32764

Ray propagation path analysis of acousto-ultrasonic
signals in composites
[NASA-TM-100148] p 62 N87-25589

ACOUSTIC MICROSCOPES
Comparison of NDE techniques for sintered-SiC
components p 51 A83-22265

Reliability of void detection in structural ceramics by use
of scanning laser acoustic microscopy
p 52 A86-39027

Quantitative void characterization in structural ceramics
by use of scanning laser acoustic microscopy
p 53 A87-51974

Reliability of void detection in structural ceramics using
scanning laser acoustic microscopy
[NASA-TM-87035] p 58 N85-32337

Reliability of scanning laser acoustic microscopy for
detecting internal voids in structural ceramics
[NASA-TM-87222] p 59 N86-16599

Factors that affect reliability of nondestructive detection
of flaws in structural ceramics
[NASA-TM-87348] p 61 N86-31912

Quantitative void characterization in structural ceramics
using scanning laser acoustic microscopy
[NASA-TM-88797] p 61 N86-31913

Application of scanning acoustic microscopy to
advanced structural ceramics
[NASA-TM-89929] p 62 N87-23987

ACOUSTIC SCATTERING
Ultrasonic attenuation of a void-containing medium for
very long wavelengths
[NASA-CR-3693] p 56 N83-28466

ACOUSTIC VELOCITY
On ultrasonic factors and fracture toughness
p 66 A82-42863

Nondestructive characterization of structural ceramics
p 46 A86-37141

ACOUSTICS
Quantitative flaw characterization with scanning laser
acoustic microscopy p 52 A86-45150

Acousto-ultrasonic characterization of fiber reinforced
composites
[NASA-TM-82651] p 54 N81-28458

Effects of specimen resonances on acoustic-ultrasonic
testing
[NASA-CR-3679] p 55 N83-21373

The acousto-ultrasonic approach
[NASA-TM-89843] p 62 N87-20562

ACTUATORS
The 20th Aerospace Mechanics Symposium
[NASA-CP-2423-REV] p 121 N87-16321

Evaluation of a high-torque backlash-free roller
actuator
p 49 N87-16336

ADDITIVES
Fatigue crack propagation of nickel-base superalloys at
650 deg C
[NASA-TM-87150] p 42 N86-12294

ADHESIVE BONDING

Interface cracks in adhesively bonded lap-shear
joints p 67 A82-46109

Fracture of composite-adhesive-composite systems
p 76 A85-27935

Nondestructive evaluation of adhesive bond strength
using the stress wave factor technique
p 53 A87-32200

Analysis of interface cracks in adhesively bonded lap
shear joints, part 4
[NASA-CR-165438] p 93 N82-26716

AERODYNAMIC BALANCE
Mass balancing of hollow fan blades
[ASME PAPER 86-GT-195] p 84 A86-48245

AERODYNAMIC CHARACTERISTICS
The effect of limiting aerodynamic and structural
coupling in models of mistuned bladed disk vibration
p 5 A86-26905

AERODYNAMIC COEFFICIENTS
Optimization of cascade blade mistuning. I - Equations
of motion and basic inherent properties
p 3 A85-42365

AERODYNAMIC CONFIGURATIONS
NASTRAN level 16 user's manual updates for
aeroelastic analysis of bladed discs
[NASA-CR-159824] p 90 N81-19481

AERODYNAMIC FORCES
The coupled aeroelastic response of turbomachinery
blading to aerodynamic excitations
[AIAA 83-0844] p 69 A83-29822

The coupled response of turbomachinery blading to
aerodynamic excitations
p 2 A84-26959

Forced response analysis of an aerodynamically
detuned supersonic turbomachine rotor
p 5 A86-26902

AERODYNAMIC LOADS
Effects of structural coupling on mistuned cascade flutter
and response
[ASME PAPER 83-GT-117] p 73 A84-33701

Three dimensional unsteady aerodynamics and
aeroelastic response of advanced turboprops
[AIAA PAPER 86-0846] p 5 A86-38894

Effect of time dependent flight loads on JT9D-7
performance deterioration
[NASA-CR-159681] p 87 N80-10515

NASTRAN level 16 theoretical manual updates for
aeroelastic analysis of bladed discs
[NASA-CR-159823] p 90 N81-19480

Effects of structural coupling on mistuned cascade flutter
and response
[NASA-TM-83049] p 96 N83-15672

AERODYNAMIC STABILITY
Effects of friction dampers on aerodynamically unstable
rotor stages
[AIAA PAPER 83-0848] p 1 A83-32791

Measurements of self-excited rotor-blade vibrations
using optical displacements
[ASME PAPER 83-GT-132] p 73 A84-33702

Effects of friction dampers on aerodynamically unstable
rotor stages
p 3 A85-21866

Optimization of cascade blade mistuning. II - Global
optimum and numerical optimization p 3 A85-45715

Stability of limit cycles in frictionally damped and
aerodynamically unstable rotor stages p 4 A86-19198

Stability of large horizontal-axis axisymmetric wind
turbines
[NASA-TM-81623] p 89 N81-12446

Coupled bending-bending-torsion flutter of a mistuned
cascade with nonuniform blades
[NASA-TM-82813] p 92 N82-21604

Large displacements and stability analysis of nonlinear
propeller structures
[NASA-TM-82850] p 94 N82-31707

Measurements of self-excited rotor-blade vibrations
using optical displacements
[NASA-TM-82953] p 95 N83-14523

AERODYNAMIC STALLING
A comparative study of some dynamic stall models
[NASA-TM-88917] p 122 N87-18883

AEROELASTICITY
Status of NASA full-scale engine aeroelasticity
research p 63 A80-35906

Effects of mistuning on bending-torsion flutter and response of a cascade in incompressible flow
[AIAA 81-0602] p 65 A81-29465

The coupled aeroelastic response of turbomachinery blading to aerodynamic excitations
[AIAA 83-0844] p 69 A83-29822

Flutter and forced response of mistuned rotors using standing wave analysis
[AIAA 83-0845] p 69 A83-29823

The coupled response of turbomachinery blading to aerodynamic excitations p 2 A84-26959

Effects of structural coupling on mistuned cascade flutter and response
[ASME PAPER 83-GT-117] p 73 A84-33701

Measurements of self-excited rotor-blade vibrations using optical displacements
[ASME PAPER 83-GT-132] p 73 A84-33702

Flutter analysis of advanced turbopropellers
p 73 A84-36492

Flutter of turbofan rotors with mistuned blades
p 74 A85-12716

Flutter and forced response of mistuned rotors using standing wave analysis p 74 A85-12721

Flutter of swept fan blades
[ASME PAPER 84-GT-138] p 77 A85-32962

Vibration and flutter of mistuned bladed-disk assemblies p 3 A85-45854

Aeroelastic formulations for turbomachines and propellers p 4 A86-24677

Dynamic characteristics of an assembly of prop-fan blades
[ASME PAPER 85-GT-134] p 5 A86-32956

Three dimensional unsteady aerodynamics and aeroelastic response of advanced turboprops
[AIAA PAPER 86-0846] p 5 A86-38894

Computational engine structural analysis
[ASME PAPER 86-GT-70] p 5 A86-48141

Analytical and experimental investigation of the coupled bladed disk/shaft whirl of a cantilevered turbofan
[ASME PAPER 86-GT-98] p 6 A86-48163

Aeroelastic behavior of low aspect ratio metal and composite blades
[ASME PAPER 86-GT-243] p 84 A86-48271

Analytical flutter investigation of a composite propfan model
[AIAA PAPER 87-0738] p 87 A87-40497

Status of NASA full-scale engine aeroelasticity research
[NASA-TM-81500] p 88 N80-23678

Effects of mistuning on bending-torsion flutter and response of a cascade in incompressible flow --- turbofan engines
[NASA-TM-81674] p 89 N81-16494

Nastran level 16 theoretical manual updates for aeroelastic analysis of bladed discs
[NASA-CR-159823] p 90 N81-19480

NASTRAN level 16 user's manual updates for aeroelastic analysis of bladed discs
[NASA-CR-159824] p 90 N81-19481

NASTRAN level 16 programmer's manual updates for aeroelastic analysis of bladed discs
[NASA-CR-159825] p 90 N81-19482

NASTRAN level 16 demonstration manual updates for aeroelastic analysis of bladed discs
[NASA-CR-159826] p 90 N81-19483

Aeroelastic characteristics of a cascade of mistuned blades in subsonic and supersonic flows --- turbofan engines
[NASA-TM-82631] p 90 N81-26492

Coupled bending-bending-torsion flutter of a mistuned cascade with nonuniform blades
[NASA-TM-82813] p 92 N82-21604

Measurements of self-excited rotor-blade vibrations using optical displacements
[NASA-TM-82953] p 95 N83-14523

Effects of structural coupling on mistuned cascade flutter and response
[NASA-TM-83049] p 96 N83-15672

Aeroelastic analysis for propellers - mathematical formulations and program user's manual
[NASA-CR-3729] p 101 N84-12530

Bladed-shrouded-disc aeroelastic analyses: Computer program updates in NASTRAN level 17.7
[NASA-CR-165428] p 8 N84-15154

Flutter of swept fan blades
[NASA-TM-83547] p 102 N84-16587

Formulation of blade-flutter spectral analyses in stationary reference frame
[NASA-TP-2296] p 8 N84-20562

Flutter and forced response of mistuned rotors using standing wave analysis
[NASA-CR-173555] p 9 N84-24586

Structural response of a rotating bladed disk to rotor whirl
[NASA-CR-175605] p 11 N85-22391

Computational engine structural analysis
[NASA-TM-87231] p 116 N86-19663

Analytical flutter investigation of a composite propfan model
[NASA-TM-88944] p 122 N87-18115

Structural and aeroelastic analysis of the SR-7L propfan
[NASA-TM-86877] p 123 N87-22273

AEROSPACE ENGINEERING

Computational composite mechanics for aerospace propulsion structures
[AIAA PAPER 86-1190] p 19 A86-40596

Computational composite mechanics for aerospace propulsion structures
[NASA-TM-88965] p 31 N87-18614

AEROTHERMODYNAMICS

Digital computer program for generating dynamic turbofan engine models (DIGTEM)
[NASA-TM-83446] p 8 N84-16185

AEROTHERMOELASTICITY

Aeroelastic and dynamic finite element analyses of a bladed shrouded disk
[NASA-CR-159728] p 90 N81-19479

AGING (MATERIALS)

Ten year environmental test of glass fiber/epoxy pressure vessels
[AIAA PAPER 85-1198] p 19 A85-47022

Ten year environmental test of glass fiber/epoxy pressure vessels
[NASA-TM-87058] p 29 N85-30034

Thermomechanical deformation in the presence of metallurgical changes p 112 N85-31533

Fracture characteristics of angleplied laminates fabricated from overaged graphite/epoxy prepreg
[NASA-TM-87266] p 30 N86-25417

AIR COOLING

Nonlinear, three-dimensional finite-element analysis of air-cooled gas turbine blades
[NASA-TP-1669] p 88 N80-22734

Structural analysis of turbine blades using unified constitutive models
[NASA-TM-88807] p 119 N86-28461

AIRCRAFT CONSTRUCTION MATERIALS

Fatigue crack initiation and propagation in several nickel-base superalloys at 650 C p 33 A83-41199

Nonlinear analysis for high-temperature composites: Turbine blades/vanes p 106 N84-31699

AIRCRAFT DESIGN

Improved methods of vibration analysis of pretwisted, airfoil blades
[NASA-TM-83735] p 104 N84-30329

AIRCRAFT ENGINES

Blade loss transient dynamic analysis of turbomachinery p 2 A83-40864

Design concepts for low cost composite engine frames
[AIAA PAPER 83-2445] p 2 A83-48331

Vibration and flutter of mistuned bladed-disk assemblies p 3 A85-45854

NASA Lewis Research Center/university graduate research program on engine structures
[ASME PAPER 85-GT-159] p 80 A86-22084

Forced response analysis of an aerodynamically detuned supersonic turbomachine rotor p 5 A86-26902

The effect of limiting aerodynamic and structural coupling in models of mistuned bladed disk vibration p 5 A86-26905

Mode II fatigue crack growth specimen development p 83 A86-43566

Unified constitutive materials model development and evaluation for high-temperature structural analysis applications --- for aircraft gas turbine engines p 84 A86-49133

Effect of time dependent flight loads on JT9D-7 performance deterioration
[NASA-CR-159681] p 87 N80-10515

Integrated analysis of engine structures
[NASA-TM-82713] p 91 N82-11491

Evaluation of inelastic constitutive models for nonlinear structural analysis --- for aircraft turbine engines
[NASA-TM-82845] p 92 N82-24502

Structural tailoring of engine blades (STAEBL)
[NASA-CR-167949] p 7 N82-33391

Aerothermal modeling. Executive summary
[NASA-CR-168330] p 7 N84-15152

Design concepts for low-cost composite engine frames
[NASA-TM-83544] p 8 N84-16186

Mode 2 fatigue crack growth specimen development
[NASA-TM-83722] p 104 N84-29248

Nonlinear analysis for high-temperature composites: Turbine blades/vanes p 106 N84-31699

Turbine Engine Hot Section Technology (HOST)
[NASA-TM-83022] p 9 N85-10951

Nonlinear structural and life analyses of a turbine blade p 9 N85-10954

Nonlinear structural and life analyses of a combustor liner p 9 N85-10955

Pre-HOST high temperature crack propagation p 9 N85-10956

Structural analysis p 9 N85-10969

Component-specific modeling p 10 N85-10971

The 3-D inelastic analysis methods for hot section components: Brief description p 10 N85-10972

Constitutive model development for isotropic materials p 10 N85-10975

NASA Lewis Research Center/University Graduate Research Program on Engine Structures
[NASA-TM-86916] p 107 N85-18375

Component-specific modeling
[NASA-CR-174925] p 12 N85-32119

HOST structural analysis program overview p 12 N86-11513

Turbine Engine Hot Section Technology, 1984
[NASA-CP-2339] p 120 N87-11180

STAEBL: Structural tailoring of engine blades, phase 2 p 13 N87-17311

AIRCRAFT STRUCTURES

Numerical synthesis of tri-variate velocity realizations of turbulence p 81 A86-26654

AIRCRAFT TIRES

Temperature distribution in an aircraft tire at low ground speeds
[NASA-TP-2195] p 97 N83-33217

AIRFOIL OSCILLATIONS

A technique for the prediction of airfoil flutter characteristics in separated flow
[AIAA PAPER 87-0910] p 86 A87-33719

AIRFOIL PROFILES

The coupled aeroelastic response of turbomachinery blading to aerodynamic excitations
[AIAA 83-0844] p 69 A83-29822

The coupled response of turbomachinery blading to aerodynamic excitations p 2 A84-26959

AIRFOILS

Diffusion bonded boron/aluminum spar-shell fan blade
[NASA-CR-159571] p 23 N80-25382

Comparison of elastic and elastic-plastic structural analyses for cooled turbine blade airfoils
[NASA-TP-1679] p 88 N80-27719

Structural fatigue test results for large wind turbine blade sections p 96 N83-19246

Aerothermal modeling. Executive summary
[NASA-CR-168330] p 7 N84-15152

Formulation of blade-flutter spectral analyses in stationary reference frame p 8 N84-20562

Life prediction and constitutive models for engine hot section anisotropic materials program
[NASA-CR-174952] p 60 N86-25003

Structural tailoring of engine blades (STAEBL) theoretical manual p 12 N86-27283

Structural tailoring of engine blades (STAEBL) user's manual p 13 N86-27284

Structural analysis of turbine blades using unified constitutive models
[NASA-TM-88807] p 119 N86-28461

Turbine Engine Hot Section Technology, 1984
[NASA-CP-2339] p 120 N87-11180

ALGORITHMS

Hybrid stress finite elements for large deformations of inelastic solids p 74 A85-15894

Constrained self-adaptive solutions procedures for structure subject to high temperature elastic-plastic creep effects p 99 N83-34370

Stress and fracture analyses under elastic-plastic creep conditions: Some basic developments and computational approaches p 99 N83-34371

Slave finite elements: The temporal element approach to nonlinear analysis p 105 N84-31689

Self-adaptive solution strategies p 105 N84-31693

Augmented weak forms and element-by-element preconditioners: Efficient iterative strategies for structural finite elements. A preliminary study p 106 N85-10384

Compliance matrices for cracked bodies
[NASA-CR-179478] p 120 N86-30236

ALLOYS

Results of an interlaboratory fatigue test program conducted on alloy 800H at room and elevated temperatures p 37 A87-54370

Elastic-plastic finite-element analyses of thermally cycled double-edge wedge specimens
[NASA-TP-1973] p 92 N82-20566

Viscoplastic constitutive relationships with dependence on thermomechanical history p 108 N85-21691

Thermomechanical deformation in the presence of metallurgical changes p 112 N85-31533

Results of an interlaboratory fatigue test program conducted on alloy 800H at room and elevated temperatures
[NASA-CR-174940] p 114 N85-32340

Constitutive modeling for isotropic materials (HOST)
[NASA-CR-174980] p 115 N86-10589

Low-cycle thermal fatigue
[NASA-TM-87225] p 118 N86-26651

Effects of a high mean stress on the high cycle fatigue life of PWA 1480 and correlation of data by linear elastic fracture mechanics
[NASA-CR-175057] p 118 N86-27689

ALUMINUM

Low cycle fatigue behavior of aluminum/stainless steel composites
[AIAA 83-0806] p 16 A83-29886

Dynamic modulus and damping of boron, silicon carbide, and alumina fibers
[NASA-TM-81422] p 22 N80-20313

Predicting the time-temperature dependent axial failure of B/A1 composites
[NASA-TM-81474] p 22 N80-21452

Experimental compliance calibration of the NASA Lewis Research Center Mode 2 fatigue specimen
[NASA-TM-86908] p 107 N85-16205

Shot peening for Ti-6Al-4V alloy compressor blades
[NASA-TP-2711] p 123 N87-20566

ALUMINUM ALLOYS

On the equivalence between semiempirical fracture analyses and R-curves
p 64 A81-18792

A study of spectrum fatigue crack propagation in two aluminum alloys. I - Spectrum simplification. II - Influence of microstructures
p 36 A86-48973

The plastic compressibility of 7075-T651 aluminum-alloy plate
p 36 A86-49690

Diffusion bonded boron/aluminum spar-shell fan blade
[NASA-CR-159571] p 23 N80-25382

A study of spectrum fatigue crack propagation in two aluminum alloys. 2: Spectrum simplification
[NASA-TM-86929] p 41 N85-18124

A study of spectrum fatigue crack propagation in two aluminum alloys. 2: Influence of microstructures
[NASA-TM-86930] p 41 N85-18125

ALUMINUM BORON COMPOSITES

Predicting the time-temperature dependent axial failure of B/A1 composites
p 14 A80-35494

Analysis of crack propagation as an energy absorption mechanism in metal matrix composites
[NASA-CR-165051] p 24 N82-14288

Micromechanical predictions of crack propagation and fracture energy in a single fiber boron/aluminum model composite
[NASA-CR-168550] p 25 N82-18326

ALUMINUM GRAPHITE COMPOSITES

Select fiber composites for space applications - A mechanistic assessment
p 18 A85-16040

Select fiber composites for space applications: A mechanistic assessment
[NASA-TM-83631] p 26 N84-22702

ALUMINUM OXIDES

Fracture toughness determination of Al₂O₃ using four-point-bend specimens with straight-through and chevron notches
p 45 A80-42085

Dynamic modulus and damping of boron, silicon carbide, and alumina fibers
p 15 A80-44236

Performance of Chevron-notch short bar specimen in determining the fracture toughness of silicon nitride and aluminum oxide
p 45 A80-50696

Fracture toughness of brittle materials determined with chevron notch specimens
p 45 A81-32545

Specimen size and geometry effects on fracture toughness of Al₂O₃ measured with short rod and short bar chevron-notch specimens
[NASA-TM-83319] p 47 N83-19902

AMBIENT TEMPERATURE

Results of an interlaboratory fatigue test program conducted on alloy 800H at room and elevated temperatures
p 37 A87-54370

Results of an interlaboratory fatigue test program conducted on alloy 800H at room and elevated temperatures
[NASA-CR-174940] p 114 N85-32340

AMPLITUDES

The use of an optical data acquisition system for bladed disk vibration analysis
[NASA-TM-86891] p 106 N85-15184

ANALYSIS (MATHEMATICS)

Progressive damage, fracture predictions and post mortem correlations for fiber composites
[NASA-TM-87101] p 29 N86-10290

ANGULAR DISTRIBUTION

Joint research effort on vibrations of twisted plates, phase 1: Final results
[NASA-RP-1150] p 115 N86-10579

ANISOTROPIC MEDIA

Constitutive relationships for anisotropic high-temperature alloys
[NASA-TM-83437] p 97 N83-28493

Stress waves in transversely isotropic media: The homogeneous problem
[NASA-CR-3977] p 59 N86-25002

ANISOTROPIC PLATES

Three-dimensional finite-element analysis of layered composite plates
p 68 A83-27432

ANISOTROPY

Time-independent anisotropic plastic behavior by mechanical subelement models
p 99 N83-34369

Low cycle fatigue of MAR-M 200 single crystals at 760 and 870 deg C
[NASA-TM-86933] p 41 N85-19074

Anisotropic constitutive model for nickel base single crystal alloys: Development and finite element implementation
[NASA-CR-175015] p 117 N86-21952

ANTENNA COMPONENTS

Composite space antenna structures - Properties and environmental effects
p 20 A87-38610

Composite space antenna structures: Properties and environmental effects
[NASA-TM-88859] p 31 N87-16880

ANTIFRICTION BEARINGS

Selection of rolling-element bearing steels for long-life application
[NASA-TM-88881] p 49 N87-11993

APPLICATIONS PROGRAMS (COMPUTERS)

Integrated research in constitutive modelling at elevated temperatures, part 2
[NASA-CR-177233] p 119 N86-28455

ICAN: A versatile code for predicting composite properties
[NASA-TM-87334] p 31 N86-31664

Finite element implementation of Robinson's unified viscoplastic model and its application to some uniaxial and multiaxial problems
[NASA-TM-89891] p 123 N87-23010

ARGON

Ion beam sputter etching of orthopedic implanted alloy MP35N and resulting effects on fatigue
[NASA-TM-81747] p 38 N81-21174

ASPECT RATIO

Nonlinear finite element analysis of shells with large aspect ratio
p 105 N84-31692

Joint research effort on vibrations of twisted plates, phase 1: Final results
[NASA-RP-1150] p 115 N86-10579

ASSEMBLING

A pad perturbation method for the dynamic coefficients of tilting-pad journal bearings
p 47 A82-14400

ASSURANCE

Experience with modified aerospace reliability and quality assurance method for wind turbines
[NASA-TM-82803] p 54 N82-19550

ASTROLOGY (TRADEMARK)

Effects of fine porosity on the fatigue behavior of a powder metallurgy superalloy
p 32 A80-35495

The effect of microstructure on 650 C fatigue crack growth in P/M Astrology
p 33 A84-12395

Fatigue crack growth and low cycle fatigue of two nickel base superalloys
[NASA-CR-174534] p 39 N84-10267

ATMOSPHERIC TURBULENCE

Numerical synthesis of tri-variate velocity realizations of turbulence
p 81 A86-28654

ATTENUATION

Ultrasonic evaluation of mechanical properties of thick, multilayered, filament wound composites
[NASA-TM-87088] p 58 N86-10561

AUTOMATIC CONTROL

A computational procedure for automated flutter analysis
[NASA-TM-100171] p 125 N87-28058

AUTOREGRESSIVE PROCESSES

Numerical synthesis of tri-variate velocity realizations of turbulence
p 81 A86-28654

AXIAL COMPRESSION LOADS

Compression behavior of unidirectional fibrous composite
[NASA-TM-82833] p 25 N82-22313

AXIAL FLOW TURBINES

Stability of large horizontal-axis axisymmetric wind turbines
[NASA-TM-81623] p 89 N81-12446

AXIAL LOADS

Predicting the time-temperature dependent axial failure of B/A1 composites
p 14 A80-35494

Plasticity, viscoplasticity, and creep of solids by mechanical subelement models
p 77 A85-35048

The plastic compressibility of 7075-T651 aluminum-alloy plate
p 36 A86-49690

Axial and torsional fatigue behavior of Waspaloy
[NASA-CR-175052] p 44 N86-25454

J-integral estimates for cracks in infinite bodies
[NASA-CR-179474] p 119 N86-28467

AXIAL STRAIN

Results of an interlaboratory fatigue test program conducted on alloy 800H at room and elevated temperatures
p 37 A87-54370

Results of an interlaboratory fatigue test program conducted on alloy 800H at room and elevated temperatures
[NASA-CR-174940] p 114 N85-32340

AXIAL STRESS

Fatigue life prediction in bending from axial fatigue information
[NASA-CR-165563] p 91 N82-20564

AXISYMMETRIC FLOW

Stability of large horizontal-axis axisymmetric wind turbines
[NASA-TM-81623] p 89 N81-12446

B

BALL BEARINGS

Lubricant effects on bearing life
[NASA-TM-88875] p 49 N87-15467

BARS

Compliance and stress intensity coefficients for short bar specimens with chevron notches
p 64 A80-46032

Extended range stress intensity factor expressions for chevron-notched short bar and short rod fracture toughness specimens
p 66 A82-40357

Thermal-mechanical fatigue crack growth in Inconel X-750
p 35 A86-20982

Specimen size and geometry effects on fracture toughness of Al₂O₃ measured with short rod and short bar chevron-notch specimens
[NASA-TM-83319] p 47 N83-19902

Thermal-mechanical fatigue crack growth in Inconel X-750
[NASA-CR-174740] p 41 N85-15877

NDE for heat engine ceramics
[NASA-TM-86949] p 57 N85-20389

BAUSCHINGER EFFECT

Finite elastic-plastic deformation of polycrystalline metals
p 34 A84-43872

BEAMS (SUPPORTS)

Buckling of rotating beams
p 63 A80-20149

Comparison of beam and shell theories for the vibrations of thin turbomachinery blades
[ASME PAPER 82-GT-223] p 65 A82-35408

Effects of warping and pretwist on torsional vibration of rotating beams
[ASME PAPER 84-WA/APM-41] p 75 A85-17040

Instructions for the use of the CIVM-Jet 4C finite-strain computer code to calculate the transient structural responses of partial and/or complete arbitrarily-curved rings subjected to fragment impact
[NASA-CR-159873] p 88 N80-27720

Improved finite-difference vibration analysis of pretwisted, tapered beams
[NASA-TM-83549] p 102 N84-16588

Joint research effort on vibrations of twisted plates, phase 1: Final results
[NASA-RP-1150] p 115 N86-10579

BEARING ALLOYS

Selection of rolling-element bearing steels for long-life application
[NASA-TM-88881] p 49 N87-11993

BEARINGS

Engine dynamic analysis with general nonlinear finite element codes. II - Bearing element implementation, overall numerical characteristics and benchmarking
[ASME PAPER 82-GT-292] p 47 A82-35462

Nonlinear transient finite element analysis of rotor-bearing-stator systems
p 48 A84-20580

A blade loss response spectrum for flexible rotor systems
[ASME PAPER 84-GT-29] p 48 A84-46893

Mode II fatigue crack growth specimen development
p 83 A86-43566

Engine dynamic analysis with general nonlinear finite element codes. Part 2: Bearing element implementation overall numerical characteristics and benchmarking
[NASA-CR-167944] p 7 N82-33390

Mode 2 fatigue crack growth specimen development
[NASA-TM-83722] p 104 N84-29248

BENDING

The effect of circumferential aerodynamic detuning on coupled bending-torsion unstalled supersonic flutter
[ASME PAPER 86-GT-100] p 6 A87-25396

Finite-element modeling of layered, anisotropic composite plates and shells: A review of recent research
p 91 N82-19563

Stress intensity and displacement coefficients for radially cracked ring segments subject to three-point bending [NASA-TM-83059] p 96 N83-24874

BENDING FATIGUE

Fatigue life prediction in bending from axial fatigue information [NASA-CR-165563] p 91 N82-20564
Bending fatigue of electron-beam-welded foils. Application to a hydrodynamic air bearing in the Chrysler/DOE upgraded automotive gas turbine engine [NASA-TM-83539] p 102 N84-16589

BENDING MOMENTS

Fracture toughness determination of Al₂O₃ using four-point-bend specimens with straight-through and chevron notches p 45 A80-42085
Nonlinear flap-lag-extensional vibrations of rotating, pretwisted, precone beams including Coriolis effects [NASA-TM-87102] p 115 N85-34427

BENDING THEORY

Alternative ways for formulation of hybrid stress elements p 68 A83-14710
Three-dimensional finite-element analysis of layered composite plates p 68 A83-27432

BENDING VIBRATION

Effects of mistuning on bending-torsion flutter and response of a cascade in incompressible flow [AIAA 81-0602] p 65 A81-29465
Vibrations of twisted cantilevered plates - Experimental investigation [ASME PAPER 84-GT-96] p 73 A84-46937
Nonlinear vibration and stability of rotating, pretwisted, precone blades including Coriolis effects p 86 A87-39896

Coupled bending-bending-torsion flutter of a mistuned cascade with nonuniform blades [NASA-TM-82813] p 92 N82-21604
Nonlinear bending-torsional vibration and stability of rotating, pretwisted, precone blades including Coriolis effects [NASA-TM-87207] p 116 N86-17789

BERYLLIUM

Fracture toughness of hot-pressed beryllium p 34 A85-25835

BINARY SYSTEMS (MATERIALS)

Ultrasonic wave propagation in two-phase media - Spherical inclusions p 17 A85-11926

BIRD-AIRCRAFT COLLISIONS

Superhybrid composite blade impact studies [ASME PAPER 81-GT-24] p 1 A81-29940

BLADE TIPS

Turbine blade nonlinear structural and life analysis p 1 A83-29024

BLADES

A NASTRAN primer for the analysis of rotating flexible blades [NASA-TM-89861] p 123 N87-21375

BORON FIBERS

Dynamic modulus and damping of boron, silicon carbide, and alumina fibers p 15 A80-44236
Durability/life of fiber composites in hygrothermomechanical environments p 16 A84-27359

Dynamic modulus and damping of boron, silicon carbide, and alumina fibers [NASA-TM-81422] p 22 N80-20313
Calculation of residual principal stresses in CVD boron on carbon filaments [NASA-TM-81456] p 22 N80-20314

Predicting the time-temperature dependent axial failure of B/A1 composites [NASA-TM-81474] p 22 N80-21452
Durability/life of fiber composites in hygrothermomechanical environments [NASA-TM-82749] p 24 N82-14287

Micromechanical predictions of crack propagation and fracture energy in a single fiber boron/aluminum model composite [NASA-CR-168550] p 25 N82-18326

BORON REINFORCED MATERIALS

Durability/life of fiber composites in hygrothermomechanical environments p 16 A84-27359

Diffusion bonded boron/aluminum spar-shell fan blade [NASA-CR-159571] p 23 N80-25382
Durability/life of fiber composites in hygrothermomechanical environments [NASA-TM-82749] p 24 N82-14287

BOTTLES

Ten year environmental test of glass fiber/epoxy pressure vessels [AIAA PAPER 85-1198] p 19 A85-47022
Ten year environmental test of glass fiber/epoxy pressure vessels [NASA-TM-87058] p 29 N85-30034

BOUNDARY ELEMENT METHOD

Stress analysis of gas turbine engine structures using the boundary element method p 81 A86-34444
Advanced three-dimensional dynamic analysis by boundary element methods p 81 A86-34445
Nonlinear Structural Analysis [NASA-CP-2297] p 105 N84-31688
Three-dimensional stress analysis using the boundary element method p 106 N84-31700

BOUNDARY LAYERS

Boundary layer thermal stresses in angle-ply composite laminates, part 1 --- graphite-epoxy composites [NASA-CR-165412] p 93 N82-26713
Boundary-layer effects in composite laminates: Free-edge stress singularities, part 6 [NASA-CR-165440] p 94 N82-26718

BOUNDARY VALUE PROBLEMS

Analysis of an externally radially crack ring segment subject to three-point radial loading p 79 A86-20710
An embedding method for the steady Euler equations p 126 A86-30814
The finite analytic method, volume 3 [NASA-CR-170186] p 127 N83-23087

BRANCHING (MATHEMATICS)

A numerical analysis of contact and limit-point behavior in a class of problems of finite elastic deformation p 72 A84-27370

BREATHING APPARATUS

Ten year environmental test of glass fiber/epoxy pressure vessels [AIAA PAPER 85-1198] p 19 A85-47022
Ten year environmental test of glass fiber/epoxy pressure vessels [NASA-TM-87058] p 29 N85-30034

BRITTLE MATERIALS

Compliance and stress intensity coefficients for short bar specimens with chevron notches p 64 A80-46032
Fracture toughness of brittle materials determined with chevron notch specimens p 45 A81-32545
Fracture toughness of brittle materials determined with chevron notch specimens [NASA-TM-81607] p 38 N80-32486

BUBBLES

Vapor cavitation in dynamically loaded journal bearings [NASA-TM-83366] p 97 N83-24875

BUCKLING

Buckling of rotating beams p 63 A80-20149
Vibration and buckling of rectangular plates under in-plane hydrostatic loading p 64 A80-45364
Tensile buckling of advanced turboprops [AIAA PAPER 82-0776] p 67 A83-10900
On the solution of elastic-plastic static and dynamic postbuckling collapse of general structure p 67 A83-12746
Tensile buckling of advanced turboprops p 71 A84-11039
Tensile buckling of advanced turboprops [NASA-TM-82896] p 94 N82-31708
A solution procedure for behavior of thick plates on a nonlinear foundation and postbuckling behavior of long plates [NASA-TP-2174] p 99 N83-34373
Dynamic delamination buckling in composite laminates under impact loading: Computational simulation [NASA-TM-100192] p 31 N87-28611

BURNERS

Component-specific modeling p 12 N86-11515
Burner liner thermal-structural load modeling [NASA-CR-174892] p 117 N86-21932
High temperature stress-strain analysis p 120 N87-11209

C**CALCULATORS**

Prediction of fiber composite mechanical behavior made simple --- using a rocket calculator [NASA-TM-81404] p 22 N80-16107

CAMBER

Vibrations of twisted rotating blades [ASME PAPER 81-DET-127] p 65 A82-19341

CANTILEVER BEAMS

Natural frequency of rotating beams using non-rotating modes p 68 A83-18383
Design of dry-friction dampers for turbine blades p 2 A83-35883
Forced response of a cantilever beam with a dry friction damper attached. I - Theory. II - Experiment p 71 A84-21267
Finite difference analysis of torsional vibrations of pretwisted, rotating, cantilever beams with effects of warping p 78 A85-42047

An improved finite-difference analysis of uncoupled vibrations of tapered cantilever beams [NASA-TM-83495] p 101 N84-13610
Nonlinear flap-lag-extensional vibrations of rotating, pretwisted, precone beams including Coriolis effects [NASA-TM-87102] p 115 N85-34427

CANTILEVER MEMBERS

Vibrations of cantilevered shallow cylindrical shells of rectangular planform p 65 A82-11298
Vibrations of cantilevered circular cylindrical shells. Shallow versus deep shell theory p 69 A83-36958
On the three-dimensional vibrations of the cantilevered rectangular parallelepiped p 70 A83-37729
Vibrations of cantilevered doubly-curved shallow shells p 70 A83-39557
Analytical and experimental investigation of the coupled bladed disk/shaft whirl of a cantilevered turbofan [ASME PAPER 86-GT-98] p 6 A86-48163

CANTILEVER PLATES

Vibrations of twisted cantilevered plates - Experimental investigation [ASME PAPER 84-GT-96] p 73 A84-46937
Vibrations of twisted cantilevered plates - Summary of previous and current studies p 76 A85-22069
Vibrations of twisted cantilever plates - A comparison of theoretical results p 79 A85-47626
Joint research effort on vibrations of twisted plates, phase 1: Final results [NASA-RP-1150] p 115 N86-10579

CARBON FIBER REINFORCED PLASTICS

Impact resistance of fiber composites p 66 A82-39852

CARBON FIBERS

Thermal expansion behavior of graphite/glass and graphite/magnesium p 21 A87-38615
Calculation of residual principal stresses in CVD boron on carbon filaments [NASA-TM-81456] p 22 N80-20314
Statistical aspects of carbon fiber risk assessment modeling --- fire accidents involving aircraft [NASA-CR-159318] p 23 N80-29432

CARBON-CARBON COMPOSITES

Mechanical behavior of carbon-carbon composites [NASA-CR-174767] p 28 N84-34575

CASCADE FLOW

Effects of mistuning on bending-torsion flutter and response of a cascade in incompressible flow [AIAA 81-0602] p 65 A81-29465
Effects of structural coupling on mistuned cascade flutter and response [ASME PAPER 83-GT-117] p 73 A84-33701
Flutter of turbofan rotors with mistuned blades p 74 A85-12716
Optimization of cascade blade mistuning. II - Global optimum and numerical optimization p 3 A85-45715
The effects of strong shock loading on coupled bending-torsion flutter of tuned and mistuned cascades p 4 A86-26893
Effects of mistuning on bending-torsion flutter and response of a cascade in incompressible flow --- turbofan engines [NASA-TM-81674] p 89 N81-16494
Effects of structural coupling on mistuned cascade flutter and response [NASA-TM-83049] p 96 N83-15672

CASTING

Low cycle fatigue behavior of conventionally cast MAR-M 200 AT 1000 deg C [NASA-TM-83769] p 41 N84-33564

CAVITATION FLOW

Vapor cavitation in dynamically loaded journal bearings [NASA-TM-83366] p 97 N83-24875

CENTRIFUGING STRESS

Buckling of rotating beams p 63 A80-20149

CENTRIPETAL FORCE

Forced vibration analysis of rotating cyclic structures in NASTRAN [NASA-CR-165429] p 100 N84-11514

CEPSTRAL ANALYSIS

Ray propagation path analysis of acousto-ultrasonic signals in composites [NASA-TM-100148] p 62 N87-25589

CERAMIC COATINGS

High temperature thermomechanical analysis of ceramic coatings p 74 A84-48565
Finite element analysis of residual stress in plasma-sprayed ceramic p 46 A86-15226
Inelastic high-temperature thermomechanical response of ceramic coated gas turbine seals p 82 A86-37799

CERAMIC MATRIX COMPOSITES

Thermal expansion behavior of graphite/glass and graphite/magnesium p 21 A87-38615

CERAMICS

Quantitative ultrasonic evaluation of engineering properties in metals, composites, and ceramics

p 50 A80-39641

Fracture toughness determination of Al₂O₃ using four-point-bend specimens with straight-through and chevron notches

p 45 A80-42085

Fracture toughness of brittle materials determined with chevron notch specimens

p 45 A81-32545

Comparison of NDE techniques for sintered-SiC components

p 51 A83-22265

Development of plane strain fracture toughness test for ceramics using Chevron notched specimens

p 46 A84-11676

NDE of advanced ceramics

p 52 A86-35575

Nondestructive characterization of structural ceramics

p 46 A86-37141

Reliability of void detection in structural ceramics by use of scanning laser acoustic microscopy

p 52 A86-39027

NDE of structural ceramics

[ASME PAPER 86-GT-279]

p 52 A86-48298

Probability of detection of internal voids in structural ceramics using microfocus radiography

p 52 A87-14300

SCARE - A postprocessor program to MSC/NASTRAN for reliability analysis of structural ceramic components

[ASME PAPER 86-GT-34]

p 84 A87-17988

NDE reliability and process control for structural ceramics

[ASME PAPER 87-GT-8]

p 53 A87-48702

Quantitative void characterization in structural ceramics by use of scanning laser acoustic microscopy

p 53 A87-51974

Ultrasonic velocity for estimating density of structural ceramics

[NASA-TM-82765]

p 46 N82-14359

NDE for heat engine ceramics

[NASA-TM-86949]

p 57 N85-20389

Reliability of void detection in structural ceramics using scanning laser acoustic microscopy

[NASA-TM-87035]

p 58 N85-32337

Probability of detection of internal voids in structural ceramics using microfocus radiography

[NASA-TM-87164]

p 59 N86-13749

NDE of structural ceramics

[NASA-TM-87186]

p 59 N86-16598

Reliability of scanning laser acoustic microscopy for detecting internal voids in structural ceramics

[NASA-TM-87222]

p 59 N86-16599

Factors that affect reliability of nondestructive detection of flaws in structural ceramics

[NASA-TM-87348]

p 61 N86-31912

Quantitative void characterization in structural ceramics using scanning laser acoustic microscopy

[NASA-TM-88797]

p 61 N86-31913

NDE reliability and process control for structural ceramics

[NASA-TM-88870]

p 61 N87-12910

A constitutive law for finite element contact problems with unclassical friction

[NASA-TM-88838]

p 120 N87-12924

Surface flaw reliability analysis of ceramic components with the SCARE finite element postprocessor program

[NASA-TM-88901]

p 121 N87-17087

Nondestructive evaluation of structural ceramics

[NASA-TM-88978]

p 62 N87-18109

Application of scanning acoustic microscopy to advanced structural ceramics

[NASA-TM-89929]

p 62 N87-23987

Ultrasonic NDE of structural ceramics for power and propulsion systems

[NASA-TM-100147]

p 62 N87-26362

Fracture mechanics concepts in reliability analysis of monolithic ceramics

[NASA-TM-100174]

p 124 N87-27269

CERMETS

Fatigue behavior of SiC reinforced Ti/6Al-4V/ at 650 C

p 15 A83-12414

CHEMICAL COMPOSITION

Thermal fatigue resistance of cobalt-modified UDIMET 700

p 39 N83-11289

Creep-fatigue of low cobalt superalloys

p 39 N83-11290

CHEMICAL REACTIONS

Thermal fatigue and oxidation data of oxide dispersion-strengthened alloys

[NASA-CR-159842]

p 37 N80-25415

CHROMIUM ALLOYS

Anisotropic constitutive model for nickel base single crystal alloys: Development and finite element implementation

[NASA-CR-175015]

p 117 N86-21952

CIRCULAR PLATES

Vibration and flutter of mistuned bladed-disk assemblies

[AIAA PAPER 84-0991]

p 75 A85-16095

Vibration and flutter of mistuned bladed-disk assemblies

p 3 A85-45854

Vibration and flutter of mistuned bladed-disk assemblies

[NASA-TM-83634]

p 103 N84-23923

CIRCULAR SHELLS

Vibrations of cantilevered circular cylindrical shells

Shallow versus deep shell theory

p 69 A83-36958

CLASSICAL MECHANICS

Composite mechanics for engine structures

[NASA-TM-100176]

p 32 N88-12552

COATINGS

Turbine Engine Hot Section Technology (HOST)

[NASA-TM-83022]

p 9 N85-10951

COBALT

Thermal fatigue resistance of cobalt-modified UDIMET 700

Creep-fatigue of low cobalt superalloys

Thermal-fatigue and oxidation resistance of cobalt-modified Udimet 700 alloy

[NASA-TP-2591]

p 119 N86-28464

COBALT ALLOYS

Quasi-static solution algorithms for kinematically/materially nonlinear thermomechanical problems

Creep fatigue of low-cobalt superalloys: Waspalloy, PM U 700 and wrought U 700

[NASA-CR-168260]

p 40 N84-13265

Preliminary study of thermomechanical fatigue of polycrystalline MAR-M 200

[NASA-TP-2280]

p 40 N84-17350

The low cycle fatigue behavior of a plasma-sprayed coating material

[NASA-TM-87318]

p 44 N86-31699

CODING

Progressive damage, fracture predictions and post mortem correlations for fiber composites

[NASA-TM-87101]

p 29 N86-10290

Structural tailoring of engine blades (STAEBL) user's manual

[NASA-CR-175113]

p 13 N86-27284

COEFFICIENT OF FRICTION

Stress evaluations under rolling/sliding contacts

[NASA-CR-165561]

p 91 N82-17521

The effects of crack surface friction and roughness on crack tip stress fields

[NASA-TM-88976]

p 122 N87-18881

COLD WORKING

Ultrasonic determination of recrystallization

[NASA-TM-88855]

p 61 N87-10399

COLLOCATION

Analysis of an externally radially crack ring segment subject to three-point radial loading

[NASA-TM-88797]

p 79 A86-20710

COMBINED STRESS

Analyses of large quasistatic deformations of inelastic bodies by a new hybrid-stress finite element algorithm - Applications

On stress field near a stationary crack tip

[AD-A152863]

p 76 A85-24532

COMBUSTION

Turbine Engine Hot Section Technology (HOST)

[NASA-TM-83022]

p 9 N85-10951

Turbine Engine Hot Section Technology (HOST)

[NASA-CP-2289]

p 115 N86-11495

COMBUSTION CHAMBERS

Nonlinear structural and life analyses of a combustor liner

Toward improved durability in advanced combustors and turbines - Progress in prediction of thermomechanical loads

[ASME PAPER 86-GT-172]

p 6 A86-48224

Advances in 3-D Inelastic Analysis Methods for hot section components

[AIAA PAPER 87-0719]

p 85 A87-33645

Combustor liner durability analysis

[NASA-CR-165250]

p 7 N81-17079

Nonlinear structural and life analyses of a combustor liner

[NASA-TM-82846]

p 92 N82-24501

Fracture mechanics criteria for turbine engine hot section components

[NASA-CR-167896]

p 7 N82-25257

Nonlinear constitutive theory for turbine engine structural analysis

[NASA-CR-167967]

p 95 N82-33744

Experimental verification of the Neuber relation at room and elevated temperatures --- to predict stress-strain behavior in notched specimens of hastelloy x

[NASA-CR-167967]

p 96 N83-19121

Aerothermal modeling. Executive summary

[NASA-CR-168330]

p 7 N84-15152

Turbine Engine Hot Section Technology (HOST)

[NASA-TM-83022]

p 9 N85-10951

Nonlinear structural and life analyses of a combustor liner

Validation of structural analysis methods using the in-house liner cyclic rigs

Turner liner thermal-structural load modeling

[NASA-CR-174892]

p 117 N86-21932

Longitudinal mode combustion instabilities of a high-pressure fuel-rich LOX/RP-1 preburner

Toward improved durability in advanced combustors and turbines: Progress in the prediction of thermomechanical loads

[NASA-TM-88932]

p 13 N87-28551

Turbine Engine Hot Section Technology, 1985

[NASA-CP-2405]

p 125 N88-11140

COMBUSTION STABILITY

Longitudinal mode combustion instabilities of a high-pressure fuel-rich LOX/RP-1 preburner

Creep-rupture reliability analysis

Probabilistic structural analysis to quantify uncertainties associated with turbopump blades

[AIAA PAPER 87-0766]

p 85 A87-33581

The application of probabilistic design theory to high temperature low cycle fatigue

[NASA-CR-165488]

p 91 N82-14531

Engine cyclic durability by analysis and material testing

[NASA-TM-83577]

p 102 N84-18683

Creep-rupture reliability analysis

[NASA-CR-3790]

p 102 N84-19925

Engine cyclic durability by analysis and material testing

[NASA-CR-174765]

p 110 N85-27261

Composite loads spectra for select space propulsion structural components

[NASA-TM-100174]

p 110 N85-27953

Fracture mechanics concepts in reliability analysis of monolithic ceramics

[NASA-TM-100174]

p 124 N87-27269

COMPOSITE MATERIALS

Engine environmental effects on composite behavior --- moisture and temperature effects on mechanical properties

[AIAA 80-0695]

p 1 A80-35101

Quantitative ultrasonic evaluation of engineering properties in metals, composites, and ceramics

On composites with periodic structure

[NASA-TM-82765]

p 50 A80-39641

Composites with periodic microstructure

Environmental and high strain rate effects on composites for engine applications

[NASA-TM-82882]

p 15 A83-12734

Indentation law for composite laminates

[NASA-TM-82882]

p 16 A84-27356

Simplified composite micromechanics for predicting microstresses

Environmental and High-Strain Rate effects on composites for engine applications

[NASA-TM-82882]

p 25 N82-31449

Structural tailoring of engine blades (STAEBL)

[NASA-CR-167949]

p 7 N82-33391

INHYD: Computer code for intraply hybrid composite design. A users manual

[NASA-TP-2239]

p 26 N84-13224

A study of the stress wave factor technique for the characterization of composite materials

[NASA-CR-174870]

p 29 N85-30035

COMPOSITE STRUCTURES

- Geometrically nonlinear analysis of layered composite shells p 68 A83-27431
- Three-dimensional finite-element analysis of layered composite plates p 68 A83-27432
- Design concepts for low cost composite engine frames
- [AIAA PAPER 83-2445] p 2 A83-48331
- Characterization of composite materials by means of the ultrasonic stress wave factor p 16 A84-10430
- Design procedures for fiber composite structural components - Rods, beams, and beam columns
- p 17 A85-15636
- Fracture of composite-adhesive-composite systems
- p 76 A85-27935
- Factors influencing the ultrasonic stress wave factor evaluation of composite material structures
- p 81 A86-34257
- Composite sandwich thermostructural behavior - Computational simulation
- [AIAA PAPER 86-0948] p 82 A86-38842
- Computational composite mechanics for aerospace propulsion structures
- [AIAA PAPER 86-1190] p 19 A86-40596
- Aeroelastic behavior of low aspect ratio metal and composite blades
- [ASME PAPER 86-GT-243] p 84 A86-48271
- Design concepts/parameters assessment and sensitivity analyses of select composite structural components
- p 85 A87-25407
- A higher order theory of laminated composite cylindrical shells
- p 86 A87-35656
- Composite space antenna structures - Properties and environmental effects
- p 20 A87-38610
- Sudden stretching of a four layered composite plate
- [NASA-CR-159870] p 23 N80-25383
- Composite containment systems for jet engine fan blades
- [NASA-TM-81675] p 90 N81-17480
- Structural dynamics of shroudless, hollow fan blades with composite in-lays
- [NASA-TM-82816] p 7 N82-22266
- Compression behavior of unidirectional fibrous composite
- [NASA-TM-82833] p 25 N82-22313
- Design procedures for fiber composite structural components: Rods, columns and beam columns
- [NASA-TM-83321] p 26 N83-24559
- Design concepts for low-cost composite engine frames
- [NASA-TM-83544] p 8 N84-16186
- Composite space antenna structures: Properties and environmental effects
- [NASA-TM-88859] p 31 N87-16880
- Nondestructive evaluation of structural ceramics
- [NASA-TM-88978] p 62 N87-18109
- Computational composite mechanics for aerospace propulsion structures
- [NASA-TM-88965] p 31 N87-18614
- Composite mechanics for engine structures
- [NASA-TM-100176] p 32 N88-12552
- COMPRESSIBILITY**
- The plastic compressibility of 7075-T651 aluminum-alloy plate
- p 36 A86-49690
- Tensile and compressive constitutive response of 316 stainless steel at elevated temperatures
- p 98 N83-34353
- COMPRESSION LOADS**
- Design procedures for fiber composite structural components - Rods, beams, and beam columns
- p 17 A85-15636
- Benchmark notch test for life prediction
- [NASA-CR-165571] p 95 N83-12451
- Design procedures for fiber composite structural components: Rods, columns and beam columns
- [NASA-TM-83321] p 26 N83-24559
- COMPRESSION TESTS**
- Buckling of rotating beams
- p 63 A80-20149
- Compressive behavior of unidirectional fibrous composites
- p 16 A84-29894
- COMPRESSIVE STRENGTH**
- Longitudinal compressive failure modes in fiber composites End attachment effects on IITRI type test specimens
- p 19 A86-19999
- Compression behavior of unidirectional fibrous composite
- [NASA-TM-82833] p 25 N82-22313
- COMPRESSOR BLADES**
- Analysis of an axial compressor blade vibration based on wave reflection theory
- [ASME PAPER 83-GT-151] p 2 A83-47970
- Optimization of cascade blade mistuning. I - Equations of motion and basic inherent properties
- p 3 A85-42365
- Optimization of cascade blade mistuning. II - Global optimum and numerical optimization
- p 3 A85-45715

- Approximations to eigenvalues of modified general matrices
- [AIAA PAPER 87-0947] p 86 A87-33756
- Structural tailoring of engine blades (STAEBL) theoretical manual
- [NASA-CR-175112] p 12 N86-27283
- Structural tailoring of engine blades (STAEBL) user's manual
- [NASA-CR-175113] p 13 N86-27284
- Shot peening for Ti-6Al-4V alloy compressor blades
- [NASA-TP-2711] p 123 N87-20566
- COMPRESSOR ROTORS**
- Evaluation of the cyclic behavior of aircraft turbine disk alloys, part 2
- [NASA-CR-165123] p 38 N80-30482
- Lewis Research Center spin rig and its use in vibration analysis of rotating systems
- [NASA-TP-2304] p 9 N84-24578
- COMPRESSORS**
- Bladed-shrouded-disc aeroelastic analyses: Computer program updates in NASTRAN level 17.7
- [NASA-CR-165428] p 8 N84-15154
- COMPUTATION**
- Progressive damage, fracture predictions and post mortem correlations for fiber composites
- [NASA-TM-87101] p 29 N86-10290
- A computational procedure for automated flutter analysis
- [NASA-TM-100171] p 125 N87-28058
- COMPUTATIONAL FLUID DYNAMICS**
- NASA Lewis Research Center/university graduate research program on engine structures
- [ASME PAPER 85-GT-159] p 80 A86-22084
- The finite analytic method, volume 3
- [NASA-CR-170186] p 127 N83-23087
- The finite analytic method, volume 4
- [NASA-CR-170187] p 127 N83-23088
- The finite analytic method, volume 5
- [NASA-CR-170188] p 127 N83-23089
- NASA Lewis Research Center/University Graduate Research Program on Engine Structures
- [NASA-TM-86916] p 107 N85-18375
- COMPUTATIONAL GRIDS**
- Rational approach for assumed stress finite elements
- p 74 A85-12029
- COMPUTER AIDED DESIGN**
- Computer code for intraply hybrid composite design
- p 15 A81-44662
- Structural tailoring of engine blades (STAEBL)
- [AIAA 83-0828] p 1 A83-29737
- Finite element engine blade structural optimization
- [AIAA PAPER 85-0645] p 76 A85-30313
- Structural tailoring of advanced turboprops
- [AIAA PAPER 87-0753] p 85 A87-33648
- Structural tailoring of engine blades (STAEBL)
- [NASA-CR-167949] p 7 N82-33391
- Burner liner thermal-structural load modeling
- [NASA-CR-174892] p 117 N86-21932
- STAEBL: Structural tailoring of engine blades, phase 2
- p 13 N87-11731
- COMPUTER PROGRAMMING**
- NASTRAN level 16 programmer's manual updates for aeroelastic analysis of bladed discs
- [NASA-CR-159825] p 90 N81-19482
- COMPUTER PROGRAMS**
- Computer code for intraply hybrid composite design
- p 15 A81-44662
- On the automatic generation of FEM models for complex gears - A work-in-progress report
- p 47 A82-48243
- ICAN - Integrated composites analyzer
- [AIAA PAPER 84-0974] p 18 A85-16094
- A simplified method for elastic-plastic-creep structural analysis
- [ASME PAPER 84-GT-191] p 76 A85-23150
- A study of interply layer effects on the free edge stress field of angleplied laminates
- p 18 A85-41127
- DEAN - A program for Dynamic Engine Analysis
- [AIAA PAPER 85-1354] p 3 A86-14430
- Dynamic stress analysis of smooth and notched fiber composite flexural specimens
- p 20 A86-41070
- Advances in 3-D Inelastic Analysis Methods for hot section components
- [AIAA PAPER 87-0719] p 85 A87-33645
- Analytical flutter investigation of a composite propfan model
- [AIAA PAPER 87-0738] p 87 A87-40497
- Instructions for the use of the CIVM-Jet 4C finite-strain computer code to calculate the transient structural responses of partial and/or complete arbitrarily-curved rings subjected to fragment impact
- [NASA-CR-159873] p 88 N80-27720
- NASTRAN level 16 demonstration manual updates for aeroelastic analysis of bladed discs
- [NASA-CR-159826] p 90 N81-19483
- Computer code for intraply hybrid composite design
- [NASA-TM-82593] p 24 N81-25151

- Integrated analysis of engine structures
- [NASA-TM-82713] p 91 N82-11491
- Bird impact analysis package for turbine engine fan blades
- [NASA-TM-82831] p 92 N82-26701
- Large displacements and stability analysis of nonlinear propeller structures
- [NASA-TM-82850] p 94 N82-31707
- Large displacements and stability analysis of nonlinear propeller structures
- p 95 N83-12460
- A simplified method for elastic-plastic-creep structural analysis
- [NASA-TM-83509] p 101 N84-14542
- Aerothermal modeling. Executive summary
- [NASA-CR-168330] p 7 N84-15152
- Digital computer program for generating dynamic turbofan engine models (DIGTEM)
- [NASA-TM-83446] p 8 N84-16185
- Development of a simplified procedure for cyclic structural analysis
- [NASA-TP-2243] p 103 N84-20878
- Dynamic stress analysis of smooth and notched fiber composite flexural specimens
- [NASA-TM-83694] p 27 N84-25770
- ICAN: Integrated composites analyzer
- [NASA-TM-83700] p 27 N84-26755
- A computer program for predicting nonlinear uniaxial material responses using viscoplastic models
- [NASA-TM-83675] p 104 N84-29247
- Application of finite element substructuring to composite micromechanics
- [NASA-TM-83729] p 27 N84-31288
- Fracture modes in notched angleplied composite laminates
- [NASA-TM-83802] p 28 N84-34576
- A study of interply layer effects on the free-edge stress field of angleplied laminates
- [NASA-TM-86924] p 28 N85-15822
- 3-D inelastic analysis methods for hot section components (base program) --- turbine blades, turbine vanes, and combustor liners
- [NASA-CR-174700] p 107 N85-21686
- Component-specific modeling
- [NASA-CR-174765] p 110 N85-27261
- Composite loads spectra for select space propulsion structural components: Probabilistic load model development
- p 110 N85-27954
- Probabilistic finite element development
- p 111 N85-27956
- DEAN: A program for dynamic engine analysis
- [NASA-TM-87033] p 11 N85-28945
- A comparison of smooth specimen and analytical simulation techniques for notched members at elevated temperatures
- p 114 N85-31546
- Component-specific modeling
- [NASA-CR-174925] p 12 N85-32119
- Component-specific modeling
- [NASA-CR-174765] p 12 N85-34140
- Progressive damage, fracture predictions and post mortem correlations for fiber composites
- [NASA-TM-87101] p 29 N86-10290
- Integrated Composite Analyzer (ICAN): Users and programmers manual
- [NASA-TP-2515] p 30 N86-21614
- Computational simulation of progressive fracture in fiber composites
- [NASA-TM-87341] p 30 N86-26376
- Structural tailoring of engine blades (STAEBL) user's manual
- [NASA-CR-175113] p 13 N86-27284
- Surface flaw reliability analysis of ceramic components with the SCARE finite element postprocessor program
- [NASA-TM-88901] p 121 N87-17087
- Analytical flutter investigation of a composite propfan model
- [NASA-TM-88944] p 122 N87-18115
- COMPUTER SYSTEMS PROGRAMS**
- Automatic finite element generators
- p 105 N84-31695
- COMPUTER TECHNIQUES**
- Computer aided derivation of equations for composite mechanics problems and finite element analyses
- [AIAA PAPER 86-1016] p 83 A86-38873
- COMPUTERIZED SIMULATION**
- On the automatic generation of FEM models for complex gears - A work-in-progress report
- p 47 A82-48243
- Comments on some problems in computational penetration mechanics
- p 71 A84-13545
- On the development of hierarchical solution strategies for nonlinear finite element formulations
- p 126 A85-21979
- On local total strain redistribution using a simplified cyclic inelastic analysis based on an elastic solution
- [AIAA PAPER 85-1419] p 78 A85-39770
- DEAN - A program for Dynamic Engine Analysis
- [AIAA PAPER 85-1354] p 3 A86-14430

- Composite sandwich thermostructural behavior - Computational simulation
[AIAA PAPER 86-0948] p 82 A86-38842
- Computational engine structural analysis
[ASME PAPER 86-GT-70] p 5 A86-48141
- SCARE - A postprocessor program to MSC/NASTRAN for reliability analysis of structural ceramic components
[ASME PAPER 86-GT-34] p 84 A87-17988
- Simulation of transducer-couplant effects on broadband ultrasonic signals
[NASA-TM-81489] p 53 N80-22714
- Aeroelastic analysis for propellers - mathematical formulations and program user's manual
[NASA-CR-3729] p 101 N84-12530
- Evaluation of the effect of crack closure on fatigue crack growth of simulated short cracks
[NASA-TM-83778] p 40 N84-31348
- On local total strain redistribution using a simplified cyclic inelastic analysis based on an elastic solution
[NASA-TM-86913] p 108 N85-21690
- DEAN: A program for dynamic engine analysis
[NASA-TM-87033] p 11 N85-28945
- Computational engine structural analysis
[NASA-TM-87231] p 116 N86-19663
- Computational simulation of progressive fracture in fiber composites
[NASA-TM-87341] p 30 N86-26376
- Fiber composite sandwich thermostructural behavior: Computational simulation
[NASA-TM-88787] p 31 N86-31663
- Dynamic delamination buckling in composite laminates under impact loading: Computational simulation
[NASA-TM-100192] p 31 N87-28611
- CONDUCTIVE HEAT TRANSFER**
Thermal stress analysis for a wood composite blade --- wind turbines
[NASA-CR-173394] p 103 N84-21903
- CONFERENCES**
Vibrations of blades and bladed disk assemblies; Proceedings of the Tenth Biennial Conference on Mechanical Vibration and Noise, Cincinnati, OH, September 10-13, 1985
p 4 A86-26901
- Nonlinear Constitutive Relations for High Temperature Applications
[NASA-CP-2271] p 98 N83-34351
- Nonlinear Structural Analysis
[NASA-CP-2297] p 105 N84-31688
- Turbine Engine Hot Section Technology (HOST)
[NASA-TM-83022] p 9 N85-10951
- Nonlinear Constitutive Relations for High Temperature Application, 1984
[NASA-CP-2369] p 112 N85-31530
- Analytical Ultrasonics in Materials Research and Testing
[NASA-CP-2383] p 59 N86-22962
- Turbine Engine Hot Section Technology, 1984
[NASA-CP-2339] p 120 N87-11180
- The 20th Aerospace Mechanics Symposium
[NASA-CP-2423-REV] p 121 N87-16321
- Turbine Engine Hot Section Technology, 1985
[NASA-CP-2405] p 125 N88-11140
- CONSTITUTIVE EQUATIONS**
Nonlinear structural and life analyses of a combustor liner
p 68 A83-12764
- Requirements of constitutive models for two nickel-base superalloys
p 33 A83-21071
- An uncoupled viscoplastic constitutive model for metals at elevated temperature
p 69 A83-29798
- Thermodynamically consistent constitutive equations for nonisothermal large strain, elasto-plastic, creep behavior
[AIAA PAPER 85-0621] p 77 A85-38425
- Unified constitutive material models for nonlinear finite-element structural analysis --- gas turbine engine blades and vanes
[AIAA PAPER 85-1418] p 77 A85-39769
- Constitutive modeling and computational implementation for finite strain plasticity
p 78 A85-40910
- Unified constitutive materials model development and evaluation for high-temperature structural analysis applications --- for aircraft gas turbine engines
p 84 A86-49133
- Nonlinear structural and life analyses of a combustor liner
[NASA-TM-82846] p 92 N82-24501
- Nonlinear constitutive theory for turbine engine structural analysis
p 95 N82-33744
- Materials constitutive models for nonlinear analysis of thermally cycled structures
[NASA-TP-2055] p 95 N83-12449
- Research and development program for the development of advanced time-temperature dependent constitutive relationships. Volume 1: Theoretical discussion
[NASA-CR-168191-VOL-1] p 100 N84-10613
- Research and development program for the development of advanced time-temperature dependent constitutive relationships. Volume 2: Programming manual
[NASA-CR-168191-VOL-2] p 100 N84-10614
- Viscoplastic constitutive relationships with dependence on thermomechanical history
[NASA-CR-174836] p 108 N85-21691
- Unified constitutive material models for nonlinear finite-element structural analysis --- gas turbine engine blades and vanes
[NASA-TM-86985] p 108 N85-24338
- On thermomechanical testing in support of constitutive equation development for high temperature alloys
[NASA-CR-174879] p 109 N85-25894
- Nonlinear Constitutive Relations for High Temperature Application, 1984
[NASA-CP-2369] p 112 N85-31530
- A survey of unified constitutive theories
p 112 N85-31531
- Numerical considerations in the development and implementation of constitutive models
p 113 N85-31541
- On numerical integration and computer implementation of viscoplastic models
p 113 N85-31542
- Finite element analysis of notch behavior using a state variable constitutive equation
p 114 N85-31548
- Anisotropic constitutive model for nickel base single crystal alloys: Development and finite element implementation
[NASA-CR-175015] p 117 N86-21952
- Integrated research in constitutive modelling at elevated temperatures, part 1
[NASA-CR-177237] p 120 N86-30227
- CONSTRAINTS**
Locally bound constrained Newton-Raphson solution algorithms --- for modeling kinematic and material nonlinearity
p 83 A86-43771
- Constrained hierarchical least square nonlinear equation solvers --- for indefinite stiffness and large structural deformations
p 83 A86-43774
- Structural tailoring of engine blades (STAEBL) theoretical manual
[NASA-CR-175112] p 12 N86-27283
- CONSTRUCTION MATERIALS**
Ultrasonic NDE of structural ceramics for power and propulsion systems
[NASA-TM-100147] p 62 N87-26362
- CONTAINMENT**
Composite containment systems for jet engine fan blades
[NASA-TM-81675] p 90 N81-17480
- CONTINUUM MECHANICS**
Comments on some problems in computational penetration mechanics
p 71 A84-13545
- Probabilistic finite elements for transient analysis in nonlinear continua
p 80 A86-28653
- Constrained hierarchical least square nonlinear equation solvers --- for indefinite stiffness and large structural deformations
p 83 A86-43774
- CONTROL MOMENT GYROSCOPES**
Application of traction drives as servo mechanisms
p 114 N85-33520
- CONVECTIVE HEAT TRANSFER**
The finite analytic method, volume 5
[NASA-CR-170188] p 127 N83-23089
- CONVERGENCE**
Formal convergence characteristics of elliptically constrained incremental Newton-Raphson algorithms
p 126 A83-10273
- COOLING**
Aerothermal modeling. Executive summary
[NASA-CR-168330] p 7 N84-15152
- COPPER**
Nonlinear damage analysis: Postulate and evaluation
[NASA-CR-168171] p 118 N86-26652
- COPPER ALLOYS**
High temperature low cycle fatigue mechanisms for nickel base and a copper base alloy
[NASA-CR-3543] p 39 N82-26436
- CORIOLIS EFFECT**
Vibration and buckling of rotating, pretwisted, preconed beams including Coriolis effects
p 80 A86-26910
- Nonlinear vibration and stability of rotating, pretwisted, preconed blades including Coriolis effects
p 86 A87-39896
- Forced vibration analysis of rotating cyclic structures in NASTRAN
[NASA-CR-165429] p 100 N84-11514
- Vibration and buckling of rotating, pretwisted, preconed beams including Coriolis effects
[NASA-TM-87004] p 109 N85-25893
- Nonlinear flap-lag-extensional vibrations of rotating, pretwisted, preconed beams including Coriolis effects
[NASA-TM-87102] p 115 N85-34427
- Nonlinear bending-torsional vibration and stability of rotating, pretwisted, preconed blades including Coriolis effects
[NASA-TM-87207] p 116 N86-17789
- CORRELATION**
A quarter-century of progress in the development of correlation and extrapolation methods for creep rupture data
p 63 A80-38142
- Elevated temperature biaxial fatigue
[NASA-CR-175795] p 110 N85-27263
- COST ANALYSIS**
Structural tailoring of engine blades (STAEBL) user's manual
[NASA-CR-175113] p 13 N86-27284
- COST ESTIMATES**
Structural analysis and cost estimate of an eight-leg space frame as a support structure for horizontal axis wind turbines
[NASA-TM-83470] p 112 N85-30361
- COUPLED MODES**
Vibration and flutter of mistuned bladed-disk assemblies
[AIAA PAPER 84-0991] p 75 A85-16095
- The effect of circumferential aerodynamic detuning on coupled bending-torsion unstalled supersonic flutter
[ASME PAPER 86-GT-100] p 6 A87-25396
- Vibration and flutter of mistuned bladed-disk assemblies
[NASA-TM-83634] p 103 N84-23923
- Nonlinear flap-lag-extensional vibrations of rotating, pretwisted, preconed beams including Coriolis effects
[NASA-TM-87102] p 115 N85-34427
- COUPLING**
Effects of structural coupling on mistuned cascade flutter and response
[ASME PAPER 83-GT-117] p 73 A84-33701
- Effects of structural coupling on mistuned cascade flutter and response
[NASA-TM-83049] p 96 N83-15672
- CRACK CLOSURE**
Influence of load interactions on crack growth as related to state of stress and crack closure
[NASA-TM-87117] p 42 N86-12292
- Closure of fatigue cracks at high strains
[NASA-CR-175021] p 116 N86-17788
- Variables controlling fatigue crack growth of short cracks
[NASA-TM-87208] p 43 N86-21661
- Influence of fatigue crack wake length and state of stress on crack closure
[NASA-TM-87292] p 43 N86-22686
- CRACK GEOMETRY**
On the equivalence between semiempirical fracture analyses and R-curves
p 64 A81-18792
- Growth and stability of interacting surface flaws of arbitrary shape
p 68 A83-15060
- Wide-range displacement expressions for standard fracture mechanics specimens
p 79 A86-20706
- Creep crack-growth: A new path-independent T sub o and computational studies
[NASA-CR-168930] p 92 N82-24503
- Effect of crack curvature on stress intensity factors for ASTM standard compact tension specimens
[NASA-CR-168280] p 100 N84-11513
- Crack layer theory
[NASA-CR-174634] p 103 N84-22980
- CRACK INITIATION**
Cyclic behavior of turbine disk alloys at 650 C
p 32 A81-12266
- Requirements of constitutive models for two nickel-base superalloys
p 33 A83-21071
- Turbine blade nonlinear structural and life analysis
p 1 A83-29024
- Fatigue crack initiation and propagation in several nickel-base superalloys at 650 C
p 33 A83-41199
- Application of two creep fatigue life models for the prediction of elevated temperature crack initiation of a nickel base alloy
[AIAA PAPER 85-1420] p 35 A85-43979
- Three-dimensional hybrid-stress finite element analysis of composite laminates with cracks and cutouts
p 80 A86-26896
- Practical implementation of the double linear damage rule and damage curve approach for treating cumulative fatigue damage
[NASA-TM-81517] p 88 N80-23684
- Analysis of crack propagation as an energy absorption mechanism in metal matrix composites
[NASA-CR-165051] p 24 N82-14288
- Elevated temperature fatigue testing of metals
[NASA-TM-82745] p 91 N82-16419
- Mechanisms of deformation and fracture in high temperature low cycle fatigue of Rene 80 and IN 100
[NASA-CR-165498] p 93 N82-26706

A preliminary study of crack initiation and growth at stress concentration sites
[NASA-CR-169358] p 94 N82-33738

Creep fatigue of low-cobalt superalloys: Waspalloy, PM U 700 and wrought U 700
[NASA-CR-168260] p 40 N84-13265

Literature survey on oxidations and fatigue lives at elevated temperatures
[NASA-CR-174639] p 40 N84-20674

Crack layer theory
[NASA-CR-174634] p 103 N84-22980

Crack tip field and fatigue crack growth in general yielding and low cycle fatigue
[NASA-CR-174686] p 41 N84-32503

Nonlinear structural and life analyses of a combustor liner
p 9 N85-10955

Pre-HOST high temperature crack propagation
p 9 N85-10956

Life prediction and constitutive behavior: Overview
p 10 N85-10973

Constitutive model development for isotropic materials
p 10 N85-10975

Creep fatigue life prediction for engine hot section materials (isotropic)
[NASA-CR-168228] p 11 N85-31057

Fatigue crack propagation of nickel-base superalloys at 650 deg C
[NASA-TM-87150] p 42 N86-12294

Simplified cyclic structural analyses of SSME turbine blades
[NASA-TM-87214] p 116 N86-16615

Fatigue crack growth under general-yielding cyclic-loading
[NASA-CR-175049] p 117 N86-21951

Cyclic creep analysis from elastic finite-element solutions
[NASA-TM-87213] p 117 N86-25822

Low-cycle thermal fatigue
[NASA-TM-87225] p 118 N86-26651

Nonlinear damage analysis: Postulate and evaluation
[NASA-CR-168171] p 118 N86-26652

Structural analysis of turbine blades using unified constitutive models
[NASA-TM-88807] p 119 N86-28461

Compliance matrices for cracked bodies
[NASA-CR-179478] p 120 N86-30236

Flaw imaging and ultrasonic techniques for characterizing sintered silicon carbide
[NASA-TM-100177] p 63 N88-12106

Creep life prediction based on stochastic model of microstructurally short crack growth
[NASA-TM-100245] p 125 N88-12825

CRACK PROPAGATION

Simple spline-function equations for fracture mechanics calculations
p 63 A80-10832

Fracture toughness determination of Al₂O₃ using four-point-bend specimens with straight-through and chevron notches
p 45 A80-42085

Performance of Chevron-notch short bar specimen in determining the fracture toughness of silicon nitride and aluminum oxide
p 45 A80-50696

On the equivalence between semiempirical fracture analyses and R-curves
p 64 A81-18792

On a study of the $\Delta T/c$ and $C/\text{asterisk}/$ integrals for fracture analysis under non-steady creep
p 65 A82-36782

Moving singularity creep crack growth analysis with the $\Delta T/c$ and $C/\text{asterisk}/$ integrals --- path-independent vector and energy rate line integrals
p 66 A82-40066

Crack displacements for J/I testing with compact specimens
p 66 A82-40358

Moving cracks in layered composites
p 67 A83-12048

Growth and stability of interacting surface flaws of arbitrary shape
p 68 A83-15060

The effect of microstructure on the fatigue behavior of Ni base superalloys
p 33 A83-36166

Dynamic fields near a crack tip growing in an elastic-perfectly-plastic solid
p 70 A83-38528

Fatigue crack initiation and propagation in several nickel-base superalloys at 650 C
p 33 A83-41199

The effect of microstructure on 650 C fatigue crack growth in P/M Astroloy
p 33 A84-12395

The effects of frequency and hold times on fatigue crack propagation rates in a nickel base superalloy
p 34 A84-18733

Fracture toughness of hot-pressed beryllium
p 34 A85-25835

On the fatigue crack propagation behavior of superalloys at intermediate temperatures
p 35 A85-32434

Thermal-mechanical fatigue crack growth in Inconel X-750
p 35 A86-20982

Shear fatigue crack growth - A literature survey
p 80 A86-24219

Fracture mechanics applied to nonisothermal fatigue crack growth
p 36 A86-28951

The crack layer approach to toughness characterization in steel
p 36 A86-30010

Dynamic delamination crack propagation in a graphite/epoxy laminate
p 20 A86-43010

Mode II fatigue crack growth specimen development
p 83 A86-43566

Fatigue crack growth under general-yielding cyclic-loading
p 84 A86-44339

A study of spectrum fatigue crack propagation in two aluminum alloys. I - Spectrum simplification. II - Influence of microstructures
p 36 A86-48973

Orientation and temperature dependence of some mechanical properties of the single-crystal nickel-base superalloy Rene N4. II - Low cycle fatigue behavior
p 37 A86-50322

Elastic analysis of a mode II fatigue crack test specimen
p 84 A87-17799

Simplified composite micromechanics for predicting microstresses
p 20 A87-20090

Fracture toughness of Si₃N₄ measured with short bar chevron-notched specimens
p 46 A87-30621

Comparison tests and experimental compliance calibration of the proposed standard round compact plane strain fracture toughness specimen
[NASA-TM-81379] p 87 N80-13513

Sudden bending of cracked laminates
[NASA-CR-159860] p 23 N80-25384

Evaluation of the cyclic behavior of aircraft turbine disk alloys, part 2
[NASA-CR-165123] p 38 N80-30482

Analysis of crack propagation as an energy absorption mechanism in metal matrix composites
[NASA-CR-165051] p 24 N82-14288

Micromechanical predictions of crack propagation and fracture energy in a single fiber boron/aluminum model composite
[NASA-CR-168550] p 25 N82-18326

Creep crack-growth: A new path-independent T sub o and computational studies
[NASA-CR-168930] p 92 N82-24503

Fracture mechanics criteria for turbine engine hot section components
[NASA-CR-167896] p 7 N82-25257

Interlaminar crack growth in fiber reinforced composites during fatigue, part 3
[NASA-CR-165434] p 93 N82-26715

Creep crack-growth: A new path-independent integral (T sub c), and computational studies
[NASA-CR-167897] p 94 N82-29619

A preliminary study of crack initiation and growth at stress concentration sites
[NASA-CR-169358] p 94 N82-33738

A total life prediction model for stress concentration sites
[NASA-CR-170290] p 96 N83-23629

Crack layer morphology and toughness characterization in steels
[NASA-CR-168154] p 97 N83-27256

Fatigue crack growth and low cycle fatigue of two nickel base superalloys
[NASA-CR-174534] p 39 N84-10267

A total life prediction model for stress concentration sites
[NASA-CR-168225] p 100 N84-10612

Crack layer theory
[NASA-CR-174634] p 103 N84-22980

Mode 2 fatigue crack growth specimen development
[NASA-TM-83722] p 104 N84-29248

Evaluation of the effect of crack closure on fatigue crack growth of simulated short cracks
[NASA-TM-83778] p 40 N84-31348

Inelastic and dynamic fracture and stress analyses
p 106 N84-31697

Crack tip field and fatigue crack growth in general yielding and low cycle fatigue
[NASA-CR-174686] p 41 N84-32503

On stress analysis of a crack-layer
[NASA-CR-174774] p 106 N84-34774

Pre-HOST high temperature crack propagation
p 9 N85-10956

HOST high temperature crack propagation
p 10 N85-10977

Thermal-mechanical fatigue crack growth in Inconel X-750
[NASA-CR-174740] p 41 N85-15877

A study of spectrum fatigue crack propagation in two aluminum alloys. 1: Spectrum simplification
[NASA-TM-86929] p 41 N85-18124

A study of spectrum fatigue crack propagation in two aluminum alloys. 2: Influence of microstructures
[NASA-TM-86930] p 41 N85-18125

Translational and extensional energy release rates (the J- and M-integrals) for a crack layer in thermoelasticity
[NASA-CR-174872] p 107 N85-21685

Ultrasonic testing of plates containing edge cracks
[NASA-CR-3904] p 58 N85-29307

Creep-fatigue behavior of NiCoCrAlY coated PWA 1480 superalloy single crystals
[NASA-TM-87110] p 42 N86-10311

Influence of load interactions on crack growth as related to state of stress and crack closure
[NASA-TM-87117] p 42 N86-12292

Fatigue crack propagation of nickel-base superalloys at 650 deg C
[NASA-TM-87150] p 42 N86-12294

Fractured toughness of Si₃N₄ measured with short bar chevron-notched specimens
[NASA-TM-87153] p 47 N86-13495

Closure of fatigue cracks at high strains
[NASA-CR-175021] p 116 N86-17788

Estimating the R-curve from residual strength data
[NASA-TM-87182] p 116 N86-18750

Grain boundary oxidation and oxidation accelerated fatigue crack nucleation and propagation
[NASA-CR-175050] p 43 N86-20542

Variables controlling fatigue crack growth of short cracks
[NASA-TM-87208] p 43 N86-21661

Fatigue crack growth under general-yielding cyclic-loading
[NASA-CR-175049] p 117 N86-21951

Simplified composite micromechanics for predicting microstresses
[NASA-TM-87295] p 30 N86-24759

Thermal-mechanical fatigue behavior of nickel-base superalloys
[NASA-CR-175048] p 43 N86-24818

Axial and torsional fatigue behavior of Waspalloy
[NASA-CR-175052] p 44 N86-25454

Fatigue crack layer propagation in silicon-iron
[NASA-CR-175115] p 118 N86-25851

Low-cycle thermal fatigue
[NASA-TM-87225] p 118 N86-26651

Effects of a high mean stress on the high cycle fatigue life of PWA 1480 and correlation of data by linear elastic fracture mechanics
[NASA-CR-175057] p 118 N86-27689

Creep life prediction based on stochastic model of microstructurally short crack growth
[NASA-TM-100245] p 125 N88-12825

CRACK TIPS

Dynamic fields near a crack tip growing in an elastic-perfectly-plastic solid
p 70 A83-38528

On stress field near a stationary crack tip
[AD-A152863] p 76 A85-24532

Analysis of an externally radially cracked ring segment subject to three-point radial loading
p 79 A86-20710

Re-examination of cumulative fatigue damage analysis - An engineering perspective
p 85 A87-22128

Crack tip field and fatigue crack growth in general yielding and low cycle fatigue
[NASA-CR-174686] p 41 N84-32503

Re-examination of cumulative fatigue damage analysis: An engineering perspective
[NASA-TM-87325] p 118 N86-27680

The effects of crack surface friction and roughness on crack tip stress fields
[NASA-TM-88976] p 122 N87-18881

CRACKING (FRACTURING)

Interface cracks in adhesively bounded lap-shear joints
p 67 A82-46109

SCARE - A postprocessor program to MSC/NASTRAN for reliability analysis of structural ceramic components
[ASME PAPER 86-GT-34] p 84 A87-17988

Method for estimating crack-extension resistance curve from residual strength data
[NASA-TP-1753] p 89 N81-11417

Experimental compliance calibration of the compact fracture toughness specimen
[NASA-TM-81665] p 89 N81-16492

Stress intensity and displacement coefficients for radially cracked ring segments subject to three-point bending
[NASA-TM-83059] p 96 N83-24874

Crack layer theory
[NASA-CR-174634] p 103 N84-22980

Compliance matrices for cracked bodies
[NASA-CR-179478] p 120 N86-30236

CRACKS

Analysis of an internally radially cracked ring segment subject to three-point radial loading
p 71 A84-18691

Wide-range weight functions for the strip with a single edge crack
p 79 A86-20709

Modelling of crack tip deformation with finite element method and its applications
p 87 N80-13503

Analysis of cracks emanating from a circular hole in unidirectional fiber reinforced composites, part 2
[NASA-CR-165433] p 93 N82-26714

Analysis of interface cracks in adhesively bonded lap shear joints, part 4
[NASA-CR-165438] p 93 N82-26716

- Analysis of an externally radially cracked ring segment subject to three-point radial loading [NASA-TM-83482] p 100 N83-35413
- Wide range weight functions for the strip with a single edge crack [NASA-TM-83478] p 100 N84-11512
- On stress analysis of a crack-layer [NASA-CR-174774] p 106 N84-34774
- Ultrasonic testing of plates containing edge cracks [NASA-CR-3904] p 58 N85-29307
- J-integral estimates for cracks in infinite bodies [NASA-CR-179474] p 119 N86-28467
- Surface flaw reliability analysis of ceramic components with the SCARE finite element postprocessor program [NASA-TM-88901] p 121 N87-17087
- CREEP ANALYSIS**
- Moving singularity creep crack growth analysis with the $\Delta T/c$ and $C/\text{asterisk}/$ integrals --- path-independent vector and energy rate line integrals p 66 A82-40066
- Strainrange partitioning - A total strain range version --- for creep fatigue life prediction by summing inelastic and elastic strain-range-life relations for two Ni base superalloys p 34 A85-11603
- Thermodynamically consistent constitutive equations for nonisothermal large strain, elasto-plastic, creep behavior [AIAA PAPER 85-0621] p 77 A85-38425
- Creep crack-growth: A new path-independent integral (T sub c), and computational studies [NASA-CR-167897] p 94 N82-29619
- Strainrange partitioning: A total strain range version [NASA-TM-83023] p 39 N83-14246
- Fatigue crack propagation of nickel-base superalloys at 650 deg C [NASA-TM-87150] p 42 N86-12294
- Cyclic creep analysis from elastic finite-element solutions [NASA-TM-87213] p 117 N86-25822
- CREEP BUCKLING**
- On the solution of creep induced buckling in general structure p 66 A82-39514
- Algorithms for elasto-plastic-creep postbuckling p 73 A84-38480
- Dynamic creep buckling: Analysis of shell structures subjected to time-dependent mechanical and thermal loading p 111 N85-27959
- CREEP PROPERTIES**
- On a study of the $\Delta T/c$ and $C/\text{asterisk}/$ integrals for fracture analysis under non-steady creep p 65 A82-36782
- The influence of hold times on LCF and FCG behavior in a P/M Ni-base superalloy --- Low Cycle Fatigue/Fatigue Crack Growth p 35 A85-32400
- Plasticity, viscoplasticity, and creep of solids by mechanical subelement models p 77 A85-35048
- Constitutive modeling of cyclic plasticity and creep, using an internal time concept p 83 A86-41673
- Creep crack-growth: A new path-independent T sub c and computational studies [NASA-CR-168930] p 92 N82-24503
- Relation of cyclic loading pattern to microstructural fracture in creep fatigue [NASA-TM-83473] p 98 N83-34349
- Constrained self-adaptive solutions procedures for structure subject to high temperature elastic-plastic creep effects p 99 N83-34370
- Stress and fracture analyses under elastic-plastic creep conditions: Some basic developments and computational approaches p 99 N83-34371
- Fatigue crack growth and low cycle fatigue of two nickel base superalloys [NASA-CR-174534] p 39 N84-10267
- Low strain, long life creep fatigue of AF2-1DA and INCO 718 [NASA-CR-167989] p 40 N84-10268
- Research and development program for the development of advanced time-temperature dependent constitutive relationships. Volume 2: Programming manual [NASA-CR-168191-VOL-2] p 100 N84-10614
- Creep fatigue of low-cobalt superalloys: Waspalloy, PM U 700 and wrought U 700 [NASA-CR-168260] p 40 N84-13265
- Nonlinear structural and life analyses of a combustor liner p 9 N85-10955
- Reliability considerations for the total strain range version of strainrange partitioning [NASA-CR-174757] p 106 N85-11380
- Creep fatigue life prediction for engine hot section materials (isotropic) p 11 N85-31057
- A comparison of two contemporary creep-fatigue life prediction methods p 113 N85-31538
- Creep-fatigue behavior of NiCoCrAlY coated PWA 1480 superalloy single crystals [NASA-TM-87110] p 42 N86-10311
- An update of the total-strain version of SRP [NASA-TP-2499] p 42 N86-12295
- Development of constitutive models for cyclic plasticity and creep behavior of super alloys at high temperature [NASA-CR-176418] p 43 N86-14356
- Integrated research in constitutive modelling at elevated temperatures, part 2 [NASA-CR-177233] p 119 N86-28455
- Finite element implementation of Robinson's unified viscoplastic model and its application to some uniaxial and multiaxial problems [NASA-TM-89891] p 123 N87-23010
- Creep life prediction based on stochastic model of microstructurally short crack growth [NASA-TM-100245] p 125 N88-12825
- CREEP RUPTURE STRENGTH**
- A quarter-century of progress in the development of correlation and extrapolation methods for creep rupture data p 63 A80-38142
- Creep-rupture reliability analysis p 79 A85-42566
- Creep-rupture reliability analysis [NASA-CR-3790] p 102 N84-19925
- CREEP STRENGTH**
- Advanced stress analysis methods applicable to turbine engine structures [NASA-CR-175573] p 11 N85-21165
- Exposure time considerations in high temperature low cycle fatigue [NASA-TM-88934] p 125 N87-28944
- CREEP TESTS**
- Strainrange partitioning life predictions of the long time Metal Properties Council creep-fatigue tests p 63 A80-27958
- Fatigue and creep-fatigue deformation of several nickel-base superalloys at 650 C p 32 A82-47398
- A continuous damage model based on stepwise-stress creep rupture tests [NASA-CR-174941] p 114 N85-32341
- Constitutive modeling for isotropic materials (HOST) [NASA-CR-174980] p 115 N86-10589
- CROSS CORRELATION**
- Measurement of ultrasonic velocity using phase-slope and cross-correlation methods p 51 A86-13192
- Ultrasonic velocity measurement using phase-slope cross-correlation methods [NASA-CR-83794] p 57 N84-34769
- CRYOGENICS**
- Select fiber composites for space applications - A mechanistic assessment p 18 A85-16040
- Select fiber composites for space applications: A mechanistic assessment [NASA-TM-83631] p 26 N84-22702
- CRYSTAL DISLOCATIONS**
- On finite deformation elasto-plasticity p 66 A82-45869
- CUMULATIVE DAMAGE**
- Considerations for damage analysis of gas turbine hot section components [ASME PAPER 84-PVP-77] p 2 A85 18792
- A history dependent damage model for low cycle fatigue [ASME PAPER 84-PVP-112] p 75 A85-18795
- The crack layer approach to toughness characterization in steel p 36 A86-30010
- Progressive fracture of fiber composites p 19 A86-35809
- Practical implementation of the double linear damage rule and damage curve approach for treating cumulative fatigue damage [NASA-TM-81517] p 88 N80-23684
- CYCLIC LOADS**
- Strainrange partitioning life predictions of the long time Metal Properties Council creep-fatigue tests p 63 A80-27958
- Cyclic behavior of turbine disk alloys at 650 C p 32 A81-12266
- Requirements of constitutive models for two nickel-base superalloys p 33 A83-21071
- Low cycle fatigue behavior of aluminum/stainless steel composites [AIAA 83-0806] p 16 A83-29886
- Benchmark cyclic plastic notch strain measurements p 33 A84-11194
- Hygrothermomechanical evaluation of transverse filament tape epoxy/polyester fiberglass composites p 17 A85-15632
- A history dependent damage model for low cycle fatigue [ASME PAPER 84-PVP-112] p 75 A85-18795
- On local total strain redistribution using a simplified cyclic inelastic analysis based on an elastic solution [AIAA PAPER 85-1419] p 78 A85-39770
- Application of two creep fatigue life models for the prediction of elevated temperature crack initiation of a nickel base alloy [AIAA PAPER 85-1420] p 35 A85-43979
- Mode II fatigue crack growth specimen development p 83 A86-43566
- Fatigue crack growth under general-yielding cyclic-loading p 84 A86-44339
- Results of an interlaboratory fatigue test program conducted on alloy 800H at room and elevated temperatures p 37 A87-54370
- Hygrothermomechanical evaluation of transverse filament tape epoxy/polyester fiberglass composites [NASA-CR-83044] p 26 N83-15362
- Experimental verification of the Neuber relation at room and elevated temperatures --- to predict stress-strain behavior in notched specimens of hastelloy x [NASA-CR-167967] p 96 N83-19121
- Development of a simplified analytical method for representing material cyclic response [NASA-CR-168100] p 96 N83-21390
- Relation of cyclic loading pattern to microstructural fracture in creep fatigue [NASA-TM-83473] p 98 N83-34349
- Simplified method for nonlinear structural analysis [NASA-TP-2208] p 99 N83-34372
- Development of a simplified procedure for cyclic structural analysis [NASA-TP-2243] p 103 N84-20878
- Mode 2 fatigue crack growth specimen development [NASA-TM-83722] p 104 N84-29248
- Cyclic torsion testing [NASA-TM-83756] p 105 N84-31687
- Nonlinear structural and life analyses of a combustor liner p 9 N85-10955
- Design procedures for fiber composite structural components: Panels subjected to combined in-plane loads [NASA-TM-86909] p 29 N85-15823
- Low cycle fatigue of MAR-M 200 single crystals at 760 and 870 deg C [NASA-TM-86933] p 41 N85-19074
- Local strain redistribution corrections for a simplified inelastic analysis procedure based on an elastic finite-element analysis [NASA-TP-2421] p 107 N85-20396
- On local total strain redistribution using a simplified cyclic inelastic analysis based on an elastic solution [NASA-TM-86913] p 108 N85-21690
- Cyclic structural analyses of anisotropic turbine blades for reusable space propulsion systems --- ssme fuel turbopump [NASA-TM-86990] p 108 N85-24339
- Analysis of shell type structures subjected to time dependent mechanical and thermal loading [NASA-CR-175747] p 109 N85-25896
- Interaction of high-cycle and low-cycle fatigue of Haynes 188 alloy at 1400 F deg p 111 N85-27961
- Thermomechanical deformation in the presence of metallurgical changes p 112 N85-31533
- Results of an interlaboratory fatigue test program conducted on alloy 800H at room and elevated temperatures [NASA-CR-174940] p 114 N85-32340
- Closure of fatigue cracks at high strains [NASA-CR-175021] p 116 N86-17788
- Fatigue crack growth under general-yielding cyclic-loading [NASA-CR-175049] p 117 N86-21951
- Cyclic creep analysis from elastic finite-element solutions [NASA-TM-87213] p 117 N86-25822
- Experimental evaluation criteria for constitutive models of time dependent cyclic plasticity [NASA-CR-176821] p 117 N86-25850
- Low-cycle thermal fatigue [NASA-TM-87225] p 118 N86-26651
- Ultrasonic stress wave characterization of composite materials [NASA-CR-3976] p 60 N86-27665
- Effects of a high mean stress on the high cycle fatigue life of PWA 1480 and correlation of data by linear elastic fracture mechanics [NASA-CR-175057] p 118 N86-27689
- Structural analysis of turbine blades using unified constitutive models [NASA-TM-88807] p 119 N86-28461
- Estimation of high temperature low cycle fatigue on the basis of inelastic strain and strainrate [NASA-TM-88841] p 44 N87-14489
- Bithermal low-cycle fatigue behavior of a NiCoCrAlY-coated single crystal superalloy [NASA-TM-89831] p 45 N87-20408
- Environmental degradation of 316 stainless steel in high temperature low cycle fatigue [NASA-TM-89931] p 124 N87-24007
- Exposure time considerations in high temperature low cycle fatigue [NASA-TM-88934] p 125 N87-28944

CYLINDRICAL COORDINATES

Hybrid solid element with a traction-free cylindrical surface p 82 A86-34462

CYLINDRICAL SHELLS

Vibrations of cantilevered shallow cylindrical shells of rectangular planform p 65 A82-11298
Vibrations of cantilevered circular cylindrical shells
Shallow versus deep shell theory p 69 A83-36958
A higher order theory of laminated composite cylindrical shells p 86 A87-35656

D

DAMAGE

Dynamic response of damaged angleplied fiber composites [NASA-TM-79281] p 21 N80-11145
Reexamination of cumulative fatigue damage laws p 112 N85-27962
A continuous damage model based on stepwise-stress creep rupture tests [NASA-CR-174941] p 114 N85-32341
Progressive damage, fracture predictions and post mortem correlations for fiber composites [NASA-TM-87101] p 29 N86-10290

DAMAGE ASSESSMENT

A history dependent damage model for low cycle fatigue [ASME PAPER 84-PVP-112] p 75 A85-18795
Re-examination of cumulative fatigue damage analysis - An engineering perspective p 85 A87-22128
Crack layer theory [NASA-CR-174634] p 103 N84-22980
Nonlinear damage analysis: Postulate and evaluation [NASA-CR-168171] p 118 N86-26652
Ultrasonic stress wave characterization of composite materials [NASA-CR-3976] p 60 N86-27665
Re-examination of cumulative fatigue damage analysis: An engineering perspective [NASA-TM-87325] p 118 N86-27680

DAMPERS

Design of dry-friction dampers for turbine blades p 2 A83-35883

DAMPERS (VALVES)

Experimental study of uncentralized squeeze film dampers [NASA-CR-168317] p 103 N84-19927

DAMPING

The impact damped harmonic oscillator in free decay [NASA-TM-89897] p 50 N87-23978

DATA ACQUISITION

A low-cost optical data acquisition system for vibration measurement [NASA-TM-88907] p 121 N87-14730

DATA BASE MANAGEMENT SYSTEMS

Flow dynamic environment data base development for the SSME p 109 N85-26885

DATA BASES

Flow dynamic environment data base development for the SSME p 109 N85-26885
Advanced turboprop vibratory characteristics [NASA-CR-174708] p 12 N86-24693

DATA CORRELATION

Creep-rupture reliability analysis p 79 A85-42566
Creep-rupture reliability analysis [NASA-CR-3790] p 102 N84-19925

DECAY RATES

The impact damped harmonic oscillator in free decay [NASA-TM-89897] p 50 N87-23978

DEFECTS

Reliability of void detection in structural ceramics by use of scanning laser acoustic microscopy p 52 A86-39027
Quantitative flaw characterization with scanning laser acoustic microscopy p 52 A86-45150
Environmental and High-Strain Rate effects on composites for engine applications [NASA-TM-82882] p 25 N82-31449
Reliability of void detection in structural ceramics using scanning laser acoustic microscopy [NASA-TM-87035] p 58 N85-32337

DEFORMATION

On finite deformation elasto-plasticity p 66 A82-45869
Finite element analysis of steadily moving contact fields p 70 A83-49437
On the suppression of zero energy deformation modes p 72 A84-21541
Pantographing self adaptive gap elements p 77 A85-37440
The tensile and fatigue deformation structures in a single crystal Ni-base superalloy p 36 A86-35697

Bounding solutions of geometrically nonlinear viscoelastic problems [AIAA PAPER 86-0943] p 82 A86-38838

Re-examination of cumulative fatigue damage analysis - An engineering perspective p 85 A87-22128
Stress and fracture analyses under elastic-plastic creep conditions: Some basic developments and computational approaches p 99 N83-34371
Inelastic and dynamic fracture and stress analyses p 106 N84-31697
Advanced stress analysis methods applicable to turbine engine structures [NASA-CR-175573] p 11 N85-21165
On Hybrid and mixed finite element methods [NASA-CR-175551] p 108 N85-23096
Yielding and deformation behavior of the single crystal nickel-base superalloy PWA 1480 [NASA-CR-175100] p 44 N86-25455
Re-examination of cumulative fatigue damage analysis: An engineering perspective [NASA-TM-87325] p 118 N86-27680

DEGRADATION

Interply layer degradation effects on composite structural response [AIAA PAPER 84-0849] p 18 A85-16096
Interply layer degradation effects on composite structural response [NASA-TM-83702] p 27 N84-26756
Environmental degradation of 316 stainless steel in high temperature low cycle fatigue [NASA-TM-89931] p 124 N87-24007

DELAMINATING

Interply layer degradation effects on composite structural response [AIAA PAPER 84-0849] p 18 A85-16096
Dynamic delamination crack propagation in a graphite/epoxy laminate p 20 A86-43010
Interlaminar crack growth in fiber reinforced composites during fatigue, part 3 [NASA-CR-165434] p 93 N82-26715
Edge delamination in angle-ply composite laminates, part 5 [NASA-CR-165439] p 94 N82-26717
Interply layer degradation effects on composite structural response [NASA-TM-83702] p 27 N84-26756

Dynamic delamination buckling in composite laminates under impact loading: Computational simulation [NASA-TM-100192] p 31 N87-28611
Free-edge delamination: Laminate width and loading conditions effects [NASA-TM-100238] p 32 N88-12551

DENSITY (MASS/VOLUME)

Ultrasonic velocity for estimating density of structural ceramics [NASA-TM-82765] p 46 N82-14359

DENSITY MEASUREMENT

The plastic compressibility of 7075-T651 aluminum-alloy plate p 36 A86-49690

DERIVATION

Computer aided derivation of equations for composite mechanics problems and finite element analyses [AIAA PAPER 86-1016] p 83 A86-38873

DESIGN ANALYSIS

Factors that affect the fatigue strength of power transmission shafting and their impact on design p 48 A87-14656
Optimization and analysis of gas turbine engine blades [AIAA PAPER 87-0827] p 126 A87-33614
Approximations to eigenvalues of modified general matrices [AIAA PAPER 87-0947] p 86 A87-33756
Development of procedures for calculating stiffness and damping of elastomers in engineering applications, part 6 [NASA-CR-159838] p 87 N80-22733
Application of advanced reliability methods to local strain fatigue analysis [NASA-CR-168198] p 97 N83-29734
Nonlinear Constitutive Relations for High Temperature Applications [NASA-CP-2271] p 98 N83-34351
Structural tailoring of engine blades (STAEBL) theoretical manual [NASA-CR-175112] p 12 N86-27283
Structural tailoring of engine blades (STAEBL) user's manual [NASA-CR-175113] p 13 N86-27284
High temperature stress-strain analysis p 120 N87-11209
Effect of design variables, temperature gradients and speed of life and reliability of a rotating disk [NASA-TM-88883] p 49 N87-13755

DESTRUCTIVE TESTS

Wide-range displacement expressions for standard fracture mechanics specimens p 79 A86-20706

DETECTION

Radiographic detectability limits for seeded voids in sintered silicon carbide and silicon nitride p 51 A86-31745
Radiographic detectability limits for seeded voids in sintered silicon carbide and silicon nitride [NASA-TM-86945] p 58 N85-21674
Reliability of scanning laser acoustic microscopy for detecting internal voids in structural ceramics [NASA-TM-87222] p 59 N86-16599

DIES

The thermal fatigue resistance of H-13 Die Steel for aluminum die casting dies [NASA-TM-83331] p 39 N83-35103

DIFFERENTIAL EQUATIONS

The finite analytic method, volume 3 [NASA-CR-170186] p 127 N83-23087
The finite analytic method, volume 5 [NASA-CR-170188] p 127 N83-23089
Time-independent anisotropic plastic behavior by mechanical subelement models p 99 N83-34369
Theoretical investigation of the force and dynamically coupled torsional-axial-lateral dynamic response of eared rotors [NASA-CR-173013] p 127 N83-34656
Nonlinear flap-lag-extensional vibrations of rotating, pretwisted, precone beams including Coriolis effects [NASA-TM-87102] p 115 N85-34427

DIFFRACTION PROPAGATION

Quantitative flaw characterization with scanning laser acoustic microscopy p 52 A86-45150

DIFFUSION WELDING

Metal honeycomb to porous wireform substrate diffusion bond evaluation p 51 A83-39620
Diffusion bonded boron/aluminum spar-shell fan blade [NASA-CR-159571] p 23 N80-25382
Metal honeycomb to porous wireform substrate diffusion bond evaluation [NASA-TM-82793] p 54 N82-18612

DIGITAL COMPUTERS

Digital computer program for generating dynamic turbofan engine models (DIGTEM) [NASA-TM-83446] p 8 N84-16185

DIGITAL FILTERS

Numerical synthesis of tri-variate velocity realizations of turbulence p 81 A86-28654

DIGITAL TECHNIQUES

Input-output characterization of an ultrasonic testing system by digital signal analysis [NASA-CR-3756] p 56 N84-15565
Digital computer program for generating dynamic turbofan engine models (DIGTEM) [NASA-TM-83446] p 8 N84-16185
Lewis Research Center spin rig and its use in vibration analysis of rotating systems [NASA-TP-2304] p 9 N84-24578

DIMENSIONAL STABILITY

Fiber composite sandwich thermostructural behavior: Computational simulation [NASA-TM-88787] p 31 N86-31663

DIRECTIONAL SOLIDIFICATION (CRYSTALS)

Thermal fatigue and oxidation data for directionally solidified MAR-M 246 turbine blades [NASA-CR-159798] p 6 N80-21330

DISKS (SHAPES)

Low strain, long life creep fatigue of AF2-1DA and INCO 718 [NASA-CR-167989] p 40 N84-10268
NASTRAN documentation for flutter analysis of advanced turbopropellers [NASA-CR-167927] p 8 N84-15153

DISPERSIONS

The effect of stress on ultrasonic pulses in fiber reinforced composites [NASA-CR-3724] p 56 N83-33180

DISPLACEMENT

Analysis of an internally radially cracked ring segment subject to three-point radial loading p 71 A84-18691
Measurements of self-excited rotor-blade vibrations using optical displacements [ASME PAPER 83-GT-132] p 73 A84-33702
A blade loss response spectrum for flexible rotor systems [ASME PAPER 84-GT-29] p 48 A84-46893
Wide-range displacement expressions for standard fracture mechanics specimens p 79 A86-20706
Large displacements and stability analysis of nonlinear propeller structures [NASA-TM-82850] p 94 N82-31707
Large displacements and stability analysis of nonlinear propeller structures p 95 N83-12460
Measurements of self-excited rotor-blade vibrations using optical displacements [NASA-TM-82953] p 95 N83-14523

Analysis of an externally radially cracked ring segment subject to three-point radial loading
[NASA-TM-83482] p 100 N83-35413

Theoretical and software considerations for nonlinear dynamic analysis
[NASA-CR-174504] p 101 N84-15589

Nonlinear displacement analysis of advanced propeller structures using NASTRAN
[NASA-TM-83737] p 104 N84-31683

Experimental compliance calibration of the NASA Lewis Research Center Mode 2 fatigue specimen
[NASA-TM-86908] p 107 N85-16205

Recent advances in hybrid/mixed finite elements
[NASA-CR-175574] p 107 N85-21687

Wave propagation in anisotropic medium due to an oscillatory point source with application to unidirectional composites
[NASA-CR-4001] p 60 N86-27666

DISPLACEMENT MEASUREMENT

Crack displacements for J/I testing with compact specimens
p 66 A82-40358

Stress intensity and displacement coefficients for radially cracked ring segments subject to three-point bending
[NASA-TM-83059] p 96 N83-24874

A study of the stress wave factor technique for nondestructive evaluation of composite materials
[NASA-CR-4002] p 60 N86-28445

DISTRIBUTION FUNCTIONS

Determination of grain size distribution function using two-dimensional Fourier transforms of tone pulse encoded images
[NASA-TM-88790] p 61 N86-31065

DRAG

Stress evaluations under rolling/sliding contacts
[NASA-CR-165561] p 91 N82-17521

DRY FRICTION

Effects of friction dampers on aerodynamically unstable rotor stages
[AIAA PAPER 83-0848] p 1 A83-32791

Design of dry-friction dampers for turbine blades
p 2 A83-35883

Forced response of a cantilever beam with a dry friction damper attached. I - Theory. II - Experiment
p 71 A84-21267

Effects of friction dampers on aerodynamically unstable rotor stages
p 3 A85-21866

Influence of friction dampers on torsional blade flutter
[ASME PAPER 85-GT-170] p 5 A86-32957

Frequency domain solutions to multi-degree-of-freedom, dry friction damped systems under periodic excitation
p 83 A86-39485

DUCTILITY

Failure analysis of a tool steel torque shaft
p 51 A84-17546

DURABILITY

Durability/life of fiber composites in hygrothermomechanical environments
p 16 A84-27359

Durability/life of fiber composites in hygrothermomechanical environments
[NASA-TM-82749] p 24 N82-14287

DYNAMIC CHARACTERISTICS

Micromechanics of intraply hybrid composites: Elastic and thermal properties
[NASA-TM-79253] p 21 N80-11143

DYNAMIC LOADS

Approximations to eigenvalues of modified general matrices
[AIAA PAPER 87-0947] p 86 A87-33756

Vapor cavitation in dynamically loaded journal bearings
[NASA-TM-83366] p 97 N83-24875

Dynamic delamination buckling in composite laminates under impact loading: Computational simulation
[NASA-TM-100192] p 31 N87-28611

Free-edge delamination: Laminate width and loading conditions effects
[NASA-TM-100238] p 32 N88-12551

DYNAMIC MODELS

Stability of large horizontal-axis axisymmetric wind turbines
p 64 A81-22526

DYNAMIC MODULUS OF ELASTICITY

Dynamic modulus and damping of boron, silicon carbide, and alumina fibers
p 15 A80-44236

Dynamic modulus and damping of boron, silicon carbide, and alumina fibers
[NASA-TM-81422] p 22 N80-20313

DYNAMIC PROGRAMMING

Theoretical and software considerations for nonlinear dynamic analysis
[NASA-CR-174504] p 101 N84-15589

DYNAMIC RESPONSE

Dynamic response of damaged angleplied fiber composites
p 14 A80-27982

Flutter and forced response of mistuned rotors using standing wave analysis
[AIAA 83-0845] p 69 A83-29823

Flutter and forced response of mistuned rotors using standing wave analysis
p 74 A85-12721

The dynamics of a flexible bladed disc on a flexible rotor in a two-rotor system
p 4 A86-25743

Approximations to eigenvalues of modified general matrices
[AIAA PAPER 87-0947] p 86 A87-33756

Dynamic response of damaged angleplied fiber composites
[NASA-TM-79281] p 21 N80-11145

Combustor liner durability analysis
[NASA-CR-165550] p 7 N81-17079

Theoretical investigation of the force and dynamically coupled torsional-axial-lateral dynamic response of eared rotors
[NASA-CR-173013] p 127 N83-34656

Dynamic behavior of spiral-groove and Rayleigh-Step self-acting face seals
[NASA-TP-2266] p 8 N84-16181

Flutter and forced response of mistuned rotors using standing wave analysis
[NASA-CR-173555] p 9 N84-24586

Extensions of the Ritz-Galerkin method for the forced, damped vibrations of structural elements
p 117 N86-21909

The effect of nonlinearities on the dynamic response of a large shuttle payload
[NASA-TM-88941] p 121 N87-18112

A comparative study of some dynamic stall models
[NASA-TM-88917] p 122 N87-18883

DYNAMIC STRUCTURAL ANALYSIS

Vibration and buckling of rectangular plates under in-plane hydrostatic loading
p 64 A80-45364

Effects of mistuning on bending-torsion flutter and response of a cascade in incompressible flow
[AIAA 81-0602] p 65 A81-29465

A pad perturbation method for the dynamic coefficients of tilting-pad journal bearings
p 47 A82-14400

Engine dynamic analysis with general nonlinear finite element codes. II - Bearing element implementation, overall numerical characteristics and benchmarking
[ASME PAPER 82-GT-292] p 47 A82-35462

Sensitivity analysis results of the effects of various parameters on composite design
p 15 A82-37101

The coupled aeroelastic response of turbomachinery blading to aerodynamic excitations
[AIAA 83-0844] p 69 A83-29822

Blade loss transient dynamic analysis of turbomachinery
p 2 A83-40864

Vibrations of blades with variable thickness and curvature by shell theory
[ASME PAPER 83-GT-152] p 70 A83-47978

Finite element analysis of steadily moving contact fields
p 70 A83-49437

The coupled response of turbomachinery blading to aerodynamic excitations
p 2 A84-26959

NASTRAN forced vibration analysis of rotating cyclic structures
[ASME PAPER 83-DET-20] p 72 A84-29103

Effects of warping and pretwist on torsional vibration of rotating beams
[ASME PAPER 84-WA/APM-41] p 75 A85-17040

Aeroelastic formulations for turbomachines and propellers
p 4 A86-24677

Hierarchical implicit dynamic least-square solution algorithm
p 80 A86-26689

The effects of strong shock loading on coupled bending-torsion flutter of tuned and mistuned cascades
p 4 A86-26893

Vibrations of blades and bladed disk assemblies; Proceedings of the Tenth Biennial Conference on Mechanical Vibration and Noise, Cincinnati, OH, September 10-13, 1985
p 4 A86-26901

The effect of limiting aerodynamic and structural coupling in models of mistuned bladed disk vibration
p 5 A86-26905

Probabilistic finite elements for transient analysis in nonlinear continua
p 80 A86-28653

Efficient algorithms for use in probabilistic finite element analysis
p 81 A86-28655

Dynamic characteristics of an assembly of prop-fan blades
[ASME PAPER 85-GT-134] p 5 A86-32956

Advanced three-dimensional dynamic analysis by boundary element methods
p 81 A86-34445

Structural dynamics verification facility study
[NASA-TM-82675] p 90 N81-33497

Structural dynamics of shroudless, hollow fan blades with composite in-lays
[NASA-TM-82816] p 7 N82-22266

Blade loss transient dynamics analysis with flexible bladed disk
[NASA-CR-168176] p 7 N84-13193

Lewis Research Center spin rig and its use in vibration analysis of rotating systems
[NASA-TP-2304] p 9 N84-24578

Augmented weak forms and element-by-element preconditioners: Efficient iterative strategies for structural finite elements. A preliminary study
p 106 N85-10384

Overview of structural response: Probabilistic structural analysis
p 110 N85-27952

Probabilistic finite element development
p 111 N85-27956

Dynamic creep buckling: Analysis of shell structures subjected to time-dependent mechanical and thermal loading
p 111 N85-27959

Extensions of the Ritz-Galerkin method for the forced, damped vibrations of structural elements
p 117 N86-21909

Advanced turboprop vibratory characteristics
[NASA-CR-174708] p 12 N86-24693

Structural dynamic measurement practices for turbomachinery at the NASA Lewis Research Center
[NASA-TM-88857] p 13 N86-32433

The effect of nonlinearities on the dynamic response of a large shuttle payload
[NASA-TM-88941] p 121 N87-18112

Structural and aeroelastic analysis of the SR-7L propan
[NASA-TM-86877] p 123 N87-22273

Identification of structural interface characteristics using component mode synthesis
[NASA-TM-88960] p 123 N87-24006

DYNAMICAL SYSTEMS

Hierarchical implicit dynamic least-square solution algorithm
p 80 A86-26689

E

EDGE DISLOCATIONS

Finite elastic-plastic deformation of polycrystalline metals
p 34 A84-43872

EDGE LOADING

Boundary-layer effects in composite laminates. I - Free-edge stress singularities. II - Free-edge stress solutions and basic characteristics
p 67 A82-46806

EDGES

A study of interply layer effects on the free edge stress field of angleplied laminates
p 18 A85-41127

Wide-range weight functions for the strip with a single edge crack
p 79 A86-20709

Edge delamination in angle-ply composite laminates, part 5
[NASA-CR-165439] p 94 N82-26717

Boundary-layer effects in composite laminates: Free-edge stress singularities, part 6
[NASA-CR-165440] p 94 N82-26718

Wide range weight functions for the strip with a single edge crack
[NASA-TM-83478] p 100 N84-11512

A study of interply layer effects on the free-edge stress field of angleplied laminates
[NASA-TM-86924] p 28 N85-15822

Ultrasonic testing of plates containing edge cracks
[NASA-CR-3904] p 58 N85-29307

Free-edge delamination: Laminate width and loading conditions effects
[NASA-TM-100238] p 32 N88-12551

EDUCATION

NASA Lewis Research Center/university graduate research program on engine structures
[ASME PAPER 85-GT-159] p 80 A86-22084

NASA Lewis Research Center/University Graduate Research Program on Engine Structures
[NASA-TM-86916] p 107 N85-18375

EFFICIENCY

Component-specific modeling
p 10 N85-10971

EIGENVALUES

Stability of large horizontal-axis axisymmetric wind turbines
p 64 A81-22526

Approximations to eigenvalues of modified general matrices
[AIAA PAPER 87-0947] p 86 A87-33756

EIGENVECTORS

Boundary layer thermal stresses in angle-ply composite laminates, part 1 --- graphite-epoxy composites
[NASA-CR-165412] p 93 N82-26713

ELASTIC BENDING

Influence of third-degree geometric nonlinearities on the vibration and stability of pretwisted, preconed, rotating blades
p 6 A87-46228

Influence of third-degree geometric nonlinearities on the vibration and stability of pretwisted, preconed, rotating blades
[NASA-TM-87307] p 120 N86-31920

ELASTIC BODIES

Continuous analysis of stresses from arbitrary surface loads on a half space
p 64 A81-14162

- Composites with periodic microstructure
p 15 A83-12734
- A numerical analysis of contact and limit-point behavior in a class of problems of finite elastic deformation
p 72 A84-27370
- Development and testing of stable, invariant, isoparametric curvilinear 2- and 3-D hybrid-stress elements
p 75 A85-19899
- ELASTIC DAMPING**
Dynamic modulus and damping of boron, silicon carbide, and alumina fibers
p 15 A80-44236
- Dynamic modulus and damping of boron, silicon carbide, and alumina fibers
[NASA-TM-81422] p 22 N80-20313
- ELASTIC DEFORMATION**
A numerical analysis of contact and limit-point behavior in a class of problems of finite elastic deformation
p 72 A84-27370
- On the existence and stability conditions for mixed-hybrid finite element solutions based on Reissner's variational principle
p 77 A85-33847
- Thermodynamically consistent constitutive equations for nonisothermal large strain, elasto-plastic, creep behavior [AIAA PAPER 85-0621] p 77 A85-38425
- On local total strain redistribution using a simplified cyclic inelastic analysis based on an elastic solution
[AIAA PAPER 85-1419] p 78 A85-39770
- Simplified method for nonlinear structural analysis [NASA-TP-2208] p 99 N83-34372
- On local total strain redistribution using a simplified cyclic inelastic analysis based on an elastic solution
[NASA-TM-86913] p 108 N85-21690
- Analysis of large, non-isothermal elastic-visco-plastic deformations
[NASA-CR-176220] p 115 N86-10588
- Formulation of the nonlinear analysis of shell-like structures, subjected to time-dependent mechanical and thermal loading
[NASA-CR-177194] p 119 N86-28462
- ELASTIC MEDIA**
On a study of the $\Delta T/c$ and $C/\text{asterisk}/$ integrals for fracture analysis under non-steady creep
p 65 A82-36782
- Ultrasonic wave propagation in two-phase media - Spherical inclusions
p 17 A85-11926
- ELASTIC PLATES**
Ultrasonic input-output for transmitting and receiving longitudinal transducers coupled to same face of isotropic elastic plate
[NASA-CR-3506] p 54 N82-18613
- ELASTIC PROPERTIES**
Micromechanics of intraply hybrid composites: Elastic and thermal properties
p 14 A80-27994
- Prediction of fiber composite mechanical behavior made simple
p 63 A80-32067
- Path-independent integrals in finite elasticity and inelasticity, with body forces, inertia, and arbitrary crack-face conditions
p 65 A82-32303
- Elasticity solutions for a class of composite laminate problems with stress singularities
p 17 A84-33389
- Existence and stability, and discrete BB and rank conditions, for general mixed-hybrid finite elements in elasticity
p 82 A86-34464
- Elastic analysis of a mode II fatigue crack test specimen
p 84 A87-17799
- Micromechanics of intraply hybrid composites: Elastic and thermal properties
[NASA-TM-79253] p 21 N80-11143
- Prediction of fiber composite mechanical behavior made simple --- using a rocket calculator
[NASA-TM-81404] p 22 N80-16107
- Three dimensional finite-element elastic analysis of a thermally cycled double-edge wedge geometry specimen --- nickel alloy turbine parts
[NASA-TM-80980] p 37 N80-26433
- Structural dynamics verification facility study
[NASA-TM-82675] p 90 N81-33497
- Elastic-plastic finite-element analyses of thermally cycled double-edge wedge specimens
[NASA-TP-1973] p 92 N82-20566
- Constrained self-adaptive solutions procedures for structure subject to high temperature elastic-plastic creep effects
p 99 N83-34370
- A total life prediction model for stress concentration sites
[NASA-CR-168225] p 100 N84-10612
- A survey of unified constitutive theories
p 112 N85-31531
- On the use of internal state variables in thermoviscoplastic constitutive equations
p 113 N85-31536
- Simplified cyclic structural analyses of SSME turbine blades
[NASA-TM-87214] p 116 N86-16615

- Cyclic creep analysis from elastic finite-element solutions
[NASA-TM-87213] p 117 N86-25822
- Effects of a high mean stress on the high cycle fatigue life of PWA 1480 and correlation of data by linear elastic fracture mechanics
[NASA-CR-175057] p 118 N86-27689
- Fracture mechanics concepts in reliability analysis of monolithic ceramics
[NASA-TM-100174] p 124 N87-27269
- ELASTIC SCATTERING**
Fundamentals of microcrack nucleation mechanics
[NASA-CR-3851] p 57 N85-16195
- ELASTIC WAVES**
Ultrasonic input-output for transmitting and receiving longitudinal transducers coupled to same face of isotropic elastic plate
[NASA-CR-3506] p 54 N82-18613
- Phenomenological and mechanics aspects of nondestructive evaluation and characterization by sound and ultrasound of material and fracture properties
[NASA-CR-3623] p 55 N83-11506
- The transmission or scattering of elastic waves by an inhomogeneity of simple geometry: A comparison of theories
[NASA-CR-3659] p 55 N83-16773
- Fundamentals of microcrack nucleation mechanics
[NASA-CR-3851] p 57 N85-16195
- Wave propagation in anisotropic medium due to an oscillatory point source with application to unidirectional composites
[NASA-CR-4001] p 60 N86-27666
- ELASTODYNAMICS**
The determination of the elastodynamic fields of an ellipsoidal inhomogeneity
[ASME PAPER 83-APM-19] p 69 A83-37388
- Sudden stretching of a four layered composite plate
[NASA-CR-159870] p 23 N80-25383
- Sudden bending of cracked laminates
[NASA-CR-159860] p 23 N80-25384
- ELASTOHYDRODYNAMICS**
Nonlinear transient finite element analysis of rotor-bearing-stator systems
p 48 A84-20580
- ELASTOMERS**
Development of procedures for calculating stiffness and damping of elastomers in engineering applications, part 6
[NASA-CR-159838] p 87 N80-22733
- ELASTOPLASTICITY**
On finite deformation elasto-plasticity
p 66 A82-45869
- On the solution of elastic-plastic static and dynamic postbuckling collapse of general structure
p 67 A83-12746
- Dynamic fields near a crack tip growing in an elastic-perfectly-plastic solid
p 70 A83-38528
- Algorithms for elasto-plastic-creep postbuckling
p 73 A84-38480
- Finite elastic-plastic deformation of polycrystalline metals
p 34 A84-43872
- On stress field near a stationary crack tip
[AD-A152863] p 76 A85-24532
- Plasticity, viscoplasticity, and creep of solids by mechanical subelement models
p 77 A85-35048
- Thermodynamically consistent constitutive equations for nonisothermal large strain, elasto-plastic, creep behavior [AIAA PAPER 85-0621] p 77 A85-38425
- Constitutive modeling and computational implementation for finite strain plasticity
p 78 A85-40910
- Comparison of elastic and elastic-plastic structural analyses for cooled turbine blade airfoils
[NASA-TP-1679] p 88 N80-27719
- Finite-strain large-deflection elastic-viscoplastic finite-element transient response analysis of structures
[NASA-CR-159874] p 88 N80-29762
- Elastic-plastic finite-element analyses of thermally cycled single-edge wedge specimens
[NASA-TP-1982] p 91 N82-20565
- HOST high temperature crack propagation
p 10 N85-10977
- A review of path-independent integrals in elastic-plastic fracture mechanics, task 4
[NASA-CR-174956] p 114 N85-33541
- J-integral estimates for cracks in infinite bodies
[NASA-CR-179474] p 119 N86-28467
- ELASTOSTATICS**
Efficient algorithms for use in probabilistic finite element analysis
p 81 A86-28655
- ELECTRIC NETWORKS**
Preliminary investigation of an electrical network model for ultrasonic scattering
[NASA-CR-3770] p 57 N84-17606
- ELECTRIC POWER PLANTS**
Photovoltaic power system reliability considerations
[NASA-TM-79291] p 53 N80-15422

ELECTRIC POWER TRANSMISSION

- Factors that affect the fatigue strength of power transmission shafting and their impact on design
p 48 A87-14656
- Preliminary investigation of an electrical network model for ultrasonic scattering
[NASA-CR-3770] p 57 N84-17606
- ELECTROHYDRAULIC FORMING**
Results of an interlaboratory fatigue test program conducted on alloy 800H at room and elevated temperatures
p 37 A87-54370
- Results of an interlaboratory fatigue test program conducted on alloy 800H at room and elevated temperatures
[NASA-CR-174940] p 114 N85-32340
- ELECTROMAGNETIC MEASUREMENT**
Nondestructive techniques for characterizing mechanical properties of structural materials - An overview
[ASME PAPER 86-GT-75] p 52 A86-48143
- Nondestructive techniques for characterizing mechanical properties of structural materials: An overview
[NASA-TM-87203] p 59 N86-19636
- ELECTRON BEAM WELDING**
Bending fatigue of electron-beam-welded foils. Application to a hydrodynamic air bearing in the Chrysler/DOE upgraded automotive gas turbine engine [NASA-TM-83539] p 102 N84-16589
- ELLIPSOIDS**
The determination of the elastodynamic fields of an ellipsoidal inhomogeneity
[ASME PAPER 83-APM-19] p 69 A83-37388
- ELLIPTIC FUNCTIONS**
Formal convergence characteristics of elliptically constrained incremental Newton-Raphson algorithms
p 126 A83-10273
- ENERGY ABSORPTION**
Impact resistance of fiber composites - Energy-absorbing mechanisms and environmental effects
p 18 A85-46543
- Analysis of crack propagation as an energy absorption mechanism in metal matrix composites
[NASA-CR-165051] p 24 N82-14288
- Impact resistance of fiber composites: Energy absorbing mechanisms and environmental effects
[NASA-TM-83594] p 26 N84-24712
- ENERGY DISSIPATION**
Micromechanical predictions of crack propagation and fracture energy in a single fiber boron/aluminum model composite
[NASA-CR-168550] p 25 N82-18326
- ENERGY TECHNOLOGY**
Reliability and quality assurance on the MOD 2 wind system
[NASA-TM-82717] p 54 N81-33492
- ENGINE ANALYZERS**
DEAN - A program for Dynamic Engine Analysis
[AIAA PAPER 85-1354] p 3 A86-14430
- DEAN: A program for dynamic engine analysis
[NASA-TM-87033] p 11 N85-28945
- ENGINE DESIGN**
Design concepts for low cost composite engine frames
[AIAA PAPER 83-2445] p 2 A83-48331
- Analytical and experimental investigation of the coupled bladed disk/shaft whirl of a cantilevered turbofan
[ASME PAPER 86-GT-98] p 6 A86-48163
- Fabrication and quality assurance processes for superhybrid composite fan blades
p 20 A87-19123
- Optimization and analysis of gas turbine engine blades
[AIAA PAPER 87-0827] p 126 A87-33614
- Integrated analysis of engine structures
[NASA-TM-82713] p 91 N82-11491
- Engine dynamic analysis with general nonlinear finite element codes. Part 2: Bearing element implementation overall numerical characteristics and benchmarking
[NASA-CR-167944] p 7 N82-33390
- Structural tailoring of engine blades (STAEBL)
[NASA-CR-167949] p 7 N82-33391
- Design concepts for low-cost composite engine frames
[NASA-TM-83544] p 8 N84-16186
- Nonlinear analysis for high-temperature composites: Turbine blades/vanes
p 106 N84-31699
- Fabrication and quality assurance processes for superhybrid composite fan blades
[NASA-TM-83354] p 28 N85-14882
- ENGINE PARTS**
Engine dynamic analysis with general nonlinear finite element codes. II - Bearing element implementation, overall numerical characteristics and benchmarking
[ASME PAPER 82-GT-292] p 47 A82-35462
- High-temperature fatigue in metals - A brief review of life prediction methods developed at the Lewis Research Center of NASA
p 33 A84-14286

- Considerations for damage analysis of gas turbine hot section components
[ASME PAPER 84-PVP-77] p 2 A85-18792
- Finite element engine blade structural optimization
[AIAA PAPER 85-0645] p 76 A85-30313
- Effect of low temperature on fatigue and fracture properties of Ti-5Al-2.5Sn(ELI) for use in engine components p 35 A85-47972
- Probabilistic structural analysis for space propulsion system components p 81 A86-28659
- Stress analysis of gas turbine engine structures using the boundary element method p 81 A86-34444
- Computational composite mechanics for aerospace propulsion structures
[AIAA PAPER 86-1190] p 19 A86-40596
- Elevated temperature fatigue testing of metals
[NASA-TM-82745] p 91 N82-16419
- Elastic-plastic finite-element analyses of thermally cycled double-edge wedge specimens
[NASA-TP-1973] p 92 N82-20566
- Three-dimensional stress analysis using the boundary element method p 106 N84-31700
- Component-specific modeling p 10 N85-10971
- Constitutive model development for isotropic materials p 10 N85-10975
- Creep fatigue life prediction for engine hot section materials (isotropic)
[NASA-CR-168228] p 11 N85-31057
- Component-specific modeling
[NASA-CR-174925] p 12 N85-32119
- Turbine Engine Hot Section Technology (HOST)
[NASA-CP-2289] p 115 N86-11495
- Probabilistic structural analysis methods for space propulsion system components
[NASA-TM-88861] p 121 N87-13794
- Nondestructive evaluation of structural ceramics
[NASA-TM-88978] p 62 N87-18109
- Computational composite mechanics for aerospace propulsion structures
[NASA-TM-88965] p 31 N87-18614
- High temperature stress-strain analysis p 125 N88-11170
- Composite mechanics for engine structures
[NASA-TM-100176] p 32 N88-12552
- ENGINE TESTS**
- Status of NASA full-scale engine aeroelasticity research p 63 A80-35906
- Computational engine structural analysis
[ASME PAPER 86-GT-70] p 5 A86-48141
- HOST liner cyclic facilities: Facility description p 10 N85-10988
- Computational engine structural analysis
[NASA-TM-87231] p 116 N86-19663
- Longitudinal mode combustion instabilities of a high-pressure fuel-rich LOX/RP-1 preburner p 60 N86-28250
- ENGINES**
- Inelastic and dynamic fracture and stress analyses p 106 N84-31697
- ENVIRONMENT EFFECTS**
- Impact resistance of fiber composites - Energy-absorbing mechanisms and environmental effects p 18 A85-46543
- Engine environmental effects on composite behavior
[NASA-TM-81508] p 22 N80-23370
- Impact resistance of fiber composites: Energy absorbing mechanisms and environmental effects
[NASA-TM-83594] p 26 N84-24712
- ENVIRONMENTAL CHEMISTRY**
- Environmental degradation of 316 stainless steel in high temperature low cycle fatigue
[NASA-TM-89931] p 124 N87-24007
- ENVIRONMENTAL TESTS**
- Engine environmental effects on composite behavior --- moisture and temperature effects on mechanical properties
[AIAA 80-0695] p 1 A80-35101
- The effect of microstructure on the fatigue behavior of Ni base superalloys p 33 A83-36166
- Ten year environmental test of glass fiber/epoxy pressure vessels
[AIAA PAPER 85-1198] p 19 A85-47022
- Fatigue crack growth and low cycle fatigue of two nickel base superalloys
[NASA-CR-174534] p 39 N84-10267
- Ten year environmental test of glass fiber/epoxy pressure vessels
[NASA-TM-87058] p 29 N85-30034
- EPOXY COMPOUNDS**
- Ten year environmental test of glass fiber/epoxy pressure vessels
[AIAA PAPER 85-1198] p 19 A85-47022
- Ten year environmental test of glass fiber/epoxy pressure vessels
[NASA-TM-87058] p 29 N85-30034
- EPOXY MATRIX COMPOSITES**
- Prediction of composite hygral behavior made simple p 16 A84-14285
- Durability/life of fiber composites in hygrothermomechanical environments p 16 A84-27359
- Durability/life of fiber composites in hygrothermomechanical environments
[NASA-TM-82749] p 24 N82-14287
- Prediction of composite hygral behavior made simple
[NASA-TM-82780] p 24 N82-16181
- A study of the stress wave factor technique for the characterization of composite materials
[NASA-CR-3670] p 55 N83-27248
- EPOXY RESINS**
- Fiberglass epoxy laminate fatigue properties at 300 and 20 K p 19 A85-47970
- Tensile and flexural strength of non-graphitic superhybrid composites: Predictions and comparisons
[NASA-TM-79276] p 21 N80-11144
- EQUATIONS OF MOTION**
- Flutter of turbofan rotors with mistuned blades p 74 A85-12716
- Optimization of cascade blade mistuning. I - Equations of motion and basic inherent properties p 3 A85-42365
- Vibration analysis of rotating turbomachinery blades by an improved finite difference method p 3 A86-14338
- EQUILIBRIUM METHODS**
- A new formulation of hybrid/mixed finite element p 67 A83-12739
- ERROR ANALYSIS**
- Surface flaw reliability analysis of ceramic components with the SCARE finite element postprocessor program
[NASA-TM-88901] p 121 N87-17087
- ERROR DETECTION CODES**
- Structural dynamics verification facility study
[NASA-TM-82675] p 90 N81-33497
- ESTIMATING**
- Estimating the R-curve from residual strength data
[NASA-TM-87182] p 116 N86-18750
- Estimation of high temperature low cycle fatigue on the basis of inelastic strain and strainrate
[NASA-TM-88841] p 44 N87-14489
- ETCHING**
- Ion beam sputter etching of orthopedic implanted alloy MP35N and resulting effects on fatigue
[NASA-TM-81747] p 38 N81-21174
- EULER EQUATIONS OF MOTION**
- An embedding method for the steady Euler equations p 126 A86-30814
- Stress and fracture analyses under elastic-plastic creep conditions: Some basic developments and computational approaches p 99 N83-34371
- EVALUATION**
- Nondestructive techniques for characterizing mechanical properties of structural materials - An overview
[ASME PAPER 86-GT-75] p 52 A86-48143
- Ultrasonic evaluation of mechanical properties of thick, multilayered, filament wound composites
[NASA-TM-87088] p 58 N86-10561
- Nondestructive techniques for characterizing mechanical properties of structural materials: An overview
[NASA-TM-87203] p 59 N86-19636
- The acousto-ultrasonic approach
[NASA-TM-89843] p 62 N87-20562
- Ultrasonic NDE of structural ceramics for power and propulsion systems
[NASA-TM-100147] p 62 N87-26362
- EXISTENCE THEOREMS**
- Formal convergence characteristics of elliptically constrained incremental Newton-Raphson algorithms p 126 A83-10273
- Existence and stability, and discrete BB and rank conditions, for general mixed-hybrid finite elements in elasticity p 82 A86-34464
- EXPANSION**
- Method for alleviating thermal stress damage in laminates
[NASA-CASE-LEW-12493-2] p 24 N81-26179
- EXPERIMENTATION**
- On thermomechanical testing in support of constitutive equation development for high temperature alloys
[NASA-CR-174879] p 109 N85-25894
- Progressive damage, fracture predictions and post mortem correlations for fiber composites
[NASA-TM-87101] p 29 N86-10290
- EXPERT SYSTEMS**
- Composite loads spectra for select space propulsion structural components: Probabilistic load model development p 110 N85-27954
- EXPOSURE**
- Exposure time considerations in high temperature low cycle fatigue
[NASA-TM-88934] p 125 N87-28944
- EXTENSOMETERS**
- Results of an interlaboratory fatigue test program conducted on alloy 800H at room and elevated temperatures p 37 A87-54370
- Some advances in experimentation supporting development of viscoplastic constitutive models
[NASA-CR-174855] p 109 N85-27260
- Some advances in experimentation supporting development of viscoplastic constitutive models p 113 N85-31545
- Results of an interlaboratory fatigue test program conducted on alloy 800H at room and elevated temperatures
[NASA-CR-174940] p 114 N85-32340
- EXTRAPOLATION**
- A quarter-century of progress in the development of correlation and extrapolation methods for creep rupture data p 63 A80-38142
- F**
- FABRICATION**
- Fabrication and quality assurance processes for superhybrid composite fan blades p 20 A87-19123
- Fabrication and quality assurance processes for superhybrid composite fan blades
[NASA-TM-83354] p 28 N85-14882
- Fracture characteristics of angleplied laminates fabricated from overaged graphite/epoxy prepreg
[NASA-TM-87266] p 30 N86-25417
- FACTORIZATION**
- Element-by-element solution procedures for nonlinear structural analysis p 105 N84-31694
- Augmented weak forms and element-by-element preconditioners: Efficient iterative strategies for structural finite elements. A preliminary study p 106 N85-10384
- FAILURE**
- Effects of a high mean stress on the high cycle fatigue life of PWA 1480 and correlation of data by linear elastic fracture mechanics
[NASA-CR-175057] p 118 N86-27689
- FAILURE ANALYSIS**
- Prediction of fiber composite mechanical behavior made simple p 63 A80-32067
- Failure analysis of a tool steel torque shaft p 51 A84-17546
- Mode II fatigue crack growth specimen development p 83 A86-43566
- SCARE - A postprocessor program to MSC/NASTRAN for reliability analysis of structural ceramic components
[ASME PAPER 86-GT-34] p 84 A87-17988
- Re-examination of cumulative fatigue damage analysis - An engineering perspective p 85 A87-22128
- A relation between semiempirical fracture analyses and R-curves
[NASA-TP-1600] p 87 N80-15428
- Method for estimating crack-extension resistance curve from residual strength data
[NASA-TP-1753] p 89 N81-11417
- Application of advanced reliability methods to local strain fatigue analysis
[NASA-CR-168198] p 97 N83-29734
- Sensor failure detection for jet engines
[NASA-CR-168190] p 56 N83-33182
- Hygrothermomechanical fracture stress criteria for fiber composites with sense-parity
[NASA-TM-83691] p 27 N84-28918
- Mode 2 fatigue crack growth specimen development
[NASA-TM-83722] p 104 N84-29248
- A comparison of two contemporary creep-fatigue life prediction methods p 113 N85-31538
- Turbine Engine Hot Section Technology (HOST)
[NASA-CP-2289] p 115 N86-11495
- Yielding and deformation behavior of the single crystal nickel-base superalloy PWA 1480
[NASA-CR-175100] p 44 N86-25455
- Re-examination of cumulative fatigue damage analysis: An engineering perspective
[NASA-TM-87325] p 118 N86-27680
- FAILURE MODES**
- Fracture modes of high modulus graphite/epoxy angleplied laminates subjected to off-axis tensile loads p 14 A80-32069
- Predicting the time-temperature dependent axial failure of B/AI composites p 14 A80-35494
- Compressive behavior of unidirectional fibrous composites p 16 A84-29894
- Longitudinal compressive failure modes in fiber composites End attachment effects on IITRI type test specimens p 19 A86-19999

- Mode II fatigue crack growth specimen development
p 83 A86-43566
- Re-examination of cumulative fatigue damage analysis
- An engineering perspective p 85 A87-22128
- Fracture modes of high modulus graphite/epoxy
angled laminates subjected to off-axis tensile loads
[NASA-TM-81405] p 21 N80-16102
- Predicting the time-temperature dependent axial failure
of B/A1 composites
[NASA-TM-81474] p 22 N80-21452
- Mode 2 fatigue crack growth specimen development
[NASA-TM-83722] p 104 N84-29248
- A continuous damage model based on stepwise-stress
creep rupture tests
[NASA-CR-174941] p 114 N85-32341
- Computational simulation of progressive fracture in fiber
composites
[NASA-TM-87341] p 30 N86-26376
- Ultrasonic stress wave characterization of composite
materials
[NASA-CR-3976] p 60 N86-27665
- Re-examination of cumulative fatigue damage analysis:
An engineering perspective
[NASA-TM-87325] p 118 N86-27680
- Fatigue failure of regenerator screens in a high frequency
Stirling engine
[NASA-TM-88974] p 122 N87-18882
- FAN BLADES**
- Superhybrid composite blade impact studies
[ASME PAPER 81-GT-24] p 1 A81-29940
- Structural tailoring of engine blades (STAEBL)
[AIAA 83-0828] p 1 A83-29737
- Blade loss transient dynamic analysis of
turbomachinery p 2 A83-40864
- Finite element engine blade structural optimization
[AIAA PAPER 85-0645] p 76 A85-30313
- Flutter of swept fan blades
[ASME PAPER 84-GT-138] p 77 A85-32962
- Dynamic characteristics of an assembly of prop-fan
blades
[ASME PAPER 85-GT-134] p 5 A86-32956
- Mass balancing of hollow fan blades
[ASME PAPER 86-GT-195] p 84 A86-48245
- Fabrication and quality assurance processes for
superhybrid composite fan blades p 20 A87-19123
- Superhybrid composite blade impact studies
[NASA-TM-81597] p 89 N81-11412
- Composite containment systems for jet engine fan
blades
[NASA-TM-81675] p 90 N81-17480
- Structural dynamics of shroudless, hollow fan blades
with composite in-lays
[NASA-TM-82816] p 7 N82-22266
- Bird impact analysis package for turbine engine fan
blades
[NASA-TM-82831] p 92 N82-26701
- Structural tailoring of engine blades (STAEBL)
[NASA-CR-167949] p 7 N82-33391
- Flutter of swept fan blades
[NASA-TM-83547] p 102 N84-16587
- Fabrication and quality assurance processes for
superhybrid composite fan blades
[NASA-TM-83354] p 28 N85-14882
- Hub flexibility effects on propfan vibration
[NASA-TM-89900] p 124 N87-24722
- FATIGUE (MATERIALS)**
- Fatigue criterion to system design, life and reliability
[AIAA PAPER 85-1140] p 78 A85-40814
- Fatigue crack growth under general-yielding
cyclic-loading p 84 A86-44339
- Factors that affect the fatigue strength of power
transmission shafting and their impact on design
p 48 A87-14656
- Fatigue criterion to system design, life, and reliability
p 85 A87-27986
- Ion beam sputter etching of orthopedic implanted alloy
MP35N and resulting effects on fatigue
[NASA-TM-81747] p 38 N81-21174
- Interlaminar crack growth in fiber reinforced composites
during fatigue, part 3
[NASA-CR-165434] p 93 N82-26715
- A total life prediction model for stress concentration
sites
[NASA-CR-170290] p 96 N83-23629
- Evaluation of inelastic constitutive models for nonlinear
structural analysis p 98 N83-34357
- Creep fatigue of low-cobalt superalloys: Waspalloy, PM
U 700 and wrought U 700
[NASA-CR-168260] p 40 N84-13265
- Complexities of high temperature metal fatigue: Some
steps toward understanding
[NASA-TM-83507] p 101 N84-14541
- Theoretical and software considerations for nonlinear
dynamic analysis
[NASA-CR-174504] p 101 N84-15589

- Elevated temperature biaxial fatigue
[NASA-CR-173473] p 103 N84-21905
- Crack layer theory
[NASA-CR-174634] p 103 N84-22980
- Evaluation of the effect of crack closure on fatigue crack
growth of simulated short cracks
[NASA-TM-83778] p 40 N84-31348
- Crack tip field and fatigue crack growth in general yielding
and low cycle fatigue
[NASA-CR-174686] p 41 N84-32503
- Turbine Engine Hot Section Technology (HOST)
[NASA-TM-83022] p 9 N85-10951
- Experimental compliance calibration of the NASA Lewis
Research Center Mode 2 fatigue specimen
[NASA-TM-86908] p 107 N85-16205
- Fatigue criterion to system design, life and reliability
[NASA-TM-87017] p 49 N85-27226
- Elevated temperature biaxial fatigue
[NASA-CR-175795] p 110 N85-27263
- Interaction of high-cycle and low-cycle fatigue of Haynes
188 alloy at 1400 F deg p 111 N85-27961
- Reexamination of cumulative fatigue damage laws
p 112 N85-27962
- Two simplified procedures for predicting cyclic material
response from a strain history p 113 N85-31543
- Application of traction drives as servo mechanisms
p 114 N85-33520
- Turbine Engine Hot Section Technology (HOST)
[NASA-CP-2289] p 115 N86-11495
- Influence of load interactions on crack growth as related
to state of stress and crack closure
[NASA-TM-87117] p 42 N86-12292
- Fatigue crack propagation of nickel-base superalloys at
650 deg C
[NASA-TM-87150] p 42 N86-12294
- An update of the total-strain version of SRP
[NASA-TP-2499] p 42 N86-12295
- Closure of fatigue cracks at high strains
[NASA-CR-175021] p 116 N86-17788
- Grain boundary oxidation and oxidation accelerated
fatigue crack nucleation and propagation
[NASA-CR-175050] p 43 N86-20542
- Fatigue crack growth under general-yielding
cyclic-loading
[NASA-CR-175049] p 117 N86-21951
- Anisotropic constitutive model for nickel base single
crystal alloys: Development and finite element
implementation
[NASA-CR-175015] p 117 N86-21952
- Influence of fatigue crack wake length and state of stress
on crack closure
[NASA-TM-87292] p 43 N86-22686
- Thermal-mechanical fatigue behavior of nickel-base
superalloys
[NASA-CR-175048] p 43 N86-24818
- Fatigue crack layer propagation in silicon-iron
[NASA-CR-175115] p 118 N86-25851
- Low-cycle thermal fatigue
[NASA-TM-87225] p 118 N86-26651
- Micromechanisms of thermomechanical fatigue: A
comparison with isothermal fatigue
[NASA-TM-87331] p 44 N86-28164
- Fatigue and fracture: Overview p 120 N87-11183
- Fatigue failure of regenerator screens in a high frequency
Stirling engine
[NASA-TM-88974] p 122 N87-18882
- Environmental degradation of 316 stainless steel in high
temperature low cycle fatigue
[NASA-TM-89931] p 124 N87-24007
- Lewis' enhanced laboratory for research into the fatigue
and constitutive behavior of high temperature materials
p 125 N88-11177

FATIGUE LIFE

- Strainrange partitioning life predictions of the long time
Metal Properties Council creep-fatigue tests
p 63 A80-27958
- Comparative thermal fatigue resistance of several oxide
dispersion strengthened alloys p 32 A82-11399
- Turbine blade nonlinear structural and life analysis
p 1 A83-29024
- High-temperature fatigue in metals - A brief review of
life prediction methods developed at the Lewis Research
Center of NASA p 33 A84-14286
- Simplified analytical procedures for representing
material cyclic response --- for high temperature gas turbine
engine analysis p 2 A84-22877
- Advanced reliability method for fatigue analysis
p 72 A84-31596
- Strainrange partitioning - A total strain range version
--- for creep fatigue life prediction by summing inelastic
and elastic strain-range-life relations for two Ni base
superalloys p 34 A85-11603
- A study of fatigue damage mechanisms in Waspalloy
from 25 to 800 C p 34 A85-12098

- Considerations for damage analysis of gas turbine hot
section components
[ASME PAPER 84-PVP-77] p 2 A85-18792
- A history dependent damage model for low cycle
fatigue
[ASME PAPER 84-PVP-112] p 75 A85-18795
- Fracture toughness of hot-pressed beryllium
p 34 A85-25835
- On the fatigue crack propagation behavior of superalloys
at intermediate temperatures p 35 A85-32434
- Application of two creep fatigue life models for the
prediction of elevated temperature crack initiation of a
nickel base alloy
[AIAA PAPER 85-1420] p 35 A85-43979
- Fiberglass epoxy laminate fatigue properties at 300 and
20 K p 19 A85-47970
- Thermal-mechanical fatigue crack growth in Inconel
X-750 p 35 A86-20982
- A study of spectrum fatigue crack propagation in two
aluminum alloys. I - Spectrum simplification. II - Influence
of microstructures p 36 A86-48973
- Re-examination of cumulative fatigue damage analysis
- An engineering perspective p 85 A87-22128
- Effect of interference fits on roller bearing fatigue life
p 48 A87-37686
- Elevated temperature fatigue testing of metals
p 38 N82-13281
- The application of probabilistic design theory to high
temperature low cycle fatigue
[NASA-CR-165488] p 91 N82-14531
- Elevated temperature fatigue testing of metals
[NASA-TM-82745] p 91 N82-16419
- Stress evaluations under rolling/sliding contacts
[NASA-CR-165561] p 91 N82-17521
- Fatigue life prediction in bending from axial fatigue
information
[NASA-CR-165563] p 91 N82-20564
- High temperature low cycle fatigue mechanisms for
nickel base and a copper base alloy
[NASA-CR-3543] p 39 N82-26436
- Strainrange partitioning: A total strain range version
[NASA-TM-83023] p 39 N83-14246
- The thermal fatigue resistance of H-13 Die Steel for
aluminum die casting dies
[NASA-TM-83331] p 39 N83-35103
- Low strain, long life creep fatigue of AF2-1DA and INCO
718 p 40 N84-10268
- Bending fatigue of electron-beam-welded foils.
Application to a hydrodynamic air bearing in the
Chrysler/DOE upgraded automotive gas turbine engine
[NASA-TM-83539] p 102 N84-16589
- Crack tip field and fatigue crack growth in general yielding
and low cycle fatigue
[NASA-CR-174686] p 41 N84-32503
- Low cycle fatigue behavior of conventionally cast
MAR-M 200 AT 1000 deg C
[NASA-TM-83769] p 41 N84-33564
- Life prediction and constitutive behavior: Overview
p 10 N85-10973
- Thermal-mechanical fatigue crack growth in Inconel
X-750 p 41 N85-15877
- Fundamentals of microcrack nucleation mechanics
[NASA-CR-3851] p 57 N85-16195
- Creep fatigue life prediction for engine hot section
materials (isotropic)
[NASA-CR-168228] p 11 N85-31057
- A comparison of two contemporary creep-fatigue life
prediction methods p 113 N85-31538
- Nonlinear damage analysis: Postulate and evaluation
[NASA-CR-168171] p 118 N86-26652
- Re-examination of cumulative fatigue damage analysis:
An engineering perspective
[NASA-TM-87325] p 118 N86-27680
- Effects of a high mean stress on the high cycle fatigue
life of PWA 1480 and correlation of data by linear elastic
fracture mechanics
[NASA-CR-175057] p 118 N86-27689
- Thermal-fatigue and oxidation resistance of
cobalt-modified Udimet 700 alloy
[NASA-TP-2591] p 119 N86-28464
- Estimation of high temperature low cycle fatigue on the
basis of inelastic strain and strainrate
[NASA-TM-88841] p 44 N87-14489
- Lubricant effects on bearing life
[NASA-TM-88875] p 49 N87-15467
- Effects of surface removal on rolling-element fatigue
[NASA-TM-88871] p 50 N87-18820
- Bithermal low-cycle fatigue behavior of a
NiCoCrAlY-coated single crystal superalloy
[NASA-TM-89831] p 45 N87-20408
- Calculation of thermomechanical fatigue life based on
isothermal behavior
[NASA-TM-88864] p 122 N87-20565

Fatigue damage interaction behavior of PWA 1480
p 45 N87-22777

Exposure time considerations in high temperature low cycle fatigue
[NASA-TM-88934] p 125 N87-28944

FATIGUE TESTS

Strainrange partitioning life predictions of the long time Metal Properties Council creep-fatigue tests
p 63 A80-27958

Cyclic behavior of turbine disk alloys at 650 C
p 32 A81-12266

Low cycle fatigue behavior of aluminum/stainless steel composites
[AIAA 83-0806] p 16 A83-29886

Fatigue crack initiation and propagation in several nickel-base superalloys at 650 C
p 33 A83-41199

The effects of frequency and hold times on fatigue crack propagation rates in a nickel base superalloy
p 34 A84-18733

Effects of processing and microstructure on the fatigue behaviour of the nickel-base superalloy Rene95
p 34 A84-48715

Hygrothermomechanical evaluation of transverse filament tape epoxy/polyester fiberglass composites
p 17 A85-15632

Fracture mechanics applied to nonisothermal fatigue crack growth
p 36 A86-28951

The cyclic stress-strain behavior of a nickel-base superalloy at 650 C
p 36 A86-45715

Orientation and temperature dependence of some mechanical properties of the single-crystal nickel-base superalloy Rene N4. II - Low cycle fatigue behavior
p 37 A86-50322

Elastic analysis of a mode II fatigue crack test specimen
p 84 A87-17799

Results of an interlaboratory fatigue test program conducted on alloy 800H at room and elevated temperatures
p 37 A87-54370

Application of composite materials to turbofan engine fan exit guide vanes
[NASA-TM-81432] p 22 N80-18106

Evaluation of the cyclic behavior of aircraft turbine disk alloys, part 2
[NASA-CR-165123] p 38 N80-30482

Elevated temperature fatigue testing of metals
p 38 N82-13281

Mechanisms of deformation and fracture in high temperature low cycle fatigue of Rene 80 and IN 100
[NASA-CR-165498] p 93 N82-26706

Structural fatigue test results for large wind turbine blade sections
p 96 N83-19246

Statistical summaries of fatigue data for design purposes
[NASA-CR-3697] p 97 N83-29731

Fatigue crack growth and low cycle fatigue of two nickel base superalloys
[NASA-CR-174534] p 39 N84-10267

Preliminary study of thermomechanical fatigue of polycrystalline MAR-M 200
[NASA-TP-2280] p 40 N84-17350

Engine cyclic durability by analysis and material testing
[NASA-TM-83577] p 102 N84-18683

Cyclic torsion testing
[NASA-TM-83756] p 105 N84-31687

Engine cyclic durability by analysis and material testing
p 11 N85-15744

Low cycle fatigue of MAR-M 200 single crystals at 760 and 870 deg C
[NASA-TM-86933] p 41 N85-19074

Results of an interlaboratory fatigue test program conducted on alloy 800H at room and elevated temperatures
[NASA-CR-174940] p 114 N85-32340

Creep-fatigue behavior of NiCoCrAlY coated PWA 1480 superalloy single crystals
[NASA-TM-87110] p 42 N86-10311

The low cycle fatigue behavior of a plasma-sprayed coating material
[NASA-TM-87318] p 44 N86-31699

Fatigue damage interaction behavior of PWA 1480
p 45 N87-22777

A high temperature fatigue and structures testing facility
[NASA-TM-100151] p 124 N87-26399

FIBER COMPOSITES

Micromechanics of intraply hybrid composites: Elastic and thermal properties
p 14 A80-27994

Prediction of fiber composite mechanical behavior made simple
p 63 A80-32067

A review of issues and strategies in nondestructive evaluation of fiber reinforced structural composites
p 14 A80-34764

Sensitivity analysis results of the effects of various parameters on composite design
p 15 A82-37101

Prediction of composite hygral behavior made simple
p 16 A84-14285

Durability/life of fiber composites in hygrothermomechanical environments
p 16 A84-27359

Compressive behavior of unidirectional fibrous composites
p 16 A84-29894

Simplified composite micromechanics equations for strength, fracture toughness and environmental effects
p 17 A84-41858

Simplified composite micromechanics equations of hygral, thermal, and mechanical properties
p 17 A84-49377

Select fiber composites for space applications - A mechanistic assessment
p 18 A85-16040

ICAN - Integrated composites analyzer
[AIAA PAPER 84-0974] p 18 A85-16094

Interply layer degradation effects on composite structural response
[AIAA PAPER 84-0849] p 18 A85-16096

Impact resistance of fiber composites - Energy-absorbing mechanisms and environmental effects
p 18 A85-46543

Longitudinal compressive failure modes in fiber composites End attachment effects on IITRI type test specimens
p 19 A86-19999

Designing for fiber composite structural durability in hygrothermomechanical environments
p 19 A86-27734

Progressive fracture of fiber composites
p 19 A86-35809

Computer aided derivation of equations for composite mechanics problems and finite element analyses
[AIAA PAPER 86-1016] p 83 A86-38873

Dynamic stress analysis of smooth and notched fiber composite flexural specimens
p 20 A86-41070

Simplified composite micromechanics for predicting microstresses
p 87 A87-49275

Micromechanics of intraply hybrid composites: Elastic and thermal properties
[NASA-TM-79253] p 21 N80-11143

Tensile and flexural strength of non-graphitic superhybrid composites: Predictions and comparisons
[NASA-TM-79276] p 21 N80-11144

Dynamic response of damaged angleplied fiber composites
[NASA-TM-79281] p 21 N80-11145

Mechanical property characterization of intraply hybrid composites
[NASA-TM-79306] p 21 N80-12120

Prediction of fiber composite mechanical behavior made simple --- using a rocket calculator
[NASA-TM-81404] p 22 N80-16107

Application of composite materials to turbofan engine fan exit guide vanes
[NASA-TM-81432] p 22 N80-18106

Engine environmental effects on composite behavior
[NASA-TM-81508] p 22 N80-23370

Prediction of composite thermal behavior made simple
[NASA-TM-81618] p 23 N81-16132

Computer code for intraply hybrid composite design
[NASA-TM-82593] p 24 N81-25151

Durability/life of fiber composites in hygrothermomechanical environments
[NASA-TM-82749] p 24 N82-14287

Prediction of composite hygral behavior made simple
[NASA-TM-82780] p 24 N82-16181

Compression behavior of unidirectional fibrous composite
[NASA-TM-82833] p 25 N82-22313

Simplified composite micromechanics equations for hygral, thermal and mechanical properties
[NASA-TM-83320] p 26 N83-19817

Geometrically nonlinear analysis of layered composite plates and shells
[NASA-CR-168182] p 98 N83-33219

Select fiber composites for space applications: A mechanistic assessment
[NASA-TM-83631] p 26 N84-22702

Impact resistance of fiber composites: Energy absorbing mechanisms and environmental effects
[NASA-TM-83594] p 26 N84-24712

Dynamic stress analysis of smooth and notched fiber composite flexural specimens
[NASA-TM-83694] p 27 N84-25770

ICAN: Integrated composites analyzer
[NASA-TM-83700] p 27 N84-26755

Interply layer degradation effects on composite structural response
[NASA-TM-83702] p 27 N84-26756

Simplified composite micromechanics equations for strength, fracture toughness and environmental effects
[NASA-TM-83696] p 27 N84-27832

Application of finite element substructuring to composite micromechanics
[NASA-TM-83729] p 27 N84-31288

Design procedures for fiber composite structural components: Panels subjected to combined in-plane loads
[NASA-TM-86909] p 29 N85-15823

Designing for fiber composite structural durability in hygrothermomechanical environment
[NASA-TM-87045] p 29 N85-27978

Integrated Composite Analyzer (ICAN): Users and programmers manual
[NASA-TP-2515] p 30 N86-21614

Computational simulation of progressive fracture in fiber composites
[NASA-TM-87341] p 30 N86-26376

Fiber composite sandwich thermostrostructural behavior: Computational simulation
[NASA-TM-88787] p 31 N86-31663

ICAN: A versatile code for predicting composite properties
[NASA-TM-87334] p 31 N86-31664

FIBER ORIENTATION

Compression behavior of unidirectional fibrous composite
[NASA-TM-82833] p 25 N82-22313

FIBER REINFORCED COMPOSITES

Acousto-ultrasonic characterization of fiber reinforced composites
p 50 A81-44660

Computer code for intraply hybrid composite design
p 15 A81-44662

Boundary-layer effects in composite laminates. I - Free-edge stress singularities. II - Free-edge stress solutions and basic characteristics
p 67 A82-46806

Fatigue behavior of SiC reinforced Ti/6Al-4V/ at 650 C
p 15 A83-12414

Elasticity solutions for a class of composite laminate problems with stress singularities
p 17 A84-33389

Use of static indentation laws in the impact analysis of laminated composite plates
p 18 A85-29133

Ten year environmental test of glass fiber/epoxy pressure vessels
[AIAA PAPER 85-1198] p 19 A85-47022

Three-dimensional hybrid-stress finite element analysis of composite laminates with cracks and cutouts
p 80 A86-26896

Design concepts/parameters assessment and sensitivity analyses of select composite structural components
p 85 A87-25407

Laminates and reinforced metals
[NASA-TM-81591] p 23 N81-12171

Tungsten fiber reinforced superalloy composite high temperature component design considerations
[NASA-TM-82811] p 25 N82-21259

Designing with fiber-reinforced plastics (planar random composites)
[NASA-TM-82812] p 25 N82-24300

Analysis of cracks emanating from a circular hole in unidirectional fiber reinforced composites, part 2
[NASA-CR-165433] p 93 N82-26714

Interlaminar crack growth in fiber reinforced composites during fatigue, part 3
[NASA-CR-165434] p 93 N82-26715

Edge delamination in angle-ply composite laminates, part 5
[NASA-CR-165439] p 94 N82-26717

Boundary-layer effects in composite laminates: Free-edge stress singularities, part 6
[NASA-CR-165440] p 94 N82-26718

The effect of stress on ultrasonic pulses in fiber reinforced composites
[NASA-CR-3724] p 56 N83-33180

Nonlinear analysis for high-temperature composites: Turbine blades/vanes
p 106 N84-31699

Nonlinear analysis for high-temperature multilayered fiber composite structures --- turbine blades
[NASA-TM-83754] p 29 N85-21273

Nonlinear structural analysis for fiber-reinforced superalloy turbine blades
p 109 N85-26887

Ten year environmental test of glass fiber/epoxy pressure vessels
[NASA-TM-87058] p 29 N85-30034

A unique set of micromechanics equations for high temperature metal matrix composites
[NASA-TM-87154] p 30 N86-24757

Stress waves in transversely isotropic media: The homogeneous problem
[NASA-CR-3977] p 59 N86-25002

Ultrasonic stress wave characterization of composite materials
[NASA-CR-3976] p 60 N86-27665

Wave propagation in anisotropic medium due to an oscillatory point source with application to unidirectional composites
[NASA-CR-4001] p 60 N86-27666

FIBER STRENGTH

Indentation law for composite laminates
p 16 A84-27356

FILAMENT WINDING

- Ultrasonic evaluation of mechanical properties of thick, multilayered, filament wound composites
[NASA-TM-87088] p 58 N86-10561
- Acousto-ultrasonic verification of the strength of filament wound composite material
[NASA-TM-88827] p 61 N86-32764

FILLETS

- A finite element stress analysis of spur gears including fillet radii and rim thickness effects
[NASA-TM-82865] p 48 N82-28646
- On finite element stress analysis of spur gears
[NASA-CR-167938] p 48 N82-29607

FILM THICKNESS

- Dynamic behavior of spiral-groove and Rayleigh-Step self-acting face seals
[NASA-TP-2266] p 8 N84-16181

FINITE DIFFERENCE THEORY

- Finite difference analysis of torsional vibrations of pretwisted, rotating, cantilever beams with effects of warping p 78 A85-42047
- Vibration analysis of rotating turbomachinery blades by an improved finite difference method p 3 A86-14338
- Vibration and buckling of rotating, pretwisted, precone beams including Coriolis effects p 80 A86-26910
- A computer analysis program for interfacing thermal and structural codes p 126 A86-36861
- Aerothermal modeling. Executive summary
[NASA-CR-168330] p 7 N84-15152
- Improved finite-difference vibration analysis of pretwisted, tapered beams
[NASA-TM-83549] p 102 N84-16588
- Improved methods of vibration analysis of pretwisted, airfoil blades
[NASA-TM-83735] p 104 N84-30329
- Vibration and buckling of rotating, pretwisted, precone beams including Coriolis effects
[NASA-TM-87004] p 109 N85-25893
- A computer analysis program for interfacing thermal and structural codes
[NASA-TM-87021] p 110 N85-27264

FINITE ELEMENT METHOD

- Engine dynamic analysis with general nonlinear finite element codes. II - Bearing element implementation, overall numerical characteristics and benchmarking
[ASME PAPER 82-GT-292] p 47 A82-35462
- On the automatic generation of FEM models for complex gears - A work-in-progress report p 47 A82-48243
- A new formulation of hybrid/mixed finite element p 67 A83-12739
- Nonlinear structural and life analyses of a combustor liner p 68 A83-12764
- Alternative ways for formulation of hybrid stress elements p 68 A83-14710
- Growth and stability of interacting surface flaws of arbitrary shape p 68 A83-15060
- Geometrically nonlinear analysis of layered composite shells p 68 A83-27431
- Finite element analysis of steadily moving contact fields p 70 A83-49437
- Inelastic stress analyses at finite deformation through complementary energy approaches p 71 A84-13248
- Analyses of large quasistatic deformations of inelastic bodies by a new hybrid-stress finite element algorithm p 71 A84-16874
- Analyses of large quasistatic deformations of inelastic bodies by a new hybrid-stress finite element algorithm - Applications p 71 A84-16884
- Nonlinear transient finite element analysis of rotor-bearing-stator systems p 48 A84-20580
- On the suppression of zero energy deformation modes p 72 A84-21541
- A numerical analysis of contact and limit-point behavior in a class of problems of finite elastic deformation p 72 A84-27370
- The structural response of a rail acceleration p 72 A84-32039
- A mixed shear flexible finite element for the analysis of laminated plates p 73 A84-45994
- Analysis of hourglass instabilities and control in underintegrated finite element methods p 74 A85-11125
- Rational approach for assumed stress finite elements p 74 A85-12029
- Hybrid Semiloof elements for plates and shells based upon a modified Hu-Washizu principle p 74 A85-15893
- Hybrid stress finite elements for large deformations of inelastic solids p 74 A85-15894
- Development and testing of stable, invariant, isoparametric curvilinear 2- and 3-D hybrid-stress elements p 75 A85-19899
- On the development of hierarchical solution strategies for nonlinear finite element formulations p 126 A85-21979

- A simplified method for elastic-plastic-creep structural analysis
[ASME PAPER 84-GT-191] p 76 A85-23150
- Finite element engine blade structural optimization
[AIAA PAPER 85-0645] p 76 A85-30313
- Natural frequencies of twisted rotating plates p 76 A85-32343
- On the existence and stability conditions for mixed-hybrid finite element solutions based on Reissner's variational principle p 77 A85-33847
- Evolution of assumed stress hybrid finite element p 77 A85-35046
- Plasticity, viscoplasticity, and creep of solids by mechanical subelement models p 77 A85-35048
- Pantographing self adaptive gap elements p 77 A85-37440
- Unified constitutive material models for nonlinear finite-element structural analysis --- gas turbine engine blades and vanes
[AIAA PAPER 85-1418] p 77 A85-39769
- Axisymmetric solid elements by a rational hybrid stress method p 78 A85-41109
- A study of interply layer effects on the free edge stress field of angleply laminates p 18 A85-41127
- Impact resistance of fiber composites - Energy-absorbing mechanisms and environmental effects p 18 A85-46543
- Finite elements based on consistently assumed stresses and displacements p 79 A86-18123
- Hierarchical implicit dynamic least-square solution algorithm p 80 A86-26689
- Three-dimensional hybrid-stress finite element analysis of composite laminates with cracks and cutouts p 80 A86-26896
- Designing for fiber composite structural durability in hygrothermomechanical environments p 19 A86-27734
- Probabilistic finite elements for transient analysis in nonlinear continua p 80 A86-28653
- Efficient algorithms for use in probabilistic finite element analysis p 81 A86-28655
- Iterative methods for mixed finite element equations p 82 A86-34461
- Hybrid solid element with a traction-free cylindrical surface p 82 A86-34462
- Existence and stability, and discrete BB and rank conditions, for general mixed-hybrid finite elements in elasticity p 82 A86-34464
- A computer analysis program for interfacing thermal and structural codes p 126 A86-36861
- Computer aided derivation of equations for composite mechanics problems and finite element analyses
[AIAA PAPER 86-1016] p 83 A86-38873
- Locally bound constrained Newton-Raphson solution algorithms --- for modeling kinematic and material nonlinearity p 83 A86-43771
- Assessment of simplified composite micromechanics using three-dimensional finite-element analysis p 20 A87-19121
- Design concepts/parameters assessment and sensitivity analyses of select composite structural components p 85 A87-25407
- Modelling of crack tip deformation with finite element method and its applications p 87 N80-13503
- Nonlinear, three-dimensional finite-element analysis of air-cooled gas turbine blades
[NASA-TP-1669] p 88 N80-22734
- Three dimensional finite-element elastic analysis of a thermally cycled double-edge wedge geometry specimen --- nickel alloy turbine parts
[NASA-TM-80980] p 37 N80-26433
- Finite-strain large-deflection elastic-viscoplastic finite-element transient response analysis of structures
[NASA-CR-159874] p 88 N80-29762
- Aeroelastic and dynamic finite element analyses of a bladder shrouded disk
[NASA-CR-159728] p 90 N81-19479
- Elastic-plastic finite-element analyses of thermally cycled double-edge wedge specimens
[NASA-TP-1973] p 92 N82-20566
- Nonlinear structural and life analyses of a combustor liner
[NASA-TM-82846] p 92 N82-24501
- A finite element stress analysis of spur gears including fillet radii and rim thickness effects
[NASA-TM-82865] p 48 N82-28646
- Large displacements and stability analysis of nonlinear propeller structures
[NASA-TM-82850] p 94 N82-31707
- Large displacements and stability analysis of nonlinear propeller structures p 95 N83-12460
- Geometrically nonlinear analysis of layered composite plates and shells
[NASA-CR-168182] p 98 N83-33219

- Stress and fracture analyses under elastic-plastic creep conditions: Some basic developments and computational approaches p 99 N83-34371
- The structural response of a rail accelerator
[NASA-TM-83491] p 99 N83-35412
- Finite element forced vibration analysis of rotating cyclic structures p 101 N84-11515
- A simplified method for elastic-plastic-creep structural analysis p 101 N84-14542
- Bladed-shrouded-disc aeroelastic analyses: Computer program updates in NASTRAN level 17.7
[NASA-CR-165428] p 8 N84-15154
- Theoretical and software considerations for nonlinear dynamic analysis
[NASA-CR-174504] p 101 N84-15589
- Impact resistance of fiber composites: Energy absorbing mechanisms and environmental effects
[NASA-TM-83594] p 26 N84-24712
- Application of finite element substructuring to composite micromechanics
[NASA-TM-83729] p 27 N84-31288
- Nonlinear Structural Analysis p 105 N84-31688
- Slave finite elements: The temporal element approach to nonlinear analysis p 105 N84-31689
- New variational formulations of hybrid stress elements p 105 N84-31690
- Nonlinear finite element analysis of shells with large aspect ratio p 105 N84-31692
- Self-adaptive solution strategies p 105 N84-31693
- Element-by-element solution procedures for nonlinear structural analysis p 105 N84-31694
- Automatic finite element generators p 105 N84-31695
- Stability and convergence of underintegrated finite element approximations p 105 N84-31696
- Augmented weak forms and element-by-element preconditioners: Efficient iterative strategies for structural finite elements. A preliminary study p 106 N85-10384
- Constitutive model development for isotropic materials p 10 N85-10975
- A study of interply layer effects on the free-edge stress field of angleply laminates p 28 N85-15822
- Local strain redistribution corrections for a simplified inelastic analysis procedure based on an elastic finite-element analysis p 107 N85-20396
- Advanced stress analysis methods applicable to turbine engine structures
[NASA-CR-175573] p 11 N85-21165
- Nonlinear analysis for high-temperature multilayered fiber composite structures --- turbine blades
[NASA-TM-83754] p 29 N85-21273
- 3-D inelastic analysis methods for hot section components (base program) --- turbine blades, turbine vanes, and combustor liners
[NASA-CR-174700] p 107 N85-21686
- Recent advances in hybrid/mixed finite elements
[NASA-CR-175574] p 107 N85-21687
- Geometrically nonlinear analysis of laminated elastic structures
[NASA-CR-175609] p 108 N85-21720
- On Hybrid and mixed finite element methods
[NASA-CR-175551] p 108 N85-23096
- Unified constitutive material models for nonlinear finite-element structural analysis --- gas turbine engine blades and vanes
[NASA-TM-86985] p 108 N85-24338
- A computer analysis program for interfacing thermal and structural codes
[NASA-TM-87021] p 110 N85-27264
- Probabilistic finite element development p 111 N85-27956
- Probabilistic finite element: Variational theory p 111 N85-27957
- Designing for fiber composite structural durability in hygrothermomechanical environment
[NASA-TM-87045] p 29 N85-27978
- A review of path-independent integrals in elastic-plastic fracture mechanics, task 4
[NASA-CR-174956] p 114 N85-33541
- Joint research effort on vibrations of twisted plates, phase 1: Final results
[NASA-RP-1150] p 115 N86-10579
- A unique set of micromechanics equations for high temperature metal matrix composites
[NASA-TM-87154] p 30 N86-24757
- Cyclic creep analysis from elastic finite-element solutions
[NASA-TM-87213] p 117 N86-25822
- Computational simulation of progressive fracture in fiber composites
[NASA-TM-87341] p 30 N86-26376

- A constitutive law for finite element contact problems with unclassified friction
[NASA-TM-88838] p 120 N87-12924
- Composite interlaminar fracture toughness: Three-dimensional finite element modeling for mixed mode 1, 2 and 3 fracture
[NASA-TM-88872] p 31 N87-13491
- Surface flaw reliability analysis of ceramic components with the SCARE finite element postprocessor program
[NASA-TM-88901] p 121 N87-17087
- Nonlinear heat transfer and structural analyses of SSME turbine blades
p 123 N87-22779
- Finite element implementation of Robinson's unified viscoplastic model and its application to some uniaxial and multiaxial problems
[NASA-TM-89891] p 123 N87-23010
- Hub flexibility effects on propfan vibration
[NASA-TM-89900] p 124 N87-24722
- Finite element analysis of flexible, rotating blades
[NASA-TM-89906] p 124 N87-26385
- FIRES**
- Statistical aspects of carbon fiber risk assessment modeling --- fire accidents involving aircraft
[NASA-CR-159318] p 23 N80-29432
- FLEXIBILITY**
- Vibration and flutter of mistuned bladed-disk assemblies
[AIAA PAPER 84-0991] p 75 A85-16095
- Vibration and flutter of mistuned bladed-disk assemblies
[NASA-TM-83634] p 103 N84-23923
- Hub flexibility effects on propfan vibration
[NASA-TM-89900] p 124 N87-24722
- FLEXIBLE BODIES**
- A blade loss response spectrum for flexible rotor systems
[ASME PAPER 84-GT-29] p 48 A84-46893
- The dynamics of a flexible bladed disc on a flexible rotor in a two-rotor system
p 4 A86-25743
- A NASTRAN primer for the analysis of rotating flexible blades
[NASA-TM-89861] p 123 N87-21375
- Finite element analysis of flexible, rotating blades
[NASA-TM-89906] p 124 N87-26385
- FLEXIBLE SPACECRAFT**
- Frequency domain solutions to multi-degree-of-freedom, dry friction damped systems under periodic excitation
p 83 A86-39485
- The 20th Aerospace Mechanics Symposium
[NASA-CP-2423-REV] p 121 N87-16321
- FLEXING**
- Tensile and flexural strength of non-graphitic superhybrid composites: Predictions and comparisons
[NASA-TM-79276] p 21 N80-11144
- FLOQUET THEOREM**
- Some analysis methods for rotating systems with periodic coefficients
p 69 A83-32987
- FLOW EQUATIONS**
- The finite analytic method, volume 4
[NASA-CR-170187] p 127 N83-23088
- The finite analytic method, volume 5
[NASA-CR-170188] p 127 N83-23089
- FLUID DYNAMICS**
- Flow dynamic environment data base development for the SSME
p 109 N85-26885
- FLUIDIZED BED PROCESSORS**
- Elastic-plastic finite-element analyses of thermally cycled single-edge wedge specimens
[NASA-TP-1982] p 91 N82-20565
- FLUTTER**
- Effects of friction dampers on aerodynamically unstable rotor stages
[AIAA PAPER 83-0848] p 1 A83-32791
- Measurements of self-excited rotor-blade vibrations using optical displacements
[ASME PAPER 83-GT-132] p 73 A84-33702
- Vibration and flutter of mistuned bladed-disk assemblies
[AIAA PAPER 84-0991] p 75 A85-16095
- Flutter of swept fan blades
[ASME PAPER 84-GT-138] p 77 A85-32962
- Vibration and flutter of mistuned bladed-disk assemblies
p 3 A85-45854
- The effects of strong shock loading on coupled bending-torsion flutter of tuned and mistuned cascades
p 4 A86-26893
- Analytical flutter investigation of a composite propfan model
[AIAA PAPER 87-0738] p 87 A87-40497
- Status of NASA full-scale engine aeroelasticity research
[NASA-TM-81500] p 88 N80-23678
- Effects of mistuning on bending-torsion flutter and response of a cascade in incompressible flow --- turbofan engines
[NASA-TM-81674] p 89 N81-16494
- NASTRAN level 16 user's manual updates for aeroelastic analysis of bladed discs
[NASA-CR-159824] p 90 N81-19481
- Coupled bending-bending-torsion flutter of a mistuned cascade with nonuniform blades
[NASA-TM-82813] p 92 N82-21604
- Bending-torsion flutter of a highly swept advanced turboprop
[NASA-TM-82975] p 95 N83-11514
- Measurements of self-excited rotor-blade vibrations using optical displacements
[NASA-TM-82953] p 95 N83-14523
- Flutter of swept fan blades
[NASA-TM-83547] p 102 N84-16587
- Formulation of blade-flutter spectral analyses in stationary reference frame
[NASA-TP-2296] p 8 N84-20562
- Vibration and flutter of mistuned bladed-disk assemblies
[NASA-TM-83634] p 103 N84-23923
- Analytical flutter investigation of a composite propfan model
[NASA-TM-88944] p 122 N87-18115
- FLUTTER ANALYSIS**
- Effects of mistuning on blade torsional flutter
p 64 A81-29095
- Effects of mistuning on bending-torsion flutter and response of a cascade in incompressible flow
[AIAA 81-0602] p 65 A81-29465
- Flutter and forced response of mistuned rotors using standing wave analysis
[AIAA 83-0845] p 69 A83-29823
- Flutter analysis of advanced turbopropellers
[AIAA 83-0846] p 69 A83-29824
- Flutter analysis of advanced turbopropellers
p 73 A84-36492
- Flutter and forced response of mistuned rotors using standing wave analysis
p 74 A85-12721
- Flutter of swept fan blades
[ASME PAPER 84-GT-138] p 77 A85-32962
- Mass balancing of hollow fan blades
[ASME PAPER 86-GT-195] p 84 A86-48245
- A technique for the prediction of airfoil flutter characteristics in separated flow
[AIAA PAPER 87-0910] p 86 A87-33719
- Analytical and experimental investigation of mistuning in propfan flutter
[AIAA PAPER 87-0739] p 86 A87-40496
- Nastran level 16 theoretical manual updates for aeroelastic analysis of bladed discs
[NASA-CR-159823] p 90 N81-19480
- NASTRAN level 16 programmer's manual updates for aeroelastic analysis of bladed discs
[NASA-CR-159825] p 90 N81-19482
- Aeroelastic analysis for propellers - mathematical formulations and program user's manual
[NASA-CR-3729] p 101 N84-12530
- NASTRAN documentation for flutter analysis of advanced turbopropellers
[NASA-CR-167927] p 8 N84-15153
- Flutter of swept fan blades
[NASA-TM-83547] p 102 N84-16587
- Flutter and forced response of mistuned rotors using standing wave analysis
[NASA-CR-173555] p 9 N84-24586
- Experimental classical flutter results of a composite advanced turboprop model
[NASA-TM-88792] p 119 N86-29271
- Concentrated mass effects on the flutter of a composite advanced turboprop model
[NASA-TM-88854] p 120 N87-12017
- Analytical and experimental investigation of mistuning in propfan flutter
[NASA-TM-88959] p 122 N87-18116
- A computational procedure for automated flutter analysis
[NASA-TM-100171] p 125 N87-28058
- FOIL BEARINGS**
- Bending fatigue of electron-beam-welded foils. Application to a hydrodynamic air bearing in the Chrysler/DOE upgraded automotive gas turbine engine
[NASA-TM-83539] p 102 N84-16589
- FORCED VIBRATION**
- Flutter and forced response of mistuned rotors using standing wave analysis
[AIAA 83-0845] p 69 A83-29823
- Some analysis methods for rotating systems with periodic coefficients
p 69 A83-32987
- Design of dry-friction dampers for turbine blades
p 2 A83-35883
- Analysis of an axial compressor blade vibration based on wave reflection theory
[ASME PAPER 83-GT-151] p 2 A83-47970
- Forced response of a cantilever beam with a dry friction damper attached. I - Theory. II - Experiment
p 71 A84-21267
- NASTRAN forced vibration analysis of rotating cyclic structures
[ASME PAPER 83-DET-20] p 72 A84-29103
- The interaction between mistuning and friction in the forced response of bladed disk assemblies
[ASME PAPER 84-GT-139] p 73 A84-46957
- Flutter and forced response of mistuned rotors using standing wave analysis
p 74 A85-12721
- Vibration and flutter of mistuned bladed-disk assemblies
[AIAA PAPER 84-0991] p 75 A85-16095
- Forced response analysis of an aerodynamically detuned supersonic turbomachine rotor
p 5 A86-26902
- Forced vibration analysis of rotating cyclic structures in NASTRAN
[NASA-CR-165429] p 100 N84-11514
- Finite element forced vibration analysis of rotating cyclic structures
[NASA-CR-165430] p 101 N84-11515
- Vibration and flutter of mistuned bladed-disk assemblies
[NASA-TM-83634] p 103 N84-23923
- Flutter and forced response of mistuned rotors using standing wave analysis
[NASA-CR-173555] p 9 N84-24586
- NASTRAN forced vibration analysis of rotating cyclic structures
[NASA-CR-173821] p 104 N84-29252
- A study of internal and distributed damping for vibrating turbomachinery blades
[NASA-CR-175901] p 11 N85-27868
- Extensions of the Ritz-Galerkin method for the forced, damped vibrations of structural elements
p 117 N86-21909
- FORTRAN**
- Reliability of void detection in structural ceramics by use of scanning laser acoustic microscopy
p 52 A86-39027
- Reliability of void detection in structural ceramics using scanning laser acoustic microscopy
[NASA-TM-87035] p 58 N85-32337
- FOURIER TRANSFORMATION**
- Determination of grain size distribution function using two-dimensional Fourier transforms of tone pulse encoded images
[NASA-TM-88790] p 61 N86-31065
- FRACTOGRAPHY**
- A study of spectrum fatigue crack propagation in two aluminum alloys. I - Spectrum simplification. II - Influence of microstructures
p 36 A86-48973
- Correlation of processing and sintering variables with the strength and radiography of silicon nitride
p 46 A87-12938
- Microstructural effects on the room and elevated temperature low cycle fatigue behavior of Waspalloy
[NASA-CR-165497] p 93 N82-26702
- Fracture surface characteristics of notched angle-ply graphite/epoxy composites
[NASA-TM-83786] p 28 N84-33522
- FRACTURE MECHANICS**
- Simple spline-function equations for fracture mechanics calculations
p 63 A80-10832
- Fracture modes of high modulus graphite/epoxy angle-ply laminates subjected to off-axis tensile loads
p 14 A80-32069
- On a study of the $\Delta T/c$ and $C/\text{asterisk}/$ integrals for fracture analysis under non-steady creep
p 65 A82-36782
- Mechanics aspects of NDE by sound and ultrasound
p 51 A83-25571
- Dynamic fields near a crack tip growing in an elastic-perfectly-plastic solid
p 70 A83-38528
- Elasticity solutions for a class of composite laminate problems with stress singularities
p 17 A84-33389
- A study of fatigue damage mechanisms in Waspalloy from 25 to 800 C
p 34 A85-12098
- Statistics and thermodynamics of fracture
p 75 A85-19433
- On stress field near a stationary crack tip
[AD-A152863] p 76 A85-24532
- Wide-range displacement expressions for standard fracture mechanics specimens
p 79 A86-20706
- Wide-range weight functions for the strip with a single edge crack
p 79 A86-20709
- Fracture mechanics applied to nonisothermal fatigue crack growth
p 36 A86-28951
- Progressive fracture of fiber composites
p 19 A86-35809
- Quantitative flaw characterization with scanning laser acoustic microscopy
p 52 A86-45150
- SCARE - A postprocessor program to MSC/NASTRAN for reliability analysis of structural ceramic components
[ASME PAPER 86-GT-34] p 84 A87-17988

A relation between semiempirical fracture analyses and R-curves [NASA-TP-1600] p 87 N80-15428

Fracture modes of high modulus graphite/epoxy angleplied laminates subjected to off-axis tensile loads [NASA-TM-81405] p 21 N80-16102

The method of lines in three dimensional fracture mechanics [NASA-TM-81593] p 89 N80-32753

Micromechanical predictions of crack propagation and fracture energy in a single fiber boron/aluminum model composite [NASA-CR-168550] p 25 N82-18326

Creep crack-growth: A new path-independent T sub o and computational studies [NASA-CR-168930] p 92 N82-24503

Fracture mechanics criteria for turbine engine hot section components [NASA-CR-167896] p 7 N82-25257

High temperature low cycle fatigue mechanisms for nickel base and a copper base alloy [NASA-CR-3543] p 39 N82-26436

Analysis of cracks emanating from a circular hole in unidirectional fiber reinforced composites, part 2 [NASA-CR-165433] p 93 N82-26714

Analysis of interface cracks in adhesively bonded lap shear joints, part 4 [NASA-CR-165438] p 93 N82-26716

Phenomenological and mechanics aspects of nondestructive evaluation and characterization by sound and ultrasound of material and fracture properties [NASA-CR-3623] p 55 N83-11506

Nonlinear Constitutive Relations for High Temperature Applications [NASA-CP-2271] p 98 N83-34351

Wide range weight functions for the strip with a single edge crack [NASA-TM-83478] p 100 N84-11512

Simplified composite micromechanics equations for strength, fracture toughness and environmental effects [NASA-TM-83696] p 27 N84-27832

Hygrothermomechanical fracture stress criteria for fiber composites with sense-parity [NASA-TM-83691] p 27 N84-28918

HOST high temperature crack propagation p 10 N85-10977

Translational and extensional energy release rates (the J- and M-integrals) for a crack layer in thermoelasticity [NASA-CR-174872] p 107 N85-21685

Multiaxial and thermomechanical fatigue considerations in damage tolerant design [NASA-TM-87022] p 42 N85-26964

Interaction of high-cycle and low-cycle fatigue of Haynes 188 alloy at 1400 F deg p 111 N85-27961

A review of path-independent integrals in elastic-plastic fracture mechanics, task 4 [NASA-CR-174956] p 114 N85-33541

Progressive damage, fracture predictions and post mortem correlations for fiber composites [NASA-TM-87101] p 29 N86-10290

Estimating the R-curve from residual strength data [NASA-TM-87182] p 116 N86-18750

Variables controlling fatigue crack growth of short cracks [NASA-TM-87208] p 43 N86-21661

Fatigue crack layer propagation in silicon-iron [NASA-CR-175115] p 118 N86-25851

Computational simulation of progressive fracture in fiber composites [NASA-TM-87341] p 30 N86-26376

Effects of a high mean stress on the high cycle fatigue life of PWA 1480 and correlation of data by linear elastic fracture mechanics [NASA-CR-175057] p 118 N86-27689

Fatigue and fracture: Overview p 120 N87-11183

Fracture mechanics concepts in reliability analysis of monolithic ceramics [NASA-TM-100174] p 124 N87-27269

FRACTURE STRENGTH

Quantitative ultrasonic evaluation of engineering properties in metals, composites, and ceramics p 50 A80-39641

Fracture toughness determination of Al₂O₃ using four-point-bend specimens with straight-through and chevron notches p 45 A80-42085

Compliance and stress intensity coefficients for short bar specimens with chevron notches p 64 A80-46032

Performance of Chevron-notch short bar specimen in determining the fracture toughness of silicon nitride and aluminum oxide p 45 A80-50696

On the equivalence between semiempirical fracture analyses and R-curves p 64 A81-18792

Fracture toughness of brittle materials determined with chevron notch specimens p 45 A81-32545

Extended range stress intensity factor expressions for chevron-notched short bar and short rod fracture toughness specimens p 66 A82-40357

On ultrasonic factors and fracture toughness p 66 A82-42863

Development of plane strain fracture toughness test for ceramics using Chevron notched specimens p 46 A84-11676

Simplified composite micromechanics equations for strength, fracture toughness and environmental effects p 17 A84-41858

Fracture toughness of hot-pressed beryllium p 34 A85-25835

Fracture of composite-adhesive-composite systems p 76 A85-27935

Effect of low temperature on fatigue and fracture properties of Ti-5Al-2.5Sn(ELI) for use in engine components p 35 A85-47972

The crack layer approach to toughness characterization in steel p 36 A86-30010

Dynamic stress analysis of smooth and notched fiber composite flexural specimens p 20 A86-41070

Dynamic delamination crack propagation in a graphite/epoxy laminate p 20 A86-43010

Fracture toughness of Si₃N₄ measured with short bar chevron-notched specimens p 46 A87-30621

Comparison tests and experimental compliance calibration of the proposed standard round compact plane strain fracture toughness specimen [NASA-TM-81379] p 87 N80-13513

A relation between semiempirical fracture analyses and R-curves [NASA-TP-1600] p 87 N80-15428

Prediction of fiber composite mechanical behavior made simple --- using a rocket calculator [NASA-TM-81404] p 22 N80-16107

Fracture toughness of brittle materials determined with chevron notch specimens [NASA-TM-81607] p 38 N80-32486

Method for estimating crack-extension resistance curve from residual strength data [NASA-TP-1753] p 89 N81-11417

Experimental compliance calibration of the compact fracture toughness specimen [NASA-TM-81665] p 89 N81-16492

Interrelation of material microstructure, ultrasonic factors, and fracture toughness of two phase titanium alloy [NASA-TM-82810] p 54 N82-20551

Fundamental aspects in quantitative ultrasonic determination of fracture toughness: The scattering of a single ellipsoidal inhomogeneity [NASA-CR-3625] p 55 N83-11507

Specimen size and geometry effects on fracture toughness of Al₂O₃ measured with short rod and short bar chevron-notch specimens [NASA-TM-83319] p 47 N83-19902

Ultrasonic ranking of toughness of tungsten carbide [NASA-TM-83358] p 55 N83-23620

The thermal fatigue resistance of H-13 Die Steel for aluminum die casting dies [NASA-TM-83331] p 39 N83-35103

Dynamic stress analysis of smooth and notched fiber composite flexural specimens [NASA-TM-83694] p 27 N84-25770

Simplified composite micromechanics equations for strength, fracture toughness and environmental effects [NASA-TM-83696] p 27 N84-27832

Fractured toughness of Si₃N₄ measured with short bar chevron-notched specimens [NASA-TM-87153] p 47 N86-13495

Fracture characteristics of angleplied laminates fabricated from overaged graphite/epoxy prepreg [NASA-TM-87266] p 30 N86-25417

Concepts for interrelating ultrasonic attenuation, microstructure and fracture toughness in polycrystalline solids [NASA-TM-87339] p 60 N86-25812

Acousto-ultrasonic verification of the strength of filament wound composite material [NASA-TM-88827] p 61 N86-32764

Composite interlaminar fracture toughness: Three-dimensional finite element modeling for mixed mode 1, 2 and 3 fracture [NASA-TM-88872] p 31 N87-13491

FRACTURES (MATERIALS)

Creep crack-growth: A new path-independent integral (T sub c), and computational studies [NASA-CR-167897] p 94 N82-29619

Nonlinear Structural Analysis [NASA-CP-2297] p 105 N84-31688

Inelastic and dynamic fracture and stress analyses p 106 N84-31697

Fracture modes in notched angleplied composite laminates [NASA-TM-83802] p 28 N84-34576

Turbine Engine Hot Section Technology (HOST) [NASA-TM-83022] p 9 N85-10951

FRACTURING

Designing for fiber composite structural durability in hygrothermomechanical environments p 19 A86-27734

Relation of cyclic loading pattern to microstructural fracture in creep fatigue [NASA-TM-83473] p 98 N83-34349

Designing for fiber composite structural durability in hygrothermomechanical environment [NASA-TM-87045] p 29 N85-27978

Progressive damage, fracture predictions and post mortem correlations for fiber composites [NASA-TM-87101] p 29 N86-10290

FRAMES

Design concepts for low cost composite engine frames [AIAA PAPER 83-2445] p 2 A83-48331

Design concepts for low-cost composite engine frames [NASA-TM-83544] p 8 N84-16186

FREE VIBRATION

Vibrations of cantilevered shallow cylindrical shells of rectangular planform p 65 A82-11298

Comparison of beam and shell theories for the vibrations of thin turbomachinery blades [ASME PAPER 82-GT-223] p 65 A82-35408

Vibrations of cantilevered circular cylindrical shells Shallow versus deep shell theory p 69 A83-36958

On the three-dimensional vibrations of the cantilevered rectangular parallelepiped p 70 A83-37729

Vibrations of cantilevered doubly-curved shallow shells p 70 A83-39557

Vibrations of blades with variable thickness and curvature by shell theory [ASME PAPER 83-GT-152] p 70 A83-47978

Vibrations of twisted cantilevered plates - Summary of previous and current studies p 76 A85-22069

Vibrations of twisted cantilever plates - A comparison of theoretical results p 79 A84-47626

Finite-element modeling of layered, anisotropic composite plates and shells: A review of recent research p 91 N82-19563

A study of internal and distributed damping for vibrating turbomachinery blades [NASA-CR-175901] p 11 N85-27868

FREQUENCIES

Vibration and flutter of mistuned bladed-disk assemblies [AIAA PAPER 84-0991] p 75 A85-16095

Vibration and flutter of mistuned bladed-disk assemblies [NASA-TM-83634] p 103 N84-23923

FREQUENCY MEASUREMENT

Thermoviscoplastic nonlinear constitutive relationships for structural analysis of high temperature metal matrix composites [NASA-TM-87291] p 30 N86-24756

FRICTION

Stress evaluations under rolling/sliding contacts [NASA-CR-165561] p 91 N82-17521

A constitutive law for finite element contact problems with unclassical friction [NASA-TM-88838] p 120 N87-12924

FRICTION REDUCTION

Effects of friction dampers on aerodynamically unstable rotor stages [AIAA PAPER 83-0848] p 1 A83-32791

Forced response of a cantilever beam with a dry friction damper attached. I - Theory. II - Experiment p 71 A84-21267

Effects of friction dampers on aerodynamically unstable rotor stages p 3 A85-21866

Stress evaluations under rolling/sliding contacts [NASA-CR-165561] p 91 N82-17521

FUEL PUMPS

Effect of low temperature on fatigue and fracture properties of Ti-5Al-2.5Sn(ELI) for use in engine components p 35 A85-47972

G

GALERKIN METHOD

A study of internal and distributed damping for vibrating turbomachinery blades [NASA-CR-175901] p 11 N85-27868

Extensions of the Ritz-Galerkin method for the forced, damped vibrations of structural elements p 117 N86-21909

GAS BEARINGS

Dynamic behavior of spiral-groove and Rayleigh-Step self-acting face seals [NASA-TP-2266] p 8 N84-16181

GAS TURBINE ENGINES

Engine dynamic analysis with general nonlinear finite element codes. II - Bearing element implementation, overall numerical characteristics and benchmarking [ASME PAPER 82-GT-292] p 47 A82-35462

Structural tailoring of engine blades (STAEBL) [AIAA 83-0828] p 1 A83-29737

Effects of friction dampers on aerodynamically unstable rotor stages [AIAA PAPER 83-0848] p 1 A83-32791

Blade loss transient dynamic analysis of turbomachinery p 2 A83-40864

High-temperature fatigue in metals - A brief review of life prediction methods developed at the Lewis Research Center of NASA p 33 A84-14286

Simplified analytical procedures for representing material cyclic response --- for high temperature gas turbine engine analysis p 2 A84-22877

The interaction between mistuning and friction in the forced response of bladed disk assemblies [ASME PAPER 84-GT-139] p 73 A84-46957

Considerations for damage analysis of gas turbine hot section components [ASME PAPER 84-PVP-77] p 2 A85-18792

Effects of friction dampers on aerodynamically unstable rotor stages p 3 A85-21866

The effect of aerodynamic and structural detuning on turbomachine supersonic unstalled torsional flutter [AIAA PAPER 85-0761] p 3 A85-30378

Stability of limit cycles in frictionally damped and aerodynamically unstable rotor stages p 4 A86-19198

Aerodynamic and structural detuning of supersonic turbomachine rotors p 5 A86-31595

Stress analysis of gas turbine engine structures using the boundary element method p 81 A86-34444

Inelastic high-temperature thermomechanical response of ceramic coated gas turbine seals p 82 A86-37799

Unified constitutive materials model development and evaluation for high-temperature structural analysis applications --- for aircraft gas turbine engines p 84 A86-49133

Fabrication and quality assurance processes for superhybrid composite fan blades p 20 A87-19123

Optimization and analysis of gas turbine engine blades [AIAA PAPER 87-0827] p 126 A87-33614

Structural dynamics verification facility study [NASA-TM-82675] p 90 N81-33497

Evaluation of inelastic constitutive models for nonlinear structural analysis --- for aircraft turbine engines [NASA-TM-82845] p 92 N82-24502

Engine dynamic analysis with general nonlinear finite element codes. Part 2: Bearing element implementation overall numerical characteristics and benchmarking [NASA-CR-167944] p 7 N82-33390

Evaluation of inelastic constitutive models for nonlinear structural analysis p 98 N83-34357

Simplified method for nonlinear structural analysis [NASA-TP-2208] p 99 N83-34372

Low strain, long life creep fatigue of AF2-1DA and INCO 718 [NASA-CR-167989] p 40 N84-10268

Research and development program for the development of advanced time-temperature dependent constitutive relationships. Volume 2: Programming manual [NASA-CR-168191-VOL-2] p 100 N84-10614

Digital computer program for generating dynamic turbofan engine models (DIGTEM) [NASA-TM-83446] p 8 N84-16185

Bending fatigue of electron-beam-welded foils. Application to a hydrodynamic air bearing in the Chrysler/DOE upgraded automotive gas turbine engine [NASA-TM-83539] p 102 N84-16589

Engine cyclic durability by analysis and material testing [NASA-TM-83577] p 102 N84-18683

Elevated temperature biaxial fatigue [NASA-CR-173473] p 103 N84-21905

Nonlinear Structural Analysis [NASA-CP-2297] p 105 N84-31688

Nonlinear analysis for high-temperature composites: Turbine blades/vanes p 106 N84-31699

Three-dimensional stress analysis using the boundary element method p 106 N84-31700

Turbine Engine Hot Section Technology (HOST) [NASA-TM-83022] p 9 N85-10951

Nonlinear structural and life analyses of a turbine blade p 9 N85-10954

Nonlinear structural and life analyses of a combustor liner p 9 N85-10955

Pre-HOST high temperature crack propagation p 9 N85-10956

Component-specific modeling p 10 N85-10971

The 3-D inelastic analysis methods for hot section components: Brief description p 10 N85-10972

Constitutive model development for isotropic materials p 10 N85-10975

Fabrication and quality assurance processes for superhybrid composite fan blades [NASA-TM-83354] p 28 N85-14882

Engine cyclic durability by analysis and material testing p 11 N85-15744

Multiaxial and thermomechanical fatigue considerations in damage tolerant design [NASA-TM-87022] p 42 N85-26964

Creep fatigue life prediction for engine hot section materials (isotropic) [NASA-CR-168228] p 11 N85-31057

Constitutive modeling for isotropic materials (HOST) [NASA-CR-174980] p 115 N86-10589

Turbine Engine Hot Section Technology (HOST) [NASA-CP-2289] p 115 N86-11495

HOST structural analysis program overview p 12 N86-11513

Component-specific modeling p 12 N86-11515

Life prediction and constitutive models for engine hot section anisotropic materials program [NASA-CR-174952] p 60 N86-25003

STAEBL: Structural tailoring of engine blades, phase 2 p 13 N87-11731

Turbine Engine Hot Section Technology, 1985 [NASA-CP-2405] p 125 N88-11140

High temperature stress-strain analysis p 125 N88-11170

Composite mechanics for engine structures [NASA-TM-100176] p 32 N88-12552

GAS TURBINES

NASA Lewis Research Center/university graduate research program on engine structures [ASME PAPER 85-GT-159] p 80 A86-22084

Nonlinear, three-dimensional finite-element analysis of air-cooled gas turbine blades [NASA-TP-1669] p 88 N80-22734

Structural analysis p 9 N85-10969

NASA Lewis Research Center/University Graduate Research Program on Engine Structures [NASA-TM-86916] p 107 N85-18375

Micromechanisms of thermomechanical fatigue: A comparison with isothermal fatigue [NASA-TM-87331] p 44 N86-28164

GEARS

On the automatic generation of FEM models for complex gears - A work-in-progress report p 47 A82-48243

A finite element stress analysis of spur gears including fillet radii and rim thickness effects [NASA-TM-82865] p 48 N82-28646

On finite element stress analysis of spur gears [NASA-CR-167938] p 48 N82-29607

GEOMETRICAL ACOUSTICS

Phenomenological and mechanics aspects of nondestructive evaluation and characterization by sound and ultrasound of material and fracture properties [NASA-CR-3623] p 55 N83-11506

Fundamental aspects in quantitative ultrasonic determination of fracture toughness: The scattering of a single ellipsoidal inhomogeneity [NASA-CR-3625] p 55 N83-11507

GLASS

A study of the stress wave factor technique for the characterization of composite materials [NASA-CR-3670] p 55 N83-27248

GLASS FIBER REINFORCED PLASTICS

Dynamic response of damaged angleplied fiber composites p 14 A80-27982

Impact resistance of fiber composites p 66 A82-39852

Hygrothermomechanical evaluation of transverse filament tape epoxy/polyester fiberglass composites p 17 A85-15632

Fiberglass epoxy laminate fatigue properties at 300 and 20 K p 19 A85-47970

Dynamic response of damaged angleplied fiber composites [NASA-TM-79281] p 21 N80-11145

Application of composite materials to turbofan engine fan exit guide vanes [NASA-TM-81432] p 22 N80-18106

GLASS FIBERS

Mechanical property characterization of intraply hybrid composites p 13 A80-20954

Ten year environmental test of glass fiber/epoxy pressure vessels [AIAA PAPER 85-1198] p 19 A85-47022

Hygrothermomechanical evaluation of transverse filament tape epoxy/polyester fiberglass composites [NASA-TM-83044] p 26 N83-15362

Ten year environmental test of glass fiber/epoxy pressure vessels [NASA-TM-87058] p 29 N85-30034

GRAIN BOUNDARIES

Micromechanically based constitutive relations for polycrystalline solids p 99 N83-34359

Literature survey on oxidations and fatigue lives at elevated temperatures [NASA-CR-174639] p 40 N84-20674

Fatigue crack propagation of nickel-base superalloys at 650 deg C [NASA-TM-87150] p 42 N86-12294

Grain boundary oxidation and oxidation accelerated fatigue crack nucleation and propagation [NASA-CR-175050] p 43 N86-20542

GRAIN SIZE

On the fatigue crack propagation behavior of superalloys at intermediate temperatures p 35 A85-32434

Fatigue crack propagation of nickel-base superalloys at 650 deg C [NASA-TM-87150] p 42 N86-12294

Determination of grain size distribution function using two-dimensional Fourier transforms of tone pulse encoded images [NASA-TM-88790] p 61 N86-31065

GRAPHITE

Thermal expansion behavior of graphite/glass and graphite/magnesium p 21 A87-38615

GRAPHITE-EPoxy COMPOSITES

Mechanical property characterization of intraply hybrid composites p 13 A80-20954

Dynamic response of damaged angleplied fiber composites p 14 A80-27982

Fracture modes of high modulus graphite/epoxy angleplied laminates subjected to off-axis tensile loads p 14 A80-32069

Wave propagation in a graphite/epoxy laminate p 70 A83-44050

Select fiber composites for space applications - A mechanistic assessment p 18 A85-16040

Factors influencing the ultrasonic stress wave factor evaluation of composite material structures p 81 A86-34257

Progressive fracture of fiber composites p 19 A86-35809

Dynamic delamination crack propagation in a graphite/epoxy laminate p 20 A86-43010

Assessment of simplified composite micromechanics using three-dimensional finite-element analysis p 20 A87-19121

Dynamic response of damaged angleplied fiber composites [NASA-TM-79281] p 21 N80-11145

Mechanical property characterization of intraply hybrid composites [NASA-TM-79306] p 21 N80-12120

Fracture modes of high modulus graphite/epoxy angleplied laminates subjected to off-axis tensile loads [NASA-TM-81405] p 21 N80-16102

Application of composite materials to turbofan engine fan exit guide vanes [NASA-TM-81432] p 22 N80-18106

Boundary layer thermal stresses in angle-ply composite laminates, part 1 --- graphite-epoxy composites [NASA-CR-165412] p 93 N82-26713

Dynamic responses of graphite/epoxy laminated beam to impact of elastic spheres [NASA-CR-165461] p 25 N83-13173

Wave propagation in graphite/epoxy laminates due to impact [NASA-CR-168057] p 26 N83-22325

The effect of stress on ultrasonic pulses in fiber reinforced composites [NASA-CR-3724] p 56 N83-33180

Select fiber composites for space applications: A mechanistic assessment [NASA-TM-83631] p 26 N84-22702

Fracture surface characteristics of notched angleplied graphite/epoxy composites [NASA-TM-83786] p 28 N84-33522

Progressive damage, fracture predictions and post mortem correlations for fiber composites [NASA-TM-87101] p 29 N86-10290

Ultrasonic evaluation of mechanical properties of thick, multilayered, filament wound composites [NASA-TM-87088] p 58 N86-10561

Fracture characteristics of angleplied laminates fabricated from overaged graphite/epoxy prepreg [NASA-TM-87266] p 30 N86-25417

GRINDING (MATERIAL REMOVAL)

Effects of surface removal on rolling-element fatigue [NASA-TM-88871] p 50 N87-18820

GROUND SPEED

Temperature distribution in an aircraft tire at low ground speeds [NASA-TP-2195] p 97 N83-33217

GROUP VELOCITY

Stress waves in transversely isotropic media: The homogeneous problem
[NASA-CR-3977] p 59 N86-25002

GUIDE VANES

Application of composite materials to turbofan engine fan exit guide vanes
[NASA-TM-81432] p 22 N80-18106

H

HARMONIC ANALYSIS

Frequency domain solutions to multi-degree-of-freedom, dry friction damped systems under periodic excitation
p 83 A86-39485
On the equivalence of the incremental harmonic balance method and the harmonic balance-Newton Raphson method
p 83 A86-40695

HARMONIC OSCILLATION

The impact damped harmonic oscillator in free decay
[NASA-TM-89897] p 50 N87-23978

HASTELLOY (TRADEMARK)

Fracture mechanics applied to nonisothermal fatigue crack growth
p 36 A86-28951
Experimental verification of the Neuber relation at room and elevated temperatures --- to predict stress-strain behavior in notched specimens of hastelloy x
[NASA-CR-167967] p 96 N83-19121
Development of a simplified analytical method for representing material cyclic response
[NASA-CR-168100] p 96 N83-21390
Experimental verification of the number relation at room and elevated temperatures
p 98 N83-34355
Elevated temperature biaxial fatigue
[NASA-CR-175795] p 110 N85-27263
A comparison of smooth specimen and analytical simulation techniques for notched members at elevated temperatures
p 114 N85-31546

HEAT RESISTANT ALLOYS

Effects of fine porosity on the fatigue behavior of a powder metallurgy superalloy
p 32 A80-35495
Cyclic behavior of turbine disk alloys at 650 C
p 32 A81-12266
Fatigue and creep-fatigue deformation of several nickel-base superalloys at 650 C
p 32 A82-47398
Requirements of constitutive models for two nickel-base superalloys
p 33 A83-21071
Metallurgical instabilities during the high temperature low cycle fatigue of nickel-base superalloys
p 33 A83-22019
The effect of microstructure on the fatigue behavior of Ni base superalloys
p 33 A83-36166
Fatigue crack initiation and propagation in several nickel-base superalloys at 650 C
p 33 A83-41199
The effect of microstructure on 650 C fatigue crack growth in P/M Astroloy
p 33 A84-12395
The effects of frequency and hold times on fatigue crack propagation rates in a nickel base superalloy
p 34 A84-18733
Effects of processing and microstructure on the fatigue behaviour of the nickel-base superalloy Rene95
p 34 A84-48715
The influence of hold times on LCF and FCG behavior in a P/M Ni-base superalloy --- Low Cycle Fatigue/Fatigue Crack Growth
p 35 A85-32400
On the fatigue crack propagation behavior of superalloys at intermediate temperatures
p 35 A85-32434
The tensile and fatigue deformation structures in a single crystal Ni-base superalloy
p 36 A86-35697
Toward improved durability in advanced combustors and turbines - Progress in prediction of thermomechanical loads
[ASME PAPER 86-GT-172] p 6 A86-48224
Orientation and temperature dependence of some mechanical properties of the single-crystal nickel-base superalloy Rene N4. II - Low cycle fatigue behavior
p 37 A86-50322
Effects of fine porosity on the fatigue behavior of a powder metallurgy superalloy
[NASA-TM-81448] p 37 N80-21493
Thermal fatigue and oxidation data of TAZ-8A and M22 alloys and variations
[NASA-CR-165407] p 38 N82-10193
Mechanisms of deformation and fracture in high temperature low cycle fatigue of Rene 80 and IN 100
[NASA-CR-165498] p 93 N82-26706
Creep-fatigue of low cobalt superalloys
p 39 N83-11290
Constitutive relationships for anisotropic high-temperature alloys
[NASA-TM-83437] p 97 N83-28493
Relation of cyclic loading pattern to microstructural fracture in creep fatigue
[NASA-TM-83473] p 98 N83-34349

Fatigue crack growth and low cycle fatigue of two nickel base superalloys
[NASA-CR-174534] p 39 N84-10267
Creep fatigue of low-cobalt superalloys: Waspalloy, PM U 700 and wrought U 700
[NASA-CR-168260] p 40 N84-13265
Complexities of high temperature metal fatigue: Some steps toward understanding
[NASA-TM-83507] p 101 N84-14541
Preliminary study of thermomechanical fatigue of polycrystalline MAR-M 200
[NASA-TP-2280] p 40 N84-17350
Literature survey on oxidations and fatigue lives at elevated temperatures
[NASA-CR-174639] p 40 N84-20674
Nonlinear analysis for high-temperature composites: Turbine blades/vanes
p 106 N84-31699
Low cycle fatigue behavior of conventionally cast MAR-M 200 AT 1000 deg C
[NASA-TM-83769] p 41 N84-33564
Low cycle fatigue of MAR-M 200 single crystals at 760 and 870 deg C
[NASA-TM-86933] p 41 N85-19074
On thermomechanical testing in support of constitutive equation development for high temperature alloys
[NASA-CR-174879] p 109 N85-25894
Nonlinear structural analysis for fiber-reinforced superalloy turbine blades
p 109 N85-26887
On the use of internal state variables in thermoviscoplastic constitutive equations
p 113 N85-31536
Fatigue crack propagation of nickel-base superalloys at 650 deg C
[NASA-TM-87150] p 42 N86-12294
Development of constitutive models for cyclic plasticity and creep behavior of super alloys at high temperature
[NASA-CR-176418] p 43 N86-14356
Simplified cyclic structural analyses of SSME turbine blades
[NASA-TM-87214] p 116 N86-16615
Anisotropic constitutive model for nickel base single crystal alloys: Development and finite element implementation
[NASA-CR-175015] p 117 N86-21952
Thermal-mechanical fatigue behavior of nickel-base superalloys
[NASA-CR-175048] p 43 N86-24818
Life prediction and constitutive models for engine hot section anisotropic materials program
[NASA-CR-174952] p 60 N86-25003
Yielding and deformation behavior of the single crystal nickel-base superalloy PWA 1480
[NASA-CR-175100] p 44 N86-25455
Micromechanisms of thermomechanical fatigue: A comparison with isothermal fatigue
[NASA-TM-87331] p 44 N86-28164
Thermal-fatigue and oxidation resistance of cobalt-modified Udimet 700 alloy
[NASA-TP-2591] p 119 N86-28464
Integrated research in constitutive modelling at elevated temperatures, part 1
[NASA-CR-177237] p 120 N86-30227
Bithermal low-cycle fatigue behavior of a NiCoCrAlY-coated single crystal superalloy
[NASA-TM-89831] p 45 N87-20408
Fatigue damage interaction behavior of PWA 1480
p 45 N87-22777
Toward improved durability in advanced combustors and turbines: Progress in the prediction of thermomechanical loads
[NASA-TM-88932] p 13 N87-28551

HEAT TRANSFER

A computer analysis program for interfacing thermal and structural codes
p 126 A86-36861
Toward improved durability in advanced combustors and turbines - Progress in prediction of thermomechanical loads
[ASME PAPER 86-GT-172] p 6 A86-48224
Turbine Engine Hot Section Technology (HOST)
[NASA-TM-83022] p 9 N85-10951
Component-specific modeling
[NASA-CR-174765] p 110 N85-27261
A computer analysis program for interfacing thermal and structural codes
[NASA-TM-87021] p 110 N85-27264
Component-specific modeling
[NASA-CR-174765] p 12 N85-34140
HOST structural analysis program overview
p 12 N86-11513
Component-specific modeling
p 12 N86-11515
Burner liner thermal-structural load modeling
[NASA-CR-174892] p 117 N86-21932
Nonlinear heat transfer and structural analyses of SSME turbine blades
p 123 N87-22779

Toward improved durability in advanced combustors and turbines: Progress in the prediction of thermomechanical loads
[NASA-TM-88932] p 13 N87-28551

HEAT TRANSMISSION

Turbine Engine Hot Section Technology (HOST)
[NASA-CP-2289] p 115 N86-11495

HELMHOLTZ EQUATIONS

Volume integrals associated with the inhomogeneous Helmholtz equation. Part 1: Ellipsoidal region
[NASA-CR-3749] p 56 N84-14525
Volume integrals associated with the inhomogeneous Helmholtz equation. Part 2: Cylindrical region; rectangular region
[NASA-CR-3750] p 56 N84-14526

HELMHOLTZ VORTICITY EQUATION

On the use of internal state variables in thermoviscoplastic constitutive equations
p 113 N85-31536

HIERARCHIES

On the development of hierarchical solution strategies for nonlinear finite element formulations
p 126 A85-21979

HIGH STRENGTH ALLOYS

Quantitative ultrasonic evaluation of engineering properties in metals, composites, and ceramics
p 50 A80-39641

HIGH TEMPERATURE

Results of an interlaboratory fatigue test program conducted on alloy 800H at room and elevated temperatures
p 37 A87-54370
Experimental verification of the number relation at room and elevated temperatures
p 98 N83-34355
Elevated temperature biaxial fatigue
[NASA-CR-173473] p 103 N84-21905
Low cycle fatigue behavior of conventionally cast MAR-M 200 AT 1000 deg C
[NASA-TM-83769] p 41 N84-33564
Pre-HOST high temperature crack propagation
p 9 N85-10956
3-D inelastic analysis methods for hot section components (base program) --- turbine blades, turbine vanes, and combustor liners
[NASA-CR-174700] p 107 N85-21686
Multiaxial and thermomechanical fatigue considerations in damage tolerant design
[NASA-TM-87022] p 42 N85-26964
Creep fatigue life prediction for engine hot section materials (isotropic)
[NASA-CR-168228] p 11 N85-31057
On numerical integration and computer implementation of viscoplastic models
p 113 N85-31542
A comparison of smooth specimen and analytical simulation techniques for notched members at elevated temperatures
p 114 N85-31546
Results of an interlaboratory fatigue test program conducted on alloy 800H at room and elevated temperatures
[NASA-CR-174940] p 114 N85-32340
Constitutive modeling for isotropic materials (HOST)
[NASA-CR-174980] p 115 N86-10589
Turbine Engine Hot Section Technology (HOST)
[NASA-CP-2289] p 115 N86-11495
Estimation of high temperature low cycle fatigue on the basis of inelastic strain and strain rate
[NASA-TM-88841] p 44 N87-14489
Exposure time considerations in high temperature low cycle fatigue
[NASA-TM-88934] p 125 N87-28944
High temperature stress-strain analysis
p 125 N88-11170
Lewis' enhanced laboratory for research into the fatigue and constitutive behavior of high temperature materials
p 125 N88-11177

HIGH TEMPERATURE ENVIRONMENTS

Algorithms for elasto-plastic-creep postbuckling
p 73 A84-38480
Unified constitutive materials model development and evaluation for high-temperature structural analysis applications --- for aircraft gas turbine engines
p 84 A86-49133
Component-specific modeling
p 10 N85-10971
The 3-D inelastic analysis methods for hot section components: Brief description
p 10 N85-10972
Life prediction and constitutive behavior: Overview
p 10 N85-10973
HOST high temperature crack propagation
p 10 N85-10977

HIGH TEMPERATURE TESTS

Fatigue and creep-fatigue deformation of several nickel-base superalloys at 650 C
p 32 A82-47398
Metallurgical instabilities during the high temperature low cycle fatigue of nickel-base superalloys
p 33 A83-22019

- The effects of frequency and hold times on fatigue crack propagation rates in a nickel base superalloy p 34 A84-18733
- High temperature thermomechanical analysis of ceramic coatings p 74 A84-48565
- On the fatigue crack propagation behavior of superalloys at intermediate temperatures p 35 A85-32434
- The cyclic stress-strain behavior of a nickel-base superalloy at 650 C p 36 A86-45715
- Elevated temperature fatigue testing of metals [NASA-TM-82745] p 91 N82-16419
- High temperature low cycle fatigue mechanisms for nickel base and a copper base alloy [NASA-CR-3543] p 39 N82-26436
- Mechanisms of deformation and fracture in high temperature low cycle fatigue of Rene 80 and IN 100 [NASA-CR-165498] p 93 N82-26706
- Nonlinear Constitutive Relations for High Temperature Application, 1984 [NASA-CP-2369] p 112 N85-31530
- A high temperature fatigue and structures testing facility [NASA-TM-100151] p 124 N87-26399
- HOLE GEOMETRY (MECHANICS)**
- Analysis of cracks emanating from a circular hole in unidirectional fiber reinforced composites, part 2 [NASA-CR-165433] p 93 N82-26714
- HOLOGRAPHY**
- Nondestructive techniques for characterizing mechanical properties of structural materials - An overview [ASME PAPER 86-GT-75] p 52 A86-48143
- Nondestructive techniques for characterizing mechanical properties of structural materials: An overview [NASA-TM-87203] p 59 N86-19636
- HONEYCOMB STRUCTURES**
- Metal honeycomb to porous wireform substrate diffusion bond evaluation p 51 A83-39620
- Metal honeycomb to porous wireform substrate diffusion bond evaluation [NASA-TM-82793] p 54 N82-18612
- Fiber composite sandwich thermostructural behavior: Computational simulation [NASA-TM-88787] p 31 N86-31663
- HORIZONTAL ORIENTATION**
- Stability of large horizontal-axis axisymmetric wind turbines p 64 A81-22526
- HOT PRESSING**
- Effects of processing and microstructure on the fatigue behaviour of the nickel-base superalloy Rene95 p 34 A84-48715
- Fracture toughness of hot-pressed beryllium p 34 A85-25835
- The effect of microstructure, temperature, and hold-time on low-cycle fatigue of As HIP P/M Rene 95 p 35 A85-32399
- Fracture toughness of Si₃N₄ measured with short bar chevron-notched specimens p 46 A87-30621
- Fractured toughness of Si₃N₄ measured with short bar chevron-notched specimens [NASA-TM-87153] p 47 N86-13495
- HOT SURFACES**
- Advances in 3-D Inelastic Analysis Methods for hot section components [AIAA PAPER 87-0719] p 85 A87-33645
- Component-specific modeling [NASA-CR-174765] p 12 N85-34140
- Structural analysis of turbine blades using unified constitutive models [NASA-TM-88807] p 119 N86-28461
- HUBS**
- Hub flexibility effects on propfan vibration [NASA-TM-89900] p 124 N87-24722
- HYBRID STRUCTURES**
- Mechanical property characterization of intraply hybrid composites p 13 A80-20954
- Evolution of assumed stress hybrid finite element p 77 A85-35046
- Axisymmetric solid elements by a rational hybrid stress method p 78 A85-41109
- Superhybrid composite blade impact studies [NASA-TM-81597] p 89 N81-11412
- HYDRAULIC EQUIPMENT**
- The 20th Aerospace Mechanics Symposium [NASA-CP-2423-REV] p 121 N87-16321
- HYDRODYNAMICS**
- Dynamic behavior of spiral-groove and Rayleigh-Step self-acting face seals [NASA-TP-2266] p 8 N84-16181
- HYDROSTATIC PRESSURE**
- Vibration and buckling of rectangular plates under in-plane hydrostatic loading p 64 A80-45364
- HYDROTHERMAL STRESS ANALYSIS**
- Designing for fiber composite structural durability in hydrothermomechanical environments p 19 A86-27734
- Designing for fiber composite structural durability in hydrothermomechanical environment [NASA-TM-87045] p 29 N85-27978
- Fiber composite sandwich thermostructural behavior: Computational simulation [NASA-TM-88787] p 31 N86-31663
- HYGRAL PROPERTIES**
- Computer code for intraply hybrid composite design p 15 A81-44662
- Prediction of composite hygral behavior made simple p 16 A84-14285
- Hygrothermomechanical evaluation of transverse filament tape epoxy/polyester fiberglass composites p 17 A85-15632
- ICAN - Integrated composites analyzer [AIAA PAPER 84-0974] p 18 A85-16094
- Designing for fiber composite structural durability in hydrothermomechanical environments p 19 A86-27734
- Composite sandwich thermostructural behavior - Computational simulation [AIAA PAPER 86-0948] p 82 A86-38842
- Computer code for intraply hybrid composite design [NASA-TM-82593] p 24 N81-25151
- Prediction of composite hygral behavior made simple [NASA-TM-82780] p 24 N82-16181
- ICAN: Integrated composites analyzer [NASA-TM-83700] p 27 N84-26755
- Designing for fiber composite structural durability in hydrothermomechanical environment [NASA-TM-87045] p 29 N85-27978
- Fiber composite sandwich thermostructural behavior: Computational simulation [NASA-TM-88787] p 31 N86-31663
- HYGROSCOPICITY**
- Environmental and high strain rate effects on composites for engine applications p 16 A84-17444
- HYPERVELOCITY IMPACT**
- Computational engine structural analysis [ASME PAPER 86-GT-70] p 5 A86-48141
- Computational engine structural analysis [NASA-TM-87231] p 116 N86-19663
- HYSTERESIS**
- Application of traction drives as servo mechanisms p 114 N85-33520
- IMAGE ANALYSIS**
- Determination of grain size distribution function using two-dimensional Fourier transforms of tone pulse encoded images [NASA-TM-88790] p 61 N86-31065
- IMPACT**
- Dynamic responses of graphite/epoxy laminated beam to impact of elastic spheres [NASA-CR-165461] p 25 N83-13173
- The impact damped harmonic oscillator in free decay [NASA-TM-89897] p 50 N87-23978
- IMPACT DAMAGE**
- Bird impact analysis package for turbine engine fan blades [NASA-TM-82831] p 92 N82-26701
- Wave propagation in graphite/epoxy laminates due to impact [NASA-CR-168057] p 26 N83-22325
- IMPACT LOADS**
- Dynamic response of damaged angleply fiber composites p 14 A80-27982
- Wave propagation in a graphite/epoxy laminate p 70 A83-44050
- Dynamic delamination buckling in composite laminates under impact loading: Computational simulation [NASA-TM-100192] p 31 N87-28611
- IMPACT RESISTANCE**
- Impact resistance of fiber composites p 66 A82-39852
- Simplified composite micromechanics equations for strength, fracture toughness and environmental effects p 17 A84-1858
- Impact resistance of fiber composites - Energy-absorbing mechanisms and environmental effects p 18 A85-46543
- Computational engine structural analysis [ASME PAPER 86-GT-70] p 5 A86-48141
- Superhybrid composite blade impact studies [NASA-TM-81597] p 89 N81-11412
- Environmental and High-Strain Rate effects on composites for engine applications [NASA-TM-82882] p 25 N82-31449
- Impact resistance of fiber composites: Energy absorbing mechanisms and environmental effects [NASA-TM-83594] p 26 N84-24712
- Simplified composite micromechanics equations for strength, fracture toughness and environmental effects [NASA-TM-83696] p 27 N84-27832
- Computational engine structural analysis [NASA-TM-87231] p 116 N86-19663
- IMPACT TESTS**
- Superhybrid composite blade impact studies [ASME PAPER 81-GT-24] p 1 A81-29940
- Indentation law for composite laminates p 16 A84-27356
- Dynamic delamination crack propagation in a graphite/epoxy laminate p 20 A86-43010
- INCLUSIONS**
- Composites with periodic microstructure p 15 A83-12734
- Ultrasonic wave propagation in two-phase media - Spherical inclusions p 17 A85-11926
- INCOMPRESSIBLE FLOW**
- Effects of mistuning on bending-torsion flutter and response of a cascade in incompressible flow [AIAA 81-0602] p 65 A81-29465
- Effects of mistuning on bending-torsion flutter and response of a cascade in incompressible flow --- turbofan engines [NASA-TM-81674] p 89 N81-16494
- INCONEL (TRADEMARK)**
- Benchmark cyclic plastic notch strain measurements p 33 A84-11194
- Thermal-mechanical fatigue crack growth in Inconel X-750 p 35 A86-20982
- Benchmark notch test for life prediction [NASA-CR-165571] p 95 N83-12451
- Thermal-mechanical fatigue crack growth in Inconel X-750 [NASA-CR-174740] p 41 N85-15877
- Finite element analysis of notch behavior using a state variable constitutive equation p 114 N85-31548
- INDENTATION**
- Indentation law for composite laminates p 16 A84-27356
- Use of static indentation laws in the impact analysis of laminated composite plates p 18 A85-29133
- INELASTIC STRESS**
- Inelastic stress analyses at finite deformation through complementary energy approaches p 71 A84-13248
- Analyses of large quasistatic deformations of inelastic bodies by a new hybrid-stress finite element algorithm p 71 A84-16874
- Strainrange partitioning - A total strain range version --- for creep fatigue life prediction by summing inelastic and elastic strain-range-life relations for two Ni base superalloys p 34 A85-11603
- A history dependent damage model for low cycle fatigue [ASME PAPER 84-PVP-112] p 75 A85-18795
- Unified constitutive material models for nonlinear finite-element structural analysis --- gas turbine engine blades and vanes [AIAA PAPER 85-1418] p 77 A85-39769
- Inelastic high-temperature thermomechanical response of ceramic coated gas turbine seals p 82 A86-37799
- Evaluation of inelastic constitutive models for nonlinear structural analysis --- for aircraft turbine engines [NASA-TM-82845] p 92 N82-24502
- Materials constitutive models for nonlinear analysis of thermally cycled structures [NASA-TP-2055] p 95 N83-12449
- Strainrange partitioning: A total strain range version [NASA-TM-83023] p 39 N83-14246
- Development of a simplified analytical method for representing material cyclic response [NASA-CR-168100] p 96 N83-21390
- Development of a simplified procedure for cyclic structural analysis [NASA-TP-2243] p 103 N84-20878
- Nonlinear Structural Analysis [NASA-CP-2297] p 105 N84-31688
- Inelastic and dynamic fracture and stress analyses p 106 N84-31697
- The 3-D inelastic analysis methods for hot section components: Brief description p 10 N85-10972
- Local strain redistribution corrections for a simplified inelastic analysis procedure based on an elastic finite-element analysis [NASA-TP-2421] p 107 N85-20396
- 3-D inelastic analysis methods for hot section components (base program) --- turbine blades, turbine vanes, and combustor liners [NASA-CR-174700] p 107 N85-21686
- Unified constitutive material models for nonlinear finite-element structural analysis --- gas turbine engine blades and vanes [NASA-TM-86985] p 108 N85-24338

- A survey of unified constitutive theories
p 112 N85-31531
- Analysis of large, non-isothermal elastic-visco-plastic deformations
[NASA-CR-176220] p 115 N86-10588
- Nonlinear damage analysis: Postulate and evaluation
[NASA-CR-168171] p 118 N86-26652
- Estimation of high temperature low cycle fatigue on the basis of inelastic strain and strainrate
[NASA-TM-88841] p 44 N87-14489
- INHOMOGENEITY**
- Fundamental aspects in quantitative ultrasonic determination of fracture toughness: The scattering of a single ellipsoidal inhomogeneity
[NASA-CR-3625] p 55 N83-11507
- The transmission or scattering of elastic waves by an inhomogeneity of simple geometry: A comparison of theories
[NASA-CR-3659] p 55 N83-16773
- Volume integrals associated with the inhomogeneous Helmholtz equation. Part 1: Ellipsoidal region
[NASA-CR-3749] p 56 N84-14525
- Volume integrals associated with the inhomogeneous Helmholtz equation. Part 2: Cylindrical region; rectangular region
[NASA-CR-3750] p 56 N84-14526
- INJECTORS**
- Longitudinal mode combustion instabilities of a high-pressure fuel-rich LOX/JP-1 preburner
p 60 N86-28250
- INPUT/OUTPUT ROUTINES**
- Input-output characterization of an ultrasonic testing system by digital signal analysis
[NASA-CR-3756] p 56 N84-15565
- INTEGRAL EQUATIONS**
- Path-independent integrals in finite elasticity and inelasticity, with body forces, inertia, and arbitrary crack-face conditions
p 65 N84-32303
- On a study of the $\Delta T/c$ and $C/\text{asterisk}$ integrals for fracture analysis under non-steady creep
p 65 A82-36782
- Volume integrals associated with the inhomogeneous Helmholtz equation. Part 1: Ellipsoidal region
[NASA-CR-3749] p 56 N84-14525
- Volume integrals associated with the inhomogeneous Helmholtz equation. Part 2: Cylindrical region; rectangular region
[NASA-CR-3750] p 56 N84-14526
- Compliance matrices for cracked bodies
[NASA-CR-179478] p 120 N86-30236
- INTEGRALS**
- Volume integrals associated with the inhomogeneous Helmholtz equation. Part 1: Ellipsoidal region
[NASA-CR-3749] p 56 N84-14525
- Volume integrals associated with the inhomogeneous Helmholtz equation. Part 2: Cylindrical region; rectangular region
[NASA-CR-3750] p 56 N84-14526
- Translational and extensional energy release rates (the J- and M-integrals) for a crack layer in thermoelasticity
[NASA-CR-174872] p 107 N85-21685
- INTERFACES**
- Burner liner thermal-structural load modeling
[NASA-CR-174892] p 117 N86-21932
- Identification of structural interface characteristics using component mode synthesis
[NASA-TM-88960] p 123 N87-24006
- SINDA-NASTRAN interfacing program theoretical description and user's manual
[NASA-TM-100158] p 124 N87-27268
- INTERFACIAL TENSION**
- Interface cracks in adhesively bounded lap-shear joints
p 67 A82-46109
- Fatigue life prediction in bending from axial fatigue information
[NASA-CR-165563] p 91 N82-20564
- INTERNAL COMBUSTION ENGINES**
- NDE for heat engine ceramics
[NASA-TM-86949] p 57 N85-20389
- INTERNAL ENERGY**
- On the use of internal state variables in thermoviscoplastic constitutive equations
p 113 N85-31536
- INTERPOLATION**
- Slave finite elements: The temporal element approach to nonlinear analysis
p 105 N84-31689
- ION BEAMS**
- Ion beam sputter etching of orthopedic implanted alloy MP35N and resulting effects on fatigue
[NASA-TM-81747] p 38 N81-21174
- IRON ALLOYS**
- Fatigue crack layer propagation in silicon-iron
[NASA-CR-175115] p 118 N86-25851
- ISOPARAMETRIC FINITE ELEMENTS**
- A new formulation of hybrid/mixed finite element
p 67 A83-12739

- Three-dimensional finite-element analysis of layered composite plates
p 68 A83-27432
- Development and testing of stable, invariant, isoparametric curvilinear 2- and 3-D hybrid-stress elements
p 75 A85-19899
- Use of static indentation laws in the impact analysis of laminated composite plates
p 18 A85-29133
- Stability and convergence of underintegrated finite element approximations
p 105 N84-31696
- ISOTHERMAL PROCESSES**
- Calculation of thermomechanical fatigue life based on isothermal behavior
[NASA-TM-88864] p 122 N87-20565
- ISOTROPIC MEDIA**
- Unified constitutive material models for nonlinear finite-element structural analysis --- gas turbine engine blades and vanes
[AIAA PAPER 85-1418] p 77 A85-39769
- Ultrasonic attenuation of a void-containing medium for very long wavelengths
[NASA-CR-3693] p 56 N83-28466
- Unified constitutive material models for nonlinear finite-element structural analysis --- gas turbine engine blades and vanes
[NASA-TM-86985] p 108 N85-24338
- Constitutive modeling for isotropic materials (HOST)
[NASA-CR-174980] p 115 N86-10589
- Wave propagation in anisotropic medium due to an oscillatory point source with application to unidirectional composites
[NASA-CR-4001] p 60 N86-27666
- ISOTROPIC TURBULENCE**
- Ultrasonic input-output for transmitting and receiving longitudinal transducers coupled to same face of isotropic elastic plate
[NASA-CR-3506] p 54 N82-18613
- ISOTROPY**
- Constitutive model development for isotropic materials
p 10 N85-10975
- ITERATIVE SOLUTION**
- Iterative methods for mixed finite element equations
p 82 A86-34461
- Augmented weak forms and element-by-element preconditioners: Efficient iterative strategies for structural finite elements. A preliminary study
p 106 N85-10384
- Integrated research in constitutive modelling at elevated temperatures, part 2
[NASA-CR-177233] p 119 N86-28455

J

- J INTEGRAL**
- Crack displacements for J/I/ testing with compact specimens
p 66 A82-40358
- Crack tip field and fatigue crack growth in general yielding and low cycle fatigue
[NASA-CR-174686] p 41 N84-32503
- Translational and extensional energy release rates (the J- and M-integrals) for a crack layer in thermoelasticity
[NASA-CR-174872] p 107 N85-21685
- A review of path-independent integrals in elastic-plastic fracture mechanics, task 4
[NASA-CR-174956] p 114 N85-33541
- Closure of fatigue cracks at high strains
[NASA-CR-175021] p 116 N86-17788
- J-integral estimates for cracks in infinite bodies
[NASA-CR-179474] p 119 N86-28467
- JET ENGINES**
- Composite containment systems for jet engine fan blades
[NASA-TM-81675] p 90 N81-17480
- Sensor failure detection for jet engines
[NASA-CR-168190] p 56 N83-33182
- Component-specific modeling
[NASA-CR-174765] p 12 N85-34140
- JOINTS (ANATOMY)**
- Ion beam sputter etching of orthopedic implanted alloy MP35N and resulting effects on fatigue
[NASA-TM-81747] p 38 N81-21174
- JOINTS (JUNCTIONS)**
- Fracture of composite-adhesive-composite systems
p 76 A85-27935
- Improved stud configurations for attaching laminated wood wind turbine blades
[NASA-TM-87109] p 115 N86-10582
- The 20th Aerospace Mechanics Symposium
[NASA-CP-2423-REV] p 121 N87-16321
- Identification of structural interface characteristics using component mode synthesis
[NASA-TM-88960] p 123 N87-24006
- JOURNAL BEARINGS**
- A pad perturbation method for the dynamic coefficients of tilting-pad journal bearings
p 47 A82-14400

- Vapor cavitation in dynamically loaded journal bearings
[NASA-TM-83366] p 97 N83-24875

K

- KALMAN FILTERS**
- Sensor failure detection for jet engines
[NASA-CR-168190] p 56 N83-33182
- KINEMATICS**
- Time-independent anisotropic plastic behavior by mechanical subelement models
p 99 N83-34369
- Advanced stress analysis methods applicable to turbine engine structures
[NASA-CR-175573] p 11 N85-21165
- On Hybrid and mixed finite element methods
[NASA-CR-175551] p 108 N85-23096
- Dynamic creep buckling: Analysis of shell structures subjected to time-dependent mechanical and thermal loading
p 111 N85-27959
- Analysis of large, non-isothermal elastic-visco-plastic deformations
[NASA-CR-176220] p 115 N86-10588
- Formulation of the nonlinear analysis of shell-like structures, subjected to time-dependent mechanical and thermal loading
[NASA-CR-177194] p 119 N86-28462
- KINETICS**
- Dynamic creep buckling: Analysis of shell structures subjected to time-dependent mechanical and thermal loading
p 111 N85-27959
- Formulation of the nonlinear analysis of shell-like structures, subjected to time-dependent mechanical and thermal loading
[NASA-CR-177194] p 119 N86-28462

L

- LABORATORIES**
- Lewis' enhanced laboratory for research into the fatigue and constitutive behavior of high temperature materials
p 125 N88-11177
- LAGRANGE MULTIPLIERS**
- Finite elements based on consistently assumed stresses and displacements
p 79 A86-18123
- Recent advances in hybrid/mixed finite elements
[NASA-CR-175574] p 107 N85-21687
- LAGUERRE FUNCTIONS**
- Geometrically nonlinear analysis of layered composite plates and shells
[NASA-CR-168182] p 98 N83-33219
- LAMINATES**
- Mechanical property characterization of intraply hybrid composites
p 13 A80-20954
- Dynamic response of damaged angleply fiber composites
p 14 A80-27982
- Fracture modes of high modulus graphite/epoxy angleply laminates subjected to off-axis tensile loads
p 14 A80-32069
- Nonlinear laminate analysis for metal matrix fiber composites
[AIAA 81-0579] p 15 A81-29411
- Boundary-layer effects in composite laminates. I - Free-edge stress singularities. II - Free-edge stress solutions and basic characteristics
p 67 A82-46806
- Moving cracks in layered composites
p 67 A83-12048
- Geometrically nonlinear analysis of layered composite shells
p 68 A83-27431
- Three-dimensional finite-element analysis of layered composite plates
p 68 A83-27432
- Wave propagation in a graphite/epoxy laminate
p 70 A83-44050
- Indentation law for composite laminates
p 16 A84-27356
- Compressive behavior of unidirectional fibrous composites
p 16 A84-29894
- Elasticity solutions for a class of composite laminate problems with stress singularities
p 17 A84-33389
- A mixed shear flexible finite element for the analysis of laminated plates
p 73 A84-45994
- Interply layer degradation effects on composite structural response
[AIAA PAPER 84-0849] p 18 A85-16096
- Use of static indentation laws in the impact analysis of laminated composite plates
p 18 A85-29133
- A study of interply layer effects on the free edge stress field of angleply laminates
p 18 A85-41127
- Fiberglass epoxy laminate fatigue properties at 300 and 20 K
p 19 A85-47970
- Three-dimensional hybrid-stress finite element analysis of composite laminates with cracks and cutouts
p 80 A86-26896

- Progressive fracture of fiber composites p 19 A86-35809
- Dynamic delamination crack propagation in a graphite/epoxy laminate p 20 A86-43010
- Design concepts/parameters assessment and sensitivity analyses of select composite structural components p 85 A87-25407
- A higher order theory of laminated composite cylindrical shells p 86 A87-35656
- Micromechanics of intraply hybrid composites: Elastic and thermal properties [NASA-TM-79253] p 21 N80-11143
- Dynamic response of damaged angleplied fiber composites [NASA-TM-79281] p 21 N80-11145
- Fracture modes of high modulus graphite/epoxy angleplied laminates subjected to off-axis tensile loads [NASA-TM-81405] p 21 N80-16102
- Sudden bending of cracked laminates [NASA-CR-159860] p 23 N80-25384
- Laminates and reinforced metals [NASA-TM-81591] p 23 N81-12171
- Method for alleviating thermal stress damage in laminates --- metal matrix composites [NASA-CASE-LEW-12493-1] p 23 N81-17170
- Nonlinear laminate analysis for metal matrix fiber composites [NASA-TM-82596] p 24 N81-25149
- Method for alleviating thermal stress damage in laminates [NASA-CASE-LEW-12493-2] p 24 N81-26179
- Dynamic responses of graphite/epoxy laminated beam to impact of elastic spheres [NASA-CR-165461] p 25 N83-13173
- Wave propagation in graphite/epoxy laminates due to impact [NASA-CR-168057] p 26 N83-22325
- A study of the stress wave factor technique for the characterization of composite materials [NASA-CR-3670] p 55 N83-27248
- Interply layer degradation effects on composite structural response [NASA-TM-83702] p 27 N84-26756
- Thermal-stress analysis for wood composite blade --- horizontal axis wind turbines [NASA-CR-173830] p 104 N84-31685
- Nonlinear Structural Analysis [NASA-CP-2297] p 105 N84-31688
- Nonlinear analysis for high-temperature composites: Turbine blades/vanes p 106 N84-31699
- Fracture modes in notched angleplied composite laminates [NASA-TM-83802] p 28 N84-34576
- A study of interply layer effects on the free-edge stress field of angleplied laminates [NASA-TM-86924] p 28 N85-15822
- Design procedures for fiber composite structural components: Panels subjected to combined in-plane loads [NASA-TM-86909] p 29 N85-15823
- Ultrasonic evaluation of mechanical properties of thick, multilayered, filament wound composites [NASA-TM-87088] p 58 N86-10561
- Fracture characteristics of angleplied laminates fabricated from overaged graphite/epoxy prepreg [NASA-TM-87266] p 30 N86-25417
- Computational simulation of progressive fracture in fiber composites [NASA-TM-87341] p 30 N86-26376
- Ultrasonic stress wave characterization of composite materials [NASA-CR-3976] p 60 N86-27665
- Fiber composite sandwich thermostructural behavior: Computational simulation [NASA-TM-88787] p 31 N86-31663
- ICAN: A versatile code for predicting composite properties [NASA-TM-87334] p 31 N86-31664
- Composite interlaminar fracture toughness: Three-dimensional finite element modeling for mixed mode 1, 2 and 3 fracture [NASA-TM-88872] p 31 N87-13491
- LAP JOINTS**
- Interface cracks in adhesively bounded lap-shear joints p 67 A82-46109
- Analysis of interface cracks in adhesively bonded lap shear joints, part 4 [NASA-CR-165438] p 93 N82-26716
- LAPLACE EQUATION**
- The finite analytic method, volume 3 [NASA-CR-170186] p 127 N83-23087
- LARGE SPACE STRUCTURES**
- Frequency domain solutions to multi-degree-of-freedom, dry friction damped systems under periodic excitation p 83 A86-39485
- LASER INTERFEROMETRY**
- Extending the laser-specklegram technique to strain analysis of rotating components p 67 A83-12514
- A study of the stress wave factor technique for nondestructive evaluation of composite materials [NASA-CR-4002] p 60 N86-28445
- LASER MICROSCOPY**
- Quantitative flaw characterization with scanning laser acoustic microscopy p 52 A86-45150
- Quantitative void characterization in structural ceramics by use of scanning laser acoustic microscopy p 53 A87-51974
- Reliability of scanning laser acoustic microscopy for detecting internal voids in structural ceramics [NASA-TM-87222] p 59 N86-16599
- Factors that affect reliability of nondestructive detection of flaws in structural ceramics [NASA-TM-87348] p 61 N86-31912
- Quantitative void characterization in structural ceramics using scanning laser acoustic microscopy [NASA-TM-88797] p 61 N86-31913
- LAYERS**
- On stress analysis of a crack-layer [NASA-CR-174774] p 106 N84-34774
- LEAST SQUARES METHOD**
- Hierarchical implicit dynamic least-square solution algorithm p 80 A86-26689
- Constrained hierarchical least square nonlinear equation solvers --- for indefinite stiffness and large structural deformations p 83 A86-43774
- LIFE (DURABILITY)**
- Durability/life of fiber composites in hygrothermomechanical environments p 16 A84-27359
- Toward improved durability in advanced combustors and turbines - Progress in prediction of thermomechanical loads [ASME PAPER 86-GT-172] p 6 A86-48224
- Re-examination of cumulative fatigue damage analysis - An engineering perspective p 85 A87-22128
- Quantitative ultrasonic evaluation of engineering properties in metals, composites and ceramics [NASA-TM-81530] p 54 N80-26682
- Combustor liner durability analysis [NASA-CR-165250] p 7 N81-17079
- Durability/life of fiber composites in hygrothermomechanical environments [NASA-TM-82749] p 24 N82-14287
- Complexities of high temperature metal fatigue: Some steps toward understanding [NASA-TM-83507] p 101 N84-14541
- Engine cyclic durability by analysis and material testing [NASA-TM-83577] p 102 N84-18683
- Elevated temperature biaxial fatigue [NASA-CR-173473] p 103 N84-21905
- Turbine Engine Hot Section Technology (HOST) [NASA-TM-83022] p 9 N85-10951
- Nonlinear structural and life analyses of a turbine blade p 9 N85-10954
- Nonlinear structural and life analyses of a combustor liner p 9 N85-10955
- Constitutive model development for isotropic materials p 10 N85-10975
- Reliability considerations for the total strain range version of strainrange partitioning [NASA-CR-174757] p 106 N85-11380
- Engine cyclic durability by analysis and material testing p 11 N85-15744
- Reexamination of cumulative fatigue damage laws p 112 N85-27962
- Nonlinear damage analysis: Postulate and evaluation [NASA-CR-168171] p 118 N86-26652
- Re-examination of cumulative fatigue damage analysis: An engineering perspective [NASA-TM-87325] p 118 N86-27680
- Structural analysis of turbine blades using unified constitutive models [NASA-TM-88807] p 119 N86-28461
- Turbine Engine Hot Section Technology, 1984 [NASA-CP-2339] p 120 N87-11180
- Fatigue and fracture: Overview p 120 N87-11183
- High temperature stress-strain analysis p 120 N87-11209
- Selection of rolling-element bearing steels for long-life application [NASA-TM-88881] p 49 N87-11993
- Effect of design variables, temperature gradients and speed of life and reliability of a rotating disk [NASA-TM-88883] p 49 N87-13755
- Environmental degradation of 316 stainless steel in high temperature low cycle fatigue [NASA-TM-89931] p 124 N87-24007
- Toward improved durability in advanced combustors and turbines: Progress in the prediction of thermomechanical loads [NASA-TM-88932] p 13 N87-28551
- Exposure time considerations in high temperature low cycle fatigue [NASA-TM-88934] p 125 N87-28944
- Lewis' enhanced laboratory for research into the fatigue and constitutive behavior of high temperature materials p 125 N88-11177
- LIFT**
- A comparative study of some dynamic stall models [NASA-TM-88917] p 122 N87-18883
- LINEAR SYSTEMS**
- Effects of a high mean stress on the high cycle fatigue life of PWA 1480 and correlation of data by linear elastic fracture mechanics [NASA-CR-175057] p 118 N86-27689
- LINEAR VIBRATION**
- Oscillator response to nonstationary excitation [ASME PAPER 84-WA/APM-38] p 75 A85-17039
- LINEARITY**
- Sensor failure detection for jet engines [NASA-CR-168190] p 56 N83-33182
- Theoretical and software considerations for nonlinear dynamic analysis [NASA-CR-174504] p 101 N84-15589
- LININGS**
- Nonlinear structural and life analyses of a combustor liner p 68 A83-12764
- Combustor liner durability analysis [NASA-CR-165250] p 7 N81-17079
- Nonlinear structural and life analyses of a combustor liner [NASA-TM-82846] p 92 N82-24501
- Nonlinear constitutive theory for turbine engine structural analysis p 95 N82-33744
- Experimental verification of the Neuber relation at room and elevated temperatures --- to predict stress-strain behavior in notched specimens of hastelloy x [NASA-CR-167967] p 96 N83-19121
- Nonlinear structural and life analyses of a combustor liner p 9 N85-10955
- Validation of structural analysis methods using the in-house liner cyclic rigs p 10 N85-10987
- HOST liner cyclic facilities: Facility description p 10 N85-10988
- Component-specific modeling p 12 N86-11515
- Burner liner thermal-structural load modeling [NASA-CR-174892] p 117 N86-21932
- Turbine Engine Hot Section Technology, 1984 [NASA-CP-2339] p 120 N87-11180
- High temperature stress-strain analysis p 120 N87-11209
- Turbine Engine Hot Section Technology, 1985 [NASA-CP-2405] p 125 N88-11140
- LIQUID OXYGEN**
- Self-acting geometry for noncontact seals [ASLE PREPRINT 81-AM-5B-2] p 47 A81-33867
- LOAD DISTRIBUTION (FORCES)**
- Continuous analysis of stresses from arbitrary surface loads on a half space p 64 A81-14162
- Extension of constrained incremental Newton-Raphson scheme to generalized loading fields p 74 A85-13942
- A study of spectrum fatigue crack propagation in two aluminum alloys. I - Spectrum simplification. II - Influence of microstructures p 36 A86-48973
- LOAD TESTS**
- Indentation law for composite laminates p 16 A84-27356
- Use of static indentation laws in the impact analysis of laminated composite plates p 18 A85-29133
- Longitudinal compressive failure modes in fiber composites End attachment effects on IITRI type test specimens p 19 A86-19999
- Shear fatigue crack growth - A literature survey p 80 A86-24219
- Comparison tests and experimental compliance calibration of the proposed standard round compact plane strain fracture toughness specimen [NASA-TM-81379] p 87 N80-13513
- Fracture modes of high modulus graphite/epoxy angleplied laminates subjected to off-axis tensile loads [NASA-TM-81405] p 21 N80-16102
- The method of lines in three dimensional fracture mechanics [NASA-TM-81593] p 89 N80-32753
- Mechanical behavior of carbon-carbon composites [NASA-CR-174767] p 28 N84-34575
- A study of spectrum fatigue crack propagation in two aluminum alloys. 1: Spectrum simplification [NASA-TM-86929] p 41 N85-18124
- A study of spectrum fatigue crack propagation in two aluminum alloys. 2: Influence of microstructures [NASA-TM-86930] p 41 N85-18125

Composite loads spectra for select space propulsion structural components p 110 N85-27953

LOADING RATE

Experimental compliance calibration of the compact fracture toughness specimen
[NASA-TM-81665] p 89 N81-16492

LOADS (FORCES)

Moving cracks in layered composites p 67 A83-12048
Simplified composite micromechanics for predicting microstresses p 20 A87-20090
Fracture toughness of Si₃N₄ measured with short bar chevron-notched specimens p 46 A87-30621
Method for estimating crack-extension resistance curve from residual strength data

[NASA-TP-1753] p 89 N81-11417
Time-independent anisotropic plastic behavior by mechanical subelement models p 99 N83-34369
Evaluation of the effect of crack closure on fatigue crack growth of simulated short cracks

[NASA-TM-83778] p 40 N84-31348
Structural analysis p 9 N85-10969
Some advances in experimentation supporting development of viscoplastic constitutive models
[NASA-CR-174855] p 109 N85-27260
Composite loads spectra for select space propulsion structural components: Probabilistic load model development p 110 N85-27954

Dynamic creep buckling: Analysis of shell structures subjected to time-dependent mechanical and thermal loading p 111 N85-27959

A study of the stress wave factor technique for the characterization of composite materials
[NASA-CR-174870] p 29 N85-30035
Some advances in experimentation supporting development of viscoplastic constitutive models

p 113 N85-31545
A comparison of smooth specimen and analytical simulation techniques for notched members at elevated temperatures p 114 N85-31546

Fractured toughness of Si₃N₄ measured with short bar chevron-notched specimens p 47 N86-13495

Burner liner thermal-structural load modeling
[NASA-CR-174892] p 117 N86-21932
Simplified composite micromechanics for predicting microstresses

[NASA-TM-87295] p 30 N86-24759
Integrated research in constitutive modelling at elevated temperatures, part 2
[NASA-CR-177233] p 119 N86-28455

Fatigue damage interaction behavior of PWA 1480 p 45 N87-22777

SINDA-NASTRAN interfacing program theoretical description and user's manual
[NASA-TM-100158] p 124 N87-27268

LONG TERM EFFECTS

A total life prediction model for stress concentration sites
[NASA-CR-170290] p 96 N83-23629

LOUVERS

Pre-HOST high temperature crack propagation p 9 N85-10956

LOW SPEED

Temperature distribution in an aircraft tire at low ground speeds
[NASA-TP-2195] p 97 N83-33217

LOW TEMPERATURE TESTS

Fiberglass epoxy laminate fatigue properties at 300 and 20 K p 19 A85-47970
Effect of low temperature on fatigue and fracture properties of Ti-5Al-2.5Sn(ELI) for use in engine components p 35 A85-47972

LUBRICATION

Lubricant effects on bearing life
[NASA-TM-88875] p 49 N87-15467

M**MAGNESIUM**

Select fiber composites for space applications - A mechanistic assessment p 18 A85-16040

Select fiber composites for space applications: A mechanistic assessment
[NASA-TM-83631] p 26 N84-22702

MANIPULATORS

The 20th Aerospace Mechanics Symposium
[NASA-CP-2423-REV] p 121 N87-16321

MASS DISTRIBUTION

Mass balancing of hollow fan blades
[ASME PAPER 86-GT-195] p 84 A86-48245
Concentrated mass effects on the flutter of a composite advanced turboprop model
[NASA-TM-88854] p 120 N87-12017

MATERIALS

Development of a simplified analytical method for representing material cyclic response
[NASA-CR-168100] p 96 N83-21390

MATERIALS TESTS

A review of issues and strategies in nondestructive evaluation of fiber reinforced structural composites p 14 A80-34764

Concepts and techniques for ultrasonic evaluation of material mechanical properties p 50 A80-51575
Ultrasonic measurement of material properties p 50 A81-19656

Factors influencing the ultrasonic stress wave factor evaluation of composite material structures p 81 A86-34257

MATHEMATICAL MODELS

Constitutive modeling and computational implementation for finite strain plasticity p 78 A85-40910

Analytical and experimental investigation of mistuning in propfan flutter
[AIAA PAPER 87-0739] p 86 A87-40496

Analytical flutter investigation of a composite propfan model
[AIAA PAPER 87-0738] p 87 A87-40497

Modelling of crack tip deformation with finite element method and its applications p 87 N80-13503
Statistical aspects of carbon fiber risk assessment modeling --- fire accidents involving aircraft

[NASA-CR-159318] p 23 N80-29432
Combustor liner durability analysis
[NASA-CR-165250] p 7 N81-17079

Integrated analysis of engine structures
[NASA-TM-82713] p 91 N82-11491

Finite-element modeling of layered, anisotropic composite plates and shells: A review of recent research p 91 N82-19563

Evaluation of inelastic constitutive models for nonlinear structural analysis p 98 N83-34357

Analysis of shell type structures subjected to time dependent mechanical and thermal loading
[NASA-CR-175747] p 109 N85-25896

Composite loads spectra for select space propulsion structural components: Probabilistic load model development p 110 N85-27954

Numerical considerations in the development and implementation of constitutive models p 113 N85-31541

On numerical integration and computer implementation of viscoplastic models p 113 N85-31542

A continuous damage model based on stepwise-stress creep rupture tests
[NASA-CR-174941] p 114 N85-32341

Component-specific modeling
[NASA-CR-174765] p 12 N85-34140

Component-specific modeling p 12 N86-11515
A unique set of micromechanics equations for high temperature metal matrix composites

[NASA-TM-87154] p 30 N86-24757
Yielding and deformation behavior of the single crystal nickel-base superalloy PWA 1480

[NASA-CR-175100] p 44 N86-25455
Concepts for interrelating ultrasonic attenuation, microstructure and fracture toughness in polycrystalline solids

[NASA-TM-87339] p 60 N86-25812
Integrated research in constitutive modelling at elevated temperatures, part 2

[NASA-CR-177233] p 119 N86-28455
Formulation of the nonlinear analysis of shell-like structures, subjected to time-dependent mechanical and thermal loading

[NASA-CR-177194] p 119 N86-28462
Integrated research in constitutive modelling at elevated temperatures, part 1

[NASA-CR-177237] p 120 N86-30227
Turbine Engine Hot Section Technology, 1984

[NASA-CP-2339] p 120 N87-11180
Fatigue and fracture: Overview p 120 N87-11183

Analytical flutter investigation of a composite propfan model
[NASA-TM-88944] p 122 N87-18115

Analytical and experimental investigation of mistuning in propfan flutter
[NASA-TM-88959] p 122 N87-18116

A comparative study of some dynamic stall models
[NASA-TM-88917] p 122 N87-18883
Turbine Engine Hot Section Technology, 1985

[NASA-CP-2405] p 125 N88-11140
Creep life prediction based on stochastic model of microstructurally short crack growth
[NASA-TM-100245] p 125 N88-12825

MATHEMATICAL PROGRAMMING

Structural optimization using optimality criteria methods p 79 A85-48703

MATRICES (MATHEMATICS)

Time-independent anisotropic plastic behavior by mechanical subelement models p 99 N83-34369

Element-by-element solution procedures for nonlinear structural analysis p 105 N84-31694
Automatic finite element generators p 105 N84-31695

MATRIX MATERIALS

On composites with periodic structure p 67 A83-10283
Resin selection criteria for tough composite structures

[AIAA 83-0801] p 46 A83-29734
Nonlinear laminate analysis for metal matrix fiber composites

[NASA-TM-82596] p 24 N81-25149
Computer code for intraply hybrid composite design
[NASA-TM-82593] p 24 N81-25151

MATRIX METHODS

Analysis of hourglass instabilities and control in underintegrated finite element methods p 74 A85-11125

Micromechanically based constitutive relations for polycrystalline solids p 99 N83-34359

MECHANICAL DRIVES

Application of traction drives as servo mechanisms p 114 N85-33520
Evaluation of a high-torque backlash-free roller actuator p 49 N87-16336

MECHANICAL MEASUREMENT

Mechanical behavior of carbon-carbon composites
[NASA-CR-174767] p 28 N84-34575

MECHANICAL OSCILLATORS

Oscillator response to nonstationary excitation
[ASME PAPER 84-WA/APM-38] p 75 A85-17039

MECHANICAL PROPERTIES

Mechanical property characterization of intraply hybrid composites p 13 A80-20954
A review of issues and strategies in nondestructive evaluation of fiber reinforced structural composites

p 14 A80-34764
Engine environmental effects on composite behavior --- moisture and temperature effects on mechanical properties

[AIAA 80-0695] p 1 A80-35101
Concepts and techniques for ultrasonic evaluation of material mechanical properties p 50 A80-51575

Computer code for intraply hybrid composite design p 15 A81-44662
Environmental and high strain rate effects on composites for engine applications p 16 A84-17444

Simplified composite micromechanics equations of hygral, thermal, and mechanical properties p 17 A84-49377

ICAN - Integrated composites analyzer
[AIAA PAPER 84-0974] p 18 A85-16094

Quasi-static solution algorithms for kinematically/materially nonlinear thermomechanical problems p 78 A85-41983

Composite sandwich thermostructural behavior - Computational simulation
[AIAA PAPER 86-0948] p 82 A86-38842

Orientation and temperature dependence of some mechanical properties of the single-crystal nickel-base superalloy Rene N4. II - Low cycle fatigue behavior p 37 A86-50322

Correlation of processing and sintering variables with the strength and radiography of silicon nitride p 46 A87-12938

Composite space antenna structures - Properties and environmental effects p 20 A87-38610

Mechanical property characterization of intraply hybrid composites p 21 N80-12120

Concepts and techniques for ultrasonic evaluation of material mechanical properties
[NASA-TM-81523] p 53 N80-24634

Quantitative ultrasonic evaluation of engineering properties in metals, composites and ceramics
[NASA-TM-81530] p 54 N80-26682

Computer code for intraply hybrid composite design
[NASA-TM-82593] p 24 N81-25151

Simplified composite micromechanics equations for hygral, thermal and mechanical properties
[NASA-TM-83320] p 26 N83-19817

A study of the stress wave factor technique for the characterization of composite materials
[NASA-CR-3670] p 55 N83-27248

Micromechanically based constitutive relations for polycrystalline solids p 99 N83-34359

ICAN: Integrated composites analyzer
[NASA-TM-83700] p 27 N84-26755

Ultrasonic nondestructive evaluation, microstructure, and mechanical property interrelations
[NASA-TM-86876] p 57 N85-10371

- Ultrasonic evaluation of mechanical properties of thick, multilayered, filament wound composites
[NASA-TM-87088] p 58 N86-10561
- Formulation of the nonlinear analysis of shell-like structures, subjected to time-dependent mechanical and thermal loading
[NASA-CR-177194] p 119 N86-28462
- ICAN: A versatile code for predicting composite properties
[NASA-TM-87334] p 31 N86-31664
- Acousto-ultrasonic verification of the strength of filament wound composite material
[NASA-TM-88827] p 61 N86-32764
- Composite space antenna structures: Properties and environmental effects
[NASA-TM-88859] p 31 N87-16880
- MESH**
- Fatigue failure of regenerator screens in a high frequency Stirling engine
[NASA-TM-88974] p 122 N87-18882
- METAL COATINGS**
- The low cycle fatigue behavior of a plasma-sprayed coating material
[NASA-TM-87318] p 44 N86-31699
- METAL FATIGUE**
- Strainrange partitioning life predictions of the long time Metal Properties Council creep-fatigue tests
p 63 A80-27958
- Effects of fine porosity on the fatigue behavior of a powder metallurgy superalloy
p 32 A80-35495
- Comparative thermal fatigue resistance of several oxide dispersion strengthened alloys
p 32 A82-11399
- Fatigue and creep-fatigue deformation of several nickel-base superalloys at 650 C
p 32 A82-47398
- Fatigue behavior of SiC reinforced Ti/6Al-4V/ at 650 C
p 15 A83-12414
- Metallurgical instabilities during the high temperature low cycle fatigue of nickel-base superalloys
p 33 A83-22019
- The effect of microstructure on the fatigue behavior of Ni base superalloys
p 33 A83-36166
- High-temperature fatigue in metals - A brief review of life prediction methods developed at the Lewis Research Center of NASA
p 33 A84-14286
- The effects of frequency and hold times on fatigue crack propagation rates in a nickel base superalloy
p 34 A84-18733
- Strainrange partitioning - A total strain range version --- for creep fatigue life prediction by summing inelastic and elastic strain-range-life relations for two Ni base superalloys
p 34 A85-11603
- A history dependent damage model for low cycle fatigue
[ASME PAPER 84-PVP-112] p 75 A85-18795
- The effect of microstructure, temperature, and hold-time on low-cycle fatigue of As HIP P/M Rene 95
p 35 A85-32399
- The influence of hold times on LCF and FCG behavior in a P/M Ni-base superalloy --- Low Cycle Fatigue/Fatigue Crack Growth
p 35 A85-32400
- Effect of low temperature on fatigue and fracture properties of Ti-5Al-2.5Sn(ELI) for use in engine components
p 35 A85-47972
- Thermal-mechanical fatigue crack growth in Inconel X-750
p 35 A86-20982
- Shear fatigue crack growth - A literature survey
p 80 A86-24219
- Fracture mechanics applied to nonisothermal fatigue crack growth
p 36 A86-28951
- The tensile and fatigue deformation structures in a single crystal Ni-base superalloy
p 36 A86-35697
- Effects of fine porosity on the fatigue behavior of a powder metallurgy superalloy
[NASA-TM-81448] p 37 N80-21493
- Practical implementation of the double linear damage rule and damage curve approach for treating cumulative fatigue damage
[NASA-TM-81517] p 88 N80-23684
- Method for alleviating thermal stress damage in laminates
[NASA-CASE-LEW-12493-2] p 24 N81-26179
- Elevated temperature fatigue testing of metals
p 38 N82-13281
- Evaluation of inelastic constitutive models for nonlinear structural analysis --- for aircraft turbine engines
[NASA-TM-82845] p 92 N82-24502
- High temperature low cycle fatigue mechanisms for nickel base and a copper base alloy
[NASA-CR-3543] p 39 N82-26436
- Microstructural effects on the room and elevated temperature low cycle fatigue behavior of Waspaloy
[NASA-CR-165497] p 93 N82-26702
- Mechanisms of deformation and fracture in high temperature low cycle fatigue of Rene 80 and IN 100
[NASA-CR-165498] p 93 N82-26706
- Strainrange partitioning: A total strain range version
[NASA-TM-83023] p 39 N83-14246
- Statistical summaries of fatigue data for design purposes
[NASA-CR-3697] p 97 N83-29731
- Relation of cyclic loading pattern to microstructural fracture in creep fatigue
[NASA-TM-83473] p 98 N83-34349
- The thermal fatigue resistance of H-13 Die Steel for aluminum die casting dies
[NASA-TM-83331] p 39 N83-35103
- Fatigue crack growth and low cycle fatigue of two nickel base superalloys
[NASA-CR-174534] p 39 N84-10267
- Effect of crack curvature on stress intensity factors for ASTM standard compact tension specimens
[NASA-CR-168280] p 100 N84-11513
- Preliminary study of thermomechanical fatigue of polycrystalline MAR-M 200
[NASA-TP-2280] p 40 N84-17350
- Literature survey on oxidations and fatigue lives at elevated temperatures
[NASA-CR-174639] p 40 N84-20674
- Reliability considerations for the total strain range version of strainrange partitioning
[NASA-CR-174757] p 106 N85-11380
- Thermal-mechanical fatigue crack growth in Inconel X-750
[NASA-CR-174740] p 41 N85-15877
- A study of spectrum fatigue crack propagation in two aluminum alloys. 1: Spectrum simplification
[NASA-TM-86929] p 41 N85-18124
- A study of spectrum fatigue crack propagation in two aluminum alloys. 2: Influence of microstructures
[NASA-TM-86930] p 41 N85-18125
- Axial and torsional fatigue behavior of Waspaloy
[NASA-CR-175052] p 44 N86-25454
- Low-cycle thermal fatigue
[NASA-TM-87225] p 118 N86-26651
- The low cycle fatigue behavior of a plasma-sprayed coating material
[NASA-TM-87318] p 44 N86-31699
- Fatigue damage interaction behavior of PWA 1480
p 45 N87-22777
- Turbine Engine Hot Section Technology, 1985
[NASA-CP-2405] p 125 N88-11140
- METAL FIBERS**
- Low cycle fatigue behavior of aluminum/stainless steel composites
[AIAA 83-0806] p 16 A83-29886
- METAL FOILS**
- Metal honeycomb to porous wireform substrate diffusion bond evaluation
p 51 A83-39620
- Metal honeycomb to porous wireform substrate diffusion bond evaluation
[NASA-TM-82793] p 54 N82-18612
- METAL MATRIX COMPOSITES**
- Fatigue behavior of SiC reinforced titanium composites
p 13 A80-10036
- A review of issues and strategies in nondestructive evaluation of fiber reinforced structural composites
p 14 A80-34764
- Nonlinear laminate analysis for metal matrix fiber composites
[AIAA 81-0579] p 15 A81-29411
- Fatigue behavior of SiC reinforced Ti/6Al-4V/ at 650 C
p 15 A83-12414
- Low cycle fatigue behavior of aluminum/stainless steel composites
[AIAA 83-0806] p 16 A83-29886
- Thermal expansion behavior of graphite/glass and graphite/magnesium
p 21 A87-38615
- Tensile and flexural strength of non-graphitic superhybrid composites: Predictions and comparisons
[NASA-TM-79276] p 21 N80-11144
- Predicting the time-temperature dependent axial failure of B/A1 composites
[NASA-TM-81474] p 22 N80-21452
- Diffusion bonded boron/aluminum spar-shell fan blade
[NASA-CR-159571] p 23 N80-25382
- Superhybrid composite blade impact studies
[NASA-TM-81597] p 89 N81-11412
- Laminates and reinforced metals
[NASA-TM-81591] p 23 N81-12171
- Method for alleviating thermal stress damage in laminates --- metal matrix composites
[NASA-CASE-LEW-12493-1] p 23 N81-17170
- Method for alleviating thermal stress damage in laminates
[NASA-CASE-LEW-12493-2] p 24 N81-26179
- Analysis of crack propagation as an energy absorption mechanism in metal matrix composites
[NASA-CR-165051] p 24 N82-14288
- Tungsten fiber reinforced superalloy composite high temperature component design considerations
[NASA-TM-82811] p 25 N82-21259
- Nonlinear analysis for high-temperature composites: Turbine blades/vanes
p 106 N84-31699
- Nonlinear structural analysis for fiber-reinforced superalloy turbine blades
p 109 N85-26887
- Thermoviscoplastic nonlinear constitutive relationships for structural analysis of high temperature metal matrix composites
[NASA-TM-87291] p 30 N86-24756
- A unique set of micromechanics equations for high temperature metal matrix composites
[NASA-TM-87154] p 30 N86-24757
- METAL OXIDES**
- Comparative thermal fatigue resistance of several oxide dispersion strengthened alloys
p 32 A82-11399
- METAL PLATES**
- The plastic compressibility of 7075-T651 aluminum-alloy plate
p 36 A86-49690
- METAL SHEETS**
- On the equivalence between semiempirical fracture analyses and R-curves
p 64 A81-18792
- METAL SHELLS**
- Dynamic creep buckling: Analysis of shell structures subjected to time-dependent mechanical and thermal loading
p 111 N85-27959
- METAL SURFACES**
- A constitutive law for finite element contact problems with unclassical friction
[NASA-TM-88838] p 120 N87-12924
- METAL WORKING**
- Thermomechanical deformation in the presence of metallurgical changes
p 112 N85-31533
- METALLOGRAPHY**
- Microstructural effects on the room and elevated temperature low cycle fatigue behavior of Waspaloy
[NASA-CR-165497] p 93 N82-26702
- Determination of grain size distribution function using two-dimensional Fourier transforms of tone pulse encoded images
[NASA-TM-88790] p 61 N86-31065
- METALS**
- An uncoupled viscoplastic constitutive model for metals at elevated temperature
[AIAA 83-1016] p 69 A83-29798
- On the use of internal state variables in thermoviscoplastic constitutive equations
p 113 N85-31536
- On numerical integration and computer implementation of viscoplastic models
p 113 N85-31542
- Calculation of thermomechanical fatigue life based on isothermal behavior
[NASA-TM-88864] p 122 N87-20565
- MICROCRACKS**
- Simplified composite micromechanics for predicting microstresses
p 87 A87-49275
- Relation of cyclic loading pattern to microstructural fracture in creep fatigue
[NASA-TM-83473] p 98 N83-34349
- Fundamentals of microcrack nucleation mechanics
[NASA-CR-3851] p 57 N85-16195
- Closure of fatigue cracks at high strains
[NASA-CR-175021] p 116 N86-17788
- MICROFIBERS**
- Simplified composite micromechanics for predicting microstresses
p 20 A87-20090
- Simplified composite micromechanics for predicting microstresses
[NASA-TM-87295] p 30 N86-24759
- MICROMECHANICS**
- Simplified composite micromechanics equations for strength, fracture toughness and environmental effects
p 17 A84-1858
- Assessment of simplified composite micromechanics using three-dimensional finite-element analysis
p 20 A87-19121
- Simplified composite micromechanics for predicting microstresses
p 20 A87-20090
- Simplified composite micromechanics for predicting microstresses
p 87 A87-49275
- Simplified composite micromechanics equations for strength, fracture toughness and environmental effects
[NASA-TM-83696] p 27 N84-27832
- Application of finite element substructuring to composite micromechanics
[NASA-TM-83729] p 27 N84-31288
- A unique set of micromechanics equations for high temperature metal matrix composites
[NASA-TM-87154] p 30 N86-24757
- Simplified composite micromechanics for predicting microstresses
[NASA-TM-87295] p 30 N86-24759
- ICAN: A versatile code for predicting composite properties
[NASA-TM-87334] p 31 N86-31664
- MICROSTRUCTURE**
- Composites with periodic microstructure
p 15 A83-12734

The effect of microstructure on the fatigue behavior of Ni base superalloys p 33 A83-36166

The effect of microstructure on 650 C fatigue crack growth in P/M Astroloy p 33 A84-12395

Effects of processing and microstructure on the fatigue behaviour of the nickel-base superalloy Rene95 p 34 A84-48715

Simplified composite micromechanics equations of hygral, thermal, and mechanical properties p 17 A84-49377

The role of the reflection coefficient in precision measurement of ultrasonic attenuation p 51 A85-42151

Nondestructive characterization of structural ceramics p 46 A86-37141

Quantitative ultrasonic evaluation of engineering properties in metals, composites and ceramics [NASA-TM-81530] p 54 N80-26682

Computer code for intraply hybrid composite design [NASA-TM-82593] p 24 N81-25151

Ultrasonic velocity for estimating density of structural ceramics p 46 N82-14359

Interrelation of material microstructure, ultrasonic factors, and fracture toughness of two phase titanium alloy p 54 N82-20551

[NASA-TM-82810] p 54 N82-20551

Microstructural effects on the room and elevated temperature low cycle fatigue behavior of Waspaloy [NASA-CR-165497] p 93 N82-26702

Simplified composite micromechanics equations for hygral, thermal and mechanical properties [NASA-TM-83320] p 26 N83-19817

Relation of cyclic loading pattern to microstructural fracture in creep fatigue [NASA-TM-83473] p 98 N83-34349

Tensile and compressive constitutive response of 316 stainless steel at elevated temperatures p 98 N83-34353

The role of the reflection coefficient in precision measurement of ultrasonic attenuation [NASA-TM-83788] p 57 N84-32849

Fracture surface characteristics of notched angleplyed graphite/epoxy composites p 28 N84-33522

Ultrasonic nondestructive evaluation, microstructure, and mechanical property interrelations [NASA-TM-86876] p 57 N85-10371

Fundamentals of microcrack nucleation mechanics [NASA-CR-3851] p 57 N85-16195

A study of spectrum fatigue crack propagation in two aluminum alloys. 2: Influence of microstructures [NASA-TM-86930] p 41 N85-18125

Progressive damage, fracture predictions and post mortem correlations for fiber composites [NASA-TM-87101] p 29 N86-10290

Variables controlling fatigue crack growth of short cracks [NASA-TM-87208] p 43 N86-21661

Thermoviscoplastic nonlinear constitutive relationships for structural analysis of high temperature metal matrix composites [NASA-TM-87291] p 30 N86-24756

Concepts for interrelating ultrasonic attenuation, microstructure and fracture toughness in polycrystalline solids [NASA-TM-87339] p 60 N86-25812

Determination of grain size distribution function using two-dimensional Fourier transforms of tone pulse encoded images [NASA-TM-88790] p 61 N86-31065

Flaw imaging and ultrasonic techniques for characterizing sintered silicon carbide [NASA-TM-100177] p 63 N88-12106

MISSION PLANNING

Component-specific modeling [NASA-CR-174765] p 110 N85-27261

MODAL RESPONSE

Stagger angle dependence of inertial and elastic coupling in bladed disks p 72 A84-31903

Nastran level 16 theoretical manual updates for aeroelastic analysis of bladed discs [NASA-CR-159823] p 90 N81-19480

MODELS

Composite loads spectra for select space propulsion structural components p 110 N85-27953

Constitutive modeling for isotropic materials (HOST) [NASA-CR-174980] p 115 N86-10589

Experimental classical flutter results of a composite advanced turboprop model [NASA-TM-88792] p 119 N86-29271

MODULUS OF ELASTICITY

Compliance and stress intensity coefficients for short bar specimens with chevron notches p 64 A80-46032

On composites with periodic structure p 67 A83-10283

Composites with periodic microstructure p 15 A83-12734

Finite elastic-plastic deformation of polycrystalline metals p 34 A84-43872

Compliance matrices for cracked bodies [NASA-CR-179478] p 120 N86-30236

MOISTURE

Application of finite element substructuring to composite micromechanics [NASA-TM-83729] p 27 N84-31288

MOISTURE CONTENT

Engine environmental effects on composite behavior --- moisture and temperature effects on mechanical properties [AIAA 80-0695] p 1 A80-35101

MOMENTUM TRANSFER

The finite analytic method, volume 5 [NASA-CR-170188] p 127 N83-23089

MONTE CARLO METHOD

Creep life prediction based on stochastic model of microstructurally short crack growth [NASA-TM-100245] p 125 N88-12825

MULTIPATH TRANSMISSION

Ray propagation path analysis of acousto-ultrasonic signals in composites [NASA-TM-100148] p 62 N87-25589

N

NASA PROGRAMS

Status of NASA full-scale engine aeroelasticity research p 63 A80-35906

NASTRAN

On the automatic generation of FEM models for complex gears - A work-in-progress report p 47 A82-48243

NASTRAN forced vibration analysis of rotating cyclic structures [ASME PAPER 83-DET-20] p 72 A84-29103

Effect of time dependent flight loads on JT9D-7 performance deterioration [NASA-CR-159681] p 87 N80-10515

Aeroelastic and dynamic finite element analyses of a bladder shrouded disk [NASA-CR-159728] p 90 N81-19479

Nastran level 16 theoretical manual updates for aeroelastic analysis of bladed discs [NASA-CR-159823] p 90 N81-19480

NASTRAN level 16 user's manual updates for aeroelastic analysis of bladed discs [NASA-CR-159824] p 90 N81-19481

NASTRAN level 16 programmer's manual updates for aeroelastic analysis of bladed discs [NASA-CR-159825] p 90 N81-19482

Large displacements and stability analysis of nonlinear propeller structures [NASA-TM-82850] p 94 N82-31707

Large displacements and stability analysis of nonlinear propeller structures p 95 N83-12460

Finite element forced vibration analysis of rotating cyclic structures [NASA-CR-165430] p 101 N84-11515

NASTRAN documentation for flutter analysis of advanced turbopropellers [NASA-CR-167927] p 8 N84-15153

NASTRAN forced vibration analysis of rotating cyclic structures [NASA-CR-173821] p 104 N84-29252

Nonlinear displacement analysis of advanced propeller structures using NASTRAN [NASA-TM-83737] p 104 N84-31683

A NASTRAN primer for the analysis of rotating flexible blades [NASA-TM-89861] p 123 N87-21375

Hub flexibility effects on propfan vibration [NASA-TM-89900] p 124 N87-24722

Finite element analysis of flexible, rotating blades [NASA-TM-89906] p 124 N87-26385

SINDA-NASTRAN interfacing program theoretical description and user's manual [NASA-TM-100158] p 124 N87-27268

NAVIER-STOKES EQUATION

The finite analytic method, volume 3 [NASA-CR-170186] p 127 N83-23087

The finite analytic method, volume 4 [NASA-CR-170187] p 127 N83-23088

NEAR FIELDS

On stress field near a stationary crack tip [AD-A152863] p 76 A85-24532

NEWTON-RAPHSON METHOD

Formal convergence characteristics of elliptically constrained incremental Newton-Raphson algorithms p 126 A83-10273

On the solution of elastic-plastic static and dynamic postbuckling collapse of general structure p 67 A83-12746

Algorithms for elasto-plastic-creep postbuckling p 73 A84-38480

Extension of constrained incremental Newton-Raphson scheme to generalized loading fields p 74 A85-13942

On the development of hierarchical solution strategies for nonlinear finite element formulations p 126 A85-21979

On the equivalence of the incremental harmonic balance method and the harmonic balance-Newton Raphson method p 83 A86-40695

Locally bound constrained Newton-Raphson solution algorithms --- for modeling kinematic and material nonlinearity p 83 A86-43771

Self-adaptive solution strategies p 105 N84-31693

NICKEL

Low cycle fatigue behavior of conventionally cast MAR-M 200 at 1000 deg C [NASA-TM-83769] p 41 N84-33564

An update of the total-strain version of SRP [NASA-TP-2499] p 42 N86-12295

NICKEL ALLOYS

Comparative thermal fatigue resistance of several oxide dispersion strengthened alloys p 32 A82-11399

Fatigue and creep-fatigue deformation of several nickel-base superalloys at 650 C p 32 A82-47398

Requirements of constitutive models for two nickel-base superalloys p 33 A83-21071

Metallurgical instabilities during the high temperature low cycle fatigue of nickel-base superalloys p 33 A83-22019

The effect of microstructure on the fatigue behavior of Ni base superalloys p 33 A83-36166

Fatigue crack initiation and propagation in several nickel-base superalloys at 650 C p 33 A83-41199

The effects of frequency and hold times on fatigue crack propagation rates in a nickel base superalloy p 34 A84-18733

The influence of hold times on LCF and FCG behavior in a P/M Ni-base superalloy --- Low Cycle Fatigue/Fatigue Crack Growth p 35 A85-32400

On the fatigue crack propagation behavior of superalloys at intermediate temperatures p 35 A85-32434

Application of two creep fatigue life models for the prediction of elevated temperature crack initiation of a nickel base alloy [AIAA PAPER 85-1420] p 35 A85-43979

The tensile and fatigue deformation structures in a single crystal Ni-base superalloy p 36 A86-35697

The cyclic stress-strain behavior of a nickel-base superalloy at 650 C p 36 A86-45715

Orientation and temperature dependence of some mechanical properties of the single-crystal nickel-base superalloy Rene N4. II - Low cycle fatigue behavior p 37 A86-50322

Thermal fatigue and oxidation data for directionally solidified MAR-M 246 turbine blades [NASA-CR-159798] p 6 N80-21330

Thermal fatigue and oxidation data of oxide dispersion-strengthened alloys [NASA-CR-159842] p 37 N80-25415

Three dimensional finite-element elastic analysis of a thermally cycled double-edge wedge geometry specimen --- nickel alloy turbine parts [NASA-TM-80980] p 37 N80-26433

Evaluation of the cyclic behavior of aircraft turbine disk alloys, part 2 [NASA-CR-165123] p 38 N80-30482

Thermal fatigue and oxidation data of TAZ-8A and M22 alloys and variations [NASA-CR-165407] p 38 N82-10193

High temperature low cycle fatigue mechanisms for nickel base and a copper base alloy [NASA-CR-3543] p 39 N82-26436

Mechanisms of deformation and fracture in high temperature low cycle fatigue of Rene 80 and IN 100 [NASA-CR-165498] p 93 N82-26706

Creep-fatigue of low cobalt superalloys p 39 N83-11290

Relation of cyclic loading pattern to microstructural fracture in creep fatigue [NASA-TM-83473] p 98 N83-34349

Low strain, long life creep fatigue of AF2-1DA and INCO 718 [NASA-CR-167989] p 40 N84-10268

Literature survey on oxidations and fatigue lives at elevated temperatures [NASA-CR-174639] p 40 N84-20674

Low cycle fatigue of MAR-M 200 single crystals at 760 and 870 deg C [NASA-TM-86933] p 41 N85-19074

Fatigue crack propagation of nickel-base superalloys at 650 deg C [NASA-TM-87150] p 42 N86-12294

Simplified cyclic structural analyses of SSME turbine blades [NASA-TM-87214] p 116 N86-16615

- Anisotropic constitutive model for nickel base single crystal alloys: Development and finite element implementation
[NASA-CR-175015] p 117 N86-21952
- Yielding and deformation behavior of the single crystal nickel-base superalloy PWA 1480
[NASA-CR-175100] p 44 N86-25455
- Thermal-fatigue and oxidation resistance of cobalt-modified Udimet 700 alloy
[NASA-TP-2591] p 119 N86-28464
- The low cycle fatigue behavior of a plasma-sprayed coating material
[NASA-TM-87318] p 44 N86-31699
- Ultrasonic determination of recrystallization
[NASA-TM-88855] p 61 N87-10399
- Bithermal low-cycle fatigue behavior of a NiCoCrAlY-coated single crystal superalloy
[NASA-TM-89831] p 45 N87-20408
- Fatigue damage interaction behavior of PWA 1480
p 45 N87-22777
- NICKEL STEELS**
- Comparison tests and experimental compliance calibration of the proposed standard round compact plane strain fracture toughness specimen
[NASA-TM-81379] p 87 N80-13513
- NONDESTRUCTIVE TESTS**
- A review of issues and strategies in nondestructive evaluation of fiber reinforced structural composites
p 14 A80-34764
- Quantitative ultrasonic evaluation of engineering properties in metals, composites, and ceramics
p 50 A80-39641
- Concepts and techniques for ultrasonic evaluation of material mechanical properties
p 50 A80-51575
- Ultrasonic measurement of material properties
p 50 A81-19656
- Acousto-ultrasonic characterization of fiber reinforced composites
p 50 A81-44660
- Comparison of NDE techniques for sintered-SiC components
p 51 A83-22265
- Mechanics aspects of NDE by sound and ultrasound
p 51 A83-25571
- The determination of the elastodynamic fields of an ellipsoidal inhomogeneity
[ASME PAPER 83-APM-19] p 69 A83-37388
- Characterization of composite materials by means of the ultrasonic stress wave factor
p 16 A84-10430
- Measurement of ultrasonic velocity using phase-slope and cross-correlation methods
p 51 A86-13192
- NDE of advanced ceramics
p 52 A86-35575
- Nondestructive characterization of structural ceramics
p 46 A86-37141
- Reliability of void detection in structural ceramics by use of scanning laser acoustic microscopy
p 52 A86-39027
- Nondestructive techniques for characterizing mechanical properties of structural materials - An overview
[ASME PAPER 86-GT-75] p 52 A86-48143
- NDE of structural ceramics
[ASME PAPER 86-GT-279] p 52 A86-48298
- Nondestructive evaluation of adhesive bond strength using the stress wave factor technique
p 53 A87-32200
- Quantitative void characterization in structural ceramics by use of scanning laser acoustic microscopy
p 53 A87-51974
- Simulation of transducer-couplant effects on broadband ultrasonic signals
[NASA-TM-81489] p 53 N80-22714
- Concepts and techniques for ultrasonic evaluation of material mechanical properties
[NASA-TM-81523] p 53 N80-24634
- Quantitative ultrasonic evaluation of engineering properties in metals, composites and ceramics
[NASA-TM-81530] p 54 N80-26682
- Phenomenological and mechanics aspects of nondestructive evaluation and characterization by sound and ultrasound of material and fracture properties
[NASA-CR-3623] p 55 N83-11506
- Fundamental aspects in quantitative ultrasonic determination of fracture toughness: The scattering of a single ellipsoidal inhomogeneity
[NASA-CR-3625] p 55 N83-11507
- Effects of specimen resonances on acoustic-ultrasonic testing
[NASA-CR-3679] p 55 N83-21373
- Ultrasonic ranking of toughness of tungsten carbide
[NASA-TM-83358] p 55 N83-23620
- Mechanical behavior of carbon-carbon composites
[NASA-CR-174767] p 28 N84-34575
- Ultrasonic velocity measurement using phase-slope cross-correlation methods
[NASA-TM-83794] p 57 N84-34769

- Ultrasonic nondestructive evaluation, microstructure, and mechanical property interrelations
[NASA-TM-86876] p 57 N85-10371
- NDE for heat engine ceramics
[NASA-TM-86949] p 57 N85-20389
- Stress waves in an isotropic elastic plate excited by a circular transducer
[NASA-CR-3877] p 58 N85-20390
- Ultrasonic testing of plates containing edge cracks
[NASA-CR-3904] p 58 N85-29307
- A study of the stress wave factor technique for the characterization of composite materials
[NASA-CR-174870] p 29 N85-30035
- Reliability of void detection in structural ceramics using scanning laser acoustic microscopy
[NASA-TM-87035] p 58 N85-32337
- NDE of structural ceramics
[NASA-TM-87186] p 59 N86-16598
- Nondestructive techniques for characterizing mechanical properties of structural materials: An overview
[NASA-TM-87203] p 59 N86-19636
- Analytical Ultrasonics in Materials Research and Testing
[NASA-CP-2383] p 59 N86-22962
- Stress waves in transversely isotropic media: The homogeneous problem
[NASA-CR-3977] p 59 N86-25002
- Concepts for interrelating ultrasonic attenuation, microstructure and fracture toughness in polycrystalline solids
[NASA-TM-87339] p 60 N86-25812
- Ultrasonic stress wave characterization of composite materials
[NASA-CR-3976] p 60 N86-27665
- Wave propagation in anisotropic medium due to an oscillatory point source with application to unidirectional composites
[NASA-CR-4001] p 60 N86-27666
- A study of the stress wave factor technique for nondestructive evaluation of composite materials
[NASA-CR-4002] p 60 N86-28445
- Factors that affect reliability of nondestructive detection of flaws in structural ceramics
[NASA-TM-87348] p 61 N86-31912
- Quantitative void characterization in structural ceramics using scanning laser acoustic microscopy
[NASA-TM-88797] p 61 N86-31913
- Acousto-ultrasonic verification of the strength of filament wound composite material
[NASA-TM-88827] p 61 N86-32764
- Ultrasonic determination of recrystallization
[NASA-TM-88855] p 61 N87-10399
- Nondestructive evaluation of structural ceramics
[NASA-TM-88978] p 62 N87-18109
- The acousto-ultrasonic approach
[NASA-TM-89843] p 62 N87-20562
- Ray propagation path analysis of acousto-ultrasonic signals in composites
[NASA-TM-100148] p 62 N87-25589
- Ultrasonic NDE of structural ceramics for power and propulsion systems
[NASA-TM-100147] p 62 N87-26362
- Fracture mechanics concepts in reliability analysis of monolithic ceramics
[NASA-TM-100174] p 124 N87-27269
- Flaw imaging and ultrasonic techniques for characterizing sintered silicon carbide
[NASA-TM-100177] p 63 N88-12106
- NONISOTHERMAL PROCESSES**
- Thermodynamically consistent constitutive equations for nonisothermal large strain, elasto-plastic, creep behavior
[AIAA PAPER 85-0621] p 77 A85-38425
- Fracture mechanics applied to nonisothermal fatigue crack growth
p 36 A86-28951
- Thermomechanical deformation in the presence of metallurgical changes
p 112 N85-31533
- Analysis of large, non-isothermal elastic-visco-plastic deformations
[NASA-CR-176220] p 115 N86-10588
- NONLINEAR EQUATIONS**
- On the development of hierarchical solution strategies for nonlinear finite element formulations
p 126 A85-21979
- Constrained hierarchical least square nonlinear equation solvers --- for indefinite stiffness and large structural deformations
p 83 A86-43774
- Self-adaptive solution strategies
p 105 N84-31693
- Local strain redistribution corrections for a simplified inelastic analysis procedure based on an elastic finite-element analysis
[NASA-TP-2421] p 107 N85-20396
- Nonlinear flap-lag-extensional vibrations of rotating, pretwisted, precone beams including Coriolis effects
[NASA-TM-87102] p 115 N85-34427

NONLINEAR SYSTEMS

- Nonlinear structural and life analyses of a combustor liner
p 68 A83-12764
- Influence of third-degree geometric nonlinearities on the vibration and stability of pretwisted, precone, rotating blades
p 6 A87-46228
- Nonlinear structural and life analyses of a combustor liner
[NASA-TM-82846] p 92 N82-24501
- Large displacements and stability analysis of nonlinear propeller structures
p 95 N83-12460
- Nonlinear displacement analysis of advanced propeller structures using NASTRAN
[NASA-TM-83737] p 104 N84-31683
- Nonlinear Structural Analysis
[NASA-CP-2297] p 105 N84-31688
- Slave finite elements: The temporal element approach to nonlinear analysis
p 105 N84-31689
- Nonlinear finite element analysis of shells with large aspect ratio
p 105 N84-31692
- Element-by-element solution procedures for nonlinear structural analysis
p 105 N84-31694
- Nonlinear analysis for high-temperature composites: Turbine blades/vanes
p 106 N84-31699
- Constitutive modeling for isotropic materials (HOST)
[NASA-CR-174980] p 115 N86-10589
- Structural analysis of turbine blades using unified constitutive models
[NASA-TM-88807] p 119 N86-28461
- Influence of third-degree geometric nonlinearities on the vibration and stability of pretwisted, precone, rotating blades
[NASA-TM-87307] p 120 N86-31920
- The effect of nonlinearities on the dynamic response of a large shuttle payload
[NASA-TM-88941] p 121 N87-18112

NONLINEARITY

- A simplified method for elastic-plastic-creep structural analysis
[ASME PAPER 84-GT-191] p 76 A85-23150
- On local total strain redistribution using a simplified cyclic inelastic analysis based on an elastic solution
[AIAA PAPER 85-1419] p 78 A85-39770
- Bounding solutions of geometrically nonlinear viscoelastic problems
[AIAA PAPER 86-0943] p 82 A86-38838
- Nonlinear vibration and stability of rotating, pretwisted, precone blades including Coriolis effects
p 86 A87-39896
- Influence of third-degree geometric nonlinearities on the vibration and stability of pretwisted, precone, rotating blades
p 6 A87-46228
- Geometrically nonlinear analysis of layered composite plates and shells
[NASA-CR-168182] p 98 N83-33219
- A solution procedure for behavior of thick plates on a nonlinear foundation and postbuckling behavior of long plates
[NASA-TP-2174] p 99 N83-34373
- A simplified method for elastic-plastic-creep structural analysis
[NASA-TM-83509] p 101 N84-14542
- Theoretical and software considerations for nonlinear dynamic analysis
[NASA-CR-174504] p 101 N84-15589
- Development of a simplified procedure for cyclic structural analysis
[NASA-TP-2243] p 103 N84-20878
- A computer program for predicting nonlinear uniaxial material responses using viscoplastic models
[NASA-TM-83675] p 104 N84-29247
- Nonlinear analysis for high-temperature multilayered fiber composite structures --- turbine blades
[NASA-TM-83754] p 29 N85-21273
- On local total strain redistribution using a simplified cyclic inelastic analysis based on an elastic solution
[NASA-TM-86913] p 108 N85-21690
- Nonlinear Constitutive Relations for High Temperature Application, 1984
[NASA-CP-2369] p 112 N85-31530
- Analysis of large, non-isothermal elastic-visco-plastic deformations
[NASA-CR-176220] p 115 N86-10588
- Simplified cyclic structural analyses of SSME turbine blades
[NASA-TM-87214] p 116 N86-16615
- Nonlinear bending-torsional vibration and stability of rotating, pretwisted, precone blades including Coriolis effects
[NASA-TM-87207] p 116 N86-17789
- Integrated research in constitutive modelling at elevated temperatures, part 2
[NASA-CR-177233] p 119 N86-28455

- Influence of third-degree geometric nonlinearities on the vibration and stability of pretwisted, precone, rotating blades
[NASA-TM-87307] p 120 N86-31920
- NONSTABILIZED OSCILLATION**
Oscillator response to nonstationary excitation
[ASME PAPER 84-WA/APM-38] p 75 A85-17039
- NOTCH SENSITIVITY**
Fracture toughness of Si₃N₄ measured with short bar chevron-notched specimens p 46 A87-30621
Experimental verification of the Neuber relation at room and elevated temperatures --- to predict stress-strain behavior in notched specimens of hastelloy x
[NASA-CR-167967] p 96 N83-19121
Fractured toughness of Si₃N₄ measured with short bar chevron-notched specimens p 47 N86-13495
[NASA-TM-87153]
- NOTCH STRENGTH**
A preliminary study of crack initiation and growth at stress concentration sites
[NASA-CR-169358] p 94 N82-33738
Finite element analysis of notch behavior using a state variable constitutive equation p 114 N85-31548
Experimental evaluation criteria for constitutive models of time dependent cyclic plasticity
[NASA-CR-176821] p 117 N86-25850
- NOTCH TESTS**
Fracture toughness determination of Al₂O₃ using four-point-bend specimens with straight-through and chevron notches p 45 A80-42085
Compliance and stress intensity coefficients for short bar specimens with chevron notches p 64 A80-46032
Performance of Chevron-notch short bar specimen in determining the fracture toughness of silicon nitride and aluminum oxide p 45 A80-50696
Fracture toughness of brittle materials determined with chevron notch specimens p 45 A81-32545
Extended range stress intensity factor expressions for chevron-notched short bar and short rod fracture toughness specimens p 66 A82-40357
Benchmark cyclic plastic notch strain measurements p 33 A84-11194
Development of plane strain fracture toughness test for ceramics using Chevron notched specimens p 46 A84-11676
Mode II fatigue crack growth specimen development p 83 A86-43566
Fracture toughness of Si₃N₄ measured with short bar chevron-notched specimens p 46 A87-30621
Fracture toughness of brittle materials determined with chevron notch specimens p 38 N80-32486
[NASA-TM-81607]
Mode 2 fatigue crack growth specimen development [NASA-TM-83722] p 104 N84-29248
Fracture surface characteristics of notched angleplied graphite/epoxy composites p 28 N84-33522
[NASA-TM-83786]
Finite element analysis of notch behavior using a state variable constitutive equation p 114 N85-31548
Fractured toughness of Si₃N₄ measured with short bar chevron-notched specimens p 47 N86-13495
[NASA-TM-87153]
- NOTCHES**
Fracture modes in notched angleplied composite laminates
[NASA-TM-83802] p 28 N84-34576
- NUCLEATION**
Fundamentals of microcrack nucleation mechanics [NASA-CR-3851] p 57 N85-16195
Grain boundary oxidation and oxidation accelerated fatigue crack nucleation and propagation [NASA-CR-175050] p 43 N86-20542
- NUMERICAL ANALYSIS**
Boundary-layer effects in composite laminates: Free-edge stress singularities, part 6
[NASA-CR-165440] p 94 N82-26718
The finite analytic method, volume 3
[NASA-CR-170186] p 127 N83-23087
The finite analytic method, volume 4
[NASA-CR-170187] p 127 N83-23088
The finite analytic method, volume 5
[NASA-CR-170188] p 127 N83-23089
Nonlinear structural analysis for fiber-reinforced superalloy turbine blades p 109 N85-26887
- NUMERICAL INTEGRATION**
Analysis of hourglass instabilities and control in underintegrated finite element methods p 74 A85-11125
Integrated research in constitutive modelling at elevated temperatures, part 1
[NASA-CR-177237] p 120 N86-30227
- NUMERICAL STABILITY**
Formal convergence characteristics of elliptically constrained incremental Newton-Raphson algorithms p 126 A83-10273

- Comments on some problems in computational penetration mechanics p 71 A84-13545
Algorithms for elasto-plastic-creep postbuckling p 73 A84-38480
Analysis of hourglass instabilities and control in underintegrated finite element methods p 74 A85-11125
Extension of constrained incremental Newton-Raphson scheme to generalized loading fields p 74 A85-13942
Development and testing of stable, invariant, isoparametric curvilinear 2- and 3-D hybrid-stress elements p 75 A85-19899
Existence and stability, and discrete BB and rank conditions, for general mixed-hybrid finite elements in elasticity p 82 A86-34464
Locally bound constrained Newton-Raphson solution algorithms --- for modeling kinematic and material nonlinearity p 83 A86-43771

O

O RING SEALS

- Self-acting geometry for noncontact seals
[ASLE PREPRINT 81-AM-5B-2] p 47 A81-33867

OPERATING TEMPERATURE

- Turbine Engine Hot Section Technology (HOST)
[NASA-CP-2289] p 115 N86-11495

OPERATORS (MATHEMATICS)

- An embedding method for the steady Euler equations p 126 A86-30814

OPTICAL MEASUREMENT

- A study of the stress wave factor technique for nondestructive evaluation of composite materials
[NASA-CR-4002] p 60 N86-28445

OPTICAL MEASURING INSTRUMENTS

- A low-cost optical data acquisition system for vibration measurement
[NASA-TM-88907] p 121 N87-14730

OPTICAL PROPERTIES

- Measurements of self-excited rotor-blade vibrations using optical displacements
[ASME PAPER 83-GT-132] p 73 A84-33702
Measurements of self-excited rotor-blade vibrations using optical displacements
[NASA-TM-82953] p 95 N83-14523

OPTICS

- The use of an optical data acquisition system for bladed disk vibration analysis
[NASA-TM-86891] p 106 N85-15184

OPTIMIZATION

- Structural tailoring of engine blades (STAEBL)
[AIAA 83-0828] p 1 A84-29737
Optimization of cascade blade mistuning. I - Equations of motion and basic inherent properties p 3 A85-42365
Optimization of cascade blade mistuning. II - Global optimum and numerical optimization p 3 A85-45715
Structural optimization using optimality criteria methods p 79 A85-48703
Optimization and analysis of gas turbine engine blades [AIAA PAPER 87-0827] p 126 A87-33614
Structural tailoring of engine blades (STAEBL) theoretical manual
[NASA-CR-175112] p 12 N86-27283
Structural tailoring of engine blades (STAEBL) user's manual
[NASA-CR-175113] p 13 N86-27284
STAEBL: Structural tailoring of engine blades, phase 2 p 13 N87-11731

ORTHOPEDICS

- Ion beam sputter etching of orthopedic implanted alloy MP35N and resulting effects on fatigue
[NASA-TM-81747] p 38 N81-21174

ORTHOTROPIC PLATES

- A mixed shear flexible finite element for the analysis of laminated plates p 73 A84-45994

OSCILLATION DAMPERS

- Variable force, eddy-current or magnetic damper
[NASA-CASE-LEW-13717-1] p 49 N85-30333

OSCILLATORS

- Wave propagation in anisotropic medium due to an oscillatory point source with application to unidirectional composites
[NASA-CR-4001] p 60 N86-27666

OXIDATION

- Thermal fatigue and oxidation data for directionally solidified MAR-M 246 turbine blades
[NASA-CR-159798] p 6 N80-21330
Thermal fatigue and oxidation data of TAZ-8A and M22 alloys and variations
[NASA-CR-165407] p 38 N82-10193
Literature survey on oxidations and fatigue lives at elevated temperatures
[NASA-CR-174639] p 40 N84-20674

- Grain boundary oxidation and oxidation accelerated fatigue crack nucleation and propagation
[NASA-CR-175050] p 43 N86-20542
Low-cycle thermal fatigue
[NASA-TM-87225] p 118 N86-26651
Thermal-fatigue and oxidation resistance of cobalt-modified Udimet 700 alloy
[NASA-TP-2591] p 119 N86-28464

P

PAD

- A pad perturbation method for the dynamic coefficients of tilting-pad journal bearings p 47 A82-14400

PALMGREN-MINER RULE

- Re-examination of cumulative fatigue damage analysis - An engineering perspective p 85 A87-22128
Re-examination of cumulative fatigue damage analysis: An engineering perspective
[NASA-TM-87325] p 118 N86-27680

PANELS

- Design procedures for fiber composite structural components: Panels subjected to combined in-plane loads
[NASA-TM-86909] p 29 N85-15823

PARALLELEPIPEDS

- On the three-dimensional vibrations of the cantilevered rectangular parallelepiped p 70 A83-37729

PARAMETERIZATION

- Stress waves in an isotropic elastic plate excited by a circular transducer
[NASA-CR-3877] p 58 N85-20390

PARTIAL DIFFERENTIAL EQUATIONS

- The finite analytic method, volume 4
[NASA-CR-170187] p 127 N83-23088

PERFORMANCE PREDICTION

- Predicting the time-temperature dependent axial failure of B/AI composites p 14 A80-35494
Self-acting geometry for noncontact seals
[ASLE PREPRINT 81-AM-5B-2] p 47 A81-33867
Natural frequency of rotating beams using non-rotating modes p 68 A83-18383
Effect of time dependent flight loads on JT9D-7 performance deterioration
[NASA-CR-159681] p 87 N80-10515
Quantitative ultrasonic evaluation of engineering properties in metals, composites and ceramics
[NASA-TM-81530] p 54 N80-26682
Nonlinear constitutive theory for turbine engine structural analysis p 95 N82-33744
Experimental verification of the number relation at room and elevated temperatures p 98 N83-34355
High temperature stress-strain analysis p 120 N87-11209
[NASA-TM-88917] p 122 N87-18883

PERFORMANCE TESTS

- Acoustic emission evaluation of plasma-sprayed thermal barrier coatings
[ASME PAPER 84-GT-292] p 48 A84-47046
Development of procedures for calculating stiffness and damping of elastomers in engineering applications, part 6
[NASA-CR-159838] p 87 N80-22733
Lewis' enhanced laboratory for research into the fatigue and constitutive behavior of high temperature materials p 125 N88-11177

PERIODIC FUNCTIONS

- Some analysis methods for rotating systems with periodic coefficients p 69 A83-32987

PERIODIC VARIATIONS

- Composites with periodic microstructure p 15 A83-12734

PERTURBATION THEORY

- A pad perturbation method for the dynamic coefficients of tilting-pad journal bearings p 47 A82-14400

PHASE VELOCITY

- Stress waves in transversely isotropic media: The homogeneous problem
[NASA-CR-3977] p 59 N86-25002

PHOTOACOUSTIC MICROSCOPY

- NDE of structural ceramics
[ASME PAPER 86-GT-279] p 52 A86-48298
NDE of structural ceramics
[NASA-TM-87186] p 59 N86-16598

PHOTOACOUSTIC SPECTROSCOPY

- Comparison of NDE techniques for sintered-SiC components p 51 A83-22265

PHOTOELASTIC ANALYSIS

- Extending the laser-specklegram technique to strain analysis of rotating components p 67 A83-12514

PHOTOVOLTAIC CELLS

- Array structure design handbook for stand alone photovoltaic applications
[NASA-TM-82629] p 96 N83-23631

PHOTOVOLTAIC CONVERSION

Photovoltaic power system reliability considerations
[NASA-TM-79291] p 53 N80-15422

PLANE STRAIN

Moving singularity creep crack growth analysis with the $\Delta T/c$ and $C/\text{asterisk}$ integrals --- path-independent vector and energy rate line integrals p 66 A82-40066
Development of plane strain fracture toughness test for ceramics using Chevron notched specimens p 46 A84-11676

Fracture toughness of Si₃N₄ measured with short bar chevron-notched specimens p 46 A87-30621

Time-independent anisotropic plastic behavior by mechanical subelement models p 99 N83-34369

Fundamentals of microcrack nucleation mechanics [NASA-CR-3851] p 57 N85-16195

Fractured toughness of Si₃N₄ measured with short bar chevron-notched specimens [NASA-TM-87153] p 47 N86-13495

PLASMA SPRAYING

Acoustic emission evaluation of plasma-sprayed thermal barrier coatings [ASME PAPER 84-GT-292] p 48 A84-47046

Finite element analysis of residual stress in plasma-sprayed ceramic p 46 A86-15226

Creep-fatigue behavior of NiCoCrAlY coated PWA 1480 superalloy single crystals [NASA-TM-87110] p 42 N86-10311

The low cycle fatigue behavior of a plasma-sprayed coating material [NASA-TM-87318] p 44 N86-31699

PLASTIC BODIES

Dynamic fields near a crack tip growing in an elastic-perfectly-plastic solid p 70 A83-38528

Analyses of large quasistatic deformations of inelastic bodies by a new hybrid-stress finite element algorithm p 71 A84-16874

Analyses of large quasistatic deformations of inelastic bodies by a new hybrid-stress finite element algorithm - Applications p 71 A84-16884

Hybrid stress finite elements for large deformations of inelastic solids p 74 A85-15894

PLASTIC DEFORMATION

Benchmark cyclic plastic notch strain measurements p 33 A84-11194

Analyses of large quasistatic deformations of inelastic bodies by a new hybrid-stress finite element algorithm p 71 A84-16874

Analyses of large quasistatic deformations of inelastic bodies by a new hybrid-stress finite element algorithm - Applications p 71 A84-16884

Hybrid stress finite elements for large deformations of inelastic solids p 74 A85-15894

Shear fatigue crack growth - A literature survey p 80 A86-24219

Constitutive modeling of cyclic plasticity and creep, using an internal time concept p 83 A86-41673

Modelling of crack tip deformation with finite element method and its applications p 87 N80-13503

Experimental evaluation criteria for constitutive models of time dependent cyclic plasticity [NASA-CR-176821] p 117 N86-25850

Fatigue crack layer propagation in silicon-iron [NASA-CR-175115] p 118 N86-25851

PLASTIC PROPERTIES

The plastic compressibility of 7075-T651 aluminum-alloy plate p 36 A86-49690

Elastic-plastic finite-element analyses of thermally cycled double-edge wedge specimens [NASA-TP-1973] p 92 N82-20566

Constrained self-adaptive solutions procedures for structure subject to high temperature elastic-plastic creep effects p 99 N83-34370

Research and development program for the development of advanced time-temperature dependent constitutive relationships. Volume 2: Programming manual [NASA-CR-168191-VOL-2] p 100 N84-10614

Development of constitutive models for cyclic plasticity and creep behavior of super alloys at high temperature [NASA-CR-176418] p 43 N86-14356

Low-cycle thermal fatigue [NASA-TM-87225] p 118 N86-26651

PLATE THEORY

Alternative ways for formulation of hybrid stress elements p 68 A83-14710

A mixed shear flexible finite element for the analysis of laminated plates p 73 A84-45994

Hybrid Semiloof elements for plates and shells based upon a modified Hu-Washizu principle p 74 A85-15893

Vibrations of twisted cantilevered plates - Summary of previous and current studies p 76 A85-22069

Vibrations of twisted cantilever plates - A comparison of theoretical results p 79 A85-47626

Sudden stretching of a four layered composite plate [NASA-CR-159870] p 23 N80-25383

Sudden bending of cracked laminates [NASA-CR-159860] p 23 N80-25384

PLATES

Nonlinear finite element analysis of shells with large aspect ratio p 105 N84-31692

PLATES (STRUCTURAL MEMBERS)

Finite-element modeling of layered, anisotropic composite plates and shells: A review of recent research p 91 N82-19563

A solution procedure for behavior of thick plates on a nonlinear foundation and postbuckling behavior of long plates [NASA-TP-2174] p 99 N83-34373

Stress waves in an isotropic elastic plate excited by a circular transducer [NASA-CR-3877] p 58 N85-20390

Geometrically nonlinear analysis of laminated elastic structures [NASA-CR-175609] p 108 N85-21720

Ultrasonic testing of plates containing edge cracks [NASA-CR-3904] p 58 N85-29307

PLY ORIENTATION

Progressive fracture of fiber composites p 19 A86-35809

Design concepts/parameters assessment and sensitivity analyses of select composite structural components p 85 A87-25407

Simplified composite micromechanics for predicting microstresses p 87 A87-49275

Boundary layer thermal stresses in angle-ply composite laminates, part 1 --- graphite-epoxy composites [NASA-CR-165412] p 93 N82-26713

Edge delamination in angle-ply composite laminates, part 5 [NASA-CR-165439] p 94 N82-26717

Boundary-layer effects in composite laminates: Free-edge stress singularities, part 6 [NASA-CR-165440] p 94 N82-26718

INHYD: Computer code for intraply hybrid composite design. A users manual [NASA-TP-2239] p 26 N84-13224

Hygrothermomechanical fracture stress criteria for fiber composites with sense-parity [NASA-TM-83691] p 27 N84-28918

PLYWOOD

Thermal stress analysis for a wood composite blade --- wind turbines [NASA-CR-173394] p 103 N84-21903

POISSON RATIO

Indentation law for composite laminates p 16 A84-27356

POLYCRYSTALS

Finite elastic-plastic deformation of polycrystalline metals p 34 A84-43872

Micromechanically based constitutive relations for polycrystalline solids p 99 N83-34359

Concepts for interrelating ultrasonic attenuation, microstructure and fracture toughness in polycrystalline solids [NASA-TM-87339] p 60 N86-25812

POLYESTER RESINS

Hygrothermomechanical evaluation of transverse filament tape epoxy/polyester fiberglass composites [NASA-TM-83044] p 26 N83-15362

POLYMER MATRIX COMPOSITES

A review of issues and strategies in nondestructive evaluation of fiber reinforced structural composites p 14 A80-34764

POLYNOMIALS

Slave finite elements: The temporal element approach to nonlinear analysis p 105 N84-31689

POROSITY

Effects of fine porosity on the fatigue behavior of a powder metallurgy superalloy p 32 A80-35495

Effects of fine porosity on the fatigue behavior of a powder metallurgy superalloy [NASA-TM-81448] p 37 N80-21493

Fatigue damage interaction behavior of PWA 1480 p 45 N87-22777

POTENTIAL ENERGY

Translational and extensional energy release rates (the J- and M-integrals) for a crack layer in thermoelasticity [NASA-CR-174872] p 107 N85-21685

POWDER METALLURGY

Effects of fine porosity on the fatigue behavior of a powder metallurgy superalloy p 32 A80-35495

The effect of microstructure on 650 C fatigue crack growth in P/M Astroloy p 33 A84-12395

Effects of processing and microstructure on the fatigue behaviour of the nickel-base superalloy Rene95 p 34 A84-48715

The effect of microstructure, temperature, and hold-time on low-cycle fatigue of As HIP P/M Rene 95 p 35 A85-32399

The influence of hold times on LCF and FCG behavior in a P/M Ni-base superalloy --- Low Cycle Fatigue/Fatigue Crack Growth [NASA-TM-81448] p 35 A85-32400

Effects of fine porosity on the fatigue behavior of a powder metallurgy superalloy [NASA-TM-81448] p 37 N80-21493

PREBURNERS

Longitudinal mode combustion instabilities of a high-pressure fuel-rich LOX/RP-1 preburner p 60 N86-28250

PRECIPITATION HARDENING

Comparative thermal fatigue resistance of several oxide dispersion strengthened alloys p 32 A82-11399

Thermomechanical deformation in the presence of metallurgical changes p 112 N85-31533

PREDICTION ANALYSIS TECHNIQUES

Strainrange partitioning life predictions of the long time Metal Properties Council creep-fatigue tests p 63 A80-27958

Prediction of fiber composite mechanical behavior made simple p 63 A80-32067

Nonlinear laminate analysis for metal matrix fiber composites [AIAA 81-0579] p 15 A81-29411

Turbine blade nonlinear structural and life analysis p 1 A83-29024

Blade loss transient dynamic analysis of turbomachinery p 2 A83-40864

Prediction of composite hygral behavior made simple p 16 A84-14285

Prediction of fiber composite mechanical behavior made simple --- using a rocket calculator [NASA-TM-81404] p 22 N80-16107

Concepts and techniques for ultrasonic evaluation of material mechanical properties [NASA-TM-81523] p 53 N80-24634

Prediction of composite thermal behavior made simple [NASA-TM-81618] p 23 N81-16132

Prediction of composite hygral behavior made simple [NASA-TM-82780] p 24 N82-16181

Large displacements and stability analysis of nonlinear propeller structures [NASA-TM-82850] p 94 N82-31707

Simplified composite micromechanics equations for strength, fracture toughness and environmental effects [NASA-TM-83696] p 27 N84-27832

A computer program for predicting nonlinear uniaxial material responses using viscoplastic models [NASA-TM-83675] p 104 N84-29247

Nonlinear structural and life analyses of a turbine blade p 9 N85-10954

Nonlinear structural and life analyses of a combustor liner p 9 N85-10955

Life prediction and constitutive behavior: Overview p 10 N85-10973

Validation of structural analysis methods using the in-house liner cyclic rigs p 10 N85-10987

Reliability considerations for the total strain range version of strainrange partitioning [NASA-CR-174757] p 106 N85-11380

Elevated temperature biaxial fatigue [NASA-CR-175795] p 110 N85-27263

Reexamination of cumulative fatigue damage laws p 112 N85-27962

A comparison of two contemporary creep-fatigue life prediction methods p 113 N85-31538

Two simplified procedures for predicting cyclic material response from a strain history p 113 N85-31543

An update of the total-strain version of SRP [NASA-TP-2499] p 42 N86-12295

Life prediction and constitutive models for engine hot section anisotropic materials program [NASA-CR-174952] p 60 N86-25003

Computational simulation of progressive fracture in fiber composites [NASA-TM-87341] p 30 N86-26376

Micromechanisms of thermomechanical fatigue: A comparison with isothermal fatigue [NASA-TM-87331] p 44 N86-28164

Turbine Engine Hot Section Technology, 1984 [NASA-CP-2339] p 120 N87-11180

High temperature stress-strain analysis p 120 N87-11209

Creep life prediction based on stochastic model of microstructurally short crack growth [NASA-TM-100245] p 125 N88-12825

PREDICTIONS

Progressive damage, fracture predictions and post mortem correlations for fiber composites [NASA-TM-87101] p 29 N86-10290

Structural analysis of turbine blades using unified constitutive models [NASA-TM-88807] p 119 N86-28461

- Formulation of the nonlinear analysis of shell-like structures, subjected to time-dependent mechanical and thermal loading
[NASA-CR-177194] p 119 N86-28462
- Calculation of thermomechanical fatigue life based on isothermal behavior
[NASA-TM-88864] p 122 N87-20565
- Environmental degradation of 316 stainless steel in high temperature low cycle fatigue
[NASA-TM-89931] p 124 N87-24007

PREPREGS

- Fracture characteristics of angleplied laminates fabricated from overaged graphite/epoxy prepreg
[NASA-TM-87266] p 30 N86-25417

PRESSURE PULSES

- Flow dynamic environment data base development for the SSME p 109 N85-26885

PRESSURE VESSELS

- Ten year environmental test of glass fiber/epoxy pressure vessels
[AIAA PAPER 85-1198] p 19 A85-47022
- Ten year environmental test of glass fiber/epoxy pressure vessels
[NASA-TM-87058] p 29 N85-30034

PRESTRESSING

- Effects of warping and pretwist on torsional vibration of rotating beams
[ASME PAPER 84-WA/APM-41] p 75 A85-17040
- Vibration and buckling of rotating, pretwisted, precone beams including Coriolis effects p 80 A86-26910
- Nonlinear vibration and stability of rotating, pretwisted, precone blades including Coriolis effects p 86 A87-39896
- Vibration and buckling of rotating, pretwisted, precone beams including Coriolis effects
[NASA-TM-87004] p 109 N85-25893
- Nonlinear bending-torsional vibration and stability of rotating, pretwisted, precone blades including Coriolis effects
[NASA-TM-87207] p 116 N86-17789

PROBABILITY THEORY

- Creep-rupture reliability analysis p 79 A85-42566
- Probabilistic finite elements for transient analysis in nonlinear continua p 80 A86-28653
- Efficient algorithms for use in probabilistic finite element analysis p 81 A86-28655
- Probabilistic structural analysis for space propulsion system components p 81 A86-28659
- Reliability of void detection in structural ceramics by use of scanning laser acoustic microscopy p 52 A86-39027
- SCARE - A postprocessor program to MSC/NASTRAN for reliability analysis of structural ceramic components
[ASME PAPER 86-GT-34] p 84 A87-17988
- Probabilistic structural analysis to quantify uncertainties associated with turbopump blades
[AIAA PAPER 87-0766] p 85 A87-33581
- Statistical aspects of carbon fiber risk assessment modeling --- fire accidents involving aircraft
[NASA-CR-159318] p 23 N80-29432
- The application of probabilistic design theory to high temperature low cycle fatigue
[NASA-CR-165488] p 91 N82-14531
- Creep-rupture reliability analysis
[NASA-CR-3790] p 102 N84-19925
- Probabilistic structural analysis theory development p 111 N85-27955
- Probabilistic finite element development p 111 N85-27956
- Reliability of void detection in structural ceramics using scanning laser acoustic microscopy
[NASA-TM-87035] p 58 N85-32337
- Probabilistic structural analysis methods for space propulsion system components
[NASA-TM-88861] p 121 N87-13794

PROBLEM SOLVING

- The finite analytic method, volume 3
[NASA-CR-170186] p 127 N83-23087
- The finite analytic method, volume 4
[NASA-CR-170187] p 127 N83-23088
- The finite analytic method, volume 5
[NASA-CR-170188] p 127 N83-23089

PROCESS CONTROL (INDUSTRY)

- NDE reliability and process control for structural ceramics
[ASME PAPER 87-GT-8] p 53 A87-48702
- NDE reliability and process control for structural ceramics
[NASA-TM-88870] p 61 N87-12910

PRODUCT DEVELOPMENT

- Integrated analysis of engine structures
[NASA-TM-82713] p 91 N82-11491

PROJECT MANAGEMENT

- Life prediction and constitutive behavior: Overview p 10 N85-10973

PROP-FAN TECHNOLOGY

- Dynamic characteristics of an assembly of prop-fan blades
[ASME PAPER 85-GT-134] p 5 A86-32956
- Structural tailoring of advanced turboprops
[AIAA PAPER 87-0753] p 85 A87-33648
- Analytical and experimental investigation of mistuning in propfan flutter
[AIAA PAPER 87-0739] p 86 A87-40496
- Analytical flutter investigation of a composite propfan model
[AIAA PAPER 87-0738] p 87 A87-40497
- Advanced turboprop vibratory characteristics
[NASA-CR-174708] p 12 N86-24693
- Experimental classical flutter results of a composite advanced turboprop model
[NASA-TM-88792] p 119 N86-29271
- Analytical flutter investigation of a composite propfan model
[NASA-TM-88944] p 122 N87-18115
- Analytical and experimental investigation of mistuning in propfan flutter
[NASA-TM-88959] p 122 N87-18116
- Structural and aeroelastic analysis of the SR-7L propfan
[NASA-TM-86877] p 123 N87-22273
- A computational procedure for automated flutter analysis
[NASA-TM-100171] p 125 N87-28058

PROPAGATION MODES

- Dynamic fields near a crack tip growing in an elastic-perfectly-plastic solid p 70 A83-38528
- Shear fatigue crack growth - A literature survey p 80 A86-24219
- Elastic analysis of a mode II fatigue crack test specimen p 84 A87-17799

PROPAGATION VELOCITY

- Moving cracks in layered composites p 67 A83-12048

PROPELLER BLADES

- Tensile buckling of advanced turboprops
[AIAA PAPER 82-0776] p 67 A83-10900
- Flutter analysis of advanced turbopropellers
[AIAA 83-0846] p 69 A83-29824
- Tensile buckling of advanced turboprops p 71 A84-11039
- Flutter analysis of advanced turbopropellers p 73 A84-36492
- Dynamic characteristics of an assembly of prop-fan blades
[ASME PAPER 85-GT-134] p 5 A86-32956
- Structural tailoring of advanced turboprops
[AIAA PAPER 87-0753] p 85 A87-33648
- Influence of third-degree geometric nonlinearities on the vibration and stability of pretwisted, precone, rotating blades p 6 A87-46228
- Tensile buckling of advanced turboprops
[NASA-TM-82896] p 94 N82-31708
- Bending-torsion flutter of a highly swept advanced turboprop
[NASA-TM-82975] p 95 N83-11514
- Nonlinear displacement analysis of advanced propeller structures using NASTRAN
[NASA-TM-83737] p 104 N84-31683
- Experimental classical flutter results of a composite advanced turboprop model
[NASA-TM-88792] p 119 N86-29271
- Influence of third-degree geometric nonlinearities on the vibration and stability of pretwisted, precone, rotating blades p 120 N86-31920

PROPELLER FANS

- Advanced turboprop vibratory characteristics
[NASA-CR-174708] p 12 N86-24693

PROPELLERS

- Aeroelastic formulations for turbomachines and propellers p 4 A86-24677
- Large displacements and stability analysis of nonlinear propeller structures
[NASA-TM-82850] p 94 N82-31707
- Large displacements and stability analysis of nonlinear propeller structures p 95 N83-12460
- Forced vibration analysis of rotating cyclic structures in NASTRAN
[NASA-CR-165429] p 100 N84-11514
- Aeroelastic analysis for propellers - mathematical formulations and program user's manual
[NASA-CR-3729] p 101 N84-12530
- NASTRAN documentation for flutter analysis of advanced turbopropellers
[NASA-CR-167927] p 8 N84-15153

PROPULSION

- The structural response of a rail accelerator p 72 A84-32039
- The structural response of a rail accelerator
[NASA-TM-83491] p 99 N83-35412

PROPULSION SYSTEM PERFORMANCE

- Probabilistic structural analysis for space propulsion system components p 81 A86-28659
- Effect of time dependent flight loads on JT9D-7 performance deterioration
[NASA-CR-159681] p 87 N80-10515
- Structural dynamic measurement practices for turbomachinery at the NASA Lewis Research Center
[NASA-TM-88857] p 13 N86-32433

PROTECTIVE COATINGS

- Turbine Engine Hot Section Technology (HOST)
[NASA-CP-2289] p 115 N86-11495
- Life prediction and constitutive models for engine hot section anisotropic materials program
[NASA-CR-174952] p 60 N86-25003
- Thermal-fatigue and oxidation resistance of cobalt-modified Udimet 700 alloy
[NASA-TP-2591] p 119 N86-28464
- Bithermal low-cycle fatigue behavior of a NiCoCrAlY-coated single crystal superalloy
[NASA-TM-89831] p 45 N87-20408

Q**QUALITY CONTROL**

- Fabrication and quality assurance processes for superhybrid composite fan blades p 20 A87-19123
- Reliability and quality assurance on the MOD 2 wind system
[NASA-TM-82717] p 54 N81-33492
- Experience with modified aerospace reliability and quality assurance method for wind turbines
[NASA-TM-82803] p 54 N82-19550
- Fabrication and quality assurance processes for superhybrid composite fan blades
[NASA-TM-83354] p 28 N85-14882

R**RADIAL DISTRIBUTION**

- Analysis of an internally radially cracked ring segment subject to three-point radial loading p 71 A84-18691
- Analysis of an externally radially cracked ring segment subject to three-point radial loading
[NASA-TM-83482] p 100 N83-35413

RADIOGRAPHY

- Radiographic detectability limits for seeded voids in sintered silicon carbide and silicon nitride p 51 A86-31745
- Nondestructive characterization of structural ceramics p 46 A86-37141
- Nondestructive techniques for characterizing mechanical properties of structural materials - An overview
[ASME PAPER 86-GT-75] p 52 A86-48143
- Correlation of processing and sintering variables with the strength and radiography of silicon nitride p 46 A87-12938
- Probability of detection of internal voids in structural ceramics using microfocus radiography p 52 A87-14300
- NDE reliability and process control for structural ceramics
[ASME PAPER 87-GT-8] p 53 A87-48702
- Radiographic detectability limits for seeded voids in sintered silicon carbide and silicon nitride
[NASA-TM-86945] p 58 N85-21674
- Probability of detection of internal voids in structural ceramics using microfocus radiography
[NASA-TM-87164] p 59 N86-13749
- Nondestructive techniques for characterizing mechanical properties of structural materials: An overview
[NASA-TM-87203] p 59 N86-19636
- Factors that affect reliability of nondestructive detection of flaws in structural ceramics
[NASA-TM-87348] p 61 N86-31912
- NDE reliability and process control for structural ceramics
[NASA-TM-88870] p 61 N87-12910
- Flaw imaging and ultrasonic techniques for characterizing sintered silicon carbide
[NASA-TM-100177] p 63 N88-12106

RAILGUN ACCELERATORS

- The structural response of a rail accelerator p 72 A84-32039
- The structural response of a rail accelerator
[NASA-TM-83491] p 99 N83-35412

RANDOM LOADS

- Efficient algorithms for use in probabilistic finite element analysis p 81 A86-28655

RANDOM VARIABLES

- Advanced reliability method for fatigue analysis p 72 A84-31596

Application of advanced reliability methods to local strain fatigue analysis
[NASA-CR-168198] p 97 N83-29734

RANDOM VIBRATION
Oscillator response to nonstationary excitation
[ASME PAPER 84-WA/APM-38] p 75 A85-17039

RANKING
Existence and stability, and discrete BB and rank conditions, for general mixed-hybrid finite elements in elasticity p 82 A86-34464

RATIONAL FUNCTIONS
Axisymmetric solid elements by a rational hybrid stress method p 78 A85-41109

RAYLEIGH-RITZ METHOD
Vibrations of cantilevered shallow cylindrical shells of rectangular planform p 65 A82-11298

REACTION BONDING
Radiographic detectability limits for seeded voids in sintered silicon carbide and silicon nitride p 51 A86-31745
Radiographic detectability limits for seeded voids in sintered silicon carbide and silicon nitride [NASA-TM-86945] p 58 N85-21674

REACTION KINETICS
Nonlinear Constitutive Relations for High Temperature Applications [NASA-CP-2271] p 98 N83-34351

RECRYSTALLIZATION
Ultrasonic determination of recrystallization [NASA-TM-88855] p 61 N87-10399

RECTANGULAR BEAMS
Fatigue life prediction in bending from axial fatigue information [NASA-CR-165563] p 91 N82-20564

RECTANGULAR PANELS
Design concepts/parameters assessment and sensitivity analyses of select composite structural components p 85 A87-25407

RECTANGULAR PLANFORMS
Vibrations of cantilevered shallow cylindrical shells of rectangular planform p 65 A82-11298
Vibrations of cantilevered circular cylindrical shells
Shallow versus deep shell theory p 69 A83-36958

RECTANGULAR PLATES
Vibration and buckling of rectangular plates under in-plane hydrostatic loading p 64 A80-45364
Vibrations of twisted cantilevered plates - Summary of previous and current studies p 76 A85-22069

REFLECTORS
Composite space antenna structures - Properties and environmental effects p 20 A87-38610
Composite space antenna structures: Properties and environmental effects [NASA-TM-88859] p 31 N87-16880

REFRACTORY COATINGS
The low cycle fatigue behavior of a plasma-sprayed coating material [NASA-TM-87318] p 44 N86-31699

REFRACTORY MATERIALS
Nonlinear analysis for high-temperature multilayered fiber composite structures --- turbine blades [NASA-TM-83754] p 29 N85-21273
Viscoplastic constitutive relationships with dependence on thermomechanical history [NASA-CR-174836] p 108 N85-21691

REFRACTORY METAL ALLOYS
Application of two creep fatigue life models for the prediction of elevated temperature crack initiation of a nickel base alloy [AIAA PAPER 85-1420] p 35 A85-43979

REGENERATORS
Fatigue failure of regenerator screens in a high frequency Stirling engine [NASA-TM-88974] p 122 N87-18882

REINFORCED PLATES
Three-dimensional finite-element analysis of layered composite plates p 68 A83-27432

REINFORCED SHELLS
Geometrically nonlinear analysis of layered composite shells p 68 A83-27431

REINFORCING FIBERS
Fatigue behavior of SiC reinforced titanium composites p 13 A80-10036
Dynamic modulus and damping of boron, silicon carbide, and alumina fibers p 15 A80-44236
Laminates and reinforced metals [NASA-TM-81591] p 23 N81-12171

REISSNER THEORY
A new formulation of hybrid/mixed finite element p 67 A83-12739
Alternative ways for formulation of hybrid stress elements p 68 A83-14710
On the suppression of zero energy deformation modes p 72 A84-21541
Rational approach for assumed stress finite elements p 74 A85-12029

On the existence and stability conditions for mixed-hybrid finite element solutions based on Reissner's variational principle p 77 A85-33847

RELIABILITY
NDE reliability and process control for structural ceramics [ASME PAPER 87-GT-8] p 53 A87-48702
Experience with modified aerospace reliability and quality assurance method for wind turbines [NASA-TM-82803] p 54 N82-19550
Reliability of scanning laser acoustic microscopy for detecting internal voids in structural ceramics [NASA-TM-87222] p 59 N86-16599
NDE reliability and process control for structural ceramics [NASA-TM-88870] p 61 N87-12910
Effect of design variables, temperature gradients and speed of life and reliability of a rotating disk [NASA-TM-88883] p 49 N87-13755
Surface flaw reliability analysis of ceramic components with the SCARE finite element postprocessor program [NASA-TM-88901] p 121 N87-17087

RELIABILITY ANALYSIS
Advanced reliability method for fatigue analysis p 72 A84-31596
Fatigue criterion to system design, life and reliability [AIAA PAPER 85-1140] p 78 A85-40814
Fatigue criterion to system design, life, and reliability p 85 A87-27986
Reliability and quality assurance on the MOD 2 wind system [NASA-TM-82717] p 54 N81-33492
Statistical summaries of fatigue data for design purposes [NASA-CR-3697] p 97 N83-29731
Application of advanced reliability methods to local strain fatigue analysis [NASA-CR-168198] p 97 N83-29734
Reliability considerations for the total strain range version of strainrange partitioning [NASA-CR-174757] p 106 N85-11380
Fatigue criterion to system design, life and reliability [NASA-TM-87017] p 49 N85-27226
Factors that affect reliability of nondestructive detection of flaws in structural ceramics [NASA-TM-87348] p 61 N86-31912

RELIABILITY ENGINEERING
Photovoltaic power system reliability considerations [NASA-TM-79291] p 53 N80-15422

RENE 95
Effects of processing and microstructure on the fatigue behaviour of the nickel-base superalloy Rene95 p 34 A84-48715
The effect of microstructure, temperature, and hold-time on low-cycle fatigue of As HIP P/M Rene 95 p 35 A85-32399
The influence of hold times on LCF and FCG behavior in a P/M Ni-base superalloy --- Low Cycle Fatigue/Fatigue Crack Growth p 35 A85-32400
Fatigue crack growth and low cycle fatigue of two nickel base superalloys [NASA-CR-174534] p 39 N84-10267

RESEARCH FACILITIES
Lewis' enhanced laboratory for research into the fatigue and constitutive behavior of high temperature materials p 125 N88-11177

RESIDUAL STRENGTH
Estimating the R-curve from residual strength data [NASA-TM-87182] p 116 N86-18750

RESIDUAL STRESS
Finite element analysis of residual stress in plasma-sprayed ceramic p 46 A86-15226
Calculation of residual principal stresses in CVD boron on carbon filaments [NASA-TM-81456] p 22 N80-20314
Nonlinear damage analysis: Postulate and evaluation [NASA-CR-168171] p 118 N86-26652

RESIN MATRIX COMPOSITES
Resin selection criteria for tough composite structures [AIAA 83-0801] p 46 A83-29734
Superhybrid composite blade impact studies [NASA-TM-81597] p 89 N81-11412
Ray propagation path analysis of acousto-ultrasonic signals in composites [NASA-TM-100148] p 62 N87-25589

RESINS
Resin selection criteria for tough composite structures [AIAA 83-0801] p 46 A83-29734

RESISTANCE
Estimating the R-curve from residual strength data [NASA-TM-87182] p 116 N86-18750

RESONANCE
Effects of specimen resonances on acoustic-ultrasonic testing [NASA-CR-3679] p 55 N83-21373

RESONANT FREQUENCIES
Vibration and buckling of rectangular plates under in-plane hydrostatic loading p 64 A80-45364
Natural frequency of rotating beams using non-rotating modes p 68 A83-18383
Natural frequencies of twisted rotating plates p 76 A85-32343
Blade loss transient dynamics analysis with flexible bladed disk [NASA-CR-168176] p 7 N84-13193
An improved finite-difference analysis of uncoupled vibrations of tapered cantilever beams [NASA-TM-83495] p 101 N84-13610
The use of an optical data acquisition system for bladed disk vibration analysis [NASA-TM-86891] p 106 N85-15184

RESONANT VIBRATION
Vibrations of twisted cantilevered plates - Experimental investigation [ASME PAPER 84-GT-96] p 73 A84-46937
Improved finite-difference vibration analysis of pretwisted, tapered beams [NASA-TM-83549] p 102 N84-16588

RIGID STRUCTURES
Analyses of large quasistatic deformations of inelastic bodies by a new hybrid-stress finite element algorithm p 71 A84-16874

RIMS
A finite element stress analysis of spur gears including fillet radii and rim thickness effects [NASA-TM-82865] p 48 N82-28646
On finite element stress analysis of spur gears [NASA-CR-167938] p 48 N82-29607

RING STRUCTURES
Analysis of an internally radially cracked ring segment subject to three-point radial loading p 71 A84-18691
Analysis of an externally radially crack ring segment subject to three-point radial loading p 79 A86-20710
Instructions for the use of the CIVM-Jet 4C finite-strain computer code to calculate the transient structural responses of partial and/or complete arbitrarily-curved rings subjected to fragment impact [NASA-TM-159873] p 88 N80-27720
Stress intensity and displacement coefficients for radially cracked ring segments subject to three-point bending [NASA-TM-83059] p 96 N83-24874
Analysis of an externally radially cracked ring segment subject to three-point radial loading [NASA-TM-83482] p 100 N83-35413

RISK
Statistical aspects of carbon fiber risk assessment modeling --- fire accidents involving aircraft [NASA-CR-159318] p 23 N80-29432

RITZ AVERAGING METHOD
Vibrations of cantilevered doubly-curved shallow shells p 70 A83-39557
A study of internal and distributed damping for vibrating turbomachinery blades [NASA-CR-175901] p 11 N85-27868
Extensions of the Ritz-Galerkin method for the forced, damped vibrations of structural elements p 117 N86-21909

ROCKET ENGINE CASES
Ultrasonic evaluation of mechanical properties of thick, multilayered, filament wound composites [NASA-TM-87088] p 58 N86-10561

ROCKET ENGINES
Longitudinal mode combustion instabilities of a high-pressure fuel-rich LOX/RP-1 preburner p 60 N86-28250

RODS
Extended range stress intensity factor expressions for chevron-notched short bar and short rod fracture toughness specimens p 66 A82-40357
Specimen size and geometry effects on fracture toughness of Al₂O₃ measured with short rod and short bar chevron-notch specimens [NASA-TM-83319] p 47 N83-19902

ROLLER BEARINGS
Effect of interference fits on roller bearing fatigue life p 48 A87-37686
Selection of rolling-element bearing steels for long-life application [NASA-TM-88881] p 49 N87-11993
Lubricant effects on bearing life p 49 N87-15467
Effects of surface removal on rolling-element fatigue [NASA-TM-88871] p 50 N87-18820

ROLLERS
Evaluation of a high-torque backlash-free roller actuator p 49 N87-16336

ROLLING CONTACT LOADS
Finite element analysis of steadily moving contact fields p 70 A83-49437
Pantographing self adaptive gap elements p 77 A85-37440

S

- Lubricant effects on bearing life
[NASA-TM-88875] p 49 N87-15467
- Effects of surface removal on rolling-element fatigue
[NASA-TM-88871] p 50 N87-18820
- ROTARY STABILITY**
- Some analysis methods for rotating systems with periodic coefficients p 69 A83-32987
- The effect of aerodynamic and structural detuning on turbomachine supersonic unstalled torsional flutter
[AIAA PAPER 85-0761] p 3 A85-30378
- Influence of third-degree geometric nonlinearities on the vibration and stability of pretwisted, precone, rotating blades p 6 A87-46228
- Structural response of a rotating bladed disk to rotor whirl
[NASA-CR-175605] p 11 N85-22391
- Influence of third-degree geometric nonlinearities on the vibration and stability of pretwisted, precone, rotating blades
[NASA-TM-87307] p 120 N86-31920
- ROTATING BODIES**
- Vibrations of twisted rotating blades
[ASME PAPER 81-DET-127] p 65 A82-19341
- Extending the laser-specklegram technique to strain analysis of rotating components p 67 A83-12514
- Natural frequency of rotating beams using non-rotating modes p 68 A83-18383
- Effects of warping and pretwist on torsional vibration of rotating beams
[ASME PAPER 84-WA/APM-41] p 75 A85-17040
- Finite difference analysis of torsional vibrations of pretwisted, rotating, cantilever beams with effects of warping p 78 A85-42047
- Forced vibration analysis of rotating cyclic structures in NASTRAN
[NASA-CR-165429] p 100 N84-11514
- NASTRAN forced vibration analysis of rotating cyclic structures
[NASA-CR-173821] p 104 N84-29252
- Finite element analysis of flexible, rotating blades
[NASA-TM-89906] p 124 N87-26385
- ROTATING DISKS**
- Stagger angle dependence of inertial and elastic coupling in bladed disks p 72 A84-31903
- Vibration and flutter of mistuned bladed-disk assemblies
[AIAA PAPER 84-0991] p 75 A85-16095
- Vibrations of blades and bladed disk assemblies: Proceedings of the Tenth Biennial Conference on Mechanical Vibration and Noise, Cincinnati, OH, September 10-13, 1985 p 4 A86-26901
- The effect of limiting aerodynamic and structural coupling in models of mistuned bladed disk vibration p 5 A86-26905
- Analytical and experimental investigation of the coupled bladed disk/shaft whirl of a cantilevered turbofan
[ASME PAPER 86-GT-98] p 6 A86-48163
- Finite element forced vibration analysis of rotating cyclic structures
[NASA-CR-165430] p 101 N84-11515
- Vibration and flutter of mistuned bladed-disk assemblies
[NASA-TM-83634] p 103 N84-23923
- Effect of design variables, temperature gradients and speed of life and reliability of a rotating disk
[NASA-TM-88883] p 49 N87-13755
- ROTATING SHAFTS**
- Analytical and experimental investigation of the coupled bladed disk/shaft whirl of a cantilevered turbofan
[ASME PAPER 86-GT-98] p 6 A86-48163
- Development of procedures for calculating stiffness and damping of elastomers in engineering applications, part 6
[NASA-CR-159838] p 87 N80-22733
- Variable force, eddy-current or magnetic damper
[NASA-CASE-LEW-13717-1] p 49 N85-30333
- ROTATION**
- Nonlinear vibration and stability of rotating, pretwisted, precone blades including Coriolis effects p 86 A87-39896
- Nonlinear bending-torsional vibration and stability of rotating, pretwisted, precone blades including Coriolis effects
[NASA-TM-87207] p 116 N86-17789
- ROTOR AERODYNAMICS**
- Flutter and forced response of mistuned rotors using standing wave analysis
[AIAA 83-0845] p 69 A83-29823
- Flutter and forced response of mistuned rotors using standing wave analysis p 74 A85-12721
- Effects of friction dampers on aerodynamically unstable rotor stages p 3 A85-21866
- Stability of limit cycles in frictionally damped and aerodynamically unstable rotor stages p 4 A86-19198
- Aeroelastic formulations for turbomachines and propellers p 4 A86-24677

- Forced response analysis of an aerodynamically detuned supersonic turbomachine rotor p 5 A86-26902
- Aerodynamic and structural detuning of supersonic turbomachine rotors p 5 A86-31595
- Aeroelastic analysis for propellers - mathematical formulations and program user's manual
[NASA-CR-3729] p 101 N84-12530
- Flutter and forced response of mistuned rotors using standing wave analysis
[NASA-CR-173555] p 9 N84-24586
- ROTOR BLADES**
- Stagger angle dependence of inertial and elastic coupling in bladed disks p 72 A84-31903
- A blade loss response spectrum for flexible rotor systems
[ASME PAPER 84-GT-29] p 48 A84-46893
- ROTOR BLADES (TURBOMACHINERY)**
- Stability of large horizontal-axis axisymmetric wind turbines p 64 A81-22526
- Effects of mistuning on blade torsional flutter p 64 A81-29095
- NASTRAN forced vibration analysis of rotating cyclic structures
[ASME PAPER 83-DET-20] p 72 A84-29103
- Measurements of self-excited rotor-blade vibrations using optical displacements
[ASME PAPER 83-GT-132] p 73 A84-33702
- Natural frequencies of twisted rotating plates p 76 A85-32343
- The dynamics of a flexible bladed disc on a flexible rotor in a two-rotor system p 4 A86-25743
- Vibration and buckling of rotating, pretwisted, precone beams including Coriolis effects p 80 A86-26910
- Influence of friction dampers on torsional blade flutter
[ASME PAPER 85-GT-170] p 5 A86-32957
- The effect of circumferential aerodynamic detuning on coupled bending-torsion unstalled supersonic flutter
[ASME PAPER 86-GT-100] p 6 A87-25396
- Analytical and experimental investigation of mistuning in propfan flutter
[AIAA PAPER 87-0739] p 86 A87-40496
- Coupled bending-bending-torsion flutter of a mistuned cascade with nonuniform blades
[NASA-TM-82813] p 92 N82-21604
- Measurements of self-excited rotor-blade vibrations using optical displacements
[NASA-TM-82953] p 95 N83-14523
- Structural fatigue test results for large wind turbine blade sections p 96 N83-19246
- Improved methods of vibration analysis of pretwisted, airfoil blades
[NASA-TM-83735] p 104 N84-30329
- Structural analysis p 9 N85-10969
- Structural response of a rotating bladed disk to rotor whirl
[NASA-CR-175605] p 11 N85-22391
- Vibration and buckling of rotating, pretwisted, precone beams including Coriolis effects
[NASA-TM-87004] p 109 N85-25893
- Turbine Engine Hot Section Technology, 1984
[NASA-CP-2339] p 120 N87-11180
- Analytical and experimental investigation of mistuning in propfan flutter
[NASA-TM-88959] p 122 N87-18116
- ROTORS**
- Nonlinear transient finite element analysis of rotor-bearing-stator systems p 48 A84-20580
- A blade loss response spectrum for flexible rotor systems
[ASME PAPER 84-GT-29] p 48 A84-46893
- NASTRAN level 16 demonstration manual updates for aeroelastic analysis of bladed discs
[NASA-CR-159826] p 90 N81-19483
- Engine dynamic analysis with general nonlinear finite element codes. Part 2: Bearing element implementation overall numerical characteristics and benchmarking
[NASA-CR-167944] p 7 N82-33390
- Theoretical investigation of the force and dynamically coupled torsional-axial-lateral dynamic response of eared rotors
[NASA-CR-173013] p 127 N83-34656
- The use of an optical data acquisition system for bladed disk vibration analysis
[NASA-TM-86891] p 106 N85-15184
- Structural dynamic measurement practices for turbomachinery at the NASA Lewis Research Center
[NASA-TM-88857] p 13 N86-32433
- Structural and aeroelastic analysis of the SR-7L propfan
[NASA-TM-86877] p 123 N87-22273
- RUPTURING**
- A continuous damage model based on stepwise-stress creep rupture tests
[NASA-CR-174941] p 114 N85-32341

S GLASS

- Mechanical property characterization of intraply hybrid composites
[NASA-TM-79306] p 21 N80-12120

S-N DIAGRAMS

- The application of probabilistic design theory to high temperature low cycle fatigue
[NASA-CR-165488] p 91 N82-14531
- Statistical summaries of fatigue data for design purposes
[NASA-CR-3697] p 97 N83-29731

SAFETY

- Experience with modified aerospace reliability and quality assurance method for wind turbines
[NASA-TM-82803] p 54 N82-19550

SANDWICH STRUCTURES

- Composite sandwich thermostructural behavior - Computational simulation
[AIAA PAPER 86-0948] p 82 A86-38842
- Fiber composite sandwich thermostructural behavior: Computational simulation
[NASA-TM-88787] p 31 N86-31663

SCANNING

- Application of scanning acoustic microscopy to advanced structural ceramics
[NASA-TM-89929] p 62 N87-23987

SCATTERING

- Ultrasonic evaluation of mechanical properties of thick, multilayered, filament wound composites
[NASA-TM-87088] p 58 N86-10561

SCATTERING CROSS SECTIONS

- Preliminary investigation of an electrical network model for ultrasonic scattering
[NASA-CR-3770] p 57 N84-17606

SEALS (STOPPERS)

- Inelastic high-temperature thermomechanical response of ceramic coated gas turbine seals p 82 A86-37799
- Dynamic behavior of spiral-groove and Rayleigh-Step self-acting face seals
[NASA-TP-2266] p 8 N84-16181

SELECTION

- Resin selection criteria for tough composite structures
[AIAA 83-0801] p 46 A83-29734
- Selection of rolling-element bearing steels for long-life application
[NASA-TM-88881] p 49 N87-11993

SELF INDUCED VIBRATION

- The coupled aeroelastic response of turbomachinery blading to aerodynamic excitations
[AIAA 83-0844] p 69 A83-29822
- The coupled response of turbomachinery blading to aerodynamic excitations p 2 A84-26959

SENSITIVITY

- Sensitivity analysis results of the effects of various parameters on composite design p 15 A82-37101
- Radiographic detectability limits for seeded voids in sintered silicon carbide and silicon nitride p 51 A86-31745
- Radiographic detectability limits for seeded voids in sintered silicon carbide and silicon nitride
[NASA-TM-86945] p 58 N85-21674

SENSORS

- Sensor failure detection for jet engines
[NASA-CR-168190] p 56 N83-33182

SEPARATED FLOW

- A technique for the prediction of airfoil flutter characteristics in separated flow
[AIAA PAPER 87-0910] p 86 A87-33719
- A comparative study of some dynamic stall models
[NASA-TM-88917] p 122 N87-18883

SERVICE LIFE

- Fatigue criterion to system design, life and reliability
[AIAA PAPER 85-1140] p 78 A85-40814
- Fatigue criterion to system design, life, and reliability p 85 A87-27986

- Fracture mechanics criteria for turbine engine hot section components
[NASA-CR-167896] p 7 N82-25257

- Materials constitutive models for nonlinear analysis of thermally cycled structures
[NASA-TP-2055] p 95 N83-12449

- Benchmark notch test for life prediction
[NASA-CR-165571] p 95 N83-12451

- Fatigue criterion to system design, life and reliability
[NASA-TM-87017] p 49 N85-27226

- Micromechanisms of thermomechanical fatigue: A comparison with isothermal fatigue
[NASA-TM-87331] p 44 N86-28164

- Lubricant effects on bearing life
[NASA-TM-88875] p 49 N87-15467

SERVOMECHANISMS

- Application of traction drives as servo mechanisms p 114 N85-33520

SHAFTS (MACHINE ELEMENTS)

- Failure analysis of a tool steel torque shaft
p 51 A84-17546
- Factors that affect the fatigue strength of power transmission shafting and their impact on design
p 48 A87-14656
- Structural dynamic measurement practices for turbomachinery at the NASA Lewis Research Center
[NASA-TM-88857] p 13 N86-32433

SHAKERS

- Lewis Research Center spin rig and its use in vibration analysis of rotating systems
[NASA-TP-2304] p 9 N84-24578

SHALLOW SHELLS

- Vibrations of cantilevered shallow cylindrical shells of rectangular planform
p 65 A82-11298
- Vibrations of cantilevered doubly-curved shallow shells
p 70 A83-39557

SHEAR PROPERTIES

- Analysis of interface cracks in adhesively bonded lap shear joints, part 4
[NASA-CR-165438] p 93 N82-26716
- Fiber composite sandwich thermostructural behavior: Computational simulation
[NASA-TM-88787] p 31 N86-31663

SHEAR STRAIN

- A mixed shear flexible finite element for the analysis of laminated plates
p 73 A84-45994

SHEAR STRENGTH

- Ultrasonic evaluation of mechanical properties of thick, multilayered, filament wound composites
[NASA-TM-87088] p 58 N86-10561

SHEAR STRESS

- Continuous analysis of stresses from arbitrary surface loads on a half space
p 64 A81-14162
- Shear fatigue crack growth - A literature survey
p 80 A86-24219
- Simplified composite micromechanics for predicting microstresses
p 20 A87-20090
- Effect of interference fits on roller bearing fatigue life
p 48 A87-37686

Cyclic torsion testing

- [NASA-TM-83756] p 105 N84-31687
- Simplified composite micromechanics for predicting microstresses
[NASA-TM-87295] p 30 N86-24759
- Free-edge delamination: Laminate width and loading conditions effects
[NASA-TM-100238] p 32 N88-12551

SHELL STABILITY

- Analysis of shell type structures subjected to time dependent mechanical and thermal loading
[NASA-CR-175747] p 109 N85-25896
- Dynamic creep buckling: Analysis of shell structures subjected to time-dependent mechanical and thermal loading
p 111 N85-27959

SHELL THEORY

- Vibrations of twisted rotating blades
[ASME PAPER 81-DET-127] p 65 A82-19341
- Comparison of beam and shell theories for the vibrations of thin turbomachinery blades
[ASME PAPER 82-GT-223] p 65 A82-35408
- Geometrically nonlinear analysis of layered composite shells
p 68 A83-27431
- Vibrations of cantilevered circular cylindrical shells
Shallow versus deep shell theory
p 69 A83-36958
- Vibrations of blades with variable thickness and curvature by shell theory
[ASME PAPER 83-GT-152] p 70 A83-47978
- Hybrid Semiloof elements for plates and shells based upon a modified Hu-Washizu principle
p 74 A85-15893

- A higher order theory of laminated composite cylindrical shells
p 86 A87-35656
- New variational formulations of hybrid stress elements
p 105 N84-31690

- Dynamic creep buckling: Analysis of shell structures subjected to time-dependent mechanical and thermal loading
p 111 N85-27959

SHELLS (STRUCTURAL FORMS)

- Finite-element modeling of layered, anisotropic composite plates and shells: A review of recent research
p 91 N82-19563
- Nonlinear Structural Analysis
[NASA-CP-2297] p 105 N84-31688
- New variational formulations of hybrid stress elements
p 105 N84-31690
- Nonlinear finite element analysis of shells with large aspect ratio
p 105 N84-31692
- Geometrically nonlinear analysis of laminated elastic structures
[NASA-CR-175609] p 108 N85-21720
- Joint research effort on vibrations of twisted plates, phase 1: Final results
[NASA-RP-1150] p 115 N86-10579

SHOCK SPECTRA

- A blade loss response spectrum for flexible rotor systems
[ASME PAPER 84-GT-29] p 48 A84-46893

SHOCK WAVE PROPAGATION

- Dynamic responses of graphite/epoxy laminated beam to impact of elastic spheres
[NASA-CR-165461] p 25 N83-13173

SHOCK WAVES

- The effects of strong shock loading on coupled bending-torsion flutter of tuned and mistuned cascades
p 4 A86-26893

SHOT PEENING

- Shot peening for Ti-6Al-4V alloy compressor blades
[NASA-TP-2711] p 123 N87-20566

SHROUDED PROPELLERS

- Aeroelastic and dynamic finite element analyses of a bladed shrouded disk
[NASA-CR-159728] p 90 N81-19479

SHROUDED TURBINES

- The interaction between mistuning and friction in the forced response of bladed disk assemblies
[ASME PAPER 84-GT-139] p 73 A84-46957
- Vibration characteristics of mistuned shrouded blade assemblies
[ASME PAPER 85-GT-115] p 4 A86-22068

SIGNAL ANALYSIS

- The role of the reflection coefficient in precision measurement of ultrasonic attenuation
p 51 A85-42151

- Input-output characterization of an ultrasonic testing system by digital signal analysis
[NASA-CR-3756] p 56 N84-15565

- The role of the reflection coefficient in precision measurement of ultrasonic attenuation
[NASA-TM-83788] p 57 N84-32849

SIGNAL PROCESSING

- Application of homomorphic signal processing to stress wave factor analysis
[NAS 1.26:174871] p 58 N85-21673

SILICON ALLOYS

- Fatigue crack layer propagation in silicon-iron
[NASA-CR-175115] p 118 N86-25851

SILICON CARBIDES

- Fatigue behavior of SiC reinforced titanium composites
p 13 A80-10036
- Dynamic modulus and damping of boron, silicon carbide, and alumina fibers
p 15 A80-44236
- Fatigue behavior of SiC reinforced Ti/6Al-4V/ at 650 C
p 15 A83-12414
- Comparison of NDE techniques for sintered-SiC components
p 51 A83-22265
- Radiographic detectability limits for seeded voids in sintered silicon carbide and silicon nitride
p 51 A86-31745

- Nondestructive characterization of structural ceramics
p 46 A86-37141

- Reliability of void detection in structural ceramics by use of scanning laser acoustic microscopy
p 52 A86-39027

- Dynamic modulus and damping of boron, silicon carbide, and alumina fibers
[NASA-TM-81422] p 22 N80-20313

- Ultrasonic velocity for estimating density of structural ceramics
[NASA-TM-82765] p 46 N82-14359

- NDE for heat engine ceramics
[NASA-TM-86949] p 57 N85-20389

- Radiographic detectability limits for seeded voids in sintered silicon carbide and silicon nitride
[NASA-TM-86945] p 58 N85-21674

- Reliability of void detection in structural ceramics using scanning laser acoustic microscopy
[NASA-TM-87035] p 58 N85-32337

- Factors that affect reliability of nondestructive detection of flaws in structural ceramics
[NASA-TM-87348] p 61 N86-31912

- Flaw imaging and ultrasonic techniques for characterizing sintered silicon carbide
[NASA-TM-100177] p 63 N88-12106

SILICON NITRIDES

- Performance of Chevron-notch short bar specimen in determining the fracture toughness of silicon nitride and aluminum oxide
p 45 A80-50696

- Fracture toughness of brittle materials determined with chevron notch specimens
p 45 A81-32545

- Radiographic detectability limits for seeded voids in sintered silicon carbide and silicon nitride
p 51 A86-31745

- Nondestructive characterization of structural ceramics
p 46 A86-37141

- Reliability of void detection in structural ceramics by use of scanning laser acoustic microscopy
p 52 A86-39027

- Correlation of processing and sintering variables with the strength and radiography of silicon nitride
p 46 A87-12938

- Fracture toughness of Si₃N₄ measured with short bar chevron-notched specimens
p 46 A87-30621

- Quantitative void characterization in structural ceramics by use of scanning laser acoustic microscopy
p 53 A87-51974

- NDE for heat engine ceramics
[NASA-TM-86949] p 57 N85-20389

- Radiographic detectability limits for seeded voids in sintered silicon carbide and silicon nitride
[NASA-TM-86945] p 58 N85-21674

- Reliability of void detection in structural ceramics using scanning laser acoustic microscopy
[NASA-TM-87035] p 58 N85-32337

- Fractured toughness of Si₃N₄ measured with short bar chevron-notched specimens
[NASA-TM-87153] p 47 N86-13495

- Factors that affect reliability of nondestructive detection of flaws in structural ceramics
[NASA-TM-87348] p 61 N86-31912

- Quantitative void characterization in structural ceramics using scanning laser acoustic microscopy
[NASA-TM-88797] p 61 N86-31913

SINGLE CRYSTALS

- The tensile and fatigue deformation structures in a single crystal Ni-base superalloy
p 36 A86-35697

- The cyclic stress-strain behavior of a nickel-base superalloy at 650 C
p 36 A86-45715

- Low cycle fatigue of MAR-M 200 single crystals at 760 and 870 deg C
[NASA-TM-86933] p 41 N85-19074

- Creep-fatigue behavior of NiCoCrAlY coated PWA 1480 superalloy single crystals
[NASA-TM-87110] p 42 N86-10311

- Anisotropic constitutive model for nickel base single crystal alloys: Development and finite element implementation
[NASA-CR-175015] p 117 N86-21952

- Life prediction and constitutive models for engine hot section anisotropic materials program
[NASA-CR-174952] p 60 N86-25003

- Effects of a high mean stress on the high cycle fatigue life of PWA 1480 and correlation of data by linear elastic fracture mechanics
[NASA-CR-175057] p 118 N86-27689

- Bithermal low-cycle fatigue behavior of a NiCoCrAlY-coated single crystal superalloy
[NASA-TM-89831] p 45 N87-20408

SINGULARITY (MATHEMATICS)

- Moving singularity creep crack growth analysis with the /Delta T/c and C/asterisk/ integrals --- path-independent vector and energy rate line integrals
p 66 A82-40066

- Elasticity solutions for a class of composite laminate problems with stress singularities
p 17 A84-33389

SINTERING

- Reliability of void detection in structural ceramics by use of scanning laser acoustic microscopy
p 52 A86-39027

- Correlation of processing and sintering variables with the strength and radiography of silicon nitride
p 46 A87-12938

- Probability of detection of internal voids in structural ceramics using microfocus radiography
p 52 A87-14300

- Reliability of void detection in structural ceramics using scanning laser acoustic microscopy
[NASA-TM-87035] p 58 N85-32337

- Probability of detection of internal voids in structural ceramics using microfocus radiography
[NASA-TM-87164] p 59 N86-13749

SIZE DETERMINATION

- Quantitative void characterization in structural ceramics by use of scanning laser acoustic microscopy
p 53 A87-51974

- Quantitative void characterization in structural ceramics using scanning laser acoustic microscopy
[NASA-TM-88797] p 61 N86-31913

SIZE DISTRIBUTION

- Determination of grain size distribution function using two-dimensional Fourier transforms of tone pulse encoded images
[NASA-TM-88790] p 61 N86-31065

SOFTWARE ENGINEERING

- Integrated research in constitutive modelling at elevated temperatures, part 1
[NASA-CR-177237] p 120 N86-30227

SOLAR ARRAYS

- Array structure design handbook for stand alone photovoltaic applications
[NASA-TM-82629] p 96 N83-23631

SOLAR ENERGY

- Photovoltaic power system reliability considerations
[NASA-TM-79291] p 53 N80-15422

SOLID MECHANICS

Hybrid solid element with a traction-free cylindrical surface p 82 A86-34462

SOLID-SOLID INTERFACES

Interface cracks in adhesively bounded lap-shear joints p 67 A82-46109
A numerical analysis of contact and limit-point behavior in a class of problems of finite elastic deformation p 72 A84-27370

On the existence and stability conditions for mixed-hybrid finite element solutions based on Reissner's variational principle p 77 A85-33847

SOLIDIFICATION

Constitutive relationships for anisotropic high-temperature alloys [NASA-TM-83437] p 97 N83-28493

SOLIDS

Hybrid stress finite elements for large deformations of inelastic solids p 74 A85-15894
Measurement of ultrasonic velocity using phase-slope and cross-correlation methods p 51 A86-13192
Reliability of void detection in structural ceramics by use of scanning laser acoustic microscopy p 52 A86-39027

Micromechanically based constitutive relations for polycrystalline solids p 99 N83-34359
Preliminary investigation of an electrical network model for ultrasonic scattering [NASA-CR-3770] p 57 N84-17606

Ultrasonic velocity measurement using phase-slope cross-correlation methods [NASA-TM-83794] p 57 N84-34769

SOUND WAVES

Mechanics aspects of NDE by sound and ultrasound p 51 A83-25571

SPACE SHUTTLE MAIN ENGINE

Probabilistic structural analysis for space propulsion system components p 81 A86-28659
Cyclic structural analyses of anisotropic turbine blades for reusable space propulsion systems --- ssme fuel turbopump [NASA-TM-86990] p 108 N85-24339

Flow dynamic environment data base development for the SSME p 109 N85-26885
Overview of structural response: Probabilistic structural analysis p 110 N85-27952

Composite loads spectra for select space propulsion structural components p 110 N85-27953
Cyclic structural analyses of SSME turbine blades p 112 N85-27963

Simplified cyclic structural analyses of SSME turbine blades [NASA-TM-87214] p 116 N86-16615

Probabilistic structural analysis methods for space propulsion system components p 121 N87-13794
Nonlinear heat transfer and structural analyses of SSME turbine blades p 123 N87-22779

SPACE SHUTTLE PAYLOADS

The effect of nonlinearities on the dynamic response of a large shuttle payload [NASA-TM-88941] p 121 N87-18112

SPACE STATIONS

The 20th Aerospace Mechanics Symposium [NASA-CP-2423-REV] p 121 N87-16321

SPACECRAFT ANTENNAS

Composite space antenna structures - Properties and environmental effects p 20 A87-38610
Thermal expansion behavior of graphite/glass and graphite/magnesium p 21 A87-38615

Composite space antenna structures: Properties and environmental effects [NASA-TM-88859] p 31 N87-16880

SPACECRAFT COMPONENTS

Identification of structural interface characteristics using component mode synthesis [NASA-TM-88960] p 123 N87-24006

A high temperature fatigue and structures testing facility [NASA-TM-100151] p 124 N87-26399

SPACECRAFT CONSTRUCTION MATERIALS

ICAN: A versatile code for predicting composite properties [NASA-TM-87334] p 31 N86-31664

SPACECRAFT INSTRUMENTS

The 20th Aerospace Mechanics Symposium [NASA-CP-2423-REV] p 121 N87-16321

SPACECRAFT PROPULSION

Composite loads spectra for select space propulsion structural components: Probabilistic load model development p 110 N85-27954

Probabilistic structural analysis theory development p 111 N85-27955

Probabilistic finite element development p 111 N85-27956

SPECIMEN GEOMETRY

On composites with periodic structure p 67 A83-10283

Mode II fatigue crack growth specimen development p 83 A86-43566

Results of an interlaboratory fatigue test program conducted on alloy 800H at room and elevated temperatures p 37 A87-54370

Comparison tests and experimental compliance calibration of the proposed standard round compact plane strain fracture toughness specimen [NASA-TM-81379] p 87 N80-13513

Fracture toughness of brittle materials determined with chevron notch specimens [NASA-TM-81607] p 38 N80-32486

Mode 2 fatigue crack growth specimen development [NASA-TM-83722] p 104 N84-29248

Results of an interlaboratory fatigue test program conducted on alloy 800H at room and elevated temperatures [NASA-CR-174940] p 114 N85-32340

SPECKLE PATTERNS

Extending the laser-specklegram technique to strain analysis of rotating components p 67 A83-12514

SPECTRUM ANALYSIS

Formulation of blade-flutter spectral analyses in stationary reference frame [NASA-TP-2296] p 8 N84-20562

SPHERES

Ultrasonic wave propagation in two-phase media - Spherical inclusions p 17 A85-11926

SPHERICAL SHELLS

A numerical analysis of contact and limit-point behavior in a class of problems of finite elastic deformation p 72 A84-27370

SPIN TESTS

Lewis Research Center spin rig and its use in vibration analysis of rotating systems [NASA-TP-2304] p 9 N84-24578

SPLINE FUNCTIONS

Simple spline-function equations for fracture mechanics calculations p 63 A80-10832

SPRAYED COATINGS

Acoustic emission evaluation of plasma-sprayed thermal barrier coatings [ASME PAPER 84-GT-292] p 48 A84-47046

The low cycle fatigue behavior of a plasma-sprayed coating material [NASA-TM-87318] p 44 N86-31699

SPUTTERING

Ion beam sputter etching of orthopedic implanted alloy MP35N and resulting effects on fatigue [NASA-TM-81747] p 38 N81-21174

The 20th Aerospace Mechanics Symposium [NASA-CP-2423-REV] p 121 N87-16321

SQUEEZE FILMS

Engine dynamic analysis with general nonlinear finite element codes. II - Bearing element implementation, overall numerical characteristics and benchmarking [ASME PAPER 82-GT-292] p 47 A82-35462

Nonlinear transient finite element analysis of rotor-bearing-stator systems p 48 A84-20580
Experimental study of uncentralized squeeze film dampers [NASA-CR-168317] p 103 N84-19927

STABILITY

Nonlinear vibration and stability of rotating, pretwisted, precone blades including Coriolis effects p 86 A87-39896

Constrained self-adaptive solutions procedures for structure subject to high temperature elastic-plastic creep effects p 99 N83-34370

Stability and convergence of underintegrated finite element approximations p 105 N84-31696

Nonlinear bending-torsional vibration and stability of rotating, pretwisted, precone blades including Coriolis effects [NASA-TM-87207] p 116 N86-17789

STABLE OSCILLATIONS

Stability of limit cycles in frictionally damped and aerodynamically unstable rotor stages p 4 A86-19198

STAINLESS STEELS

Low cycle fatigue behavior of aluminum/stainless steel composites [AIAA 83-0806] p 16 A83-29886

Elastic-plastic finite-element analyses of thermally cycled single-edge wedge specimens [NASA-TP-1982] p 91 N82-20565

Creep crack-growth: A new path-independent T sub o and computational studies [NASA-CR-168930] p 92 N82-24503

Relation of cyclic loading pattern to microstructural fracture in creep fatigue [NASA-TM-83473] p 98 N83-34349

Tensile and compressive constitutive response of 316 stainless steel at elevated temperatures p 98 N83-34353

Environmental degradation of 316 stainless steel in high temperature low cycle fatigue [NASA-TM-89931] p 124 N87-24007

Creep life prediction based on stochastic model of microstructurally short crack growth [NASA-TM-100245] p 125 N88-12825

STANDING WAVES

Flutter and forced response of mistuned rotors using standing wave analysis [AIAA 83-0845] p 69 A83-29823

Flutter and forced response of mistuned rotors using standing wave analysis p 74 A85-12721

Vibration and flutter of mistuned bladed-disk assemblies [AIAA PAPER 84-0991] p 75 A85-16095

Vibration and flutter of mistuned bladed-disk assemblies [NASA-TM-83634] p 103 N84-23923

Flutter and forced response of mistuned rotors using standing wave analysis [NASA-CR-173555] p 9 N84-24586

STATIC LOADS

Hygrothermomechanical evaluation of transverse filament tape epoxy/polyester fiberglass composites p 17 A85-15632

Design procedures for fiber composite structural components - Rods, beams, and beam columns p 17 A85-15636

Hygrothermomechanical evaluation of transverse filament tape epoxy/polyester fiberglass composites [NASA-TM-83044] p 26 N83-15362

Design procedures for fiber composite structural components: Rods, columns and beam columns [NASA-TM-83321] p 26 N83-24559

STATISTICAL ANALYSIS

Durability/life of fiber composites in hygrothermomechanical environments p 16 A84-27359

Model development and statistical investigation of turbine blade mistuning p 2 A84-31905

Reliability of void detection in structural ceramics by use of scanning laser acoustic microscopy p 52 A86-39027

Probability of detection of internal voids in structural ceramics using microfocus radiography p 52 A87-14300

NDE reliability and process control for structural ceramics [ASME PAPER 87-GT-8] p 53 A87-48702

Statistical aspects of carbon fiber risk assessment modeling --- fire accidents involving aircraft [NASA-CR-159318] p 23 N80-29432

Durability/life of fiber composites in hygrothermomechanical environments [NASA-TM-82749] p 24 N82-14287

Statistical summaries of fatigue data for design purposes [NASA-CR-3697] p 97 N83-29731

Reliability of void detection in structural ceramics using scanning laser acoustic microscopy [NASA-TM-87035] p 58 N85-32337

Probability of detection of internal voids in structural ceramics using microfocus radiography [NASA-TM-87164] p 59 N86-13749

NDE reliability and process control for structural ceramics [NASA-TM-88870] p 61 N87-12910

STATISTICAL DISTRIBUTIONS

Creep-rupture reliability analysis p 79 A85-42566

Creep-rupture reliability analysis [NASA-CR-3790] p 102 N84-19925

STATISTICAL MECHANICS

Statistics and thermodynamics of fracture p 75 A85-19433

STATOR BLADES

Engine dynamic analysis with general nonlinear finite element codes. Part 2: Bearing element implementation overall numerical characteristics and benchmarking [NASA-CR-167944] p 7 N82-33390

STATORS

Nonlinear transient finite element analysis of rotor-bearing-stator systems p 48 A84-20580

STEADY STATE

Creep crack-growth: A new path-independent T sub o and computational studies [NASA-CR-168930] p 92 N82-24503

Digital computer program for generating dynamic turbofan engine models (DIGTEM) [NASA-TM-83446] p 8 N84-16185

STEELS

Failure analysis of a tool steel torque shaft p 51 A84-17546

- The crack layer approach to toughness characterization in steel p 36 A86-30010
- Crack layer morphology and toughness characterization in steels p 97 N83-27256
- [NASA-CR-168154] p 97 N83-27256
- The thermal fatigue resistance of H-13 Die Steel for aluminum die casting dies p 39 N83-35103
- [NASA-TM-83331] p 39 N83-35103
- Selection of rolling-element bearing steels for long-life application p 49 N87-11993
- [NASA-TM-88881] p 49 N87-11993
- STELLITE (TRADEMARK)**
- Interaction of high-cycle and low-cycle fatigue of Haynes 188 alloy at 1400 F deg p 111 N85-27961
- STIFFNESS**
- Application of traction drives as servo mechanisms p 114 N85-33520
- STIFFNESS MATRIX**
- Alternative ways for formulation of hybrid stress elements p 68 A83-14710
- On the suppression of zero energy deformation modes p 72 A84-21541
- Analysis of hourglass instabilities and control in underintegrated finite element methods p 74 A85-11125
- Finite elements based on consistently assumed stresses and displacements p 79 A86-18123
- Automatic finite element generators p 105 N84-31695
- Stability and convergence of underintegrated finite element approximations p 105 N84-31696
- STIRLING ENGINES**
- Fatigue failure of regenerator screens in a high frequency Stirling engine p 122 N87-18882
- [NASA-TM-88974] p 122 N87-18882
- STOCHASTIC PROCESSES**
- Probabilistic finite element development p 111 N85-27956
- STRAIN ENERGY METHODS**
- Moving singularity creep crack growth analysis with the $\Delta T/C$ and $C/\Delta T$ integrals --- path-independent vector and energy rate line integrals p 66 A82-40066
- On the suppression of zero energy deformation modes p 72 A84-21541
- STRAIN GAGES**
- Benchmark cyclic plastic notch strain measurements p 33 A84-11194
- STRAIN HARDENING**
- Finite elastic-plastic deformation of polycrystalline metals p 34 A84-43872
- Finite-strain large-deflection elastic-viscoplastic finite-element transient response analysis of structures [NASA-CR-159874] p 88 N80-29762
- STRAIN MEASUREMENT**
- Some advances in experimentation supporting development of viscoplastic constitutive models [NASA-CR-174855] p 109 N85-27260
- Some advances in experimentation supporting development of viscoplastic constitutive models p 113 N85-31545
- Closure of fatigue cracks at high strains [NASA-CR-175021] p 116 N86-17788
- High temperature stress-strain analysis p 125 N88-11170
- STRAIN RATE**
- On finite deformation elasto-plasticity p 66 A82-45869
- Environmental and high strain rate effects on composites for engine applications p 16 A84-17444
- Indentation law for composite laminates p 16 A84-27356
- Reliability considerations for the total strain range version of strainrange partitioning [NASA-CR-174757] p 106 N85-11380
- An update of the total-strain version of SRP [NASA-TP-2499] p 42 N86-12295
- Estimation of high temperature low cycle fatigue on the basis of inelastic strain and strainrate [NASA-TM-88841] p 44 N87-14489
- STRENGTH**
- Fundamentals of microcrack nucleation mechanics [NASA-CR-3851] p 57 N85-16195
- STRESS ANALYSIS**
- Continuous analysis of stresses from arbitrary surface loads on a half space p 64 A81-14162
- On the equivalence between semiempirical fracture analyses and R-curves p 64 A81-18792
- On the solution of creep induced buckling in general structure p 66 A82-39514
- Boundary-layer effects in composite laminates. I - Free-edge stress singularities. II - Free-edge stress solutions and basic characteristics p 67 A82-46806
- Moving cracks in layered composites p 67 A83-12048
- A new formulation of hybrid/mixed finite element p 67 A83-12739
- On the solution of elastic-plastic static and dynamic postbuckling collapse of general structure p 67 A83-12746
- Alternative ways for formulation of hybrid stress elements p 68 A83-14710
- Natural frequency of rotating beams using non-rotating modes p 68 A83-18383
- Turbine blade nonlinear structural and life analysis p 1 A83-29024
- An uncoupled viscoplastic constitutive model for metals at elevated temperature p 69 A83-29798
- [AIAA 83-1016] p 69 A83-29798
- Inelastic stress analyses at finite deformation through complementary energy approaches p 71 A84-13248
- Analyses of large quasistatic deformations of inelastic bodies by a new hybrid-stress finite element algorithm p 71 A84-16874
- Analyses of large quasistatic deformations of inelastic bodies by a new hybrid-stress finite element algorithm - Applications p 71 A84-16884
- Advanced reliability method for fatigue analysis p 72 A84-31596
- High temperature thermomechanical analysis of ceramic coatings p 74 A84-48565
- Rational approach for assumed stress finite elements p 74 A85-12029
- Hybrid stress finite elements for large deformations of inelastic solids p 74 A85-15894
- Interply layer degradation effects on composite structural response [AIAA PAPER 84-0849] p 18 A85-16096
- Development and testing of stable, invariant, isoparametric curvilinear 2- and 3-D hybrid-stress elements p 75 A85-19899
- Evolution of assumed stress hybrid finite element p 77 A85-35046
- Axisymmetric solid elements by a rational hybrid stress method p 78 A85-41109
- A study of interply layer effects on the free edge stress field of angleplated laminates p 18 A85-41127
- Finite element analysis of residual stress in plasma-sprayed ceramic p 46 A86-15226
- Finite elements based on consistently assumed stresses and displacements p 79 A86-18123
- Analysis of an externally radially crack ring segment subject to three-point radial loading p 79 A86-20710
- Stress analysis of gas turbine engine structures using the boundary element method p 81 A86-34444
- Hybrid solid element with a traction-free cylindrical surface p 82 A86-34462
- Dynamic stress analysis of smooth and notched fiber composite flexural specimens p 20 A86-41070
- Elastic analysis of a mode II fatigue crack test specimen p 84 A87-17799
- Assessment of simplified composite micromechanics using three-dimensional finite-element analysis p 20 A87-19121
- Effect of interference fits on roller bearing fatigue life p 48 A87-37686
- Simplified composite micromechanics for predicting microstresses p 87 A87-49275
- Prediction of fiber composite mechanical behavior made simple --- using a rocket calculator [NASA-TM-81404] p 22 N80-16107
- Calculation of residual principal stresses in CVD boron on carbon filaments [NASA-TM-81456] p 22 N80-20314
- Sudden stretching of a four layered composite plate [NASA-CR-159870] p 23 N80-25383
- Sudden bending of cracked laminates [NASA-CR-159860] p 23 N80-25384
- Instructions for the use of the CIVM-Jet 4C finite-strain computer code to calculate the transient structural responses of partial and/or complete arbitrarily-curved rings subjected to fragment impact [NASA-CR-159873] p 88 N80-27720
- Nonlinear laminate analysis for metal matrix fiber composites [NASA-TM-82596] p 24 N81-25149
- Elastic-plastic finite-element analyses of thermally cycled double-edge wedge specimens [NASA-TP-1973] p 92 N82-20566
- Boundary layer thermal stresses in angle-ply composite laminates, part 1 --- graphite-epoxy composites [NASA-CR-165412] p 93 N82-26713
- Analysis of cracks emanating from a circular hole in unidirectional fiber reinforced composites, part 2 [NASA-CR-165433] p 93 N82-26714
- Interlaminar crack growth in fiber reinforced composites during fatigue, part 3 [NASA-CR-165434] p 93 N82-26715
- Analysis of interface cracks in adhesively bonded lap shear joints, part 4 [NASA-CR-165438] p 93 N82-26716
- Edge delamination in angle-ply composite laminates, part 5 [NASA-CR-165439] p 94 N82-26717
- Boundary-layer effects in composite laminates: Free-edge stress singularities, part 6 [NASA-CR-165440] p 94 N82-26718
- A finite element stress analysis of spur gears including fillet radii and rim thickness effects [NASA-TM-82865] p 48 N82-28646
- On finite element stress analysis of spur gears [NASA-CR-167938] p 48 N82-29607
- Environmental and High-Strain Rate effects on composites for engine applications [NASA-TM-82882] p 25 N82-31449
- Benchmark notch test for life prediction [NASA-CR-165571] p 95 N83-12451
- Thermal stress analysis for a wood composite blade --- wind turbines [NASA-CR-173394] p 103 N84-21903
- Dynamic stress analysis of smooth and notched fiber composite flexural specimens [NASA-TM-83694] p 27 N84-25770
- Interply layer degradation effects on composite structural response [NASA-TM-83702] p 27 N84-26756
- Thermal-stress analysis for wood composite blade --- horizontal axis wind turbines [NASA-CR-173830] p 104 N84-31685
- Nonlinear Structural Analysis [NASA-CP-2297] p 105 N84-31688
- New variational formulations of hybrid stress elements p 105 N84-31690
- Inelastic and dynamic fracture and stress analyses p 106 N84-31697
- Nonlinear analysis for high-temperature composites: Turbine blades/vanes p 106 N84-31699
- On stress analysis of a crack-layer [NASA-CR-174774] p 106 N84-34774
- The 3-D inelastic analysis methods for hot section components: Brief description p 10 N85-10972
- A study of interply layer effects on the free-edge stress field of angleplated laminates [NASA-TM-86924] p 28 N85-15822
- Advanced stress analysis methods applicable to turbine engine structures [NASA-CR-175573] p 11 N85-21165
- 3-D inelastic analysis methods for hot section components (base program) --- turbine blades, turbine vanes, and combustor liners [NASA-CR-174700] p 107 N85-21686
- Component-specific modeling [NASA-CR-174765] p 110 N85-27261
- Component-specific modeling p 12 N86-11515
- Burner liner thermal-structural load modeling [NASA-CR-174892] p 117 N86-21932
- J-integral estimates for cracks in infinite bodies [NASA-CR-179474] p 119 N86-28467
- ICAN: A versatile code for predicting composite properties [NASA-TM-87334] p 31 N86-31664
- STRESS CONCENTRATION**
- Prediction of fiber composite mechanical behavior made simple p 63 A80-32067
- Development and testing of stable, invariant, isoparametric curvilinear 2- and 3-D hybrid-stress elements p 75 A85-19899
- On local total strain redistribution using a simplified cyclic inelastic analysis based on an elastic solution [AIAA PAPER 85-1419] p 78 A85-39770
- Comparison tests and experimental compliance calibration of the proposed standard round compact plane strain fracture toughness specimen [NASA-TM-81379] p 87 N80-13513
- The method of lines in three dimensional fracture mechanics [NASA-TM-81593] p 89 N80-32753
- Elevated temperature fatigue testing of metals p 38 N82-13281
- A preliminary study of crack initiation and growth at stress concentration sites [NASA-CR-169358] p 94 N82-33738
- A total life prediction model for stress concentration sites [NASA-CR-170290] p 96 N83-23629
- A total life prediction model for stress concentration sites [NASA-CR-168225] p 100 N84-10612
- Crack tip field and fatigue crack growth in general yielding and low cycle fatigue [NASA-CR-174686] p 41 N84-32503
- Local strain redistribution corrections for a simplified inelastic analysis procedure based on an elastic finite-element analysis [NASA-TP-2421] p 107 N85-20396

- On local total strain redistribution using a simplified cyclic inelastic analysis based on an elastic solution
[NASA-TM-86913] p 108 N85-21690
- On Hybrid and mixed finite element methods
[NASA-CR-175551] p 108 N85-23096
- Two simplified procedures for predicting cyclic material response from a strain history p 113 N85-31543
- Influence of load interactions on crack growth as related to state of stress and crack closure
[NASA-TM-87117] p 42 N86-12292
- A unique set of micromechanics equations for high temperature metal matrix composites
[NASA-TM-87154] p 30 N86-24757
- Experimental evaluation criteria for constitutive models of time dependent cyclic plasticity
[NASA-CR-176821] p 117 N86-25850
- STRESS CYCLES**
- Stress evaluations under rolling/sliding contacts
[NASA-CR-165561] p 91 N82-17521
- Two simplified procedures for predicting cyclic material response from a strain history p 113 N85-31543
- STRESS DISTRIBUTION**
- On stress field near a stationary crack tip
[AD-A152863] p 76 A85-24532
- A study of interply layer effects on the free edge stress field of angleplyed laminates p 18 A85-41127
- A study of interply layer effects on the free-edge stress field of angleplyed laminates
[NASA-TM-86924] p 28 N85-15822
- The effects of crack surface friction and roughness on crack tip stress fields
[NASA-TM-88976] p 122 N87-18881
- Free-edge delamination: Laminate width and loading conditions effects
[NASA-TM-100238] p 32 N88-12551
- STRESS FUNCTIONS**
- Recent advances in hybrid/mixed finite elements
[NASA-CR-175574] p 107 N85-21687
- STRESS INTENSITY FACTORS**
- Compliance and stress intensity coefficients for short bar specimens with chevron notches p 64 A80-46032
- Extended range stress intensity factor expressions for chevron-notched short bar and short rod fracture toughness specimens p 66 A82-40357
- Interface cracks in adhesively bounded lap-shear joints p 67 A82-46109
- Moving cracks in layered composites p 67 A83-12048
- Development of plane strain fracture toughness test for ceramics using Chevron notched specimens p 46 A84-11676
- Analysis of an internally radially cracked ring segment subject to three-point radial loading p 71 A84-18691
- Elasticity solutions for a class of composite laminate problems with stress singularities p 17 A84-33389
- Analysis of an externally radially crack ring segment subject to three-point radial loading p 79 A86-20710
- Experimental compliance calibration of the compact fracture toughness specimen
[NASA-TM-81665] p 89 N81-16492
- Stress intensity and displacement coefficients for radially cracked ring segments subject to three-point bending
[NASA-TM-83059] p 96 N83-24874
- Analysis of an externally radially cracked ring segment subject to three-point radial loading p 100 N83-35413
- Effect of crack curvature on stress intensity factors for ASTM standard compact tension specimens
[NASA-CR-168280] p 100 N84-11513
- On stress analysis of a crack-layer
[NASA-CR-174774] p 106 N84-34774
- Experimental compliance calibration of the NASA Lewis Research Center Mode 2 fatigue specimen
[NASA-TM-86908] p 107 N85-16205
- Influence of fatigue crack wake length and state of stress on crack closure p 43 N86-22686
- STRESS MEASUREMENT**
- On finite deformation elasto-plasticity p 66 A82-45869
- Extending the laser-specklegram technique to strain analysis of rotating components p 67 A83-12514
- Benchmark cyclic plastic notch strain measurements p 33 A84-11194
- STRESS RATIO**
- Practical implementation of the double linear damage rule and damage curve approach for treating cumulative fatigue damage
[NASA-TM-81517] p 88 N80-23684
- STRESS RELAXATION**
- Method for alleviating thermal stress damage in laminates --- metal matrix composites
[NASA-CASE-LEW-12493-1] p 23 N81-17170
- Constitutive modeling for isotropic materials (HOST)
[NASA-CR-174980] p 115 N86-10589

- Cyclic creep analysis from elastic finite-element solutions
[NASA-TM-87213] p 117 N86-25822
- STRESS WAVES**
- Acousto-ultrasonic characterization of fiber reinforced composites p 50 A81-44660
- Wave propagation in a graphite/epoxy laminate p 70 A83-44050
- Characterization of composite materials by means of the ultrasonic stress wave factor p 16 A84-10430
- Factors influencing the ultrasonic stress wave factor evaluation of composite material structures p 81 A86-34257
- Nondestructive evaluation of adhesive bond strength using the stress wave factor technique p 53 A87-32200
- Acousto-ultrasonic characterization of fiber reinforced composites
[NASA-TM-82651] p 54 N81-28458
- A study of the stress wave factor technique for the characterization of composite materials
[NASA-CR-3670] p 55 N83-27248
- The effect of stress on ultrasonic pulses in fiber reinforced composites p 56 N83-33180
- Input-output characterization of an ultrasonic testing system by digital signal analysis
[NASA-CR-3756] p 56 N84-15565
- Stress waves in an isotropic elastic plate excited by a circular transducer
[NASA-CR-3877] p 58 N85-20390
- Application of homomorphic signal processing to stress wave factor analysis
[NAS 1.26:174871] p 58 N85-21673
- A study of the stress wave factor technique for the characterization of composite materials
[NASA-CR-174870] p 29 N85-30035
- Ultrasonic evaluation of mechanical properties of thick, multilayered, filament wound composites
[NASA-TM-87088] p 58 N86-10561
- Stress waves in transversely isotropic media: The homogeneous problem
[NASA-CR-3977] p 59 N86-25002
- Ultrasonic stress wave characterization of composite materials
[NASA-CR-3976] p 60 N86-27665
- A study of the stress wave factor technique for nondestructive evaluation of composite materials
[NASA-CR-4002] p 60 N86-28445
- STRESS-STRAIN DIAGRAMS**
- Impact resistance of fiber composites p 66 A82-39852
- Simplified analytical procedures for representing material cyclic response --- for high temperature gas turbine engine analysis p 2 A84-22877
- Constitutive modeling and computational implementation for finite strain plasticity p 78 A85-40910
- Tensile and flexural strength of non-graphitic superhybrid composites: Predictions and comparisons
[NASA-TM-79276] p 21 N80-11144
- Simplified cyclic structural analyses of SSME turbine blades
[NASA-TM-87214] p 116 N86-16615
- STRESS-STRAIN RELATIONSHIPS**
- Mechanical property characterization of intraply hybrid composites p 13 A80-20954
- Nonlinear laminate analysis for metal matrix fiber composites
[AIAA 81-0579] p 15 A81-29411
- On the suppression of zero energy deformation modes p 72 A84-21541
- A simplified method for elastic-plastic-creep structural analysis
[ASME PAPER 84-GT-191] p 76 A85-23150
- Plasticity, viscoplasticity, and creep of solids by mechanical subelement models p 77 A85-35048
- Application of two creep fatigue life models for the prediction of elevated temperature crack initiation of a nickel base alloy
[AIAA PAPER 85-1420] p 35 A85-43979
- The cyclic stress-strain behavior of a nickel-base superalloy at 650 C p 36 A86-45715
- Comparison of elastic and elastic-plastic structural analyses for cooled turbine blade airfoils
[NASA-TP-1679] p 88 N80-27719
- Nonlinear laminate analysis for metal matrix fiber composites
[NASA-TM-82596] p 24 N81-25149
- Elastic-plastic finite-element analyses of thermally cycled single-edge wedge specimens
[NASA-TP-1982] p 91 N82-20565
- Elastic-plastic finite-element analyses of thermally cycled double-edge wedge specimens
[NASA-TP-1973] p 92 N82-20566

- Nonlinear constitutive theory for turbine engine structural analysis p 95 N82-33744
- Experimental verification of the Neuber relation at room and elevated temperatures --- to predict stress-strain behavior in notched specimens of hastelloy x
[NASA-CR-167967] p 96 N83-19121
- Development of a simplified analytical method for representing material cyclic response
[NASA-CR-168100] p 96 N83-21390
- Experimental verification of the number relation at room and elevated temperatures p 98 N83-34355
- Evaluation of inelastic constitutive models for nonlinear structural analysis p 98 N83-34357
- Simplified method for nonlinear structural analysis
[NASA-TP-2208] p 99 N83-34372
- A simplified method for elastic-plastic-creep structural analysis p 101 N84-14542
- Development of a simplified procedure for cyclic structural analysis
[NASA-TP-2243] p 103 N84-20878
- A computer program for predicting nonlinear uniaxial material responses using viscoplastic models
[NASA-TM-83675] p 104 N84-29247
- Local strain redistribution corrections for a simplified inelastic analysis procedure based on an elastic finite-element analysis
[NASA-TP-2421] p 107 N85-20396
- On thermomechanical testing in support of constitutive equation development for high temperature alloys
[NASA-CR-174879] p 109 N85-25894
- Cyclic structural analyses of SSME turbine blades p 112 N85-27963
- Finite element analysis of notch behavior using a state variable constitutive equation p 114 N85-31548
- Component-specific modeling
[NASA-CR-174925] p 12 N85-32119
- Experimental evaluation criteria for constitutive models of time dependent cyclic plasticity
[NASA-CR-176821] p 117 N86-25850
- Structural analysis of turbine blades using unified constitutive models p 119 N86-28461
- J-integral estimates for cracks in infinite bodies
[NASA-CR-179474] p 119 N86-28467
- Fatigue and fracture: Overview p 120 N87-11183
- Nonlinear heat transfer and structural analyses of SSME turbine blades p 123 N87-22779
- High temperature stress-strain analysis p 125 N88-11170
- STRESS-STRAIN-TIME RELATIONS**
- Constitutive modeling of cyclic plasticity and creep, using an internal time concept p 83 A86-41673
- Experimental evaluation criteria for constitutive models of time dependent cyclic plasticity
[NASA-CR-176821] p 117 N86-25850
- STRESSES**
- Theoretical and software considerations for nonlinear dynamic analysis
[NASA-CR-174504] p 101 N84-15589
- New variational formulations of hybrid stress elements p 105 N84-31690
- STRUCTURAL ANALYSIS**
- On the solution of creep induced buckling in general structure p 66 A82-39514
- On the automatic generation of FEM models for complex gears - A work-in-progress report p 47 A82-48243
- On composites with periodic structure p 67 A83-10283
- On the solution of elastic-plastic static and dynamic postbuckling collapse of general structure p 67 A83-12746
- The determination of the elastodynamic fields of an ellipsoidal inhomogeneity
[ASME PAPER 83-APM-19] p 69 A83-37388
- Comments on some problems in computational penetration mechanics p 71 A84-13545
- Analyses of large quasistatic deformations of inelastic bodies by a new hybrid-stress finite element algorithm p 71 A84-16874
- Analyses of large quasistatic deformations of inelastic bodies by a new hybrid-stress finite element algorithm - Applications p 71 A84-16884
- The structural response of a rail acceleration p 72 A84-32039
- Effects of structural coupling on mistuned cascade flutter and response
[ASME PAPER 83-GT-117] p 73 A84-33701
- Algorithms for elasto-plastic-creep postbuckling p 73 A84-38480
- Extension of constrained incremental Newton-Raphson scheme to generalized loading fields p 74 A85-13942
- Hybrid Semiloof elements for plates and shells based upon a modified Hu-Washizu principle p 74 A85-15893

- ICAN - Integrated composites analyzer
[AIAA PAPER 84-0974] p 18 A85-16094
- Interply layer degradation effects on composite structural response
[AIAA PAPER 84-0849] p 18 A85-16096
- Considerations for damage analysis of gas turbine hot section components
[ASME PAPER 84-PVP-77] p 2 A85-18792
- On the development of hierarchical solution strategies for nonlinear finite element formulations
p 126 A85-21979
- Evolution of assumed stress hybrid finite element
p 77 A85-35046
- Unified constitutive material models for nonlinear finite-element structural analysis --- gas turbine engine blades and vanes
[AIAA PAPER 85-1418] p 77 A85-39769
- On local total strain redistribution using a simplified cyclic inelastic analysis based on an elastic solution
[AIAA PAPER 85-1419] p 78 A85-39770
- NASA Lewis Research Center/university graduate research program on engine structures
[ASME PAPER 85-GT-159] p 80 A86-22084
- Hierarchical implicit dynamic least-square solution algorithm
p 80 A86-26689
- Vibration and buckling of rotating, pretwisted, precone beams including Coriolis effects
p 80 A86-26910
- Stress analysis of gas turbine engine structures using the boundary element method
p 81 A86-34444
- Iterative methods for mixed finite element equations
p 82 A86-34461
- A computer analysis program for interfacing thermal and structural codes
p 126 A86-36861
- Computer aided derivation of equations for composite mechanics problems and finite element analyses
[AIAA PAPER 86-1016] p 83 A86-38873
- Computational composite mechanics for aerospace propulsion structures
[AIAA PAPER 86-1190] p 19 A86-40596
- Computational engine structural analysis
[ASME PAPER 86-GT-70] p 5 A86-48141
- Unified constitutive materials model development and evaluation for high-temperature structural analysis applications --- for aircraft gas turbine engines
p 84 A86-49133
- Design concepts/parameters assessment and sensitivity analyses of select composite structural components
p 85 A87-25407
- Advances in 3-D Inelastic Analysis Methods for hot section components
[AIAA PAPER 87-0719] p 85 A87-33645
- Effect of time dependent flight loads on JT9D-7 performance deterioration
[NASA-CR-159681] p 87 N80-10515
- Comparison of elastic and elastic-plastic structural analyses for cooled turbine blade airfoils
[NASA-TP-1679] p 88 N80-27719
- Aeroelastic and dynamic finite element analyses of a bladed shrouded disk
[NASA-CR-159728] p 90 N81-19479
- NASTRAN level 16 programmer's manual updates for aeroelastic analysis of bladed discs
[NASA-CR-159825] p 90 N81-19482
- Integrated analysis of engine structures
[NASA-TM-82713] p 91 N82-11491
- Evaluation of inelastic constitutive models for nonlinear structural analysis --- for aircraft turbine engines
[NASA-TM-82845] p 92 N82-24502
- Bird impact analysis package for turbine engine fan blades
[NASA-TM-82831] p 92 N82-26701
- Environmental and High-Strain Rate effects on composites for engine applications
[NASA-TM-82882] p 25 N82-31449
- Nonlinear constitutive theory for turbine engine structural analysis
p 95 N82-33744
- Materials constitutive models for nonlinear analysis of thermally cycled structures
[NASA-TP-2055] p 95 N83-12449
- Effects of structural coupling on mistuned cascade flutter and response
[NASA-TM-83049] p 96 N83-15672
- Structural fatigue test results for large wind turbine blade sections
p 96 N83-19246
- Evaluation of inelastic constitutive models for nonlinear structural analysis
p 98 N83-34357
- Constrained self-adaptive solutions procedures for structure subject to high temperature elastic-plastic creep effects
p 99 N83-34370
- Simplified method for nonlinear structural analysis
[NASA-TP-2208] p 99 N83-34372
- The structural response of a rail accelerator
[NASA-TM-83491] p 99 N83-35412
- Engine cyclic durability by analysis and material testing
[NASA-TM-83577] p 102 N84-18683
- Development of a simplified procedure for cyclic structural analysis
[NASA-TP-2243] p 103 N84-20878
- Crack layer theory
[NASA-CR-174634] p 103 N84-22980
- ICAN: Integrated composites analyzer
[NASA-TM-83700] p 27 N84-26755
- Interply layer degradation effects on composite structural response
[NASA-TM-83702] p 27 N84-26756
- Nonlinear Structural Analysis
[NASA-CP-2297] p 105 N84-31688
- New variational formulations of hybrid stress elements
p 105 N84-31690
- Nonlinear finite element analysis of shells with large aspect ratio
p 105 N84-31692
- Self-adaptive solution strategies
p 105 N84-31693
- Element-by-element solution procedures for nonlinear structural analysis
p 105 N84-31694
- Inelastic and dynamic fracture and stress analyses
p 106 N84-31697
- Nonlinear analysis for high-temperature composites: Turbine blades/vanes
p 106 N84-31699
- Three-dimensional stress analysis using the boundary element method
p 106 N84-31700
- Fracture modes in notched angleply composite laminates
[NASA-TM-83802] p 28 N84-34576
- Turbine Engine Hot Section Technology (HOST)
[NASA-TM-83022] p 9 N85-10951
- Nonlinear structural and life analyses of a turbine blade
p 9 N85-10954
- Nonlinear structural and life analyses of a combustor liner
p 9 N85-10955
- Component-specific modeling
p 10 N85-10971
- The 3-D inelastic analysis methods for hot section components: Brief description
p 10 N85-10972
- Constitutive model development for isotropic materials
p 10 N85-10975
- Validation of structural analysis methods using the in-house linear cyclic rigs
p 10 N85-10987
- Engine cyclic durability by analysis and material testing
p 11 N85-15744
- NASA Lewis Research Center/University Graduate Research Program on Engine Structures
[NASA-TM-86916] p 107 N85-18375
- Nonlinear analysis for high-temperature multilayered fiber composite structures --- turbine blades
[NASA-TM-83754] p 29 N85-21273
- 3-D inelastic analysis methods for hot section components (base program) --- turbine blades, turbine vanes, and combustor liners
[NASA-CR-174700] p 107 N85-21686
- On local total strain redistribution using a simplified cyclic inelastic analysis based on an elastic solution
[NASA-TM-86913] p 108 N85-21690
- Geometrically nonlinear analysis of laminated elastic structures
[NASA-CR-175609] p 108 N85-21720
- Unified constitutive material models for nonlinear finite-element structural analysis --- gas turbine engine blades and vanes
[NASA-TM-86985] p 108 N85-24338
- Cyclic structural analyses of anisotropic turbine blades for reusable space propulsion systems --- ssme fuel turbopump
[NASA-TM-86990] p 108 N85-24339
- Vibration and buckling of rotating, pretwisted, precone beams including Coriolis effects
[NASA-TM-87004] p 109 N85-25893
- Nonlinear structural analysis for fiber-reinforced superalloy turbine blades
p 109 N85-26887
- A computer analysis program for interfacing thermal and structural codes
[NASA-TM-87021] p 110 N85-27264
- Probabilistic structural analysis theory development
p 111 N85-27955
- Probabilistic finite element: Variational theory
p 111 N85-27957
- Cyclic structural analyses of SSME turbine blades
p 112 N85-27963
- Structural analysis and cost estimate of an eight-leg space frame as a support structure for horizontal axis wind turbines
[NASA-TM-83470] p 112 N85-30361
- Two simplified procedures for predicting cyclic material response from a strain history
p 113 N85-31543
- Constitutive modeling for isotropic materials (HOST)
[NASA-CR-174980] p 115 N86-10589
- Turbine Engine Hot Section Technology (HOST)
[NASA-CP-2289] p 115 N86-11495
- HOST structural analysis program overview
p 12 N86-11513
- Component-specific modeling
p 12 N86-11515
- Simplified cyclic structural analyses of SSME turbine blades
[NASA-TM-87214] p 116 N86-16615
- Computational engine structural analysis
[NASA-TM-87231] p 116 N86-19663
- Integrated Composite Analyzer (ICAN): Users and programmers manual
[NASA-TP-2515] p 30 N86-21614
- Structural analysis of turbine blades using unified constitutive models
[NASA-TM-88807] p 119 N86-28461
- Fiber composite sandwich thermostructural behavior: Computational simulation
[NASA-TM-88787] p 31 N86-31663
- High temperature stress-strain analysis
p 120 N87-11209
- STAEBL: Structural tailoring of engine blades, phase 2
p 13 N87-1731
- Probabilistic structural analysis methods for space propulsion system components
[NASA-TM-88861] p 121 N87-13794
- Computational composite mechanics for aerospace propulsion structures
[NASA-TM-88965] p 31 N87-18614
- Nonlinear heat transfer and structural analyses of SSME turbine blades
p 123 N87-22779
- Finite element implementation of Robinson's unified viscoplastic model and its application to some uniaxial and multiaxial problems
[NASA-TM-89891] p 123 N87-23010
- Application of scanning acoustic microscopy to advanced structural ceramics
[NASA-TM-89929] p 62 N87-23987
- Finite element analysis of flexible, rotating blades
[NASA-TM-89906] p 124 N87-26385
- A high temperature fatigue and structures testing facility
[NASA-TM-100151] p 124 N87-26399
- Turbine Engine Hot Section Technology, 1985
[NASA-CP-2405] p 125 N88-11140
- High temperature stress-strain analysis
p 125 N88-11170
- ### STRUCTURAL DESIGN
- Structural tailoring of engine blades (STAEBL)
[AIAA 83-0828] p 1 A83-29737
- Finite element engine blade structural optimization
[AIAA PAPER 85-0645] p 76 A85-30313
- Probabilistic structural analysis to quantify uncertainties associated with turbopump blades
[AIAA PAPER 87-0766] p 85 A87-33581
- The application of probabilistic design theory to high temperature low cycle fatigue
[NASA-CR-165488] p 91 N82-14531
- Statistical summaries of fatigue data for design purposes
[NASA-CR-3697] p 97 N83-29731
- Design procedures for fiber composite structural components: Panels subjected to combined in-plane loads
[NASA-TM-86909] p 29 N85-15823
- ### STRUCTURAL DESIGN CRITERIA
- Sensitivity analysis results of the effects of various parameters on composite design
p 15 A82-37101
- Design procedures for fiber composite structural components - Rods, beams, and beam columns
p 17 A85-15636
- Structural optimization using optimality criteria methods
p 79 A85-48703
- Computational engine structural analysis
[ASME PAPER 86-GT-70] p 5 A86-48141
- Array structure design handbook for stand alone photovoltaic applications
[NASA-TM-82629] p 96 N83-23631
- Design procedures for fiber composite structural components: Rods, columns and beam columns
[NASA-TM-83321] p 26 N83-24559
- Nonlinear Constitutive Relations for High Temperature Applications
[NASA-CP-2271] p 98 N83-34351
- Structural analysis
p 9 N85-10969
- Overview of structural response: Probabilistic structural analysis
p 110 N85-27952
- Computational engine structural analysis
[NASA-TM-87231] p 116 N86-19663
- ### STRUCTURAL FAILURE
- On the solution of elastic-plastic static and dynamic postbuckling collapse of general structure
p 67 A83-12746
- Turbine blade nonlinear structural and life analysis
p 1 A83-29024
- Application of advanced reliability methods to local strain fatigue analysis
[NASA-CR-168198] p 97 N83-29734
- Progressive damage, fracture predictions and post mortem correlations for fiber composites
[NASA-TM-87101] p 29 N86-10290

STRUCTURAL MEMBERS

- Viscoplastic constitutive relationships with dependence on thermomechanical history
[NASA-CR-174836] p 108 N85-21691
- A comparison of smooth specimen and analytical simulation techniques for notched members at elevated temperatures p 114 N85-31546
- Extensions of the Ritz-Galerkin method for the forced, damped vibrations of structural elements p 117 N86-21909
- Identification of structural interface characteristics using component mode synthesis
[NASA-TM-88960] p 123 N87-24006

STRUCTURAL RELIABILITY

- Advanced reliability method for fatigue analysis p 72 A84-31596
- Overview of structural response: Probabilistic structural analysis p 110 N85-27952

STRUCTURAL STABILITY

- Stability of large horizontal-axis axisymmetric wind turbines p 64 A81-22526
- Growth and stability of interacting surface flaws of arbitrary shape p 68 A83-15060
- On the existence and stability conditions for mixed-hybrid finite element solutions based on Reissner's variational principle p 77 A85-33847
- Probabilistic structural analysis for space propulsion system components p 81 A86-28659
- Aeroelastic behavior of low aspect ratio metal and composite blades
[ASME PAPER 86-GT-243] p 84 A86-48271
- Large displacements and stability analysis of nonlinear propeller structures p 95 N83-12460

STRUCTURAL STRAIN

- A solution procedure for behavior of thick plates on a nonlinear foundation and postbuckling behavior of long plates
[NASA-TP-2174] p 99 N83-34373

STRUCTURAL VIBRATION

- Vibration and buckling of rectangular plates under in-plane hydrostatic loading p 64 A80-45364
- Effects of mistuning on blade torsional flutter p 64 A81-29095
- Vibrations of cantilevered shallow cylindrical shells of rectangular planform p 65 A82-11298
- Vibrations of cantilevered doubly-curved shallow shells p 70 A83-39557
- Analysis of an axial compressor blade vibration based on wave reflection theory
[ASME PAPER 83-GT-151] p 2 A83-47970
- Vibrations of blades with variable thickness and curvature by shell theory
[ASME PAPER 83-GT-152] p 70 A83-47978
- NASTRAN forced vibration analysis of rotating cyclic structures
[ASME PAPER 83-DET-20] p 72 A84-29103
- Stagger angle dependence of inertial and elastic coupling in bladed disks p 72 A84-31903
- Model development and statistical investigation of turbine blade mistuning p 2 A84-31905
- Vibration and flutter of mistuned bladed-disk assemblies
[AIAA PAPER 84-0991] p 75 A85-16095
- Natural frequencies of twisted rotating plates p 76 A85-32343
- Vibration and flutter of mistuned bladed-disk assemblies p 3 A85-45854
- Vibrations of twisted cantilever plates - A comparison of theoretical results p 79 A85-47626
- Vibration analysis of rotating turbomachinery blades by an improved finite difference method p 3 A86-14338
- Vibration characteristics of mistuned shrouded blade assemblies
[ASME PAPER 85-GT-115] p 4 A86-22068
- The dynamics of a flexible bladed disc on a flexible rotor in a two-rotor system p 4 A86-25743
- Vibrations of blades and bladed disk assemblies; Proceedings of the Tenth Biennial Conference on Mechanical Vibration and Noise, Cincinnati, OH, September 10-13, 1985 p 4 A86-26901
- On the equivalence of the incremental harmonic balance method and the harmonic balance-Newton Raphson method p 83 A86-40695
- Influence of third-degree geometric nonlinearities on the vibration and stability of pretwisted, preconed, rotating blades p 6 A87-46228
- An improved finite-difference analysis of uncoupled vibrations of tapered cantilever beams
[NASA-TM-83495] p 101 N84-13610
- Improved finite-difference vibration analysis of pretwisted, tapered beams
[NASA-TM-83549] p 102 N84-16588
- Vibration and flutter of mistuned bladed-disk assemblies
[NASA-TM-83634] p 103 N84-23923

- NASTRAN forced vibration analysis of rotating cyclic structures
[NASA-CR-173821] p 104 N84-29252
- Influence of third-degree geometric nonlinearities on the vibration and stability of pretwisted, preconed, rotating blades
[NASA-TM-87307] p 120 N86-31920

STUDS (STRUCTURAL MEMBERS)

- Improved stud configurations for attaching laminated wood wind turbine blades
[NASA-TM-87109] p 115 N86-10582

SUBSONIC FLUTTER

- Flutter of turbofan rotors with mistuned blades p 74 A85-12716
- Aeroelastic characteristics of a cascade of mistuned blades in subsonic and supersonic flows --- turbofan engines
[NASA-TM-82631] p 90 N81-26492

SUPERHYBRID MATERIALS

- Superhybrid composite blade impact studies
[ASME PAPER 81-GT-24] p 1 A81-29940
- Fabrication and quality assurance processes for superhybrid composite fan blades p 20 A87-19123
- Fabrication and quality assurance processes for superhybrid composite fan blades
[NASA-TM-83354] p 28 N85-14882

SUPERSONIC COMPRESSORS

- Mass balancing of hollow fan blades
[ASME PAPER 86-GT-195] p 84 A86-48245

SUPERSONIC FLUTTER

- The effect of aerodynamic and structural detuning on turbomachine supersonic unstalled torsional flutter
[AIAA PAPER 85-0761] p 3 A85-30378
- Aerodynamic and structural detuning of supersonic turbomachine rotors p 5 A86-31595
- Influence of friction dampers on torsional blade flutter
[ASME PAPER 85-GT-170] p 5 A86-32957
- The effect of circumferential aerodynamic detuning on coupled bending-torsion unstalled supersonic flutter
[ASME PAPER 86-GT-100] p 6 A87-25396

SUPERSONIC TURBINES

- Forced response analysis of an aerodynamically detuned supersonic turbomachine rotor p 5 A86-26902

SURFACE CRACKS

- Continuous analysis of stresses from arbitrary surface loads on a half space p 64 A81-14162
- Evaluation of the effect of crack closure on fatigue crack growth of simulated short cracks
[NASA-TM-83778] p 40 N84-31348

SURFACE DEFECTS

- Growth and stability of interacting surface flaws of arbitrary shape p 68 A83-15060

SURFACE FINISHING

- Reliability of void detection in structural ceramics by use of scanning laser acoustic microscopy p 52 A86-39027
- Reliability of void detection in structural ceramics using scanning laser acoustic microscopy
[NASA-TM-87035] p 58 N85-32337

SURFACE PROPERTIES

- Fracture surface characteristics of notched angleplied graphite/epoxy composites
[NASA-TM-83786] p 28 N84-33522
- Interaction of high-cycle and low-cycle fatigue of Haynes 188 alloy at 1400 F deg p 111 N85-27961
- A constitutive law for finite element contact problems with unclassical friction
[NASA-TM-88838] p 120 N87-12924
- Surface flaw reliability analysis of ceramic components with the SCARE finite element postprocessor program
[NASA-TM-88901] p 121 N87-17087

SURFACE ROUGHNESS

- The role of the reflection coefficient in precision measurement of ultrasonic attenuation p 51 A85-42151
- Quantitative flaw characterization with scanning laser acoustic microscopy p 52 A86-45150
- The role of the reflection coefficient in precision measurement of ultrasonic attenuation
[NASA-TM-83788] p 57 N84-32849
- The effects of crack surface friction and roughness on crack tip stress fields
[NASA-TM-88976] p 122 N87-18881

SURFACE ROUGHNESS EFFECTS

- Quantitative flaw characterization with scanning laser acoustic microscopy p 52 A86-45150

SWEEP EFFECT

- Flutter of swept fan blades
[ASME PAPER 84-GT-138] p 77 A85-32962
- Flutter of swept fan blades
[NASA-TM-83547] p 102 N84-16587

SWELLING

- Prediction of composite hygral behavior made simple p 16 A84-14285

- Prediction of composite hygral behavior made simple
[NASA-TM-82780] p 24 N82-16181

SYSTEMS ENGINEERING

- Fatigue criterion to system design, life and reliability
[AIAA PAPER 85-1140] p 78 A85-40814
- Fatigue criterion to system design, life, and reliability p 85 A87-27986
- Fatigue criterion to system design, life and reliability
[NASA-TM-87017] p 49 N85-27226

T**TANTALUM ALLOYS**

- Relation of cyclic loading pattern to microstructural fracture in creep fatigue
[NASA-TM-83473] p 98 N83-34349

TAPERED COLUMNS

- An improved finite-difference analysis of uncoupled vibrations of tapered cantilever beams
[NASA-TM-83495] p 101 N84-13610

TAPERING

- Vibrations of blades with variable thickness and curvature by shell theory
[ASME PAPER 83-GT-152] p 70 A83-47978

TAXIING

- Temperature distribution in an aircraft tire at low ground speeds
[NASA-TP-2195] p 97 N83-33217

TECHNOLOGY ASSESSMENT

- A quarter-century of progress in the development of correlation and extrapolation methods for creep rupture data p 63 A80-38142
- Concepts and techniques for ultrasonic evaluation of material mechanical properties
[NASA-TM-81523] p 53 N80-24634
- A survey of unified constitutive theories p 112 N85-31531

TEMPERATURE DEPENDENCE

- Predicting the time-temperature dependent axial failure of B/AI composites p 14 A80-35494
- Orientation and temperature dependence of some mechanical properties of the single-crystal nickel-base superalloy Rene N4. II - Low cycle fatigue behavior p 37 A86-50322
- Predicting the time-temperature dependent axial failure of B/AI composites
[NASA-TM-81474] p 22 N80-21452
- Research and development program for the development of advanced time-temperature dependent constitutive relationships. Volume 1: Theoretical discussion
[NASA-CR-168191-VOL-1] p 100 N84-10613
- A survey of unified constitutive theories p 112 N85-31531
- The low cycle fatigue behavior of a plasma-sprayed coating material
[NASA-TM-87318] p 44 N86-31699

TEMPERATURE DISTRIBUTION

- Temperature distribution in an aircraft tire at low ground speeds
[NASA-TP-2195] p 97 N83-33217
- Burner liner thermal-structural load modeling
[NASA-CR-174892] p 117 N86-21932

TEMPERATURE EFFECTS

- Engine environmental effects on composite behavior --- moisture and temperature effects on mechanical properties
[AIAA 80-0695] p 1 A80-35101
- Cyclic behavior of turbine disk alloys at 650 C p 32 A81-12266
- On the solution of creep induced buckling in general structure p 66 A82-39514
- An uncoupled viscoplastic constitutive model for metals at elevated temperature
[AIAA 83-1016] p 69 A83-29798
- Design procedures for fiber composite structural components - Rods, beams, and beam columns p 17 A85-15636
- Design procedures for fiber composite structural components: Rods, columns and beam columns
[NASA-TM-83321] p 26 N83-24559
- Mechanical behavior of carbon-carbon composites
[NASA-CR-174767] p 28 N84-34575
- Nonlinear Constitutive Relations for High Temperature Application, 1984 p 112 N85-31530
- On the use of internal state variables in thermoviscoplastic constitutive equations p 113 N85-31536
- A unique set of micromechanics equations for high temperature metal matrix composites
[NASA-TM-87154] p 30 N86-24757
- Micromechanisms of thermomechanical fatigue: A comparison with isothermal fatigue
[NASA-TM-87331] p 44 N86-28164

- Integrated research in constitutive modelling at elevated temperatures, part 2
[NASA-CR-177233] p 119 N86-28455
- Integrated research in constitutive modelling at elevated temperatures, part 1
[NASA-CR-177237] p 120 N86-30227
- TEMPERATURE GRADIENTS**
Analysis of large, non-isothermal elastic-visco-plastic deformations
[NASA-CR-176220] p 115 N86-10588
Effect of design variables, temperature gradients and speed of life and reliability of a rotating disk
[NASA-TM-88883] p 49 N87-13755
- TEMPERATURE MEASUREMENT**
Aerothermal modeling. Executive summary
[NASA-CR-168330] p 7 N84-15152
- TENSILE CREEP**
Tensile and compressive constitutive response of 316 stainless steel at elevated temperatures p 98 N83-34353
- TENSILE DEFORMATION**
Tensile buckling of advanced turboprops p 71 A84-11039
- TENSILE PROPERTIES**
Influence of fatigue crack wake length and state of stress on crack closure
[NASA-TM-87292] p 43 N86-22686
- TENSILE STRENGTH**
Simplified composite micromechanics equations for strength, fracture toughness and environmental effects p 17 A84-41858
Design procedures for fiber composite structural components - Rods, beams, and beam columns p 17 A85-15636
Tensile and flexural strength of non-graphitic superhybrid composites: Predictions and comparisons
[NASA-TM-79276] p 21 N80-11144
Design procedures for fiber composite structural components: Rods, columns and beam columns
[NASA-TM-83321] p 26 N83-24559
- TENSILE STRESS**
Tensile buckling of advanced turboprops
[AIAA PAPER 82-0776] p 67 A83-10900
Ion beam sputter etching of orthopedic implanted alloy MP35N and resulting effects on fatigue
[NASA-TM-81747] p 38 N81-21174
Tensile buckling of advanced turboprops
[NASA-TM-82896] p 94 N82-31708
Benchmark notch test for life prediction
[NASA-CR-165571] p 95 N83-12451
The effect of stress on ultrasonic pulses in fiber reinforced composites p 56 N83-33180
A continuous damage model based on stepwise-stress creep rupture tests
[NASA-CR-174941] p 114 N85-32341
- TENSILE TESTS**
Fracture modes of high modulus graphite/epoxy angleplied laminates subjected to off-axis tensile loads p 14 A80-32069
Impact resistance of fiber composites p 66 A82-39852
Fracture toughness of hot-pressed beryllium p 34 A85-25835
Constitutive modeling and computational implementation for finite strain plasticity p 78 A85-40910
The tensile and fatigue deformation structures in a single crystal Ni-base superalloy p 36 A86-35697
A study of spectrum fatigue crack propagation in two aluminum alloys. I - Spectrum simplification. II - Influence of microstructures p 36 A86-48973
Fracture modes of high modulus graphite/epoxy angleplied laminates subjected to off-axis tensile loads
[NASA-TM-81405] p 21 N80-16102
Constitutive modeling for isotropic materials (HOST)
[NASA-CR-174980] p 115 N86-10589
Yielding and deformation behavior of the single crystal nickel-base superalloy PWA 1480
[NASA-CR-175100] p 44 N86-25455
- TEST FACILITIES**
HOST liner cyclic facilities: Facility description p 10 N85-10988
A high temperature fatigue and structures testing facility
[NASA-TM-100151] p 124 N87-26399
- TEST STANDS**
HOST liner cyclic facilities: Facility description p 10 N85-10988
Simplified cyclic structural analyses of SSME turbine blades
[NASA-TM-87214] p 116 N86-16615
- THERMAL ANALYSIS**
High temperature thermomechanical analysis of ceramic coatings p 74 A84-48565
- Composite sandwich thermostructural behavior - Computational simulation
[AIAA PAPER 86-0948] p 82 A86-38842
- THERMAL BUCKLING**
Quasi-static solution algorithms for kinematically/materially nonlinear thermomechanical problems p 78 A85-41983
- THERMAL CONTROL COATINGS**
Acoustic emission evaluation of plasma-sprayed thermal barrier coatings
[ASME PAPER 84-GT-292] p 48 A84-47046
- THERMAL CYCLING TESTS**
Metallurgical instabilities during the high temperature low cycle fatigue of nickel-base superalloys p 33 A83-22019
An uncoupled viscoplastic constitutive model for metals at elevated temperature p 69 A83-29798
Simplified analytical procedures for representing material cyclic response --- for high temperature gas turbine engine analysis p 2 A84-22877
Fracture mechanics applied to nonisothermal fatigue crack growth p 36 A86-28951
The cyclic stress-strain behavior of a nickel-base superalloy at 650 C p 36 A86-45715
Three dimensional finite-element elastic analysis of a thermally cycled double-edge wedge geometry specimen --- nickel alloy turbine parts
[NASA-TM-80980] p 37 N80-26433
Thermal fatigue and oxidation data of TAZ-8A and M22 alloys and variations p 38 N82-10193
Elastic-plastic finite-element analyses of thermally cycled single-edge wedge specimens
[NASA-TP-1982] p 91 N82-20565
Elastic-plastic finite-element analyses of thermally cycled double-edge wedge specimens
[NASA-TP-1973] p 92 N82-20566
High temperature low cycle fatigue mechanisms for nickel base and a copper base alloy
[NASA-CR-3543] p 39 N82-26436
Microstructural effects on the room and elevated temperature low cycle fatigue behavior of Waspaloy
[NASA-CR-165497] p 93 N82-26702
Preliminary study of thermomechanical fatigue of polycrystalline MAR-M 200 p 40 N84-17350
Validation of structural analysis methods using the in-house liner cyclic rigs p 10 N85-10987
HOST liner cyclic facilities: Facility description p 10 N85-10988
- THERMAL EXPANSION**
Composite space antenna structures - Properties and environmental effects p 20 A87-38610
Thermal expansion behavior of graphite/glass and graphite/magnesium p 21 A87-38615
Prediction of composite thermal behavior made simple
[NASA-TM-81618] p 23 N81-16132
Fiber composite sandwich thermostructural behavior: Computational simulation p 31 N86-31663
Composite space antenna structures: Properties and environmental effects p 31 N87-16880
- THERMAL FATIGUE**
Comparative thermal fatigue resistance of several oxide dispersion strengthened alloys p 32 A82-11399
Metallurgical instabilities during the high temperature low cycle fatigue of nickel-base superalloys p 33 A83-22019
The effect of microstructure on 650 C fatigue crack growth in P/M Astroloy p 33 A84-12395
High-temperature fatigue in metals - A brief review of life prediction methods developed at the Lewis Research Center of NASA p 33 A84-14286
Simplified analytical procedures for representing material cyclic response --- for high temperature gas turbine engine analysis p 2 A84-22877
A study of fatigue damage mechanisms in Waspaloy from 25 to 800 C p 34 A85-12098
Considerations for damage analysis of gas turbine hot section components p 2 A85-18792
[ASME PAPER 84-PVP-77] p 2 A85-18792
Thermal-mechanical fatigue crack growth in Inconel X-750 p 35 A86-20982
Thermal fatigue and oxidation data for directionally solidified MAR-M 246 turbine blades p 6 N80-21330
[NASA-CR-159798] p 6 N80-21330
Thermal fatigue and oxidation data of oxide dispersion-strengthened alloys p 37 N80-25415
[NASA-CR-159842] p 37 N80-25415
Thermal fatigue and oxidation data of TAZ-8A and M22 alloys and variations p 38 N82-10193
[NASA-CR-165407] p 38 N82-10193
Thermal fatigue resistance of cobalt-modified UDIMET 700 p 39 N83-11289
- The thermal fatigue resistance of H-13 Die Steel for aluminum die casting dies p 39 N83-35103
[NASA-TM-83331] p 39 N83-35103
Preliminary study of thermomechanical fatigue of polycrystalline MAR-M 200 p 40 N84-17350
[NASA-TP-2280] p 40 N84-17350
Engine cyclic durability by analysis and material testing
[NASA-TM-83577] p 102 N84-18683
Engine cyclic durability by analysis and material testing p 11 N85-15744
Thermal-mechanical fatigue crack growth in Inconel X-750 p 41 N85-15877
[NASA-CR-174740] p 41 N85-15877
Thermal-mechanical fatigue behavior of nickel-base superalloys p 43 N86-24818
[NASA-CR-175048] p 43 N86-24818
Low-cycle thermal fatigue
[NASA-TM-87225] p 118 N86-26651
Thermal-fatigue and oxidation resistance of cobalt-modified Udimet 700 alloy
[NASA-TP-2591] p 119 N86-28464
- THERMAL PROTECTION**
Acoustic emission evaluation of plasma-sprayed thermal barrier coatings
[ASME PAPER 84-GT-292] p 48 A84-47046
- THERMAL STRESSES**
High temperature thermomechanical analysis of ceramic coatings p 74 A84-48565
Inelastic high-temperature thermomechanical response of ceramic coated gas turbine seals p 82 A86-37799
Toward improved durability in advanced combustors and turbines - Progress in prediction of thermomechanical loads p 6 A86-48224
[ASME PAPER 86-GT-172] p 6 A86-48224
Prediction of composite thermal behavior made simple
[NASA-TM-81618] p 23 N81-16132
Method for alleviating thermal stress damage in laminates --- metal matrix composites
[NASA-CASE-LEW-12493-1] p 23 N81-17170
Method for alleviating thermal stress damage in laminates p 24 N81-26179
[NASA-CASE-LEW-12493-2] p 24 N81-26179
The application of probabilistic design theory to high temperature low cycle fatigue
[NASA-CR-165488] p 91 N82-14531
Boundary layer thermal stresses in angle-ply composite laminates, part 1 --- graphite-epoxy composites
[NASA-CR-165412] p 93 N82-26713
Thermal stress analysis for a wood composite blade --- wind turbines p 103 N84-21903
[NASA-CR-173394] p 103 N84-21903
Hygrothermomechanical fracture stress criteria for fiber composites with sense-parity p 27 N84-28918
[NASA-CR-83691] p 27 N84-28918
Thermal-stress analysis for wood composite blade --- horizontal axis wind turbines p 104 N84-31685
[NASA-CR-173830] p 104 N84-31685
HOST structural analysis program overview p 12 N86-11513
- Low-cycle thermal fatigue p 118 N86-26651
[NASA-TM-87225] p 118 N86-26651
SINDA-NASTRAN interfacing program theoretical description and user's manual p 124 N87-27268
[NASA-TM-100158] p 124 N87-27268
Toward improved durability in advanced combustors and turbines: Progress in the prediction of thermomechanical loads p 13 N87-28551
[NASA-TM-88932] p 13 N87-28551
- THERMODYNAMIC CYCLES**
Evaluation of inelastic constitutive models for nonlinear structural analysis --- for aircraft turbine engines p 92 N82-24502
[NASA-TM-82845] p 92 N82-24502
Cyclic creep analysis from elastic finite-element solutions p 117 N86-25822
[NASA-TM-87213] p 117 N86-25822
- THERMODYNAMIC PROPERTIES**
Micromechanics of intraply hybrid composites: Elastic and thermal properties p 14 A80-27994
Computer code for intraply hybrid composite design p 15 A81-44662
Simplified composite micromechanics equations of hygral, thermal, and mechanical properties p 17 A84-49377
[AIAA PAPER 84-0974] p 18 A85-16094
Micromechanics of intraply hybrid composites: Elastic and thermal properties p 21 N80-11143
[NASA-TM-79253] p 21 N80-11143
Combustor liner durability analysis p 7 N81-17079
[NASA-CR-165250] p 7 N81-17079
Designing with fiber-reinforced plastics (planar random composites) p 25 N82-24300
[NASA-TM-82812] p 25 N82-24300

- Simplified composite micromechanics equations for hygral, thermal and mechanical properties
[NASA-TM-83320] p 26 N83-19817
ICAN: Integrated composites analyzer
[NASA-TM-83700] p 27 N84-26755
On thermomechanical testing in support of constitutive equation development for high temperature alloys
[NASA-CR-174879] p 109 N85-25894
Thermoviscoplastic nonlinear constitutive relationships for structural analysis of high temperature metal matrix composites
[NASA-TM-87291] p 30 N86-24756
Formulation of the nonlinear analysis of shell-like structures, subjected to time-dependent mechanical and thermal loading
[NASA-CR-177194] p 119 N86-28462

THERMODYNAMICS

- Statistics and thermodynamics of fracture
p 75 A85-19433
Thermodynamically consistent constitutive equations for nonisothermal large strain, elasto-plastic, creep behavior
[AIAA PAPER 85-0621] p 77 A85-38425
Designing for fiber composite structural durability in hygrothermomechanical environments
p 19 A86-27734
Computer code for intraply hybrid composite design
[NASA-TM-82593] p 24 N81-25151
Hygrothermomechanical evaluation of transverse filament tape epoxy/polyester fiberglass composites
[NASA-TM-83044] p 26 N83-15362
INHVD: Computer code for intraply hybrid composite design. A users manual
[NASA-TP-2239] p 26 N84-13224
Crack layer theory
[NASA-CR-174634] p 103 N84-22980
Viscoplastic constitutive relationships with dependence on thermomechanical history
[NASA-CR-174836] p 108 N85-21691
Dynamic creep buckling: Analysis of shell structures subjected to time-dependent mechanical and thermal loading
p 111 N85-27959
Designing for fiber composite structural durability in hygrothermomechanical environment
[NASA-TM-87045] p 29 N85-27978
Component-specific modeling
p 12 N86-11515
Thermal-mechanical fatigue behavior of nickel-base superalloys
[NASA-CR-175048] p 43 N86-24818
Integrated research in constitutive modelling at elevated temperatures, part 1
[NASA-CR-177237] p 120 N86-30227
Calculation of thermomechanical fatigue life based on isothermal behavior
[NASA-TM-88864] p 122 N87-20565

THERMOELASTICITY

- Quasi-static solution algorithms for kinematically/materially nonlinear thermomechanical problems
p 78 A85-41983
Translational and extensional energy release rates (the J- and M-integrals) for a crack layer in thermoelasticity
[NASA-CR-174872] p 107 N85-21685
A review of path-independent integrals in elastic-plastic fracture mechanics, task 4
[NASA-CR-174956] p 114 N85-33541

THERMOMECHANICAL TREATMENT

- Effects of processing and microstructure on the fatigue behaviour of the nickel-base superalloy Rene95
p 34 A84-48715
Select fiber composites for space applications - A mechanistic assessment
p 18 A85-16040
Quasi-static solution algorithms for kinematically/materially nonlinear thermomechanical problems
p 78 A85-41983
Simplified method for nonlinear structural analysis
[NASA-TP-2208] p 99 N83-34372
Select fiber composites for space applications: A mechanistic assessment
[NASA-TM-83631] p 26 N84-22702
Analysis of shell type structures subjected to time dependent mechanical and thermal loading
[NASA-CR-175747] p 109 N85-25896
Multiaxial and thermomechanical fatigue considerations in damage tolerant design
[NASA-TM-87022] p 42 N85-26964
Thermomechanical deformation in the presence of metallurgical changes
p 112 N85-31533

THERMOPLASTIC RESINS

- Designing with fiber-reinforced plastics (planar random composites)
[NASA-TM-82812] p 25 N82-24300

THERMOPLASTICITY

- Nonlinear structural and life analyses of a combustor liner
p 68 A83-12764
Simplified analytical procedures for representing material cyclic response --- for high temperature gas turbine engine analysis
p 2 A84-22877

- Inelastic high-temperature thermomechanical response of ceramic coated gas turbine seals
p 82 A86-37799
Nonlinear structural and life analyses of a combustor liner
[NASA-TM-82846] p 92 N82-24501
Nonlinear structural and life analyses of a combustor liner
p 9 N85-10955

THERMOSETTING RESINS

- Designing with fiber-reinforced plastics (planar random composites)
[NASA-TM-82812] p 25 N82-24300

THERMOVISCOELASTICITY

- Research and development program for the development of advanced time-temperature dependent constitutive relationships. Volume 2: Programming manual
[NASA-CR-168191-VOL-2] p 100 N84-10614
Thermoviscoplastic nonlinear constitutive relationships for structural analysis of high temperature metal matrix composites
[NASA-TM-87291] p 30 N86-24756

THICKNESS

- A finite element stress analysis of spur gears including fillet radii and rim thickness effects
[NASA-TM-82865] p 48 N82-28646

THICKNESS RATIO

- Joint research effort on vibrations of twisted plates, phase 1: Final results
[NASA-RP-1150] p 115 N86-10579

THIN BODIES

- Finite-strain large-deflection elastic-viscoplastic finite-element transient response analysis of structures
[NASA-CR-159874] p 88 N80-29762

THIN PLATES

- A mixed shear flexible finite element for the analysis of laminated plates
p 73 A84-45994

THIN WALLED SHELLS

- Dynamic creep buckling: Analysis of shell structures subjected to time-dependent mechanical and thermal loading
p 111 N85-27959
Formulation of the nonlinear analysis of shell-like structures, subjected to time-dependent mechanical and thermal loading
[NASA-CR-177194] p 119 N86-28462

THIN WALLS

- On the solution of creep induced buckling in general structure
p 66 A82-39514

THREE DIMENSIONAL BODIES

- Advanced three-dimensional dynamic analysis by boundary element methods
p 81 A86-34445
Recent advances in hybrid/mixed finite elements
[NASA-CR-175574] p 107 N85-21687
Composite interlaminar fracture toughness: Three-dimensional finite element modeling for mixed mode 1, 2 and 3 fracture
[NASA-TM-88872] p 31 N87-13491

THREE DIMENSIONAL COMPOSITES

- Three-dimensional hybrid-stress finite element analysis of composite laminates with cracks and cutouts
p 80 A86-26896
Assessment of simplified composite micromechanics using three-dimensional finite-element analysis
p 20 A87-19121

THREE DIMENSIONAL MOTION

- Three dimensional unsteady aerodynamics and aeroelastic response of advanced turboprops
[AIAA PAPER 85-0846] p 5 A86-38894

TILTING ROTORS

- A pad perturbation method for the dynamic coefficients of tilting-pad journal bearings
p 47 A82-14400

TIME DEPENDENCE

- Predicting the time-temperature dependent axial failure of B/A1 composites
p 14 A80-35494
Predicting the time-temperature dependent axial failure of B/A1 composites
[NASA-TM-81474] p 22 N80-21452
Finite-strain large-deflection elastic-viscoplastic finite-element transient response analysis of structures
[NASA-CR-159874] p 88 N80-29762
Research and development program for the development of advanced time-temperature dependent constitutive relationships. Volume 1: Theoretical discussion
[NASA-CR-168191-VOL-1] p 100 N84-10613
Some advances in experimentation supporting development of viscoplastic constitutive models
[NASA-CR-174855] p 109 N85-27260
Some advances in experimentation supporting development of viscoplastic constitutive models
p 113 N85-31545

- Exposure time considerations in high temperature low cycle fatigue
[NASA-TM-88934] p 125 N87-28944

TIME MARCHING

- On the solution of creep induced buckling in general structure
p 66 A82-39514

TIME SERIES ANALYSIS

- Numerical considerations in the development and implementation of constitutive models
p 113 N85-31541

TITANIUM

- Structural dynamics of shrouded, hollow fan blades with composite in-lays
[NASA-TM-82816] p 7 N82-22266

TITANIUM ALLOYS

- Fatigue behavior of SiC reinforced titanium composites
p 13 A80-10036
Fatigue behavior of SiC reinforced Ti/6Al-4V/ at 650 C
p 15 A83-12414
Effect of low temperature on fatigue and fracture properties of Ti-5Al-2.5Sn(ELI) for use in engine components
p 35 A85-47972
Aeroelastic behavior of low aspect ratio metal and composite blades
[ASME PAPER 86-GT-243] p 84 A86-48271
Interrelation of material microstructure, ultrasonic factors, and fracture toughness of two phase titanium alloy
[NASA-TM-82810] p 54 N82-20551
Shot peening for Ti-6Al-4V alloy compressor blades
[NASA-TP-2711] p 123 N87-20566

TOLERANCES (MECHANICS)

- Multiaxial and thermomechanical fatigue considerations in damage tolerant design
[NASA-TM-87022] p 42 N85-26964

TOPOGRAPHY

- Nonlinear damage analysis: Postulate and evaluation
[NASA-CR-168171] p 118 N86-26652

TORQUE

- Application of traction drives as servo mechanisms
p 114 N85-33520
Evaluation of a high-torque backlash-free roller actuator
p 49 N87-16336

TORSION

- The effect of circumferential aerodynamic detuning on coupled bending-torsion unstalled supersonic flutter
[ASME PAPER 86-GT-100] p 6 A87-25396
Influence of third-degree geometric nonlinearities on the vibration and stability of pretwisted, precone, rotating blades
p 6 A87-46228
Cyclic torsion testing
[NASA-TM-83756] p 105 N84-31687
Application of traction drives as servo mechanisms
p 114 N85-33520
Influence of third-degree geometric nonlinearities on the vibration and stability of pretwisted, precone, rotating blades
[NASA-TM-87307] p 120 N86-31920

TORSIONAL STRESS

- Effects of mistuning on blade torsional flutter
p 64 A81-29095
Effects of mistuning on bending-torsion flutter and response of a cascade in incompressible flow
[AIAA 81-0602] p 65 A81-29465
Failure analysis of a tool steel torque shaft
p 51 A84-17546
Constitutive modeling and computational implementation for finite strain plasticity
p 78 A85-40910

TORSIONAL VIBRATION

- Flutter of turbfan rotors with mistuned blades
p 74 A85-12716
Effects of warping and pretwist on torsional vibration of rotating beams
[ASME PAPER 84-WA/APM-41] p 75 A85-17040
The effect of aerodynamic and structural detuning on turbomachine supersonic unstalled torsional flutter
[AIAA PAPER 85-0761] p 3 A85-30378
Finite difference analysis of torsional vibrations of pretwisted, rotating, cantilever beams with effects of warping
p 78 A85-42047
Optimization of cascade blade mistuning. I - Equations of motion and basic inherent properties
p 3 A85-42365
Aerodynamic and structural detuning of supersonic turbomachine rotors
p 5 A86-31595
Influence of friction dampers on torsional blade flutter
[ASME PAPER 85-GT-170] p 5 A86-32957
Nonlinear vibration and stability of rotating, pretwisted, precone blades including Coriolis effects
p 86 A87-39896
Nonlinear bending-torsional vibration and stability of rotating, pretwisted, precone blades including Coriolis effects
[NASA-TM-87207] p 116 N86-17789

TOUGHNESS

- Resin selection criteria for tough composite structures
[AIAA 83-0801] p 46 A83-29734
Crack layer morphology and toughness characterization in steels
[NASA-CR-168154] p 97 N83-27256

- Effect of crack curvature on stress intensity factors for ASTM standard compact tension specimens
[NASA-CR-168280] p 100 N84-11513
- TOWERS**
Structural analysis and cost estimate of an eight-leg space frame as a support structure for horizontal axis wind turbines
[NASA-TM-83470] p 112 N85-30361
- TRACTION**
Stress evaluations under rolling/sliding contacts
[NASA-CR-165561] p 91 N82-17521
Application of traction drives as servo mechanisms
p 114 N85-33520
- TRANSDUCERS**
Stress waves in an isotropic elastic plate excited by a circular transducer
[NASA-CR-3877] p 58 N85-20390
- TRANSFORMATIONS (MATHEMATICS)**
Bounding solutions of geometrically nonlinear viscoelastic problems
[AIAA PAPER 86-0943] p 82 A86-38838
- TRANSIENT LOADS**
Analysis of shell type structures subjected to time dependent mechanical and thermal loading
[NASA-CR-175747] p 109 N85-25896
- TRANSIENT RESPONSE**
Engine dynamic analysis with general nonlinear finite element codes. II - Bearing element implementation, overall numerical characteristics and benchmarking
[ASME PAPER 82-GT-292] p 47 A82-35462
Blade loss transient dynamic analysis of turbomachinery
p 2 A83-40864
Probabilistic finite elements for transient analysis in nonlinear continua
p 80 A86-28653
Advanced three-dimensional dynamic analysis by boundary element methods
p 81 A86-34445
Instructions for the use of the CIVM-Jet 4C finite-strain computer code to calculate the transient structural responses of partial and/or complete arbitrarily-curved rings subjected to fragment impact
[NASA-CR-159873] p 88 N80-27720
Geometrically nonlinear analysis of layered composite plates and shells
[NASA-CR-168182] p 98 N83-33219
Blade loss transient dynamics analysis with flexible bladed disk
[NASA-CR-168176] p 7 N84-13193
- TRANSMISSION LINES**
Preliminary investigation of an electrical network model for ultrasonic scattering
[NASA-CR-3770] p 57 N84-17606
- TRAVELING WAVES**
Vibration and flutter of mistuned bladed-disk assemblies
[AIAA PAPER 84-0991] p 75 A85-16095
Bending-torsion flutter of a highly swept advanced turboprop
[NASA-TM-82975] p 95 N83-11514
Vibration and flutter of mistuned bladed-disk assemblies
[NASA-TM-83634] p 103 N84-23923
- TRIBOLOGY**
The 20th Aerospace Mechanics Symposium
[NASA-CP-2423-REV] p 121 N87-16321
- TUNGSTEN**
Tungsten fiber reinforced superalloy composite high temperature component design considerations
[NASA-TM-82811] p 25 N82-21259
- TUNGSTEN CARBIDES**
Ultrasonic ranking of toughness of tungsten carbide
[NASA-TM-83358] p 55 N83-23620
- TUNING**
Model development and statistical investigation of turbine blade mistuning
p 2 A84-31905
Effects of structural coupling on mistuned cascade flutter and response
[ASME PAPER 83-GT-117] p 73 A84-33701
Vibration and flutter of mistuned bladed-disk assemblies
[AIAA PAPER 84-0991] p 75 A85-16095
The effect of aerodynamic and structural detuning on turbomachine supersonic unstalled torsional flutter
[AIAA PAPER 85-0761] p 3 A85-30378
Optimization of cascade blade mistuning. I - Equations of motion and basic inherent properties
p 3 A85-42365
Optimization of cascade blade mistuning. II - Global optimum and numerical optimization
p 3 A85-45715
Vibration characteristics of mistuned shrouded blade assemblies
[ASME PAPER 85-GT-115] p 4 A86-22068
The effect of circumferential aerodynamic detuning on coupled bending-torsion unstalled supersonic flutter
[ASME PAPER 86-GT-100] p 6 A87-25396
- Analytical and experimental investigation of mistuning in propfan flutter
[AIAA PAPER 87-0739] p 86 A87-40496
Effects of mistuning on bending-torsion flutter and response of a cascade in incompressible flow --- turbopfan engines
[NASA-TM-81674] p 89 N81-16494
Aeroelastic characteristics of a cascade of mistuned blades in subsonic and supersonic flows --- turbopfan engines
[NASA-TM-82631] p 90 N81-26492
Effects of structural coupling on mistuned cascade flutter and response
[NASA-TM-83049] p 96 N83-15672
Vibration and flutter of mistuned bladed-disk assemblies
[NASA-TM-83634] p 103 N84-23923
Analytical and experimental investigation of mistuning in propfan flutter
[NASA-TM-88959] p 122 N87-18116
- TURBINE BLADES**
Effects of mistuning on bending-torsion flutter and response of a cascade in incompressible flow
[AIAA 81-0602] p 65 A81-29465
Requirements of constitutive models for two nickel-base superalloys
p 33 A83-21071
Turbine blade nonlinear structural and life analysis
p 1 A83-29024
Some analysis methods for rotating systems with periodic coefficients
p 69 A83-32987
Design of dry-friction dampers for turbine blades
p 2 A83-35883
Model development and statistical investigation of turbine blade mistuning
p 2 A84-31905
Effects of structural coupling on mistuned cascade flutter and response
[ASME PAPER 83-GT-117] p 73 A84-33701
Vibrations of twisted cantilevered plates - Experimental investigation
[ASME PAPER 84-GT-96] p 73 A84-46937
The interaction between mistuning and friction in the forced response of bladed disk assemblies
[ASME PAPER 84-GT-139] p 73 A84-46957
Hygrothermomechanical evaluation of transverse filament tape epoxy/polyester fiberglass composites
p 17 A85-15632
The effect of aerodynamic and structural detuning on turbomachine supersonic unstalled torsional flutter
[AIAA PAPER 85-0761] p 3 A85-30378
Unified constitutive material models for nonlinear finite-element structural analysis --- gas turbine engine blades and vanes
[AIAA PAPER 85-1418] p 77 A85-39769
Vibrations of blades and bladed disk assemblies; Proceedings of the Tenth Biennial Conference on Mechanical Vibration and Noise, Cincinnati, OH, September 10-13, 1985
p 4 A86-26901
The effect of limiting aerodynamic and structural coupling in models of mistuned bladed disk vibration
p 5 A86-26905
Aerodynamic and structural detuning of supersonic turbomachine rotors
p 5 A86-31595
Aeroelastic behavior of low aspect ratio metal and composite blades
[ASME PAPER 86-GT-243] p 84 A86-48271
Probabilistic structural analysis to quantify uncertainties associated with turbopump blades
[AIAA PAPER 87-0766] p 85 A87-33581
Optimization and analysis of gas turbine engine blades
[AIAA PAPER 87-0827] p 126 A87-33614
Advances in 3-D Inelastic Analysis Methods for hot section components
[AIAA PAPER 87-0719] p 85 A87-33645
Thermal fatigue and oxidation data for directionally solidified MAR-M 246 turbine blades
[NASA-CR-159798] p 6 N80-21330
Nonlinear, three-dimensional finite-element analysis of air-cooled gas turbine blades
[NASA-TP-1669] p 88 N80-22734
Comparison of elastic and elastic-plastic structural analyses for cooled turbine blade airfoils
[NASA-TP-1679] p 88 N80-27719
Aeroelastic characteristics of a cascade of mistuned blades in subsonic and supersonic flows --- turbopfan engines
[NASA-TM-82631] p 90 N81-26492
Tungsten fiber reinforced superalloy composite high temperature component design considerations
[NASA-TM-82811] p 25 N82-21259
Structural dynamics of shroudless, hollow fan blades with composite in-lays
[NASA-TM-82816] p 7 N82-22266
Hygrothermomechanical evaluation of transverse filament tape epoxy/polyester fiberglass composites
[NASA-TM-83044] p 26 N83-15362
- Effects of structural coupling on mistuned cascade flutter and response
[NASA-TM-83049] p 96 N83-15672
Structural fatigue test results for large wind turbine blade sections
p 96 N83-19246
Blade loss transient dynamics analysis with flexible bladed disk
[NASA-CR-168176] p 7 N84-13193
Thermal stress analysis for a wood composite blade --- wind turbines
[NASA-CR-173394] p 103 N84-21903
Thermal-stress analysis for wood composite blade --- horizontal axis wind turbines
[NASA-CR-173830] p 104 N84-31685
Nonlinear analysis for high-temperature composites: Turbine blades/vanes
p 106 N84-31699
Nonlinear structural and life analyses of a turbine blade
p 9 N85-10954
Nonlinear analysis for high-temperature multilayered fiber composite structures --- turbine blades
[NASA-TM-83754] p 29 N85-21273
Unified constitutive material models for nonlinear finite-element structural analysis --- gas turbine engine blades and vanes
[NASA-TM-86985] p 108 N85-24338
Cyclic structural analyses of anisotropic turbine blades for reusable space propulsion systems --- ssme fuel turbopump
[NASA-TM-86990] p 108 N85-24339
Nonlinear structural analysis for fiber-reinforced superalloy turbine blades
p 109 N85-26887
Cyclic structural analyses of SSME turbine blades
p 112 N85-27963
Component-specific modeling
[NASA-CR-174925] p 12 N85-32119
Joint research effort on vibrations of twisted plates, phase 1: Final results
[NASA-RP-1150] p 115 N86-10579
Improved stud configurations for attaching laminated wood wind turbine blades
[NASA-TM-87109] p 115 N86-10582
Simplified cyclic structural analyses of SSME turbine blades
[NASA-TM-87214] p 116 N86-16615
Thermoviscoplastic nonlinear constitutive relationships for structural analysis of high temperature metal matrix composites
[NASA-TM-87291] p 30 N86-24756
Structural tailoring of engine blades (STAEBL) user's manual
[NASA-CR-175113] p 13 N86-27284
Structural analysis of turbine blades using unified constitutive models
[NASA-TM-88807] p 119 N86-28461
Structural dynamic measurement practices for turbomachinery at the NASA Lewis Research Center
[NASA-TM-88857] p 13 N86-32433
STAEBL: Structural tailoring of engine blades, phase 2
p 13 N87-11731
Structural and aeroelastic analysis of the SR-7L propfan
[NASA-TM-86877] p 123 N87-22273
Nonlinear heat transfer and structural analyses of SSME turbine blades
p 123 N87-22779
Finite element analysis of flexible, rotating blades
[NASA-TM-89906] p 124 N87-26385
Turbine Engine Hot Section Technology, 1985
[NASA-CP-2405] p 125 N88-11140
- TURBINE ENGINES**
Toward improved durability in advanced combustors and turbines - Progress in prediction of thermomechanical loads
[ASME PAPER 86-GT-172] p 6 A86-48224
Superhybrid composite blade impact studies
[NASA-TM-81597] p 89 N81-11412
Elevated temperature fatigue testing of metals
[NASA-TM-82745] p 91 N82-16419
Fracture mechanics criteria for turbine engine hot section components
[NASA-CR-167896] p 7 N82-25257
Bird impact analysis package for turbine engine fan blades
[NASA-TM-82831] p 92 N82-26701
Blade loss transient dynamics analysis with flexible bladed disk
[NASA-CR-168176] p 7 N84-13193
Aerothermal modeling. Executive summary
[NASA-CR-168330] p 7 N84-15152
Lewis Research Center spin rig and its use in vibration analysis of rotating systems
[NASA-TP-2304] p 9 N84-24578
Life prediction and constitutive behavior: Overview
p 10 N85-10973
Validation of structural analysis methods using the in-house liner cyclic rigs
p 10 N85-10987

- HOST liner cyclic facilities: Facility description p 10 N85-10988
- Advanced stress analysis methods applicable to turbine engine structures [NASA-CR-175573] p 11 N85-21165
- Component-specific modeling [NASA-CR-174925] p 12 N85-32119
- Structural tailoring of engine blades (STAEBL) theoretical manual [NASA-CR-175112] p 12 N86-27283
- Turbine Engine Hot Section Technology, 1984 [NASA-CP-2339] p 120 N87-11180
- Fatigue and fracture: Overview p 120 N87-11183
- Toward improved durability in advanced combustors and turbines: Progress in the prediction of thermomechanical loads [NASA-TM-88932] p 13 N87-28551
- TURBINE PUMPS**
- Self-acting geometry for noncontact seals [ASLE PREPRINT 81-AM-5B-2] p 47 A81-33867
- Probabilistic structural analysis to quantify uncertainties associated with turbopump blades [AIAA PAPER 87-0766] p 85 A87-33581
- Cyclic structural analyses of anisotropic turbine blades for reusable space propulsion systems --- ssme fuel turbopump [NASA-TM-86990] p 108 N85-24339
- Cyclic structural analyses of SSME turbine blades p 112 N85-27963
- Nonlinear heat transfer and structural analyses of SSME turbine blades p 123 N87-22779
- TURBINE WHEELS**
- Cyclic behavior of turbine disk alloys at 650 C p 32 A81-12266
- Fatigue and creep-fatigue deformation of several nickel-base superalloys at 650 C p 32 A82-47398
- Effects of friction dampers on aerodynamically unstable rotor stages [AIAA PAPER 83-0848] p 1 A83-32791
- NASTRAN forced vibration analysis of rotating cyclic structures [ASME PAPER 83-DET-20] p 72 A84-29103
- Stagger angle dependence of inertial and elastic coupling in bladed disks p 72 A84-31903
- Model development and statistical investigation of turbine blade mistuning p 2 A84-31905
- The dynamics of a flexible bladed disc on a flexible rotor in a two-rotor system p 4 A86-25743
- Evaluation of the cyclic behavior of aircraft turbine disk alloys, part 2 [NASA-CR-165123] p 38 N80-30482
- TURBINES**
- Three dimensional finite-element elastic analysis of a thermally cycled double-edge wedge geometry specimen --- nickel alloy turbine parts [NASA-TM-80980] p 37 N80-26433
- TURBOCOMPRESSORS**
- Analysis of an axial compressor blade vibration based on wave reflection theory [ASME PAPER 83-GT-151] p 2 A83-47970
- Nastran level 16 theoretical manual updates for aeroelastic analysis of bladed discs [NASA-CR-159823] p 90 N81-19480
- NASTRAN level 16 demonstration manual updates for aeroelastic analysis of bladed discs [NASA-CR-159826] p 90 N81-19483
- TURBOFAN ENGINES**
- Status of NASA full-scale engine aeroelasticity research p 63 A80-35906
- DEAN - A program for Dynamic Engine Analysis [AIAA PAPER 85-1354] p 3 A86-14430
- The dynamics of a flexible bladed disc on a flexible rotor in a two-rotor system p 4 A86-25743
- Application of composite materials to turbofan engine fan exit guide vanes [NASA-TM-81432] p 22 N80-18106
- Status of NASA full-scale engine aeroelasticity research [NASA-TM-81500] p 88 N80-23678
- Effects of mistuning on bending-torsion flutter and response of a cascade in incompressible flow --- turbofan engines [NASA-TM-81674] p 89 N81-16494
- Aeroelastic characteristics of a cascade of mistuned blades in subsonic and supersonic flows --- turbofan engines [NASA-TM-82631] p 90 N81-26492
- DEAN: A program for dynamic engine analysis [NASA-TM-87033] p 11 N85-28945
- TURBOFANS**
- Vibration and flutter of mistuned bladed-disk assemblies [AIAA PAPER 84-0991] p 75 A85-16095
- Analytical and experimental investigation of the coupled bladed disk/shaft whirl of a cantilevered turbofan [ASME PAPER 86-GT-98] p 6 A86-48163
- Diffusion bonded boron/aluminum spar-shell fan blade [NASA-CR-159571] p 23 N80-25382
- Vibration and flutter of mistuned bladed-disk assemblies [NASA-TM-83634] p 103 N84-23923
- Structural response of a rotating bladed disk to rotor whirl [NASA-CR-175605] p 11 N85-22391
- TURBOGENERATORS**
- Stability of large horizontal-axis axisymmetric wind turbines [NASA-TM-81623] p 89 N81-12446
- Experience with modified aerospace reliability and quality assurance method for wind turbines [NASA-TM-82803] p 54 N82-19550
- TURBOJET ENGINES**
- Engine environmental effects on composite behavior --- moisture and temperature effects on mechanical properties [AIAA 80-0695] p 1 A80-35101
- Status of NASA full-scale engine aeroelasticity research p 63 A80-35906
- Environmental and high strain rate effects on composites for engine applications p 16 A84-17444
- Engine environmental effects on composite behavior [NASA-TM-81508] p 22 N80-23370
- Status of NASA full-scale engine aeroelasticity research [NASA-TM-81500] p 88 N80-23678
- Environmental and High-Strain Rate effects on composites for engine applications [NASA-TM-82882] p 25 N82-31449
- TURBOMACHINE BLADES**
- Superhybrid composite blade impact studies [ASME PAPER 81-GT-24] p 1 A81-29940
- Vibrations of twisted rotating blades [ASME PAPER 81-DET-127] p 65 A82-19341
- Comparison of beam and shell theories for the vibrations of thin turbomachinery blades [ASME PAPER 82-GT-223] p 65 A82-35408
- The coupled aeroelastic response of turbomachinery blading to aerodynamic excitations [AIAA 83-0844] p 69 A83-29822
- Vibrations of blades with variable thickness and curvature by shell theory [ASME PAPER 83-GT-152] p 70 A83-47978
- The coupled response of turbomachinery blading to aerodynamic excitations p 2 A84-26959
- Flutter of turbofan rotors with mistuned blades p 74 A85-12716
- Vibration and flutter of mistuned bladed-disk assemblies [AIAA PAPER 84-0991] p 75 A85-16095
- Vibration and flutter of mistuned bladed-disk assemblies p 3 A85-45854
- Vibrations of twisted cantilever plates - A comparison of theoretical results p 79 A85-47626
- Vibration analysis of rotating turbomachinery blades by an improved finite difference method p 3 A86-14338
- Vibration characteristics of mistuned shrouded blade assemblies [ASME PAPER 85-GT-115] p 4 A86-22068
- The effects of strong shock loading on coupled bending-torsion flutter of tuned and mistuned cascades p 4 A86-26893
- Effects of mistuning on bending-torsion flutter and response of a cascade in incompressible flow --- turbofan engines [NASA-TM-81674] p 89 N81-16494
- NASTRAN level 16 user's manual updates for aeroelastic analysis of bladed discs [NASA-CR-159824] p 90 N81-19481
- NASTRAN level 16 programmer's manual updates for aeroelastic analysis of bladed discs [NASA-CR-159825] p 90 N81-19482
- Improved finite-difference vibration analysis of pretwisted, tapered beams [NASA-TM-83549] p 102 N84-16588
- Vibration and flutter of mistuned bladed-disk assemblies [NASA-TM-83634] p 103 N84-23923
- A study of internal and distributed damping for vibrating turbomachinery blades [NASA-CR-175901] p 11 N85-27868
- Composite loads spectra for select space propulsion structural components p 110 N85-27953
- TURBOMACHINERY**
- Aeroelastic formulations for turbomachines and propellers p 4 A86-24677
- Forced vibration analysis of rotating cyclic structures in NASTRAN [NASA-CR-165429] p 100 N84-11514
- Lewis Research Center spin rig and its use in vibration analysis of rotating systems [NASA-TP-2304] p 9 N84-24578
- The use of an optical data acquisition system for bladed disk vibration analysis [NASA-TM-86891] p 106 N85-15184
- Structural dynamic measurement practices for turbomachinery at the NASA Lewis Research Center [NASA-TM-88857] p 13 N86-32433
- TURBOPROP AIRCRAFT**
- Three dimensional unsteady aerodynamics and aeroelastic response of advanced turboprops [AIAA PAPER 86-0846] p 5 A86-38894
- Bending-torsion flutter of a highly swept advanced turboprop [NASA-TM-82975] p 95 N83-11514
- Concentrated mass effects on the flutter of a composite advanced turboprop model [NASA-TM-88854] p 120 N87-12017
- TURBOPROP ENGINES**
- Flutter analysis of advanced turbopropellers [AIAA 83-0846] p 69 A83-29824
- Flutter analysis of advanced turbopropellers p 73 A84-36492
- Structural tailoring of advanced turboprops [AIAA PAPER 87-0753] p 85 A87-33648
- Experimental classical flutter results of a composite advanced turboprop model [NASA-TM-88792] p 119 N86-29271
- TURBULENCE EFFECTS**
- Numerical synthesis of tri-variate velocity realizations of turbulence p 81 A86-28654
- TWISTING**
- Vibrations of twisted rotating blades [ASME PAPER 81-DET-127] p 65 A82-19341
- Vibrations of twisted cantilevered plates - Experimental investigation [ASME PAPER 84-GT-96] p 73 A84-46937
- Vibrations of twisted cantilevered plates - Summary of previous and current studies p 76 A85-22069
- Natural frequencies of twisted rotating plates p 76 A85-32343
- Finite difference analysis of torsional vibrations of pretwisted, rotating, cantilever beams with effects of warping p 78 A85-42047
- Vibrations of twisted cantilever plates - A comparison of theoretical results p 79' A85-47626
- Joint research effort on vibrations of twisted plates, phase 1: Final results [NASA-RP-1150] p 115 N86-10579

U

UDIMET ALLOYS

- Thermal fatigue resistance of cobalt-modified UDIMET 700 p 39 N83-11289
- Thermal-fatigue and oxidation resistance of cobalt-modified Udimet 700 alloy [NASA-TP-2591] p 119 N86-28464

ULTRASONIC DENSIMETERS

- Ultrasonic velocity for estimating density of structural ceramics [NASA-TM-82765] p 46 N82-14359

ULTRASONIC FLAW DETECTION

- Ultrasonic measurement of material properties p 50 A81-19656
- On ultrasonic factors and fracture toughness p 66 A82-42863
- Comparison of NDE techniques for sintered-SiC components p 51 A83-22265
- Mechanics aspects of NDE by sound and ultrasound p 51 A83-25571
- Factors influencing the ultrasonic stress wave factor evaluation of composite material structures p 81 A86-34257
- Quantitative void characterization in structural ceramics by use of scanning laser acoustic microscopy p 53 A87-51974
- Fundamental aspects in quantitative ultrasonic determination of fracture toughness: The scattering of a single ellipsoidal inhomogeneity [NASA-CR-3625] p 55 N83-11507
- Factors that affect reliability of nondestructive detection of flaws in structural ceramics [NASA-TM-87348] p 61 N86-31912
- Quantitative void characterization in structural ceramics using scanning laser acoustic microscopy [NASA-TM-88797] p 61 N86-31913
- Ultrasonic determination of recrystallization [NASA-TM-88855] p 61 N87-10399
- ULTRASONIC RADIATION**
- Ultrasonic wave propagation in two-phase media - Spherical inclusions p 17 A85-11926
- Nondestructive characterization of structural ceramics p 46 A86-37141

- Ultrasonic input-output for transmitting and receiving longitudinal transducers coupled to same face of isotropic elastic plate
[NASA-CR-3506] p 54 N82-18613
- Ultrasonic attenuation of a void-containing medium for very long wavelengths
[NASA-CR-3693] p 56 N83-28466
- Analytical Ultrasonics in Materials Research and Testing
[NASA-CP-2383] p 59 N86-22962
- Ultrasonic determination of recrystallization
[NASA-TM-88855] p 61 N87-10399
- ULTRASONIC TESTS**
- Quantitative ultrasonic evaluation of engineering properties in metals, composites, and ceramics
p 50 A80-39641
- Concepts and techniques for ultrasonic evaluation of material mechanical properties
p 50 A80-51575
- Ultrasonic measurement of material properties
p 50 A81-19656
- Characterization of composite materials by means of the ultrasonic stress wave factor
p 16 A84-10430
- Nondestructive techniques for characterizing mechanical properties of structural materials - An overview
[ASME PAPER 86-GT-75] p 52 A86-48143
- Nondestructive evaluation of adhesive bond strength using the stress wave factor technique
p 53 A87-32200
- Simulation of transducer-couplant effects on broadband ultrasonic signals
[NASA-TM-81489] p 53 N80-22714
- Concepts and techniques for ultrasonic evaluation of material mechanical properties
[NASA-TM-81523] p 53 N80-24634
- Ultrasonic velocity for estimating density of structural ceramics
[NASA-TM-82765] p 46 N82-14359
- Interrelation of material microstructure, ultrasonic factors, and fracture toughness of two phase titanium alloy
[NASA-TM-82810] p 54 N82-20551
- Phenomenological and mechanics aspects of nondestructive evaluation and characterization by sound and ultrasound of material and fracture properties
[NASA-CR-3623] p 55 N83-11506
- Ultrasonic ranking of toughness of tungsten carbide
[NASA-TM-83358] p 55 N83-23620
- Ultrasonic nondestructive evaluation, microstructure, and mechanical property interrelations
[NASA-TM-86876] p 57 N85-10371
- Application of homomorphic signal processing to stress wave factor analysis
[NAS 1.26-174871] p 58 N85-21673
- Ultrasonic evaluation of mechanical properties of thick, multilayered, filament wound composites
[NASA-TM-87088] p 58 N86-10561
- Nondestructive techniques for characterizing mechanical properties of structural materials: An overview
[NASA-TM-87203] p 59 N86-19636
- Stress waves in transversely isotropic media: The homogeneous problem
[NASA-CR-3977] p 59 N86-25002
- Ultrasonic stress wave characterization of composite materials
[NASA-CR-3976] p 60 N86-27665
- A study of the stress wave factor technique for nondestructive evaluation of composite materials
[NASA-CR-4002] p 60 N86-28445
- Factors that affect reliability of nondestructive detection of flaws in structural ceramics
[NASA-TM-87348] p 61 N86-31912
- Acousto-ultrasonic verification of the strength of filament wound composite material
[NASA-TM-88827] p 61 N86-32764
- Nondestructive evaluation of structural ceramics
[NASA-TM-88978] p 62 N87-18109
- Ultrasonic NDE of structural ceramics for power and propulsion systems
[NASA-TM-100147] p 62 N87-26362
- Flaw imaging and ultrasonic techniques for characterizing sintered silicon carbide
[NASA-TM-100177] p 63 N88-12106
- ULTRASONIC WAVE TRANSDUCERS**
- Acousto-ultrasonic characterization of fiber reinforced composites
p 50 A81-44660
- Effects of specimen resonances on acousto-ultrasonic testing
[NASA-CR-3679] p 55 N83-21373
- Ultrasonic evaluation of mechanical properties of thick, multilayered, filament wound composites
[NASA-TM-87088] p 58 N86-10561

ULTRASONICS

- The role of the reflection coefficient in precision measurement of ultrasonic attenuation
p 51 A85-42151
- Measurement of ultrasonic velocity using phase-slope and cross-correlation methods
p 51 A86-13192
- Nondestructive characterization of structural ceramics
p 46 A86-37141
- Reliability of void detection in structural ceramics by use of scanning laser acoustic microscopy
p 52 A86-39027
- NDE of structural ceramics
[ASME PAPER 86-GT-279] p 52 A86-48298
- Quantitative ultrasonic evaluation of engineering properties in metals, composites and ceramics
[NASA-TM-81530] p 54 N80-26682
- Acousto-ultrasonic characterization of fiber reinforced composites
[NASA-TM-82651] p 54 N81-28458
- Effects of specimen resonances on acousto-ultrasonic testing
[NASA-CR-3679] p 55 N83-21373
- Input-output characterization of an ultrasonic testing system by digital signal analysis
[NASA-CR-3756] p 56 N84-15565
- The role of the reflection coefficient in precision measurement of ultrasonic attenuation
[NASA-TM-83788] p 57 N84-32849
- Ultrasonic velocity measurement using phase-slope cross-correlation methods
[NASA-TM-83794] p 57 N84-34769
- Stress waves in an isotropic elastic plate excited by a circular transducer
[NASA-CR-3877] p 58 N85-20390
- Ultrasonic testing of plates containing edge cracks
[NASA-CR-3904] p 58 N85-29307
- Reliability of void detection in structural ceramics using scanning laser acoustic microscopy
[NASA-TM-87035] p 58 N85-32337
- NDE of structural ceramics
[NASA-TM-87186] p 59 N86-16598
- Analytical Ultrasonics in Materials Research and Testing
[NASA-CP-2383] p 59 N86-22962
- Concepts for interrelating ultrasonic attenuation, microstructure and fracture toughness in polycrystalline solids
[NASA-TM-87339] p 60 N86-25812
- Wave propagation in anisotropic medium due to an oscillatory point source with application to unidirectional composites
[NASA-CR-4001] p 60 N86-27666
- The acousto-ultrasonic approach
[NASA-TM-89843] p 62 N87-20562
- Ray propagation path analysis of acousto-ultrasonic signals in composites
[NASA-TM-100148] p 62 N87-25589
- UNIQUENESS THEOREM**
- Formal convergence characteristics of elliptically constrained incremental Newton-Raphson algorithms
p 126 A83-10273
- UNIVERSITIES**
- NASA Lewis Research Center/university graduate research program on engine structures
[ASME PAPER 85-GT-159] p 80 A86-22084
- NASA Lewis Research Center/University Graduate Research Program on Engine Structures
[NASA-TM-86916] p 107 N85-18375
- UNLOADING WAVES**
- Indentation law for composite laminates
p 16 A84-27356
- UNSTEADY FLOW**
- Aeroelastic formulations for turbomachines and propellers
p 4 A86-24677
- Three dimensional unsteady aerodynamics and aeroelastic response of advanced turboprops
[AIAA PAPER 86-0846] p 5 A86-38894
- USER MANUALS (COMPUTER PROGRAMS)**
- NASTRAN level 16 user's manual updates for aeroelastic analysis of bladed discs
[NASA-CR-159824] p 90 N81-19481
- NASTRAN level 16 demonstration manual updates for aeroelastic analysis of bladed discs
[NASA-CR-159826] p 90 N81-19483
- Aeroelastic analysis for propellers - mathematical formulations and program user's manual
[NASA-CR-3729] p 101 N84-12530
- Integrated Composite Analyzer (ICAN): Users and programmers manual
[NASA-TP-2515] p 30 N86-21614
- Structural tailoring of engine blades (STAEBL) theoretical manual
[NASA-CR-175112] p 12 N86-27283
- A NASTRAN primer for the analysis of rotating flexible blades
[NASA-TM-89861] p 123 N87-21375

- SINDA-NASTRAN interfacing program theoretical description and user's manual
[NASA-TM-100158] p 124 N87-27268
- USER REQUIREMENTS**
- Structural tailoring of engine blades (STAEBL) user's manual
[NASA-CR-175113] p 13 N86-27284
- V**
- VANADIUM**
- Shot peening for Ti-6Al-4V alloy compressor blades
[NASA-TP-2711] p 123 N87-20566
- VANES**
- Advances in 3-D Inelastic Analysis Methods for hot section components
[AIAA PAPER 87-0719] p 85 A87-33645
- Nonlinear analysis for high-temperature composites: Turbine blades/vanes
p 106 N84-31699
- Turbine Engine Hot Section Technology, 1985
[NASA-CP-2405] p 125 N88-11140
- VAPOR DEPOSITION**
- Calculation of residual principal stresses in CVD boron on carbon filaments
[NASA-TM-81456] p 22 N80-20314
- VARIATIONAL PRINCIPLES**
- Alternative ways for formulation of hybrid stress elements
p 68 A83-14710
- Rational approach for assumed stress finite elements
p 74 A85-12029
- On Hybrid and mixed finite element methods
[NASA-CR-175551] p 108 N85-23096
- VARIATIONS**
- Probabilistic finite element: Variational theory
p 111 N85-27957
- VELOCITY**
- Ultrasonic evaluation of mechanical properties of thick, multilayered, filament wound composites
[NASA-TM-87088] p 58 N86-10561
- VELOCITY DISTRIBUTION**
- Numerical synthesis of tri-variate velocity realizations of turbulence
p 81 A86-28654
- VELOCITY MEASUREMENT**
- Measurement of ultrasonic velocity using phase-slope and cross-correlation methods
p 51 A86-13192
- Ultrasonic velocity measurement using phase-slope cross-correlation methods
[NASA-TM-83794] p 57 N84-34769
- VIBRATION**
- Bending-torsion flutter of a highly swept advanced turboprop
[NASA-TM-82975] p 95 N83-11514
- Dynamic behavior of spiral-groove and Rayleigh-Step self-acting face seals
[NASA-TP-2266] p 8 N84-16181
- Lewis Research Center spin rig and its use in vibration analysis of rotating systems
[NASA-TP-2304] p 9 N84-24578
- Improved methods of vibration analysis of pretwisted, airfoil blades
[NASA-TM-83735] p 104 N84-30329
- Flow dynamic environment data base development for the SSME
p 109 N85-26885
- Nonlinear flap-lag-extensional vibrations of rotating, pretwisted, precone beams including Coriolis effects
[NASA-TM-87102] p 115 N85-34427
- Hub flexibility effects on propfan vibration
[NASA-TM-89900] p 124 N87-24722
- VIBRATION DAMPING**
- Design of dry-friction dampers for turbine blades
p 2 A83-35883
- The interaction between mistuning and friction in the forced response of bladed disk assemblies
[ASME PAPER 84-GT-139] p 73 A84-46957
- Influence of friction dampers on torsional blade flutter
[ASME PAPER 85-GT-170] p 5 A86-32957
- Frequency domain solutions to multi-degree-of-freedom, dry friction damped systems under periodic excitation
p 83 A86-39485
- Development of procedures for calculating stiffness and damping of elastomers in engineering applications, part 6
[NASA-CR-159838] p 87 N80-22733
- A study of internal and distributed damping for vibrating turbomachinery blades
[NASA-CR-175901] p 11 N85-27868
- Variable force, eddy-current or magnetic damper
[NASA-CASE-LEW-13717-1] p 49 N85-30333
- Extensions of the Ritz-Galerkin method for the forced, damped vibrations of structural elements
p 117 N86-21909
- VIBRATION EFFECTS**
- Experimental study of uncentralized squeeze film dampers
[NASA-CR-168317] p 103 N84-19927

Structural analysis and cost estimate of an eight-leg space frame as a support structure for horizontal axis wind turbines

[NASA-TM-83470] p 112 N85-30361

Improved stud configurations for attaching laminated wood wind turbine blades

[NASA-TM-87109] p 115 N86-10582

WINDPOWER UTILIZATION

Stability of large horizontal-axis axisymmetric wind turbines

[NASA-TM-81623] p 89 N81-12446

Reliability and quality assurance on the MOD 2 wind system

[NASA-TM-82717] p 54 N81-33492

WINDPOWERED GENERATORS

Stability of large horizontal-axis axisymmetric wind turbines

[NASA-TM-82717] p 54 N81-33492

Experience with modified aerospace reliability and quality assurance method for wind turbines

[NASA-TM-82803] p 54 N82-19550

Structural analysis and cost estimate of an eight-leg space frame as a support structure for horizontal axis wind turbines

[NASA-TM-83470] p 112 N85-30361

WIRE CLOTH

Metal honeycomb to porous wireform substrate diffusion bond evaluation

[NASA-TM-82793] p 54 N82-18612

Metal honeycomb to porous wireform substrate diffusion bond evaluation

[NASA-TM-88974] p 122 N87-18882

Fatigue failure of regenerator screens in a high frequency Stirling engine

WOOD

Thermal-stress analysis for wood composite blade ---

horizontal axis wind turbines

[NASA-CR-173830] p 104 N84-31685

Improved stud configurations for attaching laminated wood wind turbine blades

[NASA-TM-87109] p 115 N86-10582

X

X RAY ANALYSIS

NDE of structural ceramics

[ASME PAPER 86-GT-279] p 52 A86-48298

Correlation of processing and sintering variables with the strength and radiography of silicon nitride

[NASA-TM-87186] p 59 N86-16598

Flaw imaging and ultrasonic techniques for characterizing sintered silicon carbide

[NASA-TM-100177] p 63 N88-12106

X RAY INSPECTION

Comparison of NDE techniques for sintered-SiC components

[ASME PAPER 87-GT-8] p 53 A87-48702

NDE reliability and process control for structural ceramics

[NASA-TM-87348] p 61 N86-31912

Factors that affect reliability of nondestructive detection of flaws in structural ceramics

[NASA-TM-88870] p 61 N87-12910

NDE reliability and process control for structural ceramics

[NASA-TM-88870] p 61 N87-12910

Y

YIELD STRENGTH

Time-independent anisotropic plastic behavior by mechanical subelement models

[NASA-TM-87214] p 116 N86-16615

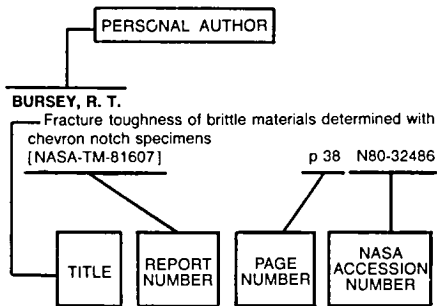
Simplified cyclic structural analyses of SSME turbine blades

[NASA-TM-87214] p 116 N86-16615

Yielding and deformation behavior of the single crystal nickel-base superalloy PWA 1480

[NASA-CR-175100] p 44 N86-25455

Typical Personal Author Index Listing



Listings in this index are arranged alphabetically by personal author. The title of the document provides the user with a brief description of the subject matter. The report number helps to indicate the type of document listed (e.g., NASA report, translation, NASA contractor report). The page and accession numbers are located beneath and to the right of the title. Under any one author's name the accession numbers are arranged in sequence with the AIAA accession numbers appearing first.

A

- ABDUL-AZIZ, A.**
Nonlinear heat transfer and structural analyses of SSME turbine blades p 123 N87-22779
- ABEL, PHILLIP B.**
Nondestructive evaluation of structural ceramics [NASA-TM-88978] p 62 N87-18109
Flaw imaging and ultrasonic techniques for characterizing sintered silicon carbide [NASA-TM-100177] p 63 N88-12106
- ABUELFOUTOUH, N.**
Finite element analysis of notch behavior using a state variable constitutive equation p 114 N85-31548
- ADAMS, D. F.**
Analysis of crack propagation as an energy absorption mechanism in metal matrix composites [NASA-CR-165051] p 24 N82-14288
Micromechanical predictions of crack propagation and fracture energy in a single fiber boron/aluminum model composite [NASA-CR-168550] p 25 N82-18326
- ADAMS, M.**
Engine dynamic analysis with general nonlinear finite element codes. II - Bearing element implementation, overall numerical characteristics and benchmarking [ASME PAPER 82-GT-292] p 47 A82-35462
Nonlinear transient finite element analysis of rotor-bearing-stator systems p 48 A84-20580
Engine dynamic analysis with general nonlinear finite element codes. Part 2: Bearing element implementation overall numerical characteristics and benchmarking [NASA-CR-167944] p 7 N82-33390
- AHMA, S.**
Advanced three-dimensional dynamic analysis by boundary element methods p 81 A86-34445
- AIELLO, R. A.**
Tensile buckling of advanced turboprops [AIAA PAPER 82-0776] p 67 A83-10900
Tensile buckling of advanced turboprops p 71 A84-11039
Composite sandwich thermostructural behavior - Computational simulation [AIAA PAPER 86-0948] p 82 A86-38842

- Structural dynamics of shroudless, hollow fan blades with composite in-lays [NASA-TM-82816] p 7 N82-22266
Large displacements and stability analysis of nonlinear propeller structures [NASA-TM-82850] p 94 N82-31707
Tensile buckling of advanced turboprops [NASA-TM-82896] p 94 N82-31708
Large displacements and stability analysis of nonlinear propeller structures p 95 N83-12460
Fiber composite sandwich thermostructural behavior: Computational simulation [NASA-TM-88787] p 31 N86-31663
- AIELLO, ROBERT**
Structural and aeroelastic analysis of the SR-7L propfan [NASA-TM-86877] p 123 N87-22273
- AIELLO, ROBERT A.**
A NASTRAN primer for the analysis of rotating flexible blades [NASA-TM-89861] p 123 N87-21375
Dynamic delamination buckling in composite laminates under impact loading: Computational simulation [NASA-TM-100192] p 31 N87-28611
- AKHTER, M. M.**
Sensor failure detection for jet engines [NASA-CR-168190] p 56 N83-33182
- ALAM, J.**
Effect of crack curvature on stress intensity factors for ASTM standard compact tension specimens [NASA-CR-168280] p 100 N84-11513
- ALAM, M.**
A blade loss response spectrum for flexible rotor systems [ASME PAPER 84-GT-29] p 48 A84-46893
- ALGER, DONALD L.**
Fatigue failure of regenerator screens in a high frequency Stirling engine [NASA-TM-88974] p 122 N87-18882
- ALLAIRE, P. E.**
A pad perturbation method for the dynamic coefficients of tilting-pad journal bearings p 47 A82-14400
- ALLEN, D. H.**
On the use of internal state variables in thermoviscoplastic constitutive equations p 113 N85-31536
Integrated research in constitutive modelling at elevated temperatures, part 2 [NASA-CR-177233] p 119 N86-28455
Integrated research in constitutive modelling at elevated temperatures, part 1 [NASA-CR-177237] p 120 N86-30227
- ALLEN, G. P.**
Self-acting geometry for noncontact seals [ASLE PREPRINT 81-AM-5B-2] p 47 A81-33867
- ANCONA, W.**
Design of dry-friction dampers for turbine blades p 2 A83-35883
- ANDERSON, WILLIAM**
Evaluation of a high-torque backlash-free roller actuator p 49 N87-16336
- ANTOLOVICH, S. D.**
Metallurgical instabilities during the high temperature low cycle fatigue of nickel-base superalloys p 33 A83-22019
The effect of microstructure on the fatigue behavior of Ni base superalloys p 33 A83-36166
A study of fatigue damage mechanisms in Waspaloy from 25 to 800 C p 34 A85-12098
The effect of microstructure, temperature, and hold-time on low-cycle fatigue of As HIP P/M Rene 95 p 35 A85-32399
A study of spectrum fatigue crack propagation in two aluminum alloys. I - Spectrum simplification. II - Influence of microstructures p 36 A86-48973
A study of spectrum fatigue crack propagation in two aluminum alloys. 1: Spectrum simplification [NASA-TM-86929] p 41 N85-18124
A study of spectrum fatigue crack propagation in two aluminum alloys. 2: Influence of microstructures [NASA-TM-86930] p 41 N85-18125

- ARD, K. E.**
Thermal expansion behavior of graphite/glass and graphite/magnesium p 21 A87-38615
- ARECHAGA, T.**
Formal convergence characteristics of elliptically constrained incremental Newton-Raphson algorithms p 126 A83-10273
- ARYA, V. K.**
Finite element implementation of Robinson's unified viscoplastic model and its application to some uniaxial and multiaxial problems [NASA-TM-89991] p 123 N87-23010
- ATLURI, S. N.**
Path-independent integrals in finite elasticity and inelasticity, with body forces, inertia, and arbitrary crack-face conditions p 65 A82-32303
On a study of the $\Delta T/c$ and $C/\text{asterisk}$ integrals for fracture analysis under non-steady creep p 65 A82-36782
Moving singularity creep crack growth analysis with the $\Delta T/c$ and $C/\text{asterisk}$ integrals p 66 A82-40066
Inelastic stress analyses at finite deformation through complementary energy approaches p 71 A84-13248
Analyses of large quasistatic deformations of inelastic bodies by a new hybrid-stress finite element algorithm p 71 A84-16874
Analyses of large quasistatic deformations of inelastic bodies by a new hybrid-stress finite element algorithm - Applications p 71 A84-16884
Hybrid stress finite elements for large deformations of inelastic solids p 74 A85-15894
Development and testing of stable, invariant, isoparametric curvilinear 2- and 3-D hybrid-stress elements p 75 A85-19899
On the existence and stability conditions for mixed-hybrid finite element solutions based on Reissner's variational principle p 77 A85-33847
Constitutive modeling and computational implementation for finite strain plasticity p 78 A85-40910
Existence and stability, and discrete BB and rank conditions, for general mixed-hybrid finite elements in elasticity p 82 A86-34464
Constitutive modeling of cyclic plasticity and creep, using an internal time concept p 83 A86-41673
Creep crack-growth: A new path-independent T sub o and computational studies [NASA-CR-168930] p 92 N82-24503
Creep crack-growth: A new path-independent integral (T sub c), and computational studies [NASA-CR-167897] p 94 N82-29619
Stress and fracture analyses under elastic-plastic creep conditions: Some basic developments and computational approaches p 99 N83-34371
Inelastic and dynamic fracture and stress analyses p 106 N84-31697
- AUGUST, R.**
Effect of design variables, temperature gradients and speed of life and reliability of a rotating disk [NASA-TM-88883] p 49 N87-13755

B

- BAKLINI, G. Y.**
Radiographic detectability limits for seeded voids in sintered silicon carbide and silicon nitride p 51 A86-31745
Reliability of void detection in structural ceramics by use of scanning laser acoustic microscopy p 52 A86-39027
Correlation of processing and sintering variables with the strength and radiography of silicon nitride p 46 A87-12938
Probability of detection of internal voids in structural ceramics using microfocus radiography p 52 A87-14300
NDE reliability and process control for structural ceramics [ASME PAPER 87-GT-8] p 53 A87-48702

- Quantitative void characterization in structural ceramics by use of scanning laser acoustic microscopy p 53 A87-51974
- The effect of stress on ultrasonic pulses in fiber reinforced composites p 56 N83-33180
- Radiographic detectability limits for seeded voids in sintered silicon carbide and silicon nitride [NASA-TM-86945] p 58 N85-21674
- Reliability of void detection in structural ceramics using scanning laser acoustic microscopy [NASA-TM-87035] p 58 N85-32337
- Probability of detection of internal voids in structural ceramics using microfocus radiography [NASA-TM-87164] p 59 N86-13749
- Reliability of scanning laser acoustic microscopy for detecting internal voids in structural ceramics [NASA-TM-87222] p 59 N86-16599
- Factors that affect reliability of nondestructive detection of flaws in structural ceramics [NASA-TM-87348] p 61 N86-31912
- Quantitative void characterization in structural ceramics using scanning laser acoustic microscopy [NASA-TM-88797] p 61 N86-31913
- NDE reliability and process control for structural ceramics [NASA-TM-88870] p 61 N87-12910
- BAKLINI, GEORGE Y.**
- Nondestructive evaluation of structural ceramics [NASA-TM-88978] p 62 N87-18109
- Ultrasonic NDE of structural ceramics for power and propulsion systems [NASA-TM-100147] p 62 N87-26362
- Flaw imaging and ultrasonic techniques for characterizing sintered silicon carbide [NASA-TM-100177] p 63 N88-12106
- BACH, L.**
- Blade loss transient dynamics analysis with flexible bladed disk [NASA-CR-168176] p 7 N84-13193
- BACH, L. J.**
- Blade loss transient dynamic analysis of turbomachinery p 2 A83-40864
- BAHNUK, E.**
- Ion beam sputter etching of orthopedic implanted alloy MP35N and resulting effects on fatigue [NASA-TM-81747] p 38 N81-21174
- BAILEY, W. J.**
- Fiberglass epoxy laminate fatigue properties at 300 and 20 K p 19 A85-47970
- BAK, M. J.**
- 3-D inelastic analysis methods for hot section components (base program) [NASA-CR-174700] p 107 N85-21686
- BALLARINI, R.**
- Compliance matrices for cracked bodies [NASA-CR-179478] p 120 N86-30236
- BALLARINI, ROBERTO**
- The effects of crack surface friction and roughness on crack tip stress fields [NASA-TM-88976] p 122 N87-18881
- BANERJEE, P. K.**
- Stress analysis of gas turbine engine structures using the boundary element method p 81 A86-34444
- Advanced three-dimensional dynamic analysis by boundary element methods p 81 A86-34445
- Three-dimensional stress analysis using the boundary element method p 106 N84-31700
- 3-D inelastic analysis methods for hot section components (base program) [NASA-CR-174700] p 107 N85-21686
- BARRETT, L. E.**
- A pad perturbation method for the dynamic coefficients of tilting-pad journal bearings p 47 A82-14400
- BARROW, B. J.**
- Thermal-fatigue and oxidation resistance of cobalt-modified Udimet 700 alloy [NASA-TP-2591] p 119 N86-28464
- BARTOLOTTA, P. A.**
- Viscoplastic constitutive relationships with dependence on thermomechanical history [NASA-CR-174836] p 108 N85-21691
- BARTOLOTTA, PAUL A.**
- A high temperature fatigue and structures testing facility [NASA-TM-100151] p 124 N87-26399
- BASHIR, S.**
- The effect of microstructure, temperature, and hold-time on low-cycle fatigue of As HIP P/M Rene 95 p 35 A85-32399
- BASKLINI, G. Y.**
- Nondestructive characterization of structural ceramics p 46 A86-37141
- BASU, P.**
- The effect of limiting aerodynamic and structural coupling in models of mistuned bladed disk vibration p 5 A86-26905
- BEATTIE, E. C.**
- Sensor failure detection for jet engines [NASA-CR-168190] p 56 N83-33182
- BECKER, E. B.**
- A numerical analysis of contact and limit-point behavior in a class of problems of finite elastic deformation p 72 A84-27370
- BEEK, J. M.**
- On the use of internal state variables in thermoviscoplastic constitutive equations p 113 N85-31536
- BEHRENDT, D. R.**
- Calculation of residual principal stresses in CVD boron on carbon filaments [NASA-TM-81456] p 22 N80-20314
- BELL, J. C.**
- Continuous analysis of stresses from arbitrary surface loads on a half space p 64 A81-14162
- BELYTSCHKO, T.**
- Probabilistic finite elements for transient analysis in nonlinear continua p 80 A86-28653
- Probabilistic finite element: Variational theory p 111 N85-27957
- BENDIKSEN, O. O.**
- Vibration characteristics of mistuned shrouded blade assemblies [ASME PAPER 85-GT-115] p 4 A86-22068
- Aeroelastic behavior of low aspect ratio metal and composite blades [ASME PAPER 86-GT-243] p 84 A86-48271
- BERKE, L.**
- Structural optimization using optimality criteria methods p 79 A85-48703
- The method of lines in three dimensional fracture mechanics [NASA-TM-81593] p 89 N80-32753
- BERKOVITS, A.**
- Estimation of high temperature low cycle fatigue on the basis of inelastic strain and strainrate [NASA-TM-88841] p 44 N87-14489
- BERNDT, C. C.**
- Acoustic emission evaluation of plasma-sprayed thermal barrier coatings [ASME PAPER 84-GT-292] p 48 A84-47046
- BESSENDORF, M.**
- Crack layer morphology and toughness characterization in steels [NASA-CR-168154] p 97 N83-27256
- BESSENDORFF, M.**
- The crack layer approach to toughness characterization in steel p 36 A86-30010
- BHAGAT, R. B.**
- Low cycle fatigue behavior of aluminum/stainless steel composites [AIAA 83-0806] p 16 A83-29886
- BHATT, R. T.**
- Fatigue behavior of SiC reinforced titanium composites p 13 A80-10036
- Fatigue behavior of SiC reinforced Ti/6Al-4V at 650 C p 15 A83-12414
- BIELAWA, R. L.**
- Aeroelastic analysis for propellers - mathematical formulations and program user's manual [NASA-CR-3729] p 101 N84-12530
- BILL, R. C.**
- Preliminary study of thermomechanical fatigue of polycrystalline MAR-M 200 [NASA-TP-2280] p 40 N84-17350
- Low cycle fatigue behavior of conventionally cast MAR-M 200 AT 1000 deg C [NASA-TM-83769] p 41 N84-33564
- Low cycle fatigue of MAR-M 200 single crystals at 760 and 870 deg C [NASA-TM-86933] p 41 N85-19074
- Multiaxial and thermomechanical fatigue considerations in damage tolerant design [NASA-TM-87022] p 42 N85-26964
- Micromechanisms of thermomechanical fatigue: A comparison with isothermal fatigue [NASA-TM-87331] p 44 N86-28164
- BIROL, Y.**
- Fatigue crack layer propagation in silicon-iron [NASA-CR-175115] p 118 N86-25851
- BIZON, P. T.**
- Comparative thermal fatigue resistance of several oxide dispersion strengthened alloys p 32 A82-11399
- Three dimensional finite-element elastic analysis of a thermally cycled double-edge wedge geometry specimen [NASA-TM-80980] p 37 N80-26433
- Thermal fatigue resistance of cobalt-modified UDIMET 700 p 39 N83-11289
- Interaction of high-cycle and low-cycle fatigue of Haynes 188 alloy at 1400 F deg p 111 N85-27961
- Thermal-fatigue and oxidation resistance of cobalt-modified Udimet 700 alloy [NASA-TP-2591] p 119 N86-28464
- BLACK, G.**
- Blade loss transient dynamic analysis of turbomachinery p 2 A83-40864
- Blade loss transient dynamics analysis with flexible bladed disk [NASA-CR-168176] p 7 N84-13193
- BODNER, S. R.**
- A survey of unified constitutive theories p 112 N85-31531
- Constitutive modeling for isotropic materials (HOST) [NASA-CR-174980] p 115 N86-10589
- BOYCE, D. A.**
- Fiberglass epoxy laminate fatigue properties at 300 and 20 K p 19 A85-47970
- BRAUN, M. J.**
- High temperature thermomechanical analysis of ceramic coatings p 74 A84-48565
- BROWN, G. V.**
- Nonlinear vibration and stability of rotating, pretwisted, precone blades including Coriolis effects p 86 A87-39896
- Lewis Research Center spin rig and its use in vibration analysis of rotating systems [NASA-TP-2304] p 9 N84-24578
- Nonlinear bending-torsional vibration and stability of rotating, pretwisted, precone blades including Coriolis effects [NASA-TM-87207] p 116 N86-17789
- A low-cost optical data acquisition system for vibration measurement [NASA-TM-88907] p 121 N87-14730
- The impact damped harmonic oscillator in free decay [NASA-TM-89897] p 50 N87-23978
- BROWN, K. W.**
- Structural tailoring of engine blades (STAEBL) [AIAA 83-0828] p 1 A83-29737
- Finite element engine blade structural optimization [AIAA PAPER 85-0645] p 76 A85-30313
- Structural tailoring of advanced turboprops [AIAA PAPER 87-0753] p 85 A87-33648
- Structural tailoring of engine blades (STAEBL) [NASA-CR-167949] p 7 N82-33391
- Structural tailoring of engine blades (STAEBL) theoretical manual [NASA-CR-175112] p 12 N86-27283
- Structural tailoring of engine blades (STAEBL) user's manual [NASA-CR-175113] p 13 N86-27284
- STAEBL: Structural tailoring of engine blades, phase 2 p 13 N87-11731
- BROWN, W. F., JR.**
- Fracture toughness of hot-pressed beryllium p 34 A85-25835
- Elastic analysis of a mode II fatigue crack test specimen p 84 A87-17799
- BUBSEY, R. T.**
- Fracture toughness determination of Al₂O₃ using four-point-bend specimens with straight-through and chevron notches p 45 A80-42085
- Compliance and stress intensity coefficients for short bar specimens with chevron notches p 64 A80-46032
- Performance of Chevron-notch short bar specimen in determining the fracture toughness of silicon nitride and aluminum oxide p 45 A80-50696
- Fracture toughness of brittle materials determined with chevron notch specimens p 45 A81-32545
- Extended range stress intensity factor expressions for chevron-notched short bar and short rod fracture toughness specimens p 66 A82-40357
- Development of plane strain fracture toughness test for ceramics using Chevron notched specimens p 46 A84-11676
- BUNDAS, D. J.**
- Flutter and forced response of mistuned rotors using standing wave analysis [AIAA 83-0845] p 69 A83-29823
- Flutter and forced response of mistuned rotors using standing wave analysis p 74 A85-12721
- Flutter and forced response of mistuned rotors using standing wave analysis [NASA-CR-173555] p 9 N84-24586
- BURGESS, G.**
- Development of procedures for calculating stiffness and damping of elastomers in engineering applications, part 6 [NASA-CR-159838] p 87 N80-2273:
- BURNSIDE, O. H.**
- Probabilistic structural analysis for space propulsion system components p 81 A86-28659
- Probabilistic structural analysis theory development p 111 N85-27955

- BURRUS, D. L.**
Aerothermal modeling. Executive summary
[NASA-CR-168330] p 7 N84-15152
- BURSEY, R. T.**
Fracture toughness of brittle materials determined with chevron notch specimens
[NASA-TM-81607] p 38 N80-32486
- BUSBEY, B. C.**
The effects of strong shock loading on coupled bending-torsion flutter of tuned and mistuned cascades
p 4 A86-26893
- BUZZARD, R. J.**
Mode II fatigue crack growth specimen development
p 83 A86-43566
Elastic analysis of a mode II fatigue crack test specimen
p 84 A87-17799
Comparison tests and experimental compliance calibration of the proposed standard round compact plane strain fracture toughness specimen
[NASA-TM-81379] p 87 N80-13513
Experimental compliance calibration of the compact fracture toughness specimen
[NASA-TM-81665] p 89 N81-16492
Mode 2 fatigue crack growth specimen development
[NASA-TM-83722] p 104 N84-29248
Experimental compliance calibration of the NASA Lewis Research Center Mode 2 fatigue specimen
[NASA-TM-86908] p 107 N85-16205
- C**
- CAREK, GERALD A.**
Shot peening for Ti-6Al-4V alloy compressor blades
[NASA-TP-2711] p 123 N87-20566
- CARLSON, C. E. K.**
Diffusion bonded boron/aluminum spar-shell fan blade
[NASA-CR-159571] p 23 N80-25382
- CARLSON, R. L.**
Thermodynamically consistent constitutive equations for nonisothermal large strain, elasto-plastic, creep behavior
[AIAA PAPER 85-0621] p 77 A85-38425
Analysis of shell type structures subjected to time dependent mechanical and thermal loading
[NASA-CR-175747] p 109 N85-25896
Dynamic creep buckling: Analysis of shell structures subjected to time-dependent mechanical and thermal loading
p 111 N85-27959
Analysis of large, non-isothermal elastic-visco-plastic deformations
[NASA-CR-176220] p 115 N86-10588
Formulation of the nonlinear analysis of shell-like structures, subjected to time-dependent mechanical and thermal loading
[NASA-CR-177194] p 119 N86-28462
- CARNEY, K. S.**
Joint research effort on vibrations of twisted plates, phase 1: Final results
[NASA-RP-1150] p 115 N86-10579
- CARNEY, KELLY S.**
The effect of nonlinearities on the dynamic response of a large shuttle payload
[NASA-TM-88941] p 121 N87-18112
- CARUSO, J. J.**
Assessment of simplified composite micromechanics using three-dimensional finite-element analysis
p 20 A87-19121
Application of finite element substructuring to composite micromechanics
[NASA-TM-83729] p 27 N84-31288
- CASSENTI, B. N.**
Research and development program for the development of advanced time-temperature dependent constitutive relationships. Volume 1: Theoretical discussion
[NASA-CR-168191-VOL-1] p 100 N84-10613
Research and development program for the development of advanced time-temperature dependent constitutive relationships. Volume 2: Programming manual
[NASA-CR-168191-VOL-2] p 100 N84-10614
Constitutive modeling for isotropic materials (HOST)
[NASA-CR-174980] p 115 N86-10589
- CHAMIS, C. C.**
Mechanical property characterization of intraply hybrid composites
p 13 A80-20954
Dynamic response of damaged angleplied fiber composites
p 14 A80-27982
Micromechanics of intraply hybrid composites: Elastic and thermal properties
p 14 A80-27994
Prediction of fiber composite mechanical behavior made simple
p 63 A80-32067
Engine environmental effects on composite behavior
[AIAA 80-0695] p 1 A80-35101

- Nonlinear laminate analysis for metal matrix fiber composites
[AIAA 81-0579] p 15 A81-29411
Superhybrid composite blade impact studies
[ASME PAPER 81-GT-24] p 1 A81-29940
Computer code for intraply hybrid composite design
p 15 A81-44662
Sensitivity analysis results of the effects of various parameters on composite design
p 15 A82-37101
Impact resistance of fiber composites
p 66 A82-39852
Tensile buckling of advanced turboprops
[AIAA PAPER 82-0776] p 67 A83-10900
Resin selection criteria for tough composite structures
[AIAA 83-0801] p 46 A83-29734
Structural tailoring of engine blades (STAEBL)
[AIAA 83-0828] p 1 A83-29737
Design concepts for low cost composite engine frames
[AIAA PAPER 83-2445] p 2 A83-48331
Tensile buckling of advanced turboprops
p 71 A84-11039
Prediction of composite hygral behavior made simple
p 16 A84-14285
Environmental and high strain rate effects on composites for engine applications
p 16 A84-17444
Durability/life of fiber composites in hygrothermomechanical environments
p 16 A84-27359
Compressive behavior of unidirectional fibrous composites
p 16 A84-29894
Simplified composite micromechanics equations for strength, fracture toughness and environmental effects
p 17 A84-41858
Simplified composite micromechanics equations of hygral, thermal, and mechanical properties
p 17 A84-49377
Hygrothermomechanical evaluation of transverse filament tape epoxy/polyester fiberglass composites
p 17 A85-15632
Design procedures for fiber composite structural components - Rods, beams, and beam columns
p 17 A85-15636
Select fiber composites for space applications - A mechanistic assessment
p 18 A85-16040
ICAN - Integrated composites analyzer
[AIAA PAPER 84-0974] p 18 A85-16094
Interply layer degradation effects on composite structural response
[AIAA PAPER 84-0849] p 18 A85-16096
Finite element engine blade structural optimization
[AIAA PAPER 85-0645] p 76 A85-30313
A study of interply layer effects on the free edge stress field of angleplied laminates
p 18 A85-41127
Impact resistance of fiber composites - Energy-absorbing mechanisms and environmental effects
p 18 A85-46543
Longitudinal compressive failure modes in fiber composites End attachment effects on ILTRI type test specimens
p 19 A86-19999
NASA Lewis Research Center/university graduate research program on engine structures
[ASME PAPER 85-GT-159] p 80 A86-22084
Designing for fiber composite structural durability in hygrothermomechanical environments
p 19 A86-27734
Composite sandwich thermostructural behavior - Computational simulation
[AIAA PAPER 86-0948] p 82 A86-38842
Computer aided derivation of equations for composite mechanics problems and finite element analyses
[AIAA PAPER 86-1016] p 83 A86-38873
Computational composite mechanics for aerospace propulsion structures
[AIAA PAPER 86-1190] p 19 A86-40596
Dynamic stress analysis of smooth and notched fiber composite flexural specimens
p 20 A86-41070
Computational engine structural analysis
[ASME PAPER 86-GT-70] p 5 A86-48141
Assessment of simplified composite micromechanics using three-dimensional finite-element analysis
p 20 A87-19121
Fabrication and quality assurance processes for superhybrid composite fan blades
p 20 A87-19123
Design concepts/parameters assessment and sensitivity analyses of select composite structural components
p 85 A87-25407
Structural tailoring of advanced turboprops
[AIAA PAPER 87-0753] p 85 A87-33648
Micromechanics of intraply hybrid composites: Elastic and thermal properties
[NASA-TM-79253] p 21 N80-11143
Tensile and flexural strength of non-graphitic superhybrid composites: Predictions and comparisons
[NASA-TM-79276] p 21 N80-11144

- Dynamic response of damaged angleplied fiber composites
[NASA-TM-79281] p 21 N80-11145
Mechanical property characterization of intraply hybrid composites
[NASA-TM-79306] p 21 N80-12120
Prediction of fiber composite mechanical behavior made simple
[NASA-TM-81404] p 22 N80-16107
Engine environmental effects on composite behavior
[NASA-TM-81508] p 22 N80-23370
Superhybrid composite blade impact studies
[NASA-TM-81597] p 89 N81-11412
Laminates and reinforced metals
[NASA-TM-81591] p 23 N81-12171
Prediction of composite thermal behavior made simple
[NASA-TM-81618] p 23 N81-16132
Nonlinear laminate analysis for metal matrix fiber composites
[NASA-TM-82596] p 24 N81-25149
Computer code for intraply hybrid composite design
[NASA-TM-82593] p 24 N81-25151
Integrated analysis of engine structures
[NASA-TM-82713] p 91 N82-11491
Durability/life of fiber composites in hygrothermomechanical environments
[NASA-TM-82749] p 24 N82-14287
Prediction of composite hygral behavior made simple
[NASA-TM-82780] p 24 N82-16181
Structural dynamics of shrouded, hollow fan blades with composite in-lays
[NASA-TM-82816] p 7 N82-22266
Compression behavior of unidirectional fibrous composite
[NASA-TM-82833] p 25 N82-22313
Designing with fiber-reinforced plastics (planar random composites)
[NASA-TM-82812] p 25 N82-24300
Environmental and High-Strain Rate effects on composites for engine applications
[NASA-TM-82882] p 25 N82-31449
Tensile buckling of advanced turboprops
[NASA-TM-82896] p 94 N82-31708
Large displacements and stability analysis of nonlinear propeller structures
p 95 N83-12460
Hygrothermomechanical evaluation of transverse filament tape epoxy/polyester fiberglass composites
[NASA-TM-83044] p 26 N83-15362
Simplified composite micromechanics equations for hygral, thermal and mechanical properties
[NASA-TM-83320] p 26 N83-19817
Design procedures for fiber composite structural components: Rods, columns and beam columns
[NASA-TM-83321] p 26 N83-24559
INHYD: Computer code for intraply hybrid composite design. A users manual
[NASA-TP-2239] p 26 N84-13224
Design concepts for low-cost composite engine frames
[NASA-TM-83544] p 8 N84-16186
Select fiber composites for space applications: A mechanistic assessment
[NASA-TM-83631] p 26 N84-22702
Impact resistance of fiber composites: Energy absorbing mechanisms and environmental effects
[NASA-TM-83594] p 26 N84-24712
Dynamic stress analysis of smooth and notched fiber composite flexural specimens
[NASA-TM-83694] p 27 N84-25770
ICAN: Integrated composites analyzer
[NASA-TM-83700] p 27 N84-26755
Interply layer degradation effects on composite structural response
[NASA-TM-83702] p 27 N84-26756
Simplified composite micromechanics equations for strength, fracture toughness and environmental effects
[NASA-TM-83696] p 27 N84-27832
Hygrothermomechanical fracture stress criteria for fiber composites with sense-parity
[NASA-TM-83691] p 27 N84-28918
Nonlinear analysis for high-temperature composites: Turbine blades/vanes
p 106 N84-31699
The 3-D inelastic analysis methods for hot section components: Brief description
p 10 N85-10972
Fabrication and quality assurance processes for superhybrid composite fan blades
[NASA-TM-83354] p 28 N85-14882
A study of interply layer effects on the free-edge stress field of angleplied laminates
[NASA-TM-86924] p 28 N85-15822
Design procedures for fiber composite structural components: Panels subjected to combined in-plane loads
[NASA-TM-86909] p 29 N85-15823

- NASA Lewis Research Center/University Graduate Research Program on Engine Structures
[NASA-TM-86916] p 107 N85-18375
Nonlinear structural analysis for fiber-reinforced superalloy turbine blades p 109 N85-26887
Overview of structural response: Probabilistic structural analysis p 110 N85-27952
Designing for fiber composite structural durability in hygrothermomechanical environment
[NASA-TM-87045] p 29 N85-27978
Computational engine structural analysis
[NASA-TM-87231] p 116 N86-19663
Integrated Composite Analyzer (ICAN): Users and programmers manual
[NASA-TP-2515] p 30 N86-21614
Thermoviscoplastic nonlinear constitutive relationships for structural analysis of high temperature metal matrix composites
[NASA-TM-87291] p 30 N86-24756
A unique set of micromechanics equations for high temperature metal matrix composites
[NASA-TM-87154] p 30 N86-24757
Simplified composite micromechanics for predicting microstresses
[NASA-TM-87295] p 30 N86-24759
Fracture characteristics of angleplied laminates fabricated from overaged graphite/epoxy prepreg
[NASA-TM-87266] p 30 N86-25417
Computational simulation of progressive fracture in fiber composites
[NASA-TM-87341] p 30 N86-26376
Fiber composite sandwich thermostructural behavior: Computational simulation
[NASA-TM-88787] p 31 N86-31663
ICAN: A versatile code for predicting composite properties
[NASA-TM-87334] p 31 N86-31664
Composite interlaminar fracture toughness: Three-dimensional finite element modeling for mixed mode 1, 2 and 3 fracture
[NASA-TM-88872] p 31 N87-13491
Probabilistic structural analysis methods for space propulsion system components
[NASA-TM-88861] p 121 N87-13794
Free-edge delamination: Laminar width and loading conditions effects
[NASA-TM-100238] p 32 N88-12551
- CHAMIS, CHRISTOS C.**
Simplified composite micromechanics for predicting microstresses p 20 A87-20090
Probabilistic structural analysis to quantify uncertainties associated with turbopump blades
[AIAA PAPER 87-0766] p 85 A87-33581
Advances in 3-D Inelastic Analysis Methods for hot section components
[AIAA PAPER 87-0719] p 85 A87-33645
Simplified composite micromechanics for predicting microstresses p 87 A87-49275
Computational composite mechanics for aerospace propulsion structures
[NASA-TM-88965] p 31 N87-18614
Dynamic delamination buckling in composite laminates under impact loading: Computational simulation
[NASA-TM-100192] p 31 N87-28611
Composite mechanics for engine structures
[NASA-TM-100176] p 32 N88-12552
- CHAN, K. S.**
A survey of unified constitutive theories p 112 N85-31531
Constitutive modeling for isotropic materials (HOST)
[NASA-CR-174980] p 115 N86-10589
- CHANG, J. P.**
On numerical integration and computer implementation of viscoplastic models p 113 N85-31542
- CHANG, S. H.**
A finite element stress analysis of spur gears including fillet radii and rim thickness effects
[NASA-TM-82865] p 48 N82-28646
On finite element stress analysis of spur gears
[NASA-CR-167938] p 48 N82-29607
- CHANG, S.-H.**
An embedding method for the steady Euler equations p 126 A86-30814
- CHANG, T. Y.**
A computer program for predicting nonlinear uniaxial material responses using viscoplastic models
[NASA-TM-83675] p 104 N84-29247
Nonlinear finite element analysis of shells with large aspect ratio p 105 N84-31692
On numerical integration and computer implementation of viscoplastic models p 113 N85-31542
- CHAO, W. C.**
Geometrically nonlinear analysis of layered composite shells p 68 A83-27431
- Geometrically nonlinear analysis of layered composite plates and shells
[NASA-CR-168182] p 98 N83-33219
- CHEN, C. J.**
The finite analytic method, volume 3
[NASA-CR-170186] p 127 N83-23087
The finite analytic method, volume 4
[NASA-CR-170187] p 127 N83-23088
The finite analytic method, volume 5
[NASA-CR-170188] p 127 N83-23089
- CHEN, D.**
On the suppression of zero energy deformation modes p 72 A84-21541
- CHEN, D.-P.**
A new formulation of hybrid/mixed finite element p 67 A83-12739
Alternative ways for formulation of hybrid stress elements p 68 A83-14710
- CHEN, E. P.**
Moving cracks in layered composites p 67 A83-12048
Sudden stretching of a four layered composite plate
[NASA-CR-159870] p 23 N80-25383
Sudden bending of cracked laminates
[NASA-CR-159860] p 23 N80-25384
- CHEN, H. C.**
The finite analytic method, volume 4
[NASA-CR-170187] p 127 N83-23088
- CHENG, W. S.**
The finite analytic method, volume 5
[NASA-CR-170188] p 127 N83-23089
- CHI, R. M.**
Aeroelastic analysis for propellers - mathematical formulations and program user's manual
[NASA-CR-3729] p 101 N84-12530
- CHIEN, C. H.**
Extending the laser-specklegram technique to strain analysis of rotating components p 67 A83-12514
- CHOE, S. J.**
The influence of hold times on LCF and FCG behavior in a P/M Ni-base superalloy p 35 A85-32400
Fatigue crack growth and low cycle fatigue of two nickel base superalloys
[NASA-CR-174534] p 39 N84-10267
- CHOI, I.**
Boundary-layer effects in composite laminates. I - Free-edge stress singularities. II - Free-edge stress solutions and basic characteristics p 67 A82-46806
Boundary layer thermal stresses in angle-ply composite laminates, part 1
[NASA-CR-165412] p 93 N82-26713
Boundary-layer effects in composite laminates: Free-edge stress singularities, part 6
[NASA-CR-165440] p 94 N82-26718
- CHRISTOPHER, M.**
Ion beam sputter etching of orthopedic implanted alloy MP35N and resulting effects on fatigue
[NASA-TM-81747] p 38 N81-21174
- CHUDNOVSKY, A.**
Statistics and thermodynamics of fracture p 75 A85-19433
The crack layer approach to toughness characterization in steel p 36 A86-30010
Crack layer morphology and toughness characterization in steels
[NASA-CR-168154] p 97 N83-27256
Crack layer theory
[NASA-CR-174634] p 103 N84-22980
On stress analysis of a crack-layer
[NASA-CR-174774] p 106 N84-34774
Translational and extensional energy release rates (the J- and M-integrals) for a crack layer in thermoelasticity
[NASA-CR-174872] p 107 N85-21685
Fatigue crack layer propagation in silicon-iron
[NASA-CR-175115] p 118 N86-25851
- CHUNG, B. T. F.**
High temperature thermomechanical analysis of ceramic coatings p 74 A84-48565
- CLINE, S.**
Blade loss transient dynamics analysis with flexible bladed disk
[NASA-CR-168176] p 7 N84-13193
- CO, C. M.**
Fundamentals of microcrack nucleation mechanics
[NASA-CR-3851] p 57 N85-16195
- COE, HAROLD H.**
Effect of interference fits on roller bearing fatigue life p 48 A87-37686
- COOK, T. S.**
Requirements of constitutive models for two nickel-base superalloys p 33 A83-21071
Considerations for damage analysis of gas turbine hot section components
[ASME PAPER 84-PVP-77] p 2 A85-18792
- CORREA, S. M.**
Aerothermal modeling. Executive summary
[NASA-CR-168330] p 7 N84-15152
- COWLES, B. A.**
Cyclic behavior of turbine disk alloys at 650 C p 32 A81-12266
Evaluation of the cyclic behavior of aircraft turbine disk alloys, part 2
[NASA-CR-165123] p 38 N80-30482
Low strain, long life creep fatigue of AF2-1DA and INCO 718
[NASA-CR-167989] p 40 N84-10268
- COY, J. J.**
A finite element stress analysis of spur gears including fillet radii and rim thickness effects
[NASA-TM-82865] p 48 N82-28646
- CRAWLEY, E. F.**
Stagger angle dependence of inertial and elastic coupling in bladed disks p 72 A84-31903
Aeroelastic formulations for turbomachines and propellers p 4 A86-24677
Analytical and experimental investigation of the coupled bladed disk/shaft whirl of a cantilevered turbofan
[ASME PAPER 86-GT-98] p 6 A86-48163
Structural response of a rotating bladed disk to rotor whirl
[NASA-CR-175605] p 11 N85-22391
- CRONENWORTH, J.**
An uncoupled viscoplastic constitutive model for metals at elevated temperature
[AIAA 83-1016] p 69 A83-29798
- CROSLEY, P. B.**
Fracture of composite-adhesive-composite systems p 76 A85-27935
- CUNNINGHAM, R. E.**
Variable force, eddy-current or magnetic damper
[NASA-CASE-LEW-13717-1] p 49 N85-30333
- CUTLER, J. L.**
Diffusion bonded boron/aluminum spar-shell fan blade
[NASA-CR-159571] p 23 N80-25382

D

- DALE, B.**
NASTRAN level 16 programmer's manual updates for aeroelastic analysis of bladed discs
[NASA-CR-159825] p 90 N81-19482
- DAME, L. T.**
Finite element analysis of notch behavior using a state variable constitutive equation p 114 N85-31548
Anisotropic constitutive model for nickel base single crystal alloys: Development and finite element implementation
[NASA-CR-175015] p 117 N86-21952
- DANIELE, C. J.**
Digital computer program for generating dynamic turbofan engine models (DIGTEM)
[NASA-TM-83446] p 8 N84-16185
- DAVID, J. W.**
Theoretical investigation of the force and dynamically coupled torsional-axial-lateral dynamic response of eared rotors
[NASA-CR-173013] p 127 N83-34656
- DAWICKE, D. S.**
A preliminary study of crack initiation and growth at stress concentration sites p 94 N82-33738
A total life prediction model for stress concentration sites
[NASA-CR-170290] p 96 N83-23629
A total life prediction model for stress concentration sites
[NASA-CR-168225] p 100 N84-10612
- DIAS, J. B.**
Efficient algorithms for use in probabilistic finite element analysis p 81 A86-28655
- DICARLO, J. A.**
Predicting the time-temperature dependent axial failure of B/A1 composites p 14 A80-35494
Dynamic modulus and damping of boron, silicon carbide, and alumina fibers p 15 A80-44236
Dynamic modulus and damping of boron, silicon carbide, and alumina fibers
[NASA-TM-81422] p 22 N80-20313
Predicting the time-temperature dependent axial failure of B/A1 composites
[NASA-TM-81474] p 22 N80-21452
- DIDELOT, R. C.**
Array structure design handbook for stand alone photovoltaic applications
[NASA-TM-82629] p 96 N83-23631
- DIRUSSO, E.**
Dynamic behavior of spiral-groove and Rayleigh-Step self-acting face seals
[NASA-TP-2266] p 8 N84-16181

- DODDS, R. H., JR.**
Theoretical and software considerations for nonlinear dynamic analysis
[NASA-CR-174504] p 101 N84-15589
- DOLGOPOLSKY, A.**
On stress analysis of a crack-layer
[NASA-CR-174774] p 106 N84-34774
- DOMAS, P. A.**
Benchmark notch test for life prediction
[NASA-CR-165571] p 95 N83-12451
- DOS REIS, HENRIQUE L. M.**
Nondestructive evaluation of adhesive bond strength using the stress wave factor technique
p 53 A87-32200
- DOUGHERTY, D.**
High temperature thermomechanical analysis of ceramic coatings p 74 A84-48565
Inelastic high-temperature thermomechanical response of ceramic coated gas turbine seals p 82 A86-37799
- DOWELL, E. H.**
Design of dry-friction dampers for turbine blades p 2 A83-35883
Forced response of a cantilever beam with a dry friction damper attached. I - Theory. II - Experiment p 71 A84-21267
Frequency domain solutions to multi-degree-of-freedom, dry friction damped systems under periodic excitation p 83 A86-39485
- DOWLING, N. E.**
Closure of fatigue cracks at high strains
[NASA-CR-175021] p 116 N86-17788
J-integral estimates for cracks in infinite bodies
[NASA-CR-179474] p 119 N86-28467
- DRAGO, R. J.**
On the automatic generation of FEM models for complex gears - A work-in-progress report p 47 A82-48243
- DRAKE, S. K.**
Three dimensional finite-element elastic analysis of a thermally cycled double-edge wedge geometry specimen
[NASA-TM-80980] p 37 N80-26433
- DRESHFIELD, R. L.**
Effects of fine porosity on the fatigue behavior of a powder metallurgy superalloy p 32 A80-35495
Effects of fine porosity on the fatigue behavior of a powder metallurgy superalloy p 37 N80-21493
- DUCHARME, E. H.**
Analytical and experimental investigation of the coupled bladed disk/shaft whirl of a cantilevered turbopfan
[ASME PAPER 86-GT-98] p 6 A86-48163
- DUGUNDJI, J.**
Flutter and forced response of mistuned rotors using standing wave analysis
[AIAA 83-0845] p 69 A83-29823
Some analysis methods for rotating systems with periodic coefficients p 69 A83-32987
Flutter and forced response of mistuned rotors using standing wave analysis p 74 A85-12721
- DUKE, J. C., JR.**
Characterization of composite materials by means of the ultrasonic stress wave factor p 16 A84-10430
Factors influencing the ultrasonic stress wave factor evaluation of composite material structures p 81 A86-34257
A study of the stress wave factor technique for the characterization of composite materials
[NASA-CR-3670] p 55 N83-27248
A study of the stress wave factor technique for the characterization of composite materials
[NASA-CR-174870] p 29 N85-30035
Ultrasonic stress wave characterization of composite materials
[NASA-CR-3976] p 60 N86-27665
A study of the stress wave factor technique for nondestructive evaluation of composite materials
[NASA-CR-4002] p 60 N86-28445
- DUNGUNDJI, J.**
Flutter and forced response of mistuned rotors using standing wave analysis
[NASA-CR-173555] p 9 N84-24586
- DUQUETTE, D. J.**
The effects of frequency and hold times on fatigue crack propagation rates in a nickel base superalloy p 34 A84-18733
The influence of hold times on LCF and FCG behavior in a P/M Ni-base superalloy p 35 A85-32400
Fatigue crack growth and low cycle fatigue of two nickel base superalloys
[NASA-CR-174534] p 39 N84-10267

E

- ELCHURI, V.**
Flutter analysis of advanced turbopropellers
[AIAA 83-0846] p 69 A83-29824

- NASTRAN forced vibration analysis of rotating cyclic structures
[ASME PAPER 83-DET-20] p 72 A84-29103
Flutter analysis of advanced turbopropellers p 73 A84-36492
Aeroelastic and dynamic finite element analyses of a bladder shrouded disk
[NASA-CR-159728] p 90 N81-19479
Nastran level 16 theoretical manual updates for aeroelastic analysis of bladed discs
[NASA-CR-159823] p 90 N81-19480
NASTRAN level 16 user's manual updates for aeroelastic analysis of bladed discs
[NASA-CR-159824] p 90 N81-19481
NASTRAN level 16 demonstration manual updates for aeroelastic analysis of bladed discs
[NASA-CR-159826] p 90 N81-19483
Forced vibration analysis of rotating cyclic structures in NASTRAN
[NASA-CR-165429] p 100 N84-11514
Finite element forced vibration analysis of rotating cyclic structures
[NASA-CR-165430] p 101 N84-11515
NASTRAN documentation for flutter analysis of advanced turbopropellers
[NASA-CR-167927] p 8 N84-15153
Bladed-shrouded-disc aeroelastic analyses: Computer program updates in NASTRAN level 17.7
[NASA-CR-165428] p 8 N84-15154
NASTRAN forced vibration analysis of rotating cyclic structures
[NASA-CR-173821] p 104 N84-29252
- ELLIS, J. R.**
Results of an interlaboratory fatigue test program conducted on alloy 800H at room and elevated temperatures p 37 A87-54370
Some advances in experimentation supporting development of viscoplastic constitutive models
[NASA-CR-174855] p 109 N85-27260
Some advances in experimentation supporting development of viscoplastic constitutive models p 113 N85-31545
Results of an interlaboratory fatigue test program conducted on alloy 800H at room and elevated temperatures
[NASA-CR-174940] p 114 N85-32340
- ENDO, T.**
A numerical analysis of contact and limit-point behavior in a class of problems of finite elastic deformation p 72 A84-27370
- ENDRES, N. M.**
Composite space antenna structures - Properties and environmental effects p 20 A87-38610
- ENDRES, NED M.**
Composite space antenna structures: Properties and environmental effects
[NASA-TM-88859] p 31 N87-16880
- ENSIGN, C. R.**
A quarter-century of progress in the development of correlation and extrapolation methods for creep rupture data p 63 A80-38142
Toward improved durability in advanced combustors and turbines - Progress in prediction of thermomechanical loads
[ASME PAPER 86-GT-172] p 6 A86-48224
- ENSIGN, C. ROBERT**
Toward improved durability in advanced combustors and turbines: Progress in the prediction of thermomechanical loads
[NASA-TM-88932] p 13 N87-28551
- ERNST, MICHAEL A.**
A NASTRAN primer for the analysis of rotating flexible blades
[NASA-TM-89861] p 123 N87-21375
Hub flexibility effects on propfan vibration
[NASA-TM-89900] p 124 N87-24722
- EWING, M. S.**
Comparison of beam and shell theories for the vibrations of thin turbomachinery blades
[ASME PAPER 82-GT-223] p 65 A82-35408

F

- FADDOUL, J. R.**
Ten year environmental test of glass fiber/epoxy pressure vessels
[AIAA PAPER 85-1198] p 19 A85-47022
Structural fatigue test results for large wind turbine blade sections p 96 N83-19246
Ten year environmental test of glass fiber/epoxy pressure vessels
[NASA-TM-87058] p 29 N85-30034

- FADOU, J. R.**
Improved stud configurations for attaching laminated wood wind turbine blades
[NASA-TM-87109] p 115 N86-10582
- FANG, J. J.**
Longitudinal mode combustion instabilities of a high-pressure fuel-rich LOX/RP-1 preburner p 60 N86-28250
- FERRI, A. A.**
Frequency domain solutions to multi-degree-of-freedom, dry friction damped systems under periodic excitation p 83 A86-39485
On the equivalence of the incremental harmonic balance method and the harmonic balance-Newton Raphson method p 83 A86-40695
- FERTIS, D.**
Engine dynamic analysis with general nonlinear finite element codes. II - Bearing element implementation, overall numerical characteristics and benchmarking
[ASME PAPER 82-GT-292] p 47 A82-35462
Nonlinear, transient finite element analysis of rotor-bearing-stator systems p 48 A84-20580
- FERTIS, J.**
Engine, dynamic analysis with general nonlinear finite element codes. Part 2: Bearing element implementation overall numerical characteristics and benchmarking
[NASA-CR-167944] p 7 N82-33390
- FISHER, D. M.**
Comparison, tests and experimental compliance calibration of the proposed standard round compact plane strain fracture toughness specimen
[NASA-TM-81379] p 87 N80-13513
Experimental compliance calibration of the compact fracture toughness specimen
[NASA-TM-81665] p 89 N81-16492
Evaluation of the effect of crack closure on fatigue crack growth of simulated short cracks
[NASA-TM-83778] p 40 N84-31348
Variables controlling fatigue crack growth of short cracks
[NASA-TM-87208] p 43 N86-21661
Influence of fatigue crack wake length and state of stress on crack closure
[NASA-TM-87292] p 43 N86-22686
- FISHER, W. J.**
Diffusion bonded boron/aluminum spar-shell fan blade
[NASA-CR-159571] p 23 N80-25382
- FLEETER, S.**
The coupled aeroelastic response of turbomachinery blading to aerodynamic excitations
[AIAA 83-0844] p 69 A83-29822
The coupled response of turbomachinery blading to aerodynamic excitations p 2 A84-26959
The effect of aerodynamic and structural detuning on turbomachine supersonic unstalled torsional flutter
[AIAA PAPER 85-0761] p 3 A85-30378
Forced response analysis of an aerodynamically detuned supersonic turbomachine rotor p 5 A86-26902
Aerodynamic and structural detuning of supersonic turbomachine rotors p 5 A86-31595
The effect of circumferential aerodynamic detuning on coupled bending-torsion unstalled supersonic flutter
[ASME PAPER 86-GT-100] p 6 A87-25396
- FLEMING, D. P.**
Structural dynamics verification facility study
[NASA-TM-82675] p 90 N81-33497
- FORTE, T. P.**
Nonlinear damage analysis: Postulate and evaluation
[NASA-CR-168171] p 118 N86-26652
- FREDERICK, G. R.**
Structural analysis and cost estimate of an eight-leg space frame as a support structure for horizontal axis wind turbines
[NASA-TM-83470] p 112 N85-30361
- FREED, A. D.**
The plastic compressibility of 7075-T651 aluminum-alloy plate p 36 A86-49690
- FRENCH, S. E.**
Instructions for the use of the CIVM-Jet 4C finite-strain computer code to calculate the transient structural responses of partial and/or complete arbitrarily-curved rings subjected to fragment impact
[NASA-CR-159873] p 88 N80-27720
- FU, K. C.**
Thermal stress analysis for a wood composite blade
[NASA-CR-173394] p 103 N84-21903
Thermal-stress analysis for wood composite blade
[NASA-CR-173830] p 104 N84-31685
- FU, L. S.**
On ultrasonic factors and fracture toughness p 66 A82-42863
Mechanics aspects of NDE by sound and ultrasound p 51 A82-25571

- The determination of the elastodynamic fields of an ellipsoidal inhomogeneity
[ASME PAPER 83-APM-19] p 69 A83-37388
- Ultrasonic wave propagation in two-phase media - Spherical inclusions p 17 A85-11926
- The transmission or scattering of elastic waves by an inhomogeneity of simple geometry: A comparison of theories
[NASA-CR-3659] p 55 N83-16773
- Volume integrals associated with the inhomogeneous Helmholtz equation. Part 1: Ellipsoidal region
[NASA-CR-3749] p 56 N84-14525
- Volume integrals associated with the inhomogeneous Helmholtz equation. Part 2: Cylindrical region; rectangular region
[NASA-CR-3750] p 56 N84-14526
- Fundamentals of microcrack nucleation mechanics
[NASA-CR-3851] p 57 N85-16195
- FU, L. S. W.**
- Phenomenological and mechanics aspects of nondestructive evaluation and characterization by sound and ultrasound of material and fracture properties
[NASA-CR-3623] p 55 N83-11506
- Fundamental aspects in quantitative ultrasonic determination of fracture toughness: The scattering of a single ellipsoidal inhomogeneity
[NASA-CR-3625] p 55 N83-11507
- FULTON, G. B.**
- Advanced turboprop vibratory characteristics
[NASA-CR-174708] p 12 N86-24693

G

- GABB, T. P.**
- On the fatigue crack propagation behavior of superalloys at intermediate temperatures p 35 A85-32434
- The tensile and fatigue deformation structures in a single crystal Ni-base superalloy p 36 A86-35697
- The cyclic stress-strain behavior of a nickel-base superalloy at 650 C p 36 A86-45715
- Orientation and temperature dependence of some mechanical properties of the single-crystal nickel-base superalloy Rene N4. II - Low cycle fatigue behavior p 37 A86-50322
- Fatigue crack propagation of nickel-base superalloys at 650 deg C
[NASA-TM-87110] p 42 N86-12294
- The low cycle fatigue behavior of a plasma-sprayed coating material
[NASA-TM-87318] p 44 N86-31699
- Bi-thermal low-cycle fatigue behavior of a NiCoCrAlY-coated single crystal superalloy
[NASA-TM-89831] p 45 N87-20408
- GAFFNEY, E. F.**
- Blade loss transient dynamic analysis of turbomachinery p 2 A83-40864
- GALLAGHER, J. P.**
- A preliminary study of crack initiation and growth at stress concentration sites
[NASA-CR-169358] p 94 N82-33738
- GALLARDO, V.**
- Blade loss transient dynamic analysis of turbomachinery p 2 A83-40864
- GALLARDO, V. C.**
- The dynamics of a flexible bladed disc on a flexible rotor in a two-rotor system p 4 A86-25743
- Blade loss transient dynamics analysis with flexible bladed disk
[NASA-CR-168176] p 7 N84-13193
- GALLO, A. M.**
- NASTRAN forced vibration analysis of rotating cyclic structures
[ASME PAPER 83-DET-20] p 72 A84-29103
- NASTRAN level 16 user's manual updates for aeroelastic analysis of bladed discs
[NASA-CR-159824] p 90 N81-19481
- NASTRAN level 16 programmer's manual updates for aeroelastic analysis of bladed discs
[NASA-CR-159825] p 90 N81-19482
- NASTRAN level 16 demonstration manual updates for aeroelastic analysis of bladed discs
[NASA-CR-159826] p 90 N81-19483
- Forced vibration analysis of rotating cyclic structures in NASTRAN
[NASA-CR-165429] p 100 N84-11514
- NASTRAN documentation for flutter analysis of advanced turbopropellers
[NASA-CR-167927] p 8 N84-15153
- Bladed-shrouded-disc aeroelastic analyses: Computer program updates in NASTRAN level 17.7
[NASA-CR-165428] p 8 N84-15154
- NASTRAN forced vibration analysis of rotating cyclic structures
[NASA-CR-173821] p 104 N84-29252
- GANGWANI, S. T.**
- Aeroelastic analysis for propellers - mathematical formulations and program user's manual
[NASA-CR-3729] p 101 N84-12530
- GAO, Y. C.**
- Dynamic fields near a crack tip growing in an elastic-perfectly-plastic solid p 70 A83-38528
- GAUGLER, R. E.**
- Nonlinear, three-dimensional finite-element analysis of air-cooled gas turbine blades
[NASA-TP-1669] p 88 N80-22734
- GAYDA, J.**
- Fatigue and creep-fatigue deformation of several nickel-base superalloys at 650 C p 32 A82-47398
- Fatigue crack initiation and propagation in several nickel-base superalloys at 650 C p 33 A83-41199
- The effect of microstructure on 650 C fatigue crack growth in P/M Astroloy p 33 A84-12395
- Effects of processing and microstructure on the fatigue behaviour of the nickel-base superalloy Rene95 p 34 A84-48715
- On the fatigue crack propagation behavior of superalloys at intermediate temperatures p 35 A85-32434
- The tensile and fatigue deformation structures in a single crystal Ni-base superalloy p 36 A86-35697
- Orientation and temperature dependence of some mechanical properties of the single-crystal nickel-base superalloy Rene N4. II - Low cycle fatigue behavior p 37 A86-50322
- Creep-fatigue behavior of NiCoCrAlY coated PWA 1480 superalloy single crystals
[NASA-TM-87110] p 42 N86-10311
- Fatigue crack propagation of nickel-base superalloys at 650 deg C
[NASA-TM-87150] p 42 N86-12294
- The low cycle fatigue behavior of a plasma-sprayed coating material
[NASA-TM-87318] p 44 N86-31699
- Bi-thermal low-cycle fatigue behavior of a NiCoCrAlY-coated single crystal superalloy
[NASA-TM-89831] p 45 N87-20408
- GELLIN, S.**
- Slave finite elements: The temporal element approach to nonlinear analysis p 105 N84-31689
- GENERAZIO, E. R.**
- The role of the reflection coefficient in precision measurement of ultrasonic attenuation p 51 A85-42151
- Quantitative flaw characterization with scanning laser acoustic microscopy p 52 A86-45150
- Quantitative void characterization in structural ceramics by use of scanning laser acoustic microscopy p 53 A87-51974
- The role of the reflection coefficient in precision measurement of ultrasonic attenuation
[NASA-TM-83788] p 57 N84-32849
- Determination of grain size distribution function using two-dimensional Fourier transforms of tone pulse encoded images
[NASA-TM-88790] p 61 N86-31065
- Quantitative void characterization in structural ceramics using scanning laser acoustic microscopy
[NASA-TM-88797] p 61 N86-31913
- Ultrasonic determination of recrystallization
[NASA-TM-88855] p 61 N87-10399
- GENERAZIO, EDWARD R.**
- Ultrasonic NDE of structural ceramics for power and propulsion systems
[NASA-TM-100147] p 62 N87-26362
- GINTY, C. A.**
- Select fiber composites for space applications - A mechanistic assessment p 18 A85-16040
- Progressive fracture of fiber composites p 19 A86-35809
- Composite space antenna structures - Properties and environmental effects p 20 A87-38610
- Select fiber composites for space applications: A mechanistic assessment
[NASA-TM-83631] p 26 N84-22702
- Hygrothermomechanical fracture stress criteria for fiber composites with sense-parity
[NASA-TM-83691] p 27 N84-28918
- Fracture surface characteristics of notched angleplied graphite/epoxy composites
[NASA-TM-83786] p 28 N84-33522
- Fracture modes in notched angleplied composite laminates
[NASA-TM-83802] p 28 N84-34576
- Fracture characteristics of angleplied laminates fabricated from overaged graphite/epoxy prepreg
[NASA-TM-87266] p 30 N86-25417
- ICAN: A versatile code for predicting composite properties
[NASA-TM-87334] p 31 N86-31664

- GINTY, CAROL A.**
- Composite space antenna structures: Properties and environmental effects
[NASA-TM-88859] p 31 N87-16880
- GOLWALKAR, S.**
- The effects of frequency and hold times on fatigue crack propagation rates in a nickel base superalloy p 34 A84-18733
- Fatigue crack growth and low cycle fatigue of two nickel base superalloys
[NASA-CR-174534] p 39 N84-10267
- GOLWALKER, S. V.**
- The influence of hold times on LCF and FCG behavior in a P/M Ni-base superalloy p 35 A85-32400
- GOMMERSTADT, B.**
- Translational and extensional energy release rates (the J- and M-integrals) for a crack layer in thermoelasticity
[NASA-CR-174872] p 107 N85-21685
- GOVADA, A.**
- A study of the stress wave factor technique for the characterization of composite materials
[NASA-CR-3670] p 55 N83-27248
- GOVADA, A. K.**
- A study of the stress wave factor technique for the characterization of composite materials
[NASA-CR-174870] p 29 N85-30035
- GRADY, J. E.**
- Dynamic delamination crack propagation in a graphite/epoxy laminate p 20 A86-43010
- GRADY, JOSEPH E.**
- Dynamic delamination buckling in composite laminates under impact loading: Computational simulation
[NASA-TM-100192] p 31 N87-28611
- GRIFFIN, J. H.**
- Effects of friction dampers on aerodynamically unstable rotor stages
[AIAA PAPER 83-0848] p 1 A83-32791
- Model development and statistical investigation of turbine blade mistuning p 2 A84-31905
- The interaction between mistuning and friction in the forced response of bladed disk assemblies
[ASME PAPER 84-GT-139] p 73 A84-46957
- Effects of friction dampers on aerodynamically unstable rotor stages p 3 A85-21866
- Stability of limit cycles in frictionally damped and aerodynamically unstable rotor stages p 4 A86-19198
- The effect of limiting aerodynamic and structural coupling in models of mistuned bladed disk vibration p 5 A86-26905
- Influence of friction dampers on torsional blade flutter
[ASME PAPER 85-GT-170] p 5 A86-32957
- GRIMES, H. H.**
- Fatigue behavior of SiC reinforced titanium composites p 13 A80-10036
- Fatigue behavior of SiC reinforced Ti/6Al-4V at 650 C p 15 A83-12414
- GROSS, B.**
- Analysis of an internally radially cracked ring segment subject to three-point radial loading p 71 A84-18691
- Wide-range displacement expressions for standard fracture mechanics specimens p 79 A86-20706
- Analysis of an externally radially cracked ring segment subject to three-point radial loading p 79 A86-20710
- Mode II fatigue crack growth specimen development p 83 A86-43566
- Elastic analysis of a mode II fatigue crack test specimen p 84 A87-17799
- Stress intensity and displacement coefficients for radially cracked ring segments subject to three-point bending
[NASA-TM-83059] p 96 N83-24874
- Analysis of an externally radially cracked ring segment subject to three-point radial loading
[NASA-TM-83482] p 100 N83-35413
- Mode 2 fatigue crack growth specimen development
[NASA-TM-83722] p 104 N84-29248
- GROSS, D.**
- Statistical aspects of carbon fiber risk assessment modeling
[NASA-CR-159318] p 23 N80-29432
- GUILLIAMS, B. P.**
- Three dimensional finite-element elastic analysis of a thermally cycled double-edge wedge geometry specimen
[NASA-TM-80980] p 37 N80-26433
- GYEKENYESI, J.**
- The method of lines in three dimensional fracture mechanics
[NASA-TM-81593] p 89 N80-32753
- GYEKENYESI, J. P.**
- SCARE - A postprocessor program to MSC/NASTRAN for reliability analysis of structural ceramic components
[ASME PAPER 86-GT-34] p 84 A87-17998
- GYEKENYESI, JOHN P.**
- Surface flaw reliability analysis of ceramic components with the SCARE finite element postprocessor program
[NASA-TM-88901] p 121 N87-17087

Fracture mechanics concepts in reliability analysis of monolithic ceramics
[NASA-TM-100174] p 124 N87-27269

H

HAFTKA, R. T.

Optimization of cascade blade mistuning. II - Global optimum and numerical optimization p 3 A85-45715

HAFTKA, RAPHAEL T.

Approximations to eigenvalues of modified general matrices
[AIAA PAPER 87-0947] p 86 A87-33756

HAISLER, W. E.

An uncoupled viscoplastic constitutive model for metals at elevated temperature
[AIAA 83-1016] p 69 A83-29798

Numerical considerations in the development and implementation of constitutive models p 113 N85-31541

Development of constitutive models for cyclic plasticity and creep behavior of super alloys at high temperature
[NASA-CR-176418] p 43 N86-14356

Integrated research in constitutive modelling at elevated temperatures, part 2
[NASA-CR-177233] p 119 N86-28455

Integrated research in constitutive modelling at elevated temperatures, part 1
[NASA-CR-177237] p 120 N86-30227

HALFORD, G. R.

Strainrange partitioning life predictions of the long time Metal Properties Council creep-fatigue tests p 63 A80-27958

Nonlinear structural and life analyses of a combustor liner p 68 A83-12764

Turbine blade nonlinear structural and life analysis p 1 A83-29024

High-temperature fatigue in metals - A brief review of life prediction methods developed at the Lewis Research Center of NASA p 33 A84-14286

Strainrange partitioning - A total strain range version p 34 A85-11603

Application of two creep fatigue life models for the prediction of elevated temperature crack initiation of a nickel base alloy p 35 A85-43979

Re-examination of cumulative fatigue damage analysis - An engineering perspective p 85 A87-22128

Practical implementation of the double linear damage rule and damage curve approach for treating cumulative fatigue damage p 88 N80-23684

Nonlinear structural and life analyses of a combustor liner p 92 N82-24501

Creep-fatigue of low cobalt superalloys p 39 N83-11290

Strainrange partitioning: A total strain range version p 39 N83-14246

Relation of cyclic loading pattern to microstructural fracture in creep fatigue p 98 N83-34349

Tensile and compressive constitutive response of 316 stainless steel at elevated temperatures p 98 N83-34353

Complexities of high temperature metal fatigue: Some steps toward understanding p 101 N84-14541

Bending fatigue of electron-beam-welded foils. Application to a hydrodynamic air bearing in the Chrysler/DOE upgraded automotive gas turbine engine p 102 N84-16589

Preliminary study of thermomechanical fatigue of polycrystalline MAR-M 200 p 40 N84-17350

Engine cyclic durability by analysis and material testing p 102 N84-18683

Life prediction and constitutive behavior: Overview p 10 N85-10973

Engine cyclic durability by analysis and material testing p 11 N85-15744

Interaction of high-cycle and low-cycle fatigue of Haynes 188 alloy at 1400 F deg p 111 N85-27961

Reexamination of cumulative fatigue damage laws p 112 N85-27962

An update of the total-strain version of SRP p 42 N86-12295

Low-cycle thermal fatigue p 118 N86-26651

Re-examination of cumulative fatigue damage analysis: An engineering perspective p 118 N86-27680

Structural analysis of turbine blades using unified constitutive models p 119 N86-28461

Fatigue and fracture: Overview p 120 N87-11183

Bithermal low-cycle fatigue behavior of a NiCoCrAlY-coated single crystal superalloy p 45 N87-20408

Exposure time considerations in high temperature low cycle fatigue p 125 N87-28944

Calculation of thermomechanical fatigue life based on isothermal behavior p 122 N87-20565

Environmental degradation of 316 stainless steel in high temperature low cycle fatigue p 124 N87-24007

Vapor cavitation in dynamically loaded journal bearings p 97 N83-24875

Vibration and buckling of rectangular plates under in-plane hydrostatic loading p 64 A80-45364

Thermal stress analysis for a wood composite blade p 103 N84-21903

Thermal-stress analysis for wood composite blade p 104 N84-31685

A preliminary study of crack initiation and growth at stress concentration sites p 94 N82-33738

A total life prediction model for stress concentration sites p 96 N83-23629

A total life prediction model for stress concentration sites p 100 N84-10612

Structural tailoring of advanced turboprops p 85 A87-33648

Creep-fatigue behavior of NiCoCrAlY coated PWA 1480 superalloy single crystals p 42 N86-10311

On composites with periodic structure p 67 A83-10283

The effect of stress on ultrasonic pulses in fiber reinforced composites p 56 N83-33180

Inelastic high-temperature thermomechanical response of ceramic coated gas turbine seals p 82 A86-37799

High temperature thermomechanical analysis of ceramic coatings p 74 A84-48565

Finite element analysis of residual stress in plasma-sprayed ceramic p 46 A86-15226

Characterization of composite materials by means of the ultrasonic stress wave factor p 16 A84-10430

A study of the stress wave factor technique for the characterization of composite materials p 55 N83-27248

A study of the stress wave factor technique for the characterization of composite materials p 29 N85-30035

Ultrasonic stress wave characterization of composite materials p 60 N86-27665

A study of the stress wave factor technique for nondestructive evaluation of composite materials p 60 N86-28445

Ultrasonic velocity for estimating density of structural ceramics p 46 N82-14359

Three dimensional finite-element elastic analysis of a thermally cycled double-edge wedge geometry specimen p 37 N80-26433

Thermal fatigue and oxidation data for directionally solidified MAR-M 246 turbine blades p 6 N80-21330

Thermal fatigue and oxidation data of oxide dispersion-strengthened alloys p 37 N80-25415

Structural dynamics verification facility study p 90 N81-33497

Stability of large horizontal-axis axisymmetric wind turbines p 64 A81-22526

Finite element engine blade structural optimization p 76 A85-30313

Stability of large horizontal-axis axisymmetric wind turbines p 89 N81-12446

Structural dynamics of shroudless, hollow fan blades with composite in-lays p 7 N82-22266

Bird impact analysis package for turbine engine fan blades p 92 N82-26701

Component-specific modeling p 10 N85-10971

STAEBL: Structural tailoring of engine blades, phase 2 p 13 N87-11731

Structural and aeroelastic analysis of the SR-7L proplan p 123 N87-22273

Elevated temperature fatigue testing of metals p 38 N82-13281

Elevated temperature fatigue testing of metals p 91 N82-16419

The finite analytic method, volume 5 p 127 N83-23089

Thermal fatigue and oxidation data of oxide dispersion-strengthened alloys p 37 N80-25415

Thermal fatigue and oxidation data of TAZ-8A and M22 alloys and variations p 38 N82-10193

Method for alleviating thermal stress damage in laminates p 23 N81-17170

Method for alleviating thermal stress damage in laminates p 24 N81-26179

Variables controlling fatigue crack growth of short cracks p 43 N86-21661

Model development and statistical investigation of turbine blade mistuning p 2 A84-31905

Optimization and analysis of gas turbine engine blades p 126 A87-33614

Nonlinear analysis for high-temperature composites: Turbine blades/vanes p 106 N84-31699

Nonlinear analysis for high-temperature multilayered fiber composite structures p 29 N85-21273

Nonlinear structural analysis for fiber-reinforced superalloy turbine blades p 109 N85-26887

Thermoviscoplastic nonlinear constitutive relationships for structural analysis of high temperature metal matrix composites p 30 N86-24756

A unique set of micromechanics equations for high temperature metal matrix composites p 30 N86-24757

Creep fatigue of low-cobalt superalloys: Waspalloy, PM U 700 and wrought U 700 p 40 N84-13265

The coupled aeroelastic response of turbomachinery blading to aerodynamic excitations p 69 A83-29822

The coupled response of turbomachinery blading to aerodynamic excitations p 2 A84-26959

The effect of aerodynamic and structural detuning on turbomachine supersonic unstalled torsional flutter p 3 A85-30378

Forced response analysis of an aerodynamically detuned supersonic turbomachine rotor p 5 A86-26902

Aerodynamic and structural detuning of supersonic turbomachine rotors p 5 A86-31595

The effect of circumferential aerodynamic detuning on coupled bending-torsion unstalled supersonic flutter p 6 A87-25396

Identification of structural interface characteristics using component mode synthesis p 123 N87-24006

Element-by-element solution procedures for nonlinear structural analysis p 105 N84-31694

HIRSCHBEIN, M. S.

Stability of large horizontal-axis axisymmetric wind turbines p 64 A81-22526

Finite element engine blade structural optimization p 76 A85-30313

Stability of large horizontal-axis axisymmetric wind turbines p 89 N81-12446

Structural dynamics of shroudless, hollow fan blades with composite in-lays p 7 N82-22266

Bird impact analysis package for turbine engine fan blades p 92 N82-26701

Component-specific modeling p 10 N85-10971

STAEBL: Structural tailoring of engine blades, phase 2 p 13 N87-11731

Structural and aeroelastic analysis of the SR-7L proplan p 123 N87-22273

Elevated temperature fatigue testing of metals p 38 N82-13281

Elevated temperature fatigue testing of metals p 91 N82-16419

The finite analytic method, volume 5 p 127 N83-23089

Thermal fatigue and oxidation data of oxide dispersion-strengthened alloys p 37 N80-25415

Thermal fatigue and oxidation data of TAZ-8A and M22 alloys and variations p 38 N82-10193

Method for alleviating thermal stress damage in laminates p 23 N81-17170

Method for alleviating thermal stress damage in laminates p 24 N81-26179

Variables controlling fatigue crack growth of short cracks p 43 N86-21661

Model development and statistical investigation of turbine blade mistuning p 2 A84-31905

Optimization and analysis of gas turbine engine blades p 126 A87-33614

Nonlinear analysis for high-temperature composites: Turbine blades/vanes p 106 N84-31699

Nonlinear analysis for high-temperature multilayered fiber composite structures p 29 N85-21273

Nonlinear structural analysis for fiber-reinforced superalloy turbine blades p 109 N85-26887

Thermoviscoplastic nonlinear constitutive relationships for structural analysis of high temperature metal matrix composites p 30 N86-24756

A unique set of micromechanics equations for high temperature metal matrix composites p 30 N86-24757

Creep fatigue of low-cobalt superalloys: Waspalloy, PM U 700 and wrought U 700 p 40 N84-13265

The coupled aeroelastic response of turbomachinery blading to aerodynamic excitations p 69 A83-29822

The coupled response of turbomachinery blading to aerodynamic excitations p 2 A84-26959

The effect of aerodynamic and structural detuning on turbomachine supersonic unstalled torsional flutter p 3 A85-30378

Forced response analysis of an aerodynamically detuned supersonic turbomachine rotor p 5 A86-26902

Aerodynamic and structural detuning of supersonic turbomachine rotors p 5 A86-31595

The effect of circumferential aerodynamic detuning on coupled bending-torsion unstalled supersonic flutter p 6 A87-25396

Identification of structural interface characteristics using component mode synthesis p 123 N87-24006

Element-by-element solution procedures for nonlinear structural analysis p 105 N84-31694

Augmented weak forms and element-by-element preconditioners: Efficient iterative strategies for structural finite elements. A preliminary study p 106 N85-10384

HULL, D. R.

Metal honeycomb to porous wireform substrate diffusion bond evaluation p 51 A83-39620
Measurement of ultrasonic velocity using phase-slope and cross-correlation methods p 51 A86-13192
Metal honeycomb to porous wireform substrate diffusion bond evaluation [NASA-TM-82793] p 54 N82-18612
Interrelation of material microstructure, ultrasonic factors, and fracture toughness of two phase titanium alloy [NASA-TM-82810] p 54 N82-20551
Ultrasonic ranking of toughness of tungsten carbide [NASA-TM-83358] p 55 N83-23620
Ultrasonic velocity measurement using phase-slope cross-correlation methods [NASA-TM-83794] p 57 N84-34769

HULL, DAVID R.

Fatigue failure of regenerator screens in a high frequency Stirling engine [NASA-TM-88974] p 122 N87-18882

HUMPHREYS, V. E.

Thermal fatigue and oxidation data for directionally solidified MAR-M 246 turbine blades [NASA-CR-159798] p 6 N80-21330
Thermal fatigue and oxidation data of oxide dispersion-strengthened alloys [NASA-CR-159842] p 37 N80-25415
Thermal fatigue and oxidation data of TAZ-8A and M22 alloys and variations [NASA-CR-165407] p 38 N82-10193

HUNT, L. E.

Elastic-plastic finite-element analyses of thermally cycled double-edge wedge specimens [NASA-TP-1973] p 92 N82-20566
Materials constitutive models for nonlinear analysis of thermally cycled structures [NASA-TP-2055] p 95 N83-12449

HUSTON, R. L.

A finite element stress analysis of spur gears including fillet radii and rim thickness effects [NASA-TM-82865] p 48 N82-28646
On finite element stress analysis of spur gears [NASA-CR-167938] p 48 N82-29607

HWANG, C.-C.

Three dimensional unsteady aerodynamics and aeroelastic response of advanced turboprops [AIAA PAPER 86-0846] p 5 A86-38894

HWANG, S. Y.

On local total strain redistribution using a simplified cyclic inelastic analysis based on an elastic solution [AIAA PAPER 85-1419] p 78 A85-39770
Local strain redistribution corrections for a simplified inelastic analysis procedure based on an elastic finite-element analysis [NASA-TP-2421] p 107 N85-20396
On local total strain redistribution using a simplified cyclic inelastic analysis based on an elastic solution [NASA-TM-86913] p 108 N85-21690
Cyclic creep analysis from elastic finite-element solutions [NASA-TM-87213] p 117 N86-25822

I**IMBRIE, P. K.**

Numerical considerations in the development and implementation of constitutive models p 113 N85-31541

INGLEHART, L. J.

Comparison of NDE techniques for sintered-SiC components p 51 A83-22265

IRVINE, T. B.

Progressive fracture of fiber composites p 19 A86-35809
Fracture surface characteristics of notched angleplated graphite/epoxy composites [NASA-TM-83786] p 28 N84-33522
Fracture modes in notched angleplated composite laminates [NASA-TM-83802] p 28 N84-34576

IWAKUMA, T.

On composites with periodic structure p 67 A83-10283
Composites with periodic microstructure p 15 A83-12734
Finite elastic-plastic deformation of polycrystalline metals p 34 A84-43872
Micromechanically based constitutive relations for polycrystalline solids p 99 N83-34359

IYER, N. S.

Closure of fatigue cracks at high strains [NASA-CR-175021] p 116 N86-17788

J**JACOBSON, B. O.**

Vapor cavitation in dynamically loaded journal bearings [NASA-TM-83366] p 97 N83-24875

JACQUOTTE, O.-P.

Analysis of hourglass instabilities and control in underintegrated finite element methods p 74 A85-11125

JAY, A.

Effect of time dependent flight loads on JT9D-7 performance deterioration [NASA-CR-159681] p 87 N80-10515

JAYARAMAN, N.

Metallurgical instabilities during the high temperature low cycle fatigue of nickel-base superalloys p 33 A83-22019

The effect of microstructure on the fatigue behavior of Ni base superalloys p 33 A83-36166
A study of fatigue damage mechanisms in Waspaloy from 25 to 800 C p 34 A85-12098

Low cycle fatigue of MAR-M 200 single crystals at 760 and 870 deg C [NASA-TM-86933] p 41 N85-19074

JOHNS, R. H.

Computational engine structural analysis [ASME PAPER 86-GT-70] p 5 A86-48141
Structural analysis p 9 N85-10969
HOST structural analysis program overview p 12 N86-11513

Computational engine structural analysis [NASA-TM-87231] p 116 N86-19663

JOHNSON, G. M.

An embedding method for the steady Euler equations p 126 A86-30814

JOHNSON, S. A.

Aeroelastic analysis for propellers - mathematical formulations and program user's manual [NASA-CR-3729] p 101 N84-12530

JONES, B. G.

Reliability and quality assurance on the MOD 2 wind system [NASA-TM-82717] p 54 N81-33492

JORDAN, E. H.

Fracture mechanics applied to nonisothermal fatigue crack growth p 36 A86-28951
Elevated temperature biaxial fatigue [NASA-CR-173473] p 103 N84-21905
Elevated temperature biaxial fatigue [NASA-CR-175795] p 110 N85-27263

K**KACHANOV, M.**

On stress analysis of a crack-layer [NASA-CR-174774] p 106 N84-34774

KAHN, E. B.

Effects of specimen resonances on acoustic-ultrasonic testing [NASA-CR-3679] p 55 N83-21373

KALLURI, S.

Exposure time considerations in high temperature low cycle fatigue [NASA-TM-88934] p 125 N87-28944

KALLURI, SREERAMESH

Environmental degradation of 316 stainless steel in high temperature low cycle fatigue [NASA-TM-89931] p 124 N87-24007

KANG, D.

A new formulation of hybrid/mixed finite element p 67 A83-12739
New variational formulations of hybrid stress elements p 105 N84-31690

KANNEL, J. W.

Stress evaluations under rolling/sliding contacts [NASA-CR-165561] p 91 N82-17521

KAPP, J. A.

Wide-range displacement expressions for standard fracture mechanics specimens p 79 A86-20706

KARAGUELLE, H.

Input-output characterization of an ultrasonic testing system by digital signal analysis [NASA-CR-3756] p 56 N84-15565

KARAGULLE, H.

Ultrasonic input-output for transmitting and receiving longitudinal transducers coupled to same face of isotropic elastic plate [NASA-CR-3506] p 54 N82-18613

Stress waves in an isotropic elastic plate excited by a circular transducer [NASA-CR-3877] p 58 N85-20390
Application of homomorphic signal processing to stress wave factor analysis [NAS 1.26:174871] p 58 N85-21673
Ultrasonic testing of plates containing edge cracks [NASA-CR-3904] p 58 N85-29307

KARLOVITZ, L. A.

On the existence and stability conditions for mixed-hybrid finite element solutions based on Reissner's variational principle p 77 A85-33847

KAUFMAN, A.

Nonlinear structural and life analyses of a combustor liner p 68 A83-12764
Turbine blade nonlinear structural and life analysis p 1 A83-29024

Simplified analytical procedures for representing material cyclic response p 2 A84-22877
A simplified method for elastic-plastic-creep structural analysis [ASME PAPER 84-GT-191] p 76 A85-23150

Unified constitutive material models for nonlinear finite-element structural analysis [AIAA PAPER 85-1418] p 77 A85-39769

On local total strain redistribution using a simplified cyclic inelastic analysis based on an elastic solution [AIAA PAPER 85-1419] p 78 A85-39770

Nonlinear, three-dimensional finite-element analysis of air-cooled gas turbine blades [NASA-TP-1669] p 88 N80-22734

Comparison of elastic and elastic-plastic structural analyses for cooled turbine blade airfoils [NASA-TP-1679] p 88 N80-27719

Elastic-plastic finite-element analyses of thermally cycled single-edge wedge specimens [NASA-TP-1982] p 91 N82-20565

Elastic-plastic finite-element analyses of thermally cycled double-edge wedge specimens [NASA-TP-1973] p 92 N82-20566

Nonlinear structural and life analyses of a combustor liner [NASA-TM-82846] p 92 N82-24501

Evaluation of inelastic constitutive models for nonlinear structural analysis [NASA-TM-82845] p 92 N82-24502

Materials constitutive models for nonlinear analysis of thermally cycled structures [NASA-TP-2055] p 95 N83-12449

Evaluation of inelastic constitutive models for nonlinear structural analysis p 98 N83-34357

Simplified method for nonlinear structural analysis [NASA-TP-2208] p 99 N83-34372

A simplified method for elastic-plastic-creep structural analysis [NASA-TM-83509] p 101 N84-14542

Engine cyclic durability by analysis and material testing [NASA-TM-83577] p 102 N84-18683

Development of a simplified procedure for cyclic structural analysis [NASA-TP-2243] p 103 N84-20878

Nonlinear structural and life analyses of a turbine blade p 9 N85-10954

Nonlinear structural and life analyses of a combustor liner p 9 N85-10955

Constitutive model development for isotropic materials p 10 N85-10975

Engine cyclic durability by analysis and material testing p 11 N85-15744

Local strain redistribution corrections for a simplified inelastic analysis procedure based on an elastic finite-element analysis [NASA-TP-2421] p 107 N85-20396

On local total strain redistribution using a simplified cyclic inelastic analysis based on an elastic solution [NASA-TM-86913] p 108 N85-21690

Unified constitutive material models for nonlinear finite-element structural analysis [NASA-TM-86985] p 108 N85-24338

Cyclic structural analyses of anisotropic turbine blades for reusable space propulsion systems [NASA-TM-86990] p 108 N85-24339

Cyclic structural analyses of SSME turbine blades p 112 N85-27963

Two simplified procedures for predicting cyclic material response from a strain history p 113 N85-31543

Simplified cyclic structural analyses of SSME turbine blades [NASA-TM-87214] p 116 N86-16615

Cyclic creep analysis from elastic finite-element solutions [NASA-TM-87213] p 117 N86-25822

Structural analysis of turbine blades using unified constitutive models [NASA-TM-88807] p 119 N86-28461

KLIMA, S. J.

- B-9

- Factors that affect reliability of nondestructive detection of flaws in structural ceramics
[NASA-TM-87348] p 61 N86-31912
- KLIMA, STANLEY J.**
Nondestructive evaluation of structural ceramics
[NASA-TM-88978] p 62 N87-18109
Application of scanning acoustic microscopy to advanced structural ceramics
[NASA-TM-89929] p 62 N87-23987
- KRAUTZ, HAROLD E.**
Nondestructive evaluation of adhesive bond strength using the stress wave factor technique
p 53 A87-32200
- KRISHNA MURTHY, A. V.**
A higher order theory of laminated composite cylindrical shells
p 86 A87-35656
- KROSEL, S. M.**
Digital computer program for generating dynamic turbfan engine models (DIGTEM)
[NASA-TM-83446] p 8 N84-16185
- KURKOV, A.**
Effects of mistuning on blade torsional flutter
p 64 A81-29095
- KURKOV, A. P.**
Measurements of self-excited rotor-blade vibrations using optical displacements
[ASME PAPER 83-GT-132] p 73 A84-33702
Measurements of self-excited rotor-blade vibrations using optical displacements
[NASA-TM-82953] p 95 N83-14523
Formulation of blade-flutter spectral analyses in stationary reference frame
[NASA-TP-2296] p 8 N84-20562
- KURTH, R.**
Composite loads spectra for select space propulsion structural components: Probabilistic load model development
p 110 N85-27954
- KVATERNIK, R. G.**
Buckling of rotating beams
p 63 A80-20149
- KWASNY, R.**
Effects of a high mean stress on the high cycle fatigue life of PWA 1480 and correlation of data by linear elastic fracture mechanics
[NASA-CR-175057] p 118 N86-27689
- L**
- LACKNEY, J.**
On the development of hierarchical solution strategies for nonlinear finite element formulations
p 126 A85-21979
Hierarchical implicit dynamic least-square solution algorithm
p 80 A86-26689
Constrained hierarchical least square nonlinear equation solvers
p 83 A86-43774
- LAFFLE, J. H.**
Requirements of constitutive models for two nickel-base superalloys
p 33 A83-21071
Turbine blade nonlinear structural and life analysis
p 1 A83-29024
Considerations for damage analysis of gas turbine hot section components
[ASME PAPER 84-PVP-77] p 2 A85-18792
Unified constitutive material models for nonlinear finite-element structural analysis
[AIAA PAPER 85-1418] p 77 A85-39769
Unified constitutive material models for nonlinear finite-element structural analysis
[NASA-TM-86985] p 108 N85-24338
- LALLI, V. R.**
Photovoltaic power system reliability considerations
[NASA-TM-79291] p 53 N80-15422
- LAM, P.**
Engine dynamic analysis with general nonlinear finite element codes. II - Bearing element implementation, overall numerical characteristics and benchmarking
[ASME PAPER 82-GT-292] p 47 A82-35462
Nonlinear transient finite element analysis of rotor-bearing-stator systems
p 48 A84-20580
Engine dynamic analysis with general nonlinear finite element codes. Part 2: Bearing element implementation overall numerical characteristics and benchmarking
[NASA-CR-167944] p 7 N82-33390
- LAPRAD, R. F.**
Sensor failure detection for jet engines
[NASA-CR-168190] p 56 N83-33182
- LARK, R. F.**
Mechanical property characterization of intraply hybrid composites
p 13 A80-20954
Dynamic response of damaged angleplied fiber composites
p 14 A80-27982
Superhybrid composite blade impact studies
[ASME PAPER 81-GT-24] p 1 A81-29940
- Hygrothermomechanical evaluation of transverse filament tape epoxy/polyester fiberglass composites
p 17 A85-15632
- Fabrication and quality assurance processes for superhybrid composite fan blades
p 20 A87-19123
Tensile and flexural strength of non-graphitic superhybrid composites: Predictions and comparisons
[NASA-TM-79276] p 21 N80-11144
Dynamic response of damaged angleplied fiber composites
[NASA-TM-79281] p 21 N80-11145
Mechanical property characterization of intraply hybrid composites
[NASA-TM-79306] p 21 N80-12120
Superhybrid composite blade impact studies
[NASA-TM-81597] p 89 N81-11412
Fabrication and quality assurance processes for superhybrid composite fan blades
[NASA-TM-83354] p 28 N85-14882
- LARK, R. L.**
Hygrothermomechanical evaluation of transverse filament tape epoxy/polyester fiberglass composites
[NASA-TM-83044] p 26 N83-15362
- LAWLER, D.**
Comparison of NDE techniques for sintered-SiC components
p 51 A83-22265
- LAWRENCE, C.**
Dynamic characteristics of an assembly of prop-fan blades
[ASME PAPER 85-GT-134] p 5 A86-32956
Nonlinear vibration and stability of rotating, pretwisted, precone blades including Coriolis effects
p 86 A87-39896
Nonlinear displacement analysis of advanced propeller structures using NASTRAN
[NASA-TM-83737] p 104 N84-31683
The use of an optical data acquisition system for bladed disk vibration analysis
[NASA-TM-86891] p 106 N85-15184
Nonlinear bending-torsional vibration and stability of rotating, pretwisted, precone blades including Coriolis effects
[NASA-TM-87207] p 116 N86-17789
Identification of structural interface characteristics using component mode synthesis
[NASA-TM-88960] p 123 N87-24006
- LAWRENCE, CHARLES**
A NASTRAN primer for the analysis of rotating flexible blades
[NASA-TM-89861] p 123 N87-21375
Structural and aeroelastic analysis of the SR-7L propan
[NASA-TM-86877] p 123 N87-22273
Hub flexibility effects on propfan vibration
[NASA-TM-89900] p 124 N87-24722
- LEE, J. K.**
Vibrations of cantilevered shallow cylindrical shells of rectangular planform
p 65 A82-11298
Vibrations of twisted rotating blades
[ASME PAPER 81-DET-127] p 65 A82-19341
Vibrations of cantilevered circular cylindrical shells
Shallow versus deep shell theory
p 69 A83-36958
Vibrations of cantilevered doubly-curved shallow shells
p 70 A83-39557
Vibrations of blades with variable thickness and curvature by shell theory
[ASME PAPER 83-GT-152] p 70 A83-47978
- LEE, S. S.**
Ultrasonic input-output for transmitting and receiving longitudinal transducers coupled to same face of isotropic elastic plate
[NASA-CR-3506] p 54 N82-18613
Effects of specimen resonances on acoustic-ultrasonic testing
[NASA-CR-3679] p 55 N83-21373
Ultrasonic attenuation of a void-containing medium for very long wavelengths
[NASA-CR-3693] p 56 N83-28466
Input-output characterization of an ultrasonic testing system by digital signal analysis
[NASA-CR-3756] p 56 N84-15565
Stress waves in an isotropic elastic plate excited by a circular transducer
[NASA-CR-3877] p 58 N85-20390
Application of homomorphic signal processing to stress wave factor analysis
[NAS 1.26:174871] p 58 N85-21673
Ultrasonic testing of plates containing edge cracks
[NASA-CR-3904] p 58 N85-29307
Wave propagation in anisotropic medium due to an oscillatory point source with application to unidirectional composites
[NASA-CR-4001] p 60 N86-27666
- LEESE, G. E.**
Cyclic torsion testing
[NASA-TM-83756] p 105 N84-31687
- Multiaxial and thermomechanical fatigue considerations in damage tolerant design
[NASA-TM-87022] p 42 N85-26964
- LEGER, G. S.**
Wide-range displacement expressions for standard fracture mechanics specimens
p 79 A86-20706
- LEIS, B. N.**
A history dependent damage model for low cycle fatigue
[ASME PAPER 84-PVP-112] p 75 A85-18795
Creep fatigue of low-cobalt superalloys: Waspalloy, PM U 700 and wrought U 700
[NASA-CR-168260] p 40 N84-13265
Nonlinear damage analysis: Postulate and evaluation
[NASA-CR-168171] p 118 N86-26652
- LEISSA, A.**
On the three-dimensional vibrations of the cantilevered rectangular parallelepiped
p 70 A83-37729
- LEISSA, A. W.**
Vibrations of cantilevered shallow cylindrical shells of rectangular planform
p 65 A82-11298
Vibrations of twisted rotating blades
[ASME PAPER 81-DET-127] p 65 A82-19341
Comparison of beam and shell theories for the vibrations of thin turbomachinery blades
[ASME PAPER 82-GT-223] p 65 A82-35408
Vibrations of cantilevered circular cylindrical shells
Shallow versus deep shell theory
p 69 A83-36958
Vibrations of cantilevered doubly-curved shallow shells
p 70 A83-39557
Vibrations of blades with variable thickness and curvature by shell theory
[ASME PAPER 83-GT-152] p 70 A83-47978
Vibrations of twisted cantilevered plates - Experimental investigation
[ASME PAPER 84-GT-96] p 73 A84-46937
Vibrations of twisted cantilevered plates - Summary of previous and current studies
p 76 A85-22069
Vibrations of twisted cantilever plates - A comparison of theoretical results
p 79 A85-47626
A study of internal and distributed damping for vibrating turbomachinery blades
[NASA-CR-175901] p 11 N85-27868
Joint research effort on vibrations of twisted plates, phase 1: Final results
[NASA-RP-1150] p 115 N86-10579
Extensions of the Ritz-Galerkin method for the forced, damped vibrations of structural elements
p 117 N86-21909
- LEMASCON, A.**
A study of the stress wave factor technique for the characterization of composite materials
[NASA-CR-3670] p 55 N83-27248
- LEMON, D. D.**
Fracture toughness of hot-pressed beryllium
p 34 A85-25835
- LEOWENTHAL, S. H.**
Factors that affect the fatigue strength of power transmission shafting and their impact on design
p 48 A87-14656
- LERCH, B. A.**
A study of fatigue damage mechanisms in Waspalloy from 25 to 800 C
p 34 A85-12098
Microstructural effects on the room and elevated temperature low cycle fatigue behavior of Waspalloy
[NASA-CR-165497] p 93 N82-26702
- LEVIT, I.**
Element-by-element solution procedures for nonlinear structural analysis
p 105 N84-31694
- LEWIS, B. L.**
Effect of time dependent flight loads on JT9D-7 performance deterioration
[NASA-CR-159681] p 87 N80-10515
- LINASK, I.**
Life prediction and constitutive models for engine hot section anisotropic materials program
[NASA-CR-174952] p 60 N86-25003
- LINDHOLM, U. S.**
Unified constitutive material models for nonlinear finite-element structural analysis
[AIAA PAPER 85-1418] p 77 A85-39769
Unified constitutive material models for nonlinear finite-element structural analysis
[NASA-TM-86985] p 108 N85-24338
A survey of unified constitutive theories
p 112 N85-31531
Constitutive modeling for isotropic materials (HOST)
[NASA-CR-174980] p 115 N86-10589
- LIU, H. W.**
Shear fatigue crack growth - A literature survey
p 80 A86-24219
Fatigue crack growth under general-yielding cyclic-loading
p 84 A86-44339
Literature survey on oxidations and fatigue lives at elevated temperatures
[NASA-CR-174639] p 40 N84-20674

- Crack tip field and fatigue crack growth in general yielding and low cycle fatigue
[NASA-CR-174686] p 41 N84-32503
- Grain boundary oxidation and oxidation accelerated fatigue crack nucleation and propagation
[NASA-CR-175050] p 43 N86-20542
- Fatigue crack growth under general-yielding cyclic-loading
[NASA-CR-175049] p 117 N86-21951
- LIU, W. K.**
Probabilistic finite elements for transient analysis in nonlinear continua p 80 A86-28653
Probabilistic finite element: Variational theory p 111 N85-27957
- LOEWENTHAL, S. H.**
Application of traction drives as servo mechanisms p 114 N85-33520
- LOEWY, R. G.**
Natural frequency of rotating beams using non-rotating modes p 68 A83-18383
- LUBOMSKI, J. F.**
Status of NASA full-scale engine aeroelasticity research p 63 A80-35906
Status of NASA full-scale engine aeroelasticity research
[NASA-TM-81500] p 88 N80-23678
Bending-torsion flutter of a highly swept advanced turboprop
[NASA-TM-82975] p 95 N83-11514
- LUCAS, L. J.**
Experimental verification of the Neuber relation at room and elevated temperatures p 96 N83-19121
Experimental verification of the number relation at room and elevated temperatures p 98 N83-34355

M

- MACBAIN, J. C.**
Vibrations of twisted cantilevered plates - Experimental investigation
[ASME PAPER 84-GT-96] p 73 A84-46937
Vibrations of twisted cantilevered plates - Summary of previous and current studies p 76 A85-22069
Vibrations of twisted cantilever plates - A comparison of theoretical results p 79 A85-47626
Joint research effort on vibrations of twisted plates, phase 1: Final results
[NASA-RP-1150] p 115 N86-10579
- MAFFEO, R.**
Burner liner thermal-structural load modeling
[NASA-CR-174892] p 117 N86-21932
- MAFFEO, R. J.**
A computer analysis program for interfacing thermal and structural codes p 126 A86-36861
A computer analysis program for interfacing thermal and structural codes
[NASA-TM-87021] p 110 N85-27264
- MAHISHI, J. M.**
Micromechanical predictions of crack propagation and fracture energy in a single fiber boron/aluminum model composite
[NASA-CR-168550] p 25 N82-18326
- MAIER, R. D.**
Fatigue and creep-fatigue deformation of several nickel-base superalloys at 650 C p 32 A82-47398
- MAISEL, J. E.**
Preliminary investigation of an electrical network model for ultrasonic scattering
[NASA-CR-3770] p 57 N84-17606
- MAJUMDAR, S.**
Effects of a high mean stress on the high cycle fatigue life of PWA 1480 and correlation of data by linear elastic fracture mechanics
[NASA-CR-175057] p 118 N86-27689
- MANDERSCHIED, J. M.**
Cyclic structural analyses of anisotropic turbine blades for reusable space propulsion systems
[NASA-TM-86990] p 108 N85-24339
Cyclic structural analyses of SSME turbine blades p 112 N85-27963
Simplified cyclic structural analyses of SSME turbine blades
[NASA-TM-87214] p 116 N86-16615
- MANDERSCHIED, JANE M.**
Fracture mechanics concepts in reliability analysis of monolithic ceramics
[NASA-TM-100174] p 124 N87-27269
- MANI, A.**
Probabilistic finite elements for transient analysis in nonlinear continua p 80 A86-28653
- MANSON, S. S.**
A quarter-century of progress in the development of correlation and extrapolation methods for creep rupture data p 63 A80-38142

- Re-examination of cumulative fatigue damage analysis - An engineering perspective p 85 A87-22128
Practical implementation of the double linear damage rule and damage curve approach for treating cumulative fatigue damage
[NASA-TM-81517] p 88 N80-23684
Fatigue life prediction in bending from axial fatigue information
[NASA-CR-165563] p 91 N82-20564
Relation of cyclic loading pattern to microstructural fracture in creep fatigue
[NASA-TM-83473] p 98 N83-34349
Tensile and compressive constitutive response of 316 stainless steel at elevated temperatures p 98 N83-34353
Complexities of high temperature metal fatigue: Some steps toward understanding
[NASA-TM-83507] p 101 N84-14541
Reexamination of cumulative fatigue damage laws p 112 N85-27962
- Re-examination of cumulative fatigue damage analysis: An engineering perspective
[NASA-TM-87325] p 118 N86-27680
Exposure time considerations in high temperature low cycle fatigue
[NASA-TM-88934] p 125 N87-28944
- MANSON, S. STANFORD**
Environmental degradation of 316 stainless steel in high temperature low cycle fatigue
[NASA-TM-89931] p 124 N87-24007
- MARCHAND, N.**
Thermal-mechanical fatigue crack growth in Inconel X-750 p 35 A86-20982
Thermal-mechanical fatigue crack growth in Inconel X-750
[NASA-CR-174740] p 41 N85-15877
Thermal-mechanical fatigue behavior of nickel-base superalloys
[NASA-CR-175048] p 43 N86-24818
- MARQUES, E. R. C.**
Stress waves in transversely isotropic media: The homogeneous problem
[NASA-CR-3977] p 59 N86-25002
Wave propagation in anisotropic medium due to an oscillatory point source with application to unidirectional composites
[NASA-CR-4001] p 60 N86-27666
- MARTIN, J. F.**
Experimental verification of the number relation at room and elevated temperatures p 98 N83-34355
A comparison of smooth specimen and analytical simulation techniques for notched members at elevated temperatures p 114 N85-31546
Experimental evaluation criteria for constitutive models of time dependent cyclic plasticity
[NASA-CR-176821] p 117 N86-25850
- MASON, W. E. B.**
Reliability and quality assurance on the MOD 2 wind system
[NASA-TM-82717] p 54 N81-33492
- MCALEESE, J. M.**
Structural dynamics verification facility study
[NASA-TM-82675] p 90 N81-33497
- MCCARTY, J. L.**
Temperature distribution in an aircraft tire at low ground speeds
[NASA-TP-2195] p 97 N83-33217
- MCDONALD, G.**
Finite element analysis of residual stress in plasma-sprayed ceramic p 46 A86-15226
- MCGAW, M. A.**
Preliminary study of thermomechanical fatigue of polycrystalline MAR-M 200
[NASA-TP-2280] p 40 N84-17350
A comparison of two contemporary creep-fatigue life prediction methods p 113 N85-31538
- MCGAW, MICHAEL A.**
Fatigue damage interaction behavior of PWA 1480 p 45 N87-22777
A high temperature fatigue and structures testing facility
[NASA-TM-100151] p 124 N87-26399
Lewis' enhanced laboratory for research into the fatigue and constitutive behavior of high temperature materials p 125 N88-11177
- MC GEE, OLIVER G.**
A NASTRAN primer for the analysis of rotating flexible blades
[NASA-TM-89861] p 123 N87-21375
Finite element analysis of flexible, rotating blades
[NASA-TM-89906] p 124 N87-26385
- MCKNIGHT, R. L.**
Turbine blade nonlinear structural and life analysis p 1 A83-29024
Component-specific modeling
[NASA-CR-174765] p 110 N85-27261

- Component-specific modeling
[NASA-CR-174925] p 12 N85-32119
- Component-specific modeling
[NASA-CR-174765] p 12 N85-34140
- MEHMED, O.**
Analytical flutter investigation of a composite propfan model
[AIAA PAPER 87-0738] p 87 A87-40497
Bending-torsion flutter of a highly swept advanced turboprop
[NASA-TM-82975] p 95 N83-11514
Experimental classical flutter results of a composite advanced turboprop model
[NASA-TM-88792] p 119 N86-29271
Analytical flutter investigation of a composite propfan model
[NASA-TM-88944] p 122 N87-18115
- MEHMED, ORAL**
Analytical and experimental investigation of mistuning in propfan flutter
[AIAA PAPER 87-0739] p 86 A87-40496
Analytical and experimental investigation of mistuning in propfan flutter
[NASA-TM-88959] p 122 N87-18116
- MELCHER, K. J.**
DEAN - A program for Dynamic Engine Analysis
[AIAA PAPER 85-1354] p 3 A86-14430
DEAN: A program for dynamic engine analysis
[NASA-TM-87033] p 11 N85-28945
- MEMMOTT, J. V. W.**
Diffusion bonded boron/aluminum spar-shell fan blade
[NASA-CR-159571] p 23 N80-25382
- MENDELSON, A.**
Effect of crack curvature on stress intensity factors for ASTM standard compact tension specimens
[NASA-CR-168280] p 100 N84-11513
- MEYER, T. G.**
Life prediction and constitutive models for engine hot section anisotropic materials program
[NASA-CR-174952] p 60 N86-25003
- MEYERS, G. J.**
Nonlinear structural and life analyses of a combustor liner p 68 A83-12764
Fracture mechanics applied to nonisothermal fatigue crack growth p 36 A86-28951
Nonlinear structural and life analyses of a combustor liner
[NASA-TM-82846] p 92 N82-24501
Fracture mechanics criteria for turbine engine hot section components
[NASA-CR-167896] p 7 N82-25257
- MEYN, E. H.**
Lewis Research Center spin rig and its use in vibration analysis of rotating systems
[NASA-TP-2304] p 9 N84-24578
The use of an optical data acquisition system for bladed disk vibration analysis
[NASA-TM-86891] p 106 N85-15184
- MILLER, D. R.**
Statistical aspects of carbon fiber risk assessment modeling
[NASA-CR-159318] p 23 N80-29432
- MILLER, T.**
A numerical analysis of contact and limit-point behavior in a class of problems of finite elastic deformation p 72 A84-27370
- MILLIGAN, W. W.**
Low cycle fatigue behavior of conventionally cast MAR-M 200 AT 1000 deg C
[NASA-TM-83769] p 41 N84-33564
Low cycle fatigue of MAR-M 200 single crystals at 760 and 870 deg C
[NASA-TM-86933] p 41 N85-19074
- MILLIGAN, W. W., JR.**
Yielding and deformation behavior of the single crystal nickel-base superalloy PWA 1480
[NASA-CR-175100] p 44 N86-25455
- MINER, R. V.**
Effects of fine porosity on the fatigue behavior of a powder metallurgy superalloy p 32 A80-35495
Fatigue and creep-fatigue deformation of several nickel-base superalloys at 650 C p 32 A82-47398
Fatigue crack initiation and propagation in several nickel-base superalloys at 650 C p 33 A83-41199
The effect of microstructure on 650 C fatigue crack growth in P/M Astroloy p 33 A84-12395
Effects of processing and microstructure on the fatigue behaviour of the nickel-base superalloy Rene95 p 34 A84-48715
On the fatigue crack propagation behavior of superalloys at intermediate temperatures p 35 A85-32434
The tensile and fatigue deformation structures in a single crystal Ni-base superalloy p 36 A86-35697

- Orientation and temperature dependence of some mechanical properties of the single-crystal nickel-base superalloy Rene N4. II - Low cycle fatigue behavior [NASA-TM-850322] p 37 A86-50322
- Creep-fatigue behavior of NiCoCrAlY coated PWA 1480 superalloy single crystals [NASA-TM-87110] p 42 N86-10311
- Fatigue crack propagation of nickel-base superalloys at 650 deg C [NASA-TM-87150] p 42 N86-12294
- Bithermal low-cycle fatigue behavior of a NiCoCrAlY-coated single crystal superalloy [NASA-TM-89831] p 45 N87-20408
- MINER, R. V., JR.**
- Cyclic behavior of turbine disk alloys at 650 C p 32 A81-12266
- Effects of fine porosity on the fatigue behavior of a powder metallurgy superalloy [NASA-TM-81448] p 37 N80-21493
- The low cycle fatigue behavior of a plasma-sprayed coating material [NASA-TM-87318] p 44 N86-31699
- MINZHONG, Z.**
- Fatigue crack growth under general-yielding cyclic-loading p 84 A86-44339
- Crack tip field and fatigue crack growth in general yielding and low cycle fatigue [NASA-CR-174686] p 41 N84-32503
- Fatigue crack growth under general-yielding cyclic-loading [NASA-CR-175049] p 117 N86-21951
- MIRDAMADI, M.**
- Axial and torsional fatigue behavior of Waspaloy [NASA-TM-175052] p 44 N86-25454
- MITCHELL, L. D.**
- Theoretical investigation of the force and dynamically coupled torsional-axial-lateral dynamic response of eared rotors [NASA-CR-173013] p 127 N83-34656
- MOKADAM, D. R.**
- Stagger angle dependence of inertial and elastic coupling in bladed disks p 72 A84-31903
- Analytical and experimental investigation of the coupled bladed disk/shaft whirl of a cantilevered turbofan [ASME PAPER 86-GT-98] p 6 A86-48163
- MOORE, T. J.**
- Ultrasonic velocity for estimating density of structural ceramics [NASA-TM-82765] p 46 N82-14359
- MOORE, THOMAS J.**
- Fatigue failure of regenerator screens in a high frequency Stirling engine [NASA-TM-88974] p 122 N87-18882
- MOORHEAD, P. E.**
- Metal honeycomb to porous wireform substrate diffusion bond evaluation p 51 A83-39620
- Metal honeycomb to porous wireform substrate diffusion bond evaluation [NASA-TM-82793] p 54 N82-18612
- MORENO, V.**
- Nonlinear structural and life analyses of a combustor liner p 68 A83-12764
- Simplified analytical procedures for representing material cyclic response p 2 A84-22877
- Application of two creep fatigue life models for the prediction of elevated temperature crack initiation of a nickel base alloy [AIAA PAPER 85-1420] p 35 A85-43979
- Combustor liner durability analysis [NASA-CR-165250] p 7 N81-17079
- Nonlinear structural and life analyses of a combustor liner [NASA-TM-82846] p 92 N82-24501
- Development of a simplified analytical method for representing material cyclic response [NASA-CR-168100] p 96 N83-21390
- Creep fatigue life prediction for engine hot section materials (isotropic) [NASA-CR-168228] p 11 N85-31057
- Two simplified procedures for predicting cyclic material response from a strain history p 113 N85-31543
- MORRIS, R. E.**
- Lewis Research Center spin rig and its use in vibration analysis of rotating systems [NASA-TP-2304] p 9 N84-24578
- MOSCARIELLO, R.**
- Pantographing self adaptive gap elements p 77 A85-37440
- Locally bound constrained Newton-Raphson solution algorithms p 83 A86-43771
- MOSS, LARRY A.**
- Analytical and experimental investigation of mistuning in propfan flutter [AIAA PAPER 87-0739] p 86 A87-40496
- Analytical and experimental investigation of mistuning in propfan flutter [NASA-TM-88959] p 122 N87-18116
- MULLEN, R. L.**
- Finite element analysis of residual stress in plasma-sprayed ceramic p 46 A86-15226
- MULLER, A.**
- Augmented weak forms and element-by-element preconditioners: Efficient iterative strategies for structural finite elements. A preliminary study p 106 N85-10384
- MUNZ, D.**
- Fracture toughness determination of Al₂O₃ using four-point-bend specimens with straight-through and chevron notches p 45 A80-42085
- Compliance and stress intensity coefficients for short bar specimens with chevron notches p 64 A80-46032
- Performance of Chevron-notch short bar specimen in determining the fracture toughness of silicon nitride and aluminum oxide p 45 A80-50696
- Fracture toughness of brittle materials determined with chevron notch specimens p 45 A81-32545
- Extended range stress intensity factor expressions for chevron-notched short bar and short rod fracture toughness specimens p 66 A82-40357
- Development of plane strain fracture toughness test for ceramics using Chevron notched specimens p 46 A84-11676
- Fracture toughness of brittle materials determined with chevron notch specimens [NASA-TM-81607] p 38 N80-32486
- MUNZ, D. G.**
- Specimen size and geometry effects on fracture toughness of Al₂O₃ measured with short rod and short bar chevron-notch specimens [NASA-TM-83319] p 47 N83-19902
- MURA, T.**
- The determination of the elastodynamic fields of an ellipsoidal inhomogeneity [ASME PAPER 83-APM-19] p 69 A83-37388
- Volume integrals associated with the inhomogeneous Helmholtz equation. Part 1: Ellipsoidal region [NASA-CR-3749] p 56 N84-14525
- MURAKAMI, Y.**
- Growth and stability of interacting surface flaws of arbitrary shape p 68 A83-15060
- MURALIDHARAN, U.**
- Fatigue life prediction in bending from axial fatigue information [NASA-CR-165563] p 91 N82-20564
- Tensile and compressive constitutive response of 316 stainless steel at elevated temperatures p 98 N83-34353
- MURPHY, D. P.**
- Analysis of crack propagation as an energy absorption mechanism in metal matrix composites [NASA-CR-165051] p 24 N82-14288
- MURTHY, D. V.**
- Analytical flutter investigation of a composite propfan model [AIAA PAPER 87-0738] p 87 A87-40497
- Analytical flutter investigation of a composite propfan model [NASA-TM-88944] p 122 N87-18115
- MURTHY, DURBHA V.**
- Approximations to eigenvalues of modified general matrices [AIAA PAPER 87-0947] p 86 A87-33756
- A computational procedure for automated flutter analysis [NASA-TM-100171] p 125 N87-28058
- MURTHY, P. L. N.**
- ICAN - Integrated composites analyzer [AIAA PAPER 84-0974] p 18 A85-16094
- A study of interply layer effects on the free edge stress field of angleplied laminates p 18 A85-41127
- Composite sandwich thermostructural behavior - Computational simulation [AIAA PAPER 86-0948] p 82 A86-38842
- Dynamic stress analysis of smooth and notched fiber composite flexural specimens p 20 A86-41070
- Dynamic stress analysis of smooth and notched fiber composite flexural specimens [NASA-TM-83694] p 27 N84-25770
- ICAN: Integrated composites analyzer [NASA-TM-83700] p 27 N84-26755
- A study of interply layer effects on the free-edge stress field of angleplied laminates [NASA-TM-86924] p 28 N85-15822
- Integrated Composite Analyzer (ICAN): Users and programmers manual [NASA-TP-2515] p 30 N86-21614
- Fiber composite sandwich thermostructural behavior: Computational simulation [NASA-TM-88787] p 31 N86-31663
- Composite interlaminar fracture toughness: Three-dimensional finite element modeling for mixed mode 1, 2 and 3 fracture [NASA-TM-88872] p 31 N87-13491
- Free-edge delamination: Laminar width and loading conditions effects [NASA-TM-100238] p 32 N88-12551
- N**
- NAGPAL, VINOD K.**
- Probabilistic structural analysis to quantify uncertainties associated with turbopump blades [AIAA PAPER 87-0766] p 85 A87-33581
- NAGTEGAAL, J.**
- Probabilistic finite element development p 111 N85-27956
- NAGTEGAAL, J. C.**
- Efficient algorithms for use in probabilistic finite element analysis p 81 A86-28655
- Iterative methods for mixed finite element equations p 82 A86-34461
- NAKAZAWA, S.**
- Iterative methods for mixed finite element equations p 82 A86-34461
- 3-D inelastic analysis methods for hot section components (base program) [NASA-CR-174700] p 107 N85-21686
- NALL, MARSHA**
- Structural and aeroelastic analysis of the SR-7L propfan [NASA-TM-86877] p 123 N87-22273
- NARAYANAN, G. V.**
- Analytical flutter investigation of a composite propfan model [AIAA PAPER 87-0738] p 87 A87-40497
- Analytical flutter investigation of a composite propfan model [NASA-TM-88944] p 122 N87-18115
- NELSON, H. D.**
- A blade loss response spectrum for flexible rotor systems [ASME PAPER 84-GT-29] p 48 A84-46893
- NEMAT-NASSER, S.**
- On finite deformation elasto-plasticity p 66 A82-45869
- On composites with periodic structure p 67 A83-10283
- Composites with periodic microstructure p 15 A83-12734
- Growth and stability of interacting surface flaws of arbitrary shape p 68 A83-15060
- Dynamic fields near a crack tip growing in an elastic-perfectly-plastic solid p 70 A83-38528
- Finite elastic-plastic deformation of polycrystalline metals p 34 A84-43872
- On stress field near a stationary crack tip [AD-A152863] p 76 A85-24532
- Micromechanically based constitutive relations for polycrystalline solids p 99 N83-34359
- NEMETH, NOEL N.**
- Surface flaw reliability analysis of ceramic components with the SCARE finite element postprocessor program [NASA-TM-88901] p 121 N87-17087
- NEWELL, J. F.**
- Composite loads spectra for select space propulsion structural components p 110 N85-27953
- NISSIM, E.**
- Optimization of cascade blade mistuning. I - Equations of motion and basic inherent properties p 3 A85-42365
- Optimization of cascade blade mistuning. II - Global optimum and numerical optimization p 3 A85-45715
- NISSLEY, D. M.**
- Application of two creep fatigue life models for the prediction of elevated temperature crack initiation of a nickel base alloy [AIAA PAPER 85-1420] p 35 A85-43979
- Life prediction and constitutive models for engine hot section anisotropic materials program [NASA-CR-174952] p 60 N86-25003
- NORRIS, P. P.**
- Life prediction and constitutive models for engine hot section anisotropic materials program [NASA-CR-174952] p 60 N86-25003
- NORTH, C. M.**
- The impact damped harmonic oscillator in free decay [NASA-TM-89897] p 50 N87-23978
- O**
- OBATA, M.**
- On stress field near a stationary crack tip [AD-A152863] p 76 A85-24532

ODEN, J. T.

Comments on some problems in computational penetration mechanics p 71 A84-13545

A numerical analysis of contact and limit-point behavior in a class of problems of finite elastic deformation p 72 A84-27370

Analysis of hourglass instabilities and control in underintegrated finite element methods p 74 A85-11125

Stability and convergence of underintegrated finite element approximations p 105 N84-31696

OHTANI, RYUICHI

Creep life prediction based on stochastic model of microstructurally short crack growth [NASA-TM-100245] p 125 N88-12825

OLDRIEVE, R. E.

Relation of cyclic loading pattern to microstructural fracture in creep fatigue [NASA-TM-83473] p 98 N83-34349

ORANGE, T. W.

Simple spline-function equations for fracture mechanics calculations p 63 A80-10832

On the equivalence between semiempirical fracture analyses and R-curves p 64 A81-18792

Crack displacements for J/I testing with compact specimens p 66 A82-40358

Wide-range weight functions for the strip with a single edge crack p 79 A86-20709

A relation between semiempirical fracture analyses and R-curves [NASA-TP-1600] p 87 N80-15428

Method for estimating crack-extension resistance curve from residual strength data [NASA-TP-1753] p 89 N81-11417

Wide range weight functions for the strip with a single edge crack [NASA-TM-83478] p 100 N84-11512

Pre-HOST high temperature crack propagation p 9 N85-10956

HOST high temperature crack propagation p 10 N85-10977

Estimating the R-curve from residual strength data [NASA-TM-87182] p 116 N86-18750

ORTH, N. W.

Method for alleviating thermal stress damage in laminates [NASA-CASE-LEW-12493-1] p 23 N81-17170

Method for alleviating thermal stress damage in laminates [NASA-CASE-LEW-12493-2] p 24 N81-26179

OSHIDA, Y.

Literature survey on oxidations and fatigue lives at elevated temperatures [NASA-CR-174639] p 40 N84-20674

Grain boundary oxidation and oxidation accelerated fatigue crack nucleation and propagation [NASA-CR-175050] p 43 N86-20542

OWCZAREK, J. A.

Analysis of an axial compressor blade vibration based on wave reflection theory [ASME PAPER 83-GT-151] p 2 A83-47970

P**PADOVAN, J.**

Engine dynamic analysis with general nonlinear finite element codes. II - Bearing element implementation, overall numerical characteristics and benchmarking [ASME PAPER 82-GT-292] p 47 A82-35462

On the solution of creep induced buckling in general structure p 66 A82-39514

Formal convergence characteristics of elliptically constrained incremental Newton-Raphson algorithms p 126 A83-10273

On the solution of elastic-plastic static and dynamic postbuckling collapse of general structure p 67 A83-12746

Finite element analysis of steadily moving contact fields p 70 A83-49437

Nonlinear transient finite element analysis of rotor-bearing-stator systems p 48 A84-20580

Algorithms for elasto-plastic-creep postbuckling p 73 A84-38480

High temperature thermomechanical analysis of ceramic coatings p 74 A84-48565

Extension of constrained incremental Newton-Raphson scheme to generalized loading fields p 74 A85-13942

On the development of hierarchical solution strategies for nonlinear finite element formulations p 126 A85-21979

Pantographing self adaptive gap elements p 77 A85-37440

Quasi-static solution algorithms for kinematically/materially nonlinear thermomechanical problems p 78 A85-41983

Hierarchical implicit dynamic least-square solution algorithm p 80 A86-26689

Inelastic high-temperature thermomechanical response of ceramic coated gas turbine seals p 82 A86-37799

Locally bound constrained Newton-Raphson solution algorithms p 83 A86-43771

Constrained hierarchical least square nonlinear equation solvers p 83 A86-43774

Engine dynamic analysis with general nonlinear finite element codes. Part 2: Bearing element implementation overall numerical characteristics and benchmarking [NASA-CR-167944] p 7 N82-33390

Constrained self-adaptive solutions procedures for structure subject to high temperature elastic-plastic creep effects p 99 N83-34370

Self-adaptive solution strategies p 105 N84-31693

Extension of constrained incremental Newton-Raphson scheme to generalized loading fields p 74 A85-13942

Quasi-static solution algorithms for kinematically/materially nonlinear thermomechanical problems p 78 A85-41983

A pad perturbation method for the dynamic coefficients of tilting-pad journal bearings p 47 A82-14400

Thermal-mechanical fatigue crack growth in Inconel X-750 p 35 A86-20982

Thermal-mechanical fatigue crack growth in Inconel X-750 [NASA-CR-174740] p 41 N85-15877

Thermal-mechanical fatigue behavior of nickel-base superalloys [NASA-CR-175048] p 43 N86-24818

Creep-rupture reliability analysis p 79 A85-42566

Creep-rupture reliability analysis [NASA-CR-3790] p 102 N84-19925

A new formulation of hybrid/mixed finite element p 67 A83-12739

Alternative ways for formulation of hybrid stress elements p 68 A83-14710

On the suppression of zero energy deformation modes p 72 A84-21541

Rational approach for assumed stress finite elements p 74 A85-12029

Hybrid Semiloof elements for plates and shells based upon a modified Hu-Washizu principle p 74 A85-15893

Evolution of assumed stress hybrid finite element p 77 A85-35046

Plasticity, viscoplasticity, and creep of solids by mechanical subelement models p 77 A85-35048

Axisymmetric solid elements by a rational hybrid stress method p 78 A85-41109

Finite elements based on consistently assumed stresses and displacements p 79 A86-18123

Hybrid solid element with a traction-free cylindrical surface p 82 A86-34462

Time-independent anisotropic plastic behavior by mechanical subelement models p 99 N83-34369

New variational formulations of hybrid stress elements p 105 N84-31690

Advanced stress analysis methods applicable to turbine engine structures [NASA-CR-175573] p 11 N85-21165

Recent advances in hybrid/mixed finite elements [NASA-CR-175574] p 107 N85-21687

On Hybrid and mixed finite element methods [NASA-CR-175551] p 108 N85-23096

Fracture toughness of brittle materials determined with chevron notch specimens p 45 A81-32545

Extended range stress intensity factor expressions for chevron-notched short bar and short rod fracture toughness specimens p 66 A82-40357

Fracture toughness of brittle materials determined with chevron notch specimens [NASA-TM-81607] p 38 N80-32486

Structural tailoring of engine blades (STAEBL) [NASA-CR-167949] p 7 N82-33391

A constitutive law for finite element contact problems with unclassical friction [NASA-TM-88838] p 120 N87-12924

The effects of crack surface friction and roughness on crack tip stress fields [NASA-TM-88976] p 122 N87-18881

Lewis Research Center spin rig and its use in vibration analysis of rotating systems [NASA-TP-2304] p 9 N84-24578

A low-cost optical data acquisition system for vibration measurement [NASA-TM-88907] p 121 N87-14730

Structural tailoring of engine blades (STAEBL) [AIAA 83-0828] p 1 A83-29737

Structural tailoring of engine blades (STAEBL) [NASA-CR-167949] p 7 N82-33391

Development and testing of stable, invariant, isoparametric curvilinear 2- and 3-D hybrid-stress elements p 75 A85-19899

Three-dimensional finite-element analysis of layered composite plates p 68 A83-27432

A mixed shear flexible finite element for the analysis of laminated plates p 73 A84-45994

Q

Experimental study of uncanceled squeeze film dampers [NASA-CR-168317] p 103 N84-19927

R

A preliminary study of crack initiation and growth at stress concentration sites [NASA-CR-169358] p 94 N82-33738

Natural frequencies of twisted rotating plates p 76 A85-32343

Concentrated mass effects on the flutter of a composite advanced turboprop model [NASA-TM-88854] p 120 N87-12017

Extending the laser-specklegram technique to strain analysis of rotating components p 67 A83-12514

Vibration and flutter of mistuned bladed-disk assemblies [AIAA PAPER 84-0991] p 75 A85-16095

Failure analysis of a tool steel torque shaft p 51 A84-17546

Factors influencing the ultrasonic stress wave factor evaluation of composite material structures p 81 A86-34257

Geometrically nonlinear analysis of layered composite shells p 68 A83-27431

Three-dimensional finite-element analysis of layered composite plates p 68 A83-27432

A mixed shear flexible finite element for the analysis of laminated plates p 73 A84-45994

Finite-element modeling of layered, anisotropic composite plates and shells: A review of recent research p 91 N82-19563

Geometrically nonlinear analysis of layered composite plates and shells [NASA-CR-168182] p 98 N83-33219

Geometrically nonlinear analysis of laminated elastic structures [NASA-CR-175609] p 108 N85-21720

A higher order theory of laminated composite cylindrical shells p 86 A87-35656

A comparative study of some dynamic stall models [NASA-TM-88917] p 122 N87-18883

Inelastic stress analyses at finite deformation through complementary energy approaches p 71 A84-13248

Analyses of large quasistatic deformations of inelastic bodies by a new hybrid-stress finite element algorithm p 71 A84-16874

Analyses of large quasistatic deformations of inelastic bodies by a new hybrid-stress finite element algorithm - Applications p 71 A84-16884

Hybrid stress finite elements for large deformations of inelastic solids p 74 A85-15894

Constitutive modeling and computational implementation for finite strain plasticity p 78 A85-40910

Stress and fracture analyses under elastic-plastic creep conditions: Some basic developments and computational approaches p 99 N83-34371

Characterization of composite materials by means of the ultrasonic stress wave factor p 16 A84-10430

RIEGER, A.

Development of procedures for calculating stiffness and damping of elastomers in engineering applications, part 6
[NASA-CR-159838] p 87 N80-22733

RIEGER, N. F.

Vibrations of blades and bladed disk assemblies; Proceedings of the Tenth Biennial Conference on Mechanical Vibration and Noise, Cincinnati, OH, September 10-13, 1985 p 4 A86-26901

RIFF, R.

Thermodynamically consistent constitutive equations for nonisothermal large strain, elasto-plastic, creep behavior [AIAA PAPER 85-0621] p 77 A85-38425

Analysis of shell type structures subjected to time dependent mechanical and thermal loading [NASA-CR-175747] p 109 N85-25896

Dynamic creep buckling: Analysis of shell structures subjected to time-dependent mechanical and thermal loading p 111 N85-27959

Analysis of large, non-isothermal elastic-visco-plastic deformations [NASA-CR-176220] p 115 N86-10588

Formulation of the nonlinear analysis of shell-like structures, subjected to time-dependent mechanical and thermal loading [NASA-CR-177194] p 119 N86-28462

RIPLING, E. J.

Fracture of composite-adhesive-composite systems p 76 A85-27935

ROBERTS, M. L.

Component-specific modeling p 12 N86-11515

ROBINSON, D. N.

Constitutive relationships for anisotropic high-temperature alloys [NASA-TM-83437] p 97 N83-28493

Viscoplastic constitutive relationships with dependence on thermomechanical history [NASA-CR-174836] p 108 N85-21691

On thermomechanical testing in support of constitutive equation development for high temperature alloys [NASA-CR-174879] p 109 N85-25894

Some advances in experimentation supporting development of viscoplastic constitutive models [NASA-CR-174855] p 109 N85-27260

Thermomechanical deformation in the presence of metallurgical changes p 112 N85-31533

Some advances in experimentation supporting development of viscoplastic constitutive models p 113 N85-31545

A continuous damage model based on stepwise-stress creep rupture tests [NASA-CR-174941] p 114 N85-32341

ROCK, S. M.

Sensor failure detection for jet engines [NASA-CR-168190] p 56 N83-33182

RODAL, J. J. A.

Instructions for the use of the CIVM-Jet 4C finite-strain computer code to calculate the transient structural responses of partial and/or complete arbitrarily-curved rings subjected to fragment impact [NASA-CR-159873] p 88 N80-27720

Finite-strain large-deflection elastic-viscoplastic finite-element transient response analysis of structures [NASA-CR-159874] p 88 N80-29762

ROHN, D. A.

Application of traction drives as servo mechanisms p 114 N85-33520

ROHN, DOUGLAS A.

Evaluation of a high-torque backlash-free roller actuator p 49 N87-16336

ROMANOSKI, G. R., JR.

Mechanisms of deformation and fracture in high temperature low cycle fatigue of Rene 80 and IN 100 [NASA-CR-165498] p 93 N82-26706

ROTH, D. J.

Radiographic detectability limits for seeded voids in sintered silicon carbide and silicon nitride p 51 A86-31745

Reliability of void detection in structural ceramics by use of scanning laser acoustic microscopy p 52 A86-39027

Quantitative flaw characterization with scanning laser acoustic microscopy p 52 A86-45150

Probability of detection of internal voids in structural ceramics using microfocus radiography p 52 A87-14300

Quantitative void characterization in structural ceramics by use of scanning laser acoustic microscopy p 53 A87-51974

Radiographic detectability limits for seeded voids in sintered silicon carbide and silicon nitride [NASA-TM-86945] p 58 N85-21674

Reliability of void detection in structural ceramics using scanning laser acoustic microscopy [NASA-TM-87035] p 58 N85-32337

Probability of detection of internal voids in structural ceramics using microfocus radiography [NASA-TM-87164] p 59 N86-13749

Reliability of scanning laser acoustic microscopy for detecting internal voids in structural ceramics [NASA-TM-87222] p 59 N86-16599

Factors that affect reliability of nondestructive detection of flaws in structural ceramics [NASA-TM-87348] p 61 N86-31912

Quantitative void characterization in structural ceramics using scanning laser acoustic microscopy [NASA-TM-88797] p 61 N86-31913

ROTH, DON J.

Ultrasonic NDE of structural ceramics for power and propulsion systems [NASA-TM-100147] p 62 N87-26362

ROZAK, G. A.

Mechanical behavior of carbon-carbon composites [NASA-CR-174767] p 28 N84-34575

RUBINSTEIN, ROBERT

Probabilistic structural analysis to quantify uncertainties associated with turbopump blades [AIAA PAPER 87-0766] p 85 A87-33581

RUNGTA, R.

Creep fatigue of low-cobalt superalloys: Waspalloy, PM U 700 and wrought U 700 [NASA-CR-168260] p 40 N84-13265

RYDER, J. T.

Effect of low temperature on fatigue and fracture properties of Ti-5Al-2.5Sn(EL) for use in engine components p 35 A85-47972

S

SADLER, G. G.

DEAN - A program for Dynamic Engine Analysis [AIAA PAPER 85-1354] p 3 A86-14430

DEAN: A program for dynamic engine analysis [NASA-TM-87033] p 11 N85-28945

SALEM, J. A.

Fractured toughness of Si3N4 measured with short bar chevron-notched specimens [NASA-TM-87153] p 47 N86-13495

SALEM, JONATHAN A.

Fracture toughness of Si3N4 measured with short bar chevron-notched specimens p 46 A87-30621

SALTSMAN, J. F.

Strainrange partitioning life predictions of the long time Metal Properties Council creep-fatigue tests p 63 A80-27958

Strainrange partitioning - A total strain range version p 34 A85-11603

Application of two creep fatigue life models for the prediction of elevated temperature crack initiation of a nickel base alloy [AIAA PAPER 85-1420] p 35 A85-43979

Strainrange partitioning: A total strain range version [NASA-TM-83023] p 39 N83-14246

Bending fatigue of electron-beam-welded foils. Application to a hydrodynamic air bearing in the Chrysler/DOE upgraded automotive gas turbine engine [NASA-TM-83539] p 102 N84-16589

An update of the total-strain version of SRP [NASA-TP-2499] p 42 N86-12295

Structural analysis of turbine blades using unified constitutive models [NASA-TM-88807] p 119 N86-28461

SALTSMAN, JAMES F.

Calculation of thermomechanical fatigue life based on isothermal behavior [NASA-TM-88864] p 122 N87-20565

SANDERS, W. A.

Correlation of processing and sintering variables with the strength and radiography of silicon nitride p 46 A87-12938

SANDOR, B. I.

The plastic compressibility of 7075-T651 aluminum-alloy plate p 36 A86-49690

SANKAR, L. N.

A technique for the prediction of airfoil flutter characteristics in separated flow [AIAA PAPER 87-0910] p 86 A87-33719

SANTNER, J. S.

Fracture of composite-adhesive-composite systems p 76 A85-27935

SARIGUL, N.

Computer aided derivation of equations for composite mechanics problems and finite element analyses [AIAA PAPER 86-1016] p 83 A86-38873

SARRAFZADEH-KHOEE, A.

A study of the stress wave factor technique for nondestructive evaluation of composite materials [NASA-CR-4002] p 60 N86-28445

SAWAMIPHAKDI, K.

Nonlinear finite element analysis of shells with large aspect ratio p 105 N84-31692

SCHEUERMANN, COULSON M.

Fatigue failure of regenerator screens in a high frequency Stirling engine [NASA-TM-88974] p 122 N87-18882

SCHMIDT, R. J.

Theoretical and software considerations for nonlinear dynamic analysis [NASA-CR-174504] p 101 N84-15589

SCHULTZ, D.

HOST liner cyclic facilities: Facility description p 10 N85-10988

SCHULTZ, K. P.

Numerical synthesis of tri-variate velocity realizations of turbulence p 81 A86-28654

SCHWARTZ, H. B.

Forced response of a cantilever beam with a dry friction damper attached. I - Theory. II - Experiment p 71 A84-21267

SHANNON, J. L., JR.

Fracture toughness determination of Al2O3 using four-point-bend specimens with straight-through and chevron notches p 45 A80-42085

Performance of Chevron-notch short bar specimen in determining the fracture toughness of silicon nitride and aluminum oxide p 45 A80-50696

Fracture toughness of brittle materials determined with chevron notch specimens p 45 A81-32545

Extended range stress intensity factor expressions for chevron-notched short bar and short rod fracture toughness specimens p 66 A82-40357

Development of plane strain fracture toughness test for ceramics using Chevron notched specimens p 46 A84-11676

Analysis of an externally radially crack ring segment subject to three-point radial loading p 79 A86-20710

Fracture toughness of brittle materials determined with chevron notch specimens [NASA-TM-81607] p 38 N80-32486

Specimen size and geometry effects on fracture toughness of Al2O3 measured with short rod and short bar chevron-notch specimens [NASA-TM-83319] p 47 N83-19902

Analysis of an externally radially cracked ring segment subject to three-point radial loading [NASA-TM-83482] p 100 N83-35413

Fractured toughness of Si3N4 measured with short bar chevron-notched specimens [NASA-TM-87153] p 47 N86-13495

SHANNON, JOHN L., JR.

Fracture toughness of Si3N4 measured with short bar chevron-notched specimens p 46 A87-30621

SHARP, G. RICHARD

Thermal expansion behavior of graphite/glass and graphite/magnesium p 21 A87-38615

SHARPE, W. N.

Benchmark notch test for life prediction [NASA-CR-165571] p 95 N83-12451

SHARPE, W. N., JR.

Benchmark cyclic plastic notch strain measurements p 33 A84-11194

SHEIKHOLESAMI, M. Z.

The finite analytic method, volume 3 [NASA-CR-170186] p 127 N83-23087

SHEN, H. D.

Fundamentals of microcrack nucleation mechanics [NASA-CR-3851] p 57 N85-16195

SHEU, Y. C.

Ultrasonic wave propagation in two-phase media - Spherical inclusions p 17 A85-11926

The transmission or scattering of elastic waves by an inhomogeneity of simple geometry: A comparison of theories [NASA-CR-3659] p 55 N83-16773

Fundamentals of microcrack nucleation mechanics [NASA-CR-3851] p 57 N85-16195

SHIH, C. I.

High temperature low cycle fatigue mechanisms for nickel base and a copper base alloy [NASA-CR-3543] p 39 N82-26436

SIH, G. C.

Moving cracks in layered composites p 67 A83-12048

Sudden stretching of a four layered composite plate [NASA-CR-159870] p 23 N80-25383

Sudden bending of cracked laminates [NASA-CR-159860] p 23 N80-25384

SIMITSES, G. J.

Thermodynamically consistent constitutive equations for nonisothermal large strain, elasto-plastic, creep behavior [AIAA PAPER 85-0621] p 77 A85-38425

Bounding solutions of geometrically nonlinear viscoelastic problems [AIAA PAPER 86-0943] p 82 A86-38838

- Analysis of shell type structures subjected to time dependent mechanical and thermal loading
[NASA-CR-175747] p 109 N85-25896
- Dynamic creep buckling: Analysis of shell structures subjected to time-dependent mechanical and thermal loading p 111 N85-27959
- Analysis of large, non-isothermal elastic-visco-plastic deformations
[NASA-CR-176220] p 115 N86-10588
- Formulation of the nonlinear analysis of shell-like structures, subjected to time-dependent mechanical and thermal loading
[NASA-CR-177194] p 119 N86-28462
- SIMS, D. L.**
Cyclic behavior of turbine disk alloys at 650 C p 32 A81-12266
- SINCLAIR, J. H.**
Mechanical property characterization of intraply hybrid composites p 13 A80-20954
Dynamic response of damaged angleplied fiber composites p 14 A80-27982
Micromechanics of intraply hybrid composites: Elastic and thermal properties p 14 A80-27994
Fracture modes of high modulus graphite/epoxy angleplied laminates subjected to off-axis tensile loads p 14 A80-32069
Nonlinear laminate analysis for metal matrix fiber composites
[AIAA 81-0579] p 15 A81-29411
Superhybrid composite blade impact studies
[ASME PAPER 81-GT-24] p 1 A81-29940
Computer code for intraply hybrid composite design p 15 A81-44662
Impact resistance of fiber composites p 66 A82-39852
Prediction of composite hygral behavior made simple p 16 A84-14285
Durability/life of fiber composites in hygrothermomechanical environments p 16 A84-27359
Compressive behavior of unidirectional fibrous composites p 16 A84-29894
Impact resistance of fiber composites - Energy-absorbing mechanisms and environmental effects p 18 A85-46543
Longitudinal compressive failure modes in fiber composites End attachment effects on IITRI type test specimens p 19 A86-19999
Micromechanics of intraply hybrid composites: Elastic and thermal properties
[NASA-TM-79253] p 21 N80-11143
Tensile and flexural strength of non-graphitic superhybrid composites: Predictions and comparisons
[NASA-TM-79276] p 21 N80-11144
Dynamic response of damaged angleplied fiber composites
[NASA-TM-79281] p 21 N80-11145
Mechanical property characterization of intraply hybrid composites
[NASA-TM-79306] p 21 N80-12120
Fracture modes of high modulus graphite/epoxy angleplied laminates subjected to off-axis tensile loads
[NASA-TM-81405] p 21 N80-16102
Superhybrid composite blade impact studies
[NASA-TM-81597] p 89 N81-11412
Nonlinear laminate analysis for metal matrix fiber composites
[NASA-TM-82596] p 24 N81-25149
Computer code for intraply hybrid composite design
[NASA-TM-82593] p 24 N81-25151
Durability/life of fiber composites in hygrothermomechanical environments
[NASA-TM-82749] p 24 N82-14287
Prediction of composite hygral behavior made simple
[NASA-TM-82780] p 24 N82-16181
Compression behavior of unidirectional fibrous composite
[NASA-TM-82833] p 25 N82-22313
INHYP: Computer code for intraply hybrid composite design. A users manual p 26 N84-13224
Impact resistance of fiber composites: Energy absorbing mechanisms and environmental effects
[NASA-TM-83594] p 26 N84-24712
- SINGH, K.**
The finite analytic method, volume 3
[NASA-CR-170186] p 127 N83-23087
- SINHA, A.**
Effects of friction dampers on aerodynamically unstable rotor stages
[AIAA PAPER 83-0848] p 1 A83-32791
The interaction between mistuning and friction in the forced response of bladed disk assemblies
[ASME PAPER 84-GT-139] p 73 A84-46957
Effects of friction dampers on aerodynamically unstable rotor stages p 3 A85-21866
- Stability of limit cycles in frictionally damped and aerodynamically unstable rotor stages p 4 A86-19198
Influence of friction dampers on torsional blade flutter
[ASME PAPER 85-GT-170] p 5 A86-32957
- SIZEMORE, R. L.**
Structural analysis and cost estimate of an eight-leg space frame as a support structure for horizontal axis wind turbines
[NASA-TM-83470] p 112 N85-30361
- SKALSKI, S. C.**
Forced vibration analysis of rotating cyclic structures in NASTRAN
[NASA-CR-165429] p 100 N84-11514
NASTRAN documentation for flutter analysis of advanced turbopropellers
[NASA-CR-167927] p 8 N84-15153
Bladed-shrouded-disc aeroelastic analyses: Computer program updates in NASTRAN level 17.7
[NASA-CR-165428] p 8 N84-15154
- SMITH, G. C. C.**
Flutter analysis of advanced turbopropellers
[AIAA 83-0846] p 69 A83-29824
NASTRAN forced vibration analysis of rotating cyclic structures
[ASME PAPER 83-DET-20] p 72 A84-29103
Flutter analysis of advanced turbopropellers p 73 A84-36492
Aeroelastic and dynamic finite element analyses of a bladed shrouded disk
[NASA-CR-159728] p 90 N81-19479
Nastran level 16 theoretical manual updates for aeroelastic analysis of bladed discs
[NASA-CR-159823] p 90 N81-19480
Finite element forced vibration analysis of rotating cyclic structures
[NASA-CR-165430] p 101 N84-11515
NASTRAN forced vibration analysis of rotating cyclic structures
[NASA-CR-173821] p 104 N84-29252
- SMITH, G. T.**
Engine environmental effects on composite behavior
[AIAA 80-0695] p 1 A80-35101
Resin selection criteria for tough composite structures
[AIAA 83-0801] p 46 A83-29734
Environmental and high strain rate effects on composites for engine applications p 16 A84-17444
Application of composite materials to turbofan engine fan exit guide vanes
[NASA-TM-81432] p 22 N80-18106
Engine environmental effects on composite behavior
[NASA-TM-81508] p 22 N80-23370
Composite containment systems for jet engine fan blades
[NASA-TM-81675] p 90 N81-17480
Environmental and High-Strain Rate effects on composites for engine applications
[NASA-TM-82882] p 25 N82-31449
- SMITH, T. E.**
Effect of design variables, temperature gradients and speed of life and reliability of a rotating disk
[NASA-TM-88883] p 49 N87-13755
- SNOW, D. W.**
Stress analysis of gas turbine engine structures using the boundary element method p 81 A86-34444
- SOKOLOWSKI, D. E.**
Toward improved durability in advanced combustors and turbines - Progress in prediction of thermomechanical loads
[ASME PAPER 86-GT-172] p 6 A86-48224
- SOKOLOWSKI, DANIEL E.**
Toward improved durability in advanced combustors and turbines: Progress in the prediction of thermomechanical loads
[NASA-TM-88932] p 13 N87-28551
- SOLAND, R. M.**
Statistical aspects of carbon fiber risk assessment modeling
[NASA-CR-159318] p 23 N80-29432
- SOLOMOS, G. P.**
Oscillator response to nonstationary excitation
[ASME PAPER 84-WA/APM-38] p 75 A85-17039
- SPANOS, P. T. D.**
Oscillator response to nonstationary excitation
[ASME PAPER 84-WA/APM-38] p 75 A85-17039
Numerical synthesis of tri-variate velocity realizations of turbulence p 81 A86-28654
- SPRAWLEY, J. E.**
Compliance and stress intensity coefficients for short bar specimens with chevron notches p 64 A80-46032
Analysis of an internally radially cracked ring segment subject to three-point radial loading p 71 A84-18691
Analysis of an externally radially crack ring segment subject to three-point radial loading p 79 A86-20710
Mode II fatigue crack growth specimen development p 83 A86-43566
- Stress intensity and displacement coefficients for radially cracked ring segments subject to three-point bending
[NASA-TM-83059] p 96 N83-24874
Mode 2 fatigue crack growth specimen development
[NASA-TM-83722] p 104 N84-29248
- SPRAWLEY, J. E.**
Analysis of an externally radially cracked ring segment subject to three-point radial loading
[NASA-TM-83482] p 100 N83-35413
- SRINIVASAN, A. V.**
Effects of mistuning on blade torsional flutter p 64 A81-29095
Dynamic characteristics of an assembly of prop-fan blades
[ASME PAPER 85-GT-134] p 5 A86-32956
Advanced turboprop vibratory characteristics
[NASA-CR-174708] p 12 N86-24693
- SRINIVASAN, M.**
Comparison of NDE techniques for sintered-SiC components p 51 A84-22265
- STAFFORD, J.**
Pantographing self adaptive gap elements p 77 A85-37440
- STAGLIANO, T. R.**
Instructions for the use of the CIVM-Jet 4C finite-strain computer code to calculate the transient structural responses of partial and/or complete arbitrarily-curved rings subjected to fragment impact
[NASA-CR-159873] p 88 N80-27720
- STALLONE, M. J.**
Blade loss transient dynamic analysis of turbomachinery p 2 A83-40864
The dynamics of a flexible bladed disc on a flexible rotor in a two-rotor system p 4 A86-25743
- STEIN, M.**
A solution procedure for behavior of thick plates on a nonlinear foundation and postbuckling behavior of long plates
[NASA-TP-2174] p 99 N83-34373
- STEIN, P. A.**
A solution procedure for behavior of thick plates on a nonlinear foundation and postbuckling behavior of long plates
[NASA-TP-2174] p 99 N83-34373
- STEINETZ, B. M.**
Application of traction drives as servo mechanisms p 114 N85-33520
A constitutive law for finite element contact problems with unclassical friction
[NASA-TM-88838] p 120 N87-12924
- STEINETZ, BRUCE M.**
Evaluation of a high-torque backlash-free roller actuator p 49 N87-16336
- STINCHCOMB, W. W.**
Characterization of composite materials by means of the ultrasonic stress wave factor p 16 A84-10430
A study of the stress wave factor technique for the characterization of composite materials
[NASA-CR-3670] p 55 N83-27248
A study of the stress wave factor technique for the characterization of composite materials
[NASA-CR-174870] p 29 N85-30035
Ultrasonic stress wave characterization of composite materials
[NASA-CR-79376] p 60 N86-27665
- STOLOFF, N. S.**
The effects of frequency and hold times on fatigue crack propagation rates in a nickel base superalloy p 34 A84-18733
The influence of hold times on LCF and FCG behavior in a P/M Ni-base superalloy p 35 A85-32400
Fatigue crack growth and low cycle fatigue of two nickel base superalloys
[NASA-CR-174534] p 39 N84-10267
- STONESIFER, R. B.**
On a study of the $\Delta T/c$ and $C/\text{asterisk}/$ integrals for fracture analysis under non-steady creep p 65 A82-36782
Moving singularity creep crack growth analysis with the $\Delta T/c$ and $C/\text{asterisk}/$ integrals p 66 A82-40066
Creep crack-growth: A new path-independent T sub o and computational studies p 92 N82-24503
Creep crack-growth: A new path-independent integral (T sub c), and computational studies
[NASA-CR-167897] p 94 N82-29619
Stress and fracture analyses under elastic-plastic creep conditions: Some basic developments and computational approaches p 99 N83-34371
- STORACE, A.**
Blade loss transient dynamics analysis with flexible bladed disk
[NASA-CR-168176] p 7 N84-13193
- STORACE, A. F.**
Blade loss transient dynamic analysis of turbomachinery p 2 A83-40864

T

STOUFFER, D. C.

Finite element analysis of notch behavior using a state variable constitutive equation p 114 N85-31548
Anisotropic constitutive model for nickel base single crystal alloys: Development and finite element implementation [NASA-CR-175015] p 117 N86-21952

STUBSTAD, J. M.

Bounding solutions of geometrically nonlinear viscoelastic problems [AIAA PAPER 86-0943] p 82 A86-38838

SUBRAHMANYAM, K. B.

Finite difference analysis of torsional vibrations of pretwisted, rotating, cantilever beams with effects of warping p 78 A85-42047
Vibration analysis of rotating turbomachinery blades by an improved finite difference method p 3 A86-14338
Vibration and buckling of rotating, pretwisted, precone beams including Coriolis effects p 80 A86-26910
Nonlinear vibration and stability of rotating, pretwisted, precone beams including Coriolis effects p 86 A87-39896

Influence of third-degree geometric nonlinearities on the vibration and stability of pretwisted, precone, rotating blades p 6 A87-46228

An improved finite-difference analysis of uncoupled vibrations of tapered cantilever beams [NASA-TM-83495] p 101 N84-13610

Improved finite-difference vibration analysis of pretwisted, tapered beams [NASA-TM-83549] p 102 N84-16588

Improved methods of vibration analysis of pretwisted, airfoil blades [NASA-TM-83735] p 104 N84-30329

Vibration and buckling of rotating, pretwisted, precone beams including Coriolis effects [NASA-TM-87004] p 109 N85-25893

Nonlinear flap-lag-extensional vibrations of rotating, pretwisted, precone beams including Coriolis effects [NASA-TM-87102] p 115 N85-34427

Nonlinear bending-torsional vibration and stability of rotating, pretwisted, precone blades including Coriolis effects [NASA-TM-87207] p 116 N86-17789

Influence of third-degree geometric nonlinearities on the vibration and stability of pretwisted, precone, rotating blades [NASA-TM-87307] p 120 N86-31920

SULLIVAN, T. L.

Structural fatigue test results for large wind turbine blade sections p 96 N83-19246

SULLIVAN, TIMOTHY L.

The effect of nonlinearities on the dynamic response of a large shuttle payload [NASA-TM-88941] p 121 N87-18112

SUMIHARA, K.

Rational approach for assumed stress finite elements p 74 A85-12029

Hybrid Semiloof elements for plates and shells based upon a modified Hu-Washizu principle p 74 A85-15893

New variational formulations of hybrid stress elements p 105 N84-31690

SUN, C. T.

Wave propagation in a graphite/epoxy laminate p 70 A83-44050

Indentation law for composite laminates p 16 A84-27356

Use of static indentation laws in the impact analysis of laminated composite plates p 18 A85-29133

Dynamic delamination crack propagation in a graphite/epoxy laminate p 20 A86-43010

Dynamic responses of graphite/epoxy laminated beam to impact of elastic spheres [NASA-CR-165461] p 25 N83-13173

Wave propagation in graphite/epoxy laminates due to impact [NASA-CR-168057] p 26 N83-22325

SUNDARAM, C. V.

Flow dynamic environment data base development for the SSME p 109 N85-26885

SWANSON, G. A.

Life prediction and constitutive models for engine hot section anisotropic materials program [NASA-CR-174952] p 60 N86-25003

SWINSON, W. F.

Extending the laser-specklegram technique to strain analysis of rotating components p 67 A83-12514

SZUCH, J. R.

Digital computer program for generating dynamic turbofan engine models (DIGTEM) [NASA-TM-83446] p 8 N84-16185

TABADDOR, F.

Pantographing self adaptive gap elements p 77 A85-37440

TAN, T. M.

Wave propagation in a graphite/epoxy laminate p 70 A83-44050

Use of static indentation laws in the impact analysis of laminated composite plates p 18 A85-29133

Wave propagation in graphite/epoxy laminates due to impact [NASA-CR-168057] p 26 N83-22325

TANNER, J. A.

Temperature distribution in an aircraft tire at low ground speeds [NASA-TP-2195] p 97 N83-33217

TELESMA, J.

A study of spectrum fatigue crack propagation in two aluminum alloys. I - Spectrum simplification. II - Influence of microstructures p 36 A86-48973

Evaluation of the effect of crack closure on fatigue crack growth of simulated short cracks [NASA-TM-83778] p 40 N84-31348

A study of spectrum fatigue crack propagation in two aluminum alloys. 1: Spectrum simplification [NASA-TM-86929] p 41 N85-18124

A study of spectrum fatigue crack propagation in two aluminum alloys. 2: Influence of microstructures [NASA-TM-86930] p 41 N85-18125

Influence of load interactions on crack growth as related to state of stress and crack closure [NASA-TM-87117] p 42 N86-12292

Variables controlling fatigue crack growth of short cracks [NASA-TM-87208] p 43 N86-21661

Influence of fatigue crack wake length and state of stress on crack closure [NASA-TM-87292] p 43 N86-22686

TEVABERWERK, J. L.

Stress evaluations under rolling/sliding contacts [NASA-CR-165561] p 91 N82-17521

THAKKER, A. B.

Low strain, long life creep fatigue of AF2-1DA and INCO 718 [NASA-CR-167989] p 40 N84-10268

THOMA, D. J.

Interaction of high-cycle and low-cycle fatigue of Haynes 188 alloy at 1400 F deg p 111 N85-27961

THOMAS, R. L.

Comparison of NDE techniques for sintered-SiC components p 51 A83-22265

THOMPSON, R. L.

A computer analysis program for interfacing thermal and structural codes p 126 A86-36861

Unified constitutive materials model development and evaluation for high-temperature structural analysis applications p 84 A86-49133

Nonlinear constitutive theory for turbine engine structural analysis p 95 N82-33744

A computer program for predicting nonlinear uniaxial material responses using viscoplastic models [NASA-TM-83675] p 104 N84-29247

Validation of structural analysis methods using the in-house liner cyclic rigs p 10 N85-10987

A computer analysis program for interfacing thermal and structural codes [NASA-TM-87021] p 110 N85-27264

On numerical integration and computer implementation of viscoplastic models p 113 N85-31542

High temperature stress-strain analysis p 120 N87-11209

THOMPSON, ROBERT L.

High temperature stress-strain analysis p 125 N88-11170

TIAN, Z.

Axisymmetric solid elements by a rational hybrid stress method p 78 A85-41109

Hybrid solid element with a traction-free cylindrical surface p 82 A86-34462

TOMPKINS, STEPHEN S.

Thermal expansion behavior of graphite/glass and graphite/magnesium p 21 A87-38615

TONG, M.

Structural analysis of turbine blades using unified constitutive models [NASA-TM-88807] p 119 N86-28461

TONG, M. T.

Unified constitutive materials model development and evaluation for high-temperature structural analysis applications p 84 A86-49133

TOTI, J. M., JR.

Fiberglass epoxy laminate fatigue properties at 300 and 20 K p 19 A85-47970

TOVICHAKCHAIKUL, S.

On the solution of creep induced buckling in general structure p 66 A82-39514

On the solution of elastic-plastic static and dynamic postbuckling collapse of general structure p 67 A83-12746

Finite element analysis of steadily moving contact fields p 70 A83-49437

Algorithms for elasto-plastic-creep postbuckling p 73 A84-38480

Constrained self-adaptive solutions procedures for structure subject to high temperature elastic-plastic creep effects p 99 N83-34370

TURNER, J. L.

Extending the laser-specklegram technique to strain analysis of rotating components p 67 A83-12514

V

VALERO, N. A.

Vibration characteristics of mistuned shrouded blade assemblies [ASME PAPER 85-GT-115] p 4 A86-22068

VANDENBRINK, D. J.

Optimization and analysis of gas turbine engine blades [AIAA PAPER 87-0827] p 126 A87-33614

VARY, A.

A review of issues and strategies in nondestructive evaluation of fiber reinforced structural composites p 14 A80-34764

Quantitative ultrasonic evaluation of engineering properties in metals, composites, and ceramics p 50 A80-39641

Concepts and techniques for ultrasonic evaluation of material mechanical properties p 50 A80-51575

Ultrasonic measurement of material properties p 50 A81-19656

Acousto-ultrasonic characterization of fiber reinforced composites p 50 A81-44660

Metal honeycomb to porous wireform substrate diffusion bond evaluation p 51 A83-39620

Measurement of ultrasonic velocity using phase-slope and cross-correlation methods p 51 A86-13192

Nondestructive techniques for characterizing mechanical properties of structural materials: An overview [ASME PAPER 86-GT-75] p 52 A86-48143

NDE of structural ceramics [ASME PAPER 86-GT-279] p 52 A86-48298

Simulation of transducer-couplant effects on broadband ultrasonic signals [NASA-TM-81489] p 53 N80-22714

Concepts and techniques for ultrasonic evaluation of material mechanical properties [NASA-TM-81523] p 53 N80-24634

Quantitative ultrasonic evaluation of engineering properties in metals, composites and ceramics [NASA-TM-81530] p 54 N80-26682

Acousto-ultrasonic characterization of fiber reinforced composites [NASA-TM-82651] p 54 N81-28458

Metal honeycomb to porous wireform substrate diffusion bond evaluation [NASA-TM-82793] p 54 N82-18612

Interrelation of material microstructure, ultrasonic factors, and fracture toughness of two phase titanium alloy [NASA-TM-82810] p 54 N82-20551

Ultrasonic ranking of toughness of tungsten carbide [NASA-TM-83358] p 55 N83-23620

Ultrasonic velocity measurement using phase-slope cross-correlation methods [NASA-TM-83794] p 57 N84-34769

Ultrasonic nondestructive evaluation, microstructure, and mechanical property interrelations [NASA-TM-86876] p 57 N85-10371

NDE of structural ceramics [NASA-TM-87186] p 59 N86-16598

Nondestructive techniques for characterizing mechanical properties of structural materials: An overview [NASA-TM-87203] p 59 N86-19636

Analytical Ultrasonics in Materials Research and Testing [NASA-CP-2383] p 59 N86-22962

Concepts for interrelating ultrasonic attenuation, microstructure and fracture toughness in polycrystalline solids [NASA-TM-87339] p 60 N86-25812

VARY, ALEX

The acousto-ultrasonic approach [NASA-TM-89843] p 62 N87-20562

Application of scanning acoustic microscopy to advanced structural ceramics [NASA-TM-89929] p 62 N87-23987

- Ultrasonic NDE of structural ceramics for power and propulsion systems
[NASA-TM-100147] p 62 N87-26362
- VERRILLI, M. J.**
Preliminary study of thermomechanical fatigue of polycrystalline MAR-M 200
[NASA-TP-2280] p 40 N84-17350

W

- WALKER, K. P.**
A survey of unified constitutive theories
p 112 N85-31531
- Constitutive modeling for isotropic materials (HOST)
[NASA-CR-174980] p 115 N86-10589
- Life prediction and constitutive models for engine hot section anisotropic materials program
[NASA-CR-174952] p 60 N86-25003
- WANAG, S. S.**
Boundary-layer effects in composite laminates: Free-edge stress singularities, part 6
[NASA-CR-165440] p 94 N82-26718
- WANG, A. J.**
Vibrations of cantilevered shallow cylindrical shells of rectangular planform p 65 A82-11298
- Vibrations of twisted rotating blades
[ASME PAPER 81-DET-127] p 65 A82-19341
- Vibrations of cantilevered circular cylindrical shells
Shallow versus deep shell theory p 69 A83-36958
- Vibrations of cantilevered doubly-curved shallow shells
p 70 A83-39557
- Vibrations of blades with variable thickness and curvature by shell theory
[ASME PAPER 83-GT-152] p 70 A83-47978
- WANG, H. T.**
Interlaminar crack growth in fiber reinforced composites during fatigue, part 3
[NASA-CR-165434] p 93 N82-26715
- WANG, P. S.**
Automatic finite element generators
p 105 N84-31695
- WANG, S.**
Ion beam sputter etching of orthopedic implanted alloy MP35N and resulting effects on fatigue
[NASA-TM-81747] p 38 N81-21174
- WANG, S. S.**
Interface cracks in adhesively bounded lap-shear joints p 67 A82-46109
- Boundary-layer effects in composite laminates. I - Free-edge stress singularities. II - Free-edge stress solutions and basic characteristics p 67 A82-46806
- Elasticity solutions for a class of composite laminate problems with stress singularities p 17 A84-33389
- Three-dimensional hybrid-stress finite element analysis of composite laminates with cracks and cutouts
p 80 A86-26896
- Boundary layer thermal stresses in angle-ply composite laminates, part 1
[NASA-CR-165412] p 93 N82-26713
- Analysis of cracks emanating from a circular hole in unidirectional fiber reinforced composites, part 2
[NASA-CR-165433] p 93 N82-26714
- Interlaminar crack growth in fiber reinforced composites during fatigue, part 3
[NASA-CR-165434] p 93 N82-26715
- Analysis of interface cracks in adhesively bonded lap shear joints, part 4
[NASA-CR-165438] p 93 N82-26716
- Edge delamination in angle-ply composite laminates, part 5
[NASA-CR-165439] p 94 N82-26717
- WANG, S. Y.**
The structural response of a rail acceleration
p 72 A84-32039
- The structural response of a rail accelerator
[NASA-TM-83491] p 99 N83-35412
- WANG, T.**
Dynamic responses of graphite/epoxy laminated beam to impact of elastic spheres
[NASA-CR-165461] p 25 N83-13173
- WARD, M.**
Benchmark cyclic plastic notch strain measurements
p 33 A84-11194
- Benchmark notch test for life prediction
[NASA-CR-165571] p 95 N83-12451
- WARREN, J. R.**
Cyclic behavior of turbine disk alloys at 650 C
p 32 A81-12266
- Evaluation of the cyclic behavior of aircraft turbine disk alloys, part 2
[NASA-CR-165123] p 38 N80-30482
- WATANABE, O.**
Constitutive modeling of cyclic plasticity and creep, using an internal time concept p 83 A86-41673

- WATSON, G. K.**
Ultrasonic velocity for estimating density of structural ceramics
[NASA-TM-82765] p 46 N82-14359
- WEBER, R. M.**
Constitutive modeling for isotropic materials (HOST)
[NASA-CR-174980] p 115 N86-10589
- WEETON, J. W.**
Method for alleviating thermal stress damage in laminates
[NASA-CASE-LEW-12493-1] p 23 N81-17170
- Method for alleviating thermal stress damage in laminates
[NASA-CASE-LEW-12493-2] p 24 N81-26179
- WELSCH, G.**
Fatigue crack layer propagation in silicon-iron
[NASA-CR-175115] p 118 N86-25851
- WELSCH, G. E.**
The cyclic stress-strain behavior of a nickel-base superalloy at 650 C p 36 A86-45715
- WENDELL, J. H.**
Some analysis methods for rotating systems with periodic coefficients p 69 A83-32987
- WESTERKAMP, E. J.**
Digital computer program for generating dynamic turbofan engine models (DIGTEM)
[NASA-TM-83446] p 8 N84-16185
- WHITE, J. F., III**
Aeroelastic behavior of low aspect ratio metal and composite blades
[ASME PAPER 86-GT-243] p 84 A86-48271
- WHITE, W. F., JR.**
Buckling of rotating beams p 63 A80-20149
- WHITTENBERGER, J. D.**
Comparative thermal fatigue resistance of several oxide dispersion strengthened alloys p 32 A82-11399
- WILLIAMS, G. C.**
Interply layer degradation effects on composite structural response
[AIAA PAPER 84-0849] p 18 A85-16096
- Interply layer degradation effects on composite structural response
[NASA-TM-83702] p 27 N84-26756
- WILLIAMS, J. H., JR.**
Ultrasonic input-output for transmitting and receiving longitudinal transducers coupled to same face of isotropic elastic plate
[NASA-CR-3506] p 54 N82-18613
- Effects of specimen resonances on acoustic-ultrasonic testing
[NASA-CR-3679] p 55 N83-21373
- Ultrasonic attenuation of a void-containing medium for very long wavelengths p 56 N83-28466
- Stress waves in an isotropic elastic plate excited by a circular transducer
[NASA-CR-3877] p 58 N85-20390
- Application of homomorphic signal processing to stress wave factor analysis
[NAS 1.26:174871] p 58 N85-21673
- Ultrasonic testing of plates containing edge cracks
[NASA-CR-3904] p 58 N85-29307
- Stress waves in transversely isotropic media: The homogeneous problem
[NASA-CR-3977] p 59 N86-25002
- Wave propagation in anisotropic medium due to an oscillatory point source with application to unidirectional composites
[NASA-CR-4001] p 60 N86-27666
- WILLIAMS, J., JR.**
Input-output characterization of an ultrasonic testing system by digital signal analysis
[NASA-CR-3756] p 56 N84-15565
- WILLIAMS, M. H.**
Three dimensional unsteady aerodynamics and aeroelastic response of advanced turboprops
[AIAA PAPER 86-0846] p 5 A86-38894
- WILLIAMS, MARC**
Analytical and experimental investigation of mistuning in propfan flutter
[AIAA PAPER 87-0739] p 86 A87-40496
- Analytical and experimental investigation of mistuning in propfan flutter
[NASA-TM-88959] p 122 N87-18116
- WILLIAMS, W.**
Dynamic modulus and damping of boron, silicon carbide, and alumina fibers p 15 A80-44236
- Dynamic modulus and damping of boron, silicon carbide, and alumina fibers
[NASA-TM-81422] p 22 N80-20313
- WILSON, R. B.**
Stress analysis of gas turbine engine structures using the boundary element method p 81 A86-34444
- Three-dimensional stress analysis using the boundary element method p 106 N84-31700

- 3-D inelastic analysis methods for hot section components (base program)
[NASA-CR-174700] p 107 N85-21686
- WINEGAR, STEVEN R.**
SINDA-NASTRAN interfacing program theoretical description and user's manual
[NASA-TM-100158] p 124 N87-27268
- WINEMILLER, J. R.**
Structural analysis and cost estimate of an eight-leg space frame as a support structure for horizontal axis wind turbines
[NASA-TM-83470] p 112 N85-30361
- WINGET, J. M.**
Element-by-element solution procedures for nonlinear structural analysis p 105 N84-31694
- WINSA, E. A.**
Tungsten fiber reinforced superalloy composite high temperature component design considerations
[NASA-TM-82811] p 25 N82-21259
- WINTUCKY, E. G.**
Ion beam sputter etching of orthopedic implanted alloy MP35N and resulting effects on fatigue
[NASA-TM-81747] p 38 N81-21174
- WIRSCHING, P. H.**
Advanced reliability method for fatigue analysis
p 72 A84-31596
- Creep-rupture reliability analysis p 79 A85-42566
- The application of probabilistic design theory to high temperature low cycle fatigue
[NASA-CR-165488] p 91 N82-14531
- Statistical summaries of fatigue data for design purposes
[NASA-CR-3697] p 97 N83-29731
- Application of advanced reliability methods to local strain fatigue analysis
[NASA-CR-168198] p 97 N83-29734
- Creep-rupture reliability analysis
[NASA-CR-3790] p 102 N84-19925
- Reliability considerations for the total strain range version of strain-range partitioning
[NASA-CR-174757] p 106 N85-11380
- WITMER, E. A.**
Instructions for the use of the CIVM-Jet 4C finite-strain computer code to calculate the transient structural responses of partial and/or complete arbitrarily-curved rings subjected to fragment impact
[NASA-CR-159873] p 88 N80-27720
- Finite-strain large-deflection elastic-viscoplastic finite-element transient response analysis of structures
[NASA-CR-159874] p 88 N80-29762
- WITZELL, W. E.**
Effect of low temperature on fatigue and fracture properties of Ti-5Al-2.5Sn(ELI) for use in engine components p 35 A85-47972
- WU, JIUNN-CHI**
A technique for the prediction of airfoil flutter characteristics in separated flow
[AIAA PAPER 87-0910] p 86 A87-33719
- WU, T. T.**
Application of advanced reliability methods to local strain fatigue analysis
[NASA-CR-168198] p 97 N83-29734
- WU, Y. T.**
Reliability considerations for the total strain range version of strain-range partitioning
[NASA-CR-174757] p 106 N85-11380
- WU, Y.-T.**
Advanced reliability method for fatigue analysis
p 72 A84-31596

X

- XUE, W.-M.**
On the existence and stability conditions for mixed-hybrid finite element solutions based on Reissner's variational principle p 77 A85-33847
- Existence and stability, and discrete BB and rank conditions, for general mixed-hybrid finite elements in elasticity p 82 A86-34464

Y

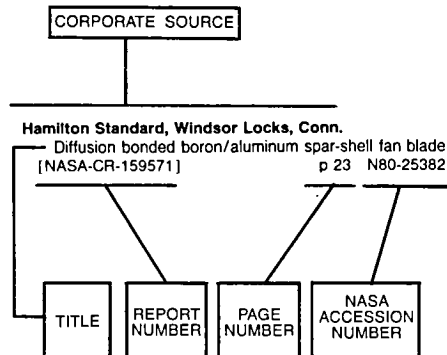
- YANG, C. Y.**
Modelling of crack tip deformation with finite element method and its applications p 87 N80-13503
- YANG, S. H.**
Indentation law for composite laminates
p 16 A84-27356
- YAU, J. F.**
Interface cracks in adhesively bounded lap-shear joints p 67 A82-46109
- Analysis of cracks emanating from a circular hole in unidirectional fiber reinforced composites, part 2
[NASA-CR-165433] p 93 N82-26714

- Analysis of interface cracks in adhesively bonded lap shear joints, part 4
[NASA-CR-165438] p 93 N82-26716
Benchmark notch test for life prediction
[NASA-CR-165571] p 95 N83-12451
- YEE, S. T.**
Structural analysis and cost estimate of an eight-leg space frame as a support structure for horizontal axis wind turbines
[NASA-TM-83470] p 112 N85-30361
- YOUNG, M. I.**
Stability of large horizontal-axis axisymmetric wind turbines p 64 A81-22526
Stability of large horizontal-axis axisymmetric wind turbines
[NASA-TM-81623] p 89 N81-12446
- YOUNG, T. H.**
Extensions of the Ritz-Galerkin method for the forced, damped vibrations of structural elements
p 117 N86-21909
- YUECE, H.**
Ultrasonic attenuation of a void-containing medium for very long wavelengths
[NASA-CR-3693] p 56 N83-28466
- YUHAS, D.**
Comparison of NDE techniques for sintered-SiC components p 51 A83-22265

Z

- ZAHIRI, F.**
Axial and torsional fatigue behavior of Waspaloy
[NASA-CR-175052] p 44 N86-25454
- ZAMRIK, S.**
Axial and torsional fatigue behavior of Waspaloy
[NASA-CR-175052] p 44 N86-25454
- ZARETSKY, E. V.**
Fatigue criterion to system design, life and reliability
[AIAA PAPER 85-1140] p 78 A85-40814
Fatigue criterion to system design, life and reliability
[NASA-TM-87017] p 49 N85-27226
Selection of rolling-element bearing steels for long-life application
[NASA-TM-88881] p 49 N87-11993
Effect of design variables, temperature gradients and speed of life and reliability of a rotating disk
[NASA-TM-88883] p 49 N87-13755
- ZARETSKY, ERWIN V.**
Effect of interference fits on roller bearing fatigue life
p 48 A87-37686
Lubricant effects on bearing life
[NASA-TM-88875] p 49 N87-15467
Effects of surface removal on rolling-element fatigue
[NASA-TM-88871] p 50 N87-18820
- ZARETSKY, ERWIN Y.**
Fatigue criterion to system design, life, and reliability
p 85 A87-27986
- ZEID, I.**
Engine dynamic analysis with general nonlinear finite element codes. II - Bearing element implementation, overall numerical characteristics and benchmarking
[ASME PAPER 82-GT-292] p 47 A82-35462
Finite element analysis of steadily moving contact fields p 70 A83-49437
Nonlinear transient finite element analysis of rotor-bearing-stator systems p 48 A84-20580
Engine dynamic analysis with general nonlinear finite element codes. Part 2: Bearing element implementation overall numerical characteristics and benchmarking
[NASA-CR-167944] p 7 N82-33390
- ZHANG, Z.-D.**
On the three-dimensional vibrations of the cantilevered rectangular parallelepiped p 70 A83-37729
- ZHONG, W. F.**
Volume integrals associated with the inhomogeneous Helmholtz equation. Part 2: Cylindrical region; rectangular region
[NASA-CR-3750] p 56 N84-14526
Fundamentals of microcrack nucleation mechanics
[NASA-CR-3851] p 57 N85-16195
- ZIENKIEWICZ, O. C.**
Iterative methods for mixed finite element equations
p 82 A86-34461
- ZORZI, E.**
Development of procedures for calculating stiffness and damping of elastomers in engineering applications, part 6
[NASA-CR-159838] p 87 N80-22733

Typical Corporate Source Index Listing



Listings in this index are arranged alphabetically by corporate source. The title of the document is used to provide a brief description of the subject matter. The page number and the accession number are included in each entry to assist the user in locating the abstract in the abstract section. If applicable, a report number is also included as an aid in identifying the document.

A

- Aerogel Technical Systems Co., Sacramento, Calif.**
Longitudinal mode combustion instabilities of a high-pressure fuel-rich LOX/RP-1 preburner p 60 N86-28250
- Air Force Academy, Colo.**
Comparison of beam and shell theories for the vibrations of thin turbomachinery blades [ASME PAPER 82-GT-223] p 65 A82-35408
- Air Force Aero Propulsion Lab., Wright-Patterson AFB, Ohio.**
Vibrations of twisted cantilevered plates - Experimental investigation [ASME PAPER 84-GT-96] p 73 A84-46937
Vibrations of twisted cantilevered plates - Summary of previous and current studies p 76 A85-22069
Vibrations of twisted cantilever plates - A comparison of theoretical results p 79 A85-47626
- Air Force Flight Dynamics Lab., Wright-Patterson AFB, Ohio.**
Structural optimization using optimality criteria methods p 79 A85-48703
- Air Force Wright Aeronautical Labs., Wright-Patterson AFB, Ohio.**
Three dimensional finite-element elastic analysis of a thermally cycled double-edge wedge geometry specimen [NASA-TM-80980] p 37 N80-26433
- Akron Univ., Ohio.**
Engine dynamic analysis with general nonlinear finite element codes. II - Bearing element implementation, overall numerical characteristics and benchmarking [ASME PAPER 82-GT-292] p 47 A82-35462
On the solution of creep induced buckling in general structure p 66 A82-39514
Formal convergence characteristics of elliptically constrained incremental Newton-Raphson algorithms p 126 A83-10273
On the solution of elastic-plastic static and dynamic postbuckling collapse of general structure p 67 A83-12746

- Finite element analysis of steadily moving contact fields p 70 A83-49437
Nonlinear transient finite element analysis of rotor-bearing-stator systems p 48 A84-20580
Algorithms for elasto-plastic-creep postbuckling p 73 A84-38480
High temperature thermomechanical analysis of ceramic coatings p 74 A84-48565
Extension of constrained incremental Newton-Raphson scheme to generalized loading fields p 74 A85-13942
On the development of hierarchical solution strategies for nonlinear finite element formulations p 126 A85-21979
Pantographing self adaptive gap elements p 77 A85-37440
Quasi-static solution algorithms for kinematically/materially nonlinear thermomechanical problems p 78 A85-41983
Hierarchical implicit dynamic least-square solution algorithm p 80 A86-26689
Inelastic high-temperature thermomechanical response of ceramic coated gas turbine seals p 82 A86-37799
Locally bound constrained Newton-Raphson solution algorithms p 83 A86-43771
Constrained hierarchical least square nonlinear equation solvers p 83 A86-43774
Results of an interlaboratory fatigue test program conducted on alloy 800H at room and elevated temperatures p 37 A87-54370
Engine dynamic analysis with general nonlinear finite element codes. Part 2: Bearing element implementation overall numerical characteristics and benchmarking [NASA-CR-167944] p 7 N82-33390
Constrained self-adaptive solutions procedures for structure subject to high temperature elastic-plastic creep effects p 99 N83-34370
Experimental study of uncentralized squeeze film dampers [NASA-CR-168317] p 103 N84-19927
Nonlinear finite element analysis of shells with large aspect ratio p 105 N84-31692
Self-adaptive solution strategies p 105 N84-31693
Viscoplastic constitutive relationships with dependence on thermomechanical history p 108 N85-21691
On thermomechanical testing in support of constitutive equation development for high temperature alloys [NASA-CR-174879] p 109 N85-25894
Some advances in experimentation supporting development of viscoplastic constitutive models [NASA-CR-174855] p 109 N85-27260
Thermomechanical deformation in the presence of metallurgical changes p 112 N85-31533
Some advances in experimentation supporting development of viscoplastic constitutive models p 113 N85-31545
Results of an interlaboratory fatigue test program conducted on alloy 800H at room and elevated temperatures [NASA-CR-174940] p 114 N85-32340
A continuous damage model based on stepwise-stress creep rupture tests [NASA-CR-174941] p 114 N85-32341
- Argonne National Lab., Ill.**
Effects of a high mean stress on the high cycle fatigue life of PWA 1480 and correlation of data by linear elastic fracture mechanics [NASA-CR-175057] p 118 N86-27689
- Arizona State Univ., Tempe.**
A blade loss response spectrum for flexible rotor systems [ASME PAPER 84-GT-29] p 48 A84-46893
- Arizona Univ., Phoenix.**
Creep-rupture reliability analysis p 79 A85-42566
- Arizona Univ., Tucson.**
Advanced reliability method for fatigue analysis p 72 A84-31596
Interply layer degradation effects on composite structural response [AIAA PAPER 84-0849] p 18 A85-16096

- The application of probabilistic design theory to high temperature low cycle fatigue [NASA-CR-165488] p 91 N82-14531
Statistical summaries of fatigue data for design purposes [NASA-CR-3697] p 97 N83-29731
Application of advanced reliability methods to local strain fatigue analysis [NASA-CR-168198] p 97 N83-29734
Creep-rupture reliability analysis [NASA-CR-3790] p 102 N84-19925
Reliability considerations for the total strain range version of strainrange partitioning [NASA-CR-174757] p 106 N85-11380
- Army Armament Research and Development Command, Watervliet, N. Y.**
Wide-range displacement expressions for standard fracture mechanics specimens p 79 A86-20706
- Army Aviation Research and Development Command, Cleveland, Ohio.**
A finite element stress analysis of spur gears including fillet radii and rim thickness effects [NASA-TM-82865] p 48 N82-28646
Micromechanisms of thermomechanical fatigue: A comparison with isothermal fatigue [NASA-TM-87331] p 44 N86-28164
- Army Propulsion Lab., Cleveland, Ohio.**
Fatigue behavior of SiC reinforced Ti/6Al-4V/ at 650 C DEAN - A program for Dynamic Engine Analysis [AIAA PAPER 85-1354] p 3 A86-14430
- Army Research and Technology Labs., Cleveland, Ohio.**
Low cycle fatigue of MAR-M 200 single crystals at 760 and 870 deg C [NASA-TM-86933] p 41 N85-19074
Multiaxial and thermomechanical fatigue considerations in damage tolerant design [NASA-TM-87022] p 42 N85-26964
DEAN: A program for dynamic engine analysis [NASA-TM-87033] p 11 N85-28945
- Army Structures Lab., Hampton, Va.**
Buckling of rotating beams p 63 A80-20149
- Auburn Univ., Ala.**
Extending the laser-specklegram technique to strain analysis of rotating components p 67 A83-12514

B

- Babcock and Wilcox Co., Akron, Ohio.**
Quasi-static solution algorithms for kinematically/materially nonlinear thermomechanical problems p 78 A85-41983
- Babcock and Wilcox Co., New York, N.Y.**
Extension of constrained incremental Newton-Raphson scheme to generalized loading fields p 74 A85-13942
- Ball Aerospace Systems Div., Boulder, Colo.**
Fracture toughness of hot-pressed beryllium p 34 A85-25835
- Battelle Columbus Labs., Ohio.**
Continuous analysis of stresses from arbitrary surface loads on a half space p 64 A81-14162
A history dependent damage model for low cycle fatigue [ASME PAPER 84-PVP-112] p 75 A85-18795
Stress evaluations under rolling/sliding contacts [NASA-CR-165561] p 91 N82-17521
Creep fatigue of low-cobalt superalloys: Waspalloy, PM U 700 and wrought U 700 [NASA-CR-168260] p 40 N84-13265
Composite loads spectra for select space propulsion structural components: Probabilistic load model development p 110 N85-27954
Nonlinear damage analysis: Postulate and evaluation [NASA-CR-168171] p 118 N86-26652
- Bell Aerospace Co., Buffalo, N. Y.**
Flutter analysis of advanced turbopropellers p 73 A84-36492
- Boeing Vertol Co., Philadelphia, Pa.**
On the automatic generation of FEM models for complex gears - A work-in-progress report p 47 A82-48243

C

Carborundum Co., Niagara Falls, N. Y.

Comparison of NDE techniques for sintered-SiC components p 51 A83-22265

Carnegie-Mellon Univ., Pittsburgh, Pa.

Effects of friction dampers on aerodynamically unstable rotor stages

[AIAA PAPER 83-0848] p 1 A83-32791

Model development and statistical investigation of turbine blade mistuning p 2 A84-31905

The interaction between mistuning and friction in the forced response of bladed disk assemblies

[ASME PAPER 84-GT-139] p 73 A84-45957

Effects of friction dampers on aerodynamically unstable rotor stages p 3 A85-21866

Stability of limit cycles in frictionally damped and aerodynamically unstable rotor stages p 4 A86-19198

The effect of limiting aerodynamic and structural coupling in models of mistuned bladed disk vibration p 5 A86-26905

Influence of friction dampers on torsional blade flutter [ASME PAPER 85-GT-170] p 5 A86-32957

Case Western Reserve Univ., Cleveland, Ohio.

A quarter-century of progress in the development of correlation and extrapolation methods for creep rupture data p 63 A80-38142

Statistics and thermodynamics of fracture p 75 A85-19433

Finite element analysis of residual stress in plasma-sprayed ceramic p 46 A86-15226

The crack layer approach to toughness characterization in steel p 36 A86-30010

The cyclic stress-strain behavior of a nickel-base superalloy at 650 C p 36 A86-45715

Re-examination of cumulative fatigue damage analysis - An engineering perspective p 85 A87-22128

Fatigue life prediction in bending from axial fatigue information

[NASA-CR-165563] p 91 N82-20564

Crack layer morphology and toughness characterization in steels

[NASA-CR-168154] p 97 N83-27256

Tensile and compressive constitutive response of 316 stainless steel at elevated temperatures p 98 N83-34353

Effect of crack curvature on stress intensity factors for ASTM standard compact tension specimens

[NASA-CR-168280] p 100 N84-11513

Crack layer theory

[NASA-CR-174634] p 103 N84-22980

Mechanical behavior of carbon-carbon composites [NASA-CR-174767] p 28 N84-34575

On stress analysis of a crack-layer

[NASA-CR-174774] p 106 N84-34774

Translational and extensional energy release rates (the J- and M-integrals) for a crack layer in thermoelasticity [NASA-CR-174872] p 107 N85-21685

Fatigue crack layer propagation in silicon-iron [NASA-CR-175115] p 118 N86-25851

Environmental degradation of 316 stainless steel in high temperature low cycle fatigue

[NASA-TM-89931] p 124 N87-24007

Chinese Academy of Sciences, Peking.

Hybrid solid element with a traction-free cylindrical surface p 82 A86-34462

Cincinnati Univ., Ohio.

Metallurgical instabilities during the high temperature low cycle fatigue of nickel-base superalloys p 33 A83-22019

The effect of microstructure on the fatigue behavior of Ni base superalloys p 33 A83-36166

A study of fatigue damage mechanisms in Waspalloy from 25 to 800 C p 34 A85-12098

High temperature low cycle fatigue mechanisms for nickel base and a copper base alloy

[NASA-CR-3543] p 39 N82-26436

Microstructural effects on the room and elevated temperature low cycle fatigue behavior of Waspalloy [NASA-CR-165497] p 93 N82-26702

Mechanisms of deformation and fracture in high temperature low cycle fatigue of Rene 80 and IN 100 [NASA-CR-165498] p 93 N82-26706

On finite element stress analysis of spur gears

[NASA-CR-167938] p 48 N82-29607

Finite element analysis of notch behavior using a state variable constitutive equation p 114 N85-31548

Anisotropic constitutive model for nickel base single crystal alloys: Development and finite element implementation

[NASA-CR-175015] p 117 N86-21952

Cleveland State Univ., Ohio.

An embedding method for the steady Euler equations p 126 A86-30814

Composite sandwich thermostructural behavior - Computational simulation

[AIAA PAPER 86-0948] p 82 A86-38842

Reliability of void detection in structural ceramics by use of scanning laser acoustic microscopy

p 52 A86-39027

Correlation of processing and sintering variables with the strength and radiography of silicon nitride

p 46 A87-12938

Probability of detection of internal voids in structural ceramics using microfocus radiography

p 52 A87-14300

Quantitative void characterization in structural ceramics by use of scanning laser acoustic microscopy

p 53 A87-51974

The effect of stress on ultrasonic pulses in fiber reinforced composites

[NASA-CR-3724] p 56 N83-33180

Preliminary investigation of an electrical network model for ultrasonic scattering

[NASA-CR-3770] p 57 N84-17606

Compliance matrices for cracked bodies

[NASA-CR-179478] p 120 N86-30236

Connecticut Univ., Storrs.

Fracture mechanics applied to nonisothermal fatigue crack growth p 36 A86-28951

Elevated temperature biaxial fatigue

[NASA-CR-173473] p 103 N84-21905

Elevated temperature biaxial fatigue

[NASA-CR-175795] p 110 N85-27263

D

Dayton Univ., Ohio.

A preliminary study of crack initiation and growth at stress concentration sites

[NASA-CR-169358] p 94 N82-33738

A total life prediction model for stress concentration sites

[NASA-CR-168225] p 100 N84-10612

Delaware Univ., Newark.

Stability of large horizontal-axis axisymmetric wind turbines

p 64 A81-22526

Deutsche Forschungs- und Versuchsanstalt fuer Luft- und Raumfahrt, Cologne (West Germany).

Compliance and stress intensity coefficients for short bar specimens with chevron notches p 64 A80-46032

Performance of Chevron-notch short bar specimen in determining the fracture toughness of silicon nitride and aluminum oxide p 45 A80-50696

Development of plane strain fracture toughness test for ceramics using Chevron notched specimens

p 46 A84-11676

Drexel Univ., Philadelphia, Pa.

Use of static indentation laws in the impact analysis of laminated composite plates p 18 A85-29133

Duke Univ., Durham, N. C.

Frequency domain solutions to multi-degree-of-freedom, dry friction damped systems under periodic excitation

p 83 A86-39485

G

Garrett Turbine Engine Co., Phoenix, Ariz.

Creep-rupture reliability analysis p 79 A85-42566

General Dynamics/Convair, San Diego, Calif.

Effect of low temperature on fatigue and fracture properties of Ti-5Al-2.5Sn(ELI) for use in engine components p 35 A85-47972

General Electric Co., Cincinnati, Ohio.

Requirements of constitutive models for two nickel-base superalloys p 33 A83-21071

Turbine blade nonlinear structural and life analysis

p 1 A83-29024

Blade loss transient dynamic analysis of turbomachinery p 2 A83-40864

Considerations for damage analysis of gas turbine hot section components

[ASME PAPER 84-PVP-77] p 2 A85-18792

Unified constitutive material models for nonlinear finite-element structural analysis

[AIAA PAPER 85-1418] p 77 A85-39769

The dynamics of a flexible bladed disc on a flexible rotor in a two-rotor system p 4 A86-25743

A computer analysis program for interfacing thermal and structural codes p 126 A86-36861

Benchmark notch test for life prediction

[NASA-CR-165571] p 95 N83-12451

Blade loss transient dynamics analysis with flexible bladed disk

[NASA-CR-168176] p 7 N84-13193

Aerothral modeling. Executive summary

[NASA-CR-168330] p 7 N84-15152

Component-specific modeling

[NASA-CR-174765] p 110 N85-27261

Component-specific modeling

[NASA-CR-174925] p 12 N85-32119

A review of path-independent integrals in elastic-plastic fracture mechanics, task 4

[NASA-CR-174956] p 114 N85-33541

Component-specific modeling

[NASA-CR-174765] p 12 N85-34140

Component-specific modeling

p 12 N86-11515

Burner liner thermal-structural load modeling

[NASA-CR-174892] p 117 N86-21932

General Motors Research Labs., Warren, Mich.

Development and testing of stable, invariant, isoparametric curvilinear 2- and 3-D hybrid-stress elements

p 75 A85-19899

General Tire and Rubber Co., Akron, Ohio.

High temperature thermomechanical analysis of ceramic coatings

p 74 A84-48565

Inelastic high-temperature thermomechanical response of ceramic coated gas turbine seals

p 82 A86-37799

George Washington Univ., Washington, D.C.

Statistical aspects of carbon fiber risk assessment modeling

[NASA-CR-159318] p 23 N80-29432

Georgia Inst. of Tech., Atlanta.

Path-independent integrals in finite elasticity and inelasticity, with body forces, inertia, and arbitrary crack-face conditions

p 65 A82-32303

On a study of the $\Delta T/c$ and $C/\text{asterisk}/$ integrals for fracture analysis under non-steady creep

p 65 A82-36782

Moving singularity creep crack growth analysis with the $\Delta T/c$ and $C/\text{asterisk}/$ integrals

p 66 A82-40066

Inelastic stress analyses at finite deformation through complementary energy approaches

p 71 A84-13248

Analyses of large quasistatic deformations of inelastic bodies by a new hybrid-stress finite element algorithm

p 71 A84-16874

Analyses of large quasistatic deformations of inelastic bodies by a new hybrid-stress finite element algorithm - Applications

p 71 A84-16884

A study of fatigue damage mechanisms in Waspalloy from 25 to 800 C

p 34 A85-12098

Hybrid stress finite elements for large deformations of inelastic solids

p 74 A85-15894

Development and testing of stable, invariant, isoparametric curvilinear 2- and 3-D hybrid-stress elements

p 75 A85-19899

The effect of microstructure, temperature, and hold-time on low-cycle fatigue of As HIP P/M Rene 95

p 35 A85-32399

On the existence and stability conditions for mixed-hybrid finite element solutions based on Reissner's variational principle

p 77 A85-33847

Thermodynamically consistent constitutive equations for nonisothermal large strain, elasto-plastic, creep behavior

[AIAA PAPER 85-0621] p 77 A85-38425

Constitutive modeling and computational implementation for finite strain plasticity

p 78 A85-40910

Existence and stability, and discrete BB and rank conditions, for general mixed-hybrid finite elements in elasticity

p 82 A86-34464

Bounding solutions of geometrically nonlinear viscoelastic problems

[AIAA PAPER 86-0943] p 82 A86-38838

On the equivalence of the incremental harmonic balance method and the harmonic balance-Newton Raphson method

- Analysis of large, non-isothermal elastic-visco-plastic deformations
[NASA-CR-176220] p 115 N86-10588
- Yielding and deformation behavior of the single crystal nickel-base superalloy PWA 1480
[NASA-CR-175100] p 44 N86-25455
- Formulation of the nonlinear analysis of shell-like structures, subjected to time-dependent mechanical and thermal loading
[NASA-CR-177194] p 119 N86-28462
- Goodrich (B. F.) Co., Akron, Ohio.**
Pantographing self adaptive gap elements
p 77 A85-37440

H

- Hamilton Standard, Windsor Locks, Conn.**
Diffusion bonded boron/aluminum spar-shell fan blade
[NASA-CR-159571] p 23 N80-25382
- Harris Corp., Melbourne, Fla.**
Thermal expansion behavior of graphite/glass and graphite/magnesium
p 21 A87-38615

I

- IIT Research Inst., Chicago, Ill.**
Thermal fatigue and oxidation data for directionally solidified MAR-M 246 turbine blades
[NASA-CR-159798] p 6 N80-21330
- Thermal fatigue and oxidation data of oxide dispersion-strengthened alloys
[NASA-CR-159842] p 37 N80-25415
- Thermal fatigue and oxidation data of TAZ-8A and M22 alloys and variations
[NASA-CR-165407] p 38 N82-10193
- Illinois Univ., Urbana.**
Interface cracks in adhesively bonded lap-shear joints
p 67 A82-46109
- Boundary-layer effects in composite laminates. I - Free-edge stress singularities. II - Free-edge stress solutions and basic characteristics
p 67 A82-46806
- Extending the laser-specklegram technique to strain analysis of rotating components
p 67 A83-12514
- Elasticity solutions for a class of composite laminate problems with stress singularities
p 17 A84-33389
- Three-dimensional hybrid-stress finite element analysis of composite laminates with cracks and cutouts
p 80 A86-26896
- Nondestructive evaluation of adhesive bond strength using the stress wave factor technique
p 53 A87-32200

- Illinois Univ., Urbana-Champaign.**
Boundary layer thermal stresses in angle-ply composite laminates, part 1
[NASA-CR-165412] p 93 N82-26713
- Analysis of cracks emanating from a circular hole in unidirectional fiber reinforced composites, part 2
[NASA-CR-165433] p 93 N82-26714
- Interlaminar crack growth in fiber reinforced composites during fatigue, part 3
[NASA-CR-165434] p 93 N82-26715
- Analysis of interface cracks in adhesively bonded lap shear joints, part 4
[NASA-CR-165438] p 93 N82-26716
- Edge delamination in angle-ply composite laminates, part 5
[NASA-CR-165439] p 94 N82-26717
- Boundary-layer effects in composite laminates: Free-edge stress singularities, part 6
[NASA-CR-165440] p 94 N82-26718
- Indian Inst. of Science, Bangalore.**
A higher order theory of laminated composite cylindrical shells
p 86 A87-35656
- Indian Inst. of Tech., Bombay.**
Low cycle fatigue behavior of aluminum/stainless steel composites
[AIAA 83-0806] p 16 A83-29886
- Indian Inst. of Tech., Madras.**
Natural frequencies of twisted rotating plates
p 76 A85-32343
- International Business Machines Corp., Bangkok (Thailand).**
Algorithms for elasto-plastic-creep postbuckling
p 73 A84-38480
- Iowa Univ., Iowa City.**
The finite analytic method, volume 3
[NASA-CR-170186] p 127 N83-23087
- The finite analytic method, volume 4
[NASA-CR-170187] p 127 N83-23088
- The finite analytic method, volume 5
[NASA-CR-170188] p 127 N83-23089

K

- Kansas Univ., Lawrence.**
Theoretical and software considerations for nonlinear dynamic analysis
[NASA-CR-174504] p 101 N84-15589
- Karlsruhe Univ. (West Germany).**
Fracture toughness of brittle materials determined with chevron notch specimens
p 45 A81-32545
- Extended range stress intensity factor expressions for chevron-notched short bar and short rod fracture toughness specimens
p 66 A82-40357
- Kent State Univ., Ohio.**
Automatic finite element generators
p 105 N84-31695
- Kernforschungszentrum, Karlsruhe (West Germany).**
Fracture toughness of brittle materials determined with chevron notch specimens
p 45 A81-32545

L

- Lehigh Univ., Bethlehem, Pa.**
Moving cracks in layered composites
p 67 A83-12048
- Analysis of an axial compressor blade vibration based on wave reflection theory
[ASME PAPER 83-GT-151] p 2 A83-47970
- Sudden stretching of a four layered composite plate
[NASA-CR-159870] p 23 N80-25383
- Sudden bending of cracked laminates
[NASA-CR-159860] p 23 N80-25384
- Lincoln Univ., Pa.**
Dynamic modulus and damping of boron, silicon carbide, and alumina fibers
p 15 A80-44236
- Lockheed-California Co., Burbank.**
Effect of low temperature on fatigue and fracture properties of Ti-5Al-2.5Sn(ELI) for use in engine components
p 35 A85-47972
- Lockheed Engineering and Management Services Co., Inc., Houston, Tex.**
Numerical synthesis of tri-variate velocity realizations of turbulence
p 81 A86-28654
- Louisiana State Univ., Baton Rouge.**
Benchmark cyclic plastic notch strain measurements
p 33 A84-11194
- Benchmark notch test for life prediction
[NASA-CR-165571] p 95 N83-12451

M

- MARC Analysis Research Corp., Palo Alto, Calif.**
Efficient algorithms for use in probabilistic finite element analysis
p 81 A86-28655
- Iterative methods for mixed finite element equations
p 82 A86-34461
- Probabilistic finite element development
p 111 N85-27956
- Martin Marietta Aerospace, Denver, Colo.**
Fiberglass epoxy laminate fatigue properties at 300 and 20 K
p 19 A85-47970
- Massachusetts Inst. of Tech., Cambridge.**
A new formulation of hybrid/mixed finite element
p 67 A83-12739
- Alternative ways for formulation of hybrid stress elements
p 68 A83-14710
- Flutter and forced response of mistuned rotors using standing wave analysis
[AIAA 83-0845] p 69 A83-29823
- Some analysis methods for rotating systems with periodic coefficients
p 69 A83-32987
- On the suppression of zero energy deformation modes
p 72 A84-21541
- Stagger angle dependence of inertial and elastic coupling in bladed disks
p 72 A84-31903
- Rational approach for assumed stress finite elements
p 74 A85-12029
- Flutter and forced response of mistuned rotors using standing wave analysis
p 74 A85-12721
- Hybrid Semiloof elements for plates and shells based upon a modified Hu-Washizu principle
p 74 A85-15893
- Evolution of assumed stress hybrid finite element
p 77 A85-35046
- Axisymmetric solid elements by a rational hybrid stress method
p 78 A85-41109
- Finite elements based on consistently assumed stresses and displacements
p 79 A86-18123
- Thermal-mechanical fatigue crack growth in Inconel X-750
p 35 A86-20982
- Aeroelastic formulations for turbomachines and propellers
p 4 A86-24677
- Hybrid solid element with a traction-free cylindrical surface
p 82 A86-34462

- Analytical and experimental investigation of the coupled bladed disk/shaft whirl of a cantilevered turbofan
[ASME PAPER 86-GT-98] p 6 A86-48163
- Instructions for the use of the CIVM-Jet 4C finite-strain computer code to calculate the transient structural responses of partial and/or complete arbitrarily-curved rings subjected to fragment impact
[NASA-CR-159873] p 88 N80-27720
- Finite-strain large-deflection elastic-viscoplastic finite-element transient response analysis of structures
[NASA-CR-159874] p 88 N80-29762
- Ultrasonic input-output for transmitting and receiving longitudinal transducers coupled to same face of isotropic elastic plate
[NASA-CR-3506] p 54 N82-18613
- Effects of specimen resonances on acoustic-ultrasonic testing
[NASA-CR-3679] p 55 N83-21373
- Ultrasonic attenuation of a void-containing medium for very long wavelengths
[NASA-CR-3693] p 56 N83-28466
- Time-independent anisotropic plastic behavior by mechanical subelement models
p 99 N83-34369
- Input-output characterization of an ultrasonic testing system by digital signal analysis
[NASA-CR-3756] p 56 N84-15565
- Flutter and forced response of mistuned rotors using standing wave analysis
[NASA-CR-173555] p 9 N84-24586
- New variational formulations of hybrid stress elements
p 105 N84-31690
- Thermal-mechanical fatigue crack growth in Inconel X-750
[NASA-CR-174740] p 41 N85-15877
- Stress waves in an isotropic elastic plate excited by a circular transducer
[NASA-CR-3877] p 58 N85-20390
- Advanced stress analysis methods applicable to turbine engine structures
[NASA-CR-175573] p 11 N85-21165
- Application of homomorphic signal processing to stress wave factor analysis
[NAS 1.26:174871] p 58 N85-21673
- Recent advances in hybrid/mixed finite elements
[NASA-CR-175574] p 107 N85-21687
- Structural response of a rotating bladed disk to rotor whirl
[NASA-CR-175605] p 11 N85-22391
- On Hybrid and mixed finite element methods
[NASA-CR-175551] p 108 N85-23096
- Ultrasonic testing of plates containing edge cracks
[NASA-CR-3904] p 58 N85-29307
- Thermal-mechanical fatigue behavior of nickel-base superalloys
[NASA-CR-175048] p 43 N86-24818
- Stress waves in transversely isotropic media: The homogeneous problem
[NASA-CR-3977] p 59 N86-25002
- Wave propagation in anisotropic medium due to an oscillatory point source with application to unidirectional composites
[NASA-CR-4001] p 60 N86-27666
- Materials Research Lab., Inc., Glenwood, Ill.**
Fracture of composite-adhesive-composite systems
p 76 A85-27935
- Max-Planck-Inst. fuer Metallforschung, Stuttgart (West Germany).**
A study of fatigue damage mechanisms in Waspaloy from 25 to 800 C
p 34 A85-12098
- McGraw-Edison Co., Buffalo, N.Y.**
Fracture mechanics applied to nonisothermal fatigue crack growth
p 36 A86-28951
- Mechanical Technology, Inc., Latham, N.Y.**
Development of procedures for calculating stiffness and damping of elastomers in engineering applications, part 6
[NASA-CR-159838] p 87 N80-22733
- Michigan State Univ., East Lansing.**
Experimental verification of the Neuber relation at room and elevated temperatures
[NASA-CR-167967] p 96 N83-19121
- Experimental verification of the number relation at room and elevated temperatures
p 98 N83-34355
- A comparison of smooth specimen and analytical simulation techniques for notched members at elevated temperatures
p 114 N85-31546
- Experimental evaluation criteria for constitutive models of time dependent cyclic plasticity
[NASA-CR-176821] p 117 N86-25850

N

- National Aeronautics and Space Administration.**
Langley Research Center, Hampton, Va.
Buckling of rotating beams
p 63 A80-20149

- Thermal expansion behavior of graphite/glass and graphite/magnesium p 21 A87-38615
- National Aeronautics and Space Administration. Lewis Research Center, Cleveland, Ohio.**
- Fatigue behavior of SiC reinforced titanium composites p 13 A80-10036
- Simple spline-function equations for fracture mechanics calculations p 63 A80-10832
- Buckling of rotating beams p 63 A80-20149
- Mechanical property characterization of intraply hybrid composites p 13 A80-20954
- Strainrange partitioning life predictions of the long time Metal Properties Council creep-fatigue tests p 63 A80-27958
- Dynamic response of damaged angleplied fiber composites p 14 A80-27982
- Micromechanics of intraply hybrid composites: Elastic and thermal properties p 14 A80-27994
- Prediction of fiber composite mechanical behavior made simple p 63 A80-32067
- Fracture modes of high modulus graphite/epoxy angleplied laminates subjected to off-axis tensile loads p 14 A80-32069
- A review of issues and strategies in nondestructive evaluation of fiber reinforced structural composites p 14 A80-34764
- Engine environmental effects on composite behavior [AIAA 80-0695] p 1 A80-35101
- Predicting the time-temperature dependent axial failure of B/AI composites p 14 A80-35494
- Effects of fine porosity on the fatigue behavior of a powder metallurgy superalloy p 32 A80-35495
- Status of NASA full-scale engine aeroelasticity research p 63 A80-35906
- A quarter-century of progress in the development of correlation and extrapolation methods for creep rupture data p 63 A80-38142
- Quantitative ultrasonic evaluation of engineering properties in metals, composites, and ceramics p 50 A80-39641
- Fracture toughness determination of Al₂O₃ using four-point-bend specimens with straight-through and chevron notches p 45 A80-42085
- Dynamic modulus and damping of boron, silicon carbide, and alumina fibers p 15 A80-44236
- Vibration and buckling of rectangular plates under in-plane hydrostatic loading p 64 A80-45364
- Compliance and stress intensity coefficients for short bar specimens with chevron notches p 64 A80-46032
- Performance of Chevron-notch short bar specimen in determining the fracture toughness of silicon nitride and aluminum oxide p 45 A80-50696
- Concepts and techniques for ultrasonic evaluation of material mechanical properties p 50 A80-51575
- Cyclic behavior of turbine disk alloys at 650 C p 32 A81-12266
- On the equivalence between semiempirical fracture analyses and R-curves p 64 A81-18792
- Ultrasonic measurement of material properties p 50 A81-19656
- Stability of large horizontal-axis axisymmetric wind turbines p 64 A81-22526
- Effects of mistuning on blade torsional flutter p 64 A81-29095
- Nonlinear laminate analysis for metal matrix fiber composites [AIAA 81-0579] p 15 A81-29411
- Effects of mistuning on bending-torsion flutter and response of a cascade in incompressible flow [AIAA 81-0602] p 65 A81-29465
- Superhybrid composite blade impact studies [ASME PAPER 81-GT-24] p 1 A81-29940
- Fracture toughness of brittle materials determined with chevron notch specimens p 45 A81-32545
- Self-acting geometry for noncontact seals [ASLE PREPRINT 81-AM-5B-2] p 47 A81-33867
- Acousto-ultrasonic characterization of fiber reinforced composites p 50 A81-44660
- Computer code for intraply hybrid composite design p 15 A81-44662
- Comparative thermal fatigue resistance of several oxide dispersion strengthened alloys p 32 A82-11399
- Sensitivity analysis results of the effects of various parameters on composite design p 15 A82-37101
- Impact resistance of fiber composites p 66 A82-39852
- Extended range stress intensity factor expressions for chevron-notched short bar and short rod fracture toughness specimens p 66 A82-40357
- Crack displacements for J/I testing with compact specimens p 66 A82-40358
- Fatigue and creep-fatigue deformation of several nickel-base superalloys at 650 C p 32 A82-47398
- Tensile buckling of advanced turboprops [AIAA PAPER 82-0776] p 67 A83-10900
- Fatigue behavior of SiC reinforced Ti/6Al-4V/ at 650 C p 15 A83-12414
- Nonlinear structural and life analyses of a combustor liner p 68 A83-12764
- Turbine blade nonlinear structural and life analysis p 1 A83-29024
- Resin selection criteria for tough composite structures [AIAA 83-0801] p 46 A83-29734
- Structural tailoring of engine blades (STAEBL) [AIAA 83-0828] p 1 A83-29737
- The coupled aeroelastic response of turbomachinery blading to aerodynamic excitations [AIAA 83-0844] p 69 A83-29822
- Low cycle fatigue behavior of aluminum/stainless steel composites [AIAA 83-0806] p 16 A83-29886
- Metal honeycomb to porous wireform substrate diffusion bond evaluation p 51 A83-39620
- Fatigue crack initiation and propagation in several nickel-base superalloys at 650 C p 33 A83-41199
- Design concepts for low cost composite engine frames [AIAA PAPER 83-2445] p 2 A83-48331
- Tensile buckling of advanced turboprops p 71 A84-11039
- Development of plane strain fracture toughness test for ceramics using Chevron notched specimens p 46 A84-11676
- The effect of microstructure on 650 C fatigue crack growth in P/M Astroloy p 33 A84-12395
- Prediction of composite hygral behavior made simple p 16 A84-14285
- High-temperature fatigue in metals - A brief review of life prediction methods developed at the Lewis Research Center of NASA p 33 A84-14286
- Environmental and high strain rate effects on composites for engine applications p 16 A84-17444
- Failure analysis of a tool steel torque shaft p 51 A84-17546
- Analysis of an internally radially cracked ring segment subject to three-point radial loading p 71 A84-18691
- Simplified analytical procedures for representing material cyclic response p 2 A84-22877
- The coupled response of turbomachinery blading to aerodynamic excitations p 2 A84-26959
- Durability/life of fiber composites in hygrothermomechanical environments p 16 A84-27359
- Compressive behavior of unidirectional fibrous composites p 16 A84-29894
- The structural response of a rail acceleration p 72 A84-32039
- Effects of structural coupling on mistuned cascade flutter and response [ASME PAPER 83-GT-117] p 73 A84-33701
- Measurements of self-excited rotor-blade vibrations using optical displacements [ASME PAPER 83-GT-132] p 73 A84-33702
- Simplified composite micromechanics equations for strength, fracture toughness and environmental effects p 17 A84-41858
- Vibrations of twisted cantilevered plates - Experimental investigation [ASME PAPER 84-GT-96] p 73 A84-46937
- Acoustic emission evaluation of plasma-sprayed thermal barrier coatings [ASME PAPER 84-GT-292] p 48 A84-47046
- High temperature thermomechanical analysis of ceramic coatings p 74 A84-48565
- Effects of processing and microstructure on the fatigue behaviour of the nickel-base superalloy Rene95 p 34 A84-48715
- Simplified composite micromechanics equations of hygral, thermal, and mechanical properties p 17 A84-49377
- Strainrange partitioning - A total strain range version p 34 A85-11603
- Flutter of turbofan rotors with mistuned blades p 74 A85-12716
- Hygrothermomechanical evaluation of transverse filament tape epoxy/polyester fiberglass composites p 17 A85-15632
- Design procedures for fiber composite structural components - Rods, beams, and beam columns p 17 A85-15636
- Select fiber composites for space applications - A mechanistic assessment p 18 A85-16040
- ICAN - Integrated composites analyzer [AIAA PAPER 84-0974] p 18 A85-16094
- Vibration and flutter of mistuned bladed-disk assemblies [AIAA PAPER 84-0991] p 75 A85-16095
- Interply layer degradation effects on composite structural response [AIAA PAPER 84-0849] p 18 A85-16096
- Effects of warping and pretwist on torsional vibration of rotating beams [ASME PAPER 84-WA/APM-41] p 75 A85-17040
- Vibrations of twisted cantilevered plates - Summary of previous and current studies p 76 A85-22069
- A simplified method for elastic-plastic-creep structural analysis [ASME PAPER 84-GT-191] p 76 A85-23150
- Fracture toughness of hot-pressed beryllium p 34 A85-25835
- Finite element engine blade structural optimization [AIAA PAPER 85-0645] p 76 A85-30313
- The effect of aerodynamic and structural detuning on turbomachine supersonic unstalled torsional flutter [AIAA PAPER 85-0761] p 3 A85-30378
- Natural frequencies of twisted rotating plates p 76 A85-32343
- On the fatigue crack propagation behavior of superalloys at intermediate temperatures p 35 A85-32434
- Flutter of swept fan blades [ASME PAPER 84-GT-138] p 77 A85-32962
- Unified constitutive material models for nonlinear finite-element structural analysis [AIAA PAPER 85-1418] p 77 A85-39769
- On local total strain redistribution using a simplified cyclic inelastic analysis based on an elastic solution [AIAA PAPER 85-1419] p 78 A85-39770
- Fatigue criterion to system design, life and reliability [AIAA PAPER 85-1140] p 78 A85-40814
- A study of interply layer effects on the free edge stress field of angleplied laminates p 18 A85-41127
- Finite difference analysis of torsional vibrations of pretwisted, rotating, cantilever beams with effects of warping p 78 A85-42047
- The role of the reflection coefficient in precision measurement of ultrasonic attenuation p 51 A85-42151
- Application of two creep fatigue life models for the prediction of elevated temperature crack initiation of a nickel base alloy [AIAA PAPER 85-1420] p 35 A85-43979
- Vibration and flutter of mistuned bladed-disk assemblies p 3 A85-45854
- Impact resistance of fiber composites - Energy-absorbing mechanisms and environmental effects p 18 A85-46543
- Ten year environmental test of glass fiber/epoxy pressure vessels [AIAA PAPER 85-1198] p 19 A85-47022
- Vibrations of twisted cantilever plates - A comparison of theoretical results p 79 A85-47626
- Structural optimization using optimality criteria methods p 79 A85-48703
- Measurement of ultrasonic velocity using phase-slope and cross-correlation methods p 51 A86-13192
- Vibration analysis of rotating turbomachinery blades by an improved finite difference method p 3 A86-14338
- DEAN - A program for Dynamic Engine Analysis [AIAA PAPER 85-1354] p 3 A86-14430
- Finite element analysis of residual stress in plasma-sprayed ceramic p 46 A86-15226
- Longitudinal compressive failure modes in fiber composites End attachment effects on IITRI type test specimens p 19 A86-19999
- Wide-range displacement expressions for standard fracture mechanics specimens p 79 A86-20706
- Wide-range weight functions for the strip with a single edge crack p 79 A86-20709
- Analysis of an externally radially crack ring segment subject to three-point radial loading p 79 A86-20710
- NASA Lewis Research Center/university graduate research program on engine structures [ASME PAPER 85-GT-159] p 80 A86-22084
- The effects of strong shock loading on coupled bending-torsion flutter of tuned and mistuned cascades p 4 A86-26893
- Vibrations of blades and bladed disk assemblies; Proceedings of the Tenth Biennial Conference on Mechanical Vibration and Noise, Cincinnati, OH, September 10-13, 1985 p 4 A86-26901
- Forced response analysis of an aerodynamically detuned supersonic turbomachine rotor p 5 A86-26902
- Vibration and buckling of rotating, pretwisted, precone beams including Coriolis effects p 80 A86-26910
- Designing for fiber composite structural durability in hygrothermomechanical environments p 19 A86-27734
- Aerodynamic and structural detuning of supersonic turbomachine rotors p 5 A86-31595
- Radiographic detectability limits for seeded voids in sintered silicon carbide and silicon nitride p 51 A86-31745
- Dynamic characteristics of an assembly of prop-fan blades [ASME PAPER 85-GT-134] p 5 A86-32956

- Influence of friction dampers on torsional blade flutter
[ASME PAPER 85-GT-170] p 5 A86-32957
- NDE of advanced ceramics p 52 A86-35575
- The tensile and fatigue deformation structures in a single crystal Ni-base superalloy p 36 A86-35697
- Progressive fracture of fiber composites p 19 A86-35809
- A computer analysis program for interfacing thermal and structural codes p 126 A86-36861
- Nondestructive characterization of structural ceramics p 46 A86-37141
- Inelastic high-temperature thermomechanical response of ceramic coated gas turbine seals p 82 A86-37799
- Composite sandwich thermostructural behavior - Computational simulation p 82 A86-38842
- [AIAA PAPER 86-0948] p 82 A86-38842
- Computer aided derivation of equations for composite mechanics problems and finite element analyses [AIAA PAPER 86-1016] p 83 A86-38873
- Reliability of void detection in structural ceramics by use of scanning laser acoustic microscopy p 52 A86-39027
- Computational composite mechanics for aerospace propulsion structures [AIAA PAPER 86-1190] p 19 A86-40596
- Dynamic stress analysis of smooth and notched fiber composite flexural specimens p 20 A86-41070
- Mode II fatigue crack growth specimen development p 83 A86-43566
- Quantitative flaw characterization with scanning laser acoustic microscopy p 52 A86-45150
- The cyclic stress-strain behavior of a nickel-base superalloy at 650 C p 36 A86-45715
- Computational engine structural analysis [ASME PAPER 86-GT-70] p 5 A86-48141
- Nondestructive techniques for characterizing mechanical properties of structural materials - An overview p 52 A86-48143
- [ASME PAPER 86-GT-75] p 52 A86-48143
- Toward improved durability in advanced combustors and turbines - Progress in prediction of thermomechanical loads [ASME PAPER 86-GT-172] p 6 A86-48224
- Mass balancing of hollow fan blades [ASME PAPER 86-GT-195] p 84 A86-48245
- NDE of structural ceramics [ASME PAPER 86-GT-279] p 52 A86-48298
- A study of spectrum fatigue crack propagation in two aluminum alloys. I - Spectrum simplification. II - Influence of microstructures p 36 A86-48973
- Unified constitutive materials model development and evaluation for high-temperature structural analysis applications p 84 A86-49133
- The plastic compressibility of 7075-T651 aluminum-alloy plate p 36 A86-49690
- Orientation and temperature dependence of some mechanical properties of the single-crystal nickel-base superalloy Rene N4. II - Low cycle fatigue behavior p 37 A86-50322
- Correlation of processing and sintering variables with the strength and radiography of silicon nitride p 46 A87-12938
- Probability of detection of internal voids in structural ceramics using microfocus radiography p 52 A87-14300
- Factors that affect the fatigue strength of power transmission shafting and their impact on design p 48 A87-14656
- Elastic analysis of a mode II fatigue crack test specimen p 84 A87-17799
- SCARE - A postprocessor program to MSC/NASTRAN for reliability analysis of structural ceramic components [ASME PAPER 86-GT-34] p 84 A87-17988
- Assessment of simplified composite micromechanics using three-dimensional finite-element analysis p 20 A87-19121
- Fabrication and quality assurance processes for superhybrid composite fan blades p 20 A87-19123
- Simplified composite micromechanics for predicting microstresses p 20 A87-20090
- Re-examination of cumulative fatigue damage analysis - An engineering perspective p 85 A87-22128
- The effect of circumferential aerodynamic detuning on coupled bending-torsion unstalled supersonic flutter [ASME PAPER 86-GT-100] p 6 A87-25396
- Design concepts/parameters assessment and sensitivity analyses of select composite structural components p 85 A87-25407
- Fracture toughness of Si3N4 measured with short bar chevron-notched specimens p 46 A87-30621
- Nondestructive evaluation of adhesive bond strength using the stress wave factor technique p 53 A87-32200
- Probabilistic structural analysis to quantify uncertainties associated with turbopump blades [AIAA PAPER 87-0766] p 85 A87-33581
- Optimization and analysis of gas turbine engine blades [AIAA PAPER 87-0827] p 126 A87-33614
- Advances in 3-D Inelastic Analysis Methods for hot section components [AIAA PAPER 87-0719] p 85 A87-33645
- Structural tailoring of advanced turboprops [AIAA PAPER 87-0753] p 85 A87-33648
- A technique for the prediction of airfoil flutter characteristics in separated flow [AIAA PAPER 87-0910] p 86 A87-33719
- Approximations to eigenvalues of modified general matrices [AIAA PAPER 87-0947] p 86 A87-33756
- A higher order theory of laminated composite cylindrical shells p 86 A87-35656
- Effect of interference fits on roller bearing fatigue life p 48 A87-37686
- Composite space antenna structures - Properties and environmental effects p 20 A87-38610
- Thermal expansion behavior of graphite/glass and graphite/magnesium p 21 A87-38615
- Nonlinear vibration and stability of rotating, pretwisted, precone blades including Coriolis effects p 86 A87-39896
- Analytical and experimental investigation of mistuning in propfan flutter [AIAA PAPER 87-0739] p 86 A87-40496
- Analytical flutter investigation of a composite propfan model [AIAA PAPER 87-0738] p 87 A87-40497
- Influence of third-degree geometric nonlinearities on the vibration and stability of pretwisted, precone, rotating blades p 6 A87-46228
- NDE reliability and process control for structural ceramics [ASME PAPER 87-GT-8] p 53 A87-48702
- Simplified composite micromechanics for predicting microstresses p 87 A87-49275
- Quantitative void characterization in structural ceramics by use of scanning laser acoustic microscopy p 53 A87-51974
- Results of an interlaboratory fatigue test program conducted on alloy 800H at room and elevated temperatures p 37 A87-54370
- Micromechanics of intraply hybrid composites: Elastic and thermal properties [NASA-TM-79253] p 21 N80-11143
- Tensile and flexural strength of non-graphitic superhybrid composites: Predictions and comparisons [NASA-TM-79276] p 21 N80-11144
- Dynamic response of damaged angleplied fiber composites [NASA-TM-79281] p 21 N80-11145
- Mechanical property characterization of intraply hybrid composites [NASA-TM-79306] p 21 N80-12120
- Comparison tests and experimental compliance calibration of the proposed standard round compact plane strain fracture toughness specimen [NASA-TM-81379] p 87 N80-13513
- Photovoltaic power system reliability considerations [NASA-TM-79291] p 53 N80-15422
- A relation between semiempirical fracture analyses and R-curves [NASA-TP-1600] p 87 N80-15428
- Fracture modes of high modulus graphite/epoxy angleplied laminates subjected to off-axis tensile loads [NASA-TM-81405] p 21 N80-16102
- Prediction of fiber composite mechanical behavior made simple [NASA-TM-81404] p 22 N80-16107
- Application of composite materials to turbofan engine fan exit guide vanes [NASA-TM-81432] p 22 N80-18106
- Dynamic modulus and damping of boron, silicon carbide, and alumina fibers [NASA-TM-81422] p 22 N80-20313
- Calculation of residual principal stresses in CVD boron on carbon filaments [NASA-TM-81456] p 22 N80-20314
- Predicting the time-temperature dependent axial failure of B/A1 composites [NASA-TM-81474] p 22 N80-21452
- Effects of fine porosity on the fatigue behavior of a powder metallurgy superalloy [NASA-TM-81448] p 37 N80-21493
- Simulation of transducer-couplant effects on broadband ultrasonic signals [NASA-TM-81489] p 53 N80-22714
- Nonlinear, three-dimensional finite-element analysis of air-cooled gas turbine blades [NASA-TP-1669] p 88 N80-22734
- Engine environmental effects on composite behavior [NASA-TM-81508] p 22 N80-23370
- Status of NASA full-scale engine aeroelasticity research [NASA-TM-81500] p 88 N80-23678
- Practical implementation of the double linear damage rule and damage curve approach for treating cumulative fatigue damage [NASA-TM-81517] p 88 N80-23684
- Concepts and techniques for ultrasonic evaluation of material mechanical properties [NASA-TM-81523] p 53 N80-24634
- Three dimensional finite-element elastic analysis of a thermally cycled double-edge wedge geometry specimen [NASA-TM-80980] p 37 N80-26433
- Quantitative ultrasonic evaluation of engineering properties in metals, composites and ceramics [NASA-TM-81530] p 54 N80-26682
- Comparison of elastic and elastic-plastic structural analyses for cooled turbine blade airfoils [NASA-TP-1679] p 88 N80-27719
- Fracture toughness of brittle materials determined with chevron notch specimens [NASA-TM-81607] p 38 N80-32486
- The method of lines in three dimensional fracture mechanics [NASA-TM-81593] p 89 N80-32753
- Superhybrid composite blade impact studies [NASA-TM-81597] p 89 N81-11412
- Method for estimating crack-extension resistance curve from residual strength data [NASA-TP-1753] p 89 N81-11417
- Laminates and reinforced metals [NASA-TM-81591] p 23 N81-12171
- Stability of large horizontal-axis axisymmetric wind turbines [NASA-TM-81623] p 89 N81-12446
- Prediction of composite thermal behavior made simple [NASA-TM-81618] p 23 N81-16132
- Experimental compliance calibration of the compact fracture toughness specimen [NASA-TM-81665] p 89 N81-16492
- Effects of mistuning on bending-torsion flutter and response of a cascade in incompressible flow [NASA-TM-81674] p 89 N81-16494
- Method for alleviating thermal stress damage in laminates [NASA-CASE-LEW-12493-1] p 23 N81-17170
- Composite containment systems for jet engine fan blades [NASA-TM-81675] p 90 N81-17480
- Ion beam sputter etching of orthopedic implanted alloy MP35N and resulting effects on fatigue [NASA-TM-81747] p 38 N81-21174
- Nonlinear laminate analysis for metal matrix fiber composites [NASA-TM-82596] p 24 N81-25149
- Computer code for intraply hybrid composite design [NASA-TM-82593] p 24 N81-25151
- Method for alleviating thermal stress damage in laminates [NASA-CASE-LEW-12493-2] p 24 N81-26179
- Aeroelastic characteristics of a cascade of mistuned blades in subsonic and supersonic flows [NASA-TM-82631] p 90 N81-26492
- Acousto-ultrasonic characterization of fiber reinforced composites [NASA-TM-82651] p 54 N81-28458
- Reliability and quality assurance on the MOD 2 wind system [NASA-TM-82717] p 54 N81-33492
- Structural dynamics verification facility study [NASA-TM-82675] p 90 N81-33497
- Integrated analysis of engine structures [NASA-TM-82713] p 91 N82-11491
- Elevated temperature fatigue testing of metals p 38 N82-13281
- Durability/life of fiber composites in hygrothermomechanical environments [NASA-TM-82749] p 24 N82-12487
- Ultrasonic velocity for estimating density of structural ceramics [NASA-TM-82765] p 46 N82-14359
- Prediction of composite hygral behavior made simple [NASA-TM-82780] p 24 N82-16181
- Elevated temperature fatigue testing of metals [NASA-TM-82745] p 91 N82-16419
- Metal honeycomb to porous wireform substrate diffusion bond evaluation [NASA-TM-82793] p 54 N82-18612
- Experience with modified aerospace reliability and quality assurance method for wind turbines [NASA-TM-82803] p 54 N82-19550

Interrelation of material microstructure, ultrasonic factors, and fracture toughness of two phase titanium alloy
[NASA-TM-82810] p 54 N82-20551

Elastic-plastic finite-element analyses of thermally cycled single-edge wedge specimens
[NASA-TP-1982] p 91 N82-20565

Elastic-plastic finite-element analyses of thermally cycled double-edge wedge specimens
[NASA-TP-1973] p 92 N82-20566

Tungsten fiber reinforced superalloy composite high temperature component design considerations
[NASA-TM-82811] p 25 N82-21259

Coupled bending-bending-torsion flutter of a mistuned cascade with nonuniform blades
[NASA-TM-82813] p 92 N82-21604

Structural dynamics of shroudless, hollow fan blades with composite in-lays
[NASA-TM-82816] p 7 N82-22266

Compression behavior of unidirectional fibrous composite
[NASA-TM-82833] p 25 N82-22313

Designing with fiber-reinforced plastics (planar random composites)
[NASA-TM-82812] p 25 N82-24300

Nonlinear structural and life analyses of a combustor liner
[NASA-TM-82846] p 92 N82-24501

Evaluation of inelastic constitutive models for nonlinear structural analysis
[NASA-TM-82845] p 92 N82-24502

Bird impact analysis package for turbine engine fan blades
[NASA-TM-82831] p 92 N82-26701

A finite element stress analysis of spur gears including fillet radii and rim thickness effects
[NASA-TM-82865] p 48 N82-28646

Environmental and High-Strain Rate effects on composites for engine applications
[NASA-TM-82882] p 25 N82-31449

Large displacements and stability analysis of nonlinear propeller structures
[NASA-TM-82850] p 94 N82-31707

Tensile buckling of advanced turboprops
[NASA-TM-82896] p 94 N82-31708

Nonlinear constitutive theory for turbine engine structural analysis
p 95 N82-33744

Thermal fatigue resistance of cobalt-modified UDIMET 700
p 39 N83-11289

Creep-fatigue of low cobalt superalloys
p 39 N83-11290

Bending-torsion flutter of a highly swept advanced turboprop
[NASA-TM-82975] p 95 N83-11514

Materials constitutive models for nonlinear analysis of thermally cycled structures
[NASA-TP-2055] p 95 N83-12449

Large displacements and stability analysis of nonlinear propeller structures
p 95 N83-12460

Strainrange partitioning: A total strain range version
[NASA-TM-83023] p 39 N83-14246

Measurements of self-excited rotor-blade vibrations using optical displacements
[NASA-TM-82953] p 95 N83-14523

Hygrothermomechanical evaluation of transverse filament tape epoxy/polyester fiberglass composites
[NASA-TM-83044] p 26 N83-15362

Effects of structural coupling on mistuned cascade flutter and response
[NASA-TM-83049] p 96 N83-15672

Structural fatigue test results for large wind turbine blade sections
p 96 N83-19246

Simplified composite micromechanics equations for hygral, thermal and mechanical properties
[NASA-TM-83320] p 26 N83-19817

Specimen size and geometry effects on fracture toughness of Al₂O₃ measured with short rod and short bar chevron-notch specimens
[NASA-TM-83319] p 47 N83-19902

Ultrasonic ranking of toughness of tungsten carbide
[NASA-TM-83358] p 55 N83-23620

A total life prediction model for stress concentration sites
[NASA-CR-170290] p 96 N83-23629

Array structure design handbook for stand alone photovoltaic applications
[NASA-TM-82629] p 96 N83-23631

Design procedures for fiber composite structural components: Rods, columns and beam columns
[NASA-TM-83321] p 26 N83-24559

Stress intensity and displacement coefficients for radially cracked ring segments subject to three-point bending
[NASA-TM-83059] p 96 N83-24874

Vapor cavitation in dynamically loaded journal bearings
[NASA-TM-83366] p 97 N83-24875

Constitutive relationships for anisotropic high-temperature alloys
[NASA-TM-83437] p 97 N83-28493

Temperature distribution in an aircraft tire at low ground speeds
[NASA-TP-2195] p 97 N83-33217

Relation of cyclic loading pattern to microstructural fracture in creep fatigue
[NASA-TM-83473] p 98 N83-34349

Nonlinear Constitutive Relations for High Temperature Applications
[NASA-CP-2271] p 98 N83-34351

Tensile and compressive constitutive response of 316 stainless steel at elevated temperatures
p 98 N83-34353

Evaluation of inelastic constitutive models for nonlinear structural analysis
p 98 N83-34357

Simplified method for nonlinear structural analysis
[NASA-TP-2208] p 99 N83-34372

A solution procedure for behavior of thick plates on a nonlinear foundation and postbuckling behavior of long plates
[NASA-TP-2174] p 99 N83-34373

The thermal fatigue resistance of H-13 Die Steel for aluminum die casting dies
[NASA-TM-83331] p 39 N83-35103

The structural response of a rail accelerator
[NASA-TM-83491] p 99 N83-35412

Analysis of an externally radially cracked ring segment subject to three-point radial loading
[NASA-TM-83482] p 100 N83-35413

Wide range weight functions for the strip with a single edge crack
[NASA-TM-83478] p 100 N84-11512

INHYD: Computer code for intraply hybrid composite design. A users manual
[NASA-TP-2239] p 26 N84-13224

An improved finite-difference analysis of uncoupled vibrations of tapered cantilever beams
[NASA-TM-83495] p 101 N84-13610

Complexities of high temperature metal fatigue: Some steps toward understanding
[NASA-TM-83507] p 101 N84-14541

A simplified method for elastic-plastic-creep structural analysis
[NASA-TM-83509] p 101 N84-14542

Dynamic behavior of spiral-groove and Rayleigh-Step self-acting face seals
[NASA-TP-2266] p 8 N84-16181

Digital computer program for generating dynamic turbofan engine models (DIGTEM)
[NASA-TM-83446] p 8 N84-16185

Design concepts for low-cost composite engine frames
[NASA-TM-83544] p 8 N84-16186

Flutter of swept fan blades
[NASA-TM-83547] p 102 N84-16587

Improved finite-difference vibration analysis of pretwisted, tapered beams
[NASA-TM-83549] p 102 N84-16588

Bending fatigue of electron-beam-welded foils. Application to a hydrodynamic air bearing in the Chrysler/DOE upgraded automotive gas turbine engine
[NASA-TM-83539] p 102 N84-16589

Preliminary study of thermomechanical fatigue of polycrystalline MAR-M 200
[NASA-TP-2280] p 40 N84-17350

Engine cyclic durability by analysis and material testing
[NASA-TM-83577] p 102 N84-18683

Formulation of blade-flutter spectral analyses in stationary reference frame
[NASA-TP-2296] p 8 N84-20562

Development of a simplified procedure for cyclic structural analysis
[NASA-TP-2243] p 103 N84-20878

Select fiber composites for space applications: A mechanistic assessment
[NASA-TM-83631] p 26 N84-22702

Vibration and flutter of mistuned bladed-disk assemblies
[NASA-TM-83634] p 103 N84-23923

Lewis Research Center spin rig and its use in vibration analysis of rotating systems
[NASA-TP-2304] p 9 N84-24578

Impact resistance of fiber composites: Energy absorbing mechanisms and environmental effects
[NASA-TM-83594] p 26 N84-24712

Dynamic stress analysis of smooth and notched fiber composite flexural specimens
[NASA-TM-83694] p 27 N84-25770

ICAN: Integrated composites analyzer
[NASA-TM-83700] p 27 N84-26755

Interply layer degradation effects on composite structural response
[NASA-TM-83702] p 27 N84-26756

Simplified composite micromechanics equations for strength, fracture toughness and environmental effects
[NASA-TM-83696] p 27 N84-27832

Hygrothermomechanical fracture stress criteria for fiber composites with sense-parity
[NASA-TM-83691] p 27 N84-28918

A computer program for predicting nonlinear uniaxial material responses using viscoplastic models
[NASA-TM-83675] p 104 N84-29247

Mode 2 fatigue crack growth specimen development
[NASA-TM-83722] p 104 N84-29248

Improved methods of vibration analysis of pretwisted, airfoil blades
[NASA-TM-83735] p 104 N84-30329

Application of finite element substructuring to composite micromechanics
[NASA-TM-83729] p 27 N84-31288

Evaluation of the effect of crack closure on fatigue crack growth of simulated short cracks
[NASA-TM-83778] p 40 N84-31348

Nonlinear displacement analysis of advanced propeller structures using NASTRAN
[NASA-TM-83737] p 104 N84-31683

Cyclic torsion testing
[NASA-TM-83756] p 105 N84-31687

Nonlinear Structural Analysis
[NASA-CP-2297] p 105 N84-31688

Nonlinear analysis for high-temperature composites: Turbine blades/vanes
p 106 N84-31699

The role of the reflection coefficient in precision measurement of ultrasonic attenuation
[NASA-TM-83788] p 57 N84-32849

Fracture surface characteristics of notched angleplied graphite/epoxy composites
[NASA-TM-83786] p 28 N84-33522

Low cycle fatigue behavior of conventionally cast MAR-M 200 AT 1000 deg C
[NASA-TM-83769] p 41 N84-33564

Fracture modes in notched angleplied composite laminates
[NASA-TM-83802] p 28 N84-34576

Ultrasonic velocity measurement using phase-slope cross-correlation methods
[NASA-TM-83794] p 57 N84-34769

Ultrasonic nondestructive evaluation, microstructure, and mechanical property interrelations
[NASA-TM-86876] p 57 N85-10371

Turbine Engine Hot Section Technology (HOST)
[NASA-TM-83022] p 9 N85-10951

Nonlinear structural and life analyses of a turbine blade
p 9 N85-10954

Nonlinear structural and life analyses of a combustor liner
p 9 N85-10955

Pre-HOST high temperature crack propagation
p 9 N85-10956

Structural analysis
p 9 N85-10969

Component-specific modeling
p 10 N85-10971

The 3-D inelastic analysis methods for hot section components: Brief description
p 10 N85-10972

Life prediction and constitutive behavior: Overview
p 10 N85-10973

Constitutive model development for isotropic materials
p 10 N85-10975

HOST high temperature crack propagation
p 10 N85-10977

Validation of structural analysis methods using the in-house liner cyclic rigs
p 10 N85-10987

HOST liner cyclic facilities: Facility description
p 10 N85-10988

Fabrication and quality assurance processes for superhybrid composite fan blades
[NASA-TM-83354] p 28 N85-14882

The use of an optical data acquisition system for bladed disk vibration analysis
[NASA-TM-86891] p 106 N85-15184

Engine cyclic durability by analysis and material testing
p 11 N85-15744

A study of interply layer effects on the free-edge stress field of angleplied laminates
[NASA-TM-86924] p 28 N85-15822

Design procedures for fiber composite structural components: Panels subjected to combined in-plane loads
[NASA-TM-86909] p 29 N85-15823

Experimental compliance calibration of the NASA Lewis Research Center Mode 2 fatigue specimen
[NASA-TM-86908] p 107 N85-16205

A study of spectrum fatigue crack propagation in two aluminum alloys. 1: Spectrum simplification
[NASA-TM-86929] p 41 N85-18124

A study of spectrum fatigue crack propagation in two aluminum alloys. 2: Influence of microstructures
[NASA-TM-86930] p 41 N85-18125

NASA Lewis Research Center/University Graduate Research Program on Engine Structures
[NASA-TM-86916] p 107 N85-18375

- Low cycle fatigue of MAR-M 200 single crystals at 760 and 870 deg C
[NASA-TM-86933] p 41 N85-19074
- NDE for heat engine ceramics
[NASA-TM-86949] p 57 N85-20389
- Local strain redistribution corrections for a simplified inelastic analysis procedure based on an elastic finite-element analysis
[NASA-TP-2421] p 107 N85-20396
- Nonlinear analysis for high-temperature multilayered fiber composite structures
[NASA-TM-83754] p 29 N85-21273
- Radiographic detectability limits for seeded voids in sintered silicon carbide and silicon nitride
[NASA-TM-86945] p 58 N85-21674
- On local total strain redistribution using a simplified cyclic inelastic analysis based on an elastic solution
[NASA-TM-86913] p 108 N85-21690
- Unified constitutive material models for nonlinear finite-element structural analysis
[NASA-TM-86985] p 108 N85-24338
- Cyclic structural analyses of anisotropic turbine blades for reusable space propulsion systems
[NASA-TM-86990] p 108 N85-24339
- Vibration and buckling of rotating, pretwisted, precone beams including Coriolis effects
[NASA-TM-87004] p 109 N85-25893
- Nonlinear structural analysis for fiber-reinforced superalloy turbine blades
[NASA-TM-86987] p 109 N85-26897
- Multiaxial and thermomechanical fatigue considerations in damage tolerant design
[NASA-TM-87022] p 42 N85-26964
- Fatigue criterion to system design, life and reliability
[NASA-TM-87017] p 49 N85-27226
- A computer analysis program for interfacing thermal and structural codes
[NASA-TM-87021] p 110 N85-27264
- Overview of structural response: Probabilistic structural analysis
[NASA-TM-87033] p 110 N85-27952
- Interaction of high-cycle and low-cycle fatigue of Haynes 188 alloy at 1400 F deg
[NASA-TM-87033] p 111 N85-27961
- Reexamination of cumulative fatigue damage laws
[NASA-TM-87033] p 112 N85-27962
- Cyclic structural analyses of SSME turbine blades
[NASA-TM-87033] p 112 N85-27963
- Designing for fiber composite structural durability in hydrothermomechanical environment
[NASA-TM-87045] p 29 N85-27978
- DEAN: A program for dynamic engine analysis
[NASA-TM-87033] p 11 N85-28945
- Ten year environmental test of glass fiber/epoxy pressure vessels
[NASA-TM-87058] p 29 N85-30034
- Variable force, eddy-current or magnetic damper
[NASA-CASE-LEW-13717-1] p 49 N85-30333
- Structural analysis and cost estimate of an eight-leg space frame as a support structure for horizontal axis wind turbines
[NASA-TM-83470] p 112 N85-30361
- Nonlinear Constitutive Relations for High Temperature Application, 1984
[NASA-CP-2369] p 112 N85-31530
- A comparison of two contemporary creep-fatigue life prediction methods
[NASA-TM-87033] p 113 N85-31538
- On numerical integration and computer implementation of viscoplastic models
[NASA-TM-87033] p 113 N85-31542
- Two simplified procedures for predicting cyclic material response from a strain history
[NASA-TM-87033] p 113 N85-31543
- Reliability of void detection in structural ceramics using scanning laser acoustic microscopy
[NASA-TM-87035] p 58 N85-32337
- Application of traction drives as servo mechanisms
[NASA-TM-87035] p 114 N85-33520
- Nonlinear flap-lag-extensional vibrations of rotating, pretwisted, precone beams including Coriolis effects
[NASA-TM-87102] p 115 N85-34427
- Progressive damage, fracture predictions and post mortem correlations for fiber composites
[NASA-TM-87101] p 29 N86-10290
- Creep-fatigue behavior of NiCoCrAlY coated PWA 1480 superalloy single crystals
[NASA-TM-87110] p 42 N86-10311
- Ultrasonic evaluation of mechanical properties of thick, multilayered, filament wound composites
[NASA-TM-87088] p 58 N86-10561
- Joint research effort on vibrations of twisted plates, phase 1: Final results
[NASA-RP-1150] p 115 N86-10579
- Improved stud configurations for attaching laminated wood wind turbine blades
[NASA-TM-87109] p 115 N86-10582
- Turbine Engine Hot Section Technology (HOST)
[NASA-CP-2289] p 115 N86-11495
- HOST structural analysis program overview
[NASA-TM-87109] p 12 N86-11513
- Influence of load interactions on crack growth as related to state of stress and crack closure
[NASA-TM-87117] p 42 N86-12292
- Fatigue crack propagation of nickel-base superalloys at 650 deg C
[NASA-TM-87150] p 42 N86-12294
- An update of the total-strain version of SRP
[NASA-TP-2499] p 42 N86-12295
- Fractured toughness of Si₃N₄ measured with short bar chevron-notched specimens
[NASA-TM-87153] p 47 N86-13495
- Probability of detection of internal voids in structural ceramics using microfocus radiography
[NASA-TM-87164] p 59 N86-13749
- NDE of structural ceramics
[NASA-TM-87186] p 59 N86-16598
- Reliability of scanning laser acoustic microscopy for detecting internal voids in structural ceramics
[NASA-TM-87222] p 59 N86-16599
- Simplified cyclic structural analyses of SSME turbine blades
[NASA-TM-87214] p 116 N86-16615
- Nonlinear bending-torsional vibration and stability of rotating, pretwisted, precone blades including Coriolis effects
[NASA-TM-87207] p 116 N86-17789
- Estimating the R-curve from residual strength data
[NASA-TM-87182] p 116 N86-18750
- Nondestructive techniques for characterizing mechanical properties of structural materials: An overview
[NASA-TM-87203] p 59 N86-19636
- Computational engine structural analysis
[NASA-TM-87231] p 116 N86-19663
- Integrated Composite Analyzer (ICAN): Users and programmers manual
[NASA-TP-2515] p 30 N86-21614
- Variables controlling fatigue crack growth of short cracks
[NASA-TM-87208] p 43 N86-21661
- Influence of fatigue crack wake length and state of stress on crack closure
[NASA-TM-87292] p 43 N86-22686
- Analytical Ultrasonics in Materials Research and Testing
[NASA-CP-2383] p 59 N86-22962
- Thermoviscoplastic nonlinear constitutive relationships for structural analysis of high temperature metal matrix composites
[NASA-TM-87291] p 30 N86-24756
- A unique set of micromechanics equations for high temperature metal matrix composites
[NASA-TM-87154] p 30 N86-24757
- Simplified composite micromechanics for predicting microstresses
[NASA-TM-87295] p 30 N86-24759
- Fracture characteristics of angle-ply laminates fabricated from overaged graphite/epoxy prepreg
[NASA-TM-87266] p 30 N86-25417
- Concepts for interrelating ultrasonic attenuation, microstructure and fracture toughness in polycrystalline solids
[NASA-TM-87339] p 60 N86-25812
- Cyclic creep analysis from elastic finite-element solutions
[NASA-TM-87213] p 117 N86-25822
- Computational simulation of progressive fracture in fiber composites
[NASA-TM-87341] p 30 N86-26376
- Low-cycle thermal fatigue
[NASA-TM-87225] p 118 N86-26651
- Re-examination of cumulative fatigue damage analysis: An engineering perspective
[NASA-TM-87325] p 118 N86-27680
- Micromechanisms of thermomechanical fatigue: A comparison with isothermal fatigue
[NASA-TM-87331] p 44 N86-28164
- Structural analysis of turbine blades using unified constitutive models
[NASA-TM-88807] p 119 N86-28461
- Thermal-fatigue and oxidation resistance of cobalt-modified Udmet 700 alloy
[NASA-TP-2591] p 119 N86-28464
- Experimental classical flutter results of a composite advanced turboprop model
[NASA-TM-88792] p 119 N86-29271
- Determination of grain size distribution function using two-dimensional Fourier transforms of tone pulse encoded images
[NASA-TM-88790] p 61 N86-31065
- Fiber composite sandwich thermostructural behavior: Computational simulation
[NASA-TM-88787] p 31 N86-31663
- ICAN: A versatile code for predicting composite properties
[NASA-TM-87334] p 31 N86-31664
- The low cycle fatigue behavior of a plasma-sprayed coating material
[NASA-TM-87318] p 44 N86-31699
- Factors that affect reliability of nondestructive detection of flaws in structural ceramics
[NASA-TM-87348] p 61 N86-31912
- Quantitative void characterization in structural ceramics using scanning laser acoustic microscopy
[NASA-TM-88797] p 61 N86-31913
- Influence of third-degree geometric nonlinearities on the vibration and stability of pretwisted, precone, rotating blades
[NASA-TM-87307] p 120 N86-31920
- Structural dynamic measurement practices for turbomachinery at the NASA Lewis Research Center
[NASA-TM-88857] p 13 N86-32433
- Acousto-ultrasonic verification of the strength of filament wound composite material
[NASA-TM-88827] p 61 N86-32764
- Ultrasonic determination of recrystallization
[NASA-TM-88855] p 61 N87-10399
- Turbine Engine Hot Section Technology, 1984
[NASA-CP-2339] p 120 N87-11180
- Fatigue and fracture: Overview
[NASA-TM-88827] p 120 N87-11183
- High temperature stress-strain analysis
[NASA-TM-88827] p 120 N87-11209
- STAEBL: Structural tailoring of engine blades, phase 2
[NASA-TM-88827] p 13 N87-11731
- Selection of rolling-element bearing steels for long-life application
[NASA-TM-88881] p 49 N87-11993
- Concentrated mass effects on the flutter of a composite advanced turboprop model
[NASA-TM-88854] p 120 N87-12017
- NDE reliability and process control for structural ceramics
[NASA-TM-88870] p 61 N87-12910
- A constitutive law for finite element contact problems with unclassical friction
[NASA-TM-88838] p 120 N87-12924
- Composite interlaminar fracture toughness: Three-dimensional finite element modeling for mixed mode 1, 2 and 3 fracture
[NASA-TM-88872] p 31 N87-13491
- Effect of design variables, temperature gradients and speed of life and reliability of a rotating disk
[NASA-TM-88883] p 49 N87-13755
- Probabilistic structural analysis methods for space propulsion system components
[NASA-TM-88861] p 121 N87-13794
- Estimation of high temperature low cycle fatigue on the basis of inelastic strain and strainrate
[NASA-TM-88841] p 44 N87-14489
- A low-cost optical data acquisition system for vibration measurement
[NASA-TM-88907] p 121 N87-14730
- Lubricant effects on bearing life
[NASA-TM-88875] p 49 N87-15467
- The 20th Aerospace Mechanics Symposium
[NASA-CP-2423-REV] p 121 N87-16321
- Evaluation of a high-torque backlash-free roller actuator
[NASA-TM-88911] p 49 N87-16336
- Composite space antenna structures: Properties and environmental effects
[NASA-TM-88859] p 31 N87-16880
- Surface flaw reliability analysis of ceramic components with the SCARE finite element postprocessor program
[NASA-TM-88901] p 121 N87-17087
- Nondestructive evaluation of structural ceramics
[NASA-TM-88978] p 62 N87-18109
- The effect of nonlinearities on the dynamic response of a large shuttle payload
[NASA-TM-88941] p 121 N87-18112
- Analytical flutter investigation of a composite propfan model
[NASA-TM-88944] p 122 N87-18115
- Analytical and experimental investigation of mistuning in propfan flutter
[NASA-TM-88959] p 122 N87-18116
- Computational composite mechanics for aerospace propulsion structures
[NASA-TM-88965] p 31 N87-18614
- Effects of surface removal on rolling-element fatigue
[NASA-TM-88971] p 50 N87-18820
- The effects of crack surface friction and roughness on crack tip stress fields
[NASA-TM-88976] p 122 N87-18881
- Fatigue failure of regenerator screens in a high frequency Stirling engine
[NASA-TM-88974] p 122 N87-18882
- A comparative study of some dynamic stall models
[NASA-TM-88917] p 122 N87-18883
- Bithermal low-cycle fatigue behavior of a NiCoCrAlY-coated single crystal superalloy
[NASA-TM-88931] p 45 N87-20408

P

- The acousto-ultrasonic approach
[NASA-TM-89843] p 62 N87-20562
Calculation of thermomechanical fatigue life based on isothermal behavior
[NASA-TM-88864] p 122 N87-20565
Shot peening for Ti-6Al-4V alloy compressor blades
[NASA-TP-2711] p 123 N87-20566
A NASTRAN primer for the analysis of rotating flexible blades
[NASA-TM-89861] p 123 N87-21375
Structural and aeroelastic analysis of the SR-7L propan
[NASA-TM-86877] p 123 N87-22273
Fatigue damage interaction behavior of PWA 1480
p 45 N87-22777
Nonlinear heat transfer and structural analyses of SSME turbine blades
p 123 N87-22779
Finite element implementation of Robinson's unified viscoplastic model and its application to some uniaxial and multiaxial problems
[NASA-TM-89891] p 123 N87-23010
The impact damped harmonic oscillator in free decay
[NASA-TM-89897] p 50 N87-23978
Application of scanning acoustic microscopy to advanced structural ceramics
[NASA-TM-89929] p 62 N87-23987
Identification of structural interface characteristics using component mode synthesis
[NASA-TM-89960] p 123 N87-24006
Environmental degradation of 316 stainless steel in high temperature low cycle fatigue
[NASA-TM-89931] p 124 N87-24007
Hub flexibility effects on propan vibration
[NASA-TM-89900] p 124 N87-24722
Ray propagation path analysis of acousto-ultrasonic signals in composites
[NASA-TM-100148] p 62 N87-25589
Ultrasonic NDE of structural ceramics for power and propulsion systems
[NASA-TM-100147] p 62 N87-26362
Finite element analysis of flexible, rotating blades
[NASA-TM-89906] p 124 N87-26385
A high temperature fatigue and structures testing facility
[NASA-TM-100151] p 124 N87-26399
SINDA-NASTRAN interfacing program theoretical description and user's manual
[NASA-TM-100158] p 124 N87-27268
Fracture mechanics concepts in reliability analysis of monolithic ceramics
[NASA-TM-100174] p 124 N87-27269
A computational procedure for automated flutter analysis
[NASA-TM-100171] p 125 N87-28058
Toward improved durability in advanced combustors and turbines: Progress in the prediction of thermomechanical loads
[NASA-TM-88932] p 13 N87-28551
Dynamic delamination buckling in composite laminates under impact loading: Computational simulation
[NASA-TM-100192] p 31 N87-28611
Exposure time considerations in high temperature low cycle fatigue
[NASA-TM-88934] p 125 N87-28944
Turbine Engine Hot Section Technology, 1985
[NASA-CP-2405] p 125 N88-11140
High temperature stress-strain analysis
p 125 N88-11170
Lewis' enhanced laboratory for research into the fatigue and constitutive behavior of high temperature materials
p 125 N88-11177
Flaw imaging and ultrasonic techniques for characterizing sintered silicon carbide
[NASA-TM-100177] p 63 N88-12106
Free-edge delamination: Laminate width and loading conditions effects
[NASA-TM-100238] p 32 N88-12551
Composite mechanics for engine structures
[NASA-TM-100176] p 32 N88-12552
Creep life prediction based on stochastic model of microstructurally short crack growth
[NASA-TM-100245] p 125 N88-12825
National Technical Systems, Hartwood, Va.
Factors influencing the ultrasonic stress wave factor evaluation of composite material structures
p 81 A86-34257
Northeastern Univ., Boston, Mass.
Engine dynamic analysis with general nonlinear finite element codes. II - Bearing element implementation, overall numerical characteristics and benchmarking
[ASME PAPER 82-GT-292] p 47 A82-35462
Northwestern Univ., Evanston, Ill.
On finite deformation elasto-plasticity
p 66 A82-45869
On composites with periodic structure
p 67 A83-10283

- Composites with periodic microstructure
p 15 A83-12734
Growth and stability of interacting surface flaws of arbitrary shape
p 68 A83-15060
The determination of the elastodynamic fields of an ellipsoidal inhomogeneity
[ASME PAPER 83-APM-19] p 69 A83-37388
Dynamic fields near a crack tip growing in an elastic-perfectly-plastic solid
p 70 A83-38528
Finite elastic-plastic deformation of polycrystalline metals
p 34 A84-43872
On stress field near a stationary crack tip
[AD-A152863] p 76 A85-24532
Probabilistic finite elements for transient analysis in nonlinear continua
p 80 A86-28653
Micromechanically based constitutive relations for polycrystalline solids
p 99 N83-34359
Probabilistic finite element: Variational theory
p 111 N85-27957

O

- Ohio State Univ., Cleveland.**
Vibrations of twisted cantilevered plates - Summary of previous and current studies
p 76 A85-22069
Ohio State Univ., Columbus.
Vibration and buckling of rectangular plates under in-plane hydrostatic loading
p 64 A80-45364
Vibrations of cantilevered shallow cylindrical shells of rectangular planform
p 65 A82-11298
Vibrations of twisted rotating blades
[ASME PAPER 81-DET-127] p 65 A82-19341
Comparison of beam and shell theories for the vibrations of thin turbomachinery blades
[ASME PAPER 82-GT-223] p 65 A82-35408
On ultrasonic factors and fracture toughness
p 66 A82-42863
Mechanics aspects of NDE by sound and ultrasound
p 51 A83-25571
Vibrations of cantilevered circular cylindrical shells
Shallow versus deep shell theory
p 69 A83-36958
The determination of the elastodynamic fields of an ellipsoidal inhomogeneity
[ASME PAPER 83-APM-19] p 69 A83-37388
On the three-dimensional vibrations of the cantilevered rectangular parallelepiped
p 70 A83-37729
Vibrations of cantilevered doubly-curved shallow shells
p 70 A83-39557
Vibrations of blades with variable thickness and curvature by shell theory
[ASME PAPER 83-GT-152] p 70 A83-47978
Vibrations of twisted cantilevered plates - Experimental investigation
[ASME PAPER 84-GT-96] p 73 A84-46937
Ultrasonic wave propagation in two-phase media - Spherical inclusions
p 17 A85-11926
Vibrations of twisted cantilever plates - A comparison of theoretical results
p 79 A85-47626
Computer aided derivation of equations for composite mechanics problems and finite element analyses
[AIAA PAPER 86-1016] p 83 A86-38873
Phenomenological and mechanics aspects of nondestructive evaluation and characterization by sound and ultrasound of material and fracture properties
[NASA-CR-3623] p 55 N83-11506
Fundamental aspects in quantitative ultrasonic determination of fracture toughness: The scattering of a single ellipsoidal inhomogeneity
[NASA-CR-3625] p 55 N83-11507
The transmission or scattering of elastic waves by an inhomogeneity of simple geometry: A comparison of theories
[NASA-CR-3659] p 55 N83-16773
Volume integrals associated with the inhomogeneous Helmholtz equation. Part 1: Ellipsoidal region
[NASA-CR-3749] p 56 N84-14525
Volume integrals associated with the inhomogeneous Helmholtz equation. Part 2: Cylindrical region; rectangular region
[NASA-CR-3750] p 56 N84-14526
Fundamentals of microcrack nucleation mechanics
[NASA-CR-3851] p 57 N85-16195
A study of internal and distributed damping for vibrating turbomachinery blades
[NASA-CR-175901] p 11 N85-27868
Extensions of the Ritz-Galerkin method for the forced, damped vibrations of structural elements
p 117 N86-21909

Pennsylvania State Univ., University Park.

- The interaction between mistuning and friction in the forced response of bladed disk assemblies
[ASME PAPER 84-GT-139] p 73 A84-46957
Effects of friction dampers on aerodynamically unstable rotor stages
p 3 A85-21866
Stability of limit cycles in frictionally damped and aerodynamically unstable rotor stages
p 4 A86-19198
Influence of friction dampers on torsional blade flutter
[ASME PAPER 85-GT-170] p 5 A86-32957
Axial and torsional fatigue behavior of Waspaloy
[NASA-CR-175052] p 44 N86-25454
Pratt and Whitney Aircraft, East Hartford, Conn.
Three-dimensional stress analysis using the boundary element method
p 106 N84-31700
3-D inelastic analysis methods for hot section components (base program)
[NASA-CR-174700] p 107 N85-21686
Creep fatigue life prediction for engine hot section materials (isotropic)
[NASA-CR-168228] p 11 N85-31057
Life prediction and constitutive models for engine hot section anisotropic materials program
[NASA-CR-174952] p 60 N86-25003
Structural tailoring of engine blades (STAEBL) theoretical manual
[NASA-CR-175112] p 12 N86-27283
Structural tailoring of engine blades (STAEBL) user's manual
[NASA-CR-175113] p 13 N86-27284
Pratt and Whitney Aircraft Group, East Hartford, Conn.
Nonlinear structural and life analyses of a combustor liner
p 68 A83-12764
Structural tailoring of engine blades (STAEBL)
[AIAA 83-0828] p 1 A83-29737
Simplified analytical procedures for representing material cyclic response
p 2 A84-22877
Finite element engine blade structural optimization
[AIAA PAPER 85-0645] p 76 A85-30313
Application of two creep fatigue life models for the prediction of elevated temperature crack initiation of a nickel base alloy
[AIAA PAPER 85-1420] p 35 A85-43979
Structural tailoring of advanced turboprops
[AIAA PAPER 87-0753] p 85 A87-33648
Effect of time dependent flight loads on JT9D-7 performance deterioration
[NASA-CR-159681] p 87 N80-10515
Combustor liner durability analysis
[NASA-CR-165250] p 7 N81-17079
Structural tailoring of engine blades (STAEBL)
[NASA-CR-167949] p 7 N82-33391
Development of a simplified analytical method for representing material cyclic response
[NASA-CR-168100] p 96 N83-21390
Sensor failure detection for jet engines
[NASA-CR-168190] p 56 N83-33182
Pratt and Whitney Aircraft Group, West Palm Beach, Fla.
Cyclic behavior of turbine disk alloys at 650 C
p 32 A81-12266
Evaluation of the cyclic behavior of aircraft turbine disk alloys, part 2
[NASA-CR-165123] p 38 N80-30482
Low strain, long life creep fatigue of AF2-1DA and INCO 718
[NASA-CR-167989] p 40 N84-10268
Princeton Univ., N. J.
Design of dry-friction dampers for turbine blades
p 2 A83-35883
Forced response of a cantilever beam with a dry friction damper attached. I - Theory. II - Experiment
p 71 A84-21267
Vibration characteristics of mistuned shrouded blade assemblies
[ASME PAPER 85-GT-115] p 4 A86-22068
Aeroelastic behavior of low aspect ratio metal and composite blades
[ASME PAPER 86-GT-243] p 84 A86-48271
Purdue Univ., West Lafayette, Ind.
Wave propagation in a graphite/epoxy laminate
p 70 A83-44050
The coupled response of turbomachinery blading to aerodynamic excitations
p 2 A84-26959
Indentation law for composite laminates
p 16 A84-27356
Use of static indentation laws in the impact analysis of laminated composite plates
p 18 A85-29133
The effect of aerodynamic and structural detuning on turbomachine supersonic unstalled torsional flutter
[AIAA PAPER 85-0761] p 3 A85-30378
Forced response analysis of an aerodynamically detuned supersonic turbomachine rotor
p 5 A86-26902

Aerodynamic and structural detuning of supersonic turbomachine rotors p 5 A86-31595
 Three dimensional unsteady aerodynamics and aeroelastic response of advanced turboprops [AIAA PAPER 86-0846] p 5 A86-38894
 Dynamic delamination crack propagation in a graphite/epoxy laminate p 20 A86-43010
 The effect of circumferential aerodynamic detuning on coupled bending-torsion unstalled supersonic flutter [ASME PAPER 86-GT-100] p 6 A87-25396
 Analytical and experimental investigation of mistuning in propfan flutter p 86 A87-40496
 Dynamic responses of graphite/epoxy laminated beam to impact of elastic spheres p 25 N83-13173
 Wave propagation in graphite/epoxy laminates due to impact [NASA-CR-168057] p 26 N83-22325

R

Rensselaer Polytechnic Inst., Troy, N.Y.
 Natural frequency of rotating beams using non-rotating modes p 68 A83-18383
 The effects of frequency and hold times on fatigue crack propagation rates in a nickel base superalloy p 34 A84-18733
 The influence of hold times on LCF and FCG behavior in a P/M Ni-base superalloy p 35 A85-32400
 Fatigue crack growth and low cycle fatigue of two nickel base superalloys [NASA-CR-174534] p 39 N84-10267
Rice Univ., Houston, Tex.
 Oscillator response to nonstationary excitation [ASME PAPER 84-WA/APM-38] p 75 A85-17039
 Numerical synthesis of tri-variate velocity realizations of turbulence p 81 A86-28654
Rockwell International Corp., Canoga Park, Calif.
 The effect of microstructure, temperature, and hold-time on low-cycle fatigue of As HIP P/M Rene 95 p 35 A85-32399
 Composite loads spectra for select space propulsion structural components p 110 N85-27953
Rose-Hulman Inst. of Tech., Terre Haute, Ind.
 The impact damped harmonic oscillator in free decay [NASA-TM-89897] p 50 N87-23978

S

Sandia National Labs., Albuquerque, N. Mex.
 Moving cracks in layered composites p 67 A83-12048
Sonoscan, Inc., Bensenville, Ill.
 Comparison of NDE techniques for sintered-SiC components p 51 A83-22265
South Carolina State Coll., Orangeburg.
 On local total strain redistribution using a simplified cyclic inelastic analysis based on an elastic solution [AIAA PAPER 85-1419] p 78 A85-39770
South Carolina Univ., Columbia.
 Extending the laser-specklegram technique to strain analysis of rotating components p 67 A83-12514
Southwest Research Inst., San Antonio, Tex.
 Unified constitutive material models for nonlinear finite-element structural analysis [AIAA PAPER 85-1418] p 77 A85-39769
 Constitutive modeling and computational implementation for finite strain plasticity p 78 A85-40910
 Probabilistic structural analysis for space propulsion system components p 81 A86-28659
 Probabilistic structural analysis theory development p 111 N85-27955
 A survey of unified constitutive theories p 112 N85-31531
 Constitutive modeling for isotropic materials (HOST) [NASA-CR-174980] p 115 N86-10589
Stanford Univ., Calif.
 Element-by-element solution procedures for nonlinear structural analysis p 105 N84-31694
 Augmented weak forms and element-by-element preconditioners: Efficient iterative strategies for structural finite elements. A preliminary study p 106 N85-10384
State Univ. of New York, Buffalo.
 Stress analysis of gas turbine engine structures using the boundary element method p 81 A86-34444
 Advanced three-dimensional dynamic analysis by boundary element methods p 81 A86-34445
Sverdrup Technology, Inc., Cleveland, Ohio.
 Unified constitutive materials model development and evaluation for high-temperature structural analysis applications p 84 A86-49133

Probabilistic structural analysis to quantify uncertainties associated with turbopump blades [AIAA PAPER 87-0766] p 85 A87-33581
 Composite space antenna structures - Properties and environmental effects p 20 A87-38610
 Analytical and experimental investigation of mistuning in propfan flutter [AIAA PAPER 87-0739] p 86 A87-40496
 Analytical flutter investigation of a composite propfan model [AIAA PAPER 87-0738] p 87 A87-40497
 Environmental degradation of 316 stainless steel in high temperature low cycle fatigue [NASA-TM-89931] p 124 N87-24007
Syracuse Univ., N. Y.
 Shear fatigue crack growth - A literature survey p 80 A86-24219
 Fatigue crack growth under general-yielding cyclic-loading p 84 A86-44339
 Modelling of crack tip deformation with finite element method and its applications p 87 N80-13503
 Literature survey on oxidations and fatigue lives at elevated temperatures p 40 N84-20674
 Crack tip field and fatigue crack growth in general yielding and low cycle fatigue [NASA-CR-174639] p 41 N84-32503
 Grain boundary oxidation and oxidation accelerated fatigue crack nucleation and propagation [NASA-CR-175050] p 43 N86-20542
 Fatigue crack growth under general-yielding cyclic-loading [NASA-CR-175049] p 117 N86-21951

T

Technion - Israel Inst. of Tech., Haifa.
 Thermodynamically consistent constitutive equations for nonisothermal large strain, elasto-plastic, creep behavior [AIAA PAPER 85-0621] p 77 A85-38425
Teledyne CAE, Toledo, Ohio.
 The effects of strong shock loading on coupled bending-torsion flutter of tuned and mistuned cascades p 4 A86-26893
Texas A&M Univ., College Station.
 An uncoupled viscoplastic constitutive model for metals at elevated temperature p 69 A83-29798
 On the use of internal state variables in thermoviscoplastic constitutive equations p 113 N85-31536
 Numerical considerations in the development and implementation of constitutive models p 113 N85-31541
 Development of constitutive models for cyclic plasticity and creep behavior of super alloys at high temperature [NASA-CR-176418] p 43 N86-14356
 Integrated research in constitutive modelling at elevated temperatures, part 2 [NASA-CR-177233] p 119 N86-28455
 Integrated research in constitutive modelling at elevated temperatures, part 1 [NASA-CR-177237] p 120 N86-30227
Texas Univ., Austin.
 Comments on some problems in computational penetration mechanics p 71 A84-13545
 A numerical analysis of contact and limit-point behavior in a class of problems of finite elastic deformation p 72 A84-27370
 Analysis of hourglass instabilities and control in underintegrated finite element methods p 74 A85-11125
 Stability and convergence of underintegrated finite element approximations p 105 N84-31696
Textron Bell Aerospace Co., Buffalo, N. Y.
 Flutter analysis of advanced turbopropellers [AIAA 83-0846] p 69 A84-29824
 NASTRAN forced vibration analysis of rotating cyclic structures [ASME PAPER 83-DET-20] p 72 A84-29103
 Aeroelastic and dynamic finite element analyses of a bladder shrouded disk [NASA-CR-159728] p 90 N81-19479
 NASTRAN level 16 theoretical manual updates for aeroelastic analysis of bladed discs [NASA-CR-159823] p 90 N81-19480
 NASTRAN level 16 user's manual updates for aeroelastic analysis of bladed discs [NASA-CR-159824] p 90 N81-19481
 NASTRAN level 16 programmer's manual updates for aeroelastic analysis of bladed discs [NASA-CR-159825] p 90 N81-19482
 NASTRAN level 16 demonstration manual updates for aeroelastic analysis of bladed discs [NASA-CR-159826] p 90 N81-19483

Forced vibration analysis of rotating cyclic structures in NASTRAN [NASA-CR-165429] p 100 N84-11514
 Finite element forced vibration analysis of rotating cyclic structures [NASA-CR-165430] p 101 N84-11515
 NASTRAN documentation for flutter analysis of advanced turbopropellers [NASA-CR-167927] p 8 N84-15153
 Bladed-shrouded-disc aeroelastic analyses: Computer program updates in NASTRAN level 17.7 [NASA-CR-165428] p 8 N84-15154
 NASTRAN forced vibration analysis of rotating cyclic structures [NASA-CR-173821] p 104 N84-29252
 Slave finite elements: The temporal element approach to nonlinear analysis p 105 N84-31689
Toledo Univ., Ohio.
 Effects of mistuning on bending-torsion flutter and response of a cascade in incompressible flow [AIAA 81-0602] p 65 A81-29465
 The effects of strong shock loading on coupled bending-torsion flutter of tuned and mistuned cascades p 4 A86-26893
 Approximations to eigenvalues of modified general matrices [AIAA PAPER 87-0947] p 86 A87-33756
 Analytical flutter investigation of a composite propfan model [AIAA PAPER 87-0738] p 87 A87-40497
 Thermal stress analysis for a wood composite blade [NASA-CR-173394] p 103 N84-21903
 Thermal-stress analysis for wood composite blade [NASA-CR-173830] p 104 N84-31685

U

United Technologies Corp., East Hartford, Conn.
 Stress analysis of gas turbine engine structures using the boundary element method p 81 A86-34444
 Fracture mechanics criteria for turbine engine hot section components [NASA-CR-167896] p 7 N82-25257
United Technologies Research Center, East Hartford, Conn.
 Effects of mistuning on blade torsional flutter p 64 A81-29095
 Dynamic characteristics of an assembly of prop-fan blades [ASME PAPER 85-GT-134] p 5 A86-32956
 Research and development program for the development of advanced time-temperature dependent constitutive relationships. Volume 1: Theoretical discussion [NASA-CR-168191-VOL-1] p 100 N84-10613
 Research and development program for the development of advanced time-temperature dependent constitutive relationships. Volume 2: Programming manual [NASA-CR-168191-VOL-2] p 100 N84-10614
 Aeroelastic analysis for propellers - mathematical formulations and program user's manual [NASA-CR-3729] p 101 N84-12530
 Advanced turboprop vibratory characteristics [NASA-CR-174708] p 12 N86-24693
University Coll. of Swansea (Wales).
 Iterative methods for mixed finite element equations p 82 A86-34461
University of Western Michigan, Kalamazoo.
 Optimization and analysis of gas turbine engine blades [AIAA PAPER 87-0827] p 126 A87-33614

V

Virginia Polytechnic Inst. and State Univ., Blacksburg.
 Geometrically nonlinear analysis of layered composite shells p 68 A83-27431
 Three-dimensional finite-element analysis of layered composite plates p 68 A83-27432
 Characterization of composite materials by means of the ultrasonic stress wave factor p 16 A84-10430
 A mixed shear flexible finite element for the analysis of laminated plates p 73 A84-45994
 Optimization of cascade blade mistuning. I - Equations of motion and basic inherent properties p 3 A85-42365
 Optimization of cascade blade mistuning. II - Global optimum and numerical optimization p 3 A85-45715
 Factors influencing the ultrasonic stress wave factor evaluation of composite material structures p 81 A86-34257
 Approximations to eigenvalues of modified general matrices [AIAA PAPER 87-0947] p 86 A87-33756

Virginia Univ., Charlottesville.

CORPORATE SOURCE

Finite-element modeling of layered, anisotropic composite plates and shells: A review of recent research p 91 N82-19563

A study of the stress wave factor technique for the characterization of composite materials [NASA-CR-3670] p 55 N83-27248

Geometrically nonlinear analysis of layered composite plates and shells [NASA-CR-168182] p 98 N83-33219

Theoretical investigation of the force and dynamically coupled torsional-axial-lateral dynamic response of eared rotors

[NASA-CR-173013] p 127 N83-34656

Geometrically nonlinear analysis of laminated elastic structures

[NASA-CR-175609] p 108 N85-21720

A study of the stress wave factor technique for the characterization of composite materials

[NASA-CR-174870] p 29 N85-30035

Closure of fatigue cracks at high strains

[NASA-CR-175021] p 116 N86-17788

Ultrasonic stress wave characterization of composite materials

[NASA-CR-3976] p 60 N86-27665

A study of the stress wave factor technique for nondestructive evaluation of composite materials

[NASA-CR-4002] p 60 N86-28445

J-integral estimates for cracks in infinite bodies

[NASA-CR-179474] p 119 N86-28467

Virginia Univ., Charlottesville.

A pad perturbation method for the dynamic coefficients of tilting-pad journal bearings p 47 A82-14400

W

Wayne State Univ., Detroit, Mich.

Comparison of NDE techniques for sintered-SiC components p 51 A83-22265

Wisconsin Univ., Madison.

The plastic compressibility of 7075-T651 aluminum-alloy plate p 36 A86-49690

Wyle Labs., Inc., Huntsville, Ala.

Flow dynamic environment data base development for the SSME p 109 N85-26885

Wyoming Univ., Laramie.

Analysis of crack propagation as an energy absorption mechanism in metal matrix composites

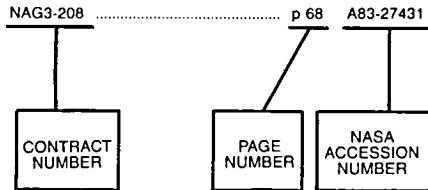
[NASA-CR-165051] p 24 N82-14288

Micromechanical predictions of crack propagation and fracture energy in a single fiber boron/aluminum model composite

[NASA-CR-168550] p 25 N82-18326

CONTRACT NUMBER INDEX

Typical Contract Number Index Listing



Listings in this index are arranged alpha-numerically by contract number. Under each contract number, the accession numbers denoting documents that have been produced as a result of research done under the contract are arranged in ascending order with the AIAA accession numbers appearing first. The accession number denotes the number by which the citation is identified in the abstract section. Preceding the accession number is the page number on which the citation may be found.

NAG3-208	p 68	A83-27431	NAG3-208	p 68	A83-27431	p 78	A85-40910
	p 68	A83-27432		p 68	A83-27432	p 82	A86-34464
	p 73	A84-45994		p 73	A84-45994	p 106	N84-31697
	p 91	N82-19563	NAG3-347	p 91	N82-19563	p 3	A85-42365
	p 98	N83-33219		p 98	N83-33219	p 3	A85-45715
	p 108	N85-21720		p 108	N85-21720	p 86	A87-33756
NAG3-210	p 75	A85-17039	NAG3-348	p 75	A85-17039	p 80	A86-24219
	p 81	A86-28654		p 81	A86-28654	p 84	A86-44339
NAG3-211	p 20	A86-43010		p 20	A86-43010	p 40	N84-20674
NAG3-214	p 69	A83-29823		p 69	A83-29823	p 41	N84-32503
	p 74	A85-12721		p 74	A85-12721	p 43	N86-20542
	p 9	N84-24586		p 9	N84-24586	p 117	N86-21951
NAG3-221	p 2	A83-35883	NAG3-362	p 2	A83-35883	p 57	N84-17606
	p 71	A84-21267		p 71	A84-21267	p 5	A86-26905
NAG3-223	p 75	A85-19433	NAG3-367	p 75	A85-19433	p 65	A82-11298
	p 36	A86-30010	NAG3-36	p 36	A86-30010	p 65	A82-19341
	p 97	N83-27256		p 97	N83-27256	p 65	A82-35408
	p 106	N84-34774		p 106	N84-34774	p 69	A83-36958
	p 107	N85-21685		p 107	N85-21685	p 70	A83-37729
	p 118	N86-25851		p 118	N86-25851	p 70	A83-39557
NAG3-22	p 34	A84-18733		p 34	A84-18733	p 70	A83-47978
	p 35	A85-32400		p 35	A85-32400	p 103	N84-21903
	p 39	N84-10267		p 39	N84-10267	p 104	N84-31685
NAG3-231	p 1	A83-32791	NAG3-373	p 1	A83-32791	p 37	A87-54370
	p 2	A84-31905		p 2	A84-31905	p 108	N85-21691
	p 73	A84-46957	NAG3-379	p 73	A84-46957	p 109	N85-25894
	p 3	A85-21866		p 3	A85-21866	p 109	N85-27260
	p 4	A86-19198		p 4	A86-19198	p 112	N85-31533
NAG3-23	p 103	N84-22980		p 103	N84-22980	p 113	N85-31545
NAG3-246	p 94	N82-33738		p 94	N82-33738	p 114	N85-32340
	p 96	N83-23629		p 96	N83-23629	p 114	N85-32341
	p 100	N84-10612		p 100	N84-10612	p 68	A83-18383
NAG3-264	p 44	N86-25454	NAG3-37	p 44	N86-25454	p 65	A82-32303
NAG3-265	p 74	A84-48565	NAG3-38	p 74	A84-48565	p 65	A82-36782
	p 82	A86-37799		p 82	A86-37799	p 66	A82-40066
NAG3-280	p 35	A86-20982		p 35	A86-20982	p 71	A84-16874
	p 41	N85-15877		p 41	N85-15877	p 71	A84-16884
	p 43	N86-24818		p 43	N86-24818	p 74	A85-15894
NAG3-298	p 105	N84-31695		p 105	N84-31695	p 92	N82-24503
NAG3-308	p 4	A86-22068		p 4	A86-22068	p 94	N82-29619
	p 84	A86-48271		p 84	A86-48271	p 99	N83-34371
NAG3-317	p 105	N84-31692		p 105	N84-31692	p 91	N82-20564
NAG3-319	p 105	N84-31694	NAG3-39	p 105	N84-31694	p 72	A84-31596
	p 106	N85-10384	NAG3-41	p 106	N85-10384	p 79	A85-42566
NAG3-31	p 69	A83-29798		p 69	A83-29798	p 91	N82-14531
	p 43	N86-14356		p 43	N86-14356	p 97	N83-29731
NAG3-323	p 16	A84-10430		p 16	A84-10430	p 97	N83-29734
	p 81	A86-34257		p 81	A86-34257	p 102	N84-19925
	p 60	N86-27665		p 60	N86-27665	p 106	N85-11380
NAG3-328	p 56	N84-15565		p 56	N84-15565	p 11	N85-27868
	p 58	N85-20390		p 58	N85-20390	p 117	N86-21909
	p 58	N85-29307		p 58	N85-29307	p 116	N86-17788
	p 59	N86-25002		p 59	N86-25002	p 119	N86-28467
	p 60	N86-27666		p 60	N86-27666	p 95	N83-12449
NAG3-329	p 71	A84-13545	NAG3-45	p 71	A84-13545	p 28	N84-34575
	p 72	A84-27370	NAG3-464	p 72	A84-27370	p 83	A86-41673
	p 74	A85-11125	NAG3-46	p 74	A85-11125	p 98	N83-34353
	p 105	N84-31696		p 105	N84-31696	p 113	N85-31536
NAG3-32	p 101	N84-15589		p 101	N84-15589	p 113	N85-31541
NAG3-337	p 124	N87-24007		p 124	N87-24007	p 119	N86-28455
	p 125	N87-28944		p 125	N87-28944	p 120	N86-30227
NAG3-339	p 126	A86-30814		p 126	A86-30814	p 5	A86-38894
NAG3-33	p 67	A83-12739	NAG3-499	p 67	A83-12739	p 44	N86-25455
	p 68	A83-14710	NAG3-503	p 68	A83-14710	p 103	N84-19927
	p 72	A84-21541	NAG3-50	p 72	A84-21541	p 114	N85-31548
	p 74	A85-12029	NAG3-511	p 74	A85-12029	p 117	N86-21952
	p 74	A85-15893		p 74	A85-15893	p 83	A86-39485
	p 77	A85-35046		p 77	A85-35046	p 83	A86-40695
	p 77	A85-35048		p 77	A85-35048	p 96	N83-19121
	p 78	A85-41109		p 78	A85-41109	p 98	N83-34355
	p 79	A86-18123		p 79	A86-18123	p 114	N85-31546
	p 82	A86-34462		p 82	A86-34462	p 117	N86-25850
	p 99	N83-34369		p 99	N83-34369	p 77	A85-38425
	p 105	N84-31690	NAG3-534	p 105	N84-31690	p 82	A86-38838
	p 11	N85-21165		p 11	N85-21165	p 109	N85-25896
	p 107	N85-21687		p 107	N85-21687	p 111	N85-27959
	p 108	N85-23096		p 108	N85-23096	p 115	N86-10588
NAG3-340	p 17	A85-11926		p 17	A85-11926	p 119	N86-28462
	p 56	N84-14526		p 56	N84-14526	p 80	A86-28653
	p 57	N85-16195		p 57	N85-16195	p 111	N85-27957
NAG3-346	p 71	A84-13248	NAG3-54	p 71	A84-13248	p 66	A82-39514
	p 75	A85-19899		p 75	A85-19899	p 126	A83-10273
	p 77	A85-33847		p 77	A85-33847	p 67	A83-12746

NAG3-553	p 70	A83-49437	NCC3-27	p 48	A84-47046	p 92	N82-20566
	p 73	A84-38480	NCC3-46	p 120	N86-30236	p 92	N82-24501
	p 74	A85-13942		p 122	N87-18881	p 92	N82-24502
	p 77	A85-37440	NGR-22-009-339	p 88	N80-27720	p 39	N82-26436
	p 78	A85-41983		p 88	N80-29762	p 93	N82-26702
	p 80	A86-26689	NSF CME-80-06265	p 68	A83-15060	p 93	N82-26706
	p 83	A86-43771	NSG-1556	p 23	N80-29432	p 95	N83-12449
	p 99	N83-34370	NSG-3044	p 67	A82-46109	p 95	N83-12451
	p 105	N84-31693		p 67	A82-46806	p 96	N83-19121
	p 124	N87-24007		p 17	A84-33389	p 47	N83-19902
	p 125	N87-28944		p 80	A86-26896	p 55	N83-21373
NAG3-6	p 48	A84-46893		p 93	N82-26713	p 97	N83-27256
NAG3-730	p 86	A87-33719		p 93	N82-26714	p 97	N83-29734
NASA ORDER C-91113-D	p 118	N86-27689		p 93	N82-26715	p 98	N83-34349
NASA ORDER C-99066-G	p 122	N87-18881		p 93	N82-26716	p 99	N83-34372
NAS3-17760	p 64	A81-14162		p 94	N82-26717	p 39	N83-35103
NAS3-17787	p 37	N80-25415		p 94	N82-26718	p 100	N84-10612
	p 38	N82-10193	NSG-3079	p 4	A86-24677	p 100	N84-11512
	p 87	N80-22733	NSG-3105	p 47	A82-14400	p 100	N84-11513
NAS3-18546	p 35	A85-47972	NSG-3139	p 4	A86-26893	p 101	N84-14541
NAS3-18896	p 6	N80-21330		p 90	N81-26492	p 40	N84-17350
NAS3-19696	p 90	N81-19479	NSG-3147	p 35	A85-32399	p 102	N84-19925
NAS3-20382	p 90	N81-19480	NSG-3172	p 55	N83-27248	p 40	N84-20674
	p 90	N81-19481	NSG-3179	p 67	A83-12048	p 103	N84-20878
	p 90	N81-19482	NSG-3185	p 70	A83-44050	p 103	N84-22980
	p 90	N81-19483		p 16	A84-27356	p 104	N84-29248
NAS3-20407	p 23	N80-25382		p 18	A85-29133	p 40	N84-31348
NAS3-20632	p 87	N80-10515		p 25	N83-13173	p 105	N84-31687
NAS3-21020	p 64	A81-14162		p 26	N83-22325	p 41	N84-33564
NAS3-21379	p 38	N80-30482	NSG-3188	p 48	N82-29607	p 106	N84-34774
NAS3-21603	p 64	A81-29095	NSG-3197	p 23	N80-25383	p 106	N85-11380
NAS3-21824	p 76	A85-27935		p 23	N80-25384	p 119	N86-28464
NAS3-21836	p 7	N81-17079	NSG-3210	p 54	N82-18613	p 54	N81-28458
NAS3-22053	p 2	A83-40864		p 55	N83-21373	p 54	N82-18612
NAS3-22143	p 47	A82-48243		p 56	N83-28466	p 25	N82-21259
NAS3-22387	p 40	N84-10268	NSG-3217	p 24	N82-14288	p 96	N83-24874
NAS3-22522	p 33	A84-11194		p 25	N82-18326	p 99	N83-34373
	p 95	N83-12451	NSG-3239	p 127	N83-34656	p 96	N83-15672
NAS3-22525	p 1	A83-29737	NSG-3251	p 100	N84-11513	p 101	N84-13610
	p 76	A85-30313	NSG-3263	p 33	A83-22019	p 102	N84-16587
	p 7	N82-33391		p 33	A83-36166	p 102	N84-16588
	p 12	N86-27283		p 34	A85-12098	p 104	N84-30329
	p 13	N86-27284		p 39	N82-26436	p 109	N85-25893
NAS3-22533	p 69	A83-29824		p 93	N82-26702	p 26	N84-22702
	p 72	A84-29103		p 93	N82-26706	p 26	N84-24712
	p 73	A84-36492	NSG-3269	p 66	A82-42863	p 27	N84-25770
	p 100	N84-11514		p 51	A83-25571	p 27	N84-26756
	p 101	N84-11515		p 69	A83-37388	p 27	N84-27832
	p 8	N84-15153		p 55	N83-11506	p 27	N84-31288
	p 8	N84-15154		p 55	N83-11507	p 28	N84-34576
	p 104	N84-29252		p 55	N83-16773	p 28	N85-15822
NAS3-22534	p 33	A83-21071		p 56	N84-14525	p 29	N85-21273
	p 2	A85-18792	NSG-3283	p 47	A82-35462	p 90	N81-26492
NAS3-22550	p 36	A86-28951		p 48	A84-20580	p 90	N81-33497
	p 7	N82-25257		p 126	A85-21979	p 92	N82-21604
NAS3-22647	p 60	N86-28250		p 83	A86-43774	p 26	N83-15362
NAS3-22753	p 101	N84-12530		p 7	N82-33390	p 97	N83-28493
NAS3-22808	p 91	N82-17521		p 103	N84-19927	p 26	N84-13224
NAS3-22821	p 96	N83-21390	NSG-3303	p 69	A83-32987	p 8	N84-16181
NAS3-22825	p 75	A85-18795	NSG-3305	p 127	N83-23087	p 8	N84-16186
	p 118	N86-26652		p 127	N83-23088	p 9	N84-24578
NAS3-23245	p 19	A85-47970		p 127	N83-23089	p 28	N85-14882
NAS3-23272	p 117	N86-21932	NSG-3328	p 58	N85-21673	p 27	N84-26755
NAS3-23273	p 100	N84-10613	NSG-350	p 27	N84-31288	p 23	N81-16132
	p 100	N84-10614	N00014-78-C-0636	p 65	A82-32303	p 24	N81-25149
NAS3-23279	p 105	N84-31689	N00014-78-C-0647	p 68	A83-27431	p 24	N81-25151
NAS3-23281	p 4	A86-25743		p 68	A83-27432	p 24	N82-14287
	p 7	N84-13193	N00014-79-C-0579	p 17	A84-33389	p 24	N82-16181
NAS3-23282	p 56	N83-33182	RESEARCH FOUNDATION PROJ.			p 7	N82-22266
NAS3-23288	p 35	A85-43979	4246	p 43	N86-14356	p 25	N82-24300
	p 11	N85-31057	W-31-109-ENG-38	p 118	N86-27689	p 93	N82-26713
NAS3-23289	p 40	N84-13265	W-7405-ENG-26	p 109	N85-27260	p 93	N82-26714
NAS3-23525	p 7	N84-15152		p 113	N85-31545	p 93	N82-26715
NAS3-23533	p 12	N86-24693	481-50-32	p 124	N87-27268	p 93	N82-26716
NAS3-23687	p 110	N85-27261	485-49-02	p 29	N85-30034	p 94	N82-26717
	p 12	N85-32119	500-33-05	p 59	N86-13749	p 94	N82-26718
	p 12	N85-34140	505-01	p 88	N80-27719	p 94	N82-31707
	p 12	N86-11515	505-02	p 87	N80-15428	p 94	N82-31708
NAS3-23697	p 81	A86-34444		p 88	N80-22734	p 7	N82-33391
	p 81	A86-34445	505-32-22	p 101	N84-14542	p 29	N85-15823
	p 82	A86-34461	505-32-42	p 48	N82-28646	p 107	N85-18375
	p 106	N84-31700		p 48	N82-29607	p 29	N85-27978
	p 107	N85-21686	505-32-52	p 26	N83-19817	p 30	N86-21614
NAS3-23698	p 114	N85-31548	505-32-6A	p 95	N83-14523	p 106	N85-15184
NAS3-23925	p 112	N85-31531	505-33-1A	p 28	N84-34575	p 115	N85-34427
	p 115	N86-10589		p 29	N86-10290	p 107	N85-16205
NAS3-23927	p 114	N85-31548		p 42	N86-10311	p 41	N85-18124
NAS3-23939	p 60	N86-25003		p 42	N86-12294	p 41	N85-18125
NAS3-23940	p 114	N85-33541		p 44	N86-31699	p 41	N85-19074
NAS3-24382	p 110	N85-27953	505-33-1B	p 97	N83-24875	p 107	N85-21685
	p 110	N85-27954	505-33-12	p 102	N84-18683	p 42	N86-12292
NAS3-24389	p 81	A86-28655	505-33-22	p 89	N81-16492	p 116	N86-17788
	p 81	A86-28659		p 91	N82-16419	p 43	N86-21661
	p 111	N85-27955		p 54	N82-18613	p 43	N86-22686
	p 111	N85-27956		p 54	N82-20551	p 97	N83-29731
NCC1-15	p 99	N83-34373		p 91	N82-20565	p 49	N85-27226

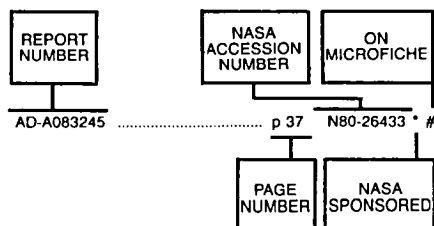
CONTRACT NUMBER INDEX

927-60-00

505-33-78	p 115	N86-10579	p 109	N85-25894
505-33-82	p 89	N81-16494	p 110	N85-27264
505-33	p 89	N81-11417	p 114	N85-32340
505-36-22	p 98	N83-33219	p 114	N85-32341
	p 29	N85-30035	p 43	N86-20542
505-40-14	p 11	N85-28945	p 117	N86-21951
505-40-5A	p 8	N84-20562	p 117	N86-25822
505-40-5B	p 8	N84-16185	p 125	N88-11140
505-45-23-01	p 97	N83-33217	p 61	N86-31912
505-53-1A	p 57	N84-32849	p 61	N86-31913
	p 57	N85-16195	p 62	N87-18109
505-53-12	p 56	N84-14526	p 124	N87-27269
505-63-01	p 45	N87-20408	p 61	N87-12910
505-63-11	p 116	N86-17789	p 121	N87-17087
	p 116	N86-18750	p 63	N88-12106
	p 116	N86-19663	p 58	N85-21674
	p 30	N86-24756	p 44	N86-25455
	p 30	N86-24757	p 121	N87-13794
	p 30	N86-24759	p 109	N85-27260
	p 43	N86-24818	p 62	N87-23987
	p 44	N86-25454	p 95	N83-11514
	p 44	N86-28164	p 120	N87-12017
	p 119	N86-28467	p 122	N87-18883
	p 31	N86-31663	p 124	N87-26385
	p 31	N86-31664	p 104	N84-31683
	p 120	N86-31920	p 119	N86-29271
	p 13	N86-32433	p 123	N87-22273
	p 49	N87-11993	p 47	N86-13495
	p 120	N87-12924	p 118	N86-27680
	p 31	N87-13491	p 122	N87-18881
	p 49	N87-13755	p 123	N87-23010
	p 44	N87-14489	p 125	N87-28944
	p 49	N87-15467	p 124	N87-24007
	p 122	N87-18115	p 105	N84-31688
	p 122	N87-18116	p 31	N87-16880
	p 31	N87-18614	p 112	N85-30361
	p 122	N87-20565	p 115	N86-10582
	p 123	N87-21375	p 96	N83-23631
	p 50	N87-23978	p 102	N84-16589
	p 123	N87-24006	p 121	N87-18112
	p 124	N87-24722		
	p 125	N87-28058		
	p 31	N87-28611		
	p 32	N88-12551		
	p 32	N88-12552		
505-63-31	p 30	N86-26376		
	p 121	N87-14730		
505-63-81	p 118	N86-25851		
506-41-11	p 61	N86-32764		
506-42-11	p 120	N86-30236		
506-43-11	p 59	N86-25002		
	p 60	N86-27666		
	p 61	N86-31065		
	p 61	N87-10399		
	p 62	N87-20562		
	p 62	N87-25589		
	p 62	N87-26362		
506-52-62	p 55	N83-11506		
	p 55	N83-16773		
	p 56	N84-14525		
506-53-1A	p 55	N83-23620		
	p 56	N84-15565		
	p 57	N84-17606		
	p 57	N84-34769		
	p 57	N85-10371		
	p 57	N85-20389		
	p 58	N85-21673		
	p 58	N85-29307		
	p 58	N85-32337		
	p 58	N86-10561		
	p 59	N86-16598		
	p 59	N86-19636		
	p 60	N86-25812		
	p 60	N86-27665		
	p 60	N86-28445		
506-55-22	p 99	N83-35412		
506-60-12	p 107	N85-20396		
	p 108	N85-24339		
	p 42	N86-12295		
	p 116	N86-16615		
506-63-1B	p 125	N88-12825		
506-63-11	p 50	N87-18820		
533-04-1A	p 104	N84-29247		
	p 9	N85-10951		
	p 107	N85-21686		
	p 108	N85-24338		
	p 12	N85-32119		
	p 12	N85-34140		
	p 115	N86-10589		
	p 115	N86-11495		
	p 120	N87-11180		
533-04-11	p 117	N86-21952		
	p 119	N86-28461		
	p 124	N87-26399		
	p 13	N87-28551		
533-04-12	p 108	N85-21691		

REPORT/ACCESSION NUMBER INDEX

Typical Report Number Index Listing



Listings in this index are arranged alpha-numerically by report number. The page number indicates the page on which the citation is located. The accession number denotes the number by which the citation is identified. An asterisk (*) indicates that the item is a NASA report. A pound sign (#) indicates that the item is available on microfiche.

AD-A083245 p 37 N80-26433 * #
 AD-A149178 p 41 N84-33584 * #
 AD-A152863 p 76 A85-24532 * #
 AD-A157112 p 42 N85-26964 * #
 AD-A171035 p 44 N86-25455 * #
 AD-A180176 p 44 N86-28164 * #

AFWAL-TR-80-2013 p 37 N80-26433 * #

AIAA PAPER 82-0776 p 67 A83-10900 * #
 AIAA PAPER 83-0848 p 1 A83-32791 * #
 AIAA PAPER 83-2445 p 2 A83-48331 * #
 AIAA PAPER 84-0849 p 18 A85-16096 * #
 AIAA PAPER 84-0974 p 18 A85-16094 * #
 AIAA PAPER 84-0991 p 75 A85-16095 * #
 AIAA PAPER 85-0621 p 77 A85-38425 * #
 AIAA PAPER 85-0645 p 76 A85-30313 * #
 AIAA PAPER 85-0761 p 3 A85-30378 * #
 AIAA PAPER 85-1140 p 78 A85-40814 * #
 AIAA PAPER 85-1198 p 19 A85-47022 * #
 AIAA PAPER 85-1354 p 3 A86-14430 * #
 AIAA PAPER 85-1418 p 77 A85-39769 * #
 AIAA PAPER 85-1419 p 78 A85-39770 * #
 AIAA PAPER 85-1420 p 35 A85-43979 * #
 AIAA PAPER 86-0846 p 5 A86-38894 * #
 AIAA PAPER 86-0943 p 82 A86-38838 * #
 AIAA PAPER 86-0948 p 82 A86-38842 * #
 AIAA PAPER 86-1016 p 83 A86-38873 * #
 AIAA PAPER 86-1190 p 19 A86-40596 * #
 AIAA PAPER 87-0719 p 85 A87-33645 * #
 AIAA PAPER 87-0738 p 87 A87-40497 * #
 AIAA PAPER 87-0739 p 86 A87-40496 * #
 AIAA PAPER 87-0753 p 85 A87-33648 * #
 AIAA PAPER 87-0766 p 85 A87-33581 * #
 AIAA PAPER 87-0827 p 126 A87-33614 * #
 AIAA PAPER 87-0910 p 86 A87-33719 * #
 AIAA PAPER 87-0947 p 86 A87-33756 * #

AIAA 80-0695 p 1 A80-35101 * #
 AIAA 81-0579 p 15 A81-29411 * #
 AIAA 81-0602 p 65 A81-29465 * #
 AIAA 83-0801 p 46 A83-29734 * #
 AIAA 83-0806 p 16 A83-29886 * #
 AIAA 83-0828 p 1 A83-29737 * #
 AIAA 83-0844 p 69 A83-29822 * #
 AIAA 83-0845 p 69 A83-29823 * #
 AIAA 83-0846 p 69 A83-29824 * #
 AIAA 83-1016 p 69 A83-29798 * #

AIAA-84-0991 p 103 N84-23923 * #
 AIAA-87-0738 p 122 N87-18115 * #
 AIAA-87-0739 p 122 N87-18116 * #

ANL-85-74 p 118 N86-27689 * #

AR-1 p 11 N85-31057 * #

ASLE PREPRINT 81-AM-5B-2 p 47 A81-33867 * #

ASME PAPER 81-DET-127 p 65 A82-19341 * #
 ASME PAPER 81-GT-24 p 1 A81-29940 * #
 ASME PAPER 82-GT-223 p 65 A82-35408 * #
 ASME PAPER 82-GT-292 p 47 A82-35462 * #
 ASME PAPER 83-APM-19 p 69 A83-37388 * #
 ASME PAPER 83-DET-20 p 72 A84-29103 * #
 ASME PAPER 83-GT-117 p 73 A84-33701 * #
 ASME PAPER 83-GT-132 p 73 A84-33702 * #
 ASME PAPER 83-GT-151 p 2 A83-47970 * #
 ASME PAPER 83-GT-152 p 70 A83-47978 * #
 ASME PAPER 84-GT-138 p 77 A85-32962 * #
 ASME PAPER 84-GT-139 p 73 A84-46957 * #
 ASME PAPER 84-GT-191 p 76 A85-23150 * #
 ASME PAPER 84-GT-292 p 48 A84-47046 * #
 ASME PAPER 84-GT-29 p 48 A84-46893 * #
 ASME PAPER 84-GT-96 p 73 A84-46937 * #
 ASME PAPER 84-PVP-112 p 75 A85-18795 * #
 ASME PAPER 84-PVP-77 p 2 A85-18792 * #
 ASME PAPER 84-WA/APM-38 p 75 A85-17039 * #
 ASME PAPER 84-WA/APM-41 p 75 A85-17040 * #
 ASME PAPER 85-GT-115 p 4 A86-22068 * #
 ASME PAPER 85-GT-134 p 5 A86-32956 * #
 ASME PAPER 85-GT-159 p 80 A86-22084 * #
 ASME PAPER 85-GT-170 p 5 A86-32957 * #
 ASME PAPER 86-GT-100 p 6 A87-25396 * #
 ASME PAPER 86-GT-172 p 6 A86-48224 * #
 ASME PAPER 86-GT-195 p 84 A86-48245 * #
 ASME PAPER 86-GT-243 p 84 A86-48271 * #
 ASME PAPER 86-GT-279 p 52 A86-48298 * #
 ASME PAPER 86-GT-34 p 84 A87-17988 * #
 ASME PAPER 86-GT-70 p 5 A86-48141 * #
 ASME PAPER 86-GT-75 p 52 A86-48143 * #
 ASME PAPER 86-GT-98 p 6 A86-48163 * #
 ASME PAPER 87-GT-8 p 53 A87-48702 * #

ASR-1 p 107 N85-21686 * #
 ASR-1 p 110 N85-27261 * #
 ASR-1 p 12 N85-34140 * #
 ASR-2 p 12 N85-32119 * #
 ASR-2 p 115 N86-10589 * #

ASRL-TR-154-15 p 88 N80-29762 * #

ASTL-MR-154-1 p 88 N80-27720 * #

AVRADCOM-TR-82-C-8 p 48 N82-28646 * #

AVSCOM-TR-83-C-6 p 40 N84-17350 * #

CCMS-84-13 p 29 N85-30035 * #

CML-82-4 p 25 N83-13173 * #

CML-82-5 p 26 N83-22325 * #

DOE/NASA/1028-29 p 89 N81-16494 * #

DOE/NASA/20305-6 p 54 N81-33492 * #

DOE/NASA/20320-38 p 54 N82-19550 * #

DOE/NASA/20320-49 p 112 N85-30361 * #

DOE/NASA/20320-66 p 115 N86-10582 * #

DOE/NASA/20370-79/19 p 53 N80-15422 * #

DOE/NASA/20485-2 p 96 N83-23631 * #

DOE/NASA/51040-35 p 46 N82-14359 * #

DOE/NASA/51040-51 p 102 N84-16589 * #

D2536-941001 p 90 N81-19479 * #

D2536-941002 p 90 N81-19480 * #

D2536-941003 p 90 N81-19481 * #

D2536-941004 p 90 N81-19482 * #

D2536-941005 p 90 N81-19483 * #

D2536-941006 p 8 N84-15154 * #

D2536-941007 p 100 N84-11514 * #

D2536-941008 p 101 N84-11515 * #

D2536-941010 p 8 N84-15153 * #

E-074 p 88 N80-22734 * #

E-1015 p 54 N81-33492 * #

E-1022 p 24 N82-16181 * #

E-1026-5 p 46 N82-14359 * #

E-1058 p 91 N82-16419 * #

E-1065 p 24 N82-14287 * #

E-1125 p 95 N83-12449 * #

E-1142 p 54 N82-19550 * #

E-1145 p 25 N82-22313 * #

E-1151 p 54 N82-20551 * #

E-1152 p 25 N82-21259 * #

E-1155 p 25 N82-24300 * #

E-1156 p 92 N82-21604 * #

E-1163 p 7 N82-22266 * #

E-1215 p 92 N82-24502 * #

E-1216 p 92 N82-24501 * #

E-1234 p 48 N82-28646 * #

E-1276 p 94 N82-31708 * #

E-1368 p 95 N83-14523 * #

E-1394 p 55 N83-16773 * #

E-1401 p 97 N83-24875 * #

E-1404 p 95 N83-11514 * #

E-1458 p 9 N85-10951 * #

E-1459 p 39 N83-14246 * #

E-1491 p 26 N83-15362 * #

E-1500 p 96 N83-19817 * #

E-1524 p 96 N83-24874 * #

E-1529 p 112 N85-30361 * #

E-1541 p 98 N83-34351 * #

E-1560 p 47 N83-19902 * #

E-1561 p 26 N83-19817 * #

E-1562 p 26 N83-24559 * #

E-1578 p 39 N83-35103 * #

E-1611 p 28 N85-14882 * #

E-1619 p 55 N83-23620 * #

E-1646 p 99 N83-34372 * #

E-164 p 21 N80-11143 * #

E-1733 p 97 N83-28493 * #

E-1748 p 8 N84-16185 * #

E-1754 p 8 N84-16181 * #

E-1755 p 26 N84-13224 * #

E-1787 p 98 N83-34349 * #

E-1794 p 100 N84-11512 * #

E-1795 p 40 N84-17350 * #

E-1804 p 100 N83-35413 * #

E-1816 p 115 N86-11495 * #

E-1820 p 99 N83-35412 * #

E-1828 p 101 N84-13610 * #

E-1829 p 9 N84-24578 * #

E-182 p 21 N80-11145 * #

E-1852 p 101 N84-14541 * #

E-1855-1 p 101 N84-14542 * #

E-1855 p 103 N84-20878 * #

E-1873 p 56 N84-15565 * #

E-1888 p 8 N84-20562 * #

E-1895 p 57 N84-17606 * #

E-1903 p 105 N84-31688 * #

E-1910 p 102 N84-16589 * #

E-1916 p 8 N84-16186 * #

E-1921 p 102 N84-16587 * #

E-1923 p 102 N84-16588 * #

E-1964 p 102 N84-18683 * #

E-1982 p 102 N84-19925 * #

E-1996 p 26 N84-24712 * #

E-2017 p 31 N86-31664 * #

E-2035 p 30 N86-21614 * #

E-203 p 21 N80-11144 * #

E-2063 p 40 N84-31348 * #

E-2069 p 26 N84-22702 * #

E-2074 p 103 N84-23923 * #

E-2108 p 104 N84-29248 * #

E-2120 p 104 N84-29247 * #

E-2146 p 27 N84-28918 * #

E-2152 p 27 N84-25770 * #

E-2154 p 27 N84-27832 * #

E-2158 p 27 N84-26755 * #

E-2160 p 27 N84-26756 * #

E-2175 p 104 N84-30329 * #

E-2185 p 57 N84-32849 * #

E-2201 p 28 N85-15822 * #

E-2203 p 27 N84-31288 * #

E-2222 p 104 N84-31683 * #

E-2232 p 105 N84-31687 * #

E-2242 p 29 N85-21273 * #

E-2260 p 41 N84-33564 * #

E-2267 p 120 N87-11180 * #

E-2284 p 28 N84-33522 * #

E-2290 p 57 N84-34769 * #

E-2296	p 57	N85-16195 * #	E-3330	p 121	N87-14730 * #	MTI-80TR29	p 87	N80-22733 * #
E-2307	p 28	N84-34576 * #	E-3342	p 122	N87-18883 * #			
E-2310	p 109	N85-25893 * #	E-3374	p 13	N87-28551 * #	NAS 1.15:100147	p 62	N87-26362 * #
E-2319	p 29	N85-15823 * #	E-3375	p 125	N87-28944 * #	NAS 1.15:100148	p 62	N87-25589 * #
E-2337	p 57	N85-10371 * #	E-3387	p 121	N87-18112 * #	NAS 1.15:100151	p 124	N87-26399 * #
E-2338	p 123	N87-22273 * #	E-3392	p 122	N87-18115 * #	NAS 1.15:100158	p 124	N87-27268 * #
E-2348	p 41	N85-18124 * #	E-3412	p 122	N87-18116 * #	NAS 1.15:100171	p 125	N87-28058 * #
E-2358	p 106	N85-15184 * #	E-3415	p 123	N87-24006 * #	NAS 1.15:100174	p 124	N87-27269 * #
E-235	p 53	N80-15422 * #	E-3430	p 123	N87-20566 * #	NAS 1.15:100176	p 32	N88-12552 * #
E-2368	p 112	N85-31530 * #	E-3443	p 122	N87-18882 * #	NAS 1.15:100177	p 63	N88-12106 * #
E-2373	p 107	N85-20396 * #	E-3445	p 122	N87-18881 * #	NAS 1.15:100192	p 31	N87-28611 * #
E-2393	p 107	N85-18375 * #	E-3446	p 62	N87-18109 * #	NAS 1.15:100238	p 32	N88-12551 * #
E-2398	p 107	N85-16205 * #	E-345	p 22	N80-20313 * #	NAS 1.15:100245	p 125	N88-12825 * #
E-2406	p 108	N85-21690 * #	E-3484	p 45	N87-20408 * #	NAS 1.15:82629	p 96	N83-23631 * #
E-241	p 88	N80-27719 * #	E-3504	p 62	N87-20562 * #	NAS 1.15:82810	p 54	N82-20551 * #
E-2439	p 41	N85-18125 * #	E-3528	p 123	N87-21375 * #	NAS 1.15:82811	p 25	N82-21259 * #
E-2444	p 41	N85-19074 * #	E-356	p 22	N80-18106 * #	NAS 1.15:82812	p 25	N82-24300 * #
E-2464	p 58	N85-21674 * #	E-3583	p 123	N87-23010 * #	NAS 1.15:82813	p 92	N82-21604 * #
E-2470	p 57	N85-20389 * #	E-3587	p 50	N87-23978 * #	NAS 1.15:82816	p 7	N82-22266 * #
E-2486	p 59	N86-22962 * #	E-3596	p 124	N87-24722 * #	NAS 1.15:82831	p 92	N82-26701 * #
E-2514	p 42	N85-26964 * #	E-3632	p 62	N87-23987 * #	NAS 1.15:82833	p 25	N82-22313 * #
E-2529	p 108	N85-24338 * #	E-3636	p 124	N87-24007 * #	NAS 1.15:82845	p 92	N82-24502 * #
E-2534	p 108	N85-24339 * #	E-3674	p 124	N87-26385 * #	NAS 1.15:82846	p 92	N82-24501 * #
E-2550	p 58	N85-29307 * #	E-367	p 37	N80-21493 * #	NAS 1.15:82850	p 94	N82-31707 * #
E-2562	p 49	N85-27226 * #	E-3705	p 62	N87-26362 * #	NAS 1.15:82865	p 48	N82-28646 * #
E-2571	p 110	N85-27264 * #	E-3706	p 62	N87-25589 * #	NAS 1.15:82882	p 25	N82-31449 * #
E-2575	p 42	N86-12295 * #	E-3712	p 124	N87-26399 * #	NAS 1.15:82896	p 94	N82-31708 * #
E-2576	p 115	N86-10579 * #	E-3720	p 124	N87-27268 * #	NAS 1.15:82953	p 95	N83-14523 * #
E-2588	p 11	N85-28945 * #	E-3736	p 125	N87-28058 * #	NAS 1.15:82975	p 95	N83-11514 * #
E-2591	p 58	N85-32337 * #	E-3743	p 124	N87-27269 * #	NAS 1.15:83022	p 9	N85-10951 * #
E-2598	p 115	N85-34427 * #	E-3750	p 32	N88-12552 * #	NAS 1.15:83023	p 39	N83-14246 * #
E-2606	p 29	N85-27978 * #	E-3753	p 63	N88-12106 * #	NAS 1.15:83044	p 26	N83-15362 * #
E-261	p 21	N80-12120 * #	E-3779	p 31	N87-28611 * #	NAS 1.15:83049	p 96	N83-15672 * #
E-2625	p 29	N85-30034 * #	E-3862	p 32	N88-12551 * #	NAS 1.15:83059	p 96	N83-24874 * #
E-2676	p 58	N86-10561 * #	E-3867	p 125	N88-12825 * #	NAS 1.15:83319	p 47	N83-19902 * #
E-2695	p 29	N86-10290 * #	E-386	p 22	N80-20314 * #	NAS 1.15:83320	p 26	N83-19817 * #
E-2704	p 119	N86-28464 * #	E-387	p 88	N80-23684 * #	NAS 1.15:83321	p 26	N83-24559 * #
E-2709	p 115	N86-10582 * #	E-408	p 22	N80-21452 * #	NAS 1.15:83331	p 39	N83-35103 * #
E-2710	p 42	N86-10311 * #	E-427	p 53	N80-22714 * #	NAS 1.15:83354	p 28	N85-14882 * #
E-2724	p 42	N86-12292 * #	E-437	p 88	N80-23678 * #	NAS 1.15:83358	p 55	N83-23620 * #
E-2727	p 125	N88-11140 * #	E-439	p 89	N81-11417 * #	NAS 1.15:83366	p 97	N83-24875 * #
E-2749	p 47	N86-13495 * #	E-446	p 22	N80-23370 * #	NAS 1.15:83437	p 97	N83-28493 * #
E-2778	p 42	N86-12294 * #	E-467	p 53	N80-24634 * #	NAS 1.15:83446	p 8	N84-16185 * #
E-2780	p 30	N86-24757 * #	E-482	p 54	N80-26682 * #	NAS 1.15:83470	p 112	N85-30361 * #
E-2782	p 30	N86-24759 * #	E-570	p 23	N81-12171 * #	NAS 1.15:83473	p 98	N83-34349 * #
E-2800	p 59	N86-13749 * #	E-576	p 89	N80-32753 * #	NAS 1.15:83478	p 100	N84-11512 * #
E-2832	p 116	N86-18750 * #	E-580	p 89	N81-11412 * #	NAS 1.15:83482	p 100	N83-35413 * #
E-2840	p 59	N86-16598 * #	E-600	p 38	N80-32486 * #	NAS 1.15:83491	p 99	N83-35412 * #
E-284	p 87	N80-13513 * #	E-624	p 23	N81-16132 * #	NAS 1.15:83495	p 101	N84-13610 * #
E-2858	p 59	N86-19636 * #	E-626	p 92	N82-20566 * #	NAS 1.15:83507	p 101	N84-14541 * #
E-2864	p 59	N86-16599 * #	E-633	p 89	N81-12446 * #	NAS 1.15:83509	p 101	N84-14542 * #
E-2865	p 43	N86-21661 * #	E-685	p 89	N81-16492 * #	NAS 1.15:83539	p 102	N84-16589 * #
E-2872	p 117	N86-25822 * #	E-687	p 91	N82-20565 * #	NAS 1.15:83544	p 8	N84-16186 * #
E-2873	p 116	N86-16615 * #	E-699	p 89	N81-16494 * #	NAS 1.15:83547	p 102	N84-16587 * #
E-2890	p 118	N86-26651 * #	E-700	p 90	N81-17480 * #	NAS 1.15:83549	p 102	N84-16588 * #
E-2898	p 116	N86-19663 * #	E-763	p 24	N81-25149 * #	NAS 1.15:83577	p 102	N84-18683 * #
E-2904	p 121	N87-16321 * #	E-782	p 38	N81-21174 * #	NAS 1.15:83594	p 26	N84-24712 * #
E-2940	p 122	N87-20565 * #	E-841	p 24	N81-25151 * #	NAS 1.15:83631	p 26	N84-22702 * #
E-2948	p 60	N86-27665 * #	E-882	p 96	N83-23631 * #	NAS 1.15:83634	p 103	N84-23923 * #
E-2949	p 59	N86-25002 * #	E-886	p 90	N81-26492 * #	NAS 1.15:83675	p 104	N84-29247 * #
E-2968	p 30	N86-25417 * #	E-910	p 54	N81-28458 * #	NAS 1.15:83691	p 27	N84-28918 * #
E-2988	p 120	N86-31920 * #	E-958	p 90	N81-33497 * #	NAS 1.15:83694	p 27	N84-25770 * #
E-2998	p 30	N86-24756 * #	E-959	p 54	N82-18612 * #	NAS 1.15:83696	p 27	N84-27832 * #
E-2999	p 43	N86-22686 * #	E-995	p 91	N82-11491 * #	NAS 1.15:83700	p 27	N84-26755 * #
E-3015	p 121	N87-13794 * #	E-9963	p 87	N80-15428 * #	NAS 1.15:83702	p 27	N84-26756 * #
E-3023	p 31	N87-18614 * #				NAS 1.15:83722	p 104	N84-29248 * #
E-3050	p 44	N86-31699 * #	FR-15652	p 40	N84-10268 * #	NAS 1.15:83729	p 27	N84-31288 * #
E-3066	p 118	N86-27680 * #				NAS 1.15:83735	p 104	N84-30329 * #
E-3075	p 44	N86-28164 * #	GT/PDL-170	p 9	N84-24586 * #	NAS 1.15:83737	p 104	N84-31683 * #
E-3081	p 60	N86-28445 * #				NAS 1.15:83754	p 29	N85-21273 * #
E-3086	p 60	N86-25812 * #	G7782	p 91	N82-17521 * #	NAS 1.15:83756	p 105	N84-31687 * #
E-3090	p 30	N86-26376 * #				NAS 1.15:83769	p 41	N84-33564 * #
E-3093	p 60	N86-27666 * #	H5ER-7698	p 23	N80-25382 * #	NAS 1.15:83778	p 40	N84-31348 * #
E-3096	p 61	N86-31912 * #				NAS 1.15:83786	p 28	N84-33522 * #
E-3112	p 31	N86-31663 * #	ICOMP-86-1	p 120	N87-12924 * #	NAS 1.15:83788	p 57	N84-32849 * #
E-3125	p 61	N86-31065 * #	ICOMP-87-1	p 122	N87-18881 * #	NAS 1.15:83794	p 57	N84-34769 * #
E-3127	p 119	N86-29271 * #				NAS 1.15:83802	p 28	N84-34576 * #
E-3155	p 119	N86-28461 * #	IFSM-80-102	p 23	N80-25383 * #	NAS 1.15:86876	p 57	N85-10371 * #
E-3158	p 120	N86-30236 * #	IFSM-80-103	p 23	N80-25384 * #	NAS 1.15:86877	p 123	N87-22273 * #
E-3166	p 61	N86-31913 * #				NAS 1.15:86891	p 106	N85-15184 * #
E-3168	p 44	N87-14489 * #	IIHR-232-III-VOL-3	p 127	N83-23087 * #	NAS 1.15:86908	p 107	N85-16205 * #
E-3181	p 120	N87-12924 * #	IIHR-232-IV-VOL-4	p 127	N83-23088 * #	NAS 1.15:86909	p 29	N85-15823 * #
E-319	p 21	N80-16102 * #	IIHR-232-V-VOL-5	p 127	N83-23089 * #	NAS 1.15:86913	p 108	N85-21690 * #
E-3201	p 61	N86-32764 * #				NAS 1.15:86916	p 107	N85-18375 * #
E-3225	p 31	N87-16880 * #	IITRI-M06001-89	p 38	N82-10193 * #	NAS 1.15:86924	p 28	N85-15822 * #
E-3229	p 121	N87-17087 * #	IITRI-M6001-82	p 37	N80-25415 * #	NAS 1.15:86929	p 41	N85-18124 * #
E-3231	p 50	N87-18820 * #	IITRI-M6003-53	p 6	N80-21330 * #	NAS 1.15:86930	p 41	N85-18125 * #
E-3245	p 13	N86-32433 * #				NAS 1.15:86933	p 41	N85-19074 * #
E-3247	p 120	N87-12017 * #	ITR-1	p 94	N82-33738 * #	NAS 1.15:86945	p 58	N85-21674 * #
E-3248	p 61	N87-10399 * #				NAS 1.15:86949	p 57	N85-20389 * #
E-3253	p 49	N87-15467 * #	L-15587	p 99	N83-34373 * #	NAS 1.15:86985	p 108	N85-24338 * #
E-3276	p 61	N87-12910 * #	L-15605	p 97	N83-33217 * #	NAS 1.15:86990	p 108	N85-24339 * #
E-3278	p 31	N87-13491 * #				NAS 1.15:87004	p 109	N85-25893 * #
E-3288	p 49	N87-11993 * #				NAS 1.15:87017	p 49	N85-27226 * #
E-3291	p 49	N87-13755 * #	MM-4998-86-13-PT-1	p 120	N86-30227 * #	NAS 1.15:87021	p 110	N85-27264 * #
E-331	p 22	N80-16107 * #	MM-4998-86-13-PT-2	p 119	N86-28455 * #	NAS 1.15:87022	p 42	N85-26964 * #

NAS 1.15:87033	p 11	N85-28945 * #	NAS 1.26:167938	p 48	N82-29607 * #	NAS 1.26:3750	p 56	N84-14526 * #
NAS 1.15:87035	p 58	N85-32337 * #	NAS 1.26:167944	p 7	N82-33390 * #	NAS 1.26:3756	p 56	N84-15565 * #
NAS 1.15:87045	p 29	N85-27978 * #	NAS 1.26:167949	p 7	N82-33391 * #	NAS 1.26:3770	p 57	N84-17606 * #
NAS 1.15:87058	p 29	N85-30034 * #	NAS 1.26:167967	p 96	N83-19121 * #	NAS 1.26:3790	p 102	N84-19925 * #
NAS 1.15:87088	p 58	N86-10561 * #	NAS 1.26:167989	p 40	N84-10268 * #	NAS 1.26:3851	p 57	N85-16195 * #
NAS 1.15:87101	p 29	N86-10290 * #	NAS 1.26:168057	p 26	N83-22325 * #	NAS 1.26:3877	p 58	N85-20390 * #
NAS 1.15:87102	p 115	N85-34427 * #	NAS 1.26:168100	p 96	N83-21390 * #	NAS 1.26:3904	p 58	N85-29307 * #
NAS 1.15:87109	p 115	N86-10582 * #	NAS 1.26:168154	p 97	N83-27256 * #	NAS 1.26:3976	p 60	N86-27665 * #
NAS 1.15:87110	p 42	N86-10311 * #	NAS 1.26:168171	p 118	N86-26652 * #	NAS 1.26:3977	p 59	N86-25002 * #
NAS 1.15:87117	p 42	N86-12292 * #	NAS 1.26:168176	p 7	N84-13193 * #	NAS 1.26:4001	p 60	N86-27666 * #
NAS 1.15:87150	p 42	N86-12294 * #	NAS 1.26:168182	p 98	N83-33219 * #	NAS 1.26:4002	p 60	N86-28445 * #
NAS 1.15:87153	p 47	N86-13495 * #	NAS 1.26:168190	p 56	N83-33182 * #	NAS 1.55:2271	p 98	N83-34351 * #
NAS 1.15:87154	p 30	N86-24757 * #	NAS 1.26:168191-VOL-1	p 100	N84-10613 * #	NAS 1.55:2289	p 115	N86-11495 * #
NAS 1.15:87164	p 59	N86-13749 * #	NAS 1.26:168191-VOL-2	p 100	N84-10614 * #	NAS 1.55:2297	p 105	N84-31688 * #
NAS 1.15:87182	p 116	N86-18750 * #	NAS 1.26:168198	p 97	N83-29734 * #	NAS 1.55:2339	p 120	N87-11180 * #
NAS 1.15:87186	p 59	N86-16598 * #	NAS 1.26:168225	p 100	N84-10612 * #	NAS 1.55:2369	p 112	N85-31530 * #
NAS 1.15:87203	p 59	N86-19636 * #	NAS 1.26:168228	p 11	N85-31057 * #	NAS 1.55:2383	p 59	N86-22962 * #
NAS 1.15:87207	p 116	N86-17789 * #	NAS 1.26:168260	p 40	N84-13265 * #	NAS 1.55:2405	p 125	N88-11140 * #
NAS 1.15:87208	p 43	N86-21661 * #	NAS 1.26:168280	p 100	N84-11513 * #	NAS 1.55:2423-REV	p 121	N87-16321 * #
NAS 1.15:87213	p 117	N86-25822 * #	NAS 1.26:168317	p 103	N84-19927 * #	NAS 1.60:1973	p 92	N82-20566 * #
NAS 1.15:87214	p 116	N86-16615 * #	NAS 1.26:168330	p 7	N84-15152 * #	NAS 1.60:1982	p 91	N82-20565 * #
NAS 1.15:87222	p 59	N86-16599 * #	NAS 1.26:168930	p 92	N82-20503 * #	NAS 1.60:2055	p 95	N83-12449 * #
NAS 1.15:87225	p 118	N86-26651 * #	NAS 1.26:169358	p 94	N82-33738 * #	NAS 1.60:2174	p 99	N83-34373 * #
NAS 1.15:87231	p 116	N86-19663 * #	NAS 1.26:170187	p 127	N83-23088 * #	NAS 1.60:2195	p 97	N83-33217 * #
NAS 1.15:87266	p 30	N86-25417 * #	NAS 1.26:170188	p 127	N83-23089 * #	NAS 1.60:2208	p 99	N83-34372 * #
NAS 1.15:87291	p 30	N86-24756 * #	NAS 1.26:170290	p 96	N83-23629 * #	NAS 1.60:2239	p 26	N84-13224 * #
NAS 1.15:87292	p 43	N86-22686 * #	NAS 1.26:173013	p 127	N83-34656 * #	NAS 1.60:2243	p 103	N84-20878 * #
NAS 1.15:87295	p 30	N86-24759 * #	NAS 1.26:173394	p 103	N84-21903 * #	NAS 1.60:2266	p 8	N84-16181 * #
NAS 1.15:87307	p 120	N86-31920 * #	NAS 1.26:173473	p 103	N84-21905 * #	NAS 1.60:2280	p 40	N84-17350 * #
NAS 1.15:87318	p 44	N86-31699 * #	NAS 1.26:173555	p 9	N84-24586 * #	NAS 1.60:2296	p 8	N84-20562 * #
NAS 1.15:87325	p 118	N86-27680 * #	NAS 1.26:173821	p 104	N84-29252 * #	NAS 1.60:2304	p 9	N84-24578 * #
NAS 1.15:87331	p 44	N86-28164 * #	NAS 1.26:173830	p 104	N84-31685 * #	NAS 1.60:2421	p 107	N85-20396 * #
NAS 1.15:87334	p 31	N86-31664 * #	NAS 1.26:174504	p 101	N84-15589 * #	NAS 1.60:2499	p 42	N86-12295 * #
NAS 1.15:87339	p 60	N86-25812 * #	NAS 1.26:174534	p 39	N84-10267 * #	NAS 1.60:2515	p 30	N86-21614 * #
NAS 1.15:87341	p 30	N86-26376 * #	NAS 1.26:174634	p 103	N84-22980 * #	NAS 1.60:2591	p 119	N86-28464 * #
NAS 1.15:87348	p 61	N86-31912 * #	NAS 1.26:174639	p 40	N84-20674 * #	NAS 1.60:2711	p 123	N87-20566 * #
NAS 1.15:88787	p 31	N86-31663 * #	NAS 1.26:174686	p 41	N84-32503 * #	NAS 1.61:1150	p 115	N86-10579 * #
NAS 1.15:88790	p 61	N86-31065 * #	NAS 1.26:174700	p 107	N85-21686 * #			
NAS 1.15:88792	p 119	N86-29271 * #	NAS 1.26:174708	p 12	N86-24693 * #	NASA-CASE-LEW-12493-1	p 23	N81-17170 *
NAS 1.15:88797	p 61	N86-31913 * #	NAS 1.26:174740	p 41	N85-15877 * #	NASA-CASE-LEW-12493-2	p 24	N81-26179 *
NAS 1.15:88807	p 119	N86-28461 * #	NAS 1.26:174757	p 106	N85-11380 * #	NASA-CASE-LEW-13717-1	p 49	N85-30333 *
NAS 1.15:88827	p 61	N86-32764 * #	NAS 1.26:174765	p 110	N85-27261 * #			
NAS 1.15:88838	p 120	N87-12924 * #	NAS 1.26:174765	p 12	N85-34140 * #	NASA-CP-2271	p 98	N83-34351 * #
NAS 1.15:88841	p 44	N87-14489 * #	NAS 1.26:174767	p 28	N84-34575 * #	NASA-CP-2289	p 115	N86-11495 * #
NAS 1.15:88854	p 120	N87-12017 * #	NAS 1.26:174774	p 106	N84-34774 * #	NASA-CP-2297	p 105	N84-31688 * #
NAS 1.15:88855	p 61	N87-10399 * #	NAS 1.26:174836	p 108	N85-21691 * #	NASA-CP-2339	p 120	N87-11180 * #
NAS 1.15:88857	p 13	N86-32433 * #	NAS 1.26:174855	p 109	N85-27260 * #	NASA-CP-2369	p 112	N85-31530 * #
NAS 1.15:88859	p 31	N87-16880 * #	NAS 1.26:174870	p 29	N85-30035 * #	NASA-CP-2383	p 59	N86-22962 * #
NAS 1.15:88861	p 121	N87-13794 * #	NAS 1.26:174871	p 58	N85-21673 * #	NASA-CP-2405	p 125	N88-11140 * #
NAS 1.15:88864	p 122	N87-20565 * #	NAS 1.26:174872	p 107	N85-21685 * #	NASA-CP-2423-REV	p 121	N87-16321 * #
NAS 1.15:88870	p 61	N87-12910 * #	NAS 1.26:174879	p 109	N85-25894 * #			
NAS 1.15:88871	p 50	N87-18820 * #	NAS 1.26:174892	p 117	N86-21932 * #	NASA-CR-159318	p 23	N80-29432 * #
NAS 1.15:88872	p 31	N87-13491 * #	NAS 1.26:174925	p 12	N85-32119 * #	NASA-CR-159571	p 23	N80-25382 * #
NAS 1.15:88875	p 49	N87-15467 * #	NAS 1.26:174940	p 114	N85-32340 * #	NASA-CR-159681	p 87	N80-10515 * #
NAS 1.15:88881	p 49	N87-11993 * #	NAS 1.26:174941	p 114	N85-32341 * #	NASA-CR-159728	p 90	N81-19479 * #
NAS 1.15:88883	p 49	N87-13755 * #	NAS 1.26:174952	p 60	N86-25003 * #	NASA-CR-159798	p 6	N80-21330 * #
NAS 1.15:88901	p 121	N87-17087 * #	NAS 1.26:174956	p 114	N85-33541 * #	NASA-CR-159823	p 90	N81-19480 * #
NAS 1.15:88907	p 121	N87-14730 * #	NAS 1.26:174980	p 115	N86-10589 * #	NASA-CR-159824	p 90	N81-19481 * #
NAS 1.15:88917	p 122	N87-18883 * #	NAS 1.26:175015	p 117	N86-21952 * #	NASA-CR-159825	p 90	N81-19482 * #
NAS 1.15:88932	p 13	N87-28551 * #	NAS 1.26:175021	p 116	N86-17788 * #	NASA-CR-159826	p 90	N81-19483 * #
NAS 1.15:88934	p 125	N87-28944 * #	NAS 1.26:175048	p 43	N86-24818 * #	NASA-CR-159838	p 87	N80-22733 * #
NAS 1.15:88941	p 121	N87-18112 * #	NAS 1.26:175049	p 117	N86-21951 * #	NASA-CR-159842	p 37	N80-25415 * #
NAS 1.15:88944	p 122	N87-18115 * #	NAS 1.26:175050	p 43	N86-20542 * #	NASA-CR-159860	p 23	N80-25384 * #
NAS 1.15:88959	p 122	N87-18116 * #	NAS 1.26:175052	p 44	N86-25454 * #	NASA-CR-159870	p 23	N80-25383 * #
NAS 1.15:88960	p 123	N87-24006 * #	NAS 1.26:175057	p 118	N86-27689 * #	NASA-CR-159873	p 88	N80-27720 * #
NAS 1.15:88965	p 31	N87-18614 * #	NAS 1.26:175100	p 44	N86-25455 * #	NASA-CR-159874	p 88	N80-29762 * #
NAS 1.15:88974	p 122	N87-18882 * #	NAS 1.26:175112	p 12	N86-27283 * #	NASA-CR-160501	p 24	N82-14288 * #
NAS 1.15:88976	p 122	N87-18881 * #	NAS 1.26:175113	p 13	N86-27284 * #	NASA-CR-165123	p 38	N80-30482 * #
NAS 1.15:88978	p 62	N87-18109 * #	NAS 1.26:175115	p 118	N86-25851 * #	NASA-CR-165250	p 7	N81-17079 * #
NAS 1.15:88981	p 45	N87-20408 * #	NAS 1.26:175551	p 108	N85-23096 * #	NASA-CR-165407	p 38	N82-10193 * #
NAS 1.15:88983	p 62	N87-20562 * #	NAS 1.26:175573	p 11	N85-21165 * #	NASA-CR-165412	p 93	N82-26713 * #
NAS 1.15:88986	p 123	N87-21375 * #	NAS 1.26:175574	p 107	N85-21687 * #	NASA-CR-165428	p 8	N84-15154 * #
NAS 1.15:88991	p 123	N87-23010 * #	NAS 1.26:175605	p 11	N85-22391 * #	NASA-CR-165429	p 100	N84-11514 * #
NAS 1.15:88997	p 50	N87-23978 * #	NAS 1.26:175609	p 108	N85-21720 * #	NASA-CR-165430	p 101	N84-11515 * #
NAS 1.15:89000	p 124	N87-24722 * #	NAS 1.26:175747	p 109	N85-25896 * #	NASA-CR-165433	p 93	N82-26714 * #
NAS 1.15:89006	p 124	N87-26385 * #	NAS 1.26:175795	p 110	N85-27263 * #	NASA-CR-165434	p 93	N82-26715 * #
NAS 1.15:89029	p 62	N87-23987 * #	NAS 1.26:175901	p 11	N85-27868 * #	NASA-CR-165438	p 93	N82-26716 * #
NAS 1.15:89031	p 124	N87-24007 * #	NAS 1.26:176220	p 115	N86-10588 * #	NASA-CR-165439	p 94	N82-26717 * #
NAS 1.26:10186	p 127	N83-23087 * #	NAS 1.26:176418	p 43	N86-14356 * #	NASA-CR-165440	p 94	N82-26718 * #
NAS 1.26:165412	p 93	N82-26713 * #	NAS 1.26:176821	p 117	N86-25850 * #	NASA-CR-165461	p 25	N83-13173 * #
NAS 1.26:165428	p 8	N84-15154 * #	NAS 1.26:177194	p 119	N86-28462 * #	NASA-CR-165488	p 91	N82-14531 * #
NAS 1.26:165429	p 100	N84-11514 * #	NAS 1.26:177233	p 119	N86-28455 * #	NASA-CR-165497	p 93	N82-26702 * #
NAS 1.26:165430	p 101	N84-11515 * #	NAS 1.26:177237	p 120	N86-30227 * #	NASA-CR-165498	p 93	N82-26706 * #
NAS 1.26:165433	p 93	N82-26714 * #	NAS 1.26:179474	p 119	N86-28467 * #	NASA-CR-165561	p 91	N82-17521 * #
NAS 1.26:165434	p 93	N82-26715 * #	NAS 1.26:179478	p 120	N86-30236 * #	NASA-CR-165563	p 91	N82-20564 * #
NAS 1.26:165438	p 93	N82-26716 * #	NAS 1.26:3543	p 39	N82-26436 * #	NASA-CR-165571	p 95	N83-12451 * #
NAS 1.26:165439	p 94	N82-26717 * #	NAS 1.26:3623	p 55	N83-11506 * #	NASA-CR-167896	p 7	N82-25257 * #
NAS 1.26:165440	p 94	N82-26718 * #	NAS 1.26:3625	p 55	N83-11507 * #	NASA-CR-167897	p 94	N82-29619 * #
NAS 1.26:165461	p 25	N83-13173 * #	NAS 1.26:3659	p 55	N83-16773 * #	NASA-CR-167927	p 8	N84-15153 * #
NAS 1.26:165497	p 93	N82-26702 * #	NAS 1.26:3670	p 55	N83-27248 * #	NASA-CR-167938	p 48	N82-29607 * #
NAS 1.26:165498	p 93	N82-26706 * #	NAS 1.26:3679	p 55	N83-21373 * #	NASA-CR-167944	p 7	N82-33390 * #
NAS 1.26:165563	p 91	N82-20564 * #	NAS 1.26:3693	p 56	N83-28466 * #	NASA-CR-167949	p 7	N82-33391 * #
NAS 1.26:165571	p 95	N83-12451 * #	NAS 1.26:3697	p 97	N83-29731 * #	NASA-CR-167967	p 96	N83-19121 * #
NAS 1.26:167896	p 7	N82-25257 * #	NAS 1.26:3724	p 56	N83-33180 * #	NASA-CR-167989	p 40	N84-10268 * #
NAS 1.26:167897	p 94	N82-29619 * #	NAS 1.26:3729	p 101	N84-12530 * #	NASA-CR-168057	p 26	N83-22325 * #
NAS 1.26:167927	p 8	N84-15153 * #	NAS 1.26:3749	p 56	N84-14525 * #	NASA-CR-168100	p 96	N83-21390 * #

NASA-CR-168154	p 97	N83-27256 * #	NASA-CR-3851	p 57	N85-16195 * #	NASA-TM-83478	p 100	N84-11512 * #
NASA-CR-168171	p 118	N86-26652 * #	NASA-CR-3877	p 58	N85-20390 * #	NASA-TM-83482	p 100	N83-35413 * #
NASA-CR-168176	p 7	N84-13193 * #	NASA-CR-3904	p 58	N85-29307 * #	NASA-TM-83491	p 99	N83-35412 * #
NASA-CR-168182	p 98	N83-33219 * #	NASA-CR-3976	p 60	N86-27665 * #	NASA-TM-83495	p 101	N84-13610 * #
NASA-CR-168190	p 56	N83-33182 * #	NASA-CR-3977	p 59	N86-25002 * #	NASA-TM-83507	p 101	N84-14541 * #
NASA-CR-168191-VOL-1	p 100	N84-10613 * #	NASA-CR-4001	p 60	N86-27666 * #	NASA-TM-83509	p 101	N84-14542 * #
NASA-CR-168191-VOL-2	p 100	N84-10614 * #	NASA-CR-4002	p 60	N86-28445 * #	NASA-TM-83539	p 102	N84-16589 * #
NASA-CR-168198	p 97	N83-29734 * #				NASA-TM-83544	p 8	N84-16186 * #
NASA-CR-168225	p 100	N84-10612 * #	NASA-RP-1150	p 115	N86-10579 * #	NASA-TM-83547	p 102	N84-16587 * #
NASA-CR-168228	p 11	N85-31057 * #				NASA-TM-83549	p 102	N84-16588 * #
NASA-CR-168260	p 40	N84-13265 * #	NASA-TM-100147	p 62	N87-26362 * #	NASA-TM-83577	p 102	N84-16683 * #
NASA-CR-168280	p 100	N84-11513 * #	NASA-TM-100148	p 62	N87-25589 * #	NASA-TM-83594	p 26	N84-24712 * #
NASA-CR-168317	p 103	N84-19927 * #	NASA-TM-100151	p 124	N87-26399 * #	NASA-TM-83631	p 26	N84-22702 * #
NASA-CR-168330	p 7	N84-15152 * #	NASA-TM-100158	p 124	N87-27268 * #	NASA-TM-83634	p 103	N84-23923 * #
NASA-CR-168550	p 25	N82-18326 * #	NASA-TM-100171	p 125	N87-28058 * #	NASA-TM-83675	p 104	N84-29247 * #
NASA-CR-168930	p 92	N82-24503 * #	NASA-TM-100174	p 124	N87-27269 * #	NASA-TM-83691	p 27	N84-28918 * #
NASA-CR-169358	p 94	N82-33738 * #	NASA-TM-100176	p 32	N88-12552 * #	NASA-TM-83694	p 27	N84-25770 * #
NASA-CR-170186	p 127	N83-23087 * #	NASA-TM-100177	p 63	N88-12106 * #	NASA-TM-83696	p 27	N84-27832 * #
NASA-CR-170187	p 127	N83-23088 * #	NASA-TM-100192	p 31	N87-28611 * #	NASA-TM-83700	p 27	N84-26755 * #
NASA-CR-170188	p 127	N83-23089 * #	NASA-TM-100238	p 32	N88-12551 * #	NASA-TM-83702	p 27	N84-26756 * #
NASA-CR-170290	p 96	N83-23629 * #	NASA-TM-100245	p 125	N88-12825 * #	NASA-TM-83722	p 104	N84-29248 * #
NASA-CR-173013	p 127	N83-34656 * #	NASA-TM-79253	p 21	N80-11143 * #	NASA-TM-83729	p 27	N84-31288 * #
NASA-CR-173394	p 103	N84-21903 * #	NASA-TM-79276	p 21	N80-11144 * #	NASA-TM-83735	p 104	N84-30329 * #
NASA-CR-173473	p 103	N84-21905 * #	NASA-TM-79281	p 21	N80-11145 * #	NASA-TM-83737	p 104	N84-31683 * #
NASA-CR-173555	p 9	N84-24586 * #	NASA-TM-79291	p 53	N80-15422 * #	NASA-TM-83754	p 29	N85-21273 * #
NASA-CR-173821	p 104	N84-29252 * #	NASA-TM-79306	p 21	N80-12120 * #	NASA-TM-83756	p 105	N84-31687 * #
NASA-CR-173830	p 104	N84-31685 * #	NASA-TM-80980	p 37	N80-26433 * #	NASA-TM-83769	p 41	N84-33564 * #
NASA-CR-174504	p 101	N84-15589 * #	NASA-TM-81379	p 87	N80-13513 * #	NASA-TM-83778	p 40	N84-31348 * #
NASA-CR-174534	p 39	N84-10267 * #	NASA-TM-81404	p 22	N80-16107 * #	NASA-TM-83786	p 28	N84-33522 * #
NASA-CR-174634	p 103	N84-22980 * #	NASA-TM-81405	p 21	N80-16102 * #	NASA-TM-83788	p 57	N84-32849 * #
NASA-CR-174639	p 40	N84-20674 * #	NASA-TM-81422	p 22	N80-20313 * #	NASA-TM-83794	p 57	N84-34769 * #
NASA-CR-174686	p 41	N84-32503 * #	NASA-TM-81432	p 22	N80-18106 * #	NASA-TM-83802	p 28	N84-34576 * #
NASA-CR-174700	p 107	N85-21686 * #	NASA-TM-81448	p 37	N80-21493 * #	NASA-TM-86876	p 57	N85-10371 * #
NASA-CR-174708	p 12	N86-24693 * #	NASA-TM-81456	p 22	N80-20314 * #	NASA-TM-86877	p 123	N87-22273 * #
NASA-CR-174740	p 41	N85-15877 * #	NASA-TM-81474	p 22	N80-21452 * #	NASA-TM-86891	p 106	N85-15184 * #
NASA-CR-174757	p 106	N85-11380 * #	NASA-TM-81489	p 53	N80-22714 * #	NASA-TM-86908	p 107	N85-16205 * #
NASA-CR-174765	p 110	N85-27261 * #	NASA-TM-81500	p 88	N80-23678 * #	NASA-TM-86909	p 29	N85-15823 * #
NASA-CR-174765	p 12	N85-34140 * #	NASA-TM-81508	p 22	N80-23370 * #	NASA-TM-86913	p 108	N85-21690 * #
NASA-CR-174767	p 28	N84-34575 * #	NASA-TM-81517	p 88	N80-23684 * #	NASA-TM-86916	p 107	N85-18375 * #
NASA-CR-174774	p 106	N84-34774 * #	NASA-TM-81523	p 53	N80-24634 * #	NASA-TM-86924	p 28	N85-15822 * #
NASA-CR-174836	p 108	N85-21691 * #	NASA-TM-81530	p 54	N80-26682 * #	NASA-TM-86929	p 41	N85-18124 * #
NASA-CR-174855	p 109	N85-27260 * #	NASA-TM-81591	p 23	N81-12171 * #	NASA-TM-86930	p 41	N85-18125 * #
NASA-CR-174870	p 29	N85-30035 * #	NASA-TM-81593	p 89	N80-32753 * #	NASA-TM-86933	p 41	N85-19074 * #
NASA-CR-174871	p 58	N85-21673 * #	NASA-TM-81597	p 89	N81-11412 * #	NASA-TM-86945	p 58	N85-21674 * #
NASA-CR-174872	p 107	N85-21685 * #	NASA-TM-81607	p 38	N80-32486 * #	NASA-TM-86949	p 57	N85-20389 * #
NASA-CR-174879	p 109	N85-25894 * #	NASA-TM-81618	p 23	N81-16132 * #	NASA-TM-86985	p 108	N85-24338 * #
NASA-CR-174892	p 117	N86-21932 * #	NASA-TM-81623	p 89	N81-12446 * #	NASA-TM-86990	p 108	N85-24339 * #
NASA-CR-174925	p 12	N85-32119 * #	NASA-TM-81665	p 89	N81-16492 * #	NASA-TM-87004	p 109	N85-25893 * #
NASA-CR-174940	p 114	N85-32340 * #	NASA-TM-81674	p 89	N81-16494 * #	NASA-TM-87017	p 49	N85-27226 * #
NASA-CR-174941	p 114	N85-32341 * #	NASA-TM-81675	p 90	N81-17480 * #	NASA-TM-87021	p 110	N85-27264 * #
NASA-CR-174952	p 60	N86-25003 * #	NASA-TM-81747	p 38	N81-21174 * #	NASA-TM-87022	p 42	N85-26964 * #
NASA-CR-174956	p 114	N85-33541 * #	NASA-TM-82593	p 24	N81-25151 * #	NASA-TM-87033	p 11	N85-28945 * #
NASA-CR-174980	p 115	N86-10589 * #	NASA-TM-82596	p 24	N81-25149 * #	NASA-TM-87035	p 58	N85-32337 * #
NASA-CR-175015	p 117	N86-21952 * #	NASA-TM-82629	p 96	N83-23631 * #	NASA-TM-87045	p 29	N85-27978 * #
NASA-CR-175021	p 116	N86-17788 * #	NASA-TM-82631	p 90	N81-26492 * #	NASA-TM-87058	p 29	N85-30034 * #
NASA-CR-175048	p 43	N86-24818 * #	NASA-TM-82651	p 54	N81-28458 * #	NASA-TM-87088	p 58	N86-10561 * #
NASA-CR-175049	p 117	N86-21951 * #	NASA-TM-82675	p 90	N81-33497 * #	NASA-TM-87101	p 29	N86-10290 * #
NASA-CR-175050	p 43	N86-20542 * #	NASA-TM-82713	p 91	N82-11491 * #	NASA-TM-87102	p 115	N85-34427 * #
NASA-CR-175052	p 44	N86-25454 * #	NASA-TM-82717	p 54	N81-33492 * #	NASA-TM-87109	p 115	N86-10582 * #
NASA-CR-175057	p 118	N86-27689 * #	NASA-TM-82745	p 91	N82-16419 * #	NASA-TM-87110	p 42	N86-10311 * #
NASA-CR-175100	p 44	N86-25455 * #	NASA-TM-82749	p 24	N82-14287 * #	NASA-TM-87117	p 42	N86-12292 * #
NASA-CR-175112	p 12	N86-27283 * #	NASA-TM-82765	p 46	N82-14359 * #	NASA-TM-87150	p 42	N86-12294 * #
NASA-CR-175113	p 13	N86-27284 * #	NASA-TM-82780	p 24	N82-16181 * #	NASA-TM-87153	p 47	N86-13495 * #
NASA-CR-175115	p 118	N86-25851 * #	NASA-TM-82793	p 54	N82-18612 * #	NASA-TM-87154	p 30	N86-24757 * #
NASA-CR-175551	p 108	N85-23096 * #	NASA-TM-82803	p 54	N82-19550 * #	NASA-TM-87164	p 59	N86-13749 * #
NASA-CR-175573	p 11	N85-21165 * #	NASA-TM-82810	p 54	N82-20551 * #	NASA-TM-87182	p 116	N86-18750 * #
NASA-CR-175574	p 107	N85-21687 * #	NASA-TM-82811	p 25	N82-21259 * #	NASA-TM-87186	p 59	N86-16598 * #
NASA-CR-175605	p 11	N85-22391 * #	NASA-TM-82812	p 25	N82-24300 * #	NASA-TM-87203	p 59	N86-19636 * #
NASA-CR-175609	p 108	N85-21720 * #	NASA-TM-82813	p 92	N82-21604 * #	NASA-TM-87207	p 116	N86-17789 * #
NASA-CR-175747	p 109	N85-25896 * #	NASA-TM-82816	p 7	N82-22266 * #	NASA-TM-87208	p 43	N86-21661 * #
NASA-CR-175795	p 110	N85-27263 * #	NASA-TM-82831	p 92	N82-26701 * #	NASA-TM-87213	p 117	N86-25822 * #
NASA-CR-175901	p 11	N85-27868 * #	NASA-TM-82833	p 25	N82-22313 * #	NASA-TM-87214	p 116	N86-16615 * #
NASA-CR-176220	p 115	N86-10588 * #	NASA-TM-82845	p 92	N82-24502 * #	NASA-TM-87222	p 59	N86-16599 * #
NASA-CR-176418	p 43	N86-14356 * #	NASA-TM-82846	p 92	N82-24501 * #	NASA-TM-87225	p 118	N86-26651 * #
NASA-CR-176821	p 117	N86-25850 * #	NASA-TM-82850	p 94	N82-31707 * #	NASA-TM-87231	p 116	N86-19663 * #
NASA-CR-177194	p 119	N86-28462 * #	NASA-TM-82865	p 48	N82-28646 * #	NASA-TM-87266	p 30	N86-25417 * #
NASA-CR-177233	p 119	N86-28455 * #	NASA-TM-82882	p 25	N82-31449 * #	NASA-TM-87291	p 30	N86-24756 * #
NASA-CR-177237	p 120	N86-30227 * #	NASA-TM-82896	p 94	N82-31708 * #	NASA-TM-87292	p 43	N86-22686 * #
NASA-CR-179474	p 119	N86-28467 * #	NASA-TM-82953	p 95	N83-14523 * #	NASA-TM-87295	p 30	N86-24759 * #
NASA-CR-179478	p 120	N86-30236 * #	NASA-TM-82975	p 95	N83-11514 * #	NASA-TM-87307	p 120	N86-31920 * #
NASA-CR-3506	p 54	N82-18613 * #	NASA-TM-83022	p 9	N85-10951 * #	NASA-TM-87318	p 44	N86-31699 * #
NASA-CR-3543	p 39	N82-26434 * #	NASA-TM-83023	p 39	N83-14246 * #	NASA-TM-87325	p 118	N86-27680 * #
NASA-CR-3623	p 55	N83-11506 * #	NASA-TM-83044	p 26	N83-15362 * #	NASA-TM-87331	p 44	N86-28164 * #
NASA-CR-3625	p 55	N83-11507 * #	NASA-TM-83049	p 96	N83-15672 * #	NASA-TM-87334	p 31	N86-31664 * #
NASA-CR-3659	p 55	N83-16773 * #	NASA-TM-83059	p 96	N83-24874 * #	NASA-TM-87339	p 60	N86-25812 * #
NASA-CR-3670	p 55	N83-27248 * #	NASA-TM-83319	p 47	N83-19902 * #	NASA-TM-87341	p 30	N86-26376 * #
NASA-CR-3679	p 55	N83-21373 * #	NASA-TM-83320	p 26	N83-19817 * #	NASA-TM-87348	p 61	N86-31912 * #
NASA-CR-3693	p 56	N83-28466 * #	NASA-TM-83321	p 26	N83-24559 * #	NASA-TM-88787	p 31	N86-31663 * #
NASA-CR-3697	p 97	N83-29731 * #	NASA-TM-83331	p 39	N83-35103 * #	NASA-TM-88790	p 61	N86-31065 * #
NASA-CR-3724	p 56	N83-33180 * #	NASA-TM-83354	p 28	N85-14882 * #	NASA-TM-88792	p 119	N86-29271 * #
NASA-CR-3729	p 101	N84-12530 * #	NASA-TM-83358	p 55	N83-23620 * #	NASA-TM-88797	p 61	N86-31913 * #
NASA-CR-3749	p 56	N84-14525 * #	NASA-TM-83366	p 97	N83-24875 * #	NASA-TM-88807	p 119	N86-28461 * #
NASA-CR-3750	p 56	N84-14526 * #	NASA-TM-83437	p 97	N83-28493 * #	NASA-TM-88827	p 61	N86-32764 * #
NASA-CR-3756	p 56	N84-15565 * #	NASA-TM-83446	p 8	N84-16185 * #	NASA-TM-88838	p 120	N87-12924 * #
NASA-CR-3770	p 57	N84-17606 * #	NASA-TM-83470	p 112	N85-30361 * #	NASA-TM-88841	p 44	N87-14489 * #
NASA-CR-3790	p 102	N84-19925 * #	NASA-TM-83473	p 98	N83-34349 * #	NASA-TM-88854	p 120	N87-12017 * #

NASA-TM-88855	p 61	N87-10399 * #	US-PATENT-APPL-SN-893857	p 24	N81-26179 * #
NASA-TM-88857	p 13	N86-32433 * #	US-PATENT-CLASS-156-292	p 23	N81-17170 * #
NASA-TM-88859	p 31	N87-16880 * #	US-PATENT-CLASS-228-118	p 23	N81-17170 * #
NASA-TM-88861	p 121	N87-13794 * #	US-PATENT-CLASS-228-118	p 24	N81-26179 * #
NASA-TM-88864	p 122	N87-20565 * #	US-PATENT-CLASS-228-170	p 23	N81-17170 * #
NASA-TM-88870	p 61	N87-12910 * #	US-PATENT-CLASS-228-174	p 23	N81-17170 * #
NASA-TM-88871	p 50	N87-18820 * #	US-PATENT-CLASS-228-190	p 23	N81-17170 * #
NASA-TM-88872	p 31	N87-13491 * #	US-PATENT-CLASS-228-190	p 24	N81-26179 * #
NASA-TM-88875	p 49	N87-15467 * #	US-PATENT-CLASS-310-77	p 49	N85-30333 * #
NASA-TM-88881	p 49	N87-11993 * #	US-PATENT-CLASS-310-93	p 49	N85-30333 * #
NASA-TM-88883	p 49	N87-13755 * #	US-PATENT-CLASS-318-611	p 49	N85-30333 * #
NASA-TM-88901	p 121	N87-17087 * #	US-PATENT-CLASS-335-100	p 49	N85-30333 * #
NASA-TM-88907	p 121	N87-14730 * #	US-PATENT-4,211,354	p 23	N81-17170 * #
NASA-TM-88917	p 122	N87-18883 * #	US-PATENT-4,211,354	p 24	N81-26179 * #
NASA-TM-88932	p 13	N87-28551 * #	US-PATENT-4,267,953	p 24	N81-26179 * #
NASA-TM-88934	p 125	N87-28944 * #	US-PATENT-4,517,505	p 49	N85-30333 * #
NASA-TM-88941	p 121	N87-18112 * #	USAAVSCOM-TR-84-C-16	p 41	N84-33564 * #
NASA-TM-88944	p 122	N87-18115 * #	USAAVSCOM-TR-85-C-10	p 11	N85-28945 * #
NASA-TM-88959	p 122	N87-18116 * #	USAAVSCOM-TR-85-C-1	p 41	N85-19074 * #
NASA-TM-88960	p 123	N87-24006 * #	USAAVSCOM-TR-85-C-5	p 42	N85-26964 * #
NASA-TM-88965	p 31	N87-18614 * #	USAAVSCOM-TR-86-C-14	p 44	N86-25454 * #
NASA-TM-88974	p 122	N87-18882 * #	USAAVSCOM-TR-86-C-18	p 44	N86-25455 * #
NASA-TM-88976	p 122	N87-18881 * #	USAAVSCOM-TR-86-C-4	p 43	N86-24818 * #
NASA-TM-88978	p 62	N87-18109 * #	USAAVSCOM-TR-86-C-7	p 44	N86-28164 * #
NASA-TM-88983	p 45	N87-20408 * #	UTRC83-6	p 101	N84-12530 * #
NASA-TM-88984	p 62	N87-20562 * #	UWME-DR-101-102-1	p 24	N82-14288 * #
NASA-TM-88986	p 123	N87-21375 * #	UWME-DR-201-101-1	p 25	N82-18326 * #
NASA-TM-88989	p 123	N87-23010 * #	VPI-E-83.10	p 98	N83-33219 * #
NASA-TM-88991	p 123	N87-23010 * #	VPI-E-84-36	p 108	N85-21720 * #
NASA-TM-88997	p 50	N87-23978 * #			
NASA-TM-88990	p 124	N87-24722 * #			
NASA-TM-88996	p 124	N87-26385 * #			
NASA-TM-88992	p 62	N87-23987 * #			
NASA-TM-88931	p 124	N87-24007 * #			
NASA-TP-1600	p 87	N80-15428 * #			
NASA-TP-1669	p 88	N80-22734 * #			
NASA-TP-1679	p 88	N80-27719 * #			
NASA-TP-1753	p 89	N81-11417 * #			
NASA-TP-1973	p 92	N82-20566 * #			
NASA-TP-1982	p 91	N82-20565 * #			
NASA-TP-2055	p 95	N83-12449 * #			
NASA-TP-2174	p 99	N83-34373 * #			
NASA-TP-2195	p 97	N83-33217 * #			
NASA-TP-2208	p 99	N83-34372 * #			
NASA-TP-2239	p 26	N84-13224 * #			
NASA-TP-2243	p 103	N84-20878 * #			
NASA-TP-2266	p 8	N84-16181 * #			
NASA-TP-2280	p 40	N84-17350 * #			
NASA-TP-2296	p 8	N84-20562 * #			
NASA-TP-2304	p 9	N84-24578 * #			
NASA-TP-2421	p 107	N85-20396 * #			
NASA-TP-2499	p 42	N86-12295 * #			
NASA-TP-2515	p 30	N86-21614 * #			
NASA-TP-2591	p 119	N86-28464 * #			
NASA-TP-2711	p 123	N87-20566 * #			
NAUFP-202-2	p 103	N84-19927 * #			
PB85-127173	p 108	N85-21720 * #			
PWA-FR-13153-PT-2	p 38	N80-30482 * #			
PWA-5512-45	p 87	N80-10515 * #			
PWA-5684-19	p 7	N81-17079 * #			
PWA-5772-23	p 7	N82-25257 * #			
PWA-5774-21	p 7	N82-33391 * #			
PWA-5774-39	p 13	N86-27284 * #			
PWA-5774-40	p 12	N86-27283 * #			
PWA-5843-13	p 96	N83-21390 * #			
PWA-5891-18	p 56	N83-33182 * #			
PWA-5894-17	p 11	N85-31057 * #			
PWA-5940-19	p 107	N85-21686 * #			
PWA-5968-19	p 60	N86-25003 * #			
RF-TECH-104	p 55	N83-16773 * #			
RFP763340/714952	p 57	N85-16195 * #			
R82AEB358	p 95	N83-12451 * #			
R83-956077-1	p 100	N84-10613 * #			
R83-956077-2	p 100	N84-10614 * #			
R84-956627-1	p 12	N86-24693 * #			
SATR-2	p 96	N83-23629 * #			
SM-8	p 101	N84-15589 * #			
SWRI-7576/30	p 115	N86-10589 * #			
UDR-TR-82-119	p 94	N82-33738 * #			
UDR-TR-83-57	p 96	N83-23629 * #			
UDR-TR-83-57	p 100	N84-10612 * #			
US-PATENT-APPL-SN-122967	p 24	N81-26179 * #			
US-PATENT-APPL-SN-463456	p 49	N85-30333 * #			
US-PATENT-APPL-SN-893857	p 23	N81-17170 * #			

Report Documentation Page

1. Report No. NASA TM-100842		2. Government Accession No.		3. Recipient's Catalog No.	
4. Title and Subtitle ENGINE STRUCTURES A Bibliography of Lewis Research Center's Research for 1980-1987				5. Report Date September 1988	
				6. Performing Organization Code	
7. Author(s)				8. Performing Organization Report No. E-4033	
				10. Work Unit No. 506-63-1B	
9. Performing Organization Name and Address National Aeronautics and Space Administration Lewis Research Center Cleveland, Ohio 44135-3191				11. Contract or Grant No.	
				13. Type of Report and Period Covered Technical Memorandum	
12. Sponsoring Agency Name and Address National Aeronautics and Space Administration Washington, D.C. 20546-0001				14. Sponsoring Agency Code	
15. Supplementary Notes Compiled by the Committee for LST '88, the Lewis Structures Technology Symposium and Exposition, Cleveland, Ohio, May 24-25, 1988.					
16. Abstract This compilation of abstracts describes and indexes the technical reporting that resulted from the scientific and engineering work performed and managed by the Structures Division of the Lewis Research Center from 1980 through 1987. All the publications were announced in the 1980-1987 issues of STAR (Scientific and Technical Aerospace Reports) and/or IAA (International Aerospace Abstracts). Included are research reports, journal articles, conference presentations, patents and patent applications, and theses.					
17. Key Words (Suggested by Author(s)) Bibliographies; Abstracts; Documentation; Indexes (documentation); Structures; Mechanics; Dynamics; Durability				18. Distribution Statement Unclassified - Unlimited Subject Category 39	
19. Security Classif. (of this report) Unclassified		20. Security Classif. (of this page) Unclassified		21. No of pages 218	
				22. Price* A10	